Volume 177 Number 1

THE BIOLOGICAL BULLETIN

AUGUST, 1989

Published by the Marine Biological Laboratory

THE
BIOLOGICAL BULLETIN

PUBLISHED BY
THE MARINE BIOLOGICAL LABORATORY

DECEMBER, 1989

Printed and Issued by
LANCASTER PRESS, Inc.
PRINCE & LEMON STS.
LANCASTER, PA

THE BIOLOGICAL BULLETIN

THE BIOLOGICAL BULLETIN is published six times a year by the Marine Biological Laboratory, MBL Street, Woods Hole, Massachusetts 02543.

Subscriptions and similar matter should be addressed to Subscription Manager, THE BIOLOGICAL BULLETIN, Marine Biological Laboratory, Woods Hole, Massachusetts 02543. Single numbers, $25.00. Subscription per volume (three issues), $57.50 ($115.00 per year for six issues).

Communications relative to manuscripts should be sent to Michael J. Greenberg, Editor-in-Chief, or Pamela L. Clapp, Managing Editor, at the Marine Biological Laboratory, Woods Hole, Massachusetts 02543. Telephone: (508) 548-3705, ext. 428. FAX: 508-540-6902.

POSTMASTER: Send address changes to THE BIOLOGICAL BULLETIN, Marine Biological Laboratory, Woods Hole, MA 02543.

Second-class postage paid at Woods Hole, MA, and additional mailing offices.
ISSN 0006-3185

INSTRUCTIONS TO AUTHORS

The Biological Bulletin accepts outstanding original research reports of general interest to biologists throughout the world. Papers are usually of intermediate length (10–40 manuscript pages). Very short papers (less than 9 manuscript pages including tables, figures, and bibliography) will be published in a separate section entitled "Notes." A limited number of solicited review papers may be accepted after formal review. A paper will usually appear within four months after its acceptance.

The Editorial Board requests that manuscripts conform to the requirements set below; those manuscripts that do not conform will be returned to authors for correction before review.

1. ***Manuscripts.*** Manuscripts, including figures, should be submitted in triplicate. (Xerox copies of photographs are not acceptable for review purposes.) The original manuscript must be typed in no smaller than 12 pitch, using double spacing (*including* figure legends, footnotes, bibliography, etc.) on one side of 16- or 20-lb. bond paper, 8½ by 11 inches. Please, no right justification. Manuscripts should be proofread carefully and errors corrected legibly in black ink. Pages should be numbered consecutively. Margins on all sides should be at least 1 inch (2.5 cm). Manuscripts should conform to the *Council of Biology Editors Style Manual*, 4th Edition (Council of Biology Editors, 1978) and to American spelling. Unusual abbreviations should be kept to a minimum and should be spelled out on first reference as well as defined in a footnote on the title page. Manuscripts should be divided into the following components: Title page, Abstract (of no more than 200 words), Introduction, Materials and Methods, Results, Discussion, Acknowledgments, Literature Cited, Tables, and Figure Legends. In addition, authors should supply a list of words and phrases under which the article should be indexed.

2. ***Title page.*** The title page consists of: a condensed title or running head of no more than 35 letters and spaces, the manuscript title, authors' names and appropriate addresses, and footnotes listing present addresses, acknowledgments or contribution numbers, and explanation of unusual abbreviations.

3. ***Figures.*** The dimensions of the printed page, 7 by 9 inches, should be kept in mind in preparing figures for publication. We recommend that figures be about 1½ times the linear dimensions of the final printing desired, and that the ratio of the largest to the smallest letter or number and of the thickest to the thinnest line not exceed 1:1.5. Explanatory matter generally should be included in legends, although axes should always be identified on the illustration itself. Figures should be prepared for reproduction as either line cuts or halftones. Figures to be reproduced as line cuts should be unmounted glossy photographic reproductions or drawn in black ink on white paper, good-quality tracing cloth or plastic, or blue-lined coordinate paper. Those to be reproduced as halftones should be mounted on board, with both designating numbers or letters and scale bars affixed directly to the figures. All figures should be numbered in consecutive order, with no distinction between text and plate figures. The author's name and an arrow indicating orientation should appear on the reverse side of all figures.

4. ***Tables, footnotes, figure legends, etc.*** Authors should follow the style in a recent issue of *The Biological Bulletin* in preparing table headings, figure legends, and the like. Because of the high cost of setting tabular material in type, authors are asked to limit such material as much as possible. Tables, with their headings and footnotes, should be typed on separate sheets, numbered with consecutive Roman numerals, and placed after the Literature Cited. Figure legends should contain enough information to make the figure intelligible separate from the text. Legends should be typed double spaced, with consecutive Arabic numbers, on a separate sheet at the end of the paper. Footnotes should be limited to authors' current addresses, acknowledgments or contribution numbers, and explanation of unusual abbreviations. All such footnotes should appear on the title page. Footnotes are not normally permitted in the body of the text.

5. ***Literature cited.*** In the text, literature should be cited by the Harvard system, with papers by more than two authors cited as Jones *et al.*, 1980. Personal communications and material in preparation or in press should be cited in the text only, with author's initials and institutions, unless the material has been formally accepted and a volume number can be supplied. The list of references following the text should be headed Literature Cited, and must be typed double spaced on separate

pages, conforming in punctuation and arrangement to the style of recent issues of *The Biological Bulletin*. Citations should include complete titles and inclusive pagination. Journal abbreviations should normally follow those of the U. S. A. Standards Institute (USASI), as adopted by BIOLOGICAL ABSTRACTS and CHEMICAL ABSTRACTS, with the minor differences set out below. The most generally useful list of biological journal titles is that published each year by BIOLOGICAL ABSTRACTS (BIOSIS List of Serials; the most recent issue). Foreign authors, and others who are accustomed to using THE WORLD LIST OF SCIENTIFIC PERIODICALS, may find a booklet published by the Biological Council of the U.K. (obtainable from the Institute of Biology, 41 Queen's Gate, London, S.W.7, England, U.K.) useful, since it sets out the WORLD LIST abbreviations for most biological journals with notes of the USASI abbreviations where these differ. CHEMICAL ABSTRACTS publishes quarterly supplements of additional abbreviations. The following points of reference style for THE BIOLOGICAL BULLETIN differ from USASI (or modified WORLD LIST) usage:

A. Journal abbreviations, and book titles, all underlined (for *italics*)

B. All components of abbreviations with initial capitals (not as European usage in WORLD LIST *e.g. J. Cell. Comp. Physiol.* NOT *J. cell. comp. Physiol.*)

C. *All* abbreviated components must be followed by a period, whole word components *must not* (*i.e. J. Cancer Res.*)

D. Space between all components (*e.g. J. Cell. Comp. Physiol.*, not *J.Cell.Comp.Physiol.*)

E. Unusual words in journal titles should be spelled out in full, rather than employing new abbreviations invented by the author. For example, use *Rit Vísindafjélags Islendinga* without abbreviation.

F. All single word journal titles in full (*e.g. Veliger, Ecology, Brain*).

G. The order of abbreviated components should be the same as the word order of the complete title (*i.e. Proc.* and *Trans.* placed where they appear, not transposed as in some BIOLOGICAL ABSTRACTS listings).

H. A few well-known international journals in their preferred forms rather than WORLD LIST or USASI usage (*e.g. Nature, Science, Evolution* NOT *Nature, Lond., Science, N.Y.; Evolution, Lancaster, Pa.*)

6. ***Reprints, page proofs, and charges.*** Authors receive their first 100 reprints (without covers) free of charge. Additional reprints may be ordered at time of publication and normally will be delivered about two to three months after the issue date. Authors (or delegates for foreign authors) will receive page proofs of articles shortly before publication. They will be charged the current cost of printers' time for corrections to these (other than corrections of printers' or editors' errors). Other than these charges for authors' alterations, *The Biological Bulletin* does not have page charges.

CONTENTS

No. 1, August 1989

No. 2, October 1989

CONSISTENCY AND VARIABILITY IN PEPTIDE FAMILIES

No. 3, December 1989

BEHAVIOR

DEVELOPMENT AND REPRODUCTION

ECOLOGY AND EVOLUTION

PHYSIOLOGY

THE
BIOLOGICAL BULLETIN

PUBLISHED BY
THE MARINE BIOLOGICAL LABORATORY

AUGUST, 1989

Printed and Issued by
LANCASTER PRESS, Inc.
PRINCE & LEMON STS.
LANCASTER, PA

THE BIOLOGICAL BULLETIN is published six times a year by the Marine Biological Laboratory, MBL Street, Woods Hole, Massachusetts 02543.

Subscriptions and similar matter should be addressed to Subscription Manager, THE BIOLOGICAL BULLETIN, Marine Biological Laboratory, Woods Hole, Massachusetts 02543. Single numbers, $25.00. Subscription per volume (three issues), $57.50 ($115.00 per year for six issues).

Communications relative to manuscripts should be sent to Michael J. Greenberg, Editor-in-Chief, or Pamela L. Clapp, Managing Editor, at the Marine Biological Laboratory, Woods Hole, Massachusetts 02543.

POSTMASTER: Send address changes to THE BIOLOGICAL BULLETIN, Marine Biological Laboratory, Woods Hole, MA 02543.

Second-class postage paid at Woods Hole, MA, and additional mailing offices.
ISSN 0006-3185

INSTRUCTIONS TO AUTHORS

The Biological Bulletin accepts outstanding original research reports of general interest to biologists throughout the world. Papers are usually of intermediate length (10–40 manuscript pages). Very short papers (less than 9 manuscript pages including tables, figures, and bibliography) will be published in a separate section entitled "Notes." A limited number of solicited review papers may be accepted after formal review. A paper will usually appear within four months after its acceptance.

The Editorial Board requests that manuscripts conform to the requirements set below; those manuscripts that do not conform will be returned to authors for correction before review.

1. ***Manuscripts.*** Manuscripts, including figures, should be submitted in triplicate. (Xerox copies of photographs are not acceptable for review purposes.) The original manuscript must be typed in no smaller than 12 pitch, using double spacing (*including* figure legends, footnotes, bibliography, etc.) on one side of 16- or 20-lb. bond paper, 8½ by 11 inches. Please, no right justification. Manuscripts should be proofread carefully and errors corrected legibly in black ink. Pages should be numbered consecutively. Margins on all sides should be at least 1 inch (2.5 cm). Manuscripts should conform to the *Council of Biology Editors Style Manual*, 4th Edition (Council of Biology Editors, 1978) and to American spelling. Unusual abbreviations should be kept to a minimum and should be spelled out on first reference as well as defined in a footnote on the title page. Manuscripts should be divided into the following components: Title page, Abstract (of no more than 200 words), Introduction, Materials and Methods, Results, Discussion, Acknowledgments, Literature Cited, Tables, and Figure Legends. In addition, authors should supply a list of words and phrases under which the article should be indexed.

2. ***Title page.*** The title page consists of: a condensed title or running head of no more than 35 letters and spaces, the manuscript title, authors' names and appropriate addresses, and footnotes listing present addresses, acknowledgments or contribution numbers, and explanation of unusual abbreviations.

3. ***Figures.*** The dimensions of the printed page, 7 by 9 inches, should be kept in mind in preparing figures for publication. We recommend that figures be about 1½ times the linear dimensions of the final printing desired, and that the ratio of the largest to the smallest letter or number and of the thickest to the thinnest line not exceed 1:1.5. Explanatory matter generally should be included in legends, although axes should always be identified on the illustration itself. Figures should be prepared for reproduction as either line cuts or halftones. Figures to be reproduced as line cuts should be unmounted glossy photographic reproductions or drawn in black ink on white paper, good-quality tracing cloth or plastic, or blue-lined coordinate paper. Those to be reproduced as halftones should be mounted on board, with both designating numbers or letters and scale bars affixed directly to the figures. All figures should be numbered in consecutive order, with no distinction between text and plate figures. The author's name and an arrow indicating orientation should appear on the reverse side of all figures.

4. ***Tables, footnotes, figure legends, etc.*** Authors should follow the style in a recent issue of *The Biological Bulletin* in preparing table headings, figure legends, and the like. Because of the high cost of setting tabular material in type, authors are asked to limit such material as much as possible. Tables, with their headings and footnotes, should be typed on separate sheets, numbered with consecutive Roman numerals, and placed after the Literature Cited. Figure legends should contain enough information to make the figure intelligible separate from the text. Legends should be typed double spaced, with consecutive Arabic numbers, on a separate sheet at the end of the paper. Footnotes should be limited to authors' current addresses, acknowledgments or contribution numbers, and explanation of unusual abbreviations. All such footnotes should appear on the title page. Footnotes are not normally permitted in the body of the text.

5. ***Literature cited.*** In the text, literature should be cited by the Harvard system, with papers by more than two authors cited as Jones *et al.*, 1980. Personal communications and material in preparation or in press should be cited in the text only, with author's initials and institutions, unless the material has been formally accepted and a volume number can be supplied. The list of references following the text should be headed Literature Cited, and must be typed double spaced on separate

pages, conforming in punctuation and arrangement to the style of recent issues of *The Biological Bulletin*. Citations should include complete titles and inclusive pagination. Journal abbreviations should normally follow those of the U. S. A. Standards Institute (USASI), as adopted by BIOLOGICAL ABSTRACTS and CHEMICAL ABSTRACTS, with the minor differences set out below. The most generally useful list of biological journal titles is that published each year by BIOLOGICAL ABSTRACTS (BIOSIS List of Serials; the most recent issue). Foreign authors, and others who are accustomed to using THE WORLD LIST OF SCIENTIFIC PERIODICALS, may find a booklet published by the Biological Council of the U.K. (obtainable from the Institute of Biology, 41 Queen's Gate, London, S.W.7, England, U.K.) useful, since it sets out the WORLD LIST abbreviations for most biological journals with notes of the USASI abbreviations where these differ. CHEMICAL ABSTRACTS publishes quarterly supplements of additional abbreviations. The following points of reference style for THE BIOLOGICAL BULLETIN differ from USASI (or modified WORLD LIST) usage:

A. Journal abbreviations, and book titles, all underlined (for *italics*)

B. All components of abbreviations with initial capitals (not as European usage in WORLD LIST *e.g. J Cell. Comp. Physiol.* NOT *J. cell. comp. Physiol.*)

C. *All* abbreviated components must be followed by a period, whole word components *must not* (*i.e. J. Cancer Res.*)

D. Space between all components (*e.g. J. Cell. Comp. Physiol.*, not *J.Cell.Comp.Physiol.*)

E. Unusual words in journal titles should be spelled out in full, rather than employing new abbreviations invented by the author. For example, use *Rit Visindafjélags Islendinga* without abbreviation.

F. All single word journal titles in full (*e.g. Veliger, Ecology, Brain*).

G. The order of abbreviated components should be the same as the word order of the complete title (*i.e. Proc.* and *Trans.* placed where they appear, not transposed as in some BIOLOGICAL ABSTRACTS listings).

H. A few well-known international journals in their preferred forms rather than WORLD LIST or USASI usage (*e.g. Nature, Science, Evolution* NOT *Nature, Lond., Science, N.Y., Evolution, Lancaster, Pa.*)

6. ***Reprints, page proofs, and charges.*** Authors receive their first 100 reprints (without covers) free of charge. Additional reprints may be ordered at time of publication and normally will be delivered about two to three months after the issue date. Authors (or delegates for foreign authors) will receive page proofs of articles shortly before publication. They will be charged the current cost of printers' time for corrections to these (other than corrections of printers' or editors' errors). Other than these charges for authors' alterations, *The Biological Bulletin* does not have page charges.

Editor's Note

For ten years, as the editor of *The Biological Bulletin*, Dr. Charles B. Metz, worked to improve the technical quality and content of the journal, and to meet the rising standards expected of it. He was eminently successful, and I am pleased to express my appreciation, and that of the Editorial Board and staff, for his efforts; he has prepared the way well for those of us who follow.

The Biological Bulletin will continue to publish outstanding papers for a general readership with interests in contemporary aspects of biology.

—M.J.G.

The Marine Biological Laboratory

Ninety-First Report for the Year 1988 One-Hundred and First Year

Officers of the Corporation

Denis M. Robinson, *Honorary Chairman of the Board of Trustees*
Prosser Gifford, *Chairman of the Board of Trustees*
Harlyn O. Halvorson, *President of the Corporation and Director*
Robert D. Manz, *Treasurer*
Kathleen Dunlap, *Clerk of the Corporation*

Contents

Report of the President and Director

Our National Marine Biological Laboratory in 1988: The Years Ahead Are Here

It will be an interesting place to watch, in the years ahead. In a rational world, things ought to go as well for the MBL as they have in the past, and it should become an even larger and more agile collective intelligence.
—Lewis Thomas

In his 1974 book, *The Lives of a Cell,* Lewis Thomas called the MBL America's unofficial "National Biological Laboratory." In the 14 years since Dr. Thomas honored the MBL with that title, we have pointed proudly to that passage on a number of occasions—because it is flattering, because it is true, and because it comes from such a distinguished participant in, and observer of, American biology.

But when you read the chapter in which the passage occurs, you find Dr. Thomas was not simply passing out compliments. In fact, his MBL chapter is a meditation on the life of institutions, and a good, hard look (from the early 1970s) at where one of America's odder institutions—the MBL—was headed. In the same sentence in which he identified the MBL as the national center for biology, Dr. Thomas identified the major challenge facing the laboratory: "It is the National Biological Laboratory without being officially designated (or yet funded) as such," he wrote. In a bit of inspired prophecy, Dr. Thomas went on to list a series of challenges the MBL was facing—and continues to face.

In this 101st director's report, I call your attention to Dr. Thomas' analysis of the MBL because we are now well into the future he anticipated so clearly back in 1974. I will return to Dr. Thomas' words shortly, after highlighting some of the milestones of our Centennial year, 1988.

Report of the year

While the years leading to up to the centennial were a time of reassessment, the centennial year itself was, in part, a celebration of the Laboratory's long and useful life. Those celebratory activities are recorded at the end of this volume and in the Autumn 1988 *Collecting Net* (vol. 6, no. 2). Here, it is sufficient to note that the national science community joined us in celebrating the Laboratory's past and, simultaneously, in reaffirming its status as a national facility for research and teaching—a place where senior investigators can do important work and where new generations of experimental biologists can receive the most rigorous training.

But if 1988 was a year for celebrating, it was also a year for building and strengthening. In August, the Howard Hughes Medical Institute awarded us a $4 million grant in support of our courses and our library. Announcing the grant, Hughes Institute President Purnell W. Choppin called the MBL "a richly productive research institute and one of the nation's most prized assets for scientific education."

The Hughes grant includes a $1 million portion earmarked for modernizing the MBL/WHOI Library. The grant comes at a time when we are facing a national crisis in information management, fired by the accelerating pace and changing nature of biological research, which has created an urgent demand for more efficient information processing and retrieval. The Hughes grant has allowed us to establish a Library Planning Committee, chaired by Dr. Edward A. Adelberg, deputy provost for the biomedical sciences at Yale. The planning committee is composed of two

subcommittees: Information Management and Technology, Research and Education, chaired by Dr. Carl Bowin, a geologist from the Woods Hole Oceanographic Institution; and Facilities and Collections, chaired by Nina Matheson, director of The Johns Hopkins University's William H. Welch Medical Library. The grant has also allowed us to establish an Office of Library Planning, directed by Catherine Norton, formerly the MBL assistant librarian. Long a leader in the pursuit of biological knowledge, the MBL is now taking a leadership role in the exploration of computer technology and scientific information management.

The same Hughes grant provides a $3 million foundation for our summer courses, including Neurobiology, Physiology, Embryology, and Microbiology. The generous grant will support those outstanding courses over a seven-year period.

Further recognition of the Laboratory's national character came in September when Congress passed and the president signed a $2.2 million appropriation toward the construction of a Marine Biomedical Institute for Advanced Studies at the MBL. The MBIAS will include a new Advanced Studies Laboratory that will house year-round researchers working in areas related to traditional MBL strengths, including cell and developmental biology, neurobiology, microbial physiology, and molecular evolution. The MBIAS will also include a new marine resources building with facilities for culturing and studying marine animals important to biomedical research.

The $2.2 million appropriation is an important first step. Beyond the initial appropriation, Congress passed a bill authorizing additional funds that will be required for construction of the new facilities. The authorization does not guarantee funding, but allows us to go back to Congress for a significant portion of the $25 million dollars that will be needed to complete the MBIAS.

In addition to locating new sources of support, we strengthened programs, put together an increasingly professional and effective staff, and broadened our base in a number of areas:

• Dr. Leslie Garrick arrived in June to direct the Office of Sponsored Programs. This critical department has prospered under his energetic, professional, and accurate style of management. One of his reorganization efforts was the redesign of the Annual Bulletin, with the goal of making it as coherent and useful as possible.

• In the summer and early autumn, two new courses got off to rousing starts. Eminently worthy of MBL tradition, the Methods in Computational Neuroscience course and the Molecular Evolution course are both operating at the forefront of their fields.

• Our summer research space rental was at or near capacity, despite the additional space opened by the departure of the year-round NINCDS laboratories.

• We worked with the American Psychological Association to develop an NIMH-funded Special Seminar Program for Minority Neuroscience Fellows, which will bring as many as 12 fellows and 4 faculty to the MBL in the summer of 1989.

• With our neighbors and colleagues at the Woods Hole Oceanographic Institution, we established an MBL/WHOI protein and nucleotide instrumentation core facility. The facility, which will open sometime in 1989, is supported by a $375,000 NSF grant.

• A committee chaired by Dr. Holger Jannasch and Dr. George Davis reviewed the Gray Museum collection to advise us on the best management of this resource.

• A committee led by Dr. Robert Barlow reviewed *The Biological Bulletin* and carried out a successful search for an editor to replace Dr. Charles Metz, the retiring editor who led the *Bulletin* with distinction for a decade. The new editor will be announced in 1989.

• On the personnel front, we worked hard in 1988 to develop the strong, professional staff the MBL needs to meet the challenges we face in the next few years. The employees of the Laboratory have long been one of its most important resources, and in the Centennial year we tried to turn special attention to employee issues and concerns. I am very happy with the results of our search for a personnel director: Susan Goux, an experienced personnel and affirmative action professional, became the MBL Human Resources Manager in December. Over the course of the year, we also improved the employees' retirement plan and made significant progress on an employee grievance procedure.

• Recognizing the increasing financial difficulties facing young investigators who want to come to the MBL, we restored Steps Toward Independence: A Program of Support for Research and Scholarship by Junior Faculty Members. Beginning in the summer of 1989, the Steps program will once again help untenured faculty from across the country come to the MBL at a time when their research careers can be most enriched by our unique facilities, associations, and training.

• I mentioned earlier that we found new sources of support in 1988—but one traditional source of support deserves special mention. The Annual Fund reached new heights in 1988, with a record number of Corporation members contributing to a record total that topped $100,000 for the first time in the Laboratory's history. This is the second consecutive year the annual Fund has broken previous records. Additionally, philanthropic support in 1988 reached record levels.

So 1988 was a year for celebrating the past and building for the future—but it was also a year for honoring those who have supported the Laboratory over the years. We had the pleasure of thanking many individuals, families, and foundations, whose names are recorded elsewhere (see the Autumn 1988 issue of *The Collecting Net* [vol 6, no 2] for a list of Centennial awards). In August, we were pleased to be able to acknowledge the support of two families with the

Ellen Grass, Albert Grass, and John Dowling at the 22 July 1988 dedication of the Grass Reference Room.

dedication of the Grass Reference Room (named for Ellen R. and Albert M. Grass, in appreciation of their long-standing support of neuroscience at the MBL) and the Bay Reading Room (named for Charles Ulrick Bay, whose foundation in 1987 made the generous gift to the library that enabled us to complete the Mellon challenge grant).

I cannot close out the Centenial year without thanking the many volunteers who served on Centennial subcommittees, and the good friends of the Laboratory who led those subcommittees: Garland Allen (History); Jelle Atema and Olivann Hobbie (Cultural Events); Robert Barlow (Scientific Events); John Pfeiffer (Public Information). Finally, I want to cite Dr. James Ebert for the distinguished leadership he provided throughout the Centennial observances. Most Corporation members know that Dr. Ebert served as Centennial chairman; few can know how patient, steady, and valuable his leadership was.

Where we are at the close of 1988

The close of our Centennial year finds us in the familiar favored position we've occupied for most of our 100-year history: we are firmly situated as a national biological facility, with important programmatic ties to other major institutions. We continued to be connected, for instance, to Boston University through the BUMP program, to the University of Pennsylvania through the Laboratory of Marine Animal Health, to our near-neighbors at the Oceanographic Institution and our distant neighbors in Naples and Japan. We are working hard to strengthen the formal, institutional ties we have and to develop new ones, where that is appropriate. At the same time, we continue to serve as a national laboratory to individual scientists—the hundreds of investigators and students who come from their home institutions to spend part of the year teaching, studying, and doing research in Woods Hole.

Moving just outside the immediate scientific community, we are attracting the interest of a national audience of historians and philosophers of science. In a 1988 book titled *The American Development of Biology*, historian Phillip J. Pauley noted, "Unlike most investigators, who experienced the 'scientific community' largely as an abstraction that referred to the variety of contacts they made in schools, journals, and professional meetings, biologists structured their professional lives around one place—the Marine Biological Laboratory, in the village of Woods Hole."

At the close of our Centennial year, the general public is a bit better acquainted with the MBL and its mission. Although the science at the MBL has long been reported in the popular press by science writers, the MBL as an institution caught the attention of the national press during the Centennial. Among other national press clippings from 1988, one PBS show (Newton's Apple) devoted a half-hour to the MBL and *Smithsonian* magazine ran a feature article about the MBL in their June issue ("A World Center of Basic Biology Celebrates a Century of Science by the Sea").

The years ahead: the challenges

"There is no way of predicting what the future will be like for an institution such as the MBL," Lewis Thomas wrote back in 1974—then proceeded to describe precisely the challenges we have faced in the last decade and a half, and are facing still today.

"One way or another," Dr. Thomas wrote, "(the MBL) will evolve. It may shift soon into a new phase,

with a year-round program for teaching and research and a year-round staff, but it will have to accomplish this without jeopardizing the immense power of its summer programs, or all institutional hell with break loose. It will have to find new ways for relating to the universities, if its graduate programs are to expand as they should. It will have to develop new symbiotic relations with the Oceanographic Institution, since both places have so much at stake. And it will have to find more money, much more—the kind of money that only federal governments possess—without losing any of its own initiative."

That is the prophecy I mentioned in the opening of this report, and I cite it here because each point in it has come to pass. The MBL has evolved, and is evolving. For some time now, year-round programs have been an essential part of the MBL, and they will have to play a larger role in the years to come—without jeopardizing the summer programs, of course. We are looking for ways to strengthen existing ties and to develop new ties to the universities we serve. We are exploring joint initiatives with WHOI, working with that institution's enthusiastic new director, Dr. Craig Dorman, to develop new symbiotic relationships.

And we are looking for money, much more. The federal government has provided some of what we need, but our needs remain large. We have aging facilities, and, like most academic institutions, we have too often deferred maintenance. We need to build major new facilities—the Advanced Studies Laboratory and a marine resources building. We need to find a permanent endowment that will support our educational program when the generous Hughes grant runs out in 1995. We must be concerned about the difficulties faced by new generations of MBL biologists—the high costs of housing and lab fees, the paucity of parking. These challenges are numerous enough and large enough that we need the help of a broad coalition of trustees and Corporation members.

The years ahead: the case for unbridled optimism

Looking at science and the national agenda, I am convinced that the last years of this century are a propitious time for the MBL to be re-dedicating itself to serving a national science community, in the classroom and in the laboratory.

In the classroom: teachers, politicians, leaders of industry, and virtually everyone else is calling for improvements in science education and training, with the sort of fervor and sense of national urgency we've not seen since the days of Sputnik. Across the country, there is a call for more and better trained young scientists—a development that bodes well for our educational program.

In the laboratory: biology's contributions to health care and agriculture (and to the nation's economy) are already well-recognized. New areas of research, such as molecular evolution, computational neuroscience, molecular parasitology, and marine microbiology are attracting the attention of industry, foundations, and governmental agencies. In an era of increasingly scarce national resources, I think we will nonetheless find that opportunities—and funding—for biological research and training are going to continue to be available to the institutions best situated to serve the nation's obvious need for better science.

Increasingly, there is a national call not only for more science but also for a more science-literate public. In this effort, too, the MBL has a role to play. In 1988, we hosted the third class of MBL Science Writing Fellows, supported by the Carnegie Corporation of New York, the Sloan Foundation, and the Foundation for Microbiology. In December, one of the 1987 fellows, *Washington Post* science writer Boyce Rensberger, published in the *Post* a remarkable five-part series on basic biology. This highly sophisticated yet completely accessible series stands as a testament to the usefulness of the MBL science writing fellowships and as a model of what science writing for the public can be.

In another effort to boost the level of public dialogue about science-related issues, we announced in 1988 the establishment of an annual Lewis Thomas Award for excellence in communicating basic research in life sciences to the general public. The first winner will be announced in 1989.

Dealing more directly with public education, we have established, with Simon's Rock of Bard College, a summer program to train high school teachers and teach marine biology to 30 high school students. In an attempt to continue our partnership with local schools, we are setting aside a number of those 30 slots for local students.

The close of our Centennial year finds us in good shape, with formidable—but surmountable—challenges before us. Where we were strong, we're still strong. Where there are national needs for biological research and education, we're well-positioned to develop appropriate new programs and new ties to complement our existing programs and ties. Most hopefully, I can report that significant national sources of support appear to be available.

We made good progress in 1988. We'll need to make more, much more, in 1989 and the years immediately beyond, but I can report this year that we are already well into the process of becoming the larger and more agile collective intelligence that Lewis Thomas predicted 14 years ago.

—Harlyn Halvorson

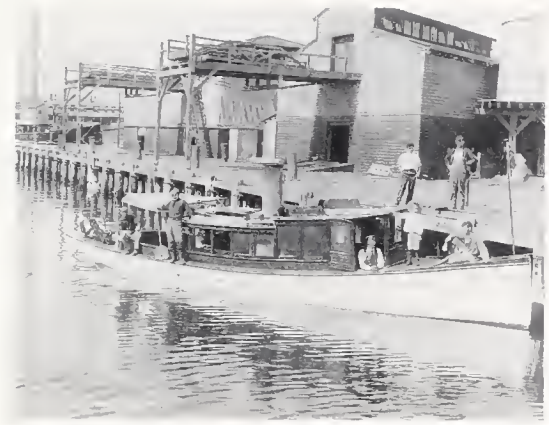

B Coolidge

Report of the Treasurer

The year 1988 was a successful one for the Laboratory. Unrestricted operations other than Housing showed a deficit of revenues to expenses of $28,637, considerably better than the budgeted deficit of $80,000. You will remember that the Executive Committee approved a one-time deficit budget for 1988, recognizing the challenges of that year of administrative transition and explicitly refusing to reduce services given the financial strength and good prospects of the Laboratory.

The Housing enterprises fund showed an excess of revenues over expenses of $151,786, of which $51,786 was applied to the reduction of debt principal and $100,000 was used to fund depreciation for Housing.

The total of the MBL's unrestricted operations, including Housing, thus showed an excess of revenues over expenses of $123,149. While this result is gratifying, we should not be satisfied until the excess of revenues over expenses has reached the total of our depreciation on plant—$561,239 in 1988.

We saw some very positive trends in 1988. For the first time since 1985, grant support of direct costs of the year-round program increased. We expect that support to increase again in 1989 and to continue to grow as the MBIAS program takes shape. Our summer research program brought in considerably more revenues in 1988—$606,218 *versus* $521,338 in 1987. That strength at the core of the Laboratory's scientific program is very heartening. 1988 saw the receipt of the first funds from the Howard Hughes Medical Institute under its $4 million grant to the Laboratory for support of instructional program overhead and modernization of Library systems. This seven-year grant will give us the time to seek endowments to underwrite the Laboratory's unique role in biological education, and will allow study of the best route to the twenty-first century for the Library.

Total expenses of the Laboratory grew by more than 8% in 1988. Almost all of the real increase, *i.e.*, in excess of the inflation rate of 4% was in administration. You will see a similar, though smaller, increase in 1989. My experience with the Laboratory leads me to conclude that that increase is fully warranted; I am confident that we have added "beef" rather than "flab." As I survey the challenges ahead of us, I am more confident of success when I look at the excellent management team that Paul Gross started, and that Harlyn Halvorson and Ray Epstein have continued to build. The continued excellence of your Laboratory depends critically on the talent and motivation of its managers.

There is one area of serious financial concern to which I want to draw your attention. As I have pointed out before, our plant renovation and replacement needs have exceeded our capital-generating capacity. The result has been that capital reserve funds have been drawn down. The Laboratory's unrestricted quasi-endowment—monies set aside by the Laboratory in the past to serve as endowment until and unless otherwise needed—have declined from $1,072,186 in 1985 to $409,997 in 1988 and are budgeted to decline to $390,000 in 1989. Any further reductions would be imprudent, but the demands of our plant for repair and modernization will not cease.

I know that we will do a better job in the near future at generating capital funds for our plant repair and replacement. By continuing to improve our financial discipline, we will generate capital through operations that can be used to renew our existing plant. In addition, as we add new facilities to our plant, we will keep our eyes on the need to assure ourselves that the necessary funds are in place, whether through operations or endowment to properly maintain them.

—Robert D. Manz

Financial Statements

Coopers
&Lybrand

certified public accountants

REPORT OF INDEPENDENT ACCOUNTANTS

To the Trustees of
Marine Biological Laboratory
Woods Hole, Massachusetts

We have audited the accompanying balance sheet of Marine Biological Laboratory as of December 31, 1988 and the related statement of support, revenues, expenses and changes in fund balances for the year then ended. We previously examined and reported upon the financial statements of the Laboratory for the year ended December 31, 1987, which condensed statements are presented for comparative purposes only. These financial statements are the responsibility of the Laboratory's management. Our responsibility is to express an opinion on these financial statements based on our audit.

We conducted our audit in accordance with generally accepted auditing standards. Those standards require that we plan and perform the audit to obtain reasonable assurance about whether the financial statements are free of material misstatement. An audit includes examining, on a test basis, evidence supporting the amounts and disclosures in the financial statements. An audit also includes assessing the accounting principles used and significant estimates made by management, as well as evaluating the overall financial statement presentation. We believe that our audit provides a reasonable basis for our opinion.

In our opinion, the financial statements referred to above present fairly, in all material respects, the financial position of Marine Biological Laboratory at December 31, 1988, and its support, revenues, expenses and changes in fund balances for the year then ended in conformity with generally accepted accounting principles.

Coopers & Lybrand

Boston, Massachusetts
April 15, 1989

(Except for the information
presented in Note J, for
which the date is May 23, 1989.)

MARINE BIOLOGICAL LABORATORY

BALANCE SHEETS

December 31, 1988 and 1987

ASSETS	*1988*	*1987*
Cash and savings deposits	$ 199,970	$ 531,705
Money market securities (Notes B and H)	1,750,000	850,000
Accounts receivable, net of allowance for uncollectible accounts	576,355	586,776
Receivables due for costs incurred on grants and contracts	836,608	595,925
Other assets	50,370	19,199
Total current assets	3,413,303	2,583,605
Investments, at market (Notes B and H)	11,401,121	10,268,985
Land, buildings and equipment (Notes B and C)	19,682,987	19,304,410
Less accumulated depreciation	(8,268,927)	(7,707,689)
	11,414,060	11,596,721
Total assets	$26,228,484	$24,449,311

LIABILITIES AND FUND BALANCES	*1988*	*1987*
Accounts payable and accrued expenses	$ 510,559	$ 449,140
Deferred income	116,345	92,800
Current portion of long-term debt	49,968	78,654
Total current liabilities	676,872	620,594
Mortgage and notes payable (Note G)	1,155,489	1,185,315
Current unrestricted fund balances:		
Current unrestricted funds	13,275	84,572
Housing enterprise funds	—	—
	13,275	84,572
Current restricted fund balances:		
Unexpended grants	264,818	459,179
Unexpended gifts	2,557,324	1,113,768
Unexpended income of endowment funds	129,520	80,387
	2,951,662	1,653,334
Endowment fund balances:		
Income for unrestricted purposes	2,850,409	2,671,519
Income for restricted purposes	3,595,974	3,053,692
	6,446,383	5,725,211
Quasi-endowment fund balances:		
Unrestricted	409,997	792,538
Restricted	3,913,255	3,766,195
	4,323,252	4,558,733
Plant fund balances:		
Unrestricted	10,251,388	10,375,536
Repairs and replacement reserve	380,241	231,016
Restricted	29,922	15,000
	10,661,551	10,621,552
Total liabilities and fund balances	$26,228,484	$24,449,311

The accompanying notes are an integral part of the financial statements.

MARINE BIOLOGICAL LABORATORY

STATEMENT OF SUPPORT, REVENUES, EXPENSES AND CHANGES IN FUND BALANCES

for the year ended December 31, 1988
(with comparative totals for 1987)

	Current Funds								Plant Funds				
					Endowment Funds		Quasi-Endowment Funds						
	Current Unrestricted Fund	Housing Enterprises Fund	Total Current Unrestricted Fund	Current Restricted Fund	Unrestricted	Restricted	Unrestricted	Restricted	Unrestricted	Restricted	Repairs and Replacement Reserve	1988 Total All Funds	1987 Total All Funds
SUPPORT AND REVENUES:													
Grant reimbursement of direct costs:													
Instruction				$ 423,309								$ 423,309	$ 359,811
Research				3,694,636								3,694,636	3,653,808
Recovery of indirect costs related to research and instruction:													
Summer program	$ 606,218		$ 606,218									606,218	521,338
Year-round program	1,840,018		1,840,018									1,840,018	1,773,586
Other	22,516		22,516									22,516	23,769
Instruction	39,107		39,107									39,107	10,827
Tuition				399,888								399,888	320,495
Support activities:													
Dormitory		$ 883,697	883,697									883,697	765,895
Dining hall	674,232		674,232									674,232	721,841
Library	209,134		209,134									209,134	207,857
Biological Bulletin	180,511		180,511									180,511	171,457
Research services	548,353		548,353									548,353	453,422
Marine resources	160,857		160,857									160,857	163,708
Other												—	95,684
Investment income	361,703		361,703	313,565								675,268	558,278
Gifts (Note I)	523,621		523,621	2,236,682		$ 400,598				$15,000		3,175,901	2,758,674
Miscellaneous revenue	113,141		113,141	230,238								343,379	101,243
Total support and revenues	5,279,411	883,697	6,163,108	7,298,318		400,598				15,000		13,877,024	12,661,693
EXPENSES:													
Instruction				1,293,092								1,293,092	1,263,867
Research				3,931,936								3,931,936	3,864,539
Scholarships and stipends				187,022								187,022	200,067
Support activities:													
Dormitory		632,666	632,666									632,666	587,432
Dining hall	590,782		590,782									590,782	654,722
Library	564,104		564,104									564,104	509,577
Biological Bulletin	165,248		165,248									165,248	139,795
Research services	657,542		657,542									657,542	632,882
Marine resources	386,358		386,358									386,358	365,900
Administration	1,393,049	99,245	1,492,294									1,492,294	1,191,794

Sponsored projects administration	266,389		266,389									266,389	333,630
Plant operations	1,242,937		1,242,937							78		1,243,015	1,085,751
Depreciation									$ 561,239			561,239	564,124
Disposal												—	4,844
Other	41,639		41,639	635,886								677,525	219,920
Total expenses	5,308,048	731,911	6,039,959	6,047,936					561,239	78		12,649,212	11,618,844
Excess (deficit) of support and revenues over expenses	(28,637)	151,786	123,149	1,250,382		400,598			(561,239)	14,922		1,227,812	1,042,849
TRANSFERS AMONG FUNDS:													
Acquisition of fixed assets	(25,573)		(25,573)	(2,912)					378,578		$(350,093)	—	—
Repayment of debt	(6,727)	(51,786)	(58,513)						58,513			—	—
Capital projects transfers							$(399,318)				399,318	—	—
Housing transfers		(100,000)	(100,000)								100,000	—	—
Instruction transfer	(10,360)		(10,360)	10,360								—	—
Other transfers				40,498				$(40,498)				—	—
Total transfers among funds	(42,660)	(151,786)	(194,446)	47,946			(399,318)	(40,498)	437,091		149,225	—	—
Realized gains on investments					$ 126,223	60,211	10,588	95,891				292,913	650,787
Unrealized gains (loss) on investment					52,667	81,473	6,189	91,667				231,996	(705,682)
Total gain (loss) on investments					178,890	141,684	16,777	187,558				524,909	(54,895)
Net change in fund balances	(71,297)		(71,297)	1,298,328	178,890	542,282	(382,541)	147,060	(124,148)	14,922	149,225	1,752,721	987,954
Fund balances, beginning of year	84,572		84,572	1,653,334	2,671,519	3,053,692	792,538	3,766,195	10,375,536	15,000	231,016	22,643,402	21,655,448
Fund balances, end of year	$ 13,275		$ 13,275	$2,951,662	$2,850,409	$3,595,974	$409,997	$3,913,255	$10,251,388	$29,922	$380,241	$24,396,125	$22,643,402

The accompanying notes are an integral part of the financial statements.

Notes to Financial Statements

A. *Purpose of the Laboratory:*

The purpose of the Marine Biological Laboratory (the "Laboratory") is to establish and maintain a laboratory or station for scientific study and investigations, and a school for instruction in biology and natural history.

B. *Significant accounting policies.*

Basis of presentation—fund accounting

In order to ensure observance of limitations and restrictions placed on the use of resources available to the Laboratory, the accounts of the Laboratory are maintained in accordance with the principles of fund accounting. This is the procedure by which resources are classified into separate funds in accordance with specified activities or objectives.

Externally restricted funds may only be utilized in accordance with the purposes established by the donor or grantor of such funds. However, the Laboratory retains full control over the utilization of unrestricted funds. Restricted gifts, grants, and other restricted resources are accounted for in the appropriate restricted funds. Restricted current funds are reported as revenue when received and as related costs are incurred.

Endowment funds are subject to restrictions requiring that the principal be invested with income available for use for restricted or unrestricted purposes by the Laboratory. Quasi-endowment funds have been established by the Laboratory for the same purposes as endowment funds; however, the principal of these funds may be expended for various restricted and unrestricted purposes.

Fixed assets

Fixed assets are recorded at cost. Depreciation is computed using the straight-line method over estimated useful lives of fixed assets.

Contracts and grants

Revenues associated with contracts and grants are recognized in the statement of support, revenues, expenses and changes in fund balances when received and as related costs are incurred. The Laboratory reimbursement of indirect costs relating to government contracts and grants is based on negotiated indirect cost rates with adjustments for actual indirect costs in future years. Any over or underrecovery of indirect costs is recognized through future adjustments of indirect cost rates.

Investments

Investments purchased by the Laboratory are carried at market value. Money market securities are carried at cost which approximates market value. Investments donated to the Laboratory are carried at fair market value at the date of the gift. For determination of gain or loss upon disposal of investments, cost is determined based on the average cost method.

The Laboratory is the beneficiary of certain endowment investments which are held in trust by others. These investments are reflected in the financial statements. Every ten years the Laboratory's status as beneficiary is reviewed to determine that the Laboratory's use of these funds is in accordance with the intent of the funds. The market value of these investments are $3,551,482 and $3,334,500 at December 31, 1988 and 1987, respectively.

Investment income and distribution

The Laboratory follows the accrual basis of accounting except that investment income is recorded on a cash basis. The difference between such basis and the accrual basis does not have a material effect on the determination of investment income earned on a year-to-year basis.

Investment income includes income from the investments of specific funds and from the pooled investment account. Income from the pooled investment account is distributed to the participating funds on the basis of their proportionate share at market value adjusted for any addition or disposals to pooled funds.

C. *Land, buildings, and equipment:*

The following is a summary of the unrestricted plant fund assets:

	1988	*1987*
Land	$ 689,660	$ 689,660
Buildings	16,694,233	16,385,099
Equipment	2,299,094	2,229,651
	19,682,987	19,304,410
Less accumulated depreciation	(8,268,927)	(7,707,689)
	$11,414,060	$11,596,721

D. *Retirement fund:*

The Laboratory has a noncontributory defined benefit pension plan for substantially all employees. Contributions are intended to provide for benefits attributed to the service date, but also those expected to be earned in the future.

Actuarial present value of accumulated benefit obligation including vested benefits of $1,604,313 as of January 1, 1988	$1,659,926
Projected benefit obligation	2,368,957
Plan assets at fair value	2,411,253
Projected benefit obligation less than plan assets	42,296
Unrecognized net (gain) or loss	(61,000)
Prior service cost not yet recognized in net periodic pension cost	—
Unrecognized net obligation at December 31, 1988	(270,946)
Prepaid pension cost (pension liability) recognized in the statement of financial position	$ (289,650)
Net pension cost for fiscal year ending December 31, 1988:	
Service cost–benefits earned during the period	160,293
Interest cost on projected benefit obligation	157,323
Actual return on plan assets	(178,653)
Net amortization and deferral	(30,835)
Net periodic pension cost	$ 108,128

The actuarial present value of the projected benefit obligation was determined using a discount rate of 7.3% and rates of increase in compensation levels of 6%. The expected long-term rate of return on assets was 8%.

In addition, the Laboratory participates in the defined contribution pension program of the Teachers Insurance and Annuity Association. Expenses amounted to $130,677 in 1988 and $103,386 in 1987.

E. *Pledges and grants:*

As of December 31, 1988, the Laboratory reported active pledge and grant commitments outstanding of $3,757,085 (unaudited) to be received as follows:

	Restricted
1989	$2,887,085
1990	810,000
1991	60,000
	$3,757,085

F. *Interfund borrowings:*

Interfund balances at December 31 are as follows:

Current Funds	*1988*	*1987*
Due from plant funds		$ 3,240
Due to restricted endowment fund	$(31,600)	(120,875)
Due to restricted quasi-endowment funds	—	(3,000)
Due from current restricted fund	—	64,318
	$(31,600)	$ (56,317)

G. *Mortgage and notes payable:*

The mortgage note payable with a term of 26 years is in the amount of $1.3 million bearing interest based on the bank's prime rate plus three quarters percent (.75%) on a floating basis for the initial five-year period with a floor of 7.50% and a ceiling of 13.00%. The interest rate at December 31, 1988 was 12.5%. The mortgage loan is collateralized by a first mortgage on the land and properties known as Memorial Circle, with recourse in the event of default limited to this land and property and the related revenue. Monthly principal and interest payments of $15,000 commenced January 19, 1987.

Other notes payable consist of the following:

Unsecured note with interest at 7.90% with monthly principal and interest payments of $221.20	$2,522
Unsecured note with interest at 6.90% with monthly principal and interest payments of $394.71	2,704
	$5,226

At December 31, 1988, these mortgages and notes payable had aggregate future annual principal payments as follows:

	Amount
1989	$ 49,968
1990	38,641
1991	43,262
1992	48,990
1993	55,477
Thereafter	969,119
	1,205,457
Less current portion	49,968
	$1,155,489

H. *Investments:*

The following is a summary of the cost and market value of investments at December 31, 1988 and 1987, and the related investment income and distribution of investment income for the years ended December 31, 1988 and 1987.

	Cost		*Market*		*Investment Income*	
	1988	*1987*	*1988*	*1987*	*1988*	*1987*
Endowment and quasi-endowment						
U.S. Government securities	$1,328,927	$1,299,763	$1,323,105	$ 1,270,857	$ 95,234	$218,919
Corporate fixed income	3,124,493	2,136,500	3,131,404	2,134,363	257,692	104,583
Common stocks	3,717,850	4,088,042	5,375,980	5,545,523	211,319	204,776
Preferred stock	—	9,611	—	14,973	250	1,019
Money market securities	916,280	1,292,097	916,280	1,287,520	49,995	42,911
Real estate	15,749	15,749	15,749	15,749	—	—
Total	9,103,299	8,841,762	10,762,518	10,268,985	614,490	572,208
Less custodian fees					(44,073)	(54,290)
					570,417	517,918
Restricted current fund						
Certificates of deposit	638,603	—	638,603	—	38,603	—
Money market securities	1,750,000	850,000	1,750,000	850,000	66,248	40,360
Total	2,388,603	850,000	2,388,603	850,000	104,851	40,360
Total investments	$11,491,902	$9,691,762	$13,151,121	$11,118,985	$675,268	$558,278

I. *Gift support for instructions.*

Unrestricted gifts includes $341,015 of gifts for the support of the Laboratory's instruction program available for indirect costs attributable to the instruction program.

J. *Subsequent event:*

On May 23, 1989, the Laboratory terminated its defined benefit pension plan. Approval of the termination is currently being reviewed by the IRS. All benefits earned by employees under the terminated plan become fully vested. The plan assets will be distributed to plan participants.

Summer Courses

Biology of Parasitism (June 12 to August 12)

Directors

Paul Englund, Johns Hopkins School of Medicine
Alan Sher, NIAID, National Institutes of Health

Faculty

Stephen Beverley, Harvard Medical School
Jennie Blackwell, University of Alabama School of Medicine
Stephen L. Hajduk, University of Alabama School of Medicine
Gerald W. Hart, Johns Hopkins School of Medicine
Carole Long, Hahnemann Medical College
David Sacks, National Institutes of Health
Phillip Scott, National Institutes of Health
Larry Simpson, University of California, Los Angeles
Mervyn J. Turner, Merck, Sharp & Dohme Laboratory
Donald L. Wassom, University of Wisconsin

Lecturers

Barry Bloom, Albert Einstein School of Medicine
Andre Capron, Pasteur Institute
Monique Capron, Pasteur Institute
Tony Cerami, Rockefeller University
Alan Cochrane, NYU Medical Center
Robert Coffman, DNAX Palo Alto, California
John Donelson, University of Iowa
Ronald Germain, National Institutes of Health
Judith Glaven, George Washington University
Michael Good, National Institutes of Health
Michael Gottlieb, Johns Hopkins School of Hygiene and Public Health
Russell Howard, DNAX, Palo Alto, California
Paul Knopf, Brown University
Wayne Masterson, Johns Hopkins School of Medicine
Ted Nash, National Institutes of Health
Tom Nutman, National Institutes of Health

B Haskell

Onesmo Ole-Moiyoi, ILRAD
Edward Pearce, NIAID, National Institutes of Health
Elmer Pfefferkorn, Dartmouth Medical School
Tom Quinn, National Institutes of Health, Johns Hopkins School of Medicine
Jonathan Ravdin, University of Virginia
Jose Ribeiro, Harvard University School of Public Health
Theresa Shapiro, Johns Hopkins School of Medicine
Ethan Shevach, National Institutes of Health
Barbara Sollner-Webb, Johns Hopkins School of Medicine
Andrew Spielman, Harvard School of Public Health
C. C. Wang, University of California, San Francisco
Kenneth Warren, Rockefeller Foundation
Rick Young, Massachusetts Institute of Technology
Fidel Zavala, New York University Medical Center

Students

Myrna C. Bonaldo, Fundaçao Oswaldo Cruz, Brazil
Clotilde K. Carlow, New England Biolabs

Glenn R. Frank, Colorado State University
Ricardo T. Gazzinelli, Federal University of Minas Gerais, Brazil
H. U. Goringer, Max-Planck Institute fur Molekulare Biologie, FRG
Jean-Murie J. Grzych, Institut Pasteur, France
Maria Lucia S. Guther, Paulista School of Medicine, Brazil
Eric R. James, Medical University of South Carolina
Jamil Kanaani, The Hebrew University, Israel
Michel E. Ledizet, Rockefeller University
Anna M. Lyles, Princeton University
Rona J. Mogil, University of Alberta, Canada
Jeffrey B. Moore, State University of New York, Albany
Silvia N. Moreno, Institute of Microbiology, Federal University of Rio de Janeiro, Brazil
Peter C. Sayles, University of Wisconsin, Madison
Mariane M. Stefani, Federal University of Goias, Brazil

Embryology: Cell Differentiation and Gene Expression in Early Development *(June 19 to July 30)*

Director
Eric H. Davidson, California Institute of Technology

Assistant director
J. Richard Whittaker, Marine Biological Laboratory

Other faculty, lecturers, and staff
Emmeline J. Chiao, Bryn Mawr College
Gary Freeman, University of Texas at Austin
John C. Gerhart, University of California, Berkeley
Judith E. Kimble, University of Wisconsin
Marc W. Kirschner, University of California, San Francisco
Mary LaGrange, University of Massachusetts
Elias Lazarides, California Institute of Technology
Howard D. Lipshitz, California Institute of Technology
Anthony P. Mahowald, Case Western Reserve University
Dennis L. Smith, University of California, Irvine
Dari K. Sweeton, Princeton University
Eric Wieschaus, Princeton University
Keith R. Yamamoto, University of California, San Francisco

Course assistants
Roberta R. Franks, California Institute of Technology
Michael Garabedian, University of California, San Francisco
Andrew D. Johnson, University of California, Irvine
David Kimelman, University of California, San Francisco
Andrew Ransic, University of Texas, Austin
Teresa R. Streeker, California Institute of Technology

Students
Miguel Allende, University of Pennsylvania
Kristin P. Carner, Scripps Institute of Oceanography
Wayne F. Daugherty, San Diego State University
James M. Denegre, Wesleyan University
Dali Ding, California Institute of Technology
Janice P. Evans, University of North Carolina
Johan J. Geysen, University of Leuven, Belgium
Neal R. Glicksman, University of North Carolina
Jill K. Hahn, Boston University Marine Program
Jeanene P. Hanley, University of Oklahoma
Alicia Hidalgo, University of Oxford, England
Jacquelyn Jarzem, University of Texas
Christopher J. Kelly, University of Chicago
Connie Lane, University of Iowa
Valeria Matranga, Instituto di Biologia dello Sviluppo del Consiglio Nazionale dello Richerche, Italy
Roberto A. Mayor, University of Chile, Chile
Brenda Ann Peculi, Johns Hopkins University
Patricia A. Pesavento, Harvard University
Wendy L. Richardson, Baylor College of Medicine
Susan M. Smith, Rensselaer Polytechnic Institute
Elly M. Tanaka, University of California, San Francisco
Henry S. Tillinghast, U. S. Air Force Academy
Kellie L. Watson, University of California, Irvine
Dineli M. Wickramasinghe, Tufts University
Joseph E. Zahner, Johns Hopkins University

Marine Ecology *(June 19 to August 13)*

Director
Richard Osman, Academy of Natural Sciences

Other faculty, lecturers, and staff
Josephine Aller, State University of New York, Stony Brook
Robert Aller, State University of New York, Stony Brook
William Ambrose, East Carolina University
Julie Berwald, University of Massachusetts, Amherst
Cheryl Ann Butman, Woods Hole Oceanographic Institution
Nina Caraco, Institute for Ecosystem Studies, New York

Hal Caswell, Woods Hole Oceanographic Institution
David Checkley, North Carolina State University
Jonathan Cole, Institute for Ecosystem Studies
Joseph Costa, Boston University Marine Program
Fred Dobbs, State University of New York, Stony Brook
Stuart Findlay, Institute for Ecosystems Studies
Marvin Freadman, Marine Biological Laboratory
Brian Fry, Marine Biological Laboratory
Steven Gaines, Brown University
Eugene Gallagher, University of Massachusetts, Boston
Anne Giblin, Marine Biological Laboratory
Patricia Glibert, Horn Point Environmental Laboratories
Diane Gould, University of Massachusetts, Boston
Frederick Grassle, Woods Hole Oceanographic Institution
Judith Grassle, Marine Biological Laboratory
Victoria Hatch, Smith College
Anson Hines, Smithsonian Environmental Research Center
Brian Howes, Woods Hole Oceanographic Institution
William Jenkins, Woods Hole Oceanographic Institution
Lisa Levin, North Carolina State University
Anton McLachlan, Oregon Institute for Marine Biology
Lauren Mullineaux, Woods Hole Oceanographic Institution
Richard Olson, University of New Hampshire
Bruce Peterson, Marine Biological Laboratory
Marshall Pregnall, Vassar College
Maribel Pregnall, Vassar College
David Policansky, National Research Council
James Porter, University of Georgia
Karen Porter, University of Georgia
Donald Rhoads, Boston University Marine Program
Donald Rice, Chesapeake Biological Laboratories
Ivan Valiela, Boston University Marine Program
John Waterbury, Woods Hole Oceanographic Institution
James Weinberg, Woods Hole Oceanographic Institution
Robert Whitlatch, University of Connecticut
Craig Young, Harbor Branch Oceanographic Institution
Roman Zajac, University of New Haven

Students

Conchita Avila, University of Barcelona, Spain
Aaron P. Corkum, Ferrum College
Sabine Dittmann, Zoologisches Institute, FRG
Saxon M. Gibson, Vanderbilt University
Todd H. Gillmore, State University of New York, New Paltz
Beatrix B. Hoecker, University of Hamburg, FRG
Susan B. Kane, University of Massachusetts, Boston
Dagmar Lackschewitz, Max-Plank Institute, FRG
Donald J. Morrisey, University of Bristol, England
Cheryl A. Ondeka, University of Massachusetts, Amherst
James L. Pickney, University of South Carolina
Rosana M. Rocha, University of Estadual de Campinas, Brazil
Robert G. Rowan, Johns Hopkins University
Roberto Sandulli, University of Naples, Italy
Carola Schmager, Institut fur Meereskunde an der Universität Kiel, FRG
Wesley W. Toller, University of California, Irvine
Mark S. Willcox, University College, Swansea, England

Microbiology: Molecular Aspects of Cellular Diversity (June 12 to July 28)

Directors

E. Peter Greenberg, University of Iowa
Ralph Wolfe, University of Illinois

Other Faculty, staff, and lecturers

Tom Baldwin, Texas A & M University
Dennis Bazylinski, Woods Hole Oceanographic Institution
Richard Blakemore, University of New Hampshire
Andreas Brune, University of Tubingen, FRG
Steven Clegg, University of Iowa
Martin Dworkin, University of Minnesota
Elizabeth Henry, Harvard University
Ralph Isberg, Tufts Medical School
Jim Ferry, Virginia Polytechnical Institute
Richard Frankel, California Polytechnical
Ronald Gibbons, Forsyth Dental Institute
Robert Gunsalus, University of California, Los Angeles
Elliot Juni, University of Michigan
Andrew Kropinski, Queens University, Canada
Carla Kuhner, University of Illinois
Margaret McFall-Ngai, Scripps Institution of Oceanography
Edward Meighan, McGill University, Canada
Karl Olson, University of Illinois
L. Nicholas Ornston, Yale University
Randy Rothmel, University of Illinois, Chicago
Rolf Schauder, Universitat Ulm, FRG
Bernhard Shink, Universitat Tubingen, FRG
Karen Sment, University of Illinois

Scott Smith, University of Illinois
Friedrich Widdel, Philips Universitat, FRG

Students
Bern Bendinger, University of Osnabruck, FRG
Bette Jo Brown, Michigan Tech.
Kevin R. Carmin, Florida State University
Frank J. Cynar, Scripps Institute of Oceanography
Eric Eisenstat, Harvard University
Mark A. Fahrina, Queens University, Canada
Kin Y. Fung, Wesleyan University
Charles Hirsch, Merck & Company
Kenneth H. Kerrick, University of Pittsburgh
Jordon Konisky, University of Illinois
Michael Lamontagne, Boston University
Kerstin Laufer, Philips University, FRG
Susanne Neuer, University of Washington
Judith A. Palmer, Oklahoma University
Sarah L. Storck, University of Illinois
John P. Walsh, University of Massachusetts
Lorraine G. Wilde, Scripps Institute of Oceanography
Fitnat Yildiz, Indiana University

Neural Systems and Behavior *(June 12 to July 30)*

Directors
Thomas Carew, Yale University
Darcy Kelley, Columbia University

Other Faculty, staff, and lecturers
Axel Borst, Max-Plank Institut fur Biologische Kybernetik, FRG
Jack Byrne, University of Texas Medical School
Ronald Calabrese, Emory University
Ellen Elliot, University of North Carolina
Russell Fernald, University of Oregon
Sally Hoskins, City University of New York
Richard Levine, University of Arizona
Eduardo Macagno, Columbia University
Laurie Tompkins, Temple University
Janis Weeks, University of California, San Diego

Students
Deborah J. Baro, University of Illinois
Glen D. Brown, University of Iowa
Sumantra Chattarji, Johns Hopkins University
Andrew K. Cheng, Johns Hopkins University
Jacqueline B. Fine-Levy, Georgia State University
Thomas M. Fischer, University of California, Riverside
Siglinde Gramol, The Hebrew University of Jerusalem, Israel
Fred J. Helmstetter, Dartmouth College
Robert Huber, Texas Tech University
Kaaren L. Johanson, Vanderbilt University
Ann M. Lohof, University of California, Los Angeles
Joseph A. Mindell, Albert Einstein College of Medicine
Lawrence I. Mortin, Brandeis University
Naomi Nagaya, University of Southern California
Clifford A. Opdyke, Emory University
Jennifer L. Raymond, University of Texas
Elian Scemes, Universidade De Sao Paulo, Brazil
Erin M. Schuman, Princeton University
Eric T. Vu, University of California, Los Angeles, School of Medicine
Laura R. Wolszon, State University of New York, Buffalo

Neurobiology (June 12 to August 20)

Director
Arthur Karlin, Columbia University

Other faculty, lecturers, and staff
Linda Amos, Cambridge University, England
Brian Andrews, National Institutes of Health
Katie Armstrong, Rice University
Cynthia Czajowski, Columbia University
Nicholas Dale, Columbia University
Douglas Fambrough, Johns Hopkins University
Gerald Fischbach, Washington University School of Medicine
Eric Frank, University of Pittsburgh School of Medicine
Robert French, University of Calgary, Alberta, Canada
Sara Garber, Stanford University
Linda Hall, Albert Einstein College of Medicine
Thomas Jessell, Howard Hughes Medical Institute
Steve Jones, Case Western Reserve University

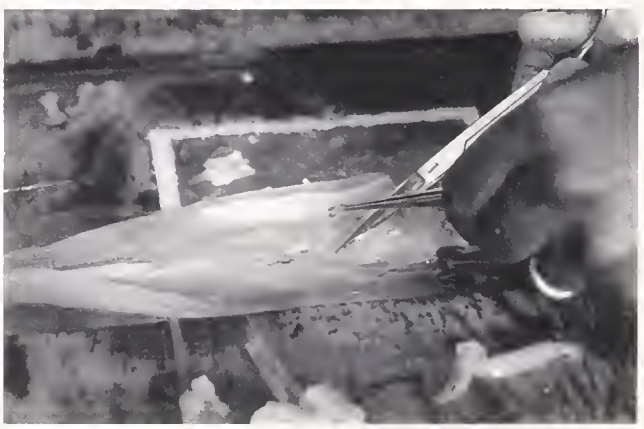

Robert Kass, University of Rochester School of Medicine
Dennis Landis, Case Western Reserve University
Story Landis, Case Western Reserve University
Rudolfo R. Llinas, New York University Medical Center
Craig Malbon, State University of New York, Stony Brook
Gail Mandel, Tufts University School of Medicine
Steven Matsumoto, University of Arizona College of Medicine
Christopher Miller, Brandeis University
Priscilla E. M. Purnick, Columbia University
Tom Reese, NINCDS, National Institutes of Health
Lewis P. Rowland, Columbia University
Bert Sakmann, Max-Plank Institute fur Biophysikalische Chemie, FRG
Bruce Schnapp, Marine Biological Laboratory
Thomas P. Segerson, New England Medical Center
Michael Sheetz, Washington University School of Medicine
Stephen Siegelbaum, Columbia University
Israel Silman, Weizmann Institute of Science, Rehovot, Israel
Carolyn Smith, University of Pittsburgh
Stefano Vicini, Georgetown University
Hsien-Yu Wang, State University of New York, Stony Brook
Monte Westerfield, University of Oregon

Students
Edward M. Blumenthal, Yale University
Kerris E. Bright, University of Sussex, England
Stephen C. Cannon, Massachusetts General Hospital
Dan P. Felsenfeld, Columbia University
Maura L. Hamrick, Johns Hopkins University
Staffan Johansson, Karolinska Institutet, Nobel Institute, Sweden
Chaya Joshi, Mayo Clinic
Margaret A. Thompson, Harvard University
Katja A. Wehner, Max-Plank Institute, FRG
Xian-Chen Yang, State University of New York, Buffalo
Rafael M. Yuste, Rockefeller University
Dayao Zhou, Harvard Medical School

Physiology: Cell and Molecular Biology
(June 12 to August 5)

Director
Robert Goldman, Northwestern University

Other faculty, staff, and lecturers
Chris Amemiya, Showa Institute
George Bloom, Worcester Foundation
Kerry Bloom, University of North Carolina
Kay O. Broshat, University of Miami
David Burgess, University of Miami
James Calvet, University of Kansas
Christine Collins, Worcester Foundation
George Dessev, Northwestern University
Yoshio Fukui, Northwestern University
Anne Goldman, Northwestern University
Elizabeth Goodwin, Brandeis University
John Hammarback, Worcester Foundation
Margaret Kenna, University of North Carolina
Leslie Leinwand, Albert Einstein College of Medicine
Gary Litman, Showa Institute
Sandra Mayrand, Worcester Foundation
Elizabeth McNally, Albert Einstein College of Medicine
Robert Obar, Worcester Foundation
Mark Paradise, Colorado College
Thoru Pederson, Worcester Foundation
Andrew Szent-Györgyi, Brandeis University
Richard Vallee, Worcester Foundation

Students
Susan Beckwith, Purdue University
Amy Boardman, University of Alabama
Alice Brown, Vanderbilt University
Isabel Cintron, University of Puerto Rico
Ian Crossley, University College of London, England
Patrick Dunn, University of Pennsylvania
David Elliot, Glasgow University, Scotland
Michael Fautsch, Mayo Clinic Foundation
Rob Fleischer, University of North Dakota
Chris Georgiou, University of Iowa
Felicia Houser, Harvard University
Jennifer Johnston, Dartmouth College
Diana Jones, Purdue University
Steve Keller, Scripps Institution/University of California, San Diego
Andreas Kiener, Harvard Medical School
David Klatte, Northwestern University
Alison Krufka, University of Wisconsin
Denis Larochelle, Stanford University
Ellen Lemosy, Duke University
Jian Li, State University of New York, Syracuse
Guohong Long, University of Massachusetts
Salim Mamajiwalla, University of Miami
Lisa Mendoza, Scripps Institution/University of California, San Diego
Dino Messina, State University of New York, Syracuse
Naomi Morrissette, University of Pennsylvania

John Oblong, University of Chicago
Scott Olsen, University of Minnesota
Matthew Rounseville, George Washington University
Alice Rushforth, University of Wisconsin
Sukanya Subramanian, Albert Einstein College of Medicine
Anthony Vattay, Rutgers University
Kevin Vaughan, Cornell University
Jin Wang, Worcester Foundation
Joseph Wolenski, Rutgers University
Connie Wolfe, Scripps Institute/University of California, San Diego
Lin Yue, Johns Hopkins University

Short Courses

Analytical and Quantitative Light Microscopy in Biology, Medicine, and Materials Science
(May 12 to 19)

Co-directors
Edward D. Salmon, University of North Carolina, Chapel Hill
D. Lansing Taylor, Cargegie-Mellon University

Other Faculty, staff, and lecturers
Brad Amos, Medical Research Council, Cambridge, England
Gordon Ellis, University of Pennsylvania
Fred Fay, University of Massachusetts Medical School
Ralph Gonzalez, Perceptics Corporation
Shinya Inoué, Marine Biological Laboratory
Fred Lanni, Carnegie-Mellon University
Katherine Luby-Phelps, Carnegie-Mellon University
Michel Nederlof, Carnegie-Mellon University
Tim O'Brien, Duke Medical Center
Alan Waggoner, Carnegie-Mellon University
Richard Walker, University of North Carolina, Chapel Hill

Commercial faculty
Richard Aikens, Photometrics, Ltd.
Dyon Anniballi, Universal Imaging Corporation
Michael Bady, Nikon Inc.
Richard Baucom, Olympus Corporation
Peter Baurschmidt, Carl Zeiss, Inc.
Gerald S. Benham, Bio-Rad Laboratories
Doug Benson, Inovision Corporation
Steve Boyd, Universal Imaging Corporation
Mel Brenner, Nikon Inc.
Cynthia Brown, Bio-Rad Laboratories
Tim Bruchman, Photometrics, Ltd.
Donald L. Commare, Photonic Microscopy, Inc.
Toni Feder, Bio-Rad Laboratories
Steve Floyd, Perceptics Corporation
Marc Friedman, Olympus Corporation
Cliff Glier, Perceptics Corporation
Dan Green, Universal Imaging Corporation
Scott Henderson, Nikon Inc.
Jan Hinsch, Wild Leitz, USA, Inc.
Mike Howard, Perceptics Corporation
Richard Inman, Inovision Corporation
Theodore Inoue, Universal Imaging Corporation
Ryozo Ito, Nikon Inc.
Ernst Keller, Carl Zeiss, Inc.
Jerry Kleifgen, Dage–MTI, Inc.
Mark J. Kuno, Wild Leitz USA, Inc.
Lloyd London, Bio-Rad Laboratories
Seth Miller, Carl Zeiss, Inc.
Masafumi Oshiro, Photonic Microscopy, Inc.
Dave Patek, Perceptics Corporation
Phillip Presley, Carl Zeiss, Inc.
Jerry Rubinow, Universal Imaging Corporation
Kevin Ryan, Perceptics Corporation
Kurt Scheier, Olympus Corporation
Stanley Schwartz, Nikon Inc.
Dan Terpstra, Perceptics Corporation
Thomas Tharp, Carl Zeiss, Inc.
Paul Thomas, Dage–MTI, Inc.
Brad Whitman, Carl Zeiss, Inc.
Robert A. Wick, Photonic Microscopy, Inc.
Richard Woods, Perceptics Corporation

Students
Karl E. Adler, E. I. DuPont De Nemours & Company
Tobias Baskin, University of California, Berkeley
Tamie J. Chilcote, The Rockefeller University
Jeffrey T. Corwin, University of Hawaii
Christopher Cullander, University of California, San Francisco
Phillip N. Dean, Lawrence Livermore National Laboratory
Jan R. De May, European Molecular Biology Laboratory, FRG
Josef Eisinger, Mount Sinai School of Medicine
Donald A. Fischman, Cornell University
Paul M. Horowitz, University of Texas Health Science Center
Bruce D. Jensen, Smith, Kline, and French Laboratories
James P. Kelly, Columbia University
Hallie M. Krider, University of Connecticut
Stephen J. Kron, Stanford University
Greta M. Lee, Duke University
Philip M. Lintilhac, University of Vermont

Nancy A. O'Rourke, University of California, Irvine
Lionel I. Rehbun, University of Virginia
Thomas F. Robinson, Albert Einstein College of Medicine
Frederick Sachs, State University of New York, Buffalo
Edwin H. Smail, University Hospital, Boston
Barbara J. Varnum-Finney, Howard Hughes Medical Institute, UCSF

Cell and Molecular Biology of Plants *(July 31 to August 19)*

Co-directors
Leon S. Dure, University of Georgia
Joe L. Key, University of Georgia

Other faculty, lecturers, and staff
Frederick M. Ausubel, Massachusetts General Hospital
Anthony Cashmore, University of Pennsylvania
Gloria Coruzzi, The Rockefeller University
Martha L. Crouch, Indiana University
Alan Darvill, USDA Russell Lab
Robert Ferl, University of Florida
Robert T. Fraley, Monsanto Company
Wilhelm Gruissem, University of California, Berkeley
Tom Guilfoyle, University of Missouri
Richard B. Hallick, University of Arizona
Robert Haselkorn, University of Chicago
R. B. Horsch, Monsanto Company
Gary Kochert, University of Georgia
C. S. Levings III, North Carolina State University
Elliot Meyerowitz, California Institute of Technology
Peter H. Quail, USDA Plant Gene Expression Center
Clarence A. Ryan, Washington State University
Carolyn D. Silflow, University of Minnesota
William Timberlake, University of Georgia
Hans D. Van Etten, Cornell University
Susan R. Wessler, University of Georgia

Students
Benita A. Brink, Marquette University
Laura G. Catignani, Hyannis, MA
Eunice A. Cronin, Belmont Abbey College
S. P. Dinesh Kumar, University of Kentucky
Sue H. Kadwell, CIBA-GEIGY Biotechnology
Jingqui Li, Marquette University
William J. Mathews, City University of New York
Lorraine Mineo, Lafayette College
Rosevelt L. Pardy, University of Nebraska
Yves Poirier, Clinical Research Institute, Canada
Daniel J. Prochska, Miami University
James Ramsay, University of Utah
Teresa Snyder, Pennsylvania State University
Frederica Sponga, Enichem Americas
William L. Steinhart, Bowdoin College
Salma N. Talhouk, Ohio State University
Stephen J. Tarapchak, Great Lakes Environmental Research Laboratory
Joanne A. West, ZOECON Research Institute

Mariculture: Culture of Marine Invertebrates for Research Purposes *(May 22 to 28)*

Director
Carl J. Berg, State of Florida, Bureau of Marine Research

Faculty
Philip Alatalo, Woods Hole Oceanographic Institution
Thomas Capo, Howard Hughes Medical Institute
Jeffrey Fisher, Eastern Connecticut State University
David Egloff, Oberlin College
Patrick M. Gaffney, University of Delaware
Scott M. Gallager, Woods Hole Oceanographic Institution
Robert Guillard, Bigelow Laboratories of Ocean Sciences
Roger Hanlon, University of Texas
Louis Leibovitz, Marine Biological Laboratory
James P. McVey, NOAA
Katherine Orr, Marathon, FL
Neal Overstrom, Sea Research Foundation, Mystic Marinelife Aquarium
Philip H. Presley, Carl Zeiss, Inc.
David Turner, Eastern Connecticut State University

Students
Ervin J. Bass, National Institutes of Health
Joseph S. Couturier, Enviro Systems Inc.
Christopher V. Davis, University of Maine
Robert I. Davidson, Trio Laboratories
Tien-Lai Hsu, University of Rhode Island
David Kohan, Hebrew University of Jerusalem, Israel
Suzanne M. Lussier, EPA Environmental Research Laboratory
Melanie Meade, Long Island University
Gloria D. Royall, George Mason University
Rafael Sarda, Boston University Marine Program
Jan Taschner, Yale University
Edward Wade, Aquatic Research Organisms
Roger G. Zirk, CFM Environmental Services Inc.

Methods in Computational Neuroscience
(August 14 to September 3)

Directors
James M. Bower, California Institute of Technology
Christof Koch, California Institute of Technology

Faculty
Paul Adams, State University of New York, Stony Brook
Thomas Albright, The Salk Institute
Daniel Alkon, NINCDS, National Institutes of Health
Thomas Anastasio, University of Southern California
Richard Andersen, Massachusetts Institute of Technology
John Hildebrand, University of Arizona
John Hopfield, California Institute of Technology
Stephen Lisberger, University of California, San Francisco, School of Medicine
Rudolfo Llinas, New York University Medical Center
Nicos Logothetis, Massachusetts Institute of Technology
Eve Marder, Brandeis University
Mark Nelson, California Institute of Technology
Alexander Pentland, Massachusetts Institute of Technology
V. S. Ramachandran, University of California, San Diego
John Rinzel, National Institutes of Health
Idan Segev, Hebrew University of Jerusalem, Israel
Terrence Sejnowski, Johns Hopkins University
Roger Traub, IBM Watson Research Center
David Van Essen, California Institute of Technology

Course assistants
Upinder S. Bhalla, California Institute of Technology
John Uhley, California Institute of Technology
Matthew Wilson, California Institute of Technology

Students
Werner Backhous, Freie Universitat Berlin, FRG
Jim Cummings, University of Pennsylvania
Allen C. Dobbins, McGill University, Canada
William N. Frost, University of Iowa
Edward W. Kairiss, Yale University
Alexander Kirillov, USSR Academy of Sciences, Moscow, USSR
Guy Major, University of Oxford, England
Yair Manor, Hebrew University, Israel
Hiroyoshi Miyakawa, New York Medical College
Barbara Moore, Massachusetts Institute of Technology
Laura J. Reece, University of Washington
Clay Reid, The Rockefeller University
John R. Rose, State University of New York, Stony Brook
Franklin H. Schuling, University of Groningen, The Netherlands
Jeffrey E. Segall, Max Planck Institute for Biochemistry, FRG
Brian H. Smith, University of Arizona
William Skaggs, University of Colorado
Xiao-Jing Wang, University of California, Berkeley
Donald J. Weir, Oxford University, England
Hagit Zabrodsky, Hebrew University, Israel

Molecular and Cellular Immunology
(July 31 to August 19)

Director
Darcy B. Wilson, Medical Biology Institute

Other faculty, lecturers, and staff
Steven Abramson, New York University Medical Center
Jenny Blackwell, London School of Hygiene and Tropical Medicine, England
Peter Brodeur, Tufts University School of Medicine
Charles Dinarello, Tufts New England Medical Center
Ann J. Feeney, Medical Biology Institute
Steve Hedrick, University of California, San Diego
Nancy Hogg, Imperial Cancer Research Fund
Richard Larson, Dana Farber Cancer Institute
Sidney Leskowitz, Tufts University Medical School
Donald Mosier, Medical Biology Institute
Lee Nadler, Dana Farber Cancer Institute
David Parker, University of Massachusetts Medical School
Jonathan Sprent, Scripps Clinic & Research Foundation
Jack Strominger, Harvard University
Geoffrey Sunshine, Tufts University School of Veterinary Medicine
Fred T. Valentine, New York University Medical Center
Gerald Weissmann, New York University Medical Center
Robert Winchester, New York University Medical Center

Students
Gina L. Adel, University of Iowa Hospital
Anthony L. Back, University of Washington

Kenneth R. Brown, Merck, Sharp, & Dohme
Nino M. Dobrovic, Stevens Institute of Technology
Verna C. Gibbs, University of California, San Francisco
Patricia A. Grady, University of Maryland
Wendy L. Niebling, Northwestern University
Marla J. O'Shea, Mount Holyoke College
Cynthia A. Pise, University of Massachusetts Medical School
Robert C. Rickert, University of North Carolina
Elizabeth M. Southard, University of Texas
N. Kanaga Sundaram, New Jersey Medical School
Susan B. Sylvers, University of Massachusetts. Amherst
Charles W. Taylor, University of Arizona
Guillermo Torre, University of Chicago
Samuel P. Wertheimer, New York University

Optical Microscopy and Imaging in the Biomedical Sciences (March 6 to 11)

Co-directors
Nina Stromgren Allen, Wake Forest University
Colin S. Izzard, State University of New York, Albany

Faculty, lecturers, and staff
Shinya Inoué, Marine Biological Laboratory
Kenneth A. Jacobson, University of North Carolina
Kenneth Orndorff, Dartmouth College
Greenfield Sluder, Worcester Foundation for Experimental Biology
Stephen J. Smith, Yale University Medical School
Kenneth R. Spring, National Institutes of Health, National Heart, Lung, and Blood Institute

Course assistant
Joseph De Pasquale, State University of New York, Albany

Student faculty
Bruce Faison Holifield, University of North Carolina

Commercial faculty
Rob Ashmead, Nikon Inc.
Michael Bady, Nikon Inc.
Gerald S. Benham, Bio-Rad Laboratories
Donald L. Commare, Photonic Microscopy, Inc.
Hermann J. Esser, Videoscope International, Ltd.
Charles Fanghella, Nikon Inc.
Barbara Foster, Reichert-Jung
David Hillman, ADCO Aerospace, Inc.
Theodore Inoué, Universal Imaging Corporation
Ernst Keller, Carl Zeiss, Inc.
Jerry Kleifgen, Dage-MTI, Inc.
Rob Klueppel, Polaroid Corporation
Mark J. Kuno, Wild Leitz USA, Inc.
Jeffrey Larson, Nikon Inc. Instrument Group
Eric Marino, Image Processing Solutions
Hugh Mellaly, Eastman Kodak Company
Patrick Moore, Molecular Probes
Raj Mundag, Bio-Rad Laboratories
Phillip Presley, Carl Zeiss, Inc.
Martin L. Scott, Eastman Kodak Company
Thomas Tharp, Carl Zeiss, Inc.
Paul Thomas, Dage-MTI, Inc.
Robert A. Wick, Photonic Microscopy, Inc.

Students
Barbara C. Boyer, Union College
Kathryn I. Casteel, University of North Carolina, Chapel Hill
Linda N. Curtis, University of North Carolina, Greensboro
Sarah C. Elgin, Washington University
Joseph Farley, Princeton University
Clare Fewtrell, Cornell University
Lorraine A. Fitzpatrick, University of Texas Health Science Center, San Antonio
Lawrence C. Katz, The Rockefeller University
Nicholas F. LaRusso, Mayo Clinic
James M. McIlvain, State University of New York, Syracuse
P. Scott Pine, Uniformed Services University of Health Sciences
Martin Reers, Harvard Medical School
Joseph F. Rizzo, Massachusetts Eye and Ear Infirmary
Allyson A. Simons, Federal Bureau of Investigation Laboratory
Mark Terasaki, Marine Biological Laboratory
Daniel Ts'o, The Rockefeller University
Michael Tytell, Wake Forest University
Hsien-yu Wang, State University of New York at Stony Brook
Patrick Weyer, Massachusetts General Hospital
R. Reid Zeigler, Merck Sharp & Dohme Research Labs

Workshop on Molecular Evolution (September 18 to 30)

Director
Mitchell L. Sogin, National Jewish Center for Immunology and Respiratory Medicine

Other faculty, lecturers, and staff

Robert Cedegren, University of Montreal, Canada
Michael Clegg, University of California, Riverside
John W. Drake, National Institute of Environmental Health Sciences
Daniel E. Dykhuuzen, State University of New York, Stony Brook
Joseph Felsenstein, University of Washington
Katherine G. Field, Oregon State University
Walter B. Goad, Los Alamos National Laboratory
Morris Goodman, Wayne State University School of Medicine
Barry G. Hall, University of Connecticut
John Lawrie, GENE-TRAK Systems
Lynn Margulis, University of Massachusetts, Amherst
Roger Milkman, University of Iowa
Gary Olsen, University of Illinois
Norman R. Pace, Indiana University
Philip J. Regal, University of Minnesota
David Shub, State University of New York, Albany
Maxine F. Singer, Carnegie Institution of Washington
Michael Syvanen, University of California, Davis
Bruce Walsh, University of Arizona
Michael S. Waterman, University of Southern California
Mark Wheelis, University of California, Davis
Carl R. Woese, University of Illinois

Students

Rogelio Alonso-Morales, Harvard School of Public Health
James W. Ammerman, Lamont-Doherty Geological Observatory of Columbia University
Ann Antlfinger, University of Nebraska
Nathalie Antoine, University of Montreal, Canada
Edgardo Ariztia, National Jewish Center for Immunology and Respiratory Medicine
Wendy J. Bailey, Wayne State University
William V. Baird, University of Georgia
David Begun, Arizona State University
Michael J. Braun, University of Cincinnati
Colleen M. Cavanaugh, Harvard University
Michael P. Cummings, Harvard University
Lloyd Demetrius, Max-Plank Institute
Paul Desjardins, Universite de Montreal, Canada
Daniel L. Distel, Woods Hole Oceanographic Institution
Hille Elwood, National Jewish Center for Immunology and Respiratory Medicine
David H. Fitch, Wayne State University
Jane C. Gallagher, City College of New York
Mark A. Gallo, Cornell University
Johann P. Gogarten, University of California, Santa Cruz
Spencer J. Greenwood, University of Guelph, Canada
Sidney Grimes, VA Medical Center, Shreveport, Louisiana
Thaddeus A. Grudzien Jr., Oakland University
John H. Gunderson, Vanderbilt University
Winston Hide, Temple University
Llewellya Hillis-Colinvaux, Ohio State University
Holly H. Hobart, University of Arizona
Volker Huss, National Jewish Center for Immunology and Respiratory Medicine
Piroska Huvos, Southern Illinois University
Thomas S. Kantz, Louisiana State University
Christopher J. Kelly, University of Chicago
Cordula Kirchgessner, University of Massachusetts Medical Center
Robert Kraft, Albert Einstein College of Medicine
Antonio A. Lazcano, National University of Mexico, Mexico
Roger D. Longley, Pacific Sciences Institute
Denis H. Lynn, University of Guelph, Canada
George M. McCorkle, Yale University
Tammy S. McCormick, University of Cincinnati
Mara A. McDonald, University of Cincinnati
J. Mitchell McGrath, University of California at Davis
Nancy Moncrief, Wayne State University
Paul A. Nelson, University of Chicago
Gokaldas C. Parikh, Quinnipiac College
Aloysius Philips, Temple University
Douglas Prasher, Woods Hole Oceanographic Institution
A. Rajaguru, University of Maryland
Thomas Redlinger, University of Massachusetts at Amherst
Rebeca Rico-Hesse, Yale University
Margaret Riley, Harvard University
Jan E. Rines, University of Rhode Island
Michael S. Roberts, Wesleyan University
Lori Sadler, University of California, Los Angeles
Patricia Sawaya, University of Cincinnati
Martin Schlegel, Universitat Tubingen, FRG
Susan Sell, Hopkins Marine Station
M. Andrew Shenk, Yale University
George N. Sideris, New York University
Scott Smiley, University of California, San Francisco
Joseph L. Staton, University of Southwestern Louisiana
Robert E. Steele, University of California, Irvine
Tamalyn Stockton, University of Massachusetts, Amherst

Diane K. Stoecker, Woods Hole Oceanographic Institution
John F. Stolz, University of Massachusetts, Amherst
Danilo Tagle, Wayne State University
John B. Waterbury, Woods Hole Oceanographic Institution
Steve A. Wolfe, Louisiana State University
Hong Y. Yan, University of Maryland
Clarice M. Yentsch, Bigelow Lab for Ocean Sciences

Workshop on Plant and Animal Cell Microinjection Techniques (May 20 to 22)

Co-directors
Robert B. Silver, University of Wisconsin
Edward B. Tucker, City University of New York

Other faculty, lecturers, and staff
Jan Blaas, Research Institute Ital, The Netherlands
Shinya Inoué, Marine Biological Laboratory
Lionel Jaffe, Marine Biological Laboratory
William Jeffrey, University of Texas
Douglas Kline, University of Connecticut Health Center
W. Langridge, Cornell University
Katherine Luby-Phelps, Carnegie Mellon University
P. McNeil, Harvard Medical School
James Maller, University of Colorado
W. Muller, Harvard Medical School
P. M. Pechan, Plant Research Center, Canada
Martin Poenie, University of Texas

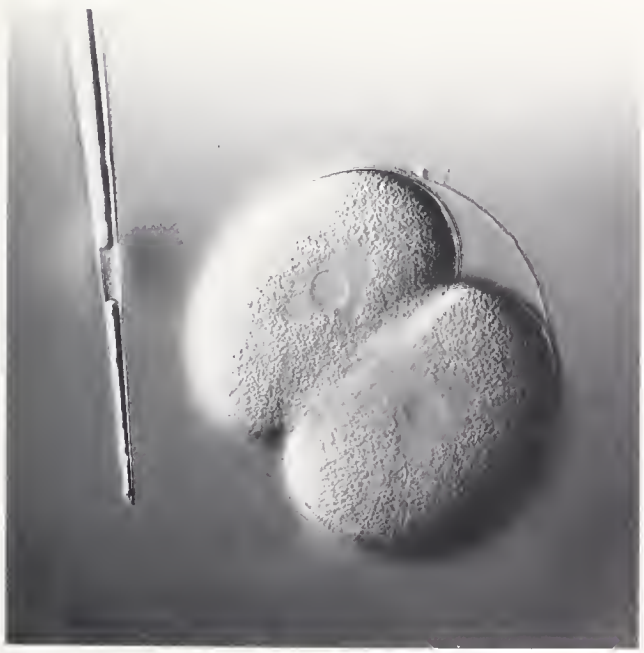

R Silver

D. Lansing Taylor, Carnegie Mellon University
B. R. Terry, The Flinders University of South Australia
R. Tsien, University of California, Berkeley

Commercial faculty
Charles Fanghella, Nikon Inc., Instrument Group
Barbara Foster, Cambridge Instruments
Daniel Green, Universal Imaging Corporation
Stuart F. Havel, Medical Systems Corporation
Theodore O. Inoué, Universal Imaging Corporation
Jerry Kleifgen, Dage-MTI, Inc.
Hans Koczinski, Carl Zeiss, Inc.
Mark John Kuno, Wild Leitz USA, Inc.
Victor P. Laronga, Atlantex & Zeiler Instrument Corporation
Charles McDonough, Cambridge Instruments
Seth Miller, Carl Zeiss, Inc.
Victor Olszewski, David Kopf Instruments
Phillip Presley, Carl Zeiss, Inc.
J. Kemp Randolph, Medical Systems Corporation
William Reid, Technical Manufacturing Corporation
Jim Schindele, Carl Zeiss, Inc.
Rick Smith, Eppendorf
Paul Thomas, Dage-MTI, Inc.
Melina Vratny, Nikon Inc., Instrument Group

Students (lectures, demonstrations and laboratory)
Lee-Ann Allen, University of Wisconsin
John Andersland, Cornell University
Thomas Bjorkman, University of Washington
Mingxin Che, Fordham University
John R. Coleman, Brown University
Frank J. Dye, Western Connecticut State University
Miles F. Epstein, University of Wisconsin
Edward A. Fisher, Medical College of Pennsylvania
Paul E. Gallant, National Institutes of Health
Stella M. Hurtley, Yale University
George M. Langford, University of North Carolina
Willy Lin, E. I. DuPont Company
Andrew Maretzki, Hawaiian Sugar Planters Association
Paul J. Millard, Cornell University
Corey Nislow, Dartmouth College
Jo Ann Render, Hamilton College
Jen Sheen, Massachusetts General Hospital
Jonathan M. Shenker, University of California
Cuthbert O. Simpkins, Howard University
Robert Turgeon, Cornell University
J. Richard Whittaker, Marine Biological Laboratory
Wayne Yunghans, State University of New York, Fredonia

Students (lectures and demonstrations)

Rosario Agnosti, University of Zurich, Switzerland
Hassan Amjad, Jafary Medical Clinic
Winston A. Anderson, Howard University
Elena Armandola, New York Medical College
Ann C. Burke, Harvard University
Andrew R. Burns, Cornell University
Robert M. Coleman, University of Lowell
Colleen Curran, University of Minnesota
Carol Dorworth, Louisiana State University
Julie Downey, City University of New York
Richard A. Fluck, Franklin and Marshall College
Donald J. Fujita, University of Calgary, Canada
Irene Garcia, University of Geneva
Edwin H. Gilland, Harvard University
Maria A. Giovino, University of Lowell
William Gordon-Kamm, DeKalb Pfizer Genetics
Thomas C. Gore, Salsbury Laboratories Inc.
Helana Hoover-Litty, Yale University
Subhash C. Juneja, Old Dominion University
P. G. Kadkade, Biotechnica International
Karen Kurvink, Moravian College
Cheryl Laursen, Molecular Genetics, Inc.
Catharina S. Lee, E. I. DuPont Company
Kersti K. Linask, Thomas Jefferson Medical College
Ming S. Lok, Denver General Hospital
Rosalind Lowen, City University of New York
Burra V. Madhukar, Michigan State University
David E. McClain, Armed Forces Radiobiology Research Institute
Raman Mocharla, Indiana University
Suresh Savarirayan, Mayo Clinic
Lewis Tilney, University of Pennsylvania
Nemat Ullah, Washington State University
Gabriele Weitz, National Institutes of Health
Yang Dar Yuan, The Upjohn Company

Summer Research Programs

Principal Investigators

Adelman, Jr., William J., NINCDS, NIH
Alkon, Daniel L., NINCDS/NIH
Anderson, Peter A. V., University of Florida
Armstrong, Clay M., University of Pennsylvania Medical School
Armstrong, Peter B., University of California
Augustine, George J., University of Southern California

Baker, Robert, New York University
Barlow, Robert B. Jr., Syracuse University
Barry, Susan R., University of Michigan
Bass, Andrew H., Cornell University
Beauge, Luis A., Instituto M. y M. Ferreyra, Argentina
Begenisich, Ted, University of Rochester School of Medicine and Dentistry
Bennett, Michael V. L., Albert Einstein College of Medicine
Bezanilla, Francisco, University of California
Bloom, George S., University of Texas Southwestern Medical Center
Bodznick, David, Wesleyan University
Borgese, Thomas A., Lehman College
Boron, Walter F., Yale University School of Medicine
Borst, David W., Illinois State University
Boyer, Barbara C., Union College
Brady, Scott T., University of Texas Southwestern Medical Center at Dallas
Brehm, Paul, Tufts University School of Medicine
Brenner, Sydney, Molecular Genetics Unit, Cambridge, England
Brown, Joel E., Washington University School of Medicine
Burdick, Carolyn J., Brooklyn College
Burger, Max M., University of Basel, Switzerland

Chang, Donald C., Baylor College of Medicine
Chappell, Richard L., Hunter College of the City University of New York
Charlton, Milton P., University of Toronto, Canada
Clay, John R., NINCDS/NIH
Cohen, William D., Hunter College
Cohen, Avis H., Cornell University
Cohen, Lawrence B., Yale University School of Medicine
Cooperstein, Sherwin J., University of Connecticut Health Center
Cresti, Mauro, University of Siena, Italy

Dowling, John E., Harvard University
Dunlap, Kathleen, Tufts Medical School
Dykens, James A., Grinnell College

Ehrlich, Barbara E., University of Connecticut Health Center

Feinman, Richard B., State University of New York Health Science Center at Brooklyn
Fine, Alan, Dalhousie University, Canada
Fink, Rachel, Mount Holyoke College
Fishman, Harvey M., University of Texas Medical Branch, Galveston

Gadsby, David C., Rockefeller University
Gainer, Harold, NIH, NINCDS
Gaze, Raymond M., University of Edinburgh, U.K.
Giuditta, Antonio, University of Naples, Italy
Glynn, Paul, AT&T Bell Laboratories
Gonzalez-Serratos, Hugo, University of Maryland School of Medicine
Gould, Robert M., Institute for Basic Research in Developmental Disabilities
Govind, C. K., University of Toronto, Canada
Graf, Werner, Rockefeller University
Green, Douglas R., University of Alberta, Canada

Haimo, Leah T., University of California, Riverside
Hepler, Peter K., University of Massachusetts, Amherst
Highstein, Stephen M., Washington University School of Medicine

Hill, Susan D., Michigan State University
Hoskin, Francis C. G., Illinois Institute of Technology
Hoy, Ronald R., Cornell University

Jeffery, William R., University of Texas, Austin
Josephson, Robert K., University of California

Kaminer, Benjamin, Boston University School of Medicine
Kao, C. Y., State University of New York Downstate Medical Center
Kaplan, Barry B., University of Pittsburgh Western Psychiatric Institute and Clinic
Katz, Paul S., Cornell University
Kirk, Mark, Boston University
Kreibel, Mahlon E., State University of New York Health Science Center

Landowne, David, University of Miami
Langford, George M., University of North Carolina School of Medicine
Lasek, Raymond J., Case Western Reserve University
Laufer, Hans, University of Connecticut
Lee, Helen M., University of Massachusetts at Amherst
Levin, Jack, Veterans Administration Medical Center
Levis, Richard A., Rush Medical Center
Levitan, Irwin, Brandeis University
Lin, Stephen S., Brandeis University
Linck, Richard, University of Minnesota
Lipicky, Raymond J., Food and Drug Administration
Lisman, John, Brandeis University
Llinas, Rudolfo, New York University
Loewenstein, Werner R., University of Miami

Matteson, Donald R., University of Maryland
McClintock, Timothy S., The Whitney Laboratory
Metuzals, Janis, University of Ottawa, Canada
Miller, Christopher, Brandeis University
Montgomery, John C., University of Auckland, New Zealand
Moore, John W., Duke University
Mooseker, Mark S., Yale University

Narahashi, Toshio, Northwestern University
Nasi, Enrico, Boston University Medical School
Nelson, Leonard, Medical College of Ohio
Noe, Bryan D., Emory University School of Medicine
Nolen, Thomas G., University of Miami

Obaid, Ana Lia, University of Pennsylvania School of Medicine
Oberhauser-Bittig, Andres, University of Pennsylvania School of Medicine
Ohki, Shinpei, State University of New York, Buffalo

Palazzo, Robert E., University of Virginia
Pappas, George D., University of Illinois College of Medicine at Chicago

Quigley, James, State University of New York

Rafferty, Nancy S., Northwestern University Medical and Dental Schools
Rakowski, Robert F., Chicago Medical School
Rebhun, Lionel I., University of Virginia
Regehr, Wade G., California Institute of Technology
Rickles, Frederick R., University of Connecticut Health Center
Ripps, Harris, University of Illinois College of Medicine at Chicago
Rose, Birgit, University of Miami School of Medicine
Ross, William N., New York Medical College
Ruderman, Joan V., Duke University
Russell, John M., University of Texas Medical Branch

Saez, Juan C., Albert Einstein College of Medicine
Salzberg, Brian M., University of Pennsylvania School of Medicine
Sanger, Jean M., University of Pennsylvania School of Medicine
Sanger, Joseph W., University of Pennsylvania School of Medicine
Scofield, Virginia L., University of California, Los Angeles School of Medicine
Segal, Sheldon J., Rockefeller Foundation
Shumway, Carolyn A., University of California, San Diego
Silver, Robert B., University of Wisconsin
Sloboda, Roger D., Dartmouth College
Smith, Stephen J., Yale University School of Medicine
Spiegel, Evelyn, Dartmouth College
Spiegel, Melvin, Dartmouth College
Stadler, Herbert, Max-Planck-Institute of Biophysical Chemistry, FRG
Steinacker, Antoinette, Washington University
Stracher, Alfred, State University of New York Health Science Center at Brooklyn
Stuart, Ann E., University of North Carolina
Suprenant, Kathy A., University of Kansas

Tanguy, Joelle, Ecole Normale Supereure, France
Telzer, Bruce R., Pomona College
Thibault, Lawrence E., University of Pennsylvania
Tilney, Lewis G., University of Pennsylvania
Treistman, Steven N., Worcester Foundation for Experimental Biology
Trinkaus, John P., Yale University
Troll, Walter, New York University Medical Center
Tucker, Edward B., Baruch College
Tytell, Michael, Bowman Gray School of Medicine

Vogel, Steven S., Columbia University

Waxman, Stephen, Yale Medical School
Wegmann, Thomas G., University of Alberta, Canada

Weiss, Dieter G., Technical University Munich, FRG
Weissmann, Gerald, New York University Medical Center
Wonderlin, William F., University of Calgary, Canada

Yeh, Jay Z., Northwestern University Medical School

Zigman, Seymour, University of Rochester School of Medicine
Zottoli, Steven J., Williams College
Zukin, R. Suzanne, Albert Einstein College of Medicine

I. Gilder

Other Research Personnel

Abramson, Charles I., State University of New York Health Science Center at Brooklyn
Adler, Elizabeth M., University of Toronto, Canada
Adra, Chaker N., University of Ottawa, Canada
Alberghinia, Mario, University of Catania, Italy
Albert, Daniel, University of Chicago Medical Center
Albrecht, Kenneth, University of Connecticut
Allen, Nina S., Wake Forest University
Altamirano, A. A., University of Texas Medical Branch
Anderson, Bruce, Medical College of Virginia
Anderson, Matthew, Howard Hughes Medical Institute

Badgerow, John P., Eastern Michigan University
Bamrungphol, Wattana, University of Pennsylvania
Bernal-Martinez, Juan, University of Connecticut Health Center
Bleakman, J., NINCDS, NIH
Brawley, Jennifer, University of Virginia
Breitwieser, Gerda E., Johns Hopkins University
Brown, Anthony, Case Western Reserve University Medical School
Brozen, Reed, Yale University
Buchanan, Jo Ann, Yale University Medical School
Butler, Derrick, Morehouse College

Callaway, Joseph C., University of Washington
Caputo, Carlo, Centro Biofisica y Bioquimica, Venezuela
Carbine, Larry, University of Virginia
Cariello, Lucio, Stazione Zoologica, Italy
Celli, Giulia, Wellesley College
Chen, Chong, California Institute of Technology
Chen, Fukuen E., Northwestern University Medical School
Chun, Xiao, Yale University School of Medicine
Church, Paul, Boston University
Cohen, Avrum, Yale University
Collin, Carlos, NINCDS, NIH
Colton, Carol A., Georgetown University Medical School
Cooper, Mark, Yale University Medical School
Cornwall, M. Carter, Boston University School of Medicine
Cottrell, Glen, New York University Medical Center
Couch, Ernest F., Texas Christian University

Davis, Graeme, Williams College
Defendi, Germaine, New York University Medical School
Dermietzel, Rolf, Albert Einstein College of Medicine
DiPolo, Reinaldo, Instituto Venezolano de Investigaciones Cientificas, Venezuela
Dome, Jeffrey S., University of Pennsylvania School of Medicine
Dostrovsky, Jonathan O., University of Toronto, Canada
Dowdall, Michael J., University of Nottingham, U.K.
Dworkin, Jonathan, Swarthmore College

Etcheberrigaray, Rene, NINCDS/NIH

Ferkowicz, Michael, Michigan State University
Flores, Roberto, INSERM, Paris, France
Floyd, Carl, Morehouse College
Forman, Robin, Medical College of Virginia

Galbraith, James, University of Pennsylvania
Gao, Pei-Qin, Baylor College of Medicine
Gee, Christine, University of Toronto, Canada
Gerosa, Daniela, Friedrich-Miescher-Institut, FRG
Gilbert, Daniel L., NINCDS/NIH
Gilbert, Susan P., Pennsylvania State University
Gill-Kumar, Pritam, Food and Drug Administration
Graff, Tracy, Syracuse University
Grant, Alan J., Worcester Foundation for Experimental Biology
Grant, Philip, NIH, NINCDS
Grassi, Dan, Fort Lauderdale, Florida

Graubard, Katherine, University of Washington
Greif, Peter, Food and Drug Administration
Greiner, Francine, Emory University School of Medicine

Haneji, Tatsuji, Population Council
Hernandez, M. R., University of Texas Medical Branch
Hess, Stephen, University of Southern California
Hice, Rita, Whitney Laboratory
Hines, Michael, Duke University
Hogan, Emilia, Yale University School of Medicine
Holbrook, Pam, University of Birmingham, England
Homola, Ellen, University of Connecticut
Hopp, Hans-Peter, Yale University School of Medicine
Hu, S. L., State University of New York Downstate Medical Center
Huddie, Patrick, NINCDS, NIH
Hunt, John R., Baylor College of Medicine
Hunter, Catherine, University of Pennsylvania
Hyrc, Krysztof, University of Miami School of Medicine

Jarrad, Hugh, Haverford College
Johansson, Steffan, Karolinska Institutet, Sweden
Jumblatt, James E., University of Louisville School of Medicine

Kadam, Arjun, Population Council
Kahana, Alon, Brandeis University
Kao, Peter N., Columbia University College of Physicians and Surgeons
Kaplan, Ehud, Rockefeller University
Klein, Kathryn, Emory University School of Medicine
Knudsen, Knud, Food and Drug Administration
Koide, Samuel S., Population Council
Kojima, Hiroshi, Northwestern University
Kolodnex, Michael, Washington University Medical School
Kosik, Kenneth S., Brigham and Women's Hospital
Kramer, Richard H., Brandeis University
Kronidou, Nafsika, Dartmouth College

Lahti, Carol, University of California at Los Angeles School of Medicine
Leddy, Scott, University of Alberta
Lederhendler, I. Izja, NINCDS, NIH
Lehman, Herman K., Syracuse University
Leighton, Stephen B., NINCDS/NIH
Li, Guan, Cornell University
Lin, Jen-Wei, New York University Medical Center
Llinas, Rafael, Washington University
Lowe, Kris, University of Rochester Medical Center
Lthi, Theres, Biozentrum, Switzerland
Luca, Frank, Duke University

Marchaterre, Margaret A., Cornell University
Marrone, M., University of Toronto, Canada
Martin, Melissa Marie, Eastern Illinois University
Matzel, Louis D., NINCDS/NIH
McDonald, John K., Emory University School of Medicine
McKee, Juliet M., University of Kansas
Menichini, Enrico, University of Naples, Italy
Milgram, Sharon, Emory University School of Medicine
Misevic, Gradimir, Friedrich-Miescher-Institut, FRG
Montgomery, John, University of Auckland, New Zealand
Murray, Sandra, University of Pittsburgh

Nemec, Vaclav, University of Connecticut
Northern, Sue, Williams College
Nuno, Claudia, University of California

Oberhauser, Andres, University of Pennsylvania
Olds, James, NINCDS/NIH

Pant, Harish, NINCDS/NIH
Parsons, Thomas D., University of Pennsylvania School of Medicine
Pearce, Joanne, University of Toronto, Canada
Perozo, Eduardo, University of California, Los Angeles
Poole, Thomas J., SUNY Health Science Center, Syracuse

Queck, Francis, University of Michigan

Rafferty, Keen A. Jr., University of Illinois Medical Center
Rasgado-Flores, Hector, University of Maryland School of Medicine
Raslavicus, Alex, Union College
Regehr, Wade G., California Institute of Technology
Robinson, Phyllis R., Brandeis University
Romero, Adarli, Washington University School of Medicine

Sanchez, Ivelisse, Hunter College
Sands, Peter J., New York University School of Medicine
Schiminovich, David, Yale University
Schneider, Melissa R., University of Rochester Medical School
Shibuya, Ellen, Duke University
Silbaugh, Timothy H., Syracuse University
Silverstein, Kurt, Baruch College
Spires, Sherrill, University of Rochester Medical Center
Spray, David C., Albert Einstein College of Medicine
Standart, Nancy, University of Cambridge, U.K.
Steffen, Walter, University of Minnesota
Stein, Philip G., University of Texas Medical Branch, Galveston

Stokes, Darrell, Emory University
Sugimori, Mutsuyuki, New York University Medical Center
Svoboda, Katherine, University of California, Los Angeles, School of Medicine
Swalla, Billie J., University of Texas, Austin
Sydlik, Mary Anne, Eastern Michigan University

Tabares, Lucia, University of Pennsylvania
Takashima, Shiro, University of Pennsylvania
Tewari, Kirti P., I. G. Medical College, Simla, India
Thompson, Jennifer, Lehman College
Tricas, Timothy, Washington University
Tyndale, Clyde, NINCDS/NIH

Uchiyama, Hiroyuki, Syracuse University
Ueno, Hiroshi, Rockefeller University

Vandenberg, Carol A., University of California, Los Angeles
Vautrin, Jean, State University of New York Health Science Center
Villanova, Lynnea, University of Miami
Vogel, Jacalyn M., Illinois State University

Wu, Jian-Young, Yale University School of Medicine

Yamoah, Ebenezer, University of Alberta, Canada
Yao, Jibin, Georgetown University Medical School

L. Gilder

Young, Steven R., New York Medical College
Yuan, Liu, University of Basel, Switzerland

Zakevicius, Jane, University of Illinois College of Medicine at Chicago
Zavilowitz, Joseph, Albert Einstein College of Medicine
Zecevic, Dejan, Institute for Biological Research, Yugoslavia
Zigman, Bunnie R., University of Rochester Medical Center

Library Readers

Allen, Garland, Washington University
Anderson, Everett, Harvard Medical School
Apter, Nathaniel, Nova University

Baccetti, Baccio, Institute of Zoology, Naples, Italy
Bang, Betsy, Marine Biological Laboratory
Barrett, Dennis, University of Denver
Benjamin, Thomas, Harvard Medical School
Bernheimer, A. W., New York, NY
Boyer, John F., Union College
Buck, John, National Institutes of Health
Burr, A. H., Simon Fraser University

Candelas, Graciela C., University of Puerto Rico
Cape Cod Planning and Economic Development
Carriere, Rita, Downstate Medical Center
Child, Frank, Trinity College
Chinard, Francis P., New Jersey Medical School
Clark, Arnold, Marine Biological Laboratory
Clark, John, University of Massachusetts
Cobb, Jewel Plumm, California State University, Fullerton
Cohen, Leonard A., American Health Foundation
Cohen, Seymour S., Marine Biological Laboratory
Constantine, Betsy J., Arthur D. Little, Inc.
Corliss, Bruce H., Duke University

DeToledo-Morrell, Leyla, Rush Presbyterian, St. Lukes Medical Center

Eder, Howard A., Albert Einstein College of Medicine
Ellner, Jerrold, Case Western Reserve University

Farb, David, SUNY
Farmanfarmian, A., Rutgers University
Finkelstein, Joan Kent, The Rockefeller University
Fisher, Saul H., NYU Medical Center
Frenkel, Krystyna, NYU Medical Center
Friedler, Gladys, Boston University School of Medicine
Fussell, Catharine P., Pennsylvania State University

Galatzer-Levy, Robert, University of Chicago
German, James L., The New York Blood Center
Goldfarb, Ronald H., Pittsburgh Cancer Inst.

Goldstein, Jr., Moise, John Hopkins University
Goodgall, S. H., University of Pennsylvania
Gordon, Erlinda, Case Western University
Grossman, Albert, NYU Medical Center
Gruner, John, NYU Medical Center
Guiseppe, D'Allesio, University of Naples, Italy
Guillemin-Meselson, Jeanne, Boston College
Guttenplan, Joseph B., NYU Dental Center

Harding, Clifford V., Wayne State University
Harrington, John P., University of Alaska
Hatten, Mary, Columbia University
Herskovits, Theodore T., Fordham University
Hill, Richard W., Michigan State University
Humphreys, Tom, University of Hawaii

Ilan, Joseph, Case Western Reserve University
Ilan, Judith, Case Western Reserve University
Inoue, Sadayuki, McGill University
Issidorides, Marietta, Athens University Medical School

Johnson, William, Goucher College
Johnston, Ardis, Harvard University

Kaltenbach, Jane C., Mount Holyoke College
Kaplan, Ilene M., Union College
Kass-Simon, Gabriele, University of Rhode Island
Kelly, Robert, University of Chicago, College of Medicine
Kemlow, Kenneth M., Wilkes College
King, Kenneth, Jr., Children's Hospital
Kirk, Mark D., Boston University
Krane, Stephen M., Massachusetts General Hospital
Kravitz, Edward A., Harvard Medical School

Laderman, Aimlee, Marine Biological Laboratory
Lau, Dian, University of Pennsylvania
Lazarow, Normand H., Rochester, MN
Lee, John, City College of CUNY
Leighton, Joseph, Medical College of Pennsylvania
Levine, Rachmiel, City of Hope Medical Center
Levitz, Mortimer, NYU Medical Center
Lewis, Larry, Millersville University
Lorand, Laszlo, Northwestern University
Lustig, Robert H., The Rockefeller University

Marine Research, Inc.
Matsumura, Fumio, University of California
Mautner, Henry G., Tufts University School of Medicine
Mauzerall, David, The Rockefeller University
McCann-Collier, Marjorie, Saint Peter's College
Meyer, Kenneth, R. E. Consulting Inc.
Mercurio, Arthur, Harvard Medical School
Miki-Noumura, Taiko, Ochanomizu University
Mitchell, Ralph, Harvard University
Mizell, Merle, Tulane University
Morrell, Frank, Rush Presbyterian, St. Lukes Medical Center
Moyer, Carolyn F., EG&G Mason Research Institute
Musacchia, X. J., University of Louisville

Nagel, Ronald L., Albert Einstein College of Medicine
Nicaise, Mari-Luz H., University of Nice, France
Nichol, Charles A., Glaxo Research Laboratories
Nickerson, Peter A., State University of New York, Buffalo
Nowotny, Alois H., University of Pennsylvania

Olins, Ada, University of Tennessee, Oak Ridge
Olins, Donald E., University of Tennessee, Oak Ridge
Olufemi, Ogunnowo, Marine Biological Laboratory

Palmer, Claude Irene, New York University
Parsons, Katharine C., Manomet Bird Observatory
Paton, David, Marine Biological Laboratory
Person, Philip, VA Medical Center, Brooklyn, NY
Prusch, Robert D., Gonzaga University

Rabinowitz, Michael, Marine Biological Laboratory
Reynolds, George T., Princeton University
Robinson, Denis, Marine Biological Laboratory
Rome, Larry, Marine Biological Laboratory
Rosenbluth, Raja, Simon Fraser University
Roth, Jay S., University of Connecticut
Russell-Hunter, W. D., Syracuse University

Salman, Edward D., University of North Carolina
Schippers, Jay, Marine Biological Laboratory
Schuel, Herbert, State University of New York, Buffalo
Schuel, Regina, State University of New York, Buffalo
Sheppard, Frank, Woods Hole Data Base
Shepro, David, Boston University
Sherman, Irwin W., University of California, Riverside
Shriftman, Mollie Starr, North Nassau Mental Health Center
Simon, Keiko O., University of Pittsburgh
Sluder, Greenfield, Worcester Foundation for Experimental Biology
Sonnenblick, Benjamin P., Rutgers University
Southeastern Massachusetts University Library
Speck, William T., Case Western Reserve University
Spector, Abraham, Columbia University
Stevens, E. Don, University of Guelph, U.K.

Tashiro, Jay Shiro, Bard College
Taylor, Rachael, Harvard University
Tilney, Lewis, University of Pennsylvania
Trager, William, The Rockefeller University
Tweedell, Kenyon S., University of Notre Dame

Van Holde, Kensal E., Oregon State University

Wagenbach, Gary, Carleton College
Wagner, Robert R., University of Virginia
Warren, Leonard, Wistar Institute
Webb, H. Marguerite, Marine Biological Laboratory
Weidner, Earl H., Louisiana State University
Weiner, Jonathan, Doylestown, PA
Weiss, Leon, University of Pennsylvania
Wheeler, George, Brooklyn College
Whittaker, J. Richard, Marine Biological Laboratory
Wichterman, Ralph, Marine Biological Laboratory
Wilber, Charles G., Colorado State University
Wittenberg, Beatrice, Albert Einstein College of Medicine
Wittenberg, Jonathan, Albert Einstein College of Medicine
Wolken, Jerome J., Carnegie Mellon University
Worth, Dyan, Harvard University

Yow, F. W., Kenyon College

Zigmond, Richard E., Harvard Medical School
Zimmerman, Morris, Zimmerman Associates

Domestic Institutions Represented

Academy of Natural Sciences
ADCO Aerospace, Inc.
Alabama, University of
Albert Einstein College of Medicine of Yeshiva University
Aquatic Research Organisms
Arizona State University
Arizona, University of
Arizona, University of, College of Medicine
Armed Forces Radiobiology Research Institute
Atlantex & Zeiler Instrument Corp.
AT&T Bell Laboratories
Axon Instruments, Inc.

Baruch College
Belmont Abbey College
Bethesda Research Laboratories
Bigelow Laboratories for Ocean Sciences
Bio-Rad Laboratories
Biotechnica International
Boston University
Boston University Marine Program
Boston University School of Medicine
Bowdoin College
Bowman Gray School of Medicine
Brandeis University
Brigham & Women's Hospital
Brooklyn College
Brown University
Bryn Mawr College

California Institute of Technology
California Polytechnical
California, University of, School of Medicine, San Francisco
California, University of, San Francisco
California, University of, Berkeley
California, University of, Davis
California, University of, Irvine
California, University of, Los Angeles
California, University of, Los Angeles, School of Medicine
California, University of, Riverside
California, University of San Diego
California, University of, San Francisco
California, University of, Santa Cruz
Cambridge Instrument, Inc.
Carnegie Institution of Washington
Carnegie-Mellon University
Case Western Reserve University
Case Western Reserve University School of Medicine
CFM Environmental Services, Inc.
Chesapeake Biological Laboratories
Chicago, University of
Chicago, University of, School of Medicine
Ciba-Geigy Biotechnology Corp.
Cincinnati, University of, School of Medicine
Colorado, College
Colorado State University
Colorado, University of
Columbia University
Columbia University College of Physicians and Surgeons
Connecticut, University of
Connecticut, University of, Health Center
Cornell University
Cornell University Medical College

Dage-MTI, Inc.
Dana Farber Cancer Institute
Dartmouth College
Dartmouth College Medical School
David Kopf Instruments
Dekalb Pfizer Genetics
Delaware, University of
Denver General Hospital
DNAX Corporation
DuPont, E. I. DeNemours & Co.
Duke University
Duke University Medical Center

E-C Apparatus Corporation
E.G.&G
Enviro Systems, Inc.
Earlham College
East Carolina University
Eastern Connecticut State University
Eastern Illinois University
Eastern Michigan University
Eastman Kodak Company
Emory University
Emory University School of Medicine
Environmental Protection Agency Research Laboratory
Enichem Americas
Eppendorf

Federal Bureau of Investigation Laboratory
Ferrum College
Florida, University of
Florida State University
Food and Drug Administration
Fordham University
Forsyth Dental Institute

GENE-TRAK Systems
George Mason University
George Washington University
Georgetown University Medical School
Georgetown University
Georgia State University
Georgia, University of
Great Lakes Environmental Research Lab
Grinnell College

Hahnemann Medical College & Hospital
Hamilton College
Harbor Branch Oceanographic Institution
Harvard Graduate School of Arts and Sciences
Harvard Medical School
Harvard School of Public Health
Harvard University
Harvard University School of Medicine

Haverford College
Hawaii, University of
Hawaiian Sugar Planters Association
Hopkins Marine Station
Horn Point Environmental Laboratories
Howard Hughes Medical Institute
Howard University

IBM, Watson Research Center
Illinois Institute of Technology
Illinois State University
Illinois, University of
Illinois, University of, College of Medicine
Illinois, University of, Medical Center
Image Processing Solutions
Indiana University
Inovision Corporation
Institute for Basic Research in Developmental Disabilities
Institute for Ecosystems Studies, New York
Iowa, University of
Iowa, University of, Hospital

JaFary Medical Clinic
Johns Hopkins University
Johns Hopkins University School of Medicine
Johns Hopkins University School of Hygiene & Public Health

Kansas, University of
Kentucky, University of

LaFayette College
Lawrence Livermore National Laboratories
Long Island University
Los Alamos National Laboratory
Louisville University of, School of Medicine
Louisiana State University
Lowell, University of

Maine, University of
Marquette University
Marine Biological Laboratory
Maryland, University of
Maryland, University of, School of Medicine
Maryland, University of, Chesapeake Biological Laboratory
Massachusetts Eye and Ear Infirmary
Massachusetts General Hospital
Massachusetts Institute of Technology
Massachusetts, University of, Amherst
Massachusetts, University of, Boston
Mayo Clinic, Rochester, MN
Mayo Graduate School of Medicine
Medical Biology Institute
Medical College of Ohio
Medical College of Pennsylvania
Medical College of Virginia
Medical Systems Corporation
Merck, Sharp & Dohme Research Laboratory
Miami, University of
Miami University of Ohio
Miami, University of, School of Medicine
Michigan State University
Michigan Tech
Michigan, University of
Minnesota, University of
Molecular Genetics, Inc.
Molecular Probes, Inc.
Moravian College
Morehouse College
Mount Sinai School of Medicine
Mystic Marinelife Aquarium

National Aeronautical & Space Administration
National Institute of Allergy and Infectious Diseases
National Institute of Environmental Health Sciences
National Institutes of Health
National Heart, Lung, & Blood Institute
National Institutes of Mental Health
National Institutes of Health
National Institute of Neurological and Communicative Disorders and Strokes
National Jewish Center For Immunology and Respiratory Medicine
National Oceanographic and Aeronautical Administration (NOAA)
National Research Council
New England Biolabs
New England Medical Center
New Haven, University of
New Hampshire, University of
New York University
New York University Medical Center
New York, City University of, Bernard M. Baruch College
New York, City University of, Brooklyn College
New York, City University of, City College
New York, City University of, Hunter College
New York, City University of, Lehman College
New York, City University of, Mt. Sinai School of Medicine
New York, State University of, Albany
New York, State University of, Buffalo
New York, State University of, Downstate Medical Center
New York, State University of, Health Sciences
New York, State University, Health Science Center at Brooklyn
New York, State University, Health Science Center at Stony Brook
New York, State University, Upstate Medical Center
New York, State University of, Fredonia
New York, State University of, New Paltz
New York, State University of, Syracuse
New York, State University of, Stony Brook
Nikon, Inc.
North Carolina State University
North Carolina, University of
North Carolina, University of, at Chapel Hill
North Carolina, University of, at Greensboro
North Carolina, University of, School of Medicine
North Dakota, University of
Northwestern University Medical School
Northwestern University Medical and Dental Schools
Northwestern University

Oakland University
Oberlin College
Oklahoma, University of
Oklahoma, University of, Health Science Center
Ohio State University
Old Dominion University
Olympic Corporation of America
Oregon Institute for Marine Biology
Oregon State University
Oregon, University of

Pacific Sciences Institute
Pennsylvania State University
Pennsylvania, University of
Pennsylvania, University of, School of Medicine
Perceptics Corporation
Photometrics, Ltd.
Photonic Microscopy, Inc.
Pittsburgh, University of, School of Medicine
Pittsburgh, University of, Western Psychiatric Institute

Polaroid Corporation
Pomona College
Population Council
Princeton University
Puerto Rico, University of
Purdue University

Quinnipiac College

Rensselaer Polytechnic Institute
Reichert-Jung
Rhode Island, University of
Rice University
Rochester, University of
Rochester, University of, Medical Center
Rochester, University of, School of Medicine and Dentistry
Rockefeller Foundation
Rockefeller University
Rush Medical Center
Rush University
Rutgers University

San Diego State University
Salk Institute
Salsbury Laboratories, Inc.
Scripps Clinic and Research Foundation
Scripps Institute of Oceanography
Sea Research Foundation
Showa University Research Institute
Smith College
Smithsonian Environmental Research Center
Smith, Kline, and French Laboratories
South Carolina, University of, Medical School
Southern California, University of
Southern California, University of, School of Medicine
Southern Louisiana State University
Southwestern Louisiana, University of
Stanford University
Stanford University Medical School
State of Florida, Bureau of Marine Research
Stevens Institute of Technology
Swarthmore College
Syracuse University

Technical Manufacturing Corporation
Technical Products International, Inc.
Temple University
Texas Agriculture and Mines
Texas Tech. University
Texas Christian University
Texas, University of, Austin
Texas, University of, Health Science Center, Dallas
Texas, University of, Health Science Center, Houston
Texas, University of, Health Science Center, San Antonio
Texas, University of, Medical Branch, Galveston
Texas, University of, Medical School
Thomas Jefferson University
Thomas Jefferson Medical College
Trio Laboratories
Tufts New England Medical Center
Tufts University
Tufts University School of Medicine
Tufts University School of Veterinary Medicine

Uniformed Services University of Health Sciences
Union College
United States Air Force Academy
United States Department of Agriculture, Russell Lab
United States Department of Agriculture, Plant Gene Expression Center
United States Environmental Protection Agency
United States Food and Drug Administration
Universal Imaging Corporation
University Hospital, Boston
University Hospitals of Cleveland
Upjohn Company, The
Utah, University of

Vanderbilt University
Vassar College
Veterans Administration Medical Center, Shreveport, LA
Videoscope International, Ltd.
Virginia Polytechnic Institute and State University
Virginia, University of

Wake Forest University
Washington State University
Washington University
Washington University School of Medicine
Washington, University of
Washington, University of, School of Medicine
Wayne State University School of Medicine
Wesleyan University
Western Connecticut State University
Whitney Laboratory
Wild Leitz USA, Inc.
Wisconsin, University of
Wisconsin, University of, School of Veterinary Medicine
Woods Hole Oceanographic Institution
Worcester Foundation for Experimental Biology

Yale University
Yale University School of Medicine
Yale University School of Public Health

Zeiss, Carl, Inc.
Zoecon Research Institute

Foreign Institutions Represented

Alberta, University of, Canada
Auckland, University of, New Zealand

Barcelona, University of, Spain
Basel, University of, Switzerland
Berlin, University of, FRG
Biozentrum, Switzerland
Birmingham, University of, U.K.
Bristol, University of, U.K.

Calgary, University of, Canada
Cambridge, University of, U.K.
Catania, University of, Italy
Catholic University of Leuven, Belgium
Central University of, Venezuela
Centre National de la Recherche Scientifique, France
Centro BioFiscia y Bioquinica, Venequela
Centro Nacional Patagonico, Argentina
Chile University, Chile
Clinical Research Institute, Canada
Cuyo, University of, Mendoza, Argentina
Dalhousie University, Canada

Ecole Normale Superieure, France
Edinburgh, University of, U.K.
European Molecular Biology Laboratory, FRG

Federal University of Goias, Brazil
Federal University of Minas Gerais, Brazil
Flinders University of South Australia, The

Freie Universitat of Berlin, FRG
Friedrich Miescher-Institut, Switzerland

Glasgow, University of, Scotland, U.K.
Groningen, University of, The Netherlands
Guelph, University of, Canada

Hamburg, University of, FRG
Hebrew University, The, Israel
Hebrew University of Jerusalem, Israel
Heidelberg, University of, FRG

Imperial Cancer Research Fund, U.K.
Imperial College of Science and Technology, U.K.
Institut fur Meereskunde, FRG
Institut fur Tierphysiologie, FRG
Institut Pasteur, France
Institute of Biological Research, Yugoslavia
Instituto de Biologia, Argentina
Instituto de Histologia y Embriologia, Argentina
Instituto de Investigacion Medica, Argentina
I.G. Medical College, Simla, India
Inserm, France
Instituto di Biologia Cellulare, Italy
Instituto de Microbiolgie, Brazil
Instituto Venezolanode Investigaciones Cientifican, Venezuela
International Lab. for Research on Animal Diseases, Kenya

Karolinska Institutet, Sweden

Leuven, University of, Belgium
London School of Hygiene and Tropical Medicine, U.K.

Max-Planck Institute, FRG
McGill University, Quebec, Canada
Medical Research Council, England, U.K.
Montreal, University of, Canada

Naples Zoological Station, Italy
Naples, University of, Italy
National University of Mexico, Mexico
Nottingham, University of, U.K.

Osnabruck, University of, FRG
Ottawa, University of, Canada
Oxford University, U.K.

Pasteur Institute, France
Paulista School of Medicine, Brazil
Philipps Universitat, FRG
Plant Research Center, Canada
Puerto Rico, University of

Research Institute, The Netherlands

Siena, University of, Italy
St. Andrews University, Scotland, U.K.
St. Georges Hospital Medical School, U.K.
Station Zoologique, France
Stazione Zoologica, Italy
Stockholm, University of, Sweden
Strathclyde, University of, Scotland, U.K.
Sussex University, U.K.
Swansea, University College at, U.K.
Sweden, University of, Stockholm

Technical University of Munich, Garching, FRG
Toronto, University of, Canada
Toyohashi University of Technology, Japan
Tromso, University of Norway
Tubingen, University of, FRG

Ulm, University of, FRG
Universidad Nacional de Mar del Plata, Argentina
Universidad de Sao Paulo, Brazil
Universidad de Estadual de Campinas, Brazil
Universidade Federal do Espirito, Brazil
Universita Degli Studi Di Napoli, Italy
Universitat Kiel, FRG
University College, Ireland
University College of London, England, U.K.
University College of North Wales, U.K.
Uppsala University, Sweden
USSR Academy of Sciences, USSR
Utrecht, University of, The Netherlands

Warwick, University of, U.K.
Weizmann Institute of Science, Israel

Yamaguchi University, Japan

Zoological Station, Italy
Zoologisches Institut der Universitat, Heidelberg, FRG
Zurich, University of, Switzerland

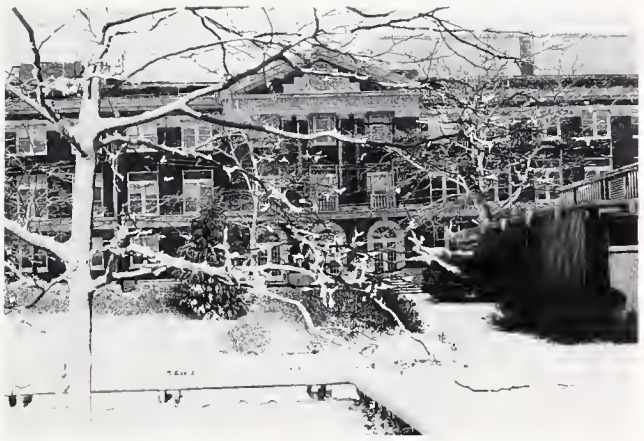

G. Liles

Year-Round Research Programs

Boston University Marine Program

Faculty

Strickler, J. Rudi, Professor of Biology, Program Director
Atema, Jelle, Professor of Biology
Humes, Arthur G., Professor of Biology Emeritus
Tamm, Sidney L., Professor of Biology
Valiela, Ivan, Professor of Biology

Visiting investigators and instructors

Baldwin, Christopher (Boston University)
Bloomer, Sherman (Boston University)
D'Avanzo, Charlene (Hampshire College)
Deegan, Linda (University of Massachusetts, Amherst)
Freadman, Marvin (Visiting Assistant Professor)
Guerrero, Ricardo (University of Barcelona)
Margulis, Lynn (University of Massachusetts, Amherst)
Marrase, Celia (University of Barcelona)
Mitchell, James (University of Barcelona)
Muscatine, Leonard (University of California, Los Angeles)
Peckol, Paulette (Smith College)
Rhoads, Donald
Richman, Sumner (Lawrence University)
Rietsma, Carol (SUNY, New Paltz)
Sarda, Rafael (University of Barcelona)

Research staff

Costa, Joseph, Research Associate
Costello, Jack, Research Associate
Tamm, Signhild, Senior Research Associate
Van Etten, Richard, Research Assistant
Voigt, Reiner, Research Associate
Zinn, Margery, Research Assistant

Staff

Corker, Amy, Course Assistant
Hahn, Dorothy, Senior Administrative Secretary
Hinckle, Greg, Course Assistant
Sunley, Madeline, Administrative Manager
Weis, Virginia, Course Assistant

Graduate students

Alber, Merryl
Banta, Gary
Brooks, Cydney
Corotto, Frank
Coughlin, David
Cowan, Diane
Elskus, Adria
Foreman, Kenneth
Gallager, Scott
Hahn, Jill
Hersh, Douglas
Krieger, Yutta
Hwang, Jiang-shiou
LaMontagne, Michael
Lavalli, Kari
Mazel, Charles
Merrill, Carl
Moore, Paul
Mulsow, Sandor
Piotrowski, Michael
Scott, Marsha
Siddiqui, Pirzada
Tamse, Armando
Trager, Geoffrey
Trott, Thomas
White, David
Wood, Susan

Undergraduate students

Batjakas, Ioanis
Bergles, Dwight
Brewer, Matthew C.
Buckley, Joseph P.

Call, Christopher A.
Casteline, Jennifer
Cochran, Wendy
Eleuterio, Daniel
Forrest, Davina
Forrester, Amy L.
Halczyn, William C.
Kennedy, S. Blain
Kenzora, Kristen T.
Kleinhans, Julie (Cornell)
Kreuger, Dana (Lawrence University)
LaPusata, David T.
Lynch, Helen M.
Massoff, Daniel A.
Mayer, Marilyn A. (University of Maryland)
Michmerhuizen, Cathy (Lawrence University)
Myers, Monique
Melvin, Mary Kay
Pacioni, Thomas D. (SUNY, Buffalo)
Parker, Todd A.
Pizzelanti, Donna M.
Rugoletti, Steven J.
Rutka, Timothy
Scholz, Nathaniel L.
Short, Graham
Siwko, Robert P.
Stone, Gayle (Skidmore)
Zeller, Robert (special honors work)

Summer undergraduate interns

Butler, Elizabeth (Hampshire College)
Coburn, Cara
Forrest, Davina (Boston University)
Gerardo, Hortense
Townsend, Susan
Rogers, Ruth
Rutka, Timothy
Sammon, Leslie
Short, Graham

Laboratory of Jelle Atema

Organisms use chemical signals as their main channel of information about the environment. These signals are transported in the marine environment by turbulent currents, viscous flow, and molecular diffusion. Receptor cells extract signals through various filtering processes. Currently, the lobster with its exquisite sense of taste and smell is our major model, to study the signal filtering capabilities of the whole animal and its narrowly tuned receptor cells. Research focuses on amino acids (food signals) and pheromones (courtship), neurophysiology of receptor cells, behavior guided or modulated by chemical signals, and computer modeling of odor plumes and neural filters.

Laboratory of Arthur G. Humes

Research interests include systematics, development, host specificity, and geographical distribution of copepods associated with marine invertebrates. Current research is on taxonomic studies of copepods from invertebrates in the tropical Indo-Pacific area, and poecilostomatoid and siphonostomatoid copepods from deep-sea hydrothermal vents and cold seeps.

Laboratory of Rudi J. Strickler

Use high-speed cinematography and special laser light optical systems with target tracking devices to observe zooplankton-algae, carnivorous-herbivorous zooplankton, and fish-zoo-plankton interactions. Lab and field results show the degree to which abiotic forces influence the evolution of species, feeding guilds, and predator-prey interactions. Additional topics in the feeding ecology of crinoids, bryozoans and other suspension feeding invertebrates enhance perception of the first consumer level in the aquatic food chain.

Laboratory of Ivan Valiela

Research emphasis is on structure and function of salt marsh ecosystems and coastal embayments, including the processes of predation, herbivory, decomposition, and nutrient cycles. A parallel line of work, with more applied aspects, is eutrophication in coastal marine communities and interactions between watersheds and coastal waters.

The Ecosystems Center

The Center was established in 1975 to promote research and education in ecosystems ecology. Eleven scientists study the terrestrial and aquatic ecology of a wide variety of ecosystems ranging from northern Europe (trace gas emission from acid-rain affected forests) and the Alaskan Arctic (long-term studies on the controls of tundra, lake and stream biota), to the Harvard Forest (long-term studies of the effects of disturbance on forest ecosystems) and Buzzard's Bay (controls of anaerobic decomposition). Many projects, such as those dealing with sulfur transformations in lakes and nitrogen cycling in the forest floor, investigate the movements of nutrients and make use of the Center's mass spectrometry laboratory (directed by Brian Fry) to measure the stable isotopes of carbon, nitrogen, and sulfur. The research results are applied wherever possible to questions of the successful management of the natural resources of the earth. In addition, the ecological expertise of the staff is made available to public affairs groups and government agencies who deal with such problems as acid rain, groundwater contamination, and possible carbon dioxide-caused climate change.

Staff and consultants

Melillo, Jerry M., Acting Director
Hobbie, John E., Director (on sabbatical)
Banta, Gary T.
Bauman, Carolyn H.
Boutwell, Anne M.
Bowles, Francis P.
Brooks, Marilyn

Davis, Sarah J.
Danforth, Carolyn
Dornblaser, Mark
Downs, Martha
Fry, Brian
Giblin, Anne E.
Griffin, Elisabeth A.
Helfrich, John V. K.
Hooper, David
Hullar, Meredith
Jordan, Marilyn
Kicklighter, David W.
Knudson, Heather N.
Laundre, James
McKerrow, Alexa
Michener, Robert H.
Nadelhoffer, Knute J.
O'Brien, Margaret
Pallant, Julie
Peterson, Bruce J.
Piterman, Oksana
Rastetter, Edward B.
Regan, Kathleen M.
Ricca, Andrea
Russell, Anne E.
Saupe, Susan
Schwamb, Carol
Semino, Suzanne J.
Shaver, Gaius R.
Steudler, Paul A.
Tucker, Jane

Postdoctorals

Bowden, Richard D.
Kling, George W.
McIvor, Carole C.
Raich, James
Ryan, Michael G.

Visiting investigators

Joyce, Linda, U.S.D.A. Forest Service
Waring, Richard, University of Oregon

Laboratory for Marine Animal Health

The laboratory provides diagnostic, consultative, research and educational services to the institutions and scientists of the Woods Hole community concerned with marine animal health. Diseases of wild, captive, and cultured animals are investigated.

Staff

Leibovitz, Louis, Director, Laboratory for Marine Animal Health, MBL, and Professor, Department of Avian & Aquatic Animal Medicine, New York State College of Veterinary Medicine
Abt, Donald A., Co-Investigator, University of Pennsylvania
Bullis, Robert A., Senior Research Associate, Cornell University
Hansen, Sandra B., Secretary, Cornell University
McCafferty, Michelle, Histological Technician, Cornell University
Moniz, Priscilla C., Administrative Secretary
Wadman, Elizabeth A., Microbiological Technician, Cornell University

Visiting investigators

Garvey, Margaret, University of Pennsylvania

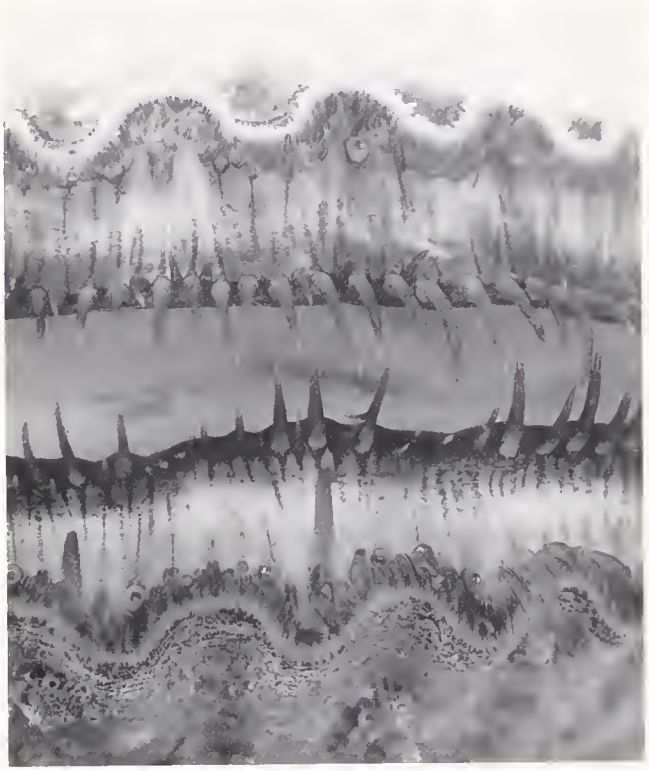

R & I. Golder

Laboratory of Aquatic Biomedicine

Our laboratory is studying hematopoietic neoplasia, a leukemia-like disease of soft shell clams. Monoclonal antibodies developed by this laboratory and techniques in molecular biology are used to investigate the differences between normal and leukemic cells and their ontogeny.

Staff

Reinisch, Carol L., Investigator, MBL, and Chairperson, Department of Comparative Medicine, Tufts University School of Medicine
Miosky, Donna, Laboratory Technician
Turano, Brian, Research Assistant

Laboratory of Cell Biochemistry

This laboratory studies developmental, metabolic, and environmental influences on the genetic regulation of cellular enzymes. Current emphasis is on hepatic heme biosynthesis and utilization in marine fish. These processes are responsive to hormonal and nutritional signals as well as to environmental pollutants such as hydrocarbons. This work is being conducted with primary cultures of hepatocytes and with cDNA probes that permit quantitation of gene activity. Other research is concerned with translocation of proteins between various subcellular compartments both in fish hepatocytes and in invertebrate eggs before and after fertilization.

Staff

Neal W. Cornell, Senior Scientist
Grace Bruning, Research Assistant
Michael Ferkowicz, Research Assistant

Laboratory of D. Eugene Copeland

Electron microscopy of luminescent organs (photophores) in deep-sea fish; gas secretion in swimbladders of deep-sea fish; and osmoregulatory tissue in *Limulus*.

Laboratory of Developmental Genetics

This research group studies the early gene control of cellular differentiation pathways (cell lineage determination) in embryos of tunicates and other marine invertebrate species.

Staff

Whittaker, J. Richard, Senior Scientist
Crowther, Robert, Research Assistant
Loescher, Jane L., Research Assistant
Meedel, Thomas H., Assistant Scientist

Visiting investigators

Arnold, John M., University of Hawaii
Collier, J. R., Brooklyn College
Heady, Judith E., University of Michigan-Dearborn (Sabbatical year, 1987–88)
Johnson, Carl D., Cambridge NeuroScience Research

Laboratory of Judith P. Grassle

Studies on the population genetics and ecology of marine invertebrates living in disturbed environments, especially of sibling species in the genus *Capitalla* (Polychaeta).

Staff

Grassle, Judith P., Senior Scientist
Mills, Susan W., Research Assistant

Laboratory of Harlyn O. Halvorson

The first project involves the study of spore germination in the bacterium *Bacillus subtilis*. A lambda genomic library has been screened and clones corresponding to the *Ger* J locus have been isolated. *Ger* J is involved in late spore germination. We wish to characterize *Ger* J and flanking sequences.

In collaboration with J. Weinberg (WHOI), we are also studying genome evolution in the marine polychaete *Nereis acuminata*. Several reproductively isolated field populations will be analyzed by comparative physical mapping, using cosmids and artificial chromosome vectors.

Staff

Halvorson, Harlyn, Principal Investigator, Director
Chikarmane, Hemant, Assistant Scientist
Pratt, Sara S., Research Assistant

Visiting investigators

Kornberg, Hans, University of Cambridge, UK
Keynan, Alex, Memorial Sloan Kettering Cancer Center
Vincent, Walter, University of Delaware

Laboratory of Shinya Inoué

Mechanism of mitosis and related motility. Development of high resolution 3-D video microscope systems.

Staff

Inoué, Shinya, Distinguished Scientist, MBL, and University of Pennsylvania
Anniballi, Dyon, Programming Engineer, Cornell University College of Engineering
Boyd, Steven, Programming Engineer, Cornell University College of Engineering
Inoué, Theodore, Programming Engineer, Cornell University College of Engineering
Shimomura, Sachi, Research Assistant, Stanford University
Taracka, Robert, Research Assistant
Woodward, Bertha M., Laboratory Manager

Visiting investigators

Bajer, Andrew S., University of Oregon
Burgos, Mario H., University of Cuyo, Mendoza, Argentina
Fukui, Yoshio, Northwestern University Medical School
Kiehart, Daniel P., Harvard University
Salmon, Edward D., University of North Carolina
Sardet, Christian, Biol. Cell. Marine, Ville France-Sur-Mer
Silver, Robert B., University of Wisconsin

Laboratory of Sensory Physiology

Since 1973, the laboratory has conducted research on various aspects of vision. Current studies focus on photoreceptor cells; on their light-absorbing pigments; and on their biochemical reactions initiated by light stimulation. Microspectrophotometric and biochemical techniques are used to study the receptors of both vertebrates (amphibia, fish, and mammals) and invertebrates (horseshoe crab and squid).

Staff

Harosi, Ference, Director. Associate Scientist, MBL, and Boston University School of Medicine
Szuts, Ete, Assistant Scientist, MBL, and Boston University School of Medicine
Trapp, Susan, Research Assistant
Zahajszky, Tibor, Research Associate

Visiting investigators

Clay, John R., Laboratory of Biophysics, NINCDS/NIH
Cornwall, Carter, Boston University School of Medicine
Eckberg, William R., Howard University
Hawryshyn, Craig W., McMaster University, Canada
Nicaise, Ghislain, University of Nice, France
Petry, Heywood M., SUNY, Stony Brook
Wood, Susan F., Boston University Marine Program

Laboratory of Neurobiology

The Laboratory of Neurobiology is concerned with the secretory mechanism underlying synaptic transmission, the mechanism of organelle movement underlying axoplasmic transport, and the organization of neural cytoplasm.

Staff

Reese, Thomas S., Chief, Laboratory of Neurobiology, MBL, NINCDS/NIH
Andrews, S. Brian, Research Associate
Bechtold-Imhof, Ruth, Research Assistant
Cheng, Toni, Research Associate
Chludzinski, John, Research Technician
Coyle, Jo-Anne, Secretary
Gallant, Paul, Research Associate
Garbus-Gooch, Cynthia, Research Assistant
Hammar, Katherine, Research Assistant
Khan, Shahid, Visiting Research Associate
Reese, Barbara F., Research Technician
Sheetz, Michael P., Visiting Research Associate
Schnapp, Bruce J., Research Associate
Tatsuoka, Hozumi, Research Associate
Terasaki, Mark, Research Associate

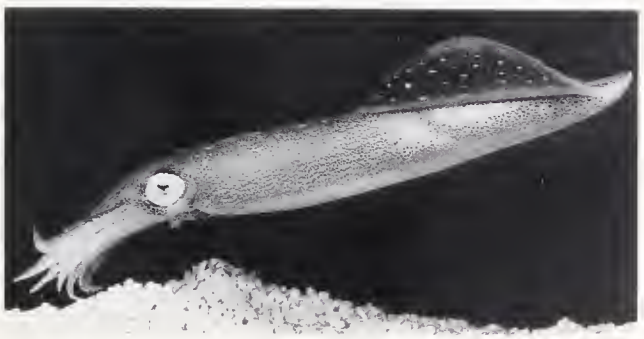

L. Golder

Laboratory of Neuroendocrinology

This laboratory studies the molecular and cellular bases of two neural programs that regulate different important behaviors in the model mollusc *Aplysia*. Research is conducted on the mechanisms of the neuronal circadian oscillators located in the eyes. These circadian oscillators drive the circadian activity rhythm of the animal, which is concerned with the daily timing of food gathering and of prolonged rest. Additional research is conducted on a group of neuroendocrine cells that produce a peptide, "egg-laying hormone," that initiates egg laying and associated behaviors. The laboratory is interested in how the three-dimensional shape of this peptide hormone allows a highly specific interaction with its receptor and the intracellular processes that are triggered by it. In another project, the laboratory has discovered and is continuing research on an anti-toxin protein that inhibits ADP-ribosylation of G-proteins induced by bacterial exotoxins.

Staff

Strumwasser, Felix, Director, Laboratory of Neuroendocrinology, Boston University School of Medicine, and MBL
Cox, Rachel L., Senior Research Assistant
Eason, Barbara, Laboratory Assistant
Glick, David, Senior Postdoctoral Fellow
Hellmich, Mark, Graduate Student (Boston University School of Medicine)
Viele, Daniel P., Senior Research Assistant

Laboratory of Michael Rabinowitz

Measurement of lead in baby teeth to see if lead exposure at different ages, recorded at different sites within teeth, are related to child development.

Staff

Rabinowitz, Michael, Investigator, MBL, and Instructor in Neurology, Harvard Medical School
Lewandowski, Ann, Research Assistant, Harvard Medical School

Laboratory of Osamu Shimomura

Biochemical studies of the various types of bioluminescent systems. Preparation of the improved forms of aequorin for measuring intracellular free calcium.

Staff

Shimomura, Osamu, Senior Scientist, MBL, and Boston University School of Medicine
Shimomura, Akemi, Research Assistant

Visiting investigators

Musicki, Branislav, Harvard University
Nakamura, Hideshi, Harvard University

Laboratory of Raymond E. Stephens

Biochemistry of microtubules in cilia, flagella, and the cytoplasm; mechanosensitivity and the control of ciliary movement.

Staff

Stephens, Raymond E., Investigator, MBL, and Boston University School of Medicine
Good, Michael J., Research Assistant
Oleszko-Szuts, Susan, Research Associate
Stommel, Elijah W., Research Associate, St. Elizabeth's Hospital

Visiting investigator

Holz, George G., Tufts University School of Medicine

Laboratory of Raquel Sussman

Investigation of the molecular mechanism of DNA damage-inducible functions. Present studies deal with the structure-function relationships of λ repressor analyzed by immunological techniques.

Staff

Sussman, Raquel, Associate Scientist
McLaughlin, Jane, Research Assistant
Cornuel, Catherine, Research Assistant

National Vibrating Probe Facility

We are exploring the roles of ionic currents, gradients, and waves in controlling development. We focus on controls *of* pattern and *by* calcium ions.

Staff

Jaffe, Lionel, Senior Scientist and Facility Director
Kuhtreiber, Wiel, Physiologist
Miller, Andrew, Research Associate
Sanger, Richard, Technician
Shipley, Alan, Technician
Williams, Phillip C., Engineer
Speksnijder, Annelies, Research Associate

Visiting investigators

Asman, Sally, Harvard University
Baumann, Steve, EPA, Research Triangle Park, NC
Biggers, John, Harvard Medical School
Bowdan, Elizabeth, University of Massachusetts
Chen, Tsung-Hsien, Academia Sinica, Taiwan
Crawford, Karen, Swarthmore College
Cullander, Chris, University of California, S. F.
Devlin, Leah, University of Rhode Island
Dickey, Joe, Clemson College
Diehl-Jones, W. L., University of Manitoba, Canada
Fink, Rachael, Mount Holyoke College
Holtug, Klars, Royal Veterinary University, Denmark
Kunkel, Joseph, University of Massachusetts
Mladenov, Phillip, Mount Allison University, New Brunswick, Canada
Payne, Richard, University of Maryland
Pethig, Ron, University College of North Wales, U. K.
Sardet, Christian, Station Marine Ville franche-sur-mer, France
Trinkaus, John, Yale University
Troxell, Cindy, University of Colorado
Ver Achtert, Barend, University of Leuven, Belgium
Wyman, Robert, Yale University

Lionel Jaffe in his laboratory.

Centennial Evening Lectures

Meredith Applebury, University of Chicago, 24 June
"Hecht and Wald: Towards the Molecular Basis of Vision"

Daniel Koshland Jr., University of California, Berkeley, 1 July
"The Future of Biological Research: What is Possible and What is Ethical"

Torsten Wiesel, The Rockefeller University, 8 July, Lang Lecture
"Neural Mechanisms of Visual Perception: The Legacy of Hartline and Kuffler"

Joshua Lederberg, The Rockefeller University, 15 July
"Genetic Maps: Fruit Flies, People, Bacteria, and Molecules—A Tribute to Morgan and Sturtevant"

Gerald Weissmann, New York University, 17 July, Dedication Day
"Loeb: The Mechanistic Conception of Life Revisited"

Joshua Lederberg delivering his Centennial Evening Lecture.

Sydney Brenner, Medical Research Council, 21, 22, July, Forbes Lectures
"Reading the Genetic Script"
"Genes and the Nervous System"

Clay Armstrong, University of Pennsylvania, 29 July
"Ionic Channels That are Gated by Voltage: A Tribute to Cole and Hodgkin"

John Hobbie, Marine Biological Laboratory, 5 August
"Ecology at Woods Hole: Baird, Bigelow, and Redfield"

Donald Kennedy, Stanford University, 6 August, Monsanto Biotechnology Lecture
"The Regulation of Science: How Much Can We Afford?"

Robert Solow, Massachusetts Institute of Technology, 7 August, Hiroshima Day Lecture
"Military Spending and Economic Health: A Great Place to Start?"

Edward Wilson, Harvard University, 12 August
"Analyzing the Superorganism: The Legacy of Whitman and Wheeler"

Clifford Slayman, Yale University, 16 August
"Channels, Pumps, and Motors in Plants: A Tribute to Osterhout"

Shinya Inoue, Marine Biological Laboratory, 19 August
"Porter and the Fine Architecture of Dividing Cells"

John Gurdon, Cambridge University, 26 August
"Determinants of Development: From Conklin and Lillie to the Present"

Fellowships

Robert Day Allen Fellowship

Suprenant, Kathy A., University of Kansas

Frederik B. Bang Fellowship Fund

Dykens, James A., Grinnell College

Frank A. Brown, Jr., Memorial Readership

Hill, Richard W., Michigan State University

Founders Fellowship

Beckwith, Susan M., Purdue University
Brown, Alice B., Vanderbilt University
Cintron, Isabel G., University of Puerto Rico
Dunn, Patrick J., University of Pennsylvania
Fautsch, Michael P., Mayo Clinic Foundation
Georgiou, Chris, University of Iowa

Hayden-Baille Fellowship

Crossley, Ian Brian, University College of London, England
Willcox, Mark S., University College at Swansea, England

William Randolph Hearst Fellowship

Gramoll, Siglnde, The Hebrew University of Jerusalem, Israel

Stephen W. Kuffler Fellowships

Nolen, Thomas G., University of Miami
Saez, Juan C., Albert Einstein College of Medicine

Frank R. Lillie Fellowship

Ding, Dali, California Institute of Technology
Dittmann, Sabine, Zoologisches Institute, FRG
Geysen, Johan J., University of Leuven, Belgium
Hidalgo, Alicia, University of Oxford, England
Lackschewitz, Dagmar, Max-Planck Institute, FRG
Mayor, Robert A., University of Chile, Chile
Morrisey, Donald J., University of Bristol, England
Rowan, Robert G., Johns Hopkins University
Wickramasinghe, Dineli M., Tufts University

Jacques Loeb Fellowship

Watson, Kellie L., University of California at Irvine

MBL Summer Fellowships

Fine, Allen, Dalhousie University, Canada
Fink, Rachel, Mount Holyoke College

Herbert W. Rand Fellowship

Gibson, Saxon M., Vanderbilt University
Kiener, Andreas M., Harvard Medical School
Mendoza, Lisa M., Scirpps Institute, University of California at San Diego

Science Writing Fellowships

Amato, Ivan, *Science News*
Crabtree, Margo, *Science World*
Golden, Frederic, Freelance, San Francisco, CA
Kanigel, Robert, Freelance, Baltimore, MD
Keller, Erie, *Smithsonian*
Knudson, Mary, *Baltimore Sun*
Kornberg, Warren, *Mosaic*
Raymond, Chris Anne, *Journal of the American Medical Association*

H. B. Steinbach Fellowships

Palazzo, Robert E., University of Virginia

Scholarships

Biology Club of City University of New York

Houser, Felicia, Harvard University

Father Arsenius Boyer Scholarship Fund

Johnson, Jennifer A., Dartmouth College

C. Lalor Burdick Scholarship

Blumenthal, Edward M., Yale University
Fautsch, Michael P., Mayo Clinic Foundation
Larochelle, Denis A., Stanford University

Gary N. Calkins Memorial Scholarship

Dunn, Patrick J., University of Pennsylvania
Lemosy, Ellen K., Duke University

Frances S. Claff Memorial Scholarship

Bright, Kerris E., University of Sussex, England
Cannon, Stephen C., Massachusetts General Hospital

Edwin Grant Conklin Memorial Scholarship

Jones, Diana C., Purdue University

Lucretia Crocker Endowment Fund

Cintron, Isabel G., University of Puerto Rico

William F. and Irene Diller Scholarship Fund

Beckwith, Susan M., Purdue University
Brown, Alice B., Vanderbilt University

Caswell Grave Scholarship

Felsenfeld, Dan P., Columbia University
Keller, Steve M., University of California, San Diego/ Scripps Institute of Oceanography

Aline D. Gross Scholarship

Klatte, D. H., Northwestern University

Merkel H. Jacobs Scholarship

Johansson, Staffan, Karolinska Institutet, Nobel Institute, Sweden

Arthur Klorfein Fund Scholarship

Krufka, Alison, University of Wisconsin
Pesavento, Patricia A., Harvard University
Scemes, Elina, Universidad de Sao Paulo, Brazil
Thompson, Margaret A., Harvard University
Vu, Eric T., University of California, Los Angeles
Wehner, Katja A., Max-Planck Institute, FRG

Lucille P. Markey Charitable Trust Scholarship

Elliott, David D., Glasgow University, Scotland
Georgiou, Chris, University of Iowa
Hoecker, Beatrix B., University of Hamburg, FRG
Mamajiwalla, Salim N., University of Miami
Messina, Dino A., State University of New York, Syracuse
Morrissette, Naomi S., University of Pennsylvania
Oblong, John E., University of Chicago
Olsen, Scott G., University of Minnesota
Rocha, Rosana M., University of Estadual de Campinas, Brazil
Rounseville, Matthew P., George Washington University
Rushforth, Alice M., University of Wisconsin
Sandulli, Roberto, University of Naples, Italy
Schmager, Carola, Institut fur Meereskunde, an der Universitat Kiel, FRG
Subramanian, Sukanya V., Albert Einstein College of Medicine
Vattay, Anthony, Rutgers University
Vanghan, Kevin T., Cornell University
Wang, Jin, Worcester Foundation for Experimental Biology
Wolenski, Joseph S., Rutgers University
Wolfe, Connie J., Scripps Institute of Oceanography, University of California, San Diego
Yue, Lin, Johns Hopkins University

S. O. Mast Founders Scholarship

Kane, Susan B., University of Massachusetts, Boston

Allen R. Memhard Scholarship

Hamrick, Maura L., Johns Hopkins University

James S. Mountain Memorial Fund Scholarship

Beckwith, Susan M., Purdue University
Brown, Alice B., Vanderbilt University
Cintron, Isabel G., University of Puerto Rico
Dunn, Patrick J., University of Pennsylvania
Fautsch, Michael P., Mayo Clinic Foundation

Planetary Biology Internship

Carman, Kevin R., Florida State University
Lackschewitz, Dagmar, Max-Planck Institute, FRG

Marjoire W. Stetten Scholarship Fund

Yang, Xian-Cheng, State University of New York, Buffalo
Yuste, Rafael M., Rockefeller University

Surdna Foundation Scholarship

Huber, Robert, Texas Technical University
Li, Jian, State University of New York, Syracuse
Long, Guohong, University of Massachusetts
Mindell, Joseph A., Albert Einstein College of Medicine
Ondeka, Cheryl A., University of Massachusetts at Amherst
Pinckney, James L., University of South Carolina
Zhao, Dayao, Harvard Medical School

William Morton Wheeler Family Founders' Scholarship

Gillmore, Todd H., State University of New York at New Paltz

Howard A. Schneiderman (center) accepts an MBL Distinguished Leadership Award from MBL Director Harlyn Halvorson (left) and Chairman Prosser Gifford (right).

Board of Trustees and Committees

Corporation Officers and Trustees

Ex officio

Honorary Chairman of the Board of Trustees, Denis M. Robinson, Key Biscayne, FL
Chairman of the Board of Trustees, Prosser Gifford, Washington, DC
President of the Corporation and Director, Harlyn O. Halvorson, Marine Biological Laboratory, Woods Hole, MA
Treasurer, Robert D. Manz, Helmer & Associates, Waltham, MA
Clerk of the Corporation, Kathleen Dunlap, Tufts University School of Medicine, Boston, MA

Class of 1992

Norman Bernstein, Bernstein Management, Inc., Washington, DC
Ellen R. Grass, Grass Foundation, Quincy, MA
Warren G. Hathaway, Hathaway Publishing, Somerset, MA
Sir Hans Kornberg, Christ's College, Cambridge, UK
George Langford, University of North Carolina, Chapel Hill, NC
Jack Levin, University of California School of Medicine, San Francisco, CA
Evelyn Spiegel, Dartmouth College, Hanover, NH
Andrew G. Szent-Györgyi, Brandeis University, Waltham, MA
Kensal E. VanHolde, Oregon State University, Corvallis, OR
Stanley W. Watson, Associates of Cape Cod, Inc., Falmouth, MA

Class of 1991

Robert B. Barlow Jr., Syracuse University, Syracuse, NY
Dieter Blennemann, Carl Zeiss, Inc., Thornwood, NY
James M. Clark, Woods Hole, MA
Wensley G. Haydon-Baillie, Porton, Int., London, UK
Laszlo Lorand, Northwestern University, Evanston, IL
Lionel I. Rebhun, University of Virginia, Charlottesville, VA
Carol L. Reinisch, Tufts University School of Veterinary Medicine, Boston, MA
Brian M. Salzberg, University of Pennsylvania, Philadelphia, PA
Howard A. Schneiderman, Monsanto Company, St. Louis, MO
Sheldon J. Segal, The Rockefeller Foundation, New York, NY

Class of 1990

John E. Dowling, Harvard University, Cambridge, MA
Gerald D. Fischbach, Washington University School of Medicine, St. Louis, MO
Robert D. Goldman, Northwestern University, Chicago, IL
John E. Hobbie, Marine Biological Laboratory, Woods Hole, MA
Richard E. Kendall, East Falmouth, MA
Irving W. Rabb, Boston, MA
Joan V. Ruderman, Duke University, Durham, NC
Ann E. Stuart, University of North Carolina, Chapel Hill, NC
D. Thomas Trigg, Wellesley, MA

Class of 1989

Garland E. Allen, Washington University, St. Louis, MO
Peter B. Armstrong, University of California, Davis, CA
Robert W. Ashton, Gaston, Snow, Beekman & Bogue, New York, NY
Jelle Atema, Marine Biological Laboratory, Woods Hole, MA
John G. Hildebrand, University of Arizona, Tucson, AZ
Thomas J. Hynes Jr., Meredith and Grew, Inc., Boston, MA
Robert Mainer, The Boston Company, Boston, MA
Birgit Rose, University of Miami School of Medicine, Miami, FL
Gerald Weissmann, New York University, New York, NY

Emeriti

John B. Buck, National Institutes of Health, Bethesda, MD
Aurin Chase, Princeton University, Princeton, NJ
Seymour S. Cohen, Woods Hole, MA
Arthur L. Colwin, Key Biscayne, FL
Laura Hunter Colwin, Key Biscayne, FL
D. Eugene Copeland, Marine Biological Laboratory, Woods Hole, MA
Sears Crowell, Indiana University, Bloomington, IN
Alexander T. Daignault, Boston, MA
William T. Golden, New York, NY
Teru Hayashi, Woods Hole, MA
Lewis Kleinholz, Reed College, Portland, OR
Maurice E. Krahl, Tucson, AZ
Charles B. Metz, Miami, FL
Keith R. Porter, University of Pennsylvania, Philadelphia, PA
C. Ladd Prosser, University of Illinois, Urbana, IL
S. Meryl Rose, Waquoit, MA
John Saunders, Jr., Waquoit, MA
Mary Sears, Woods Hole, MA
Homer P. Smith, Woods Hole, MA
W. Randolph Taylor, University of Michigan, Ann Arbor, MI
George Wald, Cambridge, MA

Executive Committee of the Board of Trustees

Prosser Gifford, Chairman*
Robert B. Barlow Jr., 1991
John E. Dowling, 1990
Ray L. Epstein*
Gerald D. Fischbach, 1989
Harlyn O. Halvorson*
Robert D. Manz*
Irving W. Rabb, 1991
Sheldon J. Segal, 1989
D. Thomas Trigg, 1990

* *ex officio*

Trustee Committees 1988

Audit

Robert Mainer, Chairman
Ray L. Epstein*
Robert D. Manz*
Sheldon J. Segal
Andrew G. Szent-Györgyi
D. Thomas Trigg
Kensal E. Van Holde
Stanley W. Watson

Compensation

Thomas J. Hynes Jr., Chairman
James M. Clark
John E. Dowling

Investment

D. Thomas Trigg, Chairman
Ray L. Epstein*
William T. Golden
Maurice Lazarus
Werner R. Loewenstein
Robert D. Manz
Irving W. Rabb
W. Nicholas Thorndike

Centennial

James D. Ebert, Chairman
Pamela L. Clapp, Coordinator*
Garland E. Allen
Robert B. Barlow Jr.
Paul R. Gross
Harlyn O. Halvorson*
Olivann Hobbie
Richard E. Kendall
John Pfeiffer
Keith Porter
Frank Press
C. Ladd Prosser
John S. Reed
D. Thomas Trigg
John Valois

Standing Committees for the Year 1988

Animal Care Committee

Carol L. Reinisch, Chairman
Ray L. Epstein*
Leslie D. Garrick*
Linda Huffer
Edward Jaskun
Andrew Mattox*
Roxanna Smolowitz
J. Richard Whittaker

Buildings & Grounds

Kenyon Tweedell, Chairman
Lawrence B. Cohen
Richard Cutler*
Alan Fein
Daniel Gilbert
Clifford Harding, Jr.
Ferenc Harosi
Donald B. Lehy*
Thomas Meedel
Philip Person
Lionel Rebhun
Thomas Reese
Evelyn Spiegel

Employee Relations

Ellen Binda, Chairwoman
Ida Baker
Peg Corbett
H. Tom Fischer
Lionel Hall
Alan Shipley
Frank Sylvia
John MacLeod

Fellowships

Thoru Pederson, Chairman
Ray L. Epstein*
Leslie D. Garrick*
Judith Grassle
John G. Hildebrand
George M. Langford
Eduardo Macagno
Carol L. Reinisch

Housing, Food Service, and Child Care

Jelle Atema, Chairman
Robert B. Barlow, Jr.
Gail Burd
Stephen Highstein
Lou Ann King*
Thomas Reese
Joan Ruderman

Institutional Biosafety

Raquel Sussman, Chairman
Paul DeWeer
Paul Englund
Harlyn O. Halvorson*
Paul Lee
Donald B. Lehy*
Joseph Martyna
Andrew Mattox*
Alfred W. Senft

Instruction

Judith Grassle, Chairman
Ray L. Epstein*
Brian Fry
Leslie D. Garrick*
John G. Hildebrand
Ron Hoy
Tom Humphreys
Hans Laufer
Brian Salzberg
Roger Sloboda
Andrew Szent-Györgyi

Library Joint Management

Harlyn O. Halvorson, Chairman*
Garland Allen
George Grice, WHOI
John W. Speer*
John Steele, WHOI
Gary Walker, WHOI

Library Joint Users

Garland Allen, Chairman
Wilfred Bryan, WHOI
A. Farmanfarmaian
Jane Fessenden*
Lionel Jaffe
Catherine Norton*
John Schlee, USGS
John Teal, WHOI
Edward Sholkovitz, WHOI
Carole Winn, WHOI*
Oliver C. Zafiriou

* *ex officio*

Marine Resources

Robert Goldman, Chairman
William Cohen
Richard Cutler*
Louis Leibovitz
Toshio Narahashi
George Pappas
Roger Sloboda
Melvin Spiegel
Antoinette Steinacher
John Valois*

Radiation Safety

Paul DeWeer, Chairman
David W. Borst
Richard L. Chappell
Sherwin J. Cooperstein
Louis M. Kerr*
Andrew Mattox*
Ete Z. Szuts
Walter Vincent

Research Services

Birgit Rose, Chairman
Peter Armstrong
Robert B. Barlow Jr.
Richard Cutler*
Barbara Ehrlich
Ehud Kaplan
Samuel S. Koide
Aimlee Laderman

* *ex officio*

Andrew Mattox*
Bryan Noe
Bruce J. Peterson
Rudi Strickler

Research Space

Joseph Sanger, Chairman
Clay Armstrong
Ray L. Epstein*
Leslie D. Garrick*
David Landowne
Hans Laufer
Laszlo Lorand
Eduardo Macagno
Jerry Melillo
Joan V. Ruderman
Roger Sloboda
Evelyn Spiegel
Steven Treistman
Ivan Valiela

Safety

John Hobbie, Chairman
Daniel Alkon
D. Eugene Copeland
Richard Cutler*
Edward Enos*
Louis Kerr*
Alan Kuzirian
Donald B. Lehy*
Andrew Mattox*
Edward Sadowski
Ray Stephens
Paul Steudler

Laboratory Support Staff*

Biological Bulletin
Metz, Charles, B., Editor
Bauer, Diane
Clapp, Pamela L.
Mountford, Rebecca J.

Controller's Office
Speer, John W., Controller

Accounting Services
Binda, Ellen F.
Blain, Harriet
Campbell, Ruth B.
Davis, Doris C.
Gilmore, Mary F.
Godin, Frances T.
Hobbs, Roger W., Jr.
Hough, Rose A.
O'Brien-Sibson, Patricia J.
Oliver, Elizabeth
Poravas, Maria

Chem Room
Clough, Lisa A.
LaMontagne, Michael
Mercurio, Kimberley
Ross, Darcy
Sadowski, Edward A.

Computer Services
Tollios, Constantine

Purchasing
Evans, William A.
Hall, Lionel E., Jr.

Copy Service Center
Gibson, Caroline F.
Jackson, Jacquelyn F.
Mountford, Rebecca J.

Development Office
Ayers, Donald E., Director
Berthel, Dorothy
Lyons, Elaine D.

* Including persons who joined or left the staff during 1988

O'Hara, Aqua
Thimas, Lisa M.

Director's Office
Halvorson, Harlyn O., President and Director
Berthel, Dorothy
Epstein, Ray L.
Kinneally, Kathleen R.
Watkins, Joan E.

Human Resources
Goux, Susan P.

Gray Museum
Bush, Louise, Curator
Armstrong, Ellen P.
Montiero, Eva

Housing
King, LouAnn D., Conference Center and Housing Manager
Crocker, Susan J.
Eddy, Kristine A.
Johnson, Frances N.
Klopfer, Katherine
Krajewski, Viola I.
Kuil, Elisabeth
Leach, Adele
McNamara, Noreen
Morrill, Barbara J.
Perry, Ann R.
Potter, Maryellen
Price, Dale L.
Roderick, Cynthia F.
Sadovsky, Sebastian
Taylor, Tobey
Tedeschi, Christine R.

Library
Fessenden, Jane, Librarian
Ashmore, Judith A.
Costa, Marguerite E.
Mirra, Anthony J.
Mountford, Rebecca J.
Nelson, Heidi
Norton, Catherine N.
Pratson, Patricia G.
deVeer, Joseph M.

MBL Associates Liaison
Scanlon, Deborah

Public Information Office
Liles, George W., Jr., Director
Anderson, Judith L.
Dzierzeski, Michelle J.
Stone, Beth R.

Services, Projects, and Facilities
Cutler, Richard D., Manager

Buildings and Grounds
Lehy, Donald B., Superintendent
Anderson, Lewis B.
Baldic, David P.
Blunt, Hugh F.
Bourgoin, Lee E.
Carini, Robert J.
Collins, Paul J.
Conlin, Henry P.
Conlin, Mary E.
Fish, David L., Jr.
Fuglister, Charles K.
Gibbons, Roberto G.
Gonsalves, Walter W., Jr.
Klinger, Michael
Krajewski, Chester J.
Lochhead, William M.
Lunn, Alan G.
Lynch, Henry L.
MacLeod, John B.
McAdams, Herbert, III
Mills, Stephen A.
Rattacasa, Frank D.
Rossetti, Michael F., Jr.
Schoepf, Claude
Schwamb, Peter J.
Simonelli, Bernard R.
Simonelli, Guy S.
deVeer, Robert L.
Ward, Frederick
Weeks, Gordon W.
Wilson, Mitchell J.
Windle, Irvin

Machine Shop
Sylvia, Frank E.

Marine Resources Center
Valois, John J., Manager
DeGiorgis, Joseph
Enos, Edward G., Jr.
Enos, Joyce B.
Fisher, Harry T., Jr.
Frank, Donald S.
Hanley, Janice S.
Moniz, Priscilla C.
Revellese, Christopher
Sullivan, Daniel A.
Tassinari, Eugene

Photolab
Golder, Linda M.
Golder, Robert J.
Rugh, Douglas E.

Sponsored Programs
Garrick, Leslie D., Assistant Administrator
Casiles, Phyllis B.
Dwane, Florence
Huffer, Linda
Lynch, Kathleen F.

Telephone Office
Baker, Ida M.
Geggatt, Agnes L.
Ridley, Alberta W.

Animal Care Facility
Briggs, Kimberly A.
Hamilton, Kathryn R.
Povio, Sandra C.
Sohn, Marcus J.
Tripp, Gretchen

Radiation Safety
Mattox, Andrew H., Safety Officer

Apparatus
Barnes, Franklin D.
Haskins, William A.
Martin, Lowell V.
Nichols, Francis H., Jr.
Sanger, Richard H., Jr.

Shipping and Receiving
Geggatt, Richard E.
Illgen, Robert F.
Monteiro, Dana

Electron Microscopy Lab
Hodge, Alan J.
Kerr, Louis M.

1988 Summer Support Staff
Allen, Carin T.
Allen, Tania L.
Amon, Tyler C.
Anger, Susan R.
Ashmore, Lynne E.
Avery, Kenneth C.
Bezanilla, Pilar M.
Bolton, Hugh
Braunlich, Denise E.
Cadwalader, George, Jr.
Campbell, Andrew
Capobianco, James A.
Child, Malcolm S.
Dettbarn, Donata A.
Dino, Victor H.
Dodge, Michael F.
Dodge, Susan A.
Donovan, Christine B.
Donovan, Jason P.
Dooley, Kimberly A.
Francisco, Manuel A.
Green, Pamela A.
Grossman, Howard
Hadamard, John
Haldiman, Susan M.
Hamilton, Elizabeth R.
Hines, Eric M.
Hines, Kristen A.
Jones, Leeland A.
Kinneally, Kara J.
Manheim, Francesca
Marini, Michael F.
McMenamin-Balano, Jonathan
Minner, Eugene W.
Peal, Richard W.
Relyea, Timothy J.
Remsen, Andrew W.
Revellese, Christopher
Rickles, Andrew H.
Riemer, Daniel J.
Roche, Theseus
Roderick, Ann J.
Rook, Kellyann
Rossetti, Michael P.
Rudin, Erik
Rugh, Douglas E.
Schauer, Caroline L.
Schopf, Kenneth M.
Shaw, Trevor P.
Showalter, Carl J.
Silverstein, Susan M.
Sintoni, Michael A.
Sohn, Marcus J.
Valois, Francis X.
Valyou, Patricia M.
Wetzel, Ernest D.

Members of the MBL community watch the Coast Guard's nautical salute to the MBL's Centennial.

Members of the Corporation*

Life Members

Abbott, Marie, c/o Vaughn Abbott, Flyer Rd., East Hartland, CT 06027

Adolph, Edward F., University of Rochester, School of Medicine and Dentistry, Rochester, NY 14642 (deceased)

Beams, Harold W., Department of Biology, University of Iowa, Iowa City, IA 52242

Behre, Ellinor, Black Mountain, NC 28711 (deceased)

Bernheimer, Alan W., Department of Microbiology, New York University Medical Center, 550 First Ave., New York, NY 10016

Bertholf, Lloyd M., Westminster Village #2114, 2025 E. Lincoln St., Bloomington, IL 61701

Bishop, David W., Department of Physiology, Medical College of Ohio, C. S. 10008, Toledo, OH 43699

Bold, Harold C., Department of Botany, University of Texas, Austin, TX 78712

Bridgman, A. Josephine, 715 Kirk Rd., Decatur, GA 30030

Buck, John B., NIH, Laboratory of Physical Biology, Room 112, Building 6 Bethesda, MD 20892

Burbanck, Madeline P., Box 15134, Atlanta, GA 30333

Burbanck, William D., Box 15134, Atlanta, GA 30333

Carpenter, Russell L., 60-H Lake St., Winchester, MA 01890

Chase, Aurin, Department of Biology, Princeton University, Princeton, NJ 08544

Clark, Arnold M., 53 Wilson Rd., Woods Hole, MA 02543

Cohen, Seymour S., 10 Carrot Hill Rd., Woods Hole, MA 02543-1206

Colwin, Arthur, 320 Woodcrest Rd., Key Biscayne, FL 33149

Colwin, Laura Hunter, 320 Woodcrest, Key Biscayne, FL 33149

Copeland, D. E., 41 Fern Lane, Woods Hole, MA 02543

Costello, Helen M., Carolina Meadows, Villa 137, Chapel Hill, NC 27514

Crouse, Helen, Institute of Molecular Biophysics, Florida State University, Tallahassee, FL 32306

Diller, Irene C., Rydal Park, Apartment 660, Rydal, PA 19046 (deceased 2/88)

Elliott, Alfred M., 428 Lely Palm Ext., Naples, FL 33962-8903 (deceased 1/20/88)

Failla, Patricia M., 2149 Loblolly Lane, Johns Island, SC 29455

Ferguson, Frederick P., National Institute of General Medical Science, NIH, Bethesda, MD 20892 (deceased 9/27/88)

Ferguson, James K. W., 56 Clarkehaven St., Thornhill, Ontario L4J 2B4 CANADA

Fries, Erik F., 41 High Street, Woods Hole, MA 02543

Graham, Herbert, 36 Wilson Rd., Woods Hole, MA 02543

Green, James W., 409 Grant Ave., Highland Park, NJ 08904

Grosch, Daniel S., 1222 Duplin Road, Raleigh, NC 27607

Hamburger, Viktor, Department of Biology, Washington University, St. Louis, MO 63130

Hamilton, Howard L., Department of Biology, University of Virginia, Charlottesville, VA 22901

Hisaw, F. L., 5925 SW Plymouth Drive, Corvallis, OR 97330

Hollaender, Alexander, Council for Research Planning, 1717 Massachusetts Ave. NW, Washington, DC 20036

Humes, Arthur G., Marine Biological Laboratory, Woods Hole, MA 02543

Johnson, Frank H., Department of Biology, Princeton University, Princeton, NJ 08540

Kaan, Helen W., Royal Megansett Nursing Home, Room 205, P. O. Box 408, N. Falmouth, MA 02556

Karush, Fred, Department of Microbiology, University of Pennsylvania School of Medicine, Philadelphia, PA 19104-6076

Kille, Frank R., 1111 S. Lakemont Ave. #444, Winter Park, FL 32792

* Including action of the 1988 Annual Meeting.

Kingsbury, John M., Department of Plant Biology, Cornell University, Ithaca, NY 14853
Kleinholz, Lewis, Department of Biology, Reed College, Portland, OR 97202

Laderman, Ezra, P. O. Box 689, 18 Agassiz Road, Woods Hole, MA 02543
Lauffer, Max A., Department of Biophysics, University of Pittsburgh, Pittsburgh, PA 15260
LeFevre, Paul G., 15 Agassiz Road, Woods Hole, MA 02543
Levine, Rachmiel, 2024 Canyon Rd., Arcadia, CA 91006
Lochhead, John H., 49 Woodlawn Rd., London SW6 6PS, England, U. K.
Lynn, W. Gardner, Department of Biology, Catholic University of America, Washington, DC 20017

Magruder, Samuel R., 270 Cedar Lane, Paducah, KY 42001
Manwell, Reginald D., Syracuse University, Lyman Hall, Syracuse, NY 13210
Miller, James A., 307 Shorewood Drive, E. Falmouth, MA 02536
Milne, Lorus J., Department of Zoology, University of New Hampshire, Durham, NH 03824 (deceased)
Moore, John A., Department of Biology, University of California, Riverside, CA 92521
Moul, E. T., Woodbriar, 339 Gifford St., Falmouth, MA 02540

Nace, Paul F., P. O. Box 529, Cutchogue, NY 11935

Page, Irving H., Box 516, Hyannisport, MA 02647
Pollister, A. W., 8 Euclid Ave., Belle Mead, NJ 08502
Prosser, C. Ladd, Department of Physiology and Biophysics, Burrill Hall 524, University of Illinois, Urbana, IL 61801
Provasoli, Luigi, Via Stazione 43, 21025 Comerio (VA), ITALY
Prytz, Margaret McDonald, Address unknown

Renn, Charles E., Route 2, Hempstead, MD 21074
Richards, A. Glenn, 942 Cromwell Ave., St. Paul, MN 55114
Richards, Oscar W., Route 1, Box 79F, Oakland, OR 97462
Rockstein, Morris, 600 Biltmore Way, Apt. 805, Coral Gables, FL 33134
Ronkin, Raphael R., 3212 McKinley St., NW, Washington, DC 20015

Sanders, Howard, Woods Hole Oceanographic Institution, Woods Hole, MA 02543
Scharrer, Berta, Department of Anatomy, Albert Einstein College of Medicine, 1300 Morris Park Avenue, Bronx, NY 10461
Schlesinger, R. Walter, University of Medicine and Dentistry of New Jersey, Department of Molecular Genetics and Microbiology, Robert Wood Johnson Medical School, Piscataway, NJ 08854-5635
Schmitt, F. O., Room 16-512, Massachusetts Institute of Technology, Cambridge, MA 02139
Scott, Allan C., 1 Nudd St., Waterville, ME 04901
Shemin, David, 33 Lawrence Farm Rd., Woods Hole, MA 02543
Smith, Homer P., 8 Quissett Ave., Woods Hole, MA 02543
Smith, Paul F., P. O. Box 264, Woods Hole, MA 02543
Sonnenblick, B. P., 91 Chestnut St., Millburn, NJ 07041
Steinhardt, Jacinto, 1508 Spruce St., Berkeley, CA 94709
Stunkard, Horace W., American Museum of Natural History, Central Park West at 79th St., New York, NY 10024

Taylor, Robert E., 20 Harbor Hill Rd., Woods Hole, MA 02543
Taylor, W. Randolph, The Herbarium, North University Bldg., University of Michigan, Ann Arbor, MI 48109
Taylor, W. Rowland, 152 Cedar Park Road, Annapolis, MD 21401
TeWinkel, Lois E., 4 Sanderson Ave., Northampton, MA 01060
Trager, William, The Rockefeller University, 1230 York Ave., New York, NY 10021

Wald, George, 21 Lakeview Ave., Cambridge, MA 02138
Waterman, T. H., Yale University, Biology Department, Box 6666, New Haven, CT 06511
Weiss, Paul A., Address unknown
Wichterman, Ralph, 31 Buzzards Bay Ave., Woods Hole, MA 02543
Wiercinski, Floyd J., Department of Biology, Northeastern Illinois University, Chicago, IL 60625
Wilber, Charles G., Department of Zoology, Colorado State University, Fort Collins, CO 80523

Young, D. B., 1137 Main St., N. Hanover, MA 02339

Zinn, Donald J., P. O. Box 589, Falmouth, MA 02541
Zorzoli, Anita, 18 Wilbur Blvd., Poughkeepsie, NY 12603
Zweifach, Benjamin W., 8811 Nottingham Place, La Jolla, CA 92037

Regular Members

Abt, Donald A., University of Pennsylvania School of Veterinary Medicine, 3800 Spruce Street, Philadelphia, PA 19104-6044
Ache, Barry W., Whitney Marine Laboratory, 9505 Ocean Shore Blvd., St. Augustine, FL 32086
Acheson, George H., 25 Quissett Ave., Woods Hole, MA 02543
Adams, James A., Department of Natural Sciences, University of Maryland, Princess Anne, MD 21853
Adelberg, Edward A., Provost's Office, 115 Hall of Graduate Studies, Yale University, New Haven, CT 06510
Adelman, William J., Jr., NIH, Bldg. 9, Rm. 1E-127, Bethesda, MD 20892
Afzelius, Bjorn, Wenner-Gren Institute, University of Stockholm, Stockholm, SWEDEN
Alberte, Randall S., Oceanic Biology Program, Code 1122B, Office of Naval Research, 800 North Quincy St., Arlington, VA 22217-5000
Alkon, Daniel, Laboratory of Cellular and Molecular Neurobiology, NINDDS/NIH, Bldg. 5, Rm. 435, Bethesda, MD 20892
Allen, Garland E., Department of Biology, Washington University, St. Louis, MO 63130

Allen, Nina S., Department of Biology, Wake Forest University, Box 7325, Winston-Salem, NC 27109

Allen, Suzanne T., Department of Medical Oncology, Boston University Medical Center, 75 E. Newton Street, Boston, MA 02118-2393

Amatniek, Ernest, 4797 Boston Post Rd., Pelham Manor, NY 10803

Anderson, Everett, Department of Anatomy, LHRBB, Harvard Medical School, 45 Shattuck St., Boston, MA 02115

Anderson, J. M., 110 Roat St., Ithaca, NY 14850

Armet-Kibel, Christine, Biology Department, University of Massachusetts-Boston, Boston, MA 02125

Armstrong, Clay M., Department of Physiology, Medical School, University of Pennsylvania, Philadelphia, PA 19174

Armstrong, Peter B., Department of Zoology, University of California, Davis, CA 95616

Arnold, John M., Pacific Biomedical Research Center, 209 Snyder Hall, 2538 The Mall, Honolulu, HI 96822

Arnold, William A., 102 Balsam Rd., Oak Ridge, TN 37830

Ashton, Robert W., Gaston Snow Beekman and Bogue, 14 Wall St., Suite 1600 New York, NY 10005

Atema, Jelle, Marine Biological Laboratory, Woods Hole, MA 02543

Atwood, Kimball C., P. O. Box 673, Woods Hole, MA 02543

Augustine, George J., Section of Neurobiology, Department of Biological Sciences, University of Southern California, Los Angeles, CA 90089-0371

Austin, Mary L., 506 1/2 N. Indiana Ave., Bloomington, IN 47401

Ayers, Donald E., Marine Biological Laboratory, Woods Hole, MA 02543

Bacon, Robert, P. O. Box 723, Woods Hole, MA 02543

Baker, Robert G., New York University Medical Center, 550 First Ave., New York, NY 10016

Baldwin, Thomas O., Department of Biochemistry and Biophysics, Texas A&M University, College Station, TX 77843

Bang, Betsy, 76 F. R. Lillie Rd., Woods Hole, MA 02543

Barlow, Robert B., Jr., Institute for Sensory Research, Syracuse University, Merrill Lane, Syracuse, NY 13210

Barry, Daniel T., Department of Physical Medicine and Rehabilitation, ID204, University of Michigan Hospital, Ann Arbor, MI 48109-0042

Barry, Susan R., Department of Physical Medicine and Rehabilitation, ID204, University of Michigan Hospital, Ann Arbor, MI 48109-0042

Bartell, Clelmer K., 2000 Lake Shore Drive, New Orleans, LA 70122

Bartlett, James H., Department of Physics, Box 870324, University of Alabama, Tuscaloosa, AL 35487-0324

Bass, Andrew H., Seely Mudd Hall, Department of Neurobiology, Cornell University, Ithaca, NY 14853

Battelle, Barbara-Anne, Whitney Laboratory, 9505 Ocean Shore Blvd., St. Augustine, FL 32086

Bauer, G. Eric, Department of Anatomy, University of Minnesota, Minneapolis, MN 55455

Beauge, Luis Alberto, Instituto de Investigacion Medica, Casilla de Correo 389, 5000 Cordoba, ARGENTINA

Beck, L. V., School of Experimental Medicine, Department of Pharmacology, Indiana University, Bloomington, IN 47401

Begenisich, Ted, Department of Physiology, University of Rochester, Rochester, NY 14642

Begg, David A., LHRRB, Harvard Medical School, 45 Shattuck St., Boston, MA 02115

Bell, Eugene, Organogenesis, Inc., 83 Rogers St., Cambridge, MA 02142

Benjamin, Thomas L., Department of Pathology, Harvard Medical School, 25 Shattuck St., Boston, MA 02115

Bennett, M. V. L., Albert Einstein College of Medicine, Department of Neuroscience, 1300 Morris Park Ave., Bronx, NY 10461

Bennett, Miriam F., Department of Biology, Colby College, Waterville, ME 04901

Berg, Carl J., Jr., Bureau of Marine Research, 13365 Overseas Highway, Marathon, FL 33050

Berne, Robert M., University of Virginia, School of Medicine, Charlottesville, VA 22908

Bezanilla, Francisco, Department of Physiology, University of California, Los Angeles, CA 90052

Biggers, John D., Department of Physiology, Harvard Medical School, Boston, MA 02115

Bishop, Stephen H., Department of Zoology, Iowa State University, Ames, IA 50010

Blaustein, Mordecai P., Department of Physiology, School of Medicine, University of Maryland, 655 W. Baltimore Street, Baltimore, MD 21201

Bloom, Kerry S., Department of Biology, University of North Carolina, Chapel Hill, NC 27514

Bodian, David, Department of Otolaryngology, 1721 Madison, Johns Hopkins University, Baltimore, MD 21205

Bodznick, David A., Department of Biology, Wesleyan University, Middletown, CT 06457

Boettiger, Edward G., 29 Juniper Point, Woods Hole, MA 02543

Boolootian, Richard A., Science Software Systems, Inc., 3576 Woodcliff Rd., Sherman Oaks, CA 91403

Borei, Hans G., Long Cove, Stanley Point Road, Minturn, ME 04659

Borgese, Thomas A., Department of Biology, Lehman College, CUNY, Bronx, NY 10468

Borisy, Gary G., Laboratory of Molecular Biology, University of Wisconsin, Madison, WI 53706

Borst, David W., Jr., Department of Biological Sciences, Illinois State University, Normal, IL 61761

Bosch, Herman F., 17 Damon Drive, Falmouth, MA 02540

Bowles, Francis P., P. O. Box 674, Woods Hole, MA 02543

Boyer, Barbara C., Department of Biology, Union College, Schenectady, NY 12308

Brandhorst, Bruce P., Biology Department, McGill University, 1205 Avenue Dr. Penfield, Montreal, P. Q. H3A 1B1, CANADA

Brehm, Paul, Department of Physiology, Tufts Medical School, Boston, MA 02111

Brinley, F. J., Neurological Disorders Program, NINCDS, 812 Federal Building, Bethesda, MD 20892

Brown, Joel E., Department of Ophthalmology, Box 8096 Sciences Center, Washington University, 660 S. Euclid Ave., St. Louis, MO 63110

Brown, Stephen C., Department of Biological Sciences, SUNY, Albany, NY 12222

Burd, Gail Deerin, Department of Molecular and Cell Biology, University of Arizona, Tucson, AZ 85721

Burdick, Carolyn J., Department of Biology, Brooklyn College, Brooklyn, NY 11210

Burger, Max, Department of Biochemistry, Biocenter, Klingelbergstrasse 70, CH-4056 Basel, SWITZERLAND

Burky, Albert, Department of Biology, University of Dayton, Dayton, OH 45469

Burstyn, Harold Lewis, Melvin and Melvin, 700 Merchants Bank Bldg., Syracuse, NY 13224

Bursztajn, Sherry, Neurology Department, Program in Neuroscience, Baylor College of Medicine, Houston, TX 77030

Bush, Louise, 7 Snapper Lane, Falmouth, MA 02540

Calabrese, Ronald L., Department of Biology, Emory University, 1555 Pierce Drive, Atlanta, GA 30322

Candelas, Graciela C., Department of Biology, University of Puerto Rico, Rio Piedras, PR 00931

Carew, Thomas J., Department of Psychology, Yale University, P. O. Box 11A, Yale Station, New Haven, CT 06520

Cariello, Lucio, Stazione Zoologica, Villa Comunale, 80120 Naples, ITALY

Carlson, Francis D., Department of Biophysics, Johns Hopkins University, Baltimore, MD 21218

Carriere, Rita M., Department of Anatomy and Cell Biology, Box 5, SUNY Health Science Center, 450 Clarkson Ave., Brooklyn, NY 11203

Case, James, Office of Research Development, Cheadle Hall, University of California, Santa Barbara, CA 93106

Cassidy, Rev. J. D., Pope John Center, 186 Forbes Rd., Braintree, MA 02184

Cebra, John J., Department of Biology, Leidy Labs, G-6, University of Pennsylvania, Philadelphia, PA 19174

Chaet, Alfred B., University of West Florida, Pensacola, FL 32504

Chambers, Edward L., Department of Physiology and Biophysics, University of Miami, School of Medicine, P. O. Box 016430, Miami, FL 33101

Chang, Donald C., Department of Physiology and Molecular Biophysics, Baylor College of Medicine, One Baylor Plaza, Houston, TX 77030

Chappell, Richard L., Department of Biological Sciences, Hunter College, Box 210, 695 Park Ave., New York, NY 10021

Charlton, Milton P., Physiology Department MSB, University of Toronto, Toronto, Ontario, M5S 1A8 CANADA

Chauncey, Howard H., 30 Falmouth St., Wellesley Hills, MA 02181

Child, Frank M., Department of Biology, Trinity College, Hartford, CT 06106

Chisholm, Rex L., Department of Cell Biology and Anatomy, Northwestern University Medical School, 303 E. Chicago Avenue, Chicago, IL 60611

Citkowitz, Elena, 410 Livingston St., New Haven, CT 06511

Clark, Eloise E., Vice President for Academic Affairs, Bowling Green State University, Bowling Green, OH 43403

Clark, Hays, 26 Deer Park Drive, Greenwich, CT 06830

Clark, James M., Shearson Lehman Brothers Inc., 14 Wall St., 9th Floor, New York, NY 10005

Clark, Wallis H., Jr., Bodega Marine Laboratory, P. O. Box 247, Bodega Bay, CA 94923

Claude, Philippa, Primate Center, Capitol Court, Madison, WI 53706

Clay, John R., Laboratory of Biophysics, NIH, Building 9, Room 1E-127, Bethesda, MD 20892

Clowes, George H. A., Jr., The Cancer Research Institute, 194 Pilgrim Rd., Boston, MA 02215 (deceased 9/10/88)

Clutter, Mary, Office of the Director, Room 518, National Science Foundation, Washington, DC 20550

Cobb, Jewel Plummer, California State University, Fullerton, CA 92634

Cohen, Adolph I., Department of Ophthalmology, School of Medicine, Washington University, 660 S. Euclid Ave., St. Louis, MO 63110

Cohen, Carolyn, Rosenstiel Basic Medical Sciences Research Center, Brandeis University, Waltham, MA 02254

Cohen, Lawrence B., Department of Physiology, Yale University School of Medicine, B-106 SHM, P. O. Box 3333, New Haven, CT 06510-8026

Cohen, Leonard A., 279 King St., Chappaqua, NY 10514

Cohen, Maynard, Department of Neurological Sciences, Rush Medical College, 600 South Paulina, Chicago, IL 60612

Cohen, Rochelle S., Department of Anatomy, University of Illinois, 808 W. Wood Street, Chicago, IL 60612

Cohen, William D., Department of Biological Sciences, Hunter College, 695 Park Ave., New York, NY 10021

Cole, Jonathan J., Institute for Ecosystems Studies, Cary Arboretum, Millbrook, NY 12545 (resigned 3/7/88)

Coleman, Annette W., Division of Biology and Medicine, Brown University, Providence, RI 02912

Collier, Jack R., Department of Biology, Brooklyn College, Brooklyn, NY 11210

Collier, Marjorie McCann, Biology Department, Saint Peter's College, Kennedy Boulevard, Jersey City, NJ 07306

Cook, Joseph A., The Edna McConnell Clark Foundation, 250 Park Ave., New York, NY 10017

Cooperstein, S. J., University of Connecticut, School of Medicine, Farmington Ave., Farmington, CT 06032

Corliss, John O., P. O. Box 53008, Albuquerque, NM 87153

Cornell, Neal W., Marine Biological Laboratory, Woods Hole, MA 02543

Cornwall, Melvin C., Jr., Department of Physiology L714, Boston University School of Medicine, 80 E. Concord St., Boston, MA 02118

Corson, David Wesley, Jr., 1034 Plantation Lane, Mt. Pleasant, SC 29464

Corwin, Jeffrey T., Department of Otolaryngology, University of Virginia Medical Center, Box 430, Charlottesville, VA 22908

Costello, Walter J., College of Medicine, Ohio University, Athens, OH 45701
Couch, Ernest F., Department of Biology, Texas Christian University, Fort Worth, TX 76129
Cremer-Bartels, Gertrud, Universitats Augenklinik, 44 Munster, WEST GERMANY
Crow, Terry J., Department of Physiology, University of Pittsburgh, School of Medicine, Pittsburgh, PA 25261
Crowell, Sears, Department of Biology, Indiana University, Bloomington, IN 47405
Crowther, Robert, Marine Biological Laboratory, Woods Hole, MA 02543
Currier, David L., P. O. Box 2476, Vineyard Haven, MA 02568

Daignault, Alexander T., 280 Beacon St., Boston, MA 02116
Dan, Katsuma, Tokyo Metropolitan Union, Meguro-ku, Tokyo, JAPAN
D'Avanzo, Charlene, School of Natural Science, Hampshire College, Amherst, MA 01002
David, John R., Seeley G. Mudd Building, Room 504, Harvard Medical School, 250 Longwood Ave., Boston, MA 02115
Davidson, Eric H., Division of Biology, 156-29, California Institute of Technology, Pasadena, CA 91125
Davis, Bernard D., Bacterial Physiology Unit, Harvard Medical School, Boston, MA 02115
Davis, Joel P., Seapuit, Inc., P. O. Box G, Osterville, MA 02655
Daw, Nigel W., 78 Aberdeen Place, Clayton, MO 63105
DeGroof, Robert C., E. R. Squibb & Sons, P. O. Box 4000, Princeton, NJ 08543-4000
DeHaan, Robert L., Department of Anatomy and Cell Biology, Emory University School of Medicine, Atlanta, GA 30322
DeLanney, Louis E., Institute for Medical Research, 2260 Clove Drive, San Jose, CA 95128
DePhillips, Henry A., Jr., Department of Chemistry, Trinity College, Hartford, CT 06106
DeTerra, Noel, 215 East 15th St., New York, NY 10003
Dettbarn, Wolf-Dietrich, Department of Pharmacology, School of Medicine, Vanderbilt University, Nashville, TN 37127
DeWeer, Paul J., Department of Physiology, School of Medicine, Washington University, St. Louis, MO 63110
Dixon, Keith E., School of Biological Sciences, Flinders University, Bedford Park, South Australia, AUSTRALIA
Donelson, John E., Department of Biochemistry, University of Iowa, Iowa City, IA 52242
Dowdall, Michael J., Department of Zoology, School of Biological Sciences, University of Nottingham, University Park, Nottingham N672 UH, England, UK
Dowling, John E., The Biological Laboratories, Harvard University, 16 Divinity St., Cambridge, MA 02138
DuBois, Arthur Brooks, John B. Pierce Foundation Laboratory, 290 Congress Ave., New Haven, CT 06519
Dudley, Patricia L., Department of Biological Sciences, Barnard College, Columbia University, New York, NY 10027
Duncan, Thomas K., Department of Environmental Sciences, Nichols College, Dudley, MA 01570
Dunham, Philip B., Department of Biology, Syracuse University, Syracuse, NY 13244
Dunlap, Kathleen, Department of Physiology, Tufts University Medical School, Boston, MA 02111

Ebert, James D., Office of the Director, Chesapeake Bay Institute, The Johns Hopkins University, Suite 340, The Rotunda, 771 West 40th St., Baltimore, MD 21211
Eckberg, William R., Department of Zoology, Howard University, Washington, DC 20059
Edds, Kenneth T., Department of Anatomical Sciences, SUNY, Buffalo, NY 14214
Eder, Howard A., Albert Einstein College of Medicine, 1300 Morris Park Ave., Bronx, NY 10461
Edstrom, Joan E., 2515 Milton Hills Drive, Charlottesville, VA 22901
Edwards, Charles, University of Southern Florida College of Medicine, MDC Box 40, 12901 Bruce B. Downs Blvd., Tampa, FL 33612
Egyud, Laszlo G., 18 Skyview, Newton, MA 02150
Ehrenstein, Gerald, NIH, Bethesda, MD 20892
Ehrlich, Barbara E., Division of Cardiology, University of Connecticut Health Center, Farmington, CT 06032
Eisen, Arthur Z., Division of Dermatology, Washington University, St. Louis, MO 63110
Eisenman, George, Department of Physiology, University of California Medical School, Los Angeles, CA 90024
Elder, Hugh Young, Institute of Physiology, University of Glasgow, Glasgow, Scotland, UK G12 8QQ
Elliott, Gerald F., The Open University Research Unit, Foxcombe Hall, Berkeley Rd., Boars Hill, Oxford, England, UK
Englund, Paul T., Department of Biological Chemistry, Johns Hopkins School of Medicine, Baltimore, MD 21205
Epel, David, Hopkins Marine Station, Pacific Grove, CA 93950
Epstein, Herman T., Department of Biology, Brandeis University, Waltham, MA 02254
Epstein, Ray L., Marine Biological Laboratory, Woods Hole, MA 02543
Erulkar, Solomon D., 318 Kent Rd., Bala Cynwyd, PA 19004
Essner, Edward S., Kresge Eye Institute, Wayne State University, 540 E. Canfield Ave., Detroit, MI 48201

Farb, David H., SUNY Health Science Center, Brooklyn, NY 11203
Farmanfarmaian, A., Department of Biological Sciences, Nelson Biological Laboratory, Rutgers University, Piscataway, NJ 08854
Fein, Alan, Physiology Department, University of Connecticut Health Center, Farmington, CT 06032
Feinman, Richard D., Box 8, Department of Biochemistry, SUNY Health Science Center, Brooklyn, NY 11203
Feldman, Susan C., Department of Anatomy, University of Medicine and Dentistry of New Jersey, New Jersey Medical School, 100 Bergen St., Newark, NJ 07103
Fessenden, Jane, Marine Biological Laboratory, Woods Hole, MA 02543

Festoff, Barry W., Neurology Service (127), Veterans Administration Medical Center, 4801 Linwood Blvd., Kansas City, MO 64128

Fink, Rachel D., Clapp Biology Laboratory, Mount Holyoke College, South Hadley, MA 01075

Finkelstein, Alan, Albert Einstein College of Medicine, 1300 Morris Park Ave., Bronx, NY 10461

Fischbach, Gerald, Department of Anatomy and Neurobiology, Washington University School of Medicine, St. Louis, MO 63110

Fischman, Donald A., Department of Cell Biology and Anatomy, Cornell University Medical College, 1300 York Ave., New York, NY 10021

Fishman, Harvey M., Department of Physiology, University of Texas Medical Branch, Galveston, TX 77550

Flanagan, Dennis, 12 Gay St., New York, NY 10014

Fox, Maurice S., Department of Biology, Massachusetts Institute of Technology, Cambridge, MA 02138

Frank, Peter W., Department of Biology, University of Oregon, Eugene, OR 97403

Franzini-Armstrong, Clara, Department of Biology G-5, School of Medicine, University of Pennsylvania, Philadelphia, PA 19174

Frazier, Donald T., Department of Physiology, University of Kentucky Medical Center, Lexington, KY 40536

Freeman, Gary L., Department of Zoology, University of Texas, Austin, TX 78172 (resigned 3/31/88)

Freinkel, Norbert, Center for Endocrinology, Metabolism & Nutrition, Northwestern University Medical School, 303 E. Chicago Avenue, Chicago, IL 60611

French, Robert J., Department of Medical Physiology, University of Calgary, 3330 Hospital Dr., NW, Calgary, Alberta, T2N 4N1, CANADA

Freygang, Walter J., Jr., 6247 29th St., NW, Washington, DC 20015

Fry, Brian, Marine Biological Laboratory, Woods Hole, MA 02543

Fukui, Yoshio, Department of Cell Biology and Anatomy, Northwestern University Medical School, Chicago, IL 60201

Fulton, Chandler M., Department of Biology, Brandeis University, Waltham, MA 02154

Furshpan, Edwin J., Department of Neurophysiology, Harvard Medical School, Boston, MA 02115

Fuseler, John W., Department of Biology, University of Southwestern Louisiana, Lafayette, LA 70504

Futrelle, Robert P., College of Computer Science, Northeastern University, 360 Huntington Avenue, Boston, MA 02115

Fye, Paul, P. O. Box 309, Woods Hole, MA 02543 (deceased 3/11/88)

Gabriel, Mordecai, Department of Biology, Brooklyn College, Brooklyn, NY 11210

Gadsby, David C., Laboratory of Cardiac Physiology, The Rockefeller University, 1230 York Avenue, New York, NY 10021

Gainer, Harold, Section of Functional Neurochemistry, NIH, Bldg. 36, Room 4D-20, Bethesda, MD 20892

Galatzer-Levy, Robert M., 180 N. Michigan Avenue, Chicago, IL 60601

Gall, Joseph G., Carnegie Institution, 115 West University Parkway, Baltimore, MD 21210

Gallant, Paul E., Laboratory of Preclinical Studies, Bldg. 36, NIAAA/NIH, 1250 Washington Ave., Rockville, MD 20892

Gascoyne, Peter, Department of Experimental Pathology, Box 85E, University of Texas System Cancer Center, M. D. Anderson Hospital and Tumor Institute, Texas Medical Center, 6723 Bertner Avenue, Houston, TX 77030

Gelfant, Seymour, Department of Dermatology, Medical College of Georgia, Augusta, GA 30904

Gelperin, Alan, Department of Biology, Princeton University, Princeton, NJ 08540

German, James L., III, The New York Blood Center, 310 East 67th St., New York, NY 10021

Gibbs, Martin, Institute for Photobiology of Cells and Organelles, Brandeis University, Waltham, MA 02254

Giblin, Anne E., Ecosystems Center, Marine Biological Laboratory, Woods Hole, MA 02543

Gibson, A. Jane, Wing Hall, Cornell University, Ithaca, NY 14850

Gifford, Prosser, 560 N Street, SW, N705, Washington, DC 20024

Gilbert, Daniel L., NIH, Bldg. 9, Room 1E-124, Bethesda, MD 20892

Giudice, Giovanni, Via Archirafi 22, Universita di Palermo, Palermo, ITALY

Glusman, Murray, New York State Psychiatric Institute, Box 70, 722 W. 168th St., New York, NY 10032

Golden, William T., 40 Wall St., Room 4201, New York, NY 10005

Goldman, David E., 63 Loop Rd., Falmouth, MA 02540

Goldman, Robert D., Department of Cell Biology and Anatomy, Northwestern University, 303 E. Chicago Ave., Chicago, IL 60611

Goldsmith, Paul K., NIH, Bldg. 10, Room 9C-101, Bethesda, MD 20892

Goldsmith, Timothy H., Department of Biology, Yale University, New Haven, CT 06510

Goldstein, Moise H., Jr., ECE Department, Barton Hall, Johns Hopkins University, Baltimore, MD 21218

Goodman, Lesley Jean, Department of Biological Sciences, Queen Mary College, Mile End Road, London, E1 4NS, England, UK

Goudsmit, Esther, M., Department of Biology, Oakland University, Rochester, MI 48309

Gould, Robert Michael, Institute for Basic Research in Developmental Disabilities, 1050 Forest Hill Rd., Staten Island, NY 10314

Gould, Stephen J., Museum of Comparative Zoology, Harvard University, Cambridge, MA 02138

Govind, C. K., Zoology Department—Scarborough, University of Toronto, 1265 Military Trail, West Hill, Ontario, M1C 1A4 CANADA

Graf, Werner, Rockefeller University, 1230 York Ave., New York, NY 10021

Grant, Philip, 120 Center Drive #308, Bethesda, MD 20814

Grass, Albert M., The Grass Foundation, 77 Reservoir Rd., Quincy, MA 02170

Grass, Ellen R., The Grass Foundation, 77 Reservoir Rd., Quincy, MA 02170

Grassle, Judith, Marine Biological Laboratory, Woods Hole, MA 02543

Green, Jonathan P., Department of Biology, Roosevelt University, 430 S. Michigan Avenue, Chicago, IL 60605 (resigned 2/5/88)

Greenberg, Everett Peter, Department of Microbiology, Stocking Hall, Cornell University, Ithaca, NY 14853

Greenberg, Michael J., C. V. Whitney Laboratory, 9505 Ocean Shore Blvd., St. Augustine, FL 32086

Griffin, Donald R., The Rockefeller University, 1230 York Ave., New York, NY 10021

Gross, Paul R., Office of the Vice President and Provost, University of Virginia, Charlottesville, VA 22906-9014

Grossman, Albert, New York University, Medical School, New York, NY 10016

Gruner, John, Department of Neurosurgery, New York University Medical Center, 550 First Ave., New York, NY 10016

Gunning, A. Robert, P. O. Box 165, Falmouth, MA 02541

Gwilliam, G. P., Department of Biology, Reed College, Portland, OR 97202

Hall, Linda M., Department of Molecular Genetics, Albert Einstein College of Medicine, 1300 Morris Park Ave., Bronx, NY 10461

Hall, Zack W., Department of Physiology, University of California, San Francisco, CA 94143

Halvorson, Harlyn O., Marine Biological Laboratory, Woods Hole, MA 02543

Hamlett, Nancy Virginia, Department of Biology, Swarthmore College, Swarthmore, PA 19081

Hanna, Robert B., College of Environmental Science and Forestry, SUNY, Syracuse, NY 13210

Harding, Clifford V., Jr., Wayne State University School of Medicine, Department of Ophthalmology, Detroit, MI 48201

Harosi, Ferene I., Laboratory of Sensory Physiology, Marine Biological Laboratory, Woods Hole, MA 02543

Harrigan, June F., 7415 Makaa Place, Honolulu, HI 96825

Harrington, Glenn W., Division of Cell Biology and Biophysics, 403 Biological Sciences Building, University of Missouri, Kansas City, MO 64110

Harris, Andrew L., Department of Biophysics, Johns Hopkins University, 34th & Charles Sts., Baltimore, MD 21218

Haschemeyer, Audrey E. V., 21 Glendon Road, Woods Hole, MA 02543

Hastings, J. W., Harvard University, 16 Divinity Street, Cambridge, MA 02138

Hauschka, Theodore S., RD1, Box 781, Damariscotta, ME 04543

Hayashi, Teru, 7105 SW 112 Place, Miami, FL 33173

Hayes, Raymond L., Jr., Department of Anatomy, Howard University, College of Medicine, 520 W St., NW, Washington, DC 20059

Henley, Catherine, 5225 Pooks Hill Rd., #1127 North, Bethesda, MD 20034

Hepler, Peter K., Department of Botany, University of Massachusetts, Amherst, MA 01003

Herndon, Walter R., University of Tennessee, Department of Botany, Knoxville, TN 37996-1100

Hessler, Anita Y., 1360 Tourmaline Ave., San Diego, CA 92109-1915

Heuser, John, Department of Biophysics, Washington University, School of Medicine, St. Louis, MO 63110

Hiatt, Howard H., Brigham and Women's Hospital, 75 Francis Street, Boston, MA 02115

Highstein, Stephen M., Department of Otolaryngology, Washington University, St. Louis, MO 63110

Hildebrand, John G., Arizona Research Laboratories, ARL Division of Neurobiology, 603 Gould-Simpson Science Building, University of Arizona, Tucson, AZ 85721

Hill, Richard W., Department of Zoology, Michigan State University, E. Lansing, MI 48824

Hill, Susan D., Department of Zoology, Michigan State University, E. Lansing, MI 48824

Hillis-Colinvaux, Llewellya, Department of Zoology, Ohio State University, 484 W. 12th Ave., Columbus, OH 43210

Hillman, Peter, Department of Biology, Life Sciences & Neurobiology, Hebrew University, Jerusalem, ISRAEL

Hinegardner, Ralph T., Division of Natural Sciences, University of California, Santa Cruz, CA 95064

Hinsch, Gertrude, W., Department of Biology, University of South Florida, Tampa, FL 33620

Hobbie, John E., Ecosystems Center, Marine Biological Laboratory, Woods Hole, MA 02543

Hodge, Alan J., Marine Biological Laboratory, Woods Hole, MA 02543

Hoffman, Joseph, Department of Physiology, School of Medicine, Yale University, New Haven, CT 06510

Hollyfield, Joe G., Baylor School of Medicine, Texas Medical Center, Houston, TX 77030

Holtzman, Eric, Department of Biological Sciences, Columbia University, New York, NY 10017

Holz, George G., Jr., Department of Microbiology, SUNY, Syracuse, NY 13210

Hoskin, Francis C. G., Department of Biology, Illinois Institute of Technology, Chicago, IL 60616

Houghton, Richard A., III, Woods Hole Research Center, P. O. Box 296, Woods Hole, MA 02543

Houston, Howard E., 2500 Virginia Ave., NW, Washington, DC 20037

Howarth, Robert, Section of Ecology & Systematics, Corson Hall, Cornell University, Ithaca, NY 14853 (resigned 3/9/88)

Hoy, Ronald R., Section of Neurobiology and Behavior, Cornell University, Ithaca, NY 14850

Hubbard, Ruth, 67 Gardner Road, Woods Hole, MA 02543

Hufnagel, Linda A., Department of Microbiology, University of Rhode Island, Kingston, RI 02881

Hummon, William D., Department of Zoology, Ohio University, Athens, OH 45701

Humphreys, Susie H., 810 Waukegan Rd., Glenview, IL 60025

Humphreys, Tom D., University of Hawaii, PBRC, 41 Ahui St., Honolulu, HI 96813
Hunter, Robert D., Department of Biological Sciences, Oakland University, Rochester, MI 48309-4401
Hunter, W. Bruce, Box 321, Lincoln Center, MA 01773
Hunziker, Herbert E., Esq., P. O. Box 547, Falmouth, MA 02541
Hurwitz, Charles, Basic Science Research Lab, Veterans Administration Hospital, Albany, NY 12208
Hurwitz, Jerard, Sloan Kettering Institute for Cancer Research, 1275 York Avenue, New York, NY 11021
Huxley, Hugh E., Department of Biology, Rosenstiel Center, Brandeis University, Waltham, MA 02154
Hynes, Thomas J., Jr., Meredith and Grew, Inc., 160 Federal Street, Boston, MA 02110-1701

Han, Joseph, Department of Anatomy, Case Western Reserve University, Cleveland, OH 44106
Ingoglia, Nicholas, Department of Physiology, New Jersey Medical School, 100 Bergen St., Newark, NJ 07103
Inoué, Saduyki, McGill University Cancer Centre, Department of Anatomy, 3640 University St., Montreal, PQ, H3A 2B2, CANADA
Inoué, Shinya, Marine Biological Laboratory, Woods Hole, MA 02543
Issadorides, Marietta, R., Department of Psychiatry, University of Athens, Monis Petraki 8, Athens, 140 GREECE
Isselbacher, Kurt J., Massachusetts General Hospital, 32 Fruit Street, Boston, MA 02114
Izzard, Colin S., Department of Biological Sciences, SUNY, Albany, NY 12222

Jacobson, Antone G., Department of Zoology, University of Texas, Austin, TX 78712
Jaffe, Lionel, Marine Biological Laboratory, Woods Hole, MA 02543
Jahan-Parwar, Behrus, Center for Laboratories & Research, New York State Department of Health, Empire State Plaza, Albany, NY 12201
Jannasch, Holger W., Department of Biology, Woods Hole Oceanographic Institution, Woods Hole, MA 02543
Jeffery, William R., Department of Zoology, University of Texas, Austin, TX 78712
Jones, Meredith L., Division of Worms, Museum of Natural History, Smithsonian Institution, Washington, DC 20560
Josephson, Robert K., School of Biological Sciences, University of California, Irvine, CA 92664

Kabat, E. A., Department of Microbiology, College of Physicians and Surgeons Columbia University, 630 West 168th St., New York, NY 10032
Kaley, Gabor, Department of Physiology, Basic Sciences Building, New York Medical College, Valhalla, NY 10595
Kaltenbach, Jane, Department of Biological Sciences, Mount Holyoke College, South Hadley, MA 01075
Kaminer, Benjamin, Department of Physiology, School of Medicine, Boston University, 80 East Concord St., Boston, MA 02118
Kammer, Ann E., Department of Zoology, Arizona State University, Tempe, AZ 85281
Kane, Robert E., PBRC, University of Hawaii, 41 Ahui St., Honolulu, HI 96813
Kaneshiro, Edna S., Department of Biological Sciences, University of Cincinnati, Cincinnati, OH 45221
Kao, Chien-yuan, Department of Pharmacology, Box 29, SUNY, Downstate Medical Center, 450 Clarkson Avenue, Brooklyn, NY 11203
Kaplan, Ehud, The Rockefeller University, 1230 York Ave., New York, NY 10021
Karakashian, Stephen J., Apt. 16-F, 165 West 91st St., New York, NY 10024
Karlin, Arthur, Department of Biochemistry and Neurology, Columbia University, 630 West 168th St., New York, NY 10032
Katz, George M., Fundamental and Experimental Research, Merck Sharpe and Dohme, Rahway, NJ 07065
Kean, Edward L., Department of Ophthalmology and Biochemistry, Case Western Reserve University, Cleveland, OH 44101 (resigned 10/27/88)
Kelley, Darcy Brisbane, Department of Biological Sciences, 1018 Fairchild, Columbia University, New York, NY 10032
Kelly, Robert E., Department of Anatomy, College of Medicine, University of Illinois, P. O. Box 6998, Chicago, IL 60680
Kemp, Norman E., Department of Biology, University of Michigan, Ann Arbor, MI 48104
Kendall, John P., Faneuil Hall Associates, Suite 1620, One Boston Place, Boston, MA 02108
Kendall, Richard E., 26 Green Harbor Rd., East Falmouth, MA 02536
Keynan, Alexander, Hebrew University, Jerusalem, ISRAEL
Kiehart, Daniel P., Department of Cellular and Developmental Biology, Harvard University, 16 Divinity Street, Cambridge, MA 02138
Klein, Morton, Department of Microbiology, Temple University, Philadelphia, PA 19103
Klotz, Irving M., Department of Chemistry, Northwestern University, Evanston, IL 60201
Koide, Samuel S., Population Council, The Rockefeller University, 1230 York Avenue, New York, NY 10021
Konigsberg, Irwin R., Department of Biology, Gilmer Hall, University of Virginia, Charlottesville, VA 22903
Kornberg, Sir Hans, The Master's Lodge, Christ's College, Cambridge CB2 3BU, England, UK
Kosower, Edward M., Ramat-Aviv, Tel Aviv, 69978 ISRAEL
Krahl, M. E., 2783 W. Casas Circle, Tucson, AZ 85741
Krane, Stephen M., Massachusetts General Hospital, Fruit Street, Boston, MA 02114
Krassner, Stuart M., Department of Developmental and Cell Biology, University of California, Irvine, CA 92717
Krauss, Robert, FASEB, 9650 Rockville Pike, Bethesda, MD 20814
Kravitz, Edward A., Department of Neurobiology, Harvard Medical School, 25 Shattuck St., Boston, MA 02115
Kriebel, Mahlon E., Department of Physiology, B.S.B., Upstate Medical Center, 766 Irving Ave., Syracuse, NY 13210

Kristan, William B., Jr., Department of Biology B-022, University of California San Diego, La Jolla, CA 92093

Kuhns, William J., Hospital for Sick Children, Department of Biochemistry Research, Toronto, Ontario M5G 1X8, CANADA

Kusano, Kiyoshi, NIH, Bldg. 36, Room 4D-20, Bethesda, MD 20892

Kuzirian, Alan M., Marine Biological Laboratory, Woods Hole, MA 02543

Laderman, Aimlee, P. O. Box 689, Woods Hole, MA 02543

LaMarche, Paul H., Eastern Maine Medical Center, 489 State St., Bangor, ME 04401

Landis, Dennis M. D., Department of Neurology, Case Western Reserve School of Medicine, Cleveland, OH 44106

Landis, Story C., Department of Pharmacology, Case Western Reserve University School of Medicine, Cleveland, OH 44106

Landowne, David, Department of Physiology, P. O. Box 016430, University of Miami School of Medicine, Miami, FL 33101

Langford, George M., Department of Physiology, Medical Sciences Research Wing 206H, University of North Carolina, Chapel Hill, NC 27599-7545

Lasek, Raymond J., Case Western Reserve University, Department of Anatomy, Cleveland, OH 44106

Laster, Leonard, University of Massachusetts Medical School, 55 Lake Avenue, North, Worcester, MA 01655

Laufer, Hans, Biological Science, Molecular and Cell Biology, Group U-125, University of Connecticut, Storrs, CT 06268

Lazarow, Paul B., The Rockefeller University, 1230 York Avenue, New York, NY 10021

Lazarus, Maurice, Federated Department Stores, Inc., 50 Cornhill, Boston, MA 02108

Leadbetter, Edward R., Department of Molecular and Cell Biology, U-131, University of Connecticut, Storrs, CT 06268

Lederberg, Joshua, The Rockefeller University, 1230 York Ave., New York, NY 10021

Lederhendler, Izja I., Laboratory of Cellular and Molecular Neurobiology, NINCDS/NIH, Park 5 Building, Room 435, Bethesda, MD 20892

Lee, John J., Department of Biology, City College of CUNY, Convent Ave. and 138th St., New York, NY 10031

Lehy, Donald B., Marine Biological Laboratory, Woods Hole, MA 02543

Leibovitz, Louis, 3 Kettle Hole Road, Woods Hole, MA 02543

Leighton, Joseph, 1201 Waverly Rd., Gladwyne, PA 19035

Leighton, Stephen, NIH, Bldg. 13 3W13, Bethesda, MD 20892

Leinwand, Leslie Ann, Department of Microbiology and Immunology, Albert Einstein College of Medicine, 1300 Morris Park Ave., Bronx, NY 10461

Lerman, Sidney, Eye Research Lab, Room 41, New York Medical College, 100 Grasslands Ave., Valhalla, NY 10595

Lerner, Aaron B., Yale University, School of Medicine, New Haven, CT 06510

Lester, Henry A., 156-29 California Institute of Technology, Pasadena, CA 91125

Levin, Jack, Clinical Pathology Service, VA Hospital, 113A, 4150 Clement St., San Francisco, CA 94121

Levinthal, Cyrus, Department of Biological Sciences, Columbia University, Broadway and 116th Street, New York, NY 10026

Levitan, Herbert, Department of Zoology, University of Maryland, College Park, MD 20742

Linck, Richard W., Department of Anatomy, Jackson Hall, University of Minnesota, 321 Church Street, S. E., Minneapolis, MN 55455

Lipicky, Raymond J., Department of Cardio-Renal/HFD 110, FDA Bureau of Drugs, Rm. 16B-45, 5600 Fishers Lane, Rockville, MD 20857

Lisman, John E., Department of Biology, Brandeis University, Waltham, MA 02254

Liuzzi, Anthony, 55 Fay Rd., Box 184, Woods Hole, MA 02543

Llinas, Rodolfo R., Department of Physiology and Biophysics, New York University Medical Center, 550 First Ave., New York, NY 10016

Loew, Franklin M., Tufts University School of Veterinary Medicine, 200 Westboro Rd., N. Grafton, MA 01536

Loewenstein, Werner R., Department of Physiology and Biophysics, University of Miami, P. O. Box 016430, Miami, FL 33101

Loewus, Frank A., Institute of Biological Chemistry, Washington State University, Pullman, WA 99164

Loftfield, Robert B., Department of Chemistry, School of Medicine, University of New Mexico, 900 Stanford, NE, Albuquerque, NM 87131

London, Irving M., Massachusetts Institute of Technology, E-25-551, Cambridge, MA 02139

Longo, Frank J., Department of Anatomy, University of Iowa, Iowa City, IA 52442

Lorand, Laszlo, Department of Biochemistry and Molecular Biology, Northwestern University, Evanston, IL 60208

Luckenbill-Edds, Louise, 155 Columbia Ave., Athens, OH 45701

Luria, Salvador E., 48 Peacock Farm Rd., Lexington, MA 02173

Macagno, Eduardo R., 1003B Fairchild, Department of Biosciences, Columbia University, New York, NY 10022

MacNichol, E. F., Jr., Department of Physiology, Boston University School of Medicine, 80 E. Concord St., Boston, MA 02118

Maglott-Duffield, Donna R. S., American Type Culture Collection, 12301 Parklawn Drive, Rockville, MD 20852-1776

Maienschein, Jane Ann, Department of Philosophy, Arizona State University, Tempe, AZ 85287-2004

Mainer, Robert, The Boston Company, One Boston Place, 5-D, Boston, MA 02108

Malbon, Craig Curtis, Department of Pharmacology, Health Sciences Center, SUNY, Stony Brook, NY 11794-8651

Malkiel, Saul, Allergic Diseases, Inc., 130 Lincoln St., Worcester, MA 01605

Manalis, Richard S., Department of Biological Sciences, Indiana University—Purdue University at Fort Wayne, Fort Wayne, IN 46805

Mangum, Charlotte P., Department of Biology, College of William and Mary, Williamsburg, VA 23185

Margulis, Lynn, Botany Department, University of Massachusetts, Morrill Science Center, Amherst, MA 01003

Marinucci, Andrew C., 102 Nancy Drive, Mercerville, NJ 08619

Marsh, Julian B., Department of Biochemistry and Physiology, Medical College of Pennsylvania, 3300 Henry Ave., Philadelphia, PA 19129

Martin, Lowell V., Marine Biological Laboratory, Woods Hole, MA 02543

Martinez-Palomo, Adolfo, Seccion de Patologia Experimental, Cinvesav-ipn, 07000 Mexico, D.F. A.P., 140740, MEXICO

Maser, Morton, P. O. Box EM, Woods Hole Education Assoc., Woods Hole, MA 02543

Mastroianni, Luigi, Jr., Department of Obstetrics and Gynecology, Hospital of the University of Pennsylvania, 106 Dulles, Philadelphia, PA 19174

Mathews, Rita W., Department of Medicine, NYU Medical Center, 550 First Ave., New York, NY 10016

Matteson, Donald R., Department of Physiology, G4, School of Medicine, University of Pennsylvania, Philadelphia, PA 19104

Mautner, Henry G., Department of Biochemistry, Tufts University, 136 Harrison Ave., Boston, MA 02111

Mauzerall, David, The Rockefeller University, 1230 York Ave., New York, NY 10021

Mazia, Daniel, Hopkins Marine Station, Pacific Grove, CA 93950

Mazzella, Lucia, Laboratorio di Ecologia del Benthos, Stazione Zoologica di Napoli, P.ta S. Pietro 80077, Ischia Porto (NA), ITALY

McCann, Frances, Department of Physiology, Dartmouth Medical School, Hanover, NH 03755

McLaughlin, Jane A., Marine Biological Laboratory, Woods Hole, MA 02543

McMahon, Robert F., Department of Biology, Box 19498, University of Texas, Arlington, TX 76019

Meedel, Thomas, Marine Biological Laboratory, Woods Hole, MA 02543

Meinertzhagen, Ian A., Department of Psychology, Life Sciences Center, Dalhousie University, Halifax, Nova Scotia B3H 451, CANADA

Meiss, Dennis E., 462 Soland Avenue, Hayward, CA 94541

Melillo, Jerry A., Ecosystems Center, Marine Biological Laboratory, Woods Hole, MA 02543

Mellon, Richard P., P. O. Box 187, Laughlintown, PA 15655

Mellon, DeForest, Jr., Department of Biology, University of Virginia, Charlottesville, VA 22903

Metuzals, Janis, Department of Anatomy, Faculty of Medicine, University of Ottawa, Ottawa, Ontario K1N 9A9, CANADA

Metz, Charles B., 7220 SW 124th St., Miami, FL 33156

Milkman, Roger, Department of Biology, University of Iowa, Iowa City, IA 52242

Mills, Eric L., Oceanography Dept., Dalhousie University, Halifax, Nova Scotia B3H 4J1, CANADA

Mills, Robert, 10315 44th Avenue, W 12 H Street, Bradenton, FL 33507-1535

Mitchell, Ralph, Pierce Hall, Harvard University, Cambridge, MA 02138

Miyamoto, David M., Department of Biology, Drew University, Madison, NJ 07940

Mizell, Merle, Laboratory of Tumor Cell Biology, Tulane University, New Orleans, LA 70118

Moore, John W., Department of Physiology, Duke University Medical Center, Durham, NC 27710

Moore, Lee E., Department of Physiology and Biophysics, University of Texas Medical Branch, Galveston, TX 77550

Morin, James G., Department of Biology, University of California, Los Angeles, CA 90024

Morrell, Frank, Department of Neurological Sciences, Rush Medical Center, 1753 W. Congress Parkway, Chicago, IL 60612

Morse, M. Patricia, Marine Science Center, Northeastern University, Nahant, MA 01908

Morse, Richard S., 193 Winding River Rd., Wellesley, MA 02181 (deceased 7/1/88)

Morse, Robert W., Box 574, N. Falmouth, MA 02556

Morse, Stephen Scott, The Rockefeller University, 1230 York Ave., Box 2, New York, NY 10021-6399

Moscona, Arthur A., Department of Molecular Genetics and Cell Biology, University of Chicago, 920 East 58th St., Chicago, IL 60637

Mote, Michael I., Department of Biology, Temple University, Philadelphia, PA 19122

Mountain, Isabel, Vinson Hall #112, 6251 Old Dominion Drive, McLean, VA 22101

Mullins, Lorin J., University of Maryland, School of Medicine, Baltimore, MD 21201

Musacchia, Xavier J., Department of Physiology and Biophysics, University of Louisville School of Medicine, Louisville, KY 40292

Nabrit, S. M., 686 Beckwith St., SW, Atlanta, GA 30314

Nadelhoffer, Knute, Marine Biological Laboratory, Woods Hole, MA 02543

Naka, Ken-ichi, PHL 821, Department of Ophthalmology, NYU Medical Center, 550 First Avenue, New York, NY 10016

Nakajima, Shigehiro, University of Illinois College of Medicine at Chicago, 835 S. Wolcott Avenue, Chicago, IL 60612

Nakajima, Yasuko, University of Illinois College of Medicine at Chicago, Department of Anatomy and Cell Biology, M/C 512, Chicago, IL 60612

Narahashi, Toshio, Department of Pharmacology, Medical Center, Northwestern University, 303 East Chicago Ave., Chicago, IL 60611

Nasatir, Maimon, Department of Biology, University of Toledo, Toledo, OH 43606

Nelson, Leonard, Department of Physiology, Medical College of Ohio, Toledo, OH 43699

Nelson, Margaret C., Section of Neurobiology and Behavior, Cornell University, Ithaca, NY 14850

Nicholls, John G., Biocenter, Klingelbergstr. 70, Basel 4056, SWITZERLAND

Nicosia, Santo V., Department of Pathology, University of South Florida, College of Medicine, Box 11, 12901 North 30th St., Tampa, FL 33612

Nielsen, Jennifer B. K., Merck Sharp & Dohme Laboratories, RY 80-210, Rahway, NJ 07065

Noe, Bryan D., Department of Anatomy, Emory University, Atlanta, GA 30345

Obaid, Ana Lia, Department of Physiology and Pharmacy, University of Pennsylvania, 4001 Spruce St., Philadelphia, PA 19104-6003

Oertel, Donata, Department of Neurophysiology, University of Wisconsin, 281 Medical Science Bldg., Madison, WI 53706

O'Herron, Jonathan, 45 Swifts Lane, Darien, CT 06820

Olins, Ada L., University of Tennessee-Oak Ridge, Graduate School of Biomedical Sciences, Biology Division ORNL, P. O. Box Y, Oak Ridge, TN 37830

Olins, Donald E., University of Tennessee-Oak Ridge, Graduate School of Biomedical Sciences, Biology Division ORNL, P. O. Box Y, Oak Ridge, TN 37830

O'Melia, Anne F., 16 Evergreen Lane, Chappaqua, New York 10514

Oschman, James L., 9 George Street, Woods Hole, MA 02543

Palmer, John D., Department of Zoology, University of Massachusetts, Amherst, MA 01002

Palti, Yoram, Rappaport Institution, Technion, POB 9697, Haifa, ISRAEL

Pant, Harish C., NINCDS/NIH, Bldg. 36, Room 4D-20, Bethesda, MD 20892

Pappas, George D., Department of Anatomy, College of Medicine, University of Illinois, 808 South Wood St., Chicago, IL 60612

Pardee, Arthur B., Department of Pharmacology, Harvard Medical School, Boston, MA 02115

Pardy, Roosevelt L., School of Life Sciences, University of Nebraska, Lincoln, NE 68588

Parmentier, James L., Becton Dickinson Research Center, P. O. Box 12016, Research Triangle Park, NC 27709

Passano, Leonard M., Department of Zoology, Birge Hall, University of Wisconsin, Madison, WI 53706

Pearlman, Alan L., Department of Physiology, School of Medicine, Washington University, St. Louis, MO 63110

Pederson, Thorn, Worcester Foundation for Experimental Biology, Shrewsbury, MA 01545

Perkins, C. D., 400 Hilltop Terrace, Alexandria, VA 22301

Person, Philip, Research Testing Labs, Inc., 167 E. 2nd St., Huntington Station, NY 11746

Peterson, Bruce J., Ecosystems Center, Marine Biological Laboratory, Woods Hole, MA 02543

Pethig, Ronald, School of Electronic Engineering Science, University College of N. Wales, Dean St., Bangor, Gwynedd, LL57 1UT, UK

Pfohl, Ronald J., Department of Zoology, Miami University, Oxford, OH 45056

Pierce, Sidney K., Jr., Department of Zoology, University of Maryland, College Park, MD 20740

Poindexter, Jeanne S., Science Division, Long Island University, Brooklyn Campus, Brooklyn, NY 11201

Pollard, Harvey B., NIH, NIDDKD, Bldg. 8, Rm. 401, Bethesda, MD 20892

Pollard, Thomas D., Department of Cell Biology and Anatomy, Johns Hopkins University, 725 North Wolfe St., Baltimore, MD 21205

Pollock, Leland W., Department of Zoology, Drew University, Madison, NJ 07940 (resigned 12/17/88)

Poole, Alan F., P. O. Box 533, Woods Hole, MA 02543

Porter, Beverly H., 13617 Glenoble Drive, Rockville, MD 20853

Porter, Keith R., Department of Biology, Leidy Laboratories, Rm. 303, University of Pennsylvania, Philadelphia, PA 19104-6018

Porter, Mary E., Department MCD Biology, Campus Box 347, University of Colorado, Boulder, CO 80309

Potter, David, Department of Neurobiology, Harvard Medical School, Boston, MA 02115

Potts, William T., Department of Biology, University of Lancaster, Lancaster, England, UK

Pratt, Melanie M., Department of Anatomy and Cell Biology, University of Miami School of Medicine (R124), P. O. Box 016960, Miami, FL 33101

Prendergast, Robert A., Wilmer Institute, Johns Hopkins Hospital, Baltimore, MD 21205

Presley, Phillip H., Carl Zeiss, Inc., 1 Zeiss Drive, Thornwood, NY 10594

Price, Carl A., Waksman Institute of Microbiology, Rutgers University, P. O. Box 759, Piscataway, NJ 08854

Prior, David J., Department of Biological Sciences, NAU Box 5640, Northern Arizona University, Flagstaff, AZ 86011

Prusch, Robert D., Department of Life Sciences, Gonzaga University, Spokane, WA 99258

Przybylski, Ronald J., Case Western Reserve University, Department of Anatomy, Cleveland, OH 44104

Purves, Dale, Department of Anatomy, Washington University School of Medicine, 660 S. Euclid Ave., St. Louis, MO 63110

Quigley, James, Department of Microbiology, Box 44, SUNY Downstate Medical Center, 450 Clarkson Ave., Brooklyn, NY 11203

Rabb, Irving W., P.O. Box 369, Boston, MA 02101

Rabin, Harvey, DuPont Biomed. Products, BRL-2, 331 Treble Cove Road, No. Billerica, MA 01862

Rabinowitz, Michael B., Marine Biological Laboratory, Woods Hole, MA 02543

Raff, Rudolf A., Department of Biology, Indiana University, Bloomington, IN 47405

Rakowski, Robert F., Department of Physiology and Biophysics, UHS/The Chicago Medical School, 3333 Greenbay Rd., N. Chicago, IL 60064

Ramon, Fidel, Dept. de Fisiologia y Biofisea, Centro de Investigacion y de Estudius Avanzados del ipn, Apurtado Postal 14-740, D.F. 07000, MEXICO

Ranzi, Silvio, Sez Zoologia Sc Nat, Via Coloria 26, 120133, Milano, ITALY

Rastetter, Edward B., Ecosystems Center, Marine Biological Laboratory, Woods Hole, MA 02543

Ratner, Sarah, Department of Biochemistry, Public Health Research Institute, 455 First Ave., New York, NY 10016

Rebhun, Lionel I., Department of Biology, Gilmer Hall, University of Virginia, Charlottesville, VA 22901

Reddan, John R., Department of Biological Sciences, Oakland University, Rochester, MI 48063

Reese, Barbara F., NINCDS/NIH, Bldg. 36, Room 3B26, Bethesda, MD 20892

Reese, Thomas S., NINCDS/NIH, Bldg. 36, Room 2A27, Bethesda, MD 20892

Reiner, John M., Department of Biochemistry, Albany Medical College of Union University, Albany, NY 12208

Reinisch, Carol L., Tufts University School of Veterinary Medicine, 203 Harrison Avenue, Boston, MA 02115

Reuben, John P., Department of Biochemistry, Merck Sharp and Dohme, P. O. Box 2000, Rahway, NJ 07065

Reynolds, George T., Department of Physics, Jadwin Hall, Princeton University, Princeton, NJ 08540

Rice, Robert V., 30 Burnham Dr., Falmouth, MA 02540

Rich, Alexander, Department of Biology, Massachusetts Institute of Technology, Cambridge, MA 02139

Rickles, Frederick R., University of Connecticut, School of Medicine, VA Hospital, Newington, CT 06111

Ripps, Harris, Department of Ophthalmology, University of Illinois College of Medicine, 1855 W. Taylor Street, Chicago, IL 60611

Robinson, Denis M., 200 Ocean Lane Drive #908, Key Biscayne, FL 33149

Rose, Birgit, Department of Physiology and Biophysics, R-430, University of Miami School of Medicine, P. O. Box 016430, Miami, FL 33101

Rose, S. Meryl, 32 Crosby Ln., E. Falmouth, MA 02536

Rosenbaum, Joel L., Department of Biology, Kline Biology Tower, Yale University, New Haven, CT 06520

Rosenberg, Philip, School of Pharmacy, Division of Pharmacology, University of Connecticut, Storrs, CT 06268

Rosenbluth, Jack, Department of Physiology, New York University School of Medicine, 550 First Ave., New York, NY 10016

Rosenbluth, Raja, 3380 West 5th Ave., Vancouver 8, BC V6R 1R7, CANADA

Roslansky, John, Box 208, Woods Hole, MA 02543

Roslansky, Priscilla F., Box 208, Woods Hole, MA 02543

Ross, William N., Department of Physiology, New York Medical College, Valhalla, NY 10595

Roth, Jay S., 18 Millfield Street, P. O. Box 285, Woods Hole, MA 02543

Rowland, Lewis P., Neurological Institute, 710 West 168th St., New York, NY 10032

Ruderman, Joan V., Department of Zoology, Duke University, Durham, NC 27706

Rushforth, Norman B., Case Western Reserve University, Department of Biology, Cleveland, OH 44106

Russell-Hunter, W. D., Department of Biology, Lyman Hall 029, Syracuse University, Syracuse, NY 13210

Saffo, Mary Beth, Institute of Marine Sciences, 272 Applied Sciences, University of California, Santa Cruz, CA 95064

Sager, Ruth, Dana Farber Cancer Institute, 44 Binney St., Boston, MA 02115

Salama, Guy, Department of Physiology, University of Pittsburgh, Pittsburgh, PA 15261

Salmon, Edward D., Department of Zoology, University of North Carolina, Chapel Hill, NC 27514

Salzberg, Brian M., Department of Physiology, University of Pennsylvania, 4010 Locust St., Philadelphia, PA 19104-6085

Sanborn, Richard C., 11 Oak Ridge Road, Teaticket, MA 02536

Sanger, Jean M., Department of Anatomy, School of Medicine, University of Pennsylvania, 36th and Hamilton Walk, Philadelphia, PA 19174

Sanger, Joseph, Department of Anatomy, School of Medicine, University of Pennsylvania, 36th and Hamilton Walk, Philadelphia, PA 19174

Sato, Eimei, Department of Animal Science, Faculty of Agriculture, Kyoto University, Kyoto 606, JAPAN (resigned 10/20/88)

Sato, Hidemi, Sugashima Marine Biological Laboratory, Nagoya University, Sugashima-cho, Toba-shi, Mieken 517, JAPAN

Sattelle, David B., AFRC Unit-Department of Zoology, University of Cambridge, Downing St., Cambridge CB2 3EJ, England, UK

Saunders, John W., Jr., P. O. Box 381, Waquoit Station, Waquoit, MA 02536

Saz, Arthur K., Department of Immunology, Georgetown University Medical School, Washington, DC 20007

Schachman, Howard K., Department of Molecular Biology, University of California, Berkeley, CA 94720

Schatten, Gerald P., Integrated Microscopy Facility for Biomedical Research, University of Wisconsin, 1117 W. Johnson St., Madison, WI 53706

Schatten, Heide, Department of Zoology, University of Wisconsin, Madison, WI 53706

Schiff, Jerome A., Institute for Photobiology of Cells and Organelles, Brandeis University, Waltham, MA 02154

Schmeer, Arline C., Mercenene Cancer Research Institute, Hospital of Saint Raphael, New Haven, CT 06511

Schnapp, Bruce J., Department of Physiology, Boston University Medical School, 80 East Concord Street, Boston, MA 02118

Schneider, E. Gayle, Department of Obstetrics and Gynecology, Yale University School of Medicine, 333 Cedar St., New Haven, CT 06510

Schneiderman, Howard A., Monsanto Company, 800 North Lindbergh Blvd., D1W, St. Louis, MO 63166

Schotte, Oscar E., Department of Biology, Amherst College, Amherst, MA 01002 (deceased 4/12/88)

Schuel, Herbert, Department of Anatomical Sciences, SUNY, Buffalo, Buffalo, NY 14214

Schuetz, Allen W., School of Hygiene and Public Health, Johns Hopkins University, Baltimore, MD 21205

Schwartz, James H., Center for Neurobiology and Behavior, New York State Psychiatric Institute—Research Annex, 722 W. 168th St., 7th Floor, New York, NY 10032

Scofield, Virginia Lee, Department of Microbiology and Immunology, UCLA School of Medicine, Los Angeles, CA 90024

Sears, Mary, P. O. Box 152, Woods Hole, MA 02543

Segal, Sheldon J., Population Division, The Rockefeller Foundation, 1133 Avenue of the Americas, New York, NY 10036

Seliger, Howard H., Johns Hopkins University, McCollum-Pratt Institute, Baltimore, MD 21218 (resigned 1/31/88)

Selman, Kelly, Department of Anatomy, College of Medicine, University of Florida, Gainesville, FL 32601

Senft, Joseph, Biology Department, Juniata College, Huntingdon, PA 16652

Shanklin, Douglas R., Department of Pathology, Room 584, University of Tennessee College of Medicine, Memphis, TN 38163

Shapiro, Herbert, 6025 North 13th St., Philadelphia, PA 19141

Shaver, Gaius R., Ecosystems Center, Marine Biological Laboratory, Woods Hole, MA 02543

Shaver, John R., Department of Biology, Cayey Regional Campus, University of Puerto Rico, Cayey, PR 00633

Sheetz, Michael P., Department of Cell Biology and Physiology, Washington University Medical School, 606 S. Euclid Ave., St. Louis, MO 63110

Shepard, David C., P. O. Box 44, Woods Hole, MA 02543

Shepro, David, Department of Biology, Boston University, 2 Cummington St., Boston, MA 02215

Sher, F. Alan, Immunology and Cell Biology Section, Laboratory of Parasitic Disease, NIAID, Building 5, Room 114, NIH, Bethesda, MD 20892

Sheridan, William F., Biology Department, University of North Dakota, Box 8238, University Station, Grand Forks, ND 58202-8238

Sherman, I. W., Division of Life Sciences, University of California, Riverside, CA 92502

Shilo, Moshe, Department of Microbial and Molecular Biology, The Hebrew University, 91904 Jerusalem, ISRAEL

Shimomura, Osamu, Marine Biological Laboratory, Woods Hole, MA 02543

Shoukimas, Jonathan J., 45 Dillingham Avenue, Falmouth, MA 02540

Siegel, Irwin M., Department of Ophthalmology, New York University Medical Center, 550 First Avenue, New York, NY 10016

Siegelman, Harold W., Department of Biology, Brookhaven National Laboratory, Upton, NY 11973

Silver, Robert B., Department of Physiology, Cornell University, 822 Veterinary Research Tower, Ithaca, NY 14853-6401

Silverstein, Arthur M., Wilmer Institute, The Johns Hopkins Hospital, Baltimore, MD 21205

Sjodin, Raymond A., Department of Biophysics, University of Maryland, Baltimore, MD 21201

Skinner, Dorothy M., Oak Ridge National Laboratory, P. O. Box 2009, Biology Division, Oak Ridge, TN 37830

Sloboda, Roger D., Department of Biological Sciences, Dartmouth College, Hanover, NH 03755

Sluder, Greenfield, Cell Biology Group, Worcester Foundation for Experimental Biology, 222 Maple Ave., Shrewsbury, MA 01545

Smith, Homer P., 8 Quissett Avenue, Woods Hole, MA 02543

Smith, Michael A., Jl Sinabung, Buntu #7, Semarang, Java, INDONESIA

Smith, Ralph I., Department of Zoology, University of California, Berkeley, CA 94720

Sorenson, Martha M., Depto de Bioquimica-RFRJ, Centro de Ciencias da Saude-I. C. B., Cidade Universitaria-Fundad, Rio de Janeiro, BRASIL 21.910

Speck, William T., Case Western Reserve University, Department of Pediatrics, Cleveland, OH 44106

Spector, Abraham, College of Physicians and Surgeons, Columbia University, 630 West 168th Street, New York, NY 10032

Speer, John W., Marine Biological Laboratory, Woods Hole, MA 02543

Spiegel, Evelyn, Department of Biological Sciences, Dartmouth College, Hanover, NH 03755

Spiegel, Melvin, Department of Biological Sciences, Dartmouth College, Hanover, NH 03755

Spray, David C., Albert Einstein College of Medicine, Department of Neurosciences, 1300 Morris Park Avenue, Bronx, NY 10461

Steele, John Hyslop, Woods Hole Oceanographic Institution, Woods Hole, MA 02543

Steinacher, Antoinette, Dept. of Otolaryngology, Washington University, School of Medicine, 4911 Barnes Hospital, St. Louis, MO 63110

Steinberg, Malcolm, Department of Biology, Princeton University, Princeton, NJ 08540

Stephens, Grover C., Department of Developmental and Cell Biology, University of California, Irvine, CA 92717

Stephens, Raymond E., Marine Biological Laboratory, Woods Hole, MA 02543

Stetten, DeWitt, Jr., NIH, Bldg. 16, Room 118, Bethesda, MD 20892

Stetten, Jane Lazarow, 2 W Drive, Bethesda, MD 20814

Steudler, Paul A., Ecosystems Center, Marine Biological Laboratory, Woods Hole, MA 02543

Stokes, Darrell R., Department of Biology, Emory University, Atlanta, GA 30322

Stommel, Elijah W., Marine Biological Laboratory, Woods Hole, MA 02543

Stracher, Alfred, Downstate Medical Center, SUNY, 450 Clarkson Ave., Brooklyn, NY 11203

Strehler, Bernard L., 2235 25th St., #217, San Pedro, CA 90732

Strumwasser, Felix, Marine Biological Laboratory, Woods Hole, MA 02543

Stuart, Ann E., Department of Physiology, Medical Sciences Research Wing 206H, University of North Carolina, Chapel Hill, NC 27514

Sugimori, Mutsuyuki, Department of Physiology and Biophysics, New York University Medical Center, 550 First Avenue, New York, NY 10016
Summers, William C., Huxley College of Environmental Studies, Western Washington University, Bellingham, WA 98225
Suprenant, Kathy A., Department of Physiology and Cell Biology, 4010 Haworth Hall, University of Kansas, Lawrence, KS 66045
Sussman, Maurice, 72 Carey Lane, Falmouth, MA 02540
Szabo, George, Harvard School of Dental Medicine, 188 Longwood Avenue, Boston, MA 02115
Szent-Gyorgyi, Andrew, Department of Biology, Brandeis University, Waltham, MA 02254
Szent-Gyorgyi, Eva Szentkiraly, Department of Biology, Brandeis University, Waltham, MA 02254 (deceased 3/22/88)
Szuts, Ete Z., Laboratory of Sensory Physiology, Marine Biological Laboratory, Woods Hole, MA 02543

Tamm, Sidney L., Boston University Marine Program, Marine Biological Laboratory, Woods Hole, MA 02543
Tanzer, Marvin L., Department of Oral Biology, Medical School, University of Connecticut, Farmington, CT 06032
Tasaki, Ichiji, Laboratory of Neurobiology, Bldg. 36, Rm. 2B-16, NIMH/NIH, Bethesda, MD 20892
Taylor, Douglass L., Biological Sciences, Mellon Institute, 440 Fifth Avenue, Pittsburgh, PA 15213
Teal, John M., Department of Biology, Woods Hole Oceanographic Institution, Woods Hole, MA 02543
Telfer, William H., Department of Biology, University of Pennsylvania, Philadelphia, PA 19174
Thorndike, W. Nicholas, Wellington Management Company, 28 State St., Boston, MA 02109
Trager, William, Rockefeller University, 1230 York Ave., New York, NY 10021
Travis, D. M., Veterans Administration Medical Center, 2101 Elm Street, Fargo, ND 58102
Treistman, Steven N., Worcester Foundation for Experimental Biology, Shrewsbury, MA 01545
Trigg, D. Thomas, 125 Grove St., Wellesley, MA 02181
Trinkaus, J. Philip, Department of Biology, Box 6666, Yale University, New Haven, CT 06510
Troll, Walter, Department of Environmental Medicine, College of Medicine, New York University, New York, NY 10016
Troxler, Robert F., Department of Biochemistry, School of Medicine, Boston University, 80 East Concord St., Boston, MA 02118
Tucker, Edward B., Department of Natural Sciences, Baruch College, 17 Lexington Ave., New York, NY 10010
Turner, Ruth D., Mollusk Department, Museum of Comparative Zoology, Harvard University, Cambridge, MA 02138
Tweedell, Kenyon S., Department of Biology, University of Notre Dame, Notre Dame, IN 46656
Tytell, Michael, Department of Anatomy, Bowman Gray School of Medicine, Wake Forest University, Winston-Salem, NC 27103

Ueno, Hiroshi, Department of Biochemistry, The Rockefeller University, 1230 York Ave., New York, NY 10021
Uretz, Robert B., Division of Biological Sciences, University of Chicago, 950 East 59th St., Chicago, IL 60637

Valiela, Ivan, Boston University Marine Program, Marine Biological Laboratory, Woods Hole, MA 02543
Vallee, Richard, Cell Biology Group, Worcester Foundation for Experimental Biology, Shrewsbury, MA 01545
Valois, John, Marine Biological Laboratory, Woods Hole, MA 02543
Van Holde, Kensal, Department of Biochemistry and Biophysics, Oregon State University, Corvallis, OR 97331
Villee, Claude A., Parcel B, Room 122, Harvard Medical School, 25 Shattuck St., Boston, MA 02115
Vincent, Walter S., School of Life and Health Sciences, University of Delaware, Newark, DE 19711

Waksman, Byron, National Multiple Sclerosis Society, 205 East 42nd St., New York, NY 10017
Wall, Betty, 9 George St., Woods Hole, MA 02543
Wallace, Robin A., Whitney Laboratory, 9505 Ocean Shore Blvd., St. Augustine, FL 32086
Wang, An, Wang Laboratories, Inc., One Industrial Ave., Lowell, MA 01851
Wang, Ching Chung, Department of Pharmaceutical Chemistry, University of California, San Francisco, CA 94143
Warner, Robert C., Department of Molecular Biology and Biochemistry, University of California, Irvine, CA 92717
Warren, Kenneth S., MacMillan, Inc., 866 Third Avenue, New York, NY 10022
Warren, Leonard, Wistar Institute, 36th and Spruce Streets, Philadelphia, PA 19104
Watson, Stanley, Associates of Cape Cod, Inc., P. O. Box 224, Woods Hole, MA 02543
Waxman, Stephen G., Department of Neurology, LCI 708, Yale School of Medicine, 333 Cedar Street, New Haven, CT 06510
Webb, H. Marguerite, Marine Biological Laboratory, Woods Hole, MA 02543
Weber, Annemarie, Department of Biochemistry and Biophysics, School of Medicine, University of Pennsylvania, Philadelphia, PA 19104
Webster, Ferris, Box 765, Lewes, DE 19958
Weidner, Earl, Department of Zoology and Physiology, Louisiana State University, Baton Rouge, LA 70803
Weiss, Dieter, G., Institut fur Zoologie, Technische Universitat Munchen, 8046 Garching, FRG
Weiss, Leon P., Department of Animal Biology, School of Veterinary Medicine, University of Pennsylvania, Philadelphia, PA 19104
Weissmann, Gerald, New York University Medical Center, 550 First Avenue, New York, NY 10016
Werman, Robert, Neurobiology Unit, The Hebrew University, Jerusalem, ISRAEL
Westerfield, R. Monte, The Institute of Neuroscience, University of Oregon, Eugene, OR 37403
Wexler, Nancy Sabin, 15 Claremont Avenue, Apt. 92, New York, NY 10027

White, Roy L., Department of Neuroscience, Albert Einstein College, 1300 Morris Park Avenue, Bronx, NY 10461

Whittaker, J. Richard, Marine Biological Laboratory, Woods Hole, MA 02543

Wigley, Roland L., 35 Wilson Road, Woods Hole, MA 02543

Wilson, Darcy B., Medical Biology Institute, 11077 North Torrey Pines Road, La Jolla, CA 92037

Wilson, Edward O., Museum, Comparative Zoology, Harvard University, Cambridge, MA 02138

Wilson, T. Hastings, Department of Physiology, Harvard Medical School, Boston, MA 02115

Wilson, Walter L., 743 Cambridge Drive, Rochester Hills, MI 48063 (deceased 3/1/88)

Witkovsky, Paul, Department of Ophthalmology, New York University Medical Center, 550 First Ave., New York, NY 10016

Wittenberg, Jonathan B., Department of Physiology and Biochemistry, Albert Einstein College, 1300 Morris Park Ave., Bronx, NY 10016

Wolfe, Ralph, Department of Microbiology, 131 Burrill Hall, University of Illinois, Urbana, IL 61801

Wolken, Jerome J., Department of Biological Sciences, Carnegie Mellon University, 440 Fifth Ave., Pittsburgh, PA 15213

Worgul, Basil V., Department of Ophthalmology, Columbia University, 630 West 168th St., New York, NY 10032

Wu, Chau Hsiung, Department of Pharmacology, Northwestern University Medical School, Chicago, IL 60611

Wyttenbach, Charles R., Department of Physiology and Cell Biology, University of Kansas, Lawrence, KS 66045

Yeh, Jay Z., Department of Pharmacology, Northwestern University Medical School, Chicago, IL 60611

Young, Richard, Mentor O & O, Inc., 3000 Longwater Dr., Norwell, MA 02061

Zackroff, Robert, 80 Kersey Rd., Peacedale, RI 02883

Zigman, Seymour, School of Medicine and Dentistry, University of Rochester, 260 Crittenden Blvd., Rochester, NY 14620

Zigmond, Richard E., Center for Neurosciences, School of Medicine, Case Western Reserve University, Cleveland, OH 44106

Zimmerberg, Joshua J., Bldg. 12A, Room 2007, NIH, Bethesda, MD 20892

Zottoli, Steven J., Department of Biology, Williams College, Williamstown, MA 01267

Zucker, Robert S., Neurobiology Division, Department of Molecular and Cellular Biology, University of California, Berkeley, CA 94720

Associate Members

Ackroyd, Dr. Frederick W.
Adams, Dr. Paul
Adelberg, Dr. and Mrs. Edward A.
Ahearn, Mr. and Mrs. David
Alden, Mr. John M.
Allard, Dr. and Mrs. Dean C., Jr.
Allen, Miss Camilla K.
Allen, Dr. Nina S.
Amon, Mr. Carl H. Jr
Anderson, Mr. J. Gregory
Anderson, Drs. James L. and Helene M.
Antonucci, Dr. Robert V.
Armstrong, Dr. and Mrs. Samuel C.
Arnold, Mrs. Lois
Aspinwall, Mr. and Mrs. Duncan
Atwood, Dr. and Mrs. Kimball C., III
Ayers, Mrs. Donald
Backus, Mrs. Nell
Baker, Mrs. C. L.
Ball, Mrs. Eric G.
Ballantine, Dr. and Mrs. H. T., Jr.
Bang, Mrs. Frederik B.
Bang, Miss Molly
Banks, Mr. and Mrs. William L.
Barkan, Mr. and Mrs. Mel A.
Barrows, Mrs. Albert W.
Baum, Mr. Richard T.
Baylor, Drs. Edward and Martha
Beers, Dr. and Mrs. Yardley
Belesir, Mr. Tasos
Bennett, Dr. and Mrs. Michael V. L.
Berg, Mr. and Mrs. C. John
Bernheimer, Dr. Alan W.
Bernstein, Mr. and Mrs. Norman
Bicker, Mr. Alvin
Bigelow, Mr. and Mrs. Robert O.
Bird, Mr. William R.
Bleck, Dr. Thomas B.
Boche, Mr. Robert
Bodeen, Mr. and Mrs. George H.
Boettiger, Dr. and Mrs. Edward G.
Boettiger, Mrs. Julie
Bolton, Mr. and Mrs. Thomas C.
Bonn, Mr. and Mrs. Theodore H.
Borg, Dr. and Mrs. Alfred F.
Borgese, Dr. and Mrs. Thomas
Bowles, Dr. and Mrs. Francis P.
Bradley, Dr. and Mrs. Charles C.
Bradley, Mr. Richard
Brown, Mrs. Frank A., Jr.
Brown, Mr. and Mrs. Henry
Brown, Mrs. James
Brown, Mrs. Neil
Brown, Mr. and Mrs. T. A.
Brown, Dr. and Mrs. Thornton
Broyles, Dr. Robert H.
Buck, Dr. and Mrs. John W.
Buckley, Mr. George D.
Bunts, Mr. and Mrs. Frank E.
Burt, Mrs. Charles E.
Burwell, Dr. and Mrs. E. Langdon
Bush, Dr. Louise
Buxton, Mr. and Mrs. Bruce E.

MBL Associates Joel and Ruth Davis.

Buxton, Mr. E. Brewster
Cadwalader, Mr. George
Calkins, Mr. and Mrs. G. N., Jr.
Campbell, Dr. and Mrs. David G.
Carlson, Dr. and Mrs. Francis
Carlton, Mr. and Mrs. Winslow G.
Case, Dr. and Mrs. James
Chandler, Mr. Robert
Chase, Mr. Thomas H.
Child, Dr. and Mrs. Frank M., III
Chisholm, Dr. Sallie W.
Church, Dr. Wesley
Claff, Mr. and Mrs. Mark
Clark, Dr. and Mrs. Arnold
Clark, Mr. and Mrs. Hays
Clark, Mr. and Mrs. James McC.
Clark, Mr. and Mrs. Leroy, Jr.
Clark, Dr. Peter L.
Clarke, Dr. Barbara J.
Clement, Mrs. Anthony C.
Cloud, Dr. Laurence P.
Clowes Fund, Inc.
Clowes, Dr. and Mrs. Alexander W.
Clowes, Mr. Allen W.
Clowes, Mrs. G. H. A., Jr.
Coburn, Mr. and Mrs. Lawrence
Cohen, Mrs. Seymour S.
Coleman, Drs. John and Annette
Collum, Mrs. Peter
Colt, Dr. LeBaron C., Jr.
Connell, Mr. and Mrs. W. J.
Cook, Dr. and Mrs. Joseph
Cook, Dr. and Mrs. Paul W., Jr.
Copel, Mrs. Marcia N.
Copeland, Dr. and Mrs. D. Eugene
Copeland, Mr. Frederick C.
Copeland, Mr. and Mrs. Preston S.
Costello, Mrs. Donald P.
Cowan, Mr. and Mrs. James F., III
Crabb, Mr. and Mrs. David L.
Crain, Mr. and Mrs. Melvin C.
Cramer, Mr. and Mrs. Ian D. W.
Crane, Mrs. John O.
Crane, Josephine B., Foundation
Crane, Mr. Thomas S.
Crosby, Miss Carol
Cross, Mr. and Mrs. Norman C.
Crossley, Miss Dorothy
Crossley, Miss Helen
Crowell, Dr. and Mrs. Sears
Currier, Mr. and Mrs. David L.
Daignault, Mr. and Mrs. Alexander T.
Daniels, Mr. and Mrs. Bruce G.
Davidson, Dr. Morton
Davis, Mr. and Mrs. Joel P.
Day, Mr. and Mrs. Pomeroy
Decker, Dr. Raymond F.
DeMello, Mr. John
DiBerardino, Dr. Marie A.
DiCecca, Dr. and Mrs. Charles
Dickson, Dr. Willim A.
Dierolf, Dr. Shirley H.
Donovan, Mr. David L.
Dreyer, Mrs. Frank
Drummey, Mr. and Mrs. Charles E.
Drummey, Mr. Todd A.
DuBois, Dr. and Mrs. Arthur B.
Dudley, Dr. Patricia
DuPont, Mr. A. Felix, Jr.
Dutton, Mr. and Mrs. Roderick L.
Ebert, Dr. and Mrs. James D.
Egloff, Dr. and Mrs. F. R. L.
Elliott, Mrs. Alfred M.
Enos, Mr. Edward, Jr.
Eppel, Mr. and Mrs. Dudley
Epstein, Mr. and Mrs. Ray L.
Estabrooks, Mr. Gordon C.
Evans, Mr. and Mrs. Dudley
Farley, Miss Joan
Farmer, Miss Mary
Faull, Mr. J. Horace, Jr.
Ferguson, Mrs. James J., Jr.
Fisher, Mrs. B. C.
Fisher, Mr. Frederick S., III
Fisher, Dr. and Mrs. Saul H.
Fluck, Mr. Richard A.
Folino, Mr. John W., Jr.
Forbes, Mr. John M.
Ford, Mr. John H.
Fowlkes, Mr. Aaron
Francis, Mr. and Mrs. Lewis W., Jr.
Frenkel, Dr. Krystina
Fribourgh, Dr. James H.
Friendship Fund
Fries, Dr. and Mrs. E. F. B.
Frosch, Dr. and Mrs. Robert A.
Fye, Mrs. Paul M.
Gabriel, Dr. and Mrs. Mordecai L.
Gagnon, Mr. Michael
Gaiser, Mrs. David W.
Gallagher, Mr. Robert O.
Garcia, Dr. Ignacio
Garfield, Miss Eleanor
Gellis, Dr. and Mrs. Sydney
Gephard, Mr. Stephen
German, Dr. and Mrs. James L., III
Gewecke, Mr. and Mrs. Thomas H.
Gifford, Mr. and Mrs. Cameron
Gifford, Mr. John A.
Gifford, Dr. and Mrs. Prosser
Gilbert, Drs. Daniel L. and Claire
Gilbert, Mrs. Carl J.
Gildea, Dr. Margaret C. L.
Gillette, Mr. and Mrs. Robert S.
Glad, Mr. Robert
Glass, Dr. and Mrs. H. Bentley
Glazebrook, Mr. James G.
Glazebrook, Mrs. James R.
Goldman, Mrs. Mary
Goldring, Mr. Michael
Goldstein, Dr. and Mrs. Moise H., Jr.
Goodwin, Mr. and Mrs. Charles
Gould, Miss Edith
Grace, Miss Priscilla B.
Grant, Dr. and Mrs. Philip
Grassle, Mrs. J. K.
Green, Mrs. Davis Crane
Greenberg, Noah and Mosher, Diane
Greer, Mr. and Mrs. W. H., Jr.
Griffin, Mrs. Robert W.
Griffith, Dr. and Mrs. B. Herold
Grosch, Dr. and Mrs. Daniel S.
Gross, Mrs. Mona
Gunning, Mr. and Mrs. Robert
Haakonsen, Dr. Harry O.
Haigh, Mr. and Mrs. Richard H.
Hall, Mr. and Mrs. Peter A.
Hall, Mr. Warren C.
Halvorson, Dr. and Mrs. Harlyn O.
Hamstrom, Miss Mary Elizabeth
Harrington, Mr. Robert D., Jr.
Harvey, Dr. and Mrs. Richard B.
Hassett, Mr. and Mrs. Charles
Hastings, Dr. and Mrs. J. Woodland
Haubrich, Mr. Robert R.
Hay, Mr. John
Hays, Dr. David S.
Hedberg, Mrs. Frances
Hedberg, Dr. Mary
Hersey, Mrs. George L.
Hiatt, Dr. and Mrs. Howard
Hichar, Mrs. Barbara
Hill, Mrs. Samuel E.
Hirschfeld, Mrs. Nathan B.
Hobbie, Dr. and Mrs. John
Hocker, Mr. and Mrs. Lon
Hodge, Mrs. Stuart
Hokin, Mr. Richard
Hornor, Mr. Townsend
Horwitz, Dr. and Mrs. Norman H.
Hoskin, Dr. and Mrs. Francis C. G.
Houston, Mr. and Mrs. Howard E.
Howard, Mrs. L. L.
Hoyle, Dr. Merrill C.
Huettner, Dr. and Mrs. Robert J.
Hutchison, Mr. Alan D.
Hyde, Mr. and Mrs. Robinson
Hynes, Mr. and Mrs. Thomas J., Jr.
Inouë, Dr. and Mrs. Shinya
Issokson, Mr. and Mrs. Israel
Jackson, Miss Elizabeth B.
Jaffe, Dr. and Mrs. Ernst R.
Janney, Mrs. F. Wistar
Jewett, G. F., Foundation
Jewett, Mr. and Mrs. G. F., Jr.
Jones, Mr. and Mrs. DeWitt C., III
Jones, Mr. and Mrs. Frederick, II

Harlyn Halvorson presents Lilyan Saunders with a Centennial poster in appreciation for her efforts in the Associates' Gift Shop.

Jones, Mr. Frederick S., III
Jordan, Dr. and Mrs. Edwin P.
Kaan, Dr. Helen W.
Kahler, Mrs. Robert W.
Kaminer, Dr. and Mrs. Benjamin
Karplus, Mrs. Alan K.
Karush, Dr. and Mrs. Fred
Kelleher, Mr. and Mrs. Paul R.
Kendall, Mr. and Mrs. Richard E.
Keosian, Mrs. Jessie
Keoughan, Miss Patricia
Ketchum, Mrs. Paul
Kien, Mr. and Mrs. Pieter
Kinnard, Mrs. L. Richard
Kirschenbaum, Mrs. Donald
Kissam, Mr. and Mrs. William M.
Kivy, Dr. and Mrs. Peter
Koller, Dr. Lewis R.
Korgen, Dr. Ben J.
Kravitz, Dr. and Mrs. Edward
Kuffler, Mrs. Stephen W.
Laderman, Mr. and Mrs. Ezra
Lafferty, Miss Nancy
Larmon, Mr. Jay
Laster, Dr. and Mrs. Leonard
Laufer, Dr. and Mrs. Hans
Laufer, Jessica, and Weiss, Malcolm
LaVigne, Mrs. Richard J.
Lawrence, Mr. Frederick V.
Lawrence, Mr. and Mrs. William
Leach, Dr. Berton J.
Leatherbee, Mrs. John H.
LeBlond, Mr. and Mrs. Arthur
Leeson, Mr. and Mrs. A. Dix
LeFevre, Dr. Marian E.
Lehman, Miss Robin
Lenher, Dr. and Mrs. Samuel
Leprohon, Mr. Joseph
Levine, Mr. Joseph
Levine, Dr. and Mrs. Rachmiel
Levitz, Dr. Mortimer
Levy, Mr. and Mrs. Stephen R.
Lindner, Mr. Timothy P.
Little, Mrs. Elbert
Livingstone, Mr. and Mrs. Robert
Lloyd, Mr. and Mrs. James
Loeb, Mrs. Robert F.
Loessel, Mrs. Edward
Lovell, Mr. and Mrs. Hollis R.
Lovering, Mr. Richard C.
Low, Miss Doris
Lowe, Dr. and Mrs. Charles V.
Lowengard, Mrs. Joseph
Mackey, Mr. and Mrs. William K.
MacLeish, Mrs. Margaret
MacNary, Mr. and Mrs. B. Glenn
MacNichol, Dr. and Mrs. Edward F., Jr.
Maher, Miss Anne Camille
Mahler, Mrs. Henry
Mahler, Mrs. Suzanne
Mansworth, Miss Marie
Maples, Dr. Philip B.
Marsh, Dr. and Mrs. Julian
Martyna, Mr. and Mrs. Joseph C.
Mason, Mr. Appleton
Mastroianni, Dr. and Mrs. Luigi, Jr.
Mather, Mr. and Mrs. Frank J., III
Matherly, Mr. and Mrs. Walter
Matthiessen, Dr. and Mrs. G. C.
McCusker, Mr. and Mrs. Paul T.
McElroy, Mrs. Nella W.
McIlwain, Dr. Susan G.
McMurtrie, Mrs. Cornelia Hanna
Meigs, Mr. and Mrs. Arthur
Meigs, Dr. and Mrs. J. Wister
Melillo, Dr. and Mrs. Jerry M.
Mellon, Richard King, Trust
Mellon, Mr. and Mrs. Richard P.
Mendelson, Dr. Martin
Metz, Dr. and Mrs. Charles B.
Meyers, Mr. and Mrs. Richard
Miller, Dr. Daniel A.
Miller, Mr. and Mrs. Paul
Mixter, Mr. and Mrs. William J., Jr.
Mizell, Dr. and Mrs. Merle
Monroy, Mrs. Alberto
Montgomery, Dr. and Mrs. Charles H.
Montgomery, Mrs. Raymond B.
Moore, Drs. John and Betty
Morgan, Miss Amy
Morse, Mrs. Charles L., Jr.
Morse, Dr. M. Patricia
Moul, Mrs. Edwin T.
Murray, Mr. David M.
Myles-Tochko, Drs. Christina J. and John
Nace, Dr. and Mrs. Paul
Nace, Mr. Paul F., Jr.
Neall, Mr. William G.
Nelson, Dr. and Mrs. Leonard
Nelson, Dr. Pamela
Newton, Mr. William F.
Nickerson, Mr. and Mrs. Frank L.
Norman, Mr. and Mrs. Andrew E.
Norman Foundation
Norris, Mr. and Mrs. Barry
Norris, Mr. and Mrs. John A.
Norris, Mr. William
Norton, Mrs. Thomas J.
O'Herron, Mr. and Mrs. Jonathan
Olszowka, Miss Janice S.
O'Neil, Mr. and Mrs. Barry T.
O'Rand, Mr. and Mrs. Michael
O'Sullivan, Dr. Renee Bennett
Pappas, Dr. and Mrs. George D.
Park, Mr. and Mrs. Malcolm S.
Parmenter, Dr. Charles
Parmenter, Miss Carolyn L.
Peltz, Mr. and Mrs. William L.
Pendergast, Mrs. Claudia
Pendleton, Dr. and Mrs. Murray E.
Peri, Mrs. Barbara Anne
Perkins, Mr. and Mrs. Courtland D.
Person, Dr. and Mrs. Philip
Peterson, Mr. and Mrs. E. Gunnar
Peterson, Mr. and Mrs. E. Joel
Peterson, Mr. Raymond W.
Petty, Mr. Richard F.
Pfeiffer, Mr. and Mrs. John
Plough, Mr. and Mrs. George H.
Plough, Mrs. Harold H.
Pointe, Mr. Albert
Pointe, Mr. Charles
Porter, Dr. and Mrs. Keith R.
Pothier, Dr. and Mrs. Aubrey
Press, Drs. Frank and Billie
Proskauer, Mr. Joseph H.
Proskauer, Mr. Richard
Prosser, Dr. and Mrs. C. Ladd
Psaledakis, Mr. Nicholas
Psychoyos, Dr. Alexandre
Putnam, Mr. Allan Ray
Putnam, Mr. and Mrs. William A., III
Raymond, Dr. and Mrs. Samuel
Reese, Miss Bonnie
Reingold, Mr. Stephen C.
Reynolds, Dr. and Mrs. George
Reynolds, Mr. and Mrs. Robert M.
Reznikoff, Mrs. Paul
Ricca, Dr. and Mrs. Renato A.
Righter, Mr. and Mrs. Harold
Riley, Dr. Monica
Riina, Mr. John R.
Robb, Mrs. Alison A.
Roberts, Miss Jean
Roberts, Mr. Mervin F.
Robertson, Mrs. C. W.
Robinson, Dr. Denis M.
Root, Mrs. Walter S.
Rosenthal, Miss Hilde
Roslansky, Drs. John and Priscilla
Ross, Dr. and Mrs. Donald
Ross, Dr. Robert
Ross, Dr. Virginia
Roth, Dr. and Mrs. Stephen
Rowan, Mr. Edward
Rowe, Mr. Don
Rowe, Mr. and Mrs. William S.
Rugh, Mrs. Roberts
Ryder, Mr. and Mrs. Francis C.
Sager, Dr. Ruth
Sardinha, Mr. George H.
Saunders, Dr. and Mrs. John W.
Saunders, Mrs. Lawrence
Saunders, Lawrence, Fund
Sawyer, Mr. and Mrs. John E.
Saz, Mrs. Ruth L.
Schlesinger, Dr. and Mrs. R. Walter
Schwamb, Mr. Peter
Scott, Mrs. George T.
Scott, Mr. and Mrs. Norman E.
Sears, Mr. Clayton C.
Sears, Mr. and Mrs. Harold B.
Sears, Mr. Harold H.
Seaver, Mr. George
Segal, Dr. and Mrs. Sheldon J.
Selby, Dr. Cecily
Senft, Dr. and Mrs. Alfred
Shapiro, Mr. and Mrs. Howard
Shapley, Dr. Robert
Shemin, Dr. and Mrs. David
Shepro, Dr. and Mrs. David
Siegel, Mr. and Mrs. Alvin
Simmons, Mr. Tim
Singer, Mr. and Mrs. Daniel M.
Smith, Drs. Frederick E. and Marguerite A.
Smith, Mrs. Homer P.
Smith, Mr. Van Dorn C.
Snyder, Mr. Robert M.
Solomon, Dr. and Mrs. A. K.
Speck, Dr. William T.
Specht, Mr. and Mrs. Heinz
Spiegel, Dr. and Mrs. Melvin
Spotte, Mr. Stephen
Steele, Mrs. John H.
Stein, Mr. Ronald
Steinbach, Mrs. H. Burr
Stetson, Mrs. Thomas J.
Stetten, Dr. Gail
Stetten, Dr. and Mrs. H. DeWitt, Jr.
Stunkard, Dr. Horace
Sudduth, Dr. William
Swanson, Dr. and Mrs. Carl P.
Swope, Mrs. Gerard, Jr.
Swope, Mr. and Mrs. Gerard L.
Szent-Györgyi, Dr. Andrew
Taber, Mr. George H.
Taylor, Mr. James K.
Taylor, Dr. and Mrs. W. Randolph
Tietje, Mr. and Mrs. Emil D., Jr.
Timmins, Mrs. William
Todd, Mr. and Mrs. Gordon F.
Tolkan, Mr. and Mrs. Norman N.
Trager, Mrs. William
Trigg, Mr. and Mrs. D. Thomas

Troll, Dr. and Mrs. Walter
Trousof, Miss Natalie
Tucker, Miss Ruth
Tully, Mr. and Mrs. Gordon F.
Ulbrich, Mr. and Mrs. Volker
Valois, Mr. and Mrs. John
Van Buren, Mrs. Harold
Van Holde, Mrs. Kensal E.
Veeder, Mrs. Ronald A.
Vincent, Mr. and Mrs. Samuel W.
Vincent, Dr. Walter S.
Wagner, Mr. Mark
Waksman, Dr. and Mrs. Byron H.
Ward, Dr. Robert T.
Ware, Mr. and Mrs. J. Lindsay
Warren, Dr. Henry B.
Warren, Dr. and Mrs. Leonard
Watt, Mr. and Mrs. John B.
Weeks, Mr. and Mrs. John T.
Weinstein, Miss Nancy B.
Weisberg, Mr. and Mrs. Alfred M.
Weissmann, Dr. and Mrs. Gerald
Wheeler, Dr. and Mrs. Paul S.
Whitehead, Mr. and Mrs. Fred
Whitney, Mr. and Mrs. Geoffrey G., Jr.
Wichterman, Dr. and Mrs. Ralph
Wickersham, Mr. and Mrs. A. A. Tilney
Wiese, Dr. Konrad
Wilhelm, Dr. Hazel S.
Wilson, Mr. and Mrs. T. Hastings
Wilson, Mr. and Mrs. Leslie J.
Winn, Dr. William M.
Winsten, Dr. Jay A.
Witting, Miss Joyce
Wofinsohn, Mrs. Wolfe
Woodwell, Dr. and Mrs. George M.
Yntema, Mrs. Chester L.
Young, Miss Nina L.
Zinn, Dr. and Mrs. Donald J.
Zipf, Dr. Elizabeth

B Coolidge

Certificate of Organization Articles of Amendment Bylaws of the MBL

Certificate of Organization

(On File in the Office of the Secretary of the Commonwealth)

No. 3170

We, Alpheus Hyatt, President, William Stanford Stevens, Treasurer, and William T. Sedgwick, Edward G. Gardiner, Susan Mims and Charles Sedgwick Minot being a majority of the Trustees of the Marine Biological Laboratory in compliance with the requirements of the fourth section of chapter one hundred and fifteen of the Public Statutes do hereby certify that the following is a true copy of the agreement of association to constitute said Corporation, with the names of the subscribers thereto:

We, whose names are hereto subscribed, do, by this agreement, associate ourselves with the intention to constitute a Corporation according to the provisions of the one hundred and fifteenth chapter of the Public Statutes of the Commonwealth of Massachusetts, and the Acts in amendment thereof and in addition thereto.

The name by which the Corporation shall be known is
THE MARINE BIOLOGICAL LABORATORY.

The purpose for which the Corporation is constituted is to establish and maintain a laboratory or station for scientific study and investigations, and a school for instruction in biology and natural history.

The place within which the Corporation is established or located is the city of Boston within said Commonwealth.

The amount of its capital stock is none.

In Witness Whereof, we have hereunto set our hands, this twenty seventh day of February in the year eighteen hundred and eighty-eight, Alpheus Hyatt, Samuel Mills, William T. Sedgwick, Edward G. Gardiner, Charles Sedgwick Minot, William G. Farlow, William Stanford Stevens, Anna D. Phillips, Susan Mims, B. H. Van Vleck.

That the first meeting of the subscribers to said agreement was held on the thirteenth day of March in the year eighteen hundred and eighty-eight.

In Witness Whereof, we have hereunto signed our names, this thirteenth day of March in the year eighteen hundred and eighty-eight, Alpheus Hyatt, President, William Stanford Stevens, Treasurer, Edward G. Gardiner, William T. Sedgwick, Susan Mims, Charles Sedgwick Minot.

(Approved on March 20, 1888 as follows:

I hereby certify that it appears upon an examination of the within written certificate and the records of the corporation duly submitted to my inspection, that the requirements of sections one, two and three of chapter one hundred and fifteen, and sections eighteen, twenty and twenty-one of chapter one hundred and six, of the Public Statutes, have been complied with and I hereby approve said certificate this twentieth day of March A.D. eighteen hundred and eighty-eight.

Charles Endicott
Commissioner of Corporations)

Articles of Amendment

(On File in the Office of the Secretary of the Commonwealth)

We, James D. Ebert, President, and David Shepro, Clerk of the Marine Biological Laboratory, located at Woods Hole, Massachusetts 02543, do hereby certify that the following amendment to the Articles of Organization of the Corporation was duly adopted at a meeting held on August 15, 1975, as adjourned to August 29, 1975, by vote of 444 members, being at least two-thirds of its members legally qualified to vote in the meeting of the corporation:

Voted: That the Certificate of Organization of this corporation be and it hereby is amended by the addition of the following provisions:

"No Officer, Trustee or Corporate Member of the corporation shall be personally liable for the payment or satisfaction of any obligation or liabilities incurred as a result of, or otherwise in connection with, any commitments, agreements, activities or affairs of the corporation.

"Except as otherwise specifically provided by the Bylaws of the corporation, meetings of the Corporate Members of the corporation may be held anywhere in the United States.

"The Trustees of the corporation may make, amend or repeal the Bylaws of the corporation in whole or in part, except with respect to any provisions thereof which shall by law, this Certificate or the bylaws of the corporation, require action by the Corporate Members."

The foregoing amendment will become effective when these articles of amendment are filed in accordance with Chapter 180, Section 7 of the General Laws unless these articles specify, in accordance with the vote adopting the amendment, a later effective date not more than thirty days after such filing, in which event the amendment will become effective on such later date.

In Witness whereof and Under the Penalties of Perjury, we have hereto signed our names this 2nd day of September, in the year 1975, James D. Ebert, President; David Shepro, Clerk.

(Approved on October 24, 1975, as follows:

I hereby approve the within articles of amendment and, the filing fee in the amount of $10 having been paid, said articles are deemed to have been filed with me this 24th day of October, 1975.

Paul Guzzi
Secretary of the Commonwealth)

Bylaws of the Corporation of the Marine Biological Laboratory

(Revised August 14, 1987)

I. (A) The name of the Corporation shall be The Marine Biological Laboratory. The Corporation's purpose shall be to establish and maintain a laboratory or station for scientific study and investigation, and a school for instruction in biology and natural history.

(B) Marine Biological Laboratory admits students without regard to race, color, sex, national and ethnic origin to all the rights, privileges, programs and activities generally accorded or made available to students in its courses. It does not discriminate on the basis of race, color, sex, national and ethnic origin in employment, administration or its educational policies, admissions policies, scholarship and other programs.

II. (A) The members of the Corporation ("Members") shall consist of persons elected by the Board of Trustees, upon such terms and conditions and in accordance with such procedures, not inconsistent with law or these Bylaws, as may be determined by said Board of Trustees. Except as provided below, any Member may vote at any meeting either in person or by proxy executed no more than six months prior to the date of such meeting. Members shall serve until their death or resignation unless earlier removed with or without cause by the affirmative vote of two-thirds of the Trustees then in office. Any member who has attained the age of seventy years or has retired from his home institution shall automatically be designated a Life Member provided he signifies his wish to retain his membership. Life Members shall not have the right to vote and shall not be assessed for dues.

(B) The Associates of the Marine Biological Laboratory shall be an unincorporated group of persons (including associations and corporations) interested in the Laboratory and shall be organized and operated under the general supervision and authority of the Trustees.

III. The officers of the Corporation shall consist of a Chairman of the Board of Trustees, President, Director, Treasurer, and Clerk, elected or appointed by the Trustees as set forth in Article IX.

IV. The Annual Meeting of the Members shall be held on the Friday following the Second Tuesday in August in each year at the Laboratory in Woods Hole, Massachusetts, at 9:30 a.m. Subject to the provisions of Article VIII(2), at such meeting the Members shall choose by ballot six Trustees to serve four years, and shall transact such other business as may properly come before the meeting. Special meetings of the Members may be called by the Chairman or Trustees to be held at such time and place as may be designated.

V. Twenty-five Members shall constitute a quorum at any meeting. Except as otherwise required by law or these Bylaws, the affirmative vote of a majority of the Members voting in person or by proxy at a meeting attended by a quorum (present in person or by proxy) shall constitute action on behalf of the Members.

VI. (A) Inasmuch as the time and place of the Annual Meeting of Members are fixed by these Bylaws, no notice of the Annual Meeting need be given. Notice of any special meeting of Members, however, shall be given by the Clerk by mailing notice of the time and place and purpose of such meeting, at least 15 days before such meeting, to each Member at his or her address as shown on the records of the Corporation.

(B) Any meeting of the Members may be adjourned to any other time and place by the vote of a majority of those Members present or represented at the meeting, whether or not such Members constitute a quorum. It shall not be necessary to notify any Members of any adjournment.

VII. The Annual Meeting of the Trustees shall be held promptly after the Annual Meeting of the Corporation at the Laboratory in Woods Hole, Massachusetts. Special meetings of the Trustees shall be called by the Chairman, the President, or by any seven Trustees, to be held at such time and place as may be designated. Notice of Trustees' meetings may be given orally, by telephone, telegraph or in writing; and notice given in time to enable the Trustees to attend, or in any case notice sent by mail or telegraph to a Trustee's usual or last known place of residence, at least one week before the meeting shall be sufficient. Notice of a meeting need not be given to any Trustee if a written waiver of notice, executed by him before or after the meeting is filed with the records of the meeting, or if he shall attend the meeting without protesting prior thereto or at its commencement the lack of notice to him.

VIII. (A) There shall be four groups of Trustees:

(1) Trustees (the "Corporate Trustees") elected by the Members according to such procedures, not inconsistent with these Bylaws, as the Trustees shall have determined. Except as provided below, such Trustees shall be divided into four classes of six, one class to be elected each year to serve for a term of four years. Such classes shall be designated by the year of expiration of their respective terms.

(2) Trustees ("Trustees-at-large") approved by members according to such procedures, not inconsistent with these Bylaws, as the Trustees shall have determined. Except as provided below, such Trustees-at-large shall be divided into four classes of *four*, one class to be elected each year to serve for a term of four years. Such classes shall be designated by the year of expiration of their respective terms. It is contemplated that, unless otherwise determined by the Trustees for good reason, Trustees-at-large, shall be individuals who have not been considered for election as Corporate Trustees.

(3) Trustees ex officio, who shall be the Chairman, the President, the Director, the Treasurer, and the Clerk.

(4) Trustees emeriti, who shall include any Member who has attained the age of seventy years (or the age of sixty-five and has retired from his home institution) and who has served a full elected term as a regular Trustee, provided he signifies his wish to serve the Laboratory in that capacity. Any Trustee who qualifies for emeritus status shall continue to serve as a regular Trustee until the next Annual Meeting whereupon his office as regular Trustee shall become vacant and be filled by election by the Members or by the Board, as the case may be. The Trustees ex officio and emeriti shall have all the rights of the Trustees, except that Trustees emeriti shall not have the right to vote.

(B) The aggregate number of Corporate Trustees and Trustees-at-large elected in any year (excluding Trustees elected to fill vacancies which do not result from expiration of a term) shall not exceed ten. The number of Trustees-at-large so elected shall not exceed four and unless otherwise determined by vote of the Trustees, the number of Corporate Trustees so elected shall not exceed six. Corporate Trustees shall always constitute a majority on the Board of those elected or approved by the Corporation.

(C) The Trustees and Officers shall hold their respective offices until their successors are chosen in their stead.

(D) Any Trustee may be removed from office at any time with or without cause, by vote of a majority of the Members entitled to vote in the election of Trustees; or for cause, by vote of two-thirds of the Trustees then in office. A Trustee may be removed for cause only if notice of such action shall have been given to all of the Trustees or Members entitled to vote, as the case may be, prior to the meeting at which such action is to be taken and if the Trustee so to be removed shall have been given reasonable notice and opportunity to be heard before the body proposing to remove him.

(E) Any vacancy in the number of Trustees, however arising, may be filled by the Trustees then in office unless and until filled by the Members at the next Annual Meeting.

(F) A Corporate Trustee or a Trustee-at-large who has served an initial term of at least two years duration shall be eligible for re-election to a second term, but shall be ineligible for re-election to any subsequent term until two years have elapsed after he last served as Trustee.

IX. (A) The Trustees shall have the control and management of the affairs of the Corporation. They shall elect a Chairman of the Board of Trustees who shall be elected annually and shall serve until his successor is selected and qualified and who shall also preside at meetings of the Corporation. They shall elect a President of the Corporation who shall also be the Vice Chairman of the Board of Trustees and Vice Chairman of meetings of the Corporation, and who shall be elected annually and shall serve until his successor is selected and qualified. They shall annually elect a Treasurer who shall serve until his successor is selected and qualified. They shall elect a Clerk (a resident of Massachusetts) who shall serve for a term of four years. Eligibility for re-election shall be in accordance with the content of Article VIII(F) as applied to Corporate or Board Trustees. They shall elect Board Trustees as described in Article VIII(B). They shall appoint a Director of the Laboratory for a term not to exceed five years, provided the term shall not exceed one year if the candidate has attained the age of 65 years prior to the date of the appointment. They may choose such other officers and agents as they may think best. They may fix the compensation and define the duties of all the officers and agents of the Corporation and may remove them at any time. They may fill vacancies occurring in any of the offices. The Board of Trustees shall have the power to choose an Executive Committee from their own number as provided in Article X, and to delegate to such Committee such of their own powers as they may deem expedient in addition to those powers conferred by Article X. They shall from time to time elect Members to the Corporation upon such terms and conditions as they shall have determined, not inconsistent with law or these Bylaws.

(B) The Board of Trustees shall also have the power, by vote of a majority of the Trustees then in Office, to elect an Investment Committee and any other committee and, by like vote, to delegate thereto some or all of their powers except those which by law, the Articles of Organization or these Bylaws they are prohibited from delegating. The members of any such committee shall have tenure and duties as the Trustees shall determine; provided that the Investment Committee, which shall oversee the management of the Corporation's endowment funds and marketable securities, shall include the Chairman of the Board of Trustees, the Treasurer of the Corporation, and the Chairman of the Corporation's Budget Committee, as ex officio members, together with such Trustees as may be required for not less than two-thirds of the Investment Committee to consist of Trustees. Except as otherwise provided by these Bylaws or determined by the Trustees, any such committee may make rules for the conduct of its business; but, unless otherwise provided by the Trustees or in such rules, its business shall be conducted as nearly as possible in the same manner as is provided by these Bylaws for the Trustees.

X. (A) The Executive Committee is hereby designated to consist of not more than ten members, including the ex officio Members (Chairman of the Board of Trustees, President, Director, and Treasurer); and six additional Trustees, two of whom shall be elected by the Board of Trustees each year, to serve for a three-year term. Beginning with the members elected for terms ending in 1990, one of the Trustees elected to serve on the Executive Committee should be a Trustee-at-large. This procedure will be repeated in the class of 1991, and henceforth the Trustees will elect to the Executive Committee Trustees to ensure that the composition of the Committee is four Corporate Trustees and two Trustees-at-large.

(B) The Chairman of the Board of Trustees shall act as Chairman of the Executive Committee, and the President as Vice Chairman. A majority of the members of the Executive Committee shall constitute a quorum and the affirmative vote of a majority of those voting at any meeting at which a quorum is present shall constitute action on behalf of the Executive Committee. The Executive Committee shall meet at such times and places and upon such notice and appoint such subcommittees as the Committee shall determine.

(C) The Executive Committee shall have and may exercise all the powers of the Board during the intervals between meetings of the Board of Trustees except those powers specifically withheld from time to time by vote of the Board or by law. The Executive Committee may also appoint such committees, including persons who are not Trustees, as it may from time to time approve to make recommendations with respect to matters to be acted upon by the Executive Committee or the Board of Trustees.

(D) The Executive Committee shall keep appropriate minutes of its meetings and its action shall be reported to the Board of Trustees.

(E) The elected Members of the Executive Committee shall constitute a standing "Committee for the Nomination of Officers," responsible for making nominations, at each Annual Meeting of the Corporation, and of the Board of Trustees, for candidates to fill each office as the respective terms of office expire (Chairman of the Board, President, Director, Treasurer, and Clerk).

XI. A majority of the Trustees, the Executive Committee, or any other committee elected by the Trustees shall constitute a quorum; and a lesser number than a quorum may adjourn any meeting from time to time without further notice. At any meeting of the Trustees, the Executive Committee, or any other committee elected by the Trustees, the vote of a majority of those present, or such different vote as may be specified by law, the Articles of Organization or these Bylaws, shall be sufficient to take any action.

XII Any action required or permitted to be taken at any meeting of the Trustees, the Executive Committee or any other committee elected by the Trustees as referred to under Article IX may be taken without a meeting if all of the Trustees or members of such committee, as the case may be, consent to the action in writing and such written consents are filed with the records of meetings. The Trustees or members of the Executive Committee or any other committee appointed by the Trustees may also participate in meeting by means of conference telephone, or otherwise take action in such a manner as may from time to time be permitted by law.

XIII. The consent of every Trustee shall be necessary to dissolution of the Marine Biological Laboratory. In case of dissolution, the property shall be disposed of in such a manner and upon such terms as shall be determined by the affirmative vote of two-thirds of the Board of Trustees then in office.

XIV. These Bylaws may be amended by the affirmative vote of the Members at any meeting, provided that notice of the substance of the proposed amendment is stated in the notice of such meeting. As authorized by the Articles of Organization, the Trustees, by a majority of their number then in office, may also make, amend, or repeal these Bylaws, in whole or in part, except with respect to (a) the provisions of these Bylaws governing (i) the removal of Trustees and (ii) the amendment of these Bylaws and (b) any provisions of these Bylaws which by law, the Articles of Organization or these Bylaws, requires action by the Members.

No later than the time of giving notice of the meeting of Members next following the making, amending or repealing by the Trustees of any Bylaw, notice thereof stating the substance of such change shall be given to all Corporation Members entitled to vote on amending the Bylaws.

Any Bylaw adopted by the Trustees may be amended or repealed by the Members entitled to vote on amending the Bylaws.

XV. The account of the Treasurer shall be audited annually by a certified public accountant.

XVI. Except as otherwise provided below, the Corporation shall, to the extent legally permissible, indemnify each person who is, or shall have been, a Trustee, director or officer of the Corporation or who is serving, or shall have served, at the request of the Corporation as a Trustee, director or officer of another organization in which the Corporation directly or indirectly has any interest, as a shareholder, creditor or otherwise, against all liabilities and expenses (including judgments, fines, penalties and reasonable attorneys' fees and all amounts paid, other than to the Corporation or such other organization, in compromise or settlement) imposed upon or incurred by any such person in connection with, or arising out of, the defense or disposition of any action, suit or other proceeding, whether civil or criminal, in which he or she may be a defendant or with which he or she may be threatened or otherwise involved, directly or indirectly, by reason of his or her being or having been such a Trustee, director or officer.

The Corporation shall provide no indemnification with respect to any matter as to which any such Trustee, director or officer shall be finally adjudicated in such action, suit or proceeding not to have acted in good faith in the reasonable belief that his or her action was in the best interests of the Corporation. The Corporation shall provide no indemnification with respect to any matter settled or compromised, pursuant to a consent decree or otherwise, unless such settlement or compromise shall have been approved as in the best interests of the Corporation, after notice that indemnification is involved, by (i) a disinterested majority of the Board of Trustees or of the Executive Committee or, (ii) a majority of the Corporation's Members.

Indemnification may include payment by the Corporation of expenses in defending a civil or criminal action or proceeding in advance of the final disposition of such action or proceeding upon receipt of an undertaking by the person indemnified to repay such payment if it is ultimately determined that such person is not entitled to indemnification under the provisions of this Article XVI, or under any applicable law.

As used in this Article, the terms "Trustee," "director" and "officer" include their respective heirs, executors, administrators and legal representatives, and an "interested" Trustee, director or officer is one against whom in such capacity the proceeding in question or another proceeding on the same or similar grounds is then pending.

To assure indemnification under this Article of all persons who are determined by the Corporation or otherwise to be or to have been "fiduciaries" of any employee benefit plan of the Corporation which may exist from time to time, this Article shall be interpreted as follows: (i) "another organization" shall be deemed to include such an employee benefit plan, including without limitation, any plan of the Corporation which is governed by the Act of Congress entitled "Employee Retirement Income Security Act of 1974," as amended from time to time ("ERISA"); (ii) "Trustee" shall be deemed to include any person requested by the Corporation to serve as such for an employee benefit plan where the performance by such person of his or her duties to the Corporation also imposes duties on, or otherwise involves services by, such person to the plan or participants or beneficiaries of the plan; (iii) "fines" shall be deemed to include any excise taxes assessed on a person with respect to an employee benefit plan pursuant to ERISA; and (iv) actions taken or omitted by a person with respect to an employee benefit plan in the performance of such person's duties for a purpose reasonably believed by such person to be in the interest of the participants and beneficiaries of the plan shall be deemed to be for a purpose which is in the best interests of the Corporation.

The right of indemnification provided in this Article shall not be exclusive of or affect any other rights to which any Trustee, director or officer may be entitled under any agreement, statute, vote of members or otherwise. The Corporation's obligation to provide indemnification under this Article shall be offset to the extent of any other source of indemnification or any otherwise applicable insurance coverage under a policy maintained by the Corporation or any other person. Nothing contained in this Article shall affect any rights to which employees and corporate personnel other than Trustees, directors or officers may be entitled by contract, by vote of the Board of Trustees or of the Executive Committee or otherwise.

E. F. Armstrong

Jean-Pierre Rampal and Jelle Atema perform in the 14 August 1988 Centennial Benefit Concert.

Centennial Events Calendar

March

16 *Hoya Crystal reception* for the MBL.

April

29 *Panel Discussion on Learning and Memory.* Speakers included Daniel Alkon, Jerome Kagan, and David Hubel.

May

22–25 *The Cellular Basis of Morphogenesis* symposium honoring Dr. J. P. Trinkaus on his retirement from Yale University.

24 *Futures in Science* Student Presentations.

June

9, 10 *MBL Update.* Science writers and Science Writing Fellowship alumni met to learn about and discuss science as it is performed at the MBL.

15 *"Science in a Social World"* five-part, weekly lecture series, sponsored by the Boston University Marine Program Graduate Student Organization.

23–25 *Ionic Channels: Structure, Function, and Morphology* symposium.

24 *Centennial Evening Lecture:* Meredith Applebury, speaker.

26 *Associates' Brunch.*

30 *Cape Cod: A Diversity of Life* photo contest and exhibit (6/30 to 7/15).

July

1 *Centennial Evening Lecture:* Daniel Koshland, speaker.

1, 2 *"To See What Everyone Has Seen, To Think What No One Has Thought."* A symposium honoring the late Albert Szent-Györgyi.

8 *Centennial Evening Lecture* (Lang Lecture): Torsten Wiesel, speaker.

8 *Scientific Illustration—1560–1988 exhibit.*

9 *"Study Nature Not Books"* botany field trip.

14 *"Roadblocks and Breakthroughs in Scientific Discovery"* weekly history of science series opened.

15 *Centennial Evening Lecture:* Joshua Lederberg, speaker.

16 *Associates' Nautical Treasure Hunt.*

17 *Dedication Day* (the 100th anniversary of the MBL's opening)
Opening of Centennial Art Exhibit
Centennial Evening Lecture: Gerald Weissmann, speaker
MBL Birthday Party

21, 22 *Forbes Lectures:* Sydney Brenner, speaker.

22 *Albert M. and Ellen R. Grass Reference Room Dedication.*

29 *Centennial Evening Lecture:* Clay Armstrong, speaker.

P. L. Clapp

(From left) Katsuma Dan, former Dan Fellow Melanie Pratt, Daniel Mazia, Shinya Inoué, former Dan Fellow Ron Vale, and (kneeling) former Dan Fellow Carl Johnson at the 11 August 1988 "Reflections with Katsuma Dan and Daniel Mazia" centennial event.

August

4 *Cape and Islands Chamber Music Festival Concert.*

5 *Centennial Evening Lecture:* John Hobbie, speaker.

6 *National Academy of Sciences Reception.*

7 *Hiroshima Day Lecture:* Donald Kennedy, speaker.

11 *Reflections with Katsuma Dan and Daniel Mazia.*

12–19 *MBL Centennial Celebratory Week:*

12 Corporation Meeting
Dedication of Charles Ulrick Bay Reading Room
Trustees Meeting
Opening Ceremony
Centennial Evening Lecture: E. O. Wilson, speaker

14 Open Rehearsal for Benefit Concert
MBL Centennial Benefit Concert featuring new composition by Ezra Laderman. Performed by Jean-Pierre Rampal, Jelle Atema, and the Colorado Quartet

Old Timers return from their 16 August 1988 collecting trip.

15 Biomedical Applications of Basic Research symposium
16 Old Timers' Collecting Trip
Centennial Evening Lecture: Clifford Slaman, speaker
17 Old Timers' Day
19 Centennial Evening Lecture: Shinya Inoué, speaker
Closing Ceremony
20 *Cape and Islands Chamber Music Concert.*
22–24 *MBL General Scientific Meetings.*
26 *Centennial Evening Lecture:* John Gurdon, speaker.
27–30 *Developmental Biology of Sea Urchins* symposium.

September

3–6 *Ionic Currents in Development* symposium.

Reference: *Biol. Bull.* 177: 77–82. (August, 1989)

Contrasting Modes of Reproduction in Two Antarctic Asteroids of the Genus *Porania*, With a Description of Unusual Feeding and Non-feeding Larval Types

ISIDRO BOSCH

Institute of Marine Sciences and Biology Board of Studies, University of California, Santa Cruz, California 95064 and Department of Larval Ecology, Harbor Branch Institution Inc., Ft. Pierce, Florida 34946

Abstract. Reproduction and development were markedly different in two morphologically similar asteroids of the genus *Porania* that occur in shallow waters of McMurdo Sound, Antarctica. Adults of the recognized species, *Porania antarctica* (Perrier, 1894), are large (R_{max} = 70 mm) and have genital pores that are situated aborally on the disc; females broadcast spawn large numbers ($3–4 \times 10^4$) of buoyant eggs that measure 0.55 mm and develop into unusual, yolky planktotrophic larvae. In contrast, adults of the undescribed *Porania* sp. are considerably smaller (R_{max} = 30 mm) and their genital pores are located orally on the disc. Female fecundity is low (100–310 eggs); the few eggs produced measure 0.55 mm, are heavier than seawater, and develop into demersal lecithotrophic larvae. These differences conform to general patterns reported for echinoderms with divergent types of reproduction. However, other differences contradict established trends; specifically, *P. antarctica* with planktotrophic development has a shorter embryonic and larval phase (65 days *vs.* 78 days) and a larger juvenile size at metamorphosis (0.8 *vs.* 0.6 mm) than *Porania* sp., which has lecithotrophic development. The reproduction of *P. antarctica* incorporates advantages of both planktotrophic and lecithotrophic strategies and may be particularly well-suited for environmental conditions in the Antarctic Ocean.

Introduction

The larval development of echinoderms can be classified into general categories on the basis of mode of nutrition and habitat (Chia, 1974). Larvae may be lecithotrophic (non-feeding) or planktotrophic (feeding on particulate material); lecithotrophic larvae can be pelagic, demersal, or brooded, whereas planktotrophic larvae are nearly always pelagic (Young and Chia, 1987). Species with lecithotrophic development typically have a larger maximum egg size, reduced fecundity, abbreviated larval development, and greater juvenile size at metamorphosis than species with planktotrophic development (Strathmann, 1985; Emlet *et al.*, 1987). Intermediate reproductive strategies (*e.g.*, facultative planktotrophy), considered transitional and evolutionarily unstable by some theoretical modelers (Vance, 1973; Christiansen and Fenchel, 1979), are known or implied for several species of echinoids (Strathmann, 1979; Emlet, 1986) but seem to be generally rare among echinoderms.

Phylogenetically proximate echinoderm species that are nearly indistinguishable by morphological criteria often occur sympatrically and exhibit contrasting developmental strategies. With such strong similarities between species, these complexes provide useful systems for reliable analyses of the interrelationship between different reproductive traits (*e.g.*, egg size, larval type, juvenile size) and as such they have been the focus of several investigations (Atwood, 1973; Menge, 1975; Lawson-Kerr and Anderson, 1978; Emson and Crump, 1979; Scheibling and Lawrence, 1982; Emlet, 1986).

A pair of morphologically similar asteroids of the genus *Porania* co-occur in shallow waters of McMurdo Sound, Antarctica. The two types can be distinguished reliably by the position of the genital pores, which are found on the aboral surface in the recognized species, *Porania antarctica* (Perrier, 1894), and on the oral surface in the undescribed form, referred to here as *Porania* sp. This contrast was first recognized by H. E. S. Clark

Received 24 March 1989; accepted 31 May 1989.

(1963) and A. M. Clark (1962), who argued that a higher taxonomic ranking was warranted for the undescribed form. However, their observations did not lead to the description of a new species and at present the taxonomic standing of *Porania* sp. is unresolved (H. E. S. Clark, pers. comm.).

This paper describes differences in reproduction and development between *Porania antarctica* and *Porania* sp. that substantiate Clark's (1962) recommendation of distinct species rankings for the two forms. The findings of this study are compared to general patterns of reproduction in other echinoderms and discussed in the context of life-history evolution.

Materials and Methods

Adult sea stars were collected haphazardly by SCUBA divers at depths of 10–33 m beneath the annual sea ice in McMurdo Sound between Sept. 1984 and Dec. 1985. Immediately after collection, individuals were transported to McMurdo Station in ice chests filled with ambient seawater and maintained for up to several months in laboratory sea tables with flow-through seawater (−1.5°C). Spawning was induced by injection of 1-methyladenine (1-MA at 1×10^{-4} *M* in seawater) into the coelom. For each species, the diameters of 30–35 eggs selected haphazardly from two spawning females were measured using a compound microscope equipped with an ocular micrometer. The annual fecundity of females was estimated by direct count of spawned eggs for *Porania* sp. and by counting a known portion of the total spawn for *P. antarctica*. Spawned females were maintained in the laboratory for at least one week after a spawning event and treated daily with 1-MA to assure that most mature oocytes had been shed.

Embryos and larvae were reared at temperatures near their ambient (−1.5 to −1.0°C) in gently stirred or unstirred 4 L culture vessels following procedures established by Strathmann (1971), as modified for Antarctic asteroid larvae by Pearse and Bosch (1986). Larvae of *Porania antarctica* were fed every two days with equal amounts of xenic *Isochrysis galbana* and *Dunaliella tertiolecta* to a final concentration of $5–10 \times 10^3$ cells/ml in 5 μm-filtered seawater. No cultured food was added to vessels containing lecithotrophic larvae of *Porania* sp. Brachiolariae with well-developed rudiments were isolated in small glass dishes and induced to settle with substrates (*e.g.*, shell debris, small rocks, sediment) collected from adult habitats. Since competent brachiolariae of *P. antarctica* were usually buoyant, glass slides covered with a bacterial-algal film were suspended horizontally in midwater to facilitate settlement.

Results

Distribution and spawning

Porania antarctica were collected primarily at New Harbor (Fig. 1) during the austral spring and summer,

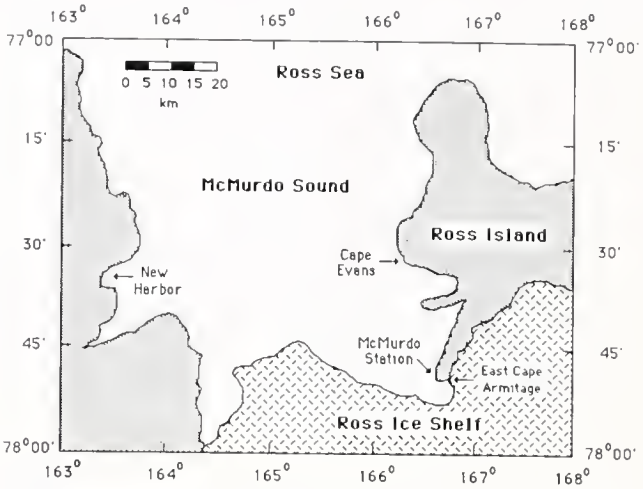

Figure 1. Sites in McMurdo Sound, Antarctica, where *Porania antarctica* and *Porania* sp. were collected.

1984 and 1985, when weather and sea ice conditions permitted access to this remote site. Only a few specimens were collected at E. Cape Armitage and McMurdo Station, usually below depths of 30 m. Adults were large, measuring up to 70 mm from the tip of the longest ray to the center of the disc (R). The ovaries of all females (n = 11) examined during the austral spring, 1984 and 1985, were small and contained only a few oocytes of the largest size class. Individuals (n = 9) collected in early February, 1985 did not respond to 1-MA; the dissected ovaries of one female were relatively small and devoid of fully grown oocytes. The remaining eight sea stars were maintained in laboratory sea tables until mid October and treated with 1-MA about every two months. Two of four females spawned in late September and the other two in early October. Males contained active sperm from early August to mid-October, as revealed by partial spawnings and biopsies of testicular lobes. Gametes were broadcast through aboral genital pores. Spawned oocytes, approximately $3–4 \times 10^4$ in number (n = 2 females), were of moderate size (548 ± 10 μm, n = 30), opaque yellow in color, and buoyant.

Individuals of *Porania* sp. were generally rare and only 20 were collected during this study: 14 from East Cape Armitage, and 3, 2, and 1 from McMurdo Station, Cape Evans, and New Harbor, respectively. Adults were small, with R ranging from 10–30 mm. Females were induced to spawn with 1-MA in November (n = 2) and December (n = 1), 1984, and in February (n = 1), April (n = 2), and July (n = 1), 1985. Males examined during each of these sampling dates contained active sperm. Although similar in size (554 ± 16 μm, n = 35) and lipid content (50–60% of dry weight; J. McClintock, unpubl. data) to the eggs of *Porania antarctica*, the few eggs (100–310, n = 4) produced by *Porania* sp. were free-spawned through oral

Table I

Embryonic and planktotrophic larval development of Porania antarctica *reared at −1.5 to −1.0°C*

Developmental stage	First appearance (days)	Size* (mm)
Zygote	0	0.55
Two-cell embryo	0.42	—
Coeloblastula	3.2	—
Hatched blastula	5.8	—
Gastrula	12	0.70
Bi-lobed larva	20	0.76
Bipinnaria	22	0.80
Brachiolaria	40	1.1
Juvenile	65	0.79

* Refer to the diameter of zygotes and juveniles and the maximum length of all other stages.

genital pores and immediately settled onto the bottom of culture dishes.

Planktotrophic development of Porania antarctica

With several important exceptions described below, the development from fertilization to metamorphosis of *Porania antarctica* is similar to that of the north temperate asteroid *Porania pulvillus* (Gemmill, 1915) and generally follows the typical pattern of asteroids with feeding larvae (Table I).

Early cleavage divisions were slow at −1.5 to −1.0°C; morula and blastula stages were reached approximately 2.0 and 3.2 days after fertilization, respectively. By the fifth day of development, blastulae had developed a rich, active ciliary field. Hatched blastulae were highly buoyant and seemed to have little control over their vertical position; they usually floated near the water surface in stirred as well as unstirred culture vessels. Gastrulation by invagination was accompanied by substantial expansion of the larva, which attained a length of nearly 0.7 mm by the 12th day of development.

Young bipinnariae were large, and judging from their coloration and buoyancy, retained a substantial proportion of the maternal yolk. At this stage the mouth is open and connects to the digestive tract, which is divided into an esophagus, stomach, and intestine. There followed a period of significant differentiation but of little apparent increase in size, as evidenced by the extension of the axohydrocoels, which by the 27th day had fused anteriorly forming a U-shape around the esophagus.

After 32 days of development, an adhesive disc formed in the presumptive region of the brachiolarian complex. Brachiolarian arms were first observed on the 40th day of development. The various ciliated arms characteristic of planktotrophic asteroid larvae are lacking in *Porania antarctica*. Early brachiolariae measured 1.1 mm in length and grew very little to attain their final form (Fig. 2). Over the next 25 days, the brachiolarian arms increased gradually in size and developed an arrangement of adhesive papillae. Sixty-five days after fertilization, the larvae were competent to metamorphose. Some would swim along the bottom of dishes and temporarily attach themselves by their brachiolarian arms. However, most fully developed brachiolariae (83%, n = 53) were positively buoyant and remained near the water surface. They attached and metamorphosed on the sides of dishes and underneath floating objects rather than on the bottom. Newly metamorphosed juveniles (0.79 ± .04 mm diameter, n = 9) had well-differentiated arms and retained the opaque, yellowish coloration of the egg.

Lecithotrophic development of Porania *sp.*

A chronology of development is given in Table II. Early cleavage followed the typical pattern of asteroids, but the rate of development was extremely slow; an early blastula stage was not reached until 12 days after fertilization. Embryos hatched as ciliated blastulae that were negatively buoyant and moved along the bottom of culture vessels by ciliary action. Gastrulation was by invagination, leading to the formation of a blastopore that was widely open at first, but gradually narrowed and disappeared during later stages of development. The gastrula reached 0.6 mm by the 26th day of development, when a small lobe first became evident on the anterior end (Fig. 3A). Continued expansion in this fashion resulted in the formation of a generally ciliated, pear-shaped larva that consisted of a large, rounded posterior lobe and a narrow

Figure 2. Feeding brachiolaria of *Porania antarctica*. The opacity of this larva is likely due to an abundance of yolk. Note the absence of ciliated larval arms, which are typically used in swimming and feeding by planktotrophic asteroid larvae.

Table II

Embryonic and lecithotrophic larval development of the undescribed asteroid Porania *sp. reared at −1.5 to −1.0°C*

Developmental stage	First appearance (days)	Size* (mm)
Zygote	0	0.55
Hatched blastula	15	—
Early gastrula	21	0.57
Late gastrula	26	0.60
Pear-shaped larva	38	0.76
Early brachiolaria	47	0.80
Late brachiolaria	68	1.20
Juvenile	75	0.60

* Refer to the diameter of zygotes and juveniles and the maximum length of all other stages.

anterior lobe and was entirely lacking feeding structures (Fig. 3B). These larvae were negatively buoyant and usually swam near or on the bottom of stirred and unstirred culture vessels with the anterior lobe foremost and the anterioposterior axis in a horizontal attitude.

Three bulbous arms first formed 47 days after fertilization: a single median anterodorsal arm, and a pair of ventrolateral arms that occupy a region near the base of the narrow anterior lobe (Fig. 3C). Soon after, each arm was able to adhere temporarily to glass surfaces, and an adhesive disc had differentiated central to them. Therefore, the larva can be considered a modified brachiolaria. Fully developed brachiolariae (Fig. 3D) measured 1.2 mm in length. Attachment to a substratum was initially accomplished by the brachiolarian arms and the adhesive disc. Metamorphosis included the complete degeneration of the anterior lobe, and lasted from one to two weeks. During this period, some larvae detached from the bottom and continued to swim for hours to days. Final attachment was facilitated by the tube feet of the juvenile rudiment. The newly metamorphosed sea star, about 0.60 ± 0.03 mm across (n = 10), had two pairs of tube feet on each of its 5 arms. The arms were short and difficult to distinguish due to the presence of yolk on the aboral surface of the disc.

Discussion

In echinoderms, and particularly asteroids, there are considerable differences (*e.g.*, egg size, larval morphology) between planktotrophic and lecithotrophic developmental strategies (Strathmann, 1974; Emlet *et al.*, 1987). One interpretation of this phenomenon is that types of development intermediate of planktotrophy and lecithotrophy are evolutionarily transitional and short lived (Vance, 1973). However, possible intermediate strategies do appear in some species, particularly among echinoids. Planktotrophic echinoplutei of *Clypeaster rosaceus* develop from relatively large eggs and do not require particulate food to complete development to metamorphosis (Emlet, 1986). A similar mode of development (*i.e.*, facultative planktotrophy) is suggested for echinoplutei of the spatangoid *Brisaster latifrons* (Strathmann, 1979) and judging from some egg sizes reported by Emlet *et al.* (1987) may occur in several other echinoids (*e.g., Sterechinus agassizi, Brisaster fragilis*).

Additional studies are necessary to adequately evaluate the ecological and evolutionary significance of the unusual development described here for *Porania antarctica*. Nonetheless, it is evident that features of both lecithotrophic and planktotrophic strategies are manifested in this species. The larvae feed on bacteria (Rivkin *et al.*,

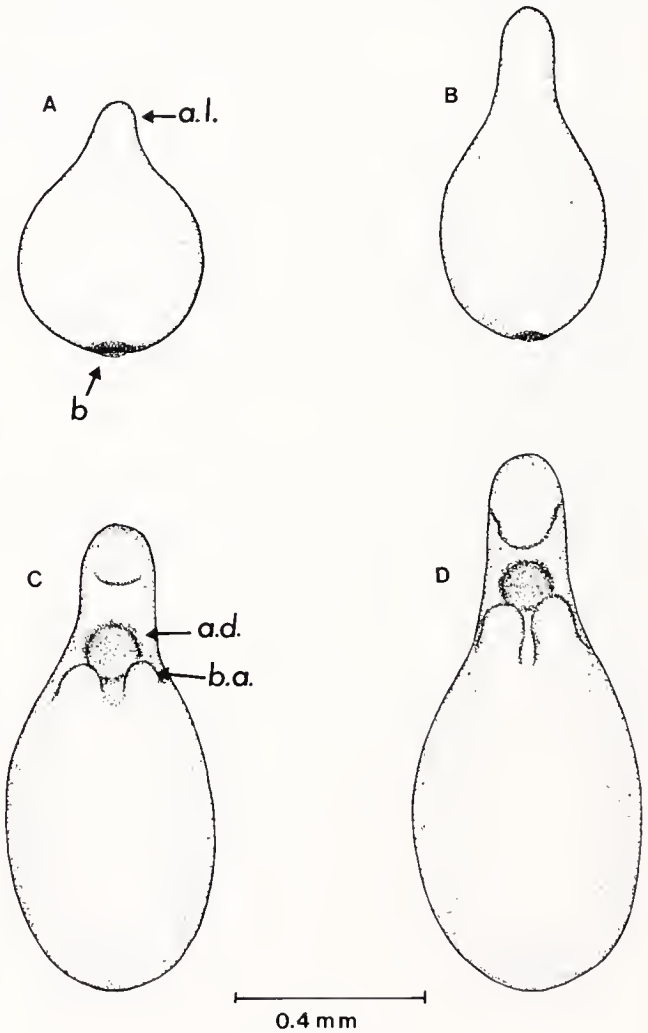

Figure 3. Larval stages of *Porania* sp. (A) Post-gastrula 26 days after fertilization with a small anterior lobe, large posterior lobe, and blastopore. (B) Pear-shaped larva (38 days) showing increased development of the anterior lobe. (C) Early modified brachiolaria 47 days after spawning. Three brachiolarian arms and an adhesive disc have formed on the preoral lobe. (D) Fully developed brachiolaria 68 days after spawning. ad, adhesive disc; al, anterior lobe; b, blastopore; ba, brachiolarian arms.

1986) but, unlike other planktotrophic asteroid larvae, they develop from buoyant eggs containing large lipid yolk reserves (J. McClintock, unpubl. data) and produce an unusually large juvenile at metamorphosis. The characters cited above may contribute to several other unique developmental features of *P. antarctica*. These include: (1) an absence of ciliated arms that aid swimming and feeding in other larvae (Strathmann, 1974), and (2) the metamorphosis of larvae almost exclusively on the sides of culture dishes and undersides of suspended glass slides.

One possible advantage conferred on feeding larvae that develop from larger eggs is an abbreviated larval phase (Vance, 1973; McEdward, 1984; Emlet, 1986). Accordingly, the period from fertilization to metamorphosis of *P. antarctica* is less than half that of another planktotrophic antarctic asteroid, *Odontaster validus* (Pearse and Bosch, 1986). Indeed, at 65 days the developmental period of *P. antarctica* is similar to that of some temperate asteroids reared at their ambient temperatures (Emlet *et al.*, 1987). The production of a fully developed feeding larva from a larger, yolk-laden egg apparently requires less growth and differentiation. In low temperature environments such as the Antarctic, these differences are translated into a considerable reduction in development time, presumably leading to a concomitant decrease in the risk of mortality associated with a pelagic feeding larval phase.

In contrast to *Porania antarctica*, eggs spawned by *Porania* sp. were negatively buoyant. The larvae were lecithotrophic, and judging from their distribution and swimming behavior in culture vessels most likely are demersal in nature. As in *Porania* sp., larvae of *Asterina minor* also are heavier than seawater and pass through a pear-shaped brachiolaria stage (Komatsu *et al.*, 1979). Hatching of *A. minor* brachiolariae from an attached egg case occurs on the 9th day of development and is followed by a brief (*ca.* 1 day) demersal stage that precedes metamorphosis. In *Porania* sp., the free-swimming demersal larval phase lasts about two months. With the exception of one other Antarctic sea star, *Acodontaster hodgsoni* (Bosch and Pearse, in press), this is the longest period of development to first metamorphosis reported for asteroids with lecithotrophic larvae (Emlet *et al.*, 1987).

In previous studies of morphologically similar, sympatric asteroids with contrasting developmental strategies (Atwood, 1973; Lawson-Kerr and Anderson, 1978; Emson and Crump, 1979; Scheibling and Lawrence, 1982), distinction of the morphs or species has been made principally on the basis of egg size and embryonic or larval habitat (*e.g.*, pelagic *vs.* brooded). By comparison, the differences reported here for *Porania* sp. and *P. antarctica* (Table III), including sharp contrasts in larval form and mode of nutrition, represent a case of extensive divergence. Such cases are relatively common in some invertebrate taxa, particularly polychaete annelids and gastropod molluscs (Perron, 1981; Hoagland and Robertson, 1988), but seem to be unusual in the Echinodermata.

Table III

Summary of major known differences between Porania antarctica *and* Porania *sp.*

Trait	*Porania antarctica*	*Porania* sp.
1) Morphology	Aboral genital pores	Oral genital pores
2) Adult size (R)	Maximum 70 mm	Maximum 30 mm
3) Timing of reproduction	Seasonal (Sept.?–Oct.)	Year-round
4) Fecundity (# eggs)	*ca.* 35,000	100–310
5) Larval type	Modified planktotrophic, pelagic	Lecithotrophic, demersal

Among related, sympatric echinoderms, those with larger adults tend to have an extended planktonic larval phase and produce relatively small juveniles at metamorphosis. Small adult size is associated with brooding or an abbreviated non-feeding larval phase and the production of fewer, larger offspring which presumably have a greater chance of survival (*e.g.*, Schoener, 1972; Menge, 1975; Lawson-Kerr and Anderson, 1978; Hendler, 1979). Strathmann and Strathmann (1982) reviewed several possible explanations for this phenomenon. One common explanation links brooding and other forms of non-pelagic development to energetic constraints on reproductive output (Menge, 1975). According to this hypothesis, small adults cannot produce sufficient offspring to benefit from the enhanced dispersal of a typically high-risk pelagic larval phase. In the *Porania* studied here, pelagic feeding development was associated with large adult size and high fecundity in *P. antarctica*. The smaller *Porania* sp. have considerably lower fecundity (*ca.* two orders of magnitude less) and develop non-pelagically. On the other hand, planktotrophic larvae of *P. antarctica* had a shorter developmental period and produced larger juveniles. Therefore, Menge's (1975) hypothesis is applicable only if larval mortality rates in the plankton are much higher than near the bottom. Comparisons of this type have not been made (see Strathmann, 1985; Young and Chia, 1987). One possible consideration is the tendency for pelagic larvae to be swept by currents far from areas suitable for settlement and post-settlement survival, as shown, for example, for continental slope ophiuroids by Gage and Tyler (1981). A second possibility is that predation is much lower on demersal larvae. However, possible larval predators such as polychaetes and small crustaceans are common in shallow antarctic benthic habitats (Oliver, 1979; Marinovic,

1987). Indeed, several species, including the tanaid *Nototanais dimorphus* and the small infaunal actinian *Edwardsia meridionalis* often attain mean densities of more than 15,000 m^{-2} (Oliver, 1979). How a few larvae produced by *Porania* sp. escape these predators over several weeks of development and recruit successfully into benthic populations is a question of considerable interest.

Acknowledgments

I thank B. Marinovic, R. Britton, and J. Bernhard for assistance in collecting animals; H. E. S. Clark for invaluable help in identifying sea stars; A. Russell for assistance with graphics; and the Antarctic Services Inc. of ITT, the Antarctic support services of the National Science Foundation, and the U.S. Navy Antarctic Support Force for their logistic support. M. Barker, J. McClintock, A. T. Newberry, and J. Pearse reviewed drafts of the manuscript and I thank them for their valuable suggestions. This work was supported by an NSF grant (#DPP-8317082) to John S. Pearse and by a Harbor Branch Institution postdoctoral fellowship. Harbor Branch Oceanographic Institution Contribution # 713.

Literature Cited

Atwood, D. G. 1973. Larval development of the asteroid *Echinaster echinophorous*. *Biol. Bull.* **144:** 1–11.

Bosch, I., and J. S. Pearse. 1989. Developmental types of shallow-water asteroids in McMurdo Sound, Antarctica. *Mar. Biol.*, in press.

Chia, F.-S. 1974. Classification and adaptive significance of developmental patterns in marine invertebrates. *Thalassia Jugosl.* **10:** 121–130.

Christiansen, F. B., and T. M. Fenchel. 1979. Evolution of marine invertebrate reproductive patterns. *Theor. Popul. Biol.* **16:** 267–284.

Clark, A. M. 1962. Asteroidea. *British Museum Antarctic Exped. Rpts.* Series B, 9: 1–143.

Clark, H. E. S. 1963. The fauna of the Ross Sea. Part 3. Asteroidea. *N. Z. Dept. Sci. Ind. Res. Bull.* **151:** 1–84.

Emlet, R., 1986. Facultative planktotrophy in the tropical echinoid *Clypeaster roseaceus* and a comparison with obligate planktotrophy in *Clypeaster subdepressus* (Clypeasteroidea: Echinoidea). *J. Exp. Mar. Biol. Ecol.* **95:** 183–202.

Emlet, R., L. R. McEdward, and R. R. Strathmann. 1987. Echinoderm larval ecology viewed from the egg. Pp. 145–156 in *Echinoderm Studies 2*, M. Jangoux and J. M. Lawrence, eds. Balkema Press, Holland.

Emson, R. H., and R. G. Crump. 1979. Description of a new species of *Asterina* (Asteroidea), with an account of its ecology. *J. Mar. Biol. Assoc. U. K.* **59:** 77–94.

Gage, J. D., and P. A. Tyler. 1981. Non-viable seasonal settlement of larvae of the upper bathyal brittle star *Ophiocten gracilis* in the Rockall Trough abyssal. *Mar. Biol.* **64:** 153–161.

Gemmill, J. 1915. The larva of the starfish *Porania pulvillus*. *Q. J. Microsc. Sci.* **61:** 27–53.

Hendler, G. 1979. Sex-reversal and viviparity in *Ophiolepis keiri*, n. sp., with notes on viviparous brittlestars from the Caribbean (Echinodermata: Ophiuroidea). *Proc. Biol. Soc. Wash.* **92:** 783–795.

Hoagland, K. E., and R. Robertson. 1988. An assessment of poecilogony in marine invertebrates: phenomenon or fantasy? *Biol. Bull.* **174:** 109–125.

Komatsu, M., Y. T. Kano, H. Yoshizawa, S. Akabane, and C. Oguro. 1979. Reproduction and development of the hermaphroditic sea star, *Asterina minor* Hayashi. *Biol. Bull.* **157:** 258–274.

Lawson-Kerr, C., and D. T. Anderson. 1979. Reproduction, spawning and development of the starfish *Patiriella exigua* (Lamarck) (Asteroidea: Asterinidae) and some comparisons with *P. calcar* (Lamarck). *Aust. J. Mar. Freshwater Res.* **29:** 45–53.

Marinovic, B. 1987. Reproductive biology of the protogynous hermaphrodite *Nototanais dimorphus* (Beddard), an antarctic tanaid. Masters Thesis, Univ. of California, Santa Cruz, CA.

Menge, B. A. 1975. Brood or broadcast? The adaptive significance of different reproductive strategies in the two intertidal sea stars *Leptasterias hexactis* and *Pisaster ochraceus*. *Mar. Biol.* **31:** 87–100.

McEdward, L. 1984. Some relationships between egg size and the allometry of larval growth in echinoid plutei. *Am. Zool.* **24:** 46A.

Oliver, J. S. 1979. Processes affecting the organization of marine soft bottom communities in Monterey Bay, California and McMurdo Sound, Antarctica. Doctoral Dissertation, Scripps Inst. of Oceanogr., La Jolla, CA.

Pearse, J. S., and I. Bosch. 1986. Are the feeding larvae of the commonest Antarctic asteroid really demersal? *Bull. Mar. Sci.* **39:** 477–484.

Perron, F. E. 1981. Larval biology of six species of the genus *Conus* (Gastropoda: Toxoglossa) in Hawaii, USA. *Mar. Biol.* **61:** 215–220.

Rivkin, R. B., I. Bosch, J. S. Pearse, and E. J. Lessard. 1986. Bacterivory: a novel feeding mode in asteroid larvae. *Science* **233:** 1311–1314.

Scheibling, R. E., and J. M. Lawrence. 1982. Differences in reproductive strategies of morphs of the genus *Echinaster* (Echinodermata: Asteroidea) from the eastern Gulf of Mexico. *Mar. Biol.* **70:** 51–62.

Schoener, A. 1972. Fecundity and possible mode of development of some deep-sea ophiuroids. *Limnol. Oceanogr.* **17:** 193–199.

Strathmann, R. R. 1971. The feeding behavior of planktotrophic echinoderm larvae: mechanisms, regulation and rates of suspension feeding. *J. Exp. Mar. Biol. Ecol.* **6:** 109–150.

Strathmann, R. R. 1974. Introduction to function and adaptation in echinoderm larvae. *Thalassia Jugosl.* **10:** 321–339.

Strathmann, R. R. 1979. Echinoid larvae from the northeast Pacific (with a key and comment on an unusual type of planktotrophic development). *Can. J. Zool.* **57:** 610–616.

Strathmann R. R. 1985. Feeding and nonfeeding larval development and life-history evolution in marine invertebrates. *Ann. Rev. Ecol. Syst.* **16:** 339–361.

Strathmann R. R., and M. F. Strathmann. 1982. The relation between adult size and brooding in marine invertebrates. *Am. Nat.* **119:** 91–101.

Vance, R. R. 1973. On reproductive strategies in marine benthic invertebrates. *Am. Nat.* **107:** 339–352.

Young C. M. and F.-S. Chia. 1987. Abundance and distribution of pelagic larvae as influenced by predation, behavior, and hydrography. Pp. 385–442 in *Reproduction of Marine Invertebrates*, Vol IX, A. C. Giese, J. S. Pearse and V. B. Pearse, eds. Blackwell/Boxwood, Palo Alto, CA.

Reference: *Biol. Bull.* **177**: 83–95. (August, 1989)

Bilateral Asymmetry in the Shell Morphology and Microstructure of Early Ontogenetic Stages of *Anomia simplex*

S. CYNTHIA FULLER, RICHARD A. LUTZ, AND YA-PING HU

Institute of Marine and Coastal Sciences, Rutgers University, New Brunswick, New Jersey 08903

Abstract. Scanning electron microscopic examination of the valves of *Anomia simplex* larvae and postlarvae provides details of bilateral asymmetry in shell morphology and microstructure. Central provincular denticles and larger anterior and posterior hinge teeth develop in both valves. The umbo of the left valve becomes increasingly prominent with larval development, whereas no umbo is evident in the right valve. Thus, right and left valves of the prodissoconch differ markedly in height.

In the left valve of the dissoconch, union of antero- and posterodorsal shell margins above the hinge causes lateral, exterior displacement of the umbo. The internal ligament extends ventrally to the right valve. Thin antero- and posterodorsal shell margins of the right valve extend centrally against the substrate and eventually unite exterior to the ligament. An increasingly larger byssal foramen, with a flexible, organic covering, is formed in the right valve.

The outer layer of the left valve of the dissoconch is foliated calcite, whereas the outer layer of the right valve is composed of short, calcitic prisms. Inner shell layers consist of crossed lamellar and complex crossed lamellar microstructure, as well as myostracal prisms.

Introduction

The Anomiidae are noted for striking dissimilarity of the right and left valves. Bilateral asymmetry of the shell, which ultimately is an adaptation for secure attachment to the substrate (Yonge, 1977), begins in early larval stages. A prominent umbo characterizes the highly convex left valve; in contrast, an umbo is not apparent in the nearly flat right valve (Stafford, 1912; Miyazaki, 1935; Lebour, 1938; Jørgensen, 1946; Sullivan, 1948; Loosanoff *et al.*, 1966; Chanley and Andrews, 1971; Yonge, 1977; Le Pennec, 1978; Booth, 1979). Larval hinge dentition in the Anomiidae is taxodont; each valve has a series of small, central teeth and 2–5 anterior and posterior teeth, which enlarge during the larval period (Jørgensen, 1946; Yonge, 1977; Le Pennec, 1978, 1980). In some anomiids, formation of additional anterior and posterior provincular teeth in the left valve results in bilateral asymmetry of the larval hinge (Le Pennec, 1978, 1980).

After metamorphosis, the right (lower) valve develops an expansive foramen through which a calcified byssus attaches to the substrate (except in some free-living anomiids), while the left valve shows heightened shell growth along the antero- and posterodorsal margins, which eventually unite dorsally, above the hinge (Taylor *et al.*, 1969; Yonge, 1977; Le Pennec, 1978; Prezant, 1984). This "supradorsal" growth in the left valve leads to lateral displacement of the umbo and ventral extension of the ligament to the dorsal region of the crurum of the right valve (Yonge, 1977). [Crurum, used in the sense of Beu (1967) and Yonge (1977, 1980), refers to the prominent chondrophore in the right valve of the Anomiacea.]

In some anomiids, calcitic foliated microstructure is the principal structural type in both right and left adult valves, while in other anomiids, the left valve is predominantly foliated calcite, and the right valve is primarily prismatic calcite (Beu, 1967; Kobayashi, 1969; Taylor *et al.*, 1969; Waller, 1978; Yonge, 1980). An inner layer of aragonitic crossed or complex crossed lamellar microstructure surrounds the muscle scars in the left valve and the byssal foramen and muscle scar in the right valve (Taylor *et al.*, 1969; Waller, 1978). As in other bivalves, the myostracum is prismatic aragonite (Taylor *et al.*, 1969; Waller, 1978; Carter, 1980a).

The present scanning electron microscopic study pro-

Received 28 November 1988; accepted 23 May 1989.

vides a comprehensive description of the bilateral asymmetry in shell morphology and microstructure of early ontogenetic stages of *Anomia simplex* d'Orbigny, the common jingle shell of the western Atlantic. Details of shell morphological development are documented with micrographs of sequential stages. Comparison of early shell morphology in various North Atlantic anomiids reveals features useful in studies concerning species identification and taxonomy. A summary of the bilateral asymmetry in shell morphology and microstructure of early ontogenetic stages of four other common, inequivalve pteriomorphs from the North Atlantic is included.

Materials and Methods

Adult specimens of *Anomia simplex* were collected in Wachapreague Inlet, Virginia, and were spawned by raising the ambient water temperature from 25 to 30°C. Larvae were cultured in filtered (50 μm mesh) baywater (salinity = 32–34 ‰; temperature = 22.4–32.0°C) using standard techniques (Loosanoff and Davis, 1963). When larvae approached metamorphosis, a layer of eggshells was placed at the bottom of the culture tank. Spat on the eggshells and on the sides of the tank were attached loosely and were removed easily for sampling.

Samples from larval cultures were treated with a 5.25% solution of sodium hypochlorite for 10 min to remove soft tissues (after Rees, 1950); disarticulated valves were rinsed with distilled water. Soft tissues were dissected from postlarval specimens with a small brush. The pliable nature of postlarval right valves required careful placement as shells were mounted on silver tape. All specimens were coated with approximately 600 Å of gold-palladium and were documented with an ETEC Autoscan scanning electron microscope. Positioning disarticulated valves with selected points on the shell margin aligned in a plane normal to the electron beam of the microscope resulted in consistent orientation for documentation of shape. Photographs of a standard grid at the same magnification as each shell specimen provided accurate dimensions of shell features. Shell length is defined as the greatest anteroposterior shell dimension; shell height refers to the greatest measurement perpendicular to the hinge line. Terminology for juvenile and adult ligament components is that of Yonge (1977, 1980). Microstructural terminology is taken from Carter (1980b) and Carter and Clark (1985). Microstructural varieties of inner shell layers were determined by examination with reflected light and scanning electron microscopy.

Results

Right and left valves of the prodissoconch I range from 75 to 80 μm long ($\bar{x} \pm SD = 76.4 \pm 2.1$; n = 10). The inequivalve nature of *Anomia simplex* is evident at a

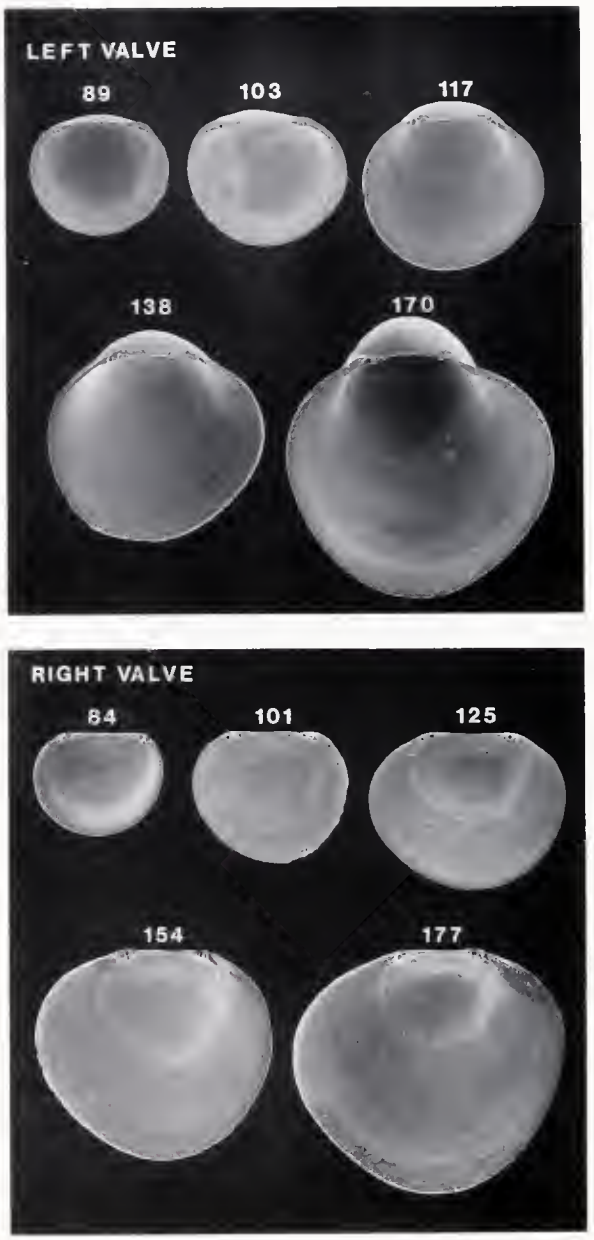

Figure 1. Scanning electron micrographs of disarticulated valves of *Anomia simplex* larvae. Numbers indicate shell lengths in μm.

shell length of 85–90 μm, as a result of formation of a low, rounded umbo in the left valve (Figs. 1, 2). Left valves are equidimensional at approximately 140 μm; shell height exceeds shell length during late larval stages. In the right valve, shell height is less than shell length throughout the larval period (Fig. 1).

Provinculum length ranges from 54 to 62 μm ($\bar{x} \pm SD = 57.1 \pm 2.8$ μm; n = 18). A series of minute, irregular denticles extends across the central portion of the provinculum in early larval valves; these interlocking denticles are slightly larger and more distinct in late larval stages (Fig. 2). Pairs of teeth, which also grow with larval devel-

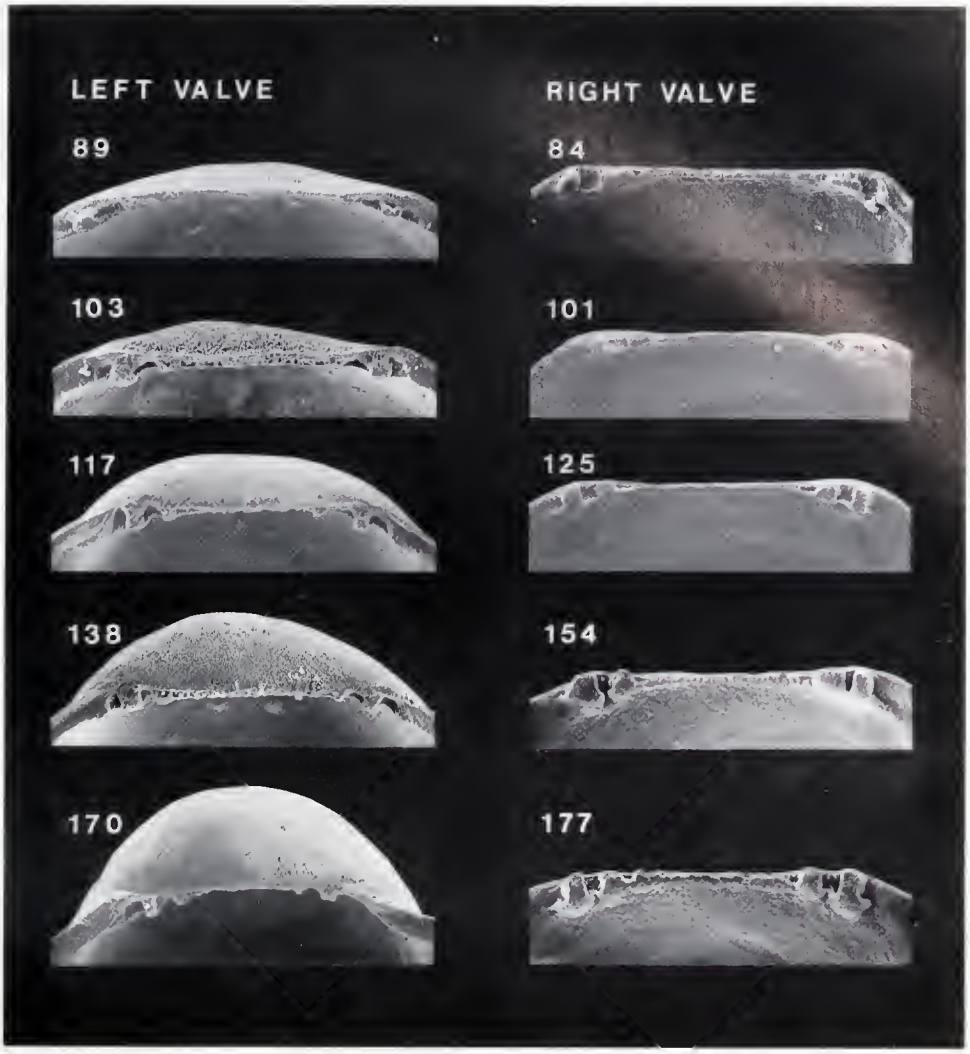

Figure 2. Scanning electron micrographs of the hinge of disarticulated valves of *Anomia simplex* larvae seen in Figure 1. Numbers indicate shell lengths in μm.

opment, form at the anterior and posterior extremes of the provinculum (Fig. 2). Articulation of the hinge teeth shifts gradually from a lateral to a dorsoventral orientation; in the right valve at a length of approximately 155 μm, anterior and posterior provincular teeth extend dorsally over the shell margin (Fig. 2).

The first morphological evidence of postlarval development is formation of a ligament pit at a shell length of approximately 190 μm, at which size central provincular denticles are mostly obliterated (Figs. 3, 4). Lengths of right and left valves are equal at this stage, but the left valve is approximately 24 μm higher than the right valve. Supradorsal growth of the left valve begins at a shell length of approximately 240 μm (Fig. 3). Bold margins of foliated microstructure expand first dorsally and then centrally across the umbo (Figs. 3, 5). By a shell length of approximately 1050 μm, supradorsal extensions are as high as the umbo, and anterior and posterior provincular teeth are obsolete (Figs. 3, 4). Anterior and posterior shell margins extend approximately 200 μm above the hinge before they unite centrally (Fig. 6). Supradorsal union of the antero- and posterodorsal shell extensions is complete in specimens approximately 1600 μm long (Fig. 3). The gap between the two margins is no longer visible in juvenile specimens approximately 5.5 mm long (Figs. 7, 8). At this size, several adult shell morphological features are recognizable, including the laterally displaced umbo, the differentiated inner and outer layers of the ligament, and three central muscle scars of myostracal prisms (Figs. 7–9). The inner layer surrounding the muscle scars is mostly fine and irregular complex crossed lamellar aragonite (Figs. 8, 10). The principal microstructural component of the left valve is foliated calcite (Figs. 7, 11).

A semicircular ligament pit, which is approximately 21 μm long, lies in the center of the hinge of the right valve of early postlarval specimens ranging from 190 to

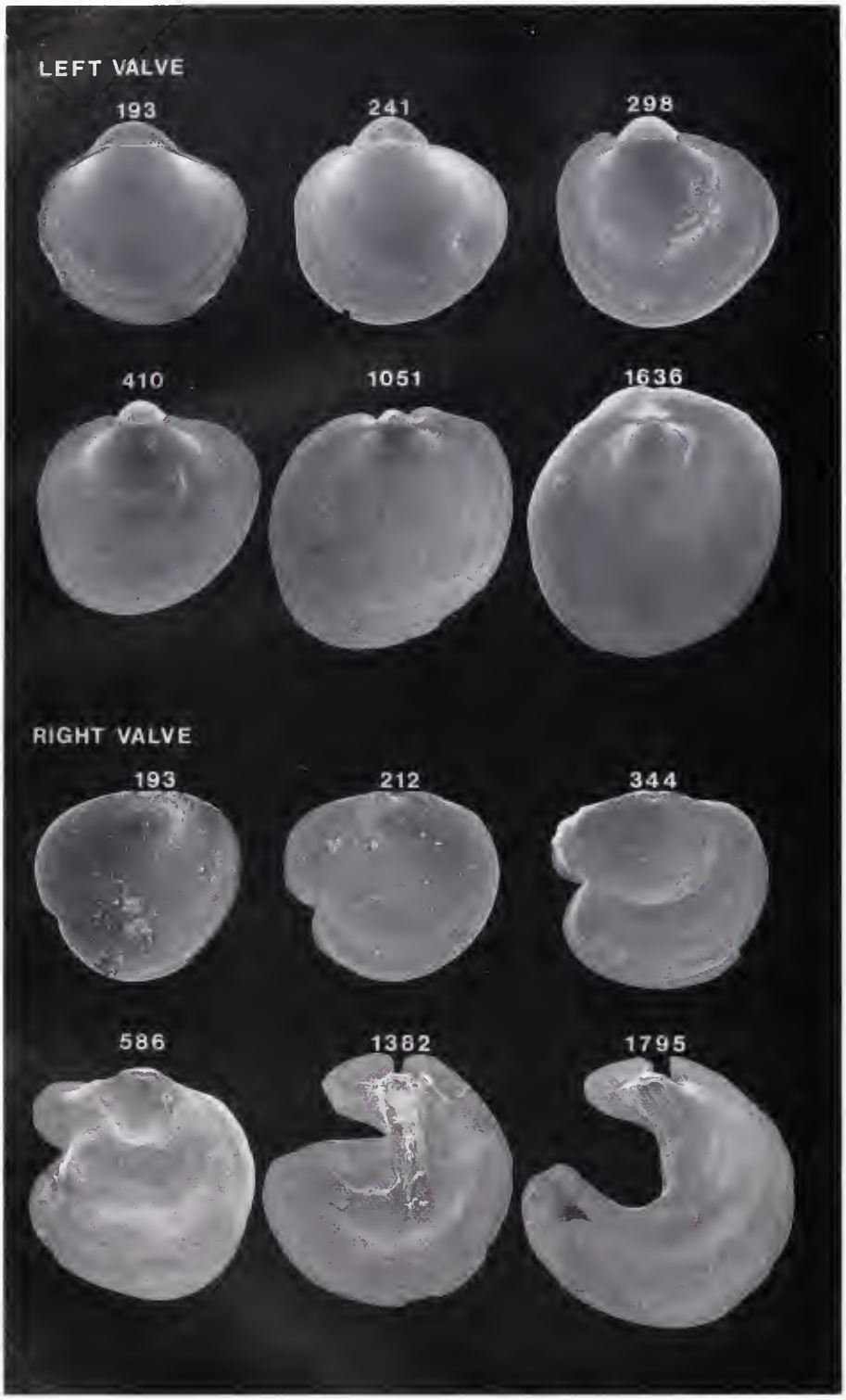

Figure 3. Scanning electron micrographs of disarticulated valves of *Anomia simplex* postlarvae. Numbers indicate shell lengths in μm.

240 μm long (Figs. 3, 4). In specimens approximately 350 μm long, anterior and posterior provincular teeth are obscured, and the ligament pit is positioned dorsally to the hinge (Fig. 4). At a shell length of 500–700 μm, the anterodorsal and anteroventral shell margins are united immediately adjacent to the byssal notch but are separated anteriorly by the byssal foramen (Figs. 3, 12, 13). At a shell length of 700–900 μm, the posteroventral re-

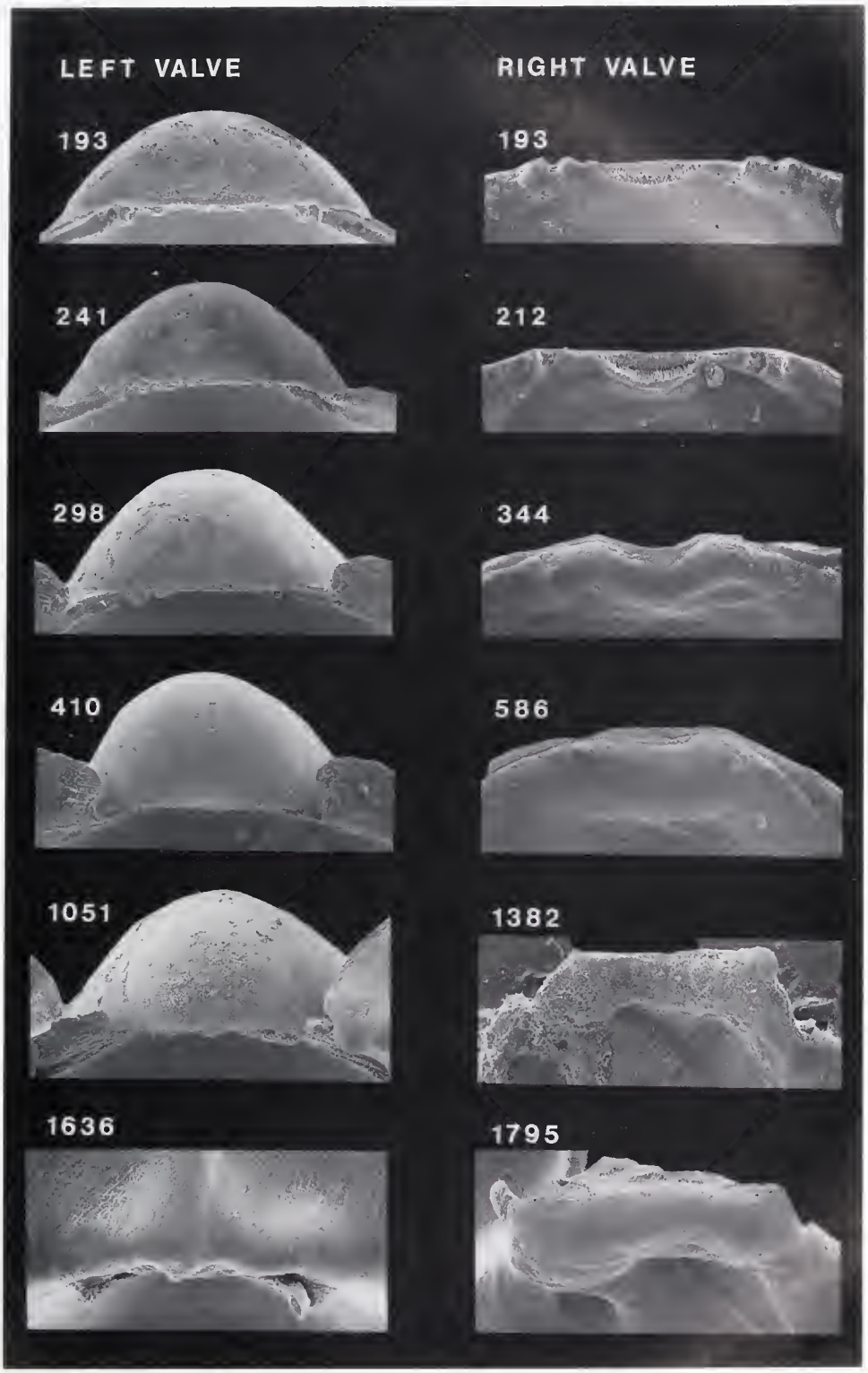

Figure 4. Scanning electron micrographs of the hinge of disarticulated valves of *Anomia simplex* postlarvae seen in Figure 3. Numbers indicate shell lengths in μm.

gion of the byssal foramen is covered by a flexible, organic sheet, which is continuous with the adjacent prismatic outer shell layer and is mostly calcified along the anterior edge (Figs. 14–16). Expansion of the anterodorsal and anteroventral shell margins enlarges the byssal foramen anteriorly, while resorption of the shell extends

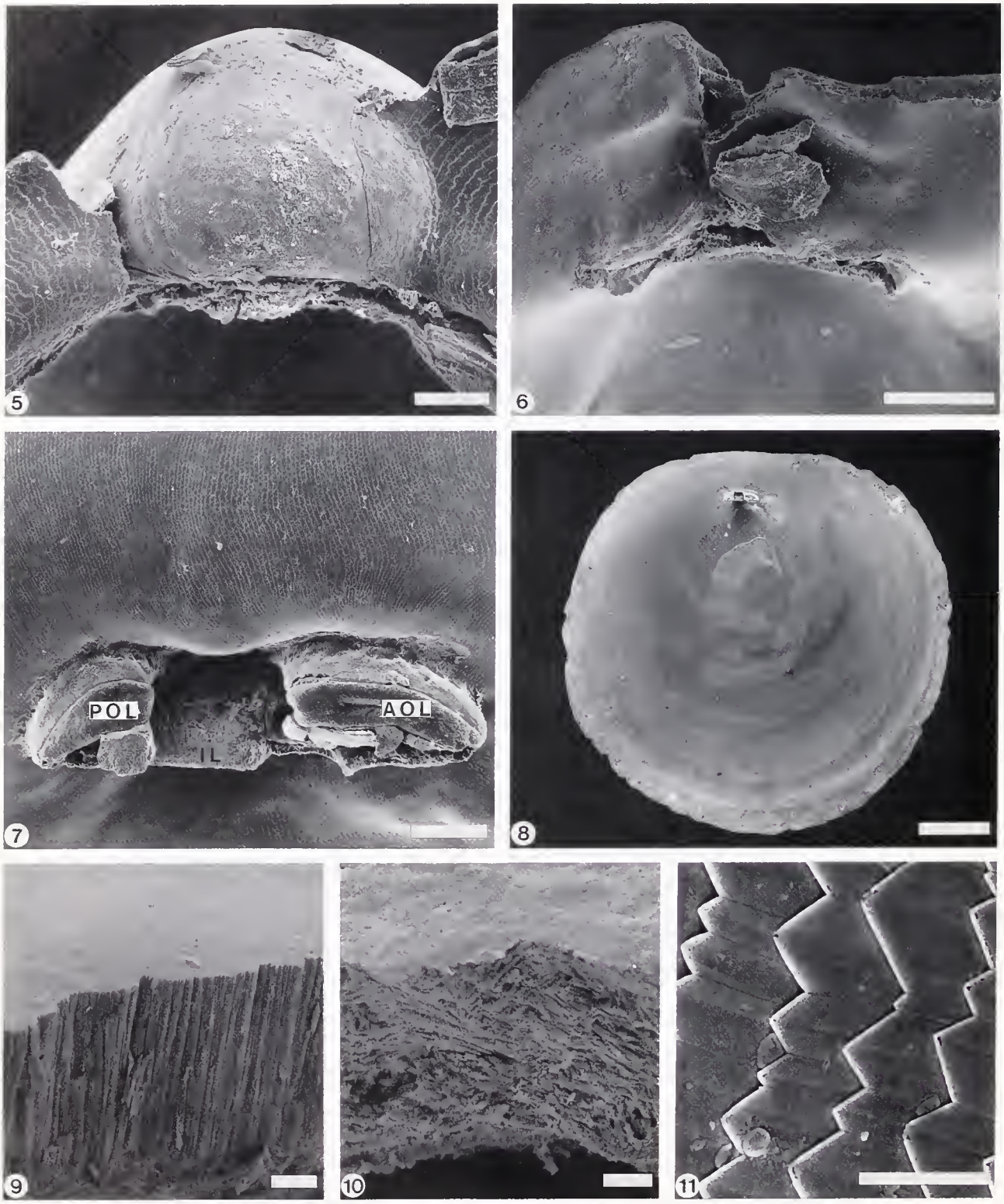

Figures 5–11. Scanning electron micrographs of the left valve of postlarval specimens of *Anomia simplex*.

Figure 5. Posterior expansion of the anterodorsal shell margin across the umbo. Scale bar = 20 μm.

Figure 6. Supradorsal extension of anterior and posterior shell margins. Scale bar = 100 μm.

Figure 7. Ligament and supradorsal shell region after union of anterodorsal and posterodorsal shell margins in a juvenile specimen. Note the vertical pattern of outcropping edges of folia on the growth surface of the supradorsal shell region. Scale bar = 100 μm. POL, posterior outer layer of the ligament; AOL, anterior outer layer of the ligament; IL, inner layer of the ligament.

the foramen in a posterior direction (Fig. 14). The extent of the covering, across the posteroventral portion of the foramen, remains constant during shell growth (Fig. 14).

A calcitic outer layer of short prisms comprises most of the right valve of the early dissoconch (Fig. 17). An inner layer, which is mostly crossed lamellar aragonite, surrounds the byssal foramen and single muscle scar (Fig. 18). No obvious surface features were observed on a narrow band of the inner shell layer closest to the byssal foramen; a fractured section of this region is illustrated in Figure 19. No foliated microstructure was observed during thorough examinations of the right valve of postlarval specimens at several developmental stages. As the crurum increases in thickness and complexity, adjacent antero- and posterodorsal shell margins extend dorsally and centrally in a thin shell layer and are united at a shell length of 8.0 mm (Figs. 20, 21). In late postlarval stages, the crurum is comprised of several prismatic layers that overgrow and obscure the prodissoconch (Figs. 22, 23).

Discussion

Yonge (1977) described development of the ligament in the left valve of anomiids as a rounding of the anterior and posterior outer layers over the dorsal side of the inner layer. He pointed out that, in *Anomia*, the supradorsally extended mantle lobes and antero- and posterodorsal shell margins unite, but anterior and posterior outer layers of the ligament remain separate. As a result of intense growth in the supradorsal region of the left valve, the outer layers of the ligament lie laterally interior to the inner layer (Yonge, 1977).

Development of the ligament in the right valve of anomiids has been poorly understood; however, examination of postlarval shells of *Anomia simplex* in the present study reveals a developmental process similar to that in the left valve. In the right valve, lateral (interior) displacement of the prodissoconch and dorsally extending ligament gives rise to the crurum (Fig. 3). Anterior and posterior outer layers of the ligament extend centrally around the crurum and thus are positioned laterally exterior to the inner layer and in vertical alignment with the corresponding layers in the left valve (Fig. 22). Concealment of the prodissoconch during postlarval developmental stages is illustrated in Figure 22; layers of prisms mask the early shell and thicken the crurum.

Shell morphological changes in the left valve of *A. simplex* during postlarval stages are similar to those described by Yonge (1977) for *Pododesmus cepio* (Gray). Early dissoconch growth is uniform along anterior, posterior, and ventral margins. Heightened dorsal extension followed by central growth across the umbo results in supradorsal union of shell margins, displacement of the umbo to an exterior position, and dorsoventral orientation of the ligament.

Shell morphological changes in the right valve of *A. simplex* during initial postlarval developmental stages also are similar to those described by Yonge (1977) for *P. cepio* in that the byssal foramen is formed between the anterodorsal and anteroventral dissoconch regions, which are united posteriorly. In the present study, documentation of further postlarval developmental stages in *A. simplex* reveals that as adjacent shell margins expand, the byssal foramen is lengthened anteriorly, while shell resorption extends the foramen posteriorly. In late postlarval developmental stages, the anterodorsal shell margin continues to expand slightly, but exaggerated growth of the anteroventral margin substantially increases the size of the byssal foramen (Figs. 3, 21). Further enlargement of the byssal foramen to the adult size occurs by shell resorption (Jackson, 1890; Yonge, 1977). Similar expansion of the adult byssal notch is found in the pectinid *Pedum spondyloideum* (Gmelin) (Yonge, 1967; Waller, 1972).

A sheet of decalcified prisms covers the posteroventral region of the byssal foramen in postlarvae of *A. simplex* (Figs. 14–16). A similar structure has been described in some of the Propeamussiidae (Waller, 1984), a family with close ancestry to the Anomiacea (Waller, 1978). The covering in these glass scallops is an extension of the prismatic outer layer of the right valve; with growth of the byssal fasciole, the covering becomes "an appliqué on the surface of the fasciole" (Waller, 1984).

Several features of the shell morphology and internal anatomy of adult *A. simplex* and *Anomia ephippium* L., the common jingle shell of Europe, are similar (Yonge, 1977, 1980). Some authors (*e.g.*, Fischer-Piette, 1973; Porter, 1974; Rios, 1985) have listed these two species as synonymous, while others (*e.g.*, Dall, 1898; Olsson and Harbison, 1953; Abbott, 1974) preserve separate species. Comparison of larval and early postlarval shell morphological features of *A. simplex* with those of *A. ephippium*, described by Le Pennec (1978, 1980), suggests similarity in the two species. Shell length during the straight-hinge developmental stage is 75 μm in *A. ephippium* (Le Pen-

Figure 8. Shell after supradorsal union of anterior and posterior shell margins; specimen is the same as that in Figure 7. Scale bar = 1.0 mm.

Figure 9. Fracture section through the prismatic layer of the dorsal muscle scar. Scale bar = 5 μm.

Figure 10. Fracture section through the inner shell layer in the region adjacent to the dorsal muscle scar; note complex crossed lamellar microstructure. Scale bar = 5 μm.

Figure 11. Folia of the interior surface of the outer shell layer. Scale bar = 5 μm.

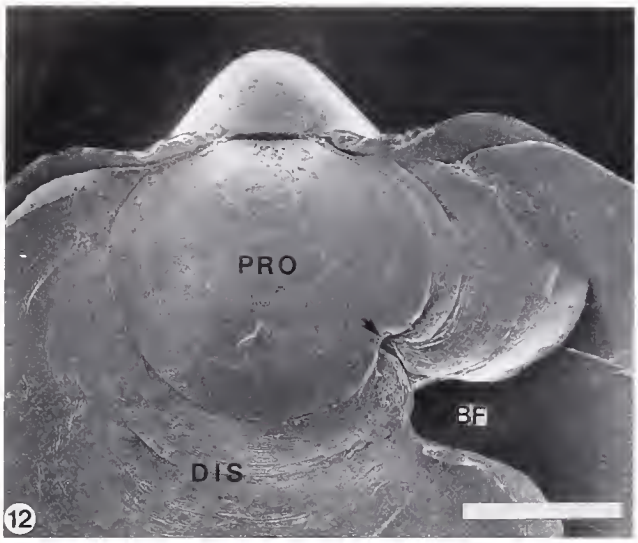

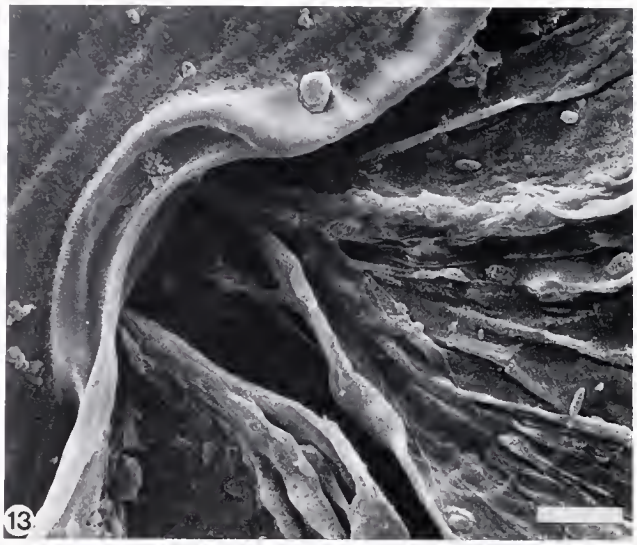

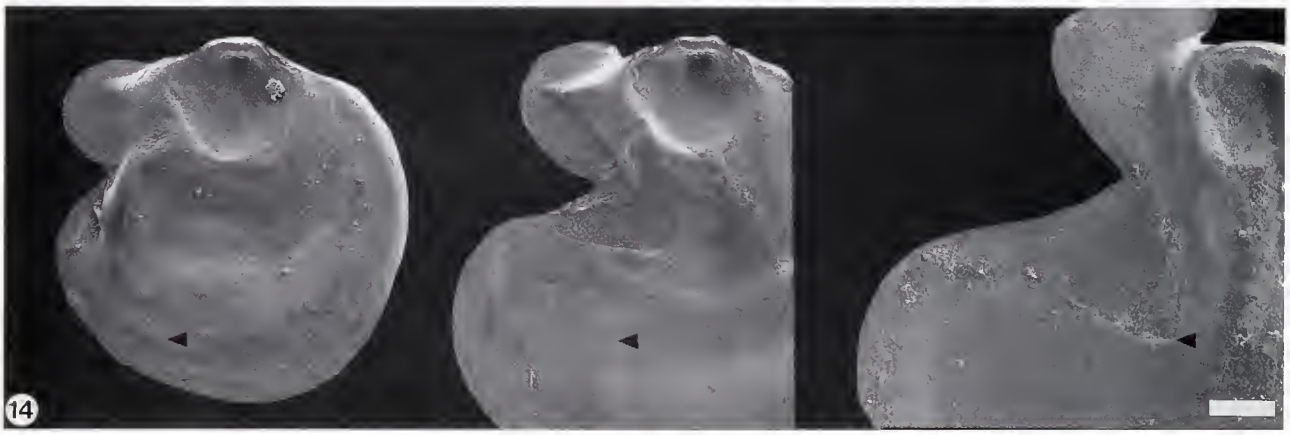

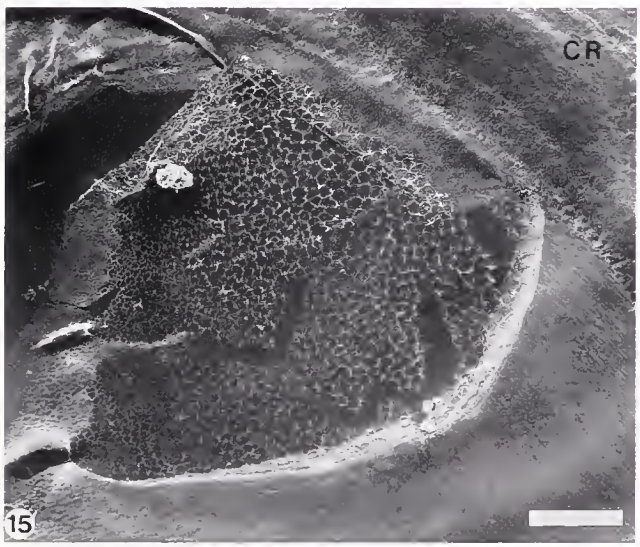

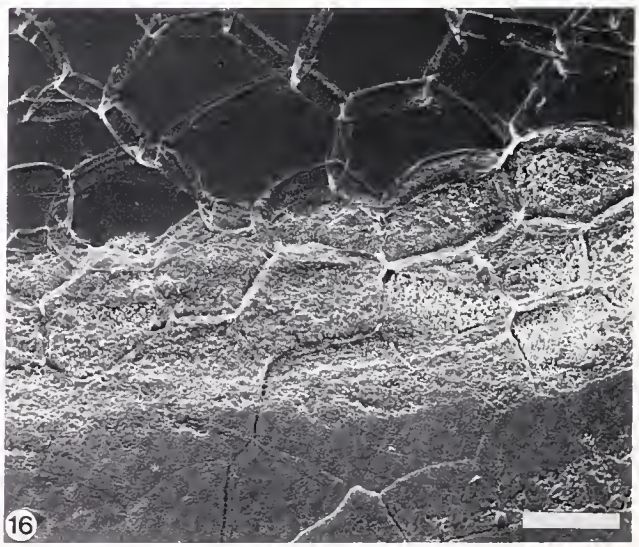

Figures 12–16. Scanning electron micrographs of the right valve of postlarval specimens of *Anomia simplex*.

Figure 12. Exterior surface of a shell 620 μm long. Arrow marks region of detail in Figure 13. Scale bar = 100 μm. PRO, prodissoconch; DIS, dissoconch; BF, byssal foramen.

Figure 13. Prismatic secretions at the byssal notch. Scale bar = 5 μm.

Figure 14. Interior surface at three sequential stages to illustrate enlargement of the byssal-foramen covering by shell resorption. Arrow marks the same spot on the three specimens, which are figured to scale. Scale bar = 100 μm.

nec, 1978); initial shell length of *A. simplex* ranged from 75 to 80 μm in the present study, although individuals as small as 58–60 μm long have been reported (Loosanoff *et al.*, 1966; Chanley and Andrews, 1971). Le Pennec (1978) described formation of an early umbo in the left valve of *A. ephippium* at a length of 100 μm and prominence of the umbo at a length of 110 μm. In specimens of the left valve of *A. simplex* depicted in Figures 1 and 2, an umbo is evident at a shell length of 89 μm and is well-developed at a shell length of 117 μm. Chanley and Andrews (1971) described development of a rounded umbo in the left valve of *A. simplex* specimens 90–110 μm long. Larval hinge dentition in both species consists of a central region of denticles and a pair of larger teeth at the anterior and posterior ends of the provinculum. In the left valve of *A. ephippium*, a third tooth is added at the anterior and posterior extremes of the hinge at a shell length of approximately 100 μm (Le Pennec, 1978, 1980). A third tooth is evident in the same position in *A. simplex* when shells are 117 μm long (Fig. 2), but these new teeth are not well-developed in either species. In *A. ephippium*, formation of a ligament pit occurs when shell height and shell length average 190 μm (Le Pennec, 1978). In specimens of *A. simplex* in the present study, a ligament pit is formed in shells 193 μm long; these post-larvae also are equidimensional. Previous workers reported that metamorphosis in *A. simplex* occurred when animals were 180–215 μm long (Loosanoff *et al.*, 1966; Chanley and Andrews, 1971). Finally, at a shell length of 250 μm, right and left valves of *A. ephippium* differ by 60 μm in length and by 70 μm in height (Le Pennec, 1978). Inequality of dimensions of right and left valves of the dissoconch of *A. simplex* is illustrated in an articulated specimen approximately 485 μm long (Fig. 24). Right and left valves of this specimen differ by 70 μm in length and by 50 μm in height.

Despite similarities in shell morphologies of early ontogenetic stages in the two species, examination of shell microstructure of early stages reveals a significant difference between *A. simplex* (= *glabra*) and *A. ephippium* and a basis for taxonomic separation (Jackson, 1890). The right valve of the dissoconch of *A. simplex* is comprised largely of prismatic microstructure, and the left valve is predominantly foliated (Jackson, 1890; present study). On the other hand, both valves of the early dissoconch of *A. ephippium* are predominantly foliated; prismatic microstructure is confined to a relatively thin outer layer of the right valve (Carpenter, 1848; Jackson, 1890). Clearly, further studies are necessary to determine the genetic distance between *A. simplex* and *A. ephippium*.

Historically, presence of a byssal notch has been a major distinguishing character used in the identification of early ontogenetic stages of anomiid species from the North Atlantic. Previously, a byssal notch was found in only the right valve of *A. simplex* and *A. ephippium*, whereas *Anomia squamula* (= *aculeata*) L. and *Anomia patelliformis* L. have a notch in both right and left valves (the notch in the left valve is shallower than the notch in the right valve) (Jackson, 1890; Ranson and Desjardin, 1941; Jørgensen, 1946; Merrill, 1962; Yonge, 1977; Le Pennec, 1978). However, data in the present study indicate that a notch sometimes occurs in the left valve of *A. simplex* (Fig. 25). Because of this variability, use of this feature for species identification may result in error.

Other details of early shell morphology of *A. squamula* and *A. patelliformis* are not well-documented. Because larval anomiids are distinctive and easily separated from other bivalve larvae by their bilateral asymmetry and conspicuous byssal notch [or pedal sinus (Yonge, 1977)], most descriptions of larval stages are limited to these two features. However, larval hinge dentition has been described for *A. squamula;* the provinculum of this species has central denticles and 3–5 larger teeth at the extremes (Jørgensen, 1946). The anterior and posterior hinge teeth of *A. squamula* are more pronounced (see Jørgensen, 1946, Fig. 162) than those of *A. simplex;* larval hinge morphology, therefore, would provide a reliable means of distinguishing these two sympatric species during planktonic stages.

Jackson (1890) described the prodissoconch of *A. simplex* (= *glabra*) as having "homogeneous" microstructure and fine commarginal lines on the exterior surface. He described the left valve of the dissoconch as "subnacreous" (foliated), with an inner "porcelaneous" region surrounding the muscle scars, and the right valve of the dissoconch as "prismatic," with a white, "porcelaneous" band around the byssal foramen. The previously reported foliated and prismatic microstructures of the outer layers are confirmed in the present study; secretion of these layers begins at the clearly delineated prodissoconch-dissoconch boundary (Figs. 12, 24, 25). In addition, reflected light and scanning electron microscopic examination of the inner shell layers has enabled categorization of the "porcelaneous" microstructure. Most of the surface of the inner shell layer of the right valve of the early dissoconch has well-defined first order lamellae, and the microstructure is distinctly crossed lamellar. Ex-

Figure 15. Interior surface view of the byssal-foramen covering of a specimen 1.5 mm long. Scale bar = 100 μm. CR, crurum.

Figure 16. Interior surface at the junction of the byssal-foramen covering and the anteroventral shell margin. Scale bar = 10 μm.

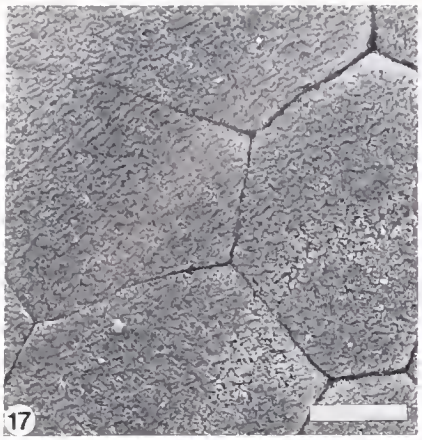

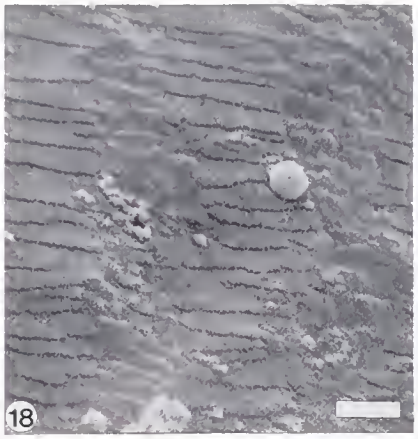

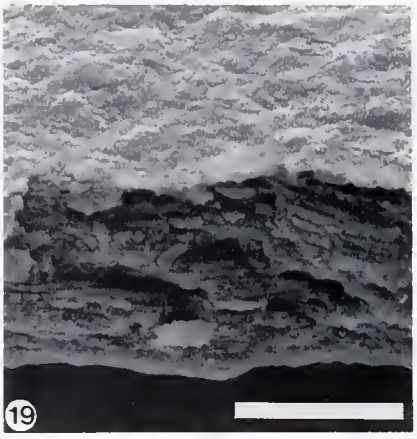

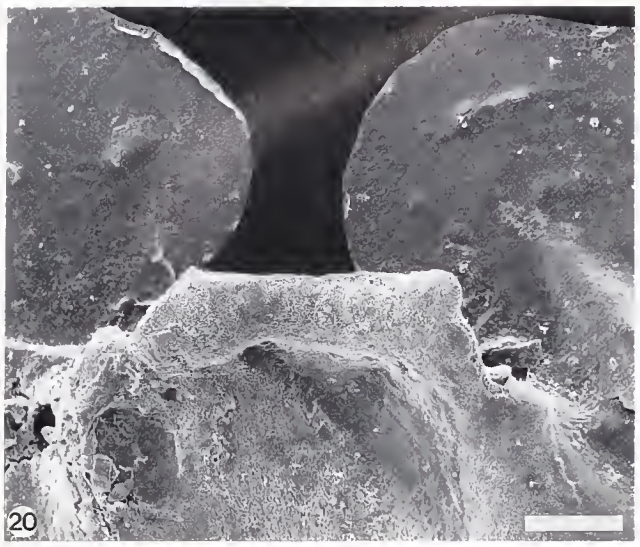

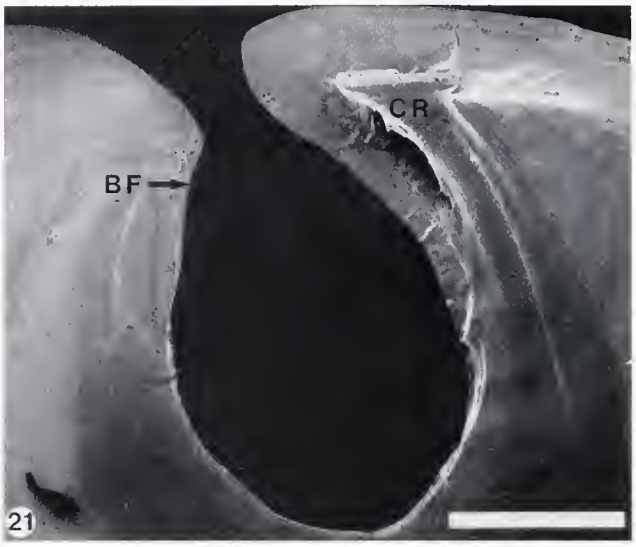

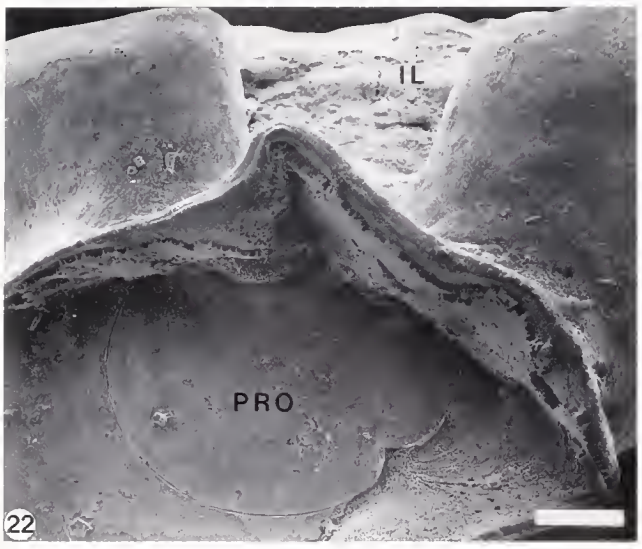

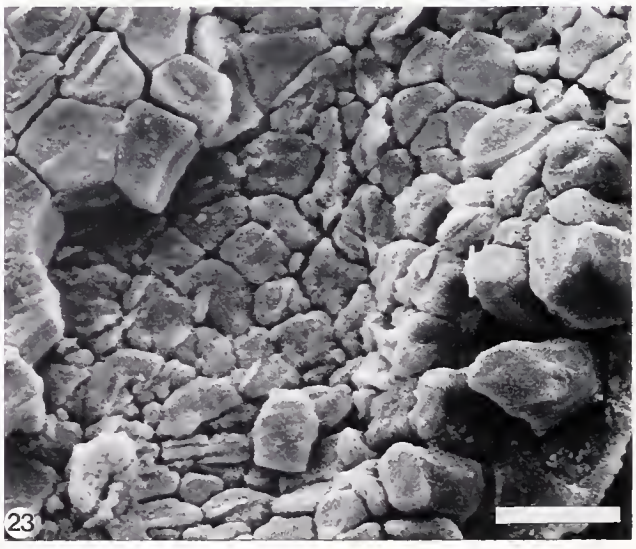

Figures 17–23. Scanning electron micrographs of the right valve of postlarval specimens of *Anomia simplex*.

Figure 17. Interior surface view of the prismatic outer layer. Scale bar = 5 μm.

Figure 18. Surface view of the crossed lamellar inner layer. Scale bar = 20 μm.

Figure 19. Fracture section of a specimen 2.0 mm long through the region of the inner shell layer closest to the byssal foramen. Scale bar = 5 μm.

Figure 20. Hinge region of the right valve before supradorsal union of shell margins. Scale bar = 50 μm.

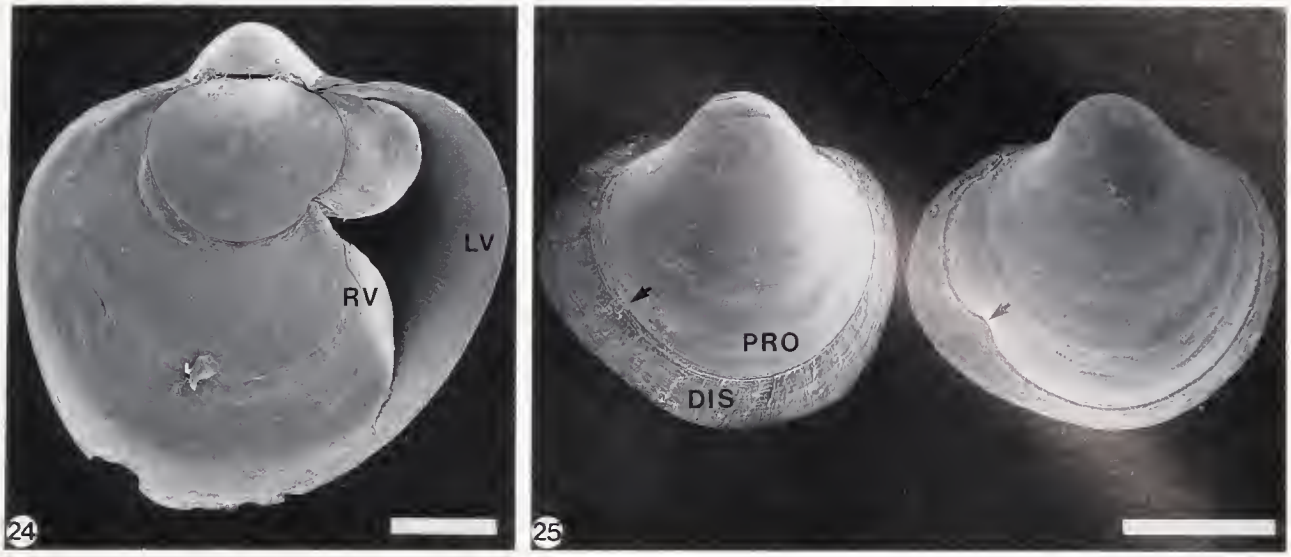

Figures 24–25. Scanning electron micrographs of postlarval specimens of *Anomia simplex*.
Figure 24. Lateral view of articulated shell. Scale bar = 100 μm. RV, right valve; LV, left valve.
Figure 25. Exterior surface of two left valves to show variation in byssal notch structure. Scale bar = 100 μm. PRO, prodissoconch; DIS, dissoconch.

amination of the fractured section of the interior region of this inner layer (depicted in Fig. 19) indicates a variety of complex crossed lamellar microstructure with a low dip angle (J. Carter, pers. comm.). The inner layer of the left valve of the early dissoconch has fine and irregular complex crossed lamellae.

The right valve of *A. squamula* (= *aculeata*) also is predominantly prismatic calcite (Jackson, 1890). In contrast, both valves of adult specimens of *Anomia trigonopsis* Hutton examined by Beu (1967) and of *A. ephippium* and *Anomia peruviana* d'Orbigny examined by Taylor *et al.* (1969) were mostly foliated calcite. Few studies subsequent to those conducted by Jackson (1890) have reported prismatic microstructure in the right valve in *Anomia*. Beu (1967) found that the right valve of three species of *Patro* is comprised primarily of prismatic microstructure and suggested that this character generally separates *Patro* from *Anomia*. Although *Patro* and *Anomia* have several other morphological differences in shell and ligament structure (Yonge, 1980), microstructure of the right valve is not a reliable character for separating these two genera.

Several of the bilaterally asymmetric early shell features characteristic of *A. simplex* are seen in other pteriomorphs common in the Northwestern Atlantic. Prodissoconch II specimens of *Crassostrea virginica* (Gmelin) and *Ostrea edulis* L. show greater convexity and umbonal protrusion in the left valve than in the right valve (Carriker and Palmer, 1979; Carriker *et al.*, 1980; Waller, 1981). Convexity of right and left valves is nearly equal through late larval stages of *Argopecten irradians* (Lamarck) (Waller, 1976); although in *Placopecten magellanicus* (Gmelin), the left valve is slightly deeper than the right valve, and the left umbo projects further than the right umbo (Merrill, 1961; Culliney, 1974). In early postlarval specimens of these visibly inequivalve species, shell height is greater in the left valve, which is the attached valve in ostreids and the upper valve in pectinids and anomiids (Fig. 26).

Microstructure of early postlarval shells of these species differs in right and left valves. Both valves of the early dissoconch of *C. virginica* and *O. edulis* have a predominant inner foliated layer; however, relative thickness of the outer layer, as well as size of its component prisms, differs in right and left valves of both species (Carriker and Palmer, 1979; Carriker *et al.*, 1980; Waller, 1981). In *A. irradians* and *P. magellanicus* postlarvae, foliated calcite comprises most of the shell; the thin outer layer of prismatic calcite present in the right valve is absent in the left valve (Merrill, 1961; Waller, 1976, 1978). Bilateral asymmetry in shell microstructure is most extreme in the early dissoconch of *A. simplex* as microstructures

Figure 21. Crurum and byssal foramen of the right valve after supradorsal union of shell margins. Scale bar = 1.0 mm. BF, byssal foramen; CR, crurum.
Figure 22. Exterior surface of the crurum. Scale bar = 50 μm. PRO, prodissoconch; IL, inner layer of the ligament.
Figure 23. Exterior surface of prismatic layers of the crurum. Scale bar = 5 μm.

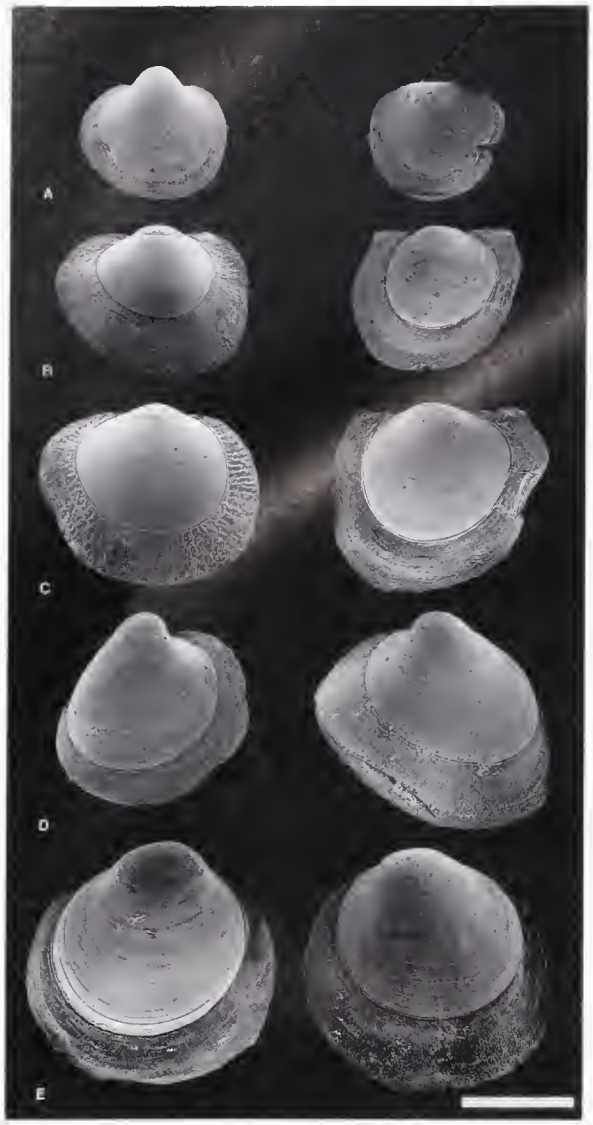

Figure 26. Scanning electron micrographs of the exterior surface of disarticulated valves of early postlarval specimens of A. *Anomia simplex*, B. *Argopecten irradians*, C. *Placopecten magellanicus*, D. *Crassostrea virginica*, and E. *Ostrea edulis*. Scale bar = 200 μm. Note marked morphological differences between right and left valves. Left valves are on the left, and right valves are on the right.

of both inner and outer layers differ in right and left valves.

Acknowledgments

Special thanks are extended to Dr. Joseph G. Carter for guidance and assistance in describing shell microstructural varieties. Valuable comments and suggestions from two anonymous reviewers are gratefully acknowledged. We thank Professor Michael Castagna for providing laboratory facilities and Joy Goodsell for giving advice on culturing larvae and postlarvae of *Anomia simplex*. Specimens of *Placopecten magellanicus* and *Ostrea edulis* were kindly provided by Samuel Chapman. New Jersey Agricultural Experiment Station Publication No. D-32401-2-89, supported by New Jersey State funds, NSF Grant EAR-84-17011, and various NOAA Sea Grants to Rutgers University.

Literature Cited

Abbott, R. T. 1974. *American Seashells*, 2nd edition, Van Nostrand Reinhold Company, New York. 663 pp.

Beu, A. G. 1967. Notes on Australasian Anomiidae (Mollusca, Bivalvia). *Trans. R. Soc. N.Z. Zool.* **9:** 225–243.

Booth, J. D. 1979. Common bivalve larvae from New Zealand: Pteriacea, Anomiacea, Ostreacea. *N. Z. J. Mar. Freshwater Res.* **13:** 131–139.

Carpenter, W. 1848. Report on the microscopic structure of shells. Part II. *Rep. Br. Assoc. Adv. Sci.* **1847:** 93–134.

Carriker, M. R., and R. E. Palmer. 1979. Ultrastructural morphogenesis of prodissoconch and early dissoconch valves of the oyster *Crassostrea virginica*. *Proc. Natl. Shellfish. Assoc.* **69:** 103–128.

Carriker, M. R., R. E. Palmer, and R. S. Prezant. 1980. Functional ultramorphology of the dissoconch valves of the oyster *Crassostrea virginica*. *Proc. Natl. Shellfish. Assoc.* **70:** 139–183.

Carter, J. G. 1980a. Environmental and biological controls of bivalve shell mineralogy and microstructure. Pp. 69–113 in *Skeletal Growth of Aquatic Organisms*, D. C. Rhoads and R. A. Lutz, eds. Plenum Press, New York.

Carter, J. G. 1980b. Guide to bivalve shell microstructures. Pp. 645–673 in *Skeletal Growth of Aquatic Organisms*, D. C. Rhoads and R. A. Lutz, eds. Plenum Press, New York.

Carter, J. G., and G. R. Clark, II. 1985. Classification and phylogenetic significance of molluscan shell microstructure. Pp. 50–71 in *Mollusks, Notes for a Short Course*, T. W. Broadhead, ed. University of Tennessee Department of Geological Sciences Studies in Geology 13.

Chanley, P., and J. D. Andrews. 1971. Aids for identification of bivalve larvae of Virginia. *Malacologia* **11:** 45–119.

Culliney, J. L. 1974. Larval development of the giant scallop *Placopecten magellanicus* (Gmelin). *Biol. Bull.* **147:** 321–332.

Dall, W. H. 1898. Tertiary fauna of Florida. *Trans. Wagner Free Inst. Sci. Phila.* **3:** 571–916.

Fischer-Piette, E. 1973. Mollusques lamellibranches et scaphopodes. *Ann. Inst. Oceanogr.* **47:** 231–262.

Jackson, R. T. 1890. Phylogeny of the pelecypoda, the Aviculidae and their allies. *Mem. Boston Soc. Nat. Hist.* **4:** 277–400.

Jørgensen, C. B. 1946. Reproduction and larval development of Danish marine bottom invertebrates, with special reference to the planktonic larvae in the Sound (Øresund). 9. Lamellibranchia. *Medd. Dan. Fisk. Havunders. Serie: Plankton* **4:** 277–311.

Kobayashi, I. 1969. Internal microstructure of the shell of bivalve molluscs. *Am. Zool.* **9:** 663–672.

Lebour, M. V. 1938. Notes on the breeding of some lamellibranchs from Plymouth and their larvae. *J. Mar. Biol. Assoc. U. K.* **23:** 119–144.

Le Pennec, M. 1978. Génèse de la coquille larvaire et postlarvaire chez divers Bivalves marins. Thèse d'Etat, Université de Bretagne Occidentale Laboratoire de Zoologie, Brest. 229 pp. + 108 pls.

Le Pennec, M. 1980. The larval and post-larval hinge of some families of bivalve molluscs. *J. Mar. Biol. Assoc. U. K.* **60:** 601–617.

Loosanoff, V. L., and H. C. Davis. 1963. Rearing of bivalve mollusks. *Adv. Mar. Biol.* **1:** 1–136.

Loosanoff, V. L., H. C. Davis, and P. E. Chanley. 1966. Dimensions and shapes of larvae of some marine bivalve mollusks. *Malacologia* **4:** 351–435.

Merrill, A. S. 1961. Shell morphology in the larval and postlarval stages of the sea scallop, *Placopecten magellanicus* (Gmelin). *Bull. Mus. Comp. Zool.* **125:** 1–20.

Merrill, A. S. 1962. Variation and change in surface sculpture in *Anomia aculeata*. *Nautilus* **75:** 131–138.

Miyazaki, I. 1935. On the development of some marine bivalves, with special reference to the shelled larvae. *J. Imp. Fish. Inst.* **31:** 1–10.

Olsson, A. A., and A. Harbison. 1953. Pliocene mollusca of southern Florida with special reference to those from North Saint Petersburg. *Monogr. Acad. Nat. Sci. Phila.* **8:** 1–457.

Porter, H. 1974. *The North Carolina Marine and Estuarine Mollusca.* University of North Carolina. 351 pp.

Prezant, R. S. 1984. Functional microstructure and mineralogy of the byssal complex of *Anomia simplex* Orbigny (Bivalvia: Anomiidae). *Am. Malacol. Bull.* **2:** 41–50.

Ranson, G., and M. Desjardin. 1941. Note sur la prodissoconque d'*Anomia* (Moll. Lamellibr.). *Bull. Mus. Paris. Series 2* **13:** 567–570.

Rees, C. B. 1950. The identification and classification of lamellibranch larvae. *Hull Bull. Mar. Ecol.* **3:** 73–104.

Rios, E. C. 1985. *Seashells of Brazil.* Universidade do Rio Grande. Museu Oceanográfico, Rio Grande. 329 pp., 102 pls.

Stafford, J. 1912. On the recognition of bivalve larvae in plankton collections. *Contrib. Can. Biol.* **1906–1910:** 221–242.

Sullivan, C. M. 1948. Bivalve larvae of Malpeque Bay, P.E.I. *Bull. Fish. Res. Board Can.* **77:** 1–36.

Taylor, J. D., W. J. Kennedy, and A. Hall. 1969. The shell structure and mineralogy of the Bivalvia: introduction. Nuculacea–Trigonacea. *Bull. Br. Mus. (Nat. Hist.) Zool. Suppl.* **3:** 1–125.

Waller, T. R. 1972. The Pectinidae (Mollusca: Bivalvia) of Eniwetok Atoll, Marshall Islands. *Veliger* **14:** 221–264.

Waller, T. R. 1976. The development of the larval and early postlarval shell of the bay scallop, *Argopecten irradians*. *Bull. Am. Malacol. Union Inc.* **1976:** 46.

Waller, T. R. 1978. Morphology, morphoclines and a new classification of the Pteriomorphia (Mollusca: Bivalvia). *Philos. Trans. R. Soc. Lond. B Biol. Sci.* **284:** 345–365.

Waller, T. R. 1981. Functional morphology and development of veliger larvae of the European oyster, *Ostrea edulis* Linné. *Smithson. Contrib. Zool.* No. 328, 70 pp.

Waller, T. R. 1984. The ctenolium of scallop shells: functional morphology and evolution of a key family-level character in the Pectinacea (Mollusca: Bivalvia). *Malacologia* 25: 203–219.

Yonge, C. M. 1967. Observations on *Pedum spondyloideum* (Chemnitz) Gmelin, a scallop associated with reef-building corals. *Proc. Malacol. Soc. Lond.* **37:** 311–323.

Yonge, C. M. 1977. Form and evolution in the Anomiacea (Mollusca: Bivalvia)—*Pododesmus, Anomia, Patro, Enigmonia* (Anomiidae): *Placunanomia, Placuna* (Placunidae Fam. Nov.) *Philos. Trans. R. Soc. Lond. B Biol. Sci.* **276:** 453–524.

Yonge, C. M. 1980. On *Patro australis* with comparisons of structure throughout the Anomiidae (Bivalvia). *Malacologia* **20:** 143–151.

Reference: *Biol. Bull.* **177:** 96–109. (August, 1989)

Direct Development in the Sea Urchin *Phyllacanthus parvispinus* (Cidaroidea): Phylogenetic History and Functional Modification

ANNETTE L. PARKS, BRENT W. BISGROVE, GREGORY A. WRAY, AND RUDOLF A. RAFF

Institute for Molecular and Cellular Biology, and Department of Biology, Indiana University, Bloomington, Indiana 47405

Abstract. Development in the Australian sea urchin *Phyllacanthus parvispinus* (Echinoidea: Cidaroidea) is of interest because it has a highly modified, lecithotrophic larva, and because it belongs to an echinoid group whose development has been little studied. This study documents early development and metamorphosis in *P. parvispinus* and considers the evolution of features unusual in echinoid ontogeny. Some features, such as lack of a vestibule, occur in other cidaroids, and are likely a product of ancestry. Other unusual features, such as larger gametes, an equal fourth cleavage, a wrinkled blastula, and accelerated development of the adult rudiment, are characteristic of other direct developing echinoids, and are probably functional modifications for altered developmental mode. Since the Cidaroidea form the sister group to the more derived Euechinoidea, cidaroid development is critical in assessing the phylogeny of ontogeny among echinoids. The distribution of developmental features among extant echinoids suggests that the extinct ancestor of cidaroids and euechinoids had planktotrophic larvae that lacked a vestibule during formation of the juvenile rudiment.

Introduction

Sea urchins and sand dollars, which comprise the echinoderm class Echinoidea, display a wide range of developmental modes. These include planktotrophic (indirect) and lecithotrophic (direct) free-swimming larvae, as well as brooded embryos (reviewed in Emlet *et al.*, 1987; Raff, 1987). Lecithotrophy has evolved independently in at least six orders of echinoids. Alterations in early echinoid development are tractable to experimental analysis, providing an excellent framework within which to analyze evolutionary changes in ontogeny (Raff *et al.*, 1989). To date, the best characterized direct developing echinoid is the Australian sea urchin *Heliocidaris erythrogramma* (Williams and Anderson, 1975). Despite the suffix, *Heliocidaris* is a euechinoid not a cidaroid. We have begun to analyze cellular and molecular alterations that accompany the evolution of direct development in this species (Parks *et al.*, 1988; Wray and Raff, 1989; Bisgrove and Raff, 1989). Predictions about ontogenetic alterations underlying direct development derived from this work can now be tested in echinoids that have independently evolved altered life history patterns.

Extant echinoids comprise two subclasses, which diverged during the Triassic: the Cidaroidea and the Euechinoidea (Smith, 1984a). The sizable literature on echinoid ontogeny deals almost exclusively with planktotrophic, or indirect, development in euechinoids. Comparatively few studies have examined development in cidaroids. Since cidaroids form the outgroup to euechinoids (Smith, 1984a), cidaroid ontogeny is important in assessing the polarity of ontogenetic transformations during echinoid evolution. Development in five planktotrophic cidaroids, three of them congeners, has been described: *Cidaris cidaris* (Prouho, 1887), *Prionocidaris baculosa* (Mortensen, 1938), *Eucidaris tribuloides* (Tennent, 1914, 1922; Schroeder, 1981; Wray and McClay, 1988), *E. metularia* (Mortensen, 1937), and *E. thouarsi* (Emlet, 1988). Although conforming to that of planktotrophic euechinoids in many regards, development in these cidaroids diverges in other respects (Emlet, 1988).

A variety of developmental modes has evolved in the

Received 24 January 1989; accepted 30 May 1989.

Cidaroidea, yet only brief descriptions of direct development in cidaroids are available: brooding in *Goniocidaris umbraculum* (Barker, 1985) and lecithotrophic development in *Phyllacanthus parvispinus* (Raff, 1987) and *P. imperialis* (Olsen *et al.*, 1988). This report extends initial observations on *P. parvispinus*, and provides a detailed characterization of early development and metamorphosis in a cidaroid with lecithotrophic larvae. Since alterations in cell lineages have evolved in *H. erythrogramma* (Wray and Raff, 1989), particular attention is given to two differentiated cell types: skeletogenic mesenchyme cells and serotonergic neurons. Several aspects of *P. parvispinus* ontogeny are discussed with reference to the phylogeny of echinoids and the evolution of novel life history strategies.

Materials and Methods

Adult and embryo culture

Adult *Eucidaris tribuloides* were purchased from Carolina Biological. Adult *Phyllacanthus parvispinus* were collected at 2–10 m depth from rock crevasses near Sydney, New South Wales, Australia. Adults of both species were maintained in aquaria with circulating filtered seawater at 23°C for up to two weeks. *E. tribuloides* gametes were obtained, and embryos cultured, by standard methods (Hinegardner, 1967). Gametes of *P. parvispinus* were obtained by cutting open tests and teasing the gonads apart. Sperm of both species were collected "dry" and stored up to 24 h at 5°C; eggs were washed and immediately fertilized with dilute sperm suspensions. Embryos were cultured at low densities in unfiltered seawater at 23°C in 3 l glass beakers with gentle stirring. To encourage metamorphosis of *P. parvispinus*, some embryos were cultured singly in plastic tissue culture dishes (Costar). These dishes were "preconditioned" with seawater from aquaria holding adults for 2–3 days before addition of embryos. Formalin-fixed *Asthenosoma ijimai* embryos from Sagami Bay, Japan, were provided by Dr. Shonan Amemiya.

Light microscopy

Embryos were fixed for 1 h in 2% formalin in seawater, washed three times in Millipore-filtered seawater, and stored in 70% ethanol until prepared for examination. Some specimens were partially cleared by dehydration through a standard ethanol series into xylene, and mounted in Permount (Fisher Scientific). Other embryos were prepared for sectioning by dehydration and embedding in Paraplast (Monoject Scientific). Sections (6 μm) were stained with eosin and Harris hematoxylin according to standard methods (Lillie, 1965), or Alizarin red and methylene blue as in Parks *et al.* (1988). Live embryos were photographed using epi-illumination.

Total mesenchyme cell counts were obtained by staining 6-μm *P. parvispinus* sections with 0.3 mg/ml 4,6 Diamidino-2-phenylindole (DAPI) to visualize nuclei. Photographs were taken of a representative cross section and total mesenchyme nuclei counted. These numbers were used to extrapolate to whole embryo cell counts by comparing section volume to whole embryo volume. Msp130 positive cell numbers were obtained by staining serial sections with monoclonal antibody B2C2 (see below) and counting all labeled cells.

Immunohistochemistry

To reveal the distribution of the protein msp130, 6-μm paraffin sections were rehydrated and incubated with 10% normal goat serum in phosphate-buffered saline (PBS: 20 m*M* Na_2HPO_4, 140 m*M* NaCl, pH 7.6) for 30 min at room temperature, followed by a 1-h incubation in undiluted culture fluid containing monoclonal antibody B2C2 (Anstrom *et al.*, 1987). Sections were then washed in PBS, incubated in goat anti-mouse IgG-conjugated fluorescein isothiocyanate (Hyclone; diluted 1:100 in PBS), and washed. Serotonergic neurons were revealed by incubating whole embryos in Tris buffer (1% sodium metabisulfite, 0.05 *M* Tris, 1% sodium chloride) containing 0.3% Triton X-100 and 10% normal goat serum for 30 min at room temperature. This was followed by incubation in polyclonal rabbit anti-serotonin antibody (Incstar; 1:100 in Tris buffer) for 2 h at room temperature. Embryos were then washed in Tris buffer and incubated for 2 h in goat anti-rabbit IgG-conjugated fluorescein isothiocyanate (Hyclone; diluted 1:100 in Tris buffer). Stained embryos were washed and mounted in glycerol/PBS (7:3) containing 1.5% n-propylgallate for viewing.

Results

Gametes and fertilization

Neither males nor females of *Phyllacanthus parvispinus* could be induced to shed gametes by intracoelomic injection of 0.55 *M* KCl; eggs and sperm were obtained directly from the gonads. By gently dissecting apart the gonadal sheath, over 2 ml of eggs could easily be obtained from each female. The reproductive season of *P. parvispinus* found in the Sydney area is apparently restricted to February and March. Even during that time, some morphologically mature batches of eggs did not fertilize.

P. parvispinus eggs are approximately 700 μm in diameter (Mortensen, 1921), much larger than those of planktotrophic cidaroids (90–170 μm; Emlet *et al.*,

Table I

Developmental timecourses among echinoids

	Species: *P. parvispinus* Subclass: Cidaroidea Larvae: lecithotrophic	*E. tribuloides* Cidaroidea planktotrophic	*H. erythrogramma* Euechinoidea lecithotrophic	*H. tuberculata* Euechinoidea planktotrophic
Stage:				
2-cell	1.5	1.5	1.5	1.5
8-cell	2.5	2.5	2.5	2.5
Wr. blastula	8–12	—	6–9	—
Blastula	13–15	7–13	10–11	6–13
Early gastr.	18	18	17	16
Mes. ingress.	??	23	12	14
Late gastr.	30	40	20	20
Coeloms	33	50	22	22
Prism	—	55	—	24
Pluteus	—	90	—	39
Rudiment	37	(25 days)	30	??
Metamorphosis	5 days	(30 days)	3.5 days	??

Developmental timecourses for representative lecithotrophic and planktotrophic developers from the Cidaroidea and Euechinoidea are listed for purposes of comparison. Note that stages being compared between lecithotrophic and planktotrophic larvae are similar but not literally equivalent, because some developmental events have undergone temporal shifts (heterochronies). Approximate times required to reach the listed stages of development at 23°C are in hours unless otherwise noted (bracketed time points in second column are based on *E. thouarsi* reared at 28°C); approximate durations are provided for blastulae. Dashes indicate absence of a particular stage; question marks indicate stages whose timing is not known. In the two euechinoids, mesenchyme ingression preceeds gastrulation, while the reverse is true of *E. tribuloides;* when mesenchyme cells first ingress in *P. parvispinus* remains to be determined. Sources: *Phyllacanthus parvispinus* (this study); *Eucidaris tribuloides/E. thouarsi* (Schroeder, 1983; Emlet, 1988; Wray and McClay, 1988); *Heliocidaris erythrogramma* (Williams and Anderson, 1975; Parks *et al.*, 1988); *Heliocidaris tuberculata* (Parks *et al.*, 1988). Abbreviations: wr. blastula = wrinkled blastula; gastr. = gastrula; mes. ingress. = initial mesenchyme cell ingression; coeloms = initiation of coeloms; pluteus = 2-armed pluteus.

1987). The buoyant eggs are gray and opaque, and possess no visible asymmetries in pigment distribution. As with other direct developing echinoids, sperm heads are longer and narrower than those of related planktotrophic species (Raff *et al.*, in prep).

Early development

Table I presents a timecourse of developmental events in *P. parvispinus.* Early development of *P. parvispinus* proceeds at approximately the same rate as that of a planktotrophic cidaroid species, *Eucidaris tribuloides.* Beginning with the formation of adult structures, however, *P. parvispinus* develops much more rapidly, resulting in a juvenile within 5 days instead of a month. This parallel timing of early development followed by acceleration of metamorphosis is also characteristic of euechinoid lecithotrophic development (Table I).

Zygotes cleave approximately 90 min after fertilization; thereafter, cleavage divisions occur at about 35-min intervals. Early cleavages are essentially equal, with slight variations in blastomere size apparently arising at random. During fourth cleavage (2.8 h), transient 12-cell embryos are occasionally observed. The 16-cell embryo (3 h) is composed of two tiers of eight blastomeres of approximately equal size (Fig. 1a). During fifth cleavage (3.5 h), some 20–30 cells are present; blastomeres at one end of the embryo are distinctly smaller than those at the other end (Figs. 1b, 2a). Together, these observations suggest that cleavages become asynchronous as early as the fourth division, with blastomeres at one pole of the embryo cleaving at a slightly faster rate. This stands in contrast to another direct developing echinoid, *H. erythrogramma,* which has synchronous, equal cleavage through at least the seventh division (Wray and Raff, 1989).

The blastular epithelium of *P. parvispinus* undergoes a pronounced wrinkling during the next several hours (Fig. 1c). The formation of wrinkled blastulae is a common feature in direct developing echinoderms with large eggs (Mladenov, 1979; Strathmann, 1987). Wrinkled blastulae also occur in the lecithotrophic euechinoids *Heliocidaris erythrogramma* (Williams and Anderson, 1975), *Holopneustes inflatus* (V. B. Morris, unpub. obs.), and *Asthenosoma ijimai* (Amemiya and Tsuchiya, 1979). Both depth and number of wrinkles in *P. parvispinus* reach a maximum at about 10 h (Figs. 2b, 3a). Wrinkles differ from those of other direct developing echinoderms in their depth, which often exceeds the radius of the blastula, and in the occurrence of branches

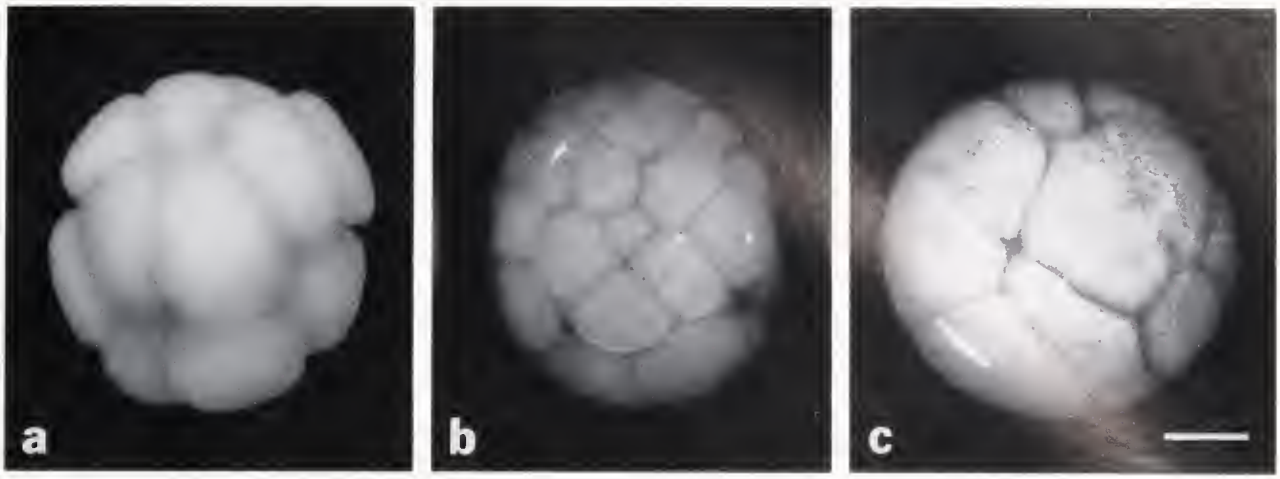

Figure 1. Early development of *Phyllacanthus parvispinus*, whole mounts of fixed and live embryos. a. 16 cell fixed embryo (3 h). The first four cleavages are equal. b. Approximately 30-cell live embryo (3.5 h). Note blastomeres are of different sizes. c. Live wrinkled blastula (11.5 h). At this stage, the wrinkles are decreasing in number. The embryo is still inside the fertilization envelope.

(Fig. 3a). At this stage, the epithelium is composed of cuboidal cells. Over the next several hours, wrinkles gradually egress in concert with a distinct increase in epithelial thickness. By 13 h, the blastula is lobate and irregular in appearance, and most embryos have only one or two very deep wrinkles remaining (Fig. 2c). The epithelium at 13 h is columnar, and approximately twice as thick as at 10 h (compare Figs. 3a and 3b). Throughout the appearance and disappearance of wrinkles, the diameter of the blastula does not change appreciably; it remains within the fertilization envelope. A similar situation exists in *H. erythrogramma* (Williams and Anderson, 1975).

Wrinkles have completely disappeared from the surface of the embryo by the beginning of gastrulation. At 21 h, the archenteron extends approximately one third of the distance across the blastocoel. The archenteron is unusually wide for an echinoid. Many mesenchyme cells are present by this time. The tip of the archenteron begins to widen into the presumptive coelom by 26 h (Figs. 2d, 3c). Archenteron elongation then ceases, and the coelom continues to elaborate over the next several hours. The 33-h larva contains a bilobed coelom, one side of which can be distinguished as hydrocoel and is already branching into five buds (Fig. 3d), marking the beginning of morphogenesis of the echinus rudiment.

An unusual feature of larval development in *P. parvispinus* is the presence of cylindrical pits, up to 100 μm deep, opening onto the ectodermal surface (Figs. 2f and 3c, arrows). These pits, which number about four to six per embryo, seem to be distributed randomly. It is not clear how pits arise, but it seems unlikely that they are remnants of the one or two wrinkles present in lobate blastulae because of their greater number and distribution over the whole of the embryo. Pits are present through metamorphosis (Fig. 2f, arrow).

Larval development in *P. parvispinus* occurs near the air and water interface. Embryos hatch from the fertilization envelope at about 18 h, just prior to the beginning of gastrulation. Hatched larvae float with the animal end up; the adult oral-aboral axis is oriented perpendicular to the embryonic animal-vegetal axis. Larvae spin slowly about the animal-vegetal axis. *P. parvispinus* larvae are uniformly ciliated and lack a ciliary band. Unlike most other echinoid larvae, these embryos do not swim in a directed manner in culture.

Development of echinus rudiment and metamorphosis

By about 37 h, a cluster of five podial buds is evident on the lateral larval ectoderm. These nascent primary podia (tube feet) surround the location of the future adult mouth and define the adult rudiment; they are the first external manifestation of pentamerous adult symmetry. During the next several hours, podia grow rapidly, and by 47 h are beginning to achieve their final form (Figs. 2e, 3e). As reported previously (Raff, 1987), no ectodermal invagination forms a vestibule around the adult rudiment of *P. parvispinus* (Fig. 3e, f). By 48 h, larval ectoderm contains numerous, brightly pigmented cells.

The floating larva becomes denser as larval development proceeds. On the fourth day of development, it sinks and begins to move about on the substratum using its primary podia. The first spines are composed of three parallel rods interconnected by short crossbridges. These are juvenile spines based on their development of charac-

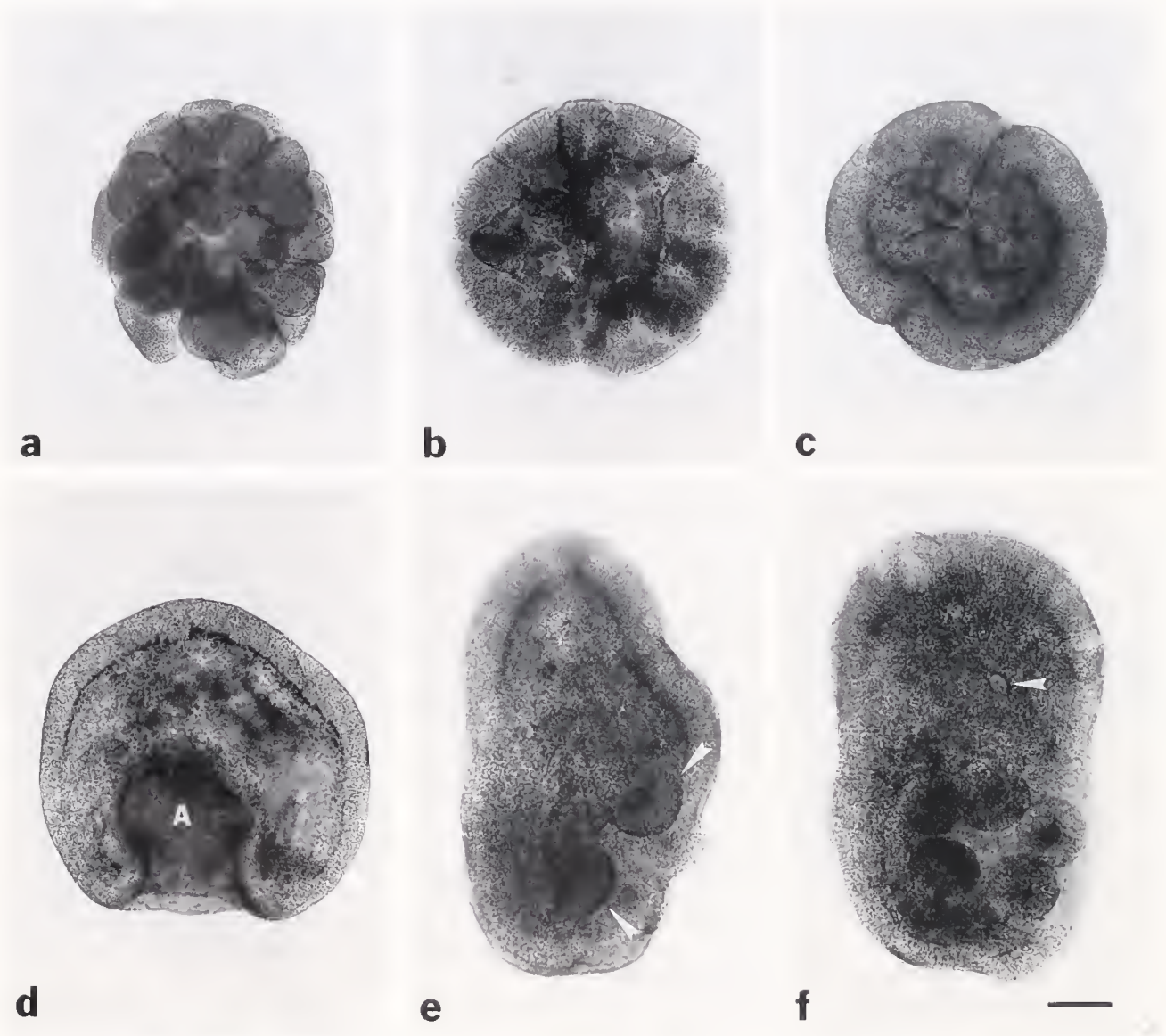

Figure 2. Development of *Phyllacanthus parvispinus*, xylene cleared whole mounts. a. Approximately 30-cell embryo (3.5 h). Note size differences in blastomeres. b. Wrinkled blastula (10 h). The surface is maximally wrinkled at this stage. c. Lobate blastula (13.5 h). Only a few wrinkles remain at this stage. d. Gastrula (26.5 h). The blastopore is quite wide. e. Early larva (45 h). Podial buds are present (arrows). f. Late larva (69 h). The five primary podia surrounding the future adult oral surface are clearly visible, as is a pit opening (arrow). Embryos in panels d–f are oriented animal end up. Formalin-fixed embryos were cleared in xylene before micrography. A, archenteron. Scale bar = 100 μm.

teristic flared ends, and on the fact that they are the first spines to appear. However, these spines differ from the juvenile spines of planktotrophic cidaroids in their cluster arrangement on the test and in the fine structure of the lateral processes (Emlet, 1988). Pedicellaria are not yet present, and a large lobe, corresponding to the animal end of the larva, protrudes from one side. During the next few days, metamorphosis is gradually completed: the larval animal lobe is resorbed, circumoral spines develop the characteristic lateral processes and flared ends of echinoid juvenile spines, and additional spines appear. By 141 h, the surface is covered by juvenile spines, and five apical test plates are evident (Fig. 4). At this point, test diameter is approximately 500 μm.

Although juveniles at six days of development contain nascent adult test plates, there is no evidence of calcification in the adult oral field. It is not known when juveniles begin to feed, but development of the lantern and

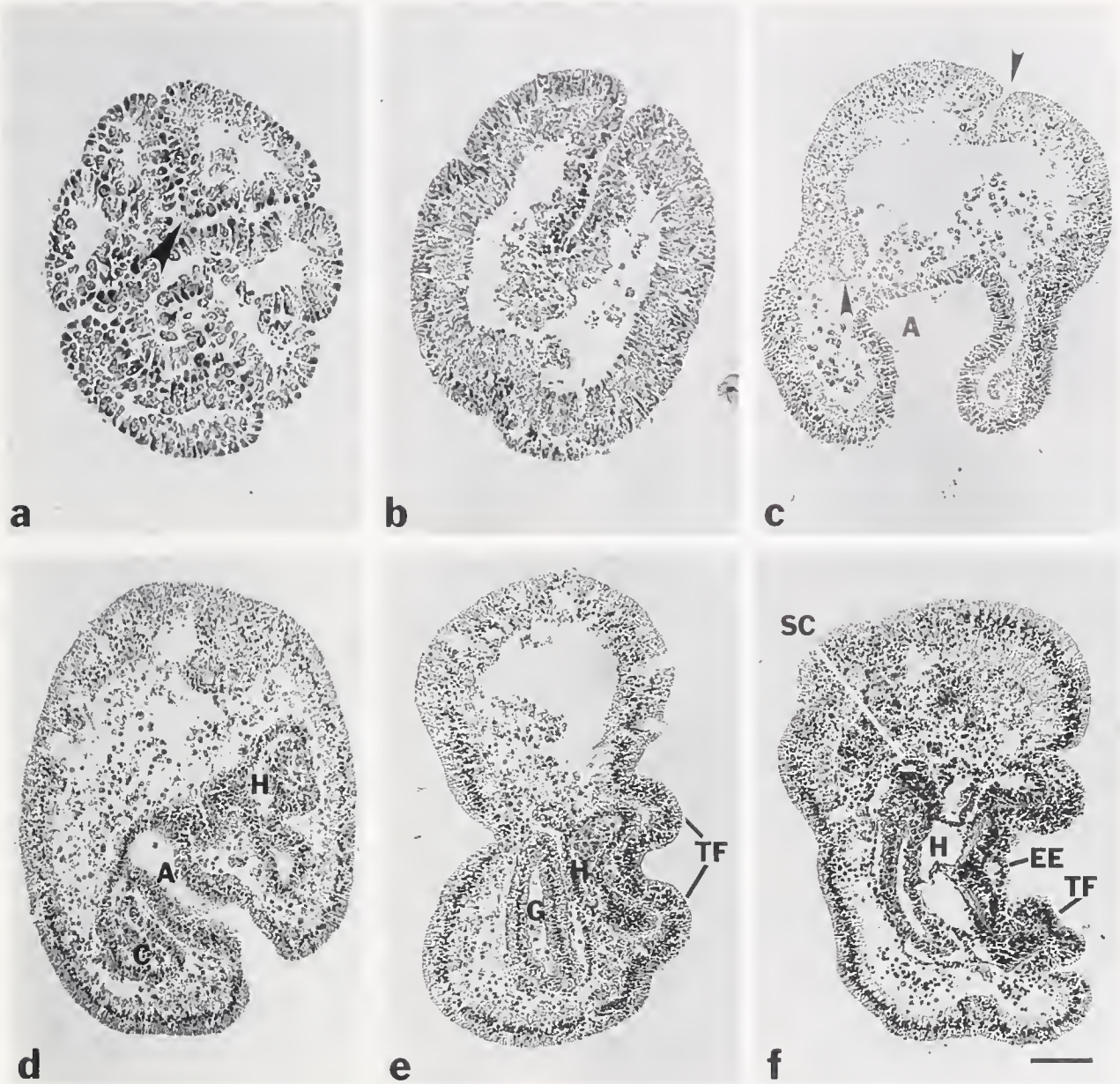

Figure 3. Development of *Phyllacanthus parvispinus*, sections. a. Wrinkled blastula (10 h). The highly convoluted surface is composed of loosely organized epithelium. A branchpoint is labeled (arrow). b. Lobate blastula (13.5 h). A single, deep wrinkle is visible; ectoderm is now much thicker. c. Gastrula (26.5 h). Numerous mesenchyme cells have ingressed from the tip of the archenteron (A). Note pits (arrows). d. Late gastrula (33 h). Mesenchyme cell ingression is complete and the coelom (C) and hydrocoel (H), a coelomic derivative, are forming. e. Early larva (45 h). Section passes through the adult rudiment and two primary podia (TF). Branches of the hydrocoel invest the podial buds. Note the lack of a vestibule enclosing the rudiment. f. Late larva (95 h). Podia have terminal discs and will support locomotion. Micrographs are of 6-μm paraffin sections prepared from formalin-fixed embryos and stained with eosin and Harris hematoxylin. Embryos in panels c–f are oriented with the animal pole at the top of the photo. EE, epineural epithelium; G, gut; SC, stone canal. Scale bar = 100 μm.

teeth evidently occurs some time after completion of most other metamorphic events. Pedicellaria and definitive adult spines are not present in six day juveniles (Fig. 4), but both are evident a week later (not shown). These later spines lack the characteristic flared ends of earlier juvenile spines.

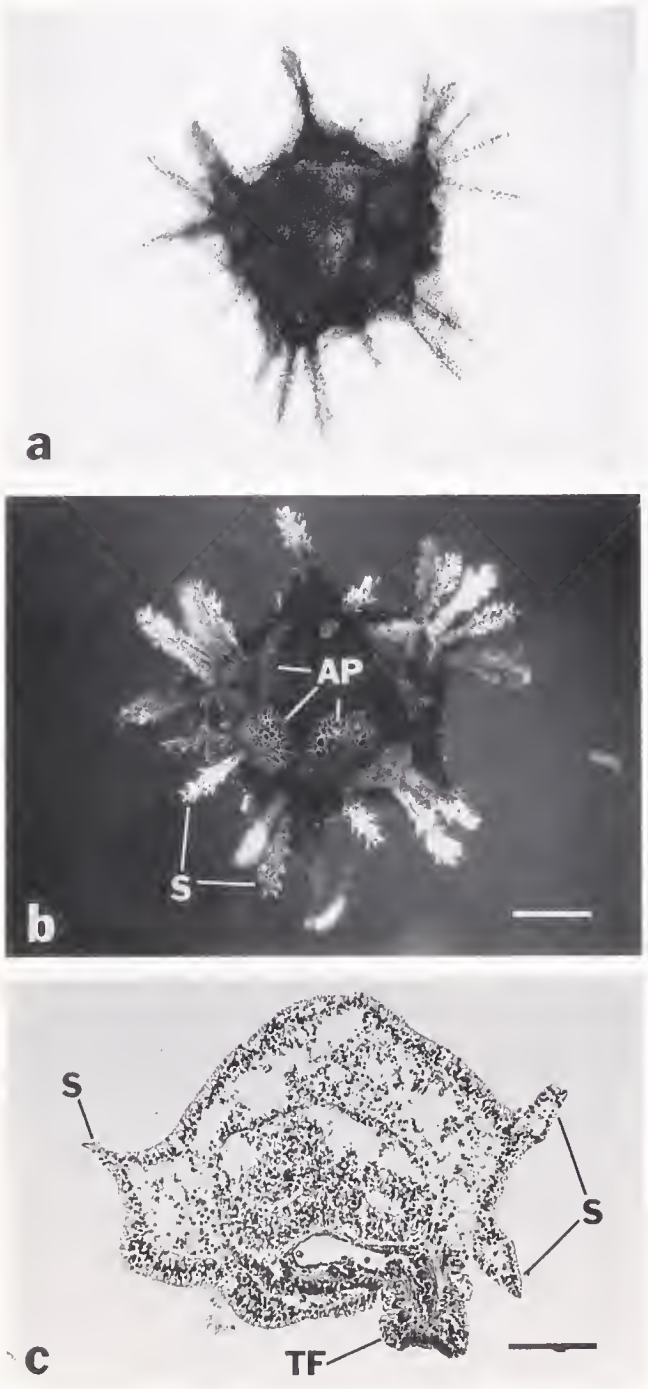

Figure 4. Juvenile *Phyllacanthus parvispinus.* Three views of 141-h juveniles. a. Xylene-cleared whole mount, aboral view. Note "webbing" between spines. b. Polarized light view of the same specimen. Secretion of the five apical plates (AP) has begun; three are visible in this phase of polarized light. Spines (S) are all of the juvenile type. c. Six-μm eosin and Harris hematoxylin cross section. A single podium (TF) is visible, as are three spines. The section is oriented oral surface down. Scale bars: a, b = 200 μm; c = 150 μm.

The larval ectoderm of planktotrophic euechinoids is largely lost during metamorphosis, the adult ectoderm deriving primarily from vestibular ectoderm (Cameron and Hinegardner, 1978). In contrast, the larval ectoderm of the cidaroid *Eucidaris thouarsi* is retained through metamorphosis (Emlet, 1988). Indirect evidence suggests that a similar situation exists in *P. parvispinus.* The ectoderm is topologically in the same position in late larvae and juveniles, because no inversion of a vestibule takes place. Larval ectoderm retracts onto the aboral surface of the juvenile as metamorphosis proceeds (Figs. 4a, c).

Differentiation of mesenchyme cells

The differentiation of skeletogenic mesenchyme cells and the pattern of skeletogenesis is highly modified in lecithotrophic echinoids (Raff, 1987; Parks *et al.,* 1988). The protein msp130 provides a specific probe for these cells. This protein is produced only by primary mesenchyme cells in euechinoid embryos (Anstrom *et al.,* 1987; Wray and McClay, 1989) and by skeletogenic cells in adults (Parks *et al.,* 1988). In planktotrophic larvae of the cidaroid *Eucidaris tribuloides,* there are 16 spicule-forming cells, homologous to euechinoid primary mesenchyme cells, that express msp130 (Wray and McClay, 1988). In *E. tribuloides,* msp130 expression begins after spicule-forming cell ingression is complete, and just before secretion of the larval skeleton.

To examine expression of msp130 during *P. parvispinus* development, embryos were stained using indirect immunofluorescence with the monoclonal antibody B2C2, which binds specifically to msp130 (Anstrom *et al.,* 1987). In early gastrulae containing hundreds of mesenchyme cells (22 h), no staining is apparent. By the time coeloms are elaborating (33 h), cell counts reveal that there are 6,000–10,000 mesenchyme cells present, of which approximately 5% exhibit B2C2 staining (Fig. 5a, b). In premetamorphic larvae, B2C2-positive cells are closely associated with calcareous spicules being elaborated into juvenile spines and test stereom (Fig. 5c, d). By 95 h, B2C2-positive cells are also present in podial terminal discs and the oral region, where additional spicule synthesis will take place. Only those mesenchyme cells adjacent to, and probably participating in, synthesis of the calcareous spicules are B2C2 positive (compare Figs. 5d and 5f).

Larval serotonergic nervous system

The evolution of direct development in several echinoids results in the reduction of structures at the apical end of the pluteus, including the larval arms and the circumoral ciliary band. *P. parvispinus* larvae lack both arms and a ciliated band. The pluteus' serotonergic ner-

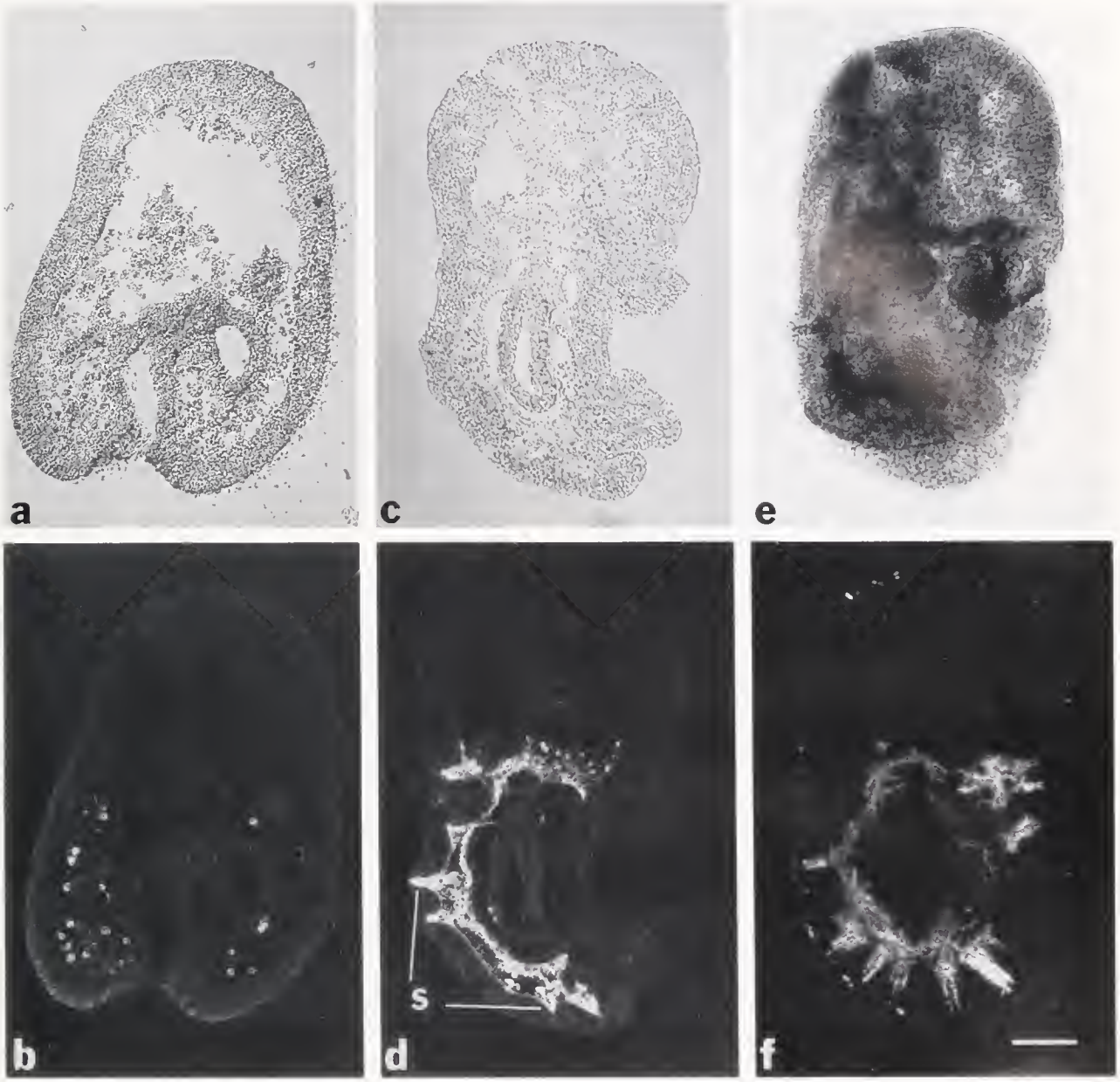

Figure 5. msp130 expression. a–d. Indirect immunofluorescent staining of sectioned embryos with monoclonal antibody B2C2. a, b. Paired brightfield and fluorescent micrographs of late gastrula (33 h). A scattering of positive cells are present in the vegetal end of the embryo. c, d. Paired brightfield and fluorescent micrographs of late larva (95 h). Many more positive cells are present. Staining is strong near nascent juvenile spines (S) on adult aboral side (left in these panels). Staining is also present in podia and adult oral region (not shown). e, f. Paired brightfield and polarized light micrographs of a late larva (95 h) xylene-cleared whole mount. Embryo is oriented with the future adult oral field facing the viewer. This larva shows the extent and position of adult test and spine secretion for comparison with the specimen in panels c and d. Scale bar = 100 μm.

vous system, which has an unknown function, also lies at the apical end of the pluteus larva. Serotonergic neurons provide an identifiable cell lineage that has been used to document echinoid nervous system development. These studies have also allowed comparisons of temporal and morphological variation in nervous system differentiation among planktotrophic and lecithotrophic species. We asked if these neurons are reduced or modified in *P. parvispinus*.

Development of larval serotonergic neurons in *P. par-*

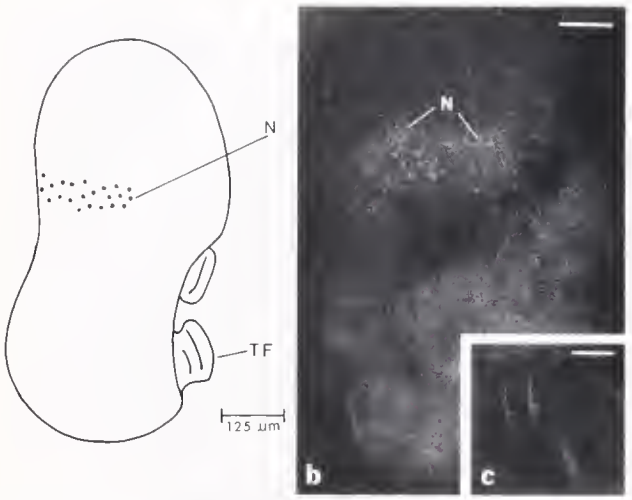

Figure 6. Distribution of serotonergic neurons in *P. parvispinus* larvae (114 h). a,b. The cluster of serotonergic neurons (N) is located in the larval epidermis opposite the echinus rudiment. Larva contains 30–50 loosely clustered neurons located medially in the larval epidermis opposite to the rudiment. View of larva in b is of side directly opposite rudiment. c. High magnification view of the neurons from b showing cell bodies and apical processes. TF, tube foot. Scale bars: b = 100 μm; c = 25 μm.

vispinus was studied using a polyclonal antibody that binds specifically to serotonergic cells. Anti-serotonin immunoreactive cells could be resolved in 92 h and older larvae. In these larvae, 30–50 serotonergic cells are present, loosely clustered in the epidermis of the larva, opposite to the oral field of the adult rudiment (Fig. 6). The serotonergic neurons are 9 μm (basal diameter) flask-shaped cells with a basal nucleus and a long apical process (about 20 μm) that extends to the surface of the epidermis (Fig. 6c). One or two axons project basally from the neurons; the organization of the axons is difficult to resolve through the thick larval epidermis. Although we were unable to resolve serotonergic neurons in larvae younger than 92 h, these cells presumably arise earlier than we have documented. This organization is quite different from the larval serotonergic nervous systems of both planktotrophic and lecithotrophic euechinoids (Bisgrove and Burke, 1986, 1987; Nakajima, 1987; Bisgrove and Raff, 1989), which have paired, interconnected clusters of neurons at the animal end of the larva.

Because the presence and location of a serotonergic nervous system has not been previously demonstrated in planktotrophic cidaroids, larvae of a planktotrophic cidaroid, *Eucidaris tribuloides*, were stained to reveal the serotonergic nervous system for comparison. In early plutei (8 day), six immunopositive cells are present; the number and location of neurons (Fig. 7a) was almost invariant among larvae of the same age despite some variation in morphological development. These 8–9 μm (basal diameter) cells lie within the epidermis along the base of the circumoral ciliary band. Bilaterally symmetrical pairs of neurons occur at the ventrolateral margins of the preoral hood, and a single cell lies at the base of each postoral arm (Fig. 7b, c). An axon up to 40 μm long extends from each neuron at the base of the postoral arms along the ciliary band toward the ipsilateral neurons in the preoral hood (Fig. 7c, d). Short (5–7 μm), axons extend, in no preferred direction, from the neurons in the preoral hood.

The vestibule in direct developing echinoids

Planktotrophic euechinoids possess a vestibule, or amniotic invagination, formed from the ectoderm overlying the hydrocoel (Hyman, 1955). This feature is absent from *Eucidaris thouarsi*, the only indirect developing cidaroid whose metamorphosis has been carefully described (Emlet, 1988). No vestibule is formed by *P. parvispinus* (Fig. 3), which is consistent with its position as a cidaroid.

A vestibule is present in euechinoid direct developers *H. erythrogramma* (Parks *et al.*, 1988), *Peronella japonica* (Okazaki, 1975), *Holopneustes inflatus* (Henry and Raff, unpub. obs.), and *Abatus cordatus* (Schatt, 1985). Thus the vestibule is apparently not lost as a consequence of direct development. To cast light on the phylogenetic origin of this feature in echinoid evolution, we re-examined metamorphosis in *Asthenosoma ijimai*, an echinothurioid. The published description of *A. ijimai* development (Amemiya and Tsuchiya, 1979), which carefully documents external features, shows no vestibule. We have serially sectioned *A. ijimai* larvae (Fig. 8) for direct comparison with *P. parvispinus*, and find no trace of an ectodermal vestibular invagination.

Discussion

Development in *Phyllacanthus parvispinus* diverges in several respects from "typical" echinoid ontogeny. Differences have arisen throughout development in molecular and cellular processes, as well as in morphological and behavioral features. Some differences are likely common to all cidaroids, and date to the evolutionary separation of cidaroids and euechinoids during the Triassic. Other differences may represent evolutionary novelties associated with the evolution of a lecithotrophic developmental mode. In this discussion, we attempt to distinguish between developmental patterns in *P. parvispinus* that result from phylogenetic history and those that result from abbreviated development.

Cidaroid early development

The few planktotrophic cidaroids whose development has been studied share a set of developmental features

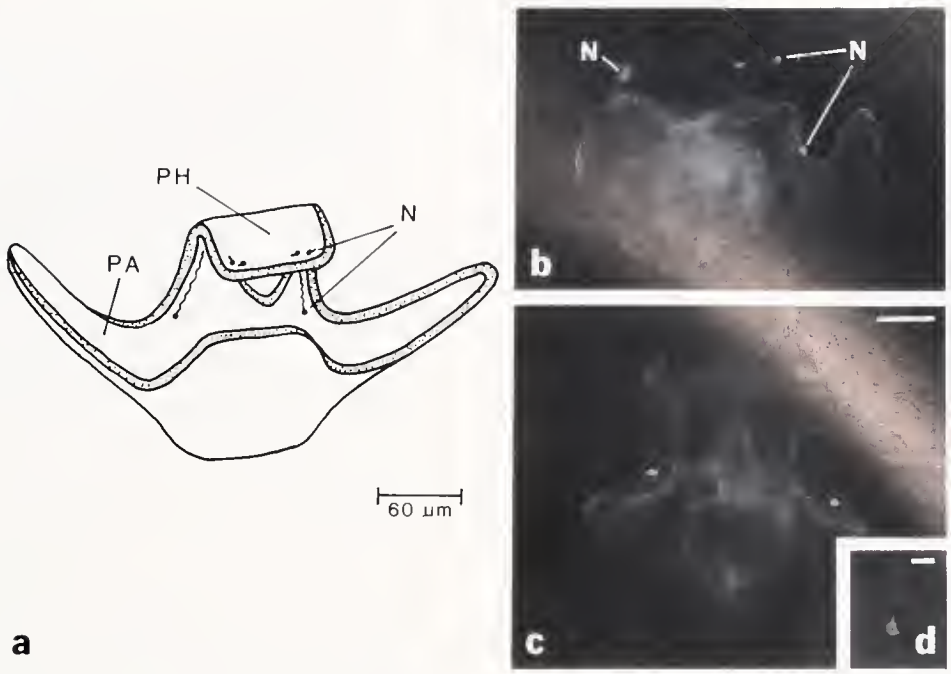

Figure 7. Distribution of serotonergic neurons in *E. tribuloides* early pluteus larvae (8 day). a. Larvae at this stage contain six bilaterally distributed serotonergic neurons (N). A single neuron lies near the base of the postoral arms, and extends an axon to a pair of neurons at the top of the preoral hood; no connections between contralateral axons are present. In all panels, larvae are oriented animal end up. b. Ventral view; a pair of neurons in the preoral hood and a single neuron at the base of the postoral arm are visible on the left side of the larva. c. Dorsal view showing the bilaterally symmetric arrangement of neurons at the base of the postoral arms. Each of these neurons (shown at higher magnification in d), extends an axon toward the preoral hood. PA, postoral arms; PH, preoral hood. Scale bars: b, c = 40 μm; d = 10 μm.

that distinguish them from euechinoids. These features, which have been documented for one or more species, include: a relatively thin hyaline layer; absence of maternal α-subtype histone mRNA in the egg; a variable number of micromeres at the 16-cell stage; lack of an apical tuft following hatching; absence of mesenchyme cell ingression prior to gastrulation; relatively slow development; several morphological features of the pluteus larva; and the lack of a vestibule during echinus rudiment formation (Prouho, 1887; Tennent, 1914, 1922; Mortensen, 1937, 1938; Schroeder, 1981; Raff *et al.*, 1984; Emlet, 1988; Wray and McClay, 1988). Planktotrophic euechinoids differ from cidaroids in each of these features (reviewed in Okazaki, 1975, and Emlet, 1988).

Direct developing euechinoids display several modifications from planktotrophic euechinoid development. These include: larger, yolky eggs; larger, more elongate sperm heads; alterations in the geometry of the fourth cleavage; transient "wrinkling" of the blastula; reduced or absent larval skeleton; and a general acceleration of adult rudiment formation (Okazaki, 1975; Williams and Anderson, 1975; Amemiya and Tsuchiya, 1979; Raff, 1987; Emlet *et al.*, 1987; Parks *et al.*, 1988; Bisgrove and Raff, 1989; Wray and Raff, 1989; Raff *et al.*, in prep.). Because planktotrophic development via a pluteus larva is likely a primitive feature in post-Paleozoic echinoids (Strathmann, 1975, 1978; Emlet *et al.*, 1987; Raff, 1987), ontogenetic alterations shared by direct developers in separate orders are derived features, and constitute parallelisms (Raff *et al.*, 1989; Wray and Raff, 1989).

P. parvispinus displays developmental features typical of cidaroids: development is slower than in euechinoids with a comparable developmental mode (Table I), and there is no vestibule present in the larvae. Because the described lecithotrophic euechinoids do not share these characters, it is probable that they are the result of phylogenetic history and not adaptations peculiar to lecithotrophic development. We expect that additional features characteristic of cidaroid development, such as the absence of mesenchyme cell ingression prior to gastrulation, will also be found in *P. parvispinus* upon further examination.

It is also significant that in many regards *P. parvispinus* conforms to the general characteristics of echinoid lecithotrophic development: elongate sperm heads, large eggs, lack of micromeres at the 16-cell stage, a transient wrinkled blastula, lack of a larval skeleton, and heterochronies in morphogenesis. Because these are aspects of

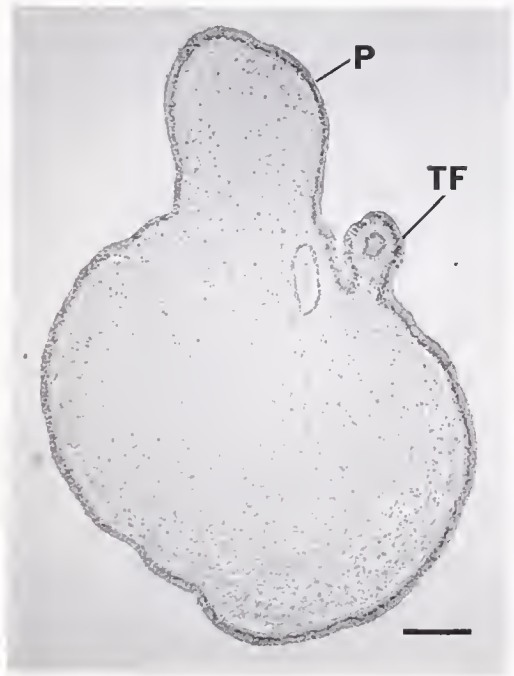

Figure 8. *Asthenosoma ijimai* lacks a vestibule. 6 μm Alizarin red and methylene blue stained section of a 101-h *A. ijimai* larvae showing one psuedo arm (P) and a developing tube foot (TF). Embryos of several stages (35, 45, 56, 75, and 101 h) were serial sectioned and no evidence of a vestibule was found at any stage across the developing adult rudiment. Scale bar = 150 μm.

early development in lecithotrophic echinoids of three, independently evolved euechinoid lineages [Echinometridae, Echinothuriidae, Temnopleuridae (Raff, 1987)], they are likely to represent functional adaptations to, or are consequences of, a change in developmental mode. This hypothesis is strengthened by the fact that these features are not characteristic of planktotrophic development in either cidaroids or euechinoids.

Skeletogenic mesenchyme cells and expression of msp130

We can distinguish three distinct classes of mesenchyme cells in the *P. parvispinus* larva: skeletogenic and nonskeletogenic mesenchyme (msp130 positive and negative) cells in the blastocoel, and pigment cells inserted in the ectoderm. Indirect developing cidaroid and euechinoid embryos contain these same three classes of mesenchyme cells (Gibson and Burke, 1985; Wray and McClay, 1988).

One of the most striking features of lecithotrophic development in *Heliocidaris erythrogramma*, a euechinoid, is the elimination of the larval pattern of skeleton formation and its replacement by an accelerated adult skeleton assembly. The expression pattern of msp130, a protein produced in larval and adult spicule-forming cells of echinoids, is also altered in direct developing echinoids (Parks *et al.*, 1988). In planktotrophic euechinoid larvae, msp130 is first expressed at, or some time before, synthesis of the larval skeleton (Wray and McClay, 1989). In *H. erythrogramma*, msp130 expression is delayed relative to that in planktotrophic larvae: expression commences hours after mesenchyme cell ingression, and is concurrent with the initiation of the echinus rudiment (Parks *et al.*, 1988). Expression of msp130 in *P. parvispinus* follows a similar timecourse. It seems likely that expression of msp130 and spicule synthesis have undergone parallel changes in these two independently derived lecithotrophic larvae: the larval program of spicule synthesis has been excised, and the adult program is initiated earlier relative to coelom formation and accelerated.

Echinoid larval nervous systems

Serotonergic nervous systems in planktotrophic euechinoids from two families have been characterized (Stronglyocentrotidae and Echinometridae; Bisgrove and Burke, 1986, 1987; Bisgrove and Raff, 1989). Although it has not been characterized in detail, the nervous system of a planktotrophic cidaroid, *Eucidaris tribuloides*, described here differs substantially from that of planktotrophic euechinoids. At a comparable stage of development (2-armed pluteus), *E. tribuloides* has fewer neurons than euechinoid plutei, the number of neurons is almost invariant, and neurons in the preoral hood lack long axonal processes extending between contralateral clusters. In addition, neurons are present at the base of the postoral arms, whereas in euechinoids, serotonergic neurons are confined to the preoral hood. Additional data will be required to characterize more fully cidaroid larval serotonergic nervous systems, but differences have clearly arisen since the euechinoids and cidaroids diverged.

The position and distribution of the larval serotonergic nervous system in *P. parvispinus* differs from that in *E. tribuloides* as well as planktotrophic euechinoids in that neurons are located medially in a single large cluster rather than as bilaterally symmetric clusters at the animal end of the larva. The *P. parvispinus* larval nervous system also differs from that of *Heliocidaris erythrogramma*, a euechinoid with lecithotrophic development (Bisgrove and Raff, 1989). In *H. erythrogramma*, serotonergic neurons are organized in two large, interconnected clusters at the animal end of the larva. Therefore, the altered organization and position of the larval nervous system in *P. parvispinus* is not solely a consequence of lecithotrophic larval development as it has been modified in ways distinct from those observed in *H. erythro-*

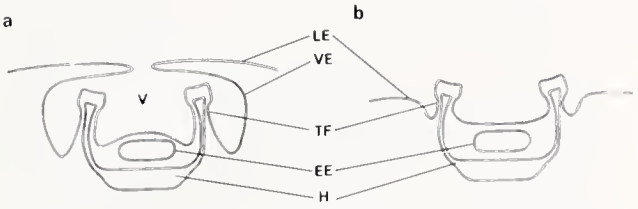

Figure 9. Comparison of adult rudiment in echinoids. Diagrammatic cross sections through the rudiment of a non-echinothurioid euechinoid (a) and a cidaroid or echinothurioid euechinoid (b). EE, epineural epithelium; H, hydrocoel; LE, larval ectoderm; TF, tube foot; V, vestibule; VE, vestibular ectoderm. Summarized from: Raff (1987), Emlet (1988), and this study (Cidaroidea); Amemiya and Tsuchiya (1979) and this study (Echinothurioida); and Okazaki (1975), Cameron and Hinegardner (1978), and Parks *et al.* (1988) (other Euechinoidea).

gramma. The orientation of the cluster of serotonergic neurons with respect to the oral-aboral axis of the echinus rudiment in *P. parvispinus* is also unusual. In *E. tribuloides* and the planktotrophic and lecithotrophic euechinoids that have been examined, the axis along the clusters of neurons lies oblique to the oral-aboral axis of the echinus rudiment, not perpendicular to it, as appears to be the case in *P. parvispinus.* The significance of the modifications in position, distribution, and orientation of the nervous system in *P. parvispinus* remains unknown.

Cidaroid metamorphosis

The adult rudiment in euechinoid sea urchins arises from the left coelomic pouch, which produces the hydrocoel (Bury, 1895; Fukushi, 1959, 1960; Cameron and Hinegardner, 1978; Okazaki, 1975). The vestibule forms as an invagination of larval ectoderm over the hydrocoel. Vestibular ectoderm encloses the adult rudiment, and its floor eventually becomes adult oral epithelium (Fig. 9a). It should be noted that analogous structures termed "vestibules" are present in some members of other echinoderm classes (Hyman, 1955), but cannot be considered homologous to the vestibules of euechinoids (Emlet, 1988).

The only cidaroid whose metamorphosis has been described in detail is *Eucidaris thouarsi,* a species with planktotrophic larvae (Emlet, 1988). As in euechinoids, the adult rudiment of *E. thouarsi* arises from the left coelomic pouch; however there is no vestibule (Fig. 9b). Metamorphosis in *E. thouarsi* is also distinguished from that of euechinoids by the presence of numerous juvenile spines on the echinus rudiment and retention of the larval ectoderm.

There is no vestibule present in *P. parvispinus,* nor in its congener, *P. imperialis,* which also undergoes lecithotrophic development (Olsen *et al.,* 1988). The absence of a larval mouth in *P. parvispinus* makes it unclear whether the adult rudiment arises exclusively from the left coelomic pouch. Metamorphosis in *P. parvispinus* is gradual, and like *E. thouarsi,* many juvenile spines are present, and much of the larval ectoderm appears to be retained. These similarities in mode of metamorphosis may prove characteristic of cidaroids in general.

The Echinothurioida, usually considered the most primitive euechinoid order (Jensen, 1981; Smith, 1984a), is the only euechinoid order in which all described species lack a vestibule. In the echinothurioid *Asthenosoma ijimai,* the adult rudiment develops on the larval surface, and is never surrounded by a vestibule (Amemiya and Tsuchiya, 1979; this paper). Since all echinothurioids appear to be direct developers (Emlet *et al.,* 1987), it has not been clear whether this is an adaptation for lecithotrophic development or a primitive feature of echinoid ontogeny. However, the presence of a vestibule in four independently evolved direct developing euechinoids (*Peronella japonica,* Okazaki and Dan, 1954; *H. erythrogramma,* Parks *et al.,* 1988; *Abatus cordatus,* Schatt, 1985; *Holopneustes inflatus,* Henry and Raff, unpub. obs.), and its absence in *E. thouarsi* demonstrates that loss of the vestibule is not a requirement of lecithotrophic development, but instead a feature of phylogenetic history.

Phylogeny of echinoid ontogeny

The Cidaroidea have been proposed as the sister group to the other extant echinoids, the Euechinoidea. This position is supported by several features of adult morphology (Jensen, 1981; Smith, 1984a, b), as well as by patterns of gene expression (Raff *et al.,* 1984; Wray and McClay, 1989). Cidaroids are characterized by lantern supports called apophyses, simple ambulacral plates, a narrow upright lantern, and the morphology of the pedicellaria. The euechinoid orders are united by several shared, derived features that distinguish them from cidaroids: lantern supports called auricles, compound ambulacral plates, lanterns with a deep foramen magnum, and details of plate arrangement. Within euechinoids, the Echinothurioida are distinguished by several primitive features absent in other orders, and by unique, derived features, including pseudocompounding of plates.

The absence of a vestibule is a character shared by cidaroids and echinothurioids and might be seen as a derived feature uniting these groups phylogenetically. However, this is probably not the case. Even if the presence of a vestibule and nature of lantern supports alone are considered, parsimony still places echinothurioids and the remaining euechinoids as a monophyletic group (Fig. 10a). The other two possible phylogenetic relationships each require not only more changes, but parallel

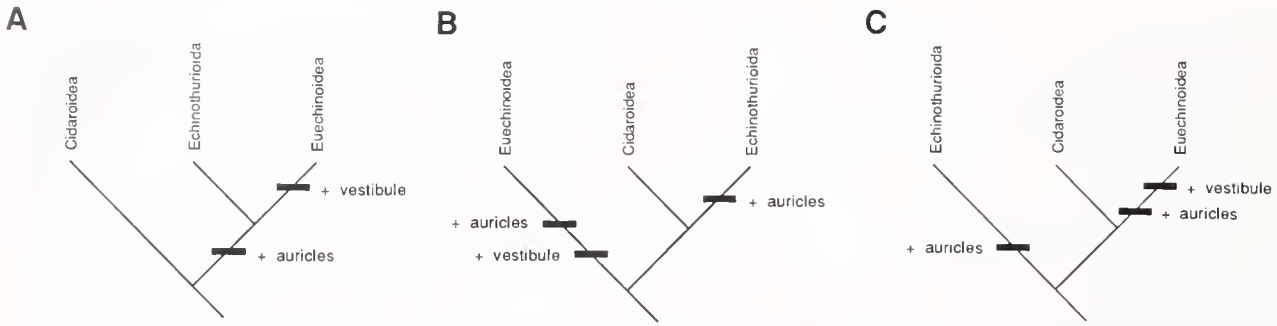

Figure 10. Echinoid phylogeny. The three possible phylogenetic relationships between cidaroids, echinothurioids, and nonechinothurioid euechinoids are shown. The states of two characters are noted in each case: presence of a vestibule during metamorphosis and the nature of lantern supports. Here we assume that the ancestor of post-Paleozoic echinoids lacked a vestibule and possessed cidaroid-type lantern supports. Acquisition of a vestibule and of lantern supports attached to ambulacral rows (euechinoid-type) are indicated "+ vestibule" and "+ auricles," respectively. The most parsimonious phylogenetic hypothesis is represented by cladogram a; cladograms b and c require more changes and parallel evolution of auricles. This hypothesis is supported by additional morphological and molecular data (see text).

evolution of auricles, which are complex morphological characters (Fig. 10b, c). Although they differ in details, the pluteus larvae of cidaroids and euechinoids are sufficiently similar that the pluteus is likely a primitive feature of post-Paleozoic echinoids. Therefore, the extinct common ancestor to cidaroids and euechinoids probably developed via a pluteus larva and lacked a vestibule. A vestibule was probably acquired after echinothurioids split from the remaining euechinoid orders, during early radiation of the euechinoids.

P. parvispinus illustrates the diversity of developmental patterns exhibited by echinoids. The lack of a vestibule, more simple metamorphosis, and the slower rate of development than comparable euechinoids are features common to cidaroids. Other characteristics such as large gametes, the absence of micromeres, a wrinkled blastula, altered msp130 expression, and accelerated echinus rudiment formation appear to be associated with the evolution of lecithotrophic development. The ability to differentiate between features attributable to ancestry and those due to the evolution of lecithotrophy should enable us to begin to decipher the molecular and cellular changes necessary to alter developmental mode.

Acknowledgments

We thank Drs. Ian Hume, Donald Anderson, Valerie Morris, and Jane Chrystal for their help and collaboration, and Heather and Craig Sowden for invaluable assistance during visits to the University of Sydney. Dr. Louis Herlands generously prepared samples of *Phyllacanthus parvispinus* embryos and provided photographs of some living embryos. Dr. Shonan Amemiya kindly provided specimens of *Asthenosoma ijimai* for comparison. We thank Drs. Brian Parr and Jonathan Henry for valuable discussions and comments. This research was supported by an NSERC Postgraduate Scholarship to BWB, by NIH Postdoctoral Fellowship GM12495 to GAW, and by NIH HD21337 and a N.S.F. U.S./Australian Cooperative Program grant to RAR.

Literature Cited

Amemiya, S. and T. Tsuchiya. 1979. Development of the echinothurioid sea urchin *Asthenosoma ijimai*. *Mar. Biol.* **52:** 93–96.

Anstrom, J. A., J.-E. Chin, D. S. Leaf, A. L. Parks, and R. A. Raff. 1987. Localization and expression of msp130, a primary mesenchyme cell lineage-specific glycoprotein in the sea urchin embryo. *Development* **101:** 225–265.

Barker, M. F. 1985. Reproduction and development in *Gonocidaris umbraculum*, a brooding echinoid. Pp. 207–214 in *Proceedings of the Fifth International Echinoderm Conference*, B. F. Keegan and B. D. S. O'Conner, eds. Balkema, Amsterdam.

Bisgrove, B. W., and R. D. Burke. 1986. Development of the serotonergic neurons in embryos of the sea urchin, *Strongylocentrotus purpuratus*. *Dev. Growth Differ* **28:** 569–574.

Bisgrove, B. W., and R. D. Burke. 1987. Development of the nervous system of the pluteus larva of *Strongylocentrotus droebachiensis*. *Cell and Tissue Res.* **248:** 335–343.

Bisgrove, B. W., and R. A. Raff. 1989. Evolutionary conservation of the larval serotonergic nervous system in a direct developing sea urchin. *Dev. Growth Differ.* **31:** 363–370.

Bury, H. 1895. The metamorphosis of echinoderms. *Q. J. Microsc. Sci.* **38:** 45–137.

Cameron, R. A., and R. T. Hinegardner. 1978. Early events in sea urchin metamorphosis. Description and analysis. *J. Morphol.* **157:** 21–32.

Emlet, R. B. 1988. Larval form and metamorphosis of a "primitive" sea urchin, *Eucidaris thouarsi* (Echinodermata: Echinoidea: Cidaroida), with implications for developmental and phylogenetic studies. *Biol. Bull.* **174:** 4–19.

Emlet, R. B., L. R. McEdward, and R. R. Strathmann. 1987. Echinoderm larval ecology viewed from egg. Pp. 55–136 in *Echinoderm Studies*, Vol. 2, J. Lawrence and M. Jangoux, eds. Balkema, Amsterdam.

Fukushi, T. 1959. On the cell mass observed on the left side of the pluteus of the sea urchin, *Temnopleurus hardwickii*. *Bull. Mar. Biol. Stat. Asamushi* **9:** 133–135.

Fukushi, T. 1960. Formation of the echinus rudiment and the development of the larval form in the sea urchin, *Temnopleurus hardwickii*. *Bull. Mar. Biol. Stat. Asamushi* **10:** 65–72.

Gibson, A. W. and R. D. Burke. 1985. The origin of pigment cells in embryos of the sea urchin *Strongylocentrotus purpuratus*. *Dev. Biol.* **107:** 414–419.

Hinegardner, R. T. 1967. Echinoderms. Pp. 139–156 in *Methods in Developmental Biology*, F. H. Wilt and N. K. Wessels, eds. T. Y. Crowell, New York.

Hyman, L. H. 1955. *The Invertebrates: Echinodermata.* McGraw-Hill, New York.

Jensen, M. 1981. Morphology and classification of the Euechinoidea Bronn, 1860—a cladistic analysis. *Vidensk. Meddr. Dansk. Naturh. Foren.* **143:** 7–99.

Lillie, R. D. 1965. *Histopathologic Technique and Practical Histochemistry*, 3 ed. McGraw-Hill, New York. Pp. 176–177.

Mladenov, P. V. 1979. Unusual lecithotrophic development of the Caribbean brittle star, *Ophiothrix oerstedi*. *Mar. Biol.* **55:** 55–62.

Mortensen, T. H. 1921. *Studies of the Development and Larval Forms of Echinoderms.* G. E. C. Gad, Copenhagen.

Mortensen, T. H. 1937. Contributions to the study of the development and larval forms of echinoderms. III. *Kgl. Dan. Vidensk. Selsk. Skr. Naturvid. Math. Ser. 9* **7**(1): 1–65.

Mortensen, T. H. 1938. Contributions to the study of the development and larval forms of echinoderms. IV. *Kgl. Dan. Vidensk. Selsk. Skr. Naturvid. Math. Ser. 9* **7**(3): 1–59.

Nakajima, Y. 1987. Developmental study on nervous system of *Hemicentrotus pulcherrimus* larva. *Dev. Growth Differ.* **29:** 408.

Okazaki, K. 1975. Normal development to metamorphosis. Pp. 177–232 in G. Czihak, ed. *The Sea Urchin Embryo.* Springer-Verlag, Berlin.

Okazaki, K. and K. Dan. 1954. The metamorphosis of partial larvae of *Peronella japonica* Mortensen, a sand dollar. *Biol. Bull.* **106:** 83–99.

Olsen, R. R., J. L. Cameron, and C. M. Young. 1988. Larval development of the pencil urchin *Phyllacanthus imperialis*: lecithotrophic echinopluteus. P. 807 in *Echinoderm Biology: Proceedings of the Sixth International Echinoderm Conference*, R. D. Burke, P. V. Mladenov, P. Lambert, and R. L. Parsley, eds. Balkema, Rotterdam.

Parks, A. L., B. A. Parr, J.-E. Chin, D. S. Leaf, and R. A. Raff. 1988. Molecular analysis of heterochronic changes in the evolution of direct developing sea urchins. *J. Evol. Biol.* **1:** 27–44.

Prouho, H. 1887. Recherches sur le *Dorocidaris papillata* et quelques autres echinides de la Méditerranée. *Arch. Zool. Exp. Gén. Ser. 2* **5:** 213–380.

Raff, R. A. 1987. Constraint, flexibility, and phylogenetic history in the evolution of direct development in sea urchins. *Dev. Biol.* **119:** 6–19.

Raff, R. A., J. A. Anstrom, C. J. Huffman, D. S. Leaf, J. H. Loo, R. M. Showman, and D. E. Wells. 1984. Origin of a gene regulatory mechanism in the evolution of echinoderms. *Nature* **310:** 312–314.

Raff, R. A., B. A. Parr, A. L. Parks, and G. A. Wray. 1989. Heterochrony and other mechanisms of radical evolutionary change. In *The Origin of Evolutionary Innovation*, M. H. Nitekki and D. V. Nitekki, eds. University Chicago Press, Chicago, IL. In press.

Schatt, P. 1985. L'édification de la face orale au cours du developpement direct de *Abatus cordatus*, oursin incubant subantartique. Pp. 339–345 in *Echinodermata: Proceedings of the Fifth International Echinoderm Conference*, B. R. Keegan and B. D. S. O'Connor, eds. Balkema, Amsterdam.

Schroeder, T. 1981. Development of a "primitive" sea urchin (*Eucidaris tribuloides*): irregularities in the hyaline layer, micromeres, and primary mesenchyme. *Biol. Bull.* **161:** 141–151.

Smith, A. B. 1984a. Classification of the Echinoidea. *Paleontology* **27:** 431–459.

Smith, A. B. 1984b. *Echinoid Paleobiology.* Allen and Unwin, London.

Strathmann, M. F. 1987. *Reproduction and Development of Marine Invertebrates of the Northern Pacific Coast.* Univ. of Washington Press, Seattle, WA.

Strathmann, R. R. 1975. Larval feeding in echinoderms. *Am. Zool.* **15:** 717–730.

Strathmann, R. R. 1978. The evolution and loss of feeding larval stages of marine invertebrates. *Evolution* **32:** 894–906.

Tennent, D. H. 1914. The early influence of the spermatozoan upon the characters of echinoid larvae. *Carn. Inst. Wash. Publ.* **182:** 129–138.

Tennent, D. H. 1922. Studies on the hybridization of echinoids. Part I. Embryology and hybridization of *Cidaris*. *Carn. Inst. Wash. Publ.* **312:** 3–43.

Williams, D. H. C., and D. T. Anderson. 1975. The reproductive system, embryonic development, larval development and metamorphosis of the sea urchin *Heliocidaris erythrogramma* (Val.) (Echinoidea: Echinometridae). *Aust. J. Zool.* **23:** 371–403.

Wray, G. A., and D. R. McClay. 1988. The origin of spicule-forming cells in a "primitive" sea urchin (*Eucidaris tribuloides*) which appears to lack primary mesenchyme cells. *Development* **103:** 305–315.

Wray, G. A., and D. R. McClay. 1989. Molecular heterochronies and heterotopies in early echinoid development. *Evolution* **43:** 803–813.

Wray, G. A., and R. A. Raff. 1989. Evolution of cell lineage and fate in the direct developing sea urchin *Heliocidaris erythrogramma*. *Dev. Biol.* **132:** 458–470.

Reference: *Biol. Bull.* **177:** 110–129. (August, 1989)

Ecology and Life History of an Amoebomastigote, *Paratetramitus jugosus,* from a Microbial Mat: New Evidence for Multiple Fission

MICHAEL ENZIEN, HEATHER I. McKHANN[1], AND LYNN MARGULIS[2]

Boston University, Department of Biology, 2 Cummington Street, Boston, Massachusetts 02215

Abstract. Five microbial habitats (gypsum crust, gypsum photosynthetic community, *Microcoleus* mat, *Thiocapsa* scum, and black mud) were sampled for the presence of the euryhaline, rapidly growing amoebomastigote, *Paratetramitus jugosus.* Field investigations of microbial mats from Baja California Norte, Mexico, and Salina Bido near Matanzas, Cuba, reveal that *P. jugosus* is most frequently found in the *Thiocapsa* layer of microbial mats.

Various stages of the life history were studied using phase-contrast, differential-interference, and transmission electron microscopy. Mastigote stages were induced and studied by electron microscopy; mastigotes that actively feed on bacteria bear two or more undulipodia*. A three-dimensional drawing of the kinetid ("basal apparatus") based on electron micrographs is presented.

Although promitoses were occasionally observed, it is unlikely that they can account for the rapid growth of *P. jugosus* populations on culture media. Dense, refractile, spherical, and irregular-shaped bodies were seen at all times in all cultures along with small mononucleate (approximately 2–7 μm diameter) amoebae. Cytochemical studies employing two different fluorescent stains for DNA (DAPI, mithramycin) verified the presence of DNA in these small bodies. Chromatin-like material seen in electron micrographs within the cytoplasm and blebbing off nuclei were interpreted to be chromatin bodies. Our interpretation, consistent with the data but not proven, is that propagation by multiple fission of released chromatin bodies that become small amoebae may occur in *Paratetramitus jugosus.* These observations are consistent with descriptions of amoeba propagules in the early literature (Hogue, 1914).

Received 12 December 1988; accepted 31 May 1989.

[1] Current address: Department of Biology, University of California at Los Angeles, Los Angeles, CA 90024.

[2] Current address: Department of Botany, University of Massachusetts, Amherst, MA 01003.

* The term mastigote refers to an organism that bears undulipodia ("eukaryotic flagella"), *i.e.,* microtubular motility organelles with [9(2) + 2] microtubules in transverse section (Margulis, 1980; Margulis and Sagan, 1985).

Introduction

We report here field and laboratory studies of a rapidly growing, hardy, encysting, and desiccation-resistant amoebomastigote, *Paratetramitus jugosus.* Responsive to recent changes in systematics, we provide the classification of *P. jugosus* (Page, 1983) in the Protoctista (rather than animal) kingdom (Table I) (Margulis, 1988; Margulis *et al.,* 1989). Our strain *P. jugosus bajacaliforniensis* (Read *et al.,* 1983), isolated from sediments of a microbial mat in an evaporated marine salt pond, is unusually euryhaline for the genus. All other isolates were taken from freshwater and soil environments (Darbyshire *et al.,* 1976).

Approximately once a year since a two-year episode of flooding that began in 1979, *P. j. bajacaliforniensis* has been taken from both submerged and re-emerged field samples of the *Microcoleus* mats at North Pond and at the south salinas area of Laguna Figueroa, Baja California Norte, Mexico (Fig. 1). *P. jugosus* amoebae were recovered in impressive numbers from nearly every mat sample transferred onto permissive plates in the years during and just after the floods (1979–80). Even after the recession of the flood waters and the return of the region to its more typical dry conditions, we have collected fresh isolates of *Paratetramitus jugosus* at the same geographic

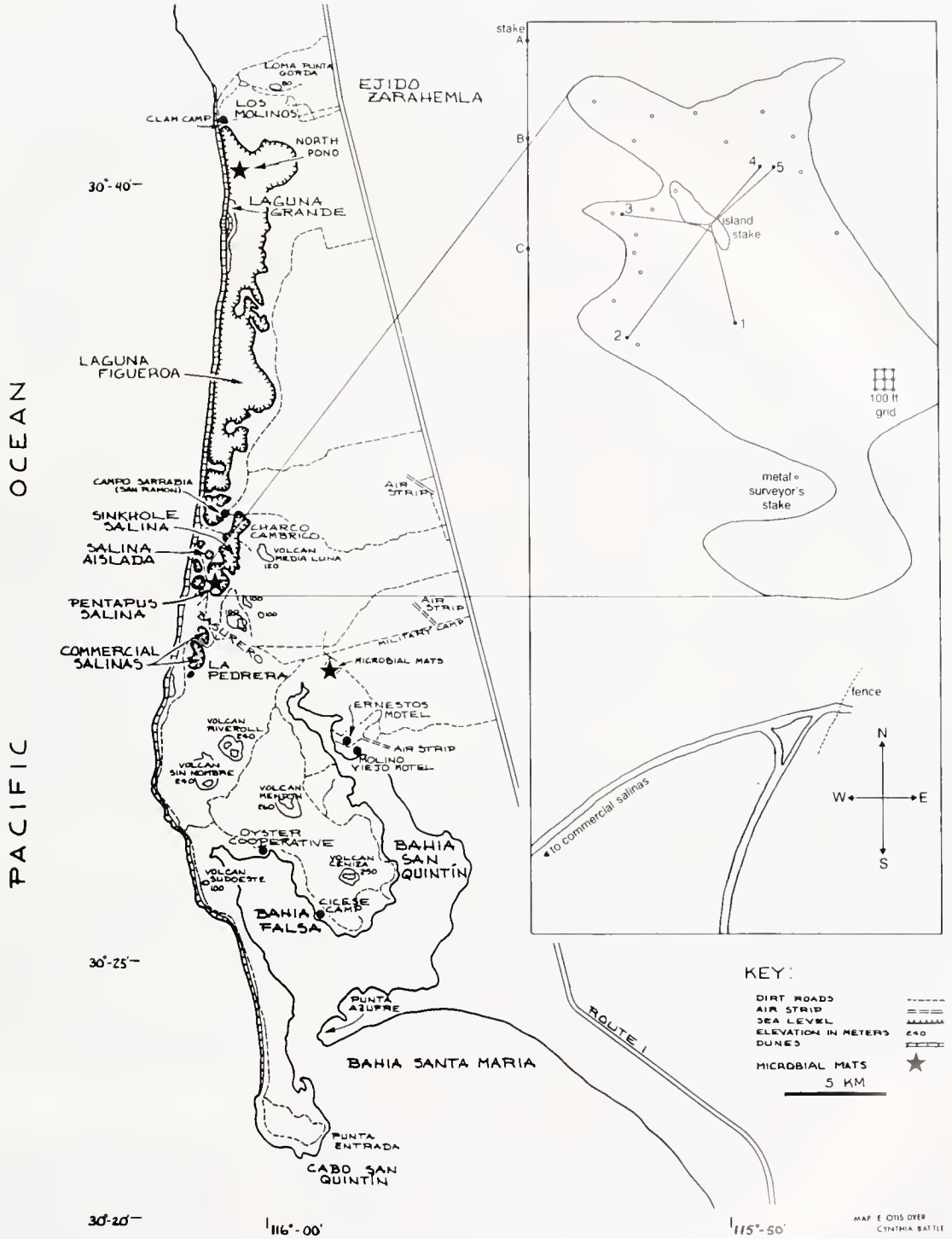

Figure 1. Map of field site in Baja California, Mexico. Samples were collected from both North Pond and Pentapus Salinas. Inset map indicates specific sampling sites at Pentapus Salinas. Sites 1–5 correspond to Figures 2A–E.

locations. A continuation of previous work (Read *et al.*, 1983), this study verifies the occurrence of *P. jugosus* in similar microbial habitats, *e.g.*, in Cuba and Mexico, and presents effective methods of ecological sampling to demonstrate its presence.

In live microscopic preparations of *P. jugosus*, every

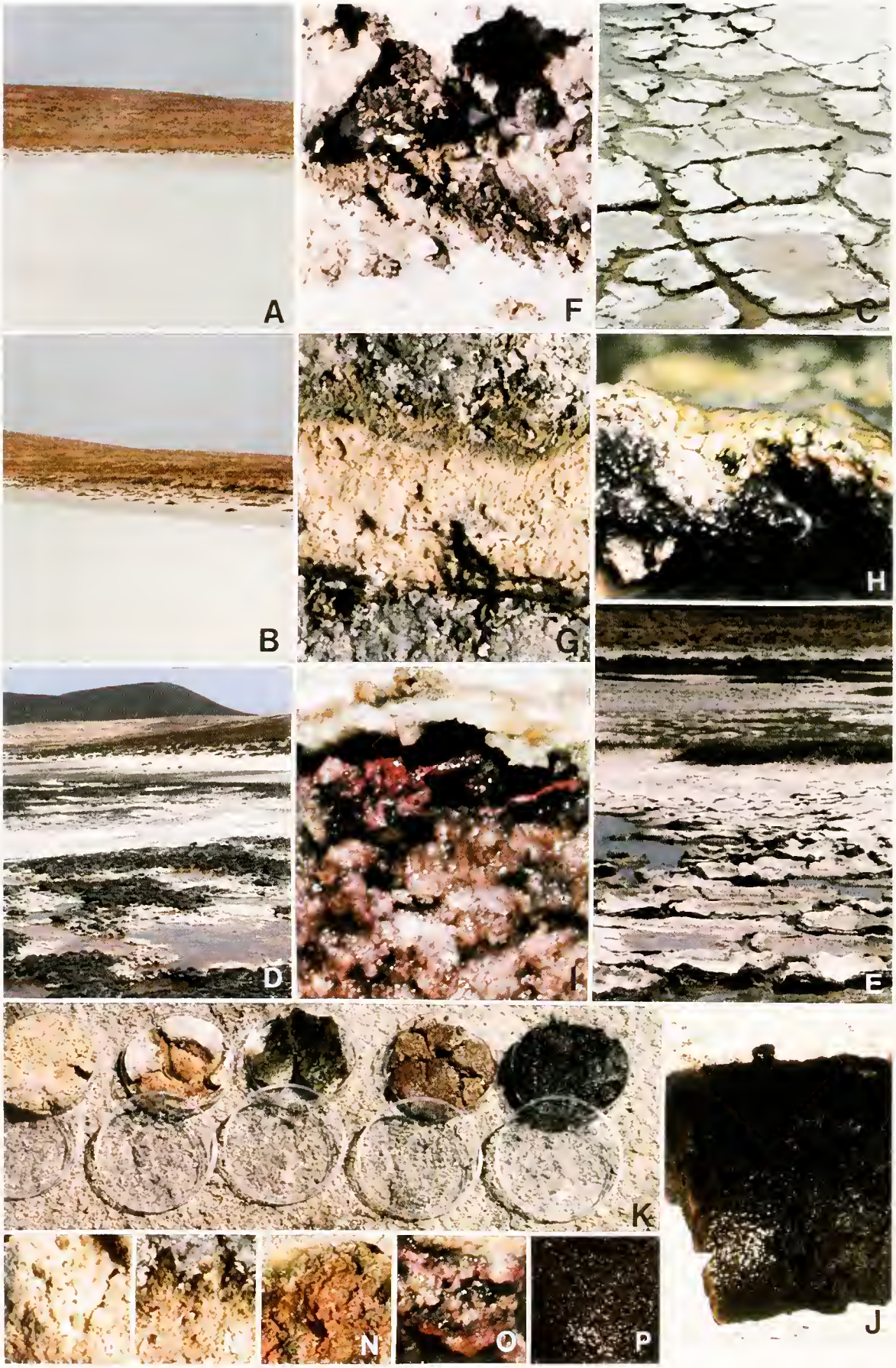
A
F
C
B
G
H
D
I
E
K
J
N
O
P

Table I

Classification of Paratetramitus jugosus

		Taxon references
KINGDOM	Protoctista	Margulis *et al.*, 1990
PHYLUM	Zoomastigina	Margulis *et al.*, 1990
CLASS	Amoebomastigota	Margulis *et al.*, 1990
ORDER	Schizopyrenida	Singh, 1952 in Page, 1983
FAMILY	Vahlkampfiidae	Jollos, 1917; Zulueta, 1917 in Page, 1983
GENUS	*Paratetramitus*	Darbyshire *et al.*, 1976
SPECIES	*jugosus*	Page, 1967
strains	*bajacaliforniensis*, Cuba	Read *et al.*, 1983 this paper

stage in the reproductive life history has been sought; yet, in spite of continued attempts, the complete process of standard vahlkampfid promitotic division has never been observed. [Promitosis is defined as karyokinesis followed by cytokinesis in which the nuclear membrane is preserved throughout; *i.e.*, closed nuclear division with an intranuclear spindle (Page, 1983; Raikov, 1982).]

The presence of small spherical and irregular shaped bodies (2–7 μm diameter) always found in our cultures, chromatin-like bodies, nuclear blebbing, and apparent cytoplasmic "budding," led us to hypothesize the existence of multiple fission in the reproduction of this small eukaryote and thus to examine the localization of DNA in actively growing and reproducing cultures. Electron microscopic studies and cytochemical observations on amoebae stained with fluorescent dyes specific for DNA (DAPI, mithramycin) coupled with DNase enzyme treatments, led us to our interpretation of the life history of this amoebomastigote.

"Chromidia," *i.e.*, chromatin bodies in large vahlkampfid amoebae parasitic on oysters, were described by Hogue (1914) from live and fixed material using nonspecific nuclear stains; apparently ours is the first cytochemical study since that time that employs DNA-specific stains of comparable structures.

Materials and Methods

Field studies

Sampling for most of the fieldwork reported here was done at Pentapus Salina (inset, Fig. 1), a small member of the south salina complex of Laguna Figueroa, Baja California Norte, Mexico. Unlike the larger salinas to the south, Pentapus is not used for commercial salt production. Although more microbial community-dominated surfaces could be distinguished than were studied, five of those easiest to recognize were chosen as sources for sampling. Each corresponds to major surface cover at the five survey sites shown on the inset map of Pentapus. Descriptively named for the appearance of the surface sediment they are (Fig. 2): (1) gypsum crust (black-and-white sediment only, no macroscopic evidence for green or red phototrophic bacterial communities); (2) gypsum photosynthetic mat (green-layered pink-underlain community of phototrophic bacteria beneath the white gypsum crust); (3) *Microcoleus* mat (cohesive microbial mat community, often polygonal at surface, dominated by the sheathed, green, filamentous cyanobacterium *Microcoleus chthonoplastes*); (4) *Thiocapsa* scum (purple-pink, dense, gelatinous community dominated by the purple phototroph *Thiocapsa sp.*); and (5) black mud (sulfurous, homogeneous black mud sample taken subaqueously from standing water in the channels or from beneath the *Microcoleus* mat). Additional samples were collected from sediment rich with sulfur-oxidizing bacteria (Fig. 3A) and from microbial mats from a mangrove area in Salina de Bido, Cuba (Fig. 3B, C).

Figure 2. Field sites in Pentapus Salina. A–E. Scenes. A. Gypsum crust, Pacific Ocean is at other side of vegetation-covered dune. B. Gypsum mat develops where enough water seeps under the dune to support it. C. *Microcoleus chthonoplastes* stratified microbial community tends to split into polygons covered with evaporite minerals on the surface in tidal channels on the seaward side of the salina. D. *Thiocapsa* scum community tends to have rumpled sediment cover and black coloration due to complex communities of coccoid cyanobacteria and other microbes in the oxygenic surface layers. E. Black muds reside in many places, but at site 5 where water is abundant, they approach the surface and can be seen without cutting into the sediment beneath the cyanobacterial community. F–J. Unaided-eye views of typical sediment profiles from sites 1–5. F. Gypsum crust which grades directly from oxidized calcium sulfate to black sulfide-rich mud tends to be dry, lacking evidence of colored phototrophic bacterial communities indicating low populations of these organisms. G. Gypsum mat in which laminae of green cyanobacterial populations are underlain by a paper-thin layer of purple phototrophs. H. Fully developed *Microcoleus* mat community (Stolz, 1983) I. *Thiocapsa* scum, which contains several types of purple phototrophs including the salmon-colored *Thiocapsa pfennigii* and the orange-colored microbe *T. roseopercicina*. J. Amorphous sulfurous gelatinous mud, which underlies most mat communities, contains many heterotrophs and evidence for degradation of the phototrophic community. K. Samples of each of the five community types are placed in sterile Petri dishes for further study. L–P. Close-up of samples used as source inocula from each of the five field sites: L. Gypsum crust, M. Gypsum mat, N. *Microcoleus* mat, O. *Thiocapsa* scum, P. Black mud. See Table II for results from each of the five sites.

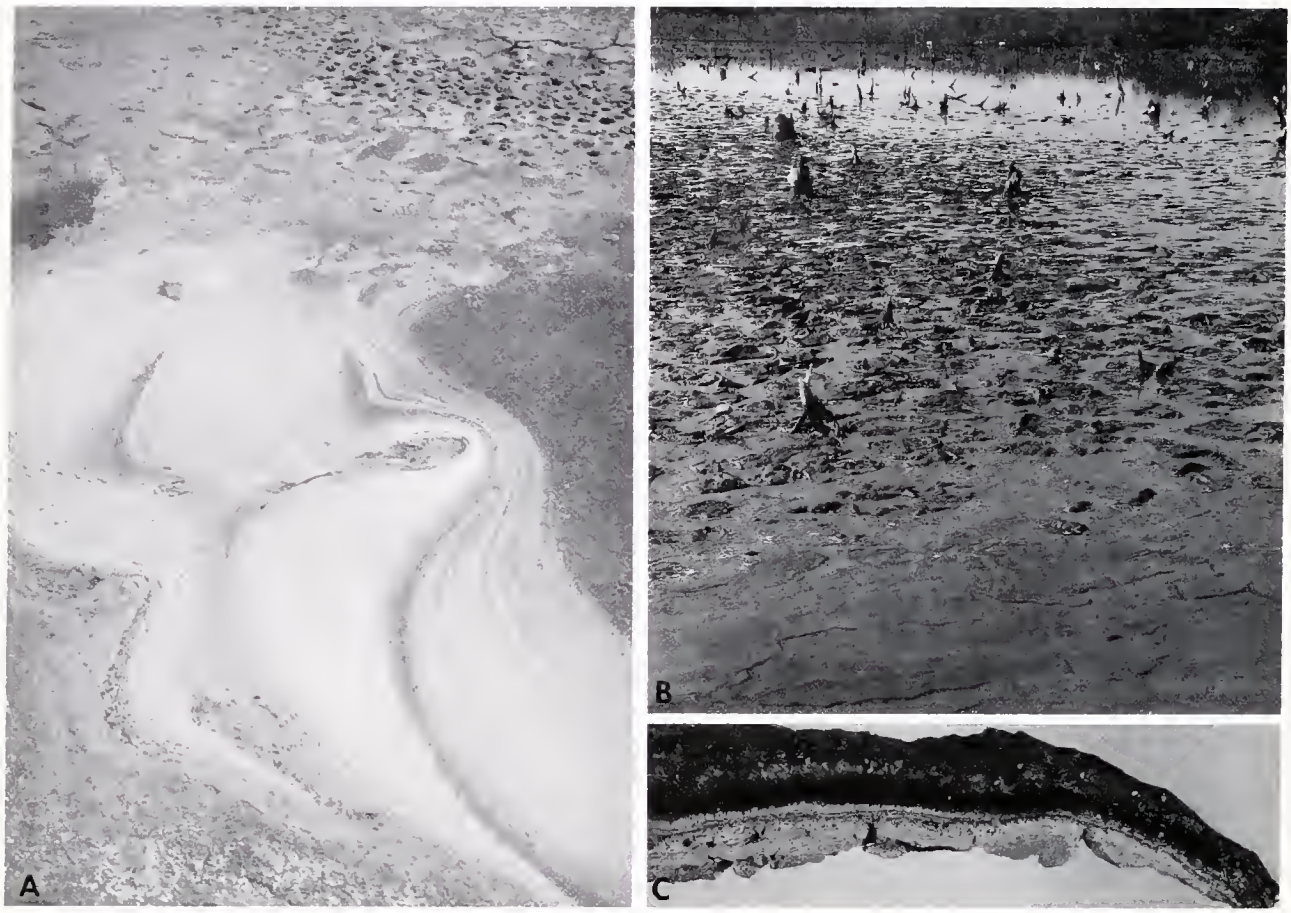

Figure 3. A. Salt pond scum community dominated by sulfide oxidizing bacteria to the west of stake marked 4 on inset of Figure 1. B. Salina Bido, Matanzas Cuba, site of collection of the Cuba strain of *Paratetramitus jugosus*. Mangrove trees form the barrier between the mats and the open ocean. C. *Microcoleus* mat from Salina Bido, hand sample.

With the help of two Earthwatch teams (1983) the Laguna Figueroa sites were extensively surveyed and marked with a permanent stake ("metal surveyor's stake," Fig. 1). Wooden stakes were placed as indicated by the open circles, including three reference stakes ("stakes A, B, C," Fig. 1). Sediment samples from the five sites were placed on petri plates to enrich for *P. jugosus* in early May; the experiments were repeated six weeks later in June 1983. Collections involving samples from the five different sediment types at Pentapus were twice made again in March and October 1988.

Agar plates were prepared with two kinds of thinly poured sterile enrichment media: "modified-K" and "manganese-acetate" (MnAc) (Margulis *et al.*, 1980; Read *et al.*, 1983). These plates were taken to the field study site where a sample about 1 mm^3 of each of the five sediment types was placed directly at the center of both kinds of sterile plates.

Immediately after samples were in place, they were covered with approximately 1 ml of sterile distilled water to suspend the organisms and initiate reproduction and perhaps excystment. When vigorous growth was evident, plates were monitored and scored for the presence of cysts and amoebae. These were subcultured as needed onto fresh medium by streaking with a sterile platinum loop.

The organisms were routinely grown at room temperature on either modified K or MnAc media, both of which contain half-concentrated seawater. The food source for *P. jugosus* is a gram-positive, flagellated, facultatively aerobic rod (designated "B bacillus") that grows readily on both media. Because it is morphologically indistinguishable, the B bacillus is likely to be a strain of the organism reported by Gong-Collins (1986).

Maintenance and storage of stock cultures is described in Read *et al.* (1983).

Light microscopy

Culture slides. Hanging-drop culture slides were made for observation of live *P. jugosus*. A very small drop of

Table II

Paratetramitus jugosus *on field plates*

Observation scored on	Day 1		Day 8		Day 10–11		Day 16–18		Day 19		Day 28		Day 30	
MEDIUM	K	MnAc	K	MnAc	K	MnAc	K	MnAc	K	MnAc	K	MnAc	K	MnAc
Sites														
1. Gypsum crust	−	−			+	+	+	+						
2. Gypsum mat	−	−			−	+	−	+						
3. *Microcoleus* mat	−	−			−, −, −	+, +, +	+, +, +	+, +, +						
4. *Thiocapsa* scum	−	−			−	+, +, −	−, +	+, +, +						
1. Gypsum crust	−	−	−	−	−, +	+, +	−, +	+, +	−	+	−	+, −	−	+
2. Gypsum mat	−	−	−	+	−, +	+, +, +	−, −	+, +	−	++	−	−	−	++
3. *Microcoleus* mat	−	−	++	+	++, −	+, +, N	++, +	+, +	++	+	−, F	+, −	++	++
4. *Thiocapsa* scum	−	−	++	+	+, −	+, +, −	++, −	+, +	++	+	++	+	+	+
5. black mud	−	−	−	−	−	−	+	−	−	−	++	++	−	−

Top: May–June 1983

Bottom: March 1988, except for day 28 which corresponds to August experiment

Key: −, no or very few cysts; +, cysts abundant; ++ at 25× magnification every field on plate has cysts; N, F nematodes, fungi obscure readings

Notes: *Acanthamoeba* sp. cysts (larger and more crenulated than those of *Paratetramitus*) also tend to appear on plates where *P. jugosus* cysts are abundant. Commas between entries indicate entirely different sets of experiments; each entry represents the value on 1 to 4 plates.

MnAc medium was placed on a glass coverslip, inoculated with amoeba cysts, and then covered with a depression slide. Petroleum jelly was used to adhere and seal the coverslip to the slide. Fresh preparations were viewed immediately with a Nikon Diaphot inverted microscope. The excysting amoebae grew on the coverslips mounted over the inverted glass depression slides. After amoebae were detected with the inverted scope, the slides were flipped upright and observed at higher magnification with the Nikon Fluophot phase-fluorescence microscope.

Amoebomastigote transformation. Monoprotist cultures were grown from fresh microbial mat material collected by the above method at Salina de Bido, Matanzas, Cuba. The cultures, started within two weeks of collection, contained various types of bacteria, including food bacteria, and were used to obtain amoebomastigote transformation. Plates were flooded with distilled water and allowed to stand for 10 min. The water was then pipetted off and placed in a sterile test tube. Several drops of this aqueous suspension were placed on a K plate, and the plate was monitored for the presence of amoebae and mastigotes by light microscopy over a 48-h period.

Nuclear fluorescent staining

Fixation. Cultures necessary for monitoring the reproductive processes of *P. jugosus* had to contain growing amoebae. Active trophic amoebae were acquired by the following technique: five glass coverslips were aseptically placed in a circle on a MnAc plate. The center of the circle made by the coverslips was then inoculated with a monoprotist culture of *P. jugosus* and flooded with sterile MnAc medium (lacking agar) up to the edge of the coverslips. One to two drops K medium (lacking agar) were added to the surface of the five coverslips. The amoebae were incubated at room temperature for one to four days, or until the growing edge of the culture could be detected on the surface of the coverslips using an inverted microscope. The coverslips were removed and immediately immersed in Columbia jars containing a modified Carnoy's fixative (70% ethanol, glacial acetic acid, in a 3:1 ratio). The coverslips containing the amoebae were then rinsed twice in 70% ethanol and stored at 4°C in 70% ethanol until they were stained.

Unlike the agar culture slides used previously (Read *et al.*, 1983) it was not necessary to coat the coverslips with agar. No step in the staining procedure was needed to insure the adherence of the amoebae to the coverslips. Apparently enough adhesive substance from the K medium and any proteinaceous substances secreted by or from lysed bacteria caused excellent adhesion of fixed amoebae. Eliminating the necessity of coating coverslips with Parlodion® or other substances decreased the amount of background debris including spurious fluorescence in stained samples.

Staining. Two fluorescent DNA stains were used in this study: 4′-6-diamidino-2-phenylindole (DAPI) and mithramycin (both purchased from Sigma Chemical Co., St. Louis, Missouri). Staining procedures were those of Coleman *et al.* (1981). Stain concentrations were 0.5 μg/ml DAPI in McIlvaine's pH 4.4, or 50 μg/ml mithramycin in McIlvaine's pH 7.0 with 10 mM $MgSO_4$. Fixed coverslips were rehydrated briefly through an ethanol series, washed twice in dH_2O, and then twice in the appropriate buffer.

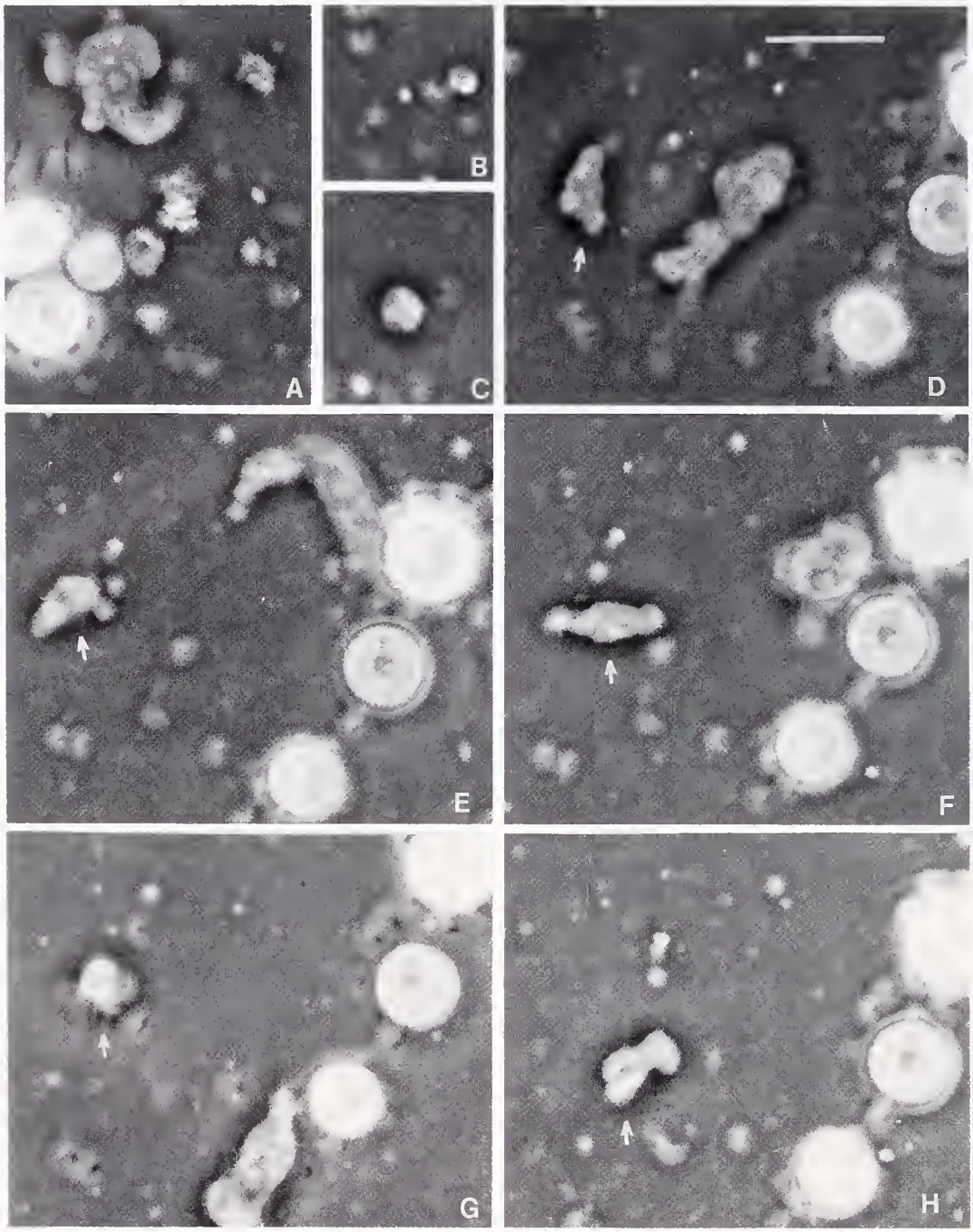

Figure 4. Photomicrographs of live *Paratetramitus jugosus*. A. Amoeba with visible nucleus and several small spherical and irregular-shaped bodies. Cyst in bottom left corner. B,C. Small spherical bodies frequently found in cultures. D–H. Sequential photos showing movement of small amoeba (arrow). The small amoeba closely resembles many other small irregular objects in our cultures. (Compare 4C with 4G) Bar scale = 10 μm.

Coverslips were placed on blotting paper, sample-side up, and flooded with approximately 200 μl of stain solution. A clean glass slide placed over the coverslip was turned over and allowed to stand for one to three hours in the dark. The slide was then blotted dry and sealed around the edges with clear nail polish. Some slide preparations were treated with pancreatic RNase before staining to remove background binding of DAPI to RNA (Coleman *et al.*, 1981). Samples treated with bovine DNase I (Coleman *et al.*, 1981) allowed distinction of stained DNA from

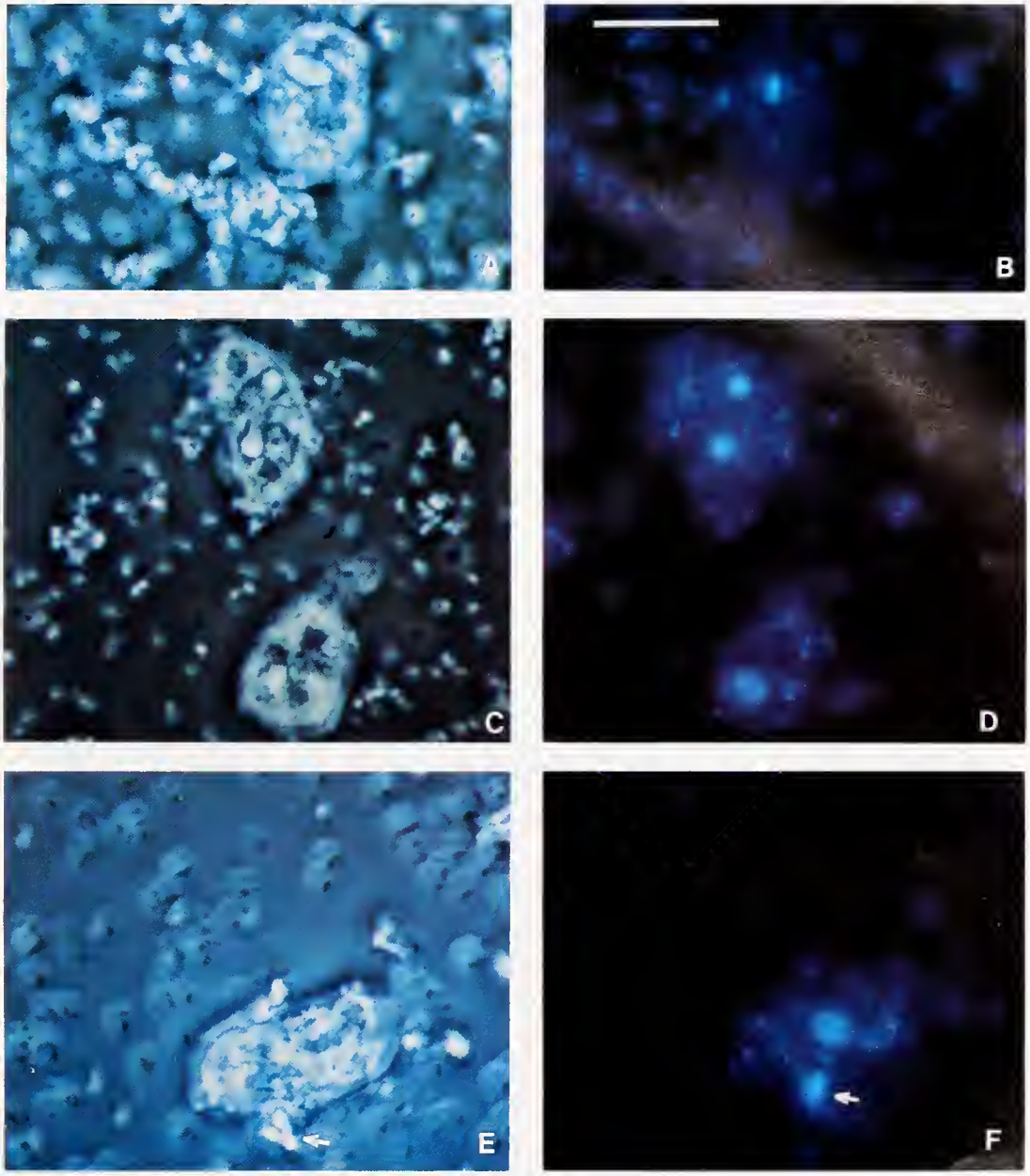

Figure 5. Phase/fluorescence micrographs of DAPI-stained amoebae. A,B. Amoeba with metaphase nucleus. Phase micrograph shows nucleus clearly intact and under fluorescence, DNA is seen condensed in the center. C,D. Amoebae with telophase nucleus. D,F. Cytoplasmic DNA is faintly visible in the amoebae. E,F. Arrow indicates a structure which may be a chromatin body extruded by the amoeba. Its size and fluorescent properties differ from cytoplasmic fluorescence. Bar scale = 10 μm.

nonspecific brightly staining material in the preparations. Unstained amoeba slide preparations were also used as controls to detect and distinguish autofluorescence from authentic DNA staining. Excitation filter sets on the Nikon Fluophot in the UV and blue (approximately 365 nm and 490 nm) were used for epifluorescence observations of DAPI and mithramycin samples, respectively. Photomicrographs were made with a Nikon Microflex AFX photomicrographic attachment. Films used for photomicroscopy were Scotch 640 ASA tungsten film and Kodak Tri-X 400 ASA pushed to 1600.

Electron microscopy

Fixation and embedding of the Cuba strain of P. jugosus. Amoebae inoculated into aqueous suspension (de-

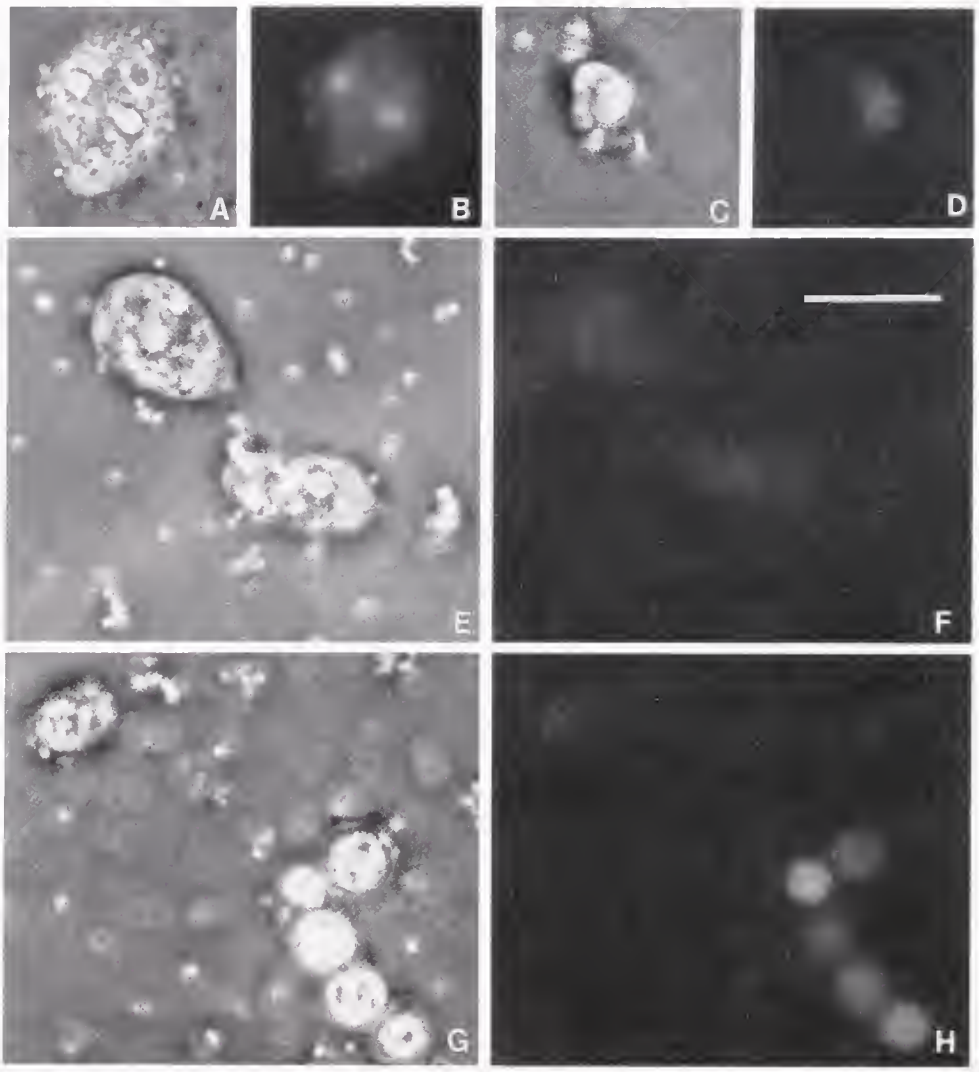

Figure 6. A,B. Phase/fluorescence micrographs of DAPI-stained amoebae with nuclei in telophase. C–H. Phase and fluorescence; Autofluorescence with blue filter (490nm) of small bodies, amoebae, and cysts. Bar scales = 10 μm.

scribed above) were allowed to grow for two days. Several milliliters of distilled water were added to the suspension and 3 ml of this water were transferred to a centrifuge tube to which 0.15 ml of glutaraldehyde was added to make the final concentration of the fixative 5%. After fixation overnight at room temperature and pelleting in a clinical centrifuge, the samples were washed twice in 0.1 *M* cacodylate buffer (10 min each wash). The pellet was post-fixed for 10 min in 2% osmium tetroxide, washed twice with distilled water, and then stained with 0.5% uranyl acetate for 30 min. Samples were then washed with distilled water (10 min) and dehydrated through an ethanol series as follows: 70% (5 min), 80% (5 min), 90% (5 min), 95% (10 min), 100% 3× 10 min. For embedding, the pelleted sample was placed in propylene oxide for 30 min, followed by 30 min in a 1:1 mixture of propylene oxide: Spurr's resin. After transferring to a beam capsule, it was recentrifuged and left in Spurr's for 5 h after which the spent Spurr's was poured off and fresh Spurr's added; the resin was polymerized for 16 h at 70°C.

Mat material from North Pond, Laguna Figueroa, Baja California, was fixed at the site according to the methods of Stolz (1983).

Sectioning and observations. The blocks were sectioned by Floyd Craft (Boston University) on a Porter Blum MT2B ultramicrotome, post-stained with 2% uranyl acetate for 15 min, lead citrate for 5 min, and then observed on a Philips model 410 transmission electron microscope at 20 kV.

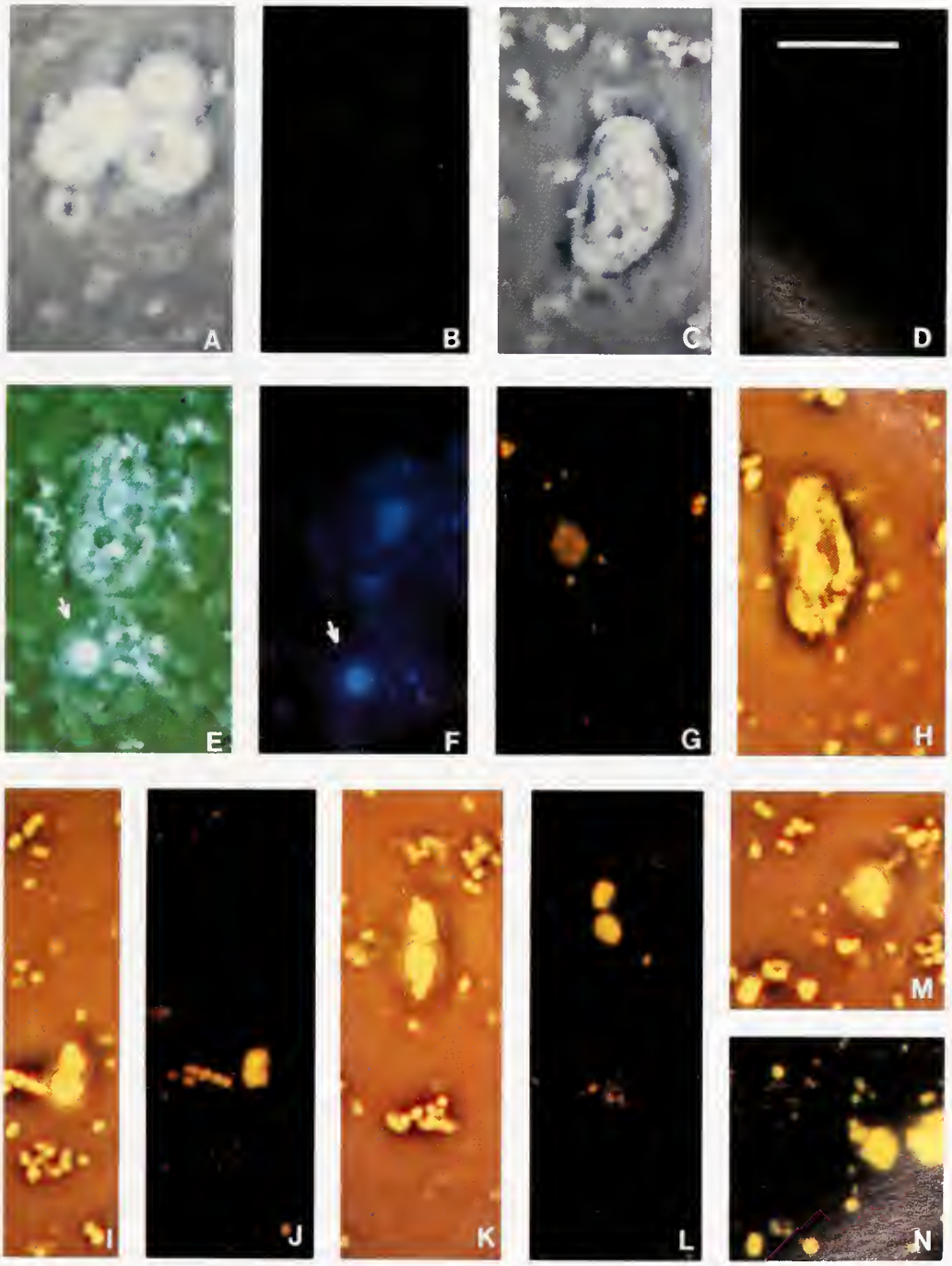

Figure 7. A–D. Phase and fluorescence; DNase treatment of amoebae stained with mithramycin. Nuclear and cytoplasmic fluorescence is completely removed. E,F. Phase/fluorescence; DAPI stained amoeba and associated small spherical body (arrow). Small body has stronger fluorescence than the amoeba nucleus. G,H. Fluorescence and phase; Mithramycin staining clearly showing nucleus of amoeba and possibly other DNA containing organelles inside cell. I–N. Phase and fluorescence; Mithramycin staining of small spherically and irregularly shaped bodies. The fluorescence of these bodies is stronger than the nuclei of the amoebae. Bar scale = 10 μm.

Isoenzyme analysis

Slant cultures of the amoebomastigote isolate from Cuba were sent for isoenzyme analysis to the American Type Culture Collection (ATCC, Rockville, Maryland). Starch gel electrophoretic techniques for isoenzyme patterns were conducted by Tom Nerad (Nerad and Daggett, 1979). The Cuban strain was tested for three isoen-

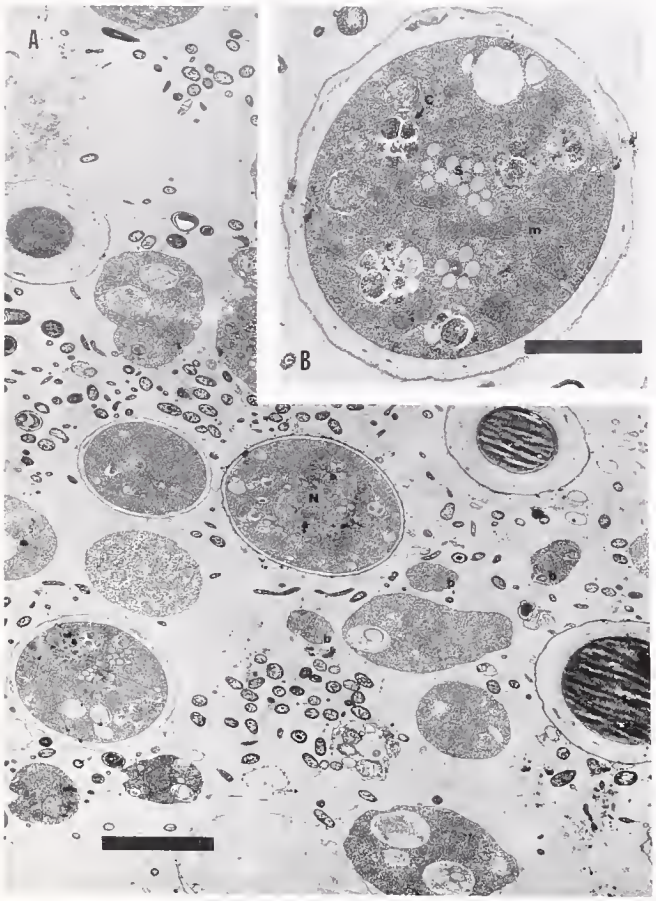

Figure 8. A. Cysts of cultured *Paratetramitus jugosus* in many different stages: from completely desiccated to recently excysting. Arrow indicates a nucleolus in a nucleus (N). Small bodies (b) are also seen which may represent released chromatin bodies or equivalent that develops into small amoebae. Bar scale = 5 μm. B. Cyst showing inner and outer walls, mitochondria (m), storage granules (s), and chromatin body (C) in division (arrow). Bar scale = 2.5 μm. Transmission electron micrograph (TEM) of material from Cuba strain of *P. jugosus*.

zyme systems: proprionyl esterase (PE), leucine aminopeptidase (LA), and acid phosphatase (AP) (Daggett and Nerad, 1983).

Results and Discussion

Field studies

More than eight sets of field studies were undertaken in 1979 and 1980 after the discovery of the extraordinary abundance of small cysts on agar plates designed to detect the presence of algae, cyanobacteria, manganese-oxidizing bacteria, and other organisms. In earlier studies, lack of consistency among samples, presence of nematodes and contamination, especially by an unidentified black manganese-oxidizing fungus, precluded orderly collection of data. The last four sets of observations (May and June 1983; March and August 1988) led to repeatable results (Table II). The appearance of cysts smaller than those of *Acanthamoeba* was taken as putative evidence for *P. jugosus*. Three or four times (by high power light and once by electron microscopy) we verified that the cysts indeed were *P. jugosus*.

Here we summarize the general experience after the eight sets of experiments in which each medium (K, MnAc) was represented by two to four plates per site. *P. jugosus*, or encysting small amoebae indistinguishable morphologically from *P. jugosus*, are invariably present in the laminated sediment when the *Thiocapsa* layer (the red layer, Fig. 2I) is well-developed. *P. jugosus* is usually recoverable from the laminated *Microcoleus* mats such as that depicted in Figures 2E and 2H. *P. jugosus* populations do develop but less frequently in the gypsum mat and black mud samples. They are least frequent in the white gypsum crust.

Our practice now is to collect mats with *Thiocapsa* scums to insure recovery of large populations of healthy *P. jugosus* cysts, amoebae, and in the case of the Cuba samples, amoebae that readily transformed to mastigotes (Fig. 3C).

In order to see abundant populations of *P. jugosus*, plates should be read several times, especially between 10 and 30 days after returning from the field. After this, plates become overgrown with many kinds of bacteria and some fungi as reported by Brown *et al.* (1985). Except for the common presence of *Acanthamoeba*, no other protists have been routinely seen on K plates. It is important to control the quantities of added distilled water, however; if water is too abundant a plethora of encysting ciliates appear that have not been studied. Due to the more limited nutrients on MnAc plates algae (for example the tiny encysting chlorella-like *Mychonastes desiccatus* BROWN, Margulis *et al.*, 1988) may appear on plates incubated in the light.

We have always used two sets of media because more abundant growth of *P. jugosus* (and most other microbes) develops on K plates whereas these amoebae are more easily recognized on the less permissive MnAc plates. We score the presence of *P. jugosus* at a site (e.g., "+" in Table II) only when the small cysts are present on all of the plates of both media.

We assess *P. jugosus* to be a normal component of the microbial mat community whose population develops especially well in the layer dominated by *Thiocapsa*, below *Microcoleus*. Our data are consistent with the interpretation that during the spring rainy season, enormous populations develop and during the hot dry summer when halite and gypsum crystals dominate the mat surface, *P. jugosus* survives by encysting. We have observed excystment in 10–20 min. Upon desiccation, encystment apparently takes place rapidly as well (certainly

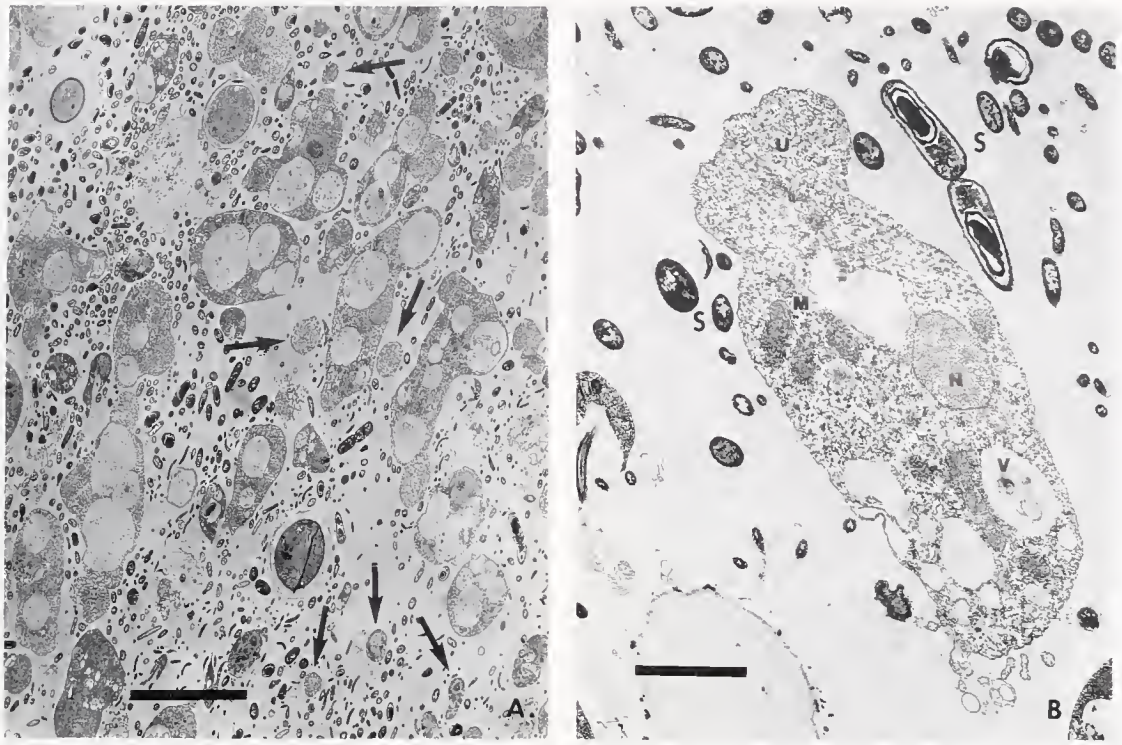

Figure 9. Healthy trophic amoebae, TEMs. A. Highly vacuolated (v) amoebae in a dense population of food bacteria. Small bodies (arrows) could be products of amoebae fission. Bar scale = 10 μm. B. Amoeba with uroid (U), nucleus (N), vacuoles (v) and mitochondria (M); bacterial spores (S). Bar scale = 2.5 μm.

overnight). Because anaerobic bacteria abound in the *Thiocapsa* mat layer, it is also likely that both cysts and amoebae of *P. jugosus* tolerate low oxygen or even totally anoxic conditions. To develop techniques to most reliably detect the greatest number of small cysts on plates by low power microscopic examinations, we compared flooding the agar plates immediately upon collection of the field samples to drying them out entirely before flooding. Because early drying out selects for rapidly growing fungi and spore forming bacteria which may overgrow the amoebae, our best results were with samples flooded with 1 ml distilled water in the field and permitted to dry for the weeks after collection. In conclusion, the optimal collecting conditions for *P. jugosus* involve recognition of small cysts from plated samples of 1-mm cubes of distilled water-flooded *Thiocapsa* layer mat samples. The cysts should be recoverable on both K and MnAc media from 20 to 30 days after return from the field. For further purification to monoprotist cultures see Read *et al.* (1983).

Light microscopy

Culture slides. Observations of live material never revealed amoebae in division. Conditions for normal promitotic amoebic division may not have been favorable under the growth conditions used, yet small bodies were frequently observed (Fig. 4A–H). These bodies were also seen frequently from cultures grown on agar plates with both light and electron microscopy (Fig. 6C, D; 7I–N; 8A; 9A). Many of these small bodies may be pieces of cytoplasm left behind by the amoeba or in EM sections through a small portion of the amoeba, however, on one occasion, a small body was observed budding off a parent amoeba followed by changes in its shape and monopodial movement (Fig. 4D–H) suggesting this body was a small amoeba. We cannot rigorously preclude the possibility that this small body was already present in the culture and that the larger amoeba passed over it, making it look as if it were extruded.

Amoebomastigote transformation. Aqueous suspensions examined 24 h after their preparation were observed to contain both amoebae and cysts. When the distilled water suspension was plated, even six weeks after its preparation, it gave rise to viable *P. jugosus* amoebae and mastigotes; however, whether cysts, mastigotes, or amoebae dominated the suspension was not determined. Amoebae were dominant 24 h after plating, while mastigotes dominated after 48 h. Mastigotes were conspicuous enough in these suspensions to warrant harvesting the cultures for electron microscopic analysis of kinetid structure.

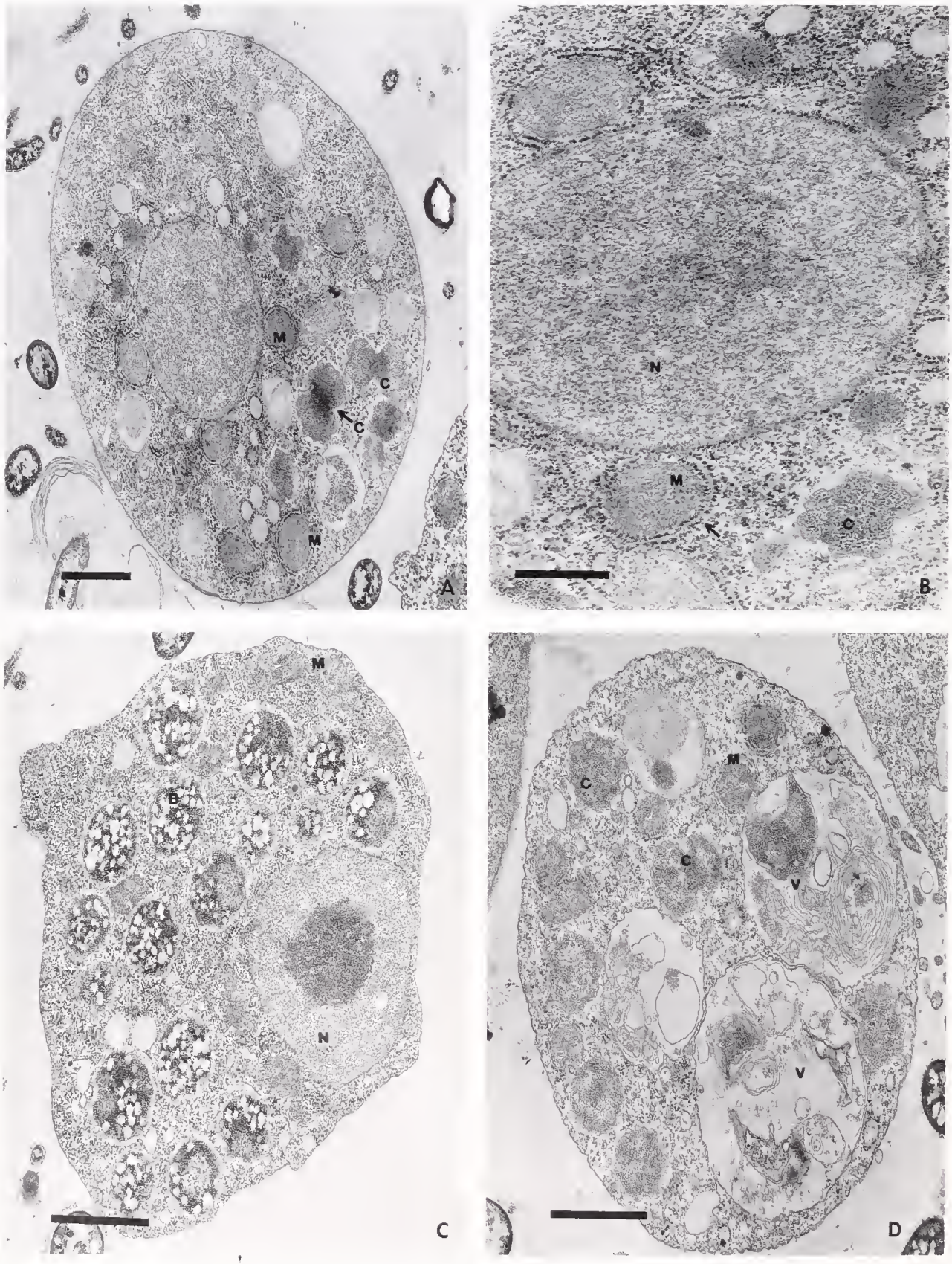

Figure 10. Rounded amoebae, TEMs. A. Dumbbell-shaped chromatin bodies (C) with condensed material (arrow), which are clearly distinguishable from mitochondria (M). Bar scale = 1.0 μm. B. Ribosome-

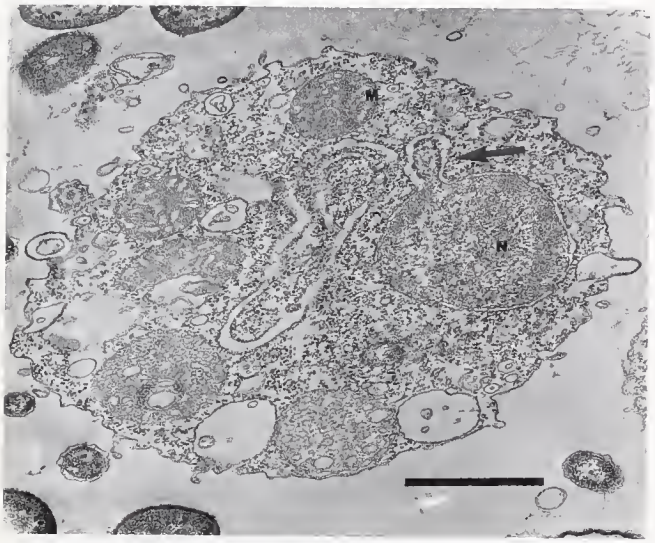

Figure 11. Amoeba with small bleb (arrow) off nucleus (N). Mitochondria (M) are also seen; chromatin bodies are lacking. TEM. Bar scale = 1.0 μm.

Nuclear fluorescent staining. In both DAPI and mithramycin-stained preparations, the nuclei of amoebae were clearly visible with epifluorescence microscopy (Fig. 5; 6A, B; 7E–H). Two stages of nuclear division were revealed: telophase (Fig. 5C, D; 6A, B) and metaphase (Fig. 5A, B). Cytoplasmic DNA was also seen in these preparations although less clearly. DAPI-stained slides tend to show high background fluorescence, making cytoplasmic DNA difficult to see (Fig. 5B, D, F; 7F). This problem has been reported in studies of other protists as well (Coleman *et al.*, 1981). Because mithramycin stains DNA more specifically, preparations made with this stain displayed less background fluorescence (Fig. 7G) and allowed for clear identification of cytoplasmic DNA. Autofluorescence and DNase controls of amoebae showed no nuclear or cytoplasmic fluorescence verifying the presence of DNA (Fig. 6E–H; 7A–D).

Fixed amoeba cultures always contained small irregular and spherically shaped bodies that displayed stronger fluorescence than the nuclei of amoebae, cytoplasmic DNA or the nucleoids of the bacteria upon which the amoebae feed. Strong fluorescence was clearly removed by DNase treatment, indicating that at least some of the small bodies contain DNA. A large number of the small spherical bodies (Fig. 6G, H) and some of the irregularly shaped bodies (Fig. 6C, D) were autofluorescent. Small spherical bodies may be nuclei of ruptured cells or dried-out collapsed cysts. However the amount of autofluorescence in some of the irregularly shaped bodies was insufficient to account for the strong fluorescence seen in stained material (Fig. 7I–N). Several small bodies seen in close proximity to normal-size amoebae (Fig. 5E, F; 7E, F) differ in both extent and intensity from nuclear and cytoplasmic fluorescence: the intensity of fluorescence is greater and the fluorescent structures are intermediate in size between large nuclei and cytoplasmic DNA. Cytoplasmic DNA in DAPI and mithramycin stained preparations is most easily interpreted to be due, at least in part, to mitochondrial nucleoids. Chromatin bodies (described below) detected in electron micrographs are approximately the same size as mitochondria therefore DNA in these structures might also be represented by cytoplasmic fluorescence. However, the more diffuse cytoplasmic DNA (regardless of its origin) stains less brightly and its fluorescence emanates from smaller structures relative to whatever DNA is causing the fluorescence of the five small bodies (as seen e.g., in Fig. 7I–N). Specific correlation between cytoplasmic and the sources of extracellular (*i.e.*, small body) fluorescence could not be made.

The relative abundance of small bodies containing DNA was not measured; attempts to quantify were thwarted by small numbers of irregularly shaped and spherical bodies together in the same field, brightness of the preparation, and variations in population densities of both the amoebae and the bacterial lawns. Quantification would require synchronously grown amoebae with fixation at the same stages of development.

Although their small size precludes definitive identification of these DNA-containing bodies, they may represent the fate of chromatin bodies, *i.e.*, the released "chromidia" reported in the early amoeba literature (Hogue, 1914). We hypothesize that these irregularly shaped bodies represent highly condensed packages of parental DNA that presumably contain information required for the full development of the organism. Although we routinely see irregular bodies in our cultures of *P. jugosus*, including those purchased from the American Type Culture Collection, we have never observed in a single specimen the entire cycle of budding off, followed by development into small and then standard-sized trophic amoebae. Yet such bodies, uncannily like the "buds" Hogue

studded mitochondria (M) adjacent to nucleus (N) with its outer membrane also studded with ribosomes. Chromatin bodies (c) shown at higher magnification. Bar scale = 0.5 μm. C. Amoeba with highly vacuolated bodies which may be a form of chromatin bodies. Mitochondria (M), nucleus (N). Bar scale = 1.0 μm. D. Amoeba with large food vacuoles (v) containing membranous material. Both mitochondria (M) and chromatin bodies (C) are also present. Bar scale = 1.0 μm.

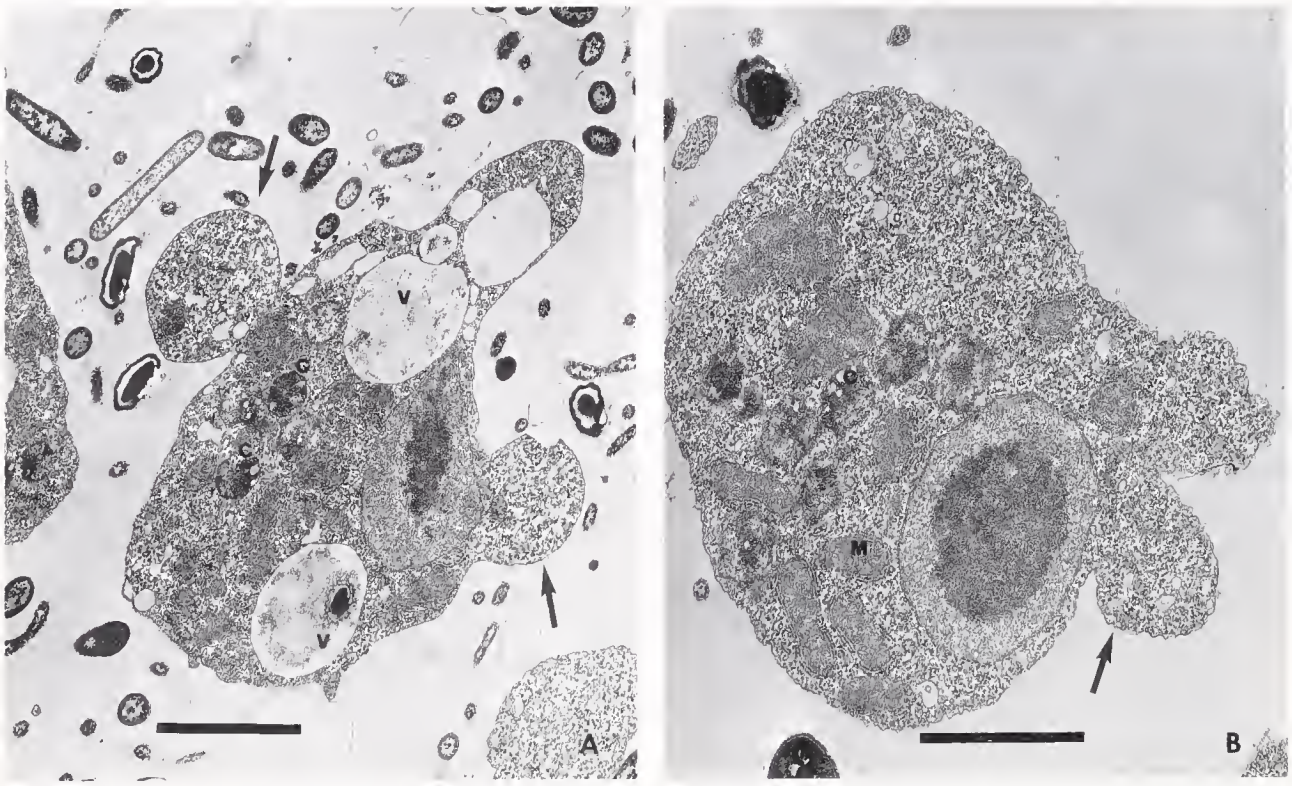

Figure 12. TEMs of amoebae. A,B. Arrows pointing to cytoplasmic buds. Chromatin bodies (C), vacuoles (V) and mitochondria (m) are also visible. Bar scale = A. 2.5 μm, B. 2.0 μm.

(1914) described in larger amoebae parasitic in oysters, are always found if sought in cultures of *P. jugosus*. Promitotic division of amoeba nuclei has also clearly been seen in our preparations (but never in live material) (Figs. 5A–D; 6A, B) suggesting more than one form of reproduction may be responsible for the growth of this organism.

The definitive solution of the problem of multiple fission in this tiny amoeba requires cloning in pure culture of a single isolated 2–4 μm diameter "bud" after the observation of its prior presence in the cytoplasm of the adult amoeba as a chromatin body. Cloning studies coupled with DAPI or mithramycin as a vital stain may eventually resolve the question of nucleus-derived cytoplasmic chromatin bodies which are released as propagules to the medium under conditions of maximal growth on dense, well-fed cultures. Extrusion of these tiny bodies from the nucleus and then from the cell would have to be directly observed to confirm this scenario. Fluorescent DNA stains would facilitate these observations by tracking nuclear DNA.

Electron microscopy

Cell structure and reproduction. Electron microscopy of cultures from Cuban mat samples revealed at least three different forms: cysts, amoebae, and mastigotes. Cysts were roughly spherical with a single, smooth outer layer, 500 nm thick (Fig. 8A,B). Cysts contained a nucleus with a prominent nucleolus, numerous dense mitochondria with tubular cristae surrounded by ribosome-studded endoplasmic reticulum, vacuoles containing various materials (*e.g.*, degrading spore-forming bacteria, stacks or whorls of membranes and unidentifiable structures, most likely degraded remnants of food). They also contain small electron-lucent spheres that may contain storage material (*e.g.*, at least 18 can be seen in Fig. 8B). Other cytoplasmic structures, distinguishable from mitochondria by their lack of cristae, darker staining, amorphous shape, and lack of surrounding endoplasmic reticulum, are here termed chromatin bodies. As indicated by their dumbbell shape, some of these bodies appear to be in division. The combination of these structures is indicative of a metabolically active rather than a dormant cell.

Trophic amoebae characteristic of this species are monopodial ("limax") (Fig. 9). The posterior region of the cell possesses an uroid (Fig. 9B) similar to other isolates of this organism. A more-or-less centrally located nucleus with a prominent nucleolus is seen in many thin sections. The nuclear membrane is surrounded by ribo-

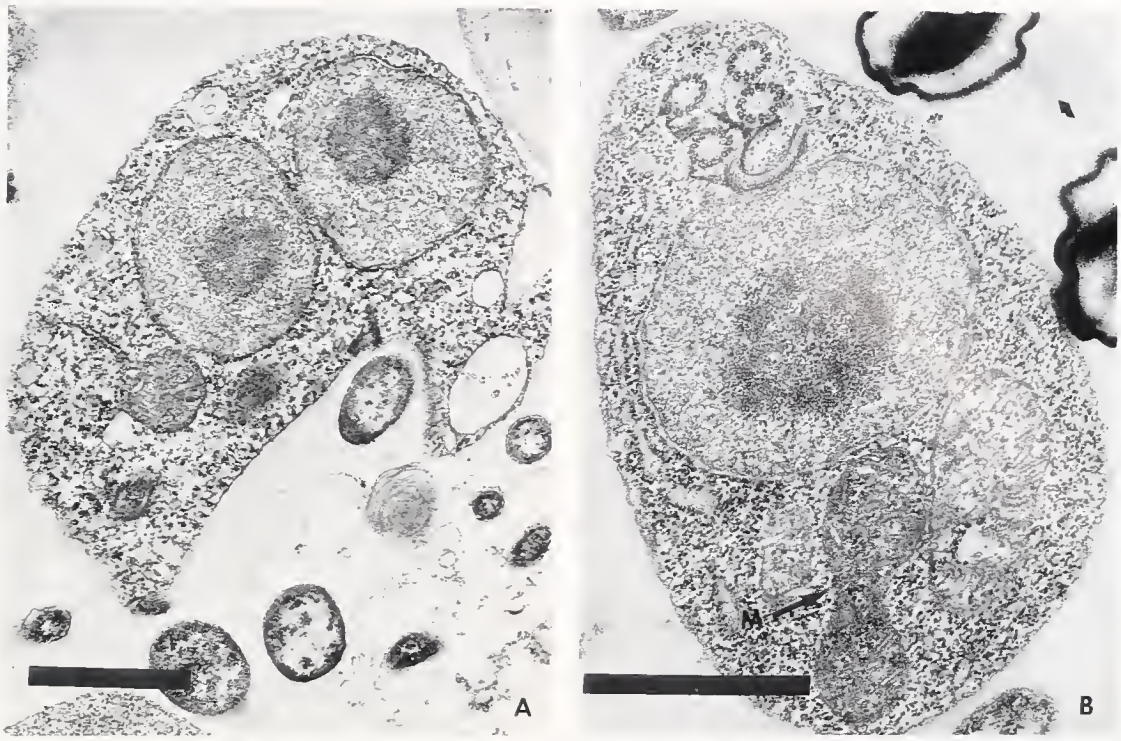

Figure 13. A. Binucleated mastigote with tubules, probably derived from rhizoplast transverse microtubules that extend subcortically (see Fig. 16). B. Mastigote with four [9(2) + 0] kinetosomes showing approach of connecting rhizoplast to the nucleus. Mitochondria (M) interpreted to be in division. A,B. Bar scale = 1.0 μm.

somes (Fig. 10B). Densely staining mitochondria with tubular cristae are often surrounded by ribosome-studded endoplasmic reticulum (Fig. 10A, B, D). Large vacuoles containing bacteria and membranous whorls are often present (Figs. 9; 10D; 17). In some amoebae, these vacuoles occupy a large portion of the cytoplasm (Figs. 9A; 10D; 12A; 17).

Chromatin bodies are almost always found in rounded amoeba, but rarely in amoebae that clearly appear trophic. Rounded amoebae may represent an early stage of encystment in which degeneration of mitochondria to chromatin bodies is caused by the onset of metabolic dormancy. We think this is unlikely because encysted and rounded pre-cyst amoeba always contain both mitochondria and chromatin bodies. Mitochondria including dumbbell-shaped forms (Fig. 11B, 13) are clearly distinguishable from chromatin bodies. Their presence in amoebae, mastigotes, and cysts suggests *P. jugosus* is fundamentally aerobic even though it apparently tolerates high sulfide and anaerobic conditions. Some chromatin bodies contain centrally located, dark-staining masses resembling nucleolar material (Fig. 10A); others are arguably in the process of division (Figs. 8B; 10A, D). Some amoebae contain dark-staining structures that differ from chromatin bodies, *e.g.*, the vacuolated structures of Figure 10C. These vacuolated structures, because they are similar in stain density, size, and number per cell, may represent some developmental form of chromatin bodies. We suggest that these bodies represent "blebs" of nuclear origin containing DNA. Nuclear blebbing was reported by Stevens *et al.* (1980) in *Naegleria.* We also observed nuclear blebs in *P. jugosus* (Fig. 11), although because they are smaller than the chromatin bodies, they may be early developmental stages that then provide the means for their formation. We have not been able to determine at the light microscopic level if any cytoplasmic fluorescent staining comes from these bodies, nor have we done ultrastructural autoradiography for DNA to distinguish these from mitochondria, yet the electron micrographic appearance of the interior of these bodies is that of chromatin (Fig. 10B, D). Our interpretation is entirely consistent with that of the chromatin bodies in oyster parasitic amoebae called "chromidia" (Hogue, 1914).

Cytoplasmic "budding," of interest because of the presence in cultures of numerous small bodies detectable by light microscopy (Figs. 4A–C; 5 E, F; 6C, D; 7E, F, I–M), is found in many sections (Fig. 12). Corresponding small bodies are difficult to identify at the ultrastructural level because the orientation of the amoebae cannot be determined with certainty; however, bodies that may

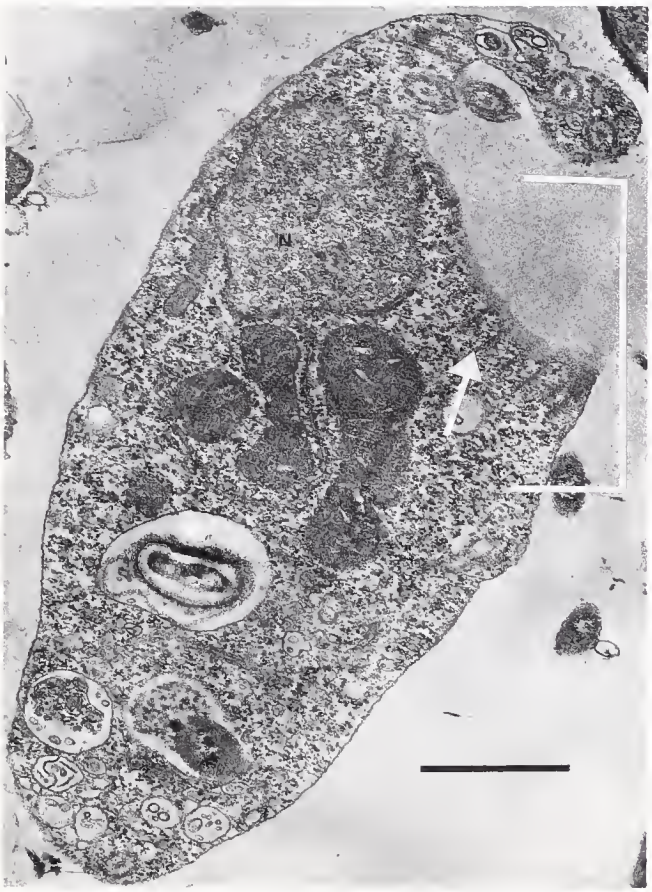

Figure 14. Cortical tubules (arrow) presumably originating from rtm of Figure 16, closely associated with the anteriorly positioned nucleus (N) of mastigote. Bracket indicates "rostral ridge" (rr). TEM. Bar scale = 1.0 μm.

correspond to those observed with light microscopy are depicted (Figs. 8A; 9A). The "buds," at least in Figure 12, are continuous with the cell cytoplasm and probably not an artifact resulting from overlapping amoebae. The "buds" lack both mitochondria and chromatin bodies in this particular micrograph, but this may simply be a function of orientation of this thin section. Because the details of mitotic division remain elusive, the case for multiple fission in this organism is incomplete and we still have no comprehensive view of how the luxuriant, rapid growth of this organism is achieved. The "buds" represent frequently observed oddities; they may or may not represent part of the amoeba reproduction process. If chromatin bodies originate from the nucleus, which is not yet clear, then budding could represent a means of their dispersion.

Although mitosis has never been observed in ultrastructural studies of *Paratetramitus jugosus* amoebae or mastigotes, some events associated with mitosis are evident in thin sections. We have seen dumbbell-shaped chromatin bodies (Fig. 10A, D) and a single binuclear cell: a mastigote in which karyokinesis but not cytokinesis apparently has occurred (Fig. 13).

Mastigotes share many features with amoebae and cysts, including mitochondria surrounded by rough endoplasmic reticulum (RER), large vacuoles, strands of rough endoplasmic reticulum, nuclei with a prominent nucleolus, and nuclear membrane surrounded by ribosomes (Figs. 13, 14). However, the three forms do differ significantly. The nucleus, anteriorly located in mastigotes and attached by rhizoplast microtubules to the nucleus, is in close proximity to the kinetosomes. This differs from previous descriptions of mastigotes in this organism (Darbyshire *et al.*, 1976) in which nuclei were centrally located. The groove seen in the anterior region of the cell adjacent to the kinetid (Fig. 14, 15) may represent a common feature observed in light micrographic studies called the "rostral ridge" of *P. jugosus* mastigotes. Chromatin bodies and the other dark-staining, vacuolated structures observed in thin sections of amoebae and cysts are apparently absent in micrographs of mastigotes.

Kinetid structure. Kinetid structure, reconstructed

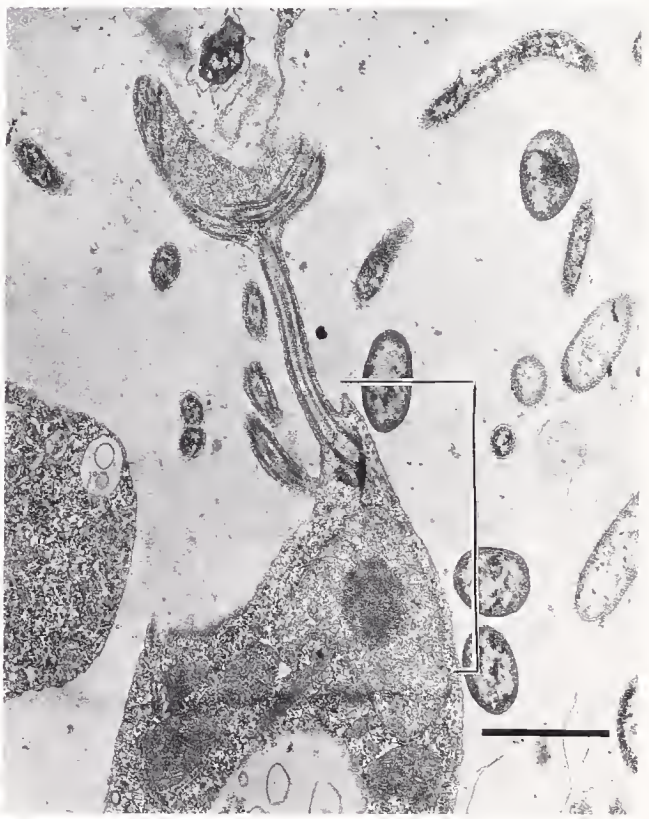

Figure 15. Microtubules of axoneme are seen here in a tangential section, the distal portion of the axoneme is probably resorbing. The cortical tubules from the kinetid are in close association with the nucleus. Bracket indicates "rostral ridge" (rr). TEM of mastigote. Bar scale = 1.0 μm.

Table III

Kinetid structure

Structure or orientation	Abbreviation
Axoneme 1	ax1
Axoneme 2	ax2
Kinetosome 1	K1
Kinetosome 2	K2
Basal sphere	bs
Lateral sphere	ls
Connecting fiber	cf
Nuclear fiber	nf
Rhizoplast	RZ
Rhizoplast microtubules: transverse	rtm
Rhizoplast microtubules: parallel	rpm
Right	R
Left	L
Anterior	A
Posterior	P
Ventral	V
Dorsal	D
Nucleus	n

from numerous electron micrographs (Figs. 13–15), and labeled according to Table III is summarized diagrammatically in Figure 16. The standard [9(2) + 0] kinetosomes (Fig. 13B), and [9(2) + 2] axonemes (Fig. 14) are present in this dikinetid that shows mirror image symmetry. A microtubular rhizoplast containing both parallel and transverse tubules arises between the kinetosomes and runs posteriorly toward the nucleus (Figs. 13A, 14, 15). The parallel kinetosomes are underlain by a basal sphere connected to the nucleus; each possesses a protruding lateral sphere also connected to the nucleus by rhizoplast nuclear fibers (K1/lsnf, K2/lsnf). The mastigote in Figure 15 may either be extending or retracting its undulipodium. Because a large portion of degraded axonemal material is visible with cytoplasm at the distal extremity, resorption of the axoneme is more likely. A row of single microtubules (seen in cross section in Fig. 14 and tangential section in Fig. 15) originates from between the kinetosomes and runs anteriorly and cortically along and past the nucleus. The sheet of microtubules presumably originating from rhizoplast transverse microtubules (rtm, Fig. 16) and supporting the anterior end of the mastigote give the cell the conical appearance that prompted Darbyshire *et al.* (1976) to identify the "rostral ridge." The number of undulipodia, usually two as determined by light microscopy, may vary greatly. While difficult to assess their precise positioning by transmission electron microscopy, four [9(2) + 0] kinetosomes can be seen in a single cell (Fig. 13B).

Amoebae in situ *in a microbial mat.* Although *P. jugosus* is infrequently observed in live mat during dry conditions, it was prevalent throughout the period of freshwa-

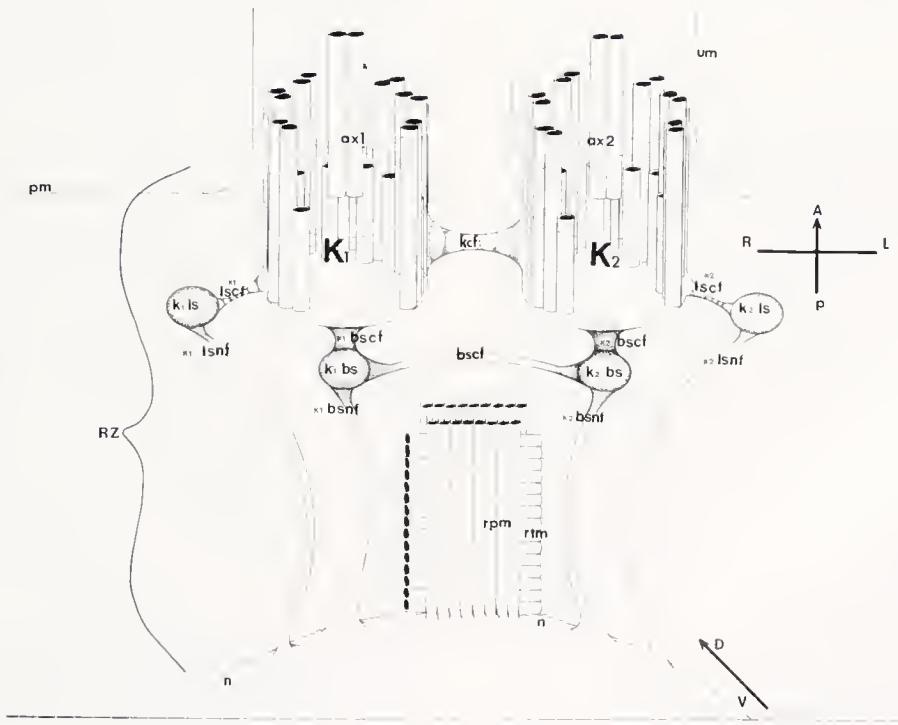

Figure 16. Kinetid structure, diagrammatic representation. See Table III for description of labels. (Drawing by Sheila Manion Artz).

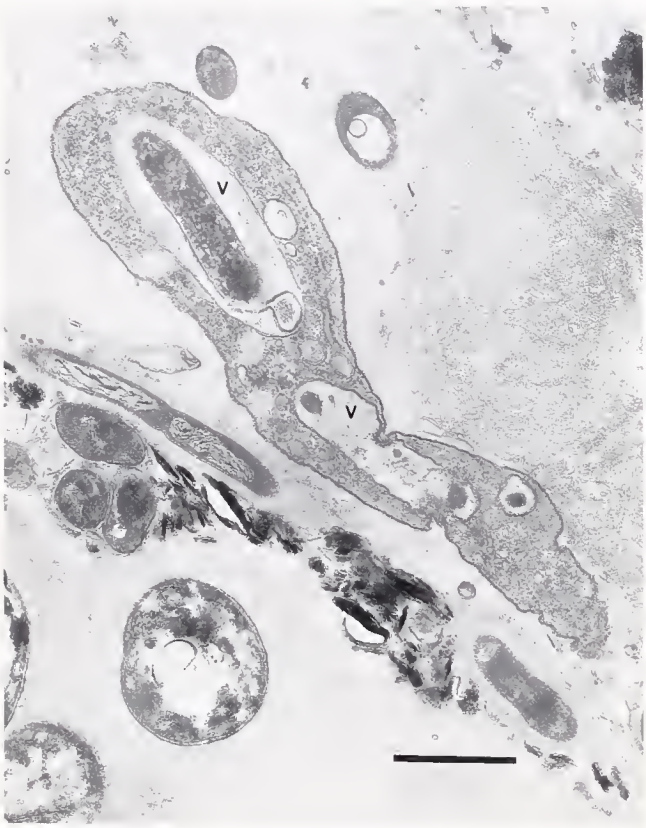

Figure 17. Amoeba from embedded microbial mat with large food vacuoles (v), taken directly from a microbial mat sample at North Pond, Laguna Figueroa, Baja California, Mexico. TEM. Bar scale = 1.0 μm.

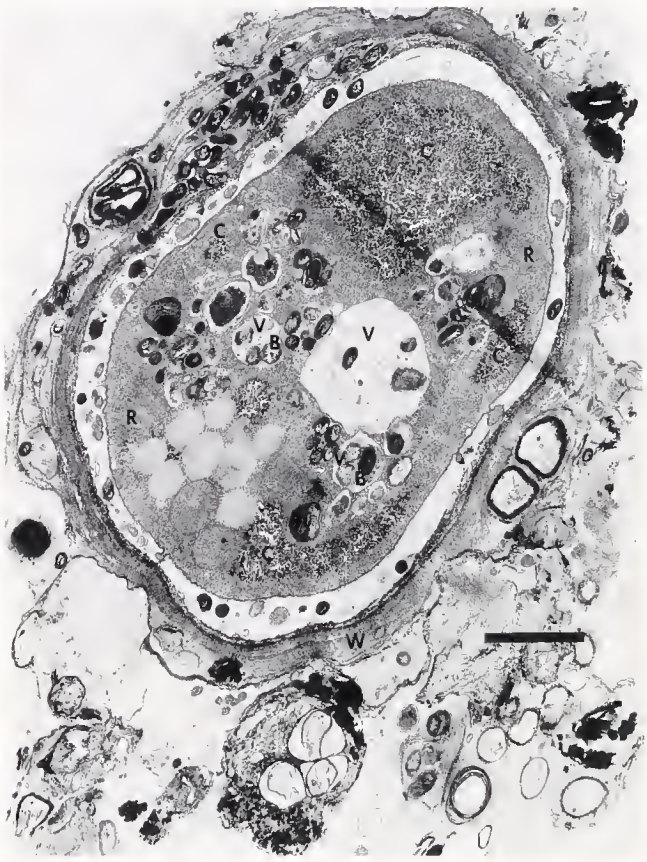

Figure 18. Organism from the *Thiocapsa sp.* layer of the microbial mat from North Pond interpreted to be an ectoplasmic cyst of *P. jugosus*. Although enclosed in a cyst wall (W), the ribosome-studded cytoplasm (R), active digestion of bacteria (B) in vacuoles (V) and the well-developed chromatin (C) indicate metabolic activity in this amoebomastigote. TEM courtesy of John F. Stolz. Bar scale = 2.0 μm.

ter inundation. Electron microscopy of fresh mat from North Pond (Laguna Figueroa, Baja California Norte, taken October 1987) reveals an amoeba similar in form to *P. jugosus* (Fig. 17). The trophic amoeba appears to have uroid and large digestive vacuoles containing bacteria. The only other amoeba regularly seen in these field samples are larger acanthamoebae with acanthopodia. The organism greatly resembles in size and cell structure the limax amoebae in our cultures (Fig. 17); it is not an acanthamoeba. Thus, we interpret it to be a free-living *P. jugosus* photographed under natural conditions in association with purple phototrophic and other mat bacteria.

An encysted amoeba, with at least five areas of active-looking chromatin, can be seen in embedded material from the *Thiocapsa* layer at North Pond, Laguna Figueroa (Fig. 18). Bacterial digestion is evident, emphasizing the rapidity with which temporary encystment can occur. Photographed by John F. Stolz during his study of phototrophic bacteria, we interpret Figure 18 to be a second example of *P. jugosus in situ* in a stratified microbial community. The electron micrograph corresponds to the

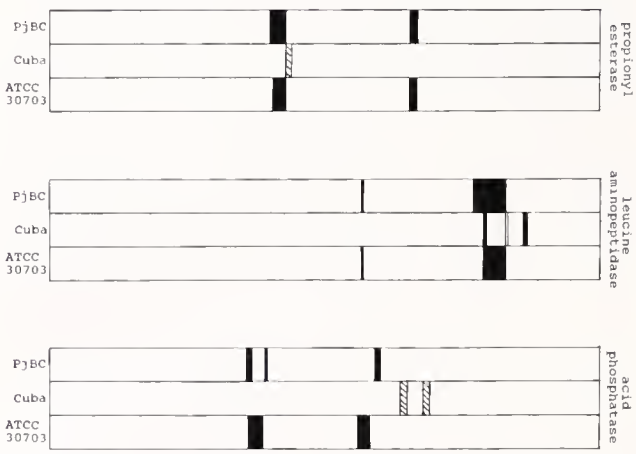

Figure 19. Diagram of isoenzyme analysis of three different isoenzymes. PjBC: the original bajacaliforniensis of Read *et al.* (1983) Cuba: the Cuban strain reported here, ATCC 30703: The standard soil isolate of Darbyshire *et al.* (1976). Black represents a strong band on starch gel electrophoresis, cross-hatching a less conspicuous band, and white represents a very faint band.

"ectoplasmic cysts" reported in light micrographs in Read *et al.* (1983; Figs. 7B–H, 13, and 14H).

Isoenzyme analysis

The results of the stock gel isoenzyme analysis run on amoebae and cysts of the Cuban *P. jugosus* strain compared to the ATCC-type strain (ATCC #30703) and *P. jugosus bajacaliforniensis* are shown in Figure 19. The pattern is unique for any amoebae in the ATCC collection (T. Nerad, ATCC, pers. comm.). The propionyl esterase (PE) and acid phosphatase (AP) each display bands resembling those enzyme patterns present in the Baja California and ATCC *P. jugosus* strains. The three narrow bands of the pattern of leucine aminopeptidase (LAP) of the Cuban strain seem to be unique.

The most abundant protist in the purple phototrophic bacterial layer of microbial mat sediments, *Paratetramitus jugosus* displays a complex life history that correlates with rapid environmental changes in water abundance and salinity. Our evidence for this life history is consistent with Hogue's (1914) assertion that some amoebae reproduce by multiple fission and disperse by "chromidial" propagules.

Acknowledgments

We are grateful to Rene Fester, Gail Fleischaker, Wendy Lazar, Dorion Sagan, and Rae Wallhausser for assistance in manuscript preparation, including cartography. We are especially grateful to Annette Coleman, Floyd Craft, Tom Nerad, and Jane Gifford for their technical assistance with fluorescence staining, electron microscopy, isoenzyme analysis, and field photography, respectively. We are immensely grateful to the members of Earthwatch team 1 & 2 (May, June 1983) for aid in the surveying and mapping of Pentapus Salina and the collection of field data. We thank Sheila Manion Artz for drawing Figure 16 and John F. Stolz for use of his electron micrograph (Fig. 18). We acknowledge helpful suggestions for observing live amoebae from Prof. F. Schuster. Support for this research came from NASA Life Sciences Offices (NGR-004-042 to L.M. at Boston University), the Boston University MacDonald award and The Evolution Fund (to L.M.), the NASA Planetary Biology Internship Program (administered through the Marine Biological Laboratory, Woods Hole, Massachusetts), the University of Massachusetts Amherst Research Trust Funds, and the Richard Lounsbery Foundation.

Literature Cited

Brown, S., L. Margulis, S. Ibarra, and D. Siqueiros. 1985. Desiccation resistance and contamination as mechanisms of Gaia. *Biosystems* **17:** 337–360.

Coleman, A. W., M. J. Maguire, and J. R. Coleman. 1981. Mithramycin- and 4′-6-diamidino-2-phenylindole (DAPI)-DNA staining for fluorescence microspectrophotometric measurement of DNA in nuclei, plastids and virus particles. *J. Histochem. Cytochem.* **29:** 959–968.

Daggett, P. M., and T. A. Nerad. 1983. The biomedical identification of Vahlkampfid amoebae. *J. Protozool.* **30:** 126–128.

Darbyshire, J. F., F. C. Page, and L. P. Goodfellow. 1976. *Paratetramitus jugosus*, an amoebo-flagellate of soils and fresh water, type-species of *Paratetramitus nov. gen. Protistologica* **12:** 375–387.

Gong-Collins, E. 1986. A euryhalic, manganese- and iron-oxidizing *Bacillus megaterium* from a microbial mat at Laguna Figueroa, Baja California Mexico. *Microbios* **48:** 109–126.

Hogue, M. J. 1914. Studies of the life history of an amoeba of the Limax group. *Arch. Protistenkd.* **35:** 154–163.

Margulis, L. 1980. Undulipodia, flagella, and cilia. *Biosystems* **12:** 105–108.

Margulis, L. 1988. Systematics: the view from the origin and early evolution of life. Secession of the Protoctista from the animal and plant kingdoms. Pp. 430–443 in *Prospects in Systematics*, D. L. Hawksworth, ed. Clarendon Press, Oxford.

Margulis, L., E. S. Barghoorn, D. Ashendorf, S. Banerjee, D. Chase, S. Francis, S. Giovannoni, and J. Stolz. 1980. The microbial community in the layered sediments at Laguna Figueroa, Baja California, Mexico: does it have PreCambrian analogues? *Precamb. Res.* **11:** 93–123.

Margulis, L., S. W. Brown, G. Hinkle, H. McKhann, and B. Moynihan. 1988. *Mychonastes desiccatus* BROWN *sp. nova* (Chlorococcales, Chlorophyte)—an intertidal alga forming achlorophyllous dessication-resistant cysts. *Arch. Hydrobiol. Suppl.* **78:** 425–446.

Margulis, L., J. O. Corliss, M. Melknonian, and D. J. Chapman. 1990. *Handbook of Protoctista:* the structure, cultivation, habitats and life cycles of the eurkaryotic microorganisms and their descendants exclusive of animals, plants and fungi. Jones and Bartlett Publishers, Inc. Boston, MA.

Margulis, L., and D. Sagan. 1985. Order amidst animalcules: the Protoctista kingdom and its undulipodiated cells. *Biosystems* **18:** 141–147.

Nerad, T., and P. M. Daggett. 1979. Starch electrophoresis; an effective method for separation of pathogenic and non-pathogenic *Naegleria* strains. *J. Protozool.* **26:** 613–615.

Page, F. C. 1967. Taxonomic criteria for limax amoebae, with descriptions of 3 new species of 3 *Hartmannella* and of 3 *Vahlkampfia*. *J. Protozool.* **14:** 499–521.

Page, F. C. 1983. *Marine Gymnoamoebae.* Institute of Terrestrial Ecology, Culture Centre of Algae and Protozoa, Cambridge, England. 54 pp.

Raikov, I. B. 1982. The Protozoan Nucleus: morphology and evolution. Springer-Verlag, New York. Pp. 73, 112.

Read, L. K., L. Margulis, J. Stolz, R. Obar, and T. K. Sawyer. 1983. A new strain of *Paratetramitus jugosus* from Laguna Figueroa, Baja California, Mexico. *Biol. Bull.* **165:** 241–264.

Stevens, A. R., J. De Jonckheere, and E. Willaert. 1980. *Naegleria lovaniensis* new species: isolation and identification of six thermophilic strains of a new species found in association with *Naegleria fowleri Int. J. Parasitol.* **10:** 51–64.

Stolz, J. F. 1983. Fine structure of the stratified microbial community at Laguna Figueroa, Baja California Mexico. I. Methods of *in situ* study of the laminated sediments. *Precamb. Res.* **20:** 479–492.

Reference: *Biol. Bull.* **177:** 130–140. (August, 1989)

Bacterial Aggregates Within the Epidermis of the Sea Anemone *Aiptasia pallida*

EDWARD E. PALINCSAR, WARREN R. JONES, JOAN S. PALINCSAR, MARY ANN GLOGOWSKI, AND JOSEPH L. MASTRO

Department of Biology, Loyola University, Chicago, Illinois 60626

Abstract. Bacteria in cyst-like aggregates have been observed in the sea anemone *Aiptasia pallida*. Algal symbionts, common in certain Cnidaria, including *Aiptasia*, are located in the gastrodermis, while the bacteria described in the present study were found exclusively in the epidermis. They were gram-negative and packed closely together within what appeared to be a single cell. The bacterial sac varied in size according to the number of bacteria it contained. Ultrastructural features of the bacteria included numbers of large vacuoles or inclusions often intertwined with web-like nucleoids in the central region. Aggregates *in situ* showed a whorled arrangement of the bacteria and maintained this pattern and their structural organization after extrusion from anemone epidermis. A fatty acid profile suggested that the bacteria may belong to the genus *Vibrio*.

Introduction

Single bacterial cells have often been observed as endosymbionts in cells of many types of organisms. Vesicles containing small numbers of bacteria and *Chlorella* were found in gastrodermal cells of *Hydra* (Margulis *et al.*, 1978; Thorington *et al.*, 1979). Wilkinson (1978) cultured and characterized bacteria associated with marine sponges, most of which inhabited the connective tissue-like mesohyl and thus were not usually intimately associated with the sponge cells. Some individual bacteria, as well as cyanobacteria, were located inside sponge cells.

In some animals, endosymbiotic bacteria inhabit specific cell-like structures called bacteriocytes, such as cells noted by Vacelet (1975) in the marine sponge, *Verongia*. Palincsar *et al.* (1988) found many bacteria inside aggregates in the epidermis of *Aiptasia pallida*. Peters *et al.* (1983) and Peters (1984) identified bacteria in "basophilic ovoid bodies" in septa and calicoblast tissue of *Acropora palmata* and *A. cervicornis*, and in mesoglea of *Porites astreoides* in the Caribbean. Gills of *Spisula subtruncata* have bacteriocytes containing a "bacteriophore" with over 200 bacteria (Soyer *et al.*, 1987). Because we found no nuclei directly associated with bacterial aggregates in *A. pallida*, and the origin of the membrane surrounding the bacteria is uncertain at present, we will use the term bacterial aggregate for large numbers of bacteria packed together, bounded by a discrete membrane, which are located either intracellularly or extracellularly.

The bulk of trophosome tissue in vestimentarian tube worms, *Riftia pachyptila*, of the Galapagos Rift was observed by Jones (1981) to be mostly bacteria; on inspection under the electron microscope, Cavanaugh (1983) found that these bacteria were located in bacteriocytes. The tissues of other smaller pogonophorans not from hydrothermal vent communities also contained bacteria, mostly within host cells (Southward *et al.*, 1981). The gutless marine oligochaete *Phallodrillus* (Felbeck *et al.*, 1983) contained bacteria within its tissues. In addition, Cavanaugh (1983) described bacteriocytes in gills of the hydrothermal vent clams, *Calyptogena magnifica*, *C. pacifica*, two non-vent clams, *Solemya velum* and *Lucinoma annulata*, and an additional pogonophoran. Fischer and Hand (1984) studied bacteriocytes in *Lucina floridana*, a clam living in an aerobic high-sulfide environment. Dando *et al.* (1985) found several species of lucinid clams inhabiting low sulfide environments. The clams contained bacterial symbionts that accumulated sulfur as an energy source. Bouvy *et al.* (1986) and Soyer *et al.* (1987) described packets of bacteria which they

Received 12 October 1988; accepted 31 May 1989.

termed bacteriophores, in *Spisula subtruncata,* a surf clam living in a highly aerobic environment. These bacteria were of two types, were spatially separated in the gill, and used reduced nitrogen and sulfur compounds as energy sources.

Although it is well known that the gastrodermis of *A. pallida* harbors the symbiotic dinoflagellate *Symbiodinium microadriaticum,* here we describe bacteria in aggregates at both light and electron microscopic levels, in a different location in the epidermis of the anemone *Aiptasia pallida.* In addition, we have begun chemical characterization of the bacteria with fatty acid analysis. We have also studied control of the bacterial population *in situ* to learn whether interrelationships exist between population levels of the two different symbionts, algal and bacterial.

Materials and Methods

Individuals of *Aiptasia pallida* were obtained from Carolina Biological Supply Company (Burlington, North Carolina 27215). The anemones were kept in 38-l aquaria in Instant Ocean (Aquarium Systems, Mentor, Ohio 44060) made with tap water at a specific gravity of 1.020 at 25°C. The anemones were cultured under fluorescent light with 16 h of light and 8 h of darkness, using a 35 W GE Lite-white and a 40 W Sylvania Grolux fluorescent tube at an intensity of 24 $\mu Em^{-2}\ s^{-1}$, measured with a LI Photometer Model LI185A with an underwater sensor (Lambda Instrument Corporation). The anemones were fed to repletion with *Artemia* nauplii (San Francisco Bay Brand, Newark, California 94560) twice a week. The H_2S level in the culture tank was 0.015 mg/l (Hach kit #2238); the sulfate level was 200 mg/l (Hach kit #2251); the nitrate level was 7.95 mg/l and the nitrite level was 0.048 mg/l, measured with Model NI14 nitrate and nitrite kit (Hach Company, Loveland, Colorado 80539). *A. pallida* were maintained for two years in culture. The tentacles contained clear ovoid structures as seen under the dissecting microscope. (In the ensuing 2 years, we have seen over 200 anemones with these structures.) Higher magnification revealed bacteria inside the ovoid structures. New orders of *Aiptasia* from Carolina, and from Ward's Natural Science Establishment, examined immediately upon arrival, also contained aggregates in the tentacular epidermis. Samples of *Aiptasia pallida* from the Shedd Aquarium, Chicago, and from Bermuda were examined; no aggregates were found (S. Kenney and M. Lesser, pers. comm.). *A. pallida* individuals collected immediately before shipment from their natural habitat at Morehead City, North Carolina by Lawrence Wallace (Carolina Biological Supply Company) had the largest numbers of bacteria seen to date, averaging 75 aggregates per sample (sampled according to methods given for antibiotic sensitivity determinations).

For electron microscope studies, 10 anemones containing aggregates were anesthetized in 3% $MgSO_4$ for 1 h. Tentacle tips 2–4 mm long were clipped and immersed for 1 h at 4°C in a modified Karnovsky's fixative (2.5% glutaraldehyde and 2% paraformaldehyde, Karnovsky, 1967) made up in Instant Ocean, postfixed in 2% osmium tetroxide at room temperature for 30 min, dehydrated in a graded series of acetone, and embedded in Epon 812. Sections were cut on an LKB Nova Ultratome, stained with uranyl acetate (Hayat, 1969) and lead citrate (Reynolds, 1963), and viewed in a JEOL model 1200EX transmission electron microscope at 80 kV. One μm sections from the same preparations were cut and stained in toluidine blue for light microscopic evaluation.

Estimates of numbers of bacteria inside a small, typical (20 μm diameter) aggregate were made by comparing the volume of a aggregate with that of a bacterium, according to methods described by Boatman (1986). Bacterial vacuole or inclusion numbers, diameters, and volumes were measured with the Bioquant Image Analysis System (R & M Biometrics, Inc., Nashville, Tennessee 37209) with Hipad electronic digitizer. All vacuoles in the sample were counted regardless of level of section through the sphere of the vacuole.

Tentacles were removed and placed in two washes of Instant Ocean to obtain isolated aggregates for observation, analysis, and culture. This procedure stimulated the release of intact aggregates into the medium. The isolated aggregates were also washed twice in Instant Ocean to minimize collection of any surface microflora. Both intact aggregates and individual bacteria released from broken aggregates were stained with Gram's stain for type of wall structure and with Sudan Black for lipids (Humason, 1972).

A sample of isolated aggregates was lyophilized and sent to Microbial ID, Inc. (Newark, Delaware 19711) for fatty acid analysis by gas chromatography. The cellular fatty acid profile, showing types and relative amounts of fatty acids by chain length, saturation, and side groups, was compared to a Hewlett Packard computer data bank of fatty acid profiles of bacterial genera and species. Identification by fatty acid analysis is comparable to that by rapid biochemical strips, is effective for far more genera, and is often more specific than biochemical tests. Matching of similarities between the sample and known bacterial species provided a reliable index to the identification of bacteria (Moss and Lewis, 1967; Miller, 1984; Sasser *et al.,* 1984).

The effects of antibiotics on the control of the numbers of bacterial aggregates of *Aiptasia* were determined.

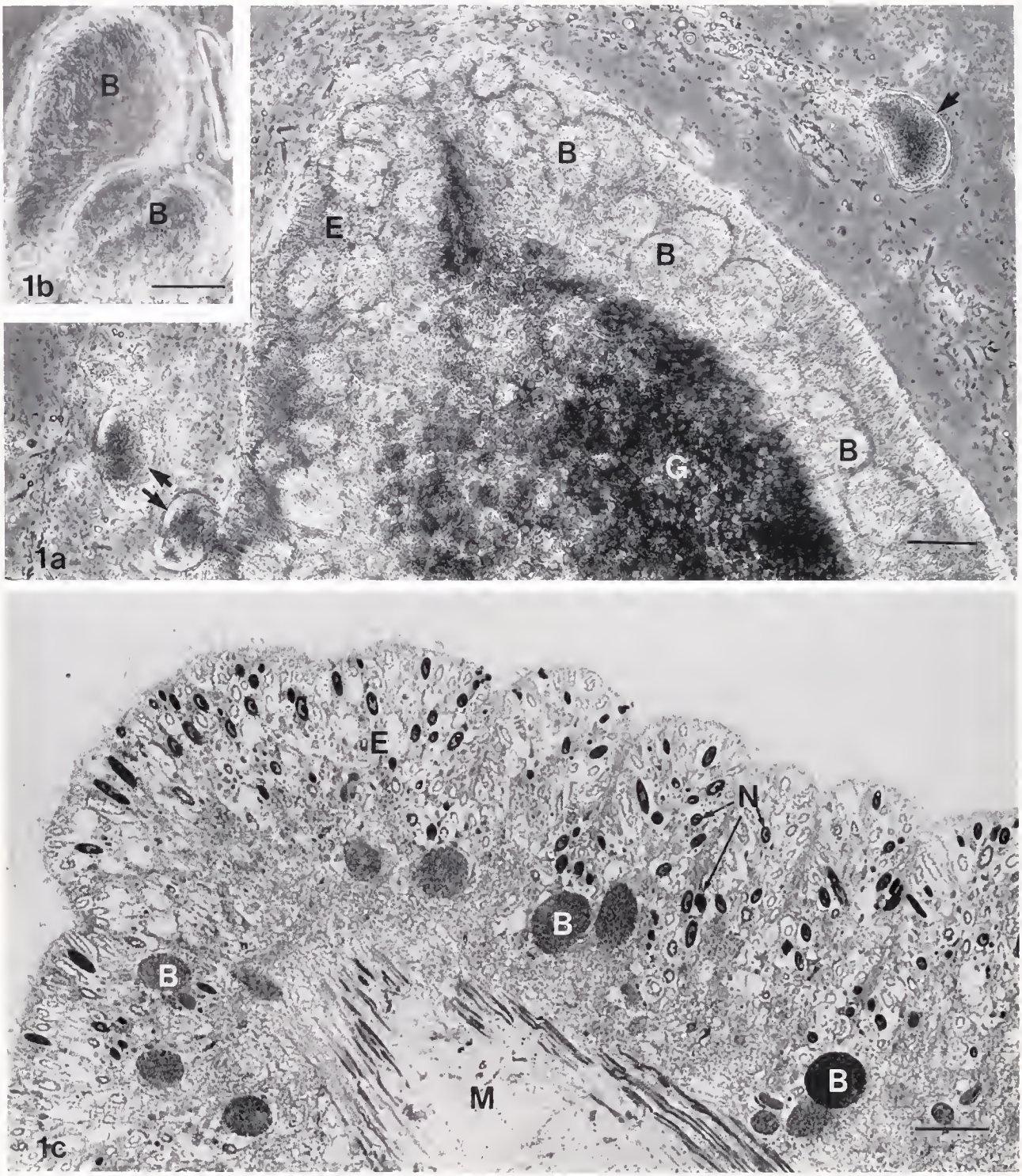

Figure 1. A. Phase contrast view of living tentacle containing numerous balloon-like aggregates in *Aiptasia pallida* epidermis. Note extruded aggregate (arrow) outside the tentacle. Bar = 100 μm. B. Phase contrast view of two extruded aggregates. Bar = 25 μm. C. Light microscope view of toluidine blue stained section of epidermis of anemone tentacle showing aggregates among epidermal cells. Aggregate (B), epidermis (E), gastrodermis containing symbiotic dinoflagellates (*Symbiodinium microadriaticum*) (G), mesoglea (M), nematocyst (N). Bar = 100 μm.

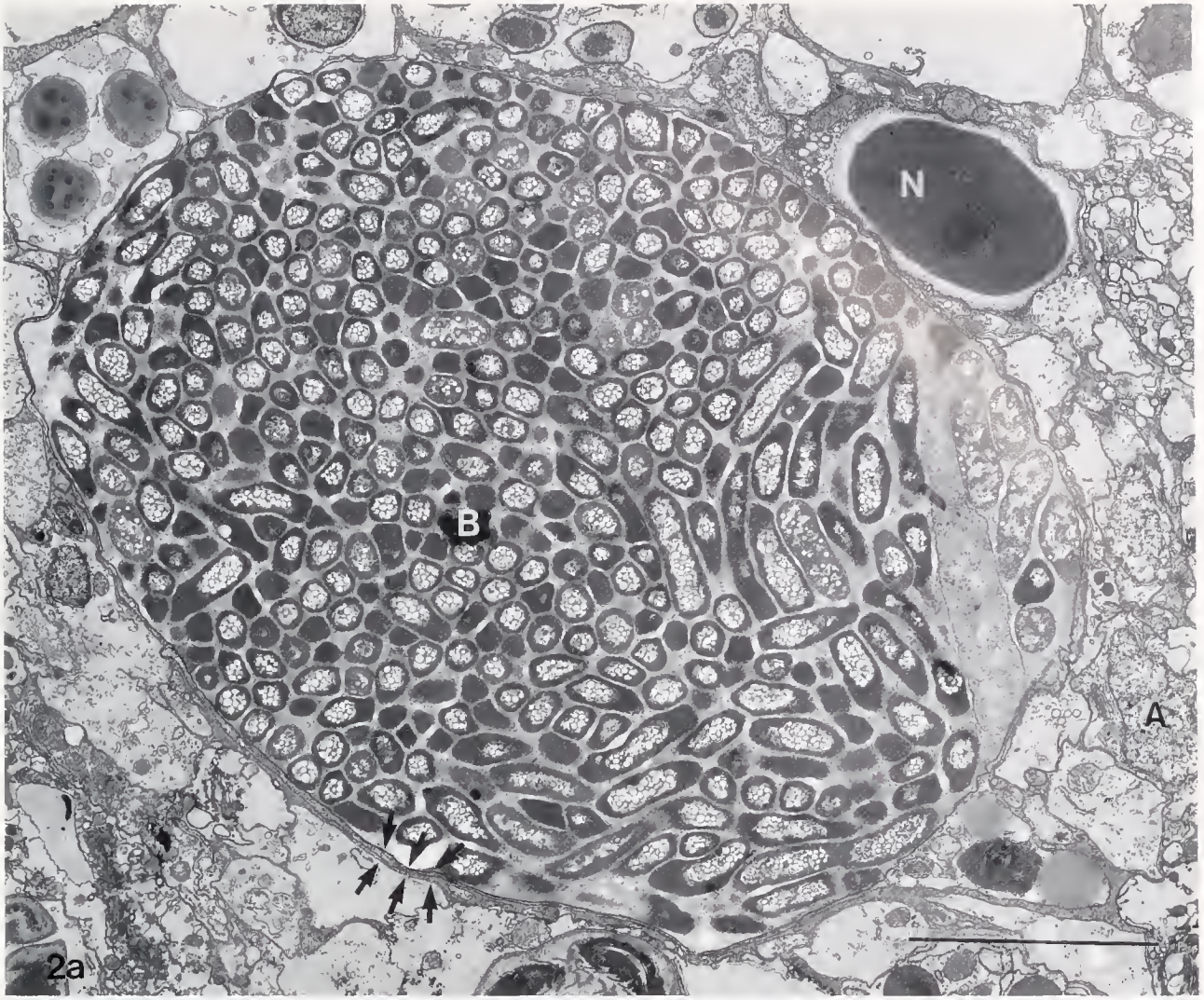

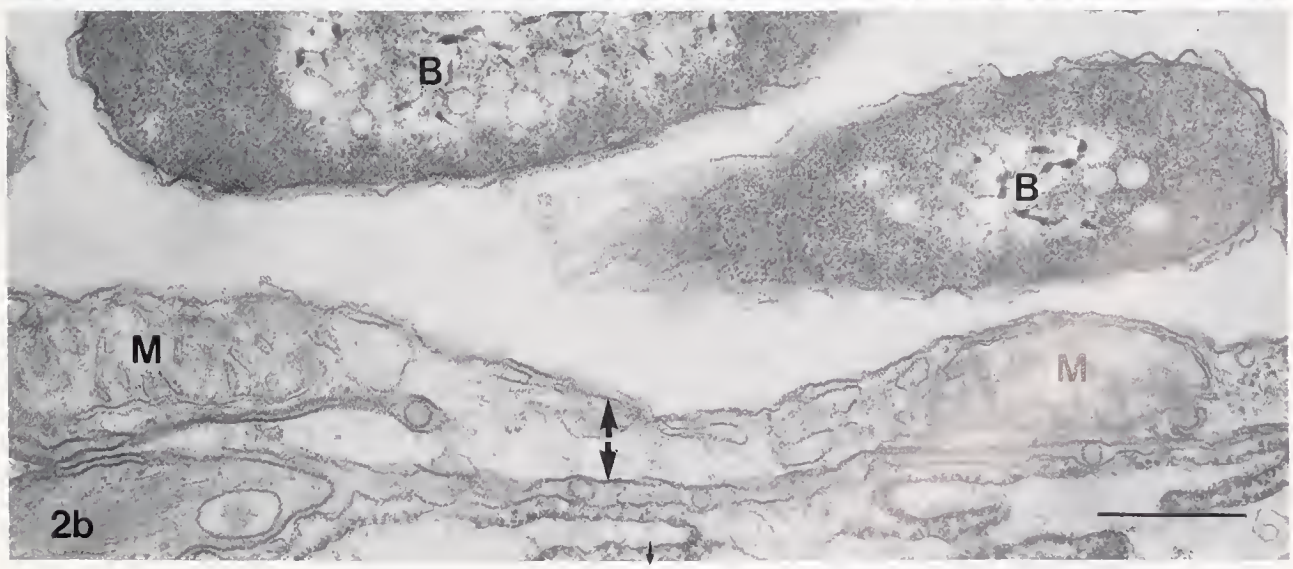

Figure 2. A. Transmission electron microscope section of entire aggregate containing numerous bacteria. Note thin membrane surrounding aggregate and associated anemone membranes (facing arrows). Several anemone cells abut the bacterial enclosure. Anemone epidermal nucleus (A), aggregate (B), nematocyst (N). Bar = 5.0 μm. B. Portion of aggregate-anemone interface. Note small amount of anemone cytoplasm with mitochondria between membrane of aggregate vacuole and plasma membrane. Bacteria (B), mitochondrion (M); Arrows span width of anemone cytoplasm. Bar = 0.5 μm.

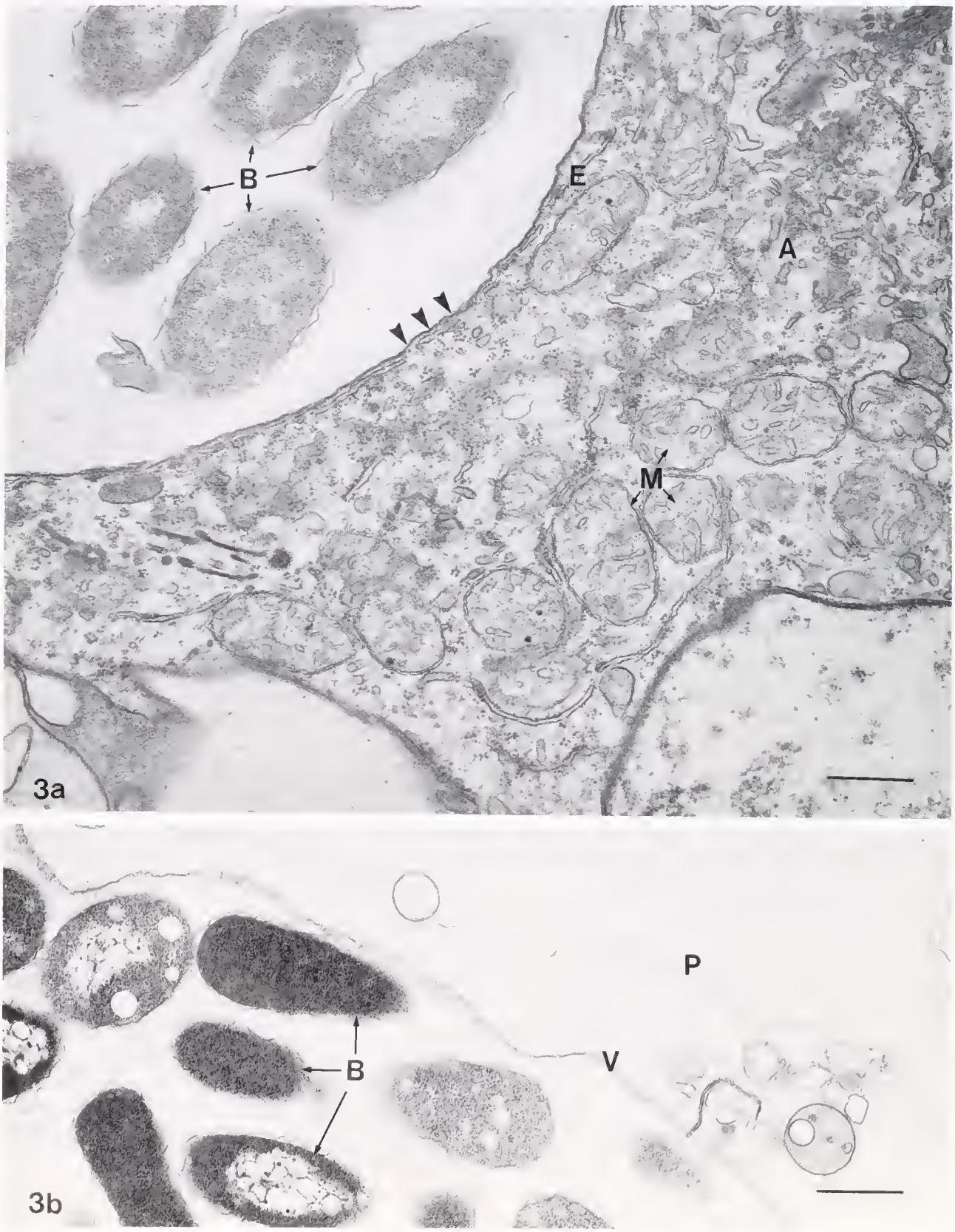

Figure 3. A. Portion of small aggregate. There is a relatively large amount of anemone cytoplasm in this specimen. Endoplasmic reticulum (E). Bar = 0.5 μm. B. High power view of membranes of isolated

Three aquaria, each containing 10 anemones with their aggregates, were set up. One contained 125 mg/ml streptomycin sulfate in Instant Ocean, a second contained 25 mg/ml chloramphenicol (d'Agostino, 1975), and a third contained Instant Ocean alone, as a control. Conditions were the same as for the stock cultures. Aggregate populations were sampled every 5 days over a 3-week period by clipping a tentacle from each anemone and counting bacteriocytes visible in the epidermis on one side of the tentacle from the tip toward the base for 0.6 mm.

To determine whether decreased populations of *Symbiodinium* would affect the population of bacteria, anemones were placed in 3 l of aerated Instant Ocean at 17°C that contained 10^{-3} *M* 3-(3,4-dichlorophenyl)-1,1-dimethylurea (DCMU) (Sigma Chemical Company) in light of 580 $\mu Em^{-2}\ s^{-1}$ intensity from 2 GE 120 W reflector floodlights, for 3 days. This procedure was adapted from the technique of Pardy (1976) which, when applied over a longer period of time, or at a higher light intensity, resulted in nearly total destruction of algal symbionts. Pardy used this procedure to obtain aposymbiotic cnidarians for controls in symbiosis experiments. Aggregates were counted using the same procedure as that used for the antibiotic sensitivity determinations. Cell numbers of *S. microadriaticum* were sampled by counting the cells found in a 0.2-mm transect. The distribution of *S. microadriaticum* was homogeneous in the tentacle preparations.

Results

In intact tentacles viewed under phase contrast microscopy, aggregates appeared as lucent spherical bodies within the epidermis of *Aiptasia pallida* (Fig. 1a). Their position varied from near the mesoglea to the free surface of the epidermis. While the aggregates were most common at the tips of anemone tentacles, they were also observed proximally on the tentacles, on the oral disc, and at low density throughout the column of the anemones. The size of aggregates shown in Figures 1–3 varied from about 10 to 100 μm. The number of aggregates varied greatly from one anemone to another. Bacterial aggregates (counted according to the method for antibiotic sampling) from each of a sample of 44 different anemones showed that 6 (14%) anemones had no aggregates in the area of the sample, and 10 (23%) anemones had 25 or more aggregates in the same sample area. The mean number of aggregates for all 44 anemones was 14.86 per 0.6 mm sample. Under higher magnification, the aggregates had a characteristic "finger print" appearance due to the tendency of adjacent rod-shaped bacteria to orient parallel to each other, producing a whorled pattern (Fig. 1b). The organization of the aggregate, and the characteristic whorled arrangement of the bacteria, was maintained after isolation of the aggregate from the epidermis.

Toluidine blue-stained aggregates seen in tentacular epidermis of *A. pallida* under light magnification appeared as dark oval spots in the epidermal layer (Fig. 1c). Cnidocytes, ciliated cells, and other cells normally present in the epidermis surrounded the aggregates. An aggregate 20 μm in diameter contained up to about 1200 individual bacteria.

Examination of the ultrastructure of an aggregate in its place in anemone epidermis shows the bacteria packed closely together (Fig. 2a). The tendency of the bacteria to remain parallel to one another within the aggregate results in many adjacent longitudinal or many adjacent cross sections. Even this relatively small aggregate is many times larger than the epidermal cells of the anemone peripheral to it. Membranes of the anemone cells intersect the thin dark aggregate membrane and either merge with it or run parallel to it for some distance. The interface between the bacteria-containing structure and the anemone cell may contain cytoplasm and cell organelles (Fig. 2b). Very small aggregates may be surrounded by a wide band of cytoplasm (Fig. 3a), containing the usual complement of cell organelles, including a layer of endoplasmic reticulum parallel to the aggregate. Following extrusion from the anemone epidermis, isolated aggregates are surrounded by a double membrane strong enough to withstand the stress of up to 6 transfers to fresh Instant Ocean (Fig. 3b). Occasionally, when aggregates ruptured, the bacteria exhibited pronounced motility on contact with seawater.

The size of the aggregate was close to the size of the intergrid space of the section support medium so that the ultrastructure of entire full-sized aggregates could not be observed. The size of the aggregate (observed range about 10–100 μm) was determined by the number of bacteria it contained, since the bacteria were packed closely together in every aggregate observed.

The individual bacteria of the aggregates were gram-negative rods, averaging 1.0 μm × 4.0 μm in size. Viewed

aggregate. Disruption of anemone cytoplasm was not due to fixation, since the same procedures were used on all tissues, but probably due to mechanical disruption during handling of individual aggregates. Bacteria (B), anemone cytoplasm (A), mitochondrion (M), membranes of aggregate (P) and (V). Arrowheads indicate membrane of aggregate vacuole. Bar = 0.5 μm.

under the electron microscope, the cytoplasm contained numerous electron-lucent vacuoles or granules that were not membrane bound (Fig. 4a, b). Calculations from measurements of 370 vacuoles showed that they occupied up to 6.66 ± 0.74% of the volume of the cell, appeared randomly distributed and had a mean diameter of 162 ± 6.98 nm. Using the light microscope, we observed the bacteria accumulating the lipid stain, Sudan Black. Web-like nucleoid material was centrally located. The bacterial wall had the layered structure typical of Gram-negative bacteria, and stained negatively in Gram's stain. The outer wall of the bacterial cell appeared loose and undulating or ridged, leaving regular spaces between the wall and cell membrane (Fig. 4a, b). This appearance may be a fixation artifact in gram negative bacteria, according to studies of *E. coli*, as described by Dubochet *et al.* (1983). Bacteria were regularly observed to be dividing by fission (Fig. 4c). The bacteria were observed only within aggregates in *A. pallida*, and we did not observe single bacterial cells in, or between, anemone cells. Some aggregates observed in electron microscope sections also contained one or two less electron-dense bacteria that were about twice as large as the other bacteria. Southward (1986) also observed two different types of bacteria in the same aggregate in deep sea thyasirids. Two types of bacteria were also seen by Soyer *et al.* (1987), although not within the same bacteriophore.

Aggregate fatty acid analysis showed 11 fatty acids with chains from 9 to 18 carbons in length. Comparison of the aggregate fatty acid profile with the Hewlett Packard bacterial classification data bank indicated most similarities to the genus *Vibrio* (pers. comm., Microbial ID). Comparisons of aggregate fatty acids with *Vibrio mimicus* (Microbial ID) and *V. anguillarum* (Boe and Gjerde, 1980) were made by setting the 16-carbon straight chain fatty acid in all three samples to 100%. Amounts of fatty acids having different chain lengths were calculated as percentages of this base value (Table I).

During treatment with chloramphenicol, the aggregate population decreased from 17.5 aggregates per 0.6 mm sample of one side of a tentacle tip from each of 10 anemones, to 5.0 in 5 days, a decrease of 75% as compared to the control, reaching a minimum of 1.4 after 10 days. In streptomycin, the number of aggregates decreased by 50% after 10 days from 14.9 to 7.8, and reached a minimum of 6.0 after 20 days. After 20 days, the number of aggregates was 4 times lower in chloramphenicol than in streptomycin. On day 1, the means of the three groups showed no significant differences (using one-way analysis of variance, the F statistic is 0.20 and the *P*-value is 0.82). Also, this and subsequent observations on the control group made on days 1, 5, 10, 16, and 20, showed no significant changes in the mean of the control group over this time period (using one-way analysis of variance, the F statistic is 0.15 and the *P*-value is 0.96). However, there was a sharp decline in both the mean and the variance of the number of bacteriocytes in the group treated with chloramphenicol when compared to the control group. A two-sample t test for independent samples with unequal variances, using the Satterwaite approximation for the degrees of freedom in computing the *P*-value, indicated a significant difference in the mean number of aggregates in the anemones undergoing chloramphenicol treatment when compared to the control group of the fifth day ($t = 4.54$, d.f. = 17, P-value < 0.0001). Separate t tests comparing these groups on days 10, 16, and 20 also indicated significant differences (on the 20th day, $t = 4.28$, d.f. = 9, P-value = 0.002). The same method comparison showed no significant difference in the means of the streptomycin group and the control group until the 20th day. (On the 20th day $t = 2.18$, d.f. = 17, P-value = 0.043). Nonparametric methods, using Mann-Whitney statistics in place of the t statistics, gave similar results. For example, the difference in the control and the streptomycin group after 20 days remained statistically significant (P-value = 0.017). The anemones undergoing chloramphenicol treatment began to show deleterious effects during the third week, indicated by tentacular retraction.

Following treatment with light and DCMU, much of the *Symbiodinium* population was lost and the number of aggregates increased, from a mean of 8.8 ± 2.61 per 0.6 mm tentacle sample before treatment, to 11.3 ± 4.86 after three days of treatment, to 27.4 ± 3.15 three days following return to normal culture conditions. Mean numbers of *Symbiodinium* decreased during treatment from 26.6 ± 1.38 to 11.6 ± 1.73, and then to a further reduction of 5.2 ± 1.70 one week later. Seven days following the return to normal culture conditions, the number of aggregates was still elevated (15.1 ± 3.33 per tentacle). The standard errors are relatively high because of the previously mentioned great variation in numbers of aggregates from one anemone to another. Even so, t-test values demonstrated that the mean number of aggregates per tentacle at the beginning of the experiment was significantly different at the 0.01 confidence level from the mean number at day 6 and day 10.

Discussion

Bacteria in the aggregates from *Aiptasia pallida* specimens were not individually surrounded by host vacuoles and host cytoplasm as observed by Cavanaugh (1983) in *Solemya velum*, *Riftia pachyptila* and *Calyptogena magnifica* or Fischer and Hand (1984) in *Lucina floridana* but instead the bacteria were clumped together in one

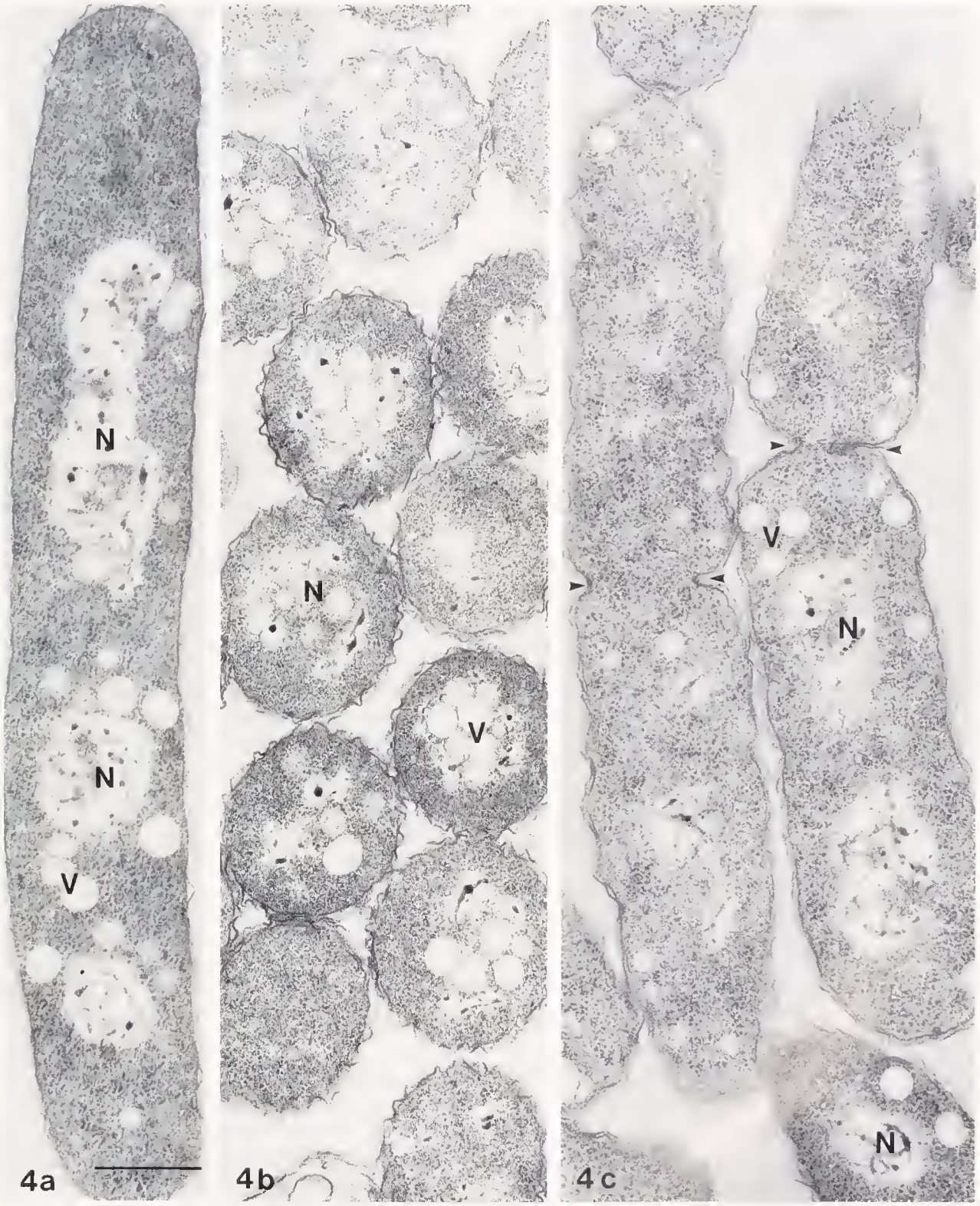

Figure 4. A. Longitudinal section of bacterium inside aggregate. B. Cross sections of bacteria in aggregate. C. Longitudinal section of bacteria undergoing fission (arrowheads) inside aggregate. Nucleosome (N), vacuole (V). Bar = 0.5 μm.

Table I

Percentage distribution of fatty acids of aggregates found in Aiptasia

	Fatty acids as a percent of 16-C fatty acid		
	Aggregate	*Vibrio mimicus*[1]	*V. anguillarum*[2]
Fatty acid chain length			
9:0[3]	5.30	0	0
12:0	8.00	0	16.50
12:0 3 OH	4.81	13.80	0
14:0	23.84	20.76	32.10
15:0 anteiso	11.29	0	1.90
16:0 iso	14.62	5.90	28.90
16:1 cis 9	117.32	128.00	251.00
16:0	100.00	100.00	100.00
18:1 cis 9	33.02	0	62.50
18:0	19.09	6.92	9.10

[1] Data from Microbial ID Hewlett Packard data base.

[2] Mean of 10 subcultures from Boe and Gjerde (1980).

[3] The first number indicates the carbon chain length; the number following the colon gives the number of double bonds; any notations to the right give modifications in structure from a straight chain fatty acid.

large vacuole. The appearance of the aggregate was more similar to those described by Peters (1983), Bouvy *et al.* (1986), and Soyer *et al.* (1987). The presence of numerous dividing bacteria (Fig. 4a) inside the aggregate indicated that they were metabolically active and that the aggregate was not a static cyst.

The data suggest that there are two possible theories of the structural origin of aggregates in *A. pallida*. Our observations of small aggregates (Fig. 3a) suggest that the aggregate is an anemone cell that is distorted by a vacuole swollen by the multiplication of invading bacteria. Micrographs of isolated aggregates also showed that there were organized structures between two membranes surrounding the aggregate. Figure 3a shows endoplasmic reticulum next to the bacterial compartment. Chesnick and Cox (1986) suggest that the membranes of the bacteriophore in the dinoflagellate *Peridinium baltica* may be derived from endoplasmic reticulum. These observations indicate that the aggregate enclosure is not of bacterial origin, but an anemone cell with the cytoplasm stretched into a thin shell surrounding the vacuole containing the bacteria. On the other hand, pictures of larger aggregates (Fig. 2a) indicate that the bacteria are enclosed in a membrane separate from the anemone structure. Figure 2a shows several anemone cells around the periphery of the bacterial enclosure, none of which enclose the aggregate. The great size difference between anemone cells and aggregates makes it seem unlikely that an anemone cell could enlarge to the necessary degree. Also, no nuclei were observed in aggregates.

No series of parallel intracytoplasmic membranes such as those characteristic of photosynthetic bacteria were seen in the bacteria of *A. pallida*. In this respect, bacteria from *A. pallida* were similar to bacteria from marine sponges (Vacelet, 1975; Wilkinson, 1978), *R. pachyptila*, other vestimentiferans, the clams *Solemya velum, C. magnifica, C. pacifica, Lucinoma annulata* (Cavanaugh, 1983), and *L. floridana* (Fischer and Hand, 1984), none of which possessed internal lamellae. In contrast, Cavanaugh *et al.* (1981) described intracytoplasmic membranes in bacteria in formalin-fixed trophosome of *R. pachyptila*. In *Hydra*, individual bacterial symbionts are located in the gastrodermis in contrast to the epidermal location in *Aiptasia* (Thorington *et al.*, 1979). Moreover, the symbiotic vesicles in *Hydra* contained very small numbers of both bacteria and *Chlorella*. Studies by Wilkerson (1980) conclude that the bacteria contribute to phosphate uptake in this organism. The bacteria in *A. pallida* differ from those in other marine animals in confinement to the epidermis and in containing numerous bacteria within a single aggregate except as noted by Peters (1983) in corals and Bouvy *et al.* (1986) in clams.

The vacuoles or granules located in the bacterial cytoplasm were a constant feature of the bacterium. Similar inclusions have been found in many other bacteria, and their contents have even been analyzed. Jones (1981) and Hand (1987) identified intracellular vacuoles similar to those seen in the bacteria found in *A. pallida*, as locations of sulfur deposits in *R. pachyptila*. A common intracellular inclusion, which is similar in appearance to vacuoles found in bacteriocytes of *A. pallida*, is associated with accumulation of poly-b-hydroxybutyrate. Lack of limiting membranes around the vacuoles does indicate that they might contain lipids. Sudan Black lipid staining under the light microscope also suggests this possibility. Lack of granular material in the vacuoles after electron microscope preparation procedures used indicated that they did not contain glycogen.

The computer matching process, based on fatty acid analysis, suggested that the bacterium found in *A. pallida* was a member of the genus *Vibrio*. This identification is supported by our structural findings, although the particular bacteria found in *A. pallida* are large for this genus. The bacteria in the aggregates were consistently gram-negative, and not variable in their Gram staining characteristics. Therefore, even though the bacteria were in various growth phases inside the aggregate, the consistency of staining shows that the cells are Gram-negative. This conclusion is further confirmed by the typical layered appearance of the cell wall (Fig. 4), not found in Gram-positive bacteria. Moreover, members of the genus *Vi-*

brio are frequently found in close association with marine animals, are Gram-negative, and can be straight rods. Most *Vibrio* require Na^+ ions for growth, often grow at 20°–30°C, and tolerate moderately alkaline conditions. These requirements are consistent with the marine environment of the aggregates. Some species store poly-b-hydroxybutyrate in intracellular granules. Many species form flagella, but others do not. They are sensitive to chloramphenicol and streptomycin, as were the bacteria in the aggregates. *Vibrio* is also sensitive to a relatively wide range of other antibiotics (Baumann *et al.*, 1984).

Because *Aiptasia* benefit from the presence of *Symbiodinium*, the possibility that changes in the bacterial population might affect the *Symbiodinium* population and consequently affect the well-being of *Aiptasia*, suggests an additional factor to be considered in studying how changes in one population may affect the other. It is unknown whether the increase of aggregates in anemones subjected to light-DCMU treatment was due to the use of substances from damaged *Symbiodinium*, or possibly to the increased availability of some substance not used by the decreased population of *Symbiodinium*. Decrease in bacterial numbers after 10 days suggests that the bacteria may have been using nutrients obtained from *S. microadriaticum* cells as they disintegrated. We have not observed detrimental effects of bacterial colonies on *A. pallida*. Individuals may develop shortened, thickened tentacles, but this condition has not been associated with certainty with increased numbers of aggregates, like Peters (1984) has associated pathological conditions in corals with the presence of bacteria.

Work is in progress to isolate and culture the bacteria, characterize them physiologically and biochemically, and determine their metabolic relationships in *A. pallida*. We now have a three-way system to study. The interrelationships between *Aiptasia* and *Symbiodinium* are already well established. The combination of bacterial, dinoflagellate, and anemone cells living together suggests curious biochemical and ecological interrelationships, knowledge of which may prove useful as a model system in cellular ecology.

Acknowledgments

The authors express grateful appreciation to the following: Drs. Myron Sasser and Margaret Roy of Microbial ID for helpful advice on sample preparation for the fatty acid analysis; Dr. Gerald Funk of the Department of Mathematics, Loyola University of Chicago, for statistical treatment of results of the antibiotics experiment; Lawrence Wallace of Carolina Biological Supply Company for freshly collected *Aiptasia pallida* from the seashore; Susan Kenney of the Shedd Aquarium in Chicago for samples of *Aiptasia pallida;* and Michael Lesser of the University of Maine at Orono for examination of *Aiptasia* from Bermuda.

Literature Cited

d'Agostino, A. 1975. Antibiotics in cultures of invertebrates. Pp. 109–133 in *Culture of Marine Invertebrate Animals*, W. L. Smith, ed. Plenum Press, New York.

Baumann, P., A. L. Furniss, and J. V. Lee. 1984. Genus I. *Vibrio*. Pp. 518–537 in *Bergey's Manual of Systematic Bacteriology*, Vol. I, J. G. Holt, ed. Williams & Wilkins, Baltimore.

Boatman, E. S. 1986. Digitizing and Quantitation. Chap. 13 in *Ultrastructural Techniques for Microorganisms*, H. C. Aldrich and W. J. Todd, eds. Plenum Press, New York.

Boe, B., and J. Gjerde. 1980. Fatty acid patterns in the classification of some representatives of the families Enterobacteriaceae and Vibrionaceae. *J. Gen. Microbiol.* **116:** 41–49.

Bouvy, M., G. Cahet, F. deBilly, J. Soyer, M.-O. Soyer-Gobillard, and C. Thiriot-Quievreux. 1986. Sur la presence de bacteries dans las branchie d'un mollusque bivelve littoral *Spisula subtruncata* *C. R. Acad. Sci Paris* **303:** 257–262.

Cavanaugh, C. M., S. L. Gardiner, M. L. Jones, H. W. Jannasch, and J. B. Waterbury. 1981. Prokaryotic cells in the hydrothermal vent tube worm *Riftia pachyptila* Jones: possible chemoautotrophic symbionts. *Science.* **213:** 340–342.

Cavanaugh, C. M. 1983. Symbiotic chemoautotrophic bacteria in marine invertebrates from sulphide rich habitats. *Nature* **302(3):** 58–61.

Chesnick, J. M. and E. R. Cox. 1986. Specialization of endoplasmic reticulum architecture in response to a bacterial symbiosis in *Peridinium balticum*. *J. Phycol.* **22:** 291–298.

Dando, P. R., A. J. Southward, E. C. Southward, N. B. Terwiliger, and R. C. Terwiliger. 1985. Sulphur-oxidising bacteria and haemoglobin in gills of the bivalve mollusc *Myrtea spinifera*. *Mar. Ecol. Prog. Ser.* **23:** 85–98.

Dubochet, J., A. W. McDowell, B. Menge, E. N. Schmid, and K. G. Lickfeld, 1983. Electron microscopy of frozen-hydrated bacteria. *J. Bacteriol.* **155:** 381–390.

Felbeck, H., G. Liebezeit, R. Dawson, and O. Giere. 1983. CO_2 fixation in tissues of marine oligochaetes (*Phallodrillus leukodermatus* and *P. planus*) containing symbiotic chemoautotrophic bacteria. *Mar. Biol.* **75:** 187–191.

Fischer, M. R. and S. C. Hand. 1984. Chemoautotrophic symbionts in the bivalve *Lucina floridana* from seagrass beds. *Biol. Bull.* **167:** 445–459.

Hand, S. C. 1987. Trophosome ultrastructure and the characterization of isolated bacteriocytes from invertebrate-sulfur bacteria symbioses. *Biol. Bull.* **173:** 260–276.

Hayat, M. A. 1969. Uranyl acetate as a stain and a fixative for heart tissue. *Proc. 27th Ann. Meeting Electron Microsc. Soc. Am.* Claitors Publ., Baton Rouge. P. 412.

Humason, G. L. 1972. *Animal Tissue Techniques.* Freeman, San Francisco.

Jones, M. L. 1981. *Riftia pachyptila* Jones: observations on the vestimentiferan worm from the Galapagos Rift. *Science.* **213:** 333–336.

Karnovsky, M. 1967. The ultrastructural basis of capillary permeability studied with peroxidase as a tracer. *J. Cell Biol.* **98:** 213–236.

Margulis, L., G. Thorington, B. Berger, and J. Stolz. 1978. Endosymbiotic bacteria associated with the intracellular green algae of *Hydra viridis*. *Current Microbiol.* **1:** 227–232.

Miller, L. T. 1984. Gas-liquid chromatography of cellular fatty acids as a bacterial identification aid. *Hewlett-Packard Application Note.* Pp. 228–237.

Moss, C. W. and V. Lewis. 1967. Characterization of *Clostridia* by gas chromatography. 1. Differentiation of species by cellular fatty acids. *Applied Micr.* **15:** 390–397.

Palincsar, E. E., W. R. Jones, and J. S. Palincsar. 1988. Bacterial aggregates within *Aiptasia pallida. Am. Zool.* **28(4):** 149.

Pardy, R. 1976. The production of aposymbiotic hydra by the photodestruction of green hydra zoochlorellae. *Biol. Bull.* **151:** 225–235.

Peters, E. C. 1984. A survey of cellular reactions to environmental stress and disease in Caribbean scleractinean corals. *Helgol. Meeresunturs.* **37:** 113–137.

Peters, E. C., J. J. Oprandy, and P. P. Yevich. 1983. Possible causal agent of "White Band Disease" in Caribbean acroporid corals. *J. Invert. Pathol.* **41:** 394–396.

Reynolds, E. S. 1963. The use of lead citrate at high pH as an electron-opaque stain in electron microscopy. *J. Cell Biol.* **23:** 271–288.

Sasser, J. M., D. H. Fieldhouse, and C. N. Carter. 1984. Computer assisted identification of bacteria based on fatty acid analysis. *Phytopathology* **74(7):** 882.

Southward, A. J., E. C. Southward, P. R. Dando, G. H. Rau, H. Felbeck, and H. Flugel. 1981. Bacterial symbionts and low 13 C/12 C ratios in tissues of Pogonophora indicate unusual nutrition and metabolism. *Nature* **293:** 616–620.

Southward, E. C. 1986. Gill symbionts in thyasirids and other bivalve molluscs. *J. Mar. Biol. Ass.* **66:** 889–914.

Soyer, J., M. Soyer-Gobillard, C. Theriot-Quievreux, M. Bouvy, and G. Cahet. 1987. Chemoautotrophic bacterial endosymbiosis in *Spisula subtruncata* Ultrastructure, metabolic significance and evolutionary implications. *Symbiosis* **3:** 301–314.

Thorington, G., B. Berger, and L. Margulis. 1979. Transmission of symbionts through the sexual cycle of *Hydra viridis* 1. Observations on living organisms. *Trans. Am. Microsc. Soc.* **98(3):** 401–413.

Vacelet, J. 1975. Etude en microscopie electronique de l'association entre bacteries et spongiaires du genre *Verongia. J. Microscopie Biol. Cell.* **23:** 271–288.

Wilkerson, F. P. 1980. Symbionts involved in phosphate uptake by green hydra. Pp. 269–277 in *Symbiosis and Cell Biology,* Vol. 1, W. Schwemmler and H. E. Schenk, eds. Walter de Gruyter, Berlin.

Wilkinson, C. R. 1978. Microbial associations in sponges. *Mar. Biol.* **49:** 161–185.

Reference: *Biol. Bull.* 177: 141–145. (August, 1989)

FMRFamide-like Immunoreactivity in the Nervous System of the Starfish *Asterias rubens*

MAURICE R. ELPHICK*, ROLAND H. EMSON**, AND MICHAEL C. THORNDYKE*,[1]

**Wolfson Laboratory, Biology Department, Royal Holloway and Bedford New College, University of London, Egham, Surrey, TW20 OEX, and **Division of Biosphere Science, King's College, University of London*

Abstract. The nervous system of the starfish *Asterias rubens* was subjected to immunocytochemical investigation using antisera raised against the molluscan neuropeptide FMRFamide. Immunoreactivity was detected in the radial nerve cords and the circumoral nerve ring, as well as in the sub-epithelial nerve plexus of the tube foot system. The hyponeural part of the radial cords contained numerous immunoreactive cell bodies. In the ectoneural tissue, immunoreactive cells were present in the epithelium, with cell bodies especially abundant in the lateral parts of the nerve, close to the site of emergence of the innervation to the tube feet. The sub-epithelial nerve plexus of the tube feet contained immunoreactive fibers that were continuous with an extensive system of ectoneural immunoreactive fibers in the radial nerve cords. Immunoreactive fibers were particularly evident in the regenerating radial nerves of previously sectioned arms.

Introduction

The isolation and characterization of FMRFamide (Phe-Met-Arg-Phe-NH_2) from the clam *Macrocallista nimbosa* by Price and Greenberg (1977) heralded an era of intense investigation into both the occurrence and functional properties of this neuropeptide in molluscs. FMRFamide has a variety of effects on molluscan hearts, visceral and somatic muscles (reviewed by Greenberg *et al.*, 1983), and molluscan neurons (reviewed by Walker, 1986).

Since its discovery, antisera raised to FMRFamide have been used to investigate the possibility that FMRFamide-like peptides occur in non-molluscan species. Indeed, such immunochemical studies have revealed that FMRFamide-like substances are present in members of most of the major animal groups, including coelenterates (Grimmelikhuijzen, 1983), platyhelminthes (Reuter *et al.*, 1984; Gustafsson *et al.*, 1985), nemertines (Varndell and Polak, 1983), nematodes (Li and Chalfie, 1986; Cowden *et al.*, 1987), annelids (Kuhlman *et al.*, 1985; Porchet and Dhainaut-Courtois, 1988), crustaceans (Hooper and Marder, 1984; Jacobs and Van Herp, 1984), a chelicerate (Watson *et al.*, 1984), insects (Boer *et al.*, 1980), and vertebrates (Boer *et al.*, 1980; Dockray *et al.*, 1981). Subsequently, several of the peptides responsible for this immunoreactivity have been identified and, at present, the peptides isolated from protostomian species appear to be quite distinct from those of non-protostomes.

The Echinodermata, a major invertebrate phylum, has so far been neglected by those interested in neuropeptide biology. Therefore, as the first step in an attempt to identify FMRFamide-related peptides in echinoderms, we have carried out an immunocytochemical study of the distribution of FMRFamide-like material in the nervous system of the starfish, *Asterias rubens*.

Materials and Methods

Specimens of *Asterias rubens* were collected on the south coast of England, transported to Kings College, and maintained there in an aerated seawater system at 11°C.

The starfish were narcotized in 3.5% magnesium chloride, and the various parts of the nervous system were then dissected into cold (4°C) Bouin's fluid in seawater. After fixation for approximately 18 h at 4°C, the tissue

Received 6 February 1989; accepted 31 May 1989.

[1] To whom correspondence should be addressed.

was embedded by routine methods in paraffin wax (58°C mp), sectioned at 7–15 μm, and mounted on poly-L-lysine coated glass slides. The primary rabbit antisera to FMRFamide (1171 from C. J. P. Grimmelikhuijzen, and L135 from G. J. Dockray) were applied at dilutions between 1:100 and 1:1000. The 1171 antiserum has been characterized by solid and liquid phase absorption tests with numerous, potentially cross-reactive peptides; it has high affinity for FMRFamide, as expected, but also some affinity for FLRFamide, FMKFamide, LTRPRYamide and RFamide (Grimmelikhuijzen, 1984).

Two methods were used to visualize the bound primary antibodies: application of a fluorescein isothiocyanate (FITC)-labelled swine anti-rabbit second antibody; or treatment with a peroxidase conjugated goat anti-rabbit second antibody, followed by rabbit peroxidase anti-peroxidase (PAP) complex and diaminobenzidine as the peroxidase substrate (the PAP method).

Three controls were carried out: the primary antibodies were pre-absorbed overnight at room temperature with 10 nmol of FMRFamide per ml of diluted antiserum; antibodies to other peptides (anti-insulin, anti-substance P, anti-cholecystokinin) were tested; and non-immune serum was also examined.

Results

General morphology

The major components of the starfish nervous system are the circumoral nerve ring and its five branches—the radial nerve cords—which extend along the ventral surface of each arm (Fig. 1a). These nerve tracts contain two distinct parts, the ectoneural and hyponeural systems (Fig. 1b). The ectoneural system is further organized into an outer epithelial region containing cell bodies and supporting cells, and an inner axonal region traversed by fibers from the supporting cells (Fig. 1b). It is continuous with an extensive sub-epithelial nerve plexus of the skin, which is thickened locally to form the marginal nerve cords and the tube foot nerve ring (Fig. 1a). The hyponeural system lies above the ectoneural tissue, separated from it by a thin basement membrane (Fig. 1b).

A minor component of the starfish nervous system is the aboral nerve ring, which is continuous, in each arm, with the apical nerve, a small strand of tissue lying along the mid-dorsal region of the coelomic epithelium (Fig. 1a).

Immunocytochemistry

Positive FMRFamide-like immunoreactivity was detected in the circumoral nerve ring and radial nerve cords of *Asterias* (Fig. 2a, b).

Bipolar immunoreactive cell bodies were evident in

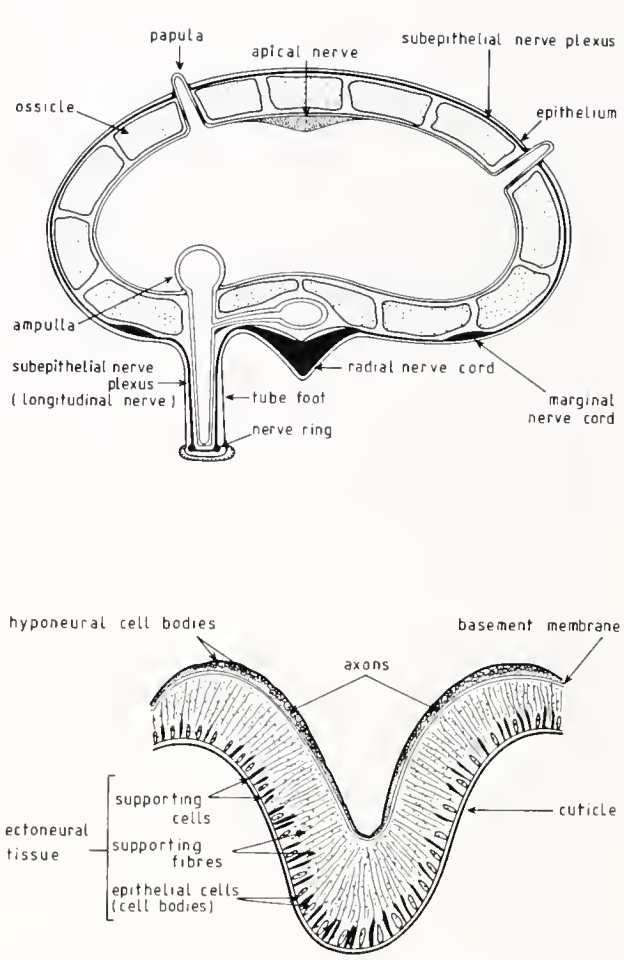

Figure 1. Diagrammatic representation of the nervous system in *Asterias*. (a) Composite cross section of an arm showing the anatomy of the nervous system at the level of a tube foot (left side) and between tube feet (right side). (b) Detailed cross section of radial nerve cord.

the ectoneural epithelium, interspersed between supporting cells (Fig. 2c). Longitudinal sections of the radial nerves show cell bodies along the entire length of the ectoneural network, with beaded fibers throughout the axonal region (Fig. 4a). Transverse sections reveal that the cell bodies and associated axonal tracts are particularly concentrated laterally, close to the points where the tube feet receive innervation from the nerve ring and cords (Figs. 2b, d; 3a).

Immunoreactive fibers occur throughout the sub-epithelial nerve plexus of the tube feet and are clearly continuous with the system of immunoreactive fibers in the ectoneural part of the adjacent nerve cord (Figs. 2b; 3a, b). No immunoreactive cell bodies were detected in the nerve plexus of the tube feet.

In the hyponeural part of the nervous system, immunoreactive cell bodies are particularly abundant, and processes could occasionally be seen directed towards the

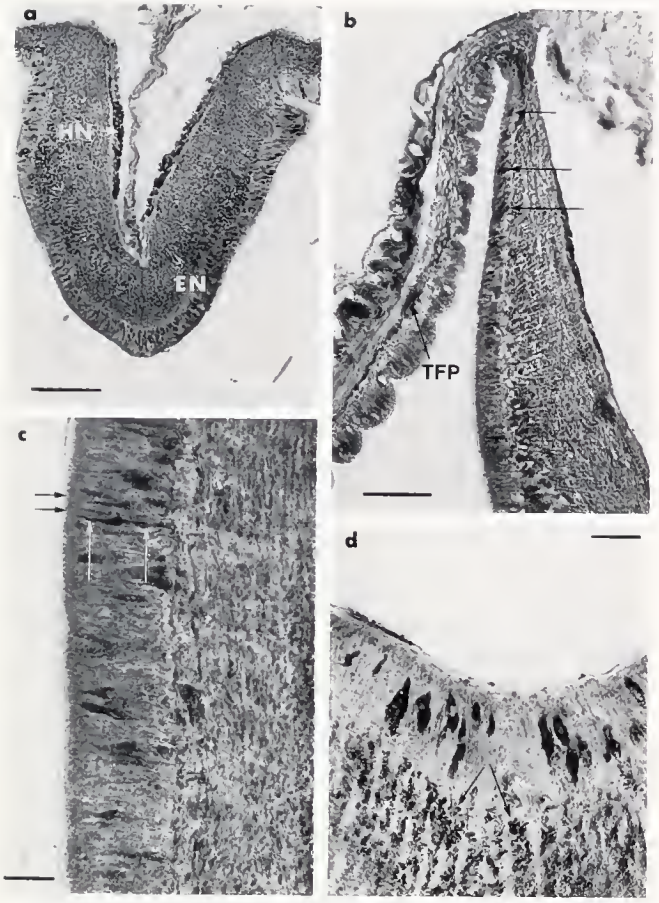

Figure 2. (a) Transverse section of radial nerve showing distribution of immunoreactivity in the ectoneural (EN) and hyponeural (HN) systems. Primary antibody, 1171, with PAP labelling. Scale bar = 100 μm.

(b) Longitudinal section of circumoral ring and part of tube foot epithelium showing lateral concentration of ectoneural cell bodies (triple arrows) and distinctive tube foot sub-epithelial nerve plexus (TFP). Primary antibody, 1171, with PAP labelling. Scale bar = 100 μm.

(c) Longitudinal section of radial nerve cord showing bipolar ectoneural cell bodies (white arrows) interspersed between supporting cells (black arrows) of the epithelium. Primary antibody, 1171, with PAP labelling. Scale bar = 30 μm.

(d) Transverse section of lateral region of the radial nerve cord near junction with tube foot showing increased concentration of immunoreactive ectoneural cell bodies and fibers (arrows). Primary antibody, L135, with PAP labelling. Scale bar = 30 μm.

basement membrane, although no fibers appeared to cross it in either direction (Fig. 4a, c).

In preliminary experiments designed to investigate the pattern of neuronal regeneration in previously sectioned arms, the concentration of immunoreactive fibers in the ectoneural system of the regenerates was noticeably increased (Fig. 4b).

Both FMRFamide antisera used gave positive results, but all of the control experiments, including those using antisera previously absorbed with FMRFamide, proved negative.

Discussion

This investigation records for the first time, the occurrence of immunoreactive FMRFamide-like molecules in the nervous system of an echinoderm. These findings have implications for both neuropeptide phylogeny and echinoderm neurobiology.

Neuropeptide phylogeny

Over the last decade, FMRFamide-like peptides have been characterized in a variety of species and appear, at present, to fall into two distinct groups. First, those isolated from protostome phyla (Nematoda, Annelida, Mollusca, and Arthropoda) share with FMRFamide the general C-terminal sequence: F(X)RFamide, where X can be methionine, leucine, or isoleucine. Second, those peptides isolated from non-protostomes (Coelenterata and Chordata) usually share with FMRFamide only the C-terminal RFamide.

Greenberg *et al.* (1988) suggested that the protostomian peptides are homologous, whereas the sharing of the RFamide C-terminus with FMRFamide among the non-protostomian peptides "may merely reflect general characteristics of associations between peptides and proteins. If there is a homology, it is likely to reside with the class of membrane proteins comprising peptide receptors." Since the echinoderms are deuterostomian inver-

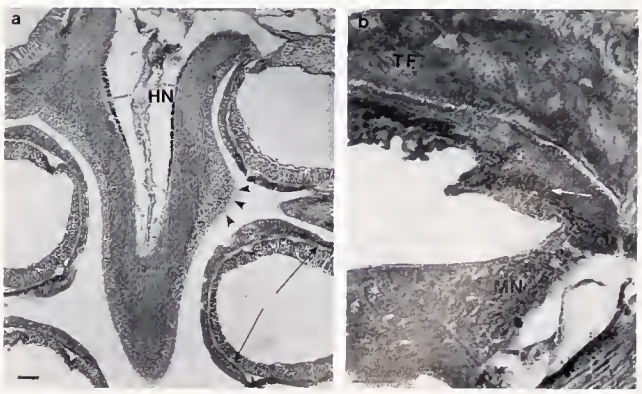

Figure 3. (a) Oblique section through radial nerve cord. Hyponeural cell bodies (HN) are clearly evident as is the sub-epithelial plexus in adjacent tube feet (arrows). Notice the high concentration of immunoreactive cells where the nerve cord branches to innervate the tube feet (arrow heads). Primary antiserum, 1171, with PAP labelling. Scale bar = 100 μm.

(b) Transverse section of marginal nerve cord (MN) and adjacent tube foot (TF). Immunoreactive fibers in the sub-epithelial plexus are clearly evident (arrow). Primary antiserum, 1171, with PAP labelling. Scale bar = 30 μm.

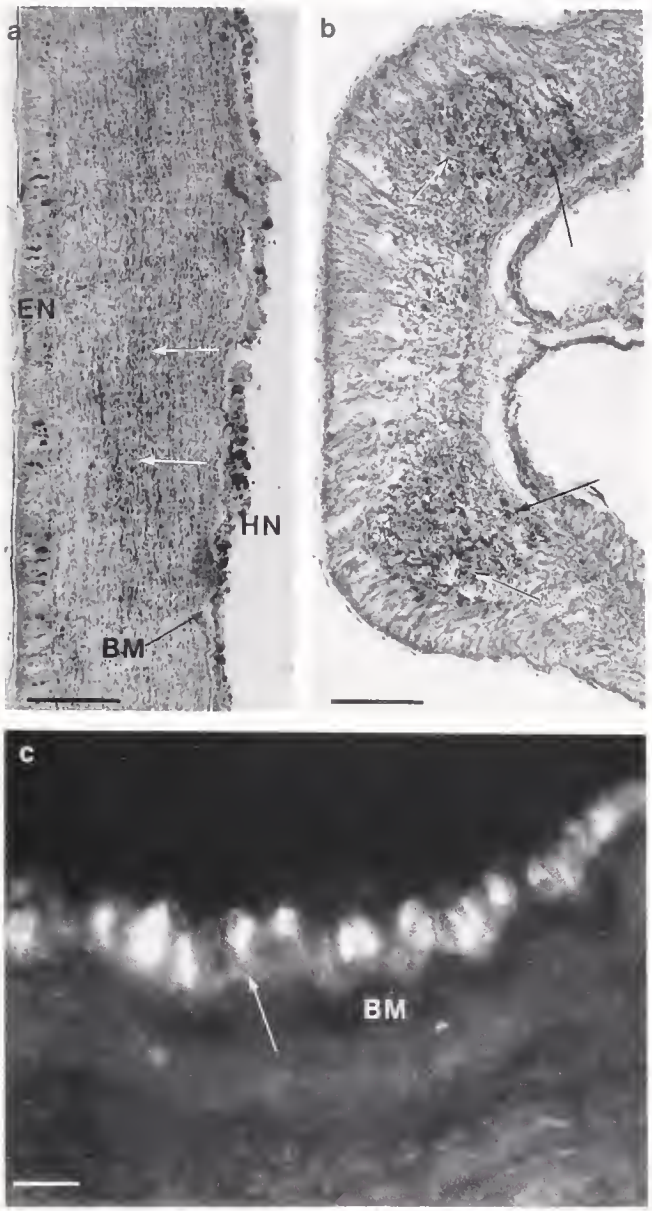

Figure 4. (a) Longitudinal section of radial nerve with cell bodies in both ectoneural (EN) and hyponeural (HN) systems as well as beaded fibers in the axonal region (arrows). BM, basement membrane. Primary antibody, L135, with PAP labelling. Scale bar = 100 μm.

(b) Transverse section of regenerating radial nerve to show dense concentration of immunoreactive fibers (arrows). The absence of immunoreactive cell bodies suggests these fibers are derived from cells distal to the region of growth. Primary antibody, L135, with PAP labelling. Scale bar = 100 μm.

(c) Longitudinal section of the radial nerve cord showing hyponeural cell bodies, one with a process (arrow) directed toward the basement membrane (BM). Primary antibody, 1171, with FITC labelling. Scale bar = 25 μm.

tebrates, the characterization of the FMRFamide-like peptides in echinoderms would provide a further test of the notion that the F(X)RFamide peptides are peculiar to protostomes.

Echinoderm neurobiology

Our current understanding of echinoderm neurobiology is far behind that of most of the other major invertebrate phyla (see Cobb, 1987, 1988). Only one native echinoderm neuropeptide has ever been thoroughly investigated: gonad stimulating substance (GSS) (see Kanatani, 1979). Discovered thirty years ago (Chaet and McConnaughy, 1959), GSS has only recently (and partially) been sequenced (Shirai, 1987).

This is the first extensive study of peptidergic neurons in an echinoderm. The distribution of FMRFamide-like immunoreactivity in the nervous system may provide some clues as to the function of these peptides in starfish. The abundance of immunoreactivity and its presence in both the ectoneural and hyponeural systems suggests that the peptides may have a general transmitter-like role. However, the immunoreactivity is particularly associated with the innervation of the tube feet. Thus the sub-epithelial nerve plexus of the tube feet contains numerous immunoreactive fibers, whereas the soma of these neurons appear to lie within the adjacent nerve cord or ring.

Florey and Cahill (1980) demonstrated that the tube feet of sea urchins are under cholinergic motor control. Their evidence indicates that chemical transmission involves the diffusion of acetylcholine (ACh) from nerve terminals of the sub-epithelial plexus to the musculature, across the intervening connective tissue layer. Peptides produced by the immunoreactive neurons described here may be modulating the motor control of tube foot activity. Some circumstantial support for this idea comes from Unger's work (1960, 1962). Using simple chromatographic methods, this author isolated two physiologically active substances from the radial nerve cords of *Asterias glacialis*. In addition to effecting color changes, both factors induced movement in whole animals, as well as in isolated arms, and one of them strongly excitated the *Helix* heart. These effects were clearly distinguishable from those of ACh, serotonin, adrenalin, noradrenalin, and histamine, and we speculate that the extracts may have contained peptidic factors, including FMRFamide-like molecules.

The immunocytochemical data presented in this report shows us relatively little about the chemical nature of the immunoreactive peptides since any peptide with a C-terminal sequence similar to that of FMRFamide might cross-react with the antisera. A good example is the family of pancreatic polypeptide-related peptides (PP-RP) which terminates in Arg-Tyr-amide (see Thorndyke, 1986, for a more complete discussion of this problem).

Experiments designed to isolate and sequence the FMRFamide-like peptides in *Asterias* are currently un-

derway. Once one or more sequences are known and synthesized, the physiological roles of the native echinoderm molecules can be established.

Note added in proof

Three novel peptides, detected with antisera to FRMFamide, have now been purified from the radial nerves of the starfish *Asterias*, and sequenced (Elphick *et al.*, 1989).

Acknowledgments

We thank Professor M. J. Greenberg, for reading the manuscript and offering helpful criticism, and Professor G. J. Dockray and Dr. C. J. P. Grimmelikhuijzen, for gifts of antisera. Thanks also to Pat Enser and Zyg Podhorodecki for help with manuscript preparation. This work was partly supported by grants from the Science and Engineering Research Council, Nuffield Foundation, and Royal Society (to MCT).

Literature Cited

Boer, H. H., L. P. C. Schot, J. A. Veenstra, and D. Reichelt. 1980. Immunocytochemical identification of neural elements in the central nervous system of a snail, some insects, a fish and a mammal with an antiserum to the molluscan cardio-excitatory tetrapeptide FMRF-amide. *Cell Tissue Res.* **213:** 21–27.

Chaet, A. B., and R. A. McConnaughy. 1959. Physiologic activity of nerve extracts. *Biol. Bull.* **117:** 407.

Cobb, J. L. S. 1987. Neurobiology of Echinodermata. Pp 483–525 in *Nervous Systems in Invertebrates*, M. A. Ali, ed. Plenum Press, New York and London.

Cobb, J. L. S. 1988. Neurohumors and neurosecretion in echinoderms: a review. *Comp. Biochem. Physiol.* **91C:** 151–158.

Cowden, C., P. Sithigorngul, J. Guastella, and A. Stretton. 1987. FMRFamide-like peptides in *Ascaris suum*. *Am. Zool.* **27:** 127A.

Dockray, G. J., C. Vaillant, R. G. Williams, R. J. Gayton, and N. Osborne. 1981. Vertebrate brain-gut peptides related to FMRFamide and Met-enkephalin-Arg^{6}Phe^7. *Peptides* **2**(suppl.2): 25–30.

Elphick, M. R., D. A. Price, T. D. Lee, and M. C. Thorndyke. 1989. The SALMFamides: a new family of neuropeptides isolated from an echinoderm. *Soc. Neurosci. Abstr.* **15:** (in press).

Florey, E., and M. A. Cahill. 1980. Cholinergic control of sea urchin tube feet: evidence for chemical transmission without synapses. *J. Exp. Biol.* **88:** 281–292.

Greenberg, M. J., S. D. Painter, K. E. Doble, G. T. Nagle, D. A. Price, and H. K. Lehman. 1983. The molluscan neurosecretory peptide FMRFamide: comparative pharmacology and relationship to the enkephalins. *Fed. Proc.* **42:** 82–86.

Greenberg, M. J., K. Payza, R. J. Nachman, G. M. Holman, and D. A. Price. 1988. Relationships between the FMRFamide-related peptides and other peptide families. *Peptides* **9**(Suppl.1): 125–135.

Grimmelikhuijzen, C. J. P. 1983. FMRFamide immunoreactivity is generally occurring in the nervous systems of coelenterates. *Histochemistry* **78:** 361–381.

Grimmelikhuijzen, C. J. P. 1984. Peptides in the nervous system of coelenterates. Pp 39–58 in *Evolution and Tumour Pathology of Neuroendocrine System*, S. Falkmer, R. Håkanson, and F. Sundler, eds. Elsevier, Amsterdam.

Gustafsson, M. K. S., M. C. Wikgren, T. J. Karhi, and L. P. C. Schot. 1985. Immunocytochemical demonstration of neuropeptides and serotonin in the tapeworm *Diphyllobothrium dendriticum*. *Cell Tissue Res.* **241:** 171–182.

Hooper, S. L., and E. Marder. 1984. Modulation of a central pattern generator by two neuropeptides, proctolin and FMRFamide. *Brain Res.* **305:** 186–191.

Jacobs, A. C., and F. Van Herp. 1984. Immunocytochemical localization of a substance in the eyestalk of the prawn, *Palaemon serratus*, reactive with an anti-FMRFamide rabbit serum. *Cell Tissue Res.* **235:** 601–605.

Kanatani, H. 1979. Hormones in echinoderms. Pp. 273–307 in *Hormones and Evolution*, E. J. W. Barrington, ed. Academic Press, London.

Kuhlman, J. R., C. Li, and R. L. Calabrese. 1985. FMRFamide-like substances in the leech: 1. Immunocytochemical localization. *J. Neurosci.* **5:** 2301–2309.

Li, C., and M. Chalfie. 1986. FMRFamide-like immunoreactivity in *C. elegans*. *Soc. Neurosci. Abstr.* **12:** 246.

Porchet M., and N. Dhainaut-Courtois. 1988. Neuropeptides and monoamines in annelids. Pp 219–234 in *Neurohormones in Invertebrates*, M. C. Thorndyke and G. J. Goldsworthy, eds. Cambridge University Press, Cambridge, U.K.

Price, D. A., and M. J. Greenberg. 1977. Structure of a molluscan cardioexcitatory neuropeptide. *Science* **197:** 670–671.

Reuter, M., T. Karhi, and L. P. C. Schot. 1984. Immunocytochemical demonstration of peptidergic neurons in the central and peripheral nervous systems of the flatworm *Microstomum lineare* with anti-serum to FMRFamide. *Cell Tissue Res.* **238:** 431–436.

Shirai, H., P. Bulet, N. Kondo, M. Isobe, K. Imai, T. Goto, and I. Kubota. 1987. Gonad-stimulating substance of starfish. *Gen. Comp. Endocrinol.* **66:** 50.

Thorndyke, M. C. 1986. Immunocytochemistry and evolutionary studies with particular reference to peptides. Pp. 308–327 in *Immunocytochemistry: Modern Methods and Applications*, J. M. Polak and S. Van Noorden, eds. J. Wright and Sons, Bristol.

Unger, H. 1960. Neurohormone bei seesternen *Marthasterias glacialis*. *Symp. Biol. Hung.* **1:** 203–207.

Unger, H. 1962. Experimentelle und histologische Untersuchungen über Wirkfaktoren aus dem Nervensystem von *Asterias (Marthasterias) glacialis*. (Asteroidea, Echinodermata). *Zool. Jahrb. Abt. Allg. Zool. Physiol. Tiere* **3 69:** 481–536.

Varndell, I. M., and J. M. Polak. 1983. Glycolytic enzymes and a peptide closely related to FMRFamide are present in neurosecretory cells in nemertean cerebral ganglia. *Am. Zool.* **23:** 924.

Walker, R. J. 1986. Transmitters and modulators. Pp 279–485 in *The Mollusca, Vol. 9, Part 2*, A.O.D. Willows, ed. Academic Press, New York.

Watson, W. H., J. R. Groome, B. M. Chronwall, J. Bishop, and T. L. O'Donohue. 1984. Presence and distribution of immunoreactive and bioactive FMRFamide-like peptides in the nervous system of the horseshoe crab, *Limulus polyphemus*. *Peptides* **5:** 585–595.

Reference: *Biol. Bull.* 177: 146–153. (August, 1989)

Protein Kinase C Activators Enhance Transmission at the Squid Giant Synapse

LUIS R. OSSES[1,3,4], SUSAN R. BARRY[2,4], AND GEORGE J. AUGUSTINE[1,3,4,*]

[1]*Section of Neurobiology, Department of Biological Sciences, University of Southern California, Los Angeles, California 90089-0371,* [2]*Department of Physical Medicine and Rehabilitation, University of Michigan, Ann Arbor, Michigan 48109,* [3]*Catalina Marine Science Center, P.O. Box 398, Avalon, California 90704, and* [4]*Marine Biological Laboratory, Woods Hole, Massachusetts 02543*

Abstract. We have examined the possible role of protein kinase C in synaptic transmission by asking whether agents that activate protein kinase C affect transmission at the squid giant synapse. Several phorbol esters and a synthetic diacylglycerol that activates the kinase produced a substantial enhancement of transmission at the squid synapse, while structurally related compounds incapable of activating the kinase did not affect transmission. These agents enhanced both postsynaptic potentials and postsynaptic currents, revealing that they were not enhancing transmission exclusively by increasing postsynaptic input resistance. The increase in transmission produced by phorbol esters was either irreversible or reversed over a time course of one hour or longer. Kinase C activators also enhanced transmission at other synapses in the squid stellate ganglion. Our results are consistent with a general role for protein kinase C in synaptic transmission and indicate that the squid giant synapse is a favorable experimental system for further elucidation of the specific function of kinase C at synapses.

Introduction

Protein kinase C (PKC) is a family of calcium-sensitive, phospholipid-dependent protein kinases (Nishizuka, 1984; Coussens *et al.*, 1986; Knopf *et al.*, 1986; Jaken and Kiley, 1987; Ono *et al.*, 1987). Although PKC is found in high concentrations in many nervous systems, including the mammalian brain (Nairn *et al.*, 1985), its physiological functions are largely unknown. The high concentrations of PKC present in presynaptic terminals (Kikkawa *et al.*, 1982; Wu *et al.*, 1982; Girard *et al.*, 1985; Unver *et al.*, 1986) suggests that this enzyme plays a role in synaptic transmission.

Kinase C could play a role in mediating or regulating neurotransmitter release (Augustine *et al.*, 1987). Because activation of PKC enhances secretion from a variety of non-neural cells (Knight and Baker, 1983; Pozzan *et al.*, 1984; Pocotte *et al.*, 1985), PKC may be a necessary component of the molecular apparatus responsible for mediating exocytosis (Baker, 1984). Consistent with such a proposal, transmission at the guinea pig ileum (Tanaka *et al.*, 1984), the frog neuromuscular junction (Publicover, 1985; Eusebi *et al.*, 1986; Haimann *et al.*, 1987; Shapira *et al.*, 1987), and certain synapses in the hippocampus (Malenka *et al.*, 1986, 1987) is potentiated by activators of PKC.

We have attempted to address the role of PKC in synaptic transmission by asking whether agents that activate PKC alter transmission at the squid giant synapse. The large size of the presynaptic terminal of this synapse makes it unusually suitable for detailed analysis of the physiological mechanisms underlying synaptic transmission (Llinas, 1982; Augustine *et al.*, 1988). Protein kinase C is also found in squid nerve terminals (Unver *et al.*, 1986), making a potential involvement of PKC in transmission at the giant synapse more plausible. We have found that agents that activate PKC dramatically enhance transmission at the giant synapse and at other synapses in the squid stellate ganglion. These observations provide further evidence in support of a general role for PKC in synaptic transmission and pave the way for a detailed analysis of the intracellular mechanisms that permit PKC to enhance synaptic transmission. A preliminary report of some of this work has appeared (Osses *et al.*, 1986).

Received 21 September 1988; accepted 23 May 1989.

* To whom reprint requests should be sent (at USC).

Materials and Methods

Stellate ganglia of the squids *Loligo pealei* and *L. opalescens* were isolated and maintained by means of techniques described in detail previously (Augustine and Eckert, 1984; Augustine *et al.*, 1985a). Conventional electrophysiological methods were used to stimulate the most distal "giant" presynaptic axon with extracellular wire electrodes. The connective containing the presynaptic axon usually was dissected (Augustine and Eckert, 1984) to eliminate other synaptic inputs that innervate the postsynaptic axon (Martin and Miledi, 1986), and to permit examination of transmission at the giant synapse in isolation. We often recorded postsynaptic potentials (PSPs) from the most distal giant postsynaptic axon with an intracellular microelectrode, although in some experiments, postsynaptic currents (PSCs) were measured with a two-microelectrode voltage clamp. Usually these signals were digitized (12-bit resolution) and stored on a Digital LSI-11/23+ computer system and analyzed with previously published procedures (Augustine *et al.*, 1985b). In a few experiments, signals were displayed on a storage oscilloscope and analyzed manually. Unless otherwise indicated, all results reported here were obtained in a minimum of five independent experiments.

To examine the effects of various PKC activating drugs on transmission, stock solutions of these compounds in DMSO were prepared, and these were then mixed with squid saline (enclosed in a capped polyethylene test tube and vigorously agitated with a Vortex mixer) to yield a final DMSO concentration of 0.1% or less. An identical concentration of DMSO routinely added to control salines had no obvious effect upon synaptic transmission. In some cases, stock solutions of 12-deoxyphorbol, 13-butyrate 20-acetate were prepared in 20 m*M* HEPES (pH 7.2) instead of in DMSO. Such solutions produced physiological responses indistinguishable from those obtained with solutions prepared in DMSO.

Giant synapses bathed in normal squid saline (454 m*M* NaCl, 54 m*M* $MgCl_2$, 11 m*M* $CaCl_2$, 10 m*M* KCl, 3 m*M* $NaHCO_3$, 10 m*M* HEPES buffer, pH 7.2) release so much transmitter that the postsynaptic response is sufficient to produce an action potential in the postsynaptic cell. We therefore lowered the extracellular Ca concentration to 2.2–2.8 m*M* (by equimolar substitution of $MgCl_2$ for $CaCl_2$) to reduce the amplitude of postsynaptic responses below the level of action potential generation, and to facilitate quantitative assessment of the effects of drugs upon transmission. Also in low Ca, the postsynaptic membrane potential was more easily controlled when the voltage clamp was used to measure PSCs. Under these conditions, transmission was often stable for many hours (*e.g.*, Fig. 2 of Augustine and Charlton, 1986).

Experimental solutions were delivered to the giant synapse by three different methods. Usually, solutions were delivered via a cannula inserted into the artery that irrigates the giant synapse (Augustine and Charlton, 1986). This technique permits more rapid delivery of solutions to the synapse than is possible by simply adding the solutions to the bulk medium surrounding the stellate ganglion. When using this technique, solutions often were dyed with Phenol Red to visualize the movement of solutions through the circulatory system and into the ganglion. Control experiments indicated that the effects reported in this paper were not caused by the presence of Phenol Red. In other experiments, solutions were delivered by a focal pipette delivery method (Augustine *et al.*, 1985a), or by simple addition to the bulk medium. Very similar results were obtained when kinase C activators were delivered by any of these three methods.

Results

To assess the role of PKC in transmission at the squid synapse, we tested known kinase activating agents for their ability to alter synaptic transmission. The selected agents all mimic diacylglycerol, a product of membrane phospholipid breakdown that is thought to be an intracellular messenger responsible for PKC activation *in vivo* (Kishimoto *et al.*, 1980; Nishizuka, 1984). Two classes of agents were examined. First, membrane-permeant phorbol esters, which apparently act at the diacylglycerol binding site of PKC to activate the enzyme (Bell, 1986; Kikkawa *et al.*, 1983; Nishizuka, 1984), were applied to the synapse. Second, we examined the action of a synthetic diacylglycerol, 1,2-oleoylacetylglycerol (OAG), which has a limited ability to permeate membranes and activate PKC when applied extracellularly (Kaibuchi *et al.*, 1982, 1983; Nishizuka, 1984). The structures of the compounds tested are shown in Figure 1.

DPBA enhances transmission

The actions of the phorbol ester, 12-deoxyphorbol, 13-butyrate 20-acetate (DPBA) were studied in particular detail. When DPBA was applied to the squid synapse, the amplitude and rate of rise of the postsynaptic potential (PSP) increased dramatically (Fig. 2A). The increase often was so large that the membrane potential of the postsynaptic axon reached threshold, causing an action potential to be elicited even though the synapse was bathed in low Ca saline to attenuate transmission. Measuring PSPs under such conditions proved difficult, because their peak and decay were obscured by the action potential. In such cases, we measured the initial rate of rise of the PSPs as an indicator of changes in transmission (Miledi and Slater, 1966; Llinas *et al.*, 1981; Augustine and Charlton, 1986). To reduce complications asso-

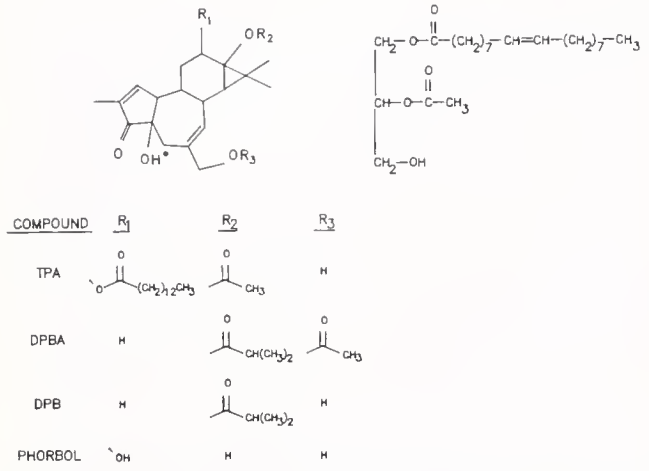

Figure 1. Structures of the compounds whose effects on synaptic transmission were examined in this study. These compounds include a variety of phorbol esters and related compounds (left) and the diacylglycerol, 1-oleoyl-2-acetylglycerol (right). The phorbol ester derivatives are tetradecanoyl phorbol-acetate (TPA), 12-deoxyphorbol, 13-butyrate 20-acetate (DPBA), 12-deoxyphorbol, 13-isobutyrate (DPB), and the phorbols, 4-α phorbol and 4-β phorbol. The structures of 4-α and 4-β phorbol are similar, except that the hydroxyl group indicated by the asterisk points down, out of the plane of the page, for 4-α phorbol but points up for 4-β phorbol. All other phorbol esters indicated have the hydroxyl group in a configuration identical to that of 4-β phorbol.

ciated with the production of postsynaptic action potentials, we often voltage clamped the postsynaptic terminal and directly measured the postsynaptic currents (PSCs) underlying the PSPs. Under such conditions, DPBA was still capable of increasing transmission (Fig. 2B), with changes in PSC amplitude being roughly equivalent to the increases in PSP amplitude produced by comparable concentrations of DPBA. Because DPBA increases PSCs as well as PSPs, DPBA does not enhance transmission solely by changing the input resistance of the postsynaptic cell.

Changes in transmission produced by DPBA usually were gradual in onset. An example of the time course of the changes in PSCs produced by DPBA, from the same experiment shown in Figure 2B, is illustrated in Figure 3. In this example, PSCs were maximally increased within 25 min of initiating DPBA perfusion. In other experiments, maximal responses were obtained at times ranging from 5 to 43 min. Part of the variability in the time course of the synaptic response to DPBA is related to the speed with which the DPBA-containing saline was delivered to the synapse via the circulatory system; *i.e.*, the speed of response could be correlated with the time required for the arrival of the tracer dye, phenol red, or high-Ca saline at the synapse. However, even after the DPBA solution had arrived at the preparation, there were delays until the maximum change in transmission occurred. Thus, the time course of the response of the synapse to DPBA treatment seems to be determined partially by the time required for DPBA to reach the giant synapse and partially by a subsequent step. Exposure of the synapse to DPBA by focal pipette delivery (Augustine *et al.*, 1985a), or addition of DPBA to the bulk solution in the recording chamber, produced similar increases in transmission, although changes in transmission were very slow when DPBA was simply added to the bath. In all subsequent experiments, drugs were delivered by arterial perfusion, unless otherwise indicated.

The reversibility of DPBA at the squid synapse was variable. In the experiment shown in Figure 3, PSC amplitude gradually recovered from DPBA treatment during a 1-h long rinse with drug-free saline. The decrease in PSC amplitude was due to a reversal of the effect of DPBA, rather than a progressive deterioration of transmission, because PSC magnitude roughly returned to its pre-treatment level and appeared to be stable for another 60 min of recording not shown on the graph. Such results were found in 7 out of 11 experiments in which stable recording conditions were maintained for more than 60 min following DPBA exposure. In the remaining experiments, the effects of DPBA did not reverse (*i.e.*, the incre-

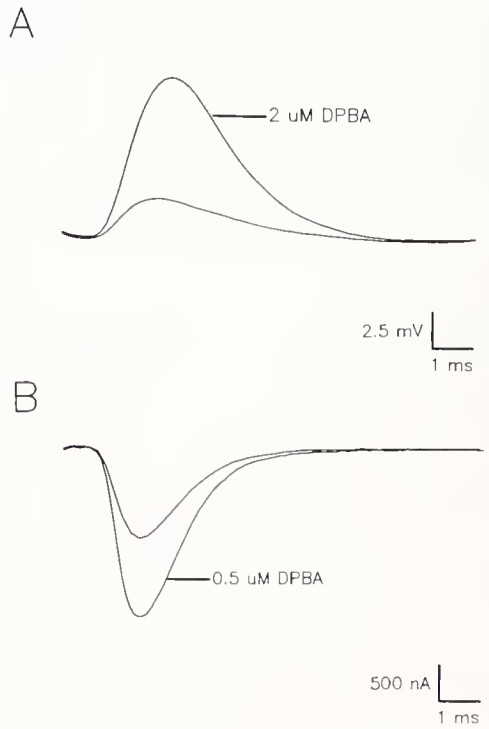

Figure 2. DPBA enhances transmission at the squid giant synapse. (A) Superimposed single traces of PSPs recorded in the absence of DPBA and after a 15-min exposure to 2 μM DPBA reveal that DPBA treatment produced a large increase in PSP magnitude. (B) Superimposed single traces of PSCs elicited in the absence of DPBA and after a 30-min exposure to 0.5 μM DPBA indicate that PSCs were increased to roughly the same extent as PSPs recorded from preparations exposed to the same concentration of DPBA.

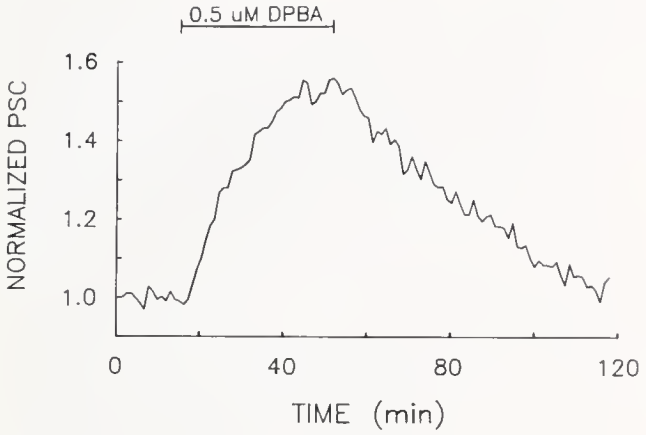

Figure 3. Time course and reversibility of DPBA effects on transmission. PSCs were elicited by stimulating the presynaptic axon every 60 s, and 0.5 μM DPBA was applied by arterial perfusion during the period indicated by the bar. DPBA produced an increase in PSC magnitude (measured by integrating each PSC record) that reached a maximum and then slowly recovered during prolonged exposure to DPBA-free saline. PSC integrals have been normalized by dividing by the mean value of the PSC integrals measured before DPBA treatment.

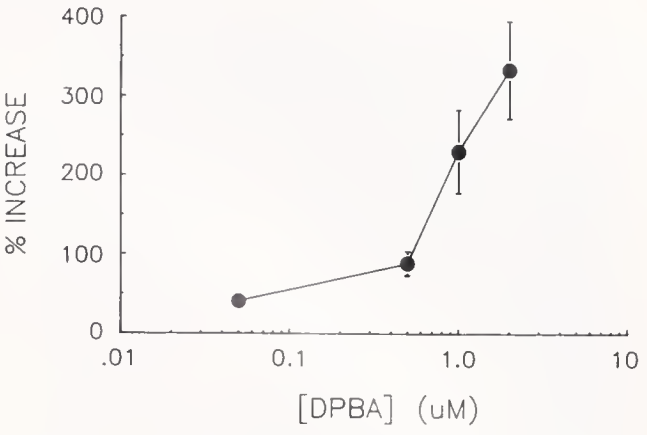

Figure 4. Concentration-dependence of DPBA effects on transmission at the squid giant synapse. Combined results of experiments examining both PSPs and PSCs reveal that DPBA concentrations as low as 50 nM increase transmission, with larger effects produced by higher concentrations of DPBA. Points are means of 4 to 12 replicates, combining measurements on both PSPs and PSCs, and error bars indicate ±S.E.M., when this value is larger than the symbol.

ment in postsynaptic response declined less than 30% after 60 min in DPBA-free saline). In these cases synaptic transmission was enhanced for hours after removal of DPBA from the saline in which the giant synapse was bathed. Such irreversibility is commonly observed with phorbol esters (*e.g.*, Publicover, 1985; Eusebi *et al.*, 1986; Shapira *et al.*, 1987; Storm, 1987) and is not unexpected, given that these molecules are hydrophobic and are also not readily metabolized within cells (Bell, 1986).

The experiments described above were performed with rather high concentrations of DPBA to optimize our ability to detect its actions on transmission. However, DPBA could enhance transmission at substantially lower concentrations. Concentrations of DPBA as low as 50 nM, the lowest concentration that we tested, increased PSP and PSC amplitude. Results of experiments with DPBA concentrations ranging from 50 nM to 2 μM are summarized in the concentration-response curve shown in Figure 4. This curve shows little sign of saturation at 2 μM, the highest DPBA concentration that we studied. Assuming that this curve can be described by a saturable function, the apparent K_D for such a function would be 1 μM or higher. Because of the hydrophobic nature of DPBA and the complex morphology of the squid stellate ganglion, we suspect that this value greatly over-estimates the actual affinity of the synapse for DPBA (see Discussion).

In summary, we find that DPBA produces concentration-dependent increases in transmission at the squid giant synapse. These observations are consistent with a role for PKC in transmission at this synapse.

Other PKC activators enhance transmission

If kinase C is involved in transmission at the squid synapse, then other PKC activators should produce changes in transmission similar to those produced by DPBA. The phorbol ester, tetradecanoyl phorbol-acetate (TPA), a compound used to activate PKC in a variety of experimental systems (Castagna *et al.*, 1982; Publicover, 1985; Caratsch *et al.*, 1986; Shapira *et al.*, 1987), was also capable of enhancing synaptic transmission (Fig. 5A). The effects of TPA upon transmission appeared similar in magnitude (Table I) and time course to those of DPBA, although the example shown in Figure 5A illustrates an

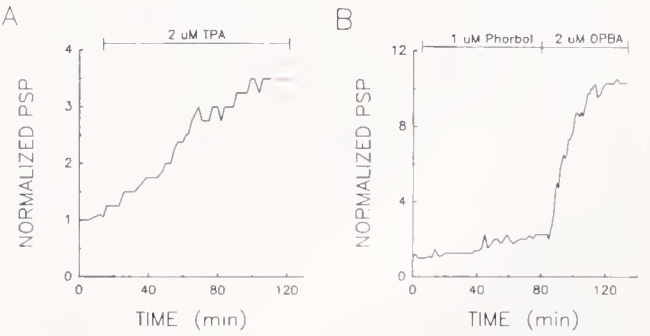

Figure 5. Other kinase C activators, such as TPA, enhance PSPs (A), while compounds that do not activate the kinase, such as 4-alpha phorbol, have little effect (B). The relatively small effect of 4-alpha phorbol is not due to an inability of the preparation to respond to phorbol esters, because subsequent treatment with 2 μM DPBA produced a robust increase in transmission. Peak amplitude of PSPs were measured in both experiments and were normalized by dividing by the mean amplitude of PSPs recorded prior to drug treatment.

Table I

Effects of various compounds on transmission at the squid giant synapse

Compound	Concentration	% Increase in synaptic response
DPBA	1 μM	229 ± 58 (n = 8)
	2 μM	321 ± 53 (n = 12)
DPB	1 μM	86 ± 9 (n = 5)
TPA	2 μM	298 ± 84 (n = 4)
4-β phorbol	1 μM	6 ± 12 (n = 10)
4-α phorbol	1 μM	1 ± 23 (n = 6)
OAG	50 μM	20 (n = 1)
	100 μM	45 ± 18 (n = 8)

Increases are expressed as mean change in PSPs or PSCs ± S.E.M.

unusually slow response to TPA. Still another phorbol ester known to activate PKC, 12-deoxyphorbol, 13-isobutyrate (Dunn and Blumberg, 1983), also increased PSP amplitude (Table I), but was less effective than DPBA. Another difference between the effect of DPB and the other kinase C activators was that, in three out of five experiments, the increase in transmission that it produced was transient. However, all three phorbol esters known to activate PKC enhanced transmission at the squid synapse.

Conversely, structurally related compounds that do not activate PKC were not able to enhance transmission. We examined two stereoisomers of the parent compound, phorbol, both of which have very weak abilities to activate PKC (Castagna *et al.*, 1982). Treatment of synapses with 1 μM concentrations of 4-α phorbol sometimes produced modest increases in transmission (Fig. 5B), but small decreases were also seen. On average, neither 4-α phorbol nor 4-β phorbol produced consistent changes in the postsynaptic response (Table I). Thus, only compounds known to activate PKC enhance transmission at the squid synapse.

To reinforce this conclusion, we tested the action of OAG, the synthetic diacylglycerol analog. OAG seemed to increase the size of evoked PSPs when applied to the synapse at concentrations of 50 μM or greater (Table I). The relatively poor efficacy of OAG, compared to the active phorbol esters, could reflect its relatively weak ability to approach and permeate synaptic membranes or the fact that phorbol esters are more potent than diacylglycerol in activating PKC (Bell, 1986). Nevertheless, the observation that OAG, too, enhances transmission strengthens the argument that activation of PKC increases transmission at the squid giant synapse. Taken together, our results obtained with six compounds suggest that activation of PKC underlies the potentiating effect of DPBA and other phorbol esters on transmission at this synapse.

DPBA enhances transmission at non-giant synapses

The postsynaptic axon of the squid synapse is innervated by at least three other presynaptic terminals, in addition to the so-called giant terminal that has been the subject of this and many other physiological studies (Young, 1939; Martin and Miledi, 1986). In some experiments, these other presynaptic inputs could be unambiguously identified and selectively stimulated. We could then ask whether the effects of PKC activators described here are restricted to the giant synapse, or are a more general feature of synapses in the squid nervous system.

An example of an experiment in which the activity of both the giant and another synapse were examined is shown in Figure 6. In this experiment, an extracellular stimulus applied to the connective innervating the stellate ganglion evoked two temporally dispersed PSCs. Examination of the electrical activity of the "giant" presynaptic terminal with an intracellular microelectrode (lower trace in Fig. 6) showed that the earlier of the two PSCs had the appropriate synaptic delay and other features characteristic of the PSC produced by the giant synapse. Addition of 0.5 μM DPBA caused this PSC (single arrow) to approximately double in amplitude, as expected (*e.g.*, Fig. 2B). In addition, DPBA caused an even more substantial increase in the amplitude of the later, non-giant PSC (double arrows). In four other experiments, we were able to evaluate the effects of various concentrations of DPBA upon transmission at these other synapses, usually in preparations in which the giant

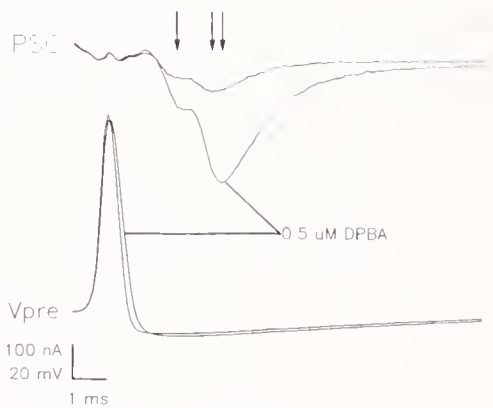

Figure 6. DPBA also enhances transmission at other squid synapses. In this experiment, extracellular stimulation of the viscero-stellate connective activated both the giant presynaptic cell (V_{pre}) and another synaptic input on to the postsynaptic axon. Both the PSC produced by the giant input (single arrow) and the non-giant PSC (double arrows) were enhanced by 0.5 μM DPBA. The action potential of the giant presynaptic terminal also was broadened by DPBA treatment.

presynaptic input had been damaged by microelectrode impalement or dissection trauma. In every case, the postsynaptic response produced by these other inputs was enhanced by DPBA. Therefore, we conclude that PKC activation regulates transmission at both the giant synapse and other synapses on the postsynaptic axon.

Discussion

Our results demonstrate that a number of activators of PKC, including three phorbol esters and a diacylglycerol compound, enhance transmission at the squid giant synapse. The effects of these compounds were concentration-dependent and long-lasting. Because structurally related compounds incapable of activating PKC had little or no physiological effect, we propose that activation of PKC is responsible for the ability of the active compounds to increase transmission. Kinase C activators enhance transmission, not only at the squid giant synapse, but also at the frog neuromuscular junction (Publicover, 1985; Eusebi *et al.*, 1986; Haimann *et al.*, 1987; Shapira *et al.*, 1987), guinea pig ileum (Tanaka *et al.*, 1984), hippocampal slices (Malenka *et al.*, 1986, 1987) and cultured hippocampal neurons (Finch and Jackson, 1987), synaptosomes from mammalian brain (Nichols *et al.*, 1987), and other neurotransmitter-secreting systems (Wakade *et al.*, 1985; Zurgil and Zisapel, 1985). These physiological consequences of PKC activation, when combined with the presence of PKC in presynaptic terminals, point to a rather general role for PKC in transmission at chemical synapses.

The concentrations of PKC activators required to alter transmission at the squid synapse are substantially higher than the concentrations used to activate purified kinase (Nishizuka, 1984) and are somewhat higher than the concentrations ordinarily applied to isolated cells (Pozzan *et al.*, 1984; Pocotte *et al.*, 1985; Rane and Dunlap, 1986). This might cast some doubt upon our conclusion that the actions of these compounds are due to PKC activation. However, the concentrations effective at the squid synapse are comparable to those that potentiate synaptic transmission in other multicellular preparations, including hippocampal slices (Malenka *et al.*, 1986, 1987; Storm, 1987). Higher concentrations are probably required in more structurally complex tissues because these compounds non-specifically partition into hydrophobic domains (*e.g.*, connective tissue) and are partially unavailable for action upon the cell under investigation. Direct microinjection of PKC into the giant pre- and postsynaptic terminals, as done with a Ca/calmodulin-dependent protein kinase (Llinas *et al.*, 1985), would provide the most definite test of the assertion that PKC activation enhances synaptic transmission.

Site and mechanism of action of kinase C activators

Our results do not allow us to state whether the action of PKC is pre- or postsynaptic. We have eliminated one possible source, namely an increase in postsynaptic input resistance, as the sole cause of the ability of DPBA to increase transmission. However, other postsynaptic actions, such as an alteration in postsynaptic sensitivity to the transmitter (Eusebi *et al.*, 1985; Caratsch *et al.*, 1986), could contribute to the effects reported here. The unknown identity of the transmitter at this synapse, combined with the small amplitude of its single-quantal events (Miledi, 1967; Mann and Joyner, 1978; Augustine and Eckert, 1984), makes it difficult to assess postsynaptic contributions to the response. In other systems, PKC activators have been shown to increase the amount of neurotransmitter released by presynaptic action potentials (Tanaka *et al.*, 1984; Wakade *et al.*, 1985; Zurgil and Zisapel, 1985). Recent experiments suggest that DPBA also acts presynaptically at the squid giant synapse (Augustine *et al.*, 1986).

PKC activation may affect transmitter release by a variety of mechanisms. PKC could increase the calcium-sensitivity of secretion, lowering the concentration of calcium necessary to stimulate transmitter release (Knight and Baker, 1983; Knight and Scrutton, 1984; Pozzan *et al.*, 1984; Pocotte *et al.*, 1985). Because transmitter release appears very sensitive to intracellular pH (Drapeau and Nachshen, 1988), PKC activation might be altering presynaptic H^+ regulation (Moolenar *et al.*, 1984; Swann and Whitaker, 1985). PKC also may enhance mobilization of transmitter (Hochner *et al.*, 1986). Finally, because PKC activators alter transmembrane ion currents (reviewed in Kaczmarek, 1986; Miller, 1986), a change in presynaptic ion currents could underlie the effect of these agents upon release. Consistent with this possibility, preliminary results suggest that PKC activation augments transmission at the squid synapse by decreasing presynaptic potassium current and consequently broadening the presynaptic action potential (Augustine *et al.*, 1986). Such an increase in presynaptic action potential duration is evident in Figure 6. These and other possible mechanisms of PKC action at synapses merit further attention.

A potpourri of protein kinase actions

Although the squid giant synapse has long been regarded as the preparation of choice for biophysical analysis of chemical synaptic transmission, it is sometimes neglected by those interested in molecular aspects of synaptic function. Our observation that PKC activators enhance transmission at this synapse, when combined with the pronounced effects observed when a Ca/calmodulin-dependent protein kinase is injected into the pre-

synaptic terminal of the squid synapse (Llinas *et al.*, 1985), makes it clear that transmission at this synapse is regulated by several of the molecular mechanisms thought to be important in determining the efficacy of other synapses. One interesting exception is the cyclic AMP-dependent protein kinase: while agents that activate this kinase alter the function of many synapses (Standaert and Dretchen, 1979; Kandel and Schwartz, 1982), they appear to have little effect on transmission at the squid synapse (G. Augustine, M. Charlton, A. Gurney, and S. Smith, unpub.). Thus, the squid synapse appears to be an appropriate model system for further explorations of the functional role of kinase C and at least some other types of regulatory molecules.

Acknowledgments

We thank D. Conly, D. Gray, and C. Nuño for technical assistance, G. Pittenger and S. Miller for providing squid, M. Charlton and R. Horn for participating in a few of these experiments, and C. Augustine, L. Byerly, M. Charlton, S. Hess, and G. Miljanich for their comments on this paper. Supported by Grass Foundation, Fogarty Foundation, and Muscular Dystrophy Association Fellowships to L.R.O., NSF Grant BNS-8506778 to S.R.B., MBL Summer Fellowships to S.R.B. and G.J.A., and USC Faculty Research and Innovation Funds and NIH Grant NS-21624 to G.J.A.

Literature Cited

Augustine, G. J., and M. P. Charlton. 1986. Calcium dependence of presynaptic calcium current and post-synaptic response at the squid giant synapse. *J. Physiol.* **381:** 619–640.

Augustine, G. J., M. P. Charlton, and S. J. Smith. 1985a. Calcium entry into voltage-clamped presynaptic terminals of squid. *J. Physiol.* **367:** 143–162.

Augustine, G. J., M. P. Charlton, and S. J. Smith. 1985b. Calcium entry and transmitter release at voltage-clamped nerve terminals of squid. *J. Physiol.* **367:** 163–181.

Augustine, G. J., M. P. Charlton, and S. J. Smith. 1987. Calcium action in synaptic transmitter release. *Ann. Rev. Neurosci.* **10:** 633–693.

Augustine, G. J., M. P. Charlton, and S. J. Smith. 1988. Toward a molecular understanding of synaptic transmitter release: physiological clues from the squid giant synapse. Pp. 157–168 in *Calcium and Ion Channel Modulation*, A. Grinnell, D. Armstrong and M. Jackson, eds., Plenum, New York.

Augustine, G. J., and R. Eckert. 1984. Divalent cations differentially support transmitter release at the squid giant synapse. *J. Physiol.* **346:** 257–271.

Augustine, G. J., L. R. Osses, S. R. Barry, and M. P. Charlton. 1986. Presynaptic mechanism of kinase C activators at the squid giant synapse. *Soc. Neurosci. Abstr.* **12:** 821.

Baker, P. F. 1984. Multiple controls for secretion. *Nature* **310:** 629–630.

Bell, R. B. 1986. Protein kinase C activation by diacylglycerol second messengers. *Cell* **45:** 631–632.

Caratsch, C. G., F. Grassi, M. Molinaro, and F. Eusebi. 1986. Postsynaptic effects of the phorbol ester TPA on frog endplates. *Pflugers Arch.* **407:** 409–413.

Castagna, M., Y. Takai, K. Kaibuchi, K. Sano, U. Kikkawa, and Y. Nishizuka. 1982. Direct activation of calcium-activated, phospholipid-dependent protein kinase by tumor-promoting phorbol esters. *J. Biol. Chem.* **257:** 7847–7851.

Coussens, L., P. J. Parker, L. Rhee, T. L. Yang-Feng, E. Chen, M. D. Waterfield, U. Francke, and A. Ullrich. 1986. Multiple, distinct forms of bovine and human protein kinase C suggest diversity in cellular signaling pathways. *Science* **233:** 859–866.

Drapeau, P., and D. A. Nachshen. 1988. Effects of lowering extracellular and cytosolic pH on calcium fluxes, cytosolic calcium levels and transmitter release in presynaptic terminals isolated from rat brain. *J. Gen. Physiol.* **91:** 305–315.

Dunn, J. A., and P. M. Blumberg. 1983. Specific binding of [20-^{3}H] 12-deoxyphorbol 13-isobutyrate to phorbol ester receptor subclasses in mouse skin particulate preparations. *Cancer Res.* **43:** 4632–4637.

Eusebi, F., M. Molinaro, and C. G. Caratsch. 1986. Effects of phorbol ester on spontaneous transmitter release at frog neuromuscular junction. *Pflugers Arch.* **406:** 181–183.

Eusebi, F., M. Molinaro, and B. M. Zani. 1985. Agents that activate protein kinase C reduce acetylcholine sensitivity in cultured myotubes. *J. Cell Biol.* **100:** 1339–1342.

Finch, D. M., and M. B. Jackson. 1987. Modulation of spontaneous synaptic currents in cultured hippocampal neurons by phorbol esters and BAY K 8644. *Soc. Neurosci. Abstr.* **13:** 310.

Girard, P. R., G. J. Mazzei, J. G. Wood, and J. F. Kuo. 1985. Polyclonal antibodies to phospholipid/Ca^{2+}-dependent protein kinase and immunocytochemical localization of the enzyme in rat brain. *Proc. Natl. Acad. Sci. USA* **82:** 3030–3034.

Haimann, C., J. Meldolesi, and B. Ceccarelli. 1987. The phorbol ester, 12-0-tetradecanoyl-phorbol-13-acetate, enhances the evoked quanta release of acetylcholine at the frog neuromuscular junction. *Pflugers Arch.* **408:** 27–31.

Hochner, B., D. Braha, M. Klein, and E. R. Kandel. 1986. Distinct processes in presynaptic facilitation contribute to sensitization and dishabituation in *Aplysia*: possible involvement of C kinase in dishabituation. *Soc. Neurosci. Abstr.* **12:** 1340.

Jaken, S., and S. C. Kiley. 1987. Purification and characterization of three types of protein kinase C from rabbit brain cytosol. *Proc. Natl. Acad. Sci. U.S.A.* **84:** 4418–4422.

Kaczmarek, L. K. 1986. Phorbol esters, protein phosphorylation and the regulation of neuronal ion channels. *J. Exp. Biol.* **124:** 375–392.

Kaibuchi, K., K. Sano, M. Hoshijima, Y. Takai, and Y. Nishizuka. 1982. Phosphatidylinositol turnover in platelet activation; calcium mobilization and protein phosphorylation. *Cell Calcium* **3:** 323–335.

Kaibuchi, K., Y. Takai, M. Sawamura, M. Hoshijima, T. Fujikura, and Y. Nishizuka. 1983. Synergistic functions of protein phosphorylation and calcium mobilization in platelet activation. *J. Biol. Chem.* **258:** 6701–6704.

Kandel, E. R., and J. H. Schwartz. 1982. Molecular biology of learning: modulation of transmitter release. *Science* **218:** 433–443.

Kikkawa, U., Y. Takai, R. Minakuchi, S. Inohara, and Y. Nishizuka. 1982. Calcium-activated, phospholipid-dependent protein kinase from rat brain: subcellular distribution, purification, and properties. *J. Biol. Chem.* **257:** 13341–13348.

Kikkawa, U., Y. Takai, Y. Tanaka, R. Miyake, and Y. Nishizuka. 1983. Protein kinase C as a possible receptor protein of tumor-promoting phorbol esters. *J. Biol. Chem.* **258:** 11442–11445.

Kishimoto, A., Y. Takai, T. Mori, U. Kikkawa, and Y. Nishizuka. 1980. Activation of calcium and phospholipid-dependent protein

kinase by diacylglycerol, its possible relation to phosphatidylinositol turnover. *J. Biol. Chem.* **255:** 2273–2276.

Knight, D. E., and P. F. Baker. 1983. The phorbol ester TPA increases the affinity of exocytosis for calcium in "leaky" adrenal medullary cells. *FEBS Lett.* **160:** 98–100.

Knight, D. E., and M. C. Scrutton. 1984. Cyclic nucleotides control a system which regulates Ca^{2+} sensitivity of platelet secretion. *Nature* **309:** 66–68.

Knopf, J. L., M. Lee, L. A. Sultzman, R. W. Kriz, C. R. Loomis, R. W. Hewick, and R. M. Bell. 1986. Cloning and expression of multiple protein kinase C cDNAs. *Cell* **46:** 491–502.

Llinas, R. R. 1982. Calcium in synaptic transmission. *Sci. Am.* **247:** 56–65.

Llinas, R., I. Z. Steinberg, and K. Walton. 1981. Relationship between presynaptic calcium current and postsynaptic potential in squid giant synapse. *Biophys. J.* **33:** 323–352.

Llinas, R., T. L. McGuinness, C. S. Leonard, M. Sugimori, and P. Greengard. 1985. Intraterminal injection of synapsin I or calcium calmodulin-dependent protein kinase II alters neurotransmitter release at the squid giant synapse. *Proc. Natl. Acad. Sci. USA* **82:** 3035–3039.

Malenka, R. C., G. S. Ayoub, and R. A. Nicoll. 1987. Phorbol esters enhance transmitter release in rat hippocampal slices. *Brain Res.* **403:** 198–203.

Malenka, R. C., D. V. Madison, and R. A. Nicoll. 1986. Potentiation of synaptic transmission in the hippocampus by phorbol esters. *Nature* **321:** 175–177.

Mann, D. W., and R. W. Joyner. 1978. Miniature synaptic potentials at the squid giant synapse. *J. Neurobiol.* **9:** 329–335.

Martin, R., and R. Miledi. 1986. The form and dimensions of the giant synapse of squids. *Phil. Trans. R. Soc. Lond. B* **312:** 355–377.

Miledi, R. 1967. Spontaneous synaptic potentials and quantal release of transmitter in the stellate ganglion of the squid. *J. Physiol.* **192:** 379–406.

Miledi, R., and C. R. Slater. 1966. The action of calcium on neuronal synapses in the squid. *J. Physiol.* **184:** 473–498.

Miller, R. J. 1986. Protein kinase C: a key regulator of neuronal excitability? *Trends Neurosci.* **9:** 538–541.

Moolenaar, W. H., L. G. J. Tertoolen, and S. W. de Laat. 1984. Phorbol ester and diacylglycerol mimic growth factors in raising cytoplasmic pH. *Nature* **312:** 371–374.

Nairn, A. C., H. C. Hemmings Jr., and P. Greengard. 1985. Protein kinases in the brain. *Ann. Rev. Biochem.* **54:** 931–976.

Nichols, R. A., J. W. Haycock, J. K.-T. Wang, and P. Greengard. 1987. Phorbol ester enhancement of neurotransmitter release from rat brain synaptosomes. *J. Neurochem.* **48:** 615–621.

Nishizuka, Y. 1984. Turnover of inositol phospholipids and signal transduction. *Science* **225:** 1365–1370.

Ono, Y., T. Fujii, K. Ogita, U. Kikkawa, K. Igarashi, and Y. Nishizuka. 1987. Identification of three additional members of rat protein kinase C family: delta, epsilon and kappa-subspecies, *FEBS Lett.* **226:** 125–128.

Osses, L., S. Barry, G. Augustine, and M. Charlton. 1986. Protein kinase C activation enhances transmission at the squid giant synapse. *Biophys. J.* **49:** 179a.

Pocotte, S. L., R. A. Frye, R. A. Senter, D. R. TerBush, S. A. Lee, and R. W. Holtz. 1985. Effects of phorbol ester on catecholamine secretion and protein phosphorylation in adrenal medullary cell cultures. *Proc. Natl. Acad. Sci. USA* **82:** 930–934.

Pozzan, T., G. Gatti, N. Dozio, L. M. Vicentini, and J. Meldolesi. 1984. Ca^{2+}-dependent and -independent release of neurotransmitters from PC12 cells: a role for protein kinase C activation? *J. Cell Biol.* **99:** 628–638.

Publicover, S. J. 1985. Stimulation of spontaneous transmitter release by the phorbol ester, 12-0-tetradecanoylphorbol-13-acetate, an activator of protein kinase C. *Brain Res.* 333: 185–187.

Rane, S. G., and K. Dunlap. 1986. Kinase C activator 1,2-oleoylacetylglycerol attenuates voltage-dependent calcium current in sensory neurons. *Proc. Natl. Acad. Sci. USA* **83:** 184–188.

Shapira, R., S. D. Silberberg, S. Ginsburg, and R. Rahamimoff. 1987. Activation of protein kinase C augments evoked transmitter release. *Nature* **325:** 58–60.

Standaert, F. G., and K. L. Dretchen. 1979. Cyclic nucleotides and neuromuscular transmission. *Fed. Proc.* **38:** 2183–2192.

Storm, J. F. 1987. Phorbol esters broaden the action potential in CA_1 hippocampal pyramidal cells. *Neurosci. Lett.* **75:** 71–74.

Swann, K., and M. Whitaker. 1985. Stimulation of the Na/H exchanger of sea urchin eggs by phorbol ester. *Nature* **314:** 274–277.

Tanaka, C., K. Taniyama, and M. Kusunoki. 1984. A phorbol ester and A23187 act synergistically to release acetylcholine from the guinea pig ileum. *FEBS Lett.* **175:** 165–169.

Unver, E., G. J. Augustine, S. R. Barry, and G. P. Miljanich. 1986. Kinase C (Ca^{2+}-phospholipid-dependent protein kinase) in squid optic lobe synaptosomes. *Soc. Neurosci. Abstr.* **12:** 821.

Wakade, A. R., R. K. Malhotra, and T. D. Wakade. 1985. Phorbol ester, an activator of protein kinase C, enhances calcium-dependent release of sympathetic neurotransmitter. *Arch. Pharmacol.* **331:** 122–124.

Wu, W. C.-S., S. I. Walaas, A. C. Nairn, and P. Greengard. 1982. Calcium/phospholipid regulates phosphorylation of a M_r "87k" substrate protein in brain synaptosomes. *Proc. Natl. Acad. Sci. USA* **79:** 5249–5253.

Young, J. Z. 1939. Fused neurons and synaptic contacts in the giant nerve fibres of cephalopods. *Phil. Trans. R. Soc. B* **229:** 465–503.

Zurgil, N., and N. Zisapel. 1985. Phorbol ester and calcium act synergistically to enhance neurotransmitter release by brain neurons in culture. *FEBS Lett.* **185:** 257–261.

Reference: *Biol. Bull.* **177**: 154–166. (August, 1989)

Effects of Hypoxia and Anoxia on Survival, Energy Metabolism, and Feeding of Oyster Larvae (*Crassostrea virginica*, Gmelin)

J. WIDDOWS[1], R. I. E. NEWELL[2], AND R. MANN[3]

[1]*Plymouth Marine Laboratory, Prospect Place, The Hoe, Plymouth PL1 3DH, England;* [2]*Horn Point Environmental Laboratories, University of Maryland, Box 775, Cambridge, Maryland 21613; and* [3]*Virginia Institute of Marine Science, Gloucester Point, Virginia, 23062*

Abstract. The tolerance of *Crassostrea virginica* larvae to anoxia increases with developmental stage and body size. Median mortality times range from 11 h for prodissoconch larvae of 82 μm (shell length) to 51 h for pediveliger larvae of 312 μm, and 150 h for juvenile oysters. Simultaneous calorimetry and respirometry showed that in response to declining oxygen tension (P_{O_2}), the rates of heat dissipation and oxygen uptake by oyster larvae are maintained independent of P_{O_2} down to low P_c values (2 kPa for prodissoconch larvae and 8 kPa for pediveliger and juveniles). Therefore, total energy metabolism is sustained mainly by aerobic metabolism down to 2 and 4 kPa for early larval stages and juveniles, respectively. Prodissoconch larvae maintain relatively high rates of heat dissipation under anoxic conditions (34% of normoxic rate), whereas pediveliger and juveniles lower their anoxic rates of heat dissipation to 3% of the normoxic rate. The ability to reduce rates of heat dissipation and thus conserve energy expenditure under anoxia appears to be related to the increase in anoxia tolerance with larval development. The larval differences in the relationship between P_{O_2} and the rate of heat dissipation are also reflected in feeding rate (ingestion rate of microspheres). Prodissoconch larvae maintain feeding activity under anoxic conditions (29% of normoxic ingestion rate), in contrast to pediveliger larvae, which lower ingestion rates to 5% of the normoxic rate.

Introduction

Many estuaries and bays regularly exhibit seasonal salinity and temperature stratification, which can lead to hypoxia and anoxia in the bottom waters. This situation is particularly pronounced in the Chesapeake Bay, where the decline in water quality over the last 25 years, caused in part by eutrophication, has contributed to a significant increase in the extent of hypoxic or anoxic waters (Taft *et al.*, 1980; Kemp and Boynton, 1984; Officer *et al.*, 1984; Seliger *et al.*, 1985; Malone *et al.*, 1986; Mackiernan, 1987). The seasonal occurrence of stratification coincides with, or partially overlaps, the period of spawning and settlement of the American oyster *Crassostrea virginica* (Gmelin). Although the spatial occurrence of hypoxia or anoxia is usually restricted to deeper waters, the seiching of deeper waters due to wind stress periodically irrigates the shallower areas—where oyster reefs abound—with hypoxic or anoxic water. Bivalve larvae appear to employ depth regulation to effect their retention in shallow, stratified estuaries (Wood and Hargis, 1971; Mann, 1986). Therefore, both larval and early post larval stages of the oyster may be subjected to hypoxic or anoxic stress in the Chesapeake Bay during summer months.

Adult oysters and other bivalves can survive prolonged anoxia, primarily by using glycogen in anaerobic metabolic pathways (de Zwaan, 1983). Larval stages may lack this capacity because (a) their nutrient reserves are relatively small (Mann and Gallager, 1985) and (b) polysaccharides form a relatively small proportion of their total energy reserves (Holland and Spencer, 1973). Energy reserves of larvae are primarily lipid and protein, and lipid cannot be used as a substrate for anaerobic catabolism. Consequently, early developmental stages of the oyster (*Crassostrea virginica*) may be particularly vulnerable to hypoxic conditions.

Received 23 January 1989; accepted 30 May 1989.

Although the rate of oxygen consumption by adult oysters (*Crassostrea virginica*) in response to hypoxia has been studied (Shumway and Koehn, 1982), little is known about the metabolic and feeding responses of oyster larvae and juveniles ('O' group or spat) to hypoxia and anoxia, nor about their overall tolerance of anoxia.

The main objectives of this study were (a) to examine the anoxia tolerance of the larval stages and spat of *Crassostrea virginica*, and (b) to determine their rates of metabolic energy expenditure and feeding under hypoxic and anoxic conditions. Simultaneous open-flow calorimetry and respirometry were used to measure metabolic activity of oyster larvae and spat, thus providing a partitioning of the rate of heat dissipation into aerobic and anaerobic components under normoxia, hypoxia, and anoxia (Widdows, 1987).

Material and Methods

Collection and maintenance of specimens

Oyster (*Crassostrea virginica*) larvae were reared and supplied by the Virginia Institute of Marine Science hatchery at Gloucester Point, Virginia; juvenile oysters (16 mm shell height) were collected from Whaley's oyster bar in the estuary of the Great Wicomico River, Virginia. All experiments were performed at 22°C and 12‰, the ambient temperature and salinity at Gloucester Point in May 1987. Larvae and juvenile oysters were maintained in static systems, receiving water changes every two days, and daily additions of algal food (*Isochrysis galbana* Parke) at a concentration of about 50×10^6 cells l^{-1}.

When the water was changed, larvae were separated, with a series of 'Nitex' nylon sieves, into various size classes, ranging from prodissoconch 'D stage' larvae to veliconcha and pediveligers. They were then resuspended in 12‰ 0.45 μm membrane filtered seawater (FSW). In addition to removing fecal material, this sieving removed the smallest size class from the larval culture, which generally included individuals that were either abnormal or dead. Only those larvae that were actively swimming in the water column were collected for an experiment.

After each experiment the larvae were sampled, and the total number of individuals, mean shell length, and dry mass (after washing in distilled water and drying at 80°C) were estimated. Shell length (the maximum dimension parallel to the hinge line) was measured with a Kontron IPS image analysis system connected to a Reichert-Jung Polyvar microscope with a calibrated graticule eyepiece. In addition, relationships between shell length, dry mass, and ash-free dry mass (weight loss at 500°C) were established for larvae (60 μm to 330 μm shell length). They are described by the following equations:

$$DM = (2.48 \times 10^{-5})SL^{2.073} \quad (r = 0.96)$$

$$AFDM = (9 \times 10^{-6})SL^{2.066} \quad (r = 0.94)$$

where DM is the total dry mass (μg), AFDM is the ash free dry mass (μg), SL is shell length (μm). Each equation is based on larvae from 10 different size classes for which the mean SL of 10 individuals was measured and the DM and AFDM of a pool of 25 larvae was determined.

Juvenile oysters (spat) of 16 mm shell height (*i.e.*, maximum dimension from the hinge to the ventral margin) were thoroughly cleaned of epibionts; the shells were first scrubbed and the surfaces were then cleaned with 1% V: V sodium hypochlorite (Newell, 1985). Before being exposed to hypoxia and anoxia, the spat were maintained overnight in tanks with flowing seawater (12‰), and ambient seston concentrations to establish that they were actively feeding and producing biodeposits. After measuring physiological responses, we removed body tissues from the shell and dried them at 80°C before weighing.

Anoxia survival experiments

Three size classes of larvae, representing prodissoconch 'D' stage, veliconch, and pediveligers (82 μm ± 2, 167 μm ± 3 and 312 μm ± 2; mean ± S.E. of shell length, respectively) and juvenile oysters (16 mm shell height), were selected for study in the anoxia tolerance experiments. Larvae were introduced into 5 ml glass syringes (100–200 larvae per syringe) and any gas bubbles were removed. A syringe filter holder containing a 20 μm 'Nitrex' mesh was attached to the syringe to retain the larvae as the volume of water in the syringe was reduced to 0.4 ml. The syringe and filter holder were then attached to a stainless steel needle that passed through a small silicone stopper at the base of a glass reservoir (1 l). The reservoir, containing 12‰ FSW, was deoxygenated by a continuous fine stream of high purity nitrogen gas (delivered via stainless steel tubing) for at least 2 h prior to sampling. The syringe was slowly filled with 5.5 ml of anoxic FSW, detached from the reservoir together with the 'Nitex' filter, and the water was then slowly expelled through the filter, reducing the volume to 0.4 ml while retaining the larvae. This procedure was repeated five times to ensure that the final 5.5 ml of water in the syringe was anoxic at the start of the anoxia tolerance experiments.

The partial pressure of oxygen in the reservoir of FSW and in the final volume contained within the glass syringes was measured with a Radiometer oxygen electrode (E5046) held in a thermostatted cell and coupled to a Radiometer oxygen meter and chart recorder. The electrode was calibrated daily with air-saturated water and oxygen-zero solution (Radiometer 54150).

The experimental procedures described above consistently maintained anoxic conditions (*i.e.*, oxygen con-

centrations in the syringes were typically zero and were always <0.2% of full air saturation and not significantly above the detection limit).

Syringes containing the larvae were sealed by inserting the stainless steel needles into a silicone stopper and incubated at 22°C in a water bath for up to three days. At intervals during the anoxia exposure period, syringes were removed and the anoxia confirmed with the oxygen sensor. The water containing the larvae was then gently reoxygenated by a stream of air bubbles for 30 min, and the larvae observed on a Sedgewick-Rafter slide under a microscope. Mortality of the larvae, defined as the absence of any ciliary activity after 30 min of normoxia, was expressed as percentage of the total number of animals. There was no evidence of further recovery after this 30-min recovery period.

Actively feeding juvenile oysters were selected and placed in 12‰ FSW in 200 ml glass containers (10 individuals per container). The containers were sealed with stoppers through which passed glass tubes for the entry and exit of high purity nitrogen gas. The contents of each container were deoxygenated for one hour and then the tubes were sealed. All containers were placed in a large glass desiccator continuously purged by a stream of nitrogen gas to prevent any diffusion of oxygen through the stoppers. Samples of water from a sealed control container were analyzed, confirming anoxic conditions. After 3 days of anoxia and daily thereafter (*i.e.*, 3–8 days of anoxia), 10 juvenile oysters were removed from sealed containers and placed in flowing aerated seawater (12‰) with ambient seston concentrations. Mortality was judged by the failure to close the shell when stimulated, and the absence of feeding activity and production of biodeposits during 24 h of recovery in air-saturated seawater with natural suspended particulates.

Measurement of rate of heat dissipation and oxygen uptake in relation to hypoxia or anoxia

Rates of metabolic energy expenditure by oyster larvae and juveniles were measured by open-flow simultaneous calorimetry and respirometry at the Plymouth Marine Laboratory (U. K.). Larvae or juveniles (from Virginia) were placed in a 25 ml stainless steel chamber modified for use as a perfusion chamber in a microcalorimeter (LKB, BioActivity Monitor). Membrane filtered (0.45 μm) seawater (22°C; 12‰ salinity) was pumped through the perfusion chamber in the calorimeter at a constant flow rate [*i.e.*, 28, 37, or 62 ml h^{-1} (±0.5) depending upon the biomass within the chamber] and then to a thermostatted Radiometer oxygen sensor via 1 mm bore stainless steel tubing. A duplicate calorespirometric system, without larvae, was a reference for monitoring baseline heat flow and inflow oxygen concentrations (for further details see Widdows, 1987). The exit ports of the perfusion chambers were fitted with 37 μm mesh to retain the larvae within the chamber. Rates of oxygen uptake by the larvae were calculated from the differences in the oxygen concentration of the outflows from the reference and experimental chambers (at a known flow rate). Flow rates of 28, 37, and 62 ml h^{-1} were selected to achieve approximately 15% removal of oxygen from the inflowing water and to enable experimental manipulation of P_{O_2}.

Preliminary calorimetric and respirometric measurements of larvae in the presence of algal food (*Isochrysis galbana*) demonstrated a significant drift in the baselines for heat flow and oxygen concentration over a 24-h period, presumably due to the attachment of cells to the surfaces and increasing microbial activity within the system. Consequently, larvae were maintained unfed in FSW during the period of measurement. An additional time-course study demonstrated that there was no significant alteration in rates of heat dissipation and oxygen uptake by 'unfed' larvae in fully air-saturated FSW over a 24-h period in the calorimeter.

The effects of hypoxia and anoxia on the metabolic rate of three larval stages (99 μm, 133 μm and >300–<376 μm shell length) and juvenile oysters (16 mm shell height) were measured by open-flow simultaneous calorimetry and respirometry. Larvae were sieved from their respective cultures, concentrated, and placed in the perfusion chamber. The number of individuals within the chamber varied with larval size (14 to 20×10^3 for 99 μm larvae, 12×10^3 for 133 μm larvae and 2 to 4×10^3 for >300–<376 μm larvae), whereas the juvenile oysters were measured as individuals. The number of prodissoconch larvae available was only sufficient for three groups of 99 μm larvae and one group of 133 μm larvae to be measured by calorespirometry, whereas six groups of >300–<376 μm larvae and five individual juvenile oysters were measured.

The calorespirometric system established an equilibrium within 3 h and the rates of heat dissipation and oxygen uptake under normoxic conditions (fully air-saturated) were continuously monitored overnight (about 8 h). By increasing the proportion of nitrogen gas to air the P_{O_2} in the reservoir of FSW was reduced step-wise through 8, 4, and 2 kPa (60, 30, and 15 mm Hg). These levels of hypoxia were maintained for a period of 2–3 h to establish steady-state conditions of heat flow and P_{O_2}. Below 2 kPa, only oxygen-free nitrogen gas was bubbled into the reservoir. This gradually reduced the P_{O_2} to zero over 6 h.

After each experimental run, the calorespirometric system was cleaned with 10% V:V sodium hypochlorite

solution, thoroughly washed with distilled water, and its baseline checked before the next experimental run.

An additional group of juvenile oysters was held at 15°C and fed *Isochrysis galbana* for 14 days before measuring the rate of oxygen uptake in air-saturated water (12‰). To quantify the emersed anoxic rate of heat dissipation, these individuals were transferred to the calorimeter chamber, which was purged with nitrogen gas.

Measurement of ingestion rate in response to hypoxia and anoxia

Ingestion rates by prodissoconch (>73–<140 μm) and pediveliger (>300–<376 μm) larvae during exposure to hypoxia and anoxia were quantified using 3.44 μm diameter 'Fluoresbrite' polystyrene fluorescent microspheres (Polyscience Inc.). To encourage their phagostimulatory nature, the microspheres were added to autoclaved 12‰ seawater containing an algal extract. This was prepared from a pellet of *Isochrysis galbana* cells that had been homogenized and centrifuged to remove cell debris.

The experimental protocol involved allowing about 50 larvae to filter and ingest the microspheres for 10 min under controlled partial pressures of oxygen, as described below. After the exposure period, further ingestion of microspheres was prevented by fixing the larvae in 4% buffered formaldehyde. Preliminary experiments demonstrated that fixation did not cause the larvae to egest or defecate any of the microspheres within the digestive system. Larvae were then washed three times in distilled water to remove loose microspheres and stored in 4% buffered formaldehyde.

The number of microspheres ingested was counted using an inverted microscope fitted with a fluorescence light source. The prodissoconch larvae had a sufficiently small gut and thin shell that the number of ingested microspheres could be counted directly. However, for the pediveligers, especially those that were actively feeding under normoxic conditions, the microspheres aggregated within the digestive system such that they could not be enumerated. For these heavily feeding larvae the percentage of individuals feeding was initially determined from the entire group. From this group, about 50 randomly selected individual larvae were transferred, using a micropipette, to wells of a flat-bottomed tissue culture plate. After the water had been evaporated at 40°C, 10 μl HCl was added to each well to dissolve the larval shell. The acid was then evaporated and 30% H_2O_2 added to dissolve most of the tissue. This digestion and disruption process was enhanced by placing the plates in a Brinkman sonicator bath. The microspheres at the bottom of each well were then counted on the inverted microscope after the H_2O_2 had evaporated. Preliminary experiments determined that these treatments did not alter the particle fluorescence or size.

The fluorescent microsphere method of assessing larval feeding rates was compared to a traditional method of measuring suspension feeding activity that involves estimating the logarithmic decline in algal cell concentration over time (Coughlan, 1969). In this comparative experiment, 1500 pediveliger larvae were maintained for 3 h in 3 replicate 250 ml flasks containing *Isochrysis galbana* at a concentration of 30×10^6 cells l^{-1}. The initial algal cell concentration was counted using a Coulter Counter and again at hourly intervals for each of the replicates. From this, a mean filtration rate of 54.1 ± 7.8 (S.E.) μl h^{-1} individual^{-1} was estimated. Filtration rate was measured using the microsphere method for 100 individual larvae from the same culture, measured at the same time. The rate was 66.2 ± 21.3 (S.E.) μl h^{-1} individual^{-1}. This indicates that the use of algal cells and microspheres gave comparable filtration rates. The larger variance associated with the microsphere method reflects the examination of 100 individual larvae. However, to obtain a measurable decrease in algal cell concentration by the Coulter Counter method, many larvae are required in each flask. This masks any high individual variability in the feeding activity of larvae.

Larvae were exposed to anoxic conditions in 5 ml glass syringes using the procedure described above (anoxia survival experiments). Ten minutes before the end of the incubation period, the anoxic seawater in the syringe was replaced by anoxic seawater containing fluorescent microspheres at a concentration of 18×10^6 l^{-1}.

Larvae were exposed to hypoxic conditions in 5 ml vials through which 22°C water of the appropriate partial pressure of oxygen was pumped (50 ml h^{-1}) from a reservoir. *Isochrysis galbana* cells (20×10^6 cells l^{-1}) were added to the reservoir, providing the larvae with a source of food. This ensured that the ingestion rate measured with the microspheres was a typical steady state value and was not an enhanced rate due to rapid gut filling by starved larvae suddenly presented with particles.

Ingestion rates in relation to exposure time were measured at three different levels of hypoxia (0.8–1.7 kPa, 2.2–3.0 kPa, and 4.0–5.6 kPa) and compared to ingestion rates by larvae at full air saturation (21 kPa). The partial pressures of oxygen within the reservoir was controlled by regulating the flows of nitrogen and compressed air; P_{O_2} was not maintained at an absolute level, but only within the stated ranges. The outflow from the 5 ml vials was passed through the Radiometer flow cell to provide a continuous record of the P_{O_2}. Ten minutes before the exposure period was complete, the flow was stopped and 10 μl of concentrated suspension of microspheres was injected through a silicone septum in the top

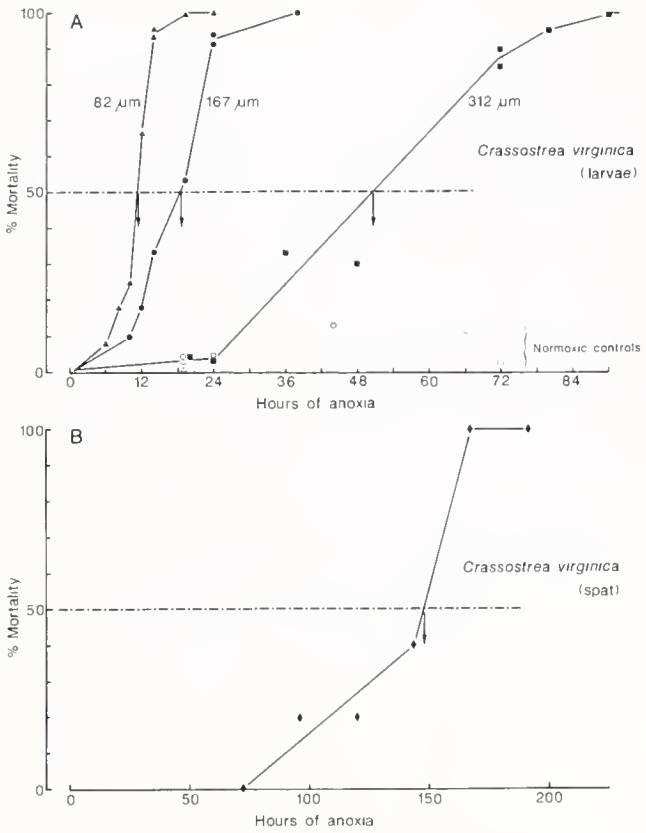

Figure 1. Relationship between mortality and duration of anoxia for (A) larval stages (▲ prodissoconch, ● veliconcha, ■ pediveliger) and (B) juvenile or spat (♦) of *Crassostrea virginica*. Open symbols represent level of mortality in the respective controls.

of each vial to give a final concentration of 18×10^6 microspheres l^{-1}. Following a 10-min incubation with microspheres, the larvae were sampled and the ingestion rate quantified using the procedures described above. Additional vials of larvae were prepared in order to examine the ability of pediveliger larvae to recover from 24 h of exposure to hypoxic conditions. The rate of ingestion of microspheres by larvae was then measured following the return of water to full air-saturation.

Results

Anoxia tolerance

Anoxic tolerance of *Crassostrea virginica* increased with developmental stage and body size (Fig. 1). The median mortality time (MMT; *i.e.*, the time required to reach a 50% mortality) was approximately 11, 18, and 51 h for the three larval stages (82 μm prodissoconch, 167 μm veliconcha, and 312 μm pediveliger, respectively). The MMT for the juvenile oysters was about 150 h. There was close agreement among replicates, and the normoxic controls typically showed only 6–10% mortality at the time of total mortality in the experimental (anoxic) groups. During the initial phase of anoxia, we observed that the larvae maintained swimming activity for at least 30 to 60 min before settling to the bottom of the syringe.

Effect of hypoxia and anoxia on the rate of heat dissipation and oxygen uptake

The effect of a reduction in the partial pressure of oxygen (P_{O_2}) on the rate of heat dissipation ($\dot{Q}$) and oxygen uptake ($\dot{N}_{O_2}$) by the three larval stages (99, 133, and 300–376 μm) and juveniles are shown in Figures 2A–D, respectively. The results demonstrate that the metabolic rate of larvae declined at reduced P_{O_2} values and the response to short-term hypoxia and anoxia (*i.e.*, duration of several hours) changed with body size or developmental stage.

The prodissoconch larvae (Fig. 2A) maintained their rates of heat dissipation and oxygen uptake independent of P_{O_2} down to 2 kPa (15 mm Hg), whereas the larger larvae (Fig. 2B, C) and juveniles (Fig. 2D) maintained their rates of heat dissipation and oxygen uptake down to only about 8 kPa (Table I). Below this P_{O_2}, generally referred to as the critical oxygen partial pressure (P_c) (Herreid, 1980), the rates of heat dissipation and oxygen uptake become dependent upon P_{O_2}. Table I also includes the oxygen partial pressure that results in a reduction in the heat dissipation rate to 50% of the normoxic and typically maximum rate. The P_{O_2} at 0.5 $\dot{Q}_{normoxia}$ was only 0.27 kPa for 99 μm larvae, increasing to 2.4 kPa for the 133 and 300–376 μm larvae and 3.1 kPa for the juveniles. These results indicate that the larvae, especially the early larval stage (99 μm), can maintain their total metabolic rate down to low P_{O_2} values. Furthermore, a comparison of the rates of heat dissipation and oxygen uptake (Fig. 2A–D) shows that oxygen consumption continues even at low P_{O_2} and forms a significant component of the total metabolic rate.

The oxycaloric equivalent in aerobic catabolism ranges from −440 to −480 kJ mol^{-1} O_2 in aquatic animals (Gnaiger, 1983). When experimentally derived oxycaloric equivalent values exceed the range of theoretical values, then partial anaerobiosis is indicated. The higher the experimental oxycaloric value the greater the reliance on anaerobic metabolism. Experimental oxycaloric equivalent values, which can be derived from the calorespirometric measurements, are presented in Table II. The values under normoxia (20.5 kPa) and above 2 kPa were not significantly different from the theoretical range of oxycaloric equivalents, commonly used to convert rates of oxygen consumption into rates of catabolic

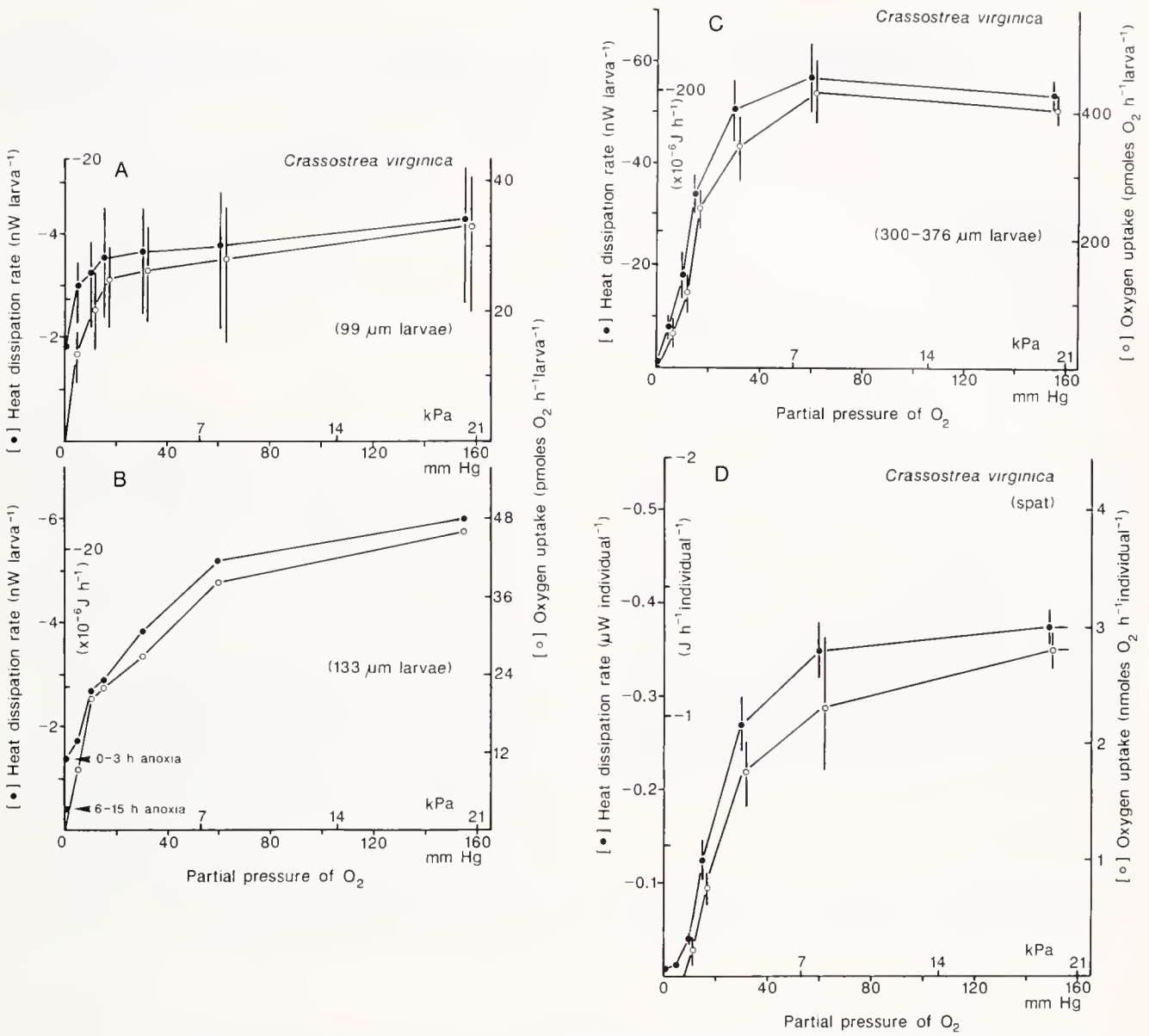

Figure 2. Effect of partial pressure of oxygen on rates of heat dissipation (●) and oxygen uptake (○) by prodissoconch larvae (A, means ± range; n = 3); veliconch larvae (B); pediveligers (C, mean ± S.E.; n = 5) and juveniles (D, mean ± S.E.; n = 5) of *Crassostrea virginica.* The rates of heat dissipation and oxygen uptake are plotted on corresponding scales using an oxycaloric equivalent of −450 kJ mol O_2^{-1} (or 1 nmoles O_2 h^{-1} = −0.125 μW; Gnaiger, 1983).

heat dissipation. However, the results indicate that the experimental oxycaloric equivalents were slightly above the theoretical range at many P_{O_2} levels. This may be due to the valve closure and quiescence of a proportion of the larvae and their reliance on anaerobic metabolism. At the lowest P_{O_2} level (0.67 kPa), the rate of heat dissipation by all larval stages had a significant anaerobic component, and 40% of the juveniles were closed and totally anaerobic. At 1.33 and 2 kPa the juveniles also had a significant (ANOVA; $P < 0.05$) anaerobic contribution to the total heat dissipation.

In Table 1, the anoxic rates of heat dissipation ($\dot{Q}_{anoxia}$) during the initial 3 h of anoxia are expressed as a proportion of the normoxic rates of heat dissipation ($\dot{Q}_{normoxia}$). The 99 μm and 133 μm larvae had relatively high values, which were 34% and 23% of $\dot{Q}_{normoxia}$, respectively. However, after 6 h of anoxia, the $\dot{Q}_{anoxia}$ of 133 μm larvae declined to 7% of $\dot{Q}_{normoxia}$ and was maintained at this

Table I

Descriptors of the effect of oxygen partial pressure (P_{O_2}) on the metabolic rate of three sizes of oyster (Crassostrea virginica) *larvae and juveniles*

	Oyster larvae (Shell length)			Spat (Shell height)
Size:	99 μm	133 μm	>300–<376 μm	16 mm
P_c (kPa)[a]	2	8	8	8
P_{O_2} (kPa) at 0.5 $\dot{Q}_{(normoxia)}$[b]	0.27	2.4	2.3	3.1
P_{O_2} (kPa) at 0.5 $\dot{N}_{O_2(normoxia)}$	1.05	2.4	2.3	3.5
$\dot{Q}_{anoxia}$[c]/$\dot{Q}_{normoxia}$	0.34	0.23	0.05	0.03

[a] P_c—critical oxygen partial pressure (P_{O_2} below which $\dot{Q}$ and $\dot{N}_{O_2}$ become P_{O_2} dependent).
[b] P_{O_2} at 0.5 $\dot{Q}_{normoxia}$—P_{O_2} that reduces rate of heat dissipation to 50% of normoxic (maximum) rate.
[c] $\dot{Q}_{anoxia}$—Rate of heat dissipation during initial 3 h of anoxia.

level for 15 h. In contrast, the pediveliger (300–376 μm) and the juveniles had relatively lower $\dot{Q}_{anoxia}$, 5% and 3% of $\dot{Q}_{normoxia}$. After 5 h of anoxia, the $\dot{Q}_{anoxia}$ of the pediveliger declined from 5% to 2% of $\dot{Q}_{normoxia}$, and was maintained at this level for 10 h.

Juvenile oysters were also held at 15°C and their rates of oxygen uptake (under normoxia) and heat dissipation (under anoxia, N_2 gas) were measured independently at 15°C. The results (Table III) show that $\dot{Q}_{anoxia}$ at 15°C was 5% of the normoxic rate of energy expenditure, which is not significantly different (ANOVA) from the $\dot{Q}$ anoxia at 22°C (*i.e.*, $Q_{10} \sim 1$). In contrast, the rate of oxygen uptake increased significantly with temperature, ($Q_{10} = 2.28$).

Recovery from anoxia

On three occasions, groups of pediveliger larvae (>300–<376 μm) were recovered after >11 h of anoxia. The P_{O_2} in the calorespirometric chamber was allowed to rise rapidly to normoxic levels while rates of heat dissipation and oxygen uptake were being monitored continuously. In each case, the response was a very rapid rise in both heat dissipation and oxygen uptake rates (Fig. 3). Due to the rapid changes in rates of heat dissipation under these conditions the apparent rate was converted to the instantaneous rate (Gnaiger, 1983), using an exponential delay correction (*i.e.*, 10 min time constant for the calorimetric system). In contrast to the slight overshoot (32%) in the rate of heat dissipation, the larvae showed a marked overshoot (*ca.* 300%) in the rate of oxygen uptake (termed the oxygen debt payment). Oxygen uptake by the larvae returned to a near steady rate after 2–3 h. The mean oxycaloric equivalent during the first hour was −180 kJ mol^{-1} O_2 and increased to −377 kJ mol^{-1} O_2 and −500 kJ mol^{-1} O_2 after 2 and 3 h, respectively. This was followed by a period (3–6 h recovery) when the oxycaloric equivalent was maintained at −583

Table II

Experimental oxycaloric equivalents (kJ mol^{-1} O_2; derived by simultaneous calorimetry and respirometry) describing the nature of energy metabolism of oyster (Crassostrea virginica) *larvae and juveniles*

	Oyster larvae (Shell length)			Spat (Shell height)
Size:	99 μm	133 μm	>300–<376 μm	
P_{O_2} (kPa)	Oxycaloric equivalents (kJ mol^{-1} O_2)			16 mm
20.5	−450 ± 14[a]	−477	−469 ± 11[b]	−486 ± 5[b]
4	−505 ± 33	−524	−548 ± 53	−508 ± 15
2	−504 ± 57	−462	−490 ± 22	−616 ± 21
1.33	−584 ± 41	−472	−549 ± 37	−658 ± 46
0.67	−694 ± 54	−644	−598 ± 50	α
0	α	α	α	α

[a] Mean ± range for 99 μm larvae.
[b] Mean ± S.E. for 300–376 μm larvae and spat.

Table III

Comparison between anoxic and normoxic metabolic rates (mean ± S.E.) by juveniles of Crassostrea virginica *(30 mg dry tissue mass) at 15°C (n = 9) and 22°C (n = 5)*

	15°C	22°C
Normoxia		
Respiration rate (μmoles O_2 h^{-1})	1.564 ± 0.144	2.789 ± 0.152
Respiration rate (J h^{-1})	0.713 ± 0.066	1.360 ± 0.071
Anoxia		
Heat dissipation rate (J h^{-1})	0.037 ± 0.005	0.035 ± 0.005
Anoxic rate as a proportion of normoxic rate	0.05	0.03

kJ mol^{-1} O_2 and then declined to −486 kJ mol^{-1} O_2 after 6 h.

Effect of hypoxia and anoxia on the rate of ingestion

The general response of prodissoconch and pediveliger larvae to hypoxia and anoxia was a reduction in the proportion of the larvae actively feeding and ingesting microspheres over 24 h exposure, and a marked decline in the rate of ingestion of microspheres within the initial 2–3 h (Fig. 4A–D; Fig. 5A–D). Although the data for prodissoconch larvae were more variable, with the percentage of larvae feeding being inexplicably depressed at certain times (*e.g.*, control or time zero and 2.75 h for P_{O_2} of 4.0–5.6 kPa, Fig. 4A; 2.25 h and 4 h for P_{O_2} of 0.8–1.7 kPa, Fig. 4C), the reduction in the rate of ingestion was small compared to the reduction shown by pediveligers under hypoxic conditions. The ingestion rates by prodissoconch larvae were generally between 5 and 8 microspheres $larva^{-1}$ per 10 min under normoxic conditions. Ingestion rates declined to about 2 microspheres $larva^{-1}$ 10 min^{-1} after 2–3 h of hypoxia (<5.6 kPa) and these rates were then maintained for the 24 h of exposure to hypoxia (Figs. 4A–D). However, prodissoconch larvae exposed to anoxia showed no evidence of ingestion after 10 h of anoxia (Fig. 4D).

Pediveligers also showed a gradual decline in the proportion of larvae ingesting microspheres with increasing duration of exposure to hypoxic and anoxic conditions (Figs. 5A–D). Under normoxia (21 kPa), the pediveligers were more consistent in their feeding activity compared to the prodissoconch stage larvae. More than 60% were actively feeding and ingesting under normoxia, and the proportion of inactive larvae increased with the duration of exposure and the degree of hypoxia. For example, ≦20% were feeding and ingesting after: 14 h at 4–5.6 kPa, 7 h at 2.2–3 kPa, 4 h at 0.8–1.7 kPa, and <1 h at 0 kPa (Figs. 5A–D). The rates of ingestion by pediveligers under fully air-saturated conditions (controls, time zero) were always above 40 microspheres $larva^{-1}$ 10 min^{-1}, whereas under hypoxic conditions (<5.6 kPa) the mean ingestion rate was always <14 microspheres $larva^{-1}$ 10 min^{-1}. However, even after 24 h at a P_{O_2} of 0.8–1.7 kPa, 4% of the larvae had ingested an average of 5 microspheres $larva^{-1}$ 10 min^{-1}. Visual observations suggested that in all conditions, the larvae exhibited some degree of activity that generally involved moving or swimming at or near the bottom of the experimental chamber.

After 24 h exposure to the three levels of hypoxia (*i.e.*, 4–5.6, 2.2–3.0, 0.8–1.7 kPa), pediveliger larvae were allowed to recover under normoxic conditions in the presence of food before measuring their ingestion rates. A high proportion (>60%) of larvae recovered after 24 h at P_{O_2} 4–5.6 kPa and showed signs of feeding, but their ingestion rates had recovered only partially (22% of the pre-exposure rate). Larvae exposed to the lower P_{O_2} conditions showed limited recovery, and only to levels of feeding and ingestion comparable to those recorded in the early stages of hypoxia (Figs. 5A–C).

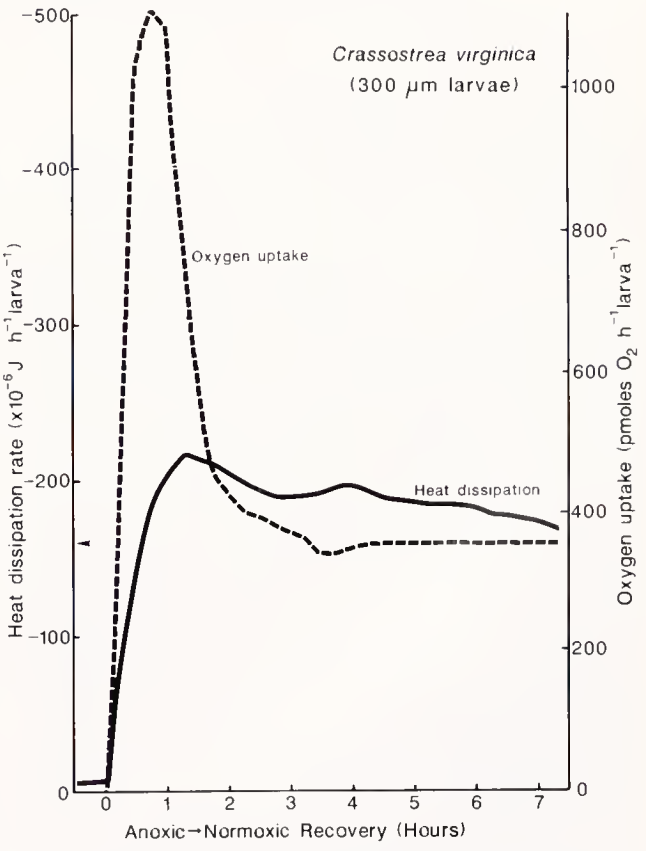

Figure 3. Recovery under normoxic conditions of rates of heat dissipation (solid line) and oxygen uptake (broken line) by pediveliger larvae of *Crassostrea virginica* following 11 hours of anoxia.

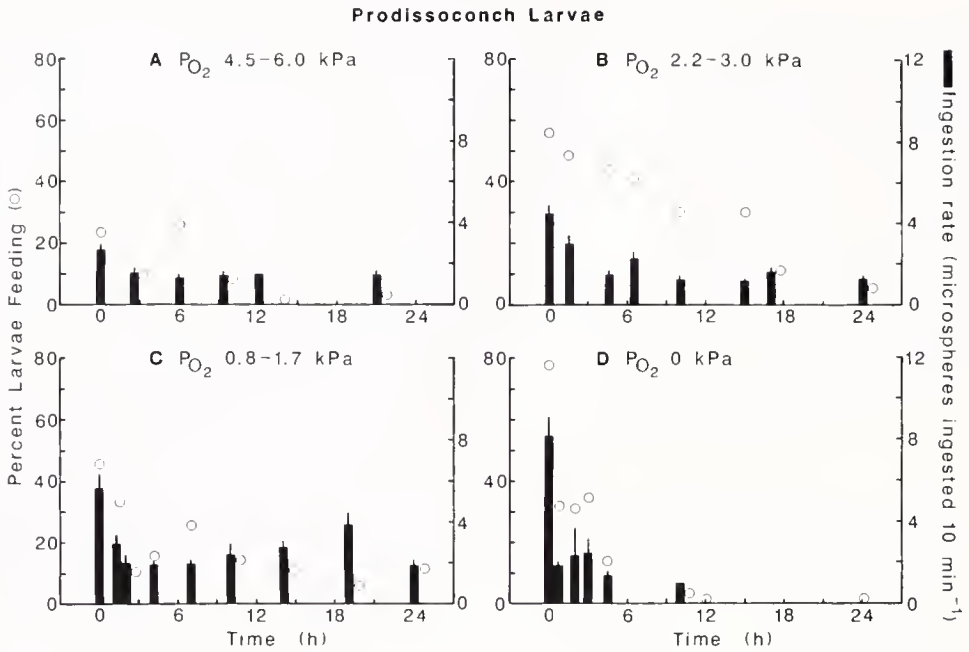

Figure 4. Effect of partial pressure of oxygen and duration of exposure on the feeding activity of prodissoconch larvae of *Crassostrea virginica*. Feeding activity is expressed in terms of the proportion of larvae feeding (○) and their ingestion rates (number of microspheres ingested per 10 min.; histograms) during hypoxia (A, 4.5 to 6 kPa; B, 2.2 to 3 kPa; C, 0.8 to 1.7 kPa) and anoxia (D, 0 kPa).

Discussion

Metabolic response to anoxia

Oyster larvae tolerate anoxia, and this tolerance increases with larval development. This suggests that all larval stages have anaerobic metabolic pathways capable of sustaining life for a limited period of time under anoxic conditions. The increase in anoxia tolerance with larval development appears to be related to an ability to lower their rates of heat dissipation and thus conserve energy expenditure under anoxia. Figure 6 illustrates such a relationship ($r = 0.99$) in a plot of $\dot{Q}_{anoxia}/\dot{Q}_{normoxia}$ against the reciprocal of anoxia tolerance (1/MMT in h). The early larval stages maintain a high rate of heat dissipation (34% of $\dot{Q}_{normoxia}$), at least during the initial 3 h of anoxia, whereas the later stages conserve energy by reducing anoxic rates of heat dissipation (3% of $\dot{Q}_{normoxia}$). These differences in the level of $\dot{Q}_{anoxia}$ appear to correlate with the relative anoxic rates of ingestion (IR) by the different larval stages. After 2 h of anoxia, $IR_{anoxia}/IR_{normoxia}$ was 29% (2.5/8.5, Fig. 4D) for the prodissoconch larvae compared to 5% (2.25/42, Fig. 5D) for the pediveliger larvae. Therefore, the higher anoxic metabolic rates by the prodissoconch compared to the pediveliger appear to be coupled to their higher levels of activity under anoxia (*i.e.*, the observed swimming activity and measured feeding activity).

These results provide evidence of differences in the type of anoxibiosis sustained by different developmental stages of the species: 'functional anoxibiosis' in the early larval stages, characterized by high power output at the expense of efficiency, compared with 'environmental anoxibiosis' in later developmental stages, characterized by low power output and a relatively high efficiency of anoxic energy conversion (Gnaiger, 1983). If the prodissoconch larvae use glycogen in anaerobic metabolic pathways, then the relatively high anoxic rates of heat dissipation represent a very high cost, at least in terms of rate of glycogen use, because of the lower biochemical efficiency or ATP yield per glycosyl unit in anaerobic metabolism (4.71 mol ATP per mol of glycogen for the succinate pathway compared to 37 mol ATP per mol of glycogen for aerobic catabolism; Gnaiger, 1983). However, in contrast to the situation in adult bivalves, polysaccharides form a relatively small proportion (*e.g.*, 2–3% of organic matter) of the energy store in bivalve larvae (Holland and Spencer, 1973; Gabbott, 1976; Mann and Gallager, 1985) and in response to nutritional and environmental stress they use lipid (especially neutral lipid) and protein substrates. While lipid represents an efficient form of energy reserve for aerobic catabolism, because of its high energy content (39.5 kJ g^{-1}), lipid cannot be used as a substrate for anaerobic metabolism. Bivalve larvae may prove to use protein and amino acids as energy substrates

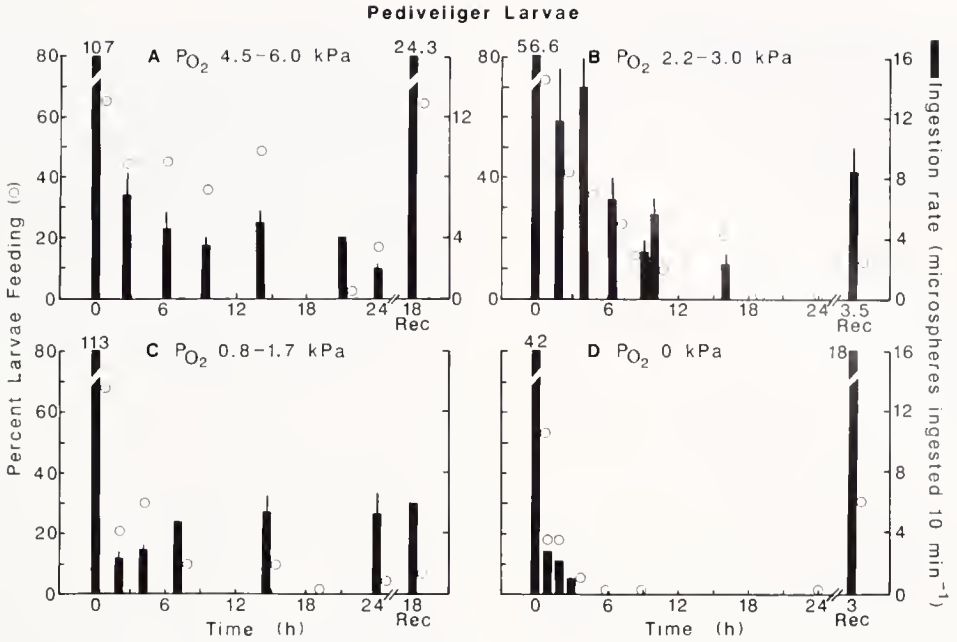

Figure 5. Effect of partial pressure of oxygen and duration of exposure on the feeding activity of pediveligers of *Crassostrea virginica*. Feeding activity is expressed in terms of the proportion of larvae feeding (○) and their ingestion rates (number of microspheres ingested per 10 min.; histograms) during hypoxia (A, 4.5 to 6 kPa; B, 2.2 to 3 kPa; C, 0.8 to 1.7 kPa), anoxia (D, 0 kPa) and after 3 to 18 h of normoxic recovery.

for anaerobic metabolism, similar to sea anemones (Anthozoa), which use protein and accumulate nitrogenous end-products during anoxia (Ellington, 1980, 1982; Navarro and Ortega, 1984).

The relatively high anoxic rate of heat dissipation by prodissoconch larvae presumably enables the larvae to maintain their observed locomotory activity and to swim away from anoxic conditions (unpub. obs. and V. S. Kennedy, pers. comm.), but at considerable cost to their energy reserves, which are relatively small in the early developmental stages (Gabbott, 1976). These high costs are likely to result in a rapid depletion of energy reserves, thus limiting the anoxia tolerance of early larval stages.

This relationship between the anoxic rate relative to the normoxic rate of energy expenditure and anoxia tolerance is also apparent in interspecific comparisons with adult bivalves. For example, the clam (*Mulinia lateralis*), has a relatively high $\dot{Q}_{anoxia}$ (*i.e.*, 97% of $\dot{Q}_{normoxia}$; Shumway *et al.*, 1983) and is relatively intolerant of prolonged anoxia (*ca.* 5 days). The high anoxic energy demands of *M. lateralis* (confirmed by direct calorimetry; Shumway *et al.*, 1983) are also related to the maintenance of locomotor and feeding activities under anoxia, which may be an adaptation to escape periodic burial in unstable, oxygen-deficient sediment. In contrast, the sessile mussel (*Mytilus edulis*) has a very low $\dot{Q}_{anoxia}$ (*i.e.*, 4% of $\dot{Q}_{normoxia}$; Widdows, 1987) which enables it to conserve energy and thus tolerate prolonged anoxia (*ca.* 35 days, Theede *et al.*, 1969).

Metabolic response to hypoxia

Oyster pediveliger larvae and juveniles maintain rates of oxygen consumption down to relatively low P_{O_2} values, as indicated by the P_C values and P_{O_2} at which the $\dot{N}_{O_2}$ is 50% of the normoxic $\dot{N}_{O_2}$ (Table I). Similar values have been recorded for adult *Crassostrea virginica* (0.4 g) under comparable conditions of 20°C and 14‰S (P_c of 8 kPa; P_{O_2} at 0.5 $\dot{Q}_{normoxia}$ of 3.4; Shumway and Koehn, 1982). The ability of the prodissoconch larvae to maintain their rates of oxygen uptake down to extremely low levels of P_{O_2} appears to be a feature of very small individuals (such as the early larval stages) as a result of the high surface area to volume ratio and the short distance for oxygen diffusion (Herreid, 1980). Furthermore, low aerobic demands permit diffusion of oxygen to meet the needs of very small animals, as long as the animals are active and keep the surrounding water stirred. Oyster larvae maintained ciliary activity on the velum down to anoxic conditions, presumably to meet their swimming, respiratory, and feeding requirements.

There is no evidence of a major anaerobic component

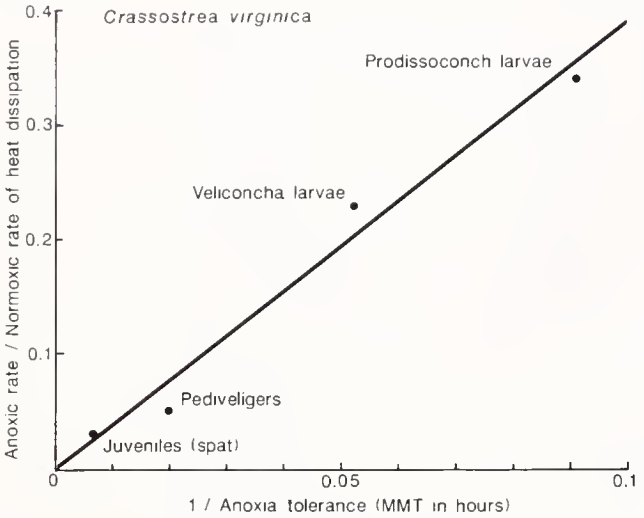

Figure 6. Relationship between anoxic rate/normoxic rate of heat dissipation and anoxic tolerance (1/median mortality time in hours) of larvae and juveniles of *Crassostrea virginica*.

of total energy metabolism by larvae and juveniles of *Crassostrea* under hypoxic conditions. Measured oxycaloric equivalents are only slightly higher than theoretical values for totally aerobic catabolism from 20.33 down to 1.33 kPa, and this increase is not significant ($P < 0.05$) until 0.67 kPa (Table II).

Recovery of pediveliger larvae (300 μm shell length) after 11 hours of anoxia (Fig. 3) shows a similar metabolic response to that previously recorded for adult mussels, *Mytilus edulis* (Shick *et al.*, 1986, 1988; Widdows, 1987). The overshoot in rate of heat dissipation was only 32%, whereas the overshoot in oxygen uptake was >300%, resulting in an experimental oxycaloric equivalent of -180 kJ mol^{-1} O_2. Experimental studies on adult bivalves have divided the overshoot in oxygen uptake (the 'oxygen debt payment') into two basic components, the metabolic component and the physical reoxygenation of water and oxygen stores within the valves of bivalves during the initial phase of normoxic recovery. This phenomenon is often recorded as a sudden 'oxygen sag' in the oxygen trace and coincides with the opening of the shell valves and the flushing out of deoxygenated water (*ca.* 15% of oxygen overshoot; Shick *et al.*, 1986). Such an 'oxygen sag' was also observed in the oxygen traces produced by the oyster larvae, and indicates that the reoxygenation of water within the shell valves of the larvae may form a significant contribution to the overshoot in oxygen uptake during the first 30 min. However, even after accounting for the physical reoxygenation in adult *M. edulis*, the heat equivalent of oxygen uptake during early aerobic recovery exceeds the total heat dissipation rate, which results in an experimental oxycaloric equivalent of about -200 kJ mol^{-1} O_2 (Shick *et al.*, 1986; Widdows, 1987). Values significantly below -440 to -480 kJ mol^{-1} O_2 indicate the conservation of heat in partially endothermic processes (biosynthesis), such as the restoration of high-energy phosphates, together with catabolic-anabolic coupled glyconeogenesis and the partial oxidation of the succinate that is accumulated by adult mussels during anoxia. However, the importance of these processes in the aerobic recovery of oyster larvae is unknown due to the absence of detailed information on the anaerobic metabolic pathways operating in larval stages and the accumulation of metabolic end products during anoxia.

Feeding rate in response to hypoxia and anoxia

The use of fluorescent microspheres provided an accurate method of quantifying ingestion rate, but may underestimate filtration rate when particles captured on the velum are rejected and not ingested (Gallager, 1988). In preliminary work using video microscopy, live larvae were observed feeding on the microspheres. These recordings showed that the microspheres were handled like algal cells and retained within the digestive system for many hours. They could also be clearly seen revolving in the crystalline style sac, thus indicating that polystyrene microspheres, which had been coated with an algal extract, were not being rapidly passed through the gut. This is in contrast to the observation of Robinson (1981) and Gallager (1988), who reported that *Mercenaria mercenaria* larvae can pass latex microspheres through their guts as fast as they are ingested. The mean ingestion rates of 55 microspheres larva^{-1} h^{-1} (prodissoconch) and 508 microspheres larva^{-1} h^{-1} (pediveliger) recorded for *Crassostrea virginica*, were similar to our measured rates of algal ingestion and the rates for *Mercenaria mercenaria* (86 *Isochrysis* cells h^{-1} for 2-day-old larvae of 100 μm and 387 cells h^{-1} for 10 day larvae of 234 μm) measured by Gallager (1988) using high-speed video microscopy.

The effect of hypoxia on the feeding and ingestion rates of oyster larvae generally reflects the relationship between P_{O_2} and rates of heat dissipation by larvae. For example, a high proportion of the prodissoconch larvae were actively feeding and maintaining relatively high ingestion rates, at least during the initial 6 h at the three levels of hypoxia (Fig. 4A–C) and this corresponded with the maintained rates of heat dissipation down to extreme hypoxic conditions (Table I). The feeding response of the early feeding prodissoconch larvae therefore appears to be an all-or-none response, and this may reflect the low nutrient reserves in these early larval stages (Mann and Gallager, 1985), which necessitates that the larvae feed almost continuously. In contrast, the pediveligers

showed a marked reduction in both the proportion of larvae feeding and their ingestion rates at more moderate levels of hypoxia (*e.g.*, 2.2–3.0 kPa), and it was at these levels that the rate of heat dissipation also declined to 50% of the normoxic rate. Although feeding and ingestion rates by pediveligers were reduced, swimming activity observed in our study was maintained even after 6 h at 0.8 kPa, thus confirming the reported uncoupling of the swimming and feeding activity of the velum of *M. mercenaria* larvae (Gallager, 1988).

The increased sensitivity of pediveligers to hypoxia may reflect problems of oxygen diffusion associated with increasing body mass and therefore reduced surface area to volume ratio. Under hypoxic conditions the supply of oxygen to pediveligers is insufficient to meet the total metabolic demands of all processes. The 30–50% reduction in oxygen consumption by pediveligers at a P_{O_2} of about 2–3 kPa is not compensated by a major contribution from anaerobic metabolism. As a result, there is a reduction in the rates of 'non-essential' (at least in the short-term) and costly processes, such as the ingestion, digestion, and absorption of food and growth. In contrast, processes with relatively low costs, such as the ciliary activity of the velum (Silvester and Sleigh, 1984), are maintained under hypoxia, thus enabling larvae to escape and to resume feeding and growth when oxygen is more readily available. In concurrent experiments, V. S. Kennedy (pers. comm.) has demonstrated the importance of upward swimming as a means for larvae to avoid hypoxic conditions. This interpretation of hypoxic responses based on metabolic costs is supported by evidence of the partitioning of energy expenditure and the costs associated with different processes in the mussel (*Mytilus edulis*). The cost of ciliary activity of the gills represents <3% of the total metabolic energy expenditure (TME), the cost of digestion and absorption of food forms is about 17% of the TME, and the cost of growth ranges from 0 to 30% of TME depending on ingestion rate (Widdows and Hawkins, 1989). Consequently, the energy conserved by markedly reducing the processes of digestion and absorption of food and growth, may largely account for the observed reduction in metabolic rate by larvae during hypoxia.

Therefore, the present study demonstrates good agreement between calorimetric, respirometric, feeding, and behavioral measurements on the larvae and juveniles of *C. virginica* in response to hypoxia and anoxia. It highlights the energetic changes associated with a change in behavior, from avoidance of anoxia in the early larval stage to tolerance in the later pediveliger larvae and juvenile oyster. It suggests that larvae are able to survive short-term (hours) hypoxia associated with low O_2 in the Chesapeake Bay. However, although the larvae can tolerate hypoxic conditions, their reduced feeding activity will reduce their growth rate and increase larval development times. This will expose the larvae for longer periods to predation by larval fishes and gelatinous carnivores, such as ctenophores (*Mnemiopsis leidyi*), hence reducing larval recruitment to the adult oyster population.

Acknowledgments

This work was supported by grant NA-86-AA-D-SG042 from the National Sea Grant Program, NOAA, to the University of Virginia, grant NA-86-AA-SG006 to the University of Maryland, and the Visiting Scientist Program of the Virginia Institute of Marine Science (J.W.). We are grateful to J. S. Rainer for assistance.

Literature Cited

Coughlan, J. 1969. The estimation of filtration rate from the clearance of suspension. *Mar. Biol.* **2:** 356–358.

Ellington, W. R. 1980. Some aspects of the metabolism of the sea anemone *Haliplanella lucia* (Verill) during air exposure and hypoxia. *Mar. Biol. Lett.* **1:** 255–262.

Ellington, W. R. 1982. Metabolic responses of the sea anemone *Bunodosoma cavernata* (Bose) to declining oxygen tensions and anoxia. *Physiol. Zool.* **55:** 240–249.

Gabbott, P. A. 1976. Energy metabolism. Pp. 293–355 in *Marine Mussels: Their Ecology and Physiology*, B. L. Bayne, ed., Cambridge University Press, Cambridge.

Gallager, S. M. 1988. Visual observations of particle manipulation during feeding in larvae of a bivalve mollusc. In *Zooplankton Behaviour Symposium*, 1987, Georgia. *Bull. Mar. Sci.* **43:** 344–365.

Gnaiger, E. 1983. Heat dissipation and energetic efficiency in animal anoxibiosis: economy contra power. *J. Exp. Zool.* **228:** 471–490.

Herreid, C. F. 1980. Hypoxia in invertebrates. *Comp. Biochem. Physiol.* **67A:** 311–320.

Holland, D. L., and B. E. Spencer. 1973. Biochemical changes in fed and starved oysters, *Ostrea edulis* L., during larval development, metamophosis, and early spat growth. *J. Mar. Biol. Assoc. U. K.* **53:** 287–298.

Kemp, W. P., and W. R. Boynton. 1984. Spatial and temporal coupling of nutrient inputs to estuarine primary production: the role of particulate transport and decomposition. *Bull. Mar. Sci.* **35:** 242–247.

Mackiernan, G. B. 1987. Dissolved oxygen in the Chesapeake Bay: processes and effects. Maryland Sea Grant publication number UM-SG-TS-87-03. 177 pp.

Malone, T. C., W. M. Kemp, H. W. Ducklow, W. R. Boynton, J. H. Tuttle, and R. B. Jonas. 1986. Lateral variation in the production and fate of phytoplankton in a partially stratified estuary. *Mar. Ecol. Prog. Ser.* **32:** 149–160.

Mann, R. 1986. Sampling of bivalve larvae. Pp 107–116 in *North Pacific Workshop on Stock Assessment and Management of Invertebrates*, G. S. Jamieson and N. Bourne, eds. Canadian Special Publication Fisheries and Aquat Sci. 92: Department of Fisheries and Oceans, Ottawa, Canada.

Mann, R., and S. M. Gallager. 1985. Physiological and biochemical energetics of larvae of *Teredo navalis* L. and *Bankia gouldi* (Bartsch) (Bivalvia: Teredinidae). *J. Exp. Mar. Biol. Ecol.* **85:** 211–228.

Navarro, E., and M. M. Ortega. 1984. Amino acid accumulation

from glucose during air exposure and anoxia in the sea anemone *Actinia equina* (L.). *Comp. Biochem. Physiol.* **78B**: 199–202.

Newell, R. I. E. 1985. Physiological effects of the MSX parasite *Haplosporidium nelsoni* (Haskin, Stauber and Mackin) on the American oyster *Crassostrea virginica* (Gmelin). *J. Shelfish Res.* **5**: 91–95.

Officer, C. B., R. B. Biggs, J. L. Taft, L. E. Cronin, M. A. Tyler, and W. R. Boynton. 1984. Chesapeake Bay anoxia: origin, development and significance. *Science* **223**: 22–27.

Robinson, W. E. 1981. Quantification of ingestion by *Mercenaria mercenaria* (L.). veligers feeding on mixed suspensions of inert material and algae using microspectrofluorimetry. *J. Moll. Stud. Suppl.* **12A**: 167–171.

Seliger, H. H., J. A. Boggs, and W. H. Biggley. 1985. Catastrophic anoxia in Chesapeake Bay in 1984. *Science* **228**: 70–73.

Shick, J. M., E. Gnaiger, J. Widdows, B. L. Bayne, and A. de Zwaan. 1986. Activity and metabolism in the mussel *Mytilus edulis* L. during intertidal hypoxia and aerobic recovery. *Physiol. Zool.* **59**: 627–642.

Shick, J. M., J. Widdows, and E. Gnaiger. 1988. Calorimetric studies of behaviour, metabolism and energetics of sessile intertidal animals. *Am. Zool.* **28**: 161–181.

Shumway, S. E., and R. K. Koehn. 1982. Oxygen consumption in the American Oyster *Crassostrea virginica*. *Mar. Ecol. Prog. Ser.* **9**: 59–68.

Shumway, S. E., T. M. Scott, and J. M. Shick. 1983. The effects of anoxia and hydrogen sulphide on survival, activity and metabolic rate in the coot clam, *Mulinia lateralis* (Say). *J. Exp. Mar. Biol. Ecol.* **71**: 135–146.

Silvester, N. R., and M. A. Sleigh. 1984. Hydrodynamic aspects of particle capture by *Mytilus*. *J. Mar. Biol. Assoc. U. K.* **64**: 859–879.

Taft, J. L., W. R. Taylor, E. D. Hartwig, and E. D. Loftus. 1980. Seasonal oxygen depletion in Chesapeake Bay. *Estuaries* **3**: 242–247.

Theede, H., A. Ponat, K. Hiroki, and C. Schlieper. 1969. Studies on the resistance of marine bottom invertebrates to oxygen-deficiency and hydrogen sulphide. *Mar. Biol.* **2**: 325–337.

Widdows, J. 1987. Application of calorimetric methods in ecological studies. Pp. 182–215 in *Thermal and Energetic Studies of Cellular Biological Systems*, A. M. James ed., Wright, Bristol.

Widdows, J., and A. J. Hawkins. 1989. Partitioning of rate of heat dissipation by *Mytilus edulis* into maintenance, feeding and growth components. *Physiol. Zool.* **62**: 764–784.

Wood, L., and W. J. Hargis. 1971. Transport of bivalve larvae in a tidal estuary. Pp. 29–114. *Fourth European Marine Biology Symposium*, D. J. Crisp, ed., Cambridge University Press, London.

de Zwaan, A. 1983. Carbohydrate catabolism in bivalves. Pp 137–175 in *The Mollusca, Vol. 1. Metabolic Biochemistry and Molecular Biomechanics*, P. W. Hochachka, ed. Academic Press, New York.

CONTENTS

Volume 177 Number 2

THE BIOLOGICAL BULLETIN

OCTOBER, 1989

Published by the Marine Biological Laboratory

THE
BIOLOGICAL BULLETIN

PUBLISHED BY

THE MARINE BIOLOGICAL LABORATORY

OCTOBER, 1989

Printed and Issued by
LANCASTER PRESS, Inc.
PRINCE & LEMON STS.
LANCASTER, PA

THE BIOLOGICAL BULLETIN

THE BIOLOGICAL BULLETIN is published six times a year by the Marine Biological Laboratory, MBL Street, Woods Hole, Massachusetts 02543.

Subscriptions and similar matter should be addressed to Subscription Manager, THE BIOLOGICAL BULLETIN, Marine Biological Laboratory, Woods Hole, Massachusetts 02543. Single numbers, $25.00. Subscription per volume (three issues), $57.50 ($115.00 per year for six issues).

Communications relative to manuscripts should be sent to Michael J. Greenberg, Editor-in-Chief, or Pamela L. Clapp, Managing Editor, at the Marine Biological Laboratory, Woods Hole, Massachusetts 02543.

POSTMASTER: Send address changes to THE BIOLOGICAL BULLETIN, Marine Biological Laboratory, Woods Hole, MA 02543.

Second-class postage paid at Woods Hole, MA, and additional mailing offices.
ISSN 0006-3185

INSTRUCTIONS TO AUTHORS

The Biological Bulletin accepts outstanding original research reports of general interest to biologists throughout the world. Papers are usually of intermediate length (10–40 manuscript pages). Very short papers (less than 9 manuscript pages including tables, figures, and bibliography) will be published in a separate section entitled "Notes." A limited number of solicited review papers may be accepted after formal review. A paper will usually appear within four months after its acceptance.

The Editorial Board requests that manuscripts conform to the requirements set below; those manuscripts that do not conform will be returned to authors for correction before review.

1. ***Manuscripts.*** Manuscripts, including figures, should be submitted in triplicate. (Xerox copies of photographs are not acceptable for review purposes.) The original manuscript must be typed in no smaller than 12 pitch, using double spacing (*including* figure legends, footnotes, bibliography, etc.) on one side of 16- or 20-lb. bond paper, 8½ by 11 inches. Please, no right justification. Manuscripts should be proofread carefully and errors corrected legibly in black ink. Pages should be numbered consecutively. Margins on all sides should be at least 1 inch (2.5 cm). Manuscripts should conform to the *Council of Biology Editors Style Manual*, 4th Edition (Council of Biology Editors, 1978) and to American spelling. Unusual abbreviations should be kept to a minimum and should be spelled out on first reference as well as defined in a footnote on the title page. Manuscripts should be divided into the following components: Title page, Abstract (of no more than 200 words), Introduction, Materials and Methods, Results, Discussion, Acknowledgments, Literature Cited, Tables, and Figure Legends. In addition, authors should supply a list of words and phrases under which the article should be indexed.

2. ***Title page.*** The title page consists of: a condensed title or running head of no more than 35 letters and spaces, the manuscript title, authors' names and appropriate addresses, and footnotes listing present addresses, acknowledgments or contribution numbers, and explanation of unusual abbreviations.

3. ***Figures.*** The dimensions of the printed page, 7 by 9 inches, should be kept in mind in preparing figures for publication. We recommend that figures be about 1½ times the linear dimensions of the final printing desired, and that the ratio of the largest to the smallest letter or number and of the thickest to the thinnest line not exceed 1:1.5. Explanatory matter generally should be included in legends, although axes should always be identified on the illustration itself. Figures should be prepared for reproduction as either line cuts or halftones. Figures to be reproduced as line cuts should be unmounted glossy photographic reproductions or drawn in black ink on white paper, good-quality tracing cloth or plastic, or blue-lined coordinate paper. Those to be reproduced as halftones should be mounted on board, with both designating numbers or letters and scale bars affixed directly to the figures. All figures should be numbered in consecutive order, with no distinction between text and plate figures. The author's name and an arrow indicating orientation should appear on the reverse side of all figures.

4. ***Tables, footnotes, figure legends, etc.*** Authors should follow the style in a recent issue of *The Biological Bulletin* in preparing table headings, figure legends, and the like. Because of the high cost of setting tabular material in type, authors are asked to limit such material as much as possible. Tables, with their headings and footnotes, should be typed on separate sheets, numbered with consecutive Roman numerals, and placed after the Literature Cited. Figure legends should contain enough information to make the figure intelligible separate from the text. Legends should be typed double spaced, with consecutive Arabic numbers, on a separate sheet at the end of the paper. Footnotes should be limited to authors' current addresses, acknowledgments or contribution numbers, and explanation of unusual abbreviations. All such footnotes should appear on the title page. Footnotes are not normally permitted in the body of the text.

5. ***Literature cited.*** In the text, literature should be cited by the Harvard system, with papers by more than two authors cited as Jones *et al.*, 1980. Personal communications and material in preparation or in press should be cited in the text only, with author's initials and institutions, unless the material has been formally accepted and a volume number can be supplied. The list of references following the text should be headed Literature Cited, and must be typed double spaced on separate

pages, conforming in punctuation and arrangement to the style of recent issues of *The Biological Bulletin*. Citations should include complete titles and inclusive pagination. Journal abbreviations should normally follow those of the U. S. A. Standards Institute (USASI), as adopted by BIOLOGICAL ABSTRACTS and CHEMICAL ABSTRACTS, with the minor differences set out below. The most generally useful list of biological journal titles is that published each year by BIOLOGICAL ABSTRACTS (BIOSIS List of Serials; the most recent issue). Foreign authors, and others who are accustomed to using THE WORLD LIST OF SCIENTIFIC PERIODICALS, may find a booklet published by the Biological Council of the U.K. (obtainable from the Institute of Biology, 41 Queen's Gate, London, S.W.7, England, U.K.) useful, since it sets out the WORLD LIST abbreviations for most biological journals with notes of the USASI abbreviations where these differ. CHEMICAL ABSTRACTS publishes quarterly supplements of additional abbreviations. The following points of reference style for THE BIOLOGICAL BULLETIN differ from USASI (or modified WORLD LIST) usage:

A. Journal abbreviations, and book titles, all underlined (for *italics*)

B. All components of abbreviations with initial capitals (not as European usage in WORLD LIST *e.g. J. Cell. Comp. Physiol.* NOT *J. cell. comp. Physiol.*)

C. *All* abbreviated components must be followed by a period, whole word components *must not* (*i.e. J. Cancer Res.*)

D. Space between all components (*e.g. J. Cell. Comp. Physiol.*, not *J.Cell.Comp.Physiol.*)

E. Unusual words in journal titles should be spelled out in full, rather than employing new abbreviations invented by the author. For example, use *Rit Vísindafjélags Islendinga* without abbreviation.

F. All single word journal titles in full (*e.g. Veliger, Ecology, Brain*).

G. The order of abbreviated components should be the same as the word order of the complete title (*i.e. Proc.* and *Trans.* placed where they appear, not transposed as in some BIOLOGICAL ABSTRACTS listings).

H. A few well-known international journals in their preferred forms rather than WORLD LIST or USASI usage (*e.g. Nature, Science, Evolution* NOT *Nature, Lond., Science, N.Y.; Evolution, Lancaster, Pa.*)

6. ***Reprints, page proofs, and charges.*** Authors receive their first 100 reprints (without covers) free of charge. Additional reprints may be ordered at time of publication and normally will be delivered about two to three months after the issue date. Authors (or delegates for foreign authors) will receive page proofs of articles shortly before publication. They will be charged the current cost of printers' time for corrections to these (other than corrections of printers' or editors' errors). Other than these charges for authors' alterations, *The Biological Bulletin* does not have page charges.

CONSISTENCY AND VARIABILITY IN PEPTIDE FAMILIES*

*Reprints of the proceedings of this symposium (pp. 167–225) are available for $9.00 from The Biological Bulletin editorial office, Woods Hole, MA 02543.

Reference: *Biol. Bull.* **177**: 167–171. (October, 1989)

Consistency and Variability in Peptide Families: Introduction*

MICHAEL J. GREENBERG[1] AND MICHAEL C. THORNDYKE[2]

[1]*The Whitney Laboratory, University of Florida, St. Augustine, Florida 32086-8623, and*
[2]*Department of Biology, RHBNC, London University, Egham, Surrey, TW20 0EX, U. K.*

Oxytocin and arginine vasopressin were sequenced and synthesized by du Vigneaud in the early '50s. Since then, and especially in recent years, the number of chemically identified peptides has increased enormously. Taking the mammals as an example, and the 1989 Peninsula Laboratories catalog as our text, we would estimate that there are roughly 55 known regulatory peptides in a standard mammalian species (*i.e.*, consensus of man, rat, ox, and pig). Of course, the number of all mammalian peptides would include species variants and would be much larger. In any event, the above estimate must be very conservative; new mammalian peptides are continually being discovered, and many of the novel invertebrate sequences being found will probably also have mammalian analogs. In the end, the total number of peptides in any mammal—and therefore in *any* species—may well be closer to 550 than to 55.

As the pool of sequences (and sequence-watchers) has increased, the tendency of peptides to occur in families characterized by substantial similarities of structure has become more apparent. For about a decade, reviewers of the field have remarked on these families and have attempted to define them, characterize them, and explain their significance (*e.g.*, Blundell and Humbel, 1980; Niall, 1982; Bloom, 1983; Iverson, 1983; Krieger *et al.*, 1983; Acher, 1984; Vigna, 1986; Greenberg and Price, 1983, 1988; Thorndyke, 1988). But peptide families are similar to human ones in their heterogeneity and their resistance to firm definition and characterization. Distinguishing between members and friends, and discerning the role of the association, are common problems.

The structure and functions of peptide families were recently re-examined at a symposium entitled "Consistency and Variability in Peptide Families[1]." The peptide families included in the symposium were meant to reflect the disparity of these groups; *e.g.*, they vary in size, diversity, and phylum of origin. The participants were also disparate in their interests, ranging from the zoological to the medical. The substance of their presentations are summarized in the ten reviews that follow, and bear on two primary issues: the synthesis and distribution of peptide families; and the effects and physiological roles of these assemblages.

Synthesis

The common feature of all secretory peptides is the manner of their synthesis. They are encoded by their genes as a segment of a larger precursor molecule and, after translation, the secretory products are processed out of the precursor by proteolytic enzymes. Steiner *et al.* (1989) suggest, referring to a model system in yeast, that the proteases and peptidases involved in post-translational processing had already appeared in early eukaryotes. Although the mechanisms have been conserved in general, substantial tissue specificity—*e.g.*, in the cleavage sites—has evolved (see the reports by Steiner *et al.*, 1989; Dockray, 1989; and Nagle *et al.*, 1989). As a practical consequence of this divergence, the products of processing cannot be unerringly predicted from conventional processing signals known only from a clone of the gene encoding the precursor. The processed peptides

* This symposium, a component of the Second International Congress of Comparative Physiology and Biochemistry, was held at the Louisiana State University in Baton Rouge on 1 August 1988. It was sponsored jointly by the Division of Comparative Physiology and Biochemistry of the American Society of Zoologists and by the Society for Experimental Biology (United Kingdom). Support for the symposium was provided by the National Science Foundation (DCB-8802916), the Monsanto Company, and ICI (Agrochemicals) U. K. The organizers and participants are pleased to acknowledge their assistance.

must be isolated and characterized chemically (Nagle *et al.*, 1989).

The structural similarity characteristic of peptide families could arise in two ways. The primary one is through the duplication of the segment of a gene encoding a particular peptide and its processing signals, or the duplication of the entire gene; subsequent point mutation in one or the other of the sister sequences would then yield a novel peptide. This mechanism is evident where very similar sequences are part of the same precursor (*e.g.*, VIP and PHI, substances P and K, the α-, β-, and γ-bag cell peptides, and FMRFamide and FLRFamide), or similar precursors [*e.g.*, the PP-RPs, the egg-laying hormone (ELH) family of *Aplysia*, and the adipokinetic hormones (AKHs) of locust]. Even where sequence similarity is low, the peptides may have similar tertiary structures (*e.g.*, the insulin/IGF family), suggesting divergence from a common genetic origin.

But peptide families—or new members of existing families—can also occur by chance, particularly when the peptides, or critical sequences, are short. Such examples of convergence are detectable when two modestly similar peptides occur on dissimilar precursors. This is the basis for relegating the tachykinins and bombesin-related peptides to separate families (see Vigna, 1989). Similarly, its distinctive precursor leads Dockray (1989) to usher the amphibian peptide caerulein out of the gastrin/CCK family. As peptides become shorter, the possibility that similar sequences are convergent increases. If the precursor organization of a short peptide is not known, convergence may not be detectable (Price and Greenberg, 1989).

Just as familial sequences can occur by chance—*i.e.*, without gene duplication—so the FMRFamide precursors in molluscs, containing 10–28 identical copies of the peptide, exemplify the possibility that replication can occur without the subsequent emergence of a novel peptide. This degree of replication, incidentally, is matched by no other peptide precursor, including prometenkephalin or the yeast α-mating factor.

Distribution

Tissues

All of our representative peptide families include one or more members that are expressed in nerve. The exception is the sub-group of insulin-related peptides in vertebrates, the long-sought insulin-like molecule in brain having yet to be sequenced. In fact, the tendency of vertebrate neuropeptides to occur, as well, in non-nervous tissue—especially the gut and its derivative glands, the heart, and the skin—has been taken as a distinguishing feature of vertebrates; most known regulatory peptides of invertebrates are secreted by neurons [*e.g.*, the AKH-, pigment dispersing hormone- (PDH-), and FMRFamide-related peptides in this symposium]. But the discovery of molluscan insulin-related peptide in snail gut (see Ebberink *et al.*, 1989), the occurrence of eledoisin (the first tachykinin) in octopus posterior salivary gland (see Vigna, 1989), and of ELH analogs in *Aplysia* atrial gland (see Nagle *et al.*, 1989) suggests that this distinction between vertebrates and invertebrates may not be valid. Possibly, the hunt for peptides in invertebrate gut and other non-neural tissues should be intensified.

Phyletic distribution

Congeners of peptides discovered in one species are routinely identified in other, more or less closely related, species. The set of all such congeners in all species constitutes an extended peptide family, and we would expect its taxonomic limits to be at least those of a phylum. We would like to know the extent to which peptide families are restricted in their phyletic distributions. This also bears on peptide evolution; extended peptide families are usually thought of as comprising congeners that have evolved from a common ancestral precursor encoded by an ancestral gene. Thus, widely ranging peptide families would have evolved earlier in metazoan phylogeny than restricted ones. Of course, the ancestral molecules are no longer available, so, as discussed above, the evidence for homology rests on the extent of the structural similarities between the genes, precursors, and peptides (as available) constituting the extant peptide family.

The phyletic limits of peptide families are varied. At one end of the range, insulin-like molecules of rather similar structure occur throughout the vertebrates and share structural similarities with the prothoracicotrophic hormone (PTTH, bombyxin) of insects and with a molluscan insulin-like peptide (MIP) from growth-regulating neurosecretory cells of the snail *Lymnaea stagnalis* (Ebberink *et al.*, 1989; Steiner *et al.*, 1989). Ebberink *et al.* (1989) argue further that, because this superfamily includes peptides sequenced in arthropods, molluscs, and vertebrates, it must have diverged from an ancestral gene present in the earliest metazoans. This hypothesis suggests that insulin-like peptides will eventually be found in all animal species.

Peptides from four protostomian phyla have sequences compellingly similar to FMRFamide, and they seem to be homologs. In contrast, the sequence similarity between FMRFamide and certain vertebrate and coelenterate peptides is probably fortuitous (reviewed by Price and Greenberg, 1989). Therefore, although the family of FMRFamide-related peptides is polyphyletic, it is more narrowly distributed than the insulin-like peptides.

If we accept only sequences as evidence, then most vertebrate peptide families appear to be restricted to that

group. The few exceptions, however, tend to inhibit dogma. These are: eledoisin, the molluscan tachykinin (see Vigna, 1989); the molluscan opioid peptides (reviewed by Greenberg and Price, 1988); and the lobster neurotensin (Kirschenbaum and Carraway, 1986). And although only vertebrate sequences are known from the large VIP/PHI/PHM/glucagon/secretin family, Thorndyke *et al.* (1989) provide evidence of similar peptides in flatworms. On the other hand, the leucosulfakinins are probably *not* members in cockroaches of the vertebrate gastrin/CCK family (see Dockray, 1989).

With the exception of the FMRFamide-related peptides, and on current evidence, the invertebrate peptide families are, like the vertebrate ones, limited to a single phylum. An encouraging finding is that congeners of the pigment-dispersing hormones (PDH) of crustaceans have now been demonstrated in insects as well (Rao and Riehm, 1989). Thus, their distribution is parallel to that of the family of peptides related to AKH of insects and red pigment-concentrating hormone (RPCH) of crustaceans.

In summary, most peptide families seem to have restricted ranges; but the restriction may only reflect the technical difficulties of identifying peptides in unusual places.

New Peptide Families

Most of the peptide families found recently have been detected by the effects of extracts on bioassays. Among the invertebrate assay preparations, the anterior byssus retractor muscle (ABRM) of *Mytilus* (Hirata *et al.*, 1987, 1988), the accessory radula closer (ARC) muscle of *Aplysia* (Cropper *et al.*, 1987; 1988), and the cockroach hindgut (G. M. Holman, references in Goldsworthy and Mordue, 1989) have been especially productive of new peptide families. Some success has also been achieved with relatively unselective chemical assays, genetic techniques, and radioimmunoassay (RIA) (see Price and Greenberg, 1989; Elphick *et al.*, 1989). However, the latter two techniques are aimed at chemical structures that are already known. Therefore, although developing new bioassay techniques in strange species is inconvenient, it provides the best hope of identifying the large number of yet unknown peptide families.

Functional Significance of Peptide Families

Tissue-specific synthesis

The co-evolution of families of peptides and their receptors is widely seen as augmenting the number and variety of regulatory agents in a species. Where the sibling peptides occur on separate precursors, the genes encoding the precursors are expressed in specific tissues and may, therefore, have distinct physiological roles. Even when two or more sibling peptides are produced from a single precursor, tissue-specific processing still permits tissue-specific function. Moreover, there is a growing roster of alternative modes of transcription and processing [considered by Dockray, 1989, and Vigna, 1989; but also see Newcomb *et al.*, 1988; and Fisher *et al.*, 1988 (ELH); Hekimi *et al.*, 1989; and Schulz-Aellen *et al.*, 1989 (AKH)]. The high degree of replication of FMRFamide in its precursors remains enigmatic, but the variety of processing signals at the C-terminals of the copies suggests that differential processing could be regulating the quantity of peptide released at specific sites, or under particular conditions.

A hierarchy of actions

Most peptides have a repertoire of fundamental actions, each initiated by binding to one of a set of complementary receptors, and mediated by one of the several common intracellular mechanisms. The many effects of FMRFamide on nerve, muscle, and gland cells are illustrative (Kobayashi and Muneoka, 1989). But for many peptides, and especially the newly discovered ones, the range of effects is not yet close to being known. An example is the insect analog of PDH which is assayed on crustacean melanophores, not present in insects (see Rao and Riehm, 1989).

Complementary actions of peptides at different sites often produce an integrated effect on organs or systems. Dockray (1989) refers to the cluster of effects as "families of actions" pointing in particular to the actions of CCK on the pancreas, gall bladder, and stomach which serve to "regulate the environment of the small intestine." Other families of actions were reported: *e.g.*, enhanced fluid and protein secretion by intestinal and digestive glands caused by VIP (Thorndyke *et al.*, 1989); inhibition of pancreatic and gastric activity and delay of gastric emptying and intestinal transport to enhance digestion and absorption in small bowel malabsorption, by PYY (Taylor, 1989); and mobilization, transport, and utilization of metabolic fuel for flight in locust by AKH (Goldsworthy and Mordue, 1989).

At the next highest level of integration, organismal functions are commonly allocated among the peptides in a family. The division of labor among sibling peptides—*e.g.*, CCK and gastrin; PPY and pancreatic polypeptide (PP); and substances P and K—in regulating aspects of vertebrate gut function is set out by Dockray (1989), Taylor (1989), and Vigna (1989), respectively. In other instances of complementarity: the ELH-gene products and atrial gland peptides affect reproductive behavior in *Aplysia*, in the latter case as secreted pheromones (Nagle *et al.*, 1989); the tetrapeptide and heptapeptide FaRPs

have distinct effects on muscle tone and posture in pulmonate snails (references in Price and Greenberg, 1989); and FMRFamide and FLRFamide modulate opposed gastropod buccal muscles (Kobayashi and Muneoka, 1989). AKH I and II may have complementary actions on the fat body of the locust (Goldsworthy and Mordue, 1989). Finally, the lack of specific actions by SCP_A and SCP_B in *Aplysia* (see Lloyd, 1986) suggests that separate receptors have not yet evolved, or have not yet been found.

Specificity of action by sibling peptides is provided by two primary mechanisms. First, the receptors can have different specificities, and this is certainly the case for some of the vertebrate gut peptides (Thorndyke *et al.*, 1989; Vigna, 1989; Dockray, 1989) and for the FaRPs (Payza, 1988; and Kobayashi and Muneoka, 1989). Moreover, the evolution of new receptors has, in some cases, occurred relatively recently (Dockray, 1989; Vigna, 1989). However, sibling peptides with different effects can act at what appears to be the same receptor; *e.g.*, egg-laying induced by atrial gland peptides (Nagle *et al.*, 1989) and vasoconstriction and inhibition of pancreatic secretion by PYY and NPY (Taylor, 1989). In such instances, specificity is ensured by differences in the timing and site of release (see especially Taylor, 1989).

Vigna (1989) cites two actions of bombesin—acid secretion by the stomach, and reduction of body temperature—demonstrable both in mammals and fish, but effected by different mechanisms in the two groups. He suggests, then, that peptide actions, if not their mechanisms, are conserved in evolution. The actions of peptides certainly appear to be conserved within classes of animals (*e.g.*, vertebrates, gastropods, crustaceans, and insects), but there has been little testing of those taxonomic limits. The regulation of growth by the insulin-like peptide of *Lymnaea* does suggest conservation, but the steroidogenic action of small PTTH-II is less convincing. Moreover, important metabolic functions of insulin in insects seem to be carried out by the AKH-like peptides (Goldsworthy and Mordue, 1989). Finally, the chromatophorotrophic hormones of crustaceans, PDH and RPCH, have actions different from those of their homologs in insects (Rao and Riehm, 1989; Goldsworthy and Mordue, 1989). Since PDH and RPCH are antagonists in crustaceans, will the PDH analogs have actions in insects opposite to those of AKH?

Finally, lest we forget, the actions of effector organs are modulated by several neuropeptides from different families, as well as by classical transmitters. This is apparent in most of the reports in this symposium, but is pointedly illustrated by the studies of Klaudiusz Weiss and his associates (Cropper *et al.*, 1987, 1988) showing that a single effector, the accessory radula closer muscle of *Aplysia*, is regulated by more than ten agents. So, the effect of a single peptide on a tissue, or cell, or even a subcellular fragment, can certainly be designated as its "action," but its "function" or "physiological role" is necessarily fractional or participatory. As for the effector, it can best be seen as a kind of olfactory organ, its physiological response dependent upon the particular combination, and relative concentrations, of regulatory agents delivered to its vicinity by neurons or the circulation. The responses of effector organs are mediated by receptors, and further study of these proteins should help to elucidate the functional and evolutionary relationships among peptides.

Literature Cited

Acher, R. 1984. Evolution of neurohormonal peptides: from genetic machinery to functional tailoring. Pp. 181–201 in *Evolution and tumour pathology of the neuroendocrine system*, S. Falkmer, R. Håkanson, and F. Sundler, eds., Elsevier Science Publishers, Amsterdam.

Bloom, F. E. 1983. The endorphins: a growing family of pharmacologically pertinent peptides. *Ann. Rev. Pharmacol. Toxicol.* **23:** 151–170.

Blundell, T. L., and R. E. Humbel. 1980. Hormone families: pancreatic hormones and homologous growth factors. *Nature* **287:** 781–787.

Cropper, E. C., P. E. Lloyd, W. Reed, R. Tenenbaum, I. Kupferman, and K. R. Weiss. 1987. Multiple neuropeptides in cholinergic motor neurons of *Aplysia*: evidence for modulation intrinsic to the motor circuit. *Proc. Natl. Acad. Sci., USA* **84:** 3486–3490.

Cropper, E. C., R. Tenenbaum, M. A. Gawinowicz Kolks, I. Kupfermann, and K. R. Weiss. 1987. Myomodulin: a bioactive neuropeptide present in an identified cholinergic buccal motor neuron of *Aplysia*. *Proc. Natl. Acad. Sci. USA* **84:** 5483–5486.

Cropper, E. C., M. W. Miller, R. Tenenbaum, M. A. G. Kolks, I. Kupfermann, and K. R. Weiss. 1988. Structure and action of buccalin: a modulatory neuropeptide localized to an identified small cardioactive peptide-containing cholinergic motor neuron of *Aplysia californica*. *Proc. Natl. Acad. Sci. USA* **85:** 6177–6181.

***Dockray, G. J. 1989.** Gastrin, cholecystokinin (CCK), and the leucosulfakinins. *Biol. Bull.* **177:** 195–197.

***Ebberink, R. H. M., A. B. Smit, and J. van Minnen. 1989.** The insulin family: evolution of structure and function in vertebrates and invertebrates. *Biol. Bull.* **177:** 176–182.

Elphick, M. R., D. A. Price, T. D. Lee, and M. C. Thorndyke. 1989. The SALMFamides: a new family of neuropeptides isolated from an echinoderm. *Neurosci. Abst.* **15:** 1276.

Fisher, J. M., W. Sossin, R. Newcomb, and R. H. Scheller. 1988. Multiple neuropeptides derived from a common precursor are differentially packaged and transported. *Cell* **54:** 813–822.

***Goldsworthy, G., and W. Mordue. 1989.** Adipokinetic hormones: functions and structures. *Biol. Bull.* **177:** 218–224.

Greenberg, M. J., and D. A. Price. 1983. Invertebrate neuropeptides: native and naturalized. *Ann. Rev. Physiol.* **45:** 271–288.

Greenberg, M. J., and D. A. Price. 1988. The phylogenetic and biomedical significance of extended neuropeptide families. Pp. 85–96 in *Biomedical Importance of Marine Organisms*, D. G. Fautin, W. Fenical and W. R. Kem, eds. Mem. California Acad. Sci., San Francisco.

Hekimi, S., W. Burkhart, M. Moyer, E. Fowler, and M. O'Shea.

1989. Dimer structure of a neuropeptide precursor established: consequences for processing. *Neuron* **2:** 1363–1368.

Hirata, T., I. Kubota, I. Takabatake, A. Kawahara, N. Shimamoto, and Y. Muneoka. 1987. Catch-relaxing peptide isolated from *Mytilus* pedal ganglia. *Brain Res.* **422:** 374–376.

Hirata, T., I. Kubota, N. Iwasawa, I. Takabatake, T. Ikeda, and Y. Muneoka. 1988. Structures and actions of *Mytilus* inhibitory peptides. *Biochem. Biophys. Res. Comm.* **152:** 1376–1382.

Iverson, L. L. 1983. Nonopioid neuropeptides in mammalian CNS. *Ann. Rev. Pharmacol. Toxicol.* **23:** 1–27.

Kirschenbaum, S. R., and R. E. Carraway. 1986. Neurotensin-like peptide in an invertebrate, (*Homarus americanus*). *Soc. Neurosci. Abstr.* **13:** 236.

***Kobayashi, M., and Y. Muneoka. 1989.** Functions, receptors, and mechanisms of the FMRFamide-related peptides. *Biol. Bull.* **177:** 206–209.

Krieger, D. T., M. J. Brownstein, and J. B. Martin. 1983. Introduction. Pp. 1–12 in *Brain Peptides,* D. T. Krieger, M. J. Brownstein and J. B. Martin, eds. Wiley, New York.

Lloyd, P. E. 1986. The small cardioactive peptides: a class of modulatory neuropeptides in *Aplysia. Trends Neurosci.* **9:** 428–432.

***Nagle, G. T., S. D. Painter, and J. E. Blankenship. 1989.** The egg-laying hormone family: precursors, products and functions. *Biol. Bull.* **177:** 210–217.

Newcomb, R., J. M. Fisher, and R. H. Scheller. 1988. Processing of the egg-laying hormone (ELH) precursor in the bag cell neurons of *Aplysia. J. Biol. Chem.* **263:** 12514–12521.

Niall, H. D. 1982. The evolution of peptide hormones. *Ann. Rev. Physiol.* **44:** 615–624.

***Price, D. A., and M. J. Greenberg. 1989.** The hunting of the FaRPs. *Biol. Bull.* **177:** 198–205.

***Rao, K. R., and J. P. Riehm. 1989.** The pigment-dispersing hormone family: chemistry, structure-activity relations, and distribution. *Biol. Bull.* **177:** 225–229.

Schulz-Aellen, M.-F., E. Roulet, J. Fischer-Lougheed, and M. O'Shea. 1989. Synthesis of a homodimer neurohormone precursor of locust adipokinetic hormone studied by *in vitro* translation and cDNA cloning. *Neuron* **2:** 1369–1373.

***Steiner, D. F., S. J. Chan, S. P. Smeekens, G. I. Bell, S. Emdin, and S. Falkmer. 1989.** Evolution of peptide hormones of the islets of Langerhans and of mechanisms of proteolytic processing. *Biol. Bull.* **177:** 172–175.

***Taylor, I. 1989.** Peptide YY: the ileo-colonic, gastric, and pancreatic inhibitor. *Biol. Bull.* **177:** 187–191.

Thorndyke, M. C. 1988. Molecular diversity and conformity of neurohormonal peptides: clues to an adaptive role in evolution. *Biol. J. Linnean Soc.* **34:** 249–267.

***Thorndyke, M. C., J. H. Riddell, D. T. Thwaites, and R. Dimaline. 1989.** Vasoactive intestinal polypeptide and its relatives: biochemistry, distribution, and functions. *Biol. Bull.* **177:** 183–186.

Vigna, S. R. 1986. Evolution of hormone and receptor diversity: cholecystokinin and gastrin. *Am. Zool.* **26:** 1033–1040.

***Vigna, S. R. 1989.** Tachykinins and the bombesin-related peptides: receptors and functions. *Biol. Bull.* **177:** 192–194.

* Reviews by the participants in this symposium.

Reference: *Biol. Bull.* **177**: 172–175. (October, 1989)

Evolution of Peptide Hormones of the Islets of Langerhans and of Mechanisms of Proteolytic Processing

D. F. STEINER[1], S. J. CHAN[1], S. P. SMEEKENS[1], G. I. BELL[1], S. EMDIN[2], AND S. FALKMER[3]

[1]*Howard Hughes Medical Institute and the Department of Biochemistry and Molecular Biology, the University of Chicago, Chicago, Illinois;* [2]*Department of Surgery, the University of Umeå, Umeå, Sweden; and* [3]*Department of Pathology, Karolinska Institute Hospital, Stockholm, Sweden*

The islets of Langerhans in vertebrates are the sources of four major peptide hormones—insulin, glucagon, pancreatic polypeptide, and somatostatin. In development, the islets probably arise from ductal precursor cells within pancreatic rudiments that grow out from the midgut region of the embryo. Various lines of evidence support the view that the islets are of endodermal origin, despite indications that islet cells seem to share some constituents and properties with nerve cells (Falkmer *et al.*, 1984; Steiner, 1984). In evolution the islets also appear to have arisen from the gut; *e.g.*, in amphioxus, the exocrine and endocrine pancreatic cells are within the gut, while in the cyclostomes the insulin-producing cells and somatostatin-producing D cells have moved out from the intestinal epithelium to form a small tissue mass—the islet organ—that lies near the entrance of the bile duct (Falkmer *et al.*, 1984).

Studies on the biosynthesis of insulin in the hagfish (*Myxine glutinosa*) have demonstrated the existence of a precursor that is closely similar in structure to the preproinsulins of higher forms (Steiner, 1984). The peptide begins with a typical 24 amino acid hydrophobic signal sequence, which is followed by the B chain, C-peptide, and A chain, making up the proinsulin molecule. The processing of the signal peptide occurs very early in biosynthesis, during or shortly after the transfer of the nascent preproinsulin chain into the cysternae of the rough endoplasmic reticulum (Steiner, 1984; Steiner *et al.*, 1986). Hagfish proinsulin has a connecting segment, or C-peptide, that is similar in length to that of human and other mammalian C-peptides. Because mutations have a rapid rate of fixation in this part of the molecule (about 15 times faster than in the insulin A and B chains), there is no sequence similarity with the C-peptides of higher vertebrates (Steiner, 1984). Nonetheless, the typical pairs of basic residues (Lys-Arg) lie at either end of the C-peptide, linking it to the B and A chains in hagfish proinsulin. The processing of proinsulin occurs in the early (pro)secretory vesicles derived from the *trans* Golgi cysternae and, although the time course is considerably slower in the hagfish, the proteolytic mechanism itself appears to be fundamentally similar.

Hagfish insulin differs at about 40% of positions from higher vertebrate insulins, which is to be expected since the cyclostomes diverged from the vertebrate line approximately 500 M years ago. Despite these substitutions, the folding of the peptide chain in crystals of hagfish insulin is almost superimposable on that derived from x-ray analyses of porcine insulin crystals (Steiner, 1984). Clearly, therefore, in the evolution of proteins, it is the "fold" (tertiary structure) that is more highly conserved than the amino acid sequence (primary structure).

Precursors similar in general structural organization to that of proinsulin have been identified for the other three principal islet hormones (Fig. 1), as well as for most other small peptide hormones, growth factors, and neuropeptides. In the majority of prohormones, proteolytic maturation occurs at pairs of basic residues, usually Lys-Arg or Arg-Arg. Occasional cleavages also occur at monobasic sites, such as Pro-Arg, Arg-Pro, Lys-Ser, etc., as well as rarely at non-tryptic sites such as Leu-Ala. Evidence suggests that a number of different proteases may be in-

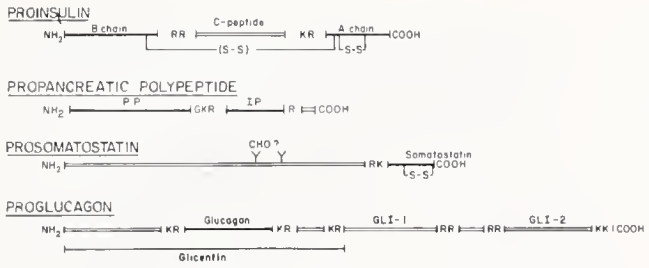

Figure 1. Schematic comparison of the primary structures of the major islet prohormones produced in the four islet cell subpopulations; *e.g.*, proinsulin (β cell), propancreatic polypeptide (PP cell), prosomatostatin (D cell), proglucagon (α cell). All four precursors are synthesized initially with an N-terminal hydrophobic signal peptide (not shown). The solid lines denote the identified product peptides. Sites of processing, at dibasic or single basic residues, are indicated by the letters K (lysine) or R (arginine); these residues are removed during the conversion process. G denotes glycine which, when it occurs at the C-terminal, serves as a substrate for amidation. Note: in *islets of Langerhans*, proglucagon is processed only at the three KR sequences to generate glucagon (heavy line) and a large C-terminal fragment (major proglucagon fragment) containing glucagon-like peptides 1 and 2 (GLI-1 and GLI-2); but in *intestinal proglucagon-expressing cells*, proglucagon is processed to liberate GLI-1 and -2 and glicentin, a larger glucagon-containing N-terminal peptide. Product peptides are usually stored and secreted together, whether biologically active or inactive. Abbreviations: PP, pancreatic peptide; IP, icosapeptide; CHO, potential N-glycosylation sites.

volved in various endocrine tissues, most having cleavage specificities similar to trypsin, but, of course, with much greater site selectivity.

Perhaps the best model system for studying these enzymes is yeast, where direct identification of several converting proteases has been achieved by applying genetic approaches. The yeast mating pheromone, α factor, is derived from a multicopy prohormone that is similar in its organization to many of the mammalian prohormones (Fuller *et al.*, 1988). In yeast, pro α factor is processed by the Kex2 proteases at Lys-Arg sequences, to liberate several copies of an extended form of the α factor peptide which is then trimmed from the N-terminus by an amino dipeptidase, and from the C-terminus by a carboxypeptidase B-like enzyme (Kex1) to yield the mature α factor peptide. Analysis of the gene encoding the Kex2 protease revealed a large open reading frame encoding an 814 amino acid protein (Fuller *et al.*, 1988; Mizuno *et al.*, 1988). Within this sequence, lying nearer the N-terminus, is a region that is homologous to the serine protease subtilisin, and near the C-terminus is a 21 residue hydrophobic region that may serve as a transmembrane domain, indicating that the protease is membrane-associated. The Kex2 product, when expressed and purified, has the expected proteolytic activity and is stimulated by calcium ions. When its gene is expressed in mammalian cell lines, Kex2 correctly cleaves neuroendocrine precursors (Thomas *et al.*, 1988).

No other proteases of comparable structure to Kex2 have yet been isolated. Recently, however, Davidson *et al.* described two calcium stimulated proteases in rat islet tumor secretory granules (Davidson *et al.*, 1988). Each of these selectively cleaves only one of the two sites, Arg-Arg or Lys-Arg, respectively, in rat proinsulin. This finding implies that mammalian enzymes somewhat similar to Kex2 may exist and, furthermore, that these enzymes may be selective for particular pairs of basic residues. A related observation of interest is that, although the insulin precursors described thus far in the most primitive vertebrates (*e.g.*, cyclostomes and teleosts) have only Lys-Arg at cleavage sites, mammalian precursors frequently contain other combinations, such as Arg-Arg. They occur, for example, in site I of proinsulin (B chain-C-peptide function), and in proglucagon, proopiomelanocortin (POMC), and many others.

Therefore, we speculate that the proteolytic converting enzymes have diverged into a superfamily comprising a range of slightly differing specificities to provide more precise control of tissue specific processing of precursors. Classic examples are the differential processing of POMC in the middle- vs. the anterior pituitary lobes, and that of proglucagon in the pancreatic α cells vs. the intestinal glicentin-producing cells (Fig. 1). The relative contributions of different levels of processing enzymes, as opposed to changes in prosecretory granule pH and calcium content, will be important areas for future research when the various processing enzymes can be identified and measured more accurately.

In contrast to the endoproteases, which in higher organisms still elude detection, a carboxypeptidase B-like processing enzyme has been identified in brain (Fricker *et al.*, 1986) and islet (Davidson and Hutton, 1987) tissues. Its amino acid sequence has been deduced by means of molecular cloning, and the enzyme has been well characterized biochemically (Fricker *et al.*, 1986). Now known as carboxypeptidase H (Skidgel, 1988), it is a homologue of the pancreatic carboxypeptidases A and B and is a soluble constituent of secretory granules, unlike the yeast Kex1 carboxypeptidase, which is membrane-bound and homologous in part to the yeast vacuolar carboxypeptidase Y (Fuller *et al.*, 1988). These differences between the yeast and higher vertebrate processing carboxypeptidases indicate that evolution has introduced significant changes, and suggests that some care should be exercised in extrapolating results from yeast to higher vertebrate processing systems.

The insulin gene provides an interesting example of the distribution and diversification of a fundamental

protein structure in the course of evolution. This gene exists in a single copy in most vertebrates and, as mentioned earlier, encodes a highly conserved preproinsulin molecule (Steiner *et al.*, 1985). Indeed, the same high degree of structural conservation is again evident when the insulin genes from a number of vertebrates are compared. From hagfish, through bony fishes, birds and mammals, this gene has retained two introns in the same relative positions, although these vary considerably in length (Steiner *et al.*, 1985). Moreover, the human insulin gene, which resides on the short arm of chromosome 11 (in man), is flanked by tyrosine hydroxylase on the 5′ side (O'Malley and Rotwein, 1988), and by the insulin like growth factor II (IGF II) gene on its 3′ side (Bell *et al.*, 1985). However, both of these flanking genes are regulated differently in terms of their tissue specificity and transcriptional control. The insulin gene is expressed only in the β cells of the pancreas in most vertebrates that have been examined and is regulated by glucose and cyclic AMP (Steiner *et al.*, 1986). The tyrosine hydroxylase gene is transiently expressed early in the development of the β cells but is repressed at about the time that insulin gene transcription begins (Alpert *et al.*, 1988). On the other hand, IGF II, while being a member of the insulin superfamily and sharing many of the structural features and activities of insulin, is expressed predominantly in the fetus and in multiple tissues (Van Wyk *et al.*, 1984).

Other members of the insulin superfamily include IGF I, relaxin, the insect prothoracicotrophic hormone, PTTH (Nagasawa *et al.*, 1986), and the recently discovered molluscan insulin-like peptide, MIP (Smit *et al.*, 1988; Ebberink *et al.*, 1989). These peptides are related to insulin in that they all conserve the characteristic tertiary "fold." However, it is unlikely that either of the two invertebrate hormones will bind to vertebrate insulin receptors, as they lack important features for binding, such as the conserved residues A21 Asn, B23 Gly, B24 Phe, B25 Phe, and B26 Tyr. Both the *Lymnaea* and *Bombyx* hormones lack these and other important groupings suggesting that they bind to different receptors. On the other hand, insulin receptors show great evolutionary conservation of their binding characteristics throughout the vertebrates (Muggeo *et al.*, 1979). The IGF I receptor is structurally homologous to the insulin receptor (Ullrich *et al.*, 1986), and a homologous receptor that preferentially binds insulin has also been found in *Drosophila* (Nishida *et al.*, 1986; Fernandez-Almonacid and Rosen, 1987). Thus, we suspect that insulin-like molecules more similar to vertebrate insulin must exist in some invertebrates. According to this view, the insulin-like peptides identified thus far in invertebrates, as well as relaxin and any other insulin-related peptides that may ultimately turn up in vertebrates, are likely the products of genes that branched away from the main insulin gene line very early. What seem to be missing at present are molecular links between these more divergent insulin-like peptides and the vertebrate insulin/IGF families with their distinctive receptor binding features (Steiner and Chan, 1988). The new genetic tools should permit us to analyze the gene lineages of peptide hormones and their precursors much more definitively than has hitherto been possible.

Literature Cited

Alpert, S., D. Hanahan, and G. Teitelman. 1988. Hybrid insulin genes reveal a developmental lineage for pancreatic endocrine cells and imply a relationship with neurons. *Cell* **53:** 295–308.

Bell, G. I., D. S. Gerhard, N. M. Fong, R. Sanchez-Pescador, and L. B. Rall. 1985. Isolation of the human insulin-like growth factor genes: the insulin-like growth factor II and insulin genes are contiguous. *Proc. Natl. Acad. Sci. USA* **82:** 6450–6454.

Davidson, H. W., and J. C. Hutton. 1987. The insulin-secretory-granule carboxypeptidase H. *Biochem. J.* **245:** 575–582.

Davidson, H. W., C. J. Rhodes, and J. C. Hutton. 1988. Intraorganellar calcium and pH control proinsulin cleavage in the pancreatic β cell via two distinct site-specific endopeptidases. *Nature* **355:** 93–96.

Ebberink, R. H. M., A. B. Smit, and J. van Minnen. 1989. The insulin family: evolution of structure and function in vertebrates and invertebrates. *Biol. Bull.* **177:** 176–182.

Falkmer, S., M. El-Salhy, and M. Titlbach. 1984. Evolution of the neuroendocrine system in vertebrates—A review with particular reference to the phylogeny and postnatal maturation of the islet parenchyma. Chapter 4, pp. 59–87 in *Evolution and Tumour Pathology of the Neuroendocrine System,* S. Falkmer, R. Håkanson, and F. Sundler, eds., Elsevier, North Holland.

Fernandez-Almonacid, R., and O. M. Rosen. 1987. Structure and ligand specificity of the *Drosophila melanogaster* insulin receptor. *Molecular Cell Biol.* **7:** 2718–2727.

Fricker, L. D., C. J. Evans, F. S. Esch, and E. Herbert. 1986. Cloning and sequence analysis of cDNA for bovine carboxypeptidase E. *Nature* **323:** 461–464.

Fuller, R. S., R. E. Sterne, and J. Thorner. 1988. Enzymes required for yeast prohormone processing. *Ann. Rev. Physiol.* **50:** 345–362.

Mizuno, K., T. Nakamura, T. Ohshima, S. Tanaka, and H. Matsuo. 1988. Yeast *Kex2* gene encodes an endopeptidase homologous to subtilisin-like serine proteases. *Biochem. Biophys. Res. Comm.* **156:** 246–254.

Muggeo, M., B. H. Ginsberg, J. Roth, D. M. Neville, Jr., P. De Meyts, and C. R. Kahn. 1979. The insulin receptor in vertebrates is functionally more conserved during evolution than insulin itself. *Endocrinology* **104:** 1393–1402.

Nagasawa, H., and H. Kataoka, A. Isogai, S. Tamura, A. Suzuki, A. Mizoguchi, Y. Fujiwara, A. Suzuki, S. Y. Takahashi, and H. Ishizaki. 1986. Amino acid sequence of a prothoracicotropic hormone of the silk worm *Bombyx mori*. *Proc. Natl. Acad. Sci. USA* **83:** 5840–5843.

Nishida, Y., M. Hata, Y. Nishizuka, W. J. Rutter, and Y. Ebina. 1986. Cloning of a *Drosophila* cDNA encoding a polypeptide similar to the human insulin receptor precursor. *Biochem. Biophys. Res. Comm.* **141:** 474–481.

O'Malley, K. L., and P. Rotwein. 1988. Human tyrosine hydroxylase

and insulin genes are contiguous on chromosome 11. *Nucleic Acid Res.* **16**: 4437–4446.

Skidgel, R. A. 1988. Basic carboxypeptidases: regulators of peptide hormone activity. *Trends in Pharmacol. Sci.* **9**: 299–304.

Smit, A. B., E. Vreugdenhil, R. H. M. Ebberink, W. P. M. Geraerts, J. Klootsijk, and J. Joosse. 1988. Growth-controlling molluscan neurons produce the precursor of an insulin-related peptide. *Nature* **331**: 535–538.

Steiner, D. F. 1984. The biosynthesis of insulin: genetic, evolutionary and pathophysiologic aspects. Pp. 191–228 in *The Harvey Lectures.* Series 78, Academic Press, New York.

Steiner, D. F., and S. J. Chan. 1988. Perspective: an overview of insulin evolution. *Hormone Metabol. Res.* **20**: 443–444.

Steiner, D. F., S. J. Chan, J. M. Welsh, D. Nielsen, J. Michael, H. S. Tager, and A. H. Rubenstein. 1986. Models of peptide biosynthesis—the molecular and cellular basis of insulin production. *Clin. Invest. Med.* **9**: 328–336.

Steiner, D. F., S. J. Chan, J. M. Welsh, and S. C. M. Kwok. 1985. Structure and evolution of the insulin gene. *Ann. Rev. Genet.* **19**: 463–484.

Thomas, G., B. A. Thorne, L. Thomas, R. G. Allen, D. E. Hruby, R. Fuller, and J. Thorner. 1988. Yeast KEX2 endopeptidase correctly cleaves a neuroendocrine prohormone in mammalian cells. *Science* **241**: 226–230.

Ullrich, A., A. Gray, A. W. Tam, T. Yang-Feng, M. Tsubokawa, C. Collins, W. Henzel, T. Le Bon, S. Kathuria, E. Chen, S. Jacobs, U. Francke, J. Ramachandran, and U. Fujita-Yamaguchi. 1986. Insulin-like growth factor 1 receptor primary structure: comparison with insulin receptor suggests structural determinants that define functional specificity. *EMBO J.* **5**: 2503–2512.

Van Wyk, J. J. 1984. The somatomedins: biological actions and physiologic control mechanisms. Pp. 81–125 in *Hormonal Proteins and Peptides.* Academic Press, NY.

Reference: *Biol. Bull.* **177**: 176–182. (October, 1989)

The Insulin Family: Evolution of Structure and Function in Vertebrates and Invertebrates

R. H. M. EBBERINK, A. B. SMIT, AND J. VAN MINNEN

Biological Laboratory, Vrije Universiteit, de Boelelaan 1087, NL-1081 HV Amsterdam, The Netherlands

Abstract. Insulin and related peptides are key hormonal integrators of growth and metabolism in vertebrates. Recently, the amino acid and DNA sequences of insulin-related peptides in invertebrates have become available. The discovery of such peptides in insects and molluscs substantiates the evidence for an early origin and widespread evolution of the insulin superfamily.

In the silkworm *Bombyx* (Insecta) the prothoracicotropic hormones (bombyxins I, II, and III; previously called PTTH) are produced in the brain and may stimulate synthesis and release of ecdysone; thus they play a central role in insect development. In the freshwater snail *Lymnaea* (Mollusca), a growth stimulating hormone (molluscan insulin-related peptide; MIP) is produced in the brain, and two other insulin-related peptides are produced in the digestive system. The MIPs are involved in body and shell growth and energy metabolism. The finding that bombyxin and MIP are involved in the control of growth fits with ideas being developed in the vertebrate field that the role of insulin is not confined to glucose metabolism, but is also related to growth.

Introduction

The structure of the insulin molecule has been highly conserved during vertebrate evolution (Chance *et al.*, 1968; Blundell *et al.*, 1972; Cutfield *et al.*, 1979, 1986; Chan *et al.*, 1981; Bajaj *et al.*, 1983; Emdin *et al.*, 1985; Le Roith *et al.*, 1987; Pollock *et al.*, 1987). At the moment, the primary structures of insulins from over 40 vertebrate species are known. In addition, the preproinsulin genes and cDNA sequences from over 12 species have been determined (Lomedica *et al.*, 1979; Hahn *et al.*, 1983; Steiner *et al.*, 1985). Therefore, for vertebrates, the structures of preproinsulins and the insulin-like growth factors could be integrated to produce an evolutionary picture of this hormone superfamily. We will not discuss the evolution of vertebrate insulins; this has already been done several times (*e.g.*, Steiner *et al.*, 1985). Rather, we will consider the varied evidence, obtained during the last few years, that modern invertebrates, and in particular the insects and the molluscs, also contain insulin-related peptides. Furthermore, we will inquire about the nature of the insulin molecule and compare its functions in insects and molluscs with those in vertebrates.

When considering the evolutionary aspects of insulins in the animal kingdom, we should keep in mind that the various phyla have had a polyphyletic origin; *i.e.*, four major groups—the chordates and vertebrates, the echinoderms and tentaculates, the coelenterates, and the molluscs, worms, and arthropods—are now considered to have evolved independently of each other (Fig. 1). An important consequence of this polyphyletic origin is that if insulin occurs in the two main branches of the phylogenetic tree, then it must have already been present in the Archaemetazoa.

Evidence for Insulins in Invertebrates

Because invertebrates as well as vertebrates rely upon the same organic molecules for metabolism, both groups should, in theory, possess insulin. The experimental evidence in support of this notion comes from two different approaches: immunocytochemistry and biochemistry.

With immunocytochemistry, rapid strides have been made in the identification of invertebrate cells and tissues that are reactive to anti-insulin. Most of the observations have been carried out with antisera raised to mammalian insulin, and positive results have been obtained

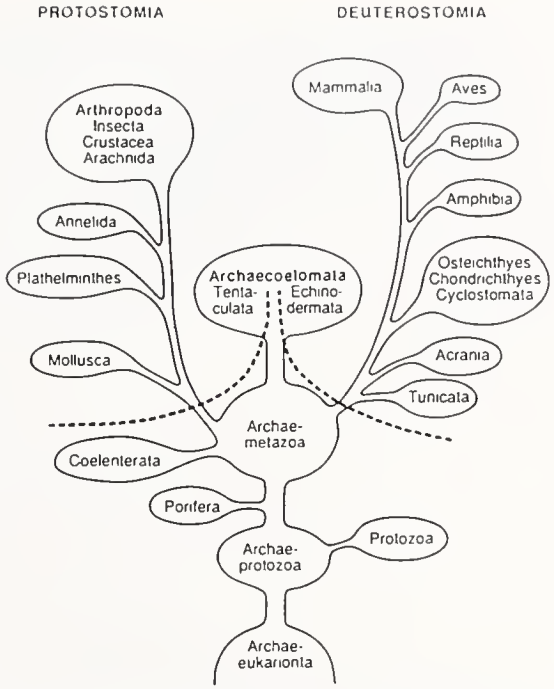

Figure 1. A phylogenetic tree, showing the polyphyletic origin of the various phyla in the animal kingdom. (Modified and extended after Karlson, 1983).

Table I

Identification of insulin-like peptides in invertebrates by immunocytochemistry

Insecta		
Calliphora vomitoria	Median neurosecretory cells	Duve and Thorpe, 1979
Bombyx mori	Median neurosecretory cells	Yui *et al.*, 1980
Locust migratoria	Median neurosecretory cells	Orchard and Loughton, 1980
Manduca sexta	Median neurosecretory cells	El-Salhy *et al.*, 1984
Eristalis aeneus	Pars intercerebralis	El-Salhy *et al.*, 1980
Apis millifera	Brain	Maier *et al.*, 1981
Mollusca		
Lymnaea stagnalis	Small cells in cerebral ganglia	Schot *et al.*, 1981
	Light green cells	van Minnen., 1987
Anodonta cygnea	Midgut	Plisetskaya, 1978
Unio pictorum	Midgut	Plisetskaya, 1978
Mytilus edulis	Hepatopancreas	Fritch *et al.*, 1976
Tunicata		
Steyla clava	Endocrine cells esophagus	Bevis and Thorndyke, 1978

* For references see literature cited in Joosse and Geraerts (1983) and Thorpe and Duve (1984).

in a range of different species, primarily insects and molluscs (Table I). In molluscs, immunoreactivity occurs not only in neuronal tissue, but also in the epithelia of the gut and hepatopancreas.

Of course, there are problems and pitfalls in immunocytochemistry. The epitope for anti-insulin deduced from structure-activity analyses, is formed by the region including residues 8, 9, and 10 of the A-chain, and residues 2, 3, and 4 of the B-chain of insulin. The ability of invertebrate tissues to bind anti-mammalian insulin is surprising because non-mammalian insulins, insulin-like growth factors, and relaxin are variable in this region and, therefore, do not bind antibodies to mammalian insulin. However, the neuroendocrine light green cells in the cerebral ganglia of the central nervous system of the freshwater snail have been identified as anti-porcine insulin immunopositive cells (Fig. 2). Indeed, these cells produce an insulin-related peptide with a different epitope region (see below).

The second approach in the identification of insulin-related peptides is biochemistry: extraction, purification, and chemical characterization. Several early reports of insulin-like substances in invertebrates relied upon rather simple or even crude tissue extraction procedures followed by heterologous bioassays (Table II). Later on, RIA and purification studies were performed. Studies on the blowfly, *Calliphora vomitoria*, by Thorpe and Duve (1984) resulted in the purification and amino acid composition of anti-insulin immunoreactive material, although no amino acid sequence analysis was done. Our recent studies on the snail *Lymnaea stagnalis* have resulted in the structural analysis of an insulin-related molecule from the CNS and the purification of two insulin-like substances from the midgut. We have cleaved and

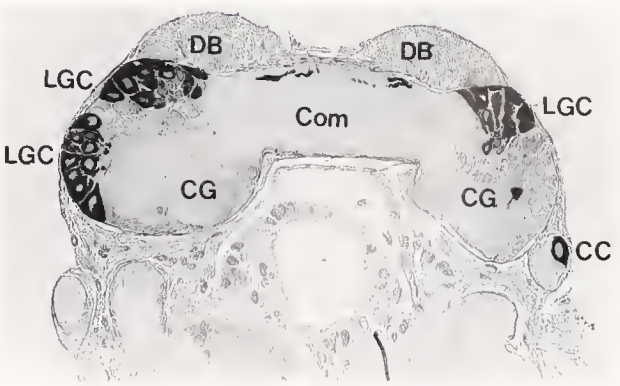

Figure 2. Transverse section through the cerebral ganglia of *Lymnaea stagnalis*. The light green cells (LGC) in the cerebral ganglia (CG) and the canopy cell (CC) in the lateral lobe are labeled by anti-porcine insulin. DB, dorsal body; Com, commissure.

Table II

Biochemical characterization of insulin-like peptides in invertebrates

Insecta		
Apis mellifera	Extract/bioassay	Patel, 1964
Drosophila melanogaster	Extract/bioassay	Meness and Ortiz, 1975
Manduca sexta	Exract/RIA/ bioassay	Kramer *et al.*, 1977
Drosophila melanogaster	Heamolymf/RIA	Seecof and Dewhurst, 1974
Manduca sexta	GPC/RIA	Tager *et al.*, 1975, 1976
Manduca sexta	Amino acid composition	Kramer, 1984
Calliphora vomitoria	GPC/IEG/HPLC	Duve *et al.*, 1979, 1982
	Amino acid composition	Thorpe and Duve, 1984
Drosophila melanogaster	GPC/RIA	Le Roith *et al.*, 1981
Bombix mori	HPLC etc. and sequence	Nagasawa *et al.*, 1984, 1986
Crustacea		
Homarus americanus	RIA/bioassay	Sanders, 1983
Mollusca		
Mya arenaria	extract/bioassay	Collip, 1923
Buccinum imdatum	extract/bioassay	Davidson, 1971
Pectum maximus	extract/bioassay	Davidson, 1971
Ostrea edulis	extract/bioassay	Martinez *et al.*, 1973
Unio pectorum	IEC/RIA	Plisetskaya, 1978
Prophysaon foliolatum	heamolymph/RIA	Plisetskaya and Deyrup, 1987
Lymnaea stagnalis	GPC/HPLC gut-insulin	Hemminga, 1984 Ebberink and Joosse, 1985
Lymnaea stagnalis	HPLC brain-insulin	Ebberink *et al.*, 1987
Lymnaea stagnalis	cDNA brain insulin	Smit *et al.*, 1988
Tunicata		
Pyura pachydermatina	HPLC/RIA	Galloway and Cutfield, 1988

* For references see literature cited in Joosse and Geraerts (1983) and Thorpe and Duve (1984).

separated the A and B chains of the midgut insulin-like substance (Fig. 3), and have determined the amino acid composition of each chain (Table III), but efforts to sequence this material using a protein sequencer have failed since both chains have a blocked N-terminal.

Structure and Function of Insulin-Related Peptides in Invertebrates

The first amino acid sequence information about an insulin-related structure in invertebrates came from the pioneer work of Nagasawa and his colleagues (Nagasawa *et al.*, 1984, 1986) on the prothoracicotrophic hormone (PTTH, now called bombyxin) of the silkworm *Bombyx mori*. Bombyxin is produced by the median neurosecretory cells of the pars intercerebrale of the brain, and controls the secretion of ecdysone from the prothoracic glands during metamorphosis (Ishizaki *et al.*, 1987). Bombyxin was not previously suspected of having any relationship to insulin. The similarity emerged only after 25 years, during which Nagasawa *et al.* purified the peptide from several million heads of *Bombyx* using a 14-step procedure.

Bombyxin II consists of two non-identical chains: the A-chain of 20 residues, and the B-chain of 28 residues (Fig. 4). Besides bombyxin II, two other peptides have been purified. Only the N-terminals of the A-chains of bombyxins I and III have been sequenced, and both have an 80% homology with bombyxin II. Four different forms of bombyxin-II have been published (Fig. 4).

Insulin-related peptides of *Lymnaea* are not only produced in the gut, but also in the neuroendocrine light green cells (LGCs). There are about 200 LGCs located in two pairs of clusters in the cerebral ganglia of the central nervous system of this snail (Fig. 2). The LGC are involved in body and shell growth (Geraerts, 1976; Joosse and Geraerts, 1983; Ebberink and Joosse, 1985). The effects on shell formation include: (1) calcium and bicar-

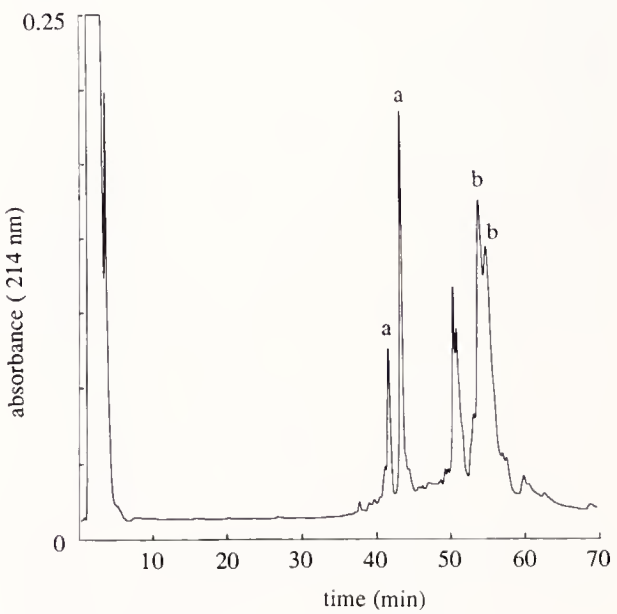

Figure 3. Reverse phase liquid chromatography of purified gut insulin of *Lymnaea stagnalis* after reduction and carboxymethylation. A mixture of two insulin-related peptides was reduced, and the A and B chains were separated on a Bakerbond wide pore C18 column with a gradient of acetonitrile (5–45% in 70 min) in 7.5 m*M* trifluoroacetic acid. The peaks at 51 min are the intact insulins.

Table III

Amino acid composition of the A- and B-chain of gut insulin of Lymnaea *and comparison with brain insulin (MIP) of* Lymnaea *and human insulin*

	A-chain				B-chain			
	Lymnaea gut insulin				*Lymnaea* gut insulin			
	I	II	*Lymnaea* brain insulin	Human insulin	I	II	*Lymnaea* brain insulin	Human insulin
Asx	2	2	1	2	3	3	6	1
Glx	2	2	4	4	2	2	2	3
Cys	~4	~4	5	4	~2	~2	3	2
His	—	1	—	—	3	2	1	2
Ser	2	1	1	2	2	3	5	1
Arg	1	1	1	—	1	1	3	1
Gly	1	1	1	1	2	3	2	3
Thr	1	1	3	1	—	—	—	2
Ala	2	2	—	—	5	6	5	1
Tyr	1	1	1	2	1	1	—	2
Val	1	1	1	1	2	3	3	3
Phe	—	1	—	—	—	—	2	3
Ile	1	1	1	2	2	2	1	—
Leu	2	2	2	2	4	4	2	4
Lys	1	—	1	—	2	2	—	1
Met	nd	nd	1	—	nd	nd	1	—
Pro	nd	nd	2	—	nd	nd	2	1
Trp	nd	nd	—	—	nd	nd	—	—

bonate incorporation into the shell; (2) formation of the periostracum (the proteinaceous component); and (3) the maintenance of high concentrations of calcium-binding protein in the cells of the mantle edge. The effects on the soft body parts are: (1) stimulation of the ornithine decarboxylase activity; (2) mobilization of glycogen stores; (3) regulation of the blood glucose concentration (Fig. 5); and (4) neurite outgrowth.

The first evidence that the LGC may contain an insulin-related peptide came from immunoytochemical data (Fig. 2). To prove that the anti-insulin immunoreactive material is a hormone, the LGCs together with the median lip nerve (the neurohemal area of the LGC), were incubated (*in vitro*) with and without 4-aminopyridine (Fig. 6). After the addition of 4-aminopyridine, the LGC show a strong increase in the number of action potentials, and they release immunoreactive insulin which reaches a maximum level within one hour. In the absence of 4-aminopyridine, only a small amount of immunoreactive insulin was released.

A-chain.

```
 1              5                  10                  15                  20
Gly-Ile-Val-Asp-Glu-Cys-Cys-Leu-Arg-Pro-Cys-Ser-Val-Asp-Val-Leu-Leu-Ser-Tyr-Cys.
```

B-chain.

```
 1              5                  10                  15                  20
Glp-Gln-Pro-Gln-Ala-Val-His-Thr-Tyr-Cys-Gly-Arg-His-Leu-Ala-Arg-Thr-Leu-Ala-Asp-

21             25          28
Leu-Cys-Trp-Glu-Ala-Gly-Val-Asp
```

```
N-terminal region of B-chain of four different forms of Bombyxin-II

Glp-Gln-Pro-Gln-Ala-Val.....
Glp-Gln-Pro-Gln-Gly-Val.....
Glp----------Gln-Ala-Val.....
Glp----------Gln-Gly-Val.....
```

Figure 4. Amino acid sequence of the A and B chains of bombyxin-II (PTTH-II) of *Bombyx mori*.

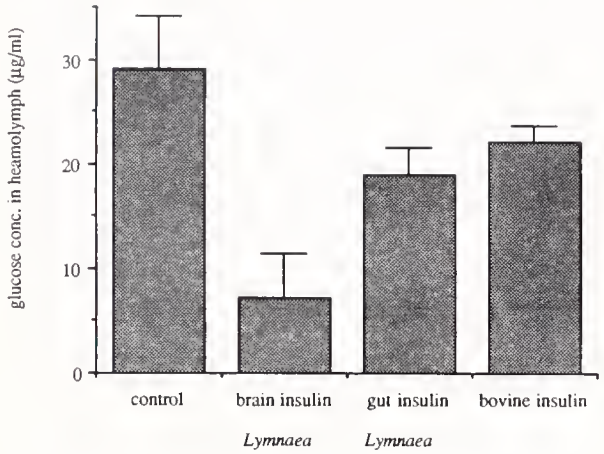

Figure 5. The effect of different insulins on the hemolymph glucose concentration of *Lymnaea stagnalis*. Purified insulins from the light green cells and gut, as well as commercial bovine insulin, were tested. The amount of brain insulin injected in each snail is about the amount stored in one animal (about 2 pmol); for gut insulin, it is the amount stored in about 0.2 animal (about 0.5 pmol); and for bovine insulin, 200 pmol. The blood volume is about 1 ml. (n = 4).

The primary structure of the insulin-related peptide was not obtained via peptide chemistry, but via the nucleotide sequence of an LGC specific cDNA clone (Smit *et al.*, 1988). A differential hybridization technique was used to isolate cerebral LGC cDNA from a central nervous system-specific library of *Lymnaea* cloned in λgt10. Therefore, replica filters of 20,000 clones were screened with a positive cDNA probe synthesized from messenger RNA of the LGC, and with a negative cDNA probe produced from other parts of the cerebral ganglia and the hepatopancreas. The LGC specificity of the clones was tested by *in situ* hybridization using histological sections of the central nervous system (Fig. 7). The LGCs in the cerebral ganglia, and the canopy cell in each lateral lobe (not shown), were the only cell types to express this clone.

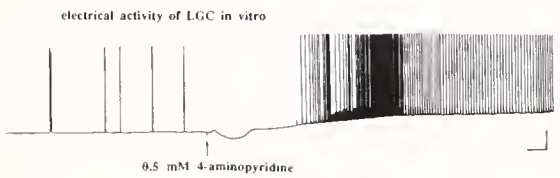

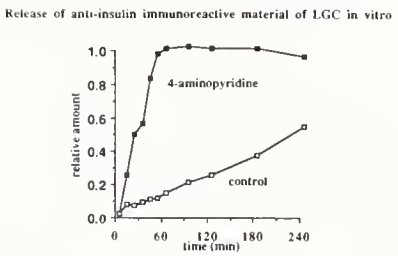

Figure 6. The effect of 4-aminopyridine on the electrical activity of the light green cells (LGC) (top panel). The release of anti-porcine immunoreactive material from the light green cells (bottom panel). Cerebral ganglia (CG) with the median lip nerves were incubated as described previously, with and without 4-aminopyridine (Ebberink *et al.*, 1987).

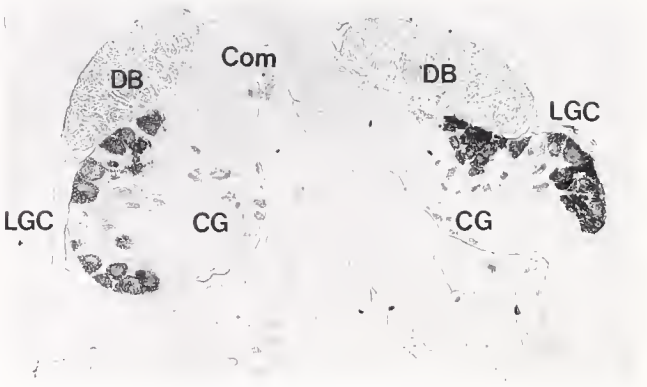

Figure 7. *In situ* hybridization with a 35S-labelled cDNA-probe in sections of the cerebral ganglia. Only hybridization of mRNA in the light green cells (LGC) and canopy cell (not shown) was observed. DB, dorsal body; CG, cerebral ganglia; Com, commissure.

The nucleotide sequence revealed a single open reading frame encoding a protein with characteristics of preproinsulin (Fig. 8) (Smit *et al.*, 1988). Thus, an A and B chain, together with a C peptide equivalent and a putative signal sequence, are present. We called this peptide molluscan insulin-related peptide (MIP).

Comparison of Invertebrate and Vertebrate Insulins

Overall, the amino acid sequences of MIP, bombyxin, and human insulin, are not very similar (Fig. 9). The se-

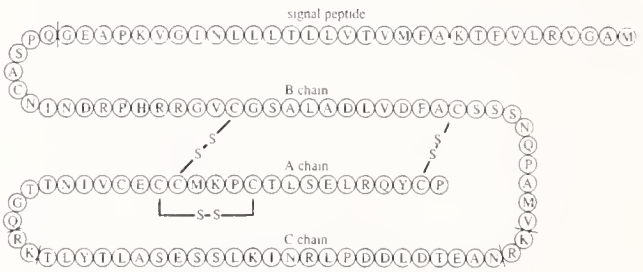

Figure 8. Amino acid sequence of prepro molluscan insulin-related peptide (preproMIP). Residues are designated by their one-letter abbreviations. The putative proteolytic processing sites are indicated (lines between some residues).

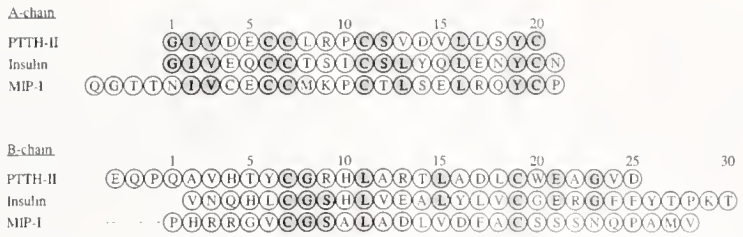

Figure 9. Comparison of the amino acid sequences of the A and B chains of bombyxin (PTTH) of *Bombyx mori*, human insulin, and molluscan insulin-related peptide (MIP) of *Lymnaea stagnalis*. The amino acids are identified by their one-letter abbreviations.

quence similarity in the A chain is about 50% between bombyxin and human insulin, and 40% between MIP and human insulin. In the B chain, the similarity is 25% and 20%, respectively. An amino acid sequence comparison of MIP and bombyxin with known insulins of all vertebrate species permits some interesting conclusions. All of these peptides have cysteines present at position A6, A7, A11, A20, B7, and B19. They have glycine at A1 (except MIP) and at B8, but glycine at B20 is only present in the vertebrate insulins. Most of the hydrophobic residues at the hydrophobic core of the globular structure of insulin are conserved in all insulins. A three-dimensional model of bombyxin and MIP has been constructed with interactive computer graphics and energy minimization techniques (Blundell *et al.*, 1972); homology with porcine insulin (the structure of which has been determined by X-ray analysis) was assumed. The model shows that both bombyxin and MIP form neither the dimers nor the hexamers characteristic of mammalian insulins. The region formed by residues B9-B19 and B22-B26 is involved in the binding of insulin to its receptor (Pullen *et al.*, 1976), and the phenylalanine in position B25 is particularly essential (Blundell and Wood, 1975). Since this region, including B25, differs from that of mammalian insulins, it has been suggested that MIP and bombyxin cannot bind to the vertebrate insulin receptor. However, gut insulin of *Lymnaea* binds very well to insulin receptors of rat fat cells (Ebberink and Joosse, 1985).

Conclusions

It is important that the structures of molluscan and insect insulins have been found at last, more than 30 years after the discovery of the first vertebrate insulin structure.

The structure of the insulin molecule is largely determined by a characteristic arrangement of certain residues in its precursor. That similar arrangements of amino acids seen in the various insulins would have arisen independently in different branches of the phylogenetic tree (Fig. 1) is extremely improbable. We cannot deduce the evolutionary pathway for insulin on the basis of nucleotide differences, since these arise predominantly from neutral mutations. Rather, the finding of insulins in two branches of the phylogenetic tree confirms the model of Blundell and Wood (1975), according to which the evolution of insulins is determined mainly by adaptive processes. The model depends critically on the relationship between such factors as the effects of sequence changes on the three-dimensional structure of the peptide, and the role of various parts of this structure in the conversion of the proinsulin to the active form, the storage of insulin, its transport to the site of action, and its interaction with the receptor. According to this hypothesis, the primary and three dimensional structures conserved in vertebrate insulins must also be conserved in the related peptides of insects and molluscs. Since MIP, the vertebrate insulins and possibly bombyxin are involved in growth, it is important to discover whether the insulin receptors of invertebrates are homologous with those of vertebrates.

According to currently accepted theory, the origin of insulin is to be found in the nervous systems of early multicellular organisms (Pearse, 1967; Pictet *et al.*, 1976; Alpert *et al.*, 1988). Indeed, the localization of an invertebrate insulin within specific neurons of the brain would seem to support such a notion. Until now, the only insulin sequences available were from the central nervous systems of invertebrates and from the pancreas of vertebrates—data that do not test the theory. But we have shown that insulins are present in the gut of molluscs, as well as in the brain. This finding suggests that, contrary to dogma, the insulins might have originated in the brain or in the gut, and possibly also in other tissues of early metazoans. Further, these considerations could imply that the brain of vertebrates also produces insulins. However, at present, the question of the synthesis of insulin in the vertebrate brain is still arguable (Baskin *et al.*, 1987; LeRoith *et al.*, 1987).

Literature Cited

Alpert, S., D. Hanahan, and G. Teitelman. 1988. Hybrid insulin genes reveal a developmental lineage for pancreatic endocrine cells and imply a relationship with neurons. *Cell* **53:** 295–308.

Bajaj, M., T. L. Blundell, J. E. Pitts, S. P. Wood, and M. A. Tatnell. 1983. Dogfish insulin. *Eur. J. Biochem.* **135:** 535–542.

Baskin, D. G., D. P. Figlewisz, S. C. Woods, D. Porte, and D. M. Dorsa. 1987. Insulin in the brain. *Ann. Rev. Physiol.* **49:** 335–347.

Blundell, T. L., J. F. Cutfield, S. M. Cutfield, E. J. Dodson, G. G. Hodgkin, and D. A. Mercola. 1972. Three-dimensional atomic structure of insulin and its relationship to activity. *Diabetes* **21, suppl 2:** 492–505.

Blundell, T. L., and S. P. Wood. 1975. Is the evolution of insulin Darwinian or due to selectively neutral mutation? *Nature* **257:** 197–203.

Chan, S. J., S. O. Emdin, S. C. M. Kwok, J. M. Kramer, S. Falkmar, and D. F. Steiner. 1981. Messenger RNA sequence and primary structure of preproinsulin in a primitive vertebrate, the Atlantic hagfish. *J. Biol. Chem.* **256:** 7595–7602.

Chance, R. E., R. M. Ellis, and W. W. Bromer. 1968. Porcine proinsulin: Characterization and amino acid sequence. *Science* **161:** 165–167.

Cutfield, J. F., S. M. Cutfield, E. J. Dodson, G. G. Dodson, S. F. Emdin, and C. D. Reynolds. 1979. Structure and biological activity of hagfish insulin. *J. Mol. Biol.* **132:** 85–100.

Cutfield, J. F., S. M. Cutfield, A. Carne, S. O. Emdin, and S. Falkmar. 1986. The isolation, purification and amino acid sequence of insulin from the teleost fish *Cottus corpius* (daddy sculpin). *Eur. J Biochem.* **158:** 117–123.

Ebberink, R. H. M., and J. Joosse. 1985. Molecular properties of various snail peptides from brain and gut. *Peptides* **6, suppl 3:** 451–457.

Ebberink, R. H. M., H. van Loenhout, J. van Beek, K. de Wilde, and J. van Minnen. 1987. Characterization of peptides isolated from growth-controlling neuroendocrine cells of *Lymnaea stagnalis* with immunoreactivity to anti-insulin. Pp. 224–227 in *Neurobiology, Molluscan Models,* H. H. Boer, W. P. M. Geraerts, and J. Joosse, eds. North Holland Publishing Company, Amsterdam.

Emdin, S. O., D. F. Steiner, S. J. Chan, and S. Falkmar. 1985. Hagfish insulin: evolution of insulin. Pp. 134 in *Evolutionary Biology of Primitive Fishes,* R. E. Foreman, A. Gorban, J. M. Dodd, and R. Olsson, eds. Plenum, New York.

Galloway, S. M., and J. F. Cutfield. 1988. Insulin-like material from the digestive tract of the tunicate *Pyura pachydermatina* (sea tulip). *Gen. Comp. Endocrinol.* **69:** 106–113.

Geraerts, W. P. M. 1976. Control of growth by the neurosecretory hormone of the light green cells of the freshwater snail *Lymnaea stagnalis*. *Gen. Comp. Endocrinol.* **29:** 61–71.

Hahn, V., J. Winkler, T. A. Rapoport, D. H. Liebscher, Ch. Coutelle, and S. Rosenthal. 1983. Carp preproinsulin cDNA sequence and evolution of genes. *Nucleic Acid Res.* **11:** 4541–4552.

Ishizaki, H., A. Suzuki, and Y. Suzuki. 1987. Prothoracicotropic hormone and functionally related peptides of the *Bombyx mori*: an overview of our studies. Pp. 55–56 in *Proc. Jpn. Soc. Comp. Endocrinol. 2.* E. Ohnishini, Y., Nagahama., H., Ishizaki, eds. Nagoya University Corporation.

Joosse, J., and W. P. M. Geraerts. 1983. Endocrinology. Pp. 317–406 in *The Mollusca, Vol. 4, Part 1, Physiology.* A. S. M. Saludin and K. M. Wilbur, eds. Academic Press, New York.

LeRoith, D., W. L. Lowe, and C. T. Roberts. 1987. Evolution of insulin and insulin receptors. Pp. 156 in *Insulin, Insulin-Like Growth Factors, and their Receptors in the Central Nervous System,* M. K. Raizada, M. I. Philips and D. LeRoith, eds. Plenum Press, New York.

Lomedico, P., N. Rosenthal, A. Erstratiadis, W. Gilbert, R. Kolodner, and R. Tizard. 1979. The structure and evolution of the two nonallelic rat preproinsulin genes. *Cell* **18:** 545–558.

Nagasawa, H., H. Kataoka, A. Isogai, S. Suzuki, A. Suzuki, H. Ishizaki, A. Mizoguchi, Y. Fujiwara, and At. Susuki. 1984. Amino-terminal amino acid sequence of the silkworm prothoracicotropic hormone: homology with insulin. *Science* **226:** 1344–1345.

Nagasawa, H., H. Kataoka, A. Isogai, S. Suzuki, A. Suzuki, H. Mizoguchi, Y. Fujiwara, At. Susuki, S. Y. Takahashi, and H. Ishizaki. 1986. Amino acid sequence of the prothoracicotropic hormone of the silkworm *Bombyx mori*. *Proc. Nat. Acad. Sci. USA* **83:** 5840–5843.

Pearse, A. G. E. 1967. Peptides in brain and intestine. *Nature* **262:** 92–94.

Pictet, R. L., L. B. Rall, P. Phelps, and W. J. Rutter. 1976. The neural crest and the origin of the insulin-producing and other gastrointestinal hormone-producing cells. *Science* **191:** 191–192.

Pollock, H. G., J. R. Kimmel, J. W. Hamilton, J. B. Rouse, K. E. Ebner, V. Lance, and A. B. Rawitch. 1987. Isolation and structures of alligator gar (*Lepisosteus spatula*) insulin and pancreatic polypeptide. *Gen. Comp. Endocrinol.* **67:** 375–382.

Pullen, R. A., G. Lindsay, W. P. Wood, I. J. Tickle, and T. L. Blundell. 1976. Receptor-binding region of insulin. *Nature* **259:** 369–373.

Smit, A. B., E. Vreugdenhil, R. H. M. Ebberink, W. P. M. Geraerts, K. Klootwijk, and J. Joosse. 1988. Growth-controlling molluscan neurons produce the precursor of an insulin-related peptide. *Nature* **331:** 535–538.

Steiner, D. F., S. J. Chan, J. M. Welsh, and S. C. M. Kwok. 1985. Structure and evolution of the insulin gene. *Ann. Rev. Genet.* **19:** 463–484.

Thorpe, A., and H. Duve. 1984. Insulin- and glucagon-like peptides in insects and molluscs. *Mol. Physiol.* **5:** 235–260.

Reference: *Biol. Bull.* 177: 183–186. (October, 1989)

Vasoactive Intestinal Polypeptide and its Relatives: Biochemistry, Distribution, and Functions

MICHAEL C. THORNDYKE[1], JENNIFER H. RIDDELL[1], DAVID T. THWAITES[2], AND RODNEY DIMALINE[2]

[1]*Department of Biology, RHBNC, London University, Egham, Surrey, TW20 OEX, U. K., and*
[2]*Physiological Laboratory, University of Liverpool, Liverpool, L69 3BX U. K.*

Introduction

Vasoactive intestinal polypeptide (VIP) was first isolated from the small intestine of the pig, the purification being monitored with a bioassay based on the vasoactive properties of the material (Said and Mutt, 1972). The new peptide had been anticipated, for in their pioneering experiments leading to the first discovery of the hormone secretin, Bayliss and Starling (1902) had noted the presence, in intestinal extracts, of a factor with vasodepressor activity. This may be the first recorded evidence of VIP activity.

Structures

Since its isolation as an octacosapeptide, VIP has been recognized as having a highly conserved sequence, not only in mammals, but throughout the vertebrates (Dimaline, 1989). The peptides from pig, man, dog, cow, and rat are identical, while the VIPs from guinea pig and chicken have only four substitutions, and dogfish and cod have five (Dimaline *et al.*, 1987; Thwaites *et al.*, 1988) (Fig. 1). Elucidation of VIP sequences also immediately revealed their structural similarities with secretin and other hormones, such as glucagon and glucose-dependent insulinotropic peptide (GIP). The subsequent characterization of growth hormone releasing factor (GRF) and a series of peptides isolated from reptilian venoms (helodermin and the helospectins)—all of which share sequence relationships with VIP—makes this assemblage one of the largest and most diverse structurally related peptide families known.

Recent structure-activity studies show that fish VIPs are equipotent to their mammalian counterparts in binding to VIP receptors on the guinea pig acinar cell or acinar cell membrane (Dimaline *et al.*, 1987; Dimaline *et al.*, 1988). This suggests that, while the C-terminal substitutions plainly influence antibody recognition sites (Dimaline *et al.*, 1986), they have little effect on biological activity. Therefore, the biologically active sites of VIP have been highly conserved during evolution.

In 1981 a peptide was isolated from pig intestine by Tatemoto and Mutt (1981) and given the notation PHI, based on its N- and C-terminal amino acids (histidine and isoleucine, respectively). The similarity between PHI and VIP was immediately noticed (Fig. 1), but not until the gene-sequence for the human VIP precursor had been determined was it apparent that both VIP and PHI are encoded within the same precursor (Itoh *et al.*, 1983). This finding strongly supports the importance of internal duplication of bioactive regions in neurohormonal peptide gene evolution.

Localization

In mammals, VIP is distributed widely throughout the central and peripheral nervous systems, and is especially concentrated in the innervation of the gastrointestinal tract. In birds, too, it is probably exclusively a neurally secreted peptide, with the rare accounts of an endocrine location being due (as in mammals) to non-specific cross-reactivity with N-terminally directed antisera. The localization of VIP in the remaining vertebrates has always been controversial. Thus, although there are reports of both neuronal and endocrine localizations throughout the lower vertebrate groups, other studies describe the sites as being of either one sort or the other (Falkmer *et al.*, 1980; Holmgren and Nilsson, 1983; El-

```
                5         10        15        20        25
COD     H S D A V F T D N Y S R F R K Q M A A K K Y L N S V L A*
DOGFISH - - - - - - - - - - - I - - - - - V - - - I - - L - -*
CHICKEN - - - - - - - - - - - - - - - - - V - - - - - - - - T*
PIG     - - - - - - - - - T - L - - - - - V - - - - - - - I - N*
pPHI    - A - V G - - S D F - - L L G - L S - - - - - E - L I*
```

Figure 1. Amino acid sequences of some members of the VIP family of peptides. The full sequence is shown for cod VIP, and the hyphens indicate an identical residue in the other peptides. p = porcine; * = amide.

Sahly, 1984). In part, these discrepancies may be due to genuine species variation, but our studies on the characterization of elasmobranch and teleost VIPs suggest that they may result from the use of inappropriate antisera and conditions of fixation (Dimaline and Thorndyke, 1986; Dimaline *et al.*, 1987). However, the duplication within the precursor in mammals suggests that the differences in localization might also reflect differential expression or processing of the precursors. Further studies of the gene sequences and precursors in lower vertebrates may provide answers to such problems.

Actions

VIP in vertebrates has two broad effects: (i) smooth muscle relaxation, and (ii) stimulation of gastrointestinal fluid and electrolyte secretion. These are fundamental activities and clearly provide for a range of actions, the extent of which is dependent upon the number of sites at which control is exerted. Indeed, VIP illustrates as well as any other peptide the idea that the same molecule may have a variety of roles, each defined according to the precision of delivery and action.

These two effects of VIP—secretion and smooth muscle relaxation—also illustrate the complementarity of such actions; thus, enhanced secretion can derive from a direct effect on epithelial secretory cells, while an augmented local blood flow (vasodilation) provides the metabolic resources for the cellular secretory activity. Elegant experiments have demonstrated such a dual effect of VIP in the gut of the cat; *i.e.*, a stimulation of intestinal and colonic blood flow accompanied by an increase in net fluid transport (Eklund *et al.*, 1979). Similarly in salivary glands, VIP dilates the submandibular arteries (thereby increasing blood flow to the glands) and, at the same time, directly enhances cellular fluid and protein secretion (Reid and Heywood, 1988).

Secretin, the founder member of the VIP family, controls pancreatic fluid and electrolyte (bicarbonate) secretion in mammals. Indeed, this effect served in the original identification of secretin by Bayliss and Starling (1902). As might have been expected from the similarity in their sequences, VIP is an effective agonist for pancreatic secretion in many mammals although, apart from pig, it is considerably less potent than secretin. This activity relationship is reversed in birds; *i.e.*, VIP is a potent stimulant of avian pancratic secretion, whereas secretin is only a weak one (Dimaline and Dockray, 1979).

The proven secretory effects of VIP in mammals have provided the basis for investigating the role of this peptide in non-mammalian species. In fishes, much attention has been focussed on water and electrolyte secretion in the gut, and VIP has clearly been implicated in the regulation of these parameters in teleosts (Foskett *et al.*, 1982).

However, contention has surrounded the actions of VIP in elasmobranchs. Much has been made of the proposed role of VIP as a stimulator of rectal gland activity, an attractive idea because it foreshadows the function of the peptide in enhancing the secretory activity of the mammalian gut. As noted above, however, glandular secretion comprises two components: ion transport at the epithelial secretory cell, and vascularization of the gland. In the spiny dogfish *Squalus,* volume expansion stimulates both flow and chloride secretion from the duct of the rectal gland (Solomon *et al.*, 1984). However, the sole evidence favoring VIP as a direct agonist of epithelial cell chloride secretion in this species appears to be the ability of somatostatin to inhibit the phenomenon (Solomon *et al.*, 1984).

VIP certainly induces vasodilation in *Squalus,* and a pilot experiment to test partially purified dogfish VIP (C. Woods, T. J. Shuttleworth, and M. C. Thorndyke, unpub. obs.) showed a potent stimulation of rectal gland flow *in vivo* (Fig. 2). At the same time, studies on rectal gland slices from *Scyliorhinus* and *Raja* show that VIP lacks a direct effect on the secretory epithelium; rather a second candidate peptide—rectin—appears to be a potent secretagogue (Shuttleworth and Thorndyke, 1984). Perhaps we are seeing here a differential dual control of rectal gland secretion: by way of the vascular supply (VIP); and by direct action on the secretory epithelium (rectin). Confirmation of the dual control hypothesis awaits the results of tests with rectin on rectal gland slices from *Squalus* and *in vivo* experiments on *Scyliorhinus.* This is important, for we need to rule out differences in response due to differences among dogfish species. In this respect, recent work on the duck salt gland shows that VIP has a potent effect on the blood supply, but that this same peptide also directly stimulates the epithelial cells (Gerstberger, 1988).

The vasodilatory effects of VIP are a reflection of its potency in smooth muscle relaxation. Indeed, one of the best recorded effects of VIP in mammals is the relaxation of the smooth muscle of the gut, which is thought by

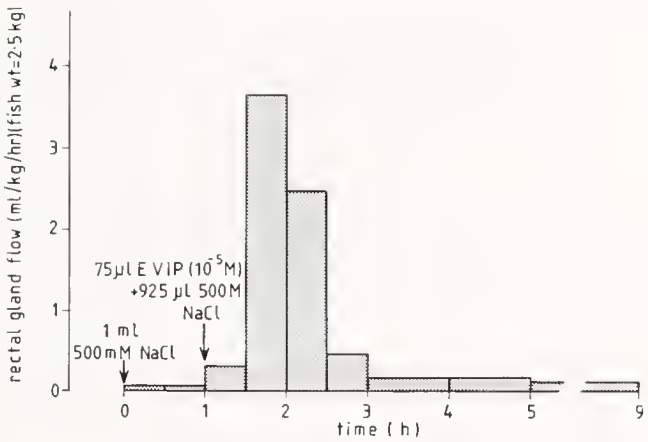

Figure 2. Effect of elasmobranch VIP on rectal gland flow in the spiny dogfish *Squalus acanthias*. The rectal gland duct is cannulated to allow collection of secreted fluid. NaCl (1 ml of 500 m*M*) is applied through the cannulated rectal gland artery at the first arrow; the test sample is applied at the second arrow. Flow rate is measured by collection of rectal gland fluid through an automated drop counter.

many to be responsible for descending relaxation in the peristaltic reflex. The roles of VIP in the gut are most often manifest when the fine control of the peptide malfunctions. For example, human pathological conditions, such as the severe Verner-Morrison syndrome (watery diarrhea), Crohn's disease, or even chronic constipation, reflect either increased (Verner-Morrison, Crohn's) or decreased (constipation) VIP levels.

Invertebrates

Until recently, VIP has not been widely sought after in invertebrates. Immunoreactive VIP has been reported only occasionally from worms, insects, and molluscs where (as has been the case with many immunochemically demonstrated vertebrate peptides) it is restricted to the nervous system (see Thorndyke and Goldsworthy, 1988, for reviews). Recent work from our own laboratories has gone some way toward redressing this lack of information, and has also thrown light on an unexpected and perhaps novel example of the inherent sophistication of adaptive evolution of host-parasite interrelationships. The digenean platyhelminth *Echinostoma liei* spends the mature phase of its life cycle in the small intestine of the mouse. We have discovered a subpopulation of tegumental cells in the flatworm which clearly elaborates an immunochemically VIP-like molecule (Thorndyke and Whitfield, 1987). The sequence of this peptide is presently unknown, although its immunological properties suggest a resemblance to the N-terminus of mammalian VIP. Since the tegumental cells generate the extracellular surface coat of the worm, there exists the fascinating possibility that the parasite may be manipulating host neuropeptide levels to its own advantage. Thus, heavy infections of *E. liei* are associated with local inflammation (vasodilation) and mucosal bloating (increased fluid secretion). These are exactly the responses that a local elevation of VIP should produce, and they are also profitable responses for *E. liei* which ingests mucus and fluid from the gut lumen. So here is a demonstration of adaptive evolution, wherein the regulatory properties of a peptide family transcends the phyletic divide to promote and encourage a parasitic association.

Acknowledgments

Much of our work has received support from the Science and Engineering Research Council (U. K.), the Nuffield Foundation, and the Royal Society (U. K.).

Literature Cited

Bayliss, W. M., and E. H. Starling. 1902. The mechanism of pancreatic secretion *J. Physiol.* **28:** 325–353.

Dimaline, R., and G. J. Dockray. 1979. Potent stimulation of the avian exocine pancreas by porcine and chicken vasoactive intestinal peptides. *J. Physiol.* **294:** 153–163.

Dimaline, R., and M. C. Thorndyke. 1986. Purification and characterization of VIP from two species of dogfish. *Peptides* **7: suppl. 1:** 21–25.

Dimaline, R., J. Young, D. T. Thwaites, C. M. Lee, T. J. Shuttleworth, and M. C. Thorndyke. 1987. A novel vasoactive intestinal peptide (VIP) from elasmobranch intestine has full affinity for mammalian pancreatic VIP receptors. *Biochim. Biophys Acta* **930:** 97–100.

Dimaline, R., M. C. Thorndyke, and J. Young. 1986. Isolation and partial sequence of elasmobranch VIP. *Reg. Peptides* **14:** 1–10.

Dimaline, R., J. Young, D. T. Thwaites, C. M. Lee, and M. C. Thorndyke. 1988. Amino acid sequence of a biologically active vasoactive intestinal peptide from the elasmobranch *Scyliorhinus canicula. Ann. N. Y. Acad. Sci.* **527:** 621–623.

Dimaline, R. 1989. Vasoactive intestinal polypeptide. Pp. 150–173 in *Comparative Physiology of Regulatory Peptides*, S. Holmgren, ed. Chapman and Hall. Publishers. Beckenham, England.

Eklund, S., M. Jodel, O. Lundgren, and A. Sjoqvist. 1979. Effects of vasoactive intestinal polypeptide on blood flow, motility and fluid transport in the gastrointestinal tract of the cat. *Acta Physiol. Scand.* **109:** 461–468.

El-Salhy, M. 1984. Immunocytochemical investigation of the gastro-entero-pancreatic (GEP) neurohormonal peptides in the pancreas and gastrointestinal tract of the dogfish *Squalus acanthias. Histochemistry* **80:** 193–205.

Falkmer, S., J. Fahrenkrug, J. Alumets, R. Hakanson, and F. Sundler. 1980. Vasoactive intestinal polypeptide (VIP) in epithelial cells of the gut mucosa of an elasmobranchious cartilaginous fish, the Ray. *Endocrinol Jpn.* **Suppl. 1:** 31–35.

Foskett, J. K., G. M. Hubbard, T. E. Macken, and H. A. Bern. 1982. Effects of epinephrine, glucagon and vasoactive intestinal polypeptide on chloride secretion by teleost opercular membrane. *J. Comp. Physiol.* **146:** 27–34.

Gerstberger, R. 1988. Functional vasoactive intestinal polypeptide (VIP)-system in salt glands of the Pekin duck. *Cell Tissue Res.* **252:** 39–48.

Holmgren, S., and S. Nilsson. 1983. Bombesin-, gastrin/CCK-, 5-hydroxytryptamine-, neurotensin-, somatostatin-, and VIP-like immunoreactivity and catecholamine fluorescence in the gut of the elasmobranch, *Squalus acanthias*. *Cell Tissue Res.* **234:** 595–618.

Itoh, N., K-I. Obata, N. Yanaihara, and H. Okamoto. 1983. Human preprovasoactive intestinal polypeptide contains a novel PHI-27-like peptide, PHM-27. *Nature* **304:** 547–549.

Reid, A. M., and L. H. Heywood. 1988. A comparison of the effects of vasoactive intestinal polypeptide on secretion from the submaxillary gland of the sheep and pig. *Reg. Peptides* **20:** 211–221.

Said, S. I., and V. Mutt. 1972. Isolation from porcine intestinal wall of a vasoactive octacosapeptide related to secretin and to glucagon. *Eur. J. Biochem.* **28:** 199–204.

Shuttleworth, T. J., and M. C. Thorndyke. 1984. An endogenous peptide stimulates secretory activity in the elasmobranch rectal gland. *Science* **225:** 319–321.

Solomon, R., M. Taylor, J. S. Stoff, P. Silva, and F. H. Epstein. 1984. *In vivo* effect of volume expansion on rectal gland function. I. Humoral factors. *Am. J. Physiol.* **246:** R63–66.

Tatemoto, K., and V. Mutt. 1981. Isolation and Characterisation of the intestinal peptide procine PHI (PHI-27), a new member of the glucagon-secretin family. *Proc. Natl. Acad. Sci. USA* **78:** 6603–6607.

Thorndyke, M. C., and P. J. Whitfield. 1987. Vasoactive intestinal polypeptide-like immunoreactive tegumental cells in the digenean helminth. *Echinostoma liei:* possible role in host-parasite interactions. *Gen. Comp. Endocrinol.* **68:** 202–207.

Thorndyke, M. C. and G. J. Goldsworthy. 1988. *Neurohormones in Invertebrates.* Cambridge University Press, Cambridge, England. 318 pp.

Thwaites, D. T., J. Young, M. C. Thorndyke, and R. Dimaline. 1988. Isolation and characterisation of two teleost VIP's. *Regulatory Peptides* **22:** 436.

Reference: *Biol. Bull.* 177: 187–191. (October, 1989)

Peptide YY: The Ileo-Colonic, Gastric, and Pancreatic Inhibitor

IAN L. TAYLOR

Department of Gastroenterology, Duke University Medical Center, Box 3913, Durham, NC 27710

Introduction

Peptide YY (PYY) was initially isolated from an extract of 400 kg of porcine duodenum using a novel chemical assay that recognizes peptides with amidated carboxyl termini (Tatemoto and Mutt, 1981; Tatemoto, 1982). This latter structural modification is a characteristic of many biologically active brain-gut peptides. Amino acid sequencing of the final purified product demonstrated that peptide YY is a 36 amino acid residue peptide that exhibits structural homology (Floyd *et al.*, 1976; Tatemoto *et al.*, 1982) to two other brain-gut peptides: pancreatic polypeptide (PP) and neuropeptide Y (NPY). These three peptides constitute the third family of structurally related peptides to be isolated from the brain-gut axis. (This family is discussed further in this issue by Price and Greenberg.)

Molecular Biology

The cDNA encoding the PYY precursor has been identified and isolated by screening a rat intestinal λgt11 cDNA library with an antiserum raised against porcine PYY (Leiter *et al.*, 1987). The nucleotide sequence of the cDNA encoded a 98-residue precursor molecule (11,121 daltons) that contained within it a sequence identical to that of porcine PYY. The rat PYY sequence was preceded within the pre-prohormone by a hydrophobic signal sequence and followed by a carboxyl terminal extension of 31 amino acids. A classic cleavage and amidation sequence (Gly-Lys-Arg) joined the carboxyl terminal extension to the carboxyl terminal tyrosine residue in PYY.

Abbreviations: PYY—Peptide YY; NPY—Neuropeptide YY; PP—Pancreatic Polypeptide.

Distribution

PYY has been localized by immunocytochemical techniques to a distinct population of cells in the mucosa of the distal small intestine and colon (El-Salhy *et al.*, 1983; Aponte *et al.*, 1985). The majority of the PYY cells in the ileum and colon are typically endocrine in form (El-Salhy *et al.*, 1983; Aponte *et al.*, 1985). These cells are of the "open-ended type" with apical projections that reach into and sample the contents of the gut lumen; the greatest density of secretory granules occur in the base of the cell in close proximity to the underlying blood vessels. In a subpopulation of these cells, PYY has been found to co-localize with enteroglucagon, demonstrating that these cells are capable of expressing both genes. Another cell type exhibits cytoplasmic processes that emanate from the basal region and extend for as long as 25–30 μM (Lundberg *et al.*, 1982). These basal processes are typically seen in paracrine cells; *i.e.*, cells that release their chemical messenger locally to exert effects on adjacent cells. Thus, PYY may act as both a paracrine and endocrine messenger. There is yet a third population of PYY immunoreactive cells that has been identified in the pancreas by immunohistochemical techniques, radioimmunoassay, and the use of molecular probes (Leiter *et al.*, 1987). The significance of this cell population remains to be determined.

Similar distribution profiles of PYY immunoreactivity have been observed in rat, dog, and man; specific radioimmunoassay were used to measure PYY in mucosal extracts (Lundberg *et al.*, 1982; Chen *et al.*, 1984; Taylor, 1985; Adrian *et al.*, 1985a). Highest concentrations of PYY are observed in the distal gut, particularly in the muscosa of the ileum and colon.

Release

The initial studies (Lundberg *et al.*, 1982; Chen *et al.*, 1984) in rat and man failed to demonstrate release of

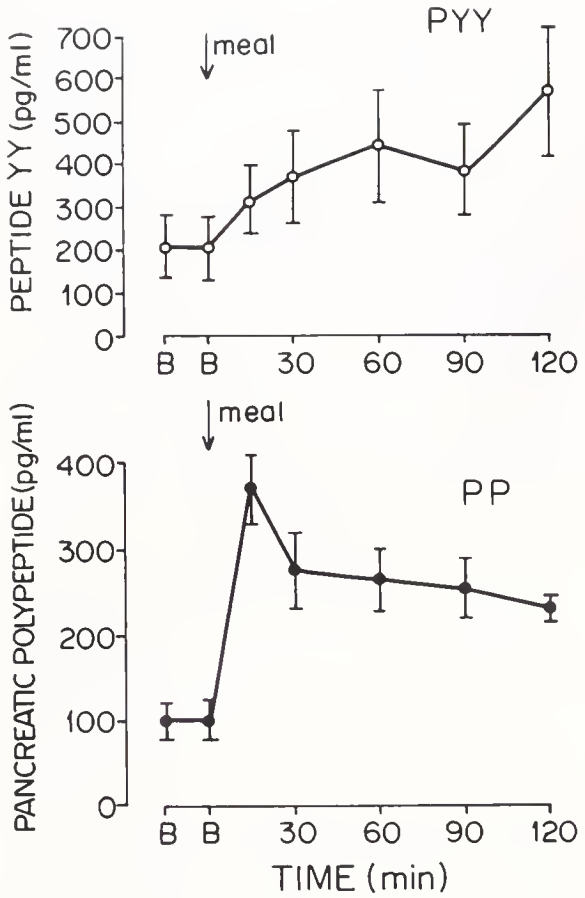

Figure 1. Comparison of the Peptide YY (PYY) and pancreatic polypeptide (PP) responses to a 15% liver extract meal in dogs.

PYY into the circulation after ingestion of a meal. These observations were held to make an endocrine role for PYY unlikely. However, subsequent studies in dog (Taylor, 1985) and man (Adrian *et al.*, 1985a) have demonstrated release of PYY into the circulation, supporting a true hormonal role for PYY. These apparently conflicting findings may reflect greater sensitivity of the radioimmunoassays employed in the latter two studies.

The PYY response to meals is distinctly different from that of its sister peptide, PP. The PP response is characterized (Floyd *et al.*, 1976; Taylor *et al.*, 1978) by an early peak approximately 15–30 min after ingestion of the meal (Fig. 1), which reflects the importance of the cephalic-vagal and gastric phases of PP release. In contrast, PYY release after a meal is not as rapid, nor does it exhibit the same vagal-cholinergic dependence that characterizes the release of its sister peptide (Taylor *et al.*, 1978; Taylor, 1985). Although significant increases in PYY levels can be observed 30 min after the ingestion of a meal, the peak response does not occur for several hours. As shown in Figure 1, PYY concentrations are still increasing in the dog 4 h after the ingestion of a meal.

The most potent stimulant of PYY release observed to date is the presence of fat in the intestinal lumen (Aponte *et al.*, 1985; Pappas *et al.*, 1986a; Adrian *et al.*, 1986). As anticipated, PYY release is markedly enhanced in patients with steatorrhea due to the presence of malabsorbed fat in the distal gut (Adrian *et al.*, 1986). As an example, patients with short bowel syndrome have markedly enhanced PYY release, and the response to ingested meals occurs much more rapidly than in normal subjects. In contrast, patients with gastrointestinal disease unassociated with rapid intestinal transit or malabsorption—*e.g.*, diverticular disease—do not exhibit enhanced PYY release (Adrian *et al.*, 1986).

Biological Actions

PYY and neuropeptide Y are both capable of inducing prolonged vasoconstriction when infused into peripheral blood vessels (Lundberg *et al.*, 1982; Edvinnson, 1985). NPY has been localized to the sympathetic nerves that innervate the smooth muscle of arteries throughout the body (Allen and Bloom, 1986), and PYY probably acts through a generic PYY-NPY receptor on vascular smooth muscle. When PYY is infused into the mesenteric circulation, the resulting vasoconstriction is associated with an inhibition of colonic motility that lasts for an hour after the peptide infusion has ceased (Lundberg *et al.*, 1982).

PYY shares with the other members of its peptide family the ability to inhibit pancreatic exocrine secretion (Tatemoto, 1982; Pappas *et al.*, 1985a, b). This inhibitory action is demonstrable whether pancreatic exocrine secretion is stimulated by a meal, or by exogenous secretagogues such as secretin and cholecystokinin. Although PYY inhibits pancreatic secretion in dog, cat, and rat (Tatemoto, 1982; Pappas *et al.*, 1985a, b; Louie *et al.*, 1985), it has no effect on pancreatic secretion in man (Adrian *et al.*, 1985c). This observation may reflect a true species difference, or the lower doses used in man compared to the other species studied.

PYY inhibits prostaglandin-induced secretion of fluid and electrolytes from the small intestine (Saria and Beubler, 1985), and disturbs the distal propagation of the interdigestive myoelectric complex (Lundberg *et al.*, 1982; Al-Saffar *et al.*, 1985). In keeping with this latter observation, treatment of animals with PYY delays transport of a labeled meal through the small intestine (Al-Saffar *et al.*, 1985). PYY also inhibits gastric emptying, delaying the entry of nutrients into the small intestine (Allen *et al.*, 1984; Pappas *et al.*, 1986a). As the peptide is also a potent inhibitor of gastric acid secretion in both man (Adrian *et al.*, 1985c) and dog (Pappas *et al.*, 1986b), it is a good candidate enterogastrone; *i.e.*, a hormonal inhibitor of gastric function.

An examination of the mechanisms by which PYY inhibits gastric secretion has given a clue to the cellular site of action of PYY (Pappas *et al.*, 1986b). Although PYY is a potent inhibitor of meal-stimulated acid secretion in the dog, it exerts no inhibitory effect on the acid secretory response to cholinomimetics such as carbachol. In addition it is, at best, a weak inhibitor of acid secretion stimulated by pentagastrin and histamine. As PYY does not block the action of the known hormonal and neurotransmitter secretogogues at the level of the parietal cell, we must assume that its effects on acid secretion are indirect. In contrast to its lack of potency in blocking the effects of external secretogogues, PYY is a very potent inhibitor of cephalic phase acid secretion, causing 95% inhibition of acid secretion induced by sham feeding in dogs. These results suggest that PYY inhibits gastric function by inhibiting vagal tone on the stomach; as such it appears to function as an endocrine neuromodulator.

Physiological Significance of PYY

Over a century ago, Ewald and Boas (1886) noted that the addition of olive oil to a test meal of gruel inhibited acid secretion and delayed gastric emptying in man. One of Pavlov's students went on to demonstrate that this inhibition of acid secretion could only be demonstrated if fat was allowed to pass beyond the stomach (Gregory, 1962). In 1930, Kosaka and Lim (1933) isolated an inhibitor of gastric secretion from the mucosa of both the small and large intestine, which they termed "enterogastrone." Despite Kosaka and Lim's initial observation (Kosaka and Lim, 1933) that colonic extracts were as potent as jejunal extracts, the search for enterogastrone largely centered on the small intestine. Interest in the distal bowel as the site of release of the gastric inhibitor (cologastrone) was rekindled by the demonstration (Seal and Debas, 1980) that perfusion of the distal bowel with a variety of nutrients—*e.g.*, fat and glucose—inhibited gastric secretion (Seal and Debas, 1980; Jian *et al.*, 1981; Kihl *et al.*, 1981).

PYY must be considered a good candidate enterogastrone or cologastrone since it is found in highest concentrations in the mucosa of the ileum and colon where it is localized to endocrine-type cells. It is also a potent inhibitor of both gastric secretion and gastric emptying. The recent demonstration that PYY is released into the circulation in amounts sufficient to inhibit gastric function after the ingestion of fatty meals (Pappas *et al.*, 1986b) establishes the peptide's credentials as an enterogastrone.

PYY may also play a pathophysiological role in disease states associated with malabsorption or maldigestion of food. For example patients with the post-vagotomy dumping syndrome—*i.e.*, those who have rapid gastric emptying after gastric surgery—exhibit markedly

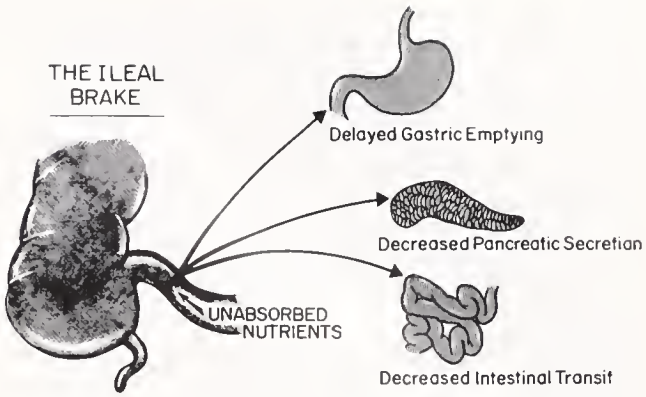

Figure 2. Schematic representation of the "ileal brake" and the potential role (arrows) of peptide YY in delaying gastric emptying, inhibiting pancreatic secretion and slowing intestinal transit.

enhanced PYY responses to glucose meals (Adrian *et al.*, 1985b). The enhanced release of PYY would be expected to delay gastric emptying. In so doing, it would help relieve some of the symptoms caused by the rapid and uncontrolled entry of hyperosmolar solutions into the small intestine.

The term "ileal brake" has been coined (MacFarlane *et al.*, 1983) to describe a phenomenon whereby perfusion of the ileum and colon with fat slows intestinal transit and delays gastric emptying in man. Undefined hormonal signals originating from the ileum and colon were proposed by the original authors to mediate this response. The ileal brake is engaged when unabsorbed nutrients pass beyond the absorptive surface of the intestine and delays the rate of delivery of unprocessed food into an already over-burdened small intestine. PYY release is markedly enhanced in diseases associated with malabsorption of food (Adrian *et al.*, 1986). In such states, the combination of delayed gastric emptying and delayed intestinal transit resulting from enhanced PYY release would allow increased time for nutrient digestion. In addition, the increased nutrient-mucosal contact time would lead to increased efficiency of nutrient absorption. PYY deserves consideration as a potential mediator of this phenomenon based on its distribution in the gut, its enhanced release in the face of malabsorption, and its unique spectrum of biological actions (Fig. 2).

PYY may also explain another biological phenomenon initially described by two different research groups working quite independently. Sarles and his co-workers (Hage *et al.*, 1974; Sarles *et al.*, 1979) described the existence of "an anti-cholecystokinin hormone" in extracts of the ileocolonic mucosa. Harper and his colleagues (Harper *et al.*, 1979a, b) described an inhibitor of pancreatic exocrine secretion, pancreotone, in the mucosa of the ileum and colon. In their initial report, Harper and coworkers (Harper *et al.*, 1979a, b) emphasized the simi-

larities between the inhibition of pancreatic secretion induced by pancreotone and that observed after infusion of PYY's sister peptide, PP. As PP could not be demonstrated in colonic mucosal extracts, the authors suggested that pancreotone might act by stimulating PP release from its cell of origin in the pancreas. The discovery of large concentrations of PYY in the mucosa of the ileum and colon precludes the necessity for postulating the existence of a PP secretogogue in the colonic mucosa. The potent inhibition by PYY of pancreatic secretion in rat, cat, and dog, and its occurrence in high concentrations in the ileum and colon, support the hypothesis that PYY is at least a component of both Harper's pancreotone and Sarle's anti-CCK hormone.

Conclusions

In summary, PYY may be of disproportionate interest to the gut endocrinologist because of the lessons it teaches about the neuro-endocrine control of gut function. First, these studies re-emphasize the importance of the ileum and colon as endocrine organs. Second, they suggest a role for the distal gut in the modulation of upper gut function. Thus, the distal gut monitors the efficiency of nutrient digestion and absorption in the upper intestine, and releases peptides that influence upper gut function in a way that will lead to increased efficiency of nutrient use. Finally, the recent demonstration that PYY acts as an endocrine neuromodulator calls into question the historic criteria used to define hormonal actions. Thus, a biological action that persists after denervation of the target organ has, in the past, been held to be hormonally mediated. Conversely, an action that is abolished by denervation of the target organ has been held to be neurally mediated. Studies with PYY demonstrate that the actions of some gastrointestinal peptides are so intimately connected with the actions of the autonomic nervous system, that they cannot be so easily differentiated. These findings suggest that the conceptional dichotomy between hormonal and neural control of gut function is an artificial one.

Acknowledgments

The author wishes to acknowledge support from the Veterans Administration and the NIH (DK38126), and from the Sarah W. Stedman Center for Nutritional Studies.

Literature Cited

Adrian, T. E., G-L. Ferri, A. J. Bacarese-Hamilton, H. S. Fuessl, J. M. Polak, and S. R. Bloom. 1985a. Human distribution and release of PYY, a putative new gut hormone. *Gastroenterology* **89:** 1070–1077.

Adrian, T. E., R. G. Long, H. S. Fuessl, and S. R. Bloom. 1985b. Plasma peptide YY (PYY) in dumping syndrome. *Dig. Dis. Sci.* **30:** 1145–1148.

Adrian, T. E., A. P. Savage, A. J. Bacarese-Hamilton, K. Wolfe, H. S. Besterman, and S. R. Bloom. 1986. Peptide YY abnormalities in gastrointestinal diseases. *Gastroenterology* **90:** 379–384.

Adrian, T. E., A. P. Savage, G. R. Sagor, J. M. Allen, A. J. Bacarese-Hamilton, K. Tatemoto, J. M. Polak, and S. R. Bloom. 1985c. Effect of peptide YY on gastric, pancreatic, and biliary function in humans. *Gastroenterology* **89:** 494–499.

Allen, Y. S., and S. R. Bloom. 1986. Neuropeptide Y: a putative neurotransmitter. *Neurochem. Int.* **8:** 1–8.

Allen, J. M., M. L. Fitzpatrick, J. C. Yeats, K. Darcy, T. E. Adrian, and S. R. Bloom. 1984. Effects of peptide YY and neuropeptide Y on gastric emptying in man. *Digestion* **30:** 255–262.

Al-Saffar, A., P. M. Hellstrom, and G. Nylander. 1985. Correlation between peptide YY-induced myoelectric activity and transit of small-intestinal contents in rats. *Scand. J. Gastroenterol.* **20:** 577–582.

Aponte, G., A. S. Fink, J. H. Meyer, K. Tatemoto, and I. L. Taylor. 1985. Regional distribution and release of peptide YY with fatty acids of different chain length. *Am. J. Physiol.* **249:** G745–G750.

Chen, M-H., A. Balasubramanian, R. F. Murphy, K. Tabata, J. E. Fischer, I-W. Chen, and S. N. Joffe. 1984. Sensitive radioimmunoassay for measurement of circulating peptide YY. *Gastroenterology* **87:** 1332–1338.

Edvinsson, L. 1985. Characterization of the contractile effect of neuropeptide Y in feline cerebral arteries. *Acta Physiol. Scand.* **125:** 33–41.

El-Salhy, M., E. Wilander, L. Juntti-Berggren, and L. Grimelius. 1983. The distribution and ontogeny of polypeptide YY (PYY)- and pancreatic polypeptide (PP)-immunoreactive cells in the gastrointestinal tract of rat. *Histochemistry* **78:** 53–60.

Ewald, C. O., and J. Boas. 1886. Beritrage zur Physiologie und Pathologie Derverlaung. *Virchows Arch.* **104:** 271–305.

Floyd, J. C., S. S. Fajans, and S. Pek. 1976. Regulation in healthy subjects of the secretion of human pancreatic polypeptide, a newly recognized pancreatic islet polypeptide. *Trans. Assoc. Am. Physicians* **98:** 146–158.

Gregory, R. A. 1962. Inhibition of gastric secretion. Pp. 103–133 in *Secretory Mechanisms of the Gastro-intestinal Tract*, R. A. Gregory, ed., Arnold, London.

Hage, G., O. Tiscornia, G. Palasciano, and H. Sarles. 1974. Inhibition of pancreatic exocrine secretion by intra-colonic oleic acid infusion in the dog. *Biomedicine* **21:** 263–267.

Harper, A. A., A. J. C. Hood, J. Mushens, and J. R. Smy. 1979a. Inhibition of external pancreatic secretion by intracolonic and intraileal infusions in the cat. *J. Physiol. Lond.* **292:** 445–454.

Harper, A. A., A. J. C. Hood, J. Mushens, and J. R. Smy. 1979b. Pancreotone, an inhibitor of pancreatic secretion in extracts of ileal and colonic mucosa. *J. Physiol. Lond.* **292:** 455–467.

Jian, R., H. S. Besterman, D. L. Sarson, C. Aymes, J. Hostein, S. R. Bloom, and J. C. Rambaud. 1981. Colonic inhibition of gastric secretion in man. *Dig. Dis. Sci.* **26:** 195–201.

Kihl, B., A. Rokaeus, S. Rosell, and L. Olbe. 1981. Fat inhibition of gastric acid secretion in man and plasma concentrations of neurotensin-like immunoreactivity. *Scand J. Gastroenterol.* **16:** 513–526.

Kosaka, T. and R. S. K. Lim. 1933. On the mechanism of the inhibition of gastric motility by fat. An inhibitory agent from the intestinal mucosa. *Chin. J. Physiol.* **7:** 5–12.

Leiter, A. B., A. Toder, H. J. Wolfe, I. L. Taylor, S. Cooperman, G. Mandel, and R. H. Goodman. 1987. Peptide YY: structure of the precursor and expression in exocrine pancreas. *J. Biol. Chem.* **262:** 12,984–12,988.

Louie, D. S., J. A. Williams, and C. Owyang. 1985. Action of pancreatic polypeptide on rat pancreatic secretion: *in vivo* and *in vitro*. *Am. J. Physiol.* **249:** G489–G495.

Lundberg, J. M., K. Tatemoto, L. Terenius, P. M. Hellstrom, V. Mutt, T. Hokfelt and B. Hamberger. 1982. Localization of peptide YY (PYY) in gastrointestinal endocrine cells and effects on intestinal blood flow and motility. *Proc. Natl. Acad. Sci. USA* **79:** 4471–4475.

MacFarlane, A., R. Kinsman, N. W. Read, and S. R. Bloom. 1983. The ileal brake: ileal fat slows small bowel transit and gastric emptying in man. *Gut* **24:** A471–A472. (Abs.).

Pappas, T. N., H. T. Debas, Y. Goto and I. L. Taylor. 1985a. Peptide YY inhibits meal-stimulated pancreatic and gastric secretion. *Am. J. Physiol.* **248:** G118–G123.

Pappas, T. N., H. T. Debas, and I. L. Taylor. 1985b. Peptide YY: metabolism and effect on pancreatic secretion in dog. *Gastroenterology* **89:** 1387–1392.

Pappas, T. N., H. T. Debas, A. M. Chang, and I. L. Taylor. 1986a. Peptide YY release by fatty acids is sufficient to inhibit gastric emptying in dogs. *Gastroenterology* **91:** 1386–1389.

Pappas, T. N., H. T. Debas, and I. L. Taylor. 1986b. Enterogastrone-like effect of peptide YY is vagally mediated in the dog. *J. Clin. Invest.* **77:** 49–53.

Saria, A., and E. Beubler. 1985. Neuropeptide Y (NPY) and peptide YY (PYY) inhibit prostaglandin E_2-induced intestinal fluid and electrolyte secretion in the rat jejunum *in vivo*. *Eur. J. Pharmacol.* **119:** 47–52.

Sarles, H., G. Hage, R. Laugier, P. Demol, and D. Bataille. 1979. Present status of the anticholecystokinin hormone. *Digestion* **19:** 73–76.

Seal, A. M., and H. T. Debas. 1980. Colonic inhibition of gastric acid secretion in the dog. *Gastroenterology* **79:** 823–826.

Tatemoto, K. 1982. Isolation and characterization of peptide YY (PYY), a candidate gut hormone that inhibits pancreatic exocrine secretion. *Proc. Natl. Acad. Sci. USA* **79:** 2514–2518.

Tatemoto, K., M. Carlquist and V. Mutt. 1982. Neuropeptide Y—a novel brain peptide with structural similarities to peptide YY and pancreatic polypeptide. *Nature* **296:** 659–660.

Tatemoto, K., and V. Mutt. 1981. Isolation of two novel candidate hormones using a chemical method for finding naturally occurring polypeptides. *Nature* **285:** 417–418.

Taylor, I. L. 1985. Distribution and release of peptide YY in dog measured by specific radioimmunoassay. *Gastroenterology* **88:** 731–737.

Taylor, I. L., M. Feldman, C. T. Richardson and J. H. Walsh. 1978. Gastric and cephalic stimulation of human pancreatic polypeptide release. *Gastroenterology* **75:** 432–437.

Reference: *Biol. Bull.* **177**: 192–194. (October, 1989)

Tachykinins and the Bombesin-Related Peptides: Receptors and Functions

STEVEN R. VIGNA

Department of Cell Biology, Duke University Medical Center, Box 3709, Durham, North Carolina 27710

Two vertebrate peptide families—the tachykinins and bombesin-related peptides—share many similarities of sequence and distribution. The amino acid sequences of the peptides in these families are similar in the carboxy-terminal region, and this is the molecular center of biological activity in both groups. All tachykinins share the C-terminal sequence -Phe-X-Gly-Leu-Met-NH_2, and many (but not all) bombesin-related peptides have -Leu-Met-NH_2 at the carboxy terminus (Table I). Furthermore, in both families, oxidation of the methionine residue at the C-terminus reduces or abolishes the biological activity of the peptides (Vigna *et al.*, 1988). Peptides from both families are expressed in nerves and gut endocrine cells of vertebrates; representatives from each group are also expressed in exocrine glands located in the skins of certain frogs. The similarity of these observations suggests that the tachykinins and bombesin-related peptide families may overlap in their functions or may even share a common origin in evolution.

The mRNAs encoding the precursor proteins for several mammalian members of these peptide families have recently been characterized. The gastrin-releasing peptides (GRPs) of human (Spindel *et al.*, 1984) and rat (Lebacq-Verheyden *et al.*, 1988) are bombesin-like and their precursors are very similar to each other. However, these precursors are both quite different from the α- and β-preprotachykinins (Nawa *et al.*, 1983) which arise from the alternate splicing of the mRNA transcribed from a single gene. Thus the mammalian tachykinins and bombesin-related peptides appear to be encoded by genes that are unrelated.

The precursor β-preprotachykinin is particularly interesting because it contains one copy each of two tachykinins, substance P and substance K. This suggests that, in the neurons that express β-preprotachykinin, both substance P and substance K are processed out of the precursor. Therefore, although both peptides may be released, their production of a functional response will be determined by the presence or absence of the appropriate postsynaptic receptor.

To begin evaluating the functions of and the interactions among the bombesin-related peptides and tachykinins in mammals, we studied the localization and properties of the receptors for various peptide members of these two families. We have also initiated comparative studies of these receptors in nonmammalian vertebrates to analyze the putative evolutionary relationship between these molecular families. Our studies have focussed on the expression of receptors in the gastrointestinal tract because the pharmacological actions of both the bombesin-related peptides and the tachykinins have been extensively studied in the guts of mammals and nonmammals.

We have shown, by quantitative autoradiography of saturable radioligand binding, that receptors specific for substance P and for substance K are expressed in the canine gastrointestinal tract (Mantyh *et al.*, 1988b). Moreover, these two receptors exhibited different patterns of anatomical localization. Therefore, separate receptors for substance P and substance K are expressed and differentially distributed in the gastrointestinal tract. No evidence for expression of receptors for the third mammalian tachykinin, neuromedin K, was observed, even though we were able to demonstrate neuromedin K receptors in the canine central nervous system.

Similar studies of bombesin receptors in the canine gastrointestinal tract revealed a pattern of binding sites specific for the radioligand ^{125}I-(Tyr^4)-bombesin. The distribution was clearly distinct from that of the substance P and substance K receptors (Vigna *et al.*, 1987).

Table I

Amino acid sequences of bombesin- and tachykinin-related peptides

	1 5 10 15 20 25
GRP Human	V P L P A G G G T V L T K M Y P R G N H W A V G H L M NH_2
Pig	A – V S V – – – – – – A – – – – – – – – – – – – – – – NH_2
Dog	A – V – G – Q – – – – D – – – – – – – – – – – – – – – NH_2
Chicken	A – – Q P – – S P A – – – I – – – – S – – – – – – – – NH_2
Dogfish[1]	A – V E N Q – S F P * * – – F – – – S – – – – – – – – NH_2
Bombesin	pQ Q R L – – Q – – – – – – – NH_2
Substance P	– P K P Q Q F F G – – NH_2
Substance K (Neurokinin A)	H K T D S F V G – – NH_2
Neuromedin K (Neurokinin B)	D M H D F F V G – – NH_2
Scyliorhinin[2]	A K F D K F Y G – – NH_2
Eledoisin[3]	pQ P S K D – F I G – – NH_2

Residues similar to those in human gastrin releasing peptide (GRP), a bombesin-related peptide, are indicated by (–).

[1] Dogfish (*Scyliorhinus*) GRP; * = position of two presumed deletions (Conlon *et al.*, 1987).

[2] A dogfish tachykinin (Conlon *et al.*, 1986).

[3] A molluscan tachykinin (Erspamer and Anastasi, 1962).

Further evidence for the distinct nature of these three neuropeptide receptors came from the demonstration of increased expression of substance P receptors, but not substance K or bombesin receptors, in inflammatory bowel disease in people (Mantyh *et al.*, 1988a).

The distribution of binding sites for iodinated bombesin was also examined in the stomach of the bony fish, *Scorpaeichthys marmoratus.* High affinity, saturable bombesin binding sites were localized on the circular and longitudinal layers of gastric smooth muscle in both the antral and oxyntic regions of the stomach (Vigna and Thorndyke, 1989); no receptors were seen in the antral mucosa, which was the richest source of bombesin binding in the dog stomach. These observations demonstrate that the simple techniques used to localize and characterize receptors in mammals are applicable to nonmammalian species and, furthermore, that putative bombesin receptors have different distributions in mammalian and nonmammalian stomachs.

Recent studies of the structure and actions of bombesin-related peptides in nonmammalian vertebrates reveal a remarkable degree of conservation. Shark GRP is reported to be nearly or completely identical to mammalian GRP at the biologically active carboxy-terminus of the peptide (Conlon *et al.*, 1987) (Table I). Of the general categories of action of bombesins in mammals—including the stimulation of release of gastrointestinal hormones, contraction of gut muscle, digestive enzyme secretion, and decrease of body temperature—most have now been demonstrated in response to bombesin administration in one or more nonmammalian vertebrate species.

Two examples of such effects deserve comment because they illustrate a phenomenon that may be of particular importance in understanding the evolution of this peptide family. First, bombesin causes acid secretion in mammals by stimulating the release of the gastric hormone, gastrin, which in turn directly initiates gastric acid secretion. Bombesin also stimulates acid secretion from the bony fish stomach (Holstein and Humphrey, 1980), but this must occur by a different mechanism, as yet unknown, because fish do not have gastrin in their stomachs.

The second comparison concerns the reduction, by bombesin, of body temperature in rats and fish. In rats, this action is caused by an unknown physiological mechanism (Brown and Vale, 1979). In carp, although bombesin has the same overall effect, it is accomplished by a behavioral mechanism (Kavaliers and Hawkins, 1981).

In both cases described above, the *actions* of bombesin have been conserved in evolution, but the *mechanisms* by which bombesin carries out these actions have changed. Future analysis of other aspects of this fascinating pattern of evolution will contribute much to our understanding of the importance of these families of regulatory peptides to biological success.

Literature Cited

Brown, M., and W. Vale. 1979. Bombesin—a putative mammalian neurogastrointestinal peptide. *Trends Neurosci.* **2:** 95–97.

Conlon, J. M., C. F. Deacon, L. O'Toole, and L. Thim. 1986. Scyliorhinin I and II: two novel tachykinins from dogfish gut. *FEBS Lett.* **200:** 111–116.

Conlon, J. M., I. W. Henderson, and L. Thim. 1987. Gastrin-releasing peptide from the intestine of the elasmobranch fish, *Scyliorhinus canicula* (common dogfish). *Gen. Comp. Endocrinol.* **68:** 415–420.

Erspamer, V., and A. Anastasi. 1962. Structure and pharmacological actions of eledoisin, the active endecapeptide of the posterior salivary gland of *Eledone. Experientia* **181:** 58–59.

Holstein, B., and C. S. Humphrey. 1980. Stimulation of gastric acid secretion and suppression of VIP-like immunoreactivity by bombesin in the Atlantic codfish, *Gadus morhua*. *Acta Physiol. Scand.* **109:** 217–223.

Kavaliers, M., and M. F. Hawkins. 1981. Bombesin alters behavioral thermoregulation in fish. *Life Sci.* **28:** 1361–1364.

Lebacq-Verheyden, A.-M., G. Krystal, O. Sartor, J. Way, and J. F. Battey. 1988. The rat prepro-gastrin releasing peptide is transcribed from two initiation sites in the brain. *Mol. Endocrinol.* **2:** 556–563.

Mantyh, C. R., T. S. Gates, R. P. Zimmerman, M. L. Welton, E. P. Passaro, Jr., S. R. Vigna, J. E. Maggio, L. Kruger, and P. W. Mantyh. 1988a. Receptor binding sites for substance P, but not substance K or neuromedin K, are expressed in high concentrations by arterioles, venule, and lymph nodules in surgical specimens obtained from patients with ulcerative colitis and Crohn disease. *Proc. Natl. Acad. Sci. USA* **85:** 3235–3239.

Mantyh, P. W., C. R. Mantyh, T. S. Gates, S. R. Vigna, and J. Maggio. 1988b. Receptor binding sites for substance P and substance K in the canine gastrointestinal tract and their possible role in inflammatory bowel disease. *Neuroscience* **25:** 817–837.

Nawa, H., T. Hirose, H. Takashima, S. Inayama, and S. Nakanishi. 1983. Nucleotide sequences of cloned cDNAs for two types of bovine brain substance P precursor. *Nature* **306:** 32–36.

Spindel, E. R., W. W. Chin, J. Price, L. H. Rees, G. M. Besser, and J. F. Habener. 1984. Cloning and characterization of cDNAs encoding human gastrin-releasing peptide. *Proc. Natl. Acad. Sci. USA* **81:** 5699–5703.

Vigna, S. R., C. R. Mantyh, A. S. Giraud, J. H. Walsh, A. H. Soll, and P. W. Mantyh. 1987. Localization of specific binding sites for bombesin in the canine gastrointestinal tract. *Gastroenterology* **93:** 1287–1295.

Vigna, S. R., A. S. Giraud, J. R. Reeve, Jr., and J. H. Walsh. 1988. Biological activity of oxidized and reduced iodinated bombesins. *Peptides* **9:** 923–926.

Vigna, S. R., and M. C. Thorndyke. 1989. Bombesin and related peptides. Pp. 34–60 in *Comparative Physiology of Regulatory Peptides*, S. Holmgren, ed. Chapman and Hall, London.

Reference: *Biol. Bull.* **177:** 195–197. (October, 1989)

Gastrin, Cholecystokinin (CCK), and the Leukosulfakinins

G. J. DOCKRAY

Physiological Laboratory, University of Liverpool, Brownlow Hill, Liverpool L69 3BX, United Kingdom

Introduction

The gastrin-CCK family is operationally defined as consisting of peptides with the common C-terminal tetrapeptide amide structure: Trp-Met-Asp-Phe-NH_2. This is also the minimal fragment with biological activity. Therefore, the distinctive patterns of activity of gastrin or CCK are determined largely by other regions of the molecule (Dockray, 1989).

In addition to the two mammalian peptides, there is an amphibian member of the group, caerulein, and an avian peptide that Rod Dimaline has characterized, which we call chicken gastrin (Dimaline *et al.*, 1986) (Fig. 1). In the invertebrates, the leucosulfakinins have been isolated by Nachman *et al.* (1986), and share several residues with the vertebrate gastrins, notably the sequence Tyr(SO_3H)-Gly-X_1-Met-X_2-Phe-NH_2 (Fig. 1). The leucosulfakinins are also similar to the FMRFamide family in terminating in Met-Arg-Phe-NH_2 (Fig. 1; see also Price and Greenberg, 1989). Whether they are phylogenetically related to gastrin and CCK is hard to say; there is no evidence of common sites of action, and the leucosulfakinin precursor is not yet known. I tend to the view that this is an example of convergent evolution.

Precursors

The genes encoding gastrin, CCK, and caerulein have been cloned and sequenced by a number of groups. Preprogastrin and preproCCK are organized on rather similar lines. The chain length is about 100 residues including the signal sequence, and there is a single copy of the major active molecular form. Away from the main active sites, however, the primary structures of the two precursors are not at all similar.

In the case of procaerulein, Kriel's group has found a variety of different possible precursors, one of which has at least two copies of caerulein and is probably quite large (Richter *et al.*, 1986; Vlasak *et al.*, 1987). Again, outside of the pentapeptide amide, there are virtually no regions of the caerulein precursor common to any in either gastrin or CCK. More important, the organization of the caerulein precursor is plainly different from that of gastrin and CCK. On this latter basis, one might reasonably question whether there is any phylogenetic relationship between caerulein and the other members of the family (Dockray, 1989).

Processing

Peptide precursors are converted by a variety of steps to the major active products. In the case of progastrin there are only two main cleavages, but in proCCK there are several. Moreover, different cells expressing these genes show different cleavage patterns. One interesting point is that, within this family, the cleavage sites are quite variable. In progastrin there is cleavage at pairs of basic residues, in proCCK mainly at single basic residues, and in procaerulein and avian gastrin there is evidence of cleavage at dibasic residues followed by dipeptidyl aminopeptidase activity.

However, other types of post-translational processing mechanisms are better conserved. The mechanisms of tyrosine sulfation follow the usual rules for sulfotransferase activity, namely an acid residue in the immediate upstream portion. However, avian gastrin is not typical in this regard (see below).

On present evidence, the mechanisms of C-terminal amidation are the same as those found in other peptides, but there is an interesting feature associated with the relevant part of the gastrin and CCK precursors. We have recently isolated the C-terminal flanking peptides of hu-

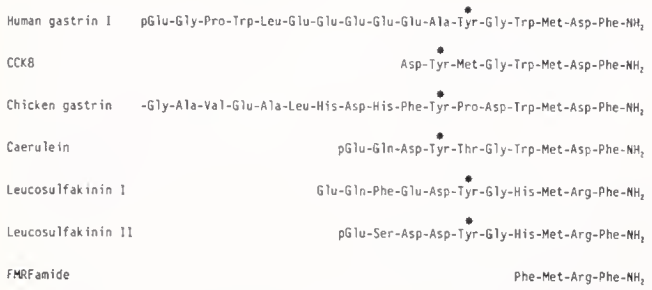

Figure 1. Amino acid sequences of human gastrin I (G17), cholecystokinin octapeptide (CCK8), chicken gastrin (20–36), caerulein (amphibian), the leucosulfakinins (cockroach), and FMRFamide (molluscs). Alignment is from the C-terminal. *Indicates sulfated tyrosine residues. pGlu = pyroglutamic acid.

man and hog progastrin, and have found two forms of each of these peptides. These forms were poorly separated by reverse phase HPLC, but were well separated on ion exchange chromatography. Using the latter method, then, we were able to demonstrate that alkaline phosphatase digestion converts one form of the peptide to the other. On sequencing, it was found that one form was phosphorylated on the N-terminal serine, and the other was not. The phosphorylation site (*i.e.*, the serine residue) seems to be a part of two consecutive consensus sequences: one (-Arg-Arg-Ser-) recognized by cyclic AMP-dependent protein kinase, and the other (-Ser-Ala-Glu-Glu-) by the casein kinase group of kinases. Interestingly, similar sequences also occur in proCCK, and at several locations in proFMRFamide. Phosphorylation may, in some way, identify, tag, or label this region as important for subsequent processing to the C-terminal amide (Dockray *et al.*, 1989).

Receptors

Throughout the vertebrates, the CCK gene is expressed both in gut endocrine cells and central neurones, particularly in forebrain regions and in the hypothalamus. An important question arising from this pattern of distribution is whether there is any functional link between brain and gut, and if not, how is specificity of action maintained in the two systems. This, in turn, is part of the larger question of how specificity is, in any case, maintained between gastrin and CCK. The results of receptor binding assays indicate that there are three types of receptors in mammals and birds: the so-called central and peripheral CCK receptors, and the gastrin receptor. We have a good antagonist for at least one of these—L-364,718—which is selective for peripheral CCK receptors.

Steven Vigna's work suggests that, in lower vertebrates, there is a single receptor in brain and gut. Whether there is also a gastrin receptor is difficult to say, particularly because there is no general agreement on whether gastrin actually exists below the reptiles (Vigna *et al.*, 1986).

The crucial feature that determines specificity of action of CCK at mammalian receptors is the position and sulfation of the tyrosine. The characteristic CCK activity depends on a sulfated tyrosine at position 7 from the C-terminus. In lower vertebrates, a sulfated tyrosine is important, but the position is less important.

The selectivity explains why mammalian gastrin, with the tyrosine at position 6 from the C-terminus, is virtually inactive at CCK receptors. But there is a problem with chicken gastrin. This peptide has a tyrosine, not in the gastrin position, but in the CCK position. The naturally occurring material is nevertheless a gastrin because it stimulates acid secretion but does not stimulate pancreatic secretion, as Rod Dimaline has shown (Dimaline *et al.*, 1986).

Recent studies comparing the sulfated and unsulfated forms of chicken gastrin confirm this pattern—both are virtually inactive on turkey pancreatic secretion and gall bladder contraction (Rod Dimaline and Caroline Lee, pers. comm.). One possibility appears to be that the chicken has found an interesting way of determining specificity for gastrin over CCK receptors. In particular, the substitution of a proline immediately adjacent to the sulfated tyrosine in chicken gastrin (Fig. 1) may introduce a conformational constraint that has the same effect as shifting the sulfate group relative to the C-terminus. It should be possible, now, to test this hypothesis by synthesis of a range of analogs.

Actions and Roles

Finally, I would like to consider families of actions, rather than families of peptides. Until recently, we knew CCK could act at a number of sites, but we didn't know whether these actions were physiologically important. Now we can study this question because we have a specific antagonist selective for the peripheral type of CCK receptor.

Applied to the pancreas, L364,718 inhibits CCK-, but not bombesin-evoked amylase release, and it has the same inhibiting effect on the gall bladder. CCK also delays gastric emptying, probably by relaxing the body of the stomach. A variety of different liquid test meals inhibit gastric emptying in the conscious gastric fistula rat. The action of protein-rich meals in delaying gastric emptying is inhibited by the CCK-antagonist, but the action of other meals is not (Green *et al.*, 1988).

We can start, then, to arrange the different actions of CCK into an integrated picture in which CCK plays a role in regulating the environment of the small intestine. Thus, on the one hand, CCK stimulates the pancreas and

gall bladder directly to control delivery of pancreatic enzymes and bile salt to the duodenum, and on the other hand, it acts to delay gastric emptying and food intake, and so balances the delivery of nutrient substrate with that of the enzymes and bile salt required for its digestion and assimilation. Some or all of these actions are found throughout the vertebrates. The appearance of gastrin in the higher vertebrates extended the role of this group of peptides to control of the stomach and may have been a later development.

The tools are at hand to examine this scheme at all levels, from the cellular and molecular to the whole animal. It should now be possible to trace the phylogeny of this family through its integrative roles in the gut.

Acknowledgments

My work is supported by grants from the Medical Research Council, the Science and Engineering Research Council, and the Agriculture and Fisheries Research Council of the United Kingdom. I am grateful to Rod Dimaline, Mike Thorndyke, and Mike Greenberg for helpful discussions.

Literature Cited

Dimaline, R., J. Young, and H. Gregory. 1986. Isolation from chicken antrum, and primary amino acid sequence of a novel 36-residue peptide of the gastrin/CCK family. *FEBS Lett.* **205:** 318–322.

Dockray, G. J. 1989. The comparative neuroendocrinology of gut peptides. In *The Neuroendocrinology of the Gut,* G. Makhlouf, ed. Handbook of Physiology. Section on the Gastrointestinal System, American Physiological Society, in press.

Dockray, G. J., R. Dimaline, S. Pauwels, and A. Varro. 1989. Gastrin and CCK-related peptides. Pp. 244–284 in *Peptide Hormones as Prohormones,* J. Martinez, ed. Ellis Horwood, Chichester.

Green, T., R. Dimaline, S. Peikin, and G. J. Dockray. 1988. Action of the cholecystokinin antagonist L-364,718 on gastric emptying in the rat. *Am. J. Physiol.* **225:** G685–689.

Nachman, R. J., G. M. Holman, B. J. Cook, W. F. Haddon, and N. Ling. 1986. Leucosulfakinin II, a blocked sulphated insect neuropeptide with homology to cholecystokinin and gastrin. *Biochem. Biophys. Res. Comm.* **140:** 357–364.

Price, David A., and Michael J. Greenberg. 1989. The hunting of the FaRPs: the distribution of FMRFamide-related peptides. *Biol. Bull.* **177:** 000–000.

Richter, K., R. Egger, and G. Kreil. 1986. Sequence of preprocaerulein cDNAs cloned from skin of *Xenopus laevis.* A small family of precursors containing one, three, or four copies of the final product. *J Biol. Chem.* **261:** 3676–3680.

Vigna, S., M. C. Thorndyke, and J. A. Williams. 1986. Evidence for a common evolutionary origin of brain and pancreas cholecystokinin receptors. *Proc. Natl. Acad. Sci. USA* **83:** 4355–4359.

Vlasak, R., O. Wiborg, K. Richter, S. Burgschwaiger, J. Vuust, and G. Kreil. 1987. Conserved exon-intron organization in two different caerulein precursor genes of *Xenopus laevis.* Additional detection of an exon potentially coding for a new peptide. *Eur. J. Biochem.* **169:** 53–58.

Reference: *Biol. Bull.* **177:** 198–205. (October, 1989)

The Hunting of the FaRPs: The Distribution of FMRFamide-Related Peptides

DAVID A. PRICE AND MICHAEL J. GREENBERG

The Whitney Laboratory of the University of Florida, 9505 Ocean Shore Blvd., St. Augustine, Florida 32086

For the FaRPs are peculiar peptides, that won't
Be caught in a commonplace way.
Do all that you know, and try all that you don't:
Not a chance must be wasted to-day![1]

Introduction

The family of *F*MRF*a*mide-*r*elated *p*eptide*s* (FaRPs) is a large assemblage of neuropeptides found throughout the Metazoa (Price *et al.*, 1987a; Greenberg *et al.*, 1988; Greenberg and Price, 1988). The first FaRP completely characterized—the tetrapeptide amide Phe-Met-Arg-Phe-NH_2 (*i.e.*, FMRFamide[2] itself) was isolated from a clam by virtue of its cardioexcitatory effect (Price and Greenberg, 1977); but we will use the term FaRP for any peptide that can be found by looking with an assay for FMRFamide, and these assays need not involve cardioexcitation or any other biological effect. A few molluscan FaRPs have been found using bioassay, but most, especially in other phyla, have been found with immunoassays. New FaRPs are constantly being added to the family rolls as the number of taxa investigated, and the detail with which each is studied, increases. Therefore, the generalizations made here, and based on only a few scattered data, will undoubtedly prove incorrect in the long term, but still provide a framework for further studies.

Our objectives in this review are to enumerate the large, heterogeneous set of FMRFamide-related peptides (FaRPs) and to classify them into more obviously related subsets. We begin by describing the molluscan peptides and our assumptions about their relatedness. We go on to identify (more or less in chronological order) the non-molluscan peptides that have been thought of as members of the FaRP family, and consider the characters that seem to relate them. From this broader perspective, we then attempt to divide the FaRPs into those that show clear evidence of homology from those that do not. Since FMRFamide is a mere tetrapeptide, we cannot establish homology by examining the peptide sequences alone; they are simply too short. Fortunately, several genes for FaRP precursors have been cloned and sequenced, and we will rely heavily on these data for demonstrating likely homologies.

Hunting the Molluscan FaRPs

By the time FMRFamide was sequenced there was already chromatographic evidence that FMRFamide-like biological activity is present throughout the Mollusca (Agarwal *et al.*, 1972). We now believe that FMRFamide itself accounts for the majority of this activity in most species, with FLRFamide as a ubiquitous and always minor component (Price, 1986, 1987). FLRFamide is typically present at 10–20% the level of FMRFamide, except in opisthobranchs (or at least *Aplysia*) where it is difficult to even detect. Two close congeners of FLRFamide (sequences in Table I) have been found as minor components in *Octopus vulgaris* by Martin and Voigt (1987).

FMRFamide is not, however, the major immunoreactive FaRP in all molluscs. In one group—the pulmonate snails and slugs—heptapeptides of the form XDPFLR-

[1] With apologies to Lewis Carroll.

[2] The uppercase letters in the name "FMRFamide" are the approved one-letter abbreviations of the amino acids constituting the peptide. Thus, "FMRFamide" conveys both the sequence of the peptide and its blocked C-terminal. FMRFamide can also be pronounced, and people often ask us how to do it. The answer is: "Anyway you want." We have heard, for example: fmerf'-amid, fuh-merf'-amid, fer-merf'-amid, fer-maf'-amid, fer-mahf'-amid, fah-mahf'-amid, and ef-em-ahr-ef-ay'-mide. All of these pronunciations, and any others that anyone can produce, are totally, and therefore equally, correct. In summary, the meaning of FMRFamide resides unambiguously and eternally in the written characters, and is independent of linguistic variability.

Table I

The FMRFamide-related peptides (FaRPs) of molluscs

The tetrapeptides and two relatives from Octopus	
Phe-Met-Arg-Phe-NH_2	FMRFamide
Phe-Leu-Arg-Phe-NH_2	FLRFamide
Thr-Phe-Leu-Arg-Phe-NH_2	TFLRFamide
Ala-Phe-Leu-Arg-Phe-NH_2	AFLRFamide
The pulmonate heptapeptides	
pGlu-Asp-Pro-Phe-Leu-Arg-Phe-NH_2	pQDPFLRFamide
Ser-Asp-Pro-Phe-Leu-Arg-Phe-NH_2	SDPFLRFamide
Gly-Asp-Pro-Phe-Leu-Arg-Phe-NH_2	GDPFLRFamide
Asn-Asp-Pro-Phe-Leu-Arg-Phe-NH_2	NDPFLRFamide

Right-hand column: the amino acids are represented by their one-letter abbreviations; pQ and pGlu are pyroglutamic acid.

Famide constitute a significant fraction of the FMRFamide-like activity. In collaboration with others (Price *et al.*, 1985; Ebberink *et al.*, 1987; Price *et al.*, 1987b), we have identified four such heptapeptides with X = Gly (G), Ser (S), pGlu (pQ), or Asn (N) (Table I).

The FMRFamide precursor gene of *Aplysia* has been sequenced (Schaefer *et al.*, 1985; Taussig and Scheller, 1986). Most of it is composed of repeated stretches of 15 or 16 amino acids, each segment containing one FMRFamide, its associated processing signals, and an acidic sequence which may only be a spacer. All together, the gene encodes 28 copies of FMRFamide, one copy of FLRFamide, and one copy of an apparently related peptide ending in -Tyr-Leu-Arg-Phe-amide. Though this last peptide has never been identified in extracts, it is expected to be a minor FaRP in *Aplysia*.

Since many of the repeated segments of the *Aplysia* gene are more than 90% identical at the nucleotide level, we suggested that they arose relatively recently (geologically speaking), and that back-extrapolation would lead to a more general molluscan precursor (Price *et al.*, 1987b). Such a hypothetical, general molluscan precursor would have only about nine copies of FMRFamide, one of FLRFamide, and one corresponding to the as yet undetected *Aplysia* peptide: -Tyr-Leu-Arg-Phe-NH_2. Such a precursor would come close to accounting for the FMRFamide/FLRFamide ratio observed in most molluscs, and, of course, assumes that all molluscs have a FMRFamide precursor homologous to, but less highly duplicated than, that of *Aplysia*.

We further hypothesized that the pulmonate heptapeptides are encoded on a separate gene, perhaps corresponding to the extreme N-terminal part of the ancestral precursor (Price *et al.*, 1987b). This hypothesis was based, not so much on the *Aplysia* gene (which is not really relevant since *Aplysia* does not have the heptapeptides), as on the disjoint tissue distributions of FMRFamide and the heptapeptides (Lehman and Price, 1987), and on their distinct biological effects on some muscles (Lehman and Greenberg, 1987) in *Helix*. Likewise, this hypothesis assumes that the heptapeptide gene is homologous to the *Aplysia* FMRFamide gene.

A recent report has given some support to parts of this hypothesis. A cDNA clone containing the entire precursor encoding region has been isolated and sequenced from the pulmonate *Lymnaea* (Linacre *et al.*, 1989). This precursor encodes nine copies of FMRFamide and two of FLRFamide, so it is only about half the size of that from *Aplysia* and is also less highly replicated. Nevertheless, the genes from the two species are clearly homologous. The *Lymnaea* precursor also encodes neither of the heptapeptides found in this snail by Ebberink *et al.* (1987). These findings support our concept of the origin of the *Aplysia* precursor, justifies our supposition that the FLRFamide/FMRFamide ratio in tissue extracts reflects the relative number of copies of the two peptides in the precursor, and bolsters the idea that the heptapeptides are encoded on a separate gene, or genes.

An unusual molluscan FaRP

Though many neurons in *Aplysia* abdominal ganglion stain with antisera against FMRFamide (Brown *et al.*, 1985), not all of them express the FMRFamide precursor gene described above. For example, neurone L5 was found to express a small precursor, dissimilar in sequence to that of FMRFamide, but containing one copy of a potentially secreted peptide ending: -Gln-Gly-Arg-Phe-NH_2 (Shyamala *et al.*, 1986). Because the substitution of Gly for Met in FMRFamide is associated with a large decrease in biological activity (Greenberg *et al.*, 1988), the *Aplysia* L5 peptide is probably not functional at FMRFamide receptors.

Though the tetrapeptides and heptapeptides have distinct effects, they are usually biologically cross-reactive, and we have always assumed that they are homologous. We argue below that the L5 peptide is not homologous to FMRFamide and, in fact, use it as an outlier in our attempts to identify those FaRPs that are most likely to be homologous.

Hunting the Non-Molluscan FaRPs

Soon after FMRFamide was sequenced, antisera were raised against it and were used in immunocytochemistry to reveal FMRFamide-like immunoreactivity throughout the animal kingdom (reviewed in Greenberg *et al.*, 1985). Even the first paper to appear (Boer *et al.*, 1980) reported FMRFamide-like immunoreactivity in arthropods and vertebrates, as well as molluscs.

Vertebrates

Immunocytochemical studies of mammalian (rat) brain (Weber *et al.*, 1981; also Williams, 1983; Dockray

Table II

Sequences of some non-molluscan FaRPs

Common name	Source	Sequence
Vertebrate peptides		
gamma$_1$-MSH	ox	YVMGHFRWDRFa
BPP	ox	APLEPQYPGDDATPEQMAQYAAELRRYINMLTRPRYa
APP	chicken	GPSQPTYPGDDAPVEDLIRFYDNLQQYLNVVTRHRYa
NPY	pig	YPSKPDNPGEDAPAEDLARYYSALRHYINLITRQRYa
PYY	pig	YPAKPEAPGEDASPEELSRYYASLRHYLNLVTRQRYa
PP	salmon	YPPKPENPGEDAPPEELAKYYTALRHYINLITRQRYa
PP	alligator	TPLQPKYPGDGAPVEDLIQFYNDLQQYLNVVTRPRFa
A18Fa	ox	AGEGLSSPFWSLAAPQRFa
F8Fa	ox	FLFQPQRFa
	chicken	LPLRFa
Invertebrate peptides		
antho-RFamide	sea anemone (*Anthopleura*)	pQGRFa
pol-RFamide	hydrozoan jellyfish (*Polyorchis*)	pQLLGGRFa
antho-RWamide	sea anemone	pQSLRWa
antho-RWamide II	sea anemone	pQGLRWa
	fruitfly (*Drosophila*)	DPKQDFMRFa
	roundworm (*Ascaris*)	KNEFIRFa
	American lobster (*Homarus*)	SDRNFLRFa
	American lobster	TNRNFLRFa
leucomyosuppressin	cockroach (*Leucophaea*)	pQDVDHVFLRFa
schistoFLRFamide	locust (*Schistocerca*)	PDVDHVFLRFa
leucosulfakinin	cockroach	pQSDDYGHMRFa
LSK II	cockroach	EQFEDYGHMRFa

References and further information about the peptides in the text. Abbreviations: MSH, melanophore stimulating hormone; BPP, bovine pancreatic polypeptide; APP, avian PP; NPY, neuropeptide tyrosine; PYY, peptide with N- and C-terminal tyrosines; LSK II, leucosulfakinin II. The one-letter abbreviations of the amino acids are used in the sequences: E, Glu; H, His; I, Ile; K, Lys; Q, Gln; pQ, pyroglutamic acid; V, Val; W, Trp; Y, Tyr; a, amide; others in Table I.

and Williams, 1983) showed extensive anti-FMRFamide staining, but most exceptionally in the cortex where few peptides are localized.

Gamma$_1$-MSH. One mammalian peptide—gamma$_1$-MSH—had been predicted to end in RFamide based on the sequence of the bovine pro-opio-melanocortin (Nakanishi *et al.,* 1979) gene (sequence in Table II). Thus, it might cross-react with FMRFamide antisera, but being restricted mainly to the pituitary, seemed unlikely to account for the cortical staining. Moreover, rats (and other rodents) do not produce the amidated peptide because their precursors lack the appropriate processing signals. Later, Ali-Rachedi *et al.* (1983) showed that some FMRFamide and gamma$_1$-MSH antisera do indeed stain the same pituitary corticotrophs in those mammalian species having the amidated form of the peptide. But gamma$_1$-MSH can only account for a small part of the total FMRFamide-like staining in the brain.

Pancreatic polypeptide. The pancreatic polypeptides are also vaguely similar to FMRFamide. The first members of the family sequenced (from pancreas, of course; Lin and Chance, 1974; Kimmel *et al.,* 1975) both ended -Arg-Tyr-NH$_2$. Though the C-terminal pentapeptide of bovine pancreatic polypeptide (BPP) lacked FMRFamide-like biological activity (Price and Greenberg, 1980), FMRFamide antisera stain vertebrate pancreas and gut, so it was argued that the PPs might be FMRFamide analogs.

Antisera to avian PP, or to the C-terminal hexapeptide of BPP also showed a pattern of staining in mammalian brain (Lundberg *et al.,* 1980) similar to that revealed by anti-FMRFamide. Were the PP antisera revealing FaRPs or were the FMRFamide antisera revealing PPs?

The issue was resolved by Tatemoto, who had developed a chromatographic method for identifying peptides with C-terminal amides and was applying it to porcine brain and gut. He isolated and sequenced two peptides that are clearly related to the pancreatic polypeptides (Tatemoto, 1982a, b; sequences in Table II). These peptides—NPY from brain and PYY from intestine—share the C-terminal sequence Arg-Tyr-amide with the pancreatic members of the family. When antisera to NPY were raised, they stained the same brain structures as the APP antiserum (Lundberg *et al.,* 1984; Moore *et al.,* 1984), so the story seemed to be that the pancreatic polypeptide-like (and possibly the FMRFamide-like) immunoreactivities of brain were due to NPY.

However, though some FMRFamide antisera stain the same brain structures as antisera to NPY, others do *not* (*e.g.*, Chronwall *et al.*, 1984; Triepel and Grimmelikhuijzen, 1984). So NPY could not account for all of the staining. When alligator PP was shown to end in Arg-Phe-NH_2, rather than Arg-Tyr-NH_2 (Lance *et al.*, 1984), it revived interest in the relation between the FaRPs and the PPs. Such a relationship would also have seemed stronger if NPY had been found using antisera to FMRFamide rather than by hunting for peptide amides.

Chicken and beef. The first peptide completely characterized by following its FMRFamide-like cross-reactivity was LPLRFamide from chicken brain (Dockray *et al.*, 1983; sequence in Table II). LPLRFamide seems to be unrelated to the pancreatic polypeptide family, is similar in size to FMRFamide, and has a tripeptide amide sequence in common with the natural FMRFamide congener FLRFamide. It even has detectable, though low, FMRFamide-like biological activity (3/10,000 of FMRFamide on the clam heart and the radula protractor). Two peptides were then isolated by Yang *et al.* (1985) from bovine brain (sequences in Table II). Both of these peptides have a glutamine where the chicken peptide has a leucine, so they are more NPY-like than the chicken peptide, but they still may well be its bovine homologs.

By 1985, therefore, the hunt for vertebrate FaRPs was winding down. Three new peptides had been discovered and characterized, and they seemed to represent a new peptide family. As for the relationship between the pancreatic polypeptide family and FMRFamide, it did not seem to be a very close one. Indeed, recent work has shown that the PP of fish is very NPY-like and has the usual C-terminal: Arg-Tyr-NH_2 (Kimmel *et al.*, 1986; sequence in Table II). So the Arg-Phe-NH_2 terminal of alligator PP is not primitive, but rather a reptilian specialization convergent to FMRFamide.

Non-molluscan invertebrates

Coelenterates. The first coelenterate FaRP was isolated from an anthozoan and named antho-RFamide (pQGRF-NH_2; Grimmelikhuijzen and Graff, 1986; see Table II). It is a tetrapeptide, like FMRFamide, but actually has more sequence in common with the L5 peptide of *Aplysia* (see Greenberg and Price, 1988). A similar, but longer peptide (pQLLGGRFamide, Grimmelikhuijzen *et al.*, 1988), has been isolated from another class (Hydrozoa) of coelenterates. It appears to be simply the hydrozoan version of anthoRFamide.

More recently, a pair of peptides that are more FMRFamide-like have been isolated from a sea anemone. These two peptides, pQSLRWamide and pQGLRWamide (antho-RWa and antho-RWa II, see Table II; Graff and Grimmelikhuijzen, 1988a, b), have a Trp-NH_2 at the C-terminal, rather than a Phe-NH_2. But they were discovered by their activity in an RIA for FMRFamide, and our structure-activity studies indicate that FMRFamide analogs with a Trp substituted for either Phe residue are effective in molluscan bioassays. They both also have the leucine residue in common with FLRFamide, so their FMRFamide-like biological potency would exceed that of the coelenterate FaRPs terminating in -GRFamide. The relationship between these two types of peptide, both coelenterate FaRPs, remains unclear.

Arthropods. A bevy of FaRPs have been flushed from a disparate group of arthropod species. Two related peptides from the American lobster (Trimmer *et al.*, 1987), one from the fruitfly, *Drosophila* (Nambu *et al.*, 1988), and one from a locust (schistoFLRFamide; Robb *et al.*, 1989) have been isolated by following their FMRFamide-like immunoreactivity and sequenced (Table II). Still, all three species had several additional peaks. Some of the additional fruitfly peaks probably represent peptides predictable from the structure of the precursor gene (Nambu *et al.*, 1988; Schneider and Taghert, 1988).

Three additional FaRPs—leucomyosuppressin (Holman *et al.*, 1986) and leucosulfakinins I and II (Nachman *et al.*, 1986a, b; Table II)—were isolated from cockroaches solely on the basis of their biological actions. Leucomyosuppressin is a single amino acid variant of schistoFLRFamide (Robb *et al.*, 1989), and the leucosulfakinins, in addition to being FaRPs, show similarities to the gastrin/CCK family, a matter discussed by G. J. Dockray in this volume (see also Greenberg and Price, 1988).

Since none of the several FaRPs predictable from the fruitfly precursor are very similar to the cockroach or locust peptides, more fly FaRPs may remain to be discovered. Thus, there are probably distinct sub-families of FaRPs in insects, just as there are in molluscs.

Nematodes. Neurons in the free-living nematode *Caenorhabditis elegans* were immunochemically stained with anti-FMRFamide sera (Li and Chalfie, 1986). Shortly thereafter, a FaRP, KNEFIRFamide, was detected by RIA in *Ascaris suum* and sequenced (Cowden *et al.*, 1989; Table II). This was the first report of a natural FaRP with an isoleucine replacing the methionine residue. Our structure-activity relations (SAR) studies indicate that this change would produce an analog with only moderately lowered FMRFamide-like biological activity on the clam heart.

The Thrill of the Hunt

The hunting of FaRPs has led to the successful identification of peptides in diverse groups of animals from coelenterates to mammals, and in some of these groups they are among the first peptides completely characterized.

How to account for this success? First, all described

antisera to FMRFamide (and virtually all bioassays sensitive to this peptide) seem to discriminate very well the amidated peptide from unamidated or C-terminally extended forms. The presence of a C-terminal amide is one unmistakable mark of a peptide that has gone through the secretory pathway, and all known peptide amides seem to be involved in intercellular communication.

Second, and beyond amidation, an RFamide is generally regarded as the minimum structural requirement for immunoreactivity with even the least selective anti-FMRFamide sera. But the stringency of this requirement for most antisera in wide use has not been evaluated. We have noted above that at least some anti-FMRFamide sera can stain NPY-containing neurons (-Arg-Tyr-NH_2) in mammalian brain, and the -Arg-Trp-NH_2 peptides in coelenterate neurons. Even the requirement for a penultimate Arg is not universal (Dockray, 1985). In summary, FMRFamide antisera are relatively unselective detectors, so the number of potentially detectable peptides in a species is large. Thus, the catch is rather good, if varied (Table II).

Subgroups of FaRPs

Come listen, my men, while I tell you again
The clear unmistakable marks
By which you may know, wheresoever you go,
The warranted genuine FaRPs.[1]

The FaRPs collected in Table II are a heterogeneous assemblage, ranging in size from 4 to 36 amino acids, with a penultimate Arg and a C-terminal amide as the only common structural features. Thus, there appears to be no natural limit to what someone might consider to be a FaRP (*e.g.*, Morris *et al.*, 1982). However, within the FaRPs, certain peptides constitute structurally related, and possibly homologous, subgroups. We are particularly interested in defining the subgroup of peptides homologous to FMRFamide.

Homologous FaRPs

Since homology implies inheritance of common features from common ancestors, detection of homology is best achieved by comparing the genes encoding the precursors. Since few FaRP genes or precursors are known, we are left, in most cases, with examining the similarity between the peptides themselves.

Sequence similarity. Unfortunately, the reliability of sequence similarity as a clue to homology declines with the length of the peptides being compared. Short stretches of amino acid sequence occur frequently by chance; Price (1983) calculated that any given sequence of four amino acids will occur at least once in the proteins of any species, but the odds go down dramatically as the sequences become longer. Thus, matches of six amino acids in a row (without gaps) are fairly unique and indicate a likely homology. The expression of FMRFamide actually requires a sequence of at least seven amino acids: Phe, Met, Arg, and Phe (the body of the peptide); Gly (to form the amide); and at least one basic amino acid (*e.g.*, Arg)—but more usually a dipeptide (Lys-Arg, Lys-Ser, or Arg-Ser)—on each end as a cleavage signal.

On the above argument, we assume a match of six residues (including processing signals) as the minimum requirement for homology. Then, for example, the *Drosophila* peptide DPKQDFMRFamide, which matches FMRFamide in six of seven residues, is a likely homolog. And so are leucomyosuppressin and schistoFLRFamide, the two lobster peptides, and the pulmonate heptapeptides; all of them have six residues in a row matching FLRFamide (compare sequences in Table I and II). The nematode peptide KNEFIRFamide, has only four residues in a row matching FMRFamide or FLRFamide. Nevertheless, it is very similar to DPKQDFMRFamide from the fruitfly; four of seven residues are identical, and the other three are conservative substitutions. So we conclude that the *Ascaris* and *Drosophila* peptides are homologous to each other and that the worm peptide is a homologous FaRP.

In contrast, the leucosulfakinins (which have the C-terminus-DYGHMRF-NH_2) have a match of only five amino acids, and the tyrosine residue is sulfated (Nachman *et al.*, 1986a, b). Thus, this peptide is an unlikely homolog of FMRFamide. Similarly, we would exclude LPLRFamide, the rest of the vertebrate FaRPs, and the coelenterate peptides.

On the basis of sequence, then, we have selected a set of homologous FaRPs that is characterized by the C-terminal structure FXRFamide (where X = M, L, or I).

Precursors. For the FaRPs that appear to be homologous on the basis of sequence, precursor genes have only been completely sequenced from *Aplysia* and *Drosophila*. Inspection of these precursors reveals several gross similarities, especially the highly repetitive nature of each (Nambu *et al.*, 1988; Schneider and Taghert, 1988). This repetitiveness can be illustrated by diagonal plots of each precursor upon itself (Fig. 1). The strong lines parallel to the main diagonal in these plots reflect the internal similarities within the precursors (Fig. 1a, b). In contrast, a diagonal plot *comparing* the *Aplysia* and *Drosophila* precursors (Fig. 1c) shows no such prominent diagonal lines, but only a series of very short diagonal dashes indicating the matching FMRFamide sequences within the two precursors. The longest such match (and also the longest stretch of exact amino acid sequence match) *between* the precursors is the heptapeptide FMRFGRS, whereas *each* precursor has 5 tandem repeats of the exact same 15 (*Aplysia*) or 11 (*Drosophila*) amino acids. Thus, the repeats within each precursor are more similar to

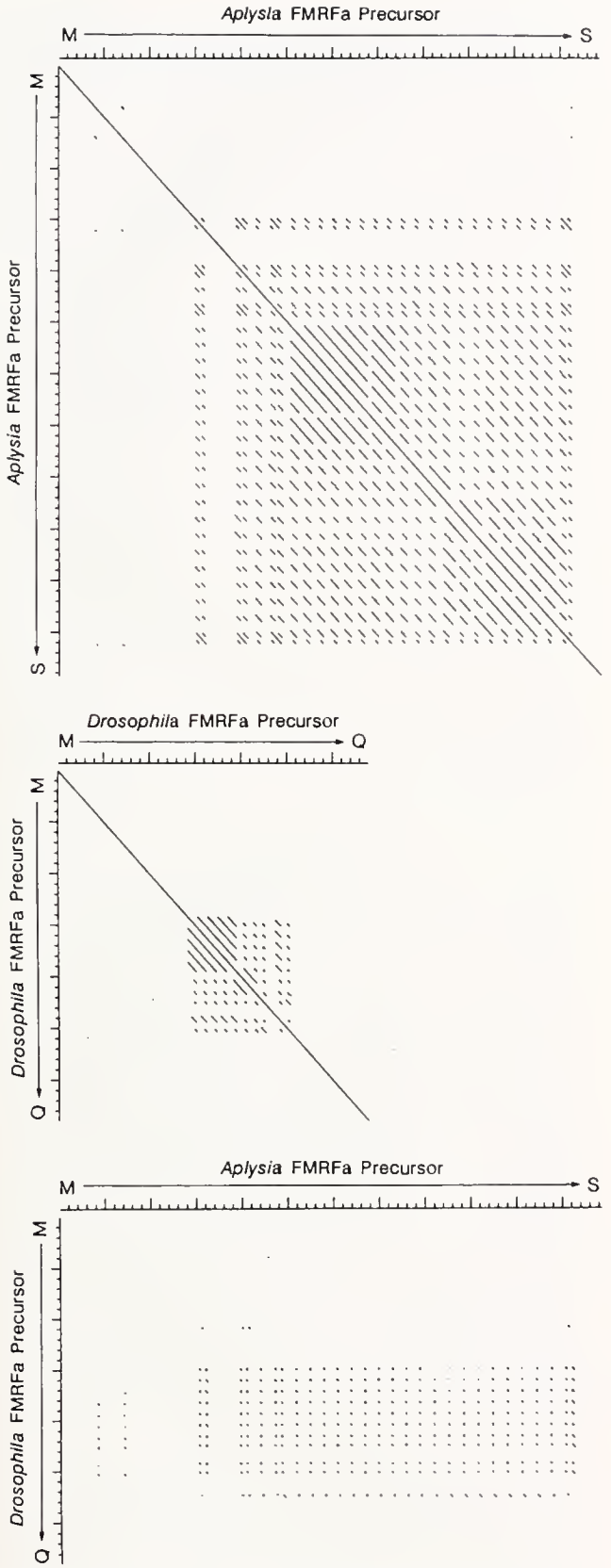

Figure 1. Diagonal plots (dot matrix plots, see Doolittle, 1986, for more explanation) comparing the *Aplysia* and *Drosophila* FaRP precursor sequences to themselves (top, middle) and to each other (bottom). The computer compares successive tetrapeptide sequences and draws a dot wherever four in a row from each protein match. The self comparisons show a complete diagonal line of self identity, and parallel lines showing internal duplications. A match of more than four amino acids in a row results in a diagonal line (down and to the right) of n-3 dots where n is the number of identical amino acids.

each other than they are to those of the other precursor. How could such a relationship develop?

The simplest explanation is that each precursor originated with an independent partial duplication of an ancestral precursor. Alternatively, as suggested by Nambu *et al.* (1988), their most recent common ancestor could have been highly duplicated and one or both of its daughters suffered partial gene conversion to regularize their repeats. These possibilities are not unconnected, and both would be favored if the FMRFamide gene contained a so-called "hot spot"; *i.e.*, a region of high recombination frequency.

Of the FaRPs that do not appear to be homologous on the basis of peptide sequence, precursors are known for the pancreatic polypeptide-like peptides (Minth *et al.*, 1984; Leiter *et al.*, 1985), gamma$_1$-MSH (Nakanishi *et al.*, 1979), and the *Aplysia* L5 peptide (Shyamala *et al.*, 1986). The precursor encoded by the L5 gene is exemplary: it is not detectably repetitive (Fig. 2a), and contains only a single stretch of sequence [RFGKR; the terminal dipeptide (RF) plus its amidation and cleavage signals] in common with either the *Aplysia* or *Drosophila* FMRFamide precursor (Fig. 2b, c). So a comparison of the genes supports our conclusion from the peptide sequences that this precursor is not homologous to that of FMRFamide.

Conclusions

The subset of FaRPs terminating in FXRFamide are probably homologs. But some members of this group may not be homologous to FMRFamide at all, while other FaRPs that lack the FXRFamide sequence will prove to be homologs once their precursors can be scrutinized. Some FaRPs that are not in the FXRFamide subset seem to fall into distinct families of peptide homologs. But lacking the requisite genetic data, we cannot yet reliably define these groups.

The plethora of metazoan FaRPs—peptides recognized by assays for FMRFamide—may reflect idiosyncracies of the eukaryotic secretory pathway. In particular, the presence of a C-terminal amide is a universal requirement for a FaRP, but not all amino acids are equally suitable substrates for the amidation system; non-polar and aromatic amino acids seem to be especially favorable. Likewise, the frequent occurrence of ar-

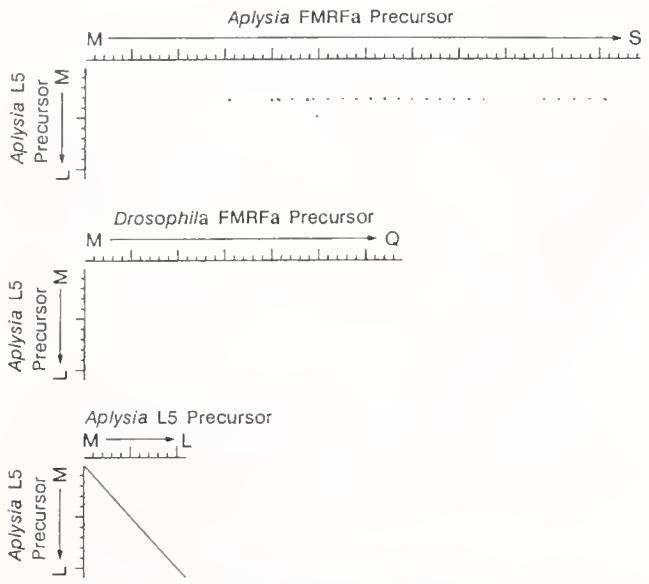

Figure 2. Diagonal plots comparing the *Aplysia* L5 gene product to itself and to the FaRP precursors of Figure 1.

ginine in the penultimate position may reflect characteristics of the trypsin-like processing system.

The FXRFamides are found in nematodes, molluscs, annelids, and arthropods. These and related phyla constitute the Protostomia, a group of invertebrates that are supposedly related because they share certain developmental characters. Of course, the leukosulfakinins and the L5 peptide show us again that every protostomian FaRP detected is not necessarily homologous to FMRFamide.

Finally, if the protostomian FXRFamides are indeed homologs, why have they been conserved? We may speculate that, since most of these peptides appear to modulate muscle contractility, they may be involved in controlling some feature unique to protostomian muscle.

Acknowledgments

The original work reported here was supported by NIH grant HL-28440 and NSF grant DCB-8616356. This is contribution #285 from the Tallahassee, Sopchoppy and Gulf Coast Marine Biological Association.

Literature Cited

Agarwal, R. A., P. J. B. Ligon, and M. J. Greenberg. 1972. The distribution of cardioactive agents among molluscan species and tissues. *Comp. Gen. Pharmacol.* **3:** 249–260.

Ali-Rachedi, A., G. L. Ferri, I. Varndell, S. Van Noorden, L. P. C. Schot, N. Ling, S. R. Bloom, and J. M. Polak. 1983. Immunocytochemical evidence for the presence of gamma$_3$-MSH-like immunoreactivity in pituitary corticotrophs and ACTH-producing tumours. *Neuroendocrinol* **37:** 427–433.

Boer, H. H., L. P. C. Schot, J. A. Veenstra, and D. Reichelt. 1980. Immunocytochemical identification of neural elements in the central nervous system of a snail, some insects, a fish and a mammal with an antiserum to the molluscan cardio-excitatory tetrapeptide FMRF-amide. *Cell Tis. Res.* **213:** 21–27.

Brown, R. O., D. Gussman, A. I. Basbaum, and E. Mayeri. 1985. Identification of *Aplysia* neurons containing immunoreactive FMRFamide. *Neuropeptides* **6:** 517–526.

Chronwall, B. M., J. A. Olschowka, and T. L. O'Donohue. 1984. Histochemical localization of FMRFamide-like immunoreactivity in the rat brain. *Peptides* **5:** 569–584.

Cowden, C., A. O. W. Stretton, and R. E. Davis. 1989. A1, a sequenced bioactive peptide isolated from the nematode *Ascaris suum*. *Neuron* **2:** 1465–1473.

Dockray, G. J. 1985. Characterization of FMRFamide-like immunoreactivity in rat spinal cord by region-specific antibodies in radioimmunoassay and HPLC. *J. Neurochem.* **45:** 152–158.

Dockray, G. J., and R. G. Williams. 1983. FMRFamide-like immunoreactivity in rat brain: development of a radioimmunoassay and its application in studies of distribution and chromatographic properties. *Brain Res.* **266:** 295–303.

Dockray, G. J., J. R. Reeve, Jr., J. Shively, R. J. Gayton, and C. S. Barnard. 1983. A novel active pentapeptide from chicken brain identified by antibodies to FMRFamide. *Nature* **305:** 328–330.

Doolittle, R. F. 1986. *Of URFs and ORFs: A Primer on How to Analyze Derived Amino Acid Sequences.* University Science Books, Mill Valley, California.

Ebberink, R. H. M., D. A. Price, H. van Loenhout, K. E. Doble, J. P. Riehm, W. P. M. Geraerts, and M. J. Greenberg. 1987. The brain of *Lymnaea* contains a family of FMRFamide-like peptides. *Peptides* **8:** 515–522.

Graff, D., and C. J. P. Grimmelikhuijzen. 1988a. Isolation of <Glu-Ser-Leu-Arg-Trp-NH_2, a novel neuropeptide from sea anemones. *Brain Res.* **442:** 354–358.

Graff, D., and C. J. P. Grimmelikhuijzen. 1988b. Isolation of <Glu-Gly-Leu-Arg-Trp-NH_2 (Antho-RWamide II), a novel neuropeptide from sea anemones. *FEBS Lett.* **239:** 137–140.

Greenberg, M. J., and D. A. Price. 1988. The phylogenetic and biomedical significance of extended neuropeptide families. Pp. 85–96 in *Biomedical Importance of Marine Organisms,* D. G. Fautin, ed. California Academy of Sciences, San Francisco.

Greenberg, M. J., D. A. Price, and H. K. Lehman. 1985. FMRFamide-like peptides of molluscs and vertebrates: distribution and evidence of function. Pp. 370–376 in *Neurosecretion and the Biology of Neuropeptides,* H. Kobayashi, H. Bern and A. Urano, ed. Japan Sci. Soc. Press, Tokyo/Springer-Verlag, Berlin.

Greenberg, M. J., K. Payza, R. J. Nachman, G. M. Holman, and D. A. Price. 1988. Relationships between the FMRFamide-related peptides and other peptide families. *Peptides* **9(Suppl. 1):** 125–135.

Grimmelikhuijzen, C. J. P., and D. Graff. 1986. Isolation of <Glu-Gly-Arg-Phe-NH_2 (Antho-RFamide), a neuropeptide from sea anemones. *Proc. Natl. Acad. Sci. USA* **83:** 9817–9821.

Grimmelikhuijzen, C. J. P., M. Hahn, K. L. Rinehart and A. N. Spencer. 1988. Isolation of <Glu-Leu-Leu-Gly-Gly-Arg-Phe-NH_2 (PolRFamide), a novel neuropeptide from hydromedusa. *Brain Res.* **475:** 198–203.

Holman, G. M., B. J. Cook, and R. J. Nachman. 1986. Isolation, primary structure and synthesis of leucomyosuppressin, an insect neuropeptide that inhibits spontaneous contractions of the cockroach hindgut. *Comp. Biochem. Physiol.* **85C:** 329–333.

Kimmel, J. R., L. J. Hayden, and H. G. Pollock. 1975. Isolation and characterization of a new pancreatic polypeptide hormone. *J. Biol. Chem.* **250:** 9369–9376.

Kimmel, J. R., E. M. Plisetskaya, H. G. Pollock, J. W. Hamilton, J. B. Rouse, K. E. Ebner, and A. B. Rawitch. 1986. Structure of a peptide from coho salmon endocrine pancreas with homology to neuropeptide Y. *Biochem. Biophys. Res. Comm.* **141:** 1084–1091.

Lance, V., J. W. Hamilton, J. B. Rouse, J. R. Kimmel and H. G. Pol-

lock. 1984. Isolation and characterization of reptilian insulin, glucagon, and pancreatic polypeptide: complete amino acid sequence of alligator (*Alligator mississippiensis*) insulin and pancreatic polypeptide. *Gen. Comp. Endocrinol.* **55:** 112–124.

Leiter, A. B., M. R. Montminy, E. Jamieson, and R. H. Goodman. 1985. Exons of the human pancreatic polypeptide gene define functional domains of the precursor. *J. Biol. Chem.* **260:** 13013–13017.

Lehman, H. K., and M. J. Greenberg. 1987. A study of a FMRFamide neuropeptide family in the gastropod mollusc, *Helix aspersa:* the actions of FMRFamide and pQDPFLRFamide. *J. Exp. Biol.* **131:** 55–68.

Lehman, H. K., and D. A. Price. 1987. Localization of FMRFamide-like peptides in the snail *Helix aspersa. J. Exp. Biol.* **131:** 37–53.

Li, C., and M. Chalfie. 1986. FMRFamide-like immunoreactivity in *C. elegans. Neurosci. Abst.* **12:** 246.

Lin, T.-M., and R. E. Chance. 1974. Bovine pancreatic polypeptide (BPP) and avian pancreatic polypeptide (APP). *Prog. Gastroenterol.* **67:** 737–738.

Linacre, A., E. Kellet, S. Saunders, K. Bright, P. Benjamin, and J. F. Burke. 1989. FMRFamide and related peptides are encoded as multiple copies in a single gene in *Lymnaea stagnalis. J. Neurosci.* (in press).

Lundberg, J. M., T. Hökfelt, A. Anggärd, J. Kimmel, M. Goldstein, and K. Markey. 1980. Coexistence of an avian pancreatic polypeptide (APP) immunoreactive substance and catecholamine in some peripheral and central neurons. *Acta Physiol. Scand.* **110:** 107–109.

Lundberg, J. M., L. Terenius, T. Hökfelt, and K. Tatemoto. 1984. Comparative immunohistochemical and biochemical analysis of pancreatic polypeptide-like peptides with special reference to presence of neuropeptide Y in central and peripheral neurons. *J. Neurosci.* **4:** 2376–2386.

Martin, R., and K. H. Voigt. 1987. The neurosecretory system of the octopus vena cava. *Experientia* **43:** 537–543.

Minth, C. D., S. R. Bloom, J. M. Polack, and J. E. Dixon. 1984. Cloning, characterization, and DNA sequence of a human cDNA encoding neuropeptide tyrosine. *Proc. Natl. Acad. Sci. USA* **81:** 4577–4581.

Moore, R. Y., E. L. Gustafson, and P. Card. 1984. Identical immunoreactivity of afferents to the rat suprachiasmatic nucleus with antisera against avian pancreatic polypeptide, molluscan cardioexcitatory peptide and neuropeptide Y. *Cell Tis. Res.* **236:** 41–46.

Morris, H. R., M. Panico, A. Karplus, P. E. Lloyd, and B. Riniker. 1982. Elucidation by FAB-MS of the structure of a new cardioactive peptide from *Aplysia. Nature* **300:** 643–645.

Nachman, R. J., G. M. Holman, B. J. Cooke, W. F. Haddon and N. Ling. 1986a. Leucosulfakinin-II, a blocked sulfated insect neuropeptide with homology to cholecystokinin and gastrin. *Biochem. Biophys. Res. Comm.* **140:** 357–364.

Nachman, R. J., G. M. Holman, W. F. Haddon, and N. Ling. 1986b. Leucosulfakinin, a sulfated insect neuropeptide with homology to gastrin and cholecystokinin. *Science* **234:** 71–73.

Nakanishi, S., A. Inoue, T. Kita, M. Nakamura, A. C. Y. Chang, S. N. Cohen, and S. Numa. 1979. Nucleotide sequence of cloned cDNA for bovine corticotropin-beta-lipotropin precursor. *Nature* **278:** 423–427.

Nambu, J. R., C. Murphy-Erdosh, P. C. Andrews, G. J. Feistner, and R. H. Scheller. 1988. Isolation and characterization of a *Drosophila* neuropeptide gene. *Neuron* **1:** 55–61.

Price, D. A. 1983. FMRFamide: assays and artifacts. Pp. 184–190 in *Molluscan Neuroendocrinology,* J. Lever and H. H. Boer, ed. North Holland Publishing Co, New York.

Price, D. A. 1986. Evolution of a molluscan cardioregulatory neuropeptide. *Am. Zool.* **26:** 1007–1015.

Price, D. A. 1987. The distribution of some FMRFamide- and SCP-related peptides in the Mollusca. Pp. 208–214 in *Neurobiology, Molluscan Models,* H. H. Boer, W. P. M. Geraerts and J. Joose, ed. Mon. Kon. Ned. Akad. Wetensch., North Holland Publ. Co., Amsterdam.

Price, D. A., and M. J. Greenberg. 1977. Structure of a molluscan cardioexcitatory neuropeptide. *Science* **197:** 670–671.

Price, D. A., and M. J. Greenberg. 1980. Pharmacology of the molluscan cardioexcitatory neuropeptide FMRFamide. *Gen. Pharmacol.* **11:** 237–241.

Price, D. A., C. G. Cobb, K. E. Doble, J. K. Kline, and M. J. Greenberg. 1987a. Evidence for a novel FMRFamide-like peptide in the pulmonate snail *Siphonaria pectinata. Peptides* **8:** 533–538.

Price, D. A., G. A. Cottrell, K. E. Doble, M. J. Greenberg, W. Jorenby, H. K. Lehman, and J. P. Riehm. 1985. A novel FMRFamide-related peptide in *Helix:* pQDPFLRFamide. *Biol. Bull.* **169:** 256–266.

Price, D. A., N. W. Davies, K. E. Doble, and M. J. Greenberg. 1987b. The variety and distribution of the FMRFamide-related peptides in molluscs. *Zool. Sci.* **4:** 395–410.

Robb, S., L. C. Packman, and P. D. Evans. 1989. Isolation, primary structure and bioactivity of schistoFLRF-amide, a FMRF-amide-like neuropeptide from the locust, *Schistocerca gregaria. Biochem. Biophys. Res. Comm.* **160:** 850–856.

Schaefer, M., M. R. Picciotto, T. Kreiner, R.-R. Kaldany, R. Taussig, and R. H. Scheller. 1985. *Aplysia* neurons express a gene encoding multiple FMRFamide neuropeptides. *Cell* **41:** 457–467.

Schneider, L. E., and P. H. Taghert. 1988. Isolation and characterization of a *Drosophila* gene that encodes multiple neuropeptides related to Phe-Met-Arg-Phe-NH_2 (FMRFamide). *Proc. Natl. Acad. Sci. USA* **85:** 1937–1997.

Shyamala, M., J. M. Fisher, and R. H. Scheller. 1986. A neuropeptide precursor expressed in *Aplysia* neuron L5. *DNA* **5:** 203–208.

Tatemoto, K. 1982a. Isolation and characterization of peptide YY (PYY), a candidate gut hormone that inhibits pancreatic exocrine secretion. *Proc. Natl. Acad. Sci. USA* **79:** 2514–2518.

Tatemoto, K. 1982b. Neuropeptide Y: complete amino acid sequence of the brain peptide. *Proc. Natl. Acad. Sci. USA* **79:** 5485–5489.

Taussig, R. and R. H. Scheller. 1986. The *Aplysia* FMRFamide gene encodes sequences related to mammalian brain peptides. *DNA* **5:** 453–462.

Triepel, J., and C. J. P. Grimmelikhuijzen. 1984. A critical examination of the occurrence of FMRFamide immunoreactivity in the brain of guinea pig and rat. *Histochemistry* **80:** 63–71.

Trimmer, B. A., L. A. Kobierski, and E. A. Kravitz. 1987. Purification and characterization of FMRFamide-like immunoreactive substances from the lobster nervous system: isolation and sequence analysis of two closely related peptides. *J. Comp. Neurol.* **265:** 16–26.

Weber, E., C. J. Evans, S. J. Samuelsson, and J. D. Barchas. 1981. Novel peptide neuronal system in rat brain and pituitary. *Science* **214:** 1248–1251.

Williams, R. G. 1983. Immunohistochemical studies of FMRFamide-like immunoreactivity in rat brain. *Brain Res.* **276:** 213–229.

Yang, H.-Y. T., W. Fratta, E. A. Majane, and E. Costa. 1985. Isolation, sequencing, synthesis, and pharmacological characterization of two brain neuropeptides that modulate the action of morphine. *Proc. Natl. Acad. Sci. USA* **82:** 7757–7761.

Reference: *Biol. Bull.* **177**: 206–209. (October, 1989)

Functions, Receptors, and Mechanisms of the FMRFamide-Related Peptides

MAKOTO KOBAYASHI AND YOJIRO MUNEOKA

Physiological Laboratory, Faculty of Integrated Arts and Sciences, Hiroshima University, Hiroshima 730, Japan

Introduction

Since the discovery of FMRFamide in the ganglia of a bivalve mollusc (*Macrocallista nimbosa*), FMRFamide and its related peptides (FaRPs) have proven to be ubiquitous in the Mollusca and to play physiological roles in various tissues, including cardiac and non-cardiac muscles, nerves, and glands (*e.g.*, Greenberg *et al.*, 1983; Lehman and Price, 1987; Kobayashi, 1987; Bulloch *et al.*, 1988; Raffa, 1988; Cottrell and Bewick, 1989). The actions of FMRFamide and other FaRPs on these tissues and cells are varied and complex. Furthermore, polyneuronal innervation and the co-localization of one peptide with other peptides or non-peptide neuroeffectors makes the assignment of function to particular agents especially complicated (*e.g.*, Weiss *et al.*, 1986; Lloyd *et al.*, 1987; Sossin *et al.*, 1987; Cropper *et al.*, 1987a, b, 1988). Therefore, rather than redescribing all of the disparate data, we have concentrated on results from a limited number of representative preparations, including heart, somatic muscle, and nerve. We ask, finally, whether any generalities are applicable to the actions of FMRFamide and its relatives.

Heart of *Rapana thomasiana*

FMRFamide is cardioexcitatory in many molluscs, but in some species it also has inhibitory effects (Painter and Greenberg, 1982; other references in Kobayashi, 1987). In the prosobranch *Rapana*, both serotonin and FMRFamide enhanced the amplitude and frequency of heart beat, with FMRFamide having the lower threshold and producing the greater enhancement (Kawakami and Kobayashi, 1984). The excitatory effects of serotonin were blocked by methysergide, a potent antagonist of serotonin receptors in molluscan hearts. On the contrary, the effects of FMRFamide were not affected by methysergide, showing that the receptors for serotonin and for FMRFamide are different.

The amplitude of heart beat was also augmented when the *r*ight or *l*eft *c*ardiac *n*erves, RCN 3a, RCN 4, or LCN 1 were electrically stimulated. The excitatory effects of nerve stimulation were not affected by the application of methysergide for 60 min or more. Thus, serotonin is probably not involved in the neurally induced excitation of this heart.

Recently, we have found, by staining with an antiserum to FMRFamide, that immunoreactive cell bodies and fibers are distributed throughout the visceral ganglia, and that such fibers also occur in the atrium (Kobayashi, 1987). Therefore, although the mechanism of action of FMRFamide is still not yet clarified, this peptide may well play a physiological role as a cardioactive agent in *Rapana*.

We have studied the structure-activity relations (SAR) of FMRFamide on the isolated *Rapana* heart (Kobayashi and Muneoka, 1986), and have shown that:

(1) The C-terminal RFamide is critical for activity; potency is markedly diminished by substitution with D-amino acids and is abolished upon removal of the amide.

(2) The N-terminal phenylalanine and the methionine could be replaced by other residues, but a total length of at least four residues is important for activity.

(3) N-terminal elongation may have little effect.

(4) FMRFamide was the most potent of 14 peptides tested.

These features are common, but not inevitable, characteristics of FMRFamide-receptor interactions. In particular, N-terminal elongation enhances the action on some pulmonate preparations, and in such cases, FMRFamide may be a relatively weak agonist (see be-

low). However, in general, the contribution to potency of the various residues in each position along a peptide needs to be examined in much greater detail.

Heart of *Achatina fulica*

The mode of action of FMRFamide on this pulmonate heart was different from that observed in *Rapana*. So far, we have identified nine neurons in the central nervous system of *Achatina* that are involved in regulating the heart beat (Furukawa and Kobayashi, 1987a, b). One giant neuron, designated the '*P*eriodically *O*scillating *N*euron' (PON), was the most potent heart excitor. Both the cardioexcitation produced by PON, and the excitatory effects of serotonin application, were depressed by methysergide, suggesting that the transmitter between the PON neuron and the heart is serotonin.

The effects of several FaRPs were tested on the atrium of *Achatina* (Hori *et al.*, unpub.). The preparation (comprising the atrium with most of the ventricle cut away, the intestinal nerve, and the central ganglia) was isolated in a bath to which the peptides were added. Of the peptides studied, only FMRFamide showed conspicuous excitatory effects. Although the threshold for the direct effects of FMRFamide on the heart was quite high (*i.e.*, 10^{-5} *M* or more), lower concentrations of FMRFamide enhanced the cardioexcitatory actions of both PON stimulation and serotonin application. The sites of action of FMRFamide (*i.e.*, pre- or post-synaptic) have not been established, but in any case, these effects were in contrast to those of SCP_B which depressed the cardioexcitatory actions. Therefore, as one of its roles in *Achatina*, FMRFamide appears to be modulating the excitatory action of a transmitter to the heart. Neither the FMRFamide- nor the SCP-containing neurons in *Achatina* have been identified.

Buccal Muscles of *Rapana*

The reciprocating movement of the radular rasp during feeding is produced in this prosobranch by the alternating contraction and relaxation of two pairs of opposing buccal muscles, the radula protractors and retractors. These muscles are innervated by the radula nerves which arise in the buccal ganglia (Furukawa and Kobayashi, 1985). In these radula muscles, the FaRPs seem to modulate the release of transmitters by acting presynaptically (Yanagawa *et al.*, 1988).

FMRFamide enhanced contractions of the radula protractor that were elicited by short pulses of electrical field stimulation (probably affecting nerve elements in the muscle), but the peptide had no such effect on the opposing muscle, the radula retractor. In contrast to FMRFamide, its close analog FLRFamide enhanced the contraction of the retractor but had no enhancing effect on the protractor. When neuromuscular transmission was blocked by application of 80 m*M* Mg^{++}, contraction of the protractor elicited by stimulation with long pulses (*i.e.*, direct muscle stimulation) was not enhanced by FMRFamide. Similarly, contraction of the retractor caused by muscle stimulation was not enhanced by FLRFamide (Yanagawa *et al.*, 1988).

Previously, we showed that the principal excitatory transmitter in the radula protractor is ACh, whereas that in the retractor is glutamate. Moreover, we know that serotonin acts to excite the protractor and to inhibit the retractor (Kobayashi and Muneoka, 1980; Muneoka and Kobayashi, 1980). Now we present the hypothesis that FMRFamide and FLRFamide act on presynaptic sites in the protractor and retractor, respectively, to enhance their contractions, possibly by increasing the release of transmitter.

Anterior Byssus Retractor Muscle (ABRM) of *Mytilus edulis*

FMRFamide also appears to have a presynaptic action on the ABRM of a bivalve mollusc (Muneoka and Matsuura, 1985). The ABRM of *Mytilus* can be set into a prolonged contracture by acetylcholine (ACh), and this catch tension is relaxed by serotonin released from the relaxing nerve; the serotonergic relaxation is blocked by mersalyl (references in Muneoka and Matsuura, 1985).

FMRFamide at low concentrations (10^{-8}–10^{-7} *M*) also relaxes ACh-induced catch tension. Moreover, this relaxation of the ABRM, like that of serotonin, was also blocked by mersalyl. However, when the muscle was denervated, ACh-induced catch tension was not relaxed by FMRFamide, although serotonin still relaxed it. These results are consistent with the notion that FMRFamide is acting on the relaxation inducing neurons in the muscle to release serotonin from their terminals.

FMRFamide showed various actions on the *Mytilus* ABRM, and catch relaxation is only one of them. The peptide also enhanced the contraction elicited by electrical stimulation of the muscle, or by application of ACh to it (Muneoka and Matsuura, 1985). The threshold for these effects was about 10^{-9} *M*. At higher concentrations (more than 10^{-7} *M*), FMRFamide caused its own contraction. These actions of FMRFamide are probably postsynaptic.

The structure-activity relations of FMRFamide for contraction of the ABRM were different from those for relaxation (Muneoka and Saitoh, 1986). Although the C-terminal RFamide was, as usual, critical for contraction, effective relaxation could still be produced when D-Arg and D-Phe (or other residues) were substituted for the C-terminal Arg and Phe, respectively. Even the C-terminal amide was not essential for relaxation. These results sug-

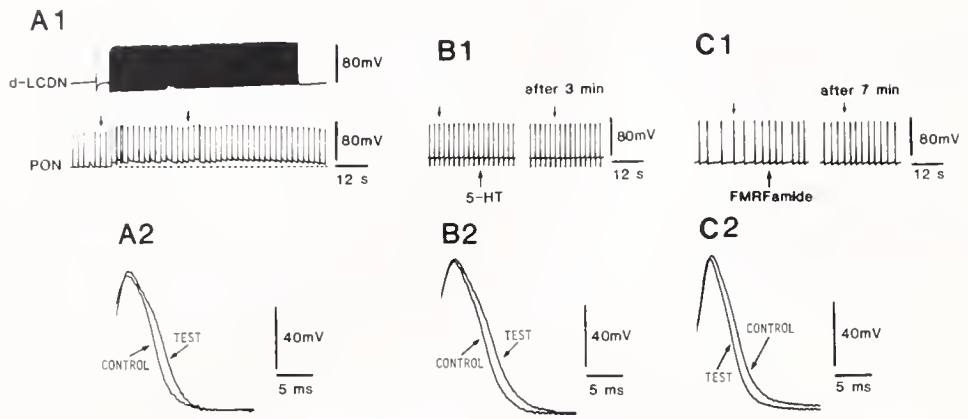

Figure 1. Duration of the action potential of the 'Periodically Oscillating Neuron' (PON) was increased by a burst of impulses in a cerebral neuron (d-LCDN) (A), and by an application of 5-HT (5×10^{-6} *M*) (B), but was decreased by FMRFamide (10^{-6} *M*) (C). In (A) and (B), PON was hyperpolarized to −50 mV (dotted line in A1) and driven to fire by a depolarizing current injection. In (C), spontaneous firings were recorded. Arrows in A1, B1, and C1 indicate selected spikes which are displayed at expanded time scale in A2, B2, and C2. (A and B; from Furukawa and Kobayashi, 1988).

gest that the *Mytilus* ABRM has at least two pharmacologically distinct classes of receptors which can be activated by FMRFamide.

Central Neurons and Synapses

Recently, the mechanisms underlying the actions of the FaRPs at central synapses have been intensively investigated (Cottrell *et al.*, 1984; Colombaioni *et al.*, 1985; Ruben *et al.*, 1986; Berladetti *et al.*, 1987; Brezina *et al.* 1987; Thompson and Ruben, 1988). In sensory neurons of *Aplysia,* the inhibitory responses to FMRFamide appear to be mediated by lipoxygenase metabolites of arachidonic acid, which open S-type K^+-channels (Piomelli *et al.*, 1987). This action of FMRFamide is in contrast to that of serotonin which closes these S-K^+-channels; *i.e.*, the effect of serotonin is mediated by cAMP by way of a different guanine nucleotide-binding protein than that coupled to the FMRFamide receptor (Volterra and Siegelbaum, 1988).

Similar results have also been obtained in the heart excitatory neuron, PON, of *Achatina.* FMRFamide increased background K^+-conductance (*i.e.*, it increased K^+-current through S-channels), and it also decreased inward Ca^{++}-current and, in turn, reduced Ca^{++}-dependent K^+-current. Moreover, these actions of FMRFamide were, again, opposite to those of serotonin. As a result, the duration of the action potential of a PON was decreased by FMRFamide, but was increased by serotonin (Fig. 1).

Serotonin is considered to act as an excitatory neurotransmitter at the synapse between a pair of command neurons in the cerebral ganglia and the PON (Furukawa and Kobayashi, 1988). Now we have found that FMRFamide is acting counter to serotonin at the same synapse (Hori *et al.*, unpub.), although the FMRFamide containing neuron has yet to be identified.

The actions of the tetra- and heptapeptide FaRPs have been examined recently on identified neurons of a pulmonate snail, *Helix aspersa* (Cottrell and Davies, 1987). The tetrapeptides were more potent than the heptapeptides at producing a slow increase in potassium conductance (gK). In addition, the tetrapeptides produced an increase in gNa, a conductance change not seen at all in response to the heptapeptides. On the other hand, the heptapeptides produced a fast increase in gK which was not observed when tetrapeptides were applied.

The exclusive actions of the tetrapeptides and heptapeptides on different ionic currents strongly suggest that multiple receptors are present. Recently, a receptor was demonstrated in *Helix* heart and brain that is specific for the tetrapeptides; *i.e.*, the heptapeptides were very ineffective at displacing radioligand bound to membranes from these tissues (Payza, 1987).

Summary

We have surveyed the functions, receptors, and mechanisms of the FMRFamide-related peptides by focussing primarily on preparations we have studied. Even these few examples clearly illustrate the versatility of the FaRPs: acting as neurotransmitters, they can directly excite or inhibit target cells; or they can potentiate or oppose the actions of a variety of other neuroeffector molecules. In the end, there are no general characteristics that can be assigned to the effects of FMRFamide or its analogs. Rather, the results show that the FaRPs exhibit multiple actions on various tissues, reflecting the struc-

tural variation, not only of the peptides, but also of their receptors.

Acknowledgments

We are grateful to Michael J. Greenberg for valuable discussions and for reviewing the manuscript. This research was supported in part by Grants-in-Aid (Nos. 62540549 and 63540575) from the Ministry of Education, Science, and Culture, Japan.

Literature Cited

Belardetti, F., E. R. Kandel, and S. A. Siegelbaum. 1987. Neuronal inhibition by the peptide FMRFamide involves opening of S K^+ channels *Nature* **325:** 153–156.

Brezina, V., R. Eckert, and C. Erxleben. 1987. Modulation of potassium conductances by an endogenous neuropeptide in neurones of *Aplysia californica*. *J. Physiol.* **382:** 267–290.

Bulloch, A. G. M., D. A. Price, A. D. Murphy, T. D. Lee, and H. N. Bowes. 1988. FMRFamide peptides in *Helisoma:* identification and physiological actions at a peripheral synapse. *J. Neurosci.* **8:** 3459–3469.

Colombaioni, L., D. Paupardin-Tritsch, P. P. Vidal, and H. M. Gerschenfeld. 1985. The neuropeptide FMRF-amide decreases both the Ca^{2+} conductance and a cyclic 3′,5′-adenosine monophosphate-dependent K^+ conductance in identified molluscan neurons. *J. Neurosci.* **5:** 2533–2538.

Cottrell, G. A., and G. S. Bewick. 1989. Novel peripheral neurotransmitters in invertebrates. *Pharmac. Ther.* **41:** 411–442.

Cottrell, G. A., and N. W. Davies. 1987. Multiple receptor sites for a molluscan peptide (FMRFamide) and related peptides of *Helix*. *J. Physiol.* **382:** 51–68.

Cottrell, G. A., N. W. Davies, and K. A. Green. 1984. Multiple actions of a molluscan cardioexcitatory neuropeptide and related peptides on identified *Helix* neurons. *J. Physiol.* **356:** 315–333.

Cropper, E. C., P. E. Lloyd, W. Reed, R. Tenenbaum, I. Kupfermann, and K. R. Weiss. 1987a. Multiple neuropeptides in cholinergic motor neurons of *Aplysia:* evidence for modulation intrinsic to the motor circuit. *Proc. Natl. Acad. Sci. USA* **84:** 3486–3490.

Cropper, E. C., R. Tenenbaum, M. A. G. Kolks, I. Kupfermann, and K. R. Weiss. 1987b. Myomodulin: a bioactive neuropeptide present in an identified cholinergic buccal motor neuron of *Aplysia*. *Proc. Natl. Acad. Sci. USA* **84:** 5483–5486.

Cropper, E. C., M. W. Miller, R. Tenenbaum, M. A. G. Kolks, I. Kupfermann, and K. R. Weiss. 1988. Structure and action of buccalin: a modulatory neuropeptide localized to an identified small cardioactive peptide-containing cholinergic motor neuron of *Aplysia californica*. *Proc. Natl. Acad. Sci. USA* **85:** 6177–6181.

Furukawa, Y., and M. Kobayashi. 1985. Neural mechanisms underlying the feeding movements of a mollusc, *Rapana thomasiana*. *Comp. Biochem. Physiol.* **81A:** 779–786.

Furukawa, Y., and M. Kobayashi. 1987a. Neural control of heart beat in the African giant snail, *Achatina fulica* Ferussac. I. Identification of the heart regulatory neurones. *J. Exp. Biol.* **129:** 279–293.

Furukawa, Y., and M. Kobayashi. 1987b. Neural control of heart beat in the African giant snail, *Achatina fulica* Ferussac. II. Interconnections among the heart regulatory neurones. *J. Exp. Biol.* **129:** 295–307.

Furukawa, Y., and M. Kobayashi. 1988. Modulation of ionic currents by synaptic action and 5-HT application in the identified heart excitatory neurone of the African giant snail, *Achatina fulica* Ferussac. *J. Exp. Biol.* **137:** 319–339.

Greenberg, M. J., S. D. Painter, K. E. Doble, G. T. Nagle, D. A. Price, and H. K. Lehman. 1983. The molluscan neurosecretory peptide FMRFamide: comparative pharmacology and relationship to the enkephalins. *Fed. Proc.* **42:** 82–86.

Kawakami, H., and M. Kobayashi. 1984. Pharmacological approach to the analysis of regulation of molluscan heart activity. *Zool. Sci.* **1:** 389–397.

Kobayashi, M. 1987. Innervation and control of the heart of a gastropod, *Rapana*. *Experientia* **43:** 981–986.

Kobayashi, M., and Y. Muneoka. 1980. Modulatory actions of octopamine and serotonin on the contraction of buccal muscles in *Rapana thomasiana*—I. Enhancement of contraction in radula protractor. *Comp. Biochem. Physiol.* **65C:** 73–79.

Kobayashi, M., and Y. Muneoka. 1986. Structural requirements for FMRFamide-like activity on the heart of the prosobranch *Rapana thomasiana*. *Comp. Biochem. Physiol.* **84C:** 349–352.

Lehman, H. K., and D. A. Price. 1987. Localization of FMRFamide-like peptides in the snail *Helix aspersa*. *J. Exp. Biol.* **131:** 37–53.

Lloyd, P. E., M. Frankfurt, P. Stevens, I. Kupfermann, and K. R. Weiss. 1987. Biochemical and immunocytological localization of the neuropeptides FMRFamide, SCP_A, SCP_B, to neurons involved in the regulation of feeding in *Aplysia*. *J. Neurosci.* **7:** 1123–1132.

Muneoka, Y., and M. Kobayashi. 1980. Modulatory actions of octopamine and serotonin on the contraction of buccal muscles in *Rapana thomasiana*—II. Inhibition of contraction in radula retractor. *Comp. Biochem. Physiol* **65C:** 81–86.

Muneoka, Y., and M. Matsuura. 1985. Effects of the molluscan neuropeptide FMRFamide and the related opioid peptide YGGFMRF-amide on *Mytilus* muscle. *Comp. Biochem. Physiol.* **81C:** 61–70.

Muneoka, Y., and H. Saitoh. 1986. Pharmacology of FMRFamide in *Mytilus* catch muscle. *Comp. Biochem. Physiol.* **85C:** 207–214.

Painter, S. D., and M. J. Greenberg 1982. A survey of the responses of bivalve hearts to the molluscan neuropeptide FMRFamide and to 5-hydroxytryptamine. *Biol. Bull.* **162:** 311–332.

Payza, K. 1987. FMRFamide receptors in *Helix aspersa*. *Peptides* **8:** 1065–1074.

Piomelli, D., A. Volterra, N. Dale, S. A. Siegelbaum, E. R. Kandel, J. H. Schwartz, and F. Belardetti. 1987. Lipoxygenase metabolites of arachidonic acid as second messengers for presynaptic inhibition of *Aplysia* sensory cells. *Nature* **328:** 38–43.

Raffa, R. B. 1988. The action of FMRFamide (Phe-Met-Arg-Phe-NH_2) and related peptides on mammals. *Peptides* **9:** 915–922.

Ruben, P., J. W. Johnson, and S. Thompson. 1986. Analysis of FMRF-amide effects on *Aplysia* bursting neurons. *J. Neurosci.* **6:** 252–259.

Sossin, W. S., M. D. Kirk, and R. H. Scheller. 1987. Peptidergic modulation of neuronal circuitry controlling feeding in *Aplysia*. *J. Neurosci.* **7:** 671–681.

Thompson, S., and P. Ruben. 1988. Inward rectification in response to FMRFamide in *Aplysia* neuron L2: summation with transient K current. *J. Neurosci.* **8:** 3200–3207.

Volterra, A. and S. A. Siegelbaum. 1988. Role of two different guanine nucleotide-binding proteins in the antagonistic modulation of the S-type K^+ channel by cAMP and arachidonic acid metabolites in *Aplysia* sensory neurons. *Proc. Natl. Acad. Sci. USA* **85:** 7810–7814.

Weiss, K. R., P. E. Lloyd, E. C. Cropper, M. Frankfurt, and I. Kupfermann. 1986. FMRF-amide is present in the arc muscle of *Aplysia* and depresses its contractions. *Soc. Neurosci. Abstr.* **12:** 947.

Yanagawa, M., M. Fujiwara, I. Takabatake, Y. Muneoka, and M. Kobayashi. 1988. Potentiating effects of some invertebrate neuropeptides on twitch contraction of the radula muscles of a mollusc; *Rapana thomasiana*. *Comp. Biochem. Physiol.* **90C:** 73–77.

Reference: *Biol Bull* **177:** 210–217. (October, 1989)

The Egg-Laying Hormone Family: Precursors, Products, and Functions

GREGG T. NAGLE, SHERRY D. PAINTER, AND JAMES E. BLANKENSHIP

The Marine Biomedical Institute and Department of Anatomy and Neurosciences, The University of Texas Medical Branch, Galveston, Texas 77550

Abstract. The marine mollusc *Aplysia* produces an egg-laying hormone (ELH), which induces ovulation and acts on central neurons to effect egg-laying behavior. ELH is synthesized in the neuroendocrine bag cells; it is encoded by the ELH gene, one of a small family of genes, each of which is expressed in a tissue-specific manner. We review what is known about post-translational processing of the ELH precursor, and report the isolation and chemical characterization of ϵ-bag-cell peptide, the seventh peptide product of the ELH precursor to be identified to date. Amino acid compositional and sequence analyses demonstrated that the primary structure of the 19-residue peptide is: NH_2-Ser-Val-Leu-Thr-Pro-Ser-Leu-Ser-Ser-Leu-Gly-Glu-Ser-Leu-Glu-Ser-Gly-Ile-Ser-COOH. Several other ELH-related genes are expressed in the atrial gland, an exocrine organ secreting into the oviduct of *Aplysia*. We review post-translational processing of these ELH-related precursors, and compare the events to those in the neuroendocrine bag cells. Finally, we compare the sequences of six ELH-related peptides from *Aplysia* with one ELH-related peptide (caudodorsal cell hormone) from *Lymnaea* to gain insight into the structure-activity relations of ELH at the ovotestis receptor.

Address reprint requests to Dr. Gregg T. Nagle, The Marine Biomedical Institute, 200 University Boulevard, University of Texas Medical Branch, Galveston, TX 77550.

Abbreviations: A-NTP, postsignal sequence NH_2-terminal peptide encoded by the A-related gene; BCP, bag-cell peptide; B-NTP, postsignal sequence NH_2-terminal peptide encoded by the B-related gene; CDCH, caudodorsal cell hormone; ELH, egg-laying hormone; AP, bag-cell acidic peptide; A-AP, an acidic peptide encoded by the A gene; A-ELH, an ELH-related peptide encoded by the A gene; HPLC, high-performance liquid chromatography; HRBP, histidine-rich basic peptide; PTH, phenylthiohydantoin; TFA, trifluoroacetic acid.

Introduction

The control of egg-laying behavior in the marine mollusc *Aplysia* has been particularly amenable to a multidisciplinary approach aimed at clarifying the cellular and molecular bases of neuroendocrine function. The neurosecretory bag cells are part of the final common pathway leading to egg deposition in these animals. Egg laying is initiated when the bag cells, which are located in the abdominal ganglion (Coggeshall, 1967; Frazier *et al.*, 1967) and are normally electrically silent, begin to fire in a prolonged and synchronous "afterdischarge" that may last 30 min or longer (Kupfermann and Kandel, 1970; Dudek and Blankenship, 1977a, b; Pinsker and Dudek, 1977). Several peptides, including the egg-laying hormone (ELH) (Table I), are released during this activity (Stuart *et al.*, 1980); they may act as classical neurohormones on peripheral targets, such as the ovotestis, or as non-synaptic neurotransmitters within the abdominal ganglion.

The peptides released by the bag cells are encoded by a single gene, known as the ELH gene, which directs the synthesis of a 37-kDa polyprotein precursor (Scheller *et al.*, 1983). A schematic diagram of the precursor (preproELH), as modified by recent peptide studies, is presented in Figure 1. Processing signals in the predicted amino acid sequence of preproELH suggest that it is post-translationally processed to generate nine or more peptide products in addition to the signal sequence. But is this processing scheme actually followed?

Seven of the nine peptides have now been identified in bag-cell extracts or releasates (Table II), and each of them, with the exception of alpha- and delta-bag-cell peptides (α-BCP, δ-BCP), has corresponded to a predicted product of the precursor. The sequence of δ-BCP

is unusual in two respects. First, it contains the only dibasic sequence in the precursor that does not appear to be cleaved during post-translational processing. Second, it is liberated from the processing intermediate (and from α-BCP, which occurs next to it on the precursor) by hydrolysis at a single arginyl residue, the only monobasic site to be cleaved during processing. Of course, this cleavage *might* have been predicted, since the region surrounding this arginyl residue has sequence characteristics that are often observed in association with cleaved monobasic sites (Benoit *et al.*, 1987). Nonetheless, as a result of these unexpected processing events, δ-BCP is 39 rather than 7 residues in length, and α-BCP is 9 rather than 40 residues in length. These observations emphasize the importance of chemically identifying peptide products—*i.e.*, of validating the processing steps that are merely predicted from precursor sequences which are, in turn, predicted from nucleotide sequence analyses of genomic or cDNA clones.

The physiological functions of most of the bag-cell products remain unclear, but their chemical properties (*e.g.*, molecular weight, NH_2- and COOH-terminal modifications) provide important clues as to their stability in biological fluids and thus to the kinds of function(s) that each could serve. Alpha-BCP, for example, probably could not act as a classical neurohormone because of its small size and lack of NH_2- or COOH-terminal modification (Mayeri and Rothman, 1985; Rothman *et al.*, 1987); it is, in fact, rapidly degraded upon release into the extracellular space. On the other hand, α-BCP could, and presumably does, act as a non-synaptic neurotransmitter within the abdominal ganglion (Rothman *et al.*, 1983; Mayeri *et al.*, 1985; Brown and Mayeri, 1986; Sigvardt *et al.*, 1986).

In this report, we describe the chemical characterization of epsilon-bag-cell peptide (ε-BCP), the seventh peptide product of the ELH gene to be identified. We also review the chemical characteristics of the ELH peptide family, since this peptide is the most frequently analyzed product of ELH-related genes and it has a well-defined physiological function (or activity)—*i.e.*, the release of mature oocytes from the ovotestis into the ducts of the reproductive tract.

Materials and Methods

Bag-cell clusters and the proximal 1 cm of the pleurovisceral connectives were removed from *A. californica* and immediately stored at −70°C until they were used. Clusters from 50 animals were heated for 3 min at 100°C and homogenized for 1 min (Brinkmann Polytron: setting 4; 4°C) in 15 ml of 1 *M* acetic acid containing 20 m*M* HCl. The extract was centrifuged (48,000 × *g*) for 20 min at 4°C, and the supernatant chromatographed at 4°C on a Sephadex G-50 superfine column (2.5 cm × 50 cm), which had previously been calibrated with molecular weight standards. Fractions were pooled based on absorbance at 280 nm, filtered (0.2 μm pore size), and the filtrate applied to a Supelcosil C18 reversed-phase HPLC column without prior Sep-Pak purification or lyophilization. The column was washed until the absorbance at 220 nm returned to baseline, and was then eluted at a flow rate of 1.0 ml/min with a gradient of Solvent A (0.1% TFA) and Solvent B (acetonitrile containing 0.1% TFA). One-minute fractions (1.0 ml) were pooled based on absorbance, and were subjected to amino acid analysis and automated amino acid sequence analysis. Samples were hydrolyzed with 5.7 *N* HCl *in vacuo* at 107°C for 24 h, and amino acid compositional analyses were carried out on a Beckman 6300 analyzer. The primary structure of the peptide was determined by microsequence analysis using an Applied Biosystems Model 475A Protein/Peptide Sequencer with an on-line 120A microbore PTH analyzer and a Model 900 data processor. The repetitive yield was 86.5%.

Results

An acid extract of heat-treated bag cells was initially chromatographed on a Sephadex G-50 column. The 0-10-kDa peptides in fraction A, a region of low absorbance at 280 nm (not shown), were filtered and fractionated by C18 reversed-phase HPLC using shallow gradient conditions to optimize peptide separation. The eluate was monitored at 220 nm (Fig. 2). Several fractions occurred as relatively broad peaks, primarily due to the shallow gradient conditions employed; however, the relatively low HPLC flow rate and the large amounts of sample loaded onto the column probably also contributed to peak broadening.

Fraction A1, which eluted from 159 through 162 min (Fig. 2), had the following amino acid composition: Thr (0.9), Ser (6.6), Glu (2.0), Pro (0.7), Gly (1.8), Val (0.8), Ile (1.0), Leu (3.8). A comparison of this composition with the reported nucleotide sequence analysis of the ELH gene (Scheller *et al.*, 1983) suggested that fraction A1 was a 19-residue peptide from the ELH precursor. Fraction A1 was subjected to quantitative microsequence analysis (10.0 nmol; 20 cycles), and the resulting amino acid sequence (Table III) was identical to that predicted for residues 156 through 174 of proELH (Scheller *et al.*, 1983). Following convention, this 19-residue peptide was termed ε-BCP. Assuming that the COOH terminus of ε-BCP was not amidated (since the last residue was not followed by Gly in the precursor), the calculated M_r is 1863. Approximately 2.6 μg (1.39

Table I

Comparison of the primary structures of bag cell, atrial gland and caudodorsal cell peptides[a]

ELH-related peptides	1	2	3	4	5	6	7	8	9	10	11	12	13	14	15	16	17
Aplysia californica ELH[b]	Ile	Ser	Ile	Asn	Gln	Asp	Leu	Lys	Ala	Ile	Thr	Asp	Met	Leu	Leu	Thr	Glu
Aplysia brasiliana ELH[c]	Ile	Ser	Ile	Asn	Gln	Asp	Leu	Lys	Ala	Ile	Thr	Asp	Met	Leu	Leu	Thr	Glu
Aplysia californica [Gln[23], Ala[27]]A-ELH[d]	Ile	Ser	Ile	Asn	Gln	Asp	Leu	Lys	Ala	Ile	Thr	Asp	Met	Leu	Leu	Thr	Glu
Aplysia californica [Ala[27]]A-ELH[d]	Ile	Ser	Ile	Asn	Gln	Asp	Leu	Lys	Ala	Ile	Thr	Asp	Met	Leu	Leu	Thr	Glu
Aplysia californica A-ELH[d]	Ile	Ser	Ile	Asn	Gln	Asp	Leu	Lys	Ala	Ile	Thr	Asp	Met	Leu	Leu	Thr	Glu
Aplysia parvula ELH[e]	Ile	Ser	Ile	Asn	Gln	Asp	Leu	Lys	Ala	Ile	Ala	Asp	Met	Leu	Ile	Val	Glu
Lymnaea stagnalis CDCH[f]	Leu	Ser	Ile	Thr	Asn	Asp	Leu	Arg	Ala	Ile	Ala	Asp	Ser	Tyr	Leu	Tyr	Asp

[a] Boxed residues indicate positions where the peptides differ from *A. californica* ELH. All of the ELH-related peptides are presumed to be amidated based on molecular genetic (Mahon *et al.*, 1985; Nambu and Scheller, 1986; Scheller *et al.*, 1983; Shyamala *et al.*, 1986) and peptide studies (Chiu *et al.*, 1979; Ebberink *et al.*, 1985).

[b] Determined by Chiu *et al.* (1979).

[c] Determined by Nagle *et al.* (1988b).

[d] Determined by Nagle *et al.* (1986) and Rothman *et al.* (1986).

[e] Predicted from nucleotide sequence analysis of an *A. parvula* bag cell genomic ELH clone (Nambu and Scheller, 1986).

[f] Determined by Ebberink *et al.* (1985).

nmol) of ϵ-BCP was recovered from each pair of bag-cell clusters. The physiological function of this peptide is not known.

The prominent fraction which eluted from 115 through 124 min (Fig. 2) was also examined. Amino acid compositional and sequence analyses demonstrated that this fraction corresponded to the myoactive 43-residue histidine-rich basic peptide (HRBP) of neurons R3-R14 (Nagle *et al.*, 1989). A wealth of data, both anatomical (Frazier *et al.*, 1967) and biochemical (Newcomb and Scheller, 1987), indicates that the R3-R14 neurons have axon terminals in the neurohemal region surrounding the bag cells.

Discussion

Chemical characterization of the peptide products predicted from the ELH gene expressed in the bag cells provides definitive information about post-translational processing in these model neuroendocrine cells. Of the seven peptides characterized to date, five are processed as predicted, in response to signals that have been empirically determined from similar studies in other systems. However, two peptides comprising contiguous segments of preproELH, are not processed as initially predicted: a dibasic site in the middle of the δ-BCP sequence is not cleaved, while a monobasic Arg separating δ-BCP from α-BCP is. Examination of the characteristics of these sites in greater detail, and their comparison to qualitatively similar sites in the precursor that are processed differently, may provide insights that will allow increasingly accurate predictions of post-translational processing events to be made in the future. Moreover, since the bag-cell ELH gene is only one of a small family of structurally related genes that are expressed in a tissue-specific manner in *Aplysia* (Scheller *et al.*, 1983), peptide characterization studies may help to distinguish between general and tissue-specific processing events. Comparisons of specific peptide sequences (*e.g.*, the ELH-related peptides) from different tissues and species may be equally useful for preliminary structure-activity analyses of peptide action.

The atrial gland, an exocrine organ secreting into the oviduct of *Aplysia* (Arch *et al.*, 1980; Beard *et al.*, 1982; Painter *et al.*, 1985), expresses several ELH-family genes (Scheller *et al.*, 1983; Mahon *et al.*, 1985). The peptide products of this gland pharmacologically elicit egg deposition when injected into a receptive animal (Arch *et al.*, 1978), but have no known physiological function inside the organism. Recent experiments suggest that the secreted peptides may be deposited onto the egg cordon as it is transported through the oviduct, and may mediate the sexual and social behaviors often associated with egg laying and egg cordons (Painter *et al.*, 1989).

Table I (*Continued*)

18	19	20	21	22	23	24	25	26	27	28	29	30	31	32	33	34	35	36
Gln	Ile	Arg	Glu	Arg	Gln	Arg	Tyr	Leu	Ala	Asp	Leu	Arg	Gln	Arg	Leu	Leu	Glu	Lys-NH_2
Gln	Ile	Arg	Glu	Arg	Gln	Arg	Tyr	Leu	Ala	Asp	Leu	Arg	Gln	Arg	Leu	Leu	Glu	Lys-NH_2
Gln	Ile	Gln	Ala	Arg	Gln	Arg	Cys	Leu	Ala	Ala	Leu	Arg	Gln	Arg	Leu	Leu	Asp	Leu-NH_2
Gln	Ile	Gln	Ala	Arg	Arg	Arg	Cys	Leu	Ala	Ala	Leu	Arg	Gln	Arg	Leu	Leu	Asp	Leu-NH_2
Gln	Ile	Gln	Ala	Arg	Arg	Arg	Cys	Leu	Asp	Ala	Leu	Arg	Gln	Arg	Leu	Leu	Asp	Leu-NH_2
Gln	Lys	Gln	Glu	Arg	Glu	Lys	Tyr	Leu	Ala	Asp	Leu	Arg	Gln	Arg	Leu	Leu	Asn	Lys-NH_2
Gln	His	Trp	Leu	Arg	Glu	Arg	Gln	Glu	Glu	Asn	Leu	Arg	Arg	Arg	Phe	Leu	Glu	Leu-NH_2

Each of the ELH-family genes expressed in the atrial gland encodes a large polyprotein precursor. Two of the precursors, preproA and preproB, are diagrammed in Figure 1; the diagrams are based on nucleotide sequence analyses of genomic and cDNA clones (Scheller *et al.*, 1983; Mahon *et al.*, 1985) and have been modified by peptide sequence analyses (Heller *et al.*, 1980; Nagle *et al.*, 1986, 1988c; Rothman *et al.*, 1986). The products that have been isolated and chemically characterized are summarized in Table IV.

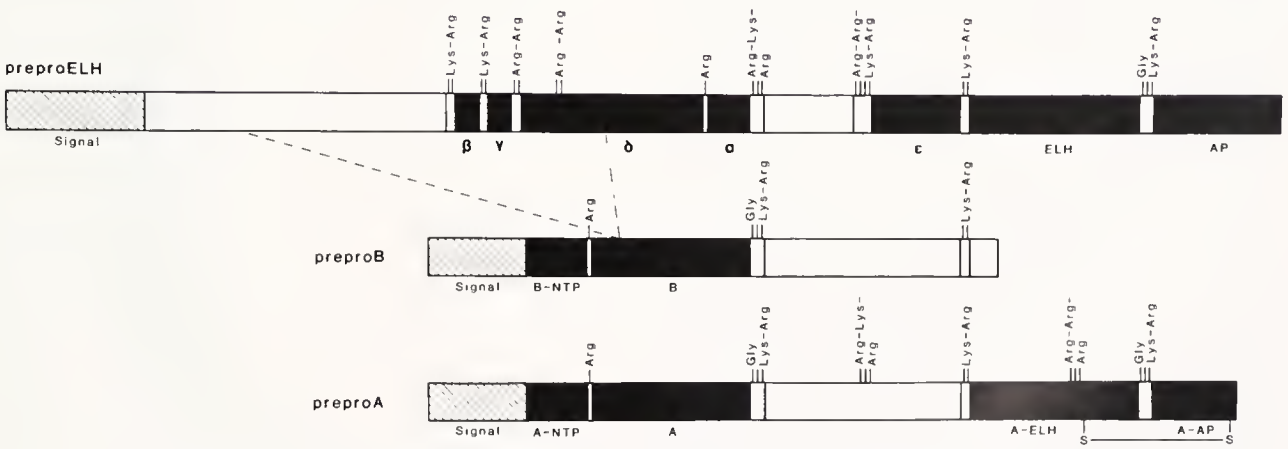

Figure 1. Schematic diagram of *Aplysia californica* preproELH, preproB, and preproA as predicted from nucleotide sequence analyses of genomic and cDNA clones (Scheller *et al.*, 1983; Mahon *et al.*, 1985) and modified by peptide studies (Nagle *et al.*, 1986, 1988c; Rothman *et al.*, 1986). Signal peptides are represented by hatched boxes. Peptides that have been identified in extracts or releasates are indicated by black boxes and have been labeled. Known or predicted mono-, di-, tri-, and tetrabasic cleavage sites, as well as the Gly-Lys-Arg signal for COOH-terminal amidation, are shown. Abbreviations are defined in a footnote on the first page of this paper.

Table II

Peptides derived from Aplysia californica *bag-cell preproELH*[a]

Peptide	Source	Means of identification	Number of residues	Function or pharmacological action
α-BCP[b]	Extracts	Sequence	7, 8, or 9	Inhibits LUQ cells Inhibits/excites bag cells
β-BCP[c]	Releasates	Comigration with Standard	5	Excites L1, R1, and bag cells in abdominal ganglion
λ-BCP[c]	Releasates	Comigration with Standard	5	Excites bag cells
δ-BCP[d]	Extracts	Sequence	39	Stimulates Ca flux into mitochondria of albumen gland secretory cells
ε-BCP[d]	Extracts	Sequence	19	Not known
ELH[e]	Extracts	Sequence	36	Induces egg release from gonad, excites R15 and LLQ cells in abdominal ganglion and B16 in buccal ganglion
AP[f]	Extracts	Sequence	27	Not known

[a] A schematic diagram of preproELH is presented in Figure 1. Abbreviations are defined in a footnote on the first page of this paper.
[b] Rothman *et al.*, 1983.
[c] Rothman *et al.*, 1985.
[d] Nagle *et al.*, 1988a.
[e] Chiu *et al.*, 1979.
[f] Scheller *et al.*, 1983.

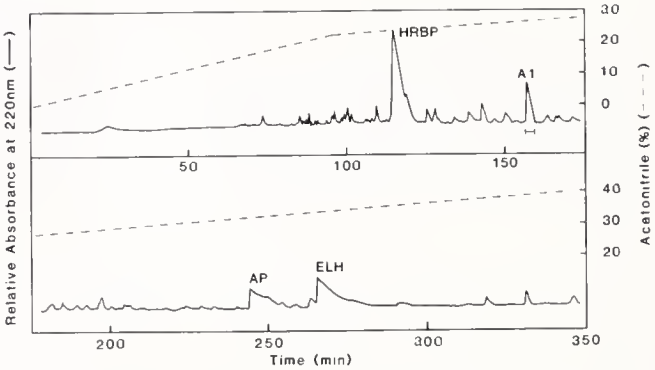

Figure 2. Reversed-phase HPLC purification of 0-10-kDa peptides from *Aplysia californica* bag cells. An extract of the bag cells was initially fractionated by Sephadex G-50 column chromatography to generate fraction A, which contained the 0-10-kDa peptides (not shown). Fraction A was filtered and then subfractionated by C18 reversed-phase HPLC using two linear gradients of 0.1% TFA and acetonitrile containing 0.1% TFA (0–22% in 96 min, 22–44% in 310 min) to generate fraction A1. A single elution profile has been divided into two panels. Abbreviations are defined in a footnote on the first page of this paper.

The atrial gland ELH-related peptides are 36-residue peptides that are identical to bag-cell ELH at residues 1–19 and at six of eight COOH-terminal residues (Table I); they are approximately equipotent to bag-cell ELH in eliciting egg deposition. Nevertheless, the atrial gland peptides differ from their homolog in the bag cells in several important characteristics. First, there is a potential tribasic cleavage site in A-ELH and [Ala^{27}]A-ELH which is missing from bag-cell ELH (Fig. 1; Table I). Second, each of the three atrial gland peptides is disulfide-bonded to an 18-residue acidic peptide, A-AP, that is located adjacent to it in the precursor. This linkage, through Cys^{25} of the ELH-related molecules, may sterically inhibit cleavage at the tribasic sequence (Arg^{22}-Arg^{23}-Arg^{24}) and explain why the site is not used during post-translational processing. The function of this heterodimeric complex is not known, but it is approximately equipotent to bag-cell ELH in eliciting egg deposition. Finally, a proportion of the A-AP/A-ELH and A-AP/[Ala^{27}]A-ELH complexes are further processed in the atrial gland by a renin-like enzyme, with cleavage occurring at the Leu^{14}-Leu^{15} and Leu^{33}-Leu^{34} bonds of the ELH-related sequences. The Leu^{11}-Leu^{12} bond in A-AP is not cleaved, however, perhaps due to differences in secondary structure that have been predicted to occur in these regions by Chou-Fasman analysis (α-helix in the ELH-related peptides, but β-sheet in A-AP) (Nagle *et al.*, 1986). Cleavage of the

Table III

Automated sequence analysis of fraction A1[a]

Edman cycle	Residue (pmol) A1
0[b]	— (10000)
1	Ser (2819)
2	Val (3836)
3	Leu (5036)
4	Thr (3540)
5	Pro (4459)
6	Ser (2317)
7	Leu (3424)
8	Ser (1890)
9	Ser (1433)
10	Leu (1960)
11	Gly (1383)
12	Glu (1148)
13	Ser (632)
14	Leu (1029)
15	Glu (643)
16	Ser (342)
17	Gly (434)
18	Ile (358)
19	Ser (127)

[a] Results obtained with gas-phase microsequencer. Phenylthiohydantoin (PTH) amino acids were quantitated by HPLC.
[b] Initial amount of peptide (pmol) applied to sequencer.

Table IV

Peptides derived from the ELH-family genes expressed in the Aplysia californica *atrial gland*[a]

Peptide	Method of identification	Number of residues	Pharmacological action
A-NTP[b]	Sequence	13	Not known
B-NTP[b]	Sequence	13	
A[c]	Sequence	34	Bag-cell activation
B[c]	Sequence	34	
A-ELH[d,e]	Sequence	36	Egg release from ovotestis
[Ala^{27}]A-ELH[d,e]	Sequence	36	
[Gln^{23}, Ala^{27}]A-ELH[d,e]	Sequence	36	
A-ELH-(1–14)[f]	Composition	14	Not known
A-ELH-(15–36)[b]	Sequence	22	
A-ELH-(1–33)[b]	Composition	33	
[Ala^{27}]A-ELH-(15–36)[b]	Sequence	22	
[Ala^{27}]A-ELH-(1–33)[b]	Composition	33	
[Gln^{23}, Ala^{27}]A-ELH-(16–36)[b]	Sequence	21	
A-AP[d,e]	Sequence	18	Not known

[a] A schematic diagram of two of the polyprotein precursors, preproA and preproB, is presented in Figure 1. Abbreviations are defined in a footnote on the first page of this paper. Peptides were isolated from tissue extracts.
[b] Nagle *et al.*, 1988c.
[c] Heller *et al.*, 1980.
[d] Nagle *et al.*, 1986.
[e] Rothman *et al.*, 1986.
[f] Rothman *et al.*, 1984.

Leu^{14}-Leu^{15} bond of the ELH-related peptides abolishes egg-laying activity. Since these atrial gland peptides do not induce egg deposition *in vivo*, however, it is not clear whether this processing step represents an activation or inactivation with regard to their actual function. It is important to note that the Leu^{14}-Leu^{15} and Leu^{33}-Leu^{34} bonds of bag-cell ELH are not cleaved during processing, even though each is predicted to occur in an α-helical segment of the molecule. The renin-related proteolysis thus appears to be a tissue-specific processing event, and one that would not be predicted to occur based on nucleotide sequence analyses of genomic or cDNA clones.

In spite of the differences in their sequences, ELH and the atrial gland ELH-related peptides are predicted to have the same secondary structure: two regions of strong α-helical potential (residues 6–21 and 26–36) separated by a β-bend (residues 22–25) (Nagle *et al.*, 1986). These observations suggest that ELH may be a U-shaped peptide, and that egg-laying activity in *Aplysia* may be correlated with conservation of the NH_2- and COOH-terminal regions of the molecule. Two additional ELH-related sequences have been reported to date—the *A. brasiliana* bag-cell ELH, determined by direct chemical characterization of the isolated peptide (Nagle *et al.*, 1988b), and the *A. parvula* bag-cell ELH, predicted from nucleotide sequence analyses of genomic clones (Nambu and Scheller, 1986). Both are 36 amino acids in length (Table I). The sequence of *A. brasiliana* ELH is identical to that of *A. californica* bag-cell ELH and so does not provide any further information about regions of the peptide important for receptor recognition and activation. The *A. parvula* ELH, in contrast, is only 78% identical to *A. californica* bag-cell ELH, and it displays the same pattern of residue conservation observed with the *A. californica* peptides: it is identical to all five sequenced peptides at 13 of 14 NH_2-terminal positions and at 6 of 8 COOH-terminal positions, but differs significantly from them in the intervening region (Table I).

More detailed structure-activity information has been obtained recently using synthetic ELH and analogs to induce egg deposition (Strumwasser *et al.*, 1987). These studies confirm that peptide chain-length is important for egg-laying activity. Removal of the NH_2-terminal Ile, or extension of the COOH terminus by one residue (ELH-Gly^{37}), results in a loss of egg-laying activity. In contrast, ELH-(1–34) and ELH-(1–35) are at least moderately active, indicating that the COOH-terminal amide is not essential for biological activity, and that the identities of the amino acids at positions 35 and 36 may be relatively unimportant. This conclusion is consistent with the comparative peptide studies outlined above, since substitutions at positions 35 and 36 of the ELH-

related peptides did not significantly decrease biological activity relative to *A. californica* bag-cell ELH (Table I).

Other positional requirements are less clear, however. The amino acids critical for receptor recognition and activation are probably concentrated at positions 1–10 and 29–34, since all six *Aplysia* ELH-related sequences are identical at these positions. If we extend the comparison to include the caudodorsal cell hormone (CDCH) of the freshwater pulmonate *Lymnaea stagnalis* (Table I; Ebberink *et al.*, 1985), an interesting pattern emerges. (CDCH is a 36-residue peptide secreted by the neuroendocrine caudodorsal cells during a burst of activity comparable to a bag-cell afterdischarge; it induces ovulation and is homologous to ELH.) Only 13 amino acid residues are conserved in all seven peptides, and 10 of the 13 (77%) occur in the regions encompassing residues 1–10 and 29–34. The number increases to 11 of 13 if we include positions 11 and 12 in the comparison, and four of them are charged (Asp^{6}, Asp^{12}, Arg^{30}, Arg^{32}). These observations strengthen the notion that the regions encompassing residues 1–12 and 29–34 may be important for receptor recognition and activation, and suggest that these positions should be modified in ELH analogs for future structure-activity studies.

Acknowledgments

This investigation was supported by NSF BNS 85 17575 (GTN) and BBS 87 11368, and by NIH NS 22079 (SDP), NS 23169 (JEB), and NS 11255.

Literature Cited

Arch, S., J. Lupatkin, T. Smock, and M. Beard. 1980. Evidence for an exocrine function of the *Aplysia* atrial gland. *J. Comp. Physiol.* **141:** 131–137.

Arch, S., T. Smock, R. Gurvis, and C. McCarthy. 1978. Atrial gland induction of the egg laying response in *Aplysia californica*. *J Comp. Physiol.* **128:** 67–70.

Beard, M., L. Millecchia, C. Masuoka, and S. Arch. 1982. Ultrastructure of secretion in the atrial gland of a mollusc (*Aplysia*). *Tissue Cell* **14:** 297–308.

Benoit, R., N. Ling, and F. Esch. 1987. A new prosomatostatin-derived peptide reveals a pattern for prohormone cleavage at monobasic sites. *Science* **238:** 1126–1129.

Brown, R. O., and E. Mayeri. 1986. Evidence for excitatory autotransmission in *Aplysia* bag cell neurons mediated by alpha-, beta-, and gamma-bag cell peptides. *Soc. Neurosci. Abstr.* **12:** 946.

Chiu, A. Y., M. W. Hunkapiller, E. Heller, D. K. Stuart, L. E. Hood, and F. Strumwasser. 1979. Purification and primary structure of the neuropeptide egg-laying hormone of *Aplysia californica*. *Proc. Natl. Acad. Sci. USA* **76:** 6656–6660.

Coggeshall, R. E. 1967. A light and electron microscope study of the abdominal ganglion of *Aplysia californica*. *J. Neurophysiol.* **30:** 1263–1287.

Dudek, F. E., and J. E. Blankenship. 1977a. Neuroendocrine cells of *Aplysia brasiliana*. I. Bag cell action potentials and afterdischarge. *J. Neurophysiol.* **40:** 1301–1311.

Dudek, F. E., and J. E. Blankenship. 1977b. Neuroendocrine cells of *Aplysia brasiliana*. II. Bag cell prepotentials and potentiation. *J. Neurophysiol.* **40:** 1312–1324.

Ebberink, R. H. M., H. van Loenhout, W. P. M. Geraerts, and J. Joosse. 1985. Purification and amino acid sequence of the ovulation neurohormone of *Lymnaea stagnalis*. *Proc. Natl. Acad. Sci. USA* **82:** 7767–7771.

Frazier, W. T., E. R. Kandel, I. Kupfermann, R. Waziri, and R. E. Coggeshall. 1967. Morphological and functional properties of identified neurons in the abdominal ganglion of *Aplysia californica*. *J. Neurophysiol.* **30:** 1288–1351.

Heller, E., L. K. Kaczmarek, M. W. Hunkapiller, L. E. Hood, and F. Strumwasser. 1980. Purification and primary structure of two neuroactive peptides that cause bag cell afterdischarge and egg-laying in *Aplysia*. *Proc. Natl. Acad. Sci. USA* **77:** 2328–2332.

Kupfermann, I., and E. R. Kandel. 1970. Electrophysiological properties and functional interconnections of two symmetrical neurosecretory clusters (bag cells) in abdominal ganglion of *Aplysia*. *J. Neurophysiol.* **33:** 865–876.

Mahon, A. C., J. R. Nambu, R. Taussig, M. Shyamala, A. Roach, and R. H. Scheller. 1985. Structure and expression of the egg-laying hormone gene family in *Aplysia*. *J. Neurosci.* **5:** 1872–1880.

Mayeri, E., and B. S. Rothman. 1985. Neuropeptides and the control of egg-laying behavior in *Aplysia*. Pp. 285–301 in *Model Neural Networks and Behavior*, A. I. Selverston, ed. Plenum, New York.

Mayeri, E., B. S. Rothman, P. H. Brownell, W. D. Branton, and L. Padgett. 1985. Non-synaptic characteristics of neurotransmission mediated by egg-laying hormone in the abdominal ganglion of *Aplysia*. *J. Neurosci.* **5:** 2060–2077.

Nagle, G. T., M. de Jong-Brink, S. D. Painter, J. E. Blankenship, and A. Kurosky. 1988a. Purification and structure of the delta and epsilon bag cell peptides of *Aplysia*. *Soc. Neurosci. Abstr.* **14:** 176.

Nagle, G. T., S. L. Knock, S. D. Painter, J. E. Blankenship, R. R. Fritz, and A. Kurosky. 1989. I. *Aplysia californica* neurons R3-R14: primary structure of the myoactive histidine-rich basic peptide and peptide I. *Peptides* (in press).

Nagle, G. T., S. D. Painter, J. E. Blankenship, J. V. A. Choate and A. Kurosky. 1988b. The bag cell egg-laying hormones of *Aplysia brasiliana* and *Aplysia californica* are identical. *Peptides* **9:** 867–872.

Nagle, G. T., S. D. Painter, J. E. Blankenship, J. D. Dixon and A. Kurosky. 1986. Evidence for the expression of three genes encoding homologous atrial gland peptides that cause egg laying in *Aplysia*. *J. Biol. Chem.* **261:** 7853–7859.

Nagle, G. T., S. D. Painter, J. E. Blankenship and A. Kurosky. 1988c. Proteolytic processing of egg-laying hormone-related precursors in *Aplysia:* identification of peptide regions critical for biological activity. *J. Biol. Chem.* **263:** 9223–9237.

Nambu, J. R., and R. H. Scheller. 1986. Egg-laying hormone genes of *Aplysia:* evolution of the ELH gene family. *J. Neurosci.* **6:** 2026–2036.

Newcomb, R., and R. H. Scheller. 1987. Proteolytic processing of the *Aplysia* egg-laying hormone and R3-R14 neuropeptide precursors. *J. Neurosci.* **7:** 854–863.

Painter, S. D., A. R. Gustavson, V. K. Kalman, G. T. Nagle, and J. E. Blankenship. 1989. Induction of copulatory behavior in *Aplysia:* atrial gland factors mimic the excitatory effects of freshly deposited egg cordons. *Behav. Neur. Biol.* **51:** 222–236.

Painter, S. D., V. K. Kalman, G. T. Nagle, R. A. Zuckerman, and J. E. Blankenship. 1985. The anatomy and functional morphology of the large hermaphroditic duct of three species of *Aplysia*, with special reference to the atrial gland. *J. Morphol.* **18:** 167–194.

Pinsker, H. M., and F. E. Dudek. 1977. Bag cell control of egg laying in freely behaving *Aplysia*. *Science* **197:** 490–493.

Rothman, B. S., D. H. Hawke, R. O. Brown, T. D. Lee, A. A. Dehghan, J. E. Shively, and E. Mayeri. 1986. Isolation and primary structure of the califins, three biologically active egg-laying hormone-like peptides from the atrial gland of *Aplysia californica*. *J. Biol. Chem.* **261:** 1616–1623.

Rothman, B. S., E. Mayeri, R. O. Brown, P.-M. Yuan, and J. E. Shively. 1983. Primary structure and neuronal effects of α-bag cell peptide, a second candidate neurotransmitter encoded by a single gene in bag cell neurons of *Aplysia*. *Proc. Natl. Acad. Sci. USA* **80:** 5753–5757.

Rothman, B. S., G. A. Phares, and T. A. Groves. 1987. Inactivation of alpha-bag cell peptide in the abdominal ganglion of *Aplysia*. *Soc. Neurosci. Abstr.* **13:** 39.

Rothman, B. S., J. Shively, D. Hawkes, R. O. Brown, and E. Mayeri. 1984. Two neuroactive peptides from a common precursor in *Aplysia* atrial gland. *Trans. Am. Soc. Neurochem.* **15:** 119.

Rothman, B. S., K. A. Sigvardt, and E. Mayeri. 1985. Co-release of five peptides, ELH, AP, α-, β-, and γ-BCP, derived from a common precursor protein of the bag cells of *Aplysia*. *Soc. Neurosci. Abstr.* **11:** 482.

Scheller, R. H., J. F. Jackson, L. B. McAllister, B. S. Rothman, E. Mayeri, and R. Axel. 1983. A single gene encodes multiple neuropeptides mediating a stereotyped behavior. *Cell* **32:** 7–22.

Shyamala, M., J. R. Nambu, and R. H. Scheller. 1986. Expression of the egg-laying hormone gene family in the head ganglia of *Aplysia*. *Brain Res.* **371:** 49–57.

Sigvardt, K. A., B. S. Rothman, R. O. Brown and E. Mayeri. 1986. The bag cells of *Aplysia* as a multitransmitter system: identification of alpha bag cell peptide as a second neurotransmitter. *J. Neurosci.* **6:** 803–813.

Strumwasser, F., D. L. Schiller, and S. B. H. Kent. 1987. Synthetic neuropeptide egg-laying hormone (ELH) of *Aplysia californica* induces normal egg-laying: structure-activity studies. *Soc. Neurosci. Abstr.* **13:** 38.

Stuart, D. K., A. Y. Chiu, and F. Strumwasser. 1980. Neurosecretion of egg-laying hormone and other peptides from electrically active bag cell neurons of *Aplysia*. *J. Neurophysiol.* **43:** 488–498.

Reference: *Biol. Bull.* 177: 218–224. (October, 1989)

Adipokinetic Hormones: Functions and Structures

GRAHAM GOLDSWORTHY[1,*] AND WILLIAM MORDUE[2]

[1]*Department of Biology, Birkbeck College, University of London, England, and*
[2]*Department of Zoology, University of Aberdeen, Scotland*

Introduction

The AKH/RPCH family of arthropod neuropeptides comprises at least eleven (see Table I) members at the time of writing. Many of these peptides were identified initially by their pharmacological activities in causing hyperlipemia in locusts and/or hypertrehalosemia in cockroaches, but in this account we will restrict our discussion to physiological functions of the endogenous peptides of locusts, and attempt to relate differences in biological activity with the variations in amino acid sequences seen in peptides from other insects.

Functions of Adipokinetic Hormones in Locusts

In locusts, two adipokinetic hormones are synthesized in the glandular lobes of the corpora cardiaca (see Hekimi and O'Shea, 1987): the decapeptide, AKH-I, and either one (depending upon species) of two octapeptides, AKH-IIL or AKH-IIS (see Goldsworthy and Wheeler, 1989). These peptides are released during flight, and the release may be under octopaminergic control (Orchard, 1987; but see Konings *et al.*, 1988) from secretomotor centers in the brain (Rademakkers, 1977). The decapeptide and the octapeptides can each stimulate the release of diacylglycerols from the fat body into the hemolymph, and thus provide fuel for migratory flight. These neuropeptides also bring about a re-organization of circulating hemolymph lipoproteins and activate fat body glycogen phosphorylase. In all these activities, AKH-I is more potent than AKH-II (Goldsworthy *et al.*, 1986a, b). However, although both peptides are thought to act on the fat body via adenylate cyclase, AKH-II increases fat body cAMP levels to a greater extent than AKH-I (Goldsworthy *et al.*, 1986a), suggesting that they may act at different receptors and that AKH-II may have other, as yet undiscovered, actions.

Actions on the fat body

Adipokinetic peptides stimulate adenylate cyclase activity in the fat body. This activation, by analogy to that of triacylglycerol lipase in vertebrates, is generally assumed to involve a conventional protein kinase cascade (see Goldsworthy, 1983; Beenakkers *et al.*, 1985; Orchard, 1987). Ca^{2+}, acting as another second messenger, may also be involved because the lipid-mobilizing action of AKH on the fat body is dependent on Ca^{2+} *in vitro*. Activation of the triacylglycerol lipase is thought to hydrolyze triacylglycerols to monoacylglycerols, which are subsequently re-acylated by a monoacylglycerol transferase to form sterospecific *sn*-1,2 diacylglycerols, and are released from the fat body (see Beenakkers *et al.*, 1985) as part of a special carrier lipoprotein (see below).

Fuel transport to the flight muscles

Neutral lipids are essentially insoluble in water and, as in vertebrate blood, their transport in hemolymph involves carrier lipoproteins; these change in composition during flight (Mayer and Candy, 1967) or after injection of AKH, and have been studied extensively by several groups (see Goldsworthy, 1983; Beenakkers *et al.*, 1985; Wheeler, 1989). Adipokinetic hormones cause a regrouping of hemolymph proteins and lipoproteins with a consequent increase in the lipid-carrying capacity of the hemolymph. Thus, a new 'activated' lipoprotein complex, or A^+ (see Fig. 1), forms in the hemolymph. Compared with the lipoprotein present at rest, A*yellow*, A^+ particles are of larger diameter (Wheeler *et al.*, 1984a), they bind large quantities of other hemolymph proteins called C_1-apoproteins (Wheeler and Goldsworthy, 1983a, b) to them, and they carry up to 18 times

* Address for correspondence: Department of Biology, Birkbeck College, Malet Street, London WC1E 7HX, U. K.

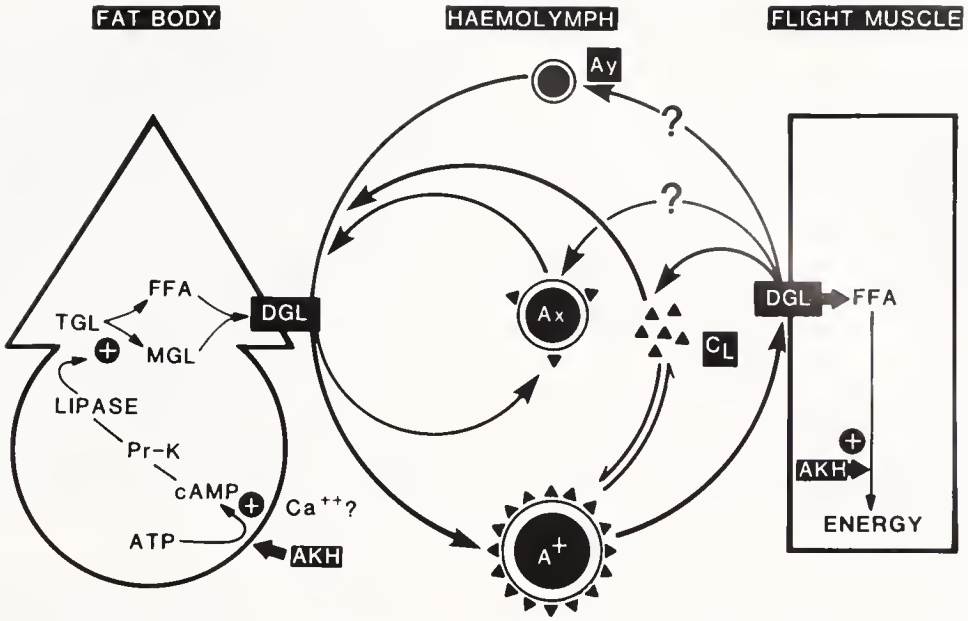

Figure 1. Diagrammatic scheme of the major actions of AKH in locusts. Diacylglycerols (DGL), made available by the action AKH in increasing triacylglycerol lipase in the fat body, are loaded onto lipoprotein A*yellow* (Ay), which forms lipoprotein A^+ which reversibly binds C_L-proteins. At the flight muscle, diacylglycerols associated with lipoprotein A^+ are hydrolyzed, and the fatty acids (FFA) are used to support flight muscle metabolism. Lipid unloading leads to the liberation of free C_L-proteins. The lipoproteins thus form a re-usable 'shuttle,' carrying energy to the flight muscles.

more neutral lipid (see Goldsworthy, 1983). The formation of A^+ lipoprotein does not require protein synthesis *de novo* and is reversible: the lipoproteins act as re-usable shuttles, carrying diacylglycerols from the fat body to the flight muscles. In the first author's laboratory, two C_L-apoproteins are recognized in the hemolymph of *Locusta* (Goldsworthy *et al.*, 1985), each of which bind to A^+ (Wheeler and Goldsworthy, 1986; Wheeler, 1989). In other laboratories, only a single locust apoprotein has been described (see Beenakkers *et al.*, 1985).

Indirect actions of AKH at the flight muscles

The unloading of diacylglycerol from A^+ lipoprotein particles at the flight muscle is also regulated by AKH, but in this case the control is indirect. A lipoprotein lipase, membrane-bound in the flight muscles, hydrolyses lipids of lipoprotein A^+ at over four times the rate of those of A*yellow*, and enzyme activity against A*yellow* is reduced by about 90% in the presence of lipoprotein A^+ (Wheeler *et al.*, 1984b; 1986; Van Heusden *et al.*, 1986). The C_L-apoproteins inhibit flight muscle lipoprotein lipase in a competitive manner at low concentrations, but this becomes mixed at higher concentrations of the apoproteins; both C_L-I and C_L-II apoproteins are effective (Wheeler *et al.*, 1986; Wheeler and Goldsworthy, 1986). This is the basis of the mechanism by which AKH controls lipoprotein lipase indirectly during rest and flight (Wheeler and Goldsworthy, 1985). That is, when the free (*i.e.*, not lipoprotein-bound) C_L-apoprotein concentration in the hemolymph is high, as it is in resting locusts, lipase activity is inhibited; but during flight, or when AKH is injected into resting locusts, C_L-apoprotein inhibition of the lipase is removed by the decrease in the concentration of free C_L-apoproteins as they bind to lipoprotein A^+.

This regulation of lipoprotein lipase by the hemolymph concentration of free C_L-apoprotein ensures rapid uptake of lipid by the flight muscles when A^+ is present in high concentrations. But more important perhaps, to prevent the flight muscles from 'stalling,' the inhibition of trehalose oxidation by products of lipid oxidation occurs only when lipoprotein A^+ (the preferred substrate) is present in sufficient quantities to sustain flight.

Histochemical staining for lipoprotein lipase in ultrathin sections of locust flight muscle confirms that the enzyme is membrane-bound, but shows also that activity is restricted to the T-tubules; therefore, the enzyme has ready access to hemolymph-borne lipoproteins. Inhibition of enzyme activity *in vitro* by free C_L-apoproteins, and activation after injection of AKH into donor locusts, can also be demonstrated by histochemical staining of

membrane preparations from flight muscles (Wheeler, 1989).

Direct actions of AKH at the flight muscles

Rates of fuel use in locusts flying under laboratory conditions can be assessed from changes in the concentrations of hemolymph metabolites; such data provide substantial circumstantial evidence that, at least during the first moments of flight, trehalose and diacylglycerols compete as fuels for the flight muscles (see Goldsworthy, 1983).

Fuel use by the flight muscles has been studied directly in half-thorax preparations of *Locusta* (Robinson and Goldsworthy, 1977). Trehalose use decreases to about 50% on addition of substrates containing hemolymph lipoproteins. This inhibition of substrate use is competitive, but in the presence of extracts of the corpora cardiaca containing AKH, or purified natural AKH-I, it becomes non-competitive. In addition, in these half thorax preparations AKH increases the rate of oxidation of lipids contained in lipoprotein preparations from AKH-injected locusts (see Goldsworthy, 1983).

Inactivation and excretion of AKH

The half life of AKH-I in the hemolymph of locusts is about 30 min (Cheeseman and Goldsworthy, 1979) but, while the hemolymph of some insects contains enzymes which degrade neuropeptides like AKH, locust hemolymph does not apparently contain AKH-degrading enzymes; the blocked peptides would presumably have some protection against non-specific peptidases. Work in Aberdeen (Mordue and Stone, 1978; Siegert and Mordue, 1987) shows that the Malpighian tubules of locusts are a potent source of degradative enzymes active against AKH-I, but we cannot be sure that inactivation by the tubules represents the major mechanism by which the AKH signal is removed: the CNS contains similar enzymes to those in the Malpighian tubules.

Siegert and Mordue (1987) have shown that AKH-I can be hydrolyzed by an endopeptidase from the Malpighian tubules. When AKH-I adopts a B-bend conformation (see below), the Asn at residue 7 could perhaps be relatively more susceptible to enzymatic attack. Analysis of the breakdown products obtained from incubating AKH-I with an homogenate of Malpighian tubules did not identify Asn, but three breakdown products present in small amounts could not be identified fully, and Asn may be contained in these. Three major breakdown products were identified, however: pGlu-Leu-Asn-Phe-Thr-Pro; Trp-Gly-Thr-NH_2; and tryptophan. Siegert and Mordue (1987) suggest that at least three proteolytic enzymes are present in the tubules: an endopeptidase cleaving at position 6–7 or 7–8; a carboxypeptidase that attacks the pGlu . . . Pro fragment at its (now) free C-terminus; and an aminopeptidase (during incubation the fragment Trp-Gly-Thr-NH_2 disappears; certainly a potent leucine aminopeptidase is present in high activity in tubules). The carboxypeptidase differs from carboxypeptidase A, because the latter did not attack the pGlu . . . Pro fragment. Certainly a carboxypeptidase and an aminopeptidase are present, but they are not responsible for the initial cleavage of AKH-I. There are no data for the breakdown of other AKH-related peptides in locusts.

We assume that AKH enters the Malpighian tubules passively and is then degraded. Molecules with larger molecular weights than AKH, such as inulin, readily permeate the tubule membrane. The relatively low molecular mass of AKH-I (1158), in combination with its lipophilic nature may mean that AKH readily enters the Malpighian tubule cells.

Adipokinetic Structure-Activity Requirements

Studying a series of synthetic peptide analogs of AKH-I, Stone *et al.* (1978) concluded that, for biological activity, peptides must be blocked by L-pyroglutamatic acid (cyclized L-glutamic acid) at the N-terminal, and by amidation at the C-terminal; they must be between 8 and 10 amino acids long; and substitutions in the area of residues 6 to 8, which were assumed to interfere with a proposed *B*-turn around residue 6 (proline), reduced biological activity. Recently the biological activities of naturally occurring analogs of AKH found in different insects have been examined (Goldsworthy *et al.*, 1986a, b; Wheeler *et al.*, 1988). While sufficiently high doses of most peptides can elicit full (maximum possible) responses, others elicit only attenuated adipokinetic (see Goldsworthy and Wheeler, 1986b) or hypertrehalosemic (Gade, 1986; Wheeler *et al.*, 1988) responses.

The sequences of naturally occurring members of the AKH family known presently are shown in Table I. In natural peptides of more than 8 residues, residue 10 is threonine and residue 9 is glycine. Residue 8 is tryptophan in all peptides. Residue 7 is either asparagine or glycine, except in *Manduca*-AKH where it is serine.

Residue 6 is proline in most of the natural peptides, the exceptions being the AKH-II's of locusts and of a grasshopper (*Romalea*), where it is alanine in *Locusta*, and threonine in *Schistocerca* and *Romalea*, and the AKH of *Manduca* in which it is serine. Residue 5 is either threonine or serine. In all peptides, residue 4 is phenylalanine. Residue 3 is either asparagine or threonine. Residue 2 is either leucine or valine. Residue 1 is always pyroglutamate.

The potencies of drugs and hormones can be represented by their ED_{50} values—the doses needed to bring about a half-maximal response (see Table I). In the first

Table I

The relative potencies of members of the AKH/RPCH family of arthropod neuropeptides in causing hyperlipaemia in Locusta *and, where indicated, in* Schistocerca

Neuropeptide	Amino acid residue 1 2 3 4 5 6 7 8 9 10	ED50 pmol	EDmax pmol	% Maximum response	CD evidence of *B*-bend
Locust AKH-I	pGlu-Leu-Asn-Phe-Thr-Pro-Asn-Trp-Gly-Thr-NH_2	1	3	100	Yes
	(assayed in *Schistocerca*)	6	20	100	
Carausius[2] HTF-II	pGlu-Leu-Thr-Phe-Thr-Pro-Asn-Trp-Gly-Thr-NH_2	2	8	100	Yes
Synthetic	Leu-Thr-Phe-Thr-Pro-Asn-Trp-Gly-Thr-NH_2		Not active		Yes
Synthetic	pGlu-Leu-Thr-Phe-Thr-Pro-Asn-Trp-Gly		Not active		Yes
Manduca[3]/*Heliothis*[4] AKH	pGlu-Leu-Thr-Phe-Thr-Ser-Ser-Trp-Gly-NH_2	10	40	45	No
		(20	40	100)	
Crustacean[5] RPCH	pGlu-Leu-Asn-Phe-Ser-Pro-Gly-Trp-NH_2	4.6	20	100	Yes
	(assayed in *Schistocerca*)	15	40	100	
Locusta[6] AKH-II	pGlu-Leu-Asn-Phe-Ser-Ala-Gly-Trp-NH_2	2	3	60	No
	(assayed in *Schistocerca*)	20	30	55	
Schistocerca[6] AKH-II	pGlu-Leu-Asn-Phe-Ser-Thr-Gly-Trp-NH_2	2	5	95–100	No
	(assayed in *Schistocerca*)	12	25	60	
Periplaneta[7] M-I	pGlu-Val-Asn-Phe-Ser-Pro-Asn-Trp-NH_2	5	30	95–100	Yes
Periplaneta[7] M-II	pGlu-Leu-Thr-Phe-Thr-Pro-Asn-Trp-NH_2	5	20	95–100	Yes
Neuphoeta[8]/ *Blaberus* HTH	pGlu-Val-Asn-Phe-Ser-Pro-Gly-Trp-Gly-Thr-NH_2	(4–5	20	100)	Yes
Romalea-I[9]	pGlu-Val-Asn-Phe-Thr-Pro-Asn-Trp-Gly-Thr-NH_2	(2	10	95–100)	Yes
Romalea-II[9]/*Gryllus*[10]	pGlu-Val-Asn-Phe-Ser-Ala-Gly-Trp-NH_2	(4–5	20	100)	No

[1] Stone *et al.* (1978); [2] Gäde and Rinehart (1987a); [3] Ziegler *et al.* (1985); [4] Jaffe *et al.* (1986); [5] Fernlund and Josefsson (1972); [6] Gäde *et al.* (1984; 1986); Siegert *et al.* (1985); [7] O'Shea *et al.* (1984); [8] Hayes and Keeley (1986); Gäde and Rinehart (1986); [9] Gäde *et al.* (1988); [10] Gäde and Rinehart (1987b).

The responses are calculated as a percentage of the maximum response obtained to a crude extract of *Locusta corpora* cardiaca (0.02 pair equivalents/locust) tested on the same batch of locusts on the same day (from Goldsworthy *et al.*, 1986b, and unpub. obs.). In our hands, with our strains of locusts, *Schistocerca* appears very much less sensitive than *Locusta* to those peptides tested. The final column shows whether CD spectroscopy indicates the presence of a *B*-bend (A. Drake, G. J. Goldsworthy, C. Wheeler, and G. Gäde, unpub. obs.). Assay data in brackets from G. Gäde (pers. comm.).

author's colony of *Locusta,* AKH-I has an ED_{50} of 1 pmol, and at doses above 3 pmol gives 'full' adipokinetic activity (ED_{max} = 3 pmol). This represents the maximum rate of lipid mobilization possible in the locusts at the time of assay, and can be used as a comparator for other peptides. *Carausius* peptide (HTF-II) has only a single residue change of threonine instead of asparagine at position 3 and, although this doubles the ED_{50} from 1 to 2 pmol, 'full' adipokinetic activity is still shown, but the ED_{max} increases so doses in excess of 8 pmol are required for a 'full' response.

From the data in Table 1 it seems that the various amino acid substitutions in the naturally occurring peptides RPCH, M-I, and M-II have little overall effect on hyperlipemic activity. However, these octapeptides all have 'weak' activity compared with AKH-I, with ED_{50} values around 5 pmol; they show 'full' adipokinetic activity, but their ED_{max} values are between 20 and 30 pmol.

Octapeptides lacking proline are particularly interesting because of the prediction of a *B*-turn at proline in AKH-I. Such predictions assess the statistical probability of there being a bend, calculated from the particular sequence of amino acids present and known secondary structures in proteins (Chou and Fasman, 1974). It is problematic whether such predictions apply to short peptides. But when the calculations are applied to the AKH family, with the exception of those members lacking proline at residue 6, all are predicted with high probability to have a turn around residue 6.

Using circular dichroism (CD) spectroscopy, we have shown at Birkbeck (A. Drake, G. J. Goldsworthy C. H. Wheeler and G. Gäde, unpub. obs.) that, in aqueous solution at room temperature, none of the naturally occurring neuropeptides of this family has a CD spectrum characteristic of a *B*-turn. However, on addition of SDS micelles or liposomes (which act as mimics of biological membranes in this system), the CD spectra of all peptides containing proline change to ones characteristic of a type-I *B*-turn (Goldsworthy and Wheeler, 1989). None

of the naturally occurring locust or grasshopper octapeptides, AKH-IIL, AKH-IIS, Ro-II, or the *Manduca*-AKH, show such changes in their CD spectra; they have no identifiable CD spectra with or without liposomes or SDS micelles (Table I).

Those members of the family that show a *B*-turn conformation, can show 'full' hyperlipemic and hypertrehalosemic activity, when tested at sufficiently high doses. However, when tested intraspecifically, the octapeptides which we have tested, and for which the CD analysis shows no evidence of a *B*-turn, all elicit attenuated hyperlipemic and hypertrehalosemic responses. Unfortunately, however, the situation is not completely clear-cut: while AKH-IIL gives an attenuated response, even at doses greater than 50 pmol, whether tested in *Locusta* or in *Schistocerca,* AKH-IIS gives an attenuated response when tested intraspecifically (in *Schistocerca*), but gives a full adipokinetic response in *Locusta* (Goldsworthy and Wheeler, 1986b). Apparently, contrary to our earlier conclusion (Goldsworthy *et al.,* 1986b), the presence of proline or of a *B*-turn is not essential for full adipokinetic activity.

Apparently, AKH receptors on the fat body of *Locusta* can discriminate between the locust AKH-II octapeptides, whereas those of *Schistocerca* cannot. When injected intraspecifically, the two locust AKH-II octapeptides do not show 'full' activity; they give truncated responses. AKH-II*L* is potent in comparison with AKH-I (ED_{50} about 2 pmol), but only gives about 60% of the maximum response in *Locusta* even at doses up to 50 pmol. AKH-II*S* is less potent in *Schistocerca* (ED_{50} = 12 pmol) and gives a truncated response. On the other hand, AKH-II*S* is very potent in *Locusta* (ED_{50} = 2 pmol) and gives a 'full' adipokinetic response. *Manduca* (and *Heliothis*)-AKH is relatively inactive in *Locusta,* having an ED_{50} of 10 pmol and giving a truncated response even at doses up to 75 pmol.

At Birkbeck, we have recently undertaken molecular modelling of members of the AKH family. A model of AKH-I has been generated using computer graphics. A type-I turn was built into the 10 residue AKH-I neurohormone using HYDRA on an Evans & Sutherland PS300 graphics system. The dihedral angles of the sequence were set to B-conformation except that the central residues of the proposed turn were set to the ideal angles for a type-I *B*-turn. Slight, by eye, adjustments produced a hydrophobic cluster of phenylalanine, tryptophan, and leucine on one side of the peptide. If, as the CD data suggests, the *B*-turn is involved in receptor binding conformation, then this hydrophobic face of the peptide may be a likely candidate for interaction with the receptor. Additional main-chain stabilizing hydrogen bonds were also built in (Leu2 main chain oxygen to Gly9 main chain NH; Thr5 main chain NH to Trp8 main chain oxygen; Thr5 main chain oxygen to Trp8 main chain NH; and Asn7 main chain NH to Thr5 side chain oxygen), and the structure was energy minimized with GROMOS. Our model differs in detail from the earlier one proposed by Mordue and his colleagues (Mordue and Morgan, 1985). Molecular dynamics suggested that the phenylalanine may flip to give a tighter hydrophobic cluster when interacting with the tryptophan ring. This hydrophobic cluster on one face of the molecule requires further investigation.

Evolutionary Considerations

The locust adipokinetic hormones and structurally similar peptides from other insects and crustacea (Table I) are commonly referred to as a family of peptides. Underlying these references are suggestions that close evolutionary relationships exist between different arthropod groups. It will be necessary to analyze closely both molecular evolution and links between and within the crustacea and the insects. It is apparent from the known structures that a number of core residues are strictly conserved in adipokinetic and related peptides: thus residues 1, 4, and 8 are constant; and in nona- and deca- peptides Gly is residue 9; and in the three known decapeptides residue 10 is Thr-NH_2.

Even this limited degree of conservation gives a strong indication of family groups, and analysis of the variability in amino acid residues in other positions adds substantially to these indications. It is essential, when dealing with molecular evolution of peptides, to give consideration to the codons that specify particular amino acids. The structure-activity relationships discussed above are integral to, and a manifestation of, the evolutionary process.

We have already discussed the variations in sequence in members of the AKH/RPCH family. The precise codons used for each amino acid in the various insects are not yet known, but routes for single point mutations to change from one amino acid residue to another can be worked out. For example, with respect to Leu or Val at position two, there are three possible routes. The variability at residue 5 is limited and involves only Thr and Ser, and for these single point mutations are also possible.

Proline is most common at residue 6, and is present in all the decapeptides; but as we have discussed above, either Thr, Ser, or Ala are present at this position in some of the natural peptides of this family. The four possible codon sequences for each amino acid residue (Pro: Thr: Ser: Ala) have identical second and third nucleotides. In consequence, single point mutations in the first nucleotide of each codon could allow mutations during evolution. One concept of peptide-families necessitates a pri-

mary peptide from which others have evolved. However, at present, we cannot predict with certainty which of the four residues at position 6 could have been present in an ancestral peptide. The first peptides to be characterized fully in this family were RPCH and AKH-I; the codon sequences for Gly and Asn, the residues present at position 7 in these two peptides respectively, indicate that single step mutations could not occur.

Other peptides of the family, which were sequenced subsequently, also contain either Asn or Gly at residue 7 (see Table I); one possible interpretation of these findings was that two separate families existed. However, a candidate link peptide exists in the adipokinetic hormone isolated from lepidoptera which has Ser at residue 7. Theoretical single steps are possible in either direction between peptides containing either Asn and Gly via the peptide found in *Manduca* (Ziegler *et al.*, 1985) or *Heliothis* (Jaffe *et al.*, 1986). It must be emphasized that in our approach so far we have been concerned only with theoretical problems. Other factors have to be taken into consideration; for example, some arthropod biologists would, on *a priori* grounds, consider insects and crustaceans to belong to separate phyla, and therefore any commonality between RPCH and AKH-peptides would stem from a peptide present in pro-arthropod stock or simply be another example of convergence in evolution. Moreover, the highly specialized lepidoptera are most unlikely candidates to provide evolutionary linkage between either crustacea and insects on the one hand or between different insect groups on the other. Nevertheless, in terms of molecular evolution within the insects, we can perhaps talk of a family of peptides, but it is unfortunate that for the largest animal classes we are attempting to construct relationships on data from so few species and from very few insect orders. There is an urgent need for data on the composition of precursor molecules. The homologies present in the AKH family may reflect both modifications from a single ancestral peptide, and their processing from a common precursor.

Are the AKH/RPCH peptides related to the leucokinins? The latter are part of a second insect peptide family, but have all been identified in a single species of cockroach, *Leucophaea maderae*, by Holman and his colleagues (1984, 1986, 1987). They have some sequence affinities with AKH and RPCH, but comparisons are not straight-forward. In the leucokinins for which structures are published, residues 4 (Phe); 6 (Ser); 7 (Trp); and 8 (Gly-NH_2) are strictly conserved. If these are considered to be analogous to residue 1–8 in the octapeptides from the AKH series, then it is possible to consider possibilities of links between the leucokinins and peptides of the AKH/RPCH family. The possibilities for mutations are slight at residue 1 (using glutamine as the residue to be cyclized to form pyroglutamate) and at residues 7 and 8. However, rather than using Phe at residue 4 as the reference point, the N-terminal Trp-Gly-NH_2 may be a more rational cross-reference point; in this situation there are many possible linkage points between the adipokinetic and leucokinin families. However, only when more is known of the structure of the precursor molecules concerned with the synthesis of insect peptide hormones, will a clearer evolutionary picture emerge.

Literature Cited

Beenakkers, A. M. Th., D. J. Van Der Horst, and W. J. A. Van Marrewijk. 1985. Biochemical processes directed to flight muscle metabolism. Pp. 451–486 in *Comprehensive Insect Physiology, Biochemistry and Pharmacology*, vol. 10, G. A. Kerkut and L. I. Gilbert, eds. Pergamon Press, Oxford.

Cheeseman, P., and G. J. Goldsworthy. 1979. The release of adipokinetic hormone during flight and starvation in *Locusta*. *Gen. Comp. Endocrinol.* **37:** 35–43.

Chou, P. Y., and G. D. Fasman. 1974. Prediction of protein conformation. *Biochemistry* **13:** 222–245.

Fernlund, P., and L. Josefsson. 1972. Crustacean color-change hormone: amino acid sequence and chemical synthesis. *Science* **177:** 173–175.

Gäde, G. 1986. Relative hypertrehalosaemic activities of naturally occurring neuropeptides from the AKH/RPCH family. *Z. Naturforsch.* **41:** 315–320.

Gäde, G., and K. L. Rinehart. 1986. Amino acid sequence of a hypertrehalosaemic neuropeptide from the corpus cardiacum of the cockroach, *Nauphoeta cinerea*. *Biochem. Biophys. Res. Comm.* **141:** 774–781.

Gäde, G., and K. L. Rinehart. 1987a. Primary structure of the hypertrehalosaemic factor II from the corpus cardiacum of the Indian stick insect, *Carausius morosus*, determined by fast atom bombardment mass spectrometry. *Biol. Chem. Hoppe-Seyler* **368:** 67–75.

Gäde, G., and K. L. Rinehart. 1987b. Primary sequence analysis by fast atom bombardment mass spectrometry of a peptide with adipokinetic activity from the corpora cardiaca of the cricket *Gryllus bimaculatus*. *Biochem. Biophys. Res. Comm.* **149:** 908–914.

Gäde, G., G. J. Goldsworthy, G. Kegel, and R. Keller. 1984. Single step purification of locust adipokinetic hormones I and II by reversed phase high-performance liquid chromatography, and amino acid composition of the hormone II. *Hoppe-Seyler's Z. Physiol. Chem.* **365:** 391–398.

Gäde, G., G. J. Goldsworthy, M. H. Schaffer, J. C. Cook, and K. L. Rinehart. 1985. Sequence analyses of adipokinetic hormones II from corpora cardiaca of *Schistocerca nitans*, *Schistocerca gregaria*, and *Locusta migratoria* by fast atom bombardment mass spectrometry. *Biochem. Biophys. Res. Comm.* **134:** 723–730.

Gäde, G., C. Hilbich, K. Beyreuther, and K. L. Rinehart. 1988. Sequence analyses of two neuropeptides of the AKH/RPCH-family from the lubber grasshopper, *Romalea microptera*. *Peptides* **9:** 681–688.

Goldsworthy, G. J. 1983. The endocrine control of flight metabolism in locusts. Pp. 149–204 in *Advances in Insect Physiology*, Vol. 17, M. J. Berridge, J. E. Treherne and V. B. Wigglesworth, eds. Academic Press, New York.

Goldsworthy, G. J., and C. H. Wheeler. 1986a. The endocrine control of flight metabolism in locusts. Pp. 49–59 in *Insect Flight Dispersal and Migration*, W. Danthanarayana, ed. Springer-Verlag, Heidelberg.

Goldsworthy, G. J., and C. H. Wheeler. 1986b. Structure/activity relationships in the adipokinetic hormone/red pigment concentrating

hormone family. Pp. 183–186 in *Insect Neurochemistry and Neurophysiology 1986*, A. B. Borkovec and D. B. Gelman, eds. Humana Press, New Jersey.

Goldsworthy, G. J., and C. H. Wheeler. 1989. Physiological and structural aspects of adipokinetic hormone function in locusts. *Pesticide Chem.* **25:** 85–95.

Goldsworthy, G. J., K. Mallison, and C. H. Wheeler. 1986a. The relative potencies of two known locust adipokinetic hormones. *J. Insect Physiol.* **32:** 95–101.

Goldsworthy, G. J., K. Mallison, C. H. Wheeler, and G. Gade. 1986b. Relative adipokinetic activities of members of the AKH/RPCH family. *J. Insect Physiol.* **32:** 433–438.

Goldsworthy, G. J., A. R. Jutsum, and N. L. Robinson. 1979. Substrate utilisation and flight speed during tethered flight in the locust. *J. Insect Physiol.* **25:** 183–185.

Goldsworthy, G. J., C. M. Miles, and C. H. Wheeler. 1985. Lipoprotein transformations during adipokinetic hormone action. *Physiol. Entomol.* **10:** 151–164.

Hayes, T. K., and L. L. Keeley. 1986. Isolation and structure of the hypertrehalosaemic hormone from *Blaberus discoidalis* cockroaches. Pp. 195–198 in *Insect Neurochemistry and Neurophysiology 1986*, A. B. Borkovec and D. B. Gelman, eds. Humana Press, New Jersey.

Hekimi, S., and M. O'Shea. 1987. Identification and purification of two precursors of the insect neuropeptide adipokinetic hormone. *J. Neurosci.* **7:** 2773–2784.

Holman, G. M., B. J. Cook, and R. M. Wagner. 1984. Isolation and partial characterization of five myotropic peptides present in head extracts of the cockroach *Leucophaea maderae*. *Comp. Biochem. Physiol.* **77C:** 1–5.

Holman, G. M., B. J. Cook, and R. J. Nachman. 1986. Isolation primary structure and synthesis of two neuropeptides from *Leucophaea maderae*: members of a new family of cephalomyotropins. *Comp. Biochem. Physiol.* **84C:** 271–276.

Holman, G. M., B. J. Cook, and R. J. Nachman. 1987. Isolation, primary structure and synthesis of leucokinins VII and VIII: the final members of this new family of cephalomyotropins isolated from head extracts of *Leucophaea maderae*. *Comp. Biochem. Physiol.* **88C:** 31–34.

Jaffe, H., A. K. Raina, C. T. Riley, B. A. Fraser, G. M. Holman, R. M. Wagner, R. L. Ridgway, and D. K. Hayes. 1986. Isolation and primary structure of a peptide from the corpora cardiaca of *Heliothis zea* with adipokinetic activity. *Biochem. Biophys. Res. Comm.* **135:** 622–628.

Konings, P. N. M., H. G. B. Vullings, M. Geffard, R. M. Buijs, J. H. B. Diederen, and W. F. Jansen. 1988. Immunocytochemical demonstration of octopamine-immunoreactive cells in the nervous system of *Locusta migratoria* and *Schistocerca gregaria*. *Cell Tissue Res.* **251:** 371–379.

Mayer, R. J., and D. J. Candy. 1967. Changes in haemolymph lipoproteins during locust flight. *Nature* **215:** 987.

Mordue, W., and P. J. Morgan. 1985. Chemistry of peptide hormones. Pp. 153–183 in *Comprehensive Insect Physiology, Biochemistry and Pharmacology*, Vol 7, G. A. Kerkut and L. I. Gilbert, eds. Pergamon Press, Oxford.

Mordue, W., and J. V. Stone. 1978. Structure and metabolism of adipokinetic hormone. Pp. 487–490 in *Comparative Endocrinology*, P. J. Gaillard and H. H. Boer, eds. Elsevier, Amsterdam.

Mwangi, R. W., and G. J. Goldsworthy. 1977. Diglyceride-transporting lipoproteins in *Locusta*. *J. Comp. Physiol. B* **114:** 177–190.

O'Shea, M., J. Witten, and M. Schaffer. 1984. Isolation and characterization of two myoactive neuropeptides: further evidence of an invertebrate peptide family. *Neuroscience* **4:** 521–529.

Orchard, I. 1987. Adipokinetic hormones—an update. *J. Insect Physiol.* **33:** 451–463.

Rademakkers, L. H. P. M. 1977. Identification of a secretomotor centre in the brain of *Locusta migratoria*, controlling the secretory activity of the adipokinetic hormone producing cells of the corpus cardiacum. *Cell Tiss. Res.* **184:** 381–395.

Robinson, N. L., and G. J. Goldsworthy. 1977. Adipokinetic hormone and the regulation of carbohydrate and lipid metabolism in a working flight muscle preparation. *J. Insect Physiol.* **23:** 9–16.

Siegert, K. J., and W. Mordue. 1987. Breakdown of locust adipokinetic hormone I by Malpighian tubules of *Schistocerca gregaria*. *Insect Biochem.* **17:** 705–710.

Siegert, K., P. J. Morgan, and W. Mordue. 1985. Primary structures of locust adipokinetic hormones II. *Biol. Chem. Hoppe-Seyle* **366:** 723–727.

Stone, J. V., W. Mordue, C. E. Broomfield, and P. M. Hardy. 1978. Structure-activity relationships for the lipid-mobilizing action of adipokinetic hormone. Synthesis and activity of a series of hormone analogues. *Eur. J. Biochem.* **89:** 195–202.

Van Heusden, M. C., D. J. Van Der Horst, J. M. Van Doorn, J. Wes, and A. M. Th. Beenakkers. 1986. Lipoprotein lipase activity in the flight muscle of *Locusta migratoria* and its specificity for haemolymph lipoproteins. *Insect Biochem.* **16:** 517–523.

Wheeler, C. H. 1989. Transport of fuels to the flight muscles. Pp. 273–303 in *Insect Flight*, G. J. Goldsworthy and C. H. Wheeler, eds. CRC Press, Boca Raton, Florida.

Wheeler, C. H., K. M. Boothby, and G. J. Goldsworthy. 1986. CL-proteins and the regulation of lipoprotein lipase activity in locust flight muscle. *Biol. Chem. Hoppe-Seyler* **367:** 1127–1133.

Wheeler, C. H., G. Gäde, and G. J. Goldsworthy. 1988. Humoral functions of insect neuropeptides. Pp. 141–157 in *Neurohormones of Invertebrates*, M. C. Thorndyke and G. J. Goldsworthy, eds. Cambridge University Press, Cambridge.

Wheeler, C. H., and G. J. Goldsworthy. 1983a. Qualitative and quantitative changes in Locusta haemolymph proteins and lipoproteins during ageing and adipokinetic hormone action. *J Insect Physiol.* **29:** 339–354.

Wheeler, C. H. and G. J. Goldsworthy. 1983b. Protein-lipoprotein interactions in the haemolymph of Locusta during the action of adipokinetic hormone: the role of C_L-proteins. *J. Insect Physiol.* **29:** 349–354.

Wheeler, C. H., and G. J. Goldsworthy. 1985. Lipid transport to the flight muscles in *Locusta* Pp. 126–135 in *Insect Locomotion*, M. Gewecke, ed. Paul Parey Press, Berlin.

Wheeler, C. H., and G. J. Goldsworthy. 1986. Lipoprotein/apoprotein interactions during adipokinetic hormone action in *Locusta*. Pp. 187–190 in *Insect Neurochemistry and Neurophysiology 1986*, A. B. Borkovec and D. B. Gelman, eds. Humana Press, New Jersey.

Wheeler, C. H., J. E. Mundy, and G. J. Goldsworthy. 1984a. Locust haemolymph lipoproteins visualised in the electron microscope. *J. Comp. Physiol.* **154:** 281–286.

Wheeler, C. H., D. J. Van Der Horst, and A. M. Th. Beenakkers. 1984b. Lipolytic activity in the flight muscles of *Locusta migratoria* measured with haemolymph lipoproteins as substrates. *Insect Biochem.* **14:** 261–266.

Ziegler, R., K. Eckart, H. Schwarz, and R. Keller. 1985. Amino acid sequence of *Manduca sexta* adipokinetic hormone elucidated by combined fast atom bombardment (FAB)/tandem mass spectrometry. *Biochem. Biophys. Res. Commun.* **133:** 337–342.

Reference: *Biol. Bull.* 177: 225–229. (October, 1989)

The Pigment-Dispersing Hormone Family: Chemistry, Structure-Activity Relations, and Distribution

K. RANGA RAO AND JOHN P. RIEHM

Department of Biology, The University of West Florida, Pensacola, Florida, 32514-5751

Abstract. This report summarizes recent work on the pigment-dispersing hormone (PDH) family, a set of related neuropeptides common to arthropods. The primary structures are known for the major form of PDH in several crustacean species (*Pandalus borealis, Uca pugilator, Cancer magister, Penaeus aztecus, Procambarus clarkii*) and for related pigment-dispersing factors from two insects (*Acheta domesticus, Romalea microptera*). In this peptide family, the amino acid chain length (18 residues), termini (N-terminal Asn, C-terminal Ala-NH_2), and at least 50% of the sequence are conserved. Synthetic analogs have been used to analyze the structure-activity relations of PDH, leading to: an evaluation of the role of specific residues; a tentative identification of the message sequence; and the preparation of stable and superpotent analogs including tyrosinated analogs for radioiodination. An enzyme-linked immunosorbant assay (ELISA) has been developed for β-PDH. Antisera raised against α-PDH and β-PDH were used to determine the distribution of PDH. This distribution and other evidence indicate that, besides its role in humoral regulation of the pigmentary system, PDH may serve extra-pigmentary functions. The functions of the PDH-related peptides in insects are unknown.

Introduction

Crustaceans display reversible color changes and eye pigment movements. The color changes result from dispersion or concentration (aggregation) of pigment granules within epithelial chromatophores. The somewhat less conspicuous eye pigment movements, associated with light or dark adaptation, may be restricted to retinular cells (photoreceptor cells), or may also involve extra-retinular ommatidial pigment cells. Whereas pigment movements within retinular cells are induced mainly by a direct action of light, the extra-retinular ommatidial pigment cells as well as epithelial chromatophores are controlled by neurosecretory hormones. The total number of pigmentary-effector hormones present in any given species is unknown, but they are separable into two sets having mutually antagonistic actions. The hormones causing chromatophoral pigment concentration and ommatidial dark adaptation belong to one set, and they are distinct from the hormones eliciting chromatophoral pigment dispersion and ommatidial light adaptation (see reviews: Rao, 1985; Rao and Riehm, 1988a, b). Among hormones in the first set, primary structure is known for only the red pigment-concentrating hormone (RPCH) isolated from eyestalks of the shrimp *Pandalus borealis* (Fernlund and Josefsson, 1972). This crustacean RPCH, an octapeptide (<Glu-Leu-Asn-Phe-Ser-Pro-Gly-Trp-NH_2), is structurally related to insect adipokinetic hormones (AKHs). The functions and structure-activity relations of the RPCH/AKH family peptides are reviewed in this issue by Goldsworthy and Mordue (1989).

Our recent work showed that an additional family of peptides, including the pigment-dispersing hormones (PDHs), is common to crustaceans and insects. This report focuses on the chemistry, structure-function relations, and distribution of PDHs and related peptides.

Structure and Relative Potency of Identified Peptides

When extracts of eyestalks are subjected to cation-exchange chromatography, several zones of PDH activity (3–5, depending on the species) can be detected. The structural basis of this heterogeneity remains unresolved, because in each of the species studied, the amino acid sequence has been deduced for only the major form of PDH. The first structural elucidation in this set of hormones was for an octadecapeptide called light-adapting

Table I

The pigment-dispersing hormone (PDH) family: structure and relative potency

Source	Sequence**																	Relative potency*
	1				6						12						18	
Uca pugilator (β-PDH)	N	S	E	L	I	N	S	I	L	G	L	P	K	V	M	N	D	A amide	1.0
Cancer magister (β-PDH)	N	S	E	L	I	N	S	I	L	G	L	P	K	V	M	N	D	A amide	1.0
Procambarus clarkii PDH	N	S	E	L	I	N	S	I	L	G	L	P	K	V	M	N	E	A amide	0.14
Penaeus aztecus PDH	N	S	E	L	I	N	S	L	L	G	I	P	K	V	M	N	D	A amide	1.0
Acheta domesticus PDF	N	S	E	I	I	N	S	L	L	G	L	P	K	V	L	N	D	A amide	0.5
Romalea microptera PDF	N	S	E	I	I	N	S	L	L	G	L	P	K	L	L	N	D	A amide	0.5
Pandalus borealis (α-PDH)	N	S	G	M	I	N	S	I	L	G	I	P	R	V	M	T	E	A amide	0.05

* Based on assays for pigment dispersion in melanophores of *Uca pugilator*; β-PDH = 1.0.

** Notation is the approved one-letter abbreviations for the amino acids. Underlined residues are those different from β-PDH.

distal retinal pigment hormone (DRPH) from eyestalks of the shrimp *Pandalus borealis* (Fernlund, 1976). This peptide elicits not only ommatidial light adaptation, but also chromatophoral pigment dispersion (Kleinholz, 1975), and is referred to as α-PDH in the recent literature.

An octadecapeptide differing from α-PDH at six positions, and designated β-PDH, has been identified as the major form of dispersing hormone in extracts of eyestalks from the crabs *Uca pugilator* (Rao *et al.*, 1985) and *Cancer magister* (Kleinholz *et al.*, 1986). Recent work in our laboratory indicated that the major forms of PDH in eyestalks of the brown shrimp *Penaeus aztecus* (Phillips *et al.*, 1988) and the crayfish *Procambarus clarkii* (McCallum *et al.*, 1988) have more sequence similarity to β-PDH than to α-PDH (Table I). Because of the substitution of Glu^3 for Gly^3, the PDHs of *Penaeus* and *Procambarus*, as well as β-PDH, are more acidic and elute faster than α-PDH in cation-exchange chromatography.

When the cation-exchange chromatography profiles were compared, α-PDH could not be detected in eyestalk extracts from *Uca*, *Cancer*, *Penaeus*, and *Procambarus*. Yet in *Pandalus*, α-PDH is the identified major form. Two faster eluting PDH zones are evident in cation-exchange chromatography of *Pandalus* eyestalk extracts, but their structural similarity to β-PDH has not been established.

Since insect head extracts are known to cause melanophore pigment dispersion in *Uca*, we have determined the primary structures of the active peptides (pigment-dispersing factors; PDFs) from two insect species: the lubber grasshopper *Romalea microptera* (Rao *et al.*, 1987), and the domestic cricket *Acheta domesticus* (Rao and Riehm, 1988b). In the latter study, we were able to identify 17 of the 18 residues, and the unidentified residue was presumed to be Arg^{13} or Lys^{13}. More recently, by comparison with synthetic peptides, we concluded that Lys is present as residue 13 in *Acheta* PDF.

The sequence similarity between insect PDFs and crustacean PDHs (Table I) shows that both groups are constituents of an authentic peptide family common to arthropods. This peptide family displays conservation of amino acid chain length (18 residues), conservation of termini (amino-terminal Asn and carboxyl-terminal Ala-amide), and at least 50% sequence similarity. The insect PDFs, like the PDHs of *Penaeus* and *Procambarus*, are more closely related to β-PDH than to α-PDH.

Since the function of PDFs in insects is unknown, these peptides, as well as crustacean PDHs, have been tested for their relative potencies by assays for melanophore pigment dispersion in *Uca*. In these assays the ratio of the highest to lowest relative potency among the PDH family peptides (*i.e.*, β-PDH/α-PDH) is 20 (Table I). *Penaeus* PDH and β-PDH are the most active and are equipotent; thus the two substitutions in the *Penaeus* peptide (Leu^8 for Ile^8, and Ile^{11} for Leu^{11}) are not critical for the potency of β-PDH. The insect PDFs, which differ from β-PDH at three or four positions, are about 50% as potent as β-PDH. Among the individual substitutions noted in the PDH family, the replacement of Asp^{17} by Glu^{17} (*e.g.*, in *Procambarus* PDH) caused a marked decline (7-fold) in potency. The least potent peptide, α-PDH, contains not only Glu^{17}, but also substitutions at five other positions (Table I).

Structure-Activity Relations of Synthetic PDH Analogs

To evaluate the contributions of specific residues to the potency differences between α-PDH and β-PDH, we synthesized several structural intermediates. Although, as noted above, replacement of Asp^{17} by Glu^{17} reduces the potency of β-PDH, replacement of Glu^{17} by Asp^{17} did not increase the potency of α-PDH. Similarly, β-PDH-

related substitutions at three other positions (Leu^{11}, Lys^{13}, or Asn^{16}) did not notably alter the potency of α-PDH. Substitutions at positions 3 and 4 (Glu^3, Leu^4) were each able to increase the potency of α-PDH (2.4 and 3.3-fold, respectively), but they did not account for the net increased potency of β-PDH. The lower potency of α-PDH appears to be due to an interactive effect of multiple substitutions.

As reviewed earlier (Rao and Riehm, 1988b), we have synthesized and assayed a number of additional analogs to evaluate the role of specific substitutions. These studies indicate that the increased potency resulting from the substitution of Glu^3 for Gly^3 may be due to a more stable ligand-receptor interaction through the formation of an ionic bond. The increased potency resulting from Leu^4 substitution for Met^4 is attributable to protection from oxidation. In α-PDH, replacement of either Met^4 or Met^{15} by norleucine (Nle) caused a three-fold increase in potency, whereas replacement of both residues led to a six-fold increase in potency. In β-PDH, which contains a single methionine residue (Met^{15}), the substitution of Nle^{15} imparted hyperpotency (16-fold) and full protection from oxidation. The latter feature proved useful in preparing tyrosinated analogs of PDH, such as the N-terminally extended [N-Tyr-Nle^{15}]-β-PDH, which could be iodinated without loss of biological activity (Rao and Riehm, 1988b).

The PDH family members share common termini, which appear to be crucial for the full potency of these peptides. Tests with truncated analogs of α-PDH showed that deamidation or deletion of C-terminal Ala, or deletion of N-terminal Asn, results in a substantial loss of potency. Further truncation produced very weak agonists, with the analog 1-9-NH_2 being the smallest carboxyl-terminal deletion peptide to display activity (0.001% potency, relative to α-PDH) and the analog 6-18-NH_2 being the smallest amino-terminal deletion peptide with activity (0.03% potency). Since these two truncated peptides share the sequence of residues 6 to 9, and because α-PDH and β-PDH share the hexapeptide sequence of residues 5–10, this region seemed to be the possible message sequence of PDH (Rao and Riehm, 1988b).

Recent work in our laboratory by Zahnow (1987) showed that peptides 5-9-NH_2, 5-10-NH_2, 6-9-NH_2, and 6-10-NH_2 were each able to cause dispersion of melanophore pigments in *Uca*, but were ineffective on leucophores. Thus, although residues 6–9 may constitute the message sequence required for melanophore activation, one or more other components of the octadecapeptide sequence may be needed for the multiple actions of PDH. More detailed studies are needed to elucidate the critical structural and sequence requirements for activation of different pigmentary effector cell types.

Immunocytochemistry

Antisera raised against α-PDH were used to detect immunoreactive somata in the brain and various optic ganglia of the crayfish *Orconectes immunis* (Schueler *et al.*, 1986). The application of β-PDH antiserum revealed immunopositive perikarya in the eyestalk ganglia and in various central ganglia of *Orconectes limosus* and *Carcinus maenas* (Mangerich *et al.*, 1987; Mangerich and Keller, 1988). These studies indicate that PDH is not only associated with neurosecretory cells terminating in the sinus gland, but is also found in apparently non-secretory neurons and in fibers not associated with neurohemal release sites. Therefore, in addition to its well known role as a blood-borne pigmentary-effector hormone, PDH may also serve as a neuromodulator or transmitter.

In eyestalk ganglia of *Orconectes limosus, Carcinus maenas* (Mangerich *et al.*, 1987), and *Penaeus aztecus* (Phillips *et al.*, 1987), some of the PDH-positive soma and nerve tracts were also reactive to a FMRFamide antiserum. In the central ganglia examined in *Orconectes*, PDH and FMRFamide immunoreactivities were not co-localized (Mangerich and Keller, 1988).

Comparable studies in the lubber grasshopper *Romalea microptera* (Zahnow *et al.*, 1987) showed that PDH-positive cells are restricted to the optic lobes, and that some of these cells are also reactive to FMRFamide antiserum. Other cells containing immunoreactive FMRFamide were widely distributed, occurring in the brain, as well as in the optic lobes of *Romalea*.

In the tobacco hawkmoth *Manduca sexta*, PDH immunoreactivity and gastrin/CCK-like immunoreactivity were co-localized in many somata that were distributed widely in the optic lobes, brain, and subesophageal ganglion (Homberg *et al.*, 1987). The physiological significance of the co-localization of immunoreactivities, and the differential distribution of PDH in the two insect species, merits further exploration.

Immunoassays

With an antiserum raised against synthetic β-PDH (Dircksen *et al.*, 1987), we developed an enzyme-linked immunosorbant assay (ELISA) and used it to evaluate antibody specificity (Bonomelli *et al.*, 1988). In competitive tests, the antiserum (diluted 1:100,000) recognized β-PDH with an IC_{50} of 160 fmol/well, but had little affinity for α-PDH (<0.001% relative to β-PDH). The antiserum showed considerable affinity for insect PDFs (13–21%) and *Penaeus* PDH (75%), which are very similar in sequence to β-PDH. The markedly lower affinity (0.4%) noted with *Procambarus* PDH was reminiscent of the low potency as a pigment disperser and could be due to its single substitution—Glu^{17} for Asp^{17}. When α-PDH

analogs containing β-PDH-related substitutions were tested, the analogs containing Asn^{16} or Asp^{17} reacted better than those with Glu^{3}, Leu^{4}, Leu^{11}, or Lys^{13}. The antiserum failed to recognize a C-terminally truncated analog of β-PDH (1-13-NH_2). These findings suggest that the antiserum needs several of the residues closer to the C-terminus in β-PDH for recognition. The specificity of the antiserum raised against α-PDH (Schueler *et al.*, 1986) was not reported.

Extra-Pigmentary Functions

The RPCH/AKH family members show considerable sequence homology, but serve distinct functions in different arthropods: chromatophoral pigment concentration in Crustacea; hyperglycemia, hypertrehalosemia, hyperlipemia, and cardioacceleration in insects (see Goldsworthy and Mordue, 1989). Since insects lack a chromatophoral system, the PDH functions (yet undetermined) are most likely to be extra-pigmentary in these animals. Immunocytochemical distribution points to a role as neuromodulator or neurotransmitter for PDH.

Recent work indicates that RPCH and PDH may also serve extra-pigmentary functions in Crustacea. RPCH has strong excitatory effects on the stomatogastric ganglion (Nusbaum and Marder, 1988). RPCH and β-PDH have stimulatory and inhibitory effects, respectively, on the secretion of methyl farnesoate by crustacean mandibular organs (Laufer *et al.*, 1987), and thus seem to have a role in the regulation of reproduction.

Perspectives

Now that the major PDH-like peptides in several species have been sequenced, and their structure-activity relations, immunoreactivity, and tissue distributions have been determined, a new arthropodan peptide family has emerged. However, because this is a very new family, most aspects of its distribution, functions, and evolution remain to be explored.

The first major problem is to define the limits of the PDH family and the variability within it. To those ends, the amino acid sequences of the unknown multiple forms of PDH in selected species must be determined, and the genetic basis of those sequences will also have to be established. Moreover, the PDH-related peptides—and the genes encoding them—should be sought in a wider selection of arthropods and crustaceans, as well as in other phyletic groups.

Second, although the pigmentary effects of the PDH family will continue to be an object of study, the extra-pigmentary effects will have to be investigated. Sites of action can be located by immunocytochemistry, and functions may be identified by correlating immunoreactive hormone titers with various physiological states. Finally, PDH receptors and receptor mechanisms must be characterized.

Acknowledgments

This investigation was supported by Grant DCB-8711403 from the National Science Foundation. The authors are thankful to Ms. Carol Hatcher for assistance in preparing the manuscript.

Literature Cited

Bonomelli, S. L., K. R. Rao, and J. P. Riehm. 1988. Development and application of an ELISA for crustacean β-PDH. *Am. Zool.* **28:** 117A.

Dircksen, H., C. A. Zahnow, G. Gaus, R. Keller, J. P. Riehm, and K. R. Rao. 1987. The ultrastructure of nerve endings containing pigment-dispersing hormone (PDH) in crustacean sinus glands: identification by an antiserum against synthetic PDH. *Cell Tissue Res.* **250:** 377–387.

Fernlund, P. 1976. Structure of a light-adapting hormone from the shrimp *Pandalus borealis*. *Biochim. Biophys. Acta* **439:** 17–25.

Fernlund, P., and L. Josefsson. 1972. Crustacean color change hormone: amino acid sequence and chemical synthesis. *Science* **177:** 173–175.

Goldsworthy, G. J., and W. Mordue. 1989. Functions and structure-activity relations of the AKH/RPCH-like peptides. *Biol. Bull.* **177:** 218–224.

Homberg, U., T. G. Kingan, and J. G. Hildebrand. 1987. Gastrin/CCK-like peptides in the brain of the tobacco hawkmoth *Manduca sexta*. *Soc. Neurosci. Abstr.* **13:** 225.

Kleinholz, L. H. 1975. Purified hormones from the crustacean eyestalks and their physiological specificity. *Nature* **258:** 256–257.

Kleinholz, L. H., K. R. Rao, J. P. Riehm, G. E. Tarr, L. Johnson, and S. Norton. 1986. Isolation and sequence analysis of pigment-dispersing hormone from eyestalks of the crab *Cancer magister*. *Biol. Bull.* **170:** 135–143.

Laufer, H., E. Homola, and M. Landau. 1987. Control of methyl farnesoate in crustacean mandibular organs. *Am. Zool.* **27:** 69A.

Mangerich, S., and R. Keller. 1988. Localization of pigment-dispersing hormone (PDH) immunoreactivity in the central nervous system of *Carcinus maenas* and *Orconectes limosus* (Crustacea), with reference to FMRFamide immunoreactivity in *O. limosus*. *Cell Tissue Res.* **253:** 199–208.

Mangerich, S., R. Keller, H. Dircksen, K. R. Rao, and J. P. Riehm. 1987. Immunocytochemical localization of pigment-dispersing hormone (PDH) and its coexistence with FMRFamide immunoreactivity in the eyestalks of the decapod crustaceans *Carcinus maenas* and *Orconectes limosus*. *Cell Tissue Res.* **250:** 365–375.

McCallum, M. L., K. R. Rao, J. P. Riehm, C. J. Mohrherr, and W. T. Morgan. 1988. Isolation of a β-PDH analog from the crayfish, *Procambarus clarkii*. *Am. Zool.* **28:** 117A.

Nusbaum, M. P., and E. Marder. 1988. A neural role for a crustacean red pigment concentrating hormone-like peptide: neuromodulation of the pyloric rhythm in the crab *Cancer borealis*. *J. Exp. Biol.* **135:** 165–181.

Phillips, J. M., C. A. Zahnow, and K. R. Rao. 1987. An immunocytochemical study of the eyestalk of *Penaeus aztecus* utilizing antisera for synthetic β-PDH and FMRFamide. *Am. Zool.* **27:** 69A.

Phillips, J. M., K. R. Rao, J. P. Riehm, and W. T. Morgan. 1988. Isolation and characterization of a pigment-dispersing hor-

mone from the shrimp *Penaeus aztecus. Soc. Neurosci. Abstr.* **14:** 534.

Rao, K. R. 1985. Pigmentary effectors. Pp. 395–462 in *The Biology of Crustacea, Vol. 9,* D. E. Bliss, and L. H. Mantel, eds. Academic Press, Orlando.

Rao, K. R., and J. P. Riehm. 1988a. Chemistry of crustacean chromatophorotropins. Pp. 407–422 in *Advances in Pigment Cell Research,* J. T. Bagnara, ed. Alan R. Liss, New York.

Rao, K. R., and J. P. Riehm. 1988b. Pigment-dispersing hormones: a novel family of neuropeptides from arthropods. *Peptides* **9, Suppl. 1:** 153–159.

Rao, K. R., J. P. Riehm, C. A. Zahnow, L. H. Kleinholz, G. E. Tarr, L. Johnson, S. Norton, M. Landau, O. J. Semmes, R. M. Sattelberg, W. H. Jorenby, and M. F. Hintz. 1985. Characterization of a pigment-dispersing hormone in eyestalks of the fiddler crab *Uca pugilator. Proc. Natl. Acad. Sci. USA* **82:** 5319–5322.

Rao, K. R., C. J. Mohrherr, J. P. Riehm, C. A. Zahnow, S. Norton, L. Johnson, and G. E. Tarr. 1987. Primary structure of an analog of crustacean pigment-dispersing hormone from the lubber grasshopper *Romalea microptera. J. Biol. Chem.* **262:** 2672–2675.

Schueler, P. A., A. J. Madsen, W. S. Herman, and R. Elde. 1986. Immunohistochemical mapping of distal retinal pigment hormone in the crayfish central nervous system. *Soc. Neurosci. Abstr* **12:** 242.

Zahnow, C. A. 1987. Synthesis and bioassay of N-terminal deletion peptides and certain "core" analogs of a crustacean pigment-dispersing hormone. Masters Thesis, The University of West Florida, Pensacola.

Zahnow, C. A., K. R. Rao, C. J. Mohrherr, and J. P. Riehm. 1987. Immunocytochemistry of neuropeptides in the cephalic neuroendocrine system of the lubber grasshopper, *Romalea microptera. Soc. Neurosci. Abstr.* **13:** 993.

Reference: *Biol. Bull.* **177**: 230–236. (October, 1989)

Modified Sperm Ultrastructure in Four Species of Soft-Bodied Echinoids (Echinodermata: Echinothuriidae) From the Bathyal Zone of the Deep Sea

KEVIN J. ECKELBARGER, CRAIG M. YOUNG, AND J. LANE CAMERON

Division of Marine Sciences, Harbor Branch Oceanographic Institution, 5600 Old Dixie Highway, Fort Pierce, Florida 34946

Abstract. Sperm of the bathyal echinothuriid echinoids *Phormosoma placenta, Sperosoma antillense, Araeosoma fenestratum,* and *A. belli* are similar to those of other echinoids, but have several unique morphological features involving the acrosomal vesicle, the nucleus, and the middlepiece. The acrosomal vesicle shows regional staining differences including a densely staining central region surrounded by an electron-opaque component. Sperm nuclei are highly elongated and abruptly taper posteriorly. With the exception of one species, the nuclei lack a distinct centriolar fossa. Intracellular droplets resembling lipid extend from the extreme posterior region of the middlepiece to form a collar around the proximal portion of the axoneme. The presence of lipid-like bodies in the middlepiece suggest that the sperm are long-lived and therefore require additional energy stores not found in most metazoan sperm. These findings are compared with a similar study of sperm ultrastructure in three shallow-water echinothuriid species, and their potential significance is discussed in relation to the present knowledge of echinothuriid reproductive biology.

Introduction

Echinothuriid echinoids have soft, flexible tests atypical of most sea urchins. The majority of species are confined to the deep sea but some littoral species are reported from the Indo-Pacific region (Amemiya *et al.*, 1980). Our knowledge of the reproductive biology of members of this family has been limited mostly to general observations of a few deep-sea species (Mortensen, 1927; Ahfeld, 1977). Tyler and Gage (1984) have examined gametogenesis in five echinothuriids from the Rockall Trough in the Northeast Atlantic Ocean using light microscopic histology. They suggest that the dominant reproductive strategy is the year-round production of large eggs undergoing benthic direct development. However, other authors have reported that echinothuriid eggs float (Amemiya and Tsuchiya, 1979; Young and Cameron, 1987; Cameron *et al.*, 1988) suggesting that the larvae are probably pelagic lecithotrophs.

Echinoderms are among the most abundant and diverse macrofaunal invertebrates in the deep sea (Pawson, 1982; Billet and Hansen, 1982), yet little is known about gamete and gonad ultrastructure in species from this habitat. The only published account deals with the ultrastructure of the highly aberrant sperm of the deep-sea concentricycloid *Xyloplax* (Healy *et al.*, 1988). General sperm morphology is known for nearly 70 shallow-water echinoids, although fewer than 10 species have been the subject of ultrastructural studies. These combined investigations show that echinoid sperm are consistently conservative in morphology and exhibit little interspecific structural variation (see Summers *et al.*, 1975; Chia and Bickell, 1983, for review).

The present paper describes ultrastructural features of the mature sperm of the bathyal echinothuriids *Phormosoma placenta, Sperosoma antillense, Araeosoma fenestratum,* and *A. belli* collected in the Bahama Islands by manned submersibles at depths ranging from 600 to 900 meters. Although their sperm are similar to those of other echinoids, significant ultrastructural differences are noted in the acrosome, nucleus, and middlepiece. Sperm morphology is influenced by the environment into which they are released prior to fertilization (Franzen, 1956, 1970; Afzelius, 1977), so structural alterations in these sperm suggest that unique selective pressures may be present in the deep sea which are absent from shallow water habitats.

Received 15 March 1989; accepted 27 June 1989.

These results are compared with an earlier ultrastructural study of sperm morphology in three species of shallow-water echinothuriids from Japanese waters (Amemiya *et al.*, 1980). The potential significance of these findings are discussed in relation to echinothuriid reproductive biology.

Materials and Methods

Live, sexually mature specimens of *Phormosoma placenta* (Fig. 1), *Sperosoma antillense*, *Araeosoma fenestratum* (Fig. 2) and *A. belli* were collected during April, May, and October, 1986, at depths ranging from 600 to 900 m in the Bahamas. The seawater temperature at the various collection sites ranged from 7 to 10°C. Collection sites included the west side of San Salvador Is. (24°02′N, 74°32.4′W), the north side of New Providence Is. (25°03.1′N, 77°31.4′W), Southwest Reef (24°53.41′N, 77°33.14′W), and the east side of Andros Is. (24°51.4′N, 77°50.62′W). Specimens were obtained using specialized collecting equipment on Johnson-Sea-Link submersibles.

In most instances, live animals were dissected on board ship shortly after collection, and testes were removed for immediate fixation. Occasionally, however, specimens were maintained on board in cooled aquaria where they remained active and healthy until later use. Whole testes were fixed for transmission electron microscopy (TEM); several methods, including those of Eckelbarger (1979) and Smiley (1988), were used, although none produced satisfactory results. Acceptable results were finally obtained with a modification of the method published by Bickell *et al.* (1980). Tissue was fixed by immersion for 1 h in a primary fixative consisting of 2.5% glutaraldehyde in filtered seawater at room temperature, followed by a 15-min wash in 2.5% $NaHCO_3$, and postfixation for 1 h in 2% OsO_4 in 1.25% $NaHCO_3$ at room temperature. Tissues were rapidly dehydrated in ascending concentrations of ethanol, transferred through two changes of propylene oxide, and embedded in Epon. Thin sections were cut with a diamond knife and stained with alcoholic uranyl acetate and aqueous lead citrate for 10 min each, then examined with a Zeiss EM9S-2 transmission electron microscope.

Live active sperm released from dissected testes were collected and fixed for scanning electron microscopy (SEM). Sperm were fixed using the same procedure as for TEM, followed by dehydration through an ascending ethanol series to 50%, air-dried on cover slips attached to aluminum stubs, and sputter-coated with gold-palladium. Sperm were then photographed using a Novascan 30 SEM with an accelerating voltage of 15 kV.

Results

The mature spermatozoa of all four species are similar in general morphology but differ in head length (acrosome, nucleus, and middlepiece) and relative dimensions. They are bullet-shaped with a small, terminal acrosome, a conical nucleus, and short middlepiece (Figs. 5–12). The sperm head length of the four species range from the longest, *Phormosoma placenta* (12 × 1.5 μm), to the shortest, *Araeosoma fenestratum* (8.5 × 1.0 μm). The sperm heads of *A. belli* and *Sperosoma antillense* each measure 9.0 × 1.25 μm. All four species have large, yolky eggs, ranging from the largest, *Araeosoma fenestratum* (1290 μm), to *Sperosoma antillense* (1060 μm), *Araeosoma belli* (965 μm), and the smallest, *Phormosoma placenta* (890 μm).

The acrosome is positioned just anterior to the nucleus and consists of a subspherical acrosomal vesicle with a flattened or slightly concave basal surface (Figs. 3, 4). The acrosomal membrane and the sperm plasmalemma are not well defined due to poor fixation. However, the posterior-lateral acrosomal membrane is thicker and more electron dense than the apical portion. The acrosomal vesicle contains two types of granular material of differing electron densities. The central portion contains a more densely staining vase-shaped region surrounded laterally by an electron-opaque component. A deep subacrosomal fossa is present just posterior to the acrosomal vesicle. Although the acrosomal region of all four species are similar, the subacrosomal fossa of *Sperosoma antillense* (Fig. 4) is narrower and deeper than that of the other species, typified by *A. belli* (Fig. 3). The subacrosomal fossa contains granular periacrosomal material extending around the basolateral sides of the acrosomal vesicles and running posteriorly between the anterolateral margin of the nucleus and sperm plasmalemma.

The nucleus contains highly condensed chromatin and gradually tapers anteriorly in all four species. Nuclear vacuoles are common in all sperm examined (Fig. 15). In the sperm of *Phormosoma placenta*, the extreme posterior region of the nucleus narrows abruptly to form a neck-like extension that extends into the middle piece (Figs. 9, 13). This posterior extension tapers more gradually in the sperm of *Sperosoma antillense* (Figs. 10, 14), *Araeosoma fenestratum* (Figs. 11, 15), and *A. belli* (Figs. 12, 16). The posterior surface of this extension is slightly concave and the axoneme-bearing distal centriole is closely associated with it (Figs. 13–16). A distinct centriolar fossa is absent except for a shallow one in *P. placenta* (Fig. 13). The proximal centriole is positioned laterally to the distal centriole and at a slight angle to the long axis of the sperm (Figs. 15, 16, 18). The distal centriole possesses a centriolar satellite consisting of nine radiating arms (Fig. 19). A single, circular mitochondrion surrounds the posterior nuclear extension (Fig. 17). In the sperm of all four species, intracellular droplets morphologically resembling lipid, extend from the extreme posterior region of the middlepiece (Figs. 13–16). They are consistently round in *P. placenta* (Fig. 13), but

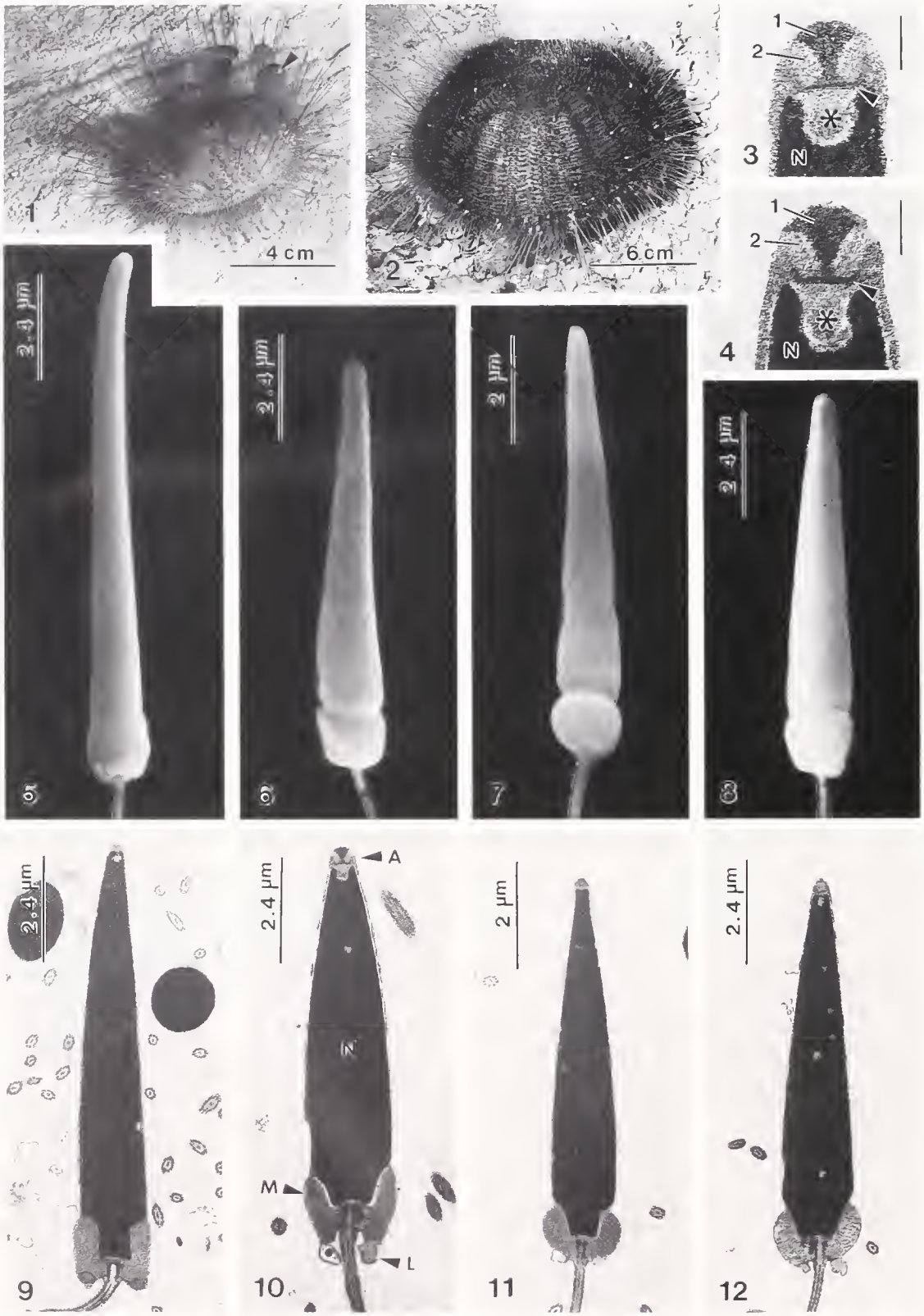

Figure 1. Adult *Phormosoma placenta* photographed *in situ* at a depth of 700 m in Bahamian waters. Arrow indicates one of several epidermal sacs of unknown function which project from the surface of the animal.

Figure 2. Adult *Araeosoma belli* photographed *in situ* at a depth of 750 m in Bahamian waters.

irregular in shape in the other species (Figs. 14–16). In cross section, a collar of lipid-like droplets surrounds the basal region of the axoneme (Fig. 20). The axoneme is of the 9 + 2 pattern.

Discussion

Recent investigations of sperm morphology from deep-sea echinoderms have revealed a variety of structural modifications that differ markedly from the sperm of shallow water species. These include a high incidence of elongated sperm heads in bathyal echinoids and holothuroids (Eckelbarger *et al.*, in press), the discovery of dimorphic sperm in the abyssal echinoid *Phrissocystis multispina* (Eckelbarger *et al.*, 1989), and the presence of highly aberrant sperm in the abyssal concentricycloid *Xyloplax turnerae* (Healy *et al.*, 1988). The present paper describes additional modifications of male gametes from four species of bathyal echinoids from Bahamian waters.

The sperm acrosomes of echinoids are morphologically conservative and have been described ultrastructurally for a number of species (see Chia and Bickell, 1983). The acrosomal vesicle typically contains a homogeneously distributed particulate material of medium electron density except for its basal region where denser material is deposited along the inner acrosomal membrane. The sperm acrosomes of all four echinothuriid species we examined resemble those of other echinoids with respect to position and superficial morphology, but show unique regional staining differences within the acrosomal vesicle. In other echinoderm classes, the contents of the acrosomal vesicle are often homogeneous, although densely staining, centrally positioned acrosomal granules have been reported in the holothuroids *Cucumaria lubrica, C. miniata,* and *Leptosynapta clarki* (Atwood and Chia, 1974), and the crinoid, *Antedon petasus* (Afzelius, 1977). Therefore, the echinothuriid acrosomal vesicle represents a morphological variant different from any observed in other echinoderm sperm. We do not believe this structural variation results from a fixation artifact because no differences were observed in sperm prepared for electron microscopy using several fixation methods. The functional significance of this novel acrosomal morphology is unknown, but it may reflect regional differences in enzyme distribution such as that observed in the cortical granules of sea urchin eggs (Alliegro and Schuel, 1988).

Echinothuriid sperm nuclei have a shape unique to echinoids. Echinoid sperm nuclei typically are wider posteriorly than anteriorly and have a relatively deep centriolar fossa into which the distal centriole and its associated axoneme are inserted (Chia and Bickell, 1983). Echinothuriid sperm nuclei abruptly taper posteriorly and a centriolar fossa is virtually absent in *Sperosoma, Araeosoma belli,* and *A. fenestratum,* and weakly developed in *Phoromosa placenta.* The presence of a deep centriolar fossa in echinoderm sperm has been suggested as a means of strengthening the connection between the tail and the elongated nucleus (Chia and Bickell, 1983). The position of the mitochondrion relative to the nucleus varies slightly in echinoderm sperm, but generally surrounds the extreme posterior end of the nucleus (Chia and Bickell, 1983). In some echinoids, such as *Paracentrotus lividus* (Anderson, 1968), *Strongylocentrotus purpuratus* (Longo and Anderson, 1969), and *Arbacia lixula* and *Echinometra lucunter* (Cruz-Landim and Beig, 1976), the mitochondrion is positioned posterior to the nucleus and forms a collar around the proximal portion of the axoneme. In the four echinothuriid species, the sperm mitochondrion wraps around the posterior portion of the nucleus, starting where the nucleus abruptly tapers. The modified sperm of the small brooding holothuroid *Cucumaria lubrica* is strikingly similar to the echinothuriid sperm with respect to nuclear shape and mitochondrial position (Atwood and Chia, 1974), although a well-developed centriolar fossa is present in *C. lubrica.*

The lipid-like droplets we observed in the middlepiece of the echinothuriid sperm closely resemble intracellular triglyceride deposits that are common in a variety of somatic cells (Bloom and Fawcett, 1968; Alberts *et al.*, 1983). To our knowledge, there are no other reports of lipid deposits in metazoan sperm aside from a few echinoderm species. Intracellular deposits that resemble lipid on morphological grounds, have been reported posterior to the middlepiece mitochondrion in the echinoids *Echinorachnius parma* (Summers and Hylander, 1974; Summers *et al.*, 1975), *Arbacia punctulata* (Bernstein, 1962; Longo and Anderson, 1969), *Echinocardium flavescens*

Figures 3, 4. Anterior region of mature sperm of *Araeosoma belli* (Fig. 3) and *Sperosoma antillense* (Fig. 4) showing acrosomal vesicle with two regions of differing electron densities. Arrow indicates dense staining posterior acrosomal membrane; *, subacrosomal fossa; N, nucleus.

Figures 5–8. Scanning electron micrographs of mature sperm of *Phormosoma placenta* (Fig. 5), *Sperosoma antillense* (Fig. 6), *Araeosoma fenestratum* (Fig. 7), and *A. belli* (Fig. 8).

Figures 9–12. Transmission electron micrographs of longitudinal sections through mature sperm of *Phormosoma placenta* (Fig. 9), *Sperosoma antillense* (Fig. 10), *Araeosoma fenestratum* (Fig. 11), and *A. belli* (Fig. 12). The sperm acrosomes in Figures 9, 11, and 12 are not clearly indicated due to the slightly oblique angle of the sections. A, acrosome; N, nucleus; M, mitochondrion; L, lipid-like deposit.

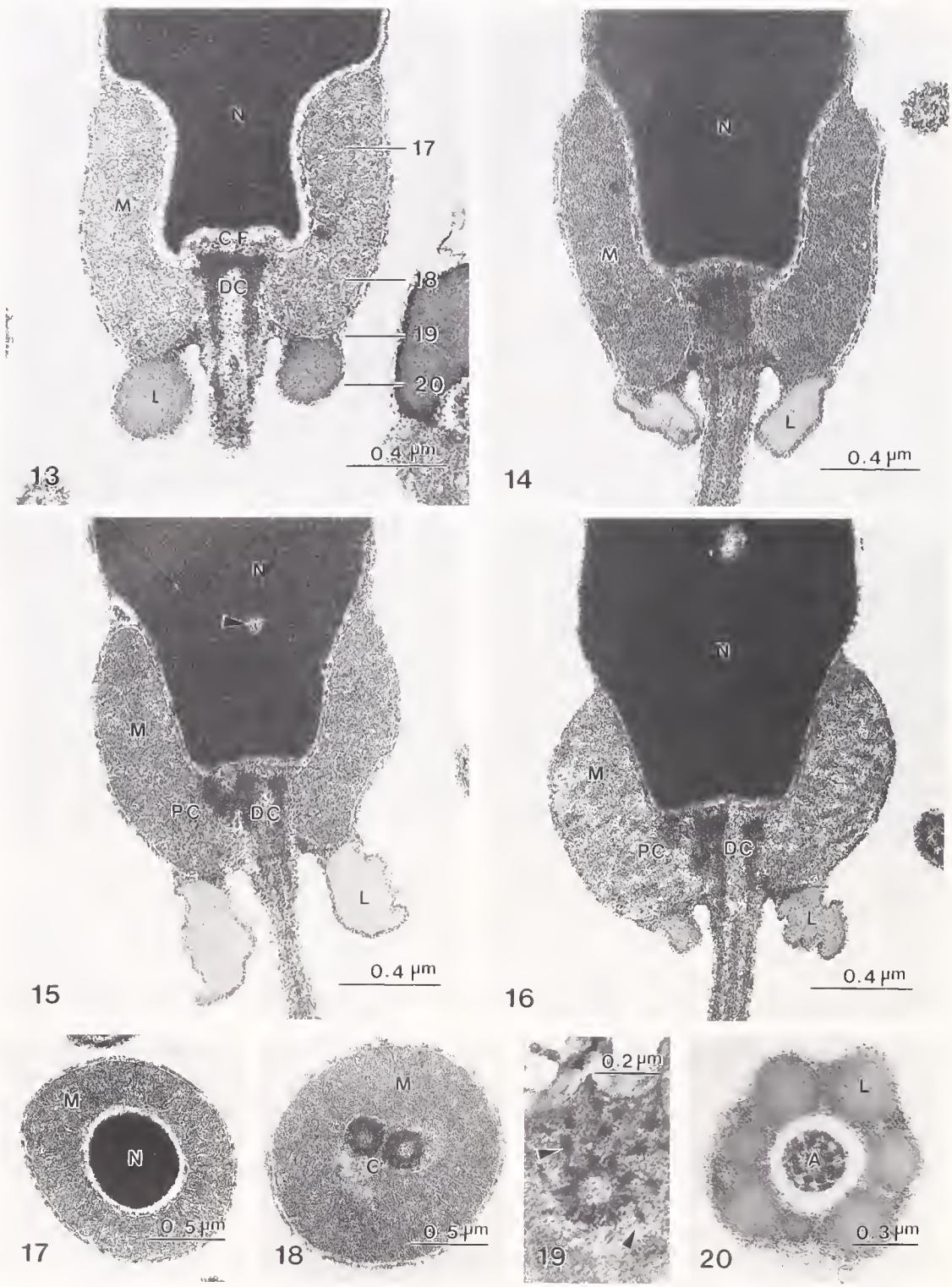

Figures 13–16. Longitudinal sections through the posterior region of the mature sperm of *Phormosoma placenta* (Fig. 13), *Sperosoma antillense* (Fig. 14), *Araeosoma fenestratum* (Fig. 15), and *A. belli* (Fig. 16). Horizontal lines in Fig. 13 indicate level of cross-sections through sperm of *Phormosoma placenta* shown in Figures 17–20. N, nucleus; M, mitochondrion; CF, centriolar fossa; DC, distal centriole; PC, proximal centriole; L, lipid-like deposit.

Figure 17. Cross section through posterior nucleus (N) and surrounding mitochondrion (M) of sperm of *P. placenta*.

and *Brissopsis lyrifera* (Afzelius and Mohri, 1966), *Hapalosoma gemmiferum* and *Araeosoma owstoni* (Amemiya *et al.*, 1980), and in the holothuroid *Cucumaria miniata* (Fontaine and Lambert, 1976). However, qualitative comparisons of micrographs from the above studies show that, with the exception of *E. parma* (Summers and Hylander, 1974) and *A. owstoni* (Amemiya *et al.*, 1980), these deposits are minor in comparison to those observed in the present study. The role of lipid deposits has not been determined in any of these echinoderm sperm.

Echinoderm spermatozoa are dependent on the metabolism of mitochondrial phospholipids during swimming (Rothschild and Cleland, 1952), or in some instances, glycogen stores (Anderson and Personne, 1975). In experiments with the sperm of the echinoid *Brissopsis lyrifera*, Afzelius and Mohri (1966) reported that prolonged swimming caused a gradual disappearance of mitochondrial cristae. They hypothesized that the sperm consume these structural phospholipids as an energy source. However, no change was observed in the lipid-like inclusions after 6 h of swimming. Triglycerides of fatty acids are used as an energy reserve, and they are commonly associated with mitochondria (Alberts *et al.*, 1983). The presence of lipid deposits in intimate association with mitochondria in some echinoderm sperm suggests that the cells are long-lived or must expend energy at a rate not commonly demanded of other metazoan sperm. We have not observed spawning in any of the echinothuriids we examined, and we know nothing of their fertilization biology or the potential life span of naturally released sperm. With the occasional exception of *Phormosoma placenta*, adult echinothuriids generally occur at very low densities in the Bahamas. The extensive lipid stores in these sperm could provide an extended window of opportunity for fertilization when males and females are widely separated. Some cidarid urchins improve fertilization success by aggregating during the breeding season (Young, unpub. data). However, echinothuriids appear not to breed seasonally (Tyler and Gage, 1984) nor to aggregate for spawning.

The present study of bathyal echinothuriid sperm morphology provides an interesting comparison to an earlier investigation of sperm ultrastructure in the three shallow-water echinothuriids *Asthenosoma ijimai*, *Araeosoma owstoni*, and *Hapalosoma gemmiferum* (Amemiya *et al.*, 1980). The latter authors described sperm morphologies very similar to those in the present study, including regional staining differences within the acrosomal vesicles, a long, tapering nucleus that abruptly narrows posteriorly, and "follicular bodies" in the middlepiece of *H. gemmiferum* and *A. owstoni* sperm, which they viewed as analagous to the lipid-like bodies reported from other echinoid sperm. However, they reported an "electron opaque rod" within the acrosomal vesicle. In addition, the lipid-like droplets appear to be smaller than those we described, and they do not extend from the posterior region of the middlepiece as they do in the deep-sea echinothuriid sperm. No information was presented regarding the process of natural spawning or sperm longevity. The most striking difference noted between our two studies is the shorter head lengths in the sperm of the shallow-water species. Sperm head length was estimated to be 7 μm for *A. ijimai*, 6 μm for *A. owstoni*, and 4 μm for *H. gemmiferum*. In contrast, we measured sperm head lengths of 12 μm for *Phormosoma placenta*, 8.5 μm for *A. fenestratum*, and 9 μm for *A. belli* and *Sperosoma antillense*. A high incidence of elongated sperm heads was noted recently in a survey of bathyal echinoids (Eckelbarger *et al.*, in press).

Ultrastructural studies of the gametes of deep-sea organisms have been rare, with only three studies of gamete morphology and sperm development in the vestimintiferan *Riftia pachyptila* (Gardiner and Jones, 1985; Cary *et al.*, 1989), and spermiogenesis in the abyssal echinoderm *Xyloplax turnerae* (Healy *et al.*, 1988) having been published recently. This is unfortunate because deep-sea habitats offer a unique laboratory for the study of gamete evolution in an environment substantially different from that of shelf waters (see Wilson and Hessler, 1987). Indeed, recent observations of unique gonadal, gamete, and larval developmental features in bathyal and abyssal echinoderms have demonstrated that deep-sea echinoderms have undergone evolutionary changes in their reproductive biology unlike that of their shallow water relatives (Eckelbarger *et al.*, in press, 1989; Young *et al.*, in press). This suggests that the deep sea is a region ripe for studies dealing with the reproductive evolution of marine invertebrates.

Acknowledgments

We thank Pamela Blades-Eckelbarger and Pat Linley for specimen preparation for scanning and transmission electron microscopy and John Miller for assistance with some specimen identification and systematics. The manuscript benefited from discussions with Dr. F. S.

Figure 18. Cross section through centrioles (C) and surrounding mitochondrion (M) in middlepiece of *P. placenta* sperm.

Figure 19. Cross section through centriolar satellite showing nine radiating arms (arrows) in middlepiece of sperm of *P. placenta*.

Figure 20. Cross section through middlepiece of sperm of *P. placenta* showing ring of lipid-like bodies (L) surrounding proximal portion of axoneme (A).

Chia. We thank the HBOI ship and submersible crews of the R/V Seward Johnson and R/V Edwin Link for their assistance. Brian Bingham, Dr. Paul Tyler, and several others assisted at sea. The research was supported in part by N.S.F. grant OCE-877922. This is contribution number 719 of Harbor Branch Oceanographic Institution.

Literature Cited

Afzelius, B. A. 1977. Spermatozoa and spermatids of the crinoid *Antedon petasus*, with a note on primitive spermatozoa from deuterostome animals. *J. Ultrastruct. Res.* **59:** 272–281.

Afzelius, B. A., and H. Mohri. 1966. Mitochondria respiring without exogenous substrate—a study of aged sea urchin spermatozoa. *Exp. Cell Res.* **42:** 10–17.

Ahfeld, T. E. 1977. A disparate seasonal study of reproduction of eight deep sea macroinvertebrate species from the Northwestern Atlantic Ocean. Ph.D. dissertation, Florida State Univ., 105 pp.

Alberts, B., D. Bray, J. Lewis, M. Raff, K. Roberts, and J. D. Watson. 1983. *Molecular Biology of the Cell.* Garland Publishing, Inc., New York. 1146 pp.

Alliegro, M. C., and H. Schuel. 1988. Immunocytochemical localization of the 35-kDa sea urchin egg trypsin-like protease and its effects upon the egg surface. *Dev. Biol.* **125:** 168–180.

Amemiya, S., and T. Tsuchiya. 1979. Development of the echinothurid sea urchin *Asthenosoma ijimai*. *Mar. Biol.* **52:** 93–96.

Amemiya, S., T. Suyemitsu, and I. Uemura. 1980. Morphological observations on the spermatozoa of echinothurid sea urchins. *Dev. Growth Diff.* **22:** 327–335.

Anderson, W. A. 1968. Cytochemistry of sea urchin gametes. I. Intramitochondrial localization of glycogen, glucose-6-phosphatase and adenosine triphosphate activity in spermatozoa of *Paracentrotus lividus*. *J. Ultrastruct. Res.* **24:** 398–441.

Anderson, W. A., and P. Personne. 1975. The form and function of spermatozoa: a comparative view. Pp. 3–14 in *The Functional Anatomy of the Spermatozoon*, B. A. Afzelius, ed. Pergamon Press, Oxford.

Atwood, D. G., and F.-S. Chia. 1974. Fine structure of an unusual spermatozoon of a brooding sea cucumber, *Cucumaria lubrica*. *Can. J. Zool.* **52:** 519–523.

Bernstein, M. H. 1962. Normal and reactive morphology of sea urchin spermatozoa. *Exp. Cell Res.* **27:** 197–209.

Bickell, L. R., F.-S. Chia, and B. J. Crawford. 1980. A fine structural study of the testicular wall and spermatogenesis in the crinoid, *Florometra serratissima* (Echinodermata). *J. Morphol.* **166:** 109–126.

Billet, D. S. M., and B. Hansen. 1982. Abyssal aggregations of *Kolga hyalina* Danielssen and Koran (Echinodermata: Holothuroidea) in the northeast Atlantic Ocean: a preliminary report. *Deep Sea Res.* **29:** 799–818.

Bloom, W., and D. W. Fawcett. 1968. *A Textbook of Histology.* W. B. Saunders Co., Philadelphia. 858 pp.

Cameron, J. L., F. S. McEuen, and C. M. Young. 1988. Floating lecithotrophic eggs from the bathyal echinothuriid sea urchin *Araeosoma fenestratum*. Pp. 177–180 in *Echinoderm Biology*, R. D. Burke, P. V. Mladenov, P. Lambert, and R. L. Parsley, eds. Balkema Press, Rotterdam.

Cary, A. C., H. Felbeck, and N. D. Holland. 1989. Observations on the reproductive biology of the hydrothermal vent tube worm *Riftia pachyptila*. *Mar. Ecol. Prog. Ser.* **52:** 89–94.

Chia, F.-S. and L. R. Bickell. 1983. Echinodermata. Pp. 545–620 in *Reproductive Biology of Invertebrates*, Vol. II: Spermatogenesis and Sperm Function, K. G., and R. G. Adiyodi, eds. John Wiley & Sons, New York.

Cruz-Landim, C. and D. Beig. 1976. Spermiogenesis in the sea urchins *Arbacia lixula* and *Echinometra lucunter* (Echinodermata). *Cytologia* **41:** 331–344.

Eckelbarger, K. J. 1979. Ultrastructural evidence for both autosynthetic and heterosynthetic yolk formation in the oocytes of an annelid (*Phragmatopoma lapidosa*: Polychaeta). *Tissue Cell* **11:** 425–443.

Eckelbarger, K. J., C. M. Young, and J. L. Cameron. In press. Modified sperm in echinoderms from the bathyal and abyssal zones of the deep sea. International Symposium Series: *23rd European Marine Biology Symposium*, P. A. Tyler and J. Ryland, eds. Olsen & Olsen, Denmark.

Eckelbarger, K. J., C. M. Young, and J. L. Cameron. 1989. Ultrastructure and development of dimorphic sperm in the abyssal echinoid *Phrissocystis multispina* (Echinodermata: Echinoidea): implications for deep sea reproductive biology. *Biol. Bull.* **176:** 257–271.

Fontaine, A. R. and P. Lambert. 1976. The fine structure of the sperm of a holothurian and an ophiuroid. *J. Morphol.* **148:** 209–226.

Franzen, A. 1956. On spermiogenesis, morphology of the spermatozoan, and biology of fertilization among invertebrates. *Zool. Bidr. Uppsala* **30:** 355–482.

Franzen, A. 1970. Phylogenetic aspects of the morphology of spermatozoa and spermiogenesis. Pp. 29–46 in *Comparative Spermatology*, B. Bacetti, ed. Academic Press, New York.

Gardiner, S. L., and M. L. Jones. 1985. Ultrastructure of spermiogenesis in the Vestimentiferan tube worm *Riftia pachyptila* (Pogonophora: Obturata). *Trans. Am. Microsc. Soc.* **104:** 19–44.

Healy, J. M., F. W. E. Rowe, and D. T. Anderson. 1988. Spermatozoa and spermiogenesis in *Xyloplax* (Class Concentricycloidea): a new type of spermatozoon in the Echinodermata. *Zool. Scripta* **17:** 297–310.

Longo, F. J., and E. Anderson. 1969. Sperm differentiation in the sea urchins *Arbacia punctulata* and *Strongylocentrotus purpuratus*. *J. Ultrastruct. Res.* **27:** 486–509.

Mortensen, T. 1927. *Handbook of the Echinoderms of the British Isles*, W. Backhuys, ed. Oxford Univ. Press. 471 pp.

Pawson, D. L. 1982. Deep-sea echinoderms in the Tongue of the Ocean, Bahama Islands: a survey using the Research Submersible ALVIN. *Aust. Mus. Mem.* **16:** 129–145.

Rothschild, L., and K. W. Cleland. 1952. The physiology of sea urchin spermatozoa. The nature and location of endogenous substrate. *J. Exp. Biol.* **29:** 66–71.

Smiley, S. 1988. The dynamics of oogenesis in *Stichopus californicus* (Echinodermata: Holothuroidea), and an explanation of its annual ovarian cycle. *Biol. Bull.* **175:** 79–93.

Summers, R. G. and B. L. Hylander. 1974. An ultrastructural analysis of early fertilization in the sand dollar, *Echinorachnius parma*. *Cell Tissue Res.* **150:** 343–368.

Summers, R. G., B. L. Hylander, L. H. Colwin, and A. L. Colwin. 1975. The functional anatomy of the echinoderm spermatozoon and its interaction with the egg at fertilization. *Am. Zool.* **15:** 523–551.

Tyler, P. A. and J. D. Gage. 1984. The reproductive biology of echinothuriid and cidarid sea urchins from the deep sea (Rockall Trough, Northeast Atlantic Ocean). *Mar. Biol.* **80:** 63–74.

Wilson, G. D. F. and R. R. Hessler. 1987. Speciation in the deep sea. *Ann. Rev. Ecol. Syst.* **18:** 185–207.

Young, C. M., and J. L. Cameron. 1987. Laboratory and *in situ* floatation rates of lecithotrophic eggs from the bathyal echinoid *Phormosoma placenta*. *Deep-Sea Res.* **34:** 1629–1639.

Young, C. M., J. L. Cameron and K. J. Eckelbarger. In press. Extended prefeeding period in planktotrophic larvae of the bathyal echinoid *Aspidodiadema jacobyi* Agassiz. *J. Mar. Biol. Assoc. U. K.*

Reference: *Biol. Bull.* 177: 237–246. (October, 1989)

Growth and Energy Imbalance During the Development of a Lecithotrophic Molluscan Larva (*Haliotis rufescens*)

WILLIAM B. JAECKLE[1] AND DONAL T. MANAHAN[2]

Department of Biological Sciences, University of Southern California, Los Angeles, California 90089-0371

Abstract. Larvae of the gastropod *Haliotis rufescens* are classified as "nonfeeding" because they cannot capture particulate foods. However, for only 1 out of 5 independent cultures was a net decrease observed in dry organic weight during the complete period of larval development (5 to 7 days). In fact, there were net increases in dry organic weight from the oocyte (day 0) to the newly formed veliger larva (2-day-old). These weight increases during early development could be explained by increases in the amounts of specific biochemical components of the larvae, relative to oocytes. The metabolic rates of larvae were measured (oxygen consumption) and used to compare (i) the required energy for development with (ii) the energy supplied from the catabolism of biochemical reserves. This analysis revealed that the cost of development for larvae could not be explained by the rates of use of the energy stores initially present in the oocyte. Larvae, from two independent cultures, could only supply 25% or 71% of their energy requirements by the use of internal reserves. Larvae of *H. rufescens* cannot use particulate foods and, thus, this energy resource cannot be invoked. Estimates of the contribution that dissolved organic material in seawater could provide to larvae, showed that this pool of exogenous material could supply the missing energy. It is suggested that "nonfeeding" larvae can feed, but that their only available nutrients are in a dissolved form.

Received 15 March 1989; accepted 31 July 1989.

[1] Present address: Harbor Branch Oceanographic Institution, 5600 Old Dixie Highway, Fort Pierce, Florida 34946.

[2] To whom reprint requests should be directed.

Introduction

The traditional separation of marine planktonic larvae into three trophic groupings (planktotrophy, facultative planktotrophy, and lecithotrophy) is based upon an ability, or lack of the ability, to concentrate and capture particulate foods from seawater (Thorson, 1946; Chia, 1974). However, this classification scheme does not consider an energy resource available to all soft-bodied invertebrate larvae, namely dissolved organic material (DOM) in seawater. By ignoring this resource, an implicit assumption has been made that planktotrophic (feeding) larvae are energetically dependent on the environment for nutrients, whereas lecithotrophic larvae are not. It follows then, that lecithotrophic (nonfeeding) larvae, using an energy source of fixed content (yolk), should continually decrease in organic weight during development. Growth, defined here as an increase in dry organic weight, can only occur in these nonfeeding forms following the development of distinct juvenile or adult feeding structures.

Changes in the biochemical composition have been well studied for embryos and larvae of marine invertebrates that produce planktotrophic larvae. There is general agreement in the literature that prefeeding embryos use internal energy stores (carbohydrate, lipid, and protein) to supply the energy requirements of early development (*e.g.*, Cognetti, 1982). Following the development of feeding structures, larvae deprived of particulate foods are also assumed to rely on an energy source of fixed content (yolk or accumulated reserves). This assumption is supported by the observed decreases in the biochemical components of starving larvae. For example, Millar and Scott (1967) reported that larvae of the bivalve *Ostrea*

edulis decreased both in dry organic weight and in all measured biochemical components during periods of starvation. Catabolism of the neutral lipid fraction provided the greatest proportion of liberated energy followed, in order, by protein and carbohydrate. Holland and Spencer (1973) also examined the changes in biochemical composition of starved *O. edulis* larvae. During starvation, the decrease in dry organic weight was explained by net decreases in lipid and protein, and again, the greatest amount of energy was made available through the catabolism of lipid. This pattern of energy use (lipid > protein > carbohydrate) was also seen during the cyprid stage of development (nonfeeding) in the barnacle *Balanus balanoides* (Lucas *et al.*, 1979). Mann and Gallager (1984, 1985) reported that the dry organic weight of larvae of the bivalves *Martesia cuneiformis, Teredo navalis,* and *Bankia gouldi* also decreased during starvation. For these larvae, the protein fraction, rather than the lipid fraction, served as the primary energy source during periods of nutrient deprivation. Studies have also been conducted examining net changes in organic weight and biochemical composition of echinoderms with nonfeeding development (Lawrence *et al.*, 1984; McClintock and Pearse, 1986). These authors have reported that, for a total of five species, there was little net change in the organic weight or energy content between eggs and juveniles. Lawrence *et al.* (1984) suggested that their results could be explained by the fact that either (i) the metabolic rates were too low to cause measurable depletion of energy reserves or (ii) the animals were gaining sufficient energy from dissolved organic material in seawater to offset the metabolic demands of development.

The only possible source of nutrients from the environment available to nonfeeding developmental stages of marine invertebrates would be in the form of DOM. Total carbon concentrations of DOM in coastal waters are at least ten times greater than those of organic carbon associated with particles (Parsons, 1975; Williams, 1975; MacKinnon, 1981; Sugimura and Suzuki, 1988). Despite the fact that only a small percentage (*ca.* 10%) of the total DOM has been chemically characterized (Williams, 1975), it is clear that biologically important compounds such as monosaccharides, amino acids, fatty acids, and nucleic acids are present in dissolved form in coastal marine environments (Testerman, 1972; Mopper *et al.*, 1980; Parkes and Taylor, 1983; Carlucci *et al.*, 1984; DeFlaun *et al.*, 1987).

There is evidence that planktotrophic larvae can take up specific compounds from the total pool of DOM (Reish and Stephens, 1969; Manahan, 1983; Manahan *et al.*, 1983; Davis and Stephens, 1984). However, the ability of nonfeeding larvae to transport specific fractions of DOM has been less extensively studied. Recently, it has been shown that nonfeeding trochophore and veliger larvae of the gastropod *Haliotis rufescens* are able to take up dissolved amino acids from seawater, and that transported alanine is rapidly used in specific anabolic and catabolic pathways in these veliger larvae (Jaeckle and Manahan, 1989).

In the present study, larvae of the gastropod *Haliotis rufescens* were cultured in natural seawater from the fertilized oocyte until they were competent to settle. The changes in dry organic weight, biochemical composition, and metabolism (oxygen consumption) were measured throughout the complete development of these larvae. An energy budget was constructed to assess the contribution of endogenous reserves to the energy demands of these larvae. This comparison revealed that larvae of *H. rufescens* are not in energy balance, suggesting that these "nonfeeding" larvae are obtaining energy from their environment, presumably in the form of dissolved organic material.

Materials and Methods

Culturing methods

Fertilized oocytes of *Haliotis rufescens* were obtained from the "Ab Lab" (Port Hueneme, California). The oocytes, embryos, and larvae were cultured in seawater at concentrations of approximately 5/ml at 16 to 17°C in 200-l culture vessels. It is known that the routine procedures (*e.g.*, sand filtering) used in marine laboratories to remove particles also affect the organic chemistry of seawater (Manahan and Stephens, 1983). To maintain the organic composition of seawater as close as possible to *in situ* conditions, all seawater used for larval culturing was passed only through a 0.2-μm (pore size, Nuclepore) polycarbonate filter. Assays for changes in the organic chemistry of seawater, caused by filtration procedures, were performed with high-performance liquid chromatography (procedures described elsewhere: Manahan, 1989). Filtered seawater samples were taken and analyzed for the concentrations of individual dissolved free amino acids. The total concentration of amino acids in the filtered seawater was always within the range reported for coastal marine environments (*i.e.*, 10 n*M* to 1 μM: Williams, 1975). Fresh seawater was collected daily, and used as soon as it had thermally equilibrated to the culture temperature. For each larval culture, following the formation of the definitive larval shell (day 2), the water was changed on a daily basis. At each sampling period, the larvae were gently sieved onto a 80-μm polyester mesh, and samples were retained for analysis of weight and biochemical composition. The culture vessel was then cleaned by a brief swabbing with a 5% sodium

hypochloride solution (bleach) followed by sequential washes of hot water, deionized water, and then filtered seawater.

Collection of oocytes and larvae

Samples of either oocytes, prior to fertilization, or larvae were placed in a graduated cylinder. The concentration of individuals was determined by counting several (usually 3 to 5) aliquots of the suspension until the coefficient of variation of the mean was less than 6%. Then, 9 samples of the suspension were removed and each sample placed in a separate 15-ml centrifuge tube. Following centrifugation, the pellet was washed with three times the sample volume using ammonium formate (3.4% w/v, isotonic with seawater). This washing procedure was then repeated twice. Replacement of seawater by ammonium formate is an important procedural step because ammonium formate is a volatile salt and there is no residual inorganic residue following drying. However, the ammonium formate solution must be passed through a 0.2-μm (pore size) filter immediately before use to avoid the carry-over of particulate material that will bias the measured weights. Six of the nine samples were placed in preashed (12 h at 500°C), preweighed aluminum boats, frozen, and retained for determinations of weights. The remaining samples were placed in 1.5-ml centrifuge tubes, frozen, and held at −20°C for biochemical analysis.

Weight determinations

Samples retained for determinations of organic weight were placed in an 80°C drying oven, and dried to constant weight (total dry weight). To determine the ash weight, organic material in each sample was combusted in a muffle furnace for 4 h at 450°C. Ashed samples were weighed, and 1-h reashing cycles repeated if the samples gained weight by hydration. Completely ashed materials do not adsorb water (Gnaiger and Bitterlich, 1984). This protocol avoids the inaccuracies associated with decomposition of $CaCO_3$ due to prolonged heating (Paine, 1971). All weight measurements were made with a Cahn Model 29 electrobalance (accurate to 0.1 μg). The amount of dry organic weight could then be calculated as the difference between the total dry weight and the ash weight. These values (dry organic and ash weight) were divided by the number of oocytes, or larvae, in each sample and the data expressed as μg material per individual.

Biochemical composition

To remove any residual fluid, samples used for determination of biochemical composition were lyophilized for at least 8 h at a pressure of 0.2 mm Hg. The lyophilized samples were then sonicated in 1 ml of glass distilled water by ultrasonic disruption (Sonics and Materials Brand, Model VC 40 fitted with a microprobe). The homogenates were centrifuged for 10 min at 12,200 × g and then sonicated a second time. Care was taken throughout the sonication procedure not to heat the samples. To determine whether the observed changes in the dry organic weight of the oocytes and larvae were accounted for by corresponding changes in biochemical composition, the amount of carbohydrate, lipid, and protein was measured. The biochemical composition of the oocytes and larvae was determined using the fractionation scheme devised by Holland and Gabbott (1971), as modified by Mann and Gallager (1985), with two additional alterations: (i) homogenates were extracted in trichloroacetic acid (TCA) for 20 min at −10°C and (ii) the total protein was assayed using Coomassie Brilliant Blue G-250 (BioRad Laboratories) as a colorimetric reagent. The TCA-insoluble pellet was dissolved in 500 μl of 1.0 M NaOH by heating at 60°C for 30 min. The alkaline protein solution was then acidified with 300 μl of 1.67 M HCl, and 200 μl of the concentrated Coomassie Blue dye solution was then added. The absorbance of the samples (at 595 nm) was determined after 10 min, and no later than 60 min, following addition of the dye solution.

Rates of larval respiration

The metabolic rates of larvae, of different ages, were measured as the rates of oxygen consumption. Larvae were placed in a conical analyzer cup (Curtin Matheson; 2 ml total volume, precalibrated to 345 μl) with filtered, then autoclaved, seawater. A Clark-type oxygen electrode (Model E5057, Radiometer Copenhagen) was placed into the cup, and excess air and seawater were discharged through a small purge hole melted into the cup. The purge hole was sealed by the membrane o-ring. The electrode was connected to a blood-gas analyzer (Model PHM 73; Radiometer Copenhagen) and, following a 5-min equilibration period, the change in the partial pressure of oxygen (mm Hg) was monitored for 20 to 30 min. During all experiments, the respiration chamber and the electrode were immersed in a 17°C water bath (Model RDL 20; Precision Instruments; ±0.02°C). Prior to the experiments with larvae, the oxygen consumption rate of the electrode itself was determined under the same conditions used for experiments with larvae. At the end of each experiment, the larvae were removed from the respiration chamber and counted (50 to 150 larvae). The rate of change in the partial pressure of oxygen was corrected for any self-consumption by the electrode, and

Table I

Changes in the amount of dry organic weight between oocytes (day 0) and veliger larvae (day 5, 6 or 7), sampled at the end of the larval life span (competent to settle), during the complete development of Haliotis rufescens

Culture 1		Culture 2		Culture 3		Culture 4		Culture 5	
Age (day)		Age (day)		Age (day)		Age (day)		Age (day)	
0	1.36 ± 0.02	0	1.41 ± 0.06	0	1.65 ± 0.03	0	1.19 ± 0.04	0	1.39 ± 0.05
7	1.17 ± 0.05	6	1.42 ± 0.08	6	1.67 ± 0.03	6	1.20 ± 0.02	5	1.59 ± 0.09
					Percent difference between beginning and end of each culture				
	(−14.0%)		(+0.7%)		(+1.2%)		(+0.8%)		(+14.4%)

Cultures 1–5 refer to batches of larvae reared from gametes obtained from five separate spawings. All data are presented as the mean dry organic weight per individual (μg ± 1 standard error of the mean). The percent difference, given at the bottom of the table, represents the net change in dry organic weight for each culture.

calculated as mm Hg larva^{-1}h^{-1}. This depletion rate was converted to moles of oxygen consumed by calibrating the electrode relative to the amount of oxygen in isothermal seawater, as determined by the Winkler titration method (Parsons *et al.*, 1984).

Results

Changes in weight during the larval life span

Figure 1 shows the changes in dry organic weight, and ash weight, from an unfertilized oocyte (day 0) to a larva competent to settle (day 7). In this culture (Culture 1), and all others studied (see Table I, Cultures 1 to 5), there was a continual linear increase in ash weight during larval development. There was a statistically significant net increase in dry organic weight from the oocyte (day 0) to the newly formed veliger larva (day 2), as can be seen in Figure 1 (Variance ratio, VR = 25.0, $F_{0.001[1,9]} = 22.9$). Similar increases during this period of development (day 0 to day 2) were seen in four other cultures. For Culture 1 (Fig. 1), there was a statistically significant net decrease from the oocyte, at 1.36 ± 0.02 μg, to the 7-day-old veliger at 1.17 ± 0.05 μg (VR = 18.3, $F_{0.01[1,8]} = 12.2$). Of the 5 cultures, reared in an identical manner (Table I), this culture (Culture 1) was the only one that showed a net decrease in dry organic weight during the larval life span. For Cultures 2, 3, and 4 there was no statistically significant change in organic weight between the oocyte and the last larval stage sampled. Larvae from Culture 5 had a net increase in organic weight, from 1.39 ± 0.05 μg (day 0) to 1.59 ± 0.09 μg (day 5).

Changes in biochemical composition and energy content

The changes in the biochemical composition of larvae, for the entire lifespan of two independent cultures (Cultures 1 and 5), are presented in Figure 2. The corresponding weight and energy values, for each total lipid and protein fraction, are given in Table II. The amount of total carbohydrate was always below the level of detection (0.1 μg per sample using a glucose standard) and, thus, a value for carbohydrate could not be included in calculations of energy budgets. The increase in dry organic weight during the first two days of development of larvae from Culture 1 (see Fig. 1) was explained by the combined increases of both the total lipid and protein fractions (Table II, Culture 1, Day 0 to 2). For Culture 5, there was also a significant increase in the dry organic weight from the oocyte (1.39 ± 0.05 μg) to the 2-day-old veliger larva (1.81 ± 0.09 μg). Again, this initial growth could be ac-

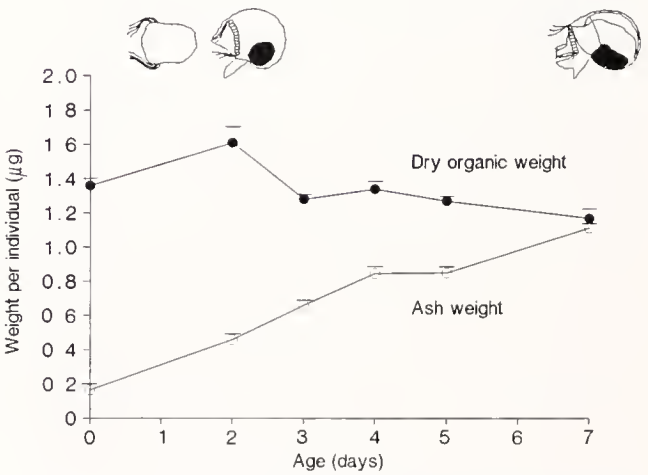

Figure 1. Change in the dry organic weight and ash weight (mean + 1 standard error of the mean) during the complete development of *Haliotis rufescens*, from the unfertilized oocyte (day 0) to a larva fully competent to settle (day 7). Diagrams of larval shape are redrawn from Leighton (1972).

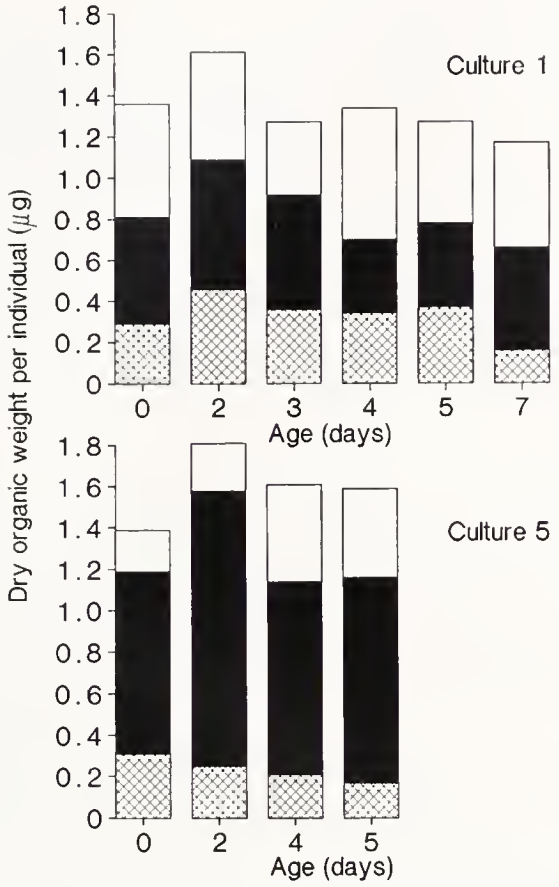

Figure 2. Changes in the biochemical composition during the complete development of *Haliotis rufescens*, from the unfertilized oocyte (day 0) to a larva fully competent to settle. Larvae in Culture 1 took 7 days to reach competence; those in Culture 5 took 5 days. For each sample the dry organic weight is represented by the sum of the weights of protein, total lipid, and the uncharacterized fraction (remainder). The cross-hatched portions of the bars represent protein; the solid portion represents total lipid; the open portions represent the remainder fraction.

counted for by the net changes in lipid and protein. There was a slight decrease in protein of −0.06 μg (day 0 to 2), and a large increase in total lipid of +0.45 μg during the same time period (Table II, Culture 5, Day 0 to 2). Following the formation of the veliger larva (day 2), the changes in protein for larvae from both Cultures 1 and 5 were qualitatively similar. There was a 65% decrease (0.30 μg) in protein content of larvae from Culture 1 (Day 2 to 7) and a 32% decrease in the amount of protein in larvae from Culture 5 (Day 2 to 5).

For lipid, the net changes were similar between Cultures 1 and 5 (day 2 to 5; day 2 to 7, respectively), following the net increases in total lipid observed during the period of day 0 to day 2 for both cultures (Table II). Larvae from Culture 1 had a decrease of 0.13 μg of lipid (21%) from day 2 to day 7. Those in Culture 5 also had a decrease in lipid content of 0.34 μg (26%) from day 2 to day 5.

The energy equivalents of the changes in weight for lipid and protein were calculated using the combustion enthalpy values for each fraction (lipid = 39.5 kJ/g, protein = 24.0 kJ/g; Gnaiger, 1983). As observed by other workers (*e.g.*, Holland and Gabbott, 1971), the sum of the weights of the measured biochemical components per individual (Fig. 2, filled bars), did not equal the dry organic weight. The "remainder" fraction (see Fig. 2, open bars), is defined as the difference between the dry organic weight and the sum of the measured biochemical components. To account for the energy represented by this material, a value of 27.0 kJ/g was given for the enthalpy of combustion of this uncharacterized fraction. This value is equal to the average of the combustion enthalpies of carbohydrate (17.5 kJ/g), lipid, and protein. In the absence of biochemical information on what comprises the remainder fraction, an average value for enthalpy of combustion was taken to be representative of the low molecular weight compounds that probably make up the majority of the remainder fraction. In Culture 1, the energy equivalent of the uncharacterized material (see "remainder," Table II) decreased from 14.85 mJ, at day 0, to 13.77 mJ by day 7. Larvae in Culture 5 had 5.40 mJ, at day 0, and increased to 11.61 mJ per larva by day 5.

The metabolic rates of larvae

The rates of oxygen consumption by veliger larvae of *Haliotis rufescens* are presented in Figure 3. The data presented in this figure are based upon the results of 47 independent determinations, obtained with larvae from 4 different cultures. The inset in Figure 3 shows the mean respiratory rate per larva, at each day of development examined. The average respiratory rate ranged from a low of 58 ± 7.2, for a 2-day-old larva, to a high of 93 ± 13 pmol O_2 $larva^{-1}$ h^{-1} for a 3-day-old larva.

Discussion

Larvae of *Haliotis rufescens* are presumed to be nonfeeding because they cannot capture particulate foods. Thus, a net loss of the organic weight contained in the oocyte would be expected during larval development. However, for four out of five cultures of larvae studied, there was a net increase in dry organic weight during early development from an oocyte (day 0) to a newly formed veliger larva at day 2 (*e.g.*, Fig. 1, day 0 to 2). These increases in dry organic weight were explained by changes in the amounts of protein and lipid during the same time period (Table II). Similarly, in only one out

Table II

Changes in dry organic weight and energy content during the complete larval development of Haliotis rufescens

Culture 1						
Weight of each biochemical fraction						
Age (day)	0	2	3	4	5	7
Dry organic weight						
Mean ± 1 SE	1.36 ± 0.02	1.61 ± 0.09	1.28 ± 0.01	1.34 ± 0.04	1.27 ± 0.03	1.17 ± 0.05
Protein						
Mean ± 1 SE	0.29 ± 0.00	0.46 ± 0.01	0.36 ± 0.01	0.34 ± 0.01	0.37 ± 0.03	0.16 ± 0.01
Total lipid						
Mean ± 1 SE	0.52 ± 0.02	0.63 ± 0.03	0.56 ± 0.07	0.36 ± 0.05	0.41 ± 0.02	0.50 ± 0.03
Energy content of each biochemical fraction						
Protein (mJ)	6.96	11.04	8.64	8.16	8.88	3.84
Total lipid (mJ)	20.54	24.89	22.12	14.22	16.20	19.75
Remainder (mJ)	14.85	14.04	9.72	17.29	13.23	13.77
Culture 5						
Weight of each biochemical fraction						
Age (day)	0	2	4	5		
Dry organic weight						
Mean ± 1 SE	1.39 ± 0.05	1.81 ± 0.09	1.61 ± 0.08	1.59 ± 0.09		
Protein						
Mean ± 1 SE	0.31 ± 0.00	0.25 ± 0.01	0.21 ± 0.01	0.17 ± 0.00		
Total lipid						
Mean ± 1 SE	0.88 ± 0.09	1.33 ± 0.05	0.93 ± 0.04	0.99 ± 0.05		
Energy content of each biochemical fraction						
Protein (mJ)	7.44	6.00	5.04	4.08		
Total lipid (mJ)	34.76	52.54	6.74	39.11		
Remainder (mJ)	5.40	6.21	12.69	11.61		

Larvae in Cultures 1 and 5 were reared from gametes obtained from separate spawnings. The weights of each protein and total lipid fractions were converted to an equivalent energy by multiplying each weight fraction by its value for enthalpy of combustion (total lipid = 39.5 kJ/g; protein = 24.0 kJ/g). The "remainder" fraction was calculated as the difference between the dry organic weight and the sum of the measured biochemical fractions. The energy value for this uncharacterized fraction was taken to be the average (27.0 kJ/g) of the combustion enthalpies for carbohydrate (17.5 kJ/g), lipid, and protein. All weight values are presented as the mean (μg) ± 1 standard error of the mean.

of five independent cultures of larvae was there a statistically significant decrease in dry organic weight from the oocyte to a competent larva (Culture 1, Fig. 1 and Table I). For the other four cultures (Table I), there was either no significant net change (Cultures 2, 3 and 4), or an increase in dry organic weight (Culture 5).

The net changes in dry organic weight, from the oocyte to a larva that is competent to settle, ranged from a decrease of 14% (Culture 1) to an increase of 14% (Culture 5) (Table I). An energy budget was constructed for each of these cultures because they represented the maximum range of weight changes observed. The amount of energy required by larvae in Cultures 1 and 5 was calculated from their respiratory rates (Fig. 3). The total rate of oxygen consumed by larvae was calculated for their entire life span. Where no measurements were made for a particular day, a value was estimated based on the rate measured for the nearest day. The energy equivalent to the rate of oxygen consumption was then compared to the available energy released by the catabolism of internal biochemical reserves (Table II). This comparison is given in Table III. For both cultures, the energy available from the net changes in lipid, protein, and the "remainder" fractions were always insufficient to account for the energy requirements of larval development. For Culture 1, there was a net decrease in all biochemical components

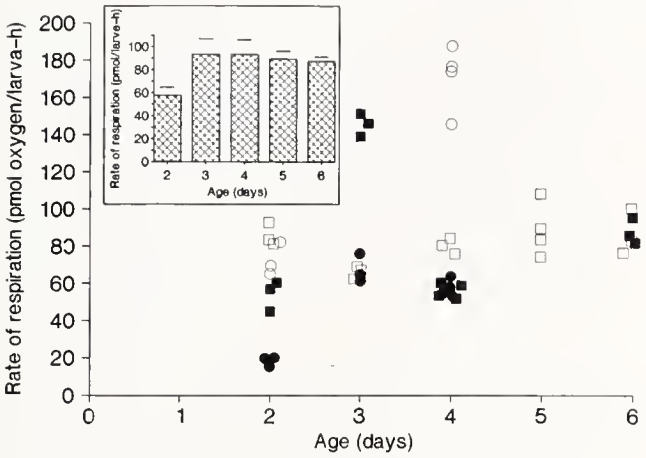

Figure 3. Metabolic rates of veliger larvae of *Haliotis rufescens*. Data are presented from four cultures, obtained from independent spawnings. The respiratory rates of larvae from Culture 1 are depicted as solid rectangles; larvae from Culture 5 are shown as solid circles. Other symbols represent larvae whose rates of respiration were not discussed in the text. The inset shows the mean respiratory rate (+1 standard error of the mean) averaged for all larvae for each day.

and the sum of the equivalent energies (−4.99 mJ) equals the amount of energy available to the larva from its reserves. In this case, 71% of the metabolic needs (+6.99 mJ) could be accounted for by the energy available from internal reserves (*i.e.*, 4.99/6.99 = 0.71, Table III). For Culture 5, there was a net increase in weight during development for both the lipid and remainder fractions (Table II). Thus, these increases represent an energy requirement for the larva. In these larvae, the amount of required energy was (i) the sum of the energy equivalent of the total amount of oxygen consumed over 5 days (+2.93 mJ) and (ii) the energy equivalent to the net increases in the biochemical components (+10.56 mJ). The amount of energy available from the net decrease in protein (−3.36 mJ) represented only 25% of the total energy required during the 5 days of development (*i.e.*, 3.36/13.49 = 0.25, Table III).

In general, larvae of *Haliotis rufescens* do not show a decrease in dry organic weight and energy content (Fig. 1, Tables I, II) during development. This finding is surprising in view of the fact that these larvae cannot use particulate foods and were cultured in natural seawater that had been passed only through a 0.2-μm (pore size) filter. Yet our results support previous findings on the net biochemical and energy changes that occurred in invertebrates unable to feed during development. When the energy content was compared between eggs, and later developmental stages, for six species of echinoderms collected from temperate and antarctic environments (Turner and Rutherford, 1976; Lawrence *et al.*, 1984; McClintock and Pearse, 1986), the results showed little net change in energy content between eggs and juveniles. Also, in a study of the energetics of embryonic development in the teleost *Sebastes schlegeli*, Boehlert *et al.* (1986) reported that the energy provided by the catabolism of endogenous reserves represented only 55% of the metabolic demand (oxygen consumption). In this latter case, the source of exogenous energy was presumed to be provided as dissolved organic compounds in ovarian fluid.

A possible alternative explanation for the observed imbalance between the rate of use of energy reserves and the measured metabolic rates of larvae, is that the latter were affected by some experimental artifact and were too high during our experiments. The average respiratory rate of all larvae of *Haliotis rufescens* measured (from Fig. 3) was 84 pmol O_2 $larva^{-1}$ h^{-1}. The dry organic weight, averaged for all veliger larvae (Cultures 1 and 5, Table II) was 1.5 μg. Thus, the average metabolic rate was 56 μmol O_2 g^{-1} h^{-1} at a temperature of 17°C. This value is at the lower end of the metabolic rates of marine invertebrate larvae (see Crisp, 1976) and is lower than that reported for a feeding larvae of the gastropod *Ilyanassa obselotus* (165 μmol O_2 g^{-1} h^{-1}, recalculated from Pechenik, 1980, assuming a Q_{10} of 2). Hence, the possibility that our reported values are artificially high is not viable. However, these analyses do suggest that within the Gastropoda, lecithotrophic larvae may have a lower metabolic rate than planktotrophic veligers. This difference may be due to the larger size of the velum of planktotrophic larvae when compared to lecithotrophic forms (Fretter and Graham, 1962). This suggestion is also supported by the work of Erickson (1984), who showed that differences in the respiratory rates of veliger larvae of the gastropod *Strombus gigas* corresponded with the extent of velar lobe expansion.

The calculated values given in Table III show that the energy reserves, initially present in the oocyte, are not being used by these larvae to supply their metabolic needs. However, this does not mean that there is insufficient energy in the oocyte to meet the metabolic demands of larval development. The energy content per oocyte (day 0) from Culture 1 was 42.35 mJ and 47.60 mJ for Culture 5. The amount of energy equivalent to the total number of moles of oxygen consumed (Fig. 3) during the complete development of larvae from these two cultures was 6.99 mJ and 2.93 mJ per larva for Cultures 1 and 5, respectively (Table III). Therefore, the amount of energy initially present in the oocyte exceeded the metabolic demand by 6-fold (*i.e.*, 42.35/6.99 = 6) for Culture 1 and 16-fold (*i.e.*, 47.60/2.93 = 16) for Culture 5. Even though there is more than enough energy contained in an oocyte to meet the metabolic demand, the

Table III

An energy budget for the complete larval development of Haliotis rufescens

Symbols used: "+" = required energy, and "−" = available energy.

Culture 1		Culture 5	
Available energy (decreases in biochemical content)		Available energy (decreases in biochemical content)	
Protein (mJ)	−3.12	Protein (mJ)	−3.36
Lipid (mJ)	−0.79	Lipid (mJ)	+4.35
Remainder (mJ)	−1.08	Remainder (mJ)	+6.21
Sum of available energy	−4.99	Sum of available energy	−3.36
Required energy (metabolic rate over 7 days)		Required energy (metabolic rate over 5 days)	
13.27 nmol O_2/larva =	+6.99 mJ	5.56 nmol O_2/larva =	+2.93 mJ
(increases in biochemical content)		(increases in biochemical content)	
None	0.00 mJ	Lipid and remainder	+10.56 mJ
Sum of required energy	+6.99	Sum of required energy	+13.49 mJ
Energy balance (available/required)		Energy balance (available/required)	
[(−4.99)/(+6.99)] = 71%*		[(−3.36)/(+13.49)] = 25%*	

*Contribution from energy stores to metabolic demand

Larvae in Cultures 1 and 5 were reared from gametes obtained from separate spawnings. The net change in total energy per individual, over the course of development, was taken from the data given in Table II (Culture 1, day 0–7; Culture 5, day 0–5). The metabolic rates of the larvae for each culture were calculated from the data provided in Figure 3. To relate the energy demand of development to the energy made available from the catabolism of internal stores, the total amount of oxygen consumed was converted to an energy equivalent. The energy reserve having the largest net decrease throughout development was protein and, therefore, the oxyenthalpic equivalent of this reserve was used (protein 527 kJ/mol O_2, from Gnaiger, 1983).

conclusions drawn from the energy budgets given in Table III are that larvae do not fully use this source of energy. Similar conclusions have been made by Lawrence *et al.* (1984) who reported that there was little change in energy content, between the egg and the juvenile, for the echinoid *Abatus cordatus* and the asteroid *Anasterias perreiri*. These authors suggested that the function of the large energy content of these eggs, 15.5 J/egg and 39.6 J/egg, respectively, was to produce a large juvenile rather than supply a large amount of energy for development. Also, Emlet *et al.* (1987) reported that, in general, juvenile asteroids that develop from nonfeeding larvae are larger than juveniles produced from feeding larvae. Thus, for development of *Haliotis rufescens*, the adaptive significance of the large amount of energy initially present in the oocyte may be related to juvenile survivorship, rather than energy metabolism during larval development.

If larvae of *Haliotis rufescens* are not using their internal reserves to fully meet the energy demands of development, there must be an input of material from the environment. Veliger larvae of *Haliotis* spp. cannot ingest particulate foods and, therefore, the most likely source of nutrients for these larvae would be in a dissolved form. Jaeckle and Manahan (1989) showed that veliger larvae can take up dissolved free amino acids from seawater, and that the rate of amino acid uptake, from a concentration of 1.6 μM, was sufficient to supply 55% of the metabolic demand of the larvae.

Larvae from Culture 5 had the higher energy imbalance, where only 25% of the metabolic cost of development could be accounted for by the use of energy stores. Could the rate of DOM uptake account for the missing energy observed for these larvae? The seawater used to culture the larvae was natural and, thus, approximated *in situ* concentrations of DOM. The calculations given below suggest that DOM could supply this missing energy. The average rate of amino acid uptake from a concentration of 1.6 μM (Jaeckle and Manahan, 1989) was 5.9 pmol amino acid larva^{-1} h^{-1}. Based on the average molecular weight of the amino acids used (140 g/mol), this equaled 826 pg larva^{-1} h^{-1}, or 99 ng larva^{-1} (5-days)$^{-1}$. Giving DOM a value for combustion enthalpy based on the average of carbohydrate, protein, and lipid (27.0 kJ/g, see Table II), 99 ng of DOM would equal 2.7 mJ/larva over a 5-day period. From Table III, it can be seen that an additional 10.13 mJ (13.49–3.36 = 10.13) was needed to balance the required energy. Thus, dis-

solved amino acids could contribute 27% of the missing energy (2.7/10.13 = 0.27). Dissolved amino acids represent less than 1% of the total pool of DOM in seawater (Williams, 1975). Thus, if only 4% of the total pool of DOM was used by larvae, at rates similar to those observed for the amino acid fraction, then 100% of the missing energy would be supplied from DOM. The requirement that 4% of the DOM has to be used is not an unreasonable estimate, given the wide variety of biologically available organic compounds that make up the pool of DOM in seawater.

The increase in both organic weight and specific biochemical components in these larvae suggests the question: are lecithotrophic invertebrate larvae really "nonfeeding"? Larvae of *Haliotis rufescens* can take up and metabolize dissolved free amino acids from seawater (Jaeckle and Manahan, 1989) and increase in organic weight (this study). This suggests that these "nonfeeding" larvae are feeding. However, the source of exogenous food exists in a dissolved form.

Acknowledgments

We would like to thank John McMullen (Ab Lab) for generously providing fertilized oocytes of *Haliotis rufescens*. This research was supported by a grant from NOAA, Office of Sea Grant (U.S.C. grant R/RD-27) and, in part, by a grant from the National Science Foundation (OCE-86-0889).

Literature Cited

Boehlert, G. W., M. Kusakari, M. Shimizu, and J. Yamada. 1986. Energetics during embryonic development of kurosoi, *Sebastes schlegeli* Hilgedorf. *J. Exp. Mar. Biol. Ecol.* **101:** 239–256.

Carlucci, A. F., D. B. Craven, and S. M. Henrichs. 1984. Diel production and microheterotrophic utilization of dissolved free amino acids in waters off southern California. *Appl. Environ. Microbiol.* **48:** 165–170.

Chia, F. S. 1974. Classification and adaptive significance of developmental patterns in marine invertebrates. *Thalass. Jugoslav.* **10:** 121–130.

Cognetti, G. 1982. Nutrition of embryos. Pp. 469–477 in *Echinoderm Nutrition,* M. Jangoux and J. M. Lawrence, eds. A. A. Balkema, Rotterdam.

Crisp, D. J. 1976. The role of the pelagic larva. Pp. 145–155 in *Perspectives in Experimental Biology,* Vol. 1, P. Spencer Davis, ed. Pergamon Press, Oxford and New York.

Davis, J. P., and G. C. Stephens. 1984. Uptake of free amino acids by bacteria-free larvae of the sand dollar *Dendraster excentricus. Am. J. Physiol.* **247:** R733–R739.

DeFlaun, M. F., J. H. Paul, and W. H. Jeffrey. 1987. Distribution and molecular weight of dissolved DNA in subtropical and estuarine and oceanic environments. *Mar. Ecol. Prog. Ser.* **36:** 65–75.

Emlet, R. E., L. R. McEdward, and R. R. Strathmann. 1987. Echinoderm larval ecology viewed from the egg. Pp. 55–136 in *Echinoderm Studies,* Vol. 2, M. Jangoux and J. M. Lawrence, eds. A. A. Balkema, Rotterdam.

Erickson, J. T. 1984. Gradient-diver respirometry applied to free-swimming larvae of the queen conch *Strombus gigas* Linne. *J. Shellfish Res.* **4:** 5–15.

Fretter, V., and A. Graham. 1962. *British Prosobranch Molluscs: The Functional Anatomy and Ecology.* The Ray Society, London. 755 pp.

Gnaiger, E. 1983. Calculation of energetic and biochemical equivalents of respiratory oxygen consumption. Pp. 337–345 in *Polarographic Oxygen Sensors* E. Gnaiger and H. Forstner, eds. Springer-Verlag, Berlin.

Gnaiger, E., and G. Bitterlich. 1984. Proximate biochemical composition and caloric concept calculated from elemental CHN analysis: a stoichiometric concept. *Oecologia* **62:** 289–298.

Holland, D. L., and P. A. Gabbott. 1971. A microanalytical scheme for the determination of protein, carbohydrate, lipid and RNA levels in marine invertebrate larvae. *J. Mar. Biol. Assoc. U.K.* **51:** 659–668.

Holland, D. L., and B. E. Spencer. 1973. Biochemical changes in fed and starved oysters, *Ostrea edulis* L. during larval development, metamorphosis and early spat growth. *J. Mar. Biol. Assoc. U.K.* **53:** 287–298.

Jaeckle, W. B., and D. T. Manahan. 1989. Feeding by a "nonfeeding" larva: uptake of dissolved amino acids from seawater by lecithotrophic larvae of the gastropod *Haliotis rufescens* Swainson. *Mar. Biol.* (in press).

Lawrence, J. M., J. B. McClintock, and A. Guille. 1984. Organic level and caloric content of eggs of brooding asteroids and an echinoid (Echinodermata) from Kerguelen (South Indian Ocean). *Int. J. Invert. Repro. Dev.* **7:** 249–257.

Leighton, D. L. 1972. Laboratory observations on the early growth of the abalone *Haliotis sorensoni,* and the effects of temperature on larval development and setting success. *Fish. Bull.* **70:** 373–381.

Lucas, M. I., G. Walker, D. L. Holland, and D. J. Crisp. 1979. An energy budget for the free-swimming and metamorphosing larvae of *Balanus balanoides* (Crustacea: Cirripedia). *Mar. Biol.* **55:** 221–229.

McClintock, J. B., and J. S. Pearse. 1986. Organic and energetic content of eggs and juveniles of antarctic echinoids and asteroids with lecithotrophic development. *Comp. Biochem. Physiol.* **85A:** 341–345.

MacKinnon, M. A. 1981. The measurement of organic carbon in seawater. Pp. 415–444 in *Marine Organic Chemistry: Evolution, Composition, Interactions and Chemistry of Organic Matter in Seawater,* E. K. Duurmsa and R. Dawson, eds. Elsevier Publ. Co., Amsterdam.

Manahan, D. T. 1983. The uptake and metabolism of dissolved amino acids by bivalve larvae. *Biol. Bull.* **164:** 236–250.

Manahan, D. T. 1989. Amino acid fluxes to and from seawater in axenic veliger larvae of a bivalve (*Crassostrea gigas*). *Mar. Ecol. Prog. Ser.* **53:** 247–255.

Manahan, D. T., J. P. Davis, and G. C. Stephens. 1983. Bacteria-free sea urchin larvae: selective uptake of neutral amino acids from seawater. *Science* **220:** 204–206.

Manahan, D. T., and G. C. Stephens. 1983. The use of high-performance liquid chromatography to measure dissolve organic compounds in bivalve aquaculture systems. *Aquaculture* **32:** 339–346.

Mann, R., and S. J. Gallager. 1984. Physiology of the wood boring bivalve mollusk, *Martesia cuneiformis* Say. *Biol. Bull.* **166:** 167–177.

Mann, R., and S. Gallager. 1985. Physiological and biochemical energetics of larvae of *Teredo navalis* L. and *Bankia gouldi* (Bartsch) (Bivalvia: Teredinidae). *J. Exp. Mar. Biol. Ecol.* **85:** 211–228.

Millar, R. H., and J. M. Scott. 1967. The larva of the oyster *Ostrea edulis* during starvation. *J. Mar. Biol. Assoc. U. K.* **47:** 475–484.

Mopper, K., R. Dawson, G. Liebezeit, and V. Ittekkot. 1980. The monosaccharide spectra of natural waters. *Mar. Chem.* **10:** 55–66.

Paine, R. T. 1971. The measurement and application of the calorie to ecological problems. *Ann. Rev. Syst. Ecol.* **2:** 145–164.

Parkes, R., and J. Taylor. 1983. Analysis of volatile acids by ion exclusion chromatography, with special reference to marine pore water. *Mar. Biol.* **77:** 113–118.

Parsons, T. 1975. Particulate organic carbon in the sea. Pp. 365–386 in *Chemical Oceanography*, Vol. 2, P. J. Riley and G. Skirrow, eds. Academic Press, London.

Parsons, T. R., Y. Maita, and C. A. Lalli. 1984. *A Manual of Chemical and Biological Methods for Seawater Analysis.* Pergamon Press, Oxford. 173 pp.

Pechenik, J. A. 1980. Growth and energy balance during the larval lives of three prosobranch gastropods. *J. Exp. Mar. Biol. Ecol.* **44:** 1–28.

Reish, D. J., and G. C. Stephens. 1969. Uptake of organic material by aquatic invertebrates. V. The influence of age on the uptake of glycine-^{14}C by the polychaete *Neanthes arenaceodentata*. *Mar. Biol.* **3:** 352–355.

Sugimura, Y., and Y. Suzuki. 1988. A high-temperature catalytic oxidation method for the determination of non-volatile dissolved organic carbon in seawater by direct injection of a liquid sample. *Mar. Chem.* **24:** 105–131.

Testerman, J. K. 1972. Accumulation of free fatty acids from sea water by marine invertebrates. *Biol. Bull.* **142:** 160–177.

Thorson, G. 1946. Reproduction and larval development of Danish marine bottom invertebrates with special reference to the planktonic larvae of the Sound (Oresund). *Medd. Komm. Danm. Fiskeriog. Havunders. Ser. Plankton* **4:** 1–523.

Turner, R. L., and J. C. Rutherford. 1976. Organic, inorganic and caloric composition of eggs, pentaculae, and adults of the brooding sea cucumber *Cucumaria curata* Cowles (Echinodermata: Holothuroidea). *J. Exp. Mar. Biol. Ecol.* **24:** 49–60.

Williams, P. J. LeB. 1975. Biological and chemical aspects of dissolved organic material in seawater. Pp. 307–364 in *Chemical Oceanography*, Vol. 2, P. J. Riley and G. Skirrow, eds. Academic Press, London.

Reference: *Biol. Bull.* 177: 247–253. (October, 1989)

Cryopreservation of Spermatophores and Seminal Plasma of the Edible Crab *Scylla serrata*

C. JEYALECTUMIE AND T. SUBRAMONIAM

Unit of Invertebrate Reproduction, Department of Zoology, University of Madras, Guindy Campus, Madras 600 025, India

Abstract. This paper describes the development of a suitable biotechnology to cryopreserve the spermatophores of the edible crab *Scylla serrata* in a viable condition. Three temperatures (−4°C, −79°C, and −196°C) were chosen to preserve the spermatophores and seminal plasma, collected from the middle region of vas deferens of mature male crabs, for 30 days. Sperm viability was determined by the eosin-nigrosin dye exclusion method, as applied to entire spermatophores. Of the three temperatures tested, the maximum percentage of sperm viability was obtained at −196°C, whereas it significantly decreased at −4°C. Biochemical alterations of the major substrates such as proteins, carbohydrates, and lipids, as well as the enzyme Lactate Dehydrogenase (LDH) occurred only at −4°C, reflecting their use in the metabolic activities of the spermatozoa contained within the spermatophores. At −4°C, the TCA-soluble total free sugars increased in correspondence with a decline in the bound sugars, suggesting that the latter may be used rapidly during sperm storage. Our data also suggest that, at −79°C and −196°C, the frozen spermatozoa retain viability but do not exhibit metabolic activity.

To investigate the role of cryoprotectants in preventing damage to the sperm cells/spermatophores during cryopreservation, four cryoprotectants, glycerol, dimethyl sulfoxide (DMSO), trehalose, and DMSO + trehalose combination, were tested. Using the phosphate buffer as the standard diluent, glycerol gave the best result. When used alone, trehalose gave only a low sperm survival, but in combination with DMSO, it gave an increased viability that equalled the result with glycerol. We recommend that glycerol is the best cryoprotectant inasmuch as the biochemical alterations in the glycerol medium is less, compared to that of DMSO + trehalose. When used alone, DMSO may be more toxic to the sperm cells as it gave a low viability value even at −196°C and −79°C.

Received 8 December 1988; accepted 31 July 1989.
DMSO—Dimethyl sulfoxide.

Introduction

Cryopreservation of gametes is a common method practiced in conjunction with artificial insemination in mammals (Leverage *et al.*, 1972). Many attempts have also been made in this respect to cryopreserve spermatozoa of the teleost fishes (Horton and Ott, 1976). Although decapod crustaceans have become important in aquaculture in recent years, cryopreservation techniques have not been employed for *in vitro* fertilization in prawns, lobsters, or crabs. However, using electroejaculation techniques, extraction of intact spermatophores and their attachment onto females have been accomplished in several decapods like shrimps and lobsters (Chow *et al.*, 1985; Ishida *et al.*, 1986). On the other hand, no work has been done on the artificial insemination or *in vitro* fertilization of crabs. Brachyuran crabs produce simple spermatophores that are carried in the fluid medium of seminal plasma. Therefore, any attempt to cryopreserve male gametes will include both the spermatophores and the seminal plasma. Previous studies on the seminal plasma of crustaceans such as crabs (Jeyalectumie and Subramoniam, 1987) and cirripede (Barnes, 1962) indicated a similarity, in terms of providing energy-yielding substrates, with the semen of mammals. The objective of the present study was to determine a suitable temperature and an extender to cryopreserve the spermatophores as well as seminal plasma of the crab, *Scylla serrata*. Fluctuations in the biochemical composition of the spermatophores and seminal plasma during cryopreservation at selected subzero temperature conditions

were also followed. LDH enzyme showed significant fluctuation during spermatophore storage in the crab, *Paratelphusa hydrodromous* (Jeyalectumie and Subramoniam, 1987) and hence, in the present study, fluctuations in the LDH activity of seminal plasma of *Scylla serrata* during cryopreservation were also determined.

Materials and Methods

Collection of sample

Seminal plasma containing vesiculate spermatophores was collected in a petri dish after puncturing the thin wall of the mid vas deferens. The samples collected were used for the cryopreservation studies.

Initial cooling, dilution, and freezing

The diluent for spermatophore preservation was prepared, according to Behlmer and Brown (1984), immediately before use by mixing 25 ml of 0.4 *M* NaCl/0.1 *M* glycine, 4 ml of 0.028 M NaH_2PO_4/0.072 *M* Na_2HPO_4, and 5 ml of glycerol. Apart from this, three other diluents were prepared by substituting glycerol with trehalose (0.25 *M*), DMSO (5%), and a combination of DMSO (5%) and trehalose (0.25 *M*). These are the cryoprotectants commonly used for various biological systems (Lovelock and Polge, 1954; Hughes, 1973; Asahina and Takahashi, 1978; Zell *et al.*, 1979; Behlmer and Brown, 1984; Chow *et al.*, 1985; Stephens, 1986; Anchordogy *et al.*, 1988). Analytical grade glycerol, trehalose, and DMSO were purchased from Sarabai Chemicals (India), BDH (England), and SD's (India), respectively.

The freshly collected sample was diluted to 20% spermatophore suspension by mixing four volumes of diluent to one volume of seminal plasma. Similarly, the spermatophoric suspensions in four different diluents were prepared separately. After dilution, the seminal plasma was aspirated into 0.5-ml semen storage straws having one end sealed. After filling, the open side of the straw was sealed with polyvinyl alcohol. Immediately after this process, all the straws containing the sample were kept for equilibration at 4°C for 16 h. Prior to freezing at −196°C in liquid nitrogen, the straws were kept exposed to the liquid nitrogen vapor for an hour and then immersed completely in the liquid nitrogen. Similarly, for −79°C, the straws were exposed to gaseous Co_2 for an hour, and then placed directly onto the dry ice. For −4°C, the straws were kept inside the freezer. All the above samples were stored for 30 days. Fresh, unfrozen semen, with appropriate diluents, were used as a control.

Our attempts to freeze the seminal plasma without adding the diluent in the three temperature conditions did not yield fruitful results. The 'dry' seminal plasma becomes coagulated after its transfer to the subzero condition. A similar problem was also mentioned by Asahina and Takahashi (1978) and Yoo *et al.* (1987), who found that removal of cryoprotectant led to agglutination of the spermatozoa of both sea urchins and salmon. Storing semen in diluent without adding any cryoprotectant resulted in the clumping of the spermatophores after thawing, thus precluding the preparation of good smear for the viability study. Moreover, in the previous studies on cryopreservation of male gametes in fishes and invertebrates such as horseshoe crabs, molluscs, and sea urchins, only the pre-frozen semen has been used as the control (Asahina and Takahashi, 1978; Zell *et al.*, 1979; Withler, 1982; Behlmer and Brown, 1984; Kurokura *et al.*, 1986).

Thawing

Thawing was accomplished by immersing the straws containing frozen seminal plasma in tap water (room temperature). The thawed seminal plasma was collected from the straws into clean test tubes by cutting open both the sealed ends.

Evaluation of viability of cryopreserved spermatophores

To evaluate sperm viability inside the spermatophore, the eosin-nigrosin staining method of Zaneveld and Polakoski (1977) was used. A smear was prepared by mixing one drop of thawed seminal plasma with one drop of 0.5% eosin and two drops of 10% nigrosin. These slides, after being air-dried, were examined using a brightfield microscope. Care was taken to complete the observation within 2 min of smear preparation. Dead sperm cells inside the spermatophores appeared pink, whereas live cells were unstained against a red background of nigrosin. For each observation, about 300–400 spermatophores were counted in a given square area. The validity of eosin-nigrosin staining method was tested using the sperm cells, intentionally killed by exposing them to room temperature for 30 min.

Biochemical analysis

Protein was estimated by the method of Lowry *et al.* (1951). The protein in 0.2 ml of diluted seminal plasma was precipitated using 10% TCA. Using bovine serum albumin as a standard, the absorbancy was recorded at 500 nm. Total free sugars (TFS) were estimated by the method of Roe (1955). Protein-bound sugars (PBS) and glycogen were estimated following the method of Caroll *et al.* (1956). After hydrolyzing the sample to release the bound sugars in 1N H_2SO_4 at 95°C, the same was treated with anthrone reagent. Glycogen was precipitated by ethanol from the supernatant obtained during protein precipitation and was dissolved in 0.5 ml distilled water and

Table I

Cryopreservation experiment on seminal plasma of Scylla serrata *with different cryoprotectants: evaluation of spermatophore viability (percentage) (mean ± S.E.)*

		Glycerol			DMSO			Trehalose			DMSO-trehalose		
Temperature		P.F	5th day	30th day	P.F	5th day	30th day	P.F	5th day	30th day	P.F	5th day	30th day
−196°C	$\bar{X}$	98.27	97.46	95.29[n]	96.96	94.80	88.99[a]	98.23	95.69	88.67[a]	98.39	97.08	94.25[n]
	S.E.	±1.217	±1.377	±1.366	±0.494	±0.425	±0.852	±0.503	±0.563	±0.676	±0.892	±0.881	±0.012
−79°C	$\bar{X}$	96.38	95.57	93.18[n]	96.98	93.40	88.76[a]	97.75	94.98	87.16[a]	97.56	96.14	92.98[n]
	S.E.	±0.858	±0.646	±1.005	±0.645	±1.022	±0.942	±0.694	±0.592	±0.489	±1.155	±1.200	±1.146
−4°C	$\bar{X}$	98.27	93.27	80.37[a]	96.96	88.19	66.75[a]	98.23	86.17	66.44[a]	98.39	92.00	78.62[a]
	S.E.	±1.217	±0.636	±1.081	±0.494	±0.965	±1.176	±0.503	±1.301	±1.602	±0.892	±0.811	±0.905

P.F. = Prefreeze. No. of observation (n) = 6. a: $P < 0.001$. n: not significant.

then treated with anthrone reagent. The color developed for PBS and glycogen was recorded as for TFS.

Total lipids were estimated using sulphophospho-vanillin method (Barnes and Blackstock, 1973), after extracting the lipid in chloroform:methanol mixture by the method of Folch *et al.* (1957). The above results were expressed in mg/ml seminal plasma.

LDH enzyme activity was measured according to Yoshida and Freese (1975), which is based on the lactate formed from pyruvate, by the oxidation of NADH. The units of enzyme per ml reaction mixture contained in a silica cell with 1 cm light path were calculated from the rate of absorbancy change at 340 nm, by using the millimolar extinction coefficient of 6.22, and expressed in units/mg protein. One unit of enzymatic activity represents the conversion of 1 μmole of NADH per minute. The enzyme protein was also assayed following Lowry *et al.* (1951).

All results were tested for significance using analysis of variance (ANOVA) and least significant difference (LSD) (Snedecor and Cochran, 1967; Winer, 1971; Zar, 1974). Arcsin transformation for proportions were used.

Results

Viability of cryopreserved spermatophores

Results of sperm (spermatophore) viability at −196°C, −79°C, and −4°C are presented in Table I. The viability test was made with every 5-day interval, but the results are given only for the 5th and 30th days for brevity. The change in sperm viability was also not markedly different between the 10th and 30th day. The viability of sperm in 30 days of storage was fairly high, but it showed a range from 95% (at −196°C) to 80% (at −4°C). This high percentage of viability was obtained in samples containing glycerol as the cryoprotectant. However, in DMSO, the viability was reduced to 89–67%. A similar trend was observed when trehalose was used as the cryoprotectant. Conversely, when DMSO + trehalose combination was used, a higher percentage of viability (between 94% and 79%) was obtained. Of the three temperatures tested, sperm viability was poor at −4°C, whereas at −196°C, sperm viability was maximum.

Biochemical analysis

The results are shown in Table II. Statistically, there was a significant difference between the three temperatures ($P < 0.001$); the LSD revealed that at −196°C, the decrease of the biochemical components was less than at −79°C and −4°C. For protein, total free sugars, glycogen, and LDH, there was no significant difference between −196°C and −79°C, whereas lipid and protein-bound sugars showed a significant difference between these two temperatures. However, at −4°C, the decrease of PBS is highly significant ($P < 0.001$); whereas glycogen and lipid do not show any significant decrease except in DMSO for glycogen ($P < 0.005$) and in trehalose for lipid ($P < 0.001$) at this temperature.

Protein, glycogen, lipid, and LDH did not show any significant difference between glycerol and DMSO + trehalose media; whereas PBS significantly decreased in DMSO + trehalose medium when compared to glycerol. Interestingly, the TFS showed a significant increase in glycerol and DMSO media at −4°C. At this temperature, TFS increased from a control (pre-freeze) value of 6.563 mg to 8.346 mg/ml in glycerol, and from 4.268 mg to 5.563 mg/ml in DMSO on the 30th day. That this increase may be due to a release of free sugars from the bound sugars was shown from a corresponding decrease of their value from 10.257 mg of the control to 6.707 mg/ml in glycerol and 7.646 mg to 3.215 mg/ml in DMSO on the 30th day (Table II). However, in media containing trehalose, there was very little difference in value of TFS between the control and the preserved seminal plasma.

Table II

Fluctuation in biochemical components of cryopreserved seminal plasma of Scylla serrata *at three different temperatures and with different cryoprotectants (mean ± S.E.)*

		Glycerol			DMSO			Trehalose			DMSO-trehalose		
Components		P.F	5th day	30th day	P.F	5th day	30th day	P.F	5th day	30th day	P.F	5th day	30th day
Protein (mg/ml)													
−196°C	$\bar{X}$	312.348	306.375	300.913^{n}	214.863	204.152	180.390^{n}	292.985	276.670	248.985^{n}	298.713	292.437	281.920^{n}
	S.E.	±12.877	±11.761	±13.934	±11.754	±11.745	±13.383	±11.496	±17.370	±8.982	±14.137	±13.318	±12.468
−79°C	$\bar{X}$	227.928	221.695	218.715^{n}	294.230	265.078	244.890^{n}	372.875	343.360	315.848^{n}	395.783	386.075	379.650^{n}
	S.E.	±12.295	±12.649	±12.771	±11.167	±12.647	±11.694	±10.033	±12.696	±10.396	±10.534	±11.209	±9.185
−4°C	$\bar{X}$	312.348	277.997	224.350^{d}	214.863	191.912	115.188^{a}	292.985	261.523	160.512^{a}	298.713	274.333	194.753^{a}
	S.E.	±12.877	±20.041	±10.961	±11.754	±7.162	±5.919	±11.496	±14.748	±8.243	±14.137	±11.046	±8.346
LDH (Units/mg protein)													
−196°C	$\bar{X}$	91.118	86.047	85.990^{n}	68.372	64.095	60.215^{n}	95.193	90.752	80.705^{n}	99.552	96.568	93.228^{n}
	S.E.	±2.176	±2.517	±3.068	±2.339	±2.853	±3.611	±3.989	±4.202	±3.638	±4.731	±4.231	±4.543
−79°C	$\bar{X}$	89.547	86.715	84.687^{n}	78.670	73.755	67.662^{n}	94.992	89.483	78.870^{n}	91.553	88.512	85.957^{n}
	S.E.	±1.789	±1.802	±1.915	±3.788	±3.753	±3.302	±3.549	±3.290	±3.597	±2.000	±2.163	±1.697
−4°C	$\bar{X}$	91.118	79.555	57.227^{a}	68.372	52.543	32.980^{a}	95.193	76.357	41.267^{a}	99.552	84.340	60.583^{a}
	S.E.	±2.176	±4.507	±5.677	±2.339	±3.789	±3.677	±3.989	±2.689	±1.674	±4.731	±2.967	±5.056
Total free sugars (mg/ml)													
−196°C	$\bar{X}$	6.563	6.337	5.966^{n}	4.268	4.069	3.588^{n}	446.672	439.036	423.371^{n}	409.324	404.885	397.177^{n}
	S.E.	±0.284	0.276	±0.289	±0.238	±0.241	±0.243	±14.069	±14.284	±12.259	±6.869	±7.899	±6.954
−79°C	$\bar{X}$	5.110	4.919	4.628^{n}	3.801	3.633	3.229^{n}	442.540	430.845	411.262^{n}	403.074	387.748	385.254^{n}
	S.E.	±0.226	±0.211	±0.222	±0.156	±0.181	±0.169	±13.451	±15.676	±13.393	±11.485	±12.478	±12.769
−4°C	$\bar{X}$	6.563	7.096	8.346^{a}	4.268	4.542	5.563^{a}	446.672	448.649	450.935^{n}	409.324	410.327	412.085^{n}
	S.E.	±0.284	±0.224	±0.115	±0.238	±0.189	±0.154	±14.069	±16.434	±20.782	±6.869	±6.410	±7.397
Protein bound sugars (mg/ml)													
−196°C	$\bar{X}$	10.257	9.992	9.569^{n}	7.646	7.350	6.726^{n}	15.294	14.688	13.828^{n}	15.012	14.433	13.953^{n}
	S.E.	±0.328	±0.323	±0.331	±0.434	±0.382	±0.443	±0.507	±0.440	±0.425	±0.609	±0.583	±0.587
−79°C	$\bar{X}$	10.193	9.868	9.434^{n}	6.913	6.666	6.043^{n}	14.669	13.801	12.896^{n}	12.075	11.606	10.654^{n}
	S.E.	±0.424	±0.421	±0.394	±0.301	±0.312	±0.338	±0.366	±0.492	±0.429	±0.316	±0.307	±0.454
−4°C	$\bar{X}$	10.257	9.062	6.707^{a}	7.646	6.303	3.215^{a}	15.294	12.141	7.440^{a}	15.012	12.588	8.013^{a}
	S.E.	±0.328	±0.304	±0.223	±0.434	±0.414	±0.423	±0.507	±0.485	±0.474	±0.609	±0.562	±0.490
Glycogen (mg/ml)													
−196°C	$\bar{X}$	0.478	0.465	0.436^{n}	0.579	0.533	0.496^{n}	1.310	1.248	1.135^{n}	2.177	2.120	1.933^{n}
	S.E.	±0.021	±0.024	±0.020	±0.019	±0.018	±0.020	±0.222	±0.233	±0.238	±0.219	±0.223	±0.235
−79°C	$\bar{X}$	0.458	0.435	0.411^{n}	0.649	0.612	0.548^{n}	2.265	2.148	1.894^{n}	2.175	2.048	1.853^{n}
	S.E.	±0.021	±0.017	±0.012	±0.029	±0.032	±0.028	±0.200	±0.225	±0.232	±0.164	±0.162	±0.160
−4°C	$\bar{X}$	0.478	0.452	0.381^{n}	0.579	0.515	0.415^{b}	1.310	1.205	0.945^{n}	2.177	1.945	1.611^{n}
	S.E.	±0.021	±0.027	±0.021	±0.019	±0.023	±0.022	±0.222	±0.232	±0.189	±0.219	±0.220	±0.242
Lipid (mg/ml)													
−196°C	$\bar{X}$	11.270	11.062	10.642^{n}	8.161	7.859	7.082^{n}	9.811	9.425	8.570^{n}	10.070	9.883	9.303^{n}
	S.E.	±0.472	±0.477	±0.461	±0.514	±0.468	±0.459	±0.407	±0.362	±0.344	±0.509	±0.478	±0.524
−79°C	$\bar{X}$	11.152	10.836	10.248^{n}	8.494	7.849	6.985^{n}	8.388	7.801	6.886^{n}	11.925	11.614	10.833^{n}
	S.E.	±0.538	±0.529	±0.513	±0.484	±0.558	±0.517	±0.590	±0.568	±0.613	±0.458	±0.434	±0.414
−4°C	$\bar{X}$	11.270	10.676	9.502^{n}	8.161	7.385	5.946^{n}	9.811	9.046	6.742^{a}	10.070	9.419	8.040^{n}
	S.E.	±0.472	±0.453	±0.467	±0.514	±0.611	±0.526	±0.407	±0.407	±0.481	±0.509	±0.532	±0.513

P.F. = Prefreeze; No. of observation (n) = 6; a: $P < 0.001$; b: $P < 0.005$; d: $P < 0.05$; n: not significant.

Table III

Conditions of cryopreservation of male gametes of Arthropoda

Sl. no.	Species	Cryoprotectant	Temperature	Preservation period	Percentage of survival	Method of testing viability	References
	Decapod Crustacea						
1.	*Sicyonia ingentis*	DMSO + Trehalose	−196°C	2 months	60–70%	Acrosome reaction	Anchordogy *et al.*, 1987
2.	*S. ingentis*	Trehalose, Sucrose, Proline, Glycerol, DMSO	−196°C	1 month	56%	Acrosome reaction	Anchordogy *et al.*, 1988
3.	*Macrobrachium rosenbergii*	Glycerol	−196°C	31 days	53%	Fertility	Chow *et al.*, 1985
4.	*Scylla serrata*	Glycerol, DMSO, Trehalose, DMSO + Trehalose	−196°C −79°C −4°C	30 days	95% (Glycerol, DMSO + Trehalose) 89% (DMSO, Trehalose)	Eosin dye exclusion	Present study
	Insecta						
5.	*Apis mellifera*	Glycerol, Seminal vesicle fluid, Spermathecal fluid	−79°C	16 days	50%	Motility	Sawada and Chang, 1964
	Arachnida						
6.	*Limulus polyphemus*	Glycerol	−74°C	50 days	64%	Eosin dye exclusion	Behlmer and Brown, 1984

There was also no interaction between temperature and media for components other than the TFS and PBS.

Discussion

The present results indicate that there is a definite influence of freezing at different subzero temperatures on sperm viability and metabolism. In *Scylla serrata,* the viability of sperm varies between 95%–67% from −196°C to −4°C. This is in accordance with Clegg and Pickett (1966), who suggested that there is no significant decrease in fertility of bull semen stored in liquid nitrogen, in contrast to the deterioration that occurs in semen stored in dry ice. Cryopreservation of sperm or spermatophore has also been carried out in selected arthropod groups (Table III). According to Behlmer and Brown (1984), 64% of the post-thawed spermatozoa of *Limulus* at −74°C showed dye exclusion against 88% of control spermatozoa. Hughes (1973) also reported a notable decrease in viability during cryopreservation of oyster sperm.

Our experiments with freshly collected spermatophores as well as spermatophores killed intentionally, further support the utility of the dye exclusion method in determining sperm viability. Intentionally killed sperm gave a 100% dye accumulation. It is of interest to note in this context that Bishop and Walton (1968) showed an increased permeability of cell membranes at the time of cell death.

Damage caused by physical change in the membrane may be responsible for the reduced sperm viability as indicated by the work on RBC (Lovelock, 1954). During freezing and thawing, cell damage is due to the destructive action of the concentrated salt solution to which the cells are exposed when water is removed as ice. Several cryoprotectants prevent the damage to cell membrane caused during cryopreservation. Polge *et al.* (1949) first showed that the spermatozoa could be frozen and thawed without losing motility if glycerol was included in their suspending medium. In glycerol, the electrolyte concentration at temperatures below the freezing point is sufficiently reduced (Lovelock and Polge, 1954).

In this study, glycerol and DMSO + trehalose gave high sperm survival. At −4°C, DMSO and trehalose are not efficient cryoprotectants, whereas, when DMSO is combined with trehalose, sperm viability increased significantly. Successful preservation of spermatophores of shrimp in glycerol at −196°C has also been reported (Chow *et al.*, 1985). Similar results were obtained by Stephens (1986) in chicken spermatozoa where the percentage of cryoinjuries to the spermatozoa was less in glycerol and DMSO + glycerol media; when DMSO was used in the place of glycerol, for *Limulus* spermatozoa, post-thawing survival of spermatozoa was nil (Behlmer and Brown, 1984).

Cryopreserved spermatozoa of *Crassostrea virginica* in DMSO fertilized 11% of eggs exposed to them

(Hughes, 1973), whereas combining DMSO with glycine and NaHCO increased the fertility to 96% (Zell *et al.*, 1979). Asahina and Takahashi (1978) showed that DMSO exhibited protection similar to that of ethylene glycol against freezing injury, whereas at room temperature DMSO was toxic. In *S. serrata,* trehalose, when used alone, is not a good cryoprotectant; however, when combined with DMSO, the viability of sperm is significantly increased. In the ridge back shrimp *Sicyonia ingentis,* Anchordogy *et al.* (1987, 1988) also found a low sperm viability when trehalose was used as the cryoprotectant. However, when the DMSO was combined with trehalose, these authors found increased viability. Interestingly, in this shrimp, the free spermatozoa stored very well with DMSO either alone or in combination with other cryoprotectants such as trehalose, sucrose, proline, and glycerol (Anchordogy *et al.*, 1988).

Obviously, the chief concern regarding spermatozoa that have undergone cryopreservation is whether they are of a quality, in terms of viability and vitality, comparable to that of fresh spermatozoa. Although fertilization is the ultimate criterion by which the quality of post-preserved spermatozoa can be assessed, it is also presently an impractical one. It is difficult to obtain ova, as the exact period of oviposition of these crabs is unknown, which, therefore, precludes routine fertility tests. Thus the quality of cryopreserved spermatozoa was assessed in lieu of fertilization, as has been determined for *Salmo salar* spermatozoa by Yoo *et al.* (1987), by estimating the biochemical fluctuations in the preserved spermatozoa.

Biochemical alterations, if any, in the spermatophores of crustaceans that have been cryopreserved have not been previously reported. However, the protein component in the ovine seminal plasma undergoes qualitative changes during cold storage (Garner and Ehlers, 1971). Yoo *et al.* (1987) reported the loss of protein from the cryopreserved spermatozoa into the outer seminal plasma in salmon, due to leakage through the cell membrane into the outer medium. In bovine semen, Pickett and Komarek (1964) also showed leakage of lipids into the seminal plasma from the cryopreserved spermatozoa. It is not known whether any such change occurs in the protein or lipid contents relative to the sperm cells and seminal plasma of *S. serrata* during cryopreservation. In the present study, there were practical difficulties in completely isolating the spermatophores from the seminal plasma after cryopreservation; even after repeated centrifugation of seminal plasma diluted with the diluents, the granular substances of the seminal plasma adhered to the spermatophores, thus making it difficult to isolate the spermatophores. It should also be noted that arthropod spermatozoa are sensitive to centrifugation (Behlmer and Brown, 1984) and hence repeated centrifugation may cause increased leakage of organic substrates and enzymes from the sperm cells to the medium, as has also been reported by Barnes and Blackstock (1974) for cirripede semen.

Biochemical results of the present study reveal an interesting pattern of substrate use during cryopreservation. At −4°C, the total carbohydrates showed a significant decline, although protein also showed a decline. In *S. serrata,* carbohydrates formed the main substrate used during sperm maintenance within the spermatheca of the mated female (Jeyalectumie, 1989). The reduction in the carbohydrate level, when preserved at −4°C, further indicates that the metabolic activity of sperm may continue using carbohydrate substrates. The activity of the LDH also declined at −4°C. This may be due to the death of sperm cells, which accounts for 18%. According to Jacobs *et al.* (1986), the dissociation and loss of LDH activity occur at low temperatures; by 45 days of storage, human serum retained 74%, 53%, and 87% of initial activity when stored at 25°C, 4°C, and −20°C, respectively. Our preliminary observations on glycosidases activity in the seminal plasma and spermatophores of this crab using different substrates such as β-D-glucopyranoside, β-D-galactopyranoside, β-D-mannopyranoside, and α-N-Acetyl galactosaminide indicate high enzyme activity (Yu-Teh Li, T. Subramoniam, and C. Jeyalectumie, unpub. obs.). All these may indicate that sperm storage in a metabolically active condition require active substrate use by spermatozoa contained in the spermatophores.

In conclusion, our results suggest that glycerol provided the best protection for the seminal plasma and maintained a high percentage of sperm viability. DMSO is toxic at room temperature; the decreased value of spermatophore viability at −4°C when DMSO was used as the cryoprotectant, may also support this view.

Acknowledgments

This work was supported by the Department of Science and Technology, Government of India, New Delhi (Grant No. 22(8p-8)/STP-II).

Literature Cited

Anchordogy, T., J. H. Crowe, W. H. Clark Jr., and F. J. Griffin. 1987. Cryopreservation of sperm from the penaeid shrimp *Sicyonia ingentis.* Abstract from 18th Annual meeting of the World Aquaculture Society, Guayaquil, Ecuador, Jan. 1987.

Anchordogy, T., J. H. Crowe, F. J. Griffin, and W. H. Clark Jr. 1988. Cryopreservation of sperm from the marine shrimp *Sicyonia ingentis. Cryobiology* **25:** 238–243.

Asahina, E., and T. Takahashi. 1978. Freezing tolerance in embryos and spermatozoa of the sea urchin. *Cryobiology* **15:** 122–127.

Barnes, H. 1962. The composition of the seminal plasma of *Balanus balanus. J. Exp. Biol.* **39:** 345–351.

Barnes, H., and J. Blackstock. 1973. Estimation of lipids in marine animals and tissue: detailed investigation of the sulphophospho-

vanillin method for 'total' lipids. *J. Exp. Mar. Biol. Ecol.* **12:** 103–118.

Barnes, H., and J. Blackstock. 1974. Biochemical composition of the seminal plasma of the cirripede *Balanus balanus* (L) with particular respect to free amino acids and proteins. *J. Exp. Mar. Biol. Ecol.* **16:** 47–85.

Behlmer, S. D., and G. Brown. 1984. Viability of cryopreserved spermatozoa of the horseshoe crab *Limulus polyphemus*. *Int. J. Invert. Reprod. Dev.* **7:** 193–199.

Bishop, M. W. H., and A. Walton. 1968. Spermatogenesis and the structure of mammalian spermatozoa. Pp. 1–101 in *Marshall's Physiology of Reproduction,* Vol. 1, Part II, A. S. Parkes, ed. Longmans, London.

Caroll, W. V., R. W. Longley, and J. H. Roe. 1956. The determination of glycogen in the liver and muscle by the use of anthrone reagent. *J. Biol. Chem.* **220:** 583–593.

Chow, S., Y. Taki, and Y. Ogasawara. 1985. Cryopreservation of spermatophore of the fresh water shrimp, *Macrobrachium rosenbergii*. *Biol. Bull.* **168:** 471–475.

Clegg, E. D., and B. W. Pickett. 1966. Effect of storage at −196°C on fertility. *A. I. Digest* Vol. XIV, No. 3.

Folch, J., M. Lees, and G. H. Bloane-Stanley. 1957. A simple method for the isolation and purification of total lipids from animal tissues. *J. Biol. Chem.* **266:** 497–509.

Garner, D. L., and M. H. Ehlers. 1971. Effect of storage at 5°C on the Disc electrophoretic patterns of ovine and bovine seminal proteins. *J. Reprod. Fert.* **27:** 43–52.

Horton, H. F., and A. G. Ott. 1976. Cryopreservation of fish spermatozoa and ova. *J. Fish. Res. Board Can.* **33:** 995–1000.

Hughes, J. B. 1973. An examination of eggs challenged with cryopreserved spermatozoa of the American oyster, *Crassostrea virginica*. *Cryobiology* **10:** 342–344.

Ishida, T., P. Talbot, and M. Kooda-Cisco. 1986. Technique for the long term storage of lobster (*Homarus*) spermatophores. *Gamete Res.* **14:** 183–195.

Jacobs, E., P. J. Hissin, W. Propper, L. Mayer, and L. Sarkozi. 1986. Stability of lactate dehydrogenase at different storage temperatures. *Clin. Biochem.* **19:** 183–188.

Jeyalectumie, C., and T. Subramoniam. 1987. Biochemical composition of seminal secretions with special reference to LDH activity in the reproductive tissues of the field crab, *Paratelphusa hydrodromous* (Herbst). *Exp. Biol.* **46:** 231–236.

Jeyalectumie, C. 1989. Biochemical investigations on the reproductive tissues and cryopreservation of seminal secretions of a brachyuran crab *Scylla serrata* (Forskal) (Decapoda: Portunidae). PhD Thesis, University of Madras, India.

Kurokura, H., H. Kumai, and M. Nakamura. 1986. Hybridization between female red sea bream (*Pagrus major*) and male crimson sea bream (*Evynnis japonica*) by means of sperm cryopreservation. Pp. 113–116 in *The First Asian Fisheries Forum,* J. L. Macleon, L. B. Dizon, and L. V. Hosillos, eds. Asian Fisheries Society, Manila, Philippines.

Leverage, W. E., D. A. Valerio, A. P. Schultz, E. Kingsbury, and C. Dorey. 1972. Comparative study on the freeze preservation of spermatozoa of primate, bovine and human. *Lab. Anim. Sci.* **22:** 882–889.

Lovelock, J. E. 1954. Physical instability and thermal shock in red cells. *Nature* **173:** 659–661.

Lovelock, J. E., and C. Polge. 1954. The immobilization of spermatozoa by freezing and thawing and the protective action of glycerol. *Biochem. J.* **58:** 618–622.

Lowry, D. H., N. J. Rosebrough, A. L. Fair, and R. J. Randall. 1951. Protein measurement with Folin phenol reagent. *J. Biol. Chem.* **193:** 265–275.

Pickett, B. W., and R. J. Komarek. 1964. Evidence for loss of lipid from bovine spermatozoa due to freezing. *J. Dairy Sci.* **47(8):** 905–908.

Polge, C., A. U. Smith, and A. S. Parkes. 1949. Revival of spermatozoa after vitrification and dehydration at low temperatures. *Nature* **164(4172):** 666.

Roe, J. H. 1955. The determination of sugar in blood and spinal fluid with anthrone reagent. *J. Biol. Chem.* **212:** 335–343.

Sawada, Y., and M. C. Chang. 1964. Tolerance of honey bee sperm to deep freezing. *J. Econ. Entomol.* **57(6):** 891–892.

Snedecor, G. W., and W. G. Cochran. 1967. *Statistical Methods.* Oxford and IBH Publishing Co. 593 pp.

Stephens, A. J. A. 1986. A comparison of diluents for cryopreservation of rooster semen. PhD Thesis, Tamil Nadu Agricultural University, Coimbatore, India.

Winer. 1971. *Statistical Principles in Experimental Design.* McGraw Hill, Inc.

Withler, F. C. 1982. Cryopreservation of spermatozoa of some freshwater fishes cultured in South and Southeast Asia. *Aquaculture* **26:** 395–398.

Yoo, B. Y., M. A. Ryan, and A. J. Wiggs. 1987. Loss of protein from spermatozoa of Atlantic salmon (*Salmo salar L.*) because of cryopreservation. *Can. J. Zool.* **65:** 9–13.

Yoshida, A., and E. Freese. 1975. Lactate dehydrogenase from *Bacillus subtilis*. Pp. 304 in *Methods in Enzymology,* Vol. XLI, W. A. Wood, ed. Academic Press, New York.

Zaneveld, L. J. D., and K. L. Polakoski. 1977. Collection and physical examination of the ejaculate. Pp. 147–172 in *Techniques of Human Andrology,* E. S. E. Hafez, ed. Elsevier/North-Holland Biomedical Press.

Zar, J. H. 1974. *Biostatistical Analysis.* Prentice-Hall, Inc. Englewood Cliffs, N.J. 620 pp.

Zell, S. R., M. H. Bamford, and H. Hidu. 1979. Cryopreservation of spermatozoa of the American oyster, *Crassostrea virginica* Gmelin. *Cryobiology* **16:** 448–460.

Reference: *Biol. Bull.* **177**: 254–276. (October, 1989)

On the Early Development of the Vestimentiferan Tube Worm *Ridgeia* sp. and Observations on the Nervous System and Trophosome of *Ridgeia* sp. and *Riftia pachyptila*

MEREDITH L. JONES[1] AND STEPHEN L. GARDINER[2]

[1]*Department of Invertebrate Zoology, National Museum of Natural History, Smithsonian Institution, Washington, D.C. 20560 and* [2]*Department of Biology, Bryn Mawr College, Bryn Mawr, Pennsylvania 19010*

Abstract. Stages in the development of the vestimentiferan *Ridgeia* sp., based on lengths of preserved specimens processed for scanning electron microscopy, were examined. Features of the nervous system and trophosome of *Riftia pachyptila* were studied by light, scanning-, and transmission-electron microscopy. Development proceeds from a trochophore-type larva with an anterior prototrochal ciliary ring and a posterior assemblage of transient larval setae, through intermediate stages, some of which lack endosymbiotic bacteria but all of which display additional transient features such as larval branchial filaments, a ventral medial process, and digestive tract, to a young juvenile stage that possesses endosymbiotic bacteria and exhibits the morphology characteristic of adult vestimentiferans. Larval branchial filaments are resorbed in later developmental stages and replaced by paired rows of ciliated branchial filaments with pinnules. The larval gut is divisible into foregut, midgut, and hindgut regions based on cytological features of the epithelium. The establishment of the symbiotic association in the midgut region is confirmed. The development of the gut and the establishment of the endosymbiotic association appear to be correlated with the timing of settlement by the young juveniles. Aspects of the development of the nervous system include the appearance of the brain near the base of the ventral medial process followed by the development of a nerve cord in the epithelium of the body wall throughout the length of the juvenile. The nerve cord includes one or two giant axons, except in its most posterior region. The trochophore larva likely serves as a dispersal stage in the life history of vestimentiferans. The trochophore larva in the early development of vestimentiferans strengthens the assertion that Vestimentifera and Annelida are closely related.

Introduction

The first vestimentiferan species, *Lamellibrachia barhami*, was described by Webb (1969) from a cold-water site in the eastern Pacific. Among other features, the absence of a gut led Webb to place this species in the phylum Pogonophora. In their description of a second vestimentiferan species, *L. luymesi*, van der Land and Nørrevang (1975) introduced the term "trophosome" for a peculiar tissue that occupies the trunk region. In a later report, van der Land and Nørrevang (1977) examined in greater detail the organization of the "parenchymatous" trophosomal tissue and stated that it consists of numerous small lobules. In each lobule, a peripheral layer of pigment cells surrounds a central region of basophilic cells filled with numerous vacuoles. Van der Land and Nørrevang suggested that the trophosome functions as a liver and is also a source of nutrients for developing spermatozoa. In the same year, Webb (1977) described and illustrated a "spongy tissue" associated with the male reproductive system of *L. barhami*, but he did not suggest a function for this tissue nor did he refer to it as trophosome. In his description of a third vestimentiferan species, *Riftia pachyptila*, Jones (1981a) noted the presence of trophosomal tissue in the trunk region. In a subsequent report, Jones (1981b) described the trophosome as consisting of many lobules, each with a central blood vessel that gives rise to numerous capillaries that ramify throughout the tissue. In their description of a third species of *Lamellibrachia*, *L. victori*, Mañé-Garzón and Montero (1986) commented on the lobular nature of the trophosome and its vascularization. Further, they stated, apparently on the basis of light microscopy, that there

are ". . . numerous accumulations of symbiotic microorganisms which are not bacteria but spores or algae" (p. 18). These observations have not been confirmed by other investigations.

Based on transmission electron microscopic (TEM) observations and analysis of lipopolysaccharide, Cavanaugh (1980) suggested that the bulk of the trophosome of *R. pachyptila* is occupied by bacteria that potentially serve as chemoautotrophic symbionts. In the first study of trophosomal tissue to include TEM micrographs, Cavanaugh *et al.* (1981) confirmed the presence of bacteria in the trophosome of *R. pachyptila*. Subsequent studies have confirmed the presence of endosymbiotic bacteria in *R. pachyptila* (Bosch and Grassé, 1984a, b; Hand, 1987), *Escarpia spicata* (Felbeck *et al.*, 1981; Cavanaugh, 1983a, b; reported as an unnamed new species), *Lamellibrachia barhami* (Felbeck *et al.*, 1981), *Ridgeia piscesae, Ridgeia phaeophiale,* and two additional undescribed species of vestimentiferans (de Burgh, 1986), *Oasisia alvinae* and *Ridgeia* sp. (the latter two species from personal TEM observations by SLG). These and other studies have also provided insight into the nature of the relationship between the bacteria and their hosts (for recent references, see Felbeck and Childress, 1988). One question that arises with respect to this association is how it is established in new individuals.

Jones (1985b, 1987, 1988b) and Jones and Gardiner (1988) noted the presence of a so-called ventral medial process (=siphon; Southward, 1988b) at the base of the branchial plume of juvenile *R. pachyptila, Ridgeia* sp., and *Oasisia alvinae*. The ciliated aperture at the distal end of the process leads to a duct that passes through the brain, through the vestimentum, and communicates with the established trophosome. They suggested that the aperture and duct are the means of entry of bacteria into the trophosome. Jones (1987) suggested that free-living bacteria are collected at random by the ciliated aperture of the process and transported to the trophosome via the duct, and if such bacteria include sulfide-oxidizing bacteria and others necessary for the worm, the worm survives; if they do not, the worm ultimately dies. Jones and Gardiner (1988) stated that the ciliated aperture at the distal end of the ventral medial process is the mouth. In addition, they described the gut and anus of a complete digestive tract in *Ridgeia,* as well as the fine structure of the foregut of *Riftia* and of cell junctions of its trophosomal bacteriocytes. Southward (1988a, b) also reported on the digestive tract in early developmental stages of *Ridgeia,* suggested an early phase of ciliary feeding, and discussed the relationship of the Vestimentifera and Pogonophora and the relationship of these to the Annelida.

Preliminary results of additional studies of early developmental stages of *Ridgeia* were presented by Jones (1988a) and form the basis of expanded results presented in this report, which includes the first description of a trochophore larva in the development of vestimentiferans. Additional new information is provided on the development of the ventral process and digestive system, the nervous system, larval and opisthosomal setae, branchial filaments, ventral ciliated field, and vestimentum. Observations on certain aspects of the development of the trophosome are presented. When appropriate, results from Southward (1988b) are compared with our findings.

Materials and Methods

Larval and juvenile specimens of *Ridgeia* sp. were collected at "Axial Seamount," Juan de Fuca Ridge (*Alvin* Dive 1413, 45°56′N; 130°01′W, 18 July 1984, 1546 m depth, and *Alvin* Dive 1924, 45°55′N; 130°02′W, 30 September 1987, 1540 m depth). Specimens of *Riftia pachyptila* were collected on the Galapagos Rift at the "Rose Garden" hydrothermal vent site (*Alvin* Dive 889, 00°48.7′N; 86°12.7′W, 14 February 1979, 2458 m depth) and a juvenile *Riftia* was collected at the "Garden of Eden" vent site (*Alvin* Dive 993, 00°47′N; 86°08′W, 10 December 1979, 2518 m depth). Additional specimens of *Riftia pachyptila* were obtained at the "Clam Acres" site on the EPR at 21° N (*Alvin* Dive 1225, 20°50′N; 109°06′W, 9 May 1982, 2618 m depth). For all specimens, except those from "Clam Acres" and the 1987 collections from "Axial Seamount," after initial fixation in 10% formalin (buffered with $CaCO_3$, pH 6.95) in seawater, the specimens were transferred to 70% ethanol.

For light microscopy, specimens were dehydrated and embedded in a mixture of epon-araldite, using propylene oxide as the infiltration solvent; semi-thin sections (1.5 or 2.0 μm) were cut on a Sorvall MT-2 ultramicrotome and were stained with Masson's triple stain. For scanning electron microscopy (SEM), specimens were placed in Ruthenium Red (as a mordant for OsO_4) for one hour, post-fixed in 1% OsO_4, on ice, for one hour, dehydrated through a graded ethanol series, and then critical-point or freeze dried. Specimens were sputter-coated with gold-palladium (about 15-nm thick) and examined in either a Cambridge 100 Stereoscan or a Hitachi S-570 scanning electron microscope. The collections from "Clam Acres" were intended for examination by transmission electron microscopy; samples of adult trophosome were fixed aboard ship at room temperature in 3.5% glutaraldehyde in 0.1 *M* phosphate buffer (pH 7.3) containing 10% sucrose and a trace of $CaCl_2$. Tissues were refrigerated and stored in glutaraldehyde fixative until their use for this study. The recent collections from "Axial Seamount" (1987) yielded *Ridgeia* larvae/juveniles for light microscopy and TEM examination from a clump of tubes of *R. piscesae,* bulk-fixed onboard ship in approximately 4% glutaraldehyde in 0.1 *M* cacodylate buffer (pH 7.2). Tis-

sues for TEM were ("Clam Acres") post-fixed in phosphate-buffered OsO_4 for 1 h at 4°C and dehydrated in a standard ethanol series, or ("Axial Seamount") post-fixed in cacodylate-buffered OsO_4 for 2 h at room temperature, pre-embedded in agar, and dehydrated in a graded series of ethanol, with 2,2-dimethyoxypropane after 70% ethanol. Trophosome was embedded in a mixture of epon-araldite and larvae/juveniles in agar blocks were embedded in Spurr's resin; propylene oxide was the infiltration solvent in both procedures. Thin-sections were cut on a Sorvall MT-2 ultramicrotome, stained with aqueous uranyl acetate and lead citrate, and examined in a JEOL 100S, JEM 1200EX, or a Zeiss EM9S-2 transmission electron microscope.

Measurements of length of the 38 specimens of *Ridgeia* examined by SEM are not "total length" (Table I). Due to the variability of contraction of branchial filaments of preserved specimens, as well as the lack of branchial filaments in early stages, lengths were measured from the prototrochal band of larvae and the base of branchial filaments of juveniles to the posterior extremity. This length, of specimens processed for SEM, is the basis for the ranking of specimens and does not necessarily reflect a true estimate of actual or relative age of the specimens. Where appropriate, rank numbers (#X) are included in the text and figure legends to identify individual specimens listed in Table I. Those illustrated specimens not ranked are noted as "nr. #X" to indicate their length relative to ranked specimens. The lengths of sectioned specimens were adjusted to take into account shrinkage due to processing for SEM. A comparison of measurements before and after critical-point drying indicated a shortening of body length by about 7.5% during processing; this factor was applied to lengths of sectioned material to make them comparable to SEM specimens. This shrinkage was variable (the 7.5%, above, is an average of shrinkage of specimens ranging from 4% to 10%), and may explain apparent inconsistencies in some of the results below. Where a comparison with the observations of Southward (1988b) was appropriate, measurements, from the base of branchial filaments to the posterior end, were based on her SEM micrograph and camera lucida drawings, using her indicated scales and correcting for shrinkage, and were converted to "nr. #'s" as follows:

Fig. 3A,—0.727 mm—nr. #27
Fig. 4, left—0.119 mm—nr. #6
Fig. 4, right—0.108 mm—nr. #5
Fig. 5A, spec. RJ—0.142 mm—nr. #9
Fig. 5C, spec. RB—1.304 mm—nr. #32
Fig. 5D, spec. RC—1.613 mm—nr. #33

Two species of *Ridgeia* are known from Axial Seamount and, although the 38 larvae and juveniles examined by SEM were sorted from clumps of *Ridgeia piscesae* tubes, it is not possible to determine their specific identity. On the basis of overall body shape, specimens with rank numbers 6, 7, 17, and 19 may be different from the rest of the series; rank numbers 15 and 22 have an unusually thick ventral process; these characteristics may be artifacts of fixation or processing.

The Vestimentiferan Body Plan and the Systematic Relationships of the Vestimentifera

The Vestimentifera presently contains ten species whose anatomy and morphology have been described to varying degrees (see Jones, 1985c; Mañé-Garzón and Montero, 1986). Although differences exist pertaining to certain aspects of the anatomy and morphology of these ten species, they, nevertheless, share a common body plan as adults. The following description, based largely on observations from Jones (1985c), is intended to familiarize the reader with this vestimentiferan body plan. It is our desire that subsequent sections of this report, which describe certain aspects of the development of *Ridgeia* sp. and the anatomy of *Riftia pachyptila,* can be examined with the characteristic adult body plan of the Vestimentifera in mind.

The body of juvenile and adult vestimentiferans is divisible externally into four distinct regions. From anterior to posterior ends, these regions are (1) the obturacular region, (2) the vestimentum, (3) the trunk, and (4) the opisthosome (Fig. 1).

The obturacular region (Fig. 1, OB) comprises the central obturaculum (Fig. 1, OBT), which supports and bears the respiratory plume, and the plume itself; the latter consists of many branchial filaments (Fig. 1, BF) that are provided with pinnules (lobes that increase the respiratory surface) and are fused as left and right series of branchial lamellae. In the case of *R. pachyptila,* the branchial lamellae extend perpendicularly from the obturaculum and are free for most of their length (class Axonobranchia). In all other vestimentiferans described to date (class Basibranchia), the branchial lamellae extend anteriorly from the base of the obturaculum and are fused for most of their length. One or two openings of the excretory organ are situated on the dorsal surface near the base of the obturaculum.

The vestimentum (Fig. 1, VS) is provided ventrally with a conspicuous pear- or teardrop-shaped ciliated field (Fig. 1, VC), which is bounded by the two parts of the separated ventral nerve cord. Plaques (Fig. 9, PL) and the openings of the so-called pyriform glands are also evident on the ventral and lateral surfaces; the latter secrete tube material at and near the open end of the tube. Dorsally, the vestimentum bears a pair of genital apertures with paired ciliated grooves extending anteriorly in the

Table I

Rankings (RK) of specimens of Ridgeia *sp. observed by scanning electron microscopy (SEM), arranged by length (L = distance from prototroch or base of branchial filaments to posterior end), and notations of presence of larval setae (LS), number of branchial filaments (BF), condition of ventral ciliated field (VCF), number of rows of opisthosomal setae (OS), state of vestimentum (VST), obturaculum (OBT) and anus (AN) and presence or absence of endosymbiotic bacteria (BA)*

RK		L (mm)	LS	BF	VCF	OS	VST	OBT	AN	BA
1		0.058	P	0	L	0	L	L	?	?
2		0.075	P	0	L	0	L	L	?	?
3		0.087	P	2	S	?	L	L	?	?
4		0.100	P	3	S	1	L	L	?	?
	*G	0.104 (0.112)	P	2	S	0	L	L	L	L
5		0.110	?	2	S	?	L	L	?	?
6		0.111	P	2	L	0	L	L	?	?
7		0.140	P	2	S	1	L	L	?P	?
8		0.141	P	3	S	1	L	L	?	?
9		0.143	P	2	S	1	L	L	P	?
	*F	0.148 (0.160)	P	2	S	1	L	L	L	L
10		0.150	P	3	S	1	L	L	P	?
11		0.155	P	3	S	1	L	L	?	?
12		0.160	P	5	S	1	L	L	?	?
13		0.162	P	2	S	1	L	L	P	?
	*D	0.163 (0.176)	?	2	S	1	L	L	L	L
14		0.169	P	2	S	1	L	L	?	?
	*H	0.176 (0.190)	P	4	S	1	L	L	P	P
	*B	0.178 (0.192)	?	4	S	1	L	L	P	L
15		0.180	P	5	S	1	L	L	?	?
16		0.180	P	4	S	2	D	L	?	?
	*E	0.182 (0.197)	P	2(?+)	?	1	L	L	L	L
17		0.184	P	2	S	1	L	L	L	?
18		0.190	P	4	S	1	L	L	?	?
19		0.214	P	2	?	1	L	L	?	?
20		0.220	?	5	S	2	D	L	?	?
	*CB7	0.247 (0.267)	?	5	?S	1	L	L	?	P
		0.257	P	?4	S	1	L	L	L	?
	*C	0.272 (0.294)	?	4	S	1	L	L	P	L
21		0.280	P	2	S	2	D	L	?	?
	*A	0.285 (0.308)	?	6	?S	1	L	L	P	P
22		0.300	P	5	S	2	L	L	?	?
23		0.400	P	4	?	2	P	L	?	?
	*CB1	0.400 (0.432)	?	8	?	3	P	L	L	P
24		0.440	P	M	F	1	P	L	?	?
25		0.540	P	8	F	2	P	L	?	?
26		0.690	L	M	F	4	P	?	?	?
27		0.750	P	M	F	4	P	?	?	?
28		1.010	P	M	F	7	P	P	?	?
29		1.060	L	M	F	?	P	?	?	?
30		1.120	?	M	F	8	P	?	?L	?
31		1.210	P	M	F	5	P	P	?	?
32		1.340	P	M	F	9	P	?	?	?
33		1.560	P	M	F	8	P	P	?	?
34		1.740	P	M	F	7	P	P	L	?
35		2.000	L	M	F	4	P	?	?	?
36		2.190	L	M	F	7	P	P	?	?
37		2.230	L	M	F	11	P	P	L	?
38		4.040	L	M	F	22	P	P	L	?

Lengths of sectioned specimens, marked with "*" and an identifying letter, are adjusted to allow for lack of shrinkage due to SEM processing and actual lengths follow, in parentheses. D: developing; F: fused; L: lacking; M: many, not countable accurately; P: present; S: segmented; ?: not known, unobservable.

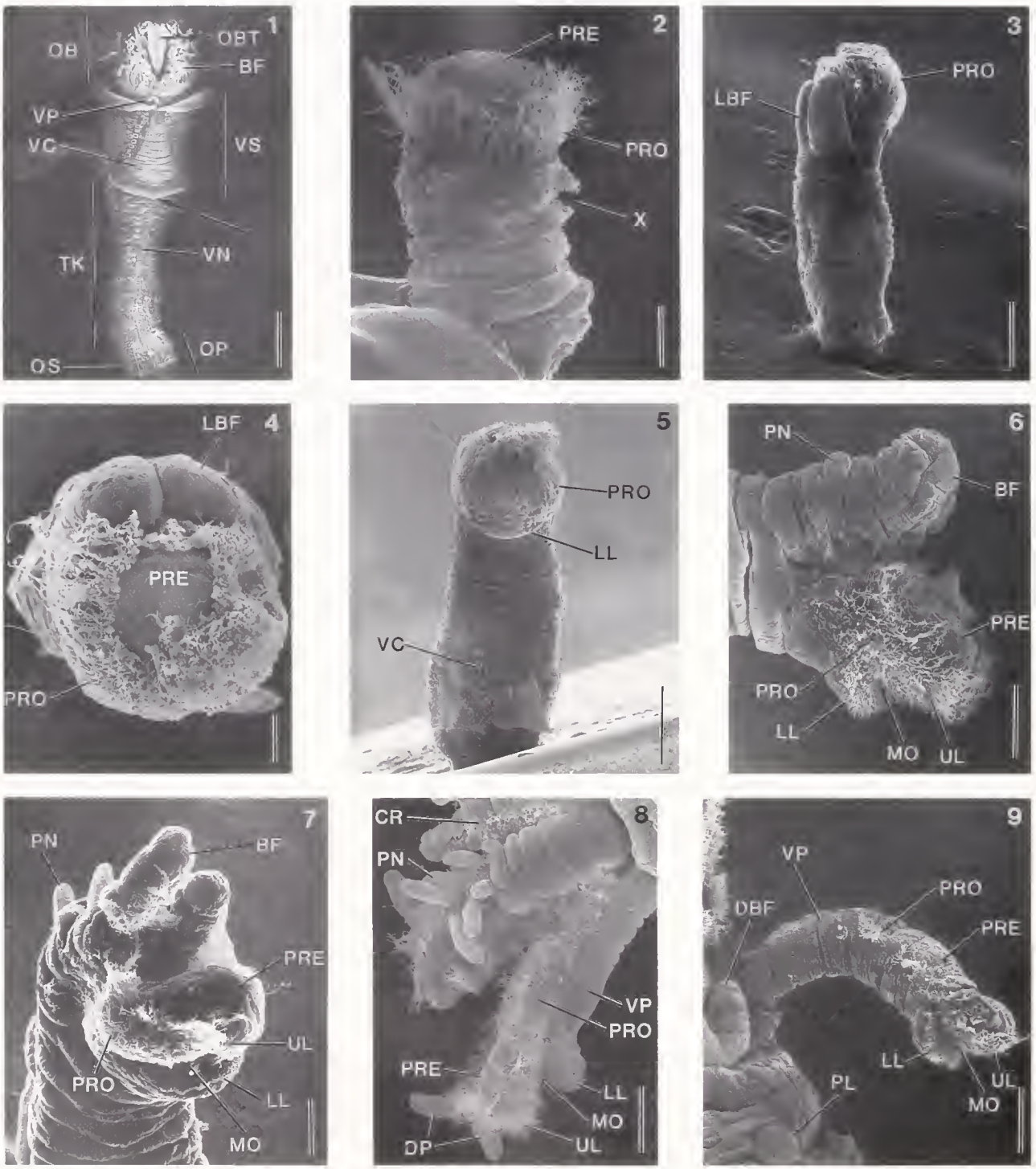

Figure 1. *Ridgeia* sp. Rank #36, SEM. Ventral view, juvenile. Arrow, posterior margin of vestimentum. Scale bar, 500 μm.

Figure 2. Rank #1, SEM. Trochophore larva. Scale bar, 15 μm.

Figure 3. Rank #3, SEM. Right dorsolateral view of larva. Scale bar, 30 μm.

Figure 4. Rank #3, SEM. Anterior view of larva of Fig. 3. Scale bar, 10 μm.

Figure 5. Rank #3, SEM. Ventral view of larva of Fig. 3. Scale bar, 30 μm.

Figure 6. Rank #5, SEM. Right lateral view, ventral process of larva. Scale bar, 20 μm.

Figure 7. Rank #14, SEM. Anterior view, anterior region of larva, developing ventral process; tip of branchial filament damaged. Scale bar, 20 μm.

case of males. Internally, the bulk of the vestimentum consists of muscles and connective tissue and these act to keep the vestimentum at the open end of the tube and maintain the position of the branchial plume of the obturacular region outside the tube; the brain is situated ventrally near the anterior margin and the excretory organ is posterior to the brain.

The trunk region (Fig. 1, TK) occupies the greatest relative portion of the body in all vestimentiferans so far described (up to 80% of total body length in the largest specimen of *R. pachyptila*; Jones, 1981a). The surface of the trunk bears the trace of the united nerve cord in the ventral midline (Fig. 1, VN) and the papillae of pyriform gland openings; secretions from the latter thicken the tube wall. Internally, the trunk contains vascular elements, the trophosome, which houses endosymbiotic bacteria, and the gonad. A digestive tract has not been observed in this region in adult specimens.

The opisthosome (Fig. 1, OP) is the only region of the body that is multisegmented in the adult. Externally, the continued trace of the nerve cord is visible in the ventral midline. Anterior segments are provided with transverse rows of opisthosomal setae (Fig. 1, OS) that act as a holdfast to the inner surface of the tube when the worm withdraws; a variable number of posterior segments lack setae but are indicated externally by furrows that mark the positions of internal septa. Internally, the coelomic space of each segment is paired due to the presence of a median mesentery that extends throughout the length of the opisthosome.

The systematic relationship of the Vestimentifera with other higher Bilateria is still unsettled. This lack of agreement among investigators centers in large part on the importance of the segmentation pattern (and the arrangement of coelomic spaces) and the manner of segment formation in the Vestimentifera relative to other segmented groups. Webb (1969) cited the long trunk and opisthosome (=metasoma) of *Lamellibrachia barhami* as distinctive pogonophoran features and placed that species in a new class and order in the phylum Pogonophora. Van der Land and Nørrevang (1975, 1977) did not attribute special phylogenetic importance to the regionation of the body of *Lamellibrachia* and considered the Vestimentifera, as well as the Pogonophora, as separate classes in the phylum Annelida. In his original description of *Riftia pachyptila,* Jones (1981a) considered the body regionation as indicating a close relationship with the pogonophorans. He retained the Pogonophora at the level of phylum and placed the Vestimentifera in it as a new subphylum, the Obturata. Jones (1985a) contrasted the arrangement of the apparent segments of the vestimentiferans and pogonophorans and the development of segments in the opisthosome. He suggested that these two groups may not be as closely related as previously thought and that their close relationship with the Annelida required reexamination. Based on previous observations and additional new information, Jones (1985b, c) separated the Vestimentifera and Pogonophora at the level of phyla. Citing, in particular, an apparent lack of difference in the development of segments in the opisthosomes of the vestimentiferans and pogonophorans, Southward (1988b) suggested that the two groups should be considered as subclasses in the class Pogonophora. In addition, she suggested that the outcome of future developmental studies would be instrumental in determining if the class Pogonophora should be placed in the phylum Annelida or phylum Brachiata.

Results

Trochophore

The trochophore larva of *Ridgeia* is provided with a prototrochal ring of cilia (Fig. 2, PRO) and lacks a neurotroch, metatroch, and an apical tuft on the pretrochal area (Fig. 2, PRE); that part of the posterior region that is not obscured by mounting adhesive does not reveal a telotroch (Fig. 2). Examination of the prototroch at higher magnification does not reveal the presence of compound cilia; this may be due to a less than optimal fixation of the original sample or may reflect the true state of the prototrochal cilia. There are no apparent mouth or anal openings. That the specimen is a vestimentiferan trochophore is confirmed by the presence of larval setae typical of later larval and juvenile stages (see Discussion, below).

Ventral process and gut

At about the time that the first pair of larval branchial filaments develop (Figs. 3, 4, LBF) (see Branchial filaments, below), a lip-like protrusion (Fig. 5, LL) arises just posterior to the prototroch (Figs. 3–5, PRO). This, in ad-

Figure 8. Rank #15, SEM. Left lateral view, ventral process of larva. Scale bar, 30 μm.

Figure 9. Rank #25, SEM. Right lateral view, ventral process of juvenile. Scale bar, 30 μm. BF, branchial filament(s); CR, ciliary row; DBF, developing branchial filament; DP, displaced pinnules; LBF, larval branchial filaments; LL, lower lip; MO, mouth; OB, obturacular region; OBT, obturaculum; OP, opisthosome; OS, opisthosomal setae; PL, vestimental plaque; PN, pinnule; PRE, pretrochal region; PRO, prototroch; TK, trunk; UL, upper lip; VC, ventral ciliated field; VN, ventral nerve cord; VP, ventral process; VS, vestimentum; X, damage during processing.

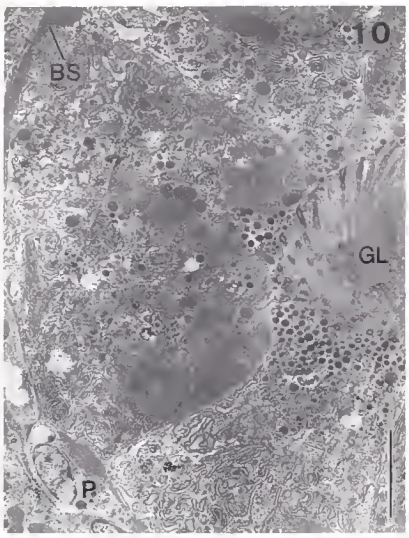
10
BS
GL
P

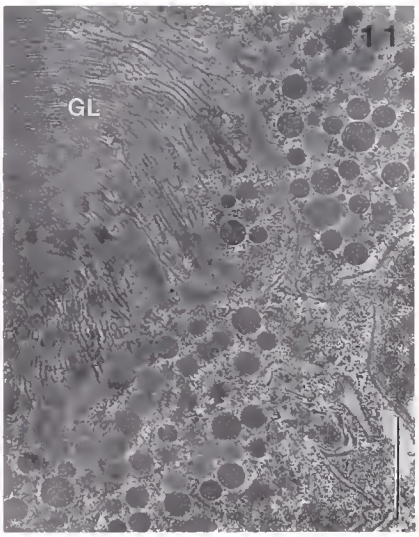
11
GL

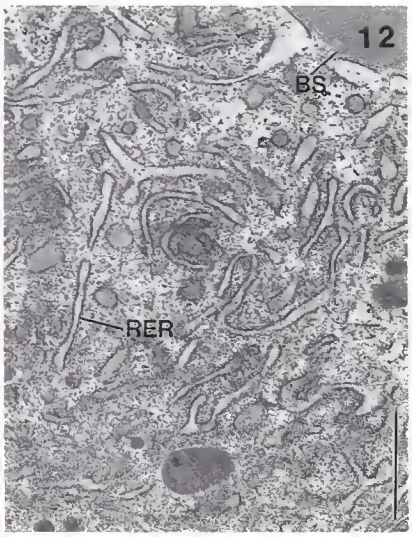
12
BS
RER

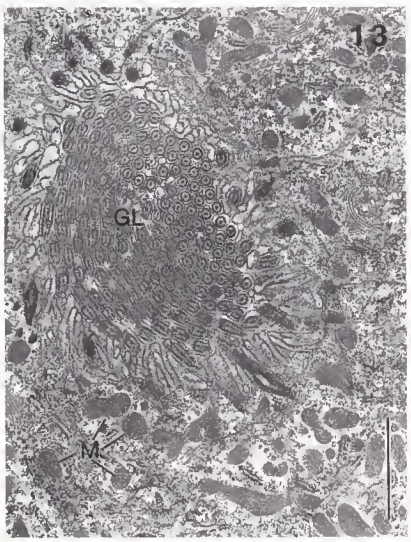
13
GL
M

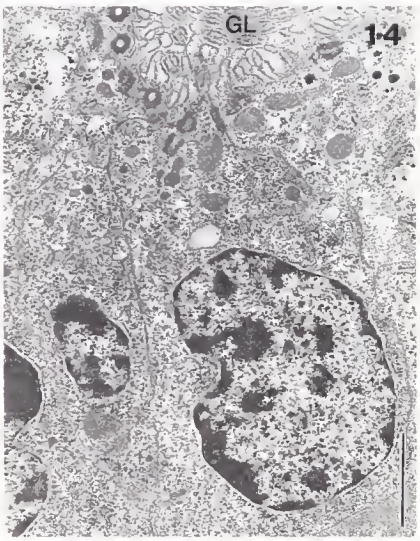
GL
14

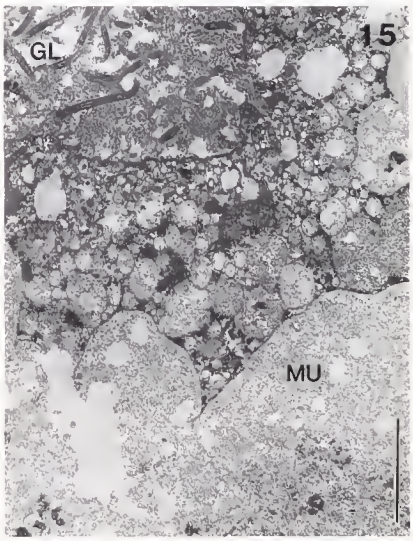
GL
15
MU

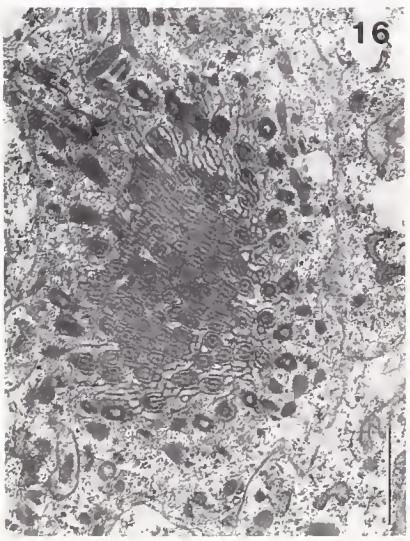
16

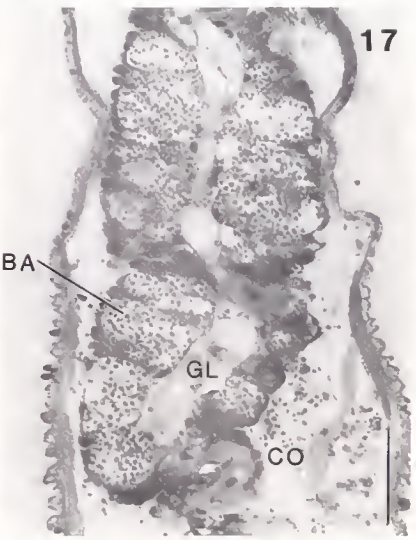
17
BA
GL
CO

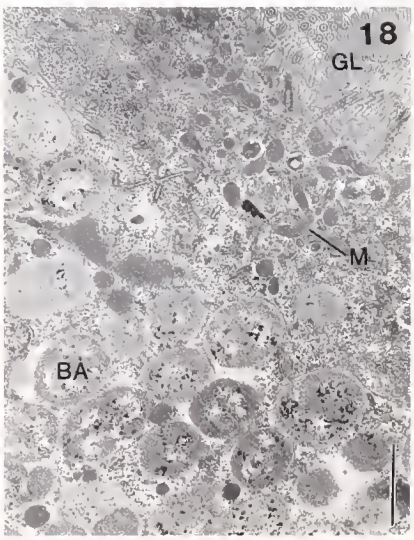
18
GL
M
BA

dition to the first appearance of the ciliated field (Fig. 5, VC), establishes the ventral surface of the developing larva. As in the case of the trochophore, close examination of the prototroch failed to reveal the presence of compound cilia. In time, the posttrochal protrusion develops cilia and becomes the lower (=posterior) lip of the mouth opening (Figs. 6, 7, LL). The mouth is formed between the lower lip and the ventral portion of the prototroch; the latter becomes the upper (=anterior) lip of the mouth (Figs. 6, 7, UL). There is a differential growth such that the prototroch is displaced ventrally and the ventral process, with its terminal mouth, is formed (Figs. 6, 7, MO). The residuum of the prototroch is distributed laterally along the length of the process (Fig. 8, PRO) and persists for some time as the process elongates (Fig. 9, rank #25, PRO). The entire pretrochal region of the trochophore appears to be restricted to the upper (=anterior) surface of the ventral process (Figs. 6–9, PRE).

Examination of sectioned specimens by light microscopy and whole specimens by SEM (see Table I) reveals details of several aspects of the early development of the gut of *Ridgeia*. First, the mouth is formed early in development (G-nr. #4) but is not connected to the foregut (F-nr. #10, D-nr. #13, E-nr. #16) until later in development (H-nr. #15, CB7-nr. #20, with endosymbionts; C-nr. #21, lacking endosymbionts). Second, the anal opening is established after the mouth is open, but the stage at which the anus appears, and a complete digestive system can be established, is variable. Third, the appearance of the anus seems to precede the establishment of the bacterial association in young juvenile stages (note specimens B-nr. #15 and C-nr. #21 in Table I). Fourth, the bacterial association is established in the midgut region of *Ridgeia*, but the time at which this association occurs is variable (in particular, note specimens H- and B-nr. #15, C- and A-nr. #21). Finally, the closure of an anus in later juvenile stages, *e.g.*, #34, #37, and #38, is correlated with the probability that the symbiotic association with bacteria has been established (see Discussion, below).

Throughout its length, the gut is lined by an epithelium of multiciliated cells whose cilia nearly obscure the lumen (Figs. 10, 13, 16). The presence of accessory centrioles and a system of rootlets associated with basal bodies of the cilia have not been confirmed. When viewed by TEM, a foregut, midgut, and hindgut are distinguishable in *Ridgeia*, based on cytological features of the epithelial cells.

The foregut epithelium is characterized by the presence of numerous electron-dense secretory granules up to 500 nm in diameter in the apical region of the cells (Figs. 10, 11). Mitochondria are scattered in the cytoplasm beneath the area occupied by the granules. Basally, the cells contain extensive profiles of rough endoplasmic reticulum (Fig. 12, RER) and numerous Golgi complexes that are actively releasing vesicles. The foregut epithelium rests on a blood sinus (Figs. 10, 12, BS), and a layer of peritoneal cells is situated between this sinus and the body wall (Fig. 10, P).

Prior to the establishment of the symbiotic association, the cytology of the epithelial cells of the midgut is rather unremarkable. Apically, the cells contain numerous mitochondria, scattered Golgi complexes, and a few electron-dense granules (Fig. 13). Nuclei of the cells are situated basally (Fig. 14) and RER is not extensively developed. A thin layer of extracellular matrix separates the epithelial cells from a layer of peritoneal cells. A blood sinus was not observed in our specimens.

When viewed by light microscopy, the hindgut appears transparent when compared with other regions of the gut (Figs. 21, 45, 49, 50). This observation is accounted for in TEM preparations in that the hindgut epithelial cells contain large vacuoles that are filled with a slightly granular, electron-translucent substance, which may represent mucus or unused yolk material (Fig. 15,

Figure 10. *Ridgeia* sp. Unranked juvenile, TEM. Cross-section of foregut epithelium. Note secretory granules in region of cells adjacent to gut lumen. Scale bar, 4 μm.

Figure 11. Unranked juvenile, TEM. Enlargement of apical region of foregut epithelium, showing numerous secretory granules. Scale bar, 1.5 μm.

Figure 12. Unranked juvenile, TEM. Enlargement of basal region of foregut epithelium, showing rough endoplasmic reticulum. Scale bar, 1.5 μm.

Figure 13. Unranked juvenile, TEM. Apical region of midgut epithelium prior to establishment of bacterial association. Scale bar, 2 μm.

Figure 14. Unranked juvenile, TEM. Cross-section of midgut epithelial cell prior to establishment of bacterial association. Scale bar, 2 μm.

Figure 15. Unranked juvenile, TEM. Hindgut epithelium. Scale bar, 3 μm.

Figure 16. Unranked juvenile, TEM. Tangential section of epithelium surrounding anal opening. Scale bar, 1.5 μm.

Figure 17. Rank A-nr. #21, frontal section, epon, 2.0 μm. Midgut of juvenile. Scale bar, 30 μm.

Figure 18. Unranked juvenile, TEM. Cross-section of midgut epithelium after establishment of bacterial association. Scale bar, 2 μm. BA, bacteria; BS, blood sinus; CO, coelom of trunk; GL, lumen of gut; M, mitochondria; MU, mucus; P, peritoneum; RER, rough endoplasmic reticulum.

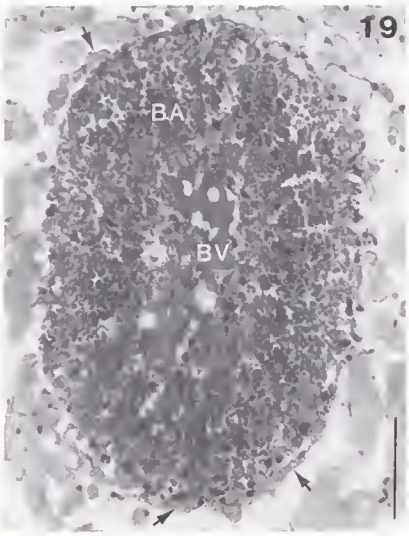
19
BA
BV

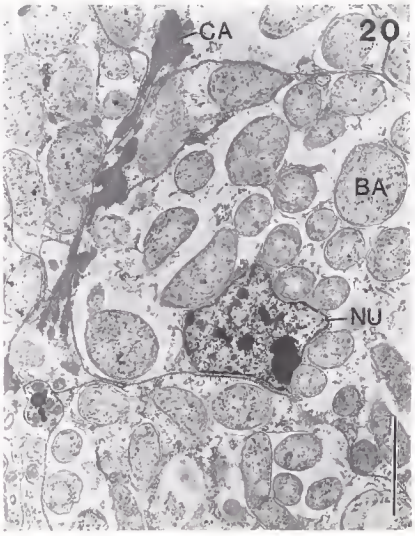
20
CA
BA
NU

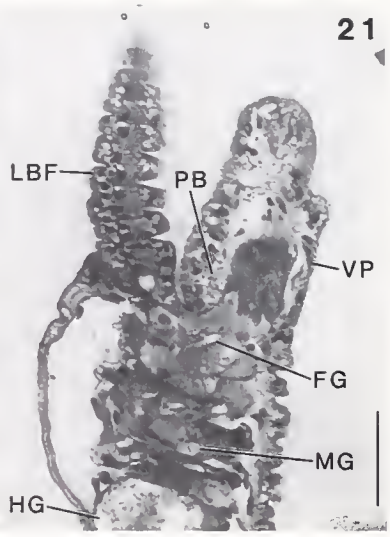
21
LBF
PB
VP
FG
MG
HG

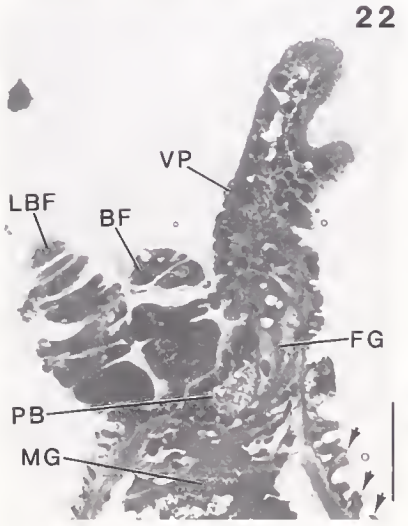
22
VP
LBF
BF
FG
PB
MG

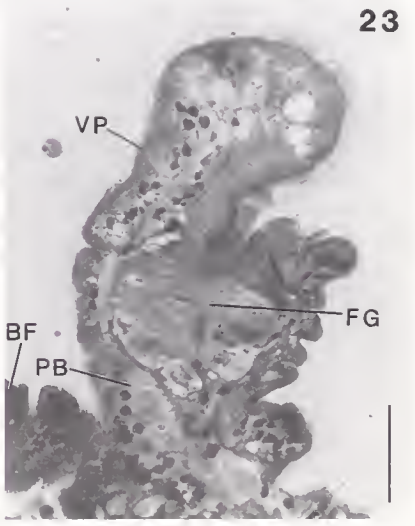
23
VP
FG
BF
PB

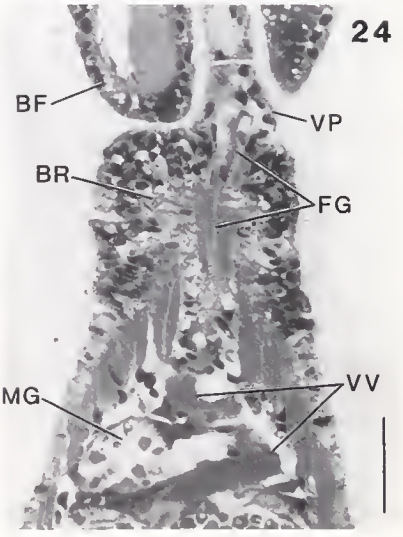
24
BF
VP
BR
FG
MG
VV

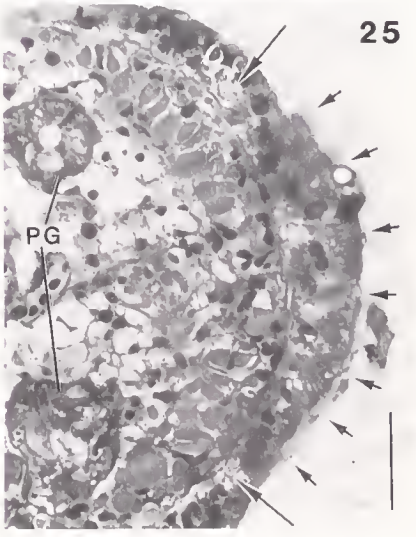
25
PG

MU). Cytoplasm is restricted to a thin layer around the periphery of the cells, adjacent to the membranes. Scattered mitochondria are present in the apical region of the cells, but nuclei and other cellular organelles have not been observed. Bacteria and other materials are present in the lumen of the hindgut. An associated layer of peritoneal cells appears to be absent. In the region of the anus, the cytology of the epithelial cells resembles that of the midgut (Fig. 16).

Bacterial association and trophosome

The bacterial association is established in the midgut region of *Ridgeia*. During early stages of the association, the lumen of the gut is open, and the bacteria appear to be scattered throughout the epithelial cells (Figs. 17, BA, GL). However, when viewed by TEM, the bacteria (Fig. 18, BA) are seen to occupy the basal area of the epithelial cells. Bacteria are coccoid in shape, up to 2.5 μm in diameter, and appear to be housed in separate vacuoles. Nuclei of the epithelial cells and mitochondria are situated in the cytoplasm surrounding the bacteria (Figs. 18, M; 20, NU). The presence of different sizes of bacteria or of the digestion of bacteria by midgut cells, as noted by Southward (1988b), were not confirmed in our specimens. At least one instance of a bacterium undergoing binary fission has been observed (pers. obs., SLG). Mitochondria, RER, and, occasionally, a Golgi complex, are observed in the apical region of the cells (Fig. 18).

As development proceeds, the lumen of the midgut disappears, and the trophosome develops through an elaboration of the original epithelial lining of the midgut. In adults of *Riftia pachyptila,* and presumably all vestimentiferans, the trophosome consists of numerous elongated lobules that appear circular or somewhat elliptical when viewed in cross-section (Fig. 19). Each lobule is provided with a central axial blood vessel from which extend numerous capillaries 1.0–3.6 μm in diameter that connect with blood vessels on the outer surface of the lobule (Fig. 19, arrows; for additional details on the vascular system of the trophosome, see Jones, 1988b). The cytology of the specialized cells that house the bacteria in the trophosome (bacteriocytes) differs from that of the original midgut epithelium mainly in the absence of most cellular organelles. Only the nucleus and a few scattered mitochondria have been observed in the cytoplasm surrounding the bacteria (Fig. 20). Analysis of TEM micrographs indicates that bacteria occupy at least 40% of the area of a bacteriocyte, in section, and that bacteriocytes account for at least 41% to 53% of the total area of the trophosome, in section.

Nervous system

In the development of the ventral process, accumulations of presumed nervous tissue are present at the base of the process (Figs. 21–23, PB), just below its dorsal (=anterior) surface. These arise between the outer layer of epithelial cells and the wall of the foregut. There are suggestions of continuity of this nervous tissue, lateral to the foregut and to just internal to the ventral surface; this growth around the foregut has yet to be confirmed at these stages. The presumptive brain, within the ventral process, has been observed in stages D-nr. #13, H-nr. #15 and C-nr. #21 (Figs. 21–23, PB), but not in presumed younger stages (G-nr. #4 and F-nr. #10). Later, the brain comes to be situated in the vestimentum, internal to the ventral process, posterior to the branchial filaments, with the foregut traversing it (Fig. 24, BR, FG).

In larval and young juvenile stages (up to C-nr. #21), a differentiated ventral nerve cord has not been observed in the epithelium of the body wall. In later juvenile stages and adults, a single nerve cord exits the brain on its ventral surface, just internal to the cuticle and epithelium of the body wall (see Jones, 1981a, 1985a, for additional descriptions of the nervous system of adult vestimentiferans). In addition to other nervous tissue, the nerve cord, here, contains a pair of giant axons. In juveniles of *Ridgeia* sp. and *Oasisia alvinae,* and, presumably, all vestimentiferans, the perikarya of these giant axons are situated adjacent to each other in the dorsal region of the brain. In contrast to other cells in the brain, the cyto-

Figure 19. *Riftia pachyptila* USNM No. 59958, adult, transverse section, paraffin, 5 μm. Cross-section of lobule of trophosome. Arrows, surface blood vessels. Scale bar, 50 μm.

Figure 20. *Riftia pachyptila,* adult, TEM. Bacteriocyte in trophosome. Scale bar, 3 μm.

Figure 21. *Ridgeia* sp. Rank D-nr. #13, sagittal section, epon, 1.5 μm. Anterior of larva. Scale bar, 30 μm.

Figure 22. Rank H-nr. #15, sagittal section, epon, 1.5 μm. Anterior of larva. Arrows, ventral ciliated field. Scale bar, 30 μm.

Figure 23. Rank C-nr. #21, sagittal section, epon, 1.5 μm. Anterior of larva. Scale bar, 30 μm.

Figure 24. Rank CB7-nr. #20, frontal section, epon, 2.0 μm. Anterior of larva. Scale bar, 30 μm.

Figure 25. Rank CB1-nr. #23, transverse section, epon, 2.0 μm. Ventral ciliated field and adjacent paired ventral nerve cords. Large arrows, nerve cords; small arrows, extent of ventral ciliated field. Scale bar, 30 μm. BA, bacteria; BF, branchial filament; BR, brain; BV, axial blood vessel; CA, capillary; FG, foregut; HG, hindgut; LBF, larval branchial filament; MG, midgut; NU, nucleus; PB, presumed brain; PG, pyriform glands; VP, ventral process; VV, ventral vessel.

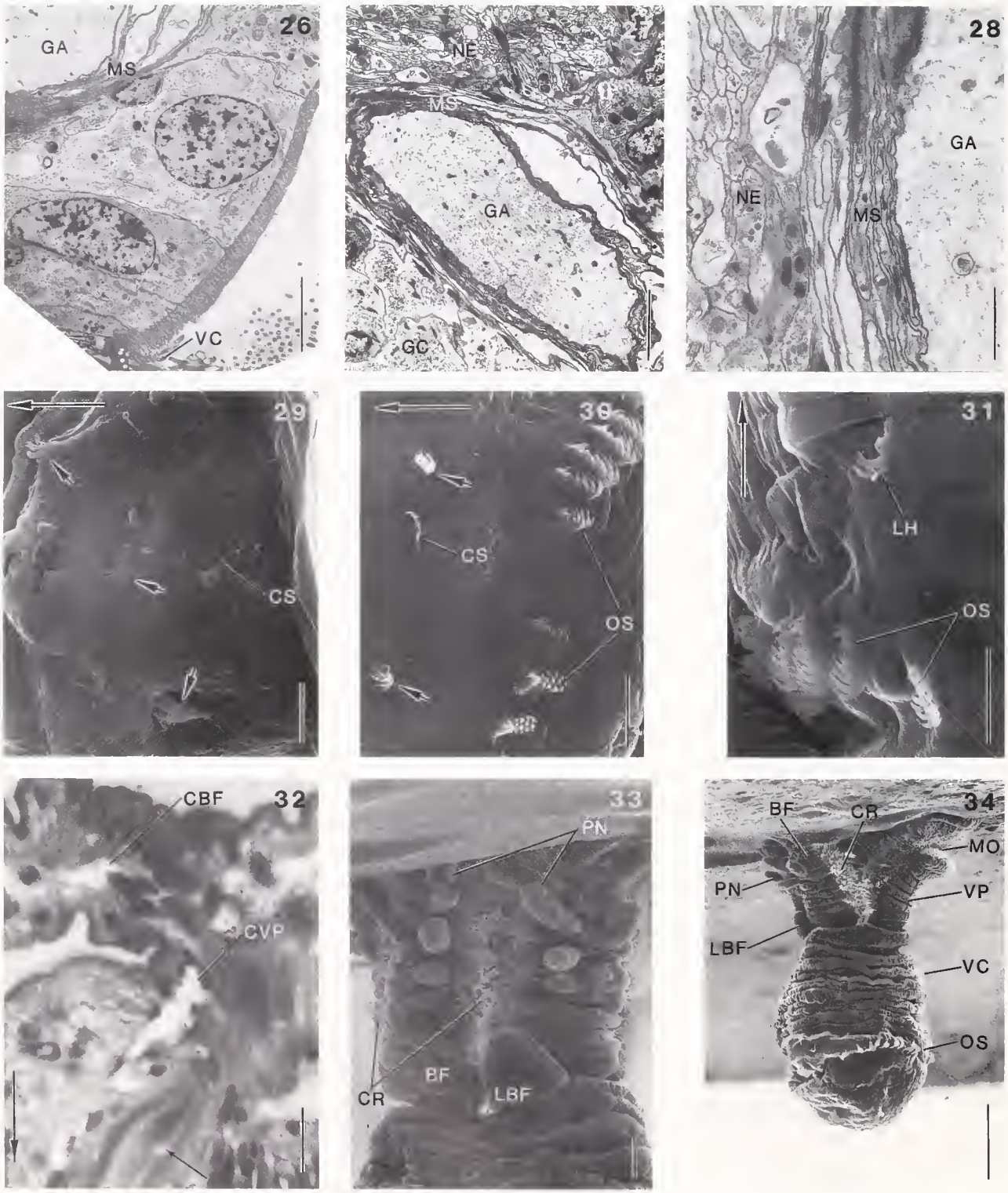

Figure 26. *Ridgeia* sp. Unranked juvenile, TEM. Cross-section of vestimentum in region of ventral ciliated field, showing portion of giant axon. Scale bar, 5 μm.

Figure 27. Unranked juvenile, TEM. Cross-section of nerve cord in vestimentum, showing giant axon, neurites and glial cell bodies of myelin sheath. Scale bar, 5 μm.

Figure 28. Unranked juvenile, TEM. Enlargement of myelin sheath of giant axon. Note varying thickness of lamellae of sheath. Scale bar, 1.5 μm.

plasm of the perikarya of the giant axons stains lightly in TEM preparations. Numerous mitochondria and dense-cored vesicles are visible in these cells. A single giant axon exits each perikaryon and extends ventrally through the neuropile of the brain. Microtubules, mitochondria, and dense-cored vesicles are present in the giant axons in this region.

Upon reaching the ventral ciliated field, the nerve cord diverges and carries one giant axon in each branch (Figs. 25, large arrows; 26, 27, GA). The cytoplasm of the giant axons in this region stains lightly in TEM preparations and contains scattered vesicles and mitochondria (Figs. 27, 29). Microtubules, however, have not been observed here. In the region of the vestimentum, each giant axon is surrounded by a myelin sheath of irregularly spaced lamellae (Figs. 26, 27, MS) derived from glial cells whose cell bodies are mostly clustered in the ventrolateral region of each nerve cord (Fig. 27, GC). Occasionally, a glial cell body is observed in the outermost lamellae of the sheaths. In one juvenile, the thickness of the sheaths varied from 0.5 μm to 2.5 μm, and each sheath consisted of about 12 lamellae, although it was difficult to determine this number precisely because the lamellae frequently branch and fold back on themselves (Fig. 28). By contrast, the number of lamellae surrounding the giant axon in the adult stage of *Riftia pachyptila* exceeds 50 (pers. obs., SLG). The layer of cytoplasm between membranes of the lamellae varies in thickness from as little as 50 nm to as much as 2 μm. Mitochondria, endoplasmic reticulum, and numerous vesicles are present in the cytoplasm of the thicker lamellae.

The nerve cords fuse at the posterior margin of the ventral ciliated field, and a single nerve cord extends through the trunk and opisthosome. In the trunk, the nerve cord contains one giant axon whose organization is similar to that of the giant axons in the vestimentum. The nerve cord in the opisthosome lacks a giant axon (Jones, 1981a, 1985a).

Further development of larvae and juveniles

If the 38 specimens examined by SEM are arranged from trochophore (Fig. 2) to established juvenile (Fig. 1), lengths from 58 μm to 4.04 mm, it is possible to determine the progressive development of a number of morphological characters (Table I; Figs. 29–52).

Larval setae. In the single trochophore observed, three larval hooks and one capillary seta are visible in one micrograph (Fig. 29, small arrows, CS), and one other hook and two other capillary setae can be seen in micrographs taken at right angles to the first; about one-half of the circumference of the trochophore, at the level of the larval setae, is obscured by mounting adhesive. We suggest that this trochophore may bear up to eight larval hooks and six to eight capillary setae. In later stages, where observed, there are two pairs of larval hooks, situated laterally, with a single, capillary seta between each pair (Fig. 30, small arrows, CS; Jones and Gardiner, 1988, Fig. 7E). Each hook bears a single cluster of three to five denticles, palmately arranged around a central one, all pointing anteriorly (Figs. 29–31, LH/small arrows). In longitudinal sections, it has been confirmed that the larval setae are situated in the trunk wall and are well-separated from the opisthosome and the opisthosomal setae (Fig. 50, LH). Larval setae persist for a longer or shorter time, apparently depending on the amount of abrasion in life or the amount of handling that the specimens receive during sorting and processing; capillary setae are lost even more readily. Figure 53 shows the presence or absence of larval setae among the ranked specimens and indicates that they are present on an individual as long as 1.74 mm.

Branchial filaments. The first (larval) branchial filaments develop as a pair on the dorsal surface of the larva, arising just posterior to the prototroch (Figs. 3, 4, 33, 34, LBF), and a second pair may develop just posterior to the first. These pairs of larval branchial filaments do not develop pinnules but bear two longitudinal rows of cilia, one dorsomedial and the other ventrolateral; both pairs are considered to be larval structures because they appear to be resorbed as development proceeds. In the youngest stage that was sectioned (G-nr. #4) there is a suggestion that the coelomic cavity of the ventral process (Fig. 32, CVP), at some time in development, communicates with the cavity of the larval branchial filaments (Fig. 32, CBF); the coelomic cavity of the ventral process was not

Figure 29. Rank #1, SEM. Larval setae on posterior of trochophore larva. Large arrow, anterior; small arrows, larval hooks. Scale bar, 5 μm.

Figure 30. Rank nr. #21, SEM. Setae on posterior of larva. Large arrow, anterior; small arrows, larval hooks. Scale bar, 10 μm.

Figure 31. Rank #15, SEM. Setae on posterior of larva. Arrow, anterior. Scale bar, 10 μm.

Figure 32. Rank G-nr. #4, sagittal section, epon, 1.5 μm. Base of branchial filament and ventral process. Small arrow, mouth/foregut; large arrow, ventral. Scale bar, 10 μm.

Figure 33. Rank #10, SEM. Dorsal view of anterior part of larva. Scale bar, 10 μm.

Figure 34. Rank #10, SEM. Left lateral view of larva. Scale bar, 50 μm. BF, branchial filament; CBF, coelom of branchial filament; CR, ciliary row(s); CS, capillary seta; CVP, coelom of ventral process; GA, giant axon; GC, glial cell bodies; LBF, larval branchial filament; LH, larval hook; MO, mouth; MS, myelin sheath; NE, neurites; OS, opisthosomal setae; PN, pinnule(s); VC, ventral ciliated field; VP, ventral process.

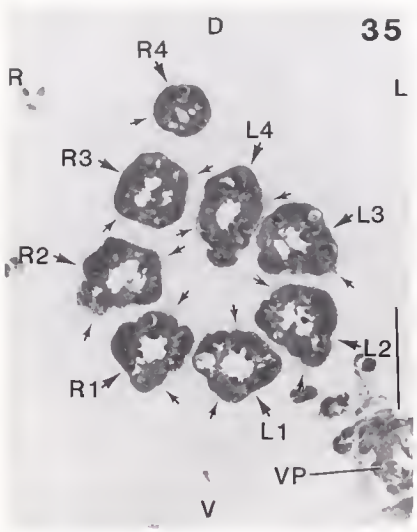
35
D
R4
R
L
L4
R3
L3
R2
L2
R1
L1
VP
V

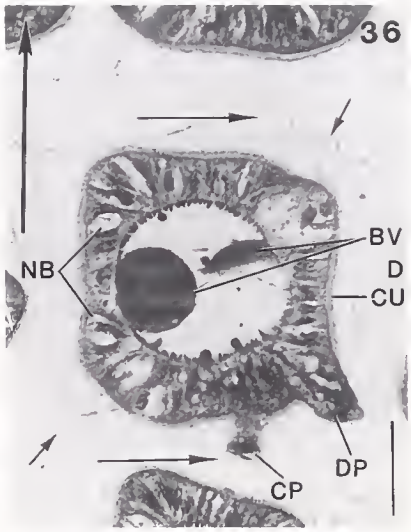
36
BV
NB
D
CU
DP
CP

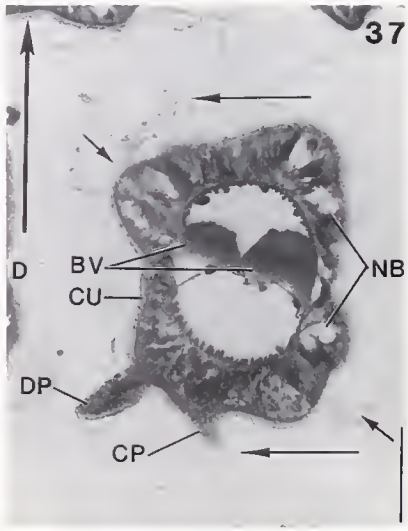
37
D
BV
NB
CU
DP
CP

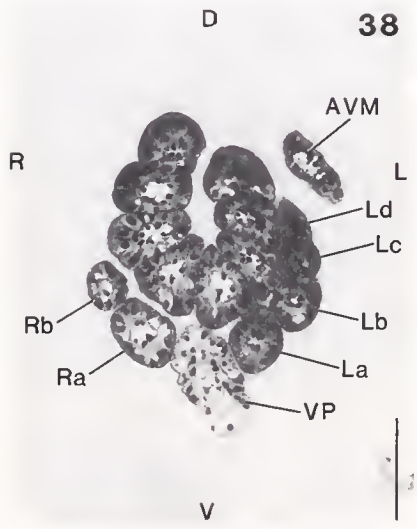
38
D
AVM
R
L
Ld
Lc
Rb
Lb
Ra
La
VP
V

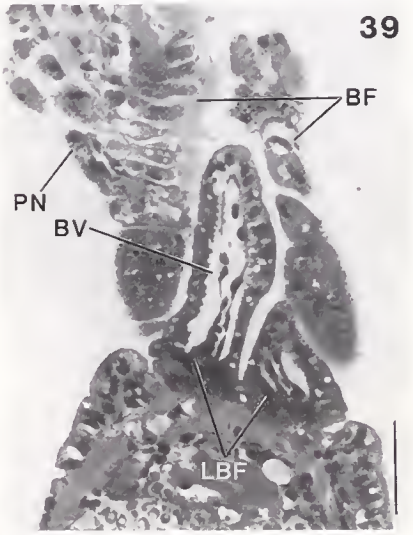
39
BF
PN
BV
LBF

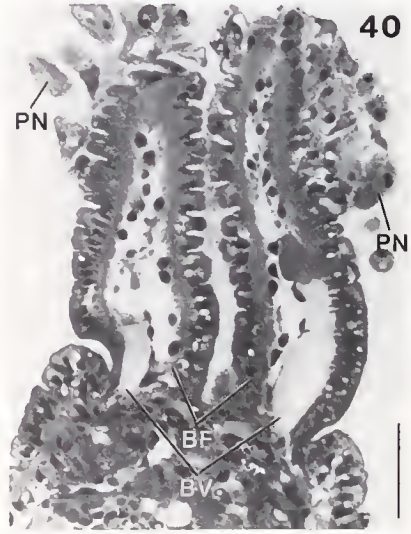
40
PN
PN
BF
BV

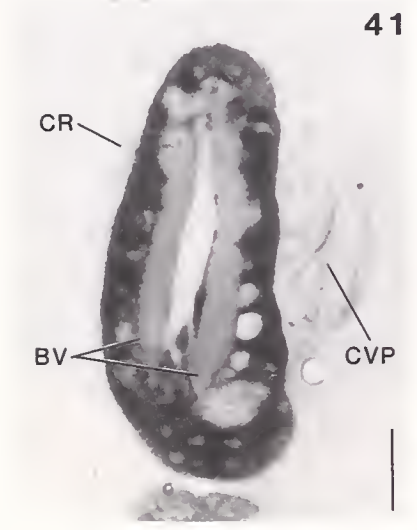
41
CR
BV
CVP

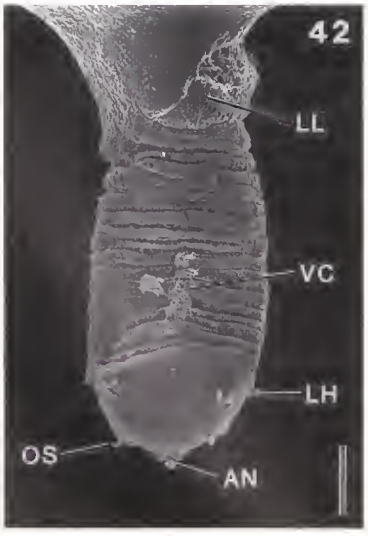
42
LL
VC
LH
OS
AN

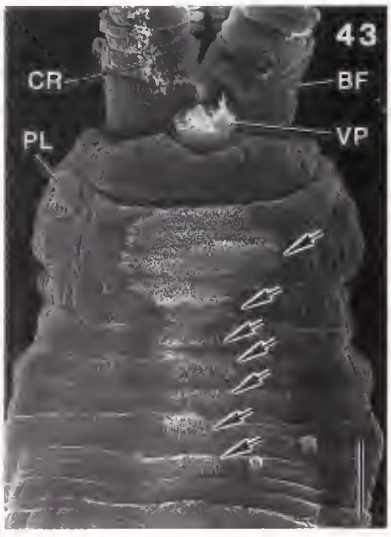
43
CR
BF
PL
VP

observed in sections of other, older, larvae. Subsequent juvenile branchial filaments develop after formation of the ventral process and mouth and, initially, are provided with two rows of pinnules on their dorsal surface and ciliary tracts on their dorsomedial and ventrolateral surfaces (Figs. 33, 34, PN, CR). The second, as well as subsequent, juvenile branchial filaments initially develop with the same disposition of pinnules and ciliary tracts as the first filaments (Figs. 8, 51, PN, CR). At about the time of appearance of the second pair of juvenile branchial filaments, the first pair of branchial filaments appears to undergo a reorientation of pinnules, which become more lateral (Fig. 8, PN), and of ventrolateral ciliary tracts, which become more ventral (Fig. 43, CR). The reorientation continues until, at a point where four pairs of branchial filaments are present in the first branchial lamella, pinnules are situated on the outer faces of filaments (Fig. 35, large arrows) and ciliary tracts are situated adjacent to the rows of pinnules, ventral or lateral, and on the surface of the filaments, directly opposite each other (Fig. 35, small arrows). This disposition of rows of cilia is continued throughout the life of the worm (Figs. 36, 37, small arrows). In adults, two rows of pinnules are on the outer face of the filament, one row is central and the other is displaced to the outer dorsal area (Figs. 36, 37, CP, DP). It may also be noted that each filament carries two bundles of nerves just below the ventral-facing surface, that the pair of branchial blood vessels is in line with the axis of the lamella, that the cuticle, generally rather thick, is quite thin over the ciliated cells and over the surface of the pinnules (Figs. 36, 39, NB, BV, CU), and that right branchial filaments are mirror images of left filaments (Figs. 35–37).

Branchial filaments are added in paired rows (Figs. 35, 38) that are the forerunners of the branchial lamellae of older specimens. The oldest filaments of a lamellar series are ventral and medial, adjacent and lateral to the ventral process or dorsal to it (Figs. 9, DBF; 35, R1, L1; 38, Ra, La), and younger filaments are added laterally and dorsally (Figs. 35, R4, L4; 38, Rb, Ld). Subsequent lamellae develop in the same manner, outside the previous lamellae (Figs. 38, 46). Relative to later-developing branchial filaments, larval filaments appear to lack well-developed longitudinal muscles, as well as pinnules (Figs. 39, 40). In earlier stages (#'s 3–9), larval branchial filaments are the primary respiratory surface for developing *Ridgeia* and are so served by simple vascular loops (Fig. 41). Later, respiratory surfaces are enhanced by the development of elongated filaments bearing pinnules (Fig. 40). Figure 54 discloses that, after they appear, there is a modest increase in the number of branchial filaments, to about eight, until a length of about 0.5 mm, after which the number of filaments is great enough to preclude their being counted.

Ventral ciliated field. There is no neurotroch on the trochophore. Up to nine tufts of cilia, linearly arranged and, perhaps, representing a late-developing neurotroch (from #3 on), are present on the mid-ventral surface of

---

Figure 35. *Ridgeia* sp. CB1-nr. #23, transverse section, epon, 2.0 μm. Cross-section, four pairs of branchial filaments. L1 (oldest)—L4 (youngest), left filaments; R1 (oldest)—R4 (youngest), right filaments; large arrows, general location of pinnules; small arrows, location of ciliary rows. Scale bar, 50 μm.

Figure 36. *Ridgeia piscesae*, USNM No. 98106, adult, transverse section, paraffin, 5 μm. Cross-section, left branchial filament. Large/thick arrow, direction to longitudinal axis of worm; long/thin arrows, direction of effective stroke of ciliary rows, *Riftia pachyptila*; short arrows, location of ciliary rows. Scale bar, 30 μm.

Figure 37. *Ridgeia piscesae*, USNM No. 98106, adult, transverse section, paraffin, 5 μm. Cross-section, right branchial filament. Large/thick arrow, direction to longitudinal axis of worm; long/thin arrows, direction of effective stroke of ciliary rows, *Riftia pachyptila*; short arrows, location of ciliary rows. Scale bar, 30 μm.

Figure 38. *Ridgeia* sp. CB1-nr. #23, transverse section, epon, 2.0 μm. Cross-section, base of branchial plume, two pairs of branchial lamellae (proximal to Fig. 35). La (oldest)—Ld (youngest) filaments of second left lamella; Ra (older)—Rb (younger) filaments of second right lamella. Scale bar, 50 μm.

Figure 39. Rank CB7-nr. #20, frontal section, epon, 2.0 μm. Base of larval branchial filaments. Scale bar, 30 μm.

Figure 40. Rank CB7-nr. #20, frontal section, epon, 2.0 μm. Base of branchial filaments. Scale bar, 30 μm.

Figure 41. Rank F-nr. #10, longitudinal section, epon, 1.5 μm. Larval branchial filament, showing vascular loop. Scale bar, 10 μm.

Figure 42. Rank #9, SEM. Ventral view showing posterior position of segmented ventral ciliated field. Scale bar, 30 μm.

Figure 43. Rank #20, SEM. Ventral view, showing segmented ventral ciliated field (arrows); ventral process damaged. Scale bar, 30 μm. AN, anus; AVM, anterior vestimental margin; BF, branchial filament(s); BV, blood vessel(s); CP, central pinnule; CR, ciliary row; CU, cuticle; CVP, cilia of ventral process; D, dorsal; DP, dorsal pinnule; L, left; LBF, larval branchial filaments; LH, larval hook; LL, lower lip; NB, nerve bundles; OS, opisthosomal seta; PL, vestimental plaque; PN, pinnule; R, right; V, ventral; VC, ventral ciliated field; VP, ventral process.

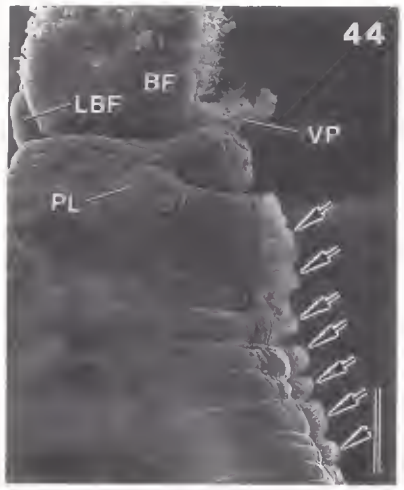

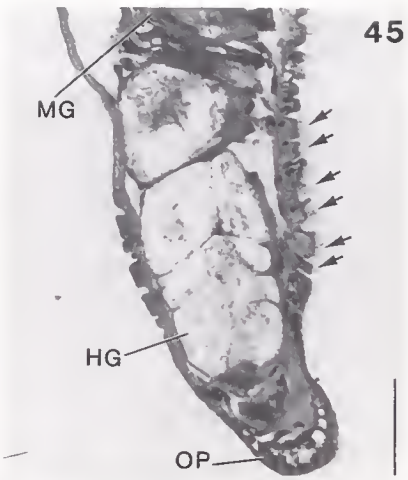

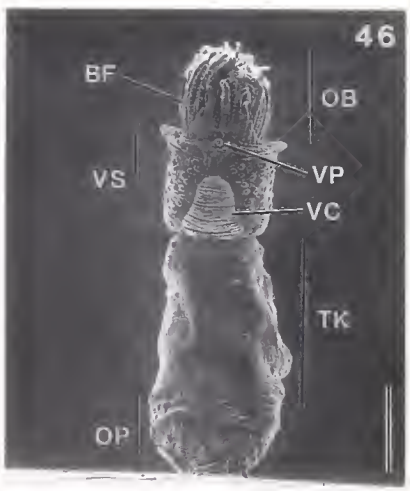

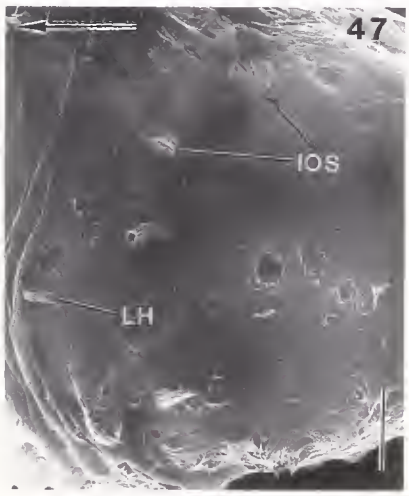

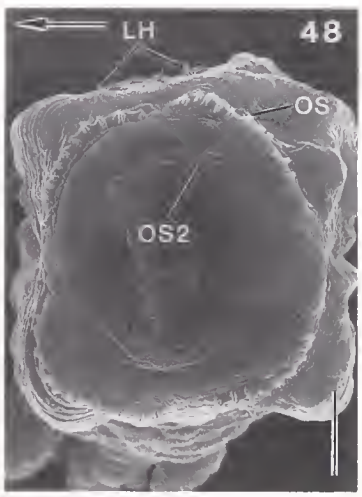

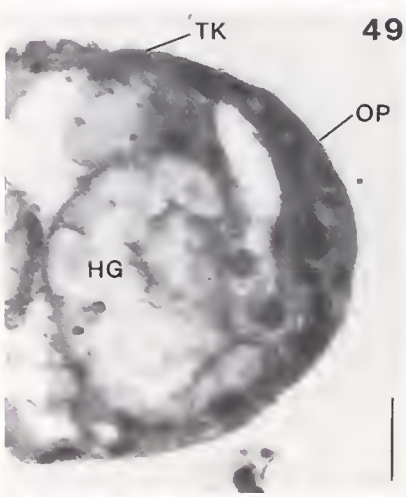

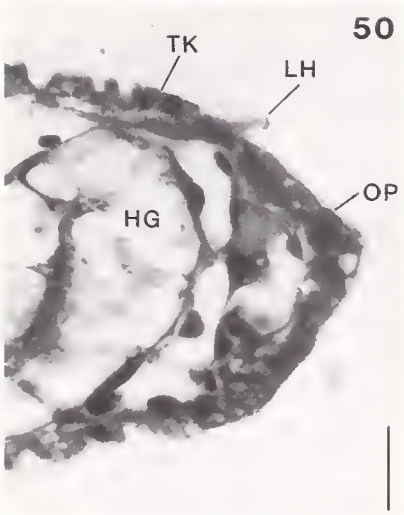

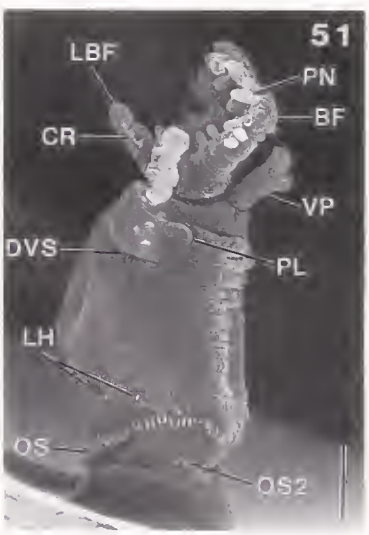

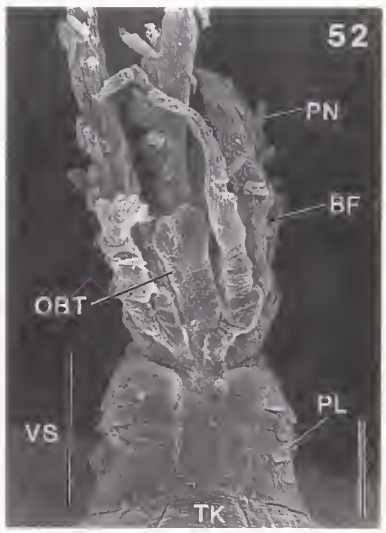

Figure 44. *Rudgeia* sp. Rank #20, SEM. Right lateral view, showing segmented ventral ciliated field (arrows); ventral process damaged. Scale bar, 30 μm.

Figure 45. Rank D-nr. #13, sagittal section, epon, 1.5 μm. Segmented ventral ciliated field (arrows). Scale bar, 30 μm.

Figure 46. Rank #33, SEM. Ventral view, showing fused ventral ciliated field. Scale bar, 30 μm.

the posterior one-half to one-third of the vestimentum-trunk of larvae and young juveniles (Fig. 42, VC); these tufts ultimately fuse to form the pear-shaped ventral ciliated field of adults (Fig. 1, VC). Although the tufts present the appearance of being segmentally arranged (Figs. 43, 44, arrows), sagittal sections through the tufts and the body wall do not reveal any indication of internal segmentation (Fig. 45, arrows). In early stages, the tufts overlie the trunk cavity and are displaced anteriorly by differential growth of the posterior trunk region. By the time the vestimentum is formed, the ciliated tufts, laterally expanded, are fused to form the ventral ciliated field (Fig. 46, VC). Figure 55 reveals that the linearly segmented ventral ciliated field persists in specimens of up to about 0.5 mm in length and the pear-shaped field of adults is present in juveniles of greater length.

Opisthosomal setae. These are confined to the anterior opisthosomal segments. As in adults, they bear two groups of denticles, the larger group projecting anteriorly and the smaller, posteriorly (Figs. 30, 31, OS; see also Jones, 1985c, Figs. 15, 48, 52). The first opisthosomal setae of juveniles may bear a superficial resemblance to larval setae and have a single set of denticles (Fig. 47, IOS). Opisthosomal setae develop in transverse rows in the four quadrants of the body (Fig. 48, OS), and those of each side meet laterally; setal rows do not appear to meet dorsally or ventrally. Semi-thin sections of the posterior end of an early larva show that, prior to the appearance of the first row of opisthosomal setae, the opisthosome is undeveloped (Fig. 49, G-nr. #4). At the time of development of the first opisthosomal setae, internal segmentation has commenced (Fig. 50, F-nr. #10). Figure 56 shows that, until juveniles are about 1.0 mm long, there are usually up to four rows of opisthosomal setae, and it is only when a length of about 2.0 mm has been attained that the number of rows of setae begins to increase rapidly; there is a quite apparent variability in the development of setal rows (see Discussion, below).

Vestimentum. Development of the vestimentum is visible externally by the delineation of a pair of dorsolateral longitudinal ridges just posterior to the branchial filaments (Fig. 51, DVS). Further development leads to an extension of the posterior ends of these ridges, laterally and ventrally, to the posterior edge of the ventral ciliated field (Fig. 46). The presence of plaques also indicates the establishment of the vestimentum (Figs. 9, 43, 44, 51, PL). Much later (#36, >2.00 mm), a flange-like posterior vestimental margin, free of the trunk, is developed (Fig. 1, arrow). Figure 57 indicates that the vestimentum is established when juveniles are 0.44 mm in length and it may be developing from a juvenile-length of 0.18 mm.

Obturaculum. The developing obturaculum has not been observed among these larval and juvenile *Ridgeia.* Most probably its development is similar to that of *Riftia* (Fig. 52, OBT) where paired, medially fused, thin lobes, each about the diameter of a branchial filament, develop on the mid-line, dorsal to all branchial filaments. Figure 58 shows that the obturaculum of *Ridgeia* is not present up to a juvenile length of about 0.5 mm; its development may be initiated during the next 0.5 mm of growth. In the case of lengths greater than 1.0 mm, the obturaculum is present to support the developing branchial filaments.

Discussion

Trochophore

The discovery of a trochophore larval stage in the life history of a vestimentiferan provides an explanation of the geographical distribution of certain species of these worms. Vent fields may occur at 100–200 km intervals (Crane, 1985). Hydrothermal vents, to which most vestimentiferan species appear to be restricted, are discrete environments that, in the same general hydrothermal field, may be as close as 3 km to one another (on the Galapagos Rift: Rose Garden site to Mussel Bed site, about 10 km; Mussel Bed to Garden of Eden site, about 3 km) (J. F. Grassle, 1986) or as far apart as the Galapagos Rift and 13°N on the East Pacific Rise (EPR) (about

Figure 47. Rank #17, SEM. Lateral view, trunk/opisthosomal region showing profile of initial opisthosomal seta. Arrow, anterior. Scale bar, 10 μm.

Figure 48. Rank nr. #21, SEM. Posterior view of opisthosome, showing disposition of four sectors of opisthosomal setae. Arrow, ventral. Scale bar, 30 μm.

Figure 49. Rank G-nr. #4, sagittal section, epon, 1.5 μm. Section through undeveloped opisthosome. Scale bar, 10 μm.

Figure 50. Rank F-nr. #10, sagittal section, epon, 1.5 μm. Section through developing opisthosome. Scale bar, 10 μm.

Figure 51. Rank #16, SEM. Right lateral view, showing developing vestimentum. Scale bar, 50 μm.

Figure 52. *Riftia pachyptila,* SEM. Dorsal view, showing developing obturaculum. Scale bar, 100 μm. BF, branchial filament(s); CR, ciliary row; DVS, developing vestimentum; HG, hindgut; IOS, initial opisthosomal setae; LBF, larval branchial filament; LH, larval hook(s); MG, midgut; OB, obturacular region; OBT, obturaculum; OP, opisthosome or opisthosomal region; OS, opisthosomal setae, first row; OS2, opisthosomal setae, second row; PL, vestimental plaque; PN, pinnule; TK, trunk; VC, ventral ciliated field; VP, ventral process; VS, vestimentum.

2500 km farther northwest) and 21°N on the EPR (about 1100 km yet farther northwest), with *Riftia pachyptila* being common to all of these localities. The trochophore represents a life stage that can be transported by sea-bottom currents to maintain genetic continuity between widespread populations of a single species.

This particular specimen of *Ridgeia* (Fig. 2) was washed from among adult tubes and, apparently having settled, had not yet developed to the point where it was permanently in place, *i.e.*, in a tube affixed to a solid substratum. The development of larval setae (Fig. 29) suggests that this trochophore had developed sufficiently so that it was nearly ready to secrete a tube that would allow the proper functioning of the larval hooks in maintaining the larva within its tube.

If, as is thought, vestimentiferans fall into the Gastroneuralia, as used by Nielsen (1987), compound cilia are to be expected in the prototroch of *Ridgeia*. That they are not present may well be due to the incidental cavalier treatment received during fixation on shipboard, when the first thought was to preserve the whole sample, primarily adults. Nielsen (1987, p. 206) specifically states that a special, gentle preservation is necessary to maintain the integrity of compound cilia.

Although Southward (1988b) had no specimens smaller than nr. #5 and #6, she compared her smallest with the patterns of ciliation noted by Nielsen (1987) and suggested that the vestimentiferan larva belongs to the "trochophore type." We confirm her suggestion.

We were able to examine only one specimen that was young enough to be identified as a trochophore larva. Although this specimen lacks openings into the digestive system, as well as an apical ciliary tuft, neurotroch, metatroch, and telotroch, the complete ring of cilia situated near the apical end, which is the characteristic position and appearance of a prototroch, confirms the larva's identity as a trochophore. The presence of larval hooks suggests that it is a late trochophore and confirms that it is a larval vestimentiferan. The absence of digestive openings is possibly correlated with the young age of the specimen, whereas the absence of ciliary bands, other than the prototroch, could be related to age of the specimen or could reflect developmental features specific to vestimentiferans. The presence of a larva of the trochophore type in the early development of vestimentiferans provides additional evidence for the belief that vestimentiferans should be placed along the evolutionary line that includes annelids, molluscs and other smaller groups of protostomes.

Ventral process and gut

On the basis of our observations, we suggest that the prototroch and pretrochal region of the trochophore are intimately involved in the formation of the ventral process. The gut appears to develop at about the same time, but the anal opening may occur early or late in development, as reflected by length (Table 1).

The pathway of the foregut through the brain to the trophosome has been established (Jones and Gardiner, 1988; Southward, 1988b; Jones, 1988b); the ventral process has been reported to be present in juveniles of *Riftia* up to 15.5 mm in overall length but is not present in young adults of about 111 mm overall length (Jones and Gardiner, 1988). In the latter, and in still older specimens, the track of the foregut, now apparently closed and functionless, can be traced through the brain and vestimental musculature to the trophosome (pers. obs., MLJ).

TEM examination of cross-sections of the cilia of the lower lip indicates that the effective stroke of these cilia is inward (pers. obs., SLG), thus justifying our contention that the mouth, indeed, might be employed in picking up free-living bacteria and/or other particulate food material. Jones and Gardiner (1988) noted that cells of the foregut are multiciliated. Southward (1988b) suggested that, prior to the installation of symbiotic bacteria, *Ridgeia* larvae are ciliary feeders; she noted, in a small specimen (nr. #9), that bacteria were in the wall of the gut, ". . . apparently undergoing digestion . . ." and that rod-shaped bacteria were present in the opisthosomal hindgut. These observations suggest at least three possibilities concerning the intracellular bacteria: (1) if all bacteria are endosymbionts, then the digestion of some by the worm indicates the early use of the endosymbionts as a food source; (2) if all bacteria are not endosymbionts, then the digestive process has been initiated for some but not for others and would confirm an early phase of ciliary feeding by the larvae; and (3) if the undigested bacteria are endosymbionts and the digested bacteria are not endosymbionts, then a period of overlap occurs between the phase of ciliary feeding and the full establishment of the symbiotic association.

There are indications that the mouth/foregut, even though morphologically developed, may not be open until H-nr. #15, based on the presence of endosymbionts. This is supported by the fact that the midgut wall, in younger, sectioned individuals, is devoid of bacterial symbionts (Table I, Figs. 21, 45; Jones and Gardiner, 1988, Fig. 7C). Likewise, the anus, although present at #7 and #9, does not appear to open to the exterior until C-nr. #21, based on light microscopy. In a small individual (G-nr. #4) we have observed a presumptive mouth and a gut, but the anus is totally lacking.

Southward (1988b) stated that, based on sections, a mouth, complete gut, and anus were present in a two-filament-stage larva (RJ, nr. #9); no trophosome was, as yet, present (see *Delayed settlement*, below).

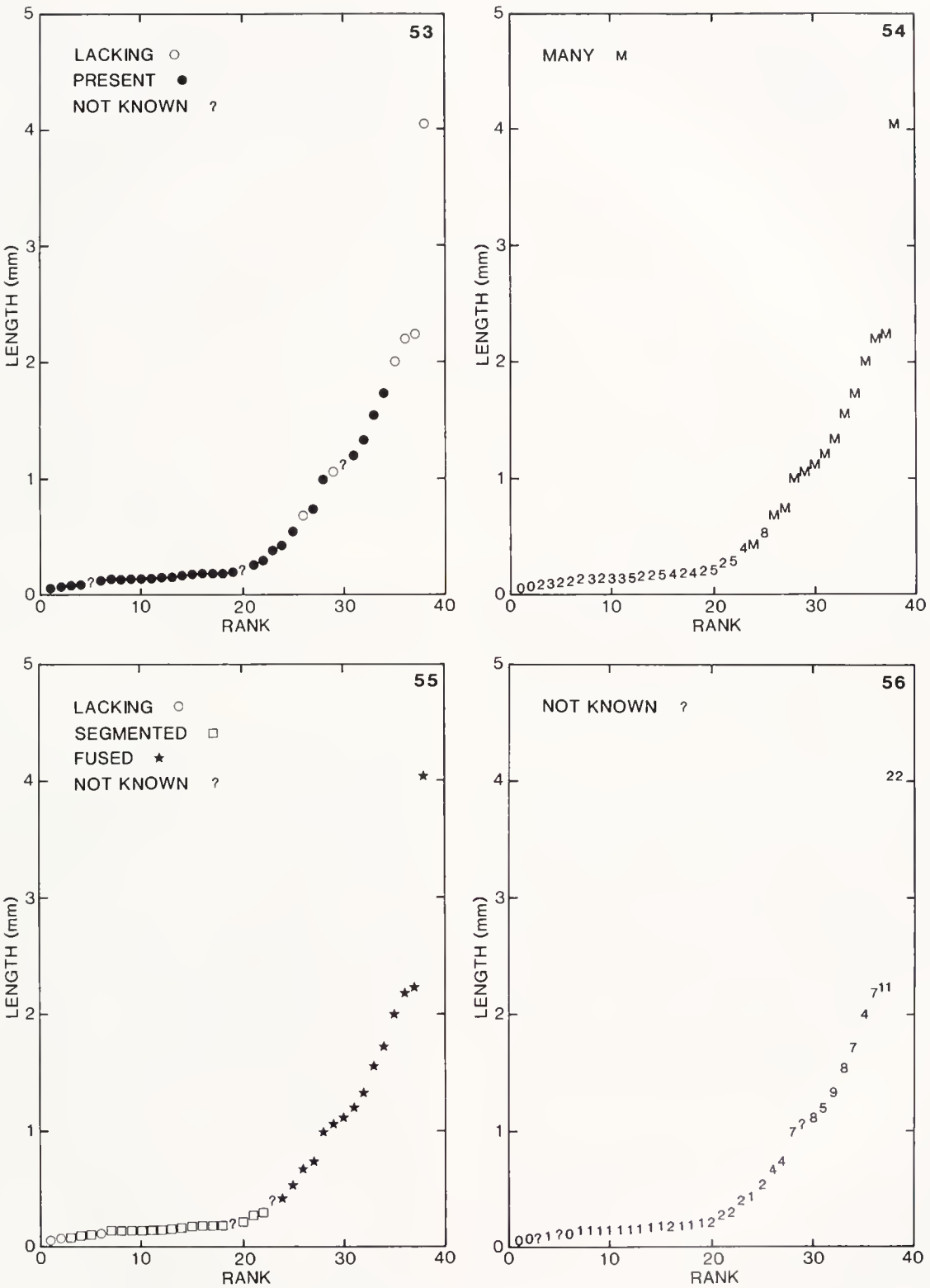

Figure 53. *Ridgeia* sp. Presence of larval setae among SEM specimens, ranked by length.
Figure 54. Numbers of branchial filaments among SEM specimens, ranked by length.
Figure 55. State of ventral ciliated field among SEM specimens, ranked by length.
Figure 56. Number of rows, opisthosomal setae, among SEM specimens, ranked by length.

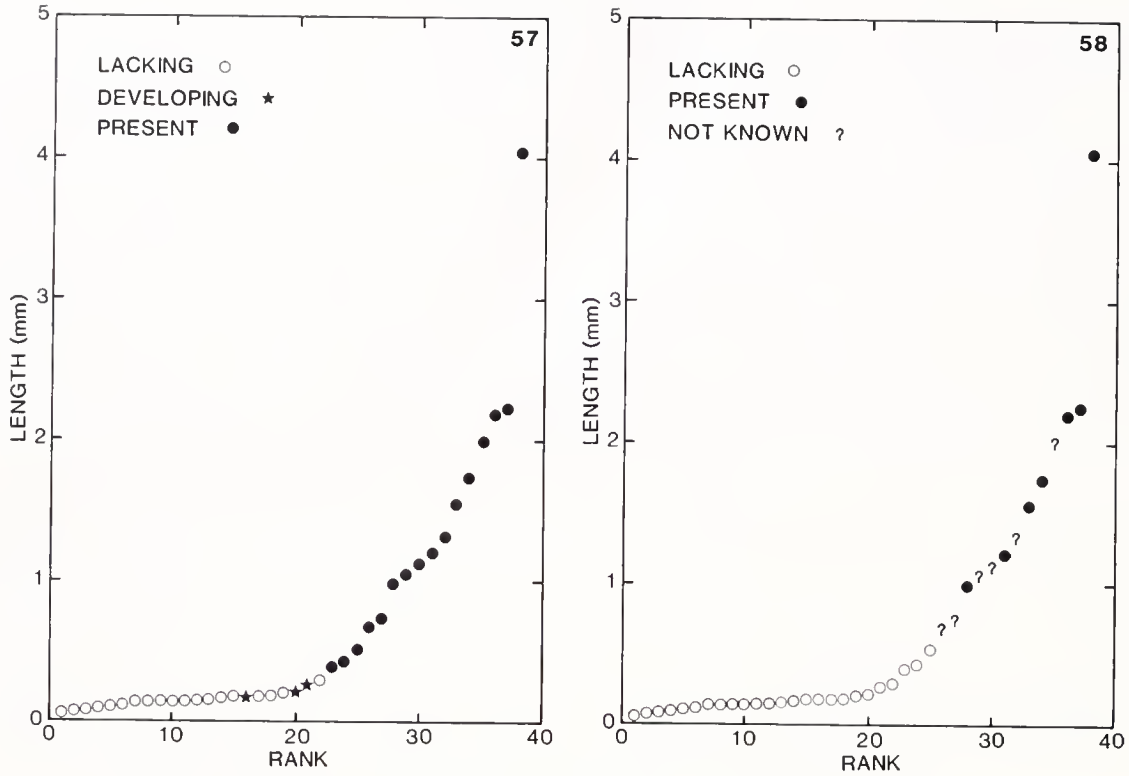

Figure 57. *Ridgeia* sp. Condition of vestimentum among SEM specimens, ranked by length.
Figure 58. Presence of obturaculum among SEM specimens, ranked by length.

Bacterial endosymbionts

Although we have not, as yet, reconstructed serial thin-sections and counted total numbers of bacteria in bacteriocytes, we have observed by TEM as many as 35 bacteria in a single section of a bacteriocyte. In this case, the bacteria occupied approximately 40% of the total area. Jones (1988b) elucidated details of the vascular system of the trophosome and observed that, in one instance, no bacterium was separated from a capillary by more than three bacteria. A chemoautotrophic mode of nutrition has been suggested for the bacteria in the trophosome of vestimentiferans (for extensive literature, see Jones and Bright, 1985, and Felbeck and Childress, 1988).

In previous accounts (Jones, 1988b; Jones and Gardiner, 1988), we suggested that the association between bacteria and the vestimentiferans *Riftia pachyptila, Oasisia alvinae,* and *Ridgeia* sp. begins with the ingestion of free-living bacteria, from surfaces available to the larvae/juveniles or from the waters surrounding the vent communities, into the transient digestive system of the worm. Once inside the gut, the appropriate bacterial strain, *i.e.,* sulfide-oxidizing, is phagocytized by midgut epithelial cells to establish the symbiotic association. Presumably other bacteria, non-essential to the vestimentiferan, not prospective endosymbionts, may be digested and used as a food source until the endosymbiotic association is established and the gut regresses.

Jannasch and Wirsen (1979) reported the presence of at least 200 different strains of free-living bacteria in vent waters and noted that most strains oxidized hydrogen sulfide or thiosulfate as their energy source. Oxidation of sulfide has been suggested as an energy source also for the endosymbiotic bacteria in *R. pachyptila* (see Arp *et al.,* 1985, for references). Distel *et al.* (1988) examined the 16S rRNA sequences of endosymbiotic bacteria from several invertebrate hosts, including *R. pachyptila.* Their data indicate that, in all cases, the host contains a single type of endosymbiont and hosts from different geographic localities possess similar types of endosymbionts. Based on these data, they concluded that the mechanism of selection of potential endosymbionts from the surrounding environment or the mechanism of transmittal of endosymbionts to new individuals must be specific. They suggested three possible mechanisms: (1) the symbiont is passed to the egg during spawning, (2) the symbiont is selected by the host during early development, and (3) the symbiont uses a host-specific "infection" (their quotation marks) mechanism.

At present, passing of endosymbionts to eggs during

spawning appears unlikely. Our TEM observations of eggs of *R. pachyptila* taken from just inside the aperture of the oviduct have not revealed the presence of endosymbionts in the egg cytoplasm or nuclei (pers. obs., SLG). TEM observations of freshly spawned eggs of *R. pachyptila* also have failed to reveal the presence of endosymbionts (Cary *et al.*, 1989). The method of establishment of the symbiotic association outlined by Jones (1988b) and Jones and Gardiner (1988) conforms to the second mechanism of Distel *et al.* (1988). However, this method also implies that midgut cells of larval/juvenile vestimentiferans are capable of distinguishing between potential endosymbionts and other, non-essential, bacteria; this method of recognition has not yet been determined.

We suggest the following possible sequence of events in the establishment of the symbiotic association: (1) engulfment of bacteria by the ventral process and their passage into the gut; (2) growth of one specific strain of bacteria close to midgut epithelial cells; and (3) phagocytosis of colonies of bacteria by midgut cells.

Nervous system

In his original description of *Lamellibrachia barhami*, Webb (1969) described the presence of a pair of tubes in the nerve cords in the vestimental region of that species. He indicated that these tubes ". . . enter the substance of the brain as very fine tubules" and that the nerve cord of the trunk contains a single tube throughout its length.

Van der Land and Nørrevang (1977) presented detailed descriptions of the organization and histology of fluid-filled "neurular tubes" in the nervous system of *Lamellibrachia luymesi*. They demonstrated that the arrangement of the tubes is similar to that described by Webb for *L. barhami*, except that a single tube extends only a short distance into the trunk region; the remaining nerve cord of the trunk lacks a neurular tube. They stated that, in the area of the brain, the tubes give off one or two side branches, which could correspond with Webb's observation. Because the opisthosome was not present on the specimens examined by Webb (see Jones, 1981a, p. 1310, 1985c, pp. 122–123) and by van der Land and Nørrevang, they could not comment on the organization of the nerve cord in that region. The wall of the tubes was described by van der Land and Nørrevang as "dense" and consisting of concentric fibers or lamellae in which nuclei are embedded.

Following the terminology of van der Land and Nørrevang (1977), Jones (1981a) described the organization of "neurular tubes" in *Riftia pachyptila*. In the vestimentum and trunk, the organization of the tubes reflects that of *L. barhami*. Because the opisthosome was present in Jones' specimens, he added the observation that the nerve cord in that region lacks a neurular tube.

Among invertebrates (excluding the "invertebrate chordate" groups), neural tubes of varying construction have been reported in the nervous systems of some Nemertea, Sipuncula, Echiura, and Hemichordata, whereas giant axons, which may present the morphological appearance of neural tubes in the light microscope, have been reported in some Nemertea, Phoronida, Sipuncula, Polychaeta, Oligochaeta, Cephalopoda, and Crustacea (for additional details and references, see Bullock and Horridge, 1965). Our TEM examination of the nerve cord of *Ridgeia* confirms the presence of paired giant axons in the paired nerve cords of the vestimentum and a single giant axon in the nerve cord of the trunk. We suggest that the nerve cords of *Lamellibrachia barhami* and *L. luymesi* be re-examined by TEM to confirm the presence of "tubes" or "neurular tubes," as reported by Webb (1969) and van der Land and Nørrevang (1977), respectively, or giant axons, as suggested by our study of *Ridgeia*. The description of the wall of the neurular tube in *L. luymesi* by van der Land and Nørrevang (1977) is consistent with the morphological appearance of the myelin sheath around the giant axons of *Ridgeia* and *R. pachyptila*, when viewed by TEM. This observation suggests that giant axons are present in *L. luymesi*. In the case of *Riftia pachyptila*, the nerve cord of the trunk has been examined by TEM (pers. obs., SLG) and the so-called "neurular tube" reported by Jones (1981a) is a giant axon surrounded by a myelin sheath.

Several alternatives may be suggested to explain the presence of two giant axons in the vestimentum and only a single axon in the trunk of *Ridgeia* and, presumably, all vestimentiferans. The single giant axon in the trunk may represent (1) the continuation of one of the giant axons that originate in the brain, (2) a third giant axon whose cell body is situated in the nerve cord near the border between the vestimentum and trunk, or (3) the product of the fusion of the two giant axons that originate in the brain. Fusion of giant axons has been reported in the nervous systems of other invertebrate groups, *e.g.*, cephalopods (Bullock and Horridge, 1965). In their description of the "neurular tubes" in *L. luymesi*, van der Land and Nørrevang (1977) included a reconstruction that shows the fusion of the tubes of the vestimentum to form the single tube of the trunk (near the posterior margin of the ventral ciliated field). Our preliminary examination of serial semi-thin sections (1.5 μm) of *Ridgeia* appears to support van der Land and Nørrevang's observation of fusion. However, additional light microscopic and TEM observations are required to confirm the exact nature of the organization of the giant axons in *Ridgeia*.

Giant axons are particularly well-developed among tube-dwelling animals, *e.g.*, the phoronids and the sabellid and serpulid polychaetes (Bullock and Horridge, 1965) and are frequently implicated as an important

component in the "startle response" of those animals, *e.g.*, the polychaete *Myxicola* (Nicol, 1948). A withdrawal response has been observed *in situ* in the case of *Riftia pachyptila* (pers. obs., MLJ). We suggest that the giant axons in vestimentiferan nervous systems have an important role in this response. In that regard, the myelin sheath observed around the giant axons of *Ridgeia* and *R. pachyptila* would enhance the speed of conduction of a nerve impulse in a manner analogous to the myelin sheath of vertebrate nerves (for additional discussion and references, see Jamieson, 1981).

Further development of larvae and juveniles

Of the characters of adult morphology followed in this study, the ventral ciliated field, vestimentum, and obturaculum are all established at a length (from prototroch or base of branchial filaments to posterior end) of 1.0 mm. There is a consistency of development of the ventral ciliated field from its "segmented" state to the fused field of the adult (Table I). Likewise, once the obturaculum appears during growth, it is always present, although it may be obscured by overlying branchial filaments. The vestimentum begins differentiation at a length of about 0.18 mm and is present, then, after a length of about 0.4 mm. There is a certain amount of variation in the initiation of vestimental development between specimens of 0.18 and 0.4 mm in length (Table I). Larval setae, having fulfilled their apparent function in providing an early holdfast for the developing larva, are of variable occurrence as they are worn, discarded, or extracted. The number of rows of opisthosomal setae remains approximately constant at one or two, until a length of about 0.5 mm, and then new rows are added with considerable variation among specimens (see *Delayed settlement*, below). Branchial filaments develop in much the same manner, except that the variability in addition occurs earlier in development, at a length of about 0.16 mm.

Delayed settlement

Of the speculations concerning the dispersion of the larvae of bivalved molluscs of the hydrothermal vents, there is a consensus that the mussel, *Bathymodiolus thermophilus*, has a pelagic (J. P. Grassle, 1985) or planktotrophic (Lutz *et al.*, 1980; Berg, 1985; Turner *et al.*, 1985; Lutz, 1988) stage that may be epipelagic (Berg, 1985) or demersal (Lutz *et al.*, 1980; Turner *et al.*, 1985). The possibility of delayed settlement of such planktotrophic larvae has been suggested by Lutz *et al.* (1980). Warén and Bouchet (1989) have concluded that gastropods of the hydrothermal vents have a lecithotrophic development and can delay settlement until the proper habitat is encountered. Van Dover *et al.* (1985) have suggested a planktotrophic stage for the crab *Bythograea thermydron* and the shrimp *Alvinocaris lusca* and mention the possibility of delayed settlement for these species.

Southward (1988b) proposed that, in the case of *Ridgeia* sp., there is early ciliary feeding in developing larvae or juveniles but did not indicate whether this would take place in a pelagic or a demersal phase. Cary *et al.* (1989) observed that spawned eggs of *Riftia pachyptila* have a positive buoyancy due, in large part, to a considerable amount of cytoplasmic lipids. They suggest a pelagic development in *Riftia*, either planktotrophic, based on the small size of eggs, or lecithotrophic, based on the lipid content of the eggs (about half of the cytoplasmic volume). They further suggest that, as development proceeds, buoyancy decreases and that, ultimately, the developing *Riftia* return to the sea floor and settle in response to cues noted by Lutz *et al.* (1980), in the case of *Bathymodiolus*.

The preceding observations bear on the following discussion.

Based upon the nine specimens sectioned (Table I), there is no apparent consistency in the presence of an anus or of internal bacteria, during development, as reflected by length. Specimens G-nr. #4 and E-nr. #16 lack an anus and bacteria; H-nr. #15 and A-nr. #21 have both an anus and bacteria; B-nr. #15 and C-nr. #21 have an anus but lack bacteria. These inconsistencies might have a reasonable explanation.

It may be assumed that a developing embryo of *Ridgeia* will be positively buoyant (Cary *et al.*, 1989). As a mouthless trochophore among the plankton, lecithotrophic development can proceed only so far and further development would be postponed until a vent site is encountered (Warén and Bouchet, 1989). If there is further development in the plankton, resulting in the formation of the ventral process and the mouth, a planktotrophic phase would be initiated (Berg, 1985; Turner *et al.*, 1985; Lutz, 1988), ciliary feeding would be possible (Southward, 1988b), and a later anal opening for the gut would establish an efficient, one-way digestive tract; along with this, there might be a reduction of larval buoyancy (Cary *et al.*, 1989). Upon finding a hydrothermal vent, using cues like those suggested by Lutz *et al.* (1980), and settling there, the developing larva would be able to acquire sulfide-oxidizing bacteria for its trophosome. Because the trophosome will become internally isolated, there would now be no necessity for a hindgut or an anus; these could be resorbed and, over time, the ventral process, the mouth, and the foregut could be resorbed or become atrophied. Under this scheme the larval branchial filaments would serve as relatively simple respiratory surfaces for an early larva still using its original supply of yolk or a later form, now feeding by cilia. The later branchial filaments, with their better-developed rows of cilia and the augmented respiratory surface afforded by

rows of pinnules, would serve as efficient structures for taking up, among other things, sulfide (for the endosymbiotic bacteria) and oxygen (for both the bacteria and the worm), both of which are crucial for the survival of the worm. If the developing larva does not quickly encounter a hydrothermal vent, then it can survive by maintaining ciliary feeding, grows more than it might otherwise and, when finally arrived at a vent site, proceeds with the acquisition of bacteria and the closing of the anal opening at a more advanced stage of development and at a length greater than its early-arriving neighbors. The following is suggested, in summary (Table I):

1. G-nr. #4, F-nr. #10, D-nr. #13, E-nr. #16, at the time of preservation, were still using yolk for nutrition or were feeding by cilia (no anus, no bacteria);
2. H-nr. #15 and A-nr. #21 had obtained endosymbiotic bacteria and the anus could atrophy (with anus, with bacteria);
3. B-nr. #15 and C-nr. #21 were still ciliary feeders, newly arrived at the vent site, not yet with endosymbionts (with anus, no bacteria).

Applying these summary statements, it might be that a larger size than expected, as in the case of D-nr. #13, A-nr. #21, and C-nr. #21 (relative to G-nr. #4, H-nr. #15, and B-nr. #15, respectively), suggests a delayed settlement. In addition, E-nr. #16, apart from size, has characters that might place it near #7 or #8 (Table I); D-nr. #13 (Fig. 21) and C-nr. #21 (Fig. 23) show about the same relative development of the ventral process; and #31 and #35 (Table I) have fewer rows of opisthosomal setae than might be expected; perhaps E-nr. #16, C-nr. #21, #31 and #35 all had a delayed settlement, as well. Further, #5 (Fig. 6) and #14 (Fig. 7) have about the same development of the ventral process, whereas #15 (Fig. 8), although of about the same length as #14, has a much better developed ventral process and its branchial filaments appear to be further along in development; this suggests that #14 might have had a delayed settlement. Of Southward's specimens RB (nr. #32) and RC (nr. #33), both about the same length (Southward, 1988b), RC agrees best with the ranked specimens near #33, as regards development of characters, and RB would fit better at about #25; perhaps RB had a delayed settlement. Finally, Southward's specimen RJ (nr. #9), with a mouth, gut (without endosymbionts), and anus, would appear to be further along in development than our F-nr. #10 and D-nr. #13, in both of which the anus has not yet appeared.

Acknowledgments

We thank Cheryl F. Bright, National Museum of Natural History, for her technical assistance and extended discussions throughout this investigation. We thank J. C. Harshbarger, Registry of Tumors of Lower Animals, for the use of his histology laboratory, W. R. Brown, S. G. Braden, and B. E. Kahn, Scanning Electron Microscope Laboratory, for the operation of their SEM instruments; both of these units are in the National Museum of Natural History. For material used in this study, we thank J. F. Grassle, Woods Hole Oceanographic Institution, Chief Scientist for the expedition to the Galapagos Rift, December 1979; A. Malahoff, University of Hawaii, Chief Scientist for the expedition to the Juan de Fuca Ridge, July 1984; K. L. Smith, Scripps Institution of Oceanography, Chief Scientist for the Oasis Expedition to the EPR at 21° North; and A. E. DeBevoise, Hatfield Marine Science Center, Oregon State University, who collected and preserved specimens during the expedition to the Juan de Fuca Ridge, September 1987, S. R. Hammond, Pacific Marine Environmental Laboratory, NOAA, Newport, OR, Chief Scientist. We thank M. H. Pettibone and K. Fauchald, National Museum of Natural History, for their reviews of the manuscript. This is Contribution No. 82 of the Galapagos Rift Biology Expedition, supported by the National Science Foundation, and a contribution of the Oasis Expedition.

Literature Cited

Arp, A. J., J. J. Childress, and C. R. Fisher Jr. 1985. Blood gas transport in *Riftia pachyptila* Pp. 289–300 in *The Hydrothermal Vents of the Eastern Pacific: An Overview*, M. L. Jones, ed. *Bull. Biol. Soc. Wash.*, No. 6.

Berg, C. J., Jr. 1985. Reproductive strategies of mollusks from abyssal hydrothermal vent communities. Pp. 185–197 in *The Hydrothermal Vents of the Eastern Pacific: An Overview*, M. L. Jones, ed. *Bull. Biol. Soc. Wash.*, No. 6.

Bosch, C., and P.-P. Grassé. 1984a. Cycle partiel des bactéries chimioautotrophes symbiotiques et leur rapports avec les bactériocytes chez *Riftia pachyptila* Jones (Pogonophore Vestimentifère). I. Le trophosome et les bactériocytes. *C. R. Acad. Sci. Paris*, Sér. III, **299:** 371–376.

Bosch, C., and P.-P. Grassé. 1984b. Cycle partiel des bactéries chimioautotrophes symbiotiques et leur rapports avec les bactériocytes chez *Riftia pachyptila* Jones (Pogonophore Vestimentifère). II. L'évolution des bactéries symbiotiques et des bactériocytes. *C. R. Acad. Sci. Paris*, Sér. III, **299:** 413–419.

Bullock, T. H. and G. A. Horridge. 1965. *Structure and Function in the Nervous Systems of Invertebrates*, Vols. I and II. W. H. Freeman and Co., San Francisco. xv+ and viii+, 1719 pp.

de Burgh, M. E. 1986. Evidence for a physiological gradient in the vestimentiferan trophosome: size-frequency analysis of bacterial populations and trophosome chemistry. *Can. J. Zool.* **64:** 1095–1103.

Cary, S. C., H. Felbeck, and N. D. Holland. 1989. Observations on the reproductive biology of the hydrothermal vent tube worm *Riftia pachyptila*. *Mar. Biol. Prog. Ser.* **52:** 89–94.

Cavanaugh, C. M. 1980. Symbiosis of chemoautotrophic bacteria and invertebrates. *Biol. Bull.* **159:** 457 (Abstr.).

Cavanaugh, C. M. 1983a. Symbiotic chemoautotrophic bacteria in marine invertebrates from sulphide-rich habitats. *Nature* **302:** 58–61.

Cavanaugh, C. M. 1983b. Chemoautotrophic bacteria in marine in-

vertebrates from sulfide-rich habitats: a new symbiosis. Pp. 699–708 in *Endocytobiology II: Intracellular Space as Oligogenetic Ecosystem,* H. E. A. Schenk and W. Schwemmler, eds. Walter de Gruyter, New York.

Cavanaugh, C. M., S. L. Gardiner, M. L. Jones, H. W. Jannasch, and J. B. Waterbury. 1981. Prokaryotic cells in the hydrothermal vent tube worm *Riftia pachyptila* Jones: possible chemoautotrophic symbionts. *Science* **213:** 340–342.

Crane, K. 1985. The distribution of geothermal fields along the Mid-Ocean Ridge. Pp. 3–18 in *The Hydrothermal Vents of the Eastern Pacific: An Overview,* M. L. Jones, ed. *Bull. Biol. Soc. Wash.,* No. 6.

Distel, D. L., D. J. Lane, G. J. Olsen, S. J. Giovannoni, B. Pace, N. R. Pace, D. A. Stahl, and H. Felbeck. 1988. Sulfur-oxidizing bacterial endosymbionts: analysis of phylogeny and specificity by 16S rRNA sequences. *J. Bacteriol.* **170:** 2506–2510.

Felbeck, H., and J. J. Childress. 1988. *Riftia pachyptila:* a highly integrated symbiosis. Pp. 131–138 in *Actes du Colloque Hydrothermalisme, Biologie et Ecologie,* L. Laubier, ed. *Oceanol. Acta,* Special Vol. No. 8.

Felbeck, H., J. J. Childress, and G. N. Somero. 1981. Calvin-Benson cycle and sulphide oxidation enzymes in animals from sulphide-rich habitats. *Nature* **293:** 291–293.

Grassle, J. F. 1986. The ecology of deep-sea hydrothermal vent communities. Pp. 301–362 in *Adv. Mar. Biol.,* vol. 23, J. H. S. Baxter and A. J. Southward, eds. Academic Press, London.

Grassle, J. P. 1985. Genetic differentiation in populations of hydrothermal vent mussels (Bathymodiolus thermophilus [sic]) from the Galapagos Rift and 13°N on the East Pacific Rise. Pp. 429–442 in *The Hydrothermal Vents of the Eastern Pacific: An Overview,* M. L. Jones, ed. *Bull. Biol. Soc. Wash.,* No. 6.

Hand, S. C. 1987. Trophosome ultrastructure and the characterization of isolated bacteriocytes from invertebrate-sulfur bacteria symbioses. *Biol. Bull.* **173:** 260–276.

Jamieson, B. G. M. 1981. *The Ultrastructure of the Oligochaeta.* Academic Press, NY. xv + 462 pp.

Jannasch, H. W., and C. O. Wirsen. 1979. Chemosynthetic primary production at east Pacific sea floor spreading centers. *BioScience* **29:** 592–598.

Jones, M. L. 1981a. *Riftia pachyptila,* new genus, new species, the vestimentiferan worm from the Galápagos Rift geothermal vents (Pogonophora). *Proc. Biol. Soc. Wash.* **93:** 1295–1313.

Jones, M. L. 1981b. *Riftia pachyptila* Jones: observations on the vestimentiferan worm from the Galápagos Rift. *Science* **213:** 333–336.

Jones, M. L. 1985a. Vestimentiferan pogonophores: their biology and affinities. Pp. 327–342 in *The Origins and Relationships of Lower Invertebrates,* S. C. Morris, J. D. George, R. Gibson and H. M. Platt, eds. The Systematics Association, Special Volume No. 28, Clarendon Press, Oxford.

Jones, M. L. 1985b. Vestimentifera, their biology and systematic and evolutionary paterns [sic]. Program for the Colloque "Les sources hydrothermales de la ride du Pacifique Oriental: Biologie et écologie," IFREMER, Paris, 4–7 November 1985 (Abstr.).

Jones, M. L. 1985c. On the Vestimentifera, new phylum: six new species, and other taxa, from the hydrothermal vents and elsewhere. Pp. 117–158 in *The Hydrothermal Vents of the Eastern Pacific: An Overview,* M. L. Jones, ed. *Bull. Biol. Soc. Wash.,* No. 6.

Jones, M. L. 1987. Recent observations on the Vestimentifera. Pp. 21–22 in *Abstracts of the 153rd Annual Meeting of the AAAS.*

Jones, M. L. 1988a. The Vestimentifera of the Pacific and elsewhere. Program for the Third International Symposium on Marine Biogeography & Evolution in the Pacific, Western Society of Naturalists/ University of Hong Kong, Hong Kong, 26 June–3 July 1988, p. 13 (Abstr.).

Jones, M. L. 1988b. The Vestimentifera, their biology, systematic and evolutionary patterns. Pp. 69–82 in *Actes du Colloque Hydrothermalisme, Biologie et Ecologie,* L. Laubier, ed. *Oceanol. Acta,* Special Vol. No. 8.

Jones, M. L., and C. F. Bright. 1985. Bibliography of hydrothermal vents and related areas, their biotas, ecological parameters and ancillary data. Pp. 495–538 in *The Hydrothermal Vents of the Eastern Pacific: An Overview,* M. L. Jones, ed. *Bull. Biol. Soc. Wash.,* No. 6.

Jones, M. L., and S. L. Gardiner. 1988. Evidence for a transient digestive tract in Vestimentifera. *Proc. Biol. Soc. Wash.* **101:** 423–433.

van der Land, J. L., and A. Nørrevang. 1975. The systematic position of Lamellibrachia [sic] (Annelida, Vestimentifera). Pp. 86–101 in *The Phylogeny and Systematic Position of Pogonophora,* A. Nørrevang, ed. *Z. Zool. Syst. Evolutionsforsch.,* Sonderheft.

van der Land, J. L., and A. Nørrevang. 1977. Structure and relationships of *Lamellibrachia* (Annelida, Vestimentifera). *K. Dan. Vidensk. Selsk. Biol. Skr.* **21**(3): 1–102.

Lutz, R. A. 1988. Dispersal of organisms at deep-sea hydrothermal vents: a review. Pp. 23–29 in *Actes du Colloque Hydrothermalisme, Biologie et Ecologie,* L. Laubier, ed. *Oceanol. Acta,* Special Vol. No. 8.

Lutz, R. A., D. Jablonski, D. C. Rhoads, and R. D. Turner. 1980. Larval dispersal of a deep-sea hydrothermal vent bivalve from the Galápagos Rift. *Mar. Biol.* **57:** 127–133.

Mañé-Garzón, F., and R. Montero. 1986. Sobre una nueva forma de verme tubicola—Lamellibrachia victori [sic] n. sp. (Vestimentifera)—Proposición de un nuevo phylum: Mesoneurophora. *Rev. Biol. Uruguay* [for 1985?] **8**(1): 1–28.

Nicol, J. A. C. 1948. The giant nerve-fibres in the central nervous system of *Myxicola* (Polychaeta, Sabellidae). *Q. J. Microsc. Sci., Ser. 2,* **89:** 1–45.

Nielsen, C. 1987. Structure and function of metazoan ciliary bands and their phylogenetic significance. *Acta Zool.* **68:** 205–262.

Southward, E. 1988a. Ultrastructure of the developmental stages of the symbiosis between bacteria and vestimentiferan Pogonophora. Program for the Fifth Deep-Sea Biology Symposium, IFREMER, Brest, France, 26 June–1 July 1988 [not paginated] (Abstr.).

Southward, E. 1988b. Development of the gut and segmentation of newly settled stages of *Ridgeia* (Vestimentifera): implications for relationship between Vestimentifera and Pogonophora. *J. Mar. Biol. Assoc. U. K.* **68:** 465–487.

Turner, R. D., Lutz, R. A., and D. Jablonski. 1985. Modes of molluscan larval development at deep-sea hydrothermal vents. Pp. 167–184 in *The Hydrothermal Vents of the Eastern Pacific: An Overview,* M. L. Jones, ed. *Bull. Biol. Soc. Wash.,* No. 6.

Van Dover, C. L., J. R. Factor, A. B. Williams, and C. J. Berg Jr. 1985. Reproductive patterns of decapod crustaceans from hydrothermal vents. Pp. 223–227 in *The Hydrothermal Vents of the Eastern Pacific: An Overview,* M. L. Jones, ed. *Bull. Biol. Soc. Wash.,* No. 6.

Warén, A. and P. Bouchet. 1989. New gastropods from East Pacific hydrothermal vents. *Zool. Scr.* **18:** 67–102.

Webb, M. 1969. *Lamellibrachia barhami,* gen. nov., sp. nov. (Pogonophora), from the northeast Pacific. *Bull. Mar. Sci.* **19:** 18–47.

Webb, M. 1977. Studies on *Lamellibrachia barhami* (Pogonophora). II. The reproductive organs. *Zool. Jahrb. Abt. Anat. Ontog. Tiere* **97:** 455–481.

Reference: *Biol. Bull.* **177:** 277–286. (October, 1989)

Variation in Growth Rate and Reproduction of the Bryozoan *Bugula neritina*

MICHAEL J. KEOUGH

Department of Zoology, University of Melbourne, Parkville, Victoria 3052 Australia

Abstract. Colonies of the arborescent cheilostome bryozoan *Bugula neritina* vary dramatically in their growth rate even when in apparently identical microhabitats. Comparison of growth rates of juveniles derived from four parent colonies at each of two sites showed only weak effects of parental colony on juvenile growth. These effects accounted for at most only 5.4% of total variation in growth. Variation in growth, and hence age at first reproduction, is interpreted as a plastic response of colonies to fine-scale environmental variation.

Bryozoans from seagrass meadows mature at a smaller size than those colonies from nearby rocky reefs (1200, *vs.* 3500 zooids at first reproduction, respectively). When juveniles from both of these habitats were grown in a common garden, there was, again, no variation among parental groups, but a highly significant effect of origin of juveniles. Juveniles matured at a size similar to that seen in their parental population, indicating that genetic or very early maternal effects influence timing of reproduction.

A *post hoc* test of the effect of onset of reproduction on colony growth showed no reduction in growth rate. Instead, colonies that reproduced grew faster than similar aged and sized colonies that did not reproduce.

Introduction

A growing body of empirical evidence suggests that, for modular organisms, many demographic variables depend more strongly on size than on age. Three of the most important such variables are mortality rates, timing of onset of reproduction, and reproductive output. Mortality rates are often size-dependent in two ways; first, the probability of a colony being eaten or overgrown may decrease with increasing size (*e.g.,* Reiswig, 1974; Werner and Caswell, 1977; Gross, 1981; Antonovics and Primack, 1982; Russ, 1982; Sebens, 1982; Hughes and Jackson, 1985; Hughes and Connell, 1987). Second, small colonies may be killed completely when attacked, while a similar attack on a larger colony may only cause damage ("partial mortality"), from which the colony subsequently recovers (Bak *et al.,* 1981; Palumbi and Jackson, 1982). Size, rather than age, may determine the onset of reproduction for many clonal animals and plants (Inouye and Taylor, 1980; van Duyl *et al.,* 1981; Gross, 1981; Wahle, 1983; Augspurger, 1985; Keough, 1986; but see Harvell and Grosberg, 1988). For a number of clonal organisms, size is correlated positively with reproductive output (Hayward, 1973; Inouye and Taylor, 1980; van Duyl *et al.,* 1981; Nakauchi, 1982; Sebens, 1983; Wahle, 1983; Augspurger, 1985), which in turn is thought to be an important component of relative fitness.

A negative correlation between size and mortality and a positive correlation between size and reproductive output both favor rapid initial growth of juveniles. However, many clonal organisms show extensive variation in growth rate. Harper (1977; 1985) reviews data for terrestrial plants, and Hughes and Jackson (1985), Jackson and Winston (1982), and Keough (1986) provide examples of such variation in clonal marine animals. For most marine organisms, the causes of this variation have not been examined in enough detail to estimate relative contributions of phenotypic responses to fine-scale environmental variation and genetic or maternal factors. For many plants, however, considerable variation in morphology and growth can be attributed to phenotypic plasticity in response to small-scale environmental variation (Silander, 1985). In animals, both genetic and environmental influences on growth rate are reported commonly (*e.g.,* Travis *et al.,* 1987).

The cosmopolitan bryozoan *Bugula neritina* appears

Received 15 March 1989; accepted 31 July 1989.

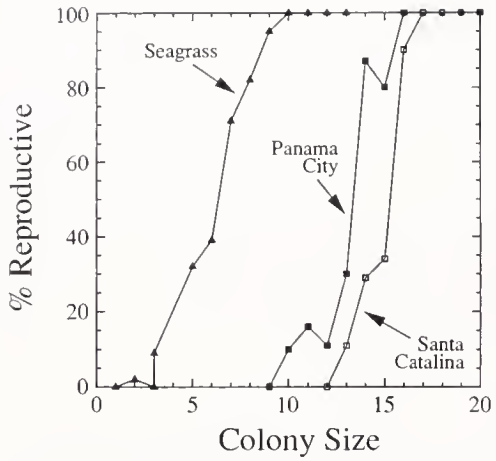

Figure 1. Onset of reproduction in *Bugula neritina*. The figure shows the percentage of colonies reproductive as a function of size for: Solid triangles: colonies in seagrass in the northeastern Gulf of Mexico. The curve is a composite from the sites and experiments reported elsewhere (Keough, 1986, Keough and Chernoff, 1987). n > 1000. Solid squares: colonies living on rock surfaces at Panama City, Florida. February 1986, n = 154. Open squares: colonies living on rock surfaces at Santa Catalina Island, California. Data from Keough (in prep.). n > 500.

to fit these emergent generalizations for clonal organisms. It is an arborescent species, in which a single colony represents the genet. Neither regrowth from dispersed fragments nor fusion between neighboring colonies has ever been observed. Fertilization is internal and larvae are brooded singly by maternal zooids in hyperstomial ovicells. The relatedness between larvae within a single colony is unclear; barring somatic mutation, the maternal zooids are genetically identical, but the number of paternal genotypes is unknown. Larvae from a single colony are at least half-sibs and at most full sibs. The onset of reproductive activity is more closely associated with size than with age, and survivorship increases with some function of size or age (Keough, 1986; Keough and Chernoff, 1987). In this paper, I re-analyze earlier data to show effects of both size and age on survivorship. When colonies are small, they suffer complete mortality, while larger colonies are frequently damaged, rather than killed outright (Keough, unpub. ob.). Growth rates vary extensively within cohorts, even when colonies are growing in what appears to be a relatively homogeneous habitat—the distal tips of artificial seagrass leaves (Keough, 1986). Similar variation occurs among cohort members attached to rock surfaces (Keough, 1989).

In addition to variation within populations, size at first reproduction also varies among populations. *Bugula neritina* colonies from seagrass meadows in the northeastern Gulf of Mexico grow rapidly in spring and fall, reproduce while small, and generally are short-lived, probably because their substratum is ephemeral (Keough, 1986; Keough and Chernoff, 1987). In contrast, colonies living on rock faces in southern California grow large, do not reproduce until they are large, and live considerably longer than one year (Keough, 1989). At Panama City, in the northeastern Gulf of Mexico, colonies live on large permanent structures, including artificial reefs, natural limestone outcroppings, and rock jetties. In this habitat, the demography of *B. neritina* appears closer to that seen in southern California (Fig. 1): they grow large, and appear not to reproduce while small.

What are the causes of this demographic variation? Here I describe experiments to determine causes of variation in growth rate and size of reproduction. I partition within-cohort variation in post-settlement growth rate of juveniles into variation occurring among and within maternal colonies, with the aim of detecting genetic components of growth rate. I also examine the basis of geographic variation in size at first reproduction.

Materials and Methods

To distinguish between effects of age and size on survivorship, I re-analyzed data from *Bugula neritina* colonies in seagrass meadows in Florida. In these experiments, cohorts of juveniles were established in the laboratory, then transplanted to the field and monitored (see Keough, 1986 for details). At any point in time, then, the experimental population comprised colonies from earlier cohorts that had grown rapidly (large, old), similar, slower-growing colonies (small, old), and small, young colonies from later cohorts. For colonies living in seagrass meadows, survivorship appears dependent on both size and age (Fig. 2).

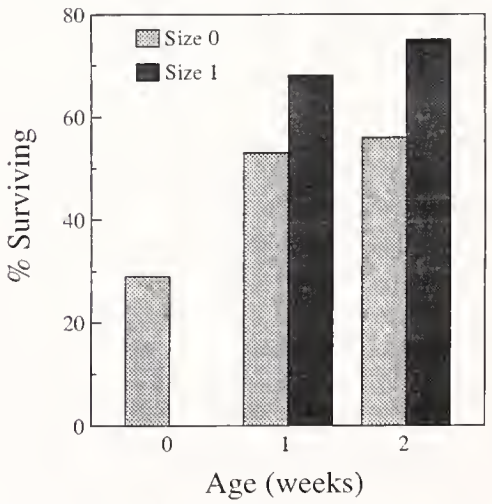

Figure 2. Effects of age and size on survivorship of *Bugula neritina* colonies. Histograms show probabilities of survival for juveniles of different sizes from a single experimental cohort, and juveniles of the same size, but of different ages. Data were taken from Keough (1986).

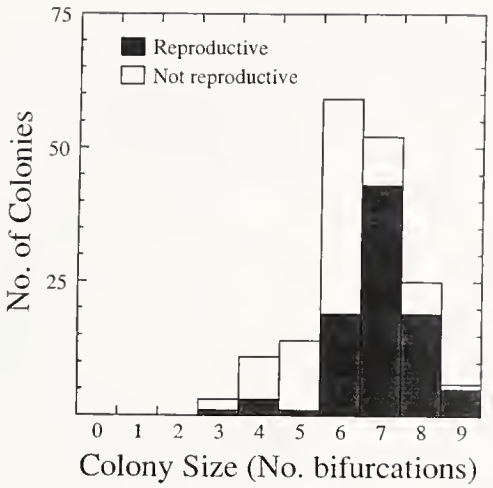

Figure 3. Reproduction as a function of size in *Bugula neritina* colonies under experimental conditions. Data are shown for experimental juveniles from Panama City after 5 weeks, and for natural recruits derived from Alligator Point after the same period of time.

Variation in growth

At the time of the first experiment (25 March 1986), there were no mature *Bugula neritina* colonies in seagrass meadows or at Alligator Point marina, which had been the source population for other demographic work (Keough, 1986; Keough and Chernoff, 1987), and where colonies mature at the same size as those from seagrass meadows (Keough, unpub. obs.). Therefore, I collected colonies from a sunken barge approximately 4 km off Panama City, at a depth of 20 m. Parental colonies were separated from each other by >10 m, to reduce the chance that they were closely related. After 2 days in the dark, the colonies were exposed to bright light and the four colonies that released the most larvae were used in the experiment.

Four or five larvae from a given colony were pipetted individually into a sterile plastic petri dish (50-mm diameter) containing seawater, and allowed to settle and metamorphose. Juveniles close to the edges of plates were removed. Without removing it from the water, each dish then had a 4-mm hole drilled into its center, and was bolted to a 60 × 20 cm piece of clear plexiglass. Each plexiglass sheet held 16 dishes in two rows of 8, with 4 dishes from each parental colony. The dishes were not arranged randomly, but in four 2 × 2 arrays, each array containing one dish from each parental colony. Two of the arrays were at ends of the plexiglass plates, and the positions of the dishes were further constrained so each parent appeared once at the corner of a plate and three times away from the corners. This design ensured that any micro-environmental variation could not bias the outcome of the experiment.

The plexiglass plates were then transported in seawater to a study site in the *Thalassia* meadow at Lanark, 1 km from the F.S.U. marine laboratory (see Keough and Chernoff, 1987, for a description of this site). There, they were bolted to a 1-m^2 PVC frame, the legs of which had been driven into the sediment until the frame was approximately 15 cm above, and parallel to, the substratum. All fasteners used in the experiment were stainless steel. The petri dishes faced downwards, with the plexiglass above them, because Young and Chia (1984) have shown that sedimentation can be a major source of mortality for some newly settled sessile animals, and my aim was to maximize the number of juveniles available for growth measurements.

At weekly intervals I returned, unbolted the plates, and transported them back to the laboratory, where I measured each juvenile. The plates were kept in running seawater, from which they were never removed for more than a few seconds.

Bugula neritina colonies in north Florida grow with regular bifurcations. New pairs of zooids are produced (budded) at the distal tip of each branch, with usually four pairs of zooids (budding events) between each bifurcation point (see Keough and Chernoff, 1987, their Fig. 2, for more details). Unless the colony has been damaged, each branch is approximately the same size, and the colony can be viewed as a series of distal buddings, with "waves" of bifurcations at regular intervals. I measured size by counting first the number of bifurcation waves and then the number of zooid pairs at the growing tip of each branch, *i.e.*, the number of budding events since the last bifurcation. This measurement can be used to estimate either the number of zooids or to compute the number of times the colony has budded. Thus, a colony of size 3.2 (bifurcated 3 times, with 2 further zooid pairs after the last bifurcation point) has budded 14 (*i.e.*, 3 bifurcations × 4 zooids/bifurcation + 2 zooids) times, and has 88 zooids. When measuring each colony I noted any missing branches, pale colored zooids, partial fouling, and the presence or absence of embryos.

After the third week, some of the juveniles were approaching a size at which they grew close to their neighbors, so I reduced their numbers to 1 or 2 per dish.

In the first experiment I used 5 such plates, with a total of 247 juveniles, distributed approximately equally among the 4 parents (57, 73, 57 and 60 juveniles).

Three weeks into the experiment, I obtained fertile colonies from Alligator Point and did a second experiment, using four parental colonies and four plexiglass sheets. The protocol for this experiment was identical to that of the first one, with colonies retained in collecting buckets for a period similar to travel time from Panama City to the laboratory, and the experiment began on 15 April

1986. There were 43, 51, 39, and 51 juveniles from the four parents.

Analysis

The plexiglass plates were a logistical convenience and were almost touching each other. They were not replaced in the same arrangement each week. A preliminary analysis of variance for the first week's growth, using mean growth of all juveniles in a dish as the dependent variable, showed neither a significant effect of plates nor a parent × plate interaction. For these reasons, I ignored plates in the analysis, and had simply a nested design, with juveniles within petri dishes within parents. The juveniles were small and well-separated from each other, so I did not expect juveniles to interfere with each other so as to make their growth non-independent. Any correlation among juveniles within a dish should reflect common responses to microhabitat conditions within dishes. This assumption does not affect the test of the main hypothesis about parental colonies, however, because growth rates of individual juveniles within dishes are not used to test the effect of parents (which is tested using variation among dishes).

I used the number of budding events as the measure of growth. Two analyses are possible from this experimental design. First, the weekly growth increment of each juvenile can be used as the dependent variable in a series of separate analyses for each week. This experiment is a simple nested design (juveniles within dishes, dishes within parent colonies), and has the drawback that statistical tests based on each week may not be independent, if juvenile growth over one period influences subsequent growth. This analysis cannot detect juveniles that grow consistently faster or slower, in successive weeks. The alternative analysis is to use only those juveniles that survived undamaged and were not culled, in a repeated measures analysis, with weekly growth increment as the dependent variable. The design is complicated, with nested factors (dishes) and repeated factors (weeks), and has two deficiencies; first, no information is gained from colonies that may have survived for most of the time, but were culled or damaged late in the experiment. The power of the analysis of very early growth is reduced by the decreased sample sizes. Second, repeated-measures analyses of variance have restrictive assumptions about the structure of covariance matrices (Winer, 1971), and the levels of the repeated factor (weeks) are always applied in a fixed, rather than random, order.

Here, I present the results of both sets of analyses, but their relative strengths and weaknesses must be considered.

Table I

Analysis of weekly growth increments for Bugula neritina *colonies from Panama City*

Variable	Week after settlement 1	2	3	4	5
Mean squares					
Among parent colonies	9.7	0.5	26.3	104.4	30.7
Dishes within colonies	2.9	7.4	26.5	78.2	57.5
"Siblings" within dishes	1.4	7.5	25.0	42.8	51.6
Degrees of freedom					
Parent colonies	3	3	3	3	3
Dishes—actual (quasi)	71 (64)	71 (58)	68 (57)	67 (57)	61
Juveniles	172	163	154	113	67
F-statistics					
Colonies	3.2*	0.1 ns	1.0 ns	1.2 ns	0.5 ns
Dishes 2.0***	1.0 ns	1.1 ns	1.8*	1.1 ns	
Variance components					
Colonies	5.4	0.0	0.0	0.8	0.0
Dishes within colonies	22.4	0.0	1.8	24.2	5.5
Siblings within dishes	72.2	102.3	98.2	75.0	96.1

The dependent variable was the number of budding events in the week concerned. The analysis was a 2-level nested analysis of variance with unequal samples sizes, using quasi F-ratios to test the main effect of parental colonies. The table shows F-ratios, mean squares, degrees of freedom, and estimated variance components. The degrees of freedom are also shown for the composite denominators used to test the main effect of parental colonies. ns, $P > 0.05$; *$0.05 > P > 0.01$; **$0.01 > P > 0.001$; ***$P < 0.001$.

Size at first reproduction

At the beginning of the experiment there was natural recruitment onto the petri dishes and the plexiglass plates. These larvae were probably produced by the population established at the Lanark site during a previous experiment using Alligator Point parents (Keough and Chernoff, 1987). To make a comparison of the size at first reproduction between colonies from Panama City and those occurring within seagrass meadows, I recorded the positions of some of these early recruits. Up through the fourth week I recorded the sizes of any *Bugula* colonies that were reproductive. In the fifth week I identified each natural recruit that had bifurcated more than four times and measured its exact size and reproductive condition.

Results

The growth rates of progeny from different Panama City colonies varied little. Only in the first week after settlement was there significant heterogeneity among parental colonies (Table I), and even then, only 5.4% of the total variation in growth rates was accounted for by parent colonies. The repeated measures analysis of vari-

Table II

Repeated measures analysis of variance using weekly growth increments of all Bugula *colonies that survived undamaged to the end of the experiment*

Source of variation	Panama City			Alligator Point		
	DF	MS	F	DF	MS	F
Among colonies	3	3.20	1.34 ns	3	11.85	4.92**
Siblings within colonies	80	2.39		145	2.41	
Among weeks	4	107.94	20.11***	1	159.25	51.84***
Colonies × weeks	12	4.36	0.81 ns	3	9.62	3.13***
Weeks × siblings	320	5.37		145	3.07	

Data were unbalanced, and sums of squares were computed by unweighted means (Winer 1971). ns, $P > 0.05$; $^{**}P < 0.01$; $^{***}P < 0.001$.

ance using only those juveniles that survived undamaged for 5 weeks showed no significant heterogeneity among parents, but highly significant variation with time (Table II). Inspection of mean weekly growth increments showed that the means did not differ by more than 1.5 buddings for the first few weeks (Table III). The clearest trend was a decline in the mean growth through the experiment, accompanied by a substantial increase in the variance (Table III).

For the juveniles from Alligator Point, the repeated measures analysis showed a highly significant effect of parent colony on growth rates (Table II), but individual weekly analyses showed only a single significant result, with parental colonies explaining a maximum of 7.4% of growth variation (Table IV). Inspection of means showed that the differences among colonies were slight in the first week after settlement and larger in the second week, although variances increased during the second week (Table III).

In both experiments, variation among dishes of juveniles from the same parent colony accounted for 15–20% of growth variation (Tables I, II, IV).

Mortality of the juveniles in this protected environment was usually <5% per week (Table V). Almost 80% of the Panama City juveniles survived for the 5 weeks of the experiment. There was no significant variation in post-settlement mortality among parental groups for the Panama City experiment, but slight variation among Alligator Point colonies (Table V). This latter result was caused by a single colony, the progeny of which suffered 23% mortality. The other three colonies did not differ significantly in the mortality rate of their juveniles ($G = 3.62$, $df = 2$, $P > 0.10$).

Panama City colonies had embryos by the fourth week, and many (46% of 154 colonies) were reproductive after the fifth week. The proportion of reproductive colonies increased with colony size (Fig. 2), and the mean size at first reproduction was 7.3 bifurcations (31.3 buddings, SD = 3.27, n = 92). Natural recruits matured at a smaller size, with a mean of 6.1 bifurcations (*i.e.*, 25 buddings, SD = 3.18, n = 58). Although most colonies were fouled by late May, there were a few unfouled Alligator Point colonies that began to reproduce. These colonies matured at a size similar to the naturally recruited juveniles (mean size at 1st reproduction 5.2, 22.3 buddings, SD = 2.6, n = 7). The natural recruits and Alligator Point juveniles did not differ significantly from each other, but both differed from the Panama City juveniles (single factor analysis of variance with unequal sample sizes, using size at first reproduction as the dependent variable, $F_{2,154} = 82.7$, $P \ll 0.001$; SNK procedure indicated that natural and Alligator Point means differed from Panama City at $P = 0.001$).

Colonies became fouled by algae during the later stages of both experiments, and large colonies often lost branches. Eight of the 21 Panama City juveniles that had begun to reproduce by the end of the fourth week had all reproductive structures removed during the fifth week, leaving them as small, asymmetric colonies.

There was no major reduction in colony growth rate associated with the onset of reproduction. No colony reproduced within the first three weeks, so I compared the growth rates of colonies that eventually reproduced to the rates of colonies that failed to reproduce. I used the growth rate for the first three weeks as a measure of pre-reproductive growth rate, and weeks 4–5 to estimate "post-reproductive" growth rates. I pooled data across parent colonies, since that factor accounted for little variation in growth rate. For each colony I used the mean growth rate for the first three weeks and the mean growth rate for weeks 4–5, and I analyzed the data using a repeated measures analysis of variance with two factors: presence or absence of reproduction, and growth period (pre- and post-reproduction). Only undamaged colonies were used in the analysis. Surprisingly, colonies that reproduced showed slightly increased growth at the onset of reproduction, while those that did not reproduce had a diminished growth rate in weeks 4 and 5 (Table VI).

Size at first reproduction was not significantly heterogeneous among parental groups for the Panama City juveniles (single factor analysis of variance using undamaged colonies, $F_{4,87} = 2.216$, $P = 0.074$). The number of reproductive colonies from the Alligator Point experiment was too small for such an analysis. Size at first reproduction was independent of growth rate for the Panama City juveniles: using mean growth rate for the first two weeks and size at first reproduction, $R^2 = 0.007$. The only significant correlation was between growth rate and age at first reproduction ($R^2 = 0.07$, $r = -0.239$, $n = 92$, $P = 0.02$), and even that relationship was weak. These

Table III

Mean weekly growth increments for Bugula *colonies from Panama City and Alligator Point*

Colony		Weeks 1	2	3	4	5
Panama City						
1	X	8.3 (1.5)	5.7 (3.1)	3.6 (3.9)	4.0 (7.5)	3.8 (7.1)
	n	57	53	48	39	26
3	X	8.3 (1.4)	5.7 (2.2)	3.0 (5.0)	2.3 (8.9)	2.7 (7.5)
	n	73	72	71	59	41
4	X	7.5 (1.1)	5.9 (2.1)	2.2 (6.5)	3.2 (7.5)	1.9 (7.9)
	n	57	57	55	43	30
6	X	7.7 (1.4)	5.7 (3.4)	3.7 (4.2)	5.8 (4.8)	4.0 (6.9)
	n	60	56	52	43	35
Alligator Point						
3	X	7.0 (1.7)	8.2 (3.5)			
	n	30	40			
4	X	6.2 (1.1)	6.4 (5.0)			
	n	51	48			
5	X	6.4 (1.6)	4.4 (7.1)			
	n	39	35			
6	X	6.5 (1.3)	5.7 (4.5)			
	n	51	47			

Data were means of the number of budding events, with standard deviations in parentheses. All undamaged colonies were included in each week, regardless of their subsequent fates.

relationships are as expected when size, rather than age, is important.

Discussion

The two demographic variables described in this study showed contrasting patterns of variation. Growth rates were very plastic, varying primarily among juveniles from the same parent, with only a minor component of variation that could be ascribed to parental colony, and little apparent variation between colonies from the two collection sites. In contrast, size at first reproduction varied strikingly among the progeny of colonies from two different sites, but showed relatively little variation within populations.

The experiments were designed to partition variation in juvenile growth into that occurring among and within "sibships." It is unclear whether these juveniles are closer to half or full sibs, because of uncertainty about the method of fertilization in most bryozoans; for *Bugula neritina*, electrophoretic attempts to resolve paternity have been thwarted by low levels of variability and few useable allozymes (Keough, unpub. obs.).

Variation among sibships reflects mostly maternal (genetic + maternal environmental), and possibly paternal genetic, effects, while variation within sibships should reflect phenotypic plasticity, genotype-environment interactions and paternal effects. In the "common garden" environment used in this study, there was little evidence of any maternal component, and, therefore, little evidence of additive genetic variation in growth rate. The largest amount of growth variation attributable to maternal colonies in any one week was 7.2%. Even when there were visible differences in mean growth rates of juveniles in a particular week, the rank order of sibships was not

Table IV

Analyses of weekly growth for Bugula neritina *juveniles from Alligator Point*

Source of variation	DF	MS	F	Var. Comp
Growth—Week 1				
Among colonies	3	5.6		2.9
Dishes within colonies	58 (54)	2.8	2.0 ns	17.3
"Siblings" within dishes	122	1.7	1.6*	79.9
Growth—Week 2				
Among colonies	3	95.3		5.1
Dishes within colonies	58 (51)	35.2	2.6 ns	19.8
"Siblings" within dishes	108	20.5	1.7*	72.2

The dependent variable was the number of buddings, and the analysis was a 2-level nested analysis of variance with unequal samples sizes, using quasi F-ratios to test the main effect. The table shows F-ratios, mean squares, degrees of freedom and variance component analysis. The degrees of freedom are also shown in parentheses for each composite denominator used to test the effect of colonies. ns, $P > 0.05$; *$0.05 > P > 0.01$.

Table V

Weekly mortality of juveniles from different Panama City and Alligator Point parents

Colony #	1	2	3	4	5	Total
Panama City						
1	10.0 (57)	3.5 (57)	3.6 (55)	15.2 (46)	2.3 (43)	16.0 (50)
3	0.0 (73)	1.4 (73)	6.9 (72)	12.5 (64)	4.2 (48)	19.0 (62)
4	0.0 (57)	1.8 (57)	12.5 (56)	9.5 (42)	5.4 (37)	25.8 (49)
6	0.0 (60)	5.0 (60)	8.8 (57)	4.2 (48)	2.2 (46)	28.6 (53)
Pooled	0.0 (247)	2.8 (247)	6.7 (240)	8.8 (217)	3.4 (174)	21.7 (214)
Alligator Pt						
3		2.3 (43)				
4		11.8 (51)				
5		23.1 (39)				
6		9.8 (51)				
Pooled		11.4 (184)				

All juveniles were pooled, regardless of dishes. Mortalities are shown as percentages, with sample size in parentheses.
G-test to compare mortality among colonies: Panama City, $G = 4.37$, $df = 3$, $P > 0.1$; Alligator Pt, $G = 9.0$, $df = 3$, $P < 0.05$.

maintained in subsequent weeks, so no groups of juveniles grew consistently faster than others. Usually about 20% of variation in growth was attributable to dishes, suggesting that there may have been slight differences in microhabitat among dishes. However, most of the variation occurred among related juveniles within single petri dishes. The causes of this latter variation are unclear. In the presence of apparently strong selection for rapid growth rates, it is not surprising to find little remaining variation that could be attributed to maternal genetic effects (Fisher 1958). However, responses to selection on single traits, such as growth rate, may depend on selection of other traits (Via and Lande, 1985), and small negative genetic correlations between traits may retard approaches to selective equilibria.

There was no noticeable difference in growth rate between juveniles from the two sites, although both cohorts showed variation through time. I have previously shown considerable seasonal variation in juvenile growth of cohorts from the Alligator Point population (Keough, 1986).

Juveniles suffered very low mortality over five weeks. The cumulative mortality over this whole period was less than most weekly mortality rates for juveniles transplanted onto distal sections of artificial seagrass leaves at the same site (Keough, 1986; Keough and Chernoff, 1987). All of these juveniles were handled in the same way. The petri dish experiments demonstrate at least that the mortality of juveniles on seagrass leaves is not a handling effect, but represents the action of crawling predators, sedimentation, or abrasion of leaves, because these processes were prevented from occurring on the petri dishes. Algal growth may kill juvenile ascidians (Young and Chia, 1984), but algae seem unimportant in my study, because the petri dishes had markedly higher standing crops of algae than do seagrass mimics or natural *Thalassia* leaves.

Growth rates of juveniles attached to artificial seagrass blades are more variable than those of juveniles in petri dishes (*cf.* Keough, 1986; Keough and Chernoff, 1987). On seagrasses, by the time the first juveniles begin to reproduce, others may not have grown since settlement. The greater variation in growth may be due to an environmental difference between the inverted petri dishes and the distal 10 cm of plastic seagrass mimics, or, more precisely, that the seagrass mimics, and by implication, seagrass leaves, are a more variable environment than the petri dishes. The two sets of experiments were done in different years, and food supply *may* have been more variable in 1985, when artificial seagrasses were used, than in 1986 in the petri dishes. However, similar results from another seagrass site in other seasons and in California suggest that juveniles on substrata mimicing natural ones generally show extensive within-cohort variation in growth (Keough, 1986; Keough and Chernoff, 1987; Keough unpub. obs.). Why do juveniles on the same part of a seagrass blade have such disparate growth rates? One plausible reason may be that the hydrodynamic "neighborhood" of a leaf is likely to vary both temporally and spatially, depending on local weather and growth and loss of surrounding blades. A single bryozoan probably experiences a range of conditions, so plasticity of growth may be more likely than specialization. Theoretical considerations of the evolution of plasticity focus on variation between, rather than within, environments (Via, 1987; Via and Lande, 1985), with genotypes dispersing between environments. It may be that for many sessile animals, dispersal between habitats, such as Alligator Point and Panama City, is rare, but that there is substantial small-scale variation within environ-

Table VI

Growth of Bugula *juveniles before and after the onset of reproduction*

Source of variation	DF	MS	F
Reproductive group	1	13.15	10.64**
Juveniles within reprod. gps	85	1.23	
Before/after onset of reprod.	1	0.47	0.26 ns
Reprod. group × onset	1	16.07	8.92**
Onset × juveniles	85	1.80	
	Wks 1–3	Wks 4–5	n
Reproduced	6.32	6.88	62
No reproduction	6.39	5.60	25

The analysis was a repeated measures analysis of variance, comparing the growth of juveniles that did and did not reproduce. The dependent variable was the average weekly growth (no. of buddings) of juveniles; the repeated measure was the growth of juveniles before (weeks 1–3) and after (weeks 4–5) the onset of reproduction. Only undamaged colonies were used in the analysis. Data were unbalanced, and sums of squares were computed by unweighted means (Winer, 1971). The figures beneath the analysis of variance table are treatment means. ns, $P > 0.05$; $^{**}P < 0.01$; $^{***}P < 0.001$.

ments. This possibility seems worthy of further investigation.

The two cohorts differed in their mean size at first reproduction, with the juveniles from the Panama City rocky reef maturing at a larger size than those from Alligator Point (31 *vs.* 25 budding events). The number of zooids increases exponentially with the number of buddings, so this apparently small difference is equivalent to Alligator Point colonies maturing after producing around 1200 zooids, while those from Panama City did not reproduce until they had >3500 zooids. The growth rates of the two cohorts were similar (Alligator Point colonies actually grew slightly faster), so Panama City colonies reproduced at least a week later than those from Alligator Point.

A difference in onset of reproduction is consistent with other life history differences between the two populations; on seagrasses, *Bugula* colonies are necessarily short-lived because of the ephemerality of their substratum. They grow rapidly, and never get very large. The largest colonies have branched 12 times, but these colonies are rare (Figs. 4, 8 in Keough and Chernoff, 1987). In contrast to seagrasses, rocky reefs and jetties are more permanent habitats. Colonies near Panama City and at Santa Catalina Island are more long-lived: newly settled colonies have survived at Santa Catalina Island for >1 year (Keough, unpub. obs.), by which time they were still considerably smaller than the largest colonies observed at that location. Colonies on rocky substrata also grow much larger than colonies on seagrasses, branching at least twice as many times, resulting in at least three orders of magnitude more zooids. Because these animals are clonal and most zooids bear embryos, later reproduction results in more embryos per colony. Thus, rocky reef *Bugula* have an early commitment to asexual (clonal) propagation of zooids, with later sexual, dispersive propagation.

Natural recruitment allowed me to test for any effect of transplantation by comparing the experimental cohorts and the natural juveniles drawn from parent colonies on seagrass. This comparison showed that transplanting had no substantial effect on size at first reproduction.

In both experimental cohorts, the juveniles matured at approximately the same size as did colonies in their parental populations, suggesting a maternal component to size at first reproduction. It is impossible to determine whether this is a genetic or environmental effect, since *Bugula* larvae develop completely within maternal ovicells. For some solitary species, egg size can have a strong influence on larval morphology and development (Sinervo and McEdward, 1988), but there are no comparable data for clonal species. It is not clear how maternal environmental effects on 400-μm larvae might influence size at first reproduction, since by this time even colonies from seagrass meadows have >1200 asexually produced zooids. I suggest that a substantial genetic component to size at first reproduction is more likely, but there are no data to resolve this question.

Reproduction did not result in any reduction in growth rate; rather, those colonies that began to reproduce actually grew faster after the onset of reproduction, while those not reproducing had a reduced growth rate during the same period. The latter observation is not surprising; failure to reproduce may be a result of insufficient food early in life or disease, which may subsequently cause reduced growth. The experiment provides no evidence for a major cost associated with reproduction. When a colony reproduces, >50% of zooids may bear spherical, 400-m diameter embryos, whose tissue masses probably exceed those of the maternal zooids. Production of larvae seems such a substantial investment of resources that it is perhaps surprising that the allocation of considerable resources for the production of embryos had no effect on the absolute amount of resources devoted to clonal growth.

Although growth variation and its causes have been examined in detail for many terrestrial and freshwater organisms (Berven and Gill, 1983; Travis, 1983), such studies are less common in marine environments. There exist relatively few documentations of the extent of growth variation that is not associated with obvious environmental gradients (*e.g.*, Koehn *et al.*, 1980; Levinton, 1983; Levinton and Monahan, 1983), or interactions with similar organisms (Peterson, 1982; Wethey, 1982), and the causes of this variation are obscure. In this case,

Bugula do not interact strongly with other sessile organisms because of the abundance of free space on seagrass leaves (Chernoff, 1985), and although some growth variation can be explained by basal-distal gradients in physical conditions (see Luckenbach, 1984; Eckman, 1987, for a discussion of flow effects), there remains a substantial amount of growth variation that presumably is a response to fine-scale environmental heterogeneity. I suggest that the variability of their environment on very small scales reduces the likelihood of within-population genetic differentiation of growth rate.

On larger, between-population scales, variation in reproductive variables is also well documented in other habitats, and is often associated with strong selection. Some marine species may switch between planktotrophy and lecithotrophy over parts of their range (Eyster, 1979) or within populations (Levin, 1984), or individuals may have the capacity to switch between iteroparity and semelparity in response to food availability (McKillup and Butler, 1979). In the present case, longevity of the substratum provides strong selection for rapid reproduction on seagrasses. Not only is the substratum short-lived relative to rocks, but there is considerable variation in life-expectancy among seagrass tips, depending on herbivory, leaf age, and storms. The short planktonic period of larvae allows population differentiation over relatively small scales, since most rocky reefs in the northern Gulf of Mexico are in water deep enough for seagrasses to be rare. Thus, larvae are only likely to encounter one kind of substratum, and there should be little genetic exchange between seagrass and rocky reef populations. McKillup and Butler (1979) suggested that species with long planktonic larval periods might have flexible reproductive patterns. Very restricted dispersal is widespread among subtidal sessile animals and some plants (Thorson, 1950, for review), and population differentiation of reproductive patterns, rather than flexibility, may be more common in these organisms.

Acknowledgments

I am grateful to Jon Schmidt for his enthusiastic assistance in the field, and A. Butler and A. Davis for their comments on the manuscript. This work was supported by National Science Foundation grant OCE-8400404. This is a publication from the Florida State University Marine Laboratory.

Literature Cited

Antonovics, J., and R. B. Primack. 1982. Experimental ecological genetics in *Plantago*. VI. The demography of seedling transplants of *P. lanceolata*. *J. Ecol.* **70:** 55–75.

Augspurger, C. K. 1985. Demography and life history variation of *Puya dasylirioides*, a long-lived rosette in tropical subalpine bogs. *Oikos* **45:** 341–352.

Bak, R. P., J. Sybesma, and F. C. van Duyl. 1981. The ecology of the tropical compound ascidian *Trididemnum solidum*. II. Abundance, growth and survival. *Mar. Ecol. Prog. Ser.* **6:** 43–52.

Berven, K. A., and D. E. Gill. 1983. Interpreting geographic variation in life-history traits. *Am. Zool.* **23:** 85–97.

Chernoff, H. 1985. The distribution and abundance of epifauna on the seagrass *Thalassia testudinum*. Thesis, Florida State University.

van Duyl, F. C., R. P. M. Bak, and J. Sybesma. 1981. The ecology of the tropical compound ascidian *Trididemnum solidum*. I. Reproductive strategy and larval behaviour. *Mar. Ecol. Prog. Ser.* **6:** 35–42.

Eckman, J. E. 1987. The role of hydrodynamics in recruitment, growth, and survival of *Argopecten irradians* (L.) and *Anomia simplex* (D'Orbigny) within eelgrass meadows. *J. Exp. Mar. Biol. Ecol.* **106:** 165–192.

Eyster, L. S. 1979. Reproduction and developmental variability in the opisthobranch *Tenellia pallida*. *Mar. Biol.* **51:** 133–140.

Fisher, R. A. 1958. *The Genetical Theory of Natural Selection*. Dover, England.

Gross, K. L. 1981. Predictions of fate from rosette size in four "biennial" plant species: *Verbascum thapsus, Oenothera biennis, Daucus carota*, and *Tragopogon dubius*. *Oecologia* **48:** 209–213.

Harper, J. H. 1977. *Population Biology of Plants*. Academic Press, New York, New York, USA.

Harper, J. L. 1985. Modules, branches, and the capture of resources. Pp. 1–34 in *Population Biology and Evolution of Clonal Organisms*, J. B. C. Jackson, L. W. Buss and R. E. Cook, eds., Yale University Press, Connecticut.

Harvell, C. D., and R. K. Grosberg. 1988. The timing of sexual maturity in clonal animals. *Ecology* **69:** 1855–1864.

Hayward, P. J. 1973. Preliminary observations on settlement and growth in populations of *Alcyonidium hirsutum* (Fleming). Pp. 107–113 in *Living and Fossil Bryozoa*, G. P. Larwood and B. R. Rosen, eds. Academic Press, New York.

Hughes, T. P., and J. H. Connell. 1987. Population dynamics based on size or age? A reef coral analysis. *Am. Nat.* **129:** 818–829.

Hughes, T. P., and J. B. C. Jackson. 1985. Population dynamics and life histories of foliaceous corals. *Ecol. Monogr.* **55:** 141–166.

Inouye, D. W., and O. R. Taylor. 1980. Variation in generation time in *Frasera speciosa* (Gentianaceae), a long-lived perennial monocarp. *Oecologia* **47:** 171–174.

Jackson, J. B. C. 1985. Distribution and ecology of clonal and aclonal benthic invertebrates. Pp. 297–356 in *Population Biology and Evolution of Clonal Organisms*, J. B. C. Jackson, L. W. Buss, and R. E. Cook, eds. Yale University Press, CT.

Jackson, J. B. C., and J. E. Winston. 1982. Ecology of cryptic coral reef communities. I. Distribution and abundance of major groups of encrusting organisms. *J. Exp. Mar. Biol. Ecol.* **57:** 135–148.

Keough, M. J. 1986. The distribution of the bryozoan on seagrass blades: settlement growth and mortality. *Ecology* **67:** 846–857.

Keough, M. J. 1989. Dispersal of the bryozoan *Bugula neritina* and effects of adults on newly settled juveniles. *Mar. Ecol. Prog. Ser.* (in press).

Keough, M. J., and H. Chernoff. 1987. Dispersal and population variation in the bryozoan. *Ecology* **68:** 199–210.

Koehn, R. K., R. J. E. Newell, and F. Immermann. 1980. Maintenance of an aminopeptidase allele frequency cline by natural selection. *Proc. Nat. Acad. Sci. USA* **77:** 5385–5389.

Levin, L. A. 1984. Multiple patterns of development in *Streblospio benedicti* Webster (Spionidae) from three coasts of North America. *Biol. Bull.* **166:** 494–508.

Levinton, J. S. 1983. The latitudinal compensation hypothesis: growth data and a model of latitudinal growth differentiation based

upon energy budgets. I. Interspecific comparison of *Ophryotrocha* (Polychaeta: Dorveillidae). *Biol. Bull.* **165:** 686–698.

Levinton, J. S., and R. K. Monahan. 1983. The latitudinal compensation hypothesis: growth data and a model of latitudinal growth differentiation based upon energy budgets. II. Intraspecific comparison between subspecies of *Ophryotrocha puerilis* (Polychaeta: Dorveillidae). *Biol. Bull.* **165:** 699–707.

Luckenbach, M. W. 1984. Sediment movements around animal tubes: the roles of hydrodynamics processes and biological activity. *Limnol. Oceanogr.* **31:** 779–787.

McKillup, S. C., and A. J. Butler. 1979. Modification of egg production and packaging in response to food availability by *Nassarius pauperatus*. *Oecologia* **43:** 221–231.

Nakauchi, M. 1982. Asexual development of ascidians: its biological significance, diversity, and morphogenesis. *Am. Zool.* **22:** 753–763.

Palumbi, S. R., and J. B. C. Jackson. 1982. Ecology of cryptic coral reef communities. II. Recovery from small disturbance events by encrusting Bryozoa: the influence of "host" species and lesion size. *J. Exp. Mar. Biol. Ecol.* **64:** 103–115.

Peterson, C. H. 1982. The importance of predation and intra- and interspecific competition in the population biology of two infaunal suspension-feeding bivalves, *Protothaca staminea* and *Chione undatella*. *Ecol. Monogr.* **52:** 437–475.

Reiswig, H. M. 1974. Water transport, respiration and energetics of three tropical marine sponges. *J. Exp. Mar. Biol. Ecol.* **14:** 231–249.

Russ, G. R. 1982. Overgrowth in a marine epifaunal community: competitive hierarchies and competitive networks. *Oecologia* **53:** 12–19.

Sebens, K. P. 1982. Competition for space: growth rate, reproductive output, and escape in size. *Am. Nat.* **120:** 189–197.

Sebens, K. P. 1983. The larval and juvenile ecology of the temperate octocoral *Alcyonium siderium* Verrill. II. Fecundity, survival, and juvenile growth. *J. Exp. Mar. Biol. Ecol.* **72:** 263–285.

Silander, J. A. 1985. Microevolution in clonal plants. Pp. 107–152 in *Population Biology and Evolution of Clonal Organisms*, J. B. C. Jackson, L. W. Buss and R. E. Cook, eds., Yale University Press, Connecticut.

Sinervo, B., and L. R. McEdward. 1988. Developmental consequences of an evolutionary change in egg size: an experimental test. *Evolution* **42:** 885–899.

Thorson, G. 1950. Reproductive and larval ecology of marine bottom invertebrates. *Biol. Rev.* **25:** 1–45.

Travis, J. 1983. Variation in development patterns of larval anurans in temporary ponds. I. Persistent variation within a *Hyla gratiosa* population. *Evolution* **37:** 496–512.

Travis, J., S. B. Emerson, and M. S. Blouin. 1987. A quantitative-genetic analysis of larval life-history traits in *Hyla crucifer*. *Evolution* **41:** 145–156.

Via, S. 1987. Genetic constraints on the evolution of phenotypic plasticity. Pp. 47–71 in *Genetic Constraints on Adaptive Evolution*, V. Loeschcke, ed., Springer-Verlag, Berlin.

Via, S., and R. Lande. 1985. Genotype-environment interaction and the evolution of phenotypic plasticity. *Evolution* **39:** 505–522.

Wahle, C. M. 1983. The role of age, size and injury in sexual reproduction among Jamaican gorgonians. *Am. Zool.* **23:** 961.

Werner, P. A., and H. Caswell. 1977. Population growth rates and age *versus* stage-distribution models for teasel (*Dipsacus sylvestris* Huds.). *Ecology* **58:** 1103–1111.

Wethey, D. S. 1983. Intrapopulation variation in growth of sessile organisms: natural populations of the intertidal barnacle *Balanus balanoides*. *Oikos* **40:** 14–23.

Winer, B. J. 1971. *Statistical Principles in Experimental Design*. McGraw-Hill, Kogakusha, Tokyo.

Young, C. M., and F.-S. Chia. 1984. Microhabitat-associated variability in survival and growth of subtidal solitary ascidians during the first 21 days after settlement. *Mar. Biol.* **81:** 61–68.

Reference: *Biol. Bull.* 177: 287–294. (October, 1989)

Population Genetics of the Common Squid *Loligo pealei* LeSueur, 1821, from Cape Cod to Cape Hatteras

RONALD L. GARTHWAITE[1], CARL J. BERG JR.[2], AND JUNE HARRIGAN[3]

Marine Biological Laboratory, Woods Hole, Massachusetts 02543

Abstract. Collections of *Loligo pealei* LeSueur, 1821 from the Atlantic seaboard between Cape Hatteras and Georges Bank differ significantly in both allele and genotype frequencies at the phosphoglucomutase locus. *Loligo pealei* collected off the coast of Virginia are distinct at this locus from all other areas surveyed. *Loligo pealei* collected from Georges Bank also differ significantly at this locus from those collected inshore off Cape Cod. These results suggest that *L. pealei* along the Atlantic seaboard consists of several distinct populations. A comparison of allele frequencies at nine allozyme loci among *L. pealei, Loligo plei* Blainville, 1823, and *Lolliguncula brevis* (Blainville, 1823) reveals that *L. pealei* differs completely from *L. plei* at five loci, *L. pealei* from *L. brevis* at six loci, and *L. plei* from *L. brevis* at three loci.

Introduction

Data collected over the past one hundred years still present a confused picture of the stock[4] characteristics of the common squid *Loligo pealei* LeSueur, 1821. The existence of two major discrete "groups" and a third "mixed group" has been demonstrated repeatedly in size frequency data from squid caught in the region extending from Georges Bank to Cape Hatteras. This size structure has been explained by invoking different sub-species (Verrill, 1882), brood stocks (Summers, 1971), or alternate generations (Mesnil, 1977). In addition, there is some uncertainty as to how many species this taxon represents throughout its range (Cohen, 1976; Summers, 1983). In reviewing the assumptions needed for statistical analysis of population structure based on size frequency distributions, Summers (1983) points out that *L. pealei* is not homogeneous either throughout its latitudinal range, across the continental shelf, through time at a single station, or even between successive tows. All of these data suggest that there are genetically discrete populations which are isolated by seasonal or geographic spawning differences. The single fishery "stock" or "population" of *L. pealei* on the eastern seaboard (*e.g.*, Lange and Sissenwine, 1980, 1983) probably consists of several stocks or populations.

To date, biochemical genetic data have not been applied to the problem of stock structure in *Loligo pealei*. In this study we used allozyme data to clarify the population or stock structure of this species along the northeastern coast of the United States. In the process, we also present a biochemical genetic comparison of *L. pealei* with the morphologically similar *Loligo plei* Blainville, 1823, and with *Lolliguncula brevis* (Blainville, 1823).

Materials and Methods

Squid were collected by trawl nets from research vessels of the Marine Biological Laboratory and the Northeast Fisheries Center of the United States National Marine Fisheries Service (NMFS). Collection data for the trawl stations are listed in Table 1. The location of these stations is illustrated in Figure 1. For purposes of analysis, mainly to increase sample sizes, these trawl samples were grouped into six regions [North Carolina, Virginia, Delaware, Woods Hole, Cape Cod, and Georges Bank (Table 1)], which we subsequently treated as six separate samples. With the exception of station 45, stations were

Received 3 October 1988; accepted 31 July 1989.

[1] Present address: Institute of Marine Sciences, University of California, Santa Cruz, CA 95064.

[2] Present address: Florida Department of Natural Resources, Marine Research Institute, 13365 Overseas Highway, Marathon, FL 33050.

[3] Present address: Department of Ocean Engineering, University of Hawaii, Honolulu, HI 96822.

[4] In this paper we use the term "stock" as defined by Ihssen *et al.* (1981): "An intraspecific group of randomly mating individuals with temporal or spatial integrity."

Table I

Collection data for squid samples used in this study

Region	NMFS station	Date	Depth (m)	Approximate Latitude	Approximate Longitude	# of *Loligo pealei* surveyed	Other species present
North Carolina	34	2 OCT 85	36–43	35°41′	75°06′	32	*L. plei*
	35	2 OCT 85	58–63	35°44′	74°56′	24	
Virginia	45	3 OCT 85	16–15	36°28′	75°48′	16	
	53	4 OCT 85	25–24	37°25′	75°25′	54	*L. plei*
	56	4 OCT 85	14	37°45′	75°27′	9	*L. brevis*
	57	4 OCT 85	19	37°54′	75°11′	10	
	58	4 OCT 85	23–25	37°57′	75°02′	20	
Delaware	83	6 OCT 85	192–197	38°32′	73°16′	75	
	85	6 OCT 85	64–67	38°52′	73°21′	40	
Woods Hole		OCT 84	10–20	41°30′	70°30′	110	
		MAY 85	10–20	41°30′	70°30′	120	
		OCT 85	10–20	41°30′	70°30′	100	
Cape Cod	371	7 NOV 85	29–33	41°57′	69°56′	48	
	372	7 NOV 85	32–34	41°59′	69°57′	137	
Georges Bank	198	21 OCT 85	99	40°42′	67°15′	199	

NMFS = National Marine Fisheries Service. See Figure 1 for station locations.

grouped on the basis of physical proximity. Station 45, which lies approximately half way between the North Carolina stations and the other Virginia stations (Fig. 1), was grouped with the Virginia stations because it represents a similar, near-shore, shallow-water habitat (Table I). The three samples collected off Woods Hole represent three different year classes (1983, 1984, and 1985). Squid collected in October of 1984 and 1985 were juveniles that hatched during the preceding summers, while the sample from May 1985 consisted of breeding adults most likely hatched in 1983.

Soon after collection, a piece of mantle tissue was removed from each animal and frozen in liquid nitrogen for later electrophoretic analysis. The remainder of each squid was then frozen at −20°C. These specimens were later thawed and their mantle lengths measured to the nearest mm using a meter ruler.

Tissue samples for electrophoresis were returned to the laboratory and stored at −70°C until analyzed. Before electrophoretic analysis, these tissue samples were sonicated on ice in approximately equal weight to volume of 0.05 *M* Tris-HCl pH 7.5 and centrifuged for 15 min in a clinical centrifuge at 2°C. Horizontal starch gel electrophoresis (Sigma starch) using filter paper wicks (Whatman #2) and buffer systems two and five of Selander *et al.* (1971) was used to determine allele frequencies in the collections at 19 biochemical loci. Buffer system two was used to survey the collections for aminopeptidase (AP), leucine aminopeptidase-1 (LAP-1), leucine aminopeptidase-2 (LAP-2), malic enzyme (ME), phosphoglucomutase (PGM), phosphoglucose isomerase-1 (PGI-1), phosphoglucose isomerase-2 (PGI-2), superoxide dismutase (SOD), and xanthine dehydrogenase (XDH). Buffer system five was used to survey the collections for α-glycerophosphate dehydrogenase (α-GPDH), alcohol dehydrogenase (ADH), esterase (EST), glutamate oxaloacetate transaminase-1 (GOT-1), glutamate oxaloacetate transaminase-2 (GOT-2), isocitrate dehydrogenase (IDH), malate dehydrogenase-1 (MDH-1), malate dehydrogenase-2 (MDH-2), nothing dehydrogenase (NDH), and sorbitol dehydrogenase-1 (SDH-1). Initially, 40 specimens of *Loligo pealei* from Woods Hole were surveyed for all 19 loci. Nine of these loci (PGM, ME, MDH-1, MDH-2, IDH, GOT-1, GOT-2, PGI-1, and PGI-2) were chosen for use in the larger survey. Enzyme stain recipes were taken from Shaw and Prasad (1970) and Ahmad *et al.* (1977) with minor modification.

Differences in size frequency distributions among trawl samples and among individuals possessing various alleles within trawl samples were tested for significance using F-tests on variances and t-tests on means. Allele frequency differences among stations and regions were tested for significance using the tables of Mainland *et al.* (1956). Genotype frequency differences among stations and regions were tested for significance using G tests on contingency tables (Sokal and Rohlf, 1969).

During our survey, we encountered one species of squid that was morphologically distinct from *Loligo*

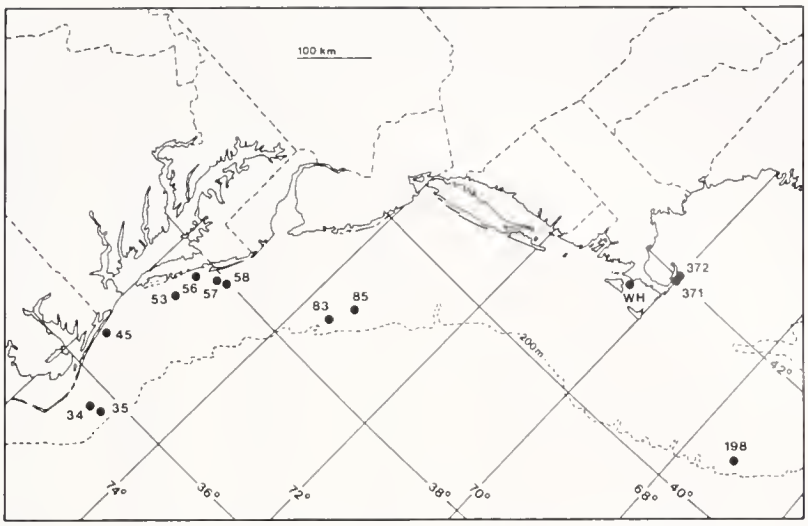

Figure 1. The location of the National Marine Fisheries Service trawl stations from which squid used in this study were collected. See Table I for collection data. WH = Woods Hole, MA.

pealei and another that was electrophoretically distinct from *L. pealei*. We suspected that these squid were *Lolliguncula brevis* and *Loligo plei*, respectively. *Loligo plei* is morphologically very similar to *L. pealei*, and the two species are not easily separated on morphological grounds (Cohen, 1976; Whitaker, 1980; Summers, 1983; Hanlon, 1988). Since the ranges of *L. pealei* and *L. plei* overlap in our study area (Whitaker, 1980), it is important that we demonstrate that we can consistently identify *L. plei* electrophoretically and that we have not accidentally included specimens of this species in our study of *L. pealei*. To confirm the identities of these species in our collections we obtained known specimens of *L. plei* and *L. brevis* from Dr. Roger Hanlon of Galveston, Texas. These Texas specimens were compared directly, on the same gels, to our specimens of *L. pealei*, *L. plei*, and *L. brevis* for the nine loci listed above.

Results

Population genetics of Loligo pealei

Significant variation in squid size distributions existed among trawl samples both within and among regions. Out of a total of 55 pair-wise comparisons among the 11 trawl samples taken in October 1985, all but 5 were significantly different in variance or mean size ($P < .05$).

Banding patterns for all loci surveyed conformed to Mendelian expectations (Harris and Hopkinson, 1976). Heterozygotes for PGM were found in both males and females, indicating that this locus is not sex linked. Alleles, allele frequencies, and sample sizes for the collections of *Loligo pealei* from all six regions are listed in Table II. Phosphoglucomutase genotype frequencies for all regions are given in Table III.

On the whole, *Loligo pealei* possessed very low levels of genetic variation. Of the 19 loci surveyed, variant alleles were found only in PGM, ME, MDH-2, IDH, GOT-1, and PGI-2. However, of these six loci, the frequencies of the variant alleles were 1% or less in all but PGM for which the maximum frequency of variant alleles in any region surveyed was only 7.5% (Georges Bank, Table II). Combining the data over all collections, only 5% of all loci surveyed in *L. pealei* were polymorphic at the 1% level and the average heterozygosity per individual was only 0.6%.

Given the low levels of genetic variation present in the collections of *Loligo pealei* surveyed, it is unlikely that differences in allele frequencies among the collections will be significant. Only PGM is polymorphic enough to reasonably give significant results with these sample sizes. No significant differences in allele or genotype frequencies were found among stations within regions for any locus. Among the three Woods Hole collections, which represent squid hatched in three different years (1983, 1984, and 1985) no significant differences in allele or genotype frequencies were found at any locus.

Individuals possessing allelic variants generally did not differ significantly in size from other squid from the same trawl; the exceptions being squid possessing PGM allele 1.18 from Georges Bank, which had a significantly larger mean length than squid which did not possess this allele ($P < .05$), and squid possessing ME allele 1.05 at Georges Bank and PGM allele 1.18 at Woods Hole (May 1985), which both had significantly larger variances than the remaining squid in each sample ($P < .05$).

Table II

Allele frequencies, and sample sizes in number of alleles surveyed (in parentheses) for collections of Loligo pealei *from the northwest Atlantic. Alleles are expressed as migration rate relative to the most common allele*

Locus	Allele	North Carolina	Virginia	Delaware	Woods Hole			Woods Hole total	Cape Cod	Georges Bank
					OCT 84	MAY 85	OCT 85			
PGM	(N)	(112)	(218)	(230)	(220)	(240)	(200)	(660)	(370)	(398)
	1.18	.054	—	.030	.036	.021	.030	.029	.022	.030
	1.00	.928	.972	.948	.946	.962	.950	.953	.967	.925
	.78	.018	.028	.022	.018	.017	.020	.018	.011	.045
ME	(N)	(112)	(146)	(164)	(220)	(240)	(200)	(660)	(370)	(398)
	1.05	—	—	—	—	—	—	—	—	.008
	1.00	1.000	1.000	1.000	1.000	1.000	1.000	1.000	1.000	.992
MDH-2	(N)	(112)	(120)	(92)	(220)	(240)	(200)	(660)	(370)	(398)
	1.00	1.000	1.000	1.000	1.000	1.000	1.000	1.000	.997	1.000
	.64	—	—	—	—	—	—	—	.003	—
IDH	(N)	(112)	(100)	(102)	(220)	(240)	(200)	(660)	(370)	(398)
	1.17	—	—	—	—	.004	—	.002	.005	—
	1.00	1.000	1.000	1.000	1.000	.996	.990	.995	.992	1.000
	.88	—	—	—	—	—	.010	.003	—	—
	.69	—	—	—	—	—	—	—	.003	—
GOT-1	(N)	(112)	(136)	(150)	(160)	(240)	(200)	(600)	(370)	(398)
	1.16	—	—	—	—	—	—	—	—	.003
	1.00	1.000	1.000	1.000	1.000	1.000	1.000	1.000	1.000	.992
	.79	—	—	—	—	—	—	—	—	.005
PGI-2	(N)	(112)	(126)	(122)	(220)	(240)	(200)	(660)	(370)	(398)
	1.00	1.000	1.000	1.000	1.000	.996	1.000	.998	1.000	1.000
	.68	—	—	—	—	.004	—	.002	—	—
MDH-1	(N)	(112)	(120)	(92)	(220)	(240)	(200)	(660)	(370)	(398)
	1.00	1.000	1.000	1.000	1.000	1.000	1.000	1.000	1.000	1.000
GOT-2	(N)	(112)	(74)	(150)	(160)	(240)	(200)	(600)	(370)	(398)
	1.00	1.000	1.000	1.000	1.000	1.000	1.000	1.000	1.000	1.000
PGI-1	(N)	(112)	(126)	(122)	(220)	(240)	(200)	(660)	(370)	(398)
	1.00	1.000	1.000	1.000	1.000	1.000	1.000	1.000	1.000	1.000

Among all pair-wise comparisons of squid collections (with the three Woods Hole collections combined and treated as a single sample), the Virginia sample stands out as being significantly different from the North Carolina sample ($P < .05$) and the Woods Hole sample ($P < .05$) in the frequency of PGM allele 1.18. In PGM ge-

Table III

Phosphoglucomutase genotype frequencies for collections of Loligo pealei *from the northwest Atlantic*

Region	Sample size	PGM genotype				
		1.18/1.00	1.18/.78	1.00/1.00	1.00/.78	.78/.78
North Carolina	56	.107	—	.857	.036	—
Virginia	109	—	—	.945	.055	—
Delaware	115	.061	—	.896	.043	—
Woods Hole						
OCT 1984	110	.064	.009	.900	.027	—
MAY 1985	120	.042	—	.925	.033	—
OCT 1985	100	.060	—	.900	.040	—
Total	330	.055	.003	.909	.033	—
Cape Cod	185	.043	—	.935	.022	—
Georges Bank	199	.060	—	.855	.080	.005

notype frequencies, the Virginia sample is significantly different from the samples from all other regions ($P < .05$). In addition, the Georges Bank sample is significantly different from its nearest neighbor, Cape Cod, in PGM genotype frequencies ($P < .05$). All other pair-wise comparisons of regions for PGM and all other loci gave nonsignificant results for both allele and genotype frequencies.

Taxonomy

Alleles, allele frequencies, and sample sizes for the comparison of allele frequencies in *Loligo pealei, Loligo plei,* and *Lolliguncula brevis* are listed in Table IV. Our specimens of *L. plei* and *L. brevis* were electrophoretically identical to the Texas specimens of these species for all loci surveyed.

Sample sizes for *Loligo plei* and *Lolliguncula brevis* were small (eight individuals apiece) and alleles with frequencies lower than approximately 6% were not likely to have been detected. However, all loci surveyed, with the exception of IDH, PGI-2, and MDH-1, showed fixed allelic differences among species such that individuals of all three species can be identified easily and unambiguously solely on the basis of the alleles they possess at these diagnostic loci. *Loligo pealei* differs completely from *L. plei* at five loci, *L. pealei* from *L. brevis* at six loci, and *L. plei* from *L. brevis* at three loci (Table IV). Nei's genetic distances (Nei, 1972) for pair-wise comparisons of the three species are: .81 for *L. pealei vs. L. plei,* 1.10 for *L. pealei vs. L. brevis,* and .40 for *L. plei vs. L. brevis.*

Discussion

Generally, biochemical genetic data, of the kind reported here, are much more appropriate and effective in determining population or stock structure than are size frequency data (Ihssen *et al.,* 1981). Size and growth rate are both affected by numerous environmental factors such as temperature and food quality or availability (Hixon, 1983; Ihssen *et al.,* 1981). Thus individuals from the same population or stock can differ significantly in these measures if they experience different environments. This is particularly a problem with *Loligo pealei,* which appears to have a rather extended spawning and hatching period (Summers, 1971; Lange and Sissenwine, 1980, 1983). Biochemical genetic data are typically not *directly* affected by the environment and thus serve as a permanent and direct measure of genetic relatedness among collections or populations (Ihssen *et al.,* 1981; Avise, 1974; Ayala, 1983). This technique has, therefore, shifted from an optional to a primary position among methods used in studies of population or stock structure (Ihssen *et al.,* 1981).

The low level of genetic variation found here in *Loligo pealei* limits the effectiveness of this technique in determining population structure in this species since only one locus (PGM) was polymorphic enough to detect differentiation among collections with reasonable sample sizes. Nevertheless, for this locus, significant differentiation was detected among collections. The patterning of this differentiation suggests that *L. pealei* in the northwest Atlantic is comprised of at least three populations. Genetically, the Virginia sample is distinct from samples from all other regions included in this study and the Georges Bank sample is distinct from its nearest neighbor, Cape Cod. However, given that *L. pealei* are migratory and highly mobile (Lange and Sissenwine, 1983), it is unlikely that the spatial arrangement of these populations is constant.

Previous studies on the population or stock structure of *Loligo pealei,* based on size frequency distributions, have postulated two groups of squid which may or may not be genetically isolated (Verrill, 1882; Summers, 1971; Mesnil, 1977; Lange and Sissenwine, 1980, 1983). We can find little genetic evidence for this structure. In no trawl sample was there an obvious bimodality in size frequency distributions. Nor did we find significant gene frequency differences among the three Woods Hole collections. While we found exceptional amounts of variation among trawl samples in size frequency distributions, there is no overall correlation between mean size and PGM gene frequency ($r^2 = .02$, $P < .05$). The fact that the Virginia trawl samples (which are genetically coherent and, as a whole, distinct from all other regions) are heterogeneous in size frequency ($P < .05$) indicates that size frequency is not a good indicator of population structure in *L. pealei.* It is possible that size frequency differences among samples are due to differences in environmental factors experienced by different groups of squid or differences in sex ratio among groups [male *L. pealei* tend to grow larger than females (Mesnil, 1977)]. Whether size frequency differences are due to environmental differences, sex ratio differences, or differences in spawning time, they do not seem to be associated with significant restrictions in gene flow.

The differences in size distributions between individuals possessing different alleles that was found in several trawl samples is interesting, but the small number of allelic variants obtained in any one sample makes analysis difficult. These differences in size distributions may be a result of selective forces acting on alleles or may indicate that our trawl samples were composed of a mixture of squid populations which differ in both size and allele frequency. In this latter case, this data would be evidence for the population structure postulated by previous workers (Verrill, 1882; Summers, 1971; Mesnil, 1977).

The degree of interpopulational genetic differentiation reported here is almost certainly a minimum value for

Table IV

Allele frequencies at nine loci in three species of squid

Locus	Allele	*Loligo pealei* (1704)	*Loligo plei* (16)	*Lolliguncula brevis* (16)
PGM	1.18	.026	—	—
	1.00	.950	—	—
	.78	.024	—	—
	.60	—	1.000	1.000
ME	1.05	.002	—	—
	1.00	.998	—	—
	.95	—	1.000	1.000
MDH-2	1.00	.999	1.000	—
	.90	—	—	1.000
	.64	.001	—	—
IDH	1.17	.002	—	—
	1.00	.996	1.000	1.000
	.88	.001	—	—
	.69	.001	—	—
GOT-1	1.16	.001	—	—
	1.00	.998	—	—
	.88	—	—	1.000
	.85	—	1.000	—
	.79	.001	—	—
PGI-2	1.00	.999	1.000	1.000
	.68	.001	—	—
MDH-1	1.00	1.000	1.000	1.000
GOT-2	1.00	1.000	—	—
	.86	—	—	1.000
	*	—	1.000	—
PGI-1	1.00	1.000	—	—
	.74	—	1.000	1.000

Minimum sample sizes (in number of alleles surveyed) are in parentheses. Alleles are expressed as migration rate relative to the most common *Loligo pealei* allele. * = no activity.

Loligo pealei. All of the collections of *L. pealei* surveyed in this study came from a limited biogeographic range extending north from Cape Hatteras to Cape Cod. The range of *L. pealei* extends south as far as the Gulf of Venezuela (Cohen, 1976; Summer, 1983) and it may be expected that comparisons of populations north of Cape Hatteras with those south of Cape Hatteras or from the Gulf of Mexico may reveal additional genetic differentiation since Cape Hatteras and Florida form natural boundaries for many other species (Briggs, 1974).

The low levels of intrapopulational genetic variation in *Loligo pealei* found in this study seem to be a general characteristic of squid. Similar low levels of genetic variation have been reported for *Loligo opalescens* Berry, 1911 (Christofferson *et al.*, 1978; Augustyn and Grant, 1988), *Loligo vulgaris* Lamarck, 1798 (Augustyn and Grant, 1988), and *Illex illecebrosus* (LeSueur, 1821) (Romero and Amaratunga, 1981). In addition, even though our data are limited both in number of loci (9) and number of individuals (8) surveyed, *Loligo plei* and *Lolliguncula brevis* also appear to fit this pattern since allelic variants for the loci surveyed here, if present at all, would likely be in frequencies of 6% or less. Table V presents a comparison of measures of genetic variation based on data taken from the literature for several squid species and for invertebrates in general.

While the lack of genetic variation in squid may limit the use of this kind of data in studies of population structure, it makes it that much more useful in taxonomic studies since banding patterns are simpler and intraspecific variation is minimized. In this study, we found biochemical data to be an excellent taxonomic tool. While *Loligo pealei* and *Loligo plei* are morphologically very similar and difficult to differentiate on morphological grounds (Cohen, 1976; Whitaker, 1980; Summer, 1983; Hanlon, 1988), they are quite distinct biochemically (differing completely at five out of nine loci) and easily distinguishable from one another. In addition, both species are easily distinguishable electrophoretically from *Lolliguncula brevis*. That *L. plei* appears to be more closely related to *L. brevis* than *L. pealei* is unexpected and interesting but this result may be an artifact of the small number of loci surveyed.

Several other studies of squid population structure and taxonomy have been performed using biochemical genetic data. Two of these studies (Ally and Keck, 1978; Christofferson *et al.*, 1978) are concerned with *Loligo opalescens* along the California coast, and both suggest a separate southern population on the basis of biochemical data. This population structure for *L. opalescens* is substantiated by data on spawning peaks (Fields, 1965) and morphological indices (Kashiwada and Recksiek, 1978). A third study concerns *Illex illecebrosus* off the eastern coast of Canada (Romero and Amaratunga, 1981). In this study, no significant differences were detected among collections, but this is not surprising considering the limited geographical range over which the collections were taken and the fact that sample sizes were small. Smith *et al.* (1981) studied *Nototodarus sloani* Gray, 1849, in New Zealand. On the basis of mainly electrophoretic evidence, Smith *et al.* found that what was previously thought to be eight sub-populations of *N. sloani* instead consisted of two species that are largely non-overlapping in their distributions. This conclusion concerning *N. sloani* was substantiated by data on morphology and parasite load. Finally, Augustyn and Grant (1988), in their morphological and biochemical study of African squid, discovered that what had previously been considered two separate species on morphological grounds (*Loligo vulgaris* and *Loligo reynaudii* d'Orbigny, 1845) actually consisted of two subspecies of *L. vulgaris* as demonstrated by biochemical data.

Table V

Genetic variability in squid

	# of Loci surveyed	# of Individuals surveyed per locus	% Polymorphic loci (1% level)	Average Ho	Average Ne	Reference
Illex illecebrosus	11	10–156	9	.005	1.01	Romero and Amaratunga, 1981
Loligo opalescens	30	45	17	.037	1.06	Augustyn and Grant, 1988
Loligo pealei	19	40–994	5	.006	1.01	This paper
Loligo plei	9	8	0	.000	1.00	This paper
Loligo vulgaris reynaudii	30	44	23	.030	1.05	Augustyn and Grant, 1988
Loligo vulgaris vulgaris	30	15	7	.011	1.01	Augustyn and Grant, 1988
Lolliguncula brevis	9	8	0	.000	1.00	This paper
Average for other invertebrates			38	.100	1.11	Nevo *et al.*, 1984

Values for *Loligo pealei* and *Illex illecebrosus* are for combined data over several collections. Ho = observed heterozygosity, Ne = effective number of alleles.

Thus, on the whole, biochemical genetic studies have proven to be very useful in the study of squid stock and population structure, furnishing data on the number of species present (Smith *et al.*, 1981; Augustyn and Grant, 1988) and the spatial distribution of breeding units within these species (Ally and Keck, 1978; Christofferson *et al.*, 1978; this paper). Obviously, this sort of information should be of central importance to fisheries management because, to use a fishery stock effectively, the number of species present, their spatial distributions, and their population structure must be considered.

Acknowledgments

This project was made possible through a collaboration of scientists and staff of the United States National Marine Fisheries Service, Northeast Fisheries Center and the Marine Biological Laboratory, both in Woods Hole, Massachusetts. We thank Y. P. Wang for technical assistance. Dr. R. T. Hanlon kindly supplied specimens through DHHS Grant RR01024. This project was supported in part by a grant from the Charles Ulrick and Josephine Bay Foundation to Dr. Garthwaite.

Literature Cited

Ahmad, M., D. O. F. Skibinski, and J. A. Beardmore. 1977. An estimate of the amount of genetic variation in the common mussel *Mytilus edulis*. *Biochem. Genet.* **15:** 833–846.

Ally, J. R. R., and S. A. Keck. 1978. A biochemical-genetic population structure study of market squid, *Loligo opalescens*, along the California coast. *Calif. Dept. Fish Game Fish Bull.* **169:** 113–121.

Augustyn, C. J., and W. S. Grant. 1988. Biochemical and morphological systematics of *Loligo vulgaris vulgaris* Lamarck and *Loligo vulgaris reynaudii* D'Orbigny NOV. COMB. (Cephalopoda: Myopsida). *Malacologia* **29:** 215–233.

Avise, J. C. 1974. Systematic value of electrophoretic data. *Syst. Zool.* **23:** 465–481.

Ayala, F. J. 1983. Enzymes as taxonomic characters. Pp. 3–26 in *Protein Polymorphism: Adaptive and Taxonomic Significance*, G. S. Oxford and D. Rollinson, eds. Academic Press, New York.

Berry, S. 1911. Notes on some cephalopods in the collection of the University of California. *Univ. Calif. Publ. Zool.* **8:** 301–310.

Blainville, H. 1823. Mémoire sur les espèces du genre calmar (*Loligo*, Lamarck). *J. Physique Chimie d'Histoire Naturelle* **96:** 116–135.

Briggs, J. C. 1974. *Marine Zoogeography*. McGraw Hill, New York. 475 pp.

Christofferson, J. P., A. Foss, W. E. Lambert, and B. Welge. 1978. An electrophoretic study of select proteins from the market squid, *Loligo opalescens* Berry. *Calif. Dept. Fish Game Fish Bull.* **169:** 123–133.

Cohen, A. C. 1976. The systematics and distribution of *Loligo* (Cephalopoda, Myopsida) in the western North Atlantic, with descriptions of two new species. *Malacologia* **15:** 299–367.

Fields, W. G. 1965. The structure, development, food relations, reproduction, and life history of the squid, *Loligo opalescens* Berry. *Calif. Dept. Fish Game Fish Bull.* **131:** 1–108.

Gray, J. E. 1849. Catalogue of the mollusca in the collection of the British Museum. Pt. 1. Cephalopoda Antepedia. British Museum, London.

Hanlon, R. T. 1988. Behavioral and body patterning characters useful in taxonomy and field identification of cephalopods. *Malacologia* **29:** 247–264.

Harris, H., and D. A. Hopkinson. 1976. *Handbook of Enzyme Electrophoresis in Human Genetics*. American Elsevier, New York.

Hixon, R. F. 1983. *Loligo opalescens*. Pp. 95–114 in *Cephalopod Life Cycles*, Vol. 1, P. R. Boyle, ed. Academic Press, New York.

Ihssen, P. E., H. E. Booke, J. M. Casselman, J. M. McGlade, N. R. Payne, and F. M. Utter. 1981. Stock identification: materials and methods. *Can. J. Fish. Aquat. Sci.* **38:** 1838–1855.

Kashiwada, J., and C. W. Recksiek. 1978. Possible morphological

indicators of population structure in the market squid, *Loligo opalescens*. *Calif. Dept. Fish Game Fish Bull.* **169:** 99–111.

Lamarck, C. 1798. Extrait d'un mémoire sur le genre de la *Sèche*, du *Calmar* et du *Poulpe*, vulgairement nommés, polypes de mer. *Bull. Société Philomatique Paris* **2:** 129–131.

Lange, A. M. T., and M. P. Sissenwine. 1980. Biological considerations relevant to the management of squid (*Loligo pealei* and *Illex illecebrosus*) of the northwest Atlantic. *Mar. Fish. Rev.* **42**(7–8)**:** 23–38.

Lange, A. M. T., and M. P. Sissenwine. 1983. Squid resources of the northwest Atlantic. *FAO Fish. Tech. Pap.* **231:** 21–54.

LeSueur, C. A. 1821. Descriptions of several new species of cuttlefish. *J. Acad. Nat. Sci. Philadelphia* **2:** 86–101.

Mainland, D., L. Herrera, and M. I. Sutcliffe. 1956. *Statistical Tables for use with Binomial Samples—Contingency Tests, Confidence Limits, and Sample Size Estimates.* Department of Medical Statistics, New York University College of Medicine, New York. 83 pp.

Mesnil, B. 1977. Growth and life cycle of squid, *Loligo pealei* and *Illex illecebrosus*, from the northwest Atlantic. *ICNAF Res. Doc.* **76/VI/65:** 55–69.

Nei, M. 1972. Genetic distance between populations. *Am. Nat.* **106**: 283–292.

Nevo, E., A. Beiles, and R. Ben-Shlomo. 1984. The evolutionary significance of genetic diversity: ecological, demographic and life history correlates. Pp. 13–213 in *Evolutionary Dynamics of Genetic Diversity*, G. S. Mani, ed. Springer-Verlag, New York.

d'Orbigny, A. 1845. Mollusques vivants et fossiles. 1. Paris.

Romero, M. C. L., and T. Amaratunga. 1981. Preliminary results of biochemical-genetic population structure study of the squid *Illex illecebrosus*. Third annual meeting of the Northwest Atlantic Fisheries Organization. *NAFO SCR Doc.* 81/IX/103. Serial No. N405.

Selander, R. K., M. H. Smith, S. Y. Yang, W. E. Johnson, and J. B. Gentry. 1971. IV. Biochemical polymorphism and systematics in the genus *Peromyscus*. I. Variation in the old-field mouse (*Peromyscus polionotus*). *Univ. Texas Publ.* **7103:** 49–90.

Shaw, C. R., and R. Prasad. 1970. Starch gel electrophoresis of enzymes—a compilation of recipes. *Biochem. Genet.* **4:** 297–320.

Smith, P. J., P. E. Roberts, and R. J. Hurst. 1981. Evidence for two species of arrow squid in the New Zealand fishery. *New Zealand J. Mar. Freshwater Res.* **15:** 247–253.

Sokal, R. R., and F. J. Rohlf. 1969. *Biometry*. W. H. Freeman & Co., San Francisco. 776 pp.

Summers, W. C. 1971. Age and growth of *Loligo pealei*, a population study of the common Atlantic Coast squid. *Biol. Bull.* **141:** 189–201.

Summers, W. C. 1983. *Loligo pealei*. Pp. 115–142 in *Cephalopod life Cycles*, Vol. 1, P. R. Boyle, ed. Academic Press, New York.

Verrill, A. E. 1882. II. Report on the cephalopods of northeastern coast of America. Pp. 211–455 in *Report to the Commissioner, 1879*. Part VII. U. S. Commission of Fish and Fisheries.

Whitaker, J. D. 1980. Squid catches resulting from trawl surveys off the southeastern United States. *Mar. Fish. Rev.* **42**(7–8)**:** 39–43.

Reference: *Biol. Bull.* **177**: 295–302. (October, 1989)

Factors Controlling Attachment of Bryozoan Larvae: A Comparison of Bacterial Films and Unfilmed Surfaces

J. S. MAKI[1], D. RITTSCHOF[2], A. R. SCHMIDT[2], A. G. SNYDER[1], AND R. MITCHELL[1]

[1] *Laboratory of Microbial Ecology, Division of Applied Sciences, Harvard University, Cambridge, Massachusetts 02138, and* [2] *Duke University Marine Laboratory, Pivers Island, Beaufort, North Carolina 28516*

Abstract. The effects of individual species of marine bacteria on the attachment of larvae of the bryozoan *Bugula neritina* were examined in the laboratory. Bacteria, grown to mid-exponential phase and allowed to adsorb to polystyrene petri dishes, attached at densities of 10^6–10^7 cells cm^{-2}. Bryozoan attachment assays (30 min) were used to compare the effects of adsorbed cells of three species of bacteria with unfilmed surfaces. Larvae permanently attached, at high percentages (65–94%), to unfilmed polystyrene, hydrophobic (*i.e.*, low wettability, low surface energy) control surfaces. This activity agrees with reports in the literature. Films of individual species of bacteria can influence bryozoan attachment. Three separate strains of the bacterial species *Deleya marina* inhibited attachment, but two other species of marine bacteria did not. Measurements indicated that all five bacteria tested differed in their cell-surface hydrophobicity, but that their films were similar in that they were all highly wettable (*i.e.*, high surface free energy). Our data indicate that factors in addition to substratum surface energy determine attachment of bryozoan larvae especially when bacterial films are present. Bacterial extracellular materials may be involved.

Introduction

Bryozoans are economically important marine fouling organisms (Ryland, 1976; Soule and Soule, 1977; Woollacott, 1984). The substratum preferences exhibited by their larvae range from the very specific to the very general (Ryland, 1974). Most bryozoans require a substratum that provides firm support for attachment, and many also prefer surfaces that have a smooth or glossy finish (Ryland, 1974, 1976). One critical characteristic in larval preference in settlement appears to be the surface free energy of the substratum (Mihm *et al.*, 1981; Woollacott, 1984). A surface with a low surface free energy has a low wettability and is hydrophobic, while a surface with a high surface free energy has a high wettability and is hydrophilic. Many bryozoan species prefer to settle and metamorphose on low surface free energy, hydrophobic substrata (Eiben, 1976; Loeb, 1977; Mihm *et al.*, 1981; Rittschof and Costlow, 1987a, 1987b, 1988).

Although a bacterial film is not essential for larval attachment (Ryland, 1976), microbial films on substrata influence the attachment of larvae from a number of different species of bryozoa (Miller *et al.*, 1948; Wisely, 1958; Crisp and Ryland, 1960; Ryland, 1974; Mihm *et al.*, 1981; Brancato and Woollacott, 1982). Mihm *et al.* (1981) demonstrated that bacterial films on polystyrene (a low surface energy substratum) caused the surface to become more wettable (higher surface free energy) and also decreased the attachment of larvae of the bryozoan *Bugula neritina*. However, Mihm *et al.* (1981) pointed out that the reduction in larval settlement could not be attributed to the change in surface free energy alone and suggested that *Bugula* larvae respond to two sensory stimuli: one for surface free energy, the second to some aspect of the bacterial-organic film. The latter stimulus could override the response to surface free energy alone (Mihm *et al.*, 1981). The response of bryozoan larvae to natural products that inhibit larval attachment may function by the same mechanism (Rittschof *et al.*, 1988).

It has been demonstrated that films, each composed of individual species of bacteria, can cause different attachment responses by spirorbid polychaete larvae (Kirchman *et al.*, 1982), barnacle cypris larvae (Maki *et al.*, 1988), and macroalgal swarmers (Thomas and Allsopp,

Received 16 September 1988; accepted 31 July 1989.

1983). Perhaps the species composition of the bacterial films may also influence attachment by bryozoan larvae. We examined the following questions: (1) could films of individual species of bacteria elicit different attachment responses from bryozoan larvae? (2) would aging the bacterial films change the larval attachment response? (3) could larval attachment be correlated with surface free energy measurements using either bacterial cell-surface hydrophobicity or bacterial film wettability? We report here the results of laboratory experiments in which we tested the attachment responses of *Bugula neritina* larvae to bacteria irreversibly attached (Marshall *et al.*, 1971) to polystyrene surfaces. Our data indicate that the attachment of bryozoan larvae varied for both films of individual bacteria and films of different ages, and that larval responses were not correlated with measurements of either the bacterial cell-surface hydrophobicity or the bacterial film wettability.

Materials and Methods

All seawater used in larval attachment experiments was passed through a septic 100,000 Dalton ultrafiltration system (Millipore) and subsequently passed through two sterile filters (0.2 μm pore size, Millipore), placed one on top of the other. This seawater is referred to as filtered seawater (FSW).

Bacteria

Five cultures of marine bacteria were used in the larval attachment experiments. Four of the pure cultures were obtained from the American Type Culture Collection, Rockville, Maryland: *Deleya marina* 25374, *D. marina* 27129, *D. marina* 35142, and *Vibrio vulnificus* 27562. The fifth bacterium was isolate DLS1, a gram negative, polarly flagellated, oxidase positive, fermentative, rod-shaped bacterium that was isolated from the estuarine waters around the Duke University Marine Laboratory using Marine Agar 2216 (Difco, Detroit, Michigan). To preserve the bacteria and their respective surface characteristics, cultures upon receipt or isolation were frozen in vials with glycerol from which new stock cultures were periodically established.

Preparation of dishes with attached bacteria

Bacteria were allowed to attach to polystyrene petri dishes (Falcon 1006, 50 × 9 mm) following the methods outlined by Fletcher (1977). Cultures were grown to exponential phase at 26°C in Marine Broth 2216 (Difco, Detroit, Michigan) and harvested by centrifugation. Bacteria were washed, centrifuged, and resuspended in FSW (10^9 cells·ml^{-1}). Petri dishes were filled with 7 ml of the bacterial suspension and incubated at 26°C for 2.5–3.0 h. Dishes were rinsed by dipping them 10× in 500 ml of FSW. Bacteria still attached to the dishes were considered irreversibly attached (Marshall *et al.*, 1971). The dishes were then filled with 5 ml of FSW. Experiments were performed using either these dishes (for convenience termed Day 1) or with dishes in which the bacteria were aged *in situ* for 1 to 5 days. Aging of the attached bacteria in the dishes was accomplished through the following manner: every day after filling the Day 1 dish with FSW, it was emptied, and fresh FSW was added. Aged dishes were rinsed as above and refilled with 5 ml of FSW immediately prior to attachment assays.

Following the larval attachment experiments, two dishes of each bacterial treatment and control were fixed with formaldehyde (final concentration 1 to 2%, v/v) for quantification of attached bacteria using acridine orange and epifluorescence microscopy (Daley and Hobbie, 1975). These dishes did not receive any larvae. At least 300 bacteria were counted per dish and the number of cells expressed as bacteria per cm^2. Aged films were streaked on Marine Agar 2216 to check for contamination.

Larvae and attachment experiments

The larval bryozoan attachment assay was that previously described by Rittschof *et al.* (1988). *Bugula neritina* colonies were collected from the Duke University Marine Laboratory floating dock and from pilings of the north end of the Atlantic Beach, North Carolina, bridge. In the laboratory, colonies were maintained at 25° ± 3°C in the dark in aerated seawater and fed cultured diatoms (*Skeletonema costatum* Greville) at 100,000 cells ml^{-1} day^{-1}. *B. neritina* larvae were released in the morning in response to exposure to artificial light. Larvae (20–80) were collected in a 250–450 μl volume of seawater and pipetted into one of two dishes of each treatment (*i.e.*, bacterial films and controls) that already contained 5 ml of FSW. Repeated transfers of larvae resulted in a maximum of 160 larvae in any one dish. Assays were for 30 min at 22° ± 2°C. Timing of the assay began with the final larval addition and was terminated by the addition of a drop of formalin. Larvae adhering to the substratum and having no visible cilia (due to involution of the corona during metamorphosis, Zimmer and Woollacott, 1977; Woollacott and Zimmer, 1978) were counted as attached, while those that either were not adherent or had visible cilia were counted as not attached (90× magnification). Colonies used as a source of larvae were replaced when larval attachment to polystyrene fell below 50% in 30 min.

Experiments examined the effect of axenic films of bacteria and bacterial film age on the attachment of larvae. The first set of experiments used bacterial films of

different ages composed of either *Deleya marina* (ATCC 25374), *Vibrio vulnificus* (ATCC 27562), or isolate DLS1. The second set of experiments used bacterial films composed of either *D. marina* ATCC 25374, ATCC 27129, or ATCC 35142. Controls were FSW with no additions (polystyrene).

Frequencies of attached and not-attached individuals pooled from the two dishes were compared between treatments by G statistic (corrected for continuity) generated from a contingency analysis (Zar, 1984). The null hypothesis for the contingency analysis was that there was no significant difference between the control (polystyrene) and any one treatment. The family and individual level of significance in each group of comparisons was determined using Bonferroni's method for multiple comparisons (Seber, 1977).

Surface free energy measurements: bacterial cell-surface hydrophobicity and film wettability

Because the surface free energy has been shown to be important in the attachment of bryozoan larvae to a substratum, we determined both the cell-surface hydrophobicity of the bacteria in solution, using the adhesion to hydrocarbon method (Rosenberg *et al.*, 1980) and the wettability of films of attached bacteria derived from the same cultures, using measurements of air bubble contact angles (Fletcher and Marshall, 1982; Dillon *et al.*, 1989). Bacteria were grown to mid-exponential phase in Marine Broth 2216 (Difco, Detroit, Michigan) and harvested by centrifugation. Bacteria were washed once and resuspended in FSW or an artificial seawater, Nine Salt Solution (NSS) (Little *et al.*, 1986) to approximately 10^9 cells ml^{-1}.

To measure cell-surface hydrophobicity by adhesion to hydrocarbons (Rosenberg *et al.*, 1980), hexadecane (0.08, 0.16, 0.32, and 0.64 ml) was added to triplicate test tubes containing 4 ml of the bacterial solution (A_{400} = 1.3–1.5) and vortexed for 2 min. The phases were allowed to separate for 15 min and the absorbance (A_{400}) of the aqueous phase was measured spectrophotometrically. The results of the adhesion to hexadecane experiments are presented as the percent absorbance (A_{400}) left in the aqueous phase (bacteria with a high surface free energy and a hydrophilic cell surface would have a value of 100%).

Air bubble contact angle determinations (Fletcher and Marshall, 1982; Dillon *et al.*, 1989) were used as a measure of the wettability of unfilmed and filmed surfaces. Coupons (approximately 1 cm × 2 cm) of the polystyrene petri dishes (Falcon 1006) were placed in larger petri dishes (100 × 15 mm, Falcon 1029) and bacteria were allowed to attach to the coupons as for the petri dishes above. After attachment, coupons were retrieved with sterile forceps and rinsed as above and placed in another large petri dish containing FSW or NSS. For bubble contact angle measurements, the coupons were placed in a stage at the top of a chamber containing FSW or NSS. An air bubble, injected from a syringe (0.25 mm ID), was allowed to rise 6–7 mm to rest against the test surface. The average diameter of the bubble was 2.0 mm. Contact angles were measured directly using a Vernier microscope with a goniometer eyepiece. Results represent the mean of at least ten observations. For air bubbles where the air came in contact with the surface, errors were within 2° unless recorded otherwise; for air bubbles that did not make contact with the surface, indicating a high surface free energy, a value of <15° was recorded (Fletcher and Marshall, 1982; Dillon *et al.*, 1989). Coupons were then fixed with formaldehyde for quantification of attached bacteria as above. Comparisons of air bubble contact angle measurements on bacterial films were made to parallel measurements on muffled glass (500°C for 4 h) and polystyrene. *Bugula neritina* larvae have known attachment responses to these last two surfaces using the above attachment assay (Rittschof and Costlow, 1987a, b; 1988).

Results

Experiments were designed to examine the attachment of *Bugula neritina* larvae to bacterial films in the laboratory and to examine the larval attachment in relationship to estimates of surface free energies. These factors were hypothesized to be involved in the larval attachment response.

Bacterial densities

Bacteria adhered in densities of 10^6–10^7 attached bacteria per cm^2 both to the polystyrene petri dishes (Tables I, II) and to polystyrene coupons (Table III). Films with lower densities of bacteria (10^6 per cm^2) were not confluent but visually appeared randomly distributed rather than patchily. Films with higher densities of bacteria were confluent. Attached bacteria were undetected on the control polystyrene dishes indicating that the filtration of the seawater was effective in removing bacteria. The densities of attached cells on the aged dishes were lower than on Day 1 dishes, suggesting that some bacteria may have desorbed from the surface or lysed. Examination of the agar plates inoculated with bacteria from the aged dishes revealed only one colony type.

Larval attachment

The percentage of *Bugula neritina* larvae that attached to polystyrene control dishes in 30 min ranged between 66% and 93% (*e.g.*, Tables I, II). Bacterial films com-

Table I

Bugula neritina *larval attachment: data from experiments using films of different ages composed of three different species of bacteria,* Deleya marina, Vibrio vulnificus, *and isolate DLS1 attached to polystyrene petri dishes*

Treatment	No. of bacteria[a] ($\times 10^7$) cm^{-2} (+SD)	Total no. of larvae[b]	% larvae attached	G statistic[c] vs polystyrene	
				G No.	*P*
Polystyrene	nd	73	91.8		
D. marina					
Day 1	5.10 (0.18)	54	7.4	99.46	<0.001
Day 2	3.52 (0.30)	55	40.0	39.12	<0.001
Day 4	0.40 (0.06)	95	60.0	21.91	<0.001
V. vulnificus					
Day 1	4.59 (0.49)	67	79.1	3.65	NS
Day 2	2.60 (0.24)	263	97.7	3.58	NS
Day 4	1.47 (0.14)	179	97.2	2.25	NS
Isolate DLS1					
Day 1	1.73 (0.28)	74	81.1	2.78	NS
Day 2	0.86 (0.04)	94	87.2	0.48	NS
Day 4	0.53 (0.04)	140	96.4	0.37	NS

[a] Mean number of attached bacteria cm^{-2} from counts of two dishes using epifluorescence microscopy after staining with 0.01% (final concentration, w/v) acridine orange. Bacteria were grown to mid-exponential phase in Marine Broth 2216 (Difco, Detroit, MI) at 26°C, harvested by centrifugation, washed, and resuspended to 10^9 cells ml^{-1}. Dishes were exposed to bacterial solution for 2.5 to 3.0 h before being rinsed and used for experiments. Day 1 dishes were prepared the same day as the experiment, while Day 2 and 4 dishes were prepared 2 and 4 days prior to the experiment, respectively. FSW in these dishes was replaced daily after their preparation. nd = none detected.

[b] Total number of larvae in two dishes.

[c] Using Bonferroni's method of multiple comparisons, the family level of significance in the experiment was $\alpha = 0.05$ with an individual significance level of $\alpha/9 = 0.0056$ with 1 df where 9 is the number of comparisons. NS = not significant.

posed of either *Deleya marina, Vibrio vulnificus,* or isolate DLS1, and aged *in situ* for different lengths of time were tested for their effect upon attachment of *B. neritina* larvae. Films of *D. marina* of all ages significantly inhibited larval attachment compared to the polystyrene controls (Table I). Films of all ages composed of *V. vulnificus* and isolate DLS1 did not significantly inhibit larval attachment when compared to polystyrene controls (Table I). Similarly, larval attachment to films composed of *D. marina* was significantly lower than attachment to films composed of the other two bacteria on all days ($38.427 < G < 110.676$, $P < 0.001$, 1 df). Larval attachment on films composed of *V. vulnificus* or isolate DLS1 was only different on films aged for 2 days ($G = 11.826$, $P < 0.001$, 1 df). For all three bacteria, the larval attachment to Day 4 films was significantly higher than attachment to Day 1 films ($P < 0.001$, G statistic with 1 df).

In an experiment using films aged up to 5 days, larval attachment on *D. marina* films was again significantly inhibited when compared to the polystyrene control (control = 93.0% out of 214 total larvae attached, *D. marina* = 3.5–10.3% out of 58–86 total larvae attached, $P < 0.001$, G statistic with 1 df, family level of significance of 0.05, individual level of significance of 0.0056). Films of *V. vulnificus* (larval attachment = 82–98% of 70–108 total larvae) were not inhibitory ($P > 0.05$, G statistic with 1 df). Films composed of isolate DLS1 aged 3 days inhibited larval attachment (45.8% out of 59 total larvae attached, $P < 0.001$, G statistic with 1 df). Larval attachment on all other DLS1 films was similar to attachment to the control. Comparisons of larval attachment between films of different bacteria showed that attachment to films composed of *D. marina* was lower than on films of the other two bacteria on all days ($28.514 < G < 171.368$, $P < 0.001$, 1 df) and that attachment on isolate DLS1 was only different from that on *V. vulnificus* on films aged 3 days ($G = 58.393$, $P < 0.001$, 1 df). Larval attachment to older and younger films of *D. marina* was not significantly different ($P > 0.05$) while attachment to older and younger films of *V. vulnificus* and DLS1 were ($P < 0.005$ and $P < 0.024$, respectively, G statistic with 1 df). The data indicate that films of individual species of bacteria can affect the attachment of *B. neritina* larvae. Although there were statistical differences in larval attachment to older and younger films of the same species (with one exception, 3-day-old films of DLS1), in general, films of inhibitory species remained inhibitory and films of non-inhibitory species remained non-inhibitory compared to the controls. Experiments were conducted with three separate cultures of bacteria, all classified as *Deleya marina,* to determine if phenotypically similar bacteria could elicit different attachment responses from bryozoan larvae. All three cultures of *D. marina* significantly inhibited larval attachment com-

Table II

Bugula neritina *larval attachment: data from experiments using films of three strains of the marine bacterium,* Deleya marina, *attached to polystyrene petri dishes*

Treatment	No. of bacteria[a] ($\times 10^7$) cm^{-2} (+SD)	Total no. of larvae[b]	% larvae attached	G statistic[c] vs polystyrene	
				G No.	*P*
A.					
Polystyrene	nd	83	84.3		
D. marina					
ATCC 25374	2.86 (0.43)	66	4.5	105.42	<0.001
ATCC 27129	1.48 (0.28)	67	7.5	96.20	<0.001
ATCC 35142	1.76 (0.21)	73	15.1	78.73	<0.001
B.					
Polystyrene	nd	43	69.8		
D. marina					
ATCC 25374	2.52 (0.43)	72	2.8	60.77	<0.001
ATCC 27129	0.65 (0.09)	73	2.7	61.35	<0.001
ATCC 35142	1.79 (0.27)	66	1.5	62.33	<0.001

[a] The mean number of attached bacteria cm^{-2} from counts of two dishes determined using epifluorescence microscopy (see Table I footnotes).
[b] Total number of larvae in two dishes.
[c] Using Bonferroni's method of multiple comparisons the family level of significance in the experiment was $\alpha = 0.05$ with an individual significance level of $\alpha/3 = 0.016$ with 1 df where 3 is the number of comparisons.

pared to polystyrene controls (Table II). There were no significant differences in larval attachment to films composed of the separate cultures ($0.006 < G < 3.310$, $P > 0.05$, 1 df).

Surface free energy measurements: bacterial cell-surface hydrophobicity and wettability of films

The test to determine cell-surface hydrophobicity by adhesion to hexadecane showed that the three cultures of *D. marina* in solution were more hydrophobic (*i.e.*, had a lower surface free energy) than the other two bacteria (Fig. 1). However, air bubble contact angle measurements on films of the attached bacteria were all <15° even after aging the bacterial films. The air bubble did not come in contact with the surface and all films had a high surface free energy (Table III). Air bubble contact angles on polystyrene controls were 90° (low surface free energy) while those on glass baked at 500°C were also <15°.

Discussion

Bryozoan larvae have well-developed mechanisms for determining a suitable substratum, and these may be species specific (Ryland, 1976; Woollacott, 1984). The process begins with larvae gliding or crawling on a surface and testing it with cilia (Woollacott and Zimmer, 1978), and is often followed by a temporary attachment that employs an acid mucopolysaccharide adhesive (Loeb and Walker, 1977). Permanent attachment involves the eversion of the metasomal sac (Woollacott and Zimmer, 1978), which releases proteins that together with acid mucopolysaccharide provide the permanent adhesive (Loeb and Walker, 1977).

Previous investigations have illustrated that natural films of microorganisms can inhibit (Crisp and Ryland, 1960; Mihm *et al.*, 1981) or facilitate (Miller *et al.*, 1948; Wisely, 1958; Ryland, 1974; Mihm *et al.*, 1981; Brancato and Woollacott, 1982) the attachment of bryozoan larvae. Mihm *et al.* (1981) demonstrated that the presence of microbial films could make an unattractive substratum (*e.g.*, glass) attractive, and an attractive substratum (*e.g.*, polystyrene) unattractive. Our data demonstrate that, on a suitable polystyrene substratum, films composed of some bacteria significantly inhibit attachment of *Bugula neritina* larvae when compared to unfilmed controls. Other bacteria did not inhibit larval attachment. These data suggest that the species composition of a film may be important in the larval attachment response. Larval attachment to aged films of bacteria was generally higher than to freshly prepared films. The aging of the films resulted in a decrease in the density of attached bacteria (Table I) suggesting that bacterial density may be one important factor in the larval response to the film. However, in our experiments films composed of bacteria that were inhibitory to larval attachment remained inhibitory regardless of the age of the film. In contrast, films composed of bacteria that did not inhibit larval attachment remained uninhibatory in comparison with unfilmed polystyrene controls (Table I). Our experi-

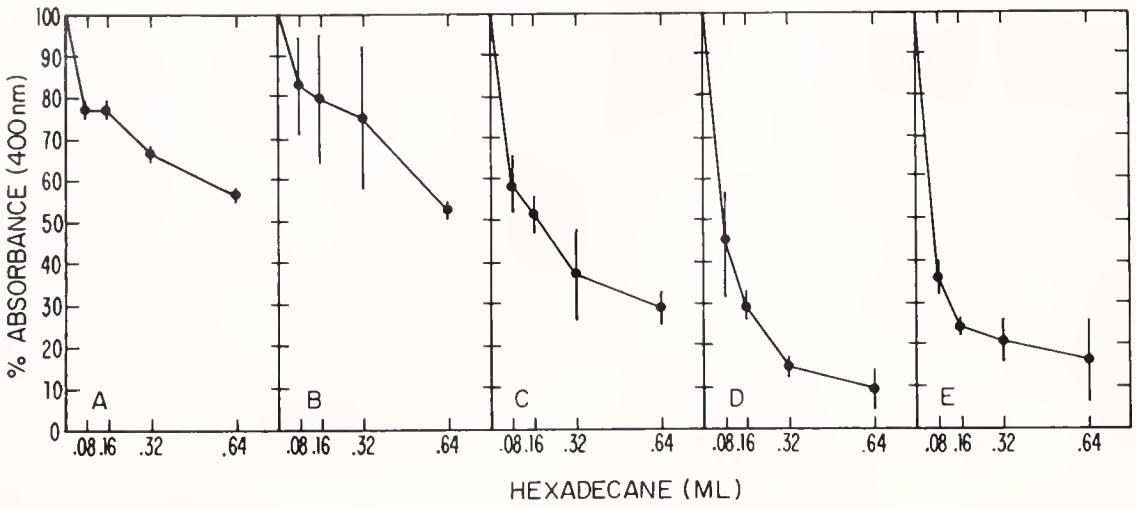

Figure 1. Affinity of mid-exponential phase bacterial cells to hexadecane as a function of hexadecane volume. Results are from three separate batch cultures and are expressed as percentage of the initial absorbance (A_{400}) remaining in the aqueous phase as a function of hexadecane volume. A. *Vibrio vulnificus* ATCC 27562. B. Isolate DLS1. C. *Deleya marina* ATCC 25374. D. *D. marina* ATCC 27129. E. *D. marina* 35142. Bars = standard deviation.

mental data indicate that the bacterial densities of 10^6 attached cells cm^{-2} were detectable by *B. neritina* larvae.

Because the surface free energy of the substratum is such an important factor in the attachment of bryozoan larvae, with larvae attaching in greater numbers to low surface energy, low wettability, hydrophobic surfaces, we used tests to measure both the cell-surface hydrophobicity and film wettability of the bacteria to determine if any correlations could be made between these measurements and larval attachment. The results of our cell-surface hydrophobicity experiments using the adhesion to hexadecane tests indicated that the three cultures of *Deleya marina* were the most hydrophobic (had the lowest surface free energy) of the five bacteria (Fig. 1). If cell-surface hydrophobicity of the bacteria was the dominant factor favoring bryozoan attachment to surfaces coated with bacteria, the larvae should have attached in greater numbers to the more hydrophobic (lowest surface free energy) bacteria (*i.e.*, the cultures of *D. marina*). However, films of *D. marina* were inhibitory to larval attachment when compared to both unfilmed polystyrene and films composed of *V. vulnificus* or isolate DLS1. Therefore, it appears that cell-surface hydrophobicity is not the dominant factor controlling the attachment of bryozoan larvae to surfaces possessing a bacterial film.

The measurements of the wettability of the bacterial film to estimate the surface free energy of the substratum may be more indicative of the surface sensed by a settling larva. Our data show that, regardless of the differences in the cell-surface hydrophobicity determinations of the bacteria, the films of all five bacteria had a similar high wettability and surface free energy (*i.e.*, they were hydrophilic) (Table III). Differences between cell-surface and colonial/film hydrophobicity have been previously reported for fish skin bacterial isolates and other bacteria (Sar, 1987; Sar and Rosenberg, 1987). The use of bubble contact angles permits the quantification of the wettabil-

Table III

Wettability measurements of bacterial films on polystyrene coupons using air bubble contact angles

Bacterium	Film age	Bubble contact angle[a]	No. of bacteria[b] ($\times 10^7$) cm^{-2} (+SD)
Deleya marina			
ATCC 25374	Day 1–Day 5	<15°	2.24 (1.37)–1.29 (0.95)[c]
ATCC 27129	Day 1	<15°	2.43 (0.14)
ATCC 35142	Day 1	<15°	2.65 (0.29)
Vibrio vulnificus	Day 1–Day 5	<15°	1.41 (0.09)–1.02 (0.13)[c]
Isolate DLS1	Day 1–Day 5	<15°	2.36 (0.09)–1.98 (0.12)[c]

[a] Bubble contact angle measurements of at least five air bubbles on surfaces of aged bacterial films on polystyrene coupons. Angles < 15° indicate that the bubble did not come in contact with the surface.

[b] Mean number of attached bacteria cm^{-2} from counts of at least five coupons using epifluorescence microscopy after staining with 0.01% (final concentration, w/v) acridine orange. Bacteria were grown and treated as in footnotes to Table I. Coupons were exposed to bacterial solution for 2.5 to 3.0 h before being rinsed and having their contact angles measured. Day 1 coupons were prepared the same day as the measurement, while Day 2, 3, 4, and 5 coupons were prepared 2, 3, 4, and 5 d before measurement, respectively. FSW for aged coupons was replaced daily after their preparation.

[c] Numbers represent the range of attached bacteria on coupons from Day 1 to Day 5.

ity (and therefore, the surface free energy) of a substratum that is normally in contact with a liquid medium (Loeb, 1985). Films of *D. marina, V. vulnificus,* and DLS1 transformed hydrophobic polystyrene (low surface free energy and wettability, contact angle = 90°) to a hydrophilic surface (high surface free energy and wettability, contact angle <15°) similar to glass, which is an unfavorable substratum for bryozoan larval attachment (Mihm *et al.,* 1981; Rittschof and Costlow, 1987a, b, 1988). If film wettability was the dominant factor that influenced bryozoan attachment in the presence of bacteria, then all the bacteria we used in our experiments should have elicited a similar unfavorable attachment response by the larvae. However, our data show that films of both *V. vulnificus* and isolate DLS1 (with one exception) were not inhibitory when compared to unfilmed polystyrene. These data support the hypothesis of Mihm *et al.* (1981) that bryozoan larvae possess a detection mechanism for an aspect of the bacterial-organic film other than its wettability (*i.e.,* surface free energy). Our data extend this hypothesis to individual species of bacteria.

Although Kirchman and Mitchell (1984) suggested that lectins on the surface of bryozoan larvae may mediate the choice of an attachment site by the larvae when bacterial films are involved, the actual sensory mechanism is unknown. However, the use of an adhesive in the temporary attachment of bryozoan larvae (Loeb and Walker, 1977) may create a situation analogous to that of attachment of barnacle cypris larvae. Crisp *et al.* (1985) have suggested that cypris larvae may not settle on, or permanently attach to, a substratum to which their temporary adhesive does not bind strongly. If bryozoan larvae function in a similar manner, then an explanation of our data may be that the temporary adhesive binds more strongly to the extracellular material of some bacteria than others. We are currently attempting to define the inhibitory factors involved in the attachment of these larvae to bacterial films.

Acknowledgments

We thank Dr. Brenda Little, NORDA, Bay St. Louis, MS, for use of the bubble contact angle measuring device. This work was supported in part by U.S. Office of Naval Research contracts #N00014-78-C-0294 and #N00014-86-K-0261 with Duke University, and U.S. Office of Naval Research contract #N00014-85-K-0061 and NOAA Sea Grant No. NA79AA-D-00091 with Harvard University.

Literature Cited

Brancato, M. S., and R. M. Woollacott. 1982. Effect of microbial films on settlement of bryozoan larvae (*Bugula simplex, B. stolonifera,* and *B. turrita*). *Mar. Biol.* **71:** 51–56.

Crisp, D. J., and J. S. Ryland. 1960. Influence of filming and of surface texture on the settlement of marine organisms. *Nature* **185:** 119.

Crisp, D. J., G. Walker, G. A. Young, and A. B. Yule. 1985. Adhesion and substrate choice in mussels and barnacles. *J. Colloid Interface Sci.* **104:** 40–50.

Daley, R. J., and J. E. Hobbie. 1975. Direct counts of aquatic bacteria by a modified epifluorescence technique. *Limnol. Oceanogr.* **20:** 875–882.

Dillon, P. S., J. S. Maki, and R. Mitchell. 1989. Adhesion of *Enteromorpha* swarmers to microbial films. *Microb. Ecol.* **17:** 39–47.

Eiben, R. 1976. Einfluss von Benetzungsspannung und Ionen auf die Substratbesiedlung und das Einsetzen der Metamorphose bei Bryozoenlarven (*Bowerbankia gracilis*). *Mar. Biol.* **37:** 249–254.

Fletcher, M. 1977. The effects of culture concentration and age, time, and temperature on bacterial attachment to polystyrene. *Can. J. Microbiol.* **23:** 1–6.

Fletcher, M., and K. C. Marshall. 1982. Bubble contact angle method for evaluating substratum interfacial characteristics and its relevance to bacterial attachment. *Appl. Environ. Microbiol.* **44:** 184–192.

Kirchman, D., S. Graham, D. Reish, and R. Mitchell. 1982. Bacteria induce settlement and metamorphosis of *Janua (Dexiospira) brasiliensis* Grube (Polychaeta: Spirorbidae). *J. Exp. Mar. Biol. Ecol.* **56:** 153–163.

Kirchman, D., and R. Mitchell. 1984. Possible role of lectins in the settlement and metamorphosis of marine invertebrate larvae on surfaces coated with bacteria. Pp. 173–177 in *Bacteriologie Marine.* Editions du CNRS, Paris.

Little, B. J., P. Wagner, J. S. Maki, M. Walch, and R. Mitchell. 1986. Factors influencing the adhesion of microorganisms to surfaces. *J. Adhesion* **20:** 187–210.

Loeb, G. I. 1977. The settlement of fouling organisms on hydrophobic surfaces. *U.S. Naval Res. Lab. Mem. Rep.* **3665,** pp. 1–9.

Loeb, G. I. 1985. The properties of nonbiological surfaces and their characterization. Pp. 111–129 in *Bacterial Adhesion: Mechanisms and Physiological Significance,* D. C. Savage and M. Fletcher, eds. Plenum Press, New York.

Loeb, M. J., and G. Walker. 1977. Origin, composition, and function of secretions from pyriform organs and internal sacs of four settling cheilo-ctenostome bryozoan larvae. *Mar. Biol.* **42:** 37–46.

Maki, J. S., D. Rittschof, J. D. Costlow, and R. Mitchell. 1988. Inhibition of attachment of larval barnacles, *Balanus amphitrite,* by bacterial surface films. *Mar. Biol.* **97:** 199–206.

Marshall, K. C., R. Stout, and R. Mitchell. 1971. Mechanism of the initial events in the sorption of marine bacteria to surfaces. *J. Gen. Microbiol.* **68:** 337–348.

Mihm, J. W., W. C. Banta, and G. I. Loeb. 1981. Effects of adsorbed organic and primary fouling films on bryozoan settlement. *J. Exp. Mar. Biol. Ecol.* **54:** 167–179.

Miller, M. A., J. C. Rapean, and W. F. Whedon. 1948. The role of slime film in the attachment of fouling organisms. *Biol. Bull.* **94:** 143–157.

Rittschof, D., and J. D. Costlow. 1987a. Macrofouling and its management by nontoxic means. *Adv. Aquat. Biol. Fish* **1987:** 1–11.

Rittschof, D., and J. D. Costlow. 1987b. Surface determination of macroinvertebrate larval settlement. In *Proc. 21st European Mar. Biol. Symp.* (in press).

Rittschof, D., and J. D. Costlow. 1988. Bryozoan and barnacle settlement in relation to initial surface wettability: a comparison of laboratory and field studies. In *Proc. 22nd European Mar. Biol. Symp.* (in press).

Rittschof, D., I. R. Hooper, and J. D. Costlow. 1988. Settlement inhibition of marine invertebrate larvae: comparison of sensitivities of

bryozoan and barnacle larvae. Pp. 599–608 in *Marine Biodeterioration,* M. Thompson, R. Sarojini, and R. Nagabhushanam, eds. Oxford & IBH Publ. Co., Pvt., Ltd., Bombay.

Rosenberg, M., D. Gutnick, and E. Rosenberg. 1980. Adherence of bacteria to hydrocarbons: a simple method of measuring cell-surface hydrophobicity. *FEMS Microbiol. Lett.* **9:** 29–33.

Ryland, J. S. 1974. Behaviour, settlement and metamorphosis of bryozoan larvae: a review. *Thalassia Jugoslav.* **10:** 239–262.

Ryland, J. S. 1976. Physiology and ecology of marine bryozoans. *Adv. Mar. Biol.* **14:** 285–443.

Sar, N. 1987. Direction of spreading (DOS): a simple method for measuring the hydrophobicity of bacterial lawns. *J. Microbiol. Meth.* **6:** 211–219.

Sar, N., and E. Rosenberg. 1987. Fish skin bacteria: colonial and cellular hydrophobicity. *Microb. Ecol.* **13:** 193–202.

Seber, G. A. F. 1977. *Linear Regression Analysis.* John Wiley & Sons, New York.

Soule, J. D., and D. F. Soule. 1977. Fouling and bioadhesion: life strategies of bryozoans. Pp. 437–457 in *Biology of Bryozoans,* R. M. Woollacott and R. L. Zimmer, eds. Academic Press, New York.

Thomas, R. W. S. P., and D. Allsopp. 1983. The effects of certain periphytic marine bacteria upon the settlement and growth of *Enteromorpha,* a fouling alga. Pp. 348–357 in *Biodeterioration 5,* T. A. Oxley and S. Barry, eds. John Wiley & Sons, New York.

Wisely, B. 1958. The settling and some experimental reactions of a bryozoan larva, *Watersipora cucullata* (Busk). *Aust. J. Mar. Freshwat. Res.* **9:** 362–371.

Woollacott, R. M. 1984. Environmental factors in bryozoan settlement. Pp. 149–154 in *Marine Biodeterioration, an Interdisciplinary Study,* J. D. Costlow and R. C. Tipper, eds. Naval Institute Press, Annapolis.

Woollacott, R. M., and R. L. Zimmer. 1978. Metamorphosis of cellularioid bryozoans. Pp. 49–63 in *Settlement and Metamorphosis of Marine Invertebrate Larvae,* F.-S. Chia and M. E. Rice, eds. Elsevier, New York.

Zar, J. H. 1984. *Biostatistical Analysis,* 2nd. ed. Prentice-Hall, Englewood Cliffs.

Zimmer, R. L., and R. M. Woollacott. 1977. Metamorphosis, ancestrulae, and coloniality in bryozoan life cycles. Pp. 91–142 in *Biology of Bryozoans,* R. M. Woollacott and R. L. Zimmer, eds. Academic Press, New York.

Reference: *Biol. Bull.* **177**: 303–312. (October, 1989)

Metabolic Adaptations of Several Species of Crustaceans and Molluscs to Hypoxia: Tolerance and Microcalorimetric Studies

WILLIAM B. STICKLE, MARTIN A. KAPPER[1], LI-LIAN LIU, ERICH GNAIGER[2], AND SHIAO Y. WANG[3]

Department of Zoology and Physiology, Louisiana State University, Baton Rouge, Louisiana 70803

Abstract. Although some species of fish, crustaceans, and molluscs may behaviorally avoid hypoxic masses of small size and limited duration, others cannot. In a series of crustaceans, tolerance of hypoxia over 28 days at 30°C, decreases as follows: *Eurypanopeus depressus* (38 Torr = LC_{50}) > *Palaemonetes pugio* > *Rhithropanopeus harrisii* > *Penaeus aztecus* > *Callinectes sapidus* (121 Torr = LC_{50}). *Callinectes sapidus* and *E. depressus* die during 12-h exposure to anoxia and their heat dissipation rates (quantified by microcalorimetry) are depressed in seawater at 25% air saturation (normoxia) to only 32 and 47% of their metabolic rate at normoxia. In contrast, starved *Crassostrea virginica* and *Thais haemastoma* are anoxia tolerant; their metabolic rates are depressed under anoxia to 75% and 9% of the normoxic rate. Hypoxia tolerance is greater at 20°C than at 30°C for *Penaeus aztecus* and *Crassostrea virginica*, but no temperature effect on tolerance exists for *Callinectes sapidus*. Hypoxia tolerance varies inversely with salinity for *Penaeus aztecus* at 20° and 30°C and for *Callinectes sapidus* at 30°C, but it varies directly with salinity at 20°C in *Callinectes sapidus*. Greater depression of metabolic rate occurs in molluscs during anoxia exposure (and is correlated with greater hypoxia tolerance) than occurs in *Callinectes sapidus* and *Penaeus aztecus*, which are not anoxia tolerant. Heavy mortality probably occurs in young *Callinectes sapidus* and *Penaeus aztecus* and in stages of the life history when the organisms are incapable of avoiding hypoxic water masses.

Received 10 November 1988; accepted 31 July 1989.

[1] Present address: Department of Zoology, Iowa State University, Ames, Iowa 50011.

[2] Permanent address: Cyclobios, Institut fur Zoologie, Abeilung Zoophysiologie, Universitat Innsbrook, A-6020 Innsbrook, Austria.

[3] Present address: Biology Division, Oak Ridge National Laboratory, Oak Ridge, Tennessee 37831.

Introduction

Mass mortality of marine and estuarine benthic communities due to hypoxia has been widely reported (Santos and Simon, 1980a, b; Harper *et al.*, 1981; Officer *et al.*, 1984; Rabalais *et al.*, 1985). The occurrence of hypoxic bottom waters off the Louisiana coast is a common, recurrent, virtually annual phenomenon, locally known as "dead water" (Bedinger *et al.*, 1981; Turner and Allen, 1982; Boesch, 1983; Renaud, 1985; 1986a; and Rabalais *et al.*, 1986a, b). Hypoxic water masses may persist for weeks. Reports suggest that fish and crustaceans avoid hypoxic waters (Pavela *et al.*, 1983). Juveniles of two species of shrimp, *Penaeus aztecus* and *Penaeus setiferus*, are capable of detecting hypoxic waters and initiating a pattern of avoidance behavior (Renaud, 1986b). Others have suggested that crustacean mortality may be taxon specific, and that hypoxia heavily affects the more susceptible forms (Garlo *et al.*, 1979). The dissolved oxygen concentrations of offshore bottom waters have been observed to be positively correlated with the combined catches of *Penaeus aztecus* and *Penaeus setiferus*, and with fish biomass (Renaud, 1986a).

The tolerance and the physiological and behavioral responses of benthic and demersal invertebrates to long-term (weeks) exposure to hypoxic water is poorly understood. Many studies of tolerance, physiology, and biochemistry are carried out only for hours to a few days. During environmental anoxia, metabolism in bivalves is reduced to a relatively greater extent than in crustaceans, suggesting that bivalves should tolerate long-term anoxia

better than crustaceans (Gade, 1983; Gnaiger 1983a, 1987).

The objectives of this study are: (1) to compare the hypoxia tolerance of five species of decapod crustaceans with that of the oyster, *Crassostrea virginica;* (2) to compare the effects of temperature and salinity on the hypoxia tolerance of *Callinectes sapidus, Crassostrea virginica,* and *Penaeus aztecus* since these species spend all or part of their lives in the estuarine environment; and (3) to correlate the hypoxia tolerance of each species [as well as that of *Thais haemastoma* (see Kapper and Stickle, 1987)], with the degree of depression of metabolic rate during exposure to hypoxia and anoxia.

Materials and Methods

Collection and maintenance

Specimens of all five species of crustaceans used in this study, and *Thais haemastoma* were collected in the vicinity of Grand Isle, LA. Crustaceans studied include the blue crab (*Callinectes sapidus*), the brown shrimp (*Penaeus aztecus*), the xanthid crabs (*Eurypanopeus depressus* and *Rhithropanopeus harrisii*), and the grass shrimp (*Palaemonetes pugio*). *Crassostrea virginica* was purchased at dockside in the same area. Almost all of the specimens were obtained in May or June, a time when the water temperature increased from 21 to 30°C. American oysters (*C. virginica* used in the 10°C experiments) were collected in late October. Specimens were returned to the laboratory in Baton Rouge (LA) where they were adapted stepwise to the experimental water temperatures and salinities. Water temperature was maintained at the desired value (±0.5°C) by placing the experimental aquaria in a constant temperature water table. Experimental salinity (±0.5‰S) was maintained by determining the salinity of Instant Ocean™ artificial seawater (ASW) with a refractometer, and adding either deionized water or an ASW made to 40‰S.

Details of the hypoxia bioassay system are given in Kapper and Stickle (1987). Briefly, each experimental chamber consisted of an aquarium (38 l), containing an undergravel filter overlaid with oyster chips. Seawater was pumped through the aquarium at a rate sufficient to ensure the water was completely exchanged several times per day. Bottled nitrogen, oxygen, and carbon dioxide were mixed with Matheson gas mixers to produce a defined mixture of desired P_{o_2} and pH. This air mixture passed through the undergravel filters at target oxygen tensions of 107, 53, 15, and 0 Torr. Ambient air was used to drive the undergravel filters of the control tanks (142–157 Torr). P_{o_2} was always within 10–15% of the target value at the three higher levels, the 15 Torr tanks were within ±5 Torr, and the P_{o_2} of the 0% air saturation tanks was usually in the range of 3–8 Torr. Each aquarium was covered with Plexiglas and the water level was maintained by a constant-level siphon that drained into a filtration unit that received water from all five experimental chambers in a bioassay series at the same temperature and salinity. Experimental conditions were checked in each chamber daily by measuring P_{o_2}, pH, and ammonium concentration (Solorzano, 1969). The pH varied between 7.6 and 8.1 and ammonium levels were consistently below 25 μM.

The range of sizes and the number of individuals used at each P_{o_2} of a bioassay series varied among species: *Crassostrea virginica,* 30–50 mm long, an average of 20 oysters per P_{o_2}; *Callinectes sapidus,* 28–54 mm carapace width, an average of 8 crabs per P_{o_2}; *Eurypanopeus depressus,* 9–16 mm carapace width, with 25 crabs per P_{o_2}; *Palaemonetes pugio,* 16–27 mm total length with 25 shrimp per P_{o_2}; *Penaeus aztecus,* 21–32 mm total length, with 20 shrimp per P_{o_2}; and *Rhithropanopeus harrisii,* 6–11 mm carapace width, with 15 crabs per P_{o_2}.

Animals were selected for each temperature series so as to minimize size differences within and among the temperature treatment. None of the crustaceans was observed to molt during the bioassay experiments.

Survival at each P_{o_2} was determined daily for 28 days for each bioassay series. LC_{50} values—the P_{o_2} at which 50 percent of the organisms were dead on each day—were calculated by the SAS Probit procedure (SAS Institute, 1982), or by the Spearman-Karber technique (Hamilton *et al.,* 1977) if mortalities in at least two of the five P_{o_2}s were not between 0 and 100%. Percent mortality in the control P_{o_2} tanks varied from 0 to 10% for *Crassostrea virginica,* from 0 to 29% for *Callinectes sapidus;* and from 0 to 50% for *Penaeus aztecus.* Control tank mortality, after 28 days exposure at 30°C and 20‰S, was 20% for *Eurypanopeus depressus,* 52% for *Palaemonetes pugio,* and 40% for *Rhithropanopeus harissii.* Abbott's correction was used to correct control tank mortalities. Significant differences in LC_{50} values among species, temperatures, and days were determined by non-overlap of the 95% fiducial limits.

LT_{50} values are the elapsed days of exposure to anoxia until 50% of the experimental animals died. Thus LT_{50} values are a measure of anoxia tolerance only, whereas LC_{50} values measure the degree of hypoxia tolerance.

Metabolic rate determinations

Rates of heat dissipation were determined by perfusion (open-flow) microcalorimetry using a system described by Gnaiger (1983a, b). Rate functions were calculated as joules·g dry $wt^{-1} \cdot h^{-1}$ and were determined at 25°C and 10‰S for *Callinectes sapidus, Penaeus aztecus,* and *E. depressus.* Rate functions were determined at 25°C and 20‰S for *Crassostrea virginica* and *T.*

haemastoma. The size of experimental animals was limited by the size of the perfusion chamber (3.5 cm^3; inner diameter = 11 mm, inner chamber height = 53 mm). Flow rate through the perfusion chamber was 20 $ml \cdot h^{-1}$. This method of determining metabolic rates has the advantage that the sum of metabolism due to aerobic and anaerobic processes can be measured (Gnaiger, 1983a, b). The metabolic rate of each individual was determined over consecutive periods of perfusion with normoxic water, anoxic water, or 25% normoxic water (=39 Torr). The P_{o_2} of the outflow water was >80% of the inflow under normoxia, and <0.5 Torr under anoxia, as measured with a Cyclobios Twin-Flow respirometer connected to the perfusion calorimeter (Gnaiger, 1983b). Hourly rates were determined from rates integrated for each minute of the hour. Steady state rates were calculated from the average of the last six hours of exposure to each experimental condition. Differences in steady state rates of heat dissipation among P_{o_2} treatments were determined by one-way analyses of variance (ANOVA), and specific differences among treatment means were determined by the Students *t*-test (SAS Inst., Inc., 1982).

Results

Hypoxia tolerance

The long term hypoxia tolerance, at 30°C and 10‰S, of the five species of crustaceans and the oyster can generally be divided into two groups. *Callinectes sapidus* and *Penaeus aztecus* were very sensitive to hypoxia with 28-day LC_{50} values of 121 and 123 Torr (79.1 and 80.4% air saturation), respectively (Table I). The remaining species all had 28-day LC_{50} values lower than 60 Torr, and their hypoxia tolerance decreased in the following order: *Eurypanopeus depressus* > *Palaemonetes pugio* > *Rhithropanopeus harrisii* > *Crassostrea virginica*. Similar results are obtained whether the LC_{50} values are calculated as Torr or percent saturation, but the variation in oxygen solubility with temperature and salinity causes the LC_{50} values calculated in terms of oxygen content (PPM) to deviate significantly from values calculated in Torr or percent saturation.

Species differences also appeared in the rate of mortality of the five species of crustaceans, and the oyster, exposed to defined levels of hypoxic or anoxic seawater. The LC_{50} values for *Callinectes sapidus* and *Penaeus aztecus* increased rapidly as a function of time of exposure; most mortalities occurred within two days exposure (Fig. 1). In contrast, LC_{50} values for *Rhithropanopeus harrisii* and *Eurypanopeus depressus* increased slowly with duration of exposure suggesting that these species are more tolerant and also more variable in their sensitivity to hypoxia (Fig. 2). LC_{50} values for *Palaemonetes pugio* increased rapidly to near the 28-day value of 46 Torr (30% saturation) on the second day of exposure with little mortality occurring thereafter (Fig. 2), whereas mortality occurred on the seventh day for *Crassostrea virginica* (Fig. 1). The rate of mortality varied directly with temperature in *Callinectes sapidus*, *Penaeus aztecus*, and *Crassostrea virginica* (Fig. 1). No mortality occurred in oysters exposed to anoxia (3–8 Torr) at 10°C for 28 days (Table I).

The 28-day LC_{50} of the crustacean species appears to be associated with differences in their natural habitats and activity levels (Fig. 3). That is, the xanthid crabs *Eurypanopeus depressus* and *Rhithropanopeus harrisii*, usually associated with oyster reefs, and the grass shrimp *Palaemonetes pugio* are significantly more tolerant to hypoxia than the potentially nektonic *Callinectes sapidus* and *Penaeus aztecus*. The molluscan species tested were more tolerant of hypoxia than the crustaceans (Fig. 1, 2, 3). The average 28-day LC_{50} for the molluscs, at 30°C and 10‰S, was 37 Torr compared with 78 Torr for the crustaceans. Furthermore, the 7-day LC_{50} at 30°C and 10‰S averaged 59% of the 28-day value for the crustaceans (range 32–89%) compared with 29% for the molluscs (range 0–57%), indicating that crustaceans die more rapidly. Although the oysters were very tolerant of hypoxia at 10 and 20°C, they were sensitive at 30°C. But they had spawned just before the 30°C experiment was conducted, which might have increased their hypoxia sensitivity.

Metabolic rate

The rate of heat dissipation was depressed in the species of crustaceans exposed to hypoxia and in *Crassostrea virginica* and *Thais haemastoma* exposed to anoxia, as shown by analysis of variance (ANOVA); but heat dissipation was considerably more depressed in *Thais haemastoma* than in the other species (Table II). There was no significant reduction in the metabolic rate of *T. haemastoma* exposed to hypoxia (ANOVA: Table II). Two each of *Callinectes sapidus*, *E. depressus*, and *Palaemonetes pugio* exposed to anoxia for 12 h in the perfusion microcalorimetry system died during the experiment. *Callinectes sapidus*, *E. depressus*, *Palaemonetes pugio*, and *T. haemastoma* were therefore treated with hypoxic water at 25% air saturation (39 Torr; Figs. 4, 5). Three *Palaemonetes pugio* died upon exposure to 25% normoxic seawater.

When *Callinectes sapidus* and *E. depressus* were exposed for consecutive 12-h periods to normoxic water, hypoxic water (25% air saturation = 39 Torr) and normoxic water, the heat dissipation rates of both species declined markedly upon exposure to hypoxic water (Fig. 4). However, the posthypoxia metabolic rate of *Callinectes sapidus* in normoxic water only returned to 75% of its pre-exposure normoxic rate, while the posthypoxia

Table I

Twenty-eight-day LC_{50} values for several species of crustaceans and molluscs

Species	T (°C)	LC_{50}[a] S (‰)	Torr	% SAT	PPM	LT_{50}[b]
Crustaceans						
Callinectes sapidus	20	10	74 ± 19	47.7	4.08	<1
		20	124 ± 0	79.9	6.44	<1
		30	123 ± 0	79.3	6.03	<1
	30	10	121 ± 0	79.1	5.63	<1
		20	119 ± 0	77.8	5.23	<1
		30	111 ± 0	72.5	4.61	<1
Eurypanopeus depressus	30	10	38 ± 6	24.8	1.76	1
Palaemonetes pugio	30	10	46 ± 6	30.1	2.14	1
Penaeus aztecus	20	10	105 ± 12	67.7	5.79	<1
		20	92 ± 14	59.3	4.78	<1
		30	93 ± 15	59.9	4.55	<1
	30	10	123 ± 0	80.4	5.72	<1
		20	122 ± 0	79.7	5.36	<1
		30	115 ± 0	75.1	4.77	<1
Rhithropanopeus harrisii	30	10	57 ± 18	37.3	2.65	<1
Molluscs						
Crassostrea virginica	10	10	<0	<0	<0	>28
		20	<0	<0	<0	>28
		30	<0	<0	<0	>28
	20	10	27 ± 8	17.4	1.49	20
		20	16 ± 4	10.3	0.83	18
		30	30 ± 5	19.3	1.47	20
	30	10	59 ± 9	38.6	2.75	8
		20	78 ± 18	51.0	3.43	4
		30	120 ± 8	78.4	4.98	3
*Thais haemastoma**	10	10	15	10	1.01	20
		20	8	5	0.50	27
		30	9	6	0.54	20
	20	10	20	13	1.10	18
		20	12	8	0.62	19
		30	29	19	1.43	20
	30	10	13	9	0.61	>28
		20	22	14	1.17	10
		30	19	12	0.79	15

[a] LC_{50} P_{O_2} causing 50% mortality after 28 days of exposure expressed in: Torr ($\bar{x}$ ± 95% confidence limits, where possible; % air saturation (% SAT); content, mgO_2/l (PPM).

[b] LT_{50}: days of exposure to anoxia causing 50% mortality.

* Data from Kapper and Stickle (1987).

metabolic rate of *E. depressus* in normoxic water returned to 101% of its pre-exposure metabolic rate.

The rate of heat dissipation of the *T. haemastoma* exposed to 25% air saturated water (39 Torr) was depressed significantly less relative to the rate under normoxia, than that of the decapods *Callinectes sapidus* and *E. depressus* (Fig. 5, Table II). Thus, *Thais* is a significantly better metabolic regulator than either species of crustacean. Furthermore, the metabolic rates of the two *T. haemastoma* exposed to various combinations of normoxia, hypoxia (39 Torr), and anoxia adjust rapidly to anoxia and exhibit an oxygen debt upon return to normoxic water (Fig. 5).

Changes in the metabolic rates of starved *Crassostrea virginica* (Fig. 6A), as well as in four of the six *T. haemastoma* (Fig. 6C) provided oysters *ad libitum* in the lab prior to their use (Fig. 6C), were examined. The heat dissipation rates of these animals did not return to the pre-exposure normoxic rate during the 12-h post-exposure period in normoxic seawater. The heat dissipation rate of *C. virginica* increased dramatically upon initial exposure to normoxic seawater, then declined to a steady state

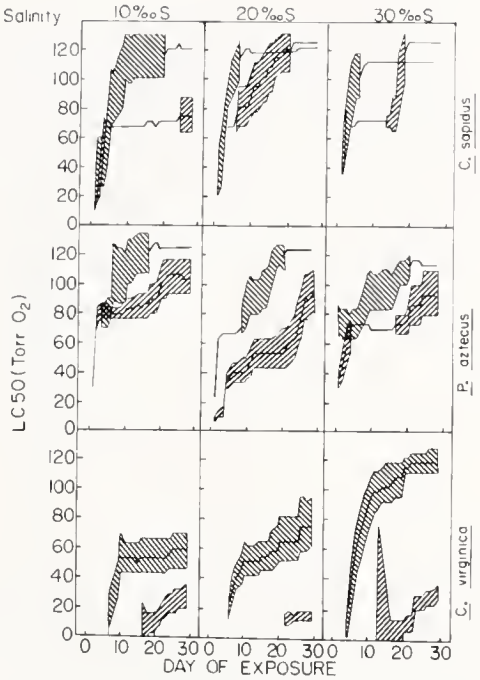

Figure 1. LC_{50} values or the oxygen tension causing 50% mortality (Torr O_2 ± 95% fiducial limits), as a function of exposure time of *Callinectes sapidus, Penaeus aztecus,* and *Crassostrea virginica.* Values were obtained over 28 days, at 10, 20, and 30‰S, and at 20 (□) and 30°C (■).

level that was unchanged during 12 h of exposure to anoxic water. Upon the return to normoxic seawater, the heat dissipation rates of the oysters increased dramatically for the first three hours, and then declined to the initial normoxic steady state level. In contrast, the heat dissipation rate of the two apparently fed *T. haemastoma* exhibited an oxygen debt upon reexposure to normoxic water after 12 h of anoxia and then returned to the initial normoxic metabolic rate (Fig. 6B).

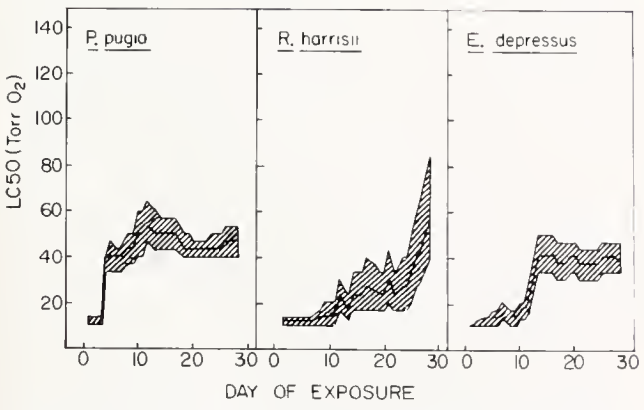

Figure 2. LC_{50} values (Torr O_2 ± 95% fiducial limits) as a function of exposure time of *Palaemonetes pugio, Rhithropanopeus harrisii,* and *Eurypanopeus depressus;* 28 days at 30°C and 10‰S.

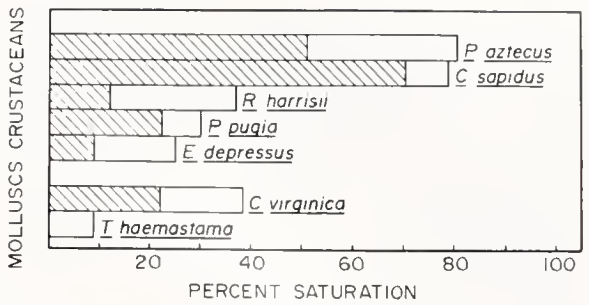

Figure 3. LC_{50} values, expressed in percent saturation, for seven species after 7 days (cross hatched portion of bars) and 28 days (total bar lengths) of exposure at 30°C and 10‰S.

As expected, the magnitude of metabolic rate depression of these crustaceans and molluscs is directly related to their LT_{50}—their mortality upon exposure to anoxia. *Callinectes sapidus, E. depressus,* and *Palaemonetes pugio* have LT_{50} values of one day or less at 20 and 30°C (Table I). Two individuals from each of these species were examined for evidence of metabolic rate depression: none was found, and all the specimens died during the 12-h exposure to anoxia. The metabolic rate of *Crassostrea virginica* exposed to anoxic water was 75% of the normoxic rate, and their LT_{50} was 18 and 4 days at 20°C and 30°C, respectively. The metabolic rate of *Thais haemastoma* under anoxia was reduced to 9% of their rates in normoxic water (Table II) and their LT_{50} was 19 and 10 days at 20 and 30°C and 20‰S, respectively (Table I).

No relationship exists between the degree of metabolic rate depression upon exposure to anoxia, and the 28-day LC_{50} values, which are indicative of hypoxia tolerance. Metabolic rate depression as a function of hypoxia appears to be inversely correlated with hypoxia tolerance. Metabolic rates during exposure to 25% air saturation are reduced to 74% of the normoxic rate for *T. haemastoma,* 32% for *Callinectes sapidus,* and 47% for *E. depressus* (Table II).

Evidence of a classical oxygen debt exists in two *T. haemastoma* upon return to normoxic seawater after exposure to anoxic water (Fig. 5, 6B). This oxygen debt is of short duration in the two oyster drills shown in Figure 5. However, four *T. haemastoma* did not exhibit an oxygen debt upon exposure to normoxic seawater after 12 h to anoxic water (Fig. 6C).

Discussion

The five species of crustaceans and two species of molluscs studied differ in their tolerance to chronic hypoxia, as well as in their sensitivity to acute exposure to anoxia. Among the crustaceans, hypoxia tolerance in each species appears to be closely correlated with activity level

Table II

Steady state rate of heat dissipation (joules · g dry wt^{-1} · h^{-1}) of four species of molluscs and crustaceans under normoxic (100% air saturation), hypoxic (25% air saturation), and anoxic (<5% air saturation) conditions

Species	n	S‰	Normoxia	Hypoxia	%	Anoxia	%
Crustaceans							
Callinectes sapidus	5	10	18.47 ± 0.31	5.91 ± 0.25*	32	N.D.	
Eurypanopeus depressus	5	10	8.70 ± 0.27	4.06 ± 0.46*	47	N.D.	
Molluscs							
Crassostrea virginica	3	20	3.16 ± 0.51	N.D.		2.38 ± 0.47*	75
Thais haemastoma	6	20	8.76 ± 0.99	N.D.		0.78 ± 0.04*	9
	2	20	19.60 ± 10.08	14.90 ± 8.55	76	N.D.	

All metabolic rates were determined at 25°C. N.D. = no data. All crabs died upon exposure to anoxic water. % = Percent of normoxic rate. * = significantly different ($P < 0.05$) from the normoxic rate.

and metabolic rate (Fig. 3). *Eurypanopeus depressus* and *Rhithropanopeus harrisii* are associated with oyster reefs; *Palaemonetes pugio* is associated with salt marsh vegetation; and juvenile *Callinectes sapidus* and *Penaeus aztecus* are active swimmers, migrating between estuaries and offshore waters during their life cycles. A two-fold difference also exists in the metabolic rates of *Eurypanopeus depressus* and *Callinectes sapidus* exposed to normoxic seawater (Table II).

Sensitivity to hypoxia has also been measured as a function of mortality in anoxic seawater, represented by LT_{50} values. The resistance of marine invertebrates to oxygen deficiency is correlated with the natural habitats of the species (Fig. 3; Theede *et al.*, 1969; Theede 1973). In this study, mortality occurred more rapidly in the crustaceans exposed to hypoxia than in the molluscs, when all of the temperature-salinity combinations tested were considered. All of the crustacean species exposed to anoxia had LT_{50} values of one day or less, whereas the LT_{50} values of *Crassostrea virginica* ranged from greater than 28 days at 10°C, to three days at 30°C and 30‰S. Moreover, the LT_{50} of *Thais haemastoma* ranged from greater than 28 days at 30°C and 10‰S, to 10 days at 30°C and 20‰S.

The LT_{50} value is not a very sensitive indicator of hypoxia tolerance, because only animals exposed to anoxia can be included in the calculation of the parameter. In contrast, the determination of a LC_{50} value requires data about survival as well as mortality, from several P_{O_2} treatments, so several degrees of hypoxia are represented. There is no correlation between the LT_{50} and the 28-day LC_{50} P_{O_2}.

If, for the species studied, the LC_{50} values for short term exposure are expressed as a function of the 28-day LC_{50}, the phylogenetic differences between crustaceans and molluscs are clearly highlighted. Thus, day 2 and day 7 LC_{50} values represent 0 and 21% of the 28-day values for the two species of molluscs at 30°C and 10‰S, whereas they represent 32 and 60% of the 28-day value for the crustaceans.

Other environmental factors have an antagonistic effect upon the tolerance of estuarine invertebrates to hypoxia and anoxia. Sensitivity to hypoxia increases with temperature in *Crassostrea virginica* and *Penaeus aztecus,* as well as in *T. haemastoma* (Kapper and Stickle, 1987), and probably results from an increased metabolic rate at elevated temperature. The survival time of oysters, experimentally buried to simulate natural sedimentation events, varied inversely with temperature, from more than 5 weeks at <5°C, to 4 days at temperatures >25°C (Dunnington, 1968). Prolonged exposure of oysters to fresh water and low salinities (<5‰S) has caused heavy mortality because they remained closed and could not feed and maintain an aerobic metabolic rate (Andrews, 1982). Oysters died, presumably because of anoxic conditions produced by dredging which resulted in an oxygen demand of spoil bank sediments and modification of the local hydrographic regime (Hoese and Ancelot, 1987).

Hypoxia tolerance varied inversely with salinity for *Penaeus aztecus* at 20 and 30°C and for *Callinectes sapidus* at 30°C, but varied directly with salinity at 20°C for *Callinectes* (Table I). The inverse relationship between tolerance and salinity noted for *Callinectes sapidus* and *Penaeus aztecus* is the opposite of that expected on the basis of theoretical osmoregulatory costs; but activity patterns associated with feeding may override the energetic costs of osmoregulation. Juvenile blue crabs and shrimp sometimes use the most brackish regions of estuaries as a nursery ground so the inverse relationship between salinity and hypoxia tolerance is correlated with the distribution of life history stages of these species.

Behavioral avoidance activities by juvenile (65 to 101 mm total length) penaeid shrimp may temporarily allow them to escape oxygen deficient water; *i.e.,* below 2.0 ppm (29% air saturation or 45 Torr at 22°C and 22‰S)

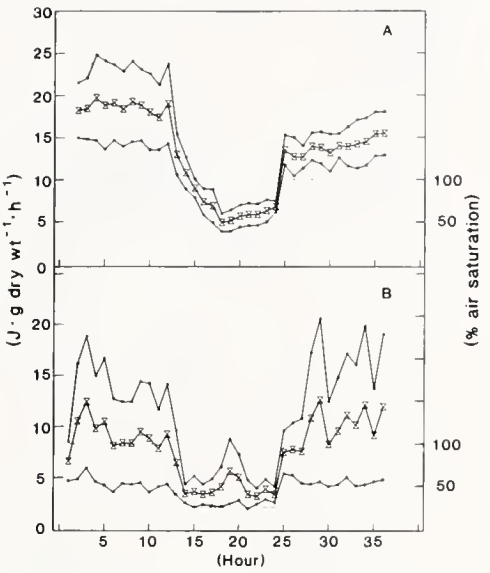

Figure 4. Hourly heat dissipation rates of 5 *Callinectes sapidus* (A) and 5 *Eurypanopeus depressus* (B) at 25°C and 10‰S. Rates expressed as J·g dry $wt^{-1} \cdot h^{-1}$ ± S.E. (mean ⊠ and standard error limits — ● —) for crabs exposed to consecutive 12 h periods of normoxia, hypoxia (25% air saturation), and normoxia. Dashed lines: percent air saturation values for ambient seawater.

for *Penaeus aztecus* and 1.5 ppm (22% air saturation or 34 Torr) for *Penaeus setiferus* (Renaud, 1986b). Juvenile shrimp may be able to alter their migration patterns to move around patches of hypoxic water (Rabalais *et al.*, 1986a, b; Renaud, 1986a), provided the patches are spatially and temporally isolated.

The values for metabolic rate depression observed in this study fall within the range of values reported in the literature and emphasize the need to consider this component of physiological adaptation in relation to the life cycle niche occupied by each species. It is not surprising that juvenile blue crabs, which are active swimmers, are intolerant of anoxia, and that their metabolic rate at 25% air saturation is depressed only to 32% of their normoxic metabolic rate. Although *Eurypanopeus depressus* is also intolerant of anoxia and exhibits metabolic rate depression to 47% of its normoxic rate upon exposure to 25% air saturated seawater, its brackish water oyster reef habitat is not exposed to hypoxic water masses of the same duration as those that develop offshore (Rabalais *et al.*, 1985). These crabs are exposed to diurnal variations in oxygen tension. In contrast, the copepod *Cyclops abyssorum*, which lives in alpine ponds that become hypoxic in the winter, exhibits metabolic rate depression to 17% of the normoxic rate upon exposure to anoxia at 6°C (Gnaiger, 1981).

The metabolic rate depression of molluscs exposed to anoxic seawater is also highly variable among species, ranging from 9% of the normoxic rate in *T. haemastoma* (Table II), 11% in *Mytilus edulis* (Famme *et al.*, 1981; Shick *et al.*, 1983), 75% in *Crassostrea virginica* to only 97% in *Mulinia lateralis* (Shumway *et al.*, 1983). Sessile and infaunal bivalves generally show a strong resistance to anoxia due in part to a reduction in activity and hence energy use (Shick *et al.*, 1986). In this study, *Crassostrea virginica* (2 to 19 mg dry weight) were starved for 35 to 65 days prior to the experiment. In bivalves, their oxygen consumption rate is directly coupled with filtration activity associated with feeding (see discussion by Bayne *et al.*, 1976). Starved *Crassostrea virginica* probably exhibited a reduced filtration activity and heat dissipation rate. In *Mytilus edulis*, the increase in oxygen consumption of starved mussels offered food is almost instantaneous (Widdows, 1973). The increased heat dissipation rate of oysters immediately after perfusion with normoxic seawater (Fig. 6A) may therefore represent "testing" of an altered ambient environment after which the active rate of the oysters was reduced to the standard, nonfeeding rate. *T. haemastoma* is exposed to diurnal and seasonal periods of anoxia, both in the water column, and when it burrows into the anoxic zone of sediments for a large portion of the winter and intermittantly in the summer (Kapper and Stickle, 1987).

The two metabolic patterns shown by *T. haemastoma*

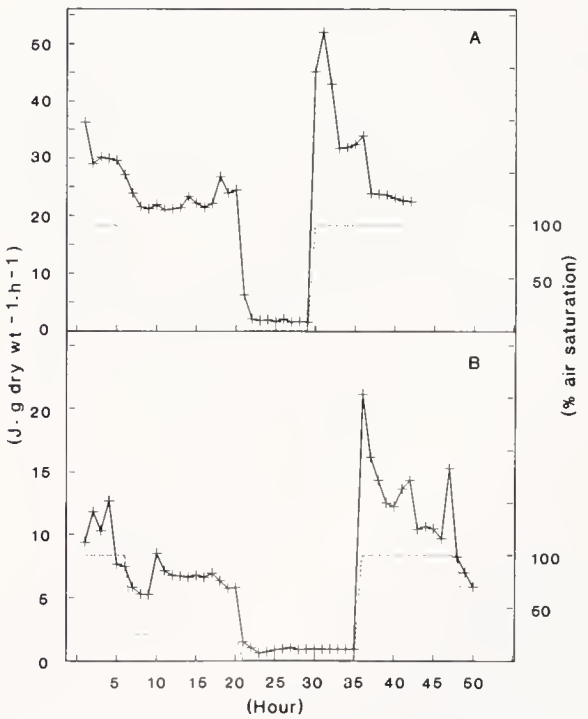

Figure 5. Hourly heat dissipation rates (at 25°C and 30‰S) of two (A and B) *Thais haemastoma* (solid lines —┼—) exposed to various combinations of normoxia (100% air saturation), hypoxia (25% air saturation), and anoxia. Dashed lines: percent air saturation values for ambient seawater.

in response to normoxic seawater after 12-h exposure to anoxic seawater (Fig. 6B, C), are probably related to the feeding history of the snails. Feeding rate is the primary bioenergetic component to become variable in gradients of environmental factors, and certain individuals cease feeding altogether under stressful conditions (Stickle, 1985). Small oyster drills, such as those used in this study, are particularly sensitive to the selection of optimum-sized bivalve prey, because prey size can limit the ingestion rate, and hence the energy budget of the predator (Garton, 1986). *T. haemastoma* prefers a number of different prey items (Butler, 1953), the importance of which may vary with the size of the snail. Oyster drills also exhibit a large specific dynamic action effect, elevated metabolic rates associated with digestion of food, in normoxic seawater, anoxic seawater, and when exposed to the air (Stickle *et al.*, 1986). All of these factors probably contributed to the variability in individual metabolic rates which resulted in two apparent patterns of response in the recovery of oyster drills from 12 h of anoxia.

The metabolic rate depression of *T. haemastoma* exposed to anoxia (Table II) suggests a switch to the relatively more efficient succinate and propionate pathways in the molluscs, compared with the well developed, but less efficient, classical glycolysis system in the crustaceans (Gade, 1983; Gnaiger, 1983a, 1987; and deZwaan and Thillart, 1985). During initial exposure to environmental anaerobiosis, the biochemically estimated ATP turnover rate may drop to about 10% of aerobic resting rates in crustaceans, and the reductions may be even larger in molluscs (deZwaan and Thillart, 1985). During the initial exposure to anoxia, when aspartate is still the precursor of succinate in the molluscs, the rate is three to five times higher than the subsequent anaerobic steady state and is fueled by both phosphagen and ATP hydrolysis (deZwaan and Thillart, 1985; Kapper and Stickle, 1987). When the steady state is reached, the glycolytic flux is reduced and channeled towards malate, whereas the phosphagen pool is somewhat depleted relative to normoxia levels (deZwaan and Thillart, 1985; Kapper and Stickle, 1987).

No evidence of oxygen debt was observed with *Callinectes sapidus* (Fig. 4A), *E. depressus* (Fig. 4B), starved *Crassostrea virginica* (Fig. 6A), or specimens of *T. haemastoma* whose metabolic rates did not even recover to the initial normoxic rate after 12-h exposure to anoxic seawater (Fig. 6C). In contrast, the *T. haemastoma* individuals that did recover to the initial normoxic rate after 12-h exposure to anoxic seawater, exhibited an oxygen debt upon their postanoxic exposure to normoxic seawater (Fig. 6B).

Two basic processes occur during recovery from environmental anoxia: (1) recharging of the phosphagen pool; and (2) the disposal of end products by excretion, oxidation, or conversion back to anaerobic substrates (Ellington, 1983). Oxygen debts are regular phenomena in free-living invertebrates and may be attributed, at the molecular level to the increased energy demands for disposal of end products and recharging of the phosphagen and ATP pools (Herreid, 1980). Patterns of oxygen debt in invertebrates tend to be highly variable from species to species, and may reflect differences in the degree of reduction of energy metabolism, hence end-product accumulation under anoxic conditions (Herreid, 1980) and the duration of exposure to anoxia. Upon exposure to anoxia for 24 h, *Thais haemastoma*, the species that exhibited the greatest metabolic rate depression in our study (Table II), showed a return of the adenylate energy charge to the pre-exposure level within 6 h. But the arginine phosphate concentration returned to only about half of its pre-exposure value 24 h after the oyster drills were returned to normoxic water (Kapper and Stickle, 1987). Lack of an oxygen debt in some *T. haemastoma* (and possibly *Crassostrea virginica*), whose postanoxia metabolic rate did not recover to the initial rate after 12-h exposure to anoxia, may be due to a reduced metabolic

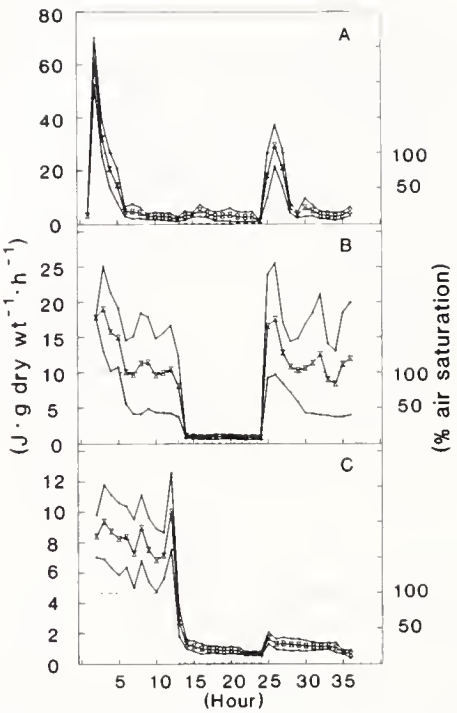

Figure 6. Hourly heat dissipation rates of three *Crassostrea virginica* (A), two *Thais haemastoma* which recovered from exposure to anoxia at 25°C and 20‰S (B), and four *T. haemastoma* which did not recover from exposure to anoxia (C). Rates expressed as: J·g dry wt^{-1}·h^{-1} ± S.E. (solid lines for the mean —⊠—; standard error limits by solid lines). The animals were exposed to consecutive 12-h periods of normoxia, anoxia, and normoxia at 25°C and 20‰S. Dashed lines: percent air saturation values for ambient seawater.

rate after long term starvation (Fig. 6C compared with 6B) coupled with a slow replenishment of the phosphagen pool and, perhaps, washout of anaerobic end products during exposure to anoxic water.

In conclusion, significant interspecies variability exists in the 28-day LC_{50} values for the five species of crustaceans studied, ranging from 38 Torr in *Eurypanopeus depressus*, to 121 Torr in *Callinectes sapidus*. In addition, species differences exist in the rate of mortality of the five species of crustaceans, and in the oyster, when exposed to defined levels of hypoxic or anoxic seawater. LC_{50} values for *Callinectes sapidus, Penaeus aztecus,* and *Palaemonetes pugio* increase rapidly during the first two days of exposure, in contrast to those of *Rhithropanopeus harrisii* and *Eurypanopeus depressus* which increased slowly over the exposure period. Sensitivity to hypoxia increased with temperature in *Callinectes sapidus, Crassostrea virginica,* and *Penaeus aztecus,* with salinity effects being less significant. Natural habitat, activity level, and seasonal differences appear to exist in the mortality rate of these five species of crustaceans. Both *Callinectes sapidus* and *Eurypanopeus depressus* died during 12 hours exposure to anoxia with little decline in the metabolic rate, and their metabolic rate in 25% air saturated seawater is reduced to only 32–40% of their metabolic rate under normoxia. In contrast, both *Crassostrea virginica* and *Thais haemastoma* are tolerant of 25% air saturated seawater, with the rate of *Thais haemastoma* being 76% of that under normoxic conditions. Metabolic rate depression occurs in both species under anoxic seawater, to 75% of the normoxic rate in *Crassostrea virginica,* and 9% in *Thais haemastoma.*

Acknowledgments

The authors acknowledge the Coastal Fisheries Institute at LSU and the Petroleum Refiners Environmental Council of Louisiana for partially funding this research. E. G. was supported by FWF Austria grants J0011 and J0187B, and by the LSU Visiting Investigator Program. Special thanks go to LKB-Thermometrics for loaning us a prototype Thermal Activity Monitor perfusion system. We are grateful to Nancy Rabalais of LUMCON for reviewing drafts of this manuscript.

Literature Cited

Andrews, J. D. 1982. Anaerobic mortalities of oysters in Virginia caused by low salinities. *J. Shellfish. Res.* **2:** 127–132.

Bayne, B. L., R. J. Thompson, and J. Widdows. 1976. Physiology I. Pp. 121–206 in *Marine Mussels: Their Ecology and Physiology,* B. L. Bayne, ed. Cambridge University Press, Cambridge.

Bedinger, C. A., R. E. Childers, J. W. Cooper, K. T. Kimball, and A. Kwok. 1981. Pollution fate and effect studies. Pp. 1–53 in *Ecological Investigations of Petroleum Production Platforms in the Central Gulf of Mexico,* Vol. 1, Pt. 1, C. A. Bedinger, ed. Final Report to the Bureau of Land Management, New Orleans, LA, Contract No. A5551-CT9-17.

Boesch, D. F. 1983. Implications of oxygen depletion on the continental shelf of the northern Gulf of Mexico. *Coastal Ocean Pollut. Assess. News.* **2:** 25–28.

Butler, P. A. 1953. The southern oyster drill. *Proc. Natl. Shellfish Assoc.* **53:** 67–75.

Dunnington, E. A., Jr. 1968. Survival time of oysters at various temperatures. *Proc. Natl. Shellfish. Assoc.* **58:** 101–103.

Ellington, W. R. 1983. The recovery from anaerobic metabolism in invertebrates. *J. Exp. Zool.* **228:** 431–444.

Famme, P., J. Knudson, and E. S. Hansen. 1981. The effect of oxygen on aerobic-anaerobic metabolism of the marine bivalve, *Mytilus edulis* L. *Mar. Biol. Lett.* **2:** 345–351.

Gade, G. 1983. Energy metabolism of arthropods and molluscs during environmental and functional anaerobiosis. *J. Exp. Zool.* **228:** 415–429.

Garlo, E. V., C. B. Milstein, and A. E. John. 1979. Impact of hypoxic conditions in the vicinity of Little Egg Inlet, New Jersey in summer 1976. *Estuar. Coast. Mar. Sci.* **8:** 421–432.

Garton, D. W. 1986. Effect of prey size on the energy budget of a predatory gastropod, *Thais haemastoma canaliculata* (Gray). *J. Exp. Mar. Biol. Ecol.* **98:** 21–33.

Gnaiger, E. 1981. Pharmacological application of animal calorimetry. *Thermochim. Acta* **49:** 75–85.

Gnaiger, E. 1983a. Heat dissipation and energetic efficiency in animal anoxibiosis: economy contra power. *J. Exp. Zool.* **228:** 471–490.

Gnaiger, E. 1983b. The twin-flow microrespirometer and simultaneous calorimetry. Pp. 134–166 in *Polarographic Oxygen Sensors, Aquatic and Physiological Applications,* E. Gnaiger and H. Forstner, eds. Springer, Berlin.

Gnaiger, E. 1987. Optimum efficiencies of energy transformation in anoxic metabolism. The strategies of power and economy. Pp. 7–36 in *Evolutionary Physiological Ecology,* P. Calow, ed. Cambridge University Press, Cambridge.

Hamilton, M. A., R. C. Russo, and R. V. Thurston. 1977. Trimmed Spearman-Karber method for estimating median lethal concentrations in toxicity bioassays. *Environ. Sci. Technol.* **11:** 714–719.

Harper, D. E., L. D. McKinney, R. R. Salzer, and R. J. Case. 1981. The occurrence of hypoxic bottom water off the upper Texas coast and its effect on the benthic biota. *Contrib. Mar. Sci.* **24:** 53–79.

Herreid, C. F. II. 1980. Review: hypoxia in invertebrates. *Comp. Biochem. Physiol.* **67A:** 311–320.

Hoese, H. D., and R. Ancelet. 1987. Anoxia induced mortality of oysters, *Crassostrea virginica,* associated with a spoil bank bisecting a bay. *J. Shellfish Res.* **6:** 41–44.

Kapper, M. A., and W. B. Stickle. 1987. Metabolic responses of the estuarine gastropod *Thais haemastoma* to hypoxia. *Physiol. Zool.* **60:** 159–173.

Officer, C. B., R. B. Biggs, J. L. Taft, L. E. Cronin, M. A. Tyler, and W. R. Boynton. 1984. Chesapeake Bay anoxia: origin, development and significance. *Science* **223:** 22–27.

Pavela, J. S., J. L. Ross, and M. E. Chittenden. 1983. Sharp reductions in abundance of fishes and benthic macroinvertebrates in the Gulf of Mexico off Texas associated with hypoxia. *Northeast Gulf Sci.* **6:** 167–172.

Rabalais, N. N., M. J. Dagg, and D. F. Boesch. 1985. Nationwide review of oxygen depletion and eutrophication in estuarine and coastal waters: Gulf of Mexico (Alabama, Mississippi, Louisiana and Texas). Final Rep. NOAA, National Ocean Service, Ocean Assessment Division, Rockville, Maryland. 60 pp.

Rabalais, N. N., R. E. Turner, W. J. Wiseman, Jr., and D. F. Boesch.

1986a. Hydrographic, biological, and nutrient characteristics of the water column in the Mississippi River Delta Bight, June, 1985 to December, 1985. Data Report No. 2, Louisiana Universities Marine Consortium, Chauvin, LA 70344. 167 pp.

Rabalais, N. N., R. E. Turner, W. J. Wiseman, Jr. and D. F. Boesch. 1986b. Hydrographic, biological and nutrient characteristics of the water column on the Louisiana Shelf, July and September, 1985. Data Report No. 3, Louisiana Universities Marine Consortium, Chauvin, LA 70344. 150 pp.

Renaud, M. L. 1985. Annotated bibliography on hypoxia and its effects on marine life, with emphasis on the Gulf of Mexico. NOAA Technical Report NMFS 21, U.S. Dept. of Commerce, Washington, DC. 9 pp.

Renaud, M. L. 1986a. Hypoxia in Louisiana coastal waters during 1983: implications for fisheries. *Fish. Bull.* **84:** 19–26.

Renaud, M. L. 1986b. Detecting and avoiding oxygen deficient sea water by brown shrimp, *Penaeus aztecus* (Ives), and white shrimp *Penaeus setiferus* (Linnaeus). *J. Exp. Mar. Biol. Ecol.* **98:** 283–292.

Santos, S. L., and J. L. Simon, 1980a. Marine soft-bottom community establishment following annual defaunation: larval or adult recruitment? *Mar. Ecol. Prog. Ser.* **2:** 233–241.

Santos, S. L., and J. L. Simon. 1980b. Response of soft-bottom benthos to annual catastrophic disturbance in a south Florida estuary. *Mar. Ecol. Prog. Ser.* **3:** 347–355.

SAS Institute, Inc. 1982. SAS User's Guide: Statistics, 1982 Edition. SAS Institute, Inc., Cary, NC. 584 pp.

Shick, J. M., A. deZwaan, and A. M. J. DeBont. 1983. Anoxic metabolic rate in the mussel *Mytilus edulis* L. estimated by simultaneous direct calorimetry and biochemical analysis. *Physiol. Zool.* **56:** 56–63.

Shick, J. M., E. Gnaiger, J. Widdows, B. L. Bayne, and A. deZwaan. 1986. Activity and metabolism in the mussel *Mytilus edulis* L. during intertidal hypoxia and aerobic recovery. *Physiol. Zool.* **59:** 627–642.

Shumway, S. E., T. M. Scott, and J. M. Shick. 1983. The effects of anoxia and hydrogen sulphide on survival, activity and metabolic rate in the coot clam, *Mulinia lateralis* (Say). *J. Exp. Mar. Biol. Ecol.* **71:** 135–146.

Solorzano, L. 1969. Determination of ammonia in natural waters by the phenolhypochlorite method. *Limnol. Oceanogr.* **14:** 799–801.

Stickle, W. B. 1985. Effects of environmental factor gradients on scope for growth in several species of carnivorous invertebrates. Pp. 601–616 in *Proc. 18th European Mar. Biol. Symp., 1983,* J. S. Gray and M. E. Christiansen, eds. Wiley, New York.

Stickle, W. B., L. L. Liu, and E. Gnaiger. 1986. Metabolic rate variation in *Thais haemastoma* as a function of exposure to anoxia, and air and during its feeding cycle. *Am. Zool.* **26:** 47A.

Theede, H., A. Ponat, K. Hiroki, and C. Schlieper. 1969. Studies on the resistance of marine bottom invertebrates to oxygen deficiency and hydrogen sulphide. *Mar. Biol.* **2:** 325–337.

Theede, H. 1973. Comparative studies on the influence of oxygen deficiency and hydrogen sulphide on marine bottom invertebrates. *Neth. J. Sea Res.* **7:** 244–252.

Turner, R. E., and R. L. Allen. 1982. Bottom water oxygen concentration in the Mississippi River Delta Bight. *Contr. Mar. Sci.* **25:** 161–172.

Widdows, J. 1973. Effect of temperature and food on the heart beat, ventilation rate and oxygen uptake of *Mytilus edulis*. *Mar. Biol.* **20:** 269–276.

deZwann, A. and G. V. D. Thillart. 1985. Low and high power output modes of anaerobic metabolism: invertebrate and vertebrate strategies. Pp. 166–192 in *Circulation, Respiration and Metabolism: Current Comparative Approaches,* R. Gilles, ed. Spring-Verlag Berlin Heidelberg.

Reference: *Biol. Bull.* **177**: 313–330. (October, 1989)

Abstracts of Papers Presented at the General Scientific Meetings of the Marine Biological Laboratory August 14–16, 1989

Abstracts are arranged alphabetically by first author within the following categories: cell motility and cytoskeleton; gametes and developmental biology; general physiology; neurobiology; pathobiology and environmental studies; and sensory biology. Author and subject references will be found in the regular volume index in the December issue.

Cell Motility and Cytoskeleton

Calcium-sensitive ATP-reactivated models of Ciona intestinalis *branchial basket cilia.* DWIGHT E. BERGLES AND SIDNEY L. TAMM (Boston University Marine Program).

The cilia lining the stigmata of the branchial basket of *Ciona intestinalis* generate the water currents necessary for feeding and gas exchange. The metachronal beating of these cilia is often interrupted by sudden stigmata-wide arrests, in which the cilia lie flat against the stigmatal opening. These arrests are always followed by a transient inactive state in which the cilia rise to an upright position before metachronal beating resumes (Takahashi *et al.* 1973, *J. Fac. Sci. U. Tokyo* **13**: 123–137). To investigate the ionic and molecular control of these motor responses, we have developed permeabilized ATP-reactivated models of *Ciona* cilia.

Cell models were produced by extracting small pieces of branchial basket in 0.1% saponin, 10 m*M* EGTA, 30 m*M* PIPES, 150 m*M* KCl, 10 m*M* $MgCl_2$, pH 7 (ES) for 4–7 min at room temperature. TEM showed that this treatment disrupted or completely removed the ciliary membranes. Transfer of extracted tissue to reactivation solution (RS: 10 m*M* EGTA, 30 m*M* PIPES, 150 m*M* KCl, 10 m*M* $MgCl_2$, 2 m*M* ATP, 1 m*M* DTT, pH 8.0) caused the cilia to beat rapidly and without metachrony for 15–30 min.

Calcium (20 μM–1 m*M*) in EGTA-free RS induces the cilia to assume an inactivated posture (stigmata closed), but not the arrested state (stigmata open). Calcium-dependent inactivation is reversed, and the cilia resume beating in the presence of 100 μM trifluoperazine (TFP) or calmidazolium, indicating that ciliary inactivation is regulated by a calcium-calmodulin pathway. The absence of a full laydown arrest in our ciliary models may be due to a loss or modification of critical control factors during extraction. Preliminary results using cAMP, phosphatases, and phosphatase inhibitors suggest that ciliary responses are mediated by protein phosphorylation levels.

Supported by NIH Grant GM 27903 to S.L.T.

Studies of membrane and cytoskeletal structures by electroporation using a radio-frequency electric field. DONALD C. CHANG AND QIANG ZHENG (Baylor College of Medicine, Houston, TX 77030).

High intensity pulsed electric fields can be used to transiently permeabilize cell membranes. This method, called "electroporation," is employed to introduce exogenous molecules into cells. Recently, we developed a new method of electroporation, in which a radio-frequency (RF) electric field, rather than a direct current (DC) field, permeabilizes cells. This new method improves cell viability and provides higher poration efficiency. In the first part of this study, we used the RF poration method to introduce rhodamine-labelled phalloidin into an attached cell line (CV-1) in order to study the microfilament system within the living cell. The CV-1 cells were grown on coverslips. In the presence of phalloidin, cells in the center region of the coverslip were exposed to pulses of RF electric field (0.8 kV/cm, 100 kHz, 1 ms wide). The cells were washed and then incubated in normal culture medium at 37°C for 30 min before being observed under a fluorescence microscope. Brilliant rhodamin-labelled stress fibers were found in nearly all cells exposed to the RF field, but none were found in the control cells. From morphological observations, we estimated that over 60% of the cells loaded with rhodamine were viable.

In the second study, we used a rapid-freezing electron microscopy technique to examine the change of membrane structure following the RF electroporation process. Human red blood cells were used in this study because their membranes had already been well characterized. Following the exposure to the electric field, volcano-shaped, pore-like structures were found in the membranes of the porated cells. Their openings were approximately 20 nm in diameter in the first few milliseconds after the pulsation. In the next 50 ms, their openings expanded and some of them were as large as 120 nm in diameter. Such expansion suggests that the electropores were shaped, not only by the electrical breakdown of the membrane, but also by secondary effects involving movement of water, ions, and other molecules.

Supported in part by a grant from the Texas Advanced Technology Program.

Quantitative motion analysis of vesicle movement in Y-1 adrenocortical cells and the use of fluorescent probes to identify the organelles. GEORGE M. LANGFORD (University of North Carolina, Chapel Hill), SANDRA A. MURRAY, BROCKTON HEFFLIN, AND KATHLEEN J. PENNY.

Video microscopy was used to study the motion of vesicular organelles in Y-1 adrenocortical tumor cells. The organelle movements were recorded in real time and subjected to quantitative motion analysis. Y-1 cells form a typical epithelial monolayer in culture, with broad extensions of very shallow depth (1–2 μm). In the extensions, vesicles can be observed moving away from (anterograde), toward (retrograde), and lateral to the nucleus. The movements observed are presumed to be microtubule-dependent, as has been shown for organelle movement in axons. When stimulated with dibutyryl cAMP (1 m*M*) for 8–24 hours, these cells showed a 3–6 fold increase in steroid production. The motion of several organelles (lipid granules) in unstimulated cells were quantitatively analyzed. Their movement can be classified as *interrupted motion II* according to the preliminary scheme of Weiss *et al.* (1986, *Cell Motil. Cytoskel.* **6:** 128). This classification refers to organelles that show pauses and reversals, and is typical of organelle movement in cultured cells. The instantaneous velocity (0.33-s intervals) was determined for three lipid granules. The fastest moving organelle had a maximum velocity of 2.0 μm/s. The velocities of the organelles fluctuated, and the average velocities for the three organelles ranged between 0.4 and 1.1 μm/s. Each organelle showed periods of movement followed by pauses. During a pause, the organelle remained in place as though tethered to the microtubule and resumed moving at maximum rates as though a force was being constantly applied to free it from an obstacle in its path. Rhodamine 123 and DIOC6 were used to identify the mitochondria and endoplasmic reticulum in these cells. Future studies are designed to determine changes in the movement pattern upon stimulation with ACTH and dibutyryl cAMP.

Supported by NSF grants DCB 8818279 to G.M.L. and RII-8402666 to S.A.M. B.H. was supported by a fellowship from the American Society for Cell Biology; K.J.P. was supported by a fellowship from the American Physiological Society.

Paddle cilia occur as artifacts in veliger larvae of Spisula solidissima *and* Lyrodus pedicellatus.

GRAHAM SHORT AND SIDNEY TAMM (Boston University Marine Program).

Cilia with paddle-shaped tips (paddle cilia or discocilia) have been described by TEM and SEM in a variety of marine invertebrates, most recently in the pretrochal ciliary bands of *Spisula solidissima* veligers (Campos *et al.* 1989, *Biol. Bull.* **175:** 343–348). We have investigated whether such modified cilia are genuine structures or artifacts of osmolarity or fixation conditions.

Living veligers of *Spisula* were observed in normal seawater by high-speed video microscopy (DIC and phase-contrast) synchronized with a strobe flash. No paddle cilia were present. The SEM fixative of Campos *et al.* (1989), consisting of 2.5% gluteraldehyde, 0.1 *M* Na cacodylate, pH 7.2, has an osmolarity of 404 mosmol; it induced paddle cilia in our *Spisula* veligers, as determined by light microscopy and SEM. Addition of 0.29 *M* NaCl to this fixative (pH 7.1) to make it isosmotic with MBL seawater (920 mOsmols) produced no paddle cilia. Similarly, an isosmotic fixative (pH 6.3) containing 2.5% gluteraldehyde, 0.13 *M* NaCl, and 50% seawater did not induce paddle cilia.

The same fixation conditions applied to shipworm larvae (*Lyrodus pedicellatus*) gave the same results as described in *Spisula*. When living *Spisula* and *Lyrodus* were placed in diluted seawater (45%; 420 mOsmols), the distal ciliary membrane vesiculated, as determined by light microscopy. This hypotonic swelling is reversible; the cilia regain their normal appearance when the larvae are returned to 100% seawater.

We conclude that paddle cilia in *Spisula* larvae, and probably in other invertebrates as well, are artifacts caused by swelling of the distal ciliary membrane in hypotonic medium. Various hydromechanical and chemosensory functions attributed to paddle cilia by previous authors (Matera *et al.* 1982, *Cell Tiss. Res.* **222:** 25–40; Stebbing *et al.*, 1972, *Mar Biol. Assoc. UK* **52:** 443–448) must therefore be abandoned.

Supported by the Woods Hole Marine Science Consortium and NIH Grant GM 27903 to S.L.T.

Cell fusion induced by a radio-frequency electric field.

QIANG ZHENG AND DONALD C. CHANG (Baylor College of Medicine, Houston, TX 77030).

Cell fusion is a very important and useful technique for hybridoma production and somatic hybridization. High intensity pulsed electric fields can be used to induce cell fusion; this is called "electrofusion." Using a new method of electrofusion developed in this laboratory, we applied a radio-frequency (RF) electric field to induce fusion of plant protoplasts and mammalian cultured cells. In the first study, protoplasts enzymatically digested from cabbage leaves were fused using three pulses of an RF field (1 kV/cm, 60 kHz, 0.2 ms). Within a few minutes after pulsation, over 70% of protoplasts fused, and microscopic observation showed very little damage to the protoplasts by the RF field. In the second study, attached mammalian cells (CV-1, COS-M6, Pam, 3T3) were fused by the RF method. We observed a high frequency of fusion in all of these cells. For example, the fusion frequency of attached CV-1 cells could reach 80% even when they were treated using a single RF pulse (1.0 kV/cm, 100 kHz, 0.2 ms); in this case, almost all cells were alive. To understand the mechanisms of cell fusion, we investigated the role of the cytoskeleton in reorganizing the cellular structures during the fusion process. The cytoskeletal changes of attached CV-1 cells were examined by fluorescence microscopy using rhodamine-phalloidin and anti-tubulin antibodies labelled with FITC. Within a few minutes after the electric pulsation, the membranes fused. During the next 20–30 min, some of the stress fibers gradually disappeared; F actin began to condense near the nucleus or at the cell periphery, while microtubules condensed between nuclei within the fusing cells. If the fusion involved only 2 or 3 neighboring cells, the fusion process was almost completed after about 90 min. Apparently normal stress fibers reappeared at this time.

Supported in part by Texas Advanced Technology Program.

Gametes and Developmental Biology

Binding of 5-hydroxytryptamine to isolated plasma membranes of Spisula *gametes.*

A. H. BANDIVDEKAR (The Population Council), S. J. SEGAL, AND S. S. KOIDE.

Serotonin (5-hydroxytryptamine, 5-HT) added *in vitro* to a suspension of *Spisula* oocytes induced germinal vesicle breakdown (GVBD). The neurotransmitter also stimulated, *in vitro*, the motility of cold-immobilized *Spisula* sperm. In the present study, the plasma membranes were prepared from *Spisula* oocytes and sperm, and the binding of [^{3}H]5-HT to the membranes was determined. 5-HT analogs were used to displace the bound [^{3}H]5-HT to determine the types of receptors present on oocytes and sperm membranes.

Plasma membranes of oocytes were prepared by suspending isolated washed *Spisula* oocytes in 50 m*M* Tris-HCl buffer, pH 7.4, containing 1 m*M* EDTA, 0.001% sodium azide. The membranes were homogenized with 2–4 light strokes in a glass-teflon homogenizer, and sedimented by centrifugation.

Spisula sperm membranes were prepared by a nitrogen cavitation method, at a pressure of 1500 psi for 30 min. The treated sperm were then centrifuged at 10,000 $\times$ *g* for 30 min at 4°C, and the supernatant centrifuged at 100,000 $\times$ *g* for 2 h at 4°C to sediment the membranes.

The radioligand binding assay system contained 100 μg of membrane

protein, and 100 μl of [^{3}H]5-HT (40 pmoles); labelled ligand was displaced with 5-HT and its analogs.

The Kd of [^{3}H]5-HT binding to *Spisula* oocyte and sperm membranes was 17.5 n*M* and 2.7 n*M*, respectively. The maximum binding capacity was 7.9 pmoles/mg and 11.25 pmoles/mg, respectively. The order of decreasing potency in the displacement of [^{3}H]5-HT binding to *Spisula* oocyte membranes by 5-HT agonists was: 5-HT > 5-CT > 8-OH-DPAT > 2-methyl-5-HT > alpha-methyl-5-HT, and that by 5-HT antagonists was ICS-205-930 > mianserin > methysergide > BMY-7378 > ketanserin > quipazine. The order of decreasing potency in the displacement of [^{3}H]5-HT bound to sperm plasma membranes by 5-HT agonists was 2-methyl-5-HT > 8-OH-DPAT > 5-HT > 5-CT > alpha-methyl-5-HT, and that by antagonists was ICS-205-930 > BMY-7378 > mianserin > methysergide.

The present findings demonstrate that plasma membranes of *Spisula* oocytes and sperm possess 5-HT_{1A} and 5-HT_3 receptors. Oocyte membrane may also contain 5-HT_2 receptor sites.

This study was supported by a grant from The Rockefeller Foundation. The 5-HT analogs were gifts from Glaxo, Sandoz, CIBA-Geigy, Roussel UCLAF, Farmatalia, Lilly, and Bristol-Myers.

Early cleavage and the role of the macromeres in the development of the polyclad flatworm Hoploplana.

BARBARA C. BOYER AND GWENDOLYN A. WALLACE (Union College).

Blastomere deletion experiments were used to investigate the role of the macromeres at the eight-cell stage (first quartet) in the development of the polyclad turbellarian *Hoploplana inquilina*. In particular, eye development, general morphology, and determination of the embryonic axes of symmetry were examined after deletion of macromeres 1A or 1C, 1B or 1D, two adjacent macromeres, three macromeres, and all four macromeres.

Normal Müller's larvae resulted in 31% of cases in which 1A or 1C was deleted, and in 23% after removal of 1B or 1D. Macromere deletions usually did not lead to loss of eyes (no more than one quarter of any experimental category included one-eyed or eyeless larvae), but often did result in formation of supernumerary eyes. The occurrence of larvae with three or more eyes ranged from one quarter of experiments in which 1A or 1C was deleted, to 77% after deletion of all four macromeres. Normal morphology was compatible with loss of no more than one macromere, while deletion of three and four macromeres resulted in almost all of the larvae exhibiting the "swollen syndrome," characterized by spherical shape, abnormal tissues, and fluid accumulation. Following deletion of 1A or 1C, 92% of the larvae exhibited bilateral symmetry, although none did when three or four macromeres were killed. These results suggest the presence of an inhibitor of eye formation in the vegetal region that is more likely to be localized in the 1B or 1D cell than in 1A or 1C. Results also indicate that normal morphology requires the presence of at least three macromeres and provide evidence that macromere-micromere interactions are involved in the determination of embryonic symmetry, in which the B or D quadrant is more likely to become dorsal than A or C.

Scanning electron microscopic studies of four and eight-cell embryos suggest that the surface of one of the macromeres is smoother (less blebbed) than that of the other three, which may be associated with localization of morphogenetic determinants.

This work was supported by NSF grant DCB-8817760 and a grant from Earthwatch.

Involvement of Ca^{2+} channels in 5-hydroxytryptamine-induced oocyte maturation in Spisula.

A. L. KADAM (The Population Council), P. A. KADAM, S. J. SEGAL, AND S. S. KOIDE.

Serotonin (5-hydroxytryptamine, 5-HT) induced *in vitro* maturation of *Spisula* oocytes. The present study was carried out to determine whether extracellular calcium is essential for 5-HT induction of maturation, and whether oocytes possess calcium channels regulated by the neurotransmitter.

5-HT induced germinal vesicle breakdown (GVBD) in *Spisula* oocytes suspended in ASW, but not in Ca^{2+}-free ASW. When Ca^{2+} is added to Ca^{2+}-free ASW to concentrations of 5, 10, 20, 30, and 50% (100% equivalent to 9.27 m*M*), the percent of GVBD induced with 5-HT at a concentration of 5 μ*M* was 2, 30, 64, 86, and 96%, respectively. The calcium channel antagonists verapamil, nitrendipine, nifedipine, nimodipine, and Cd^{2+}, at a concentration of 50 μ*M*, blocked 5-HT-induced maturation by 89, 18, 16, 5, and 1%, respectively. The 1,4-dihydropyridine agonist, BAY K8644, at a concentration of 10 μ*M*, did not induce GVBD in *Spisula* oocytes.

The capacity of 5-HT to stimulate $^{45}Ca^{2+}$ uptake by *Spisula* oocytes was determined. To a suspension of oocytes in Ca^{2+}-free ASW, $^{45}Ca^{2+}$ (0.8 μCi/μmole) and test substances were added. The reaction mixture was incubated at 20–22°C for 10 min; the reaction was stopped by adding 5 m*M* KCl buffer containing 3 m*M* EGTA, and the mixture was filtered through a GF/C filter. Radioactivity on the filter was measured using a liquid scintillation counter.

5-HT at concentrations of 0.5, 1, 2, and 5 μ*M* stimulated $^{45}Ca^{2+}$ uptake by *Spisula* oocytes. The uptake values were 0, 5.2, 17, and 24.8 nmoles/mg protein, respectively, showing a dose response. The time course of $^{45}Ca^{2+}$ uptake at 20–22°C, showed a lag period of 2 min followed by a dramatic increase at 5 and 10 min post-treatment. Verapamil, at a concentration of 10 μ*M*, inhibited 5-HT-stimulated Ca^{2+} uptake. The receptor-selective 5-HT agonists, alpha-methyl-5-HT (5-HT_2) and 8-OH-DPAT (5-HT_{1A}), at a concentration of 5 μ*M*, stimulated Ca^{2+} uptake by *Spisula* oocytes. Mianserin (5-HT_1, 5-HT_2), at a concentration of 5 μ*M*, blocked 5-HT-stimulated Ca^{2+} uptake.

In conclusion, extracellular Ca^{2+} is required for 5-HT induction of *Spisula* oocyte maturation. 5-HT acts by opening receptor-regulated calcium channels of *Spisula* oocytes.

BAY K 8644 was a gift of Miles, Inc. The study was supported by a grant from the Rockefeller Foundation.

5-hydroxytryptamine receptor types on Spisula *gametes.*

P. A. KADAM (The Population Council), A. L. KADAM, S. J. SEGAL, AND S. S. KOIDE.

Receptors for serotonin (5-hydroxytryptamine, 5-HT) are classified into various types and subtypes. To establish the biologically functional 5-HT receptor types in *Spisula* gametes, selective agonists and antagonists for the various receptor types were tested for their capacity to influence *Spisula* oocyte maturation and sperm motility.

Oocyte maturation was assayed by examining the oocytes under a light microscope for dissolution of the germinal vesicle (GVBD); sperm motility was assessed by stimulation of cold-immobilized *Spisula* sperm. The drugs were tested at final concentration ranging from 1 to 50 μ*M*

The order of decreasing potency of the 5-HT agonists to induce GVBD in *Spisula* oocyte was: 5-HT = alpha-methyl-5-HT = 8-OH-DPAT [8-hydroxy-2-(di-n-propylamino)tetralin]; both 2-methyl-5-HT and 5-CT (5-carboxyamidotryptamine) were inactive. The order of decreasing potency in stimulating sperm motility was: 5-HT = alpha-methyl-5-HT = 8-OH-DPAT > 2-methyl-5-HT > 5-CT. Phenylbiguanide and PAPP (LY-165, 163) were inactive on both gametes. The order of decreasing potency of 5-HT antagonists in blocking 5-HT induced oocyte maturation was: mianserin > ketanserin > s-(-)propanolol > GR3832F > methysergide maleate. To block 5-HT stimulation of *Spisula* sperm motility, the order of decreasing potency of 5-HT was: mianserin > ICS-250-930 > GR3832F > ketanserin.

These results indicate that *Spisula* oocytes possess biologically functional 5-HT_{1A} and 5-HT_2 receptor sites, and sperm contain 5-HT_{1A}, 5-HT_2 and 5-HT_3 receptor sites. The presence of 5-HT_{1A} and 5-HT_2 receptor sites on the oocyte membrane was validated by the finding that mianserin (5-HT_1 and 5-HT_2) and BMY-7378 (5-HT_{1A}) blocked 8-OH-DPAT-(5-HT_{1A}) induced oocyte maturation, and ketanserin (5-HT_2) and mianserin blocked alpha-methyl-5-HT-(5-HT_2) induced maturation. In conclusion, *Spisula* gametes possess 5-HT receptors of mixed or multiple types.

The 5-HT analogs were gifts from Glaxo, Sandoz, Ciba-Geigy, Rousse UCLAF, Farmatalia, Lilly, and Bristol-Myers. The study was supported by a grant from the Rockefeller Foundation.

A fluorescent study of sensory neurons in normal and regenerating squid embryos. BARBARA E. MACLAY AND RACHEL D. FINK (Mount Holyoke College).

We found two fluorescent lipophilic dyes to be vital markers specific for the ciliated sensory neurons of embryonic squid. The cationic membrane probes $DiIC_{18}$ and R 1316 were used to study the appearance, distribution, and regeneration of these neurons in embryos of *Loligo pealei*. Manually dechorionated embryos and hatched larvae were soaked in a 20 μg/ml solution of dye for 3 min, rinsed in seawater, and viewed with epifluorescence. We followed neurogenesis in organ primordia such as tentacles and fins. After 2–5 days of outgrowth and differentiation of these structures, fluorescent staining revealed populations of peripheral neurons and an extensive network of axonal projections. All stained neurons had nonmotile cilia; those on the cells of the tentacles were numerous and long, whereas those in the fins were few and short. The presence of cilia on these cells may have facilitated uptake of the dyes, explaining their selectivity. By hatching, ciliated neurons were seen on most regions of the larva, including the epithelial lines on the head, along the mantle edge and surface, and on the siphon.

We established that larval squid completely regenerate fins 5–7 days following surgical removal. Soon after the appearance of any regenerant tissue, fully differentiated sensory neurons, complete with nonmotile cilia, can be stained. This differs from normal fin development where no staining of neurons can be seen until 3–4 days after first outgrowth. Possible models to explain this rapid ennervation of regenerated tissue include migration of pre-existing neurons from neighboring tissue, dedifferentiation and redifferentiation of cells at the wound site, and the presence of a stem cell population that differentiates into ciliated sensory neurons.

This work was supported by Steps, R. D. Allen, and S. W. Kuffler Fellowships of the MBL, an MHC Howard Hughes Summer Research Fellowship, and a William and Flora Hewlett Foundation Grant of Research Corporation to R.D.F.

Metalloproteinases of sea urchin embryo and sponge: detection by gelatin-substrate polyacrylamide gel electrophoresis. JAMES P. QUIGLEY (SUNY, Stony Brook) AND PETER B. ARMSTRONG.

Tissue remodeling is a conspicuous feature of invasion, inflammation, wound repair, and embryonic and larval morphogenesis. Proteinases have been implicated in the degradation and turnover of extracellular matrix macromolecules presumed necessary for remodeling. Of particular interest are the enzymes responsible for the degradation of collagen, the principal structural element of most extracellular matrices. Two morphogenetic systems have been investigated for the presence of collagenases: the developing *Arbacia* embryo, and reaggregating *Microciona* tissue. In the first system, processes of cellular ingression, cell migration across basal lamellae, and invagination are prominent. In the second system, dissociated cells reaggregate, then sort out to reconstitute normal tissue morphology. Collagenases were identified by subjecting tissue extracts and conditioned seawater to SDS-polyacrylamide gel electrophoresis (non-reducing conditions) on gels containing gelatin. Enzymatic activity was detected as bands of clearance of the gelatin from the polyacrylamide gel matrix following removal of the SDS, incubation in buffers containing calcium (room temperature, 36–48 h.), and staining with Coomassie blue. *Arbacia* embryos showed three prominent gelatinases that migrated with approx. molecular masses of 65, 45, and 40 kDa. Gastrula and prism stage embryos released gelatinases of approx. 70 and 80 kDa into the seawater. The activity of the 65 and 40 kDa tissue gelatinases increased, and that of the 45 kDa tissue gelatinase decreased, during development. Reaggregating *Microciona* tissue released several gelatinases into the seawater; one of them, of approx. 85 kDa, was the most prominent. All of the *Arbacia* enzymes and the 85 kDa *Microciona* enzyme were EDTA-sensitive and PMSF-insensitive. Some of the low molecular mass *Microciona* gelatinases were EDTA-insensitive and PMSF-sensitive. None of the *Arbacia* enzymes had detectable caseinolytic activity.

Supported by NIH grant No. GM35185.

Comparative aspects of gossypol action. SHELDON SEGAL (The Rockefeller Foundation) AND HIROSHI UENO.

Gossypol (gp) has both anti-sperm and anti-virus activity *in vitro* (Polsky *et al.* 1989, *Contraception* **39**: 579–587). Consequently, gp may have an application in humans as an active ingredient of a vaginal protective cream (VPC). Factors influencing the use of gp in this manner were studied. The biological assay employed was the effect on motility and fertilizing capacity of *Arbacia* sperm (Segal *et al.* 1985, *Biol. Bull.* **169**: 543–544). Biological activities of gp solutions in filtered seawater, prepared from dilutions of gp in two vehicles, ethanol (roh) and cyclodextran (cd), were compared. Gp/roh concentrations of 25 μM or higher are 100% effective in destroying the fertilizing capacity of *Arbacia* sperm within 3 min. Sperm treated with 50 μM or 25 μM gp/cd retain about 30% fertilizing capacity. The anti-oxidant glutathione (gt) is proposed as an additive to a VPC in order to extend its shelf-life under non-refrigerated, non-lightproof conditions. In the *Arbacia* sperm test, gt at a concentration of 200 μM has no effect on sperm motility, nor does it reduce the activity of solutions of gp/roh. The minimal effective dose for 100% inhibition of motility is higher for human sperm than for *Arbacia* sperm. Twenty-five μM gp/roh is required to inactivate fully a normal human sperm sample within 15 min, a time at which control samples retain their motility. Immobilization of human sperm within 3 min is achieved with a gp/roh concentration of 200 μM. Gp/roh retains full spermicidal activity when exposed to ethylene oxide under conditions used for gas sterilization. These observations suggest that a VPC containing gp/roh at a concentration of 200 μM or higher, incorporating the anti-oxidant gt, and prepared in an ointment base vanishing cream that can be sterilized with ethylene oxide, may be an effective spermicidal/virucidal modality.

Interphase particulate tubulin revisited. KATHY A. SUPRENANT (University of Kansas, Lawrence).

I have repeated the experiments of Weisenberg (*J. Cell Biol.* 1972, **54**: 266–278) in order to identify the source of the particulate and sedimentable pool of tubulin described in surf clam (*Spisula solidissima*) oocytes. *Spisula* oocytes were homogenized at 21°C in 10 volumes of 1 *M* hexylene glycol, 0.01 *M* potassium phosphate at pH 6.2 (HG1) and centrifuged at 5000 rpm (JA-20) for 30 min at 4°C through a cushion of 10% (w/v) sucrose in HG1. Tubulin was extracted from the pellet with 2 volumes of ice-cold 0.1 *M* KCl, 0.01 *M* potassium phosphate, and 0.2 m*M* GTP at pH 7.0, and the sample was clarified by centrifuga-

tion at 10,000 rpm for 10 min. The tubulin in the soluble and sedimentable fractions was analyzed by a quantitative immunoblot with a monoclonal antibody against α-tubulin (DM-1α). Approximately 6–10% of the total tubulin in the oocyte sedimented at low g forces under these extraction conditions. The "tubulin-containing structure," described by Weisenberg as a 10–20 μm granular sphere, was identified by phase and differential interference contrast microscopy as the nucleolus, but is not the source of the particulate tubulin. The sedimentable tubulin fraction comprised short microtubules (5–10 μm) associated with membranes, and an amorphous granular material, as well as an aggregated and unidentified form of tubulin. The amount of particulate tubulin was determined during the first meiotic cell cycle following parthenogenetic activation with KCl. Extracts were prepared at 3-min intervals and analyzed for soluble and particulate tubulin by the immunoblot assay. The total amount of particulate tubulin decreased by 30% during germinal vesicle breakdown and formation of the first meiotic apparatus. This decline in the sedimentable tubulin fraction during the first meiotic cell cycle is presently inexplicable.

Nicotinamide suppresses Arbacia punctulata *development.* WALTER TROLL (New York University Medical Center) AND GERALYN CORCORAN.

Nicotinamide is one of a group of compounds that inhibits the formation of poly(ADP)ribose (PADPR), a polymer formed by dividing cells. The role of PADPR in cell division and differentiation can be studied by observing the effects of inhibitors of its formation. In this study, the effect of three PADPR inhibitors, nicotinamide, benzamide, and 3-aminobenzamide, on *Arbacia punctulata* development was investigated. We noted, when these PADPR inhibitors were added immediately after fertilization of *Arbacia,* that differentiation to plutei was blocked 2 days after fertilization, and that normal division proceeded to gastrula over the first 20 h. The complete blocking of a differentiation step suggests that a specific piece of information on DNA has been deleted and is responsible for this differentiation. Specific deletion of oncogenes in NIH-3T3 cells has been noted on addition of nicotinamide and other PADPR inhibitors (Nakayasu *et al.* 1988, *Proc. Natl. Acad. Sci. USA* **85:** 9066–9070). The blocking of differentiation mimics the deletion of genetic information provided by an oncogene and may serve as an assay to test other substances that may be capable of interfering with cancer development.

Supported by NIEHS Center Grant ES 00260 and Superfund Grant 1 P42 ES 048995.

Binding of gossypol and its analog to sperm proteins from Arbacia, Chaetopterus, *and* Spisula. H. UENO (Rockefeller University) AND S. J. SEGAL.

Gossypol, a known anti-fertility agent, also exhibits anti-parasite and anti-viral activities (Eid *et al.* 1988, *Exp. Parasitol.* **66:** 140–142; Polsky *et al.* 1989, *Contraception* **39:** 579–587). To elucidate the mode of action of gossypol, the biological activity of its metabolite, gossypolone, was studied. We also attempted to identify protein components in the sperm that might be involved in gossypol recognition, uptake, and inactivation. To identify such protein components, gossypol affinity resins were developed, either through the hydroxyl group via ether linkage, or through the aldehyde group via Schiff base linkage, stabilized by $NaBH_4$ reduction.

Gossypolone inhibits both the motility and fertilizing capacity of *Arbacia* and *Spisula* sperm. The dose of gossypolone required to inhibit 50% fertilization by *Arbacia* sperm is 5 μM. A slightly lower dose (1 μM) is needed for gossypol. However, gossypolone shows no effect on oxygen uptake, whereas gossypol (17 μM) acts as an uncoupler and causes a three-fold enhancement of oxygen uptake. The results suggest that the aldehyde moiety is required for inhibition of sperm motility, and that the 1-OH position is involved in oxygen uptake, presumably due to oxidation at this location.

Protein extracts from *Arbacia, Chaetopterus,* and *Spisula* sperm were prepared in a solution containing 1% Triton X-100, 0.5% deoxycholate, and 0.1% SDS (TDS). SDS-PAGE analyses of fractions, bound and unbound to gossypol affinity resins, show three predominant bands (25, 16, and 14K) in bound fractions. Our results indicate that the gossypol affinity resin is a useful tool with which to identify gossypol binding protein components, not only in sperm, but also from other cells. Analysis and identification of gossypol binding proteins may have useful pharmacological implications.

This study was supported by the Rockefeller Foundation.

General Physiology

Arachidonate and docosahexanoate as messengers in stimulus-response-coupling: evidence for effects of G-proteins in marine sponge aggregation. GIULIA CELLI, JONATHAN MCMENAMIN-BALANO, STEVEN ABRAMSON, KATHLEEN HAINES, JOANNA LESZCZINSKA, AND GERALD WEISSMANN (Marine Biological Laboratory).

The reaggregation of dissociated cells of *Microciona prolifera* in seawater is an example of stimulus-response coupling during which the twin signals, diacylglycerol and raised cytosolic Ca, $[Ca]_i$, are generated (review in Weissmann *et al.* 1988, *Biochim. Biophys. Acta.* **960:** 351–364). We have now found that arachidonic acid (20:4) and docosahexanoic acid (22:6)—at EC_{50}'s of 10–50 μM—enhance the aggregation of marine sponge cells exposed to suboptimum amounts of Ca and ionomycin (5 mM, 1 μM, respectively), while having no effect on aggregation provoked by phorbol myristate acetate (a surrogate for diacylglycerol) and ionomycin. This behavior of 20:4 and 22:6 (the major fatty acid of *Microciona* phospholipids) was mimicked by fluoroaluminate or sodium orthovanadate (5 mM, 3 mM, respectively)—agents that activate the 41 kDa alpha subunit of GTP-binding proteins of mammalian cells. Indeed, 20:4 enhanced the binding of GTPγ ^{35}S to membranes of mammalian cells (EC_{50} = 50 μM), and autoradiograms of membrane preparations of marine sponge cells showed radio-GTP binding to two classes of proteins: 36–38 kDa and 19–20 kDa. The latter resembled *ras* proteins in gels from porcine brain and human neutrophils. Moreover, ADP ribosylation of membranes from marine sponges showed twin substrates at 36–38 kDa, the ribosylation of which was enhanced by pertussis toxin. Finally, since G-proteins are often linked to phospholipases C in stimulus-response coupling, we exposed cells to protein 1 of the gonococcus phospholipase C. Protein 1 is a specific inhibitor not only of exocytosis, but also of phosphatidyl choline. Aggregation provoked by 20:4 and 22:6 was completely inhibited by protein 1 (1 μM). The data suggest that since sponge cells *cannot* metabolize 20:4 or 22:6 to prostaglandins or leukotrienes, these fatty acids act as direct messengers which can activate the G proteins of stimulus-response coupling.

Opioids in invertebrates. GIUSEPPE D'ALESSIO, RENATA PICCOLI, AND NELLO RUSSO (Department of Organic and Biological Chemistry, University of Naples, and Zoological Station, Naples, Italy)

Almost 15 years after the discovery of opiate receptors and endogeneous opioid peptides in vertebrate animals, the question of the presence of opioids in invertebrates has not been satisfactorily answered.

Opiate receptors have, in fact, been found and characterized in invertebrates (Zipser *et al.* 1988, *Brain Res.* **463**: 296–304), and a wealth of mostly immunohistochemical data have been produced on opioid-like immunoreactivity in invertebrates, from Protozoa to Urochordata. However, no reproducible and conclusive results on the isolation and chemical characterization of opioid peptides from invertebrates are available to date. Recently, we approached the problem at the genomic and the transcription levels, with the aim of identifying sequences homologous to the coding sequences of vertebrate opioid genes. By Southern blotting, we detected hybridization signals, suggesting that *Ciona intestinalis* DNA includes sequences homologous to the pro-enkephalin precursor gene; by *in situ* hybridization we found that this gene appears to be expressed in the neural gland (R. Piccoli, N. Russo, A. Spagnuolo, T. Renda, and G. D'Alessio, in prep.). Similar results were obtained with a mollusc (*Octopus*, unpub.) and a cnidarian (*Calliactis*, in collaboration with L. Cariello and coworkers at the Zoological Station, Naples).

In an attempt to expand our research to animals not available in the Bay of Naples, we prepared DNA from *Styela partita*, a tunicate, and from a mollusc, *Mytilus edulis*. Protocols were defined for obtaining suitable DNA preparations in good yields. DNA was then digested with Eco R1 and with (Eco R1 + Bam H1), and the digests analyzed by Southern blotting with a probe from *Xenopus* pro-enkephalin gene labelled with ^{32}P at a high specific activity. No clear discrete bands of hybridization were detected, which at least in the case of *Styela* would be surprising, considering its relation to *Ciona*.

Does calsequestrin facilitate calcium diffusion along the endoplasmic reticulum of eggs? LIONEL F. JAFFE (Marine Biological Laboratory).

I would suggest that egg calsequestrin (Henson *et al.*, 1989 *J. Cell Biol.* **109**: 149–161)—unlike its muscle counterpart—is freely diffusable within the endoplasmic reticulum (e.r.) and is thus able to facilitate calcium movement over long distances. Such facilitation could aid in the generation and control of steady, free calcium gradients within the cytosol of eggs. (Compare Speksnijder *et al.*, 1989 *Proc. Natl. Acad. Sci. USA* **86**: in press.) Egg calsequestrin, a 50 kDa hydrophilic protein able to bind about 15 calcium ions per molecule, seems well suited to this role. From the energetics of the well known calcium ATPase of muscle, it can be estimated that free calcium within egg e.r. does not exceed about 1 m*M*. From the total calcium within fertilized sea urchin eggs (known to be about 2 m*M*), and the volume fraction of e.r. within such eggs (morphometrically estimated to be about 5%), as well as cytochemical evidence that most of the calcium in fertilized sea urchin eggs lies within the e.r. (Poenie *et al.*, 1987; *J. Histochem. Cytochem.* **9**: 939–956), the total calcium within egg e.r. can be estimated as well over 10 m*M*. If these estimates are correct, and if egg calsequestrin is indeed freely diffusable, then most calcium movement along the e.r. can be shown to occur while the ion is bound to calsequestrin.

Calcification and proton transport in algae. TED MCCONNAUGHEY (Marine Biological Laboratory).

Inward proton currents exceeding 10 μmols m^{-2} s^{-1} were measured at localized regions of the rhizoid of the marine alga *Acetabularia mediterranea*, using a vibrating proton-specific microelectrode. These currents are light and Ca^{2+}-dependent, and are associated with $CaCO_3$ deposition. Similar light and Ca^{2+}-dependent currents were observed in the calcareous fresh water alga *Chara corallina*. A combination of techniques (electrophysiology, electron microprobe, isotope ratio mass spectrometry, ^{14}C isotopic labelling, and studies using buffers to affect proton and carbon transport) suggests that proton uptake occurs through ATP-driven electroneutral $2H^+/Ca^{2+}$ exchange, which raises the local extracellular Ca^{2+} concentration and pH. CO_2 then diffuses from the cell into the alkaline extracellular environment, and precipitates with Ca^{2+}. The protons taken up by the cell derive from CO_2 hydration and ionization.

For each $CaCO_3$ precipitated, the plant takes up two H^+. These move through the plant and are expelled at a separate surface, giving rise to electrical gradients and currents through the plant. Upon expulsion from the cell, the two H^+ convert two HCO_3^- to two CO_2, which are taken up by the plant. Since one CO_2 is subsequently consumed in calcification, there is a net gain of one CO_2 for photosynthesis when this physiology works efficiently (at pH about 8, typical of seawater). Viewed in this context, rapid and massive calcification by aquatic plants and algae-invertebrate symbioses is mainly a proton-generating mechanism for stimulating the photosynthetic utilization of bicarbonate.

Regulation of insulin release from pancreatic islet cells by norepinephrine and neuropeptide Y. SHARON L. MILGRAM, JOHN K. MCDONALD, AND BRYAN D. NOE (Emory University School of Medicine, Atlanta, GA 30322).

Insulin secretion from pancreatic islet beta cells is regulated by nutrient, hormonal, and neuronal secretagogues. Nerve fibers innervating pancreatic islets of a number of species contain both neurotransmitters and neuropeptides. Interactions between transmitters and peptides in modulating islet hormone release are poorly understood. We have recently demonstrated that a peptide with HPLC and immunoreactive characteristics identical to neuropeptide Y (NPY) is found in nerve fibers in anglerfish pancreatic islets. NPY is a 36 amino acid peptide having widespread distribution throughout the central and peripheral nervous systems in various species and is often co-localized with norepinephrine (NE) in catacholaminergic nerve terminals. Therefore, we are investigating the possibility that NPY and NE may interact in regulating basal- or glucose-stimulated insulin secretion from anglerfish islet beta cells.

Islets were decapsulated, minced, and dispersed using dispase. Dispersed cells were cultured for a minimum of 72 h in RPMI 1640 containing all amino acids, 2 m*M* glucose, and 10% fetal calf serum. Cells ($3–5 \times 10^6$) were suspended and perifused in 10 m*M* HEPES buffer containing 3 m*M* $CaCl_2$, 2 m*M* glucose, and nutrient or neural secretagogues. Perifusate fractions were collected, and aliquots were assayed for insulin by RIA. Glucose-stimulated insulin secretion in a dose-dependent fashion. Maximal increases of 2.5–3 fold over basal levels were achieved with 11.0 and 16.7 m*M* glucose, respectively. NE inhibited insulin release caused by 11 m*M* glucose in a dose-related manner, with complete inhibition accomplished at 50 n*M* NE. NE perfusion (10 n*M*) with basal glucose (2 m*M*) also reduced basal insulin release by 33–36%. Administration of NPY (1 μ*M*) with 2 m*M* glucose stimulated insulin secretion 53%. The effects of porcine NPY on glucose-stimulated insulin release and the potential interactions of NPY and NE are currently under investigation.

Supported by NSF grant DCB-8700843.

Analysis of edge birefringence observed near refractive index steps in myofibrils and KCl crystals using high resolution polarized light microscopy and spatial Fourier filtering. RUDOLF OLDENBOURG AND SHINYA INOUÉ (Marine Biological Laboratory).

In conventional polarizing microscopes, vertebrate striated muscles show a pattern of alternating strongly birefringent A-bands and weakly birefringent I-bands; both bands exhibit positive birefringence (slow axis parallel to fiber axis). Each I-band is bisected by a less birefringent Z-line. When observed at high resolution with polarization rectifiers, the Z-band appeared split into three narrow zones, with two outer positively birefringent zones flanking a central negatively birefringent, or isotropic, zone. In addition, each interface between the A- and I-bands seemed to be composed of two narrow zones of different birefringence values. These observations were made upon muscle fibers suspended in standard salt solutions that had a lower refractive index than the filaments in the fibers. When the medium was replaced with one that matched the refractive index of the filaments, the A- and I-bands each appeared uniform and exhibited their characteristic high and low intrinsic birefringence.

The appearance of narrow birefringent zones near refractive index steps in muscle is similar to the patterns observed at the edges of isotropic crystals: the side with the high refractive index medium exhibits what appears to be a thin birefringent layer with the slow axis parallel to the interface; and the low index side exhibits a birefringent layer with the slow axis perpendicular to the interface.

We explored the phenomenon of edge birefringence with inhibition measurements using thin KCl crystals and myofibrils of rabbit psoas muscle. Video images of myofibrils, several sarcomeres long, were recorded and processed using a desktop computer. Spatial filtering was applied by multiplying the Fourier spectrum of the fiber image with a mask retaining only those frequencies that were an integral multiple of the inverse sarcomere length. The back transform of the filtered spectrum gave the fiber image averaged over all sarcomeres.

Supported by grants NIH R37 GM 31617 and NSF DCB8518672.

Identification of myosin in dogfish shark and sea robin lens epithelium. NANCY S. RAFFERTY (Northwestern University), KRIS LOWE, KEEN A. RAFFERTY, AND SEYMOUR ZIGMAN.

We have been comparing the contractile proteins in the lenses of selected species with varying modes of accommodation for near-point focus. Marine fish and shark lenses, and the suspensory apparatus of those lenses, were examined for actin and myosin. SDS-polyacrylamide gel electrophoresis of extracts of these tissues, followed by Western blots with actin and myosin antibodies, were used to identify the proteins. We also used double-labeled immunofluorescence microscopy.

Standard methods of electrophoresis on 7.5% gels and blotting onto nitrocellulose paper were employed. The papers were incubated in a pan-myosin monoclonal antibody (Amersham) or in a polyclonal actin antibody (made in rabbits in N.S.R.'s laboratory). Reaction with biotinylated sheep anti-mouse or donkey anti-rabbit immunoglobulins were followed by streptavidin-peroxidase, (Amersham). The binding was visualized by incubation in 4-chloro-1-naphthol and H_2O_2. The same probes were used for immunofluorescence techniques, except that streptavidin-fluorescein and rhodamin phalloidin were substituted for the peroxidase on epithelial whole mounts.

A single band of about 200 kDa appeared in Western blots of the lens epithelial cells of both the shark and the sea robin, and in the suspensory ligaments of the shark. This band identifies the myosin in these tissues as myosin-II. Immunofluorescence microscopy revealed the myosin at the plasma membranes and perinuclear regions of the epithelial cells.

Thus, lens epithelial cells, and the structures that translate the lens for accommodation in these aquatic animals, have components of a contractile system. We suggest that they may be involved in maintaining lens shape and resisting excessive deformation of the epithelium through tonic contraction of actin and myosin filaments.

This research was supported by NIH grant EY 00698.

Spontaneous coagulation of Limulus *amebocyte releasate in the absence of detectable endotoxin.* FREDERICK R. RICKLES (University of Connecticut School of Medicine), PETER B. ARMSTRONG, CARL A. CARTA, AND JAMES P. QUIGLEY.

Activation of blood coagulation is a fundamental host response to trauma and inflammatory stimuli. The formation of a blood clot can delimit the inflammatory response. In higher mammals, these reactions have been well characterized, and a variety of endogenous and exogenous "activators" and inhibitors of the coagulation protease cascade have been described. In the most completely studied of all invertebrates, the horseshoe crab *Limulus polyphemus*, previous work has suggested that initial activation of a proclotting enzyme by gram-negative, bacterial endotoxin is obligatory for physiologic coagulation. In most of the previous studies of *Limulus* proteins, investigators have used *Limulus* amebocyte lysate (LAL), material prepared by distilled water lysis of blood cells (amebocytes) in the presence of the inhibitor n-ethylmaleimide (NEM). We report here the first biochemical evidence for an endotoxin-independent coagulation sequence in *Limulus;* its terminal components appear identical to those of the classical, endotoxin-mediated sequence in LAL described by others. Exocytosis and gelation of the granule contents of the amebocytes were observed in blood collected, without inhibitors, directly into heat-treated, endotoxin-free dishes. The gel and residual gel supernate (sn-1) were recovered from the dishes, a second supernate (sn-2) was recovered following centrifugation of the gel, and the proteins in these fractions were analyzed by SDS-polyacrylamide gel electrophoresis (reducing conditions) and western blotting. Two different rabbit antibodies prepared against purified *Limulus* coagulogen (the clottable protein) were used as immunologic probes. Contaminating endotoxin was excluded as a variable by testing all of the materials with an LAL sensitive to 10 pg/ml of endotoxin. A protein with a molecular radius (Mr) appropriate for the coagulogen (~24 kDa) was observed in extracts of intact, granulated amebocytes, and in both supernatants. Little or no 24 kDa protein remained in the "spontaneous" gel. A new protein band with an Mr appropriate for the coagulin, the matrix protein of the traditional LAL gel (~17 kDa), was observed in the resolubilized "spontaneous" gel. When probed with either of the antisera to coagulogen, both the 24 kDa and the 17 kDa proteins were detected. We interpret these data as evidence for an endotoxin-independent coagulation system in *Limulus*, perhaps mediated by one or more NEM-sensitive proteases not active in traditional preparations of LAL. These proteases use the same clottable protein (coagulogen) as substrate.

Supported by the Veterans Administration (Research Service) and grants from the Department of Health and Human Services (CA 22202; GM35185), the American Heart Association (83-957), the American Cancer Society (CH321), and the National Science Foundation (PCM80-24181).

Secretion of Microciona prolifera *aggregation factor (MAF) is required for marine sponge aggregation: quantitative analysis by means of a new assay for MAF.* WILLIAM RIESEN, GIULIA CELLI, JONATHAN MCMENAMIN-BALANO, AND GERALD WEISSMANN (Marine Biological Laboratory).

Since 1982, we have studied the reaggregation of marine sponge cells as an example of stimulus-response coupling during which the twin signals of diacylglycerol (protein kinase C) and increments of cytosolic Ca are generated in response to such stimuli as phorbol myristate acetate (PMA) and ionomycin (review in Weissmann *et al.* 1988, *Biochim. Biophys. Acta* **960:** 351–364). We have measured aggregation by re-

cording light transmission through stirred suspensions of dissociated sponge cells (approx 10^7 cells/ml in Ca- and Mg-free seawater containing 2.5 m*M* EDTA) after addition of Ca ± ionomycin, or PMA + ionomycin. We have analyzed tracings of light transmission, with respect to rate, extent, and onset of aggregation, to monitor steps in the purification of MAF by methods modified from Humphreys *et al* (1977, *J. Supramol. Struct.* **7**: 339–351) and Misevic *et al.* (1982, *J. Biol. Chem.* **257**: 6931–6936). Defining one kinetic unit (U_k MAF) as percent change in light transmission in one minute (ΔT/min), we report 100-fold purification of starting material by simple Ca precipitation (30 m*M*) and dissolution (5 m*M*), before density-gradient purification in cesium chloride. We confirmed that MAF fragments in EDTA inhibit MAF-induced cell/cell aggregation, and found that a 2.5 m*M* excess of Ca over EDTA permits sponge aggregation in response to MAF, but that 2.5 m*M* Mg (which preserves MAF integrity) does not: evidence that Ca is required to "prime" cells for aggregation via a Ca-dependent receptor. Moreover, inhibitors of secretion (protein I of the gonococcus and calmidazolium, 1 μM and 40 μM, respectively) inhibit aggregation produced by Ca and ionomycin (active aggregation), but not aggregation provoked by MAF (passive aggregation). The data provide functional support for our morphologic evidence that secretion of MAF is required for reaggregation of marine sponge cells, and that MAF appears to act both as a lectin and as a ligand.

In vivo *vectorial labeling of scallop gill ciliary membranes by NHS-LC-biotin.* L. Warren and R. E. Stephens (Marine Biological Laboratory).

To study the topology of proteins in the tubulin-rich membranes of scallop (*Aequipecten irradians*) gill cilia, we employed the water-soluble, membrane-impermeant probe NHS-LC-biotin to label surface-exposed -NH_2 groups. Excised gills were exposed, for 30 min, to 50 μg/ml of NHS-LC-biotin in bicarbonate-buffered seawater, the gills were washed exhaustively with seawater, and the still-motile cilia were released by brief exposure to hypertonic seawater and then isolated and purified by differential centrifugation. The membrane plus periaxonemal matrix was solubilized by washing twice with 0.5% NP-40 or 1.5% octyl glucoside in 3 m*M* $MgCl_2$ and 30 m*M* Tris-Cl (pH 8.0). The membrane extracts and the 9 + 2 axonemes were analyzed stoichiometrically by SDS-PAGE and electroblotting, using HRP-avidin to detect biotinylated proteins. The major biotinylated membrane protein, having a molecular weight >200 kDa, is only partially solubilized with NP-40 (which leaves part of the membrane skeleton intact), but is almost fully solubilized with octyl glucoside, indicating that it is an axoneme-associated transmembrane linkage similar to that reported in *Chlamydomonas moewusii* flagella (Bloodgood 1988, *J. Cell Sci.* **89**: 521–531). Two other proteins of lower molecular weight (140 and 44 kDa) behave similarly. These biotinylated proteins represent a small fraction of the ciliary membrane proteins, suggesting that they are either derived from a subpopulation of cilia, or correspond to transmembrane elements that do not occur along the whole length of the axoneme. Membrane tubulin subunits of cilia labeled *in vivo*, or labeled after isolation, are not biotinylated, even though labeling of the axoneme in the latter case indicates that the reagent can enter the periaxonemal space. Therefore, these tubulin subunits must be integral to the membrane, rather than peripheral proteins or proteins derived from the periaxonemal matrix, and they are not exposed at the membrane surface.

Supported by USPHS Grant GM 20,644.

Near-UV effects on the thymidine incorporation into dogfish lens. Seymour Zigman, Kris Lowe, and Nancy S. Rafferty (University of Rochester School of Medicine & Dentistry, Rochester, New York 14642).

The question of how near-UV radiation in the environment can damage the ocular lens so as to positively influence opacities has been considered from the standpoint of protein anomalies, but not from the standpoint that DNA may be damaged. The hypothesis that DNA is susceptible to such UV energy in the most anterior region, the lens epithelial cells, was tested by this work. Fresh dogfish (*Mustelus canis*) eyes were dissected to remove the cornea, and put into Ringer's medium so that the lens epithelium was facing upward toward a UV lamp emitting maximally at 365 nm with an intensity of 5 mW/cm^2 for up to 22 h. Control eyes were treated and incubated similarly, but without UV-exposure. Observations of the presence or absence of visible opacities were made, as were histological observations, using lenses fixed in formalin:glutaraldehyde. The incorporation of ^{3}H-thymidine into DNA was also measured. At 5 h of incubation, no changes in the above-stated parameters were observed. At 22 h, mild opalescence was noted in the anterior superficial cortical region only of UV-exposed, but not control, lenses. Both pyknotic and swollen epithelial cells were observed. In numerous experiments, the UV-exposed epithelia incorporated significantly greater amounts of thymidine than controls. H_2O_2 production did not occur. This finding applied, whether the radiolabeled DNA was isolated using Qiagen resins, or if it was TCA precipitated and extensively washed. Qiagen resin tubes and agarose A50 M columns were employed to obtain DNA essentially devoid of RNA and protein. No molecular weight change was observed. Two possible explanations for these observations are proposed: (1) Swollen and pyknotic epithelial cells may result from osmotic insult due to UV-induced inhibition of NaK-ATPase (as observed in mammalian lens epithelium). (2) Thymidine incorporation is enhanced as the result of the repair of single strand breaks in DNA (as observed in tissue culture mammalian lens epithelial cells exposed to H_2O_2).

Support: N.E.I. (Ey00459); Research to Prevent Blindness, Inc.; Mullie and Pledger Funds (University of Rochester).

Neurobiology

Functional and structural consequences of activation of protein kinase C (PKC) and injection of G-protein substrates of PKC in Hermissenda *neurons.* D. L. Alkon, C. Collin, I. Lederhendler, R. Etcheberigaray, P. Huddie, M. Sakakibara, S. Redlich, E. Yamoah, A. Papageorge, T. Nelson (Lab. Molec. Cell. Neurobiol., NINDS-NIH, Bethesda, MD).

In both *Hermissenda* and rabbit hippocampus neurons, PKC translocation accompanies and is probably responsible for long-lasting reduction of current flow through Ia and Ic K^+ channels (Alkon 1989, *Sci. Am.* 7: 42–50). Persistent memory-specific changes of *Hermissenda* neuronal branches were also closely correlated with memory acquisition and K^+ current reduction. Finally, a 21 kDa G-protein (CP20), a substrate for PKC in *Hermissenda* Type B cells, underwent learning-specific changes in phosphorylation (Neary *et al.* 1981, *Nature* **293**: 658–660; Nelson *et al.* 1989, *Bioessays* **10**: 75–79). Here we show that, within 20 min of exposure to phorbol ester (PDBU) in the presence of light, Type B soma area increased 10.1 ± 3.4% (n = 8), and projections ("blebs") consistently appeared on the soma surface, but not during exposure to inactive 4a-PDBU with light (n = 6), or PDBU in darkness (n = 9) (ANOVA, $P < .001$). Type B cells injected with Ni^{++}/lysine showed reduced volume of terminal branches ($P < .001$, n = 9) after the PDBU/light treatment, but not after the control treat-

ments. Iontophoresis of CP20 potently reduced Ia by 40 ± 6% and Ic by 53 ± 9%, $P < .001$, n = 7), but heat-inactivated CP20 (n = 8) or vehicle injections (n = 8) did not. Iontophoresis of *v-ras* reduced Ia by 50 ± 18% and Ic by 72 ± 26%, $P < .001$, n = 7, whereas *c-ras* injections increased the same K^+ currents by 43 ± 9% and 63 ± 12%, $P < .001$, n = 7. Vehicle injections were without effect. Thus, the G-protein substrates of PKC, when phosphorylated, may trigger molecular cascades with far-reaching structural and functional consequences in learning, development, and carcinogenesis.

What is the origin of photoreceptor noise? ROBERT B. BARLOW AND EHUD KAPLAN (Marine Biological Laboratory).

Photoreceptors are noisy in the dark. In the absence of light, both vertebrate and invertebrate photoreceptors produce discrete waves (quantum bumps) similar to those evoked by photon absorptions. The dependence of the rate of spontaneous bumps on temperature has been taken as evidence that they are produced by thermal isomerizations of rhodopsin. However, photoreceptor noise in the *Limulus* lateral eye can also be modulated by a circadian clock located in the brain. At night, efferent signals from the clock reduce the rate of spontaneous bumps without affecting those triggered by light.

How can neural activity change the effects of thermal energy without influencing those initiated by light? We investigated this question by measuring the effect of temperature on spontaneous activity of retinular and eccentric (second order) cells in the *Limulus* eye. Action potentials were recorded extracellularly from eccentric cells both day and night *in situ*, whereas quantum bumps were recorded intracellularly from retinular cells in the excized eye preparation, isolated from the circadian clock. We calculated the activation energies for eliciting spontaneous events from the Arrhenius relationship (log event rate *vs.* inverse absolute temperature).

We found that the average activation energy for eliciting action potentials from eccentric cells was 26.3 ± 7.8 kcal/mol (n = 10) during the day and 27.9 ± 6.5 (n = 12) kcal/mol at night. The average activation energy for eliciting quantum bumps from retinular cells *in vitro* was 26.5 ± 7.5 kcal/mol (n = 8).

Our results indicate that the circadian clock does not influence the energy required to elicit spontaneous events from the *Limulus* retina. Isomerization of rhodopsin by light requires energies ≥45 kcal/mol, which is more than twice that required for the thermal production of quantum bumps by photoreceptors and action potentials by eccentric cells. Therefore, the spontaneous events cannot be caused by thermal isomerization of rhodopsin.

Supported by NSF grant BNS-8709059 and NIH grants EY-00667 and EY-4888.

G-Proteins modulate calcium currents in Paramecium *and* Helix *neurons.* JUAN BERNAL (University of Connecticut, Farmington, CT) AND BARBARA EHRLICH.

Previously we reported that the calcium-dependent swimming behavior and the calcium action potential in *Paramecium* are modulated by G-proteins (McIlveen *et al.* 1987, *Biol. Bull.* **173:** 445; Bernal and Ehrlich 1988, *Biol. Bull.* **175:** 314). To test the hypothesis that both of these changes are due to modification of calcium channels, we measured the calcium currents in *Paramecium calkinsi*. In addition, the effects of G-proteins in *Paramecium* and in *Helix aspersa* neurons were compared. Although G-proteins modified the calcium currents in both cell types, we were surprised to find that the modifications were in opposite directions. To isolate the calcium currents, the cells were superfused with sodium-free solution containing potassium channel blockers (125 m*M* tetraethylammonium chloride, 5 m*M* 4-aminopyridine, 5 m*M* 3,4-diaminopyridine and 10 m*M* CsCl). The cells were studied using a two-microelectrode voltage clamp. The cell was held at −40 mV (*Paramecium*) or −50 mV (*Helix*) and depolarizing command pulses were applied to elicit the calcium currents. The compounds of interest were injected into the cell by pressure, with fast green as a dye indicator to ensure that the drug entered the cell. The effects of the injected compounds were studied only in those cells in which the holding and leakage currents were unaltered by the injection. We found that GTPγS, an analogue of GTP which binds to and activates G proteins, enhanced the magnitude of the calcium current in *Paramecium* by 20–90% (mean = 40%). GTPγS reduced the calcium current in *Helix* neurons by the same amount. GDPβS, which binds to and inactivates G-proteins, had the opposite effect of GTPγS in *Paramecium* as well as in *Helix*. These results demonstrate that "T-type" calcium channels in *Paramecium* may be activated, whereas "L-type" calcium channels in *Helix* neurons may be inhibited by G-proteins.

J.B. is a Fellow of the American Heart Association, Connecticut Affiliate. B.E.E. is a PEW Scholar in the Biomedical Sciences.

Preliminary molecular structure of FTX and synthesis of analogs that block I_{Ca} in the squid giant synapse. B. CHERKSEY, R. LLINAS, M. SUGIMORI, AND J.-W. LIN (Dept. Physiology and Biophysics, NYU Medical Center, New York, NY 10016).

FTX, a specific P channel blocker, is one of many channel blocking factors contained in the venom of the American funnel web spider. We have previously reported (Cherksey *et al.* 1988, *Biol. Bull.* **175:** 304; Llinas *et al.* 1989, *PNAS* **86:** 1686) on the use of FTX to construct an affinity gel for the isolation and characterization of P-type Ca^{++} channels from squid optic lobe and mammalian CNS.

Purification and structural analysis of FTX have been performed. FTX could not be adequately purified by reverse phase HPLC using acetonitrile:water gradients. FPLC on Superose indicated that FTX was of low molecular weight (200–400 Da), but did not effect an adequate purification. Anion exchange methods were ineffective. However, cation exchange on Mono S permitted a high level of purification of FTX, with elution of the active factor at approximately 0.8 *M* NaCl. Purified FTX exhibited a sharp UV absorption at 220 nm. No ring (aromatic) structure was detected. The absorption at 220 nm showed a pronounced shift with acidification suggesting that FTX possesses a titratable amine group. FT-IR (Fourier transform infrared spectroscopy) indicated the presence of C-C, C-N, N-H, C-H, and the absence of C=O, absorptions. These results ruled out the possibility that FTX is a small peptide and suggest that it is a polyamine. The known polyamine glutamate channel blockers (which contain ring structures) are ineffective as presynaptic blockers.

On the basis of these results, model compounds were constructed with the general structure of arginine-polyamine:

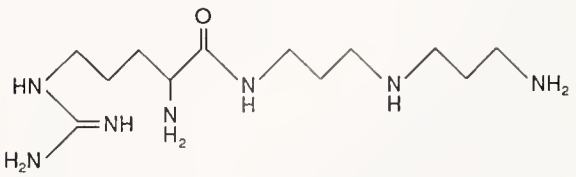

These compounds exhibited the selectivity of FTX, but not its potency. Compounds of the structure arginine-polyamine-arginine were ineffective as blockers. Thus, the free terminal amine is critical for efficacy, perhaps being the moiety that actually enters the pore of the channel. The arginyl group, perhaps via its strong charge, may act to secure the toxin in the channel. Therefore, the difference in potency between FTX and the model compounds may be due to the negative charge on

the carbonyl of the latter, which, on the basis of FT-IR spectra, is absent from FTX.

Arterial perfusion of FMRFamide-related peptides potentiate transmission at the giant synapse of the squid. G. A. COTTRELL, E. STANLEY, M. SUGIMORI, J-W. LIN, AND R. LLINAS (Department of Physiology and Biophysics, NYU Medical Center, New York, NY 10016).

Peptides of the FMRFamide (Phe-Met-Arg-Phe-NH_2) family (Price *et al.* 1987, *Zool. Sci.* **4:** 395) have several different actions on molluscan neurones, and the naturally occurring N-terminally extended forms can have different actions to the tetrapeptides on specified snail cells, suggesting the presence of more than one type of receptor (Cottrell and Davies 1987, *J. Physiol.* **382:** 51). Last year we observed that FLRFamide (L = Leu), micro-injected within the squid stellate ganglion, increases the rate of rise and amplitude of the EPSP and EPSC at the giant synapse in the absence of any observable effect on either the pre-synaptic spike or resting post-synaptic current (Cottrell *et al.* 1989, *J. Physiol.* **412:** 64P).

We have now obtained a similar response by arterial perfusion of the ganglion with solutions containing FLRFamide, using the method of Stanley and Adelman (1984, *Biol. Bull.* **167:** 467), and also by passing FLRFamide solutions directly into the stellate ganglion artery. The threshold for potentiation is less than 10 μM. SDPFLRFamide (S = Ser, D = Asp, P = Pro) has a similar effect, but we have been unable to observe any response with either Leu-enkephalin or the cephalopod peptide eledoisin. With both FLRFamide and SDPFLRFamide, potentiation of the EPSP usually wanes on exposure to the peptide for more than a few minutes. Another general feature is that the effect is more pronounced as the synapse is fatigued to a steady state by repeated high frequency stimulation. Potentiation with FLRFamide under these conditions can be greater than 2.5-fold. We must now determine which of the FMRFamide-related peptides occur in *Loligo pealeii,* and establish their modes of action in potentiating transmission at the giant synapse.

Calcium currents recorded in cells of anterior pituitary slices using the patch clamp technique. SUSAN A. DE-RIEMER, MEYER B. JACKSON, AND ARTHUR KONNERTH (Max-Planck-Institut für biophys. Chemie, Göttingen, FRG).

The patch-clamp technique was applied to analyze Ca^{++}-currents in cells found in slices of the rat anterior pituitary. Pituitary glands were removed from 15–30 day old rats, and ultrathin (60–100 μm) slices were cut on a vibratome. Single cells were visualized with an upright microscope equipped with a long-distance water immersion objective.

In the most commonly observed cell type (80–90% of all cells), even at very negative holding potentials (−120 mV), only non-inactivating Ca^{++}-currents, similar to the high-voltage activated or L-type current, could be evoked. Substitution of Ca^{++} by Ba^{++} increased the amplitude and shifted the peak current from 20 to 10 mV. Addition of 20 μM Cd^{++} blocked the current, while 100 μM Ni^{++} was ineffective. The dihydropyridine agonist BayK8644 increased the current, while nimodipine and nifedipine blocked it partially. A partial block was also seen with ω-conotoxin (50 μM). A second class of larger cells (10–20%) was observed with both the non-inactivating and an additional, transient Ca^{++}-current which was activated at holding potentials more negative than −80 mV (Carbone and Lux 1984, *Biophys. J.* **46:** 413–418; Armstrong and Matteson 1985, *Science* **227:** 65–67; Nowycky *et al.* 1985, *Nature* **316:** 440–443).

Immunocytochemistry, using antibodies to growth hormone (GH), prolactin (Prl), and lutenizing hormone (LH), showed that the primary cell type present in animals of this age contains growth hormone. Both prolactin and lutenizing hormone positive cells were distributed much more sparsely, but of the two, the Prl cells were larger. These results confirm and extend data obtained on cells in primary culture (DeRiemer and Sakmann 1986, *Exp. Brain. Res. Ser.* **14:** 139–154.)

Use of this version of the patch clamp method, in combination with immunocytochemistry *in situ,* extends the possibilities for understanding the significance of functional differences in different cell types in regulating secretion and how the local environment of cells within the pituitary affects their responses.

Supported by a fellowship from the MBL, and grants from the March of Dimes and NSF (S.A.D.); DFG (SFB 236) (A.K.).

Properties of detached nerve terminals from skate electric organ: a combined biochemical, morphological, and physiological study. M. DOWDALL, G. PAPPAS, AND M. KRIEBEL (SUNY, Health Science Center, Syracuse, NY 13210).

The electric organs of the skate (*Raja erinacea*) dissociate into functional electrocytes when incubated with 1% (w/v) collagenase. Dissociability of tissue is time and temperature dependent, and electrocytes with varying degrees of innervation can be produced according to conditions. At room temperature (26°C) most electrocytes are denervated after 6 h of treatment. These have normal resting potentials (−50 mV) and show a normal ultrastructure. After 2–4 h of treatment, innervation is present, and normal miniature end-plate potentials (MEPPs) and end-plate potentials (EPPs) can be recorded. Electron microscopy shows loosely adherent nerve terminals and detached terminals that can be concentrated by differential centrifugation. The Schwann cells migrate over newly exposed nerve terminal surfaces to encapsulate free terminals. Incubation at 6°C retards dissociation by 40-fold, although the time characteristics of the MEPPs and EPPs remain normal during dissociation of normal-appearing nerve terminals from Schwann cells and electrocytes. After 4 days of collagenase treatment at 6°C, electrocytes were washed several times, and isolated nerve terminals appeared in subsequent saline suspensions while MEPP frequencies fell and the denervated surface increased. Biochemical measurements, with choline acetyltransferase activity as a diagnostic nerve terminal marker and acetylcholinesterase activity as an auxillary marker, show that terminals became detached from electrocytes after 3–4 days at 6°C. This procedure produces isolated endings up to 5 μm in diameter, which are recognizable, with Nomarski optics, by their size and included stationary particles (mitochondria). Moreover, these nerve terminals are readily distinguished from nucleated Schwann cells.

Supported by NSF 19694 and NIH NS25683.

Very high resolution and dynamic stereo images of neurons. SHINYA INOUÉ (Marine Biological Laboratory), TED INOUÉ, ROBERT A. KNUDSON, AND RUDOLF OLDENBOURG.

We have devised a method for obtaining very high resolution stereoscopic images. A stack of 81 serial optical sections of Golgi-stained mouse neurons were recorded in 0.5-μm steps using a 100/1.35 NA Plan Apo lens (condenser NA = 1.1). In the Image-I image processing computer, each image in the stack was compressed and sheared laterally by appropriate amounts in order to generate rotated "image cubes." The angles of rotation were chosen to provide the parallax needed for stereo imaging. To retain a clear sharp view of the large number of optical sections making up each cube projected into a single plane, a sharpening convolution was applied to each section, and then

the minimum of each pixel gray value in adjoining sections was calculated. Images for the left and right eyes thus generated were placed at half height with the left image above the right in the video frame. To view in stereo, the left and right images were re-expanded vertically and projected as left- and right-circularly polarized images alternating at 120 Hz with a StereoGraphics projector. Complementary polarizing glasses worn by the viewers provide each eye with the left or right stereo image 60 times a second, giving rise to flicker-free stereoscopic images of an approximately 40-μm cube. We demonstrated very high resolution, detailed arrangements of neuronal spines on the dendrites. Rotating stereo views of the neuron at moderately high resolution (40/0.95 NA) were also demonstrated.

Supported by grants NIH R37 GM 31617 and NSF DCB 8518672.

Biphasic modulation of calcium-dependent potassium current in pituitary tumor cells examined with the perforated patch clamp technique. RICHARD H. KRAMER (Columbia University) AND EDWIN S. LEVITAN.

The pituitary tumor GH3 cell line is a model system for studying the actions of secretogogues, such as thyrotropin releasing hormone (TRH), which stimulate phosphatidylinositol hydrolysis and the formation of the intracellular messengers inositol trisphosphate (IP_3) and diacylglycerol. However, the electrophysiological effects of TRH have been difficult to study with the whole cell patch clamp method because the hormone response rapidly "washes out" of cells. To alleviate this problem, we have used the perforated patch configuration; the ionophore nystatin, contained in the patch pipette, is inserted into the membrane patch, providing a low-resistance pathway into the cell without causing washout of intracellular constituents. Using this configuration, we have elicited stable biphasic TRH responses (hyperpolarization followed by hyperexcitability). Under voltage clamp, the responses are characterized by an initial large increase in the outward current elicited during depolarizations, followed by a suppression of the outward current. The outward current, and both phases of the TRH response, are blocked by exposing the cell to the membrane-permeable calcium chelator BAPTA-AM, or by addition of charybdotoxin plus apamin, suggesting that modulation of Ca-dependent K current accounts for both phases of the TRH response. The increase in Ca-dependent K current is thought to be due to IP_3-gated Ca release from intracellular organelles. We suggest that the subsequent decrease in this current is indirect, due to TRH-induced inactivation of voltage-gated calcium channels (which we have observed) and consequent reduction of the calcium transient during depolarizations. In support of this hypothesis, we find that nimodipine, a dihydropyridine Ca channel blocker, selectively eliminates the suppression phase of calcium-dependent K current modulation.

Ontogeny of serotonergic neurons in Hermissenda: *a preliminary study.* EBENEZER YAMOAH, ALAN M. KUZIRIAN (Marine Biological Laboratory), AND CATHERINE TAMSE.

The nudibranch mollusc *Hermissenda crassicornis* is now in culture. As part of the effort to establish this invertebrate as a model system for neurobiological research, we are beginning an ontogenetic study of its nervous system. Applying function to morphology, we first undertook an immunocytological study to identify the developing serotonergic neurons in *Hermissenda.* We have observed that serotonin plays a major role in regulating feeding in adults, but one of our concerns in rearing this nudibranch is to maximize nutrition at all stages of development. Therefore, we have planned to investigate the role of these cells in feeding, and also to use them as markers documenting the developing nervous system in larvae and juveniles. Their putative role in metamorphic induction will also be examined.

Larvae raised from eggs that had been laid in the laboratory by field collected animals, were sampled on larval days: 1, 7, 14, 21, 28, and 35. We fixed the larvae in 4% paraformaldehyde and processed them for immunocytochemistry using a goat antibody to serotonin (INCSTAR); this was followed by rabbit anti-goat biotinylated secondary antibody and labeling with strep-avidin conjugated FITC (Vector Labs). Juveniles (metamorphic day-6), and adult central nervous systems (CNS) were treated similarly. Observations and photo documentations were done using epifluorescence microscopy.

Areas of anti-serotonin labeling were present in larvae at hatching (larval day-1); moreover, during development, these areas became consolidated into easily recognizable cells (day-7, 14) and finally into definite ganglia (day-21, 28, 35). Specifically, in the early larval stages, the staining occurred in the velar region and in association with the velar and larval retractor muscles. A large serotonergic cell occurred in the metapodium (day-28) and, by day-21, several positively staining cells appeared in the vicinity of the newly formed eyes. By day-35 (metamorphically competent larvae), there were clearly identifiable ganglia ventral to each eye (putative cerebropleural ganglia). Juvenile *Hermissenda* showed characteristic and numerous, scattered serotonergic sensory cells (including some proximal axons) in the outer epithelium, including the oral tentacles, rhinophores, cerata, and tail. Staining for serotonin-containing cells in the adult CNS was only minimally successful, although we used previously proven methods and had obtained positive results with the larvae. The same minimal staining was obtained in both field-collected and lab-reared adults. The findings are suggestive of a seasonality associated with the levels of serotonin in adult *Hermissenda,* and further study of this possibility is being undertaken.

This research was aided in part by the microscopic facilities sponsored by Olympus and Zeiss at the MBL and supported by a grant to A.M.K. (RR03820, NIH).

FTX blocks a calcium channel expressed by Xenopus *oocytes after injection of rat brain mRNA.* J.-W. LIN, B. RUDY, AND R. LLINAS (Dept. Physiology and Biophysics, NYU Medical Center, New York, NY 10016).

Funnel-web spider toxin (FTX) has been shown to block Ca conductances in cerebellar Purkinje cells and the presynaptic terminal of the squid giant synapse (Llinas *et al.* 1989, *PNAS* **86:** 1689). To further characterize this toxin, we studied its effect on a calcium current (I_{Ca}) appearing in *Xenopus* oocytes after injection of rat brain RNA. This current is insensitive to organic calcium channel blockers; *i.e.*, dihydropyridine or ω-conotoxin (Leonard *et al.* 1987, *J. Neurosci.* **7:** 875). Two aspects of the effect of FTX on the expressed I_{Ca} were examined: (1) the calcium-activated chloride current ($I_{Cl(Ca)}$); and (2) currents carried by barium ions through calcium channels (I_{Ba}). In the presence of 1.8 m*M* extracellular calcium, depolarizing pulses activated a mixture of inward and outward currents in the injected oocytes. Following the termination of the pulses, a prolonged tail of the Cl current could be recorded with its amplitude reflecting the magnitude of Ca influx activated during the depolarizing pulses. $I_{Cl(Ca)}$ tail current exhibited a threshold of -40 mV and reached maximal amplitude between 0 and $+10$ mV. FTX partially (57%, n = 7) and irreversibly blocked the calcium activated chloride current without changing its voltage sensitivity, and had a minimal effect on I_{Na} and I_K. This block was concentration dependent; an ED_{50} was obtained at 1500× dilution of the crude venom, and the maximum blockade was typically achieved at 600× dilution (see also Llinas *et al.* 1989, these Abstracts). In the presence of 60 m*M* Ba^{++} and blockers of sodium and potassium currents, a voltage-activated

inward current was recorded. This current (I_{Ba}), presumably mediated by calcium channels, showed little inactivation, had a higher threshold (−20 mV), and reached its peak amplitude between +20 to +30 mV. FTX blocked I_{Ba} partially and did not alter the time course of the current or its I-V characteristics. Furthermore, the extent of FTX partial block depended upon the level of RNA purification. The block is more extensive in the I_{Ba} expressed from poly(A)-mRNA (66 ± 9, n = 4), than that from whole brain RNA (41 ± 11%, n = 12). Thus, more than one population of calcium channels may exist, and they would be expressed in different proportions, depending on the degree of mRNA purification.

Dose-response for FTX blockade of presynaptic $I_{(Ca)}$ in the squid giant synapse. R. LLINAS, M. SUGIMORI, J-W. LIN, AND B. CHERKSEY (Dept. Physiology and Biophysics, NYU Medical Center, New York, NY 10016).

The dose-response relationship for the blocking action of FTX (a toxin fraction from *Agalenopsis aperta* venom, Sugimori *et al.* 1988 *Biol. Bull.* **175:** 308; Cherksey *et al.* 1988, *Biol. Bull.* **175:** 304, Llinas *et al.* 1989, *PNAS,* **86:** 1689) on the voltage-dependent presynaptic calcium current (I_{Ca}) in the squid stellate ganglion, was determined from voltage clamp measurements. In addition to the purified toxin, we tested the raw venom, and a synthetic poly-amine with an arginine at one end, constructed on the basis of chemical analysis of the FTX fraction (Cherksey *et al.* 1989, these Abstracts). These substances were added to the bathing solution in concentrations ranging from 0.2 to 190 nl/ml (volume of venom or liquid synthetic toxin in nl/ml seawater). Each of the three fractions had an ED_{50} of 5 nl/ml and produced a total blockade at 80–100 nl/ml. The block caused by 100 nl/ml had a time course of about 20 min and was very slowly reversible. Comparing the degree of calcium current block with the reduction of the post-synaptic potential, we concluded that the effect of the toxin on synaptic release is totally ascribable to its calcium blocking effect. We reached a similar conclusion about the synthetic polyamine. But because the same volume of raw venom and the synthetic polyamine produced about the same degree of block, we conclude that the active toxin may be more potent, and that the structure of the naturally occurring polyamine is therefore probably a variant of the synthetic product. Finally, we tested some polyamines with an arginine at each terminal of the chain, but I_{Ca} was not blocked. Thus, the polyamine may require the terminal amine to penetrate the channel and produce the block; the arginine group may hold the molecule in place.

Modulation of the spontaneous and evoked responses of lagenar afferents in the toadfish Opsanus tau, *by electric pulse stimulation of the efferent vestibular nuclei.* RACHEL LOCKE AND STEPHEN M. HIGHSTEIN (Marine Biological Laboratory, Woods Hole, MA).

The lagena is one of eight acoustico-lateralis mechanoreceptors innervated by the efferent vestibular nuclei (EVN). The ultrastructural morphology of efferent-afferent interactions consists of an efferent terminal on innervated hair cells and a second terminal on innervated afferents. Firing patterns of lagenar afferents encode aspects of head movement, head position, or substrate-borne vibration. Animals were lightly anesthetized with Finquel, MS222 (Ayerst), partially paralyzed by an intramuscular injection of 0.05 mg/kg of pancuronium bromide, Pavulon (Organon), placed in a lucite experimental tank atop a servo-controlled rotary table and perfused through the mouth with recirculated seawater at 15°C. Stationary animals were subjected to periods of recording of afferent activity or were oscillated with sinusoidal stimuli in the yaw plane before during and after epochs of electric pulse stimulation (100 Hz, 0.1-ms wide pulses, <100 μA amplitude constant current) via paired silver wire electrodes inserted visually into the EVN. Afferents range up to 16 μm in diameter and can be visually identified and penetrated with glass microelectrodes near the lagenar macula. Recordings reveal spontaneous excitatory post-synaptic potentials (EPSPs) and action potentials (APs). Electrical stimulation of the EVN could either increase or decrease the spontaneous or mechanically evoked firing rates of afferents (number or frequency of APs) depending upon the particular afferent studied. Effects of stimulation were generally stationary; *i.e.,* inhibition could never be converted into excitation by any experimental manipulation, and *vice versa.* Single, double, triple, *etc.* pulse stimulation of the EVN evoked monosynaptic EPSPs and APs in afferents whose spontaneous and evoked rate of APs were increased by trains of stimuli. Spontaneous miniature EPSPs from transmitter released by hair cells (EPSPs persisted when EVN axons were severed) had their amplitude and time-to-peak reduced during EVN stimulation. This reduction of "synaptic noise" from hair cells is correlated with a reduction of spontaneous and evoked firing rates. Therefore, we suggest that the EVNs exert a dual control over lagenar primary afferents via the dual innervation of lagenar receptors. We propose that actions of the axo-axonic synapses are responsible for increased firing rates while the axo-somatic synapses on hair cells may be responsible for reducing spontaneous and evoked firing rates.

The effects of GABA on retinal horizontal cells: evidence for an electrogenic uptake mechanism. ROBERT PAUL MALCHOW (Department of Ophthalmology, University of Illinois College of Medicine, Chicago, Illinois 60612).

The inhibitory effects of GABA on neurons are thought to be terminated by uptake into neurons and glia surrounding the release site. Certain classes of retinal horizontal cells avidly accumulate exogenously applied GABA. The present series of experiments were designed to determine if an electrophysiological correlate of the process of GABA uptake could be observed in such cells.

Isolated cells from the retina of the skate (*Raja erinacea* and *Raja ocellata*) were obtained by enzymatic dissociation. Voltages and currents from external horizontal cells were recorded using the whole-cell version of the patch-clamp technique. GABA (500 μM) applied via pressure ejection from pipettes placed 10–20 μm from the cell somas elicited pronounced depolarizations of the cells. When cells were voltage clamped at −70 mV, GABA produced a slow inward current of between 200–500 pA in magnitude; similar applications of 500 μM muscimol or 1 mM (−)baclofen were without effect. The response to GABA was not blocked by superfusion with either 500 μM bicuculline or 500 μM pictrotoxin. However, the response was rapidly and reversibly eliminated by superfusion with sodium-free Ringer. The I-V relationship of the GABA response was similar to that observed for glutamate uptake into glial cells (Brew and Attwell 1987, *Nature* **327**): the current decreased as cells were progressively depolarized, but did not reverse even with cells held at +70 mV.

These data indicate that the effects of GABA on horizontal cells are not due to the activation of either $GABA_a$ or $GABA_b$ receptors, but rather reflect electrogenic uptake of GABA into these cells. Skate retinal horizontal cells may prove to be an excellent model system with which to study the process of GABA uptake into neurons.

The author acknowledges the generous support for this research provided by a fellowship from the Grass Foundation.

Electric organ discharge and electrosensory reafference in the little skate, Raja erinacea. JOHN G. NEW (Dept.

of Neurosciences, A-001, School of Medicine, UCSD, La Jolla, CA 92093).

The electric organs (EO) of the little skate are located laterally along the longitudinal axis of the tail. They are innervated by a series of spinal nerves that receive descending input from the electric organ command nucleus (EOCN) situated on the midline of the rostral medulla (Szabo 1955, *J. Physiol.* **47**: 382–385). The weak and irregular discharge of the EOs consists of a head-negative, tail-positive waveform of 10–50 mV amplitude and approximately 70 ms duration (see Bass 1986, in *Electroreception,* Bullock and Heiligenberg, eds., J. Wiley, for review). The purpose of this study was to determine the effect of electric organ discharge (EOD) upon the activity of the animal's own electrosensory system.

In alert decerebrated skates, stimulation of the EOCN with a brief, high-frequency train of pulses, results in synchronous discharge of the electric organs. This evoked EOD is indistinguishable from those evoked by tactile or electric field stimuli, or the animal's spontaneous activity.

Recordings from anterior lateral line nerve (ALLN) fibers innervating the electrosensory ampullae of Lorenzini demonstrate different responses to the EOD depending upon the orientation of the receptor and the position of the ampullary pore on the body surface. ALLN fibers, with receptive fields in the caudal third of the pectoral fins, are strongly excited by the EOD (mean max. freq. = 90 spikes/s), whereas more rostral ampullae are driven more weakly or not at all. Those fibers innervating rostral ampullae and exhibiting modulation are differentially excited or inhibited depending upon ampullary orientation. Analysis of the internal and external electric fields indicates that the EOD acts similarly to an externally applied dipole, producing differential modulation of ALLN activity. This contrasts with the common-phase modulation produced by ventilatory activity.

Supported by a fellowship from the Grass Foundation and NIH NRSA NS-08114.

Stilbene derivatives or chloride replacement by impermeant anions dramatically alter a late component of the light scattering change in mammalian nerve terminals. A. L. Obaid, K. Staley, J. B. Shammash, and B. M. Salzberg. (University of Pennsylvania School of Medicine).

Electrical stimulation produces large and rapid changes in the intrinsic optical properties of the neurosecretory terminals of mammalian neurohypophyses. These signals, measured as changes in opacity, reflect alterations in large-angle light scattering, and comprised at least three components. The first of these, the E-wave, coincides with the arrival of excitation in the terminals; the second, the S-wave, is intimately related to the secretion of arginine vasopressin and oxytocin, and the third and slowest component exhibits a complex N-shaped waveform that requires seconds to return to baseline. This slow change in the transparency of the tissue suggested that volume compensation associated with chloride movement might be implicated in determining the time course of the optical signal. Chloride replacement (90%) by impermeant anions such as gluconate, isethionate, methyl-sulfate, and methane-sulfonate (Ca activity matched to that of the control Ringer's solution) resulted in the reversible loss of the N-shaped waveform and a faster return to baseline with overshoot. The same effect was obtained, although irreversibly, upon the addition of either 0.2–0.5 m*M* 4-acetamido-4-isothiocyano-stilbene-2,2′-disulfonic acid, disodium salt (SITS-Sigma) or 0.1–0.5 m*M* 4,4′-dinitrostilbene-2,2′-disulfonic acid, disodium salt (DNDS-Molecular Probes). This result suggests that the late component of the light scattering signal from the nerve terminals of the mouse neurohypophysis is prolonged by transmembrane chloride movements which may be coupled to volume changes in this tissue.

We thank Drs. Wu Jian-Young, Harvey Fishman, and M. V. L. Bennett. Supported by USPHS grant NS 16824 and by fellowships from the Nuffield Foundation (K.S.) and the Short Term Experience in Research Program of the NIH (J.B.S.).

Imaging learning-specific changes in the distribution of protein kinase C. James L. Olds, Donna L. McPhie, and Daniel L. Alkon (NINDS-NIH, Bethesda, MD 20892).

Protein kinase C (PKC) is an important second messenger in a wide variety of physiological systems. Ongoing work in this laboratory has demonstrated a statistically significant learning-specific change in the distribution of PKC in the rabbit hippocampus.

Rabbits were classically conditioned in the nictating membrane paradigm, and sacrificed either 24 h or 3 days later. Brains were prepared for quantitative autoradiography by standard methods [Olds *et al.* 1989, *Science* (in press)]. Cryosections (20 μm) were incubated with [^{3}H]-phorbol-12,13-dibutyrate (PDBU) at 2.5 n*M* for 60 min. Non-specific binding was consistently less than 9% in all assays. We analyzed film autoradiograms of rabbit brain sections and radioactive standards using with a computerized image analysis system.

Conditioned (Group C) animals showed a 49% and 43% increase, respectively, in ^{3}H-PDBU binding ($P < 0.01$, one way ANOVA) in the CA1 region of the dorsal hippocampus when compared with either unpaired control animals (Group UP), or naives (Group N), 24 h after conditioning. No significant difference was observed between Groups UP and N. Higher resolution transept-line analysis established that the stratum pyrimidale to stratum oriens ratio (SP/SO) was significantly increased over controls, thus showing not only a change in the amount of the enzyme, but also a change in its distribution. An analogous, statistically significant decrease in SP/SO was seen in group 3-C animals, which were sacrificed 3 days after the end of behavioral training. These results suggest that, after an initial increase in soma-localized PKC (24 h after conditioning), the enzyme migrates to areas corresponding to the dendritic compartments of CA1 pyramidal cells (3 days after conditioning). This conditioning-specific change represents a modification in the pattern of PKC distribution that is dependent on behavioral retention time.

A search for correlations in the spike activity of the Aplysia *abdominal ganglion during the gill withdrawal reflex.* D. Schiminovich, L. B. Cohen, A. I. Cohen, H.-P. Hopp, C. X. Falk, and J.-Y. Wu (Department of Physiology, Yale School of Medicine).

We previously made optical recordings of action potential activity in the *Aplysia* abdominal ganglion during the gill withdrawal reflex using voltage-sensitive dyes and a 124-element photodiode array. We have now searched for correlations in the spike activity of the optically detected action potentials. High correlation values were given to pairs of cells maintaining exactly the same time difference between some subset of spikes in each cell. The time differences were allowed to deviate by as much as 20 ms, although such deviations would reduce the value we assigned to the correlation. Correlations found at times of high spike activity (just after the touch to the siphon) were given lower values because of an increased probability that the correlations were due to chance.

Several trials of spike data from seven preparations were searched for correlations. No large correlations were found. To judge whether the small correlations we found were real, we looked for correlations in a file called "random." This file was obtained by taking the experimental spike file and randomly reassigning the time position of each spike in each cell in a region of 250 ms. In this way, the overall appearance of the experimental and random files were similar, while any correlations found in the experimental file should be weakened. However, the correlations found in these random files were just as large as those in the experimental file; we concluded that the correlations in the experimental file were due to chance.

We have considered two kinds of explanations for the absence of correlations. First, the optical recordings were only 20% to 40% complete, and we might have observed a special subset of cells (*e.g.*, motor neurons) that were not correlated. On the other hand, the nervous system of the *Aplysia* may not use many large fast interactions but, instead, either small fast interactions that require the activity of many pre-synaptic cells or slow interactions that would not generate precise intervals between pre- and post-synaptic spikes.

Supported by NIH grant N508437.

On-line rapid determination of [*Ca*]*i by means of Fura-II and high speed video imaging.* M. SUGIMORI AND R. LLINÁS (Dept. Physiology and Biophysics, NYU Medical Center, New York, NY 10016).

Calcium concentration changes in the soma and dendrites of mammalian Purkinje cells during spike activity have been determined with the calcium-sensitive dyes Arsenazo III (Ross and Werman 1986, *J Physiol.* **389**: 319) and more recently Fura-II (Tank *et al.* 1988, *Science* **242**: 633). In the latter study, a distinction was made between calcium entry, which occurs at the onset of plateau potentials in the peripheral dendritic branchlets, and that which occurs in the main dendritic arbor. The study suggested that the spontaneous activation of Purkinje cells is initiated by an inward calcium current at peripheral dendrites which, upon reaching sufficient amplitude, evoked calcium-dependent action potentials in the main dendritic tree. The measurements reported in that study were obtained at a maximum speed of 250 ms. With improved high speed imaging techniques (a photon counting camera and a high speed video recording system capable of recording 2.5 ms per frame), we have recorded the actual time course and distribution of calcium entry during single action potentials in Purkinje cells. Because the fluorescence measurements using Fura-II were made at only one light frequency (380 nm), the measurements indicate only relative calcium concentration changes in the cell cytosol. Simultaneous recordings of light absorption by Fura-II, and of intracellular voltage, clearly indicate that the plateau potentials preceding the activation of Purkinje cells occur in the spiny branchlets. The full action potential is then observed in the main dendrites and is followed by a synchronous, antidromic invasion into the fine dendritic tree. Averaging the calcium signal obtained immediately after the onset of a dendritic spike, and comparing it to that prior to this spike, demonstrates a large calcium influx at the main dendritic field during the spike. Moreover such signals indicate that calcium concentration transients may last for periods of 10 to 15 ms after which the calcium is buffered or pumped from the cytosol. Thus, [Ca]i is very actively modulated. This technique also allows visualization of the Fura-II response to the calcium entry in the presynaptic terminal of the squid giant synapse following a single stimulation to the presynaptic fiber.

Activation of the octavolateralis efferent system in the lateral line of free-swimming toadfish. T. C. TRICAS AND S. M. HIGHSTEIN (Washington University School of Medicine, Department of Otolaryngology, St. Louis, MO 63110).

The octavolateralis efferent system (OES) can be activated by multimodal sensory stimuli (Highstein and Baker 1985, *J. Neurophysiol.* **54**: 370) and has a predominantly inhibitory action on the firing of lateral line (LL) primary afferent fibers. We studied the OES in a semi-natural setting to determine if visual stimuli could activate it. Single LL afferents were recorded chronically with metal microelectrodes, for periods up to 9 days, in toadfish swimming freely in a small tank monitored by a video system. Primary afferents are grouped into four classes based upon their spontaneous interspike intervals: regular, irregular, bursting, and silent. Silent fibers were mechanically activated by mild 25–90 Hz vibrations of the experimental tank. Trains of bright photic stimuli (10–100 flashes/s for 1–5 s) increased spontaneous spike rates of irregular and bursting afferents, but decreased mechanically evoked afferent firing rates of silent fibers. To test a biologically relevant visual stimulus, a small prey fish was presented in a clear sealed chamber that eliminated all other sensory cues. After presentation of the prey from behind a movable blind, the spontaneous activity of some LL fibers decreased; mechanically evoked firing in silent fibers also decreased for the duration of the stimulus (up to 120 s) and recovered to pre-stimulus rates when the blind was closed. Thus, the OES can modulate the activity of LL afferents via visual input pathways in biologically relevant contexts.

Chaotic properties of quantal transmission at the skate neuro-electrocyte junction. J. VAUTRIN, J. HOLZAPPLE, AND M. KRIEBEL (SUNY Health Science Center, Syracuse, NY 13210).

Spontaneous synaptic activity at neuro-electrocyte junctions has been recorded using focal and intracellular recording techniques. After electrocyte dissociation with collagenase, nerve terminals remain in physiological contact with the electrocytes (see Dowdall *et al.*, these Abstracts). Focally recorded miniature end-plate potentials (MEPPs) from dissociated electrocytes show broad amplitude and time-to-peak distributions that are skewed towards low values. Intervals and time-to-peak plots reveal interactions between spontaneous MEPPs. Successive MEPPs often show congruent rising phases, and arise in very bursty patterns. Breaks on MEPP rising phases and changes in slope indicate a sub-structure. Many treatments increase the skew-to-bell-MEPP ratio in frog or mammalian preparations (skew class includes slow- and giant-MEPPs). Temperature changes have a reversible effect on the slope of the skate slow-MEPP. Electrocytes from intact electric organs show periods of MEPPs with the same, fast time course producing bell-shaped amplitude distributions with a subunit substructure. These periods of bell-MEPPs alternate with periods of mainly skew-MEPPs. The rapid shifts (seconds) between the two regimes of the spontaneous release process strongly suggest that each MEPP is not due to a performed packet of transmitter, but results from a deterministic process that dynamically combines subunits in different numbers and rates. A simple model, combining subminiature end-plate currents in different numbers and rates, is able to simulate all the observed MEPP amplitudes and time courses. Chaos theory shows that simple systems lead to complicated patterns. We demonstrated that a leaking faucet shows transitions, from a very organized regime with drops of regular size, to instable regimes of various drop sizes that are organized in bursts. Records of drops showing classes of volumes and interval structure are remarkably similar to those of MEPPs.

Supported by NSF 19694 and Association Française contre les Myopathies.

Pathobiology and Environmental Studies

Shell disease syndrome in Cancer *crabs.* ROSEMARIE BORKOWSKI AND ROBERT A. BULLIS (University of Pennsylvania, Laboratory for Marine Animal Health, Marine Biological Laboratory).

Gross examinations and microbiological investigations were performed on 14 *Cancer borealis* (Jonah crab) individuals and 13 *Cancer irroratus* specimens (rock crab) afflicted with shell disease syndrome. The crabs were collected from near-shore waters between the Chesapeake Bay and Martha's Vineyard. Manifestations of disease varied between and within the two species, indicating a potential for more than one pathogenic process.

Lesions in *C. borealis:* focal blackening without ulceration was the most common dorsal carapace abnormality. Mildly affected animals exhibited punctiform blackening of the dorsal shell, whereas coalescence of numerous black foci throughout at least two-thirds of this region was characteristic of extensive disease. Distribution of all such lesions ranged from markedly symmetrical to decidedly asymmetrical. Lesions of the ventral carapace and appendages included punctiform erosions and small foci of blackening with, or without, central pinpoint ulceration.

Lesions in *C. irroratus:* the most frequent dorsal carapace abnormality was focal ulceration through the exoskeleton to underlying soft tissues. Shell adjacent to such lesions was blackened and the underlying endocuticle discolored. This ulcerative abnormality occurred at random sites and affected less than one-third of the dorsal shell with the remaining dorsal carapace being normal. Circular erosions arranged in a linear fashion and cracking of the exoskeleton were the primary lesions of the ventral carapace and appendages. Eight of 13 crabs had lost entire appendages or dactylopodites.

Blackening of the gills was noted in both species, as was accumulation of black sediment between the gill bases and exoskeleton.

In *C. borealis* and *C. irroratus, Vibrio spp.* were the most frequent bacterial isolates from normal and affected areas of the exoskeleton; *Pseudomonas spp.* ranked second in number of isolates. These findings confirm earlier work regarding the genera of bacteria associated with shell disease syndrome.

This study is supported in part by grants from the Division of Research Resources, National Institutes of Health (P40-RR1333-09); Northeast Fisheries Center, National Marine Fisheries Service; and the Madison Trust.

Shell disease in impounded American lobsters, Homarus americanus. ROBERT A. BULLIS (University of Pennsylvania, Laboratory for Marine Animal Health, Marine Biological Laboratory).

Lobsters held in impoundments during the winter months for long periods can show dramatic increases in shell disease. This unsightly condition affects marketability and can spread rapidly through a population leading to wholesale losses and decreased profitability.

Twenty-five lobsters were sampled from an impoundment in Gran Manan Island, Nova Scotia, during a disease outbreak. Gross examination revealed diffuse pitting erosions covering the entire exoskeleton, but most prominently on the carapace and dorsal abdominal segments. Lesions of the ventral surface were characterized by foci of hyperpigmentation associated with abrasions and scratches. Crushing injuries were manifested by cracking of the exoskeleton and severe blackening of underlying tissues. Lesions of this type are thought to be associated with trauma induced by overcrowding and poor handling.

Microbiological examinations revealed that most individuals had concurrent bacterial septicemia. Microbial isolates from the hemolymph, internal organs, and exoskeleton included chitinolytic, lipolytic, or both types of bacteria from the genera *Acinetobacter, Flavobacter,* and *Pseudomonas.* All three genera have previously been implicated in shell disease outbreaks. Physiological and biochemical disturbances in chitin synthesis, and a resulting breakdown in exoskeletal repair, were hypothesized to be the result of stress-induced immunosuppression.

The progression of the disease was altered by placing lobsters in flow-through containment with three feedings per week of fresh squid and weekly removal of excreta. After six months, lesion severity decreased in moderately affected lobsters.

This work indicates that, although control of ubiquitous chitinolytic bacteria in captive populations is difficult, disease problems may be alleviated by increased attention to hygiene (removal of excreta and selective culling), proper husbandry (adequate nutrition and a clean water supply), and wound avoidance (minimized overcrowding).

This study was supported, in part, by a grant from the Division of Research Resources, National Institutes of Health (P40-RR1333-09) and the generosity of Paul's Lobster Co., Boston, MA.

Marketing, ecological, and policy considerations related to the New England conch fishery and Hoploplana. ILENE M. KAPLAN, BARBARA C. BOYER, AND DANIELA HOFFMANN (Union College).

Marketing procedures and ecological factors associated with the New England conch (*Busycon*) fishery, and related changes in *Hoploplana,* a turbellarian flatworm commensal in the mantle cavity of *Busycon,* are examined. Conch and pot fishermen were observed at sea on a regular basis, and interviews with fishermen, seafood buyers, processors, and fish market and restaurant owners were conducted. Data on size, width, weight, sex, and number of worms in the conch also were collected.

Conch fishermen are paid $.25–$.55 a pound for conch in the shell; markets sell conch for $.59–$1.19 per pound in the shell, and $2.75–$3.25 per pound outside the shell; and conch is sold as conch salad for $4.99–$6.99 per pound. The record of annual fluctuations over the past 20 years reveals an overall increase in the pounds of conch meat harvested in New England, as well as an increase in the market value. Conch supply has become more available due to increased fishing, and price fluctuations in the last few years have become less dramatic. Increased fishing for conch has also resulted in heightened competition between pot fishermen using traditional techniques and larger stern trawlers.

A total of 741 specimens of *Busycon canaliculatum* were examined (466 females and 264 males). Approximately 20% yielded 223 worms, 154 from females and 69 from males.

Further monitoring of the conch fishery is suggested for future research and policy considerations.

This research was supported by a grant from Earthwatch and Union College/Dana Fellowships. The authors also acknowledge the support of the Marine Policy Center, Woods Hole Oceanographic Institution, and the Marine Biological Laboratory.

The sperm cell's silent spring: herbicides and pesticides. LEONARD NELSON (Medical College of Ohio, Toledo, OH 43699).

In 1962, Rachel Carson alerted the world to the fact that the indiscriminate use of DDT and other chlorinated hydrocarbons led to reproductive failure and to the death of birds and other animals. Spermato-

zoa are also adversely affected by these pesticides, organophosphates, and organometallic compounds. Water-insoluble agents dissolve in DMSO (dimethyl sulfoxide); and because of their lipophilicity, they readily penetrate plasma membrane lipoproteins. The high surface-to-volume ratio of flagella makes sperm cells particularly vulnerable. *Arbacia punctulata* cells suspended in artificial seawater respond dose- and time-dependently.

Paraoxon, an anticholinesterase insecticide, reversibly stimulates motile progression after 5 min (0.7–70 μM). Dieldrin and lindane are chlorinated hydrocarbons that can stimulate the vertebrate central nervous system to convulsions. These compounds are effective in the micromolar range: above 30 to 100 μM dieldrin inhibits; between 1 and 15 it stimulates initially; and lindane mainly depresses (0.4–13 μM). Mirex, an inducer of the cytochrome P-450 system, is a persistent insecticide and fire-retardant (carcinogen). This compound markedly stimulates sperm (0.2–1 μM), but initially depresses them at lower ranges.

The organometallic ethyl mercuric chloride is a fungicide used to treat seeds. It inhibits sperm movement (1–5 μM), but slightly increases it (50–55 nM), apparently by deregulating sulfhydryl control systems. Tributyltin acetate, used in boat bottom paint to reduce fouling, decreases sperm movement between 0.065 and 65 nM.

These organic pesticides and their inorganic counterparts affect the function of sperm cells, which can serve as sensitive indices of toxicants in the environment.

Supported by the Sage Foundation.

Sensory Biology

Subnose I: tracking oceanic odor plumes with high spatiotemporal resolution. JELLE ATEMA, GREG GERHARDT, PAUL MOORE, AND LAURENCE MADIN (Boston University Marine Program, Marine Biological Laboratory, Woods Hole, MA 02543).

In May 1989, we employed electrochemical microelectrode techniques to measure the fine structure of an oceanic odor plume at 1000 m depth off St. Croix, USVI. To avoid interference from unknown chemical compounds, we used a dopamine tracer and a selective dopamine detection method used previously to measure dopamine diffusion in brain tissue.

"Subnose" is an underwater detector that can sample specific chemical compounds with the spatiotemporal resolution of biological noses or better. The detector was mounted on a 1.5-m long stick that could be operated by the mechanical arm of the Johnson-Sealink submersible. For "Subnose-1" we averaged the signals from three graphite-epoxy type microelectrodes, each with a sampling surface of about 30 μm diameter. An odor plume was made by releasing a 50 mM solution of dopamine, together with fluoresceine dye, from a moored platform about 15 m above the sea floor. The solution was released evenly through a small nozzle (3 mm diameter) from a 10-l reservoir over a 45-min period. Ambient turbulence created a characteristically patchy plume carried down by a 10 cm/s current. The plume was located visually and tracked for 25 min with Subnose-1, from about 50 m downcurrent, up to about 5 m from the source. The patchy distribution of visible dye was represented as a series of sharp peaks when patches of dopamine were encountered by the electrodes. Several peak parameters were measured based on peak definitions given in Moore and Atema (1988, *Biol. Bull.* **174**: 355). Peak heights and maximum onset slopes rose toward the source indicating steeper and higher peaks near the release point. Patch sizes (area) decreased toward the source. Other parameters did not show spatial gradients. Although the present, visually guided track is a rather arbitrary series of encounters with odor, peak parameters such as peak height and slope could be used by aquatic animals to orient and locate odor sources regardless of an external frame of reference (*e.g.*, seafloor). This information may be critical for midwater animals, and useful for benthic animals, in their orientation.

Response of bluefish (Pomatomus saltatrix) *to increased intracranial pressure (Cushing response).* STEPHEN H. FOX, CHRISTOPHER S. OGILVY, AND ARTHUR B. DUBOIS (The John B. Pierce Foundation Laboratory, New Haven, CT 06519).

Bluefish have vasomotor responses to hemorrhage, or to head-up tilting in air (Ogilvy *et al.* 1989, *Biol. Bull.* **176**: 176–190). Increases of intracranial pressure (ICP) induce increases of blood pressure (BP) in mammals (Cushing response). We increased ICP via metal implants in the skull and observed heart rate (HR) and BP in the ventral aorta. BP and HR increased in all 21 fish challenged, whether or not the fish were anesthetized with tricaine (1 g/40 l seawater) or were rendered flaccid with pancuronium (0.1 mg/kg). Mean BP increased from 83 (SE 4) to 126 (SE 4) mm Hg, and HR from 46 ± 4 to 75 ± 2 beats per min (BPM), as ICP was increased in 10 mm Hg steps of 20 s duration, from 3 ± 1 to 65 ± 1 mm Hg, in five bluefish. In five other bluefish, atropine (20 μg/kg) caused an increase in control heart rate and attenuated the increase of HR and BP during increases in ICP. In five more, phentolamine (400 μg/kg) lowered the resting BP and blunted the increase of BP during increased ICP. Atropine and phentolamine in combination completely eliminated the Cushing response in two fish (and the response to intraarterial epinephrine (4 μg/kg) in one of these); but in three other bluefish, the Cushing response was reduced yet not eliminated, and in two of these, epinephrine response was not blocked. The Cushing response starts in 3–5 s, stops 3–5 s after ICP drops, and can persist at least 30 min if ICP remains elevated at 16 mm Hg. The response was repeatable after recovery from atropine and phentolamine. The Cushing response was elicited by pressure exerted on the eyeballs, which raises ICP, or by an increase of air pressure over the exposed brain. Based on these experiments, the BP response in bluefish is mediated through tachyeardia and vasoconstriction. The role of this response in fish in their natural environment remains to be elucidated.

A novel chemosensory system in fish: do rocklings (Ciliata mustela, Gadidae) *use their solitary chemoreceptor cells as fish detectors?* KURT KOTRSCHAL (University of Salzburg, Austria), ROB PETERS, AND JELLE ATEMA.

Solitary chemoreceptor cells (SCC) of unknown function and biological role are scattered throughout the epidermis of most fish. Rocklings are favorable models for SCC research, as their modified anterior dorsal fin (ADF) contains several million SCC, but no taste buds (Kotrschal *et al.* 1984, *Zoomorphology* **104**: 365–372). These secondary sensory cells make synapses exclusively with recurrent facial nerve fibers (Whitear and Kotrschal 1988, *J. Zool. Lond.* **216**: 339–366), which terminate in a distinct subdivision of the brainstem facial lobe (Kotrschal and Whitear 1988, *J. Comp. Neurol.* **268**: 109–120). Body mucus dilutions of heterospecifics elicited responses in summed potential recordings (Peters *et al.* 1987, *J. Mar. Biol. Assoc. U.K.* **67**: 819–823; these abstracts).

To test the hypothesis that the ADF is a "fish detector," the breathing frequency (BTF) of four groups of rocklings (sham, closed noses, ADF removed, closed noses plus ADF removed) was recorded prior to, and during, a 2-min addition of stimulus to the tank water (*Lophius* plus *Opsanus* mucus solution 0.1% stock, or squid extract, or mucus water and squid extract simultaneously, six replicates per fish, four fish per treatment). Sham fish responded to mucus water with a significant drop

in BTF. In fish with closed noses, this response was weaker, but still significant. From fish with removed ADF, no BTF response to mucus water could be detected, even when the nose was intact. Squid juice did not affect the BTF, whereas squid juice together with body mucus produced a significant drop of BTF in the sham group. We conclude that fish body mucus is a biologically relevant stimulus for the ADF SCC in rocklings. Olfaction seems essential to interpret the ADF input. We predict, and subsequently will test with neuroanatomical techniques, that the brain connections of the ADF system are similar to that of the external taste buds, and the inputs from the ADF and the olfactory organ are integrated at prosencephalic levels.

The authors acknowledge the financial support of the Austrian Fonds zur Foerd. wiss. Forsch., proj. nr. J0367-BIO, the Royal Netherlands Acad. Sci., and the Dutch-Austrian cultural exchange program.

Potential gradient information contained within the three-dimensional structure of a laboratory odor plume. PAUL MOORE, NAT SCHOLZ, LYNNE LACOMIS, AND JELLE ATEMA (Boston University Marine Program, Marine Biological Laboratory, Woods Hole, MA 02543).

Odor plumes serve as sources of information for many animals during chemically mediated orientation. The information contained within the odor plume is poorly understood because the spatial and temporal scales at which chemoreceptor cells and organs function have been difficult to match with conventional chemical detectors. With newly introduced electrochemical microelectrodes (Moore *et al.* 1989, *Chem. Senses* **13**: in press), we can sample certain chemical tracers, such as dopamine, at micrometer space scales and millisecond time scales. In this study, we used this high resolution measurement to sample the three-dimensional structure of an odor plume under controlled laboratory conditions. An odor plume was created in a uni-directional seawater flume (90 × 250 × 20 cm). A 2-m*M* dopamine tracer flowed (50 ml/min) through a Pasteur pipette (1 mm ID) located 9 cm from the bottom in the cross-sectional center of the flume; lobsters sample in a plane about 9 cm from the bottom. After allowing the plume to establish itself for 2 min, an odor profile was recorded for 3 min using a graphite-epoxy capillary electrode and a computer-based recording system (IVEC-V). The sample sites were located at 25, 50, and 100 cm from the pipette mouth; at 3, 9, and 15 cm from the flume bottom, and at 0, 5, 10, 20, and 30 cm to the right and left of the pipette. These recordings were analyzed for odor pulse parameters by procedures developed in Moore and Atema (1988, *Biol. Bull.* **174**: 355–363). Initial three-dimensional analysis of parameters that describe odor pulse shapes and frequencies shows that spatial gradients of certain parameter values point to the source. Specifically, the frequency of large peak heights and large onset slopes increase toward the source, whereas other parameters decrease, and yet others remain constant (see also Atema *et al.*, these Abstracts). Animals may use this gradient information during orientation behavior, and their chemoreceptor filter properties may be "tuned" to certain odor pulse parameters (see abstracts by Scholz *et al.*, and Voigt and Atema).

Supported by NSF (BNS 88-12952) to J.A.

A novel chemosensory system in fish: electrophysiological evidence for mucus detection by solitary chemoreceptor cells in rocklings (Ciliata mustela, *Gadidae*). ROBERT C. PETERS (University of Utrecht, The Netherlands), KURT KOTRSCHAL, WOLF-DIETRICH KRAUTGARTNER, AND JELLE ATEMA.

Rocklings possess anterior dorsal fins (ADF) that are modified compared to other teleostean dorsal fins. The ADF consists of about 60 vibratile rays with a web only at the base; the first ray is enlarged. The vibratile rays are beset with about 5,000,000 solitary chemoreceptor cells (SCC). These SCCs are designated as chemoreceptor cells on ultrastructural criteria (Whitear 1971, *J. Zool. Lond.* **163**: 237–264; Kotrschal *et al.* 1984, *Zoomorphology* **104**: 365–372). Electrophysiological studies demonstrated "tuning" of the SCCs to mucoid stimuli (Peters *et al.* 1987, *J. Mar. Biol. Assoc. U.K.* **67**: 819–823).

The present experiments were designed to further specify the adequate stimulus and to compare the responses of the SCCs to those of taste buds (TB) in the pectoral and pelvic fins. Rocklings were anaesthetized with MS-222, and silver wire electrodes were then implanted around the recurrent facial nerve innervating the SCCs and around the facial nerves innervating the TBs. Summed potential recordings were made in unrestrained fish. Both groups of sensory organs were stimulated with body mucus of *Gadus, Ciliata, Solea, Pholis, Cottus, Mugil,* and *Zoarces,* and with the amino acids L-Arg, L-Ala, L-Cys, L-Gly, and L-Asp (1 m*M*).

The SCCs reacted to body mucus of all the fish mentioned above, except for that of conspecifics (*Ciliata*); the SCCs were insensitive to amino acids. The TBs, on the other hand, did not react to body mucus, but gave vigorous responses to amino acids.

These results suggest a specific function for the SCCs. The sensitivity of these receptors to body mucus might represent a chemosensory compensation for the limited vision of the rocklings in their highly structured and tidal habitat. This ability may help them discriminate between conspecifics and predators.

The authors gratefully acknowledge the financial support of the Royal Netherlands Academy of Sciences, the Fonds zur Förderung der Wissenschaftlichen Forschung in Österreich proj. nr. J0367-BIO, and the Austrian-Dutch cultural exchange program.

Chemo-orientation of the lobster, Homarus americanus, *to a point source in a laboratory flume.* NAT SCHOLZ, PAUL MOORE, LYNNE LACOMIS, AND JELLE ATEMA (Boston University Marine Program Marine Biological Laboratory, Woods Hole, MA 02543).

Many animals use chemical cues contained within turbulent odor plumes for orientation, but the relevant parameters of the plume are not known. Orientation studies in aquatic environments have advantages over those in terrestrial environments because odor distribution patterns can be more accurately measured, and stimulus delivery more closely controlled. We chose the lobster, *Homarus americanus,* because of its size and ease of handling, and the extensive base of neurophysiological data on the properties of its chemoreceptors. Previous behavioral studies indicate that the lobster relies heavily on chemosensory input in its natural habitat and specifically on antennular chemoreception for efficient orientation (Devine and Atema 1982, *Biol. Bull.* **163**: 144–153).

In a flow-through flume (90 × 250 × 20 cm), lobsters oriented towards a stimulus (0.5 g/l homogenized and centrifuged mussel tissue in raw seawater) constantly flowing from a pipette two meters upcurrent. The flow parameters were identical to those used for detailed plume description in Moore *et al.* (these Abstracts). Lobsters were placed on a mussel diet, and then starved for at least three days prior to testing. Tests were videotaped with a camera mounted directly overhead on a moveable track; tapes were digitized at 1 Hz with the rostrum as the reference point. From casual inspection of the resulting walking paths, we favor the hypothesis of direct chemosensory control of orientation (*i.e.*, "chemotaxis") rather than an innate behavior program (such as zig-zagging) triggered by chemical input. These preliminary results

have established the lobster as a viable model for studying chemo-orientation and chemical information extraction in turbulent odor plumes.

Supported by NSF (BNS 88-12952) to J.A.

Responses of chemoreceptor cells to controlled temporal stimulus patterns. RAINER VOIGT AND JELLE ATEMA (Boston University Marine Program, Marine Biological Laboratory, Woods Hole, MA 02543).

The lateral antennules of the lobster, *Homarus americanus,* play an important role in olfactory orientation. Taurine- (Tau) sensitive chemoreceptor cells on the antennules form a narrowly tuned and highly sensitive cell population. Tau occurs in high concentrations in lobster prey and in extremely low concentrations in coastal waters; this low natural background may enhance the value of Tau as a long distance orientation cue. Natural odor plumes can be described by stimulus pulse intensity, background concentration, and repetition rate of pulses. To determine the adaptation and dis-adaptation properties of chemoreceptor cells, we tested single chemoreceptors with a series of 10 Tau pulses in different concentrations and different background concentrations, and varied the interstimulus intervals.

Chemoreceptor cells were recorded extracellularly with suction electrodes. Single cells were identified with a standard Tau pulse (7×10^{-5} *M*). A train of 10 pulses in one of four concentrations (7×10^{-4} *M* to 7×10^{-7} *M*) was applied in a 10^{-7} *M* Tau background in one of three pulse intervals (2.5 s, 5 s, 10 s). Each of these 12 trains was separated by a 3-min recovery period. After 3 min of recovery in artificial seawater, the series of trains was repeated in 10^{-6} *M*, 10^{-5} *M*, 10^{-4} *M*, and 10^{-3} *M* Tau backgrounds.

Individual cells showed a wide range of cummulative adaptation. Stimulus-response functions revealed range fractionation. In general, shorter pulse intervals resulted in gradually stronger cumulative adaptation. Weaker pulse concentrations caused less cumulative adaptation. All but the highest background had negligible effects on response magnitude, showing the efficiency of background adaptation. Cumulative adaptation occurred mostly during the first three stimuli, and mostly with strong pulse concentrations in low background.

Thus, low-firing cells showed good response reproducibility (*i.e.,* no cumulative adaptation) even with the shortest pulse interval, whether low firing rates were caused by internal cell properties, low stimulus concentration, or high background concentration. This state of adaptation may be natural for cells operating in odor plume conditions.

Supported by a grant from NSF (BNS 88-12952) to J.A.

Spectral tuning to amino acids and mixture effects on antennular chemoreceptor cells in the lobster, Homarus americanus. ANNA WEINSTEIN, RAINER VOIGT, AND JELLE ATEMA (Boston University Marine Program, Marine Biological Laboratory, Woods Hole, MA 02543).

Lobster antennules are chemoreceptor organs that play a major role in orientation behavior. Hydroxyproline-best and taurine-best cell populations dominate their amino acid tuning spectrum. We tested the response of chemoreceptor cells on the lateral antennule to 15 amino acids and to 3 mixtures containing these amino acids to determine the effect of search mixture composition on spectral tuning.

The mixtures we used reflect the prominence of hydroxyproline (Hyp) and taurine (Tau) as best compounds for antennular chemoreceptors. All three mixtures had a total concentration of 1.5×10^{-3} *M*. "Equimolar mixture" contained all the compounds in equal concentration (10^{-4} *M*). The other two mixtures were based on the amino acid composition of a lobster prey, *Mytilus edulis,* modified by adjusting concentrations of Hyp and Tau. "Tau mixture" contained Tau at 3×10^{-4} *M* and Hyp at 10^{-4} *M*. "Tau-Hyp mixture" contained both Tau and Hyp at 10^{-4} *M*. Thus, all mixtures contained Hyp at 10^{-4} *M*. Tau mixture was used as the search mixture. The mixtures and compounds were injected at 1-min intervals into a carrier flow of artificial seawater which passed over the antennule. Action potentials were recorded with a suction electrode in excised antennules.

Twelve of the 21 cells were narrowly tuned to Hyp: three exclusively to Hyp, and nine with secondary responses mainly to glycine and arginine. Three cells were narrowly tuned to Tau, showing consistently strong responses. Four cells were tuned to glutamate, one to serine, and one to leucine.

For each Hyp-best cell, all three mixtures caused similar responses (Wilcoxon, $P > 0.05$) that were significantly less than responses to Hyp. Therefore, searching with any one of these mixtures would reveal a similar receptor population. However, cells that are completely suppressed by a search mixture only appear as "by-products" in recordings where more than one cell can be discriminated with extracellular techniques.

The results show that similar tuning spectra are revealed by searching with an equimolar "nonsense" mixture (Johnson and Atema 1983, *Neurosci. Lett.* **41:** 145–150) and natural mixtures of amino acids, all containing the same Hyp concentrations.

Supported by a grant from NSF (BNS 88-12952) to J.A.

CONTENTS

Volume 177 Number 3

THE BIOLOGICAL BULLETIN

DECEMBER, 1989

Published by the Marine Biological Laboratory

Reference: *Biol. Bull.* 177: 331–337. (December, 1989)

Female Sexual Receptivity Associated with Molting and Differences in Copulatory Behavior Among the Three Male Morphs in *Paracerceis sculpta* (Crustacea: Isopoda)

STEPHEN M. SHUSTER[1]

Department of Zoology, University of California, Berkeley, California 94720

Abstract. *Paracerceis sculpta*, a sphaeromatid isopod crustacean inhabiting the northern Gulf of California, forms harem polygynous breeding aggregations in spongocoels of intertidal sponges. Males in this species occur as three distinct morphs; α-males are large and possess modified uropods and telsons, β-males resemble females, and γ-males are small and inconspicuous. Females are semelparous, and sexual receptivity is associated with a terminal molt; the half-molted (sexually receptive) condition lasts 6–50 h. Field-collected premolt females do not contain sperm. Half-molted females possess sperm masses in both oviducts, and postmolt females contain sperm tails in their spent ovaries. The presence of an α-male does not affect the duration of female receptivity, but females can delay initiation of their reproductive molt if males are absent. Isolated premolt females are incapable of resorbing uninseminated ova. Such females molt, but do not transport ova into their marsupium and die without reproducing. All three male morphs complete similar behavioral sequences during intromission. However, β- and γ-males copulate quickly and abandon females immediately after copulation, while α-males copulate longer and retain females after mating. The duration of female receptivity may encourage multiple mating and thus influence relative fertilization success among the three male morphs.

Introduction

The details of copulatory behavior are poorly known for most sphaeromatid isopods (see Bowman and Kuhne, 1974; Buss and Iverson, 1981; Shuster, 1981). The dearth of such studies appears primarily due to the tendency for breeding pairs or harems of these animals to situate in cavities, burrows, or beneath benthic substrates (Menzies, 1954; Wieser, 1962; Glynn, 1968; Holdich, 1968; Jansen, 1971; Bowman and Kuhne, 1974; Eleftheriou *et al.*, 1981; Buss and Iverson, 1981; Shuster, 1981, 1987b; Upton, unpubl.). Direct observation of reproductive activities are, therefore, difficult or impossible for many species.

The timing of female sexual receptivity appears fundamental to the secretive nature of these isopopds. In all sphaeromatid species examined to date, female receptivity immediately follows a molt (review in Ridley, 1983; Shuster, 1981, 1986). Most Crustacea are vulnerable to predators or mechanical damage in newly molted condition. Thus, in ancestral populations, females that preferred protected habitats prior to their reproductive molt may have enjoyed greater fecundity than females preferring more exposed areas.

The association of breeding females with sheltered locations may have facilitated male attempts to monopolize access to sexually receptive females (Emlen and Oring, 1977). Most female sphaeromatids lack sperm storage organs (Menzies, 1954; Ridley, 1983; Shuster, 1986), permitting males that mate first to place their sperm closest to a female's ova (Parker, 1970). Although the effect of mating order on male fertilization success has rarely been examined in Crustacea (Diesel, 1988), males that mate first achieve the greatest fertilization success in species with reproductive tract morphology similar to that of female sphaeromatids (Parker, 1970; Ridley, 1983). By guarding females prior to their reproductive molt, an-

Received 29 May 1989; accepted 15 August 1989.

[1] Present address: Department of Ecology and Evolution, University of Chicago, 915 E. 57th Street, Chicago, IL 60637.

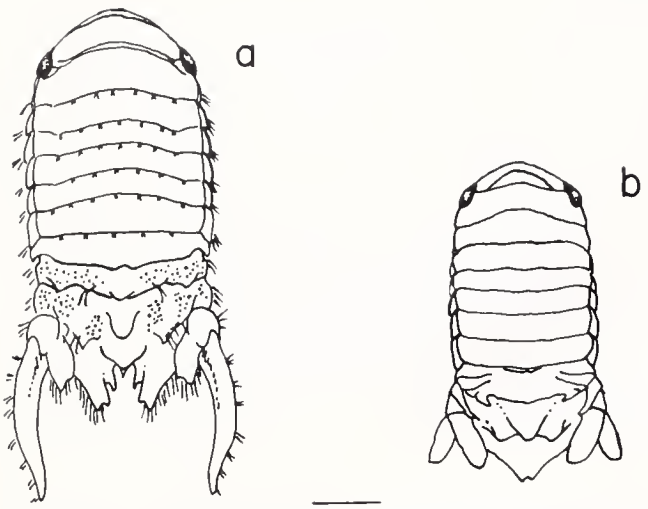

Figure 1. *Paracerceis sculpta* α-male (a) and premolt adult female (b). Horizontal line = 1 mm (redrawn from Brusca, 1980).

cestral male sphaeromatids may have enhanced their probability of mating first. Competition among males for mating priority is likely to have been intense in such species (Parker, 1970, 1978), and may have favored males capable of physically removing their mates from access by other males. An evolutionary history of male attempts to sequester their mates from reproductive competitors may have contributed to modern difficulties with observing breeding sphaeromatids (Shuster, 1981).

The timing as well as the duration of female receptivity can profoundly influence the intensity of sexual selection on males (Knowlton 1979; Shuster and Caldwell, 1989). Therefore, evolutionary analysis of male reproductive behavior must first consider how patterns of female sexual receptivity provide the context for male reproductive activities (Shuster, 1986). With respect to the characteristics of copulation itself, it is first necessary to determine when and how long females are sexually receptive, as well as how often, and with how many males, females are willing to mate.

In this paper, I report these details for *Paracerceis sculpta*, a sphaeromatid isopod crustacean inhabiting intertidal zones in the northern Gulf of California (Fig. 1). This species forms harem polygynous breeding aggregations in the spongocoels of *Leucetta losangelensis*, a common intertidal sponge (Shuster 1986, 1987a). *P. sculpta* males exhibit an unusual polymorphism involving three morphologically distinct types (Fig. 2, Shuster, 1986; 1987a, b; 1989). Alpha-males are larger than females, and possess robust telsons and elongated uropods. Alpha-males guard the entrance of spongocoels containing gravid females and defend their harems against other α-males. Beta-males are smaller than α-males, lack uropod and telsonic modifications, and resemble sexually mature females in external morphology. Beta-males mimic female courtship behavior and enter spongocoels containing reproductive females by deceiving resident α-males. Gamma-males are smaller still, also lack telsonic modification, and use their rapid movements and small size to slip around the bodies of resident α-males and into spongocoels. Gamma-males, like β-males, prefer spongocoels containing reproductive females (Shuster, 1986, 1987a; 1989). The copulatory behavior of the three male morphs is presently undescribed.

Materials and Methods

Collection of experimental animals

Leucetta losangelensis sponges grow abundantly year-round in tidepools on the coquina limestone reefs at Playa de Oro and at Station Beach, approximately 3 km southeast of Puerto Peñasco, Sonora, Mexico (Shuster, 1986). Isopods used in experiments were obtained in collections of 50–200 individuals, made every 4 to 10-days between February 1984 and November 1985. Breeding aggregations of isopods were removed from spongocoels, placed in separate vials, and examined in the laboratory within 6 h of collection. Females were identified by the possession of mature ovaries visible through the ventral cuticle or embryos in the brood pouch. Males were identified by the presence of external genitalia and were classified as α-, β-, or γ-males by their body size and external morphology. Further details of collection and animal maintenance procedures, as well as details of male and female life histories, are available in Shuster (1986). All animals were returned to the Gulf of California after experiments were completed.

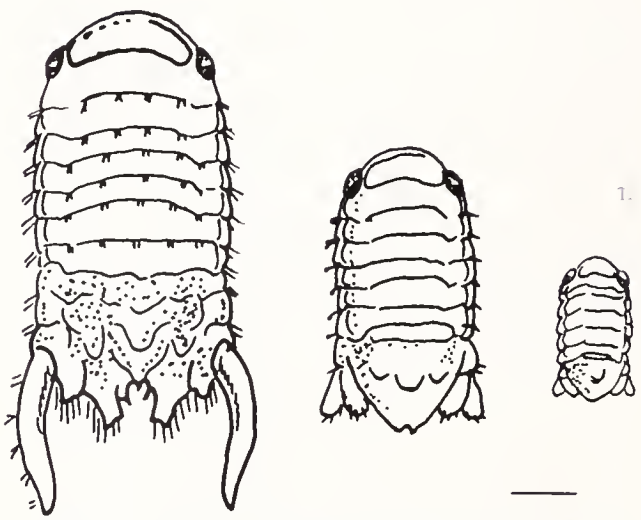

Figure 2. The relative body sizes of the three male morphs in *Paracerceis sculpta*. Left to right, α-male, β-male, γ-male. Horizontal line = 1 mm.

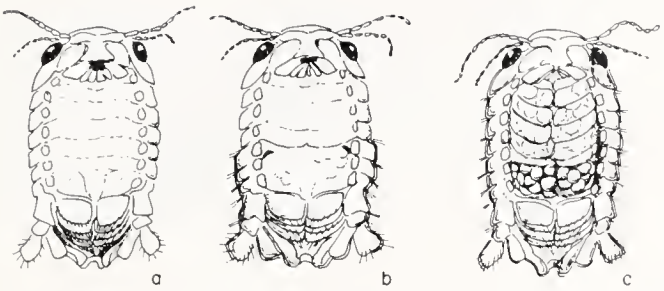

Figure 3. Diagram representing changes in female morphology associated with a sexual molt. Walking legs are not drawn. (a) Premolt female, (b) half-molted female (note genital pores in black at the base of the 5th leg), (c) postmolt female.

Sperm in the reproductive tracts of field-collected females

Females were removed from samples, measured to the nearest 0.15 mm using a stereomicroscope, and assigned to one of three categories describing their reproductive condition. Like many isopods, *P. sculpta* females undergo a biphasic molt that initiates their sexual receptivity (Ridley, 1983; Shuster, 1986). Females shed the posterior half of their cuticle below the fourth pereonal segment first, and several hours to several days later (see below) shed the anterior half of their cuticle. Unmolted females possessing mature ovaries were classified as "premolt" females (Fig. 3a). "Half-molted" females possessed mature ovaries and had shed their posterior cuticles (Fig. 3b). "Postmolt" females had completed their reproductive molts and transported their fertilized ova into their ventral marsupium (Fig. 3c). A more detailed description of female reproductive condition is provided in Shuster (1986).

Twenty females of each of the three reproductive conditions were chilled in a freezer for 10 min and then dissected in physiological saline under a stereomicroscope. The body cavities of half of the females were opened dorsally and the other half opened ventrally to permit examination of upper and lower aspects of the reproductive organs. Oviducts are transparent, and sperm, if present, are visible under low magnification (7×, Shuster, 1986). The presence or absence of sperm in the oviducts of dissected females was recorded.

Effect of α-males on the initiation and duration of female sexual receptivity

In nature, unmolted females are attracted to spongocoels containing α-males. Reproductive molting, mating, and brooding of young by females all occur within these spongocoels (Shuster, 1987b). To determine (a) the duration between female arrival in the spongocoel and the onset of sexual receptivity, (b) the duration of sexual receptivity itself (*i.e.*, the half-molted condition), and (c) the effect of the presence of an α-male on the length of these durations, 40 unmolted females were removed from samples within 2 h of collection and placed in separate 225-ml cups containing food (*Amphiroa* thalli, Shuster, 1986) and seawater. A single α-male was added to 20 of these cups and each female was examined every 4 h until she had completed her molt.

Isolation of uninseminated premolt females

To determine whether sexually mature, but uninseminated females, were capable of resorbing ova for future reproductions, 14 unmolted females were maintained in 225-ml cups with food and weekly water changes until they died. All females were examined while undergoing their molts, and postmolt females were examined every other day for evidence of feeding, changes in cuticle condition, visible changes in the character of internal organs, and activity level.

The copulatory behavior of males

Copulatory behavior was examined by placing individual half-molted females into a watch glass containing seawater and introducing a single α- (n = 8), β- (n = 3) or γ- (n = 5) male. Interactions were observed under a stereomicroscope and, after apparent copulation, the genital pores and ventral surfaces overlying the oviducts of females were inspected under a stereomicroscope at high power (70×) for evidence of sperm transfer. To determine if females mate more than once, a half-molted female was placed in a watch glass, and four males were individually introduced to the female for 10 min each in the following sequence: α-, β-, γ-, α-. All behavioral interactions were recorded on tape.

Results

Sperm in the reproductive tracts of field-collected females

Premolt females contained no sperm in their reproductive tracts (n = 21, Table I). This is not surprising

Table I

The location of spermatozoa within the reproductive tracts of premolt, half-molt, and postmolt females collected from Leucetta *spongocoels*

	Sperm present			
Female condition	In oviducts	In ovaries	No sperm	n
Premolt	0	0	21	21
Half-molt	19	0	0	19
Postmolt	19	19	0	19

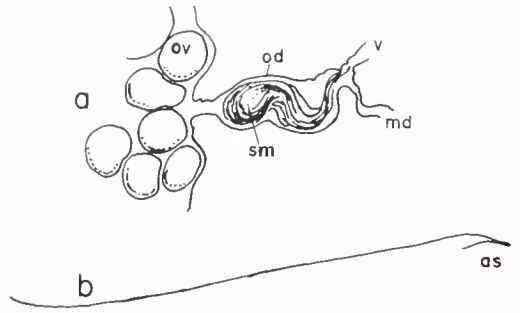

Figure 4. (a) Sperm in the oviduct of a half-molted female; (b) isolated spermatozoon; as = acrosome; md = portion of oviduct leading to marsupium; od = oviduct; ov = ovum; sm = sperm mass; v = vagina.

as the vaginae of premolt females are fused prior to the reproductive molt and are physically incapable of accomodating male genitalia (details of female reproductive morphology in Shuster, 1986).

All half-molted females collected in the field (n = 19) possessed a whitish sperm mass in each oviduct. As mentioned above, females possess simple oviducts, with no sperm storage organs (Shuster, 1986). The sperm masses of inseminated females were visible through the ventral cuticle and were located approximately 0.25 mm inside of this opening, directly within the lumen of the oviduct. Sperm in the oviduct formed a loosely organized bundle (Fig. 4a). Intact sperm are approximately 1–1.5 mm in length, consisting of a long tail and a flange-like acrosome that is clearly visible at 70× (Fig. 4b). Within the reproductive tracts of half-molt females, sperm are nonmotile.

Postmolt females transport ova through their oviducts and into ventral pouches that form the marsupium (Shuster, 1986). Spent ovaries form an H-shaped bag that lies over the brood pouches when viewed dorsally (details in Shuster, 1986). While no intact sperm were found in the reproductive tracts of postmolt females (n = 19), sperm tails, minus their acrosomes, were distributed throughout the spent ovaries and occasionally found within the oviducts.

The effect of α-males on the initiation and duration of female sexual receptivity

Premolt females retained with α-males molt significantly sooner than premolt females retained in cups alone (one-tailed U-test, $P = 0.008$). Premolt females isolated in cups molted about five days after capture (median = 126.3 h, range = 6.0–208.0 h, $\bar{x} \pm SD = 120.78 \pm 70.17$, n = 20), whereas premolt females retained in cups with an α-male molted about three days after capture (median = 87.0 h, range = 4.50–138.0 h, $\bar{x} \pm SD = 70.35 \pm 47.24$ h, n = 20). However, the duration of sexual receptivity, *i.e.*, the duration a female remains in a half-molted condition, was unaffected by the presence of an α-male. Sexual receptivity lasted about 24 h for isolated females (median h as half-molt = 24.0, range = 6.0–50.0, $\bar{x} \pm SD = 26.34 \pm 10.17$, n = 20), as well as for females retained with an α-male (median = 25.0 h, range = 7.5–41.0 h, $\bar{x} \pm SD = 25.09 \pm 8.80$ h, n = 20; U-test, $P > 0.42$).

Isolation of uninseminated premolt females

Uninseminated females do not resorb their ova. Isolated premolt females undergo sexual molts normally, and cease to feed like gravid females (Shuster, 1986). However, uninseminated females do not transport ova into their brood pouches. Within a few days after molting, the unfilled brood pouches of isolated females become opaque and slightly distended. The oostegites become progressively shriveled in appearance and begin to project outward from the body, while the ventral pereon grows large and appears to fill with fluid. Ovaries become progressively more pale, and the ova within begin to appear fuzzy and indistinct. Over several weeks, the ova diminish in size, but with no corresponding improvement in the physical condition of females. In several cases, the empty brood pouches of females became infested with fungi and protozoa while the females were still alive, and in all cases, isolated females became sluggish, deteriorated in physical condition, and died within 81 days ($\bar{x} \pm SD = 49.36 \pm 19.90$, n = 14). This period is comparable to the adult longevity of females that become gravid and release normal broods (Shuster, 1986).

The copulatory behavior of males

In watchglasses, α-males did not seem capable of detecting half-molted females from a distance of more than a centimeter. However, when females swam within this distance, α-males became active and lashed their antennae vigorously. When α-males contacted half-molted females with one of their antennae or with one of their walking legs, they immediately grasped females, adjusted them into a ventral-to-ventral position with respect to their own body, and pressed first one and then the other of the females' genital pores to their own genitalia (Fig. 5). Before being grasped, and while males adjusted their positions, females moved actively and occasionally escaped from males. However, once face-to-face with α-males, females became quiescent and permitted males to mate.

Each intromission (two per female) involved insertion of both of the male's penes into each of the female's genital pores, followed by rapid pumping of the male's first two sets of pleopods. Median intromission duration for α-males was 30 s (range = 15–120 s, $\bar{x} \pm SD = 39.08$

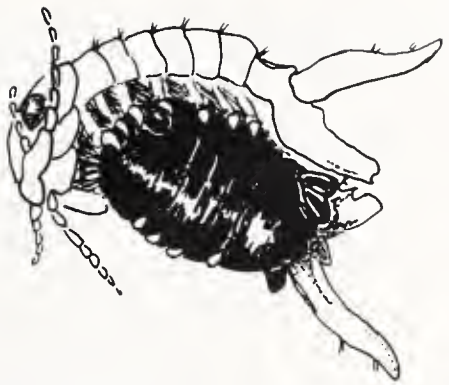

Figure 5. Alpha-male (white) in copula with half-molted female (black). Drawn from photograph.

± 28.43 s, n = 13) and the median duration of the entire copulatory sequence for α-males was 12.07 min (range = 4.40–19.92 min, $\bar{x}$ ± SD = 11.59 ± 4.60 min, n = 8). In one case, an α-male completed the above sequence, retained the female, and copulated again, intromitting both of the female's genital pores. However, most α-males copulated as described above, and relaxed their grip on the female within 10 min after mating. Females became increasingly active following copulation, and shortly after α-males appeared to relax, females freed themselves and swam off. Females examined after single copulatory bouts contained sperm masses in both oviducts. These sperm masses appeared smaller than those routinely found in half-molted females collected in the field. On two occasions, females were left in the watchglass with their α-male for an additional 4 h. Upon reexamination, both females found were embraced by their α-males, and both females contained sperm masses that appeared substantially larger than observed after their initial mating. Thus, females evidently mate more than once with an individual male.

Copulatory behavior involving females and β-males was similar in character to that observed between females and α-males. Beta-males grasped females and assumed a ventral-to-ventral position. Females became quiescent, permitted intromission, and were released by β-males almost immediately after mating. Median intromission duration for β-males was 62 (range = 30–79 s, $\bar{x}$ ± SD = 54.83 ± 20.26 s, n = 3) and the median copulatory sequence duration was 2.97 min (range = 2.00–3.36 min, $\bar{x}$ ± SD = 2.78 ± 0.70 min, n = 3). All females copulating with β-males contained sperm in both oviducts after a single copulatory sequence.

Gamma-males copulated, not by positioning females, but instead by climbing beneath them and positioning their own genitalia toward the females' genital pores. The mere contact of a male, not the act of being grasped and positioned, seems to stimulate quiescence, as females paired with γ-males ceased moving soon after γ-males assumed positions beneath them. While α- and β-males rapidly moved their anterior pleopods during copulation and engage in few or no thrusting movements, γ-males thrusted actively during copulation. Like β-males, γ-males abandoned females soon after mating. Median intromission time for γ-males was 42 s (range = 25–571 s, $\bar{x}$ ± SD = 122.86 ± 198.85 s, n = 4) and median copulatory sequence duration was 5.75 min (range = 3.00–12.60 min, $\bar{x}$ ± SD = 6.78 ± 4.10 min, n = 4), intermediate in duration between that of α- and β-males. All females mating with γ-males contained sperm masses in both oviducts. While intromission times for α-, β-, and γ-males were not significantly different (two-tailed Kruskal-Wallis test, $P > 0.05$), copulatory sequence times differed significantly among males (two-tailed Kruskal-Wallis H = 7.96, $P < 0.01$). Thus α-males evidently copulate longer than β- and γ-males.

The half-molted female introduced to an α-male, a β-male, a γ-male, and another α-male, mated with all four males in rapid succession. Copulation in the first three cases proceeded normally. In the last case, the α-male ejaculated, but was apparently unable to place all of his ejaculate into the female's genital pores. Several sperm bundles were observed trailing out of the female across her ventral pereon after the last male released her. Copulations with all four males occurred within 30 min, and, within 5 min of the final mating, the female shed her anterior cuticle and began transporting ova into her brood pouch. Thus female receptivity lasts from moments after females shed their posterior cuticle until moments before the anterior cuticle is shed. During this time, females evidently will mate with any nearby male.

Discussion

Although premolt females are attracted to spongocoels containing α-males and engage in courtship behavior (*i.e.*, premolt females are behaviorally receptive, Shuster, 1986), the genital pores of premolt females are indistinct, and the oviducts of these females do not contain sperm. Actual sexual receptivity and copulation occur only in half-molted females, substantiating observations by Menzies (1954) and Ridley (1983). Females seem capable of postponing receptivity if males are not available. This is reasonable for a species in which females must leave the habitat in which they mature to locate suitable reproductive habitat (Shuster, 1986). However, females cannot postpone their reproductive molt indefinitely even when isolated from males, and once females molt, the presence of α-males does not affect the duration of receptivity. While receptive, however, females will mate more than once and with more than one male.

Females transport ova to their brood pouches almost

immediately after shedding the anterior portion of their cuticles, and females are sexually receptive until moments before this molt. Fertilization may occur in the ovary, as sperm tails, minus their acrosomes, were abundant in spent ovaries. Within the oviduct, sperm are nonmotile, and while females may induce an acrosome reaction that initiates syngamy (P. Talbot, pers. comm.), this reaction is unlikely to propel sperm the length of the female reproductive tract. Females appear to possess contractile tissues in their oviducts that may facilitate sperm transport. Fertilization evidently does not occur in either the marsupium or in the oviduct itself, as has been suggested for some isopods (Ridley, 1983).

Females exhibit a single 24-h period of sexual receptivity. This interval seems somewhat brief until the potential density of competing males in a spongocoel is considered. Although most occupied spongocoels contain a single α-male, up to eight α-, β-, and γ-males in various combinations may simultaneously occupy the same spongocoel (Shuster, 1987a; 1989). At such male densities, 24 h of sexual receptivity introduces a high probability of multiple insemination for females, and thus presents considerable opportunities for sperm competition among males. Although it may be physically impossible for *P. sculpta* females to complete the two phases of their reproductive molt in less than 24 h, other isopod females complete their reproductive molts in a few hours or less (Ellis, 1971; review in Ridley, 1983). Furthermore, uniphasic molting (*i.e.*, shedding of the entire cuticle at once) occurs in some marine isopoda (George, 1972). The possibility must therefore be considered that *P. sculpta* females somehow benefit from a period of sexual receptivity that is sufficient in duration to permit multiple mating.

All three male types performed similar activities associated with the act of copulation and the transfer of sperm. Intromission durations among the three male morphs were also similar and were consistently rapid (the transfer, within 30 s, of several hundred 1-mm-long sperm by males no larger than 7 mm in length is an amazing feat by any standard). Furthermore, the fecundities of females mated to α-, β-, and γ-males are not significantly different (Shuster, 1986; 1989).

Despite these similarities, the amount of time males spent with individual females differed significantly among males. Alpha-males retained females for some time after mating, while β- and γ-males released females immediately. This result makes sense given descriptions of the behavior and distribution of β- and γ-males in spongocoels (Shuster, 1986, 1987b, 1989). Beta- and γ-males seem well-adapted as sperm competitors (Shuster, 1987b, 1989) and could maximize their contacts with females by avoiding post-copulatory guarding (Parker, 1974). However, the fact that α-males release females at all before females complete their reproductive molt is surprising. If females may be inseminated by other males, α-males have little to gain by releasing their half-molted mates unless other females are present.

In the field, α-males are often found gripping premolt or half-molt females with their walking legs (Shuster, 1986, 1987a). Furthermore, when single, receptive females are present in spongocoels with both an α-male and a γ-male, γ-males rarely mate successfully, suggesting successful post-copulatory guarding by α-males (Shuster, 1989). Perhaps in a watchglass and in the absence of other males, α-males are not stimulated to retain their mates. Observations of the copulatory behavior of these isopods within the confines of their natural reproductive habitat, as well as further analysis of patterns of female sexual receptivity in this species, may explain these apparently conflicting patterns of male guarding behavior and fertilization success.

Acknowledgments

I am grateful to Drs. Roy L. Caldwell, Frank A. Pitelka, Vincent H. Resh, George K. Roderick, and Eldridge S. Adams III for their comments on earlier drafts of the manuscript. Logistical support for this research was provided by Mona Radice and Mable Lee of the Department of Zoology, University of California, Berkeley, the Center for the Study of Deserts and Oceans in Puerto Peñasco, Sonora, Mexico, and the Environmental Research Laboratory in Tucson, Arizona. Financial assistance was provided by the Theodore Roosevelt Memorial Fund, and NSF dissertation improvement grant OCE-8401067, as well as by the University Regents' Fellowship, the Alice Galloway Memorial Fund, the Graduate Student Research Allocations Fund and the Departments of Zoology and Genetics of the University of California, Berkeley.

Literature Cited

Bowman, T. E., and H. Kuhne. 1974. *Cymodetta gambosa*, a new sphaeromatid isopod (Crustacea) from Australia, with notes on its mating behavior. *Rec. Aust. Mus.* **29:** 235–243.

Brusca, R. C. 1980. *Common Intertidal Invertebrates of the Gulf of California.* University of Arizona Press, Tucson, AZ. 513 pp.

Buss, L. W., and E. W. Iverson. 1981. A new genus and species of Sphaeromatidae (Crustacea: Isopoda) with experiments and observations on its reproductive biology, interspecific interactions and color polymorphisms. *Postilla* **184:** 1–23.

Diesel, R. 1988. Discrete storage of multiple mating sperm in the spider crab, *Inachus phalangium*. *Naturwissenschaften* **75:** 148–149.

Eleftheriou, A., D. M. Holdich, and K. Harrison. 1980. The systematics and ecology of a new genus of isopod (Sphaeromatidae) from the West Coast sandy beaches of India. *Estuar. Coast. Mar. Sci.* **11:** 251–262.

Ellis, R. J. 1971. Notes on the biology of the isopod *Asellus tomalensis* Hartford in an intermittent pond. *Trans. Am. Microsc. Soc.* **90:** 51–61.

Emlen, S. T., and L. W. Oring. 1977. Ecology, sexual selection and the evolution of mating systems. *Science* **197**: 215–223.

Glynn, P. W. 1968. Ecological studies on the associations of chitons in Puerto Rico, with special reference to sphaeromid isopods. *Bull. Mar. Sci.* **18**: 572–626.

George, R. Y. 1972. Biphasic moulting in isopod crustacea and the finding of an unusual mode of moulting in the antarctic genus, *Glyptonotus*. *J. Nat. Hist.* **6**: 651–656.

Holdich, D. M. 1968. Reproduction, growth and bionomics of *Dynamene bidentata* (Crustacea: Isopoda). *J. Zool. Lond* **156**: 136–153.

Jansen, K. P. 1971. Ecological studies on intertidal New Zealand Sphaeromatidae (Isopoda: Flabellifera). *Mar. Biol.* **11**: 262–285.

Knowlton, N. 1979. Reproductive synchrony, parental investment and the evollutionary dynamics of sexual selection. *Anim. Behav.* **27**: 1022–1033.

Menzies, R. J. 1954. The comparative biology of reproduction in the woodboring isopod crustacean *Limnoria*. *Bull. Mus. Comp. Zool.* **112**: 361–388.

Parker, G. A. 1970. Sperm competition and its evolutionary consequences in insects. *Biol. Rev.* **45**: 525–567.

Parker, G. A. 1974. Courtship persistence and female guarding as male time investment strategies. *Behaviour* **48**: 157–184.

Parker, G. A. 1978. Evolution of competitive mate searching. *Ann. Rev. Entomol.* **23**: 173–196.

Ridley, M. 1983. *The Explanation of Organic Diversity: The Comparative Method and Adaptations for Mating*. Oxford Science Publications, Oxford, UK. 272 pp.

Shuster, S. M. 1981. Sexual selection in the Socorro Isopod, *Thermosphaeroma thermophilum* (Cole and Bane) (Crustacea: Peracarida). *Anim. Behav.* **28**: 698–707.

Shuster, S. M. 1986. The reproductive biology of *Paracerceis sculpta* (Crustacea: Isopoda). Ph.D. Thesis, University of California, Berkeley. 279 pp.

Shuster, S. M. 1987a. Alternative reproductive behaviors: three discrete male morphs in *Paracerceis sculpta*, an intertidal isopod from the northern Gulf of California. *J. Crust. Biol.* **7**: 318–327.

Shuster, S. M. 1987b. Male body size, not reproductive habitat characteristics predicts polygyny in a sexually dimorphic intertidal isopod crustacean, *Paracerceis sculpta* (Crustacea: Isopoda). *Mem. Simp. Biol. Mar. Univ. Auton. Baja Calif.* **5**: 71–80.

Shuster, S. M. 1989. Male alternative reproductive strategies in a marine isopod crustacean (*Paracerceis sculpta*): use of genetic markers to measure differences in fertilization success among α-, β-, and γ-males. *Evolution*. **43.**

Shuster, S. M., and R. L. Caldwell. 1989. Male defense of the breeding cavity and factors affecting the persistence of breeding pairs in the stomatopod, *Gonodactylus bredini* (Crustacea: Hoplocarida). *Ethology*. **82**: 192–207.

Wieser, W. 1962. Adaptations of two intertidal isopods. I. Respiration and feeding in *Naesa bidentata* (Adams) (Sphaeromatidae). *J. Mar. Biol. Assoc. U. K.* **42**: 665–682.

Reference: *Biol. Bull.* 177: 338–343. (December, 1989)

The Role of the First Quartet Micromeres in the Development of the Polyclad *Hoploplana inquilina*

BARBARA CONTA BOYER

Department of Biological Sciences, Union College, Schenectady, New York 12308 and The Marine Biological Laboratory, Woods Hole, Massachusetts 02543

Abstract. The role of the first quartet micromeres at the eight-cell stage in the development of the polyclad flatworm *Hoploplana inquilina* was analyzed with regard to specific contributions made by these cells and their function in the determination of embryonic symmetry. The experimental series involved: (1) deletion of one micromere (1a or 1c *versus* 1b or 1d); (2) deletion of two adjacent micromeres; (3) deletion of three micromeres; (4) isolation of intact first quartets; and (5) isolation of macromere sets 1A–1D. As the number of micromeres removed was increased, the larvae became progressively more abnormal, involving reduction in number of eyes, deficiencies in lobe development, and disturbance of embryonic symmetry. After deletion of three micromeres, none of the larvae exhibited normal morphology. These experiments indicate that the determination of embryonic axes leading to a larva with bilateral symmetry may involve micromere-macromere interactions, as has been shown in mollusean embryos with equal cleavage. Isolated first quartets consistently formed spherical, bloated, transparent larvae with multiple eyes, suggesting that the macromeres play an inhibitory role in eye development. Isolated macromeres 1A–1D often failed to develop, and larval structures never differentiated. Thus, the relatively loose determination of the polyclad embryo involves both cytoplasmic localization and cell interactions.

Introduction

The establishment of cell fate has been investigated in a number of animal species having embryos that exhibit spiral cleavage. Much of our current understanding of the role that cytoplasmic determinants play in embryonic development derives from studies of higher Spiralia, which typically express early embryonic determination or mosaicism. Such investigations have revealed complexity and variety within these fundamentally mosaic systems. For example, cell interactions have been demonstrated in many spiralian embryos, and within the molluscs, two different mechanisms of achieving the embryonic axes of symmetry have evolved.

Some turbellarian platyhelminthes have spiral cleavage, and they are more primitive than the annelids and molluscs on which these investigations have been carried out. Therefore, studies of turbellarian development should provide insights, not only into the nature of cytoplasmic localization, but also into the origin and evolution of spiral cleavage and embryonic determination. The polyclads, in particular, have a typical quartet spiral cleavage that is strikingly similar to the pattern in annelids and molluscs, but there has been little experimental work done on the development of this group.

The normal development of a polyclad flatworm has been most thoroughly examined in *Hoploplana inquilina* (formerly *Planocera inquilina*) by Surface (1907). Cleavage follows the typical quartet spiral pattern in which the macomeres (A–D) divide to produce four quartets of micromeres. At the four-cell stage, the embryo consists of two equal-sized A and C blastomeres that are displaced toward the animal pole, and two equal-sized but larger B and D blastomeres that are in contact at the vegetal cross-furrow. [Surface (1907) reports that the D cell is larger than B, but I have not observed this to be the case.] The eight-cell stage (Fig. 1A) consists of the animal first quartet (1a–1d) and the vegetal macromeres (1A–1D). Later, when the cells of the fourth quartet (4a–4d) are produced, they are significantly larger than the macromeres (4A–4D) and contain most of the

Received 5 April 1989; accepted 21 September 1989.

yolk. This is characteristic of the polyclads, distinguishing them from other spiralians. Gastrulation proceeds primarily by epiboly of the micromeres over the macromeres. By the fourth day, the embryo begins to rotate, the lobes have started to form, and differentiated tissues are discernable. A fully developed Muller's larva (Fig. 1B) is produced by the fifth day.

The embryos of *Hoploplana* have the characteristic mosaic development of the Spiralia (Boyer, 1986, 1987). Blastomere deletion and isolation experiments on two- and four-cell embryos produced partial larvae with characteristic deficiencies associated with each type of experiment. "Half larvae," resulting from the separation or deletion of two-cell embryos, were abnormal in body shape, and in the development of lobes and eyes. Deletion of one cell at the four-cell stage produced less anomalous "three-quarter larvae" that were underdeveloped in one quadrant and often exhibited eye abnormalities. These results resemble those obtained from such experiments on higher spiralians—that is, development is fundamentally mosaic—but the studies did not include analysis of embryos beyond the four-cell stage, and the mechanism of determination of the embryonic axes of symmetry was not examined.

Experimental analysis of eight-cell stage (first quartet) embryos of some of the higher spiralians have focused on two different problems, the cytoplasmic contributions of the first quartet cells, and the role that these cells play in the determination of embryonic symmetry. Among the former studies are those of Wilson (1904) on *Patella*, Horstadius (1937) on *Cerebratulus*, Costello (1945) on *Nereis*, Clement (1967) on *Ilyanassa*, Morrill *et al.* (1973) on *Lymnaea*, and van Dam and Verdonk (1982) on *Bithynia*. In general, the results supported the concept of mosaic development, though there was evidence of some regulative capacity in *Bithynia* and *Lymnaea*.

Determination of the embryonic axes of symmetry has been extensively studied in gastropod molluscs, a group in which two different mechanisms are involved. In gastropods with unequal cleavage, axis determination has occurred by the four-cell stage. At this time the D blastomere, which is larger than the others, inherits cytoplasmic determinants specifying mesoderm and the dorsal quadrant. Thus, by the four-cell stage, the axes of bilateral symmetry have been established through an intracellular mechanism involving cytoplasmic localization (see Davidson, 1986, for review), and deletion of the first quartet at the eight-cell stage does not affect determination of the dorso-ventral axis (van Dam and Verdonk, 1982).

In gastropods with equal-sized blastomeres at the four-cell stage, the first quartet cells play a crucial role in establishing the embryonic axes of symmetry (van den Biggelaar, 1976, 1977; van den Biggelaar and Guerrier, 1979; Arnolds *et al.*, 1983; Martindale *et al.*, 1985). These embryos remain radially symmetrical with equipotent quadrants until after formation of the third quartet. At this time, the first quartet micromeres contact the central macromere and induce it to become dorsal (van den Biggelaar, 1976, 1977). If these interactions are delayed (Martindale *et al.*, 1985) or inhibited (van den Biggelaar and Guerrier, 1979), no D quadrant forms, and the embryo remains radially symmetrical. Thus, in these molluscs, intercellular interactions determine the embryonic axes of symmetry.

That such closely related groups should have such different mechanisms for establishing the D quadrant is surprising, because the cleavage patterns and cell lineages of these animals are very similar, and both equal and unequal cleavage occur widely in the molluscs. As Martindale *et al.* (1985) state, "We need to know more about the experimental embryology of other spiralians before the significance of the differences in the mechanisms which have been uncovered so far can be put into perspective." Because the ancestral flatworms may have been the first animals to evolve bilateral symmetry, the mechanism of symmetry determination in this group is particularly significant.

The *Hoploplana* embryo, with two equal sized A and C blastomeres and two larger but also equal sized B and D cells at the four-cell stage, does not appear to fit either model. The consistent pattern of defects occurring with deletion experiments on two- and four-cell embryos indicates that morphogenetic determinants specifying particular larval structures are organized in the zygote, but *Hoploplana* does not appear to have a designated cell corresponding to the D blastomere of higher spiralians. Therefore, I have examined the eight-cell (first quartet) stage to determine not only the specific cytoplasmic contributions of the micromeres, but also whether their interactions with the macromeres are involved in establishing the axes of symmetry.

Materials and Methods

Specimens of *Hoploplana inquilina* were collected from the mantle cavity of *Busycon* and maintained in seawater in finger bowls. Gametes were removed from the spermaducal vesicles and uterus by piercing the organs with sharp needles. Fertilization, which produced naked zygotes that lack the egg-shell membrane, occurred when eggs and sperm were mixed in plastic petri dishes containing Millipore-filtered seawater.

The blastomere deletion experiments were done by puncturing the selected cell with hand-pulled glass needles, typically about one half hour after cleavage to the eight-cell stage. The experimental embryos were examined carefully to be certain that each punctured cell had

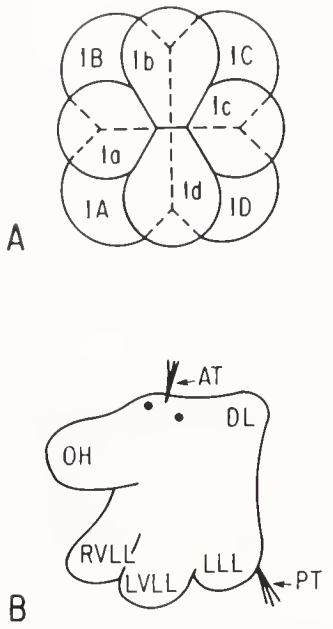

Figure 1. Normal developmental stages of *Hoploplana* (A) Eight-cell stage viewed from animal pole. (B) Muller's larva. AT: apical tuft; DL: dorsal lobe; LLL: left lateral lobe; LVLL: left ventrolateral lobe; OH: oral hood; RVLL: right ventrolateral lobe; PT: posterior tuft.

cytolyzed completely. If deletion was incomplete, the embryo was discarded. The experimental series involved: (1) deletion of first quartet micromeres 1a or 1c *versus* 1b or 1d (it is not possible to differentiate between the A and C or the B and D quadrants); (2) deletion of two adjacent micromeres; (3) deletion of three micromeres; (4) isolation of the first quartet intact by killing the macromeres; and (5) isolation of the 1A–1D macromeres intact by deleting the first quartet.

Experimental embryos were raised in Millipore-filtered seawater to which 100 units/ml penicillin and 200 μg/ml streptomycin were added. They were examined daily and analyzed on day six or seven for abnormalities in eye numbers, tufts, and morphology.

Results

The larvae became progressively more abnormal as the number of deleted micromeres increased. If larval morphology appeared normal, the larvae were categorized as Muller's larvae (Fig. 1B). If they exhibited any abnormalities similar to those resulting from deletion of one cell at the four-cell stage, such as absence or truncation of one or more lobes, they were termed "three-quarter larvae" (Fig. 2A). Larvae that were underdeveloped, asymmetric (lacking the normal axes of bilateral symmetry), and unrecognizable as Muller's larvae, were similar to those produced by deletion of one cell at the two-cell stage, and were called "half larvae" (Fig. 2B). A fourth category, not normally a product of deletion experiments on two- and four-cell embryos, appeared with deletion of three and four micromeres or isolation of the intact first quartet. These were classified as "spherical" or "swollen" embryos. The former were less well developed than half larvae, with solid but poorly differentiated tissues, and were either one-eyed or eyeless. Larvae with the "swollen syndrome" had almost perfectly spherical morphology, were greater than 100 μm, and showed very abnormal tissue development. The inner tissues typically were undifferentiated and a transparent space existed between the outer ectoderm and inner undifferentiated mass. These forms often had multiple eyes (Fig. 2C). The data for all experimental categories are summarized in Table I.

Deletion of one micromere (1a or 1c vs *1b or 1d)*

The first two columns in Table I show the results of deletion of single first quartet micromeres at the eight-cell stage. Regardless of which micromere was deleted, 16–18% of the larvae were completely normal. Most larvae (85%) exhibited normal Muller's morphology with bilateral symmetry, so that observed abnormalities were

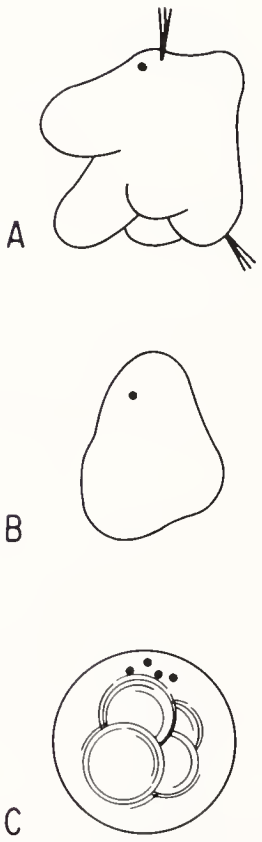

Figure 2. (A) "Three-quarter" larva. (B) "Half" larva. (C) "Swollen syndrome" larva.

Table I

Effect of deleting micromeres and macromeres on eight-cell embryos of Hoploplana inquilina

	−(1a or 1c) n = 61	−(1b or 1d) n = 50	−2 mics. n = 27	−3 mics. n = 29	−4 macs. n = 22	−4 mics. n = 20
Normal	10 (16%)	9 (18%)	0	0	0	0
Morphology						
Muller's	52 (85%)	37 (74%)	15 (56%)	0	0	0
¾ Larvae	9 (15%)	11 (22%)	10 (37%)	6 (21%)	0	0
½ Larvae	0	2 (4%)	2 (7%)	9 (31%)	0	4 (20%)
Sphere/swollen	0	0	0	14 (48%)	22 (100%)	16 (80%)
Tufts						
Normal	38 (62%)	24 (48%)	4 (15%)	0	0	0
−Apical	15 (25%)	13 (26%)	18 (67%)	8 (28%)	1 tuft: 5 (23%)	1 tuft: 2 (10%)
−Posterior	5 (8%)	5 (10%)	0	0		
−Both	3 (5%)	8 (16%)	5 (18%)	21 (72%)	17 (77%)	18 (90%)
# Eyes						
0	1 (2%)	0	2 (7%)	8 (28%)	1 (5%)	20 (100%)
1	22 (36%)	9 (18%)	19 (70%)	19 (66%)	0	0
2	35 (57%)	37 (74%)	4 (15%)	1 (3%)	4 (18%)	0
3	3 (5%)	4 (8%)	2 (7%)	1 (3%)	8 (35%)	0
4	0	0	0	0	7 (32%)	0
5	0	0	0	0	2 (9%)	0

Minus sign indicates deletion.

in the number of eyes or tufts. Three-quarter larvae, which also exhibited fundamental bilateral symmetry, constituted 15% of embryos with 1a or 1c deleted and 22% with absence of 1b or 1d. In this category the right ventrolateral lobe was truncated or missing in two larvae, the left ventrolateral lobe in four, the dorsal lobe was deficient in one, and all lobes were abnormal in two. Only a very small number were categorized as half larvae. There was no significant difference in larval morphology related to deletion of 1a or 1c *vs* 1b or 1d ($\chi^2 = 1.8$, $P > 0.05$).

Deletion of one first quartet micromere resulted in loss of a tuft in approximately half of the embryos, with the apical tuft more commonly missing than the posterior tuft. A small number were missing both tufts. There was no significant difference in tuft abnormalities with respect to the particular cell deleted ($\chi^2 = 1.88$, $P > 0.05$).

Although most larvae had two eyes, there was a significantly greater proportion of one-eyed larvae when 1a or 1c was deleted (36%) *versus* 1b or 1d (18%) ($\chi^2 = 5.2$, $P < 0.05$). Of the single-eyed larvae, when 1a or 1c was deleted, 22 (50%) had an eye on the right, 5 (23%) were left-eyed, and 6 (27%) had a centrally located eye. Deletion of 1b or 1d resulted in 5 (56%) right-eyed and 2 (22%) left-eyed larvae. One had a central eye and in one the position of the single eye could not be determined.

Deletion of two adjacent micromeres

When two micromeres rather than one were deleted (Table I, column 3), the number of larvae with normal (Muller's) morphology decreased significantly, while concomitantly the number of three-quarter larvae increased ($\chi^2 = 7.09$, $P < 0.01$). Of the latter, three had truncated or missing right ventrolateral lobes, five had comparable abnormalities of the left ventrolateral lobe, one had a deficient oral hood, one had an abnormal dorsal lobe, one had all abnormal lobes, and one was missing both ventrolateral lobes. Similarly, the number of larvae with normal tufts decreased significantly ($\chi^2 = 22$, $P < 0.01$). (For the chi square analysis, the data from both kinds of single micromere deletions were pooled because the larvae from the two groups were not significantly different in morphology or tufts.)

There was a significantly greater number of one-eyed larvae with deletion of two adjacent micromeres compared with deletion of 1a or 1c ($\chi^2 = 12.02$, $P < 0.01$) and deletion of 1b or 1d ($\chi^2 = 26.3$, $P < 0.01$). The majority of these (12 or 63%) had a central eye, 3 (16%) were right-eyed, and 4 (21%) were left-eyed.

Deletion of three micromeres

A drastic effect on development was seen when three micromeres were deleted (Table I, column 4). There were no morphologically normal larvae, and almost half fell in the highly abnormal category of spherical, swollen forms. Of the "three-quarter" larvae, one was missing the left ventrolateral lobe, two lacked both ventrolateral lobes, and in one all lobes were abnormal. Only one larva had two eyes; the remainder were almost all one-eyed or

eyeless, and 77% were missing both tufts. The number of one-eyed larvae was not significantly different between the two and three micromere experiments, but there was a significantly greater number of eyeless larvae in the latter experiments.

Isolation of the intact first quartet

Thirty-eight experiments were done in which all four macromeres were deleted leaving the four first quartet cells. Only 22 (58%) survived (Table I, column 5), and all were spherical with 95% exhibiting the "swollen syndrome." Seventy-six percent of the larvae had more than two eyes, and 77% had no tufts.

Isolation of the first quartet macromeres

The results of deleting the entire first quartet so that only the macromeres 1A–1D remain are presented in Table I, column 6. Of 105 embryos in which the 1a–1d cells were deleted, only 20 survived. These were highly aberrant; 70% were categorized as "spheres," undergoing little development beyond cleavage and no tissue differentiation. Ten percent (2) became swollen, and a small number (4) could be characterized as half larvae. None had any eyes, and 90% were tuftless.

Discussion

The results of micromere deletion experiments on *Hoploplana* corroborate the earlier four-cell deletion experiments suggesting that morphogenetic determinants are sequestered early in development, but that specific blastomeres do not receive consistently specific determinants.

Eyes and tufts

If the *Hoploplana* cell lineage conformed to the molluscan plan, only 1a and 1c should form eyes. Although deletion of one of these blastomeres results in one-eyed larvae in a statistically significant number of cases, deletion of the ventral and dorsal 1b and 1d cells also produces one-eyed larvae. Moreover, the majority have the normal two eyes. Thus, *Hoploplana* is more similar to *Bithynia* (van Dam and Verdonk, 1982) and *Lymnaea* (Morrill *et al.*, 1973), which may develop normally after deletion of first quartet micromeres, than to *Ilyanassa* (Clement, 1967), which appears to be more rigidly mosaic. The 1a and 1c blastomeres cannot be distinguished from cells 1b and 1d in the *Hoploplana* embryo; therefore the basis for the preponderance of right-eyed larvae—whether simple non-random deletion, or more complex developmental processes—cannot be determined. The occurrence of a single, centrally located eye is probably due to the disturbed cellular topography resulting from blastomere deletion.

When two adjacent micromeres are deleted, the number of one-eyed larvae is significantly larger than when one micromere is deleted; but the proportion does not reach 100% (15% still have the normal two eyes) as would be expected if eye development involved simply the localization of eye determinants in opposite micromeres. The two eyeless larvae also suggest a more complex system than can be explained by strict cytoplasmic localization. Similarly, Morrill *et al.* (1973) found that paired eyes develop in *Lymnaea* when one, two, or three micromeres are deleted at eight cells. Because cells other than 1a or 1c can produce eyes, they concluded that eye determination involves some kind of induction and that normal development is possible only when the cleavage pattern and cell arrangements are normal.

When three micromeres are deleted in *Hoploplana*, almost all of the larvae are one eyed (66%) or eyeless (28%), and isolated first quartet macromeres never produce any eyes. Thus, at least two micromeres must be present for two eyes to form. However, isolated first quartets commonly develop supernumerary eyes, suggesting that the macromeres may play an inhibitory role in eye development. Similarly, Cather (1973) has demonstrated an inhibitory role of the polar lobe in *Ilyanassa* (a macromere derivative), in the development of cilia by first quartet cells.

As the number of micromeres deleted increases, tuft abnormalities also increase. Single micromere deletions suggest that tuft determinants are localized in the first quartet micromeres, but that tufts are equally likely to be absent upon the deletion of any blastomere. Deletion of two or more micromeres almost always results in larvae missing one or both tufts.

Symmetry

Embryos in which one or two micromeres have been deleted almost always develop bilateral symmetry, as is characteristic of Muller's and three-quarter larvae. However, following deletion of three micromeres, most of the larvae fall into the half-larva or sphere/swollen categories, exhibiting either asymmetry or radial symmetry. Thus, the determination of embryonic axes resulting in a larva with bilateral symmetry may involve an interaction between the micromeres and a central cross-furrow macromere, and a minimum number of micromeres (*i.e.*, at least 2) must contact the central macromere for axis determination to occur. In these characteristics, *Hoploplana* appears to be similar to *Patella* (van den Biggelaar and Guerrier, 1979) and *Lymnaea* (Martindale *et al.*, 1985).

Survival

Though embryos consisting of only four micromeres are much smaller than those of four macromeres, they have much greater developmental potential than the latter. Their survival rate to day five is much higher, and they differentiate structures such as eyes, cilia, and sometimes tufts, though they almost always remain spherical. Wilson (1904), Horstadius (1937), and Costello (1945) observed similar development of isolated first quartets of *Patella, Cerebratulus,* and *Nereis,* respectively. The swollen syndrome that characterizes this type of embryo in *Hoploplana* may result from micromeres attempting to spread over macromeres that are not there.

Isolated, intact first quartet macromeres (1A–1D embryos), on the other hand, seldom survive, and those that do are radially symmetrical and exhibit no recognizable differentiations, such as gut, eyes, or tufts. Development of eight-cell vegetal halves in *Patella, Cerebratulus,* and *Nereis* is similar, though these embryos sometimes gastrulated. These results are in contrast to those of first quartet deletions in *Bithynia* (van Dam and Verdonk, 1982), in which the resulting larvae were bilaterally symmetrical and differentiated many larval organs, though they were missing the head.

Conclusions

The *Hoploplana* embryo apparently develops axes of bilateral symmetry only when at least two micromeres are present, and for completely normal development to occur, at least three micromeres are required. While the blastomeres apparently do express cytoplasmic localization during early cleavage, positional differences between blastomeres also appear to play a role in divergence of developmental pathways. Therefore the polyclads, with slightly unequal cleavage, and a rather loose early embryonic determination involving cytoplasmic localization, also demonstrate some complex cellular interactions during development. These studies suggest that polyclad flatworms could be an appropriate model for an ancestral form that might have given rise to the two different developmental pathways characterizing present day higher Spiralia.

Acknowledgments

This work was supported by a grant from Research Corporation, NSF grant DCB-8817760, and the Union College Faculty Research Fund.

Literature Cited

Arnolds, W. J. A., J. A. M. van den Biggelaar, and N. H. Verdonk. 1983. Spatial aspects of cell interactions involved in the determination of dorsoventral polarity in equally cleaving gastropods and regulative abilities of their embryos as studied by micromere deletions in *Lymnaea* and *Patella*. *Roux's Arch. Dev. Biol.* **192:** 75–85.

van den Biggelaar, J. A. M. 1976. Development of dorsoventral polarity preceding the formation of the mesentoblast in *Lymnaea stagnalis*. *Proc. Kon. Ned. Akad. Wet.* **C79:** 113–126.

van den Biggelaar, J. A. M. 1977. Development of dorsoventral polarity and mesentoblast determination in *Patella vulgata*. *J. Morphol.* **154:** 157–186.

van den Biggelaar, J. A. M., and P. Guerrier. 1979. Dorsoventral polarity and mesentoblast determination as concomitant results of cellular interactions in the mollusk *Patella vulgata*. *Dev. Biol.* **68:** 462–471.

Boyer, B. C. 1986. Determinative development in the polyclad turbellarian *Hoploplana inquilina*. *Int. J. Invert. Repro. Dev.* **9:** 243–251.

Boyer, B. C. 1987. Development of *in vitro* fertilized embryos of the polyclad flatworm *Hoploplana inquilina* following blastomere separation and deletion. *Roux's Arch. Dev. Biol.* **196:** 158–164.

Cather, J. N. 1973. Regulation of apical cilia development by the polar lobe of *Ilyanassa* (Gastropoda: Nassariidae). *Malacologia* **12:** 213–223.

Clement, A. C. 1967. The embryonic value of the micromeres in *Ilyanassa obsoleta* as determined by deletion experiments. I. The first quartet cells. *J. Exp. Zool.* **166:** 77–88.

Costello, D. P. 1945. Experimental studies of germinal localization in *Nereis*. I. The development of isolated blastomeres. *J. Exp. Zool.* **100:** 19–46.

van Dam, W. I., and N. H. Verdonk. 1982. The morphogenetic significance of the first quartet micromeres for the development of the snail *Bithynia tentaculata*. *Roux's Arch. Dev. Biol.* **191:** 112–118.

Davidson, E. H. 1986. *Gene Activity in Early Development,* third edition. Academic Press, New York.

Horstadius, S. 1937. Experiments on determination in the early development of *Cerebratulus lacteus*. *Biol. Bull.* **73:** 317–342.

Martindale, M. Q., C. Q. Doe, and J. B. Morrill. 1985. The role of animal-vegetal interaction with respect to the determination of dorsoventral polarity in the equal-cleaving spiralian, *Lymnaea palustris*. *Roux's Arch. Dev. Biol.* **194:** 281–295.

Morrill, J. B., C. A. Blair, and W. J. Larsen. 1973. Regulative development in the pulmonate gastropod, *Lymnaea palustris,* as determined by blastomere deletion experiments. *J. Exp. Zool.* **183:** 47–56.

Surface, F. M. 1907. The early development of a polyclad, *Planocera inquilina*. *Proc. Acad. Nat. Sci. Phila.* **59:** 514–559.

Wilson, E. B. 1904. Experimental studies on germinal localization. II. Experiments on the cleavage mosaic in *Patella* and *Dentalium*. *J. Exp. Zool.* **1:** 197–268.

Reference: *Biol. Bull.* **177**: 344–349. (December, 1989)

Cloned cDNA and Antibody for an Ovarian Cortical Granule Polypeptide of the Shrimp *Penaeus vannamei*

JAMES Y. BRADFIELD, ROBERT L. BERLIN, SUSAN M. RANKIN, AND LARRY L. KEELEY

Laboratories for Invertebrate Neuroendocrine Research, Department of Entomology, Texas A&M University, College Station, Texas 77843-2475

Abstract. A cloned cDNA was generated to a transcript for a major ovarian polypeptide (200 kDa) of the South American white shrimp, *Penaeus vannamei*. The cloned cDNA hybridized to a single transcript in ovaries but not to RNA from the hepatopancreas or muscle. For immunodetection and quantitation, a monospecific polyclonal antibody was raised against the cDNA translation product expressed in bacteria. The antibody was used to show that the 200 kDa ovarian polypeptide accumulated in cortical granules during ovarian development to comprise ~11% of the total ovarian protein and disappeared during early embryonic development. These studies begin to explain a gene-product relationship essential for reproduction in *P. vannamei*.

Introduction

Cortical granules are large and abundant in the mature oocytes of penaeid shrimp (Duronslet *et al.*, 1975; Clark and Lynn, 1977; Clark *et al.*, 1980; Anderson *et al.*, 1984; Tom *et al.*, 1987; Bell and Lightner, 1988; Tan-Fermin and Pudadera, 1989). However, despite the prominence of these organelles, shrimp cortical granule synthesis and function have received little attention. Histological studies have shown that cortical granules contain glycoproteins and lack lipids (Tan-Fermin and Pudadera, 1989), but the precise nature of the protein moieties or other potential components has not been determined.

In the present studies we have quantified cortical granule size and abundance in mature oocytes of the South American white shrimp, *Penaeus vannamei;* isolated a cloned cDNA for a major cortical granule polypeptide; and, after making a polyclonal antibody against the genetically engineered cDNA translation product, quantified the amount of that cortical granule polypeptide during ovarian and very early embryonic development. The cloned cDNA and its corresponding antibody are sensitive probes for studies on regulation of a gene that is abundantly expressed during ovarian development in *P. vannamei*.

Received 23 March 1989; accepted 22 August 1989.

Materials and Methods

Animals

Broodstock female *P. vannamei* were obtained from Laguna Madre Shrimp Farm (Los Fresnos, Texas), and Sea Critters Inc. (Tavernier, Florida). Shrimp were maintained in 2000-l circular tanks [biologically filtered, aerated, artificial seawater (35‰)] at 28°C under a 16L:8D (dim light) photoperiod, and fed squid and oysters twice daily. Under these conditions, unilateral eyestalk ablation induces ovarian development within two weeks (Rankin *et al.*, 1989). Shrimp spawn samples were obtained from Granada Genetics Inc. (College Station, Texas).

Ovarian cDNA library construction

Total RNA was isolated (Chirgwin *et al.*, 1979) from ovaries in mid-development (~150 μm oocyte diameter), and poly(A)$^+$RNA was selected by two rounds of oligodeoxythymidylate-cellulose chromatography (Aviv and Leder, 1972). Double-strand cDNA was prepared according to Gubler and Hoffman (1983), made blunt-ended with T4 DNA polymerase, and ligated to *Eco*RI/*Not*I linker-adaptors (Invitrogen). cDNAs ≥ 1.5 kb (~2 μg) were isolated by electrophoresis in agarose and glass powder adsorption (Vogelstein and Gillespie, 1979). The cDNAs were ligated to DNA of bacteriophage λgt11

(Young and Davis, 1983), and packaged with a commercial extract (Gigapack Plus, Stratagene Cloning Systems). Propagation on *Escherichia coli* Y1088 gave a library of 1.3×10^6 primary recombinants.

Isolation of a cloned cDNA representing an abundant ovarian transcript

Two mixed cDNA probes were used to isolate an ovarian cDNA representing a highly expressed transcript for a high molecular weight translation product. The first probe was ^{32}P-cDNA (Schleif and Wensink, 1981) prepared from total ovarian poly(A)$^+$RNA. The second cDNA probe was ^{32}P-cDNA prepared from 5–7 kb poly (A)$^+$RNA isolated from low-melting-temperature agarose gel. Duplicate plaque lifts on nylon filters (NEN Research Products) were hybridized with the two probes in 50% formamide, 4 X SSPE (20 X is 3.6 *M* NaCl, 0.2 *M* phosphate buffer pH 7.4, 20 m*M* EDTA), 2% SDS, 0.5% nonfat dry milk at 42°C overnight, and washes were in 15 m*M* NaCl, 10 m*M* Tris-HCl pH 7.4, 1 m*M* EDTA, 1% SDS at 60°C. Several recombinant bacteriophage hybridized strongly with both cDNA probes. A 3 kb cDNA insert from one of these recombinants was used for the experiments described below.

Production of a cDNA-derived antibody

The 3 kb ovarian cDNA (see above) was subcloned into the β-galactosidase C-terminal coding region of the plasmid expression vector pUR 291 (Ruther and Müller-Hill, 1983) for *E. coli* JM101 transformation. A fusion polypeptide (part bacterial β-galactosidase and part shrimp cDNA translation product) was induced by addition of isopropyl-β-D-thiogalactopyranoside to cell cultures in log-phase. Cellular polypeptides were separated by SDS-PAGE (Laemmli, 1970). The fusion polypeptide (205 kDa) was visualized with KCl, electroeluted (Andrews, 1986), and quantified according to Lowry *et al.* (1951). A polyclonal antibody to the gel-purified fusion polypeptide was raised in 3-month-old New Zealand white rabbits. Freund's complete adjuvant was included in the primary injection of ~600 μg protein, and the non-pyogenic adjuvant T1501 (gift from Dr. L. F. Woodard, Dept. Vet. Sciences, University of Wyoming) was used in booster injections (~150 μg protein). Rabbit serum was diluted with 15 m*M* phosphate buffer pH 6.4, and the IgG fraction isolated with a prepacked diethylaminoethyl-cellulose ion exchange column (Pharmacia LKB Biotechnology) according to the supplier's instructions. The IgG was lyophilized and stored at −80°C until use.

Ovarian transcript characterization

Total RNA was isolated from selected shrimp tissues, denatured with MeHgOH (Bailey and Davidson, 1976), and separated by electrophoresis in 1.2% agarose gel. RNA was transferred to a nylon filter (Zeta-Probe, Bio-Rad Laboratories) and hybridized with the nick-translated (Rigby *et al.*, 1977) cloned ovarian cDNA under conditions described above for cDNA isolation. Hybridization was visualized with autoradiography.

Immunoblot analysis

Polypeptides were separated by SDS-PAGE (7.5% gel) and transferred to nitrocellulose using a semi-dry electroblotting apparatus (American Bionetics) according to the manufacturer's recommendations. Polypeptides reacting with the fusion polypeptide antibody were visualized with an alkaline phosphatase detection system (Bio-Rad).

Histochemistry

Ovary fragments were fixed in 4% formaldehyde in Ott's artificial seawater (Spotte, 1979), embedded in paraffin, and sectioned (5 μm) (Sheehan and Hrapchak, 1980). Immunoreactivity in sections was located with the Bio-Rad alkaline phosphatase detection system. Control samples were incubated with IgG from uninjected rabbits. Determination of oocyte and cortical granule parameters were made on sections of 62 cells with nuclear diameter > 44 μm, using a light microscope (160×) with ocular micrometer. Analysis of cell surface sections (n = 42) was used to determine the number of cortical granules per cell.

Enzyme-linked immunosorbent assay (ELISA)

Samples in 60 m*M* carbonate buffer pH 9.6 were adsorbed to Immulon 2 Plates (Dynatech) at 4°C overnight. The plates were washed with 0.33 *M* phosphate-buffered saline pH 7.2 (PBS), and PBS adjusted to contain 0.001% Tween-20. Wells were blocked with ovalbumin (5% in carbonate buffer), washed, and incubated in PBS with rabbit IgG (see below). Immunoreactive protein was assessed at 405 nm with a peroxidase-linked antibody to rabbit IgG. For quantitation, varying quantities of fusion protein were run as standards against which the crude tissue extracts were compared. This quantitation required two preliminary experiments: (1) adsorption of the antibody with varying concentrations of a pUR 291/*E. coli* lysate. This experiment determined the concentration of cell lysate necessary to effectively remove the antibodies directed toward contaminating *E. coli* proteins. The most abundant contaminant was the 115 kDa β-galactosidase portion of the fusion protein. Adsorption of the antibody was essential to ensure that only the epitopes common to both the fusion protein and the shrimp ovary polypeptide were detected in the ELISA. Only appropriately adsorbed antibodies were used in subsequent

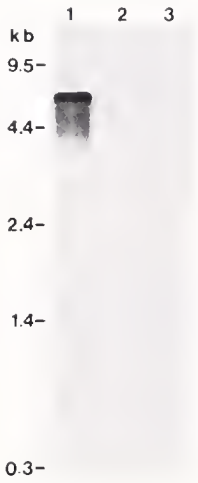

Figure 1. Total RNA samples (5 μg/lane) from mid-reproductive cycle *Penaeus vannamei* tissues were denatured, separated by electrophoresis in agarose, transferred to nylon membrane, and hybridized with the cloned 3 kb ovarian cDNA. Lane 1, ovary; lane 2, hepatopancreas; lane 3, muscle. RNA size markers are indicated at left.

experiments. (2) Incubation of extracts of various concentrations of pre-vitellogenic ovaries and nearly mature ovaries with various concentrations of fusion protein. This experiment demonstrated that the fusion polypeptide and immunoreactive native ovarian protein were adsorbed to the incubation wells with equal efficiency. We assumed that the common epitopes on the two different molecules (*i.e.*, fusion protein and ovarian polypeptide) behaved identically in the ELISA.

Results

Transcript characterization

Northern hybridization was performed to determine (1) the size of the highly expressed transcript(s) represented by the cloned ovarian cDNA and (2) which tissues expressed transcripts for production of the major ovarian polypeptide. The cDNA hybridized with a single 6 kb transcript from a mid-cycle ovary (oocyte diameter ~ 150 μm) (Fig. 1). The cDNA did not hybridize with RNA from muscle or hepatopancreas of the same animal.

Genetically engineered fusion polypeptide

A genetically engineered polypeptide consisting of shrimp ovarian polypeptide and bacterial β-galactosidase was generated for subsequent immunological identification of the shrimp ovarian cDNA translation product. For generation of this fusion polypeptide, the 3 kb cloned cDNA representing the 6 kb ovarian transcript was inserted into plasmid pUR 291 (Ruther and Müller-Hill, 1983). This recombinant construct was used for high-level expression of the fusion polypeptide in bacteria. The fusion polypeptide consisted of ~115 kDa β-galactosidase combined with a ~90 kDa *P. vannamei* ovarian polypeptide sequence (Fig. 2).

Immunoblot analysis

A polyclonal antibody raised against the fusion polypeptide was used to determine the size and tissue distribution of the ovarian 6 kb mRNA translation product. Immunoblot analysis of tissues from a shrimp with mid-cycle ovaries showed strong reaction with a ~200 kDa ovarian polypeptide (Fig. 3). There were smaller, faintly reacting polypeptides in the ovary, and one small reacting polypeptide (~35 kDa) from the hepatopancreas. The antibody did not react with muscle or hemolymph samples.

Histochemical analysis

Localization of the ovarian polypeptide was accomplished by immunocytochemical analysis. Immunoreactivity was found in the cortical granules of the mature oocytes (Fig. 4). The cortical granules were prominent club-shaped corticular organelles, ~38 μm long, 12 μm in basal diameter, and ~1.4×10^3 μm^3 in volume calculated according to conical shape. Analysis of cell surface sections indicated that there were ~420 cortical gran-

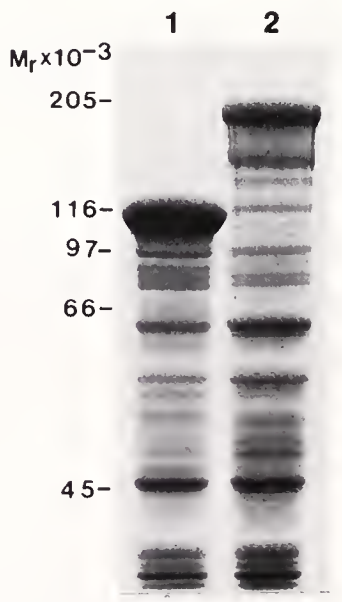

Figure 2. *E. coli* JM101 was transformed with plasmid pUR 291, and plasmid-encoded β-galactosidase was induced by addition of IPTG. Cell extracts were separated by SDS-PAGE (7.5%) and stained with Coomassie Blue R. Lane 1, native pUR 291; lane 2, recombinant pUR 291 containing the 3 kb ovarian cDNA. The heavy band at 116 kDa in lane 1 is unfused β-galactosidase. The band at 205 kDa in lane 2 is a fusion consisting of β-galactosidase linked to a polypeptide encoded by the ovarian cDNA.

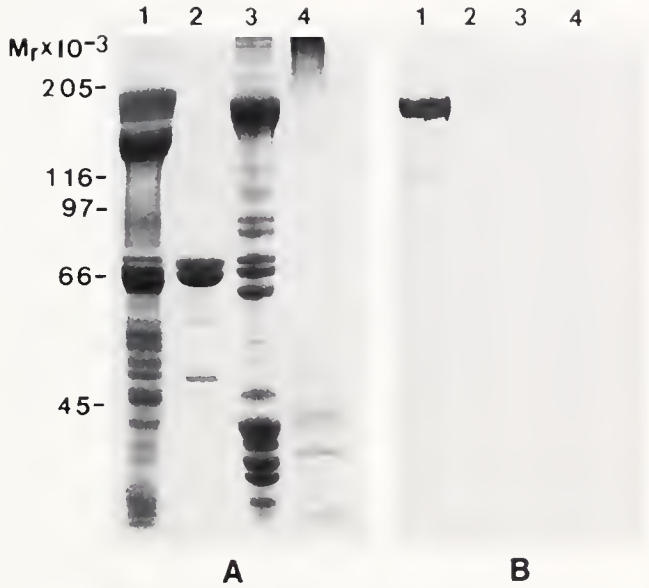

Figure 3. *Penaeus vannamei* polypeptides were separated by SDS-PAGE, and stained with Coomassie Blue R (Panel A), or blotted onto nitrocellulose and incubated with a polyclonal antibody to the genetically engineered fusion polypeptide (Panel B). Samples were from an animal with mid-cycle ovaries (oocyte diameter ~ 150 μm). Lane 1, ovary; 2, hemolymph; 3, muscle; 4, hepatopancreas. Positions of molecular weight markers are indicated at left.

ules/cell, comprising ~10% of the oocyte volume. These estimates are based on a cell diameter of ~226 μm (Table I). This cell diameter measurement was an underestimate of that in fresh tissue as a result of (a) cell shrinkage (from 320 μm, see below) during sample preparation and (b) imprecision in determining the cell center due to variations in cell morphology.

Developmental profile of the 200 kDa ovarian polypeptide

The contribution of the 200 kDa polypeptide to total protein was determined by ELISA during both ovarian development and embryonic development using the purified fusion protein as the standard. The 200 kDa polypeptide was not detected in a previtellogenic ovary (oocyte diameter = 0) (Fig. 5). It represented 4–5% of the total ovarian protein at oocyte diameter 200–240 μm and ~11% of the protein in a fully developed ovary (320 μm). In newly spawned eggs, the 200 kDa polypeptide comprised 3–4% of the protein. By 2 h after the spawn, the 200 kDa polypeptide had declined to <1% and was not detected in ≥4 h spawn. By 6 h after spawning, the first antennal, second antennal, and mandibular primordia were visible, and hatching occurred 16–18 h after spawning.

Discussion

Cortical granules are found widely in vertebrates and invertebrates; however, the size, abundance, and composition of these granules varies among species (see Guraya, 1982, for review). As shown by light and electron microscopy, cortical granules in mature ovaries of penaeid shrimp are large and plentiful (Duronslet *et al.*, 1975; Clark and Lynn, 1977; Clark *et al.*, 1980; Anderson *et al.*, 1984; Tom *et al.*, 1987; Bell and Lightner, 1988; Tan-Fermin and Pudadera, 1989). We showed that, in *P. vannamei*, the cortical granules were club-shaped structures, about 38 μm long, and occupied about 10% of the volume in fixed, mature oocytes (Fig. 4, Table I). In mature ovaries of *Penaeus aztecus*, the somewhat smaller but

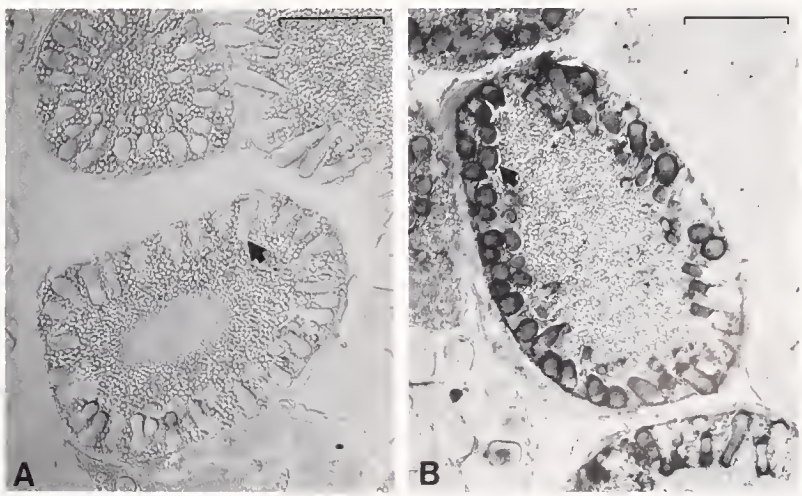

Figure 4. Localization of the 200 kDa ovarian polypeptide using immunocytochemistry. Ovarian sections (5 μm) were incubated with (Panel A) preimmune rabbit IgG and (Panel B) IgG from the rabbit inoculated with the gel-purified fusion polypeptide (see Fig. 2). Immunoreaction was visualized with an alkaline phosphatase-linked second antibody. Arrows indicate cortical granules. Scale bars = 100 μm.

Table I

Estimates of oocyte and cortical granule parameters in mature ovaries of* Penaeus vannamei

Parameter	Size ± SD
Oocyte diameter	226 ± 16 μm
Oocyte surface area	1.6×10^5 μm^2
Oocyte volume	6.0×10^6 μm^3
Cortical granule length	37.8 ± 4.3 μm
Cortical granule diameter (a)	12.0 ± 1.4 μm
Cortical granule diameter (b)	7.5 ± 1.2 μm
Vol. of cortical granules	1.4×10^3 μm^3
No. cortical granules/cell	420 ± 70
Vol. cortical granules/cell	5.9×10^5 μm^3
Vol. cortical granules/cell vol (%)	~10%

* Measurements were taken from 5 μm sections after fixation, embedding, deparafinization, and rehydration. Sections of 62 cells with nuclear diameter > 44 μm were measured for the various parameters. To determine cortical granule dimensions, three granules per cell section were measured for length, apical (a), and basal diameter (b).

more numerous cortical granules occupy about 12% of the oocyte volume (Clark *et al.*, 1980). Histological analysis shows that cortical granules of *Penaeus monodon* stain positively with alcian blue-periodic acid Schiff, indicating glycoprotein components, and negatively with Sudan black, suggesting an absence of lipids (Tan-Fermin and Pudadera, 1989).

The studies described in this paper resulted in a cloned cDNA and antibody for one highly expressed cortical granule polypeptide of the shrimp, *P. vannamei*. Using these probes, regulation of shrimp reproduction at the level of a single gene can be examined for the first time. Bacterial expression of the cloned cDNA (Fig. 2) allowed production of a monospecific antibody directed against the translation product. Immunoblot analysis showed that the major immunoreactive polypeptide (200 kDa) and several faintly reacting, smaller polypeptides were either immunologically related products of more than one gene, or, alternatively, natural or artifactual cleavage products of the 200 kDa polypeptide. We regard the latter possibilities as the more likely since the ovarian cDNA hybridized to only a single ovary-specific transcript (Fig. 1). Most likely, the immunoreactive polypeptide in the hepatopancreas originated in the ovary and, through leakage and absorption, was detected subsequently in the hepatopancreas.

We demonstrated by immunocytochemical analysis that the 200 kDa polypeptide was localized in cortical granules (Fig. 4) and that it accrued from virtually undetectable levels in the immature ovary up to ~11% of the total protein in the mature ovary of *P. vannamei* (Fig. 5). Because it is strikingly abundant (Fig. 5) and relatively insoluble (Rankin *et al.*, 1989), we speculate that the 200 kDa polypeptide contributes to the structural integrity of the cortical granules. This polypeptide is similar in size to a 180–193 kDa polypeptide found in cortical granules of the sea urchin *Strongylocentrotus purpuratus* (Kopf *et al.*, 1982; Villacorta-Moeller and Carroll, 1982). Whether sea urchin cortical granule polypeptides are immunologically related to those of *P. vannamei* remains to be determined. Indeed, determination of similarities and differences between cortical granules within single oocytes is an area of active research. Among the crustaceans, ultrastructural observations indicated two types of cortical granules in the horseshoe crab, *Limulus polyphemus* (Bannon and Brown, 1980); two in the fairy shrimp *Tanymastix* (Garreau de Loubresse, 1974); and four in the lobsters *Homarus americanus* and *H. gammarus* (Talbot and Goudeau, 1988). In the sea urchin *S. purpuratus*, immunological analysis shows a marked heterogeneity of distribution for a cortical granule polypeptide, suggesting differences between cortical granules in that species (Anstrom *et al.*, 1988).

Cortical granule contents are thought to originate in the oocytes (see Guraya, 1982, for review). For example, in crustaceans, ultrastructural evidence indicates that at least one type of cortical granule, now termed "ring-shaped inclusions," of the crab *Carcinus maenas* (Goudeau, 1984) and the lobster *Homarus* (Talbot and Goudeau, 1988) are products of oocytic machinery. We are the first to apply molecular genetic analysis to demonstrate an ovarian origin for a major cortical granule polypeptide (Figs. 1–3). It is likely that this polypeptide is synthesized in the oocytes; however, this remains to be determined by *in situ* hybridization.

The 200 kDa cortical granule polypeptide accumu-

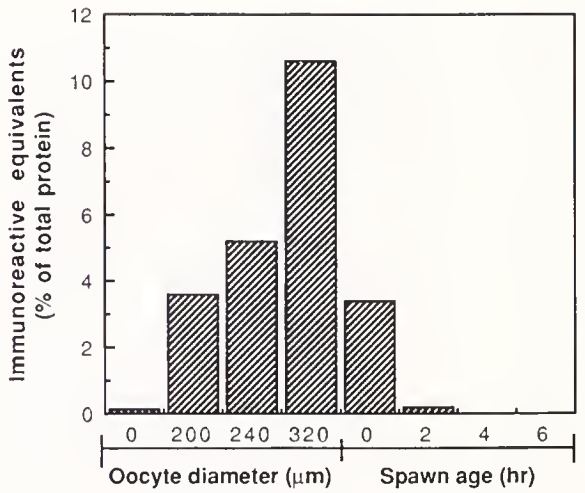

Figure 5. Enzyme-linked immunosorbent assay of the 200 kDa ovarian polypeptide, in total protein from developing ovaries and spawn. The purified fusion polypeptide (Fig. 2) was the antigen and protein standard. The fusion polypeptide antibody was preadsorbed to an *E. coli* lysate.

lated during ovarian development, from a virtually undetectable level in a previtellogenic ovary to ~11% of the total protein in a fully developed ovary. Within a few hours of spawning, the 200 kDa polypeptide had disappeared (Fig. 5), presumably through exocytosis during the cortical reaction (see Clark *et al.*, 1980). The cDNA and antibody that we have generated for this polypeptide can now be used to deduce the primary structure of a major component of the cortical granules and determine its site of synthesis precisely; to characterize the maturation of cortical granules; and to investigate the regulation of synthesis of this major ovarian component at the pretranslational and translational levels.

Acknowledgments

We thank Martha Lundberg, Pat Sistrunk, and Dr. John Ellison for technical assistance. This work was supported by institutional grant NA 85AA-D-SD128 to Texas A&M University by the National Oceanic and Atmospheric Administration's Sea Grant Program, and by the Texas Advanced Technology Research Program. The research was conducted by the Texas Agricultural Experiment Station.

Literature Cited

Anderson, S. L., E. S. Chang, and W. H. Clark Jr. 1984. Timing of postvitellogenic ovarian changes in the ridgeback prawn *Sicyonia ingentis* (Penaeidae) determined by ovarian biopsy. *Aquaculture* **42:** 257–271.

Andrews, A. T. 1986. *Electrophoresis. Theory, Techniques, and Biochemical and Clinical Applications.* 2nd ed. Clarendon Press, Oxford.

Anstrom, J. A., J. E. Chin, D. S. Leaf, A. L. Parks, and R. A. Raff. 1988. Immunocytochemical evidence suggesting heterogeneity in the population of sea urchin egg cortical granules. *Dev. Biol.* **125:** 1–7.

Aviv, H., and P. Leder. 1972. Purification of biologically active globin messenger RNA by chromatography on oligothymidylic acid-cellulose. *Proc. Natl. Acad. Sci. USA* **69:** 1408–1412.

Bailey, J. M., and N. Davidson. 1976. Methylmercury as a reversible denaturing agent for agarose gel electrophoresis. *Anal. Biochem.* **70:** 75–85.

Bannon, G. A., and G. G. Brown. 1980. Vesicle involvement in the egg cortical reaction of the horseshoe crab, *Limulus polyphemus L. Dev. Biol.* **76:** 410–417.

Bell, T. A., and D. V. Lightner. 1988. *A Handbook of Normal Penaeid Shrimp Histology.* Allen Press, Inc., Lawrence, Kansas.

Chirgwin, J. M., A. E. Przybyla, R. J. MacDonald, and W. J. Rutter. 1979. Isolation of biologically active ribonucleic acid from sources enriched in ribonuclease. *Biochemistry* **18:** 5294–5299.

Clark, W. H., Jr., and J. W. Lynn. 1977. A Mg^{++} dependent cortical reaction in the eggs of penaeid shrimp. *J. Exp. Zool.* **200:** 177–183.

Clark, W. H., Jr., J. W. Lynn, A. I. Yudin, and H. O. Persyn. 1980. Morphology of the cortical reaction in the eggs of *Penaeus aztecus. Biol. Bull.* **158:** 175–186.

Duronslet, M. J., A. I. Yudin, R. S. Wheeler, and W. H. Clark Jr. 1975. Light and fine structural studies of natural and artificially induced egg growth of penaeid shrimp. *Proc. Meet. World Mari. Soc.* **6:** 105–122.

Garreau de Loubresse, N. 1974. Etude chronologique de la mise en place des enveloppes de l'oeuf d'un crustacé phyllopode *Tanymastix lacunae. J. Microsc.* **20:** 21–38.

Goudeau, M. 1984. Fertilization in a crab. III. Cytodifferentiation of vesicles enclosing ring-shaped elements involved in the cortical reaction. *Gamete Res.* **9:** 409–424.

Gubler, U., and B. J. Hoffman. 1983. A simple and very efficient method for generating cDNA libraries. *Gene* **25:** 263–269.

Guraya, S. S. 1982. Recent progress in the structure, origin, composition, and function of cortical granules in animal eggs. *Int. Rev. Cytol.* **78:** 257–360.

Kopf, G. S., G. W. Moy, and V. D. Vaquier. 1982. Isolation and characterization of sea urchin egg cortical granules. *J. Cell Biol.* **95:** 924–932.

Laemmli, U. K. 1970. Cleavage of structural proteins during the assembly of the head of bacteriophage T4. *Nature* **277:** 680–685.

Lowry, O., N. Rosebrough, A. Farr, and R. Randall. 1951. Protein measurement with folin phenol reagent. *J. Biol. Chem.* **193:** 265–275.

Rankin, S. M., J. Y. Bradfield, and L. L. Keeley. 1989. Ovarian protein synthesis in the South American white shrimp, *Penaeus vannamei,* during the reproductive cycle. *Int. J. Invert. Reprod. Dev.* **15:** 27–33.

Rigby, P. W. J., M. Dieckmann, C. Rhoads, and P. Berg. 1977. Labelling deoxyribonucleic acid to high specific activity *in vitro* by nick-translation with DNA polymerase I. *J. Mol. Biol.* **113:** 237–251.

Ruther, U., and B. Müller-Hill. 1983. Easy identification of cDNA clones. *EMBO J.* **2:** 1791–1794.

Sehleif, R. F., and P. W. Wensink. 1981. *Practical Methods in Molecular Biology.* Springer-Verlag, New York.

Sheehan, D. C., and B. B. Hrapchak. 1980. *Theory and Practice of Histology,* 2nd ed., C. V. Mosby Co., St. Louis, Toronto and New York.

Spotte, S. H. 1979. *Fish and Invertebrate Culture; Water Management in Closed Systems,* 2nd ed. Wiley Interscience, New York.

Tom, M., G. Goren, and M. Ovadia. 1987. Localization of the vitellin and its possible precursors in various organs of *Parapenaeus longirostris* (Crustacea, Decapods, Penaeidae). *Int. J. Invert. Reprod. and Dev.* **12:** 1–12.

Talbot, P., and M. Goudeau. 1988. A complex cortical reaction leads to formation of the fertilization envelope in the lobster, *Homarus. Gamete Res.* **19:** 1–18.

Tan-Fermin, J. D., and R. A. Pudadera. 1989. Ovarian maturation stages of the wild giant tiger prawn, *Penaeus monodon* Fabricius. *Aquaculture* **77:** 229–242.

Villaeorta-Moeller, M. N., and E. J. Carroll Jr. 1982. Sea urchin embryo fertilization envelope: immunological evidence that soluble envelope proteins are derived from cortical granule secretions. *Dev. Biol.* **94:** 415–424.

Vogelstein, B., and D. Gillespie. 1979. Preparative and analytical purification of DNA from agarose. *Proc. Natl. Acad. Sci. USA* **76:** 615–619.

Young, R. A., and R. W. Davis. 1983. Efficient isolation of genes by using antibody probes. *Proc. Natl. Acad. Sci. USA* **80:** 1194–1198.

Reference: *Biol. Bull.* **177**: 350–355. (December, 1989)

Larvae of a Nudibranch Mollusc (*Phestilla sibogae*) Metamorphose when Exposed to Common Organic Solvents

J. TIMOTHY PENNINGTON[1] AND MICHAEL G. HADFIELD

Kewalo Marine Laboratory, University of Hawaii, 41 Ahui St., Honolulu, Hawaii 96813

Abstract. Larvae of the nudibranch mollusc *Phestilla sibogae* metamorphosed when exposed to 10 of 14 organic solvents. The active solvents included five alcohols and ethanolamine, acetonitrile, acetone, dichloromethane, and toluene. Inactive solvents were ethylene glycol, DMSO, benzene, and hexane. These compounds span a wide range of polarities and contain a number of functional groups. Ethanol induced metamorphosis after 1–5 days of exposure at 0.5–0.001 *M*, and maximally induced about 65% of larvae to metamorphose in 3–5 days at 0.1 *M*. Ethanol was lethal to larvae above 0.75 *M* (*ca.* 4%). Methanol was lethal only above 1.75 *M* (*ca.* 7%), but produced less metamorphosis than ethanol at most concentrations. The natural inducer of metamorphosis in *P. sibogae* produced higher percentages of metamorphosis more rapidly than did any of the solvents. The mechanism of metamorphic induction by the solvents is not known, but they probably interfere with a wide range of neuronal activities and trigger an existing metamorphic pathway. Precompetent (young) larvae did not metamorphose in response to ethanol or methanol, but juveniles produced by exposure of competent (mature) larvae to ethanol or methanol survived to reproduce. Larvae of one other mollusc species also metamorphosed in response to ethanol, suggesting that larvae of other invertebrates may also be induced to metamorphose by organic solvents. Larval biologists should be aware of this possibility.

Introduction

Many marine invertebrate species have complex life cycles, wherein a planktonic larval stage is both ecologically and morphologically distinct from the following benthic juvenile and adult stages. The planktonic and benthic segments of these life cycles are joined by relatively rapid and often drastic metamorphoses (see papers in Chia and Rice, 1978). Such metamorphoses have been subjected to considerable study (reviewed by Meadows and Campbell, 1972; Crisp, 1974, 1976; Burke, 1983), as researchers have been interested both in the ecology of metamorphosis and in the physiological and morphogenetic process of metamorphosis itself.

In nature, metamorphosis is initiated by environmental "cues" that are ecologically relevant; these cues induce larvae to metamorphose in sites where the probability of survival to adulthood is relatively high. For example, juveniles and adults of the nudibranch mollusc *Phestilla sibogae* Bergh eat only coral of the genus *Porites*, and larvae of *P. sibogae* metamorphose in response to a kairomone produced by these corals (Hadfield, 1977). However, pharmacological studies with *P. sibogae* and other invertebrates have revealed various neuroactive compounds that can also induce larvae to metamorphose (Hadfield, 1977, 1984; reviewed by Burke, 1983). These compounds are of no apparent ecological relevance, but interfere with larval nervous systems and apparently activate pre-existing metamorphic pathways. Such "artificial inducers" of metamorphosis have been useful as pharmacological probes during the study of the control of metamorphosis.

Workers in our laboratory have developed the *Phestilla:Porites* interaction as a system for the study of larval metamorphosis (reviewed by Hadfield and Pennington, in press). Here we present results of experiments with *P. sibogae* showing that organic solvents, and in particular ethanol and methanol, can serve as artificial inducers of metamorphosis. Additionally, we examine age-depen-

Received 27 June 1989; accepted 30 August 1989.

[1] Present address: Hopkins Marine Station, Stanford University, Pacific Grove, CA 93950.

dency of the response to ethanol and methanol, demonstrate that ethanol and methanol-metamorphosed nudibranchs survive to reproduce, and show that larvae of at least one other gastropod species also metamorphose in response to ethanol.

Materials and Methods

Larval culture

Routine larval culture methods for *Phestilla sibogae* have been fully described by Miller and Hadfield (1986). Briefly, embryos and early veliger larvae were raised at 25°C in their egg masses until 5 days old, when they were manually hatched. Hatched veligers were maintained in seawater with antibiotics until "competent" to metamorphose (see Hadfield, 1977, and below). Individual larvae of *P. sibogae* are either competent or not, but entire batches of larvae gradually become competent during days 7–9 of culture at 25°C.

Larvae of *Crucibulum spinosum* were provided by J. L. Bell (University of Hawaii). The hatched veligers had been fed in unstirred beakers (see Bell, 1988) for 21 days when they were tested for metamorphic response to ethanol.

Assays for metamorphic response to solvents

Most assays were conducted in soap-washed or acid-cleaned (Galigher and Kozloff, 1964, p. 25) 2-ml plastic tissue culture wells (Fisher Cat. No. 08-772-1), but where noted, assays were performed in acid-cleaned glass stender dishes. Both types of containers were covered during experiments. In experiments in culture wells, about 20 larvae were pipetted along with 200 μl of 0.22 μm-filtered seawater (FSW) into each of 2 replicate wells, each containing 1.8 ml of a given test solution. Test solutions consisted of organic solvents (analytical, HPLC, or photograde) dissolved in FSW, though where noted, a few comparisons employed MBL artificial seawater (Cavanaugh, 1956). The molar concentration of solvent in the final 2 ml of assay medium is reported. For those solvents relatively insoluble in water, a dilution series of solvent:seawater test solutions was vortexed and observed for disappearance of oily micelles. The most concentrated test solutions lacking persistent micelles were used to prepare assays of these solvents; 5 *M* stocks were used to prepare assays of solvents sufficiently soluble in water.

Larvae in the wells were counted and scored as metamorphosed or not on each of several day's exposure to solvent. Larvae were determined metamorphosed when they lost their vela and larval shells, thus becoming juvenile nudibranchs. All assays included both positive and negative controls. In negative controls, larvae were assayed as above in seawater alone, to control for any background or "spontaneous" metamorphosis. In positive controls, a living chip of *Porites compressa* (1–9 mm^3) was added to wells containing larvae and seawater to assess the competence of larvae to respond to the natural metamorphic inducer.

Several series of larval assays were conducted with *P. sibogae:*

(1) Detailed dose-response curves were constructed for both ethanol and methanol, spanning 5 orders-of-magnitude of alcohol concentration and 6 days of exposure, beginning with 11-day-old larvae. Six experiments of two replicate wells per concentration were conducted with each alcohol. Several of these experiments additionally compared responses in FSW *versus* those in MBL artificial seawater. Another experiment in this series compared responses to ethanol in acid-cleaned glass dishes and the plastic culture wells.

(2) In a second series of assays, 14 common organic solvents were surveyed for metamorphosis-inducing activity. These assays began with 11-day-old larvae and were run for 2 days over wide solvent concentrations (from lethal or near-saturated to no discernible effect).

(3) A third series of assays examined the effect of larval age (*i.e.*, precompetent-to-competent larvae) on responses to both ethanol and methanol. In these assays, larvae from the same culture but 6, 8, or 10 days old were exposed to coral, 0.5 *M* ethanol, 0.5 *M* methanol, or FSW alone and assayed for metamorphosis over the next 3 days. Four replicate wells of each of the alcohol treatments were used in this experiment.

Survival and growth of solvent-metamorphosed juveniles

An experiment was conducted to determine if juveniles of *P. sibogae* resulting from solvent-induced metamorphosis could survive and grow to adulthood. Eleven-day-old larvae were pipetted into culture wells containing 0.5 *M* ethanol, 0.75 *M* methanol, or 0.5 *M* methanol. Metamorphosed nudibranchs were removed from the solvent solutions over the next two days, counted, and transferred onto pieces of living coral. Juveniles from the different solvent solutions were placed on different pieces of coral, and each piece of coral was isolated in a small flow-through aquarium. The juveniles fed on the coral, grew, and became visible to the eye about 2 weeks after transfer. The nudibranchs were counted at this time and again at 24 days after transfer, when at least some in each basket had begun to lay eggs.

Response of Crucibulum spinosum *to ethanol*

Ten veligers of *C. spinosum* were pipetted into each of eight glass stender dishes. Two of the dishes contained 0.5 *M* ethanol in FSW, two contained 0.1 *M* ethanol in

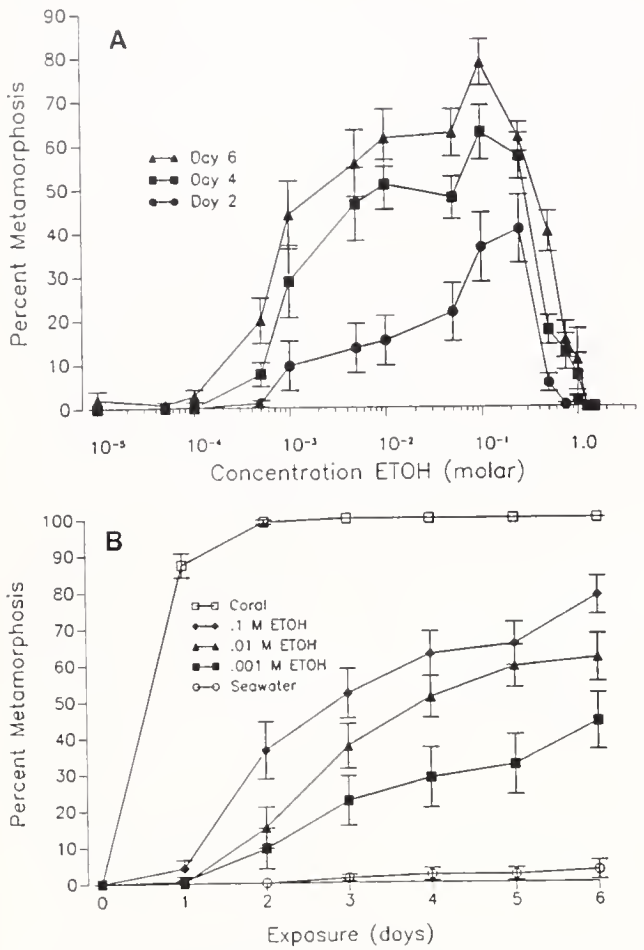

Figure 1. Cumulative percent metamorphosis of larvae of *Phestilla sibogae* exposed to a series of ethanol (ETOH) solutions for 6 days. Larvae were 11 days old at the beginning of experiments; plotted results are pooled means and S. D.'s of 6 experiments, each with 2 replicate assay wells per ETOH concentration, each well containing *ca.* 20 larvae. (A) Metamorphic response plotted as a function of ETOH concentration on days 2, 4 and 6; larvae were moribund and most eventually died at concentrations > 0.75 *M* (4%). (B) Response as a function of duration exposure to ETOH at 0.1, 0.01, and 0.001 *M*, maximal larval response was assayed with a coral chip, and "spontaneous" metamorphosis was monitored in wells containing larvae and seawater alone.

FSW, and two contained 0.01 *M* ethanol and FSW. The final pair of dishes contained FSW alone. The larvae were scored for metamorphosis on each of the next 3 days; animals were determined metamorphosed when their vela had completely disappeared.

Results

Assays for metamorphic response to solvents

Ethanol and methanol. Eleven-day-old veligers of *Phestilla sibogae* metamorphosed when exposed to both ethanol (Fig. 1A–B) and methanol (Fig. 2A–B). Very few of the larvae (<5%) metamorphosed over the 6 days of the experiments in filtered seawater alone, and 85–100% of the larvae metamorphosed within 1–2 days of exposure to a living chip of the coral *Porites compressa* (Figs. 1B, 2B). Maximal response to ethanol was between these control values, with 60–80% of larvae metamorphosing in 0.1 *M* ethanol (Fig. 1A). At least a few larvae metamorphosed at all doses between 5×10^{-4} and 1.0 *M*, but larvae were always moribund and usually died in solutions at and above 0.75 *M* (*ca.* 4%) ethanol. Maximal response to methanol was lower, with 20–35% of larvae metamorphosing in 0.1–1.0 *M* methanol (Fig. 2A). Effective doses ranged between 0.001 and 1.75 *M*, but a few metamorphoses occurred at lesser concentrations.

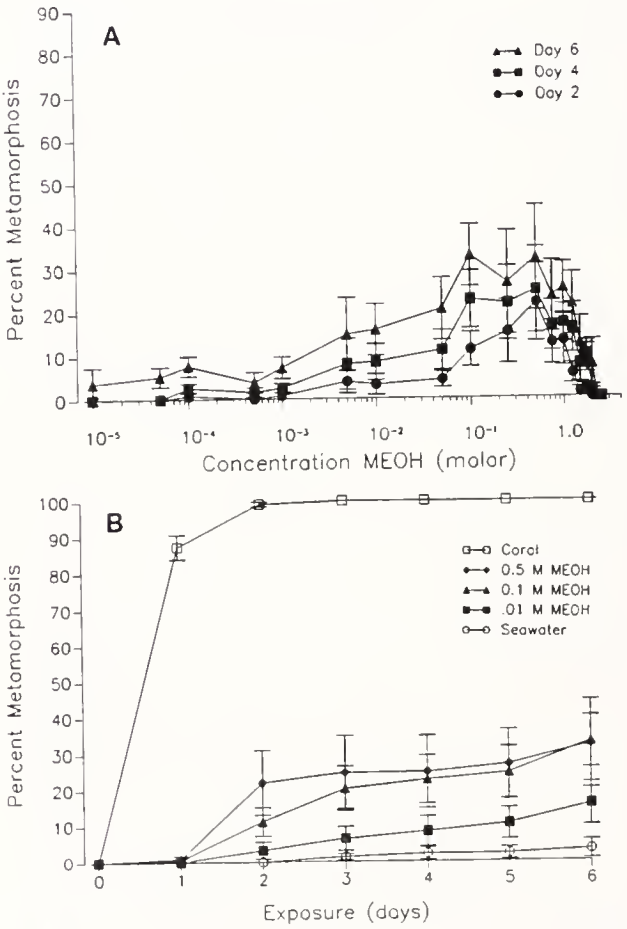

Figure 2. Cumulative percent metamorphosis of larvae of *Phestilla sibogae* exposed to a series of methanol (MEOH) solutions for 6 days. Larvae were 11 days old at the beginning of experiments; plotted results are as described under Figure 1. (A) Metamorphic response plotted as a function of MEOH concentration on Days 2, 4, and 6; larvae were moribund and most eventually died at concentrations > 1.75 *M* (7%). (B) Response as a function of duration exposure to MEOH at 0.5, 0.1, and 0.01 *M*; maximal larval response was assayed with a coral chip, and "spontaneous" metamorphosis was assayed in seawater alone.

Table I

Organic solvents assayed for capacity to induce metamorphosis of Phestilla sibogae, *listed by decreasing polarity*

Compound	Chemical family	Maximum percent metamorphosis [molar conc.]	Effective range (molar)
Ethylene glycol	diol	none —	—
Ethanolamine	amine	14 [0.01]	0.01
Methanol	alcohol	44 [0.5]	0.001–1.75
Ethanol	alcohol	39 [0.1]	0.0005–0.75
n-Propanol	alcohol	56 [0.05]	0.005–0.05
n-Butanol	alcohol	33 [0.001]	0.001–0.01
Acetonitrile	nitrile	35 [1.0]	0.1–1.0
DMSO	sulfoxide	none —	—
n-Pentanol	alcohol	18 [0.002]	0.0005–0.005
Acetone	ketone	83 [0.25]	0.05–1.0
Dichloromethane	halide	63 [0.3]	0.1–0.3*
Benzene	aromatic	3 [0.008]	0.008*
Toluene	aromatic	55 [0.003]	0.003*
Hexane(s)	alkane	none —	—

* Indicates near-saturation.

Larvae were moribund and usually died in methanol solutions above 1.75 *M* (*ca.* 7%).

The time-course of the response to both ethanol and methanol was much slower than to coral. Very few larvae metamorphosed in response to ethanol during the first day of the experiments, with increasing percentages of metamorphosis on succeeding days (Fig. 1B). Similarly, few larvae metamorphosed in methanol during the first day, with increasing percentages of metamorphosis over the second and third days (Fig. 2B). However, in methanol, few additional larvae metamorphosed after the third day.

Percentages of larvae metamorphosing in response to the alcohols in FSW or MBL artificial seawater were similar (data not shown). Experiments conducted in acid-cleaned glassware also produced similar percentages of metamorphosis to those in plastic culture wells. However, very few larvae metamorphosed in detergent-cleaned glass as compared to detergent-cleaned plastic or acid-cleaned ware of either material. Experiments were not conducted in detergent-cleaned glassware.

Other organic solvents. Including ethanol and methanol, 14 organic solvents were surveyed for their capacity to induce metamorphosis, and at least 10 solvents did so. The solvents are listed in Table I in order of decreasing polarity or water solubility, along with the general chemical family to which each belongs, the mean percent metamorphosis produced by the most effective concentration (molarity) of a solvent, and the effective ranges of concentration. Ethylene glycol, DMSO (dimethyl sulfoxide), and the hexane mixture did not produce any metamorphosis; the 3% metamorphosis observed in benzene is probably also questionable. However, the remaining solvents all produced metamorphosis in several replicate wells, and most did so at a number of concentrations. The highest solvent concentrations that did not kill or clearly incapacitate the larvae generally produced the most metamorphosis.

Response of precompetent veligers. Older, metamorphically competent larvae metamorphosed when exposed to either ethanol or methanol, but younger, precompetent larvae did not (Fig. 3A–C). When 6-day-old veligers were exposed to FSW or 0.5 *M* ethanol or methanol, essentially none metamorphosed over the next 3 days (days 6–9; Fig. 3A). At least some larvae became competent by days 8 and 9, as demonstrated by metamorphosis in the presence of coral, but few larvae metamorphosed in ethanol or methanol on these days, presumably because of the lag in response to alcohols as described above. When 8- or 10-day-old larvae were treated similarly, larvae began metamorphosing in both alcohols by day 10 (Fig. 3B) or day 11 (Fig. 3C). In these latter assays, no larvae metamorphosed in FSW alone, but at least some larvae were competent to do so during the first day of the experiments as demonstrated by the responses to coral (Fig. 3B–C). Again, larvae responded to these alcohols more slowly and less strongly than they did to coral.

Survival and growth of solvent-metamorphosed juveniles

When veligers were induced to metamorphose with ethanol or methanol and then grown on living coral, over 50% survived until at least some nudibranchs began to

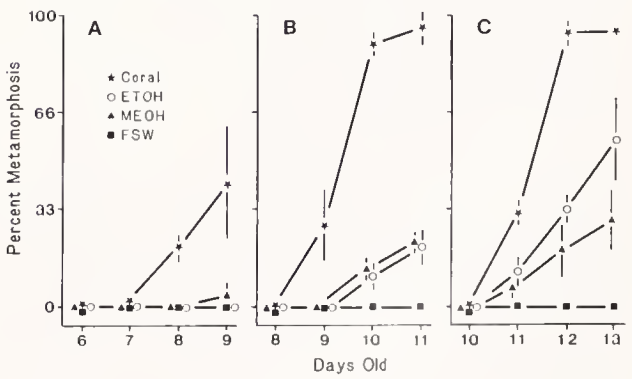

Figure 3. Cumulative percent metamorphosis of precompetent-to-competent larvae of *Phestilla sibogae* when exposed to either coral, 0.5 *M* ethanol (ETOH), 0.5 *M* methanol (MEOH), or filtered seawater (FSW) alone. Individual larvae are either metamorphically competent or not, but batches of larvae gradually become competent during days 7–9 at the culture temperatures used (25°C). Plotted results are means and S. D.'s of four replicate wells of each alcohol treatment and two replicates each of FSW and the coral treatment. (A) Response of 6-day-old, initially precompetent veligers. (B) Response of 8-day-old, mostly competent veligers. (C) Response of 10-day-old, fully competent veligers.

Table II

Phestilla sibogae: *survival of alcohol-induced nudibranchs until beginning of egg-laying*

Metamorphic inducer	Initial no. juveniles (Day 0)	Number alive (Day 14)	Number alive (Day 24)	Egg masses present? (Day 24)
Coral	10	4	3	yes
0.25 *M* ETOH	10	6	6	yes
0.5 *M* ETOH	4	4	4	yes
0.75 *M* MEOH	10	7	7	yes

lay eggs (Table II). It was usually not possible to determine which or how many of the nudibranchs in each basket had begun egg-laying. The observed survival rate was comparable to that observed when larvae were induced to metamorphose with coral (Table II), but there were no striking differences in survival among animals induced with the two ethanol doses or methanol. Nudibranchs in all treatments appeared normal. These results indicate that ethanol and methanol induce a true metamorphosis, producing juveniles that can grow to adulthood.

Response of Crucibulum spinosum *veligers to ethanol*

Veligers of *C. spinosum* metamorphosed by losing their vela when exposed to either 0.5 or 0.1 *M* ethanol for 1–3 days (Table III). No *C. spinosum* metamorphosed in either FSW or 0.01 *M* ethanol. Veligers in 0.5 *M* ethanol (*ca.* 1.5%) did not swim actively, as did larvae in the less concentrated ethanol solutions or FSW alone, but remained partly retracted or swam weakly at the bottom of the dish. J. L. Bell has successfully repeated this experiment several times (pers. comm.).

Discussion

A wide variety of common organic solvents induce metamorphosis of competent larvae of *Phestilla sibogae* (Table I). For ethanol and methanol, the response is a true metamorphosis, because precompetent larvae do not "metamorphose" in response to these alcohols (Fig. 3), and because competent larvae induced to metamorphose with ethanol or methanol can survive as juveniles and grow to adulthood (Table II). Other inducers of larval metamorphoses are suggested to be either (1) environmentally derived natural inducers, active at epidermal receptors on larval surfaces, (2) neurotransmitters, their analogues or their precursors, presumed to be active either at surface receptors or internally on larval nerves, or (3) cations thought to cause sensory cell or neuron depolarizations that activate existing metamorphic pathways (reviewed by Burke, 1983; Yool *et al.*, 1986). Because organic solvents do not normally occur in sufficient quantity to induce metamorphosis in natural seawater, are not normally involved in regulation of nerve function, and are not electrically charged, they cannot fall into any of these categories. Instead, the solvents probably penetrate larval tissues and interfere with a wide range of nervous activities, somehow activating a metamorphic pathway. This explanation is in general agreement with what is known of the pervasive and often narcotic effects of organic solvents on mammalian nervous systems (reviewed by Browning, 1965).

Because such a diversity of solvents successfully induced metamorphosis (Table I), specific functional groups of the solvent molecules are apparently not required for the induction. However, three of the solvents tested produced absolutely no metamorphosis, contrary to what might be expected if the simple presence of dissolved hydrocarbon was sufficient to induce metamorphosis. When the solvents were arrayed in order of decreasing polarity or water solubility (as in Table I), relationships between solvent polarity and maximum percent metamorphosis or effective solvent concentration were not apparent. Similarly, when arrayed by molecular weight (not shown), no obvious relationships between solvent molecular weight and percent metamorphosis or effective concentration were apparent. These simple pharmacological considerations do not clarify the means by which the active solvents induce larvae to metamorphose. Nevertheless, it was generally true that the highest concentrations of solvents that were not obviously toxic to larvae produced the highest percentages of metamorphosis.

Other artificial inducers of metamorphosis of *P. sibogae* include choline chloride (Hirata and Hadfield, 1986) and excess K^+ ions in seawater (Yool *et al.*, 1986). Additionally, epinephrine produces "partial metamorphosis," wherein veligers of *P. sibogae* lose their vela but not their shells (Hadfield, 1984). Choline maximally induces 60–70% of larvae to metamorphose at 3.75×10^{-3} *M*, after a 2–3 day latent period during which little metamorphosis occurs (Hirata and Hadfield, 1986). In con-

Table III

Ethanol-induced metamorphosis of Crucibulum spinosum

Metamorphic inducer	Percent metamorphosis		
	Day 1	Day 2	Day 3
Seawater	0	0	0
0.5 *M* ETOH	5	45	75
0.1 *M* ETOH	20	20	33
0.01 *M* ETOH	0	0	0

Values are means of 2 dishes containing 10 larvae each.

trast, live coral usually induces nearly all larvae to metamorphose within 48 h. The maximum percent metamorphosis produced by choline, the range of effective choline concentrations, and the delayed response to choline are all similar to our present results with organic solvents. Maximally effective choline doses are also just beneath toxic levels, as observed here with many of the solvents. These similarities might suggest that the solvents and choline function in the same or a similar manner. Conversely, the dose/response curves of the different solvents and choline are clearly different in some respects, and, unlike choline, the organic solvents cannot be involved in neurotransmitter biosynthesis (see Hirata and Hadfield, 1986).

Larval responses to both excess K^+ (Yool *et al.*, 1986) and epinephrine (Hadfield, 1984) are more rapid (*i.e.*, some response within 24 h) than to solvents or choline, and the maximum percentages of larvae to respond to K^+ are higher (>90%) than for solvents or choline. These differences probably indicate that solvents, K^+, and epinephrine operate via different mechanisms. Nevertheless, solvents and K^+, at least, probably induce metamorphosis through relatively nonspecific interference in nervous function.

We have had the opportunity to test larvae of only one additional invertebrate species for a metamorphic response to an organic solvent. In these experiments, larvae of the gastropod *Crucibulum spinosum* readily metamorphosed in response to ethanol. While these results are very limited, they suggest that competent larvae of other invertebrate species may also metamorphose in response to solvents. If so, ethanol in particular may prove of use to larval culturists as a widely available and relatively cheap and non-toxic inducer of metamorphosis. Conversely, in laboratories where organic solvents are commonly used, larval biologists should be aware that contamination of solutions by organic solvents may cause unwanted metamorphoses of competent larvae.

Acknowledgments

We thank Sister Phyllis Plantenberg for making the observations which led to this paper, L. Ho-Iseke and S. Miller for help in the laboratory, and J. Bell for larvae of *Crucibulum spinosum*. The work was supported by NSF Grant DCB8602149 to M.G.H.

Literature Cited

Bell, J. L. 1988. Optimal feeding by gastropod larvae: patches and picoplankton. *Am. Zool.* **28:** 167A.

Browning, E. 1965. *Toxicity and Metabolism of Industrial Solvents.* Elsevier Pub., New York. 739 pp.

Burke, R. D. 1983. The induction of metamorphosis of marine invertebrate larvae: stimulus and response. *Can. J. Zool.* **61:** 1701–1719.

Cavanaugh, G. M. 1956. *Formulae and methods VI of the Marine Biological Laboratory Chemical Room, Woods Hole, Massachusetts.* Pp. 62–69.

Chia, F. S., and M. E. Rice, eds. 1978. *Settlement and Metamorphosis of Marine Invertebrate Larvae.* Elsevier/North-Holland, New York. 290 pp.

Crisp, D. J. 1974. Factors influencing the settlement of marine invertebrate larvae. Pp. 177–265 in *Chemoreception in Marine Organisms,* P. T. Grant and A. N. Mackie, eds. Academic Press, London.

Crisp, D. J. 1976. Settlement responses in marine organisms. Pp. 83–124 in *Adaptations to Environment: Essays on the Physiology of Marine Animals,* R. C. Newell, ed. Butterworths, London.

Galigher, A. E., and E. N. Kozloff. 1964. *Essentials of Practical Microtechnique.* Lea & Febiger, Philadelphia. 484 pp.

Hadfield, M. G. 1977. Chemical interactions in larval settling of a marine gastropod. Pp. 403–413 in *Marine Natural Products Chemistry,* D. J. Faulkner and W. H. Fenical, eds. Plenum Press, New York.

Hadfield, M. G. 1984. Settlement requirements of molluscan larvae: new data on chemical and genetic roles. *Aquaculture* **39:** 283–298.

Hadfield, M. G., and J. T. Pennington. In press. The nature of the metamorphic signal and its internal transduction in larvae of the nudibranch *Phestilla sibogae. Bull. Mar. Sci.* **46**(2).

Hirata, K. Y., and M. G. Hadfield. 1986. The role of choline in metamorphic induction of *Phestilla* (Gastropoda, Nudibranchia). *Comp. Biochem. Physiol.* **84C:** 15–21.

Meadows, P. S., and J. I. Campbell. 1972. Habitat selection by aquatic invertebrates. Pp. 271–361 in *Advances in Marine Biology,* F. S. Russell and M. Yonge, eds. Academic Press, London.

Miller, S. E., and M. G. Hadfield. 1986. Ontogeny of phototaxis and metamorphic competence in larvae of the nudibranch *Phestilla sibogae* Bergh (Gastropoda: Opisthobranchia). *J. Exp. Mar. Biol. Ecol.* **97:** 95–112.

Yool, A. J., S. M. Grau, M. G. Hadfield, R. A. Jensen, D. A. Markell, and D. E. Morse. 1986. Excess potassium induces larval metamorphosis in four marine invertebrate species. *Biol. Bull.* **170:** 255–266.

Reference: *Biol. Bull.* 177: 356–362. (December, 1989)

Population Structure, Larval Dispersal, and Gene Flow in the Queen Conch, *Strombus gigas*, of the Caribbean

JEFFRY B. MITTON[1], CARL J. BERG JR.[2,*], AND KATHERINE S. ORR[2,**]

[1]*Department of Environmental, Population and Organismic Biology, University of Colorado, Boulder, Colorado 80309, and* [2]*Marine Biological Laboratory, Woods Hole, Massachusetts 02543*

Abstract. Genetic variation from 8 polymorphic enzyme loci among 17 population samples of queen conch, *Strombus gigas*, exhibits similarity of allelic frequencies throughout the species distribution. Analyses of standardized variances of allelic frequencies and of the frequencies of private alleles indicate that gene flow among populations in the Caribbean must be high. However, analyses of allelic frequencies clearly demonstrate that the populations are not panmictic. Bermuda is isolated from Caribbean populations, and there are numerous further examples of heterogeneity of allelic frequencies among populations within island groups. Limited data suggest that normal conch and samba, a slower growing, melanic form, are genetically differentiated.

Introduction

Gene flow, defined as the movement of gametes or individuals from one place to another and incorporation of the genetic material into the recipient population, influences both the population structure and geographic distribution of a species, as well as the adaptation of populations to their local environments (Slatkin, 1987). Gene flow is usually seen as a homogenizing force, preventing the differentiation of populations that exchange gametes or individuals (Mayr, 1963, 1970). Exchange of an average of just one individual per generation will prevent the fixation of neutral alleles arising from mutations within a population, regardless of its size (Wright, 1931). The importance of gene flow to population structure was illustrated in a comparative study of the degrees of differentiation of populations of three species of *Littorina* differing in their modes of reproduction and potential for gene flow (Berger, 1973, 1983). Larval *L. littorea* are planktonic, and hence have a high potential for gene flow. The egg cases of *L. obtusata* are attached to algae, and the algae may be detached from the substate and carried about by tides. *Littorina saxatalis* is restricted to the high intertidal and is ovoviviparous; because the eggs develop in the female until the juvenile adult stage, this species has little opportunity for gene flow. The potential for gene flow predicts the magnitude of genetic differentiation among populations. Populations of *L. littorea* are relatively homogeneous, populations of *L. saxatalis* are well differentiated, and populations of *L. obtusata* are intermediate in their degree of differentiation.

It is difficult to measure gene flow directly, so many biologists infer levels of gene flow from distances of migration or the potential for dispersal. But for several reasons these inferences can be seriously misleading. First, the movement of gametes and individuals may seriously overestimate gene flow. For example, pine pollen can be collected by ships 50 km from shore, yet studies of gene flow by pine pollen suggest that most genes move only a few dozen meters (Levin and Kerster, 1974). Pollen moving great distances may not reach receptive surfaces, or, having reached receptive surfaces, may have lost viability. Similarly, the flight of *Euphydryas* butterflies attests the potential for long distance dispersal, yet empirical studies reveal little or no gene flow among populations (Ehrlich *et al.*, 1975). Clearly, the distances that individuals can move and the distances that genes typically move can be profoundly disparate.

Second, the homogenizing effect of gene flow may be overridden by natural selection (Endler, 1973, 1977). A

Received 3 October 1988; accepted 18 September 1989.

* Current address: Florida Marine Research Institute, Florida Department of Natural Resources, 13365 Overseas Highway, Marathon, Florida 33050.

** Current address: 297 Anglers Drive N., Marathon, Florida 33050.

clear example has been described for the leucine aminopeptidase (Lap) polymorphism in the blue mussel, *Mytilus edulis* (Koehn and Hilbish, 1987). Mussels from estuarine and oceanic environments are differentiated at the Lap locus (Koehn *et al.*, 1976), which plays a direct role in adaptation to salinity (Koehn *et al.* 1980a; Hilbish and Koehn 1985). Populations at the eastern edge of Long Island Sound exhibit a steep cline in allelic frequency between estuarine and oceanic salinities. In the spring and early summer, tidal currents disperse planktonic larvae, obscuring the cline in allelic frequencies. Each fall, differential mortality weeds out ill-adapted genotypes, restoring the abrupt cline in frequencies (Koehn *et al.*, 1980b). A similar example can be taken from the American eel, *Anguilla rostrata* (Williams *et al.*, 1973). Although planktonic larvae from a single breeding pool are distributed by currents to the rivers of eastern North America, the environments vary from subtropical to cold temperate. Despite the redistribution of larvae each generation, several loci exhibit stable clinal variation with latitude.

Estimates of gene flow can be either direct or indirect (Slatkin, 1987). Direct methods involve tracing the dispersal of individuals, either through observation or by tagging and recapture, and subsequent estimates of reproductive success. While these methods may be applied to some species (*e.g.*, large mammals), direct methods cannot be applied to the planktonic larvae of marine organisms. Indirect methods use geographic patterns of genetic variation to infer the amount of migration that must have occurred to produce the existing pattern. Direct methods estimate the gene flow for the period of observation, but can give no indication of temporal fluctuations in gene flow through time. Indirect methods assess the cumulative effect of gene flow among populations. Consequently, indirect methods typically return higher estimates of gene flow than direct methods (Slatkin, 1987).

Here we report a study of the population structure and gene flow of a marine mesogastropod mollusk, the queen conch, *Strombus gigas* L. Laboratory studies (Ballantine and Appeldoorn, 1983; Davis and Hesse, 1983) suggest that the planktonic larvae can be dispersed by ocean currents for 12–35 days. Caribbean currents that could result in long range dispersal have typical speeds of 20–80 cm s^{-1}, but mesoscale eddies are also present that could entrain larvae and restrict their net transport (Kinder *et al.*, 1985; Lessios *et al.*, 1984). Protracted periods of larval dispersal suggest the possibility of extensive dispersal that could result in gene flow among populations in different regions of the Caribbean. In addition to describing the population structure of *S. gigas*, we have used the data on population structure to infer gene flow.

Figure 1. Collection localities for genetic studies of queen conch. 1, Bermuda; 2, Turks and Caicos Islands; 3, St. Kitts (Saint Christopher) 4, Nevis; 5, St. Lucia; 6, Bequia; 7, Grenadines; 8, Barbados; 9, Belize.

Materials and Methods

Population samples were taken throughout the range of *Strombus gigas* (Fig. 1). With the aid of fishermen and fisheries personnel, conchs were obtained by snorkeling and scuba diving. From the Atlantic we sampled the outlying populations in Oistens, Barbados, North Rock, and Bermuda. From the western Caribbean, at Ambergris Cay in Belize, we sampled both normal queen conch and the melanic morph, called samba conch. In the Turks and Caicos Is., conchs were sampled from Pine Cay, Plandon Cay, Six Hill Cay, and a samba group at French Cay. Samples were taken from the channel off Bequia, Butler's on Nevis, and at Major's Bay and Basse-Terre on St. Kitts. On St. Lucia, population samples were taken from the northern (Gros Islet) and the southern (Vieux Fort) tips of the island. Samples were collected from Saline Cay, Petit St. Vincent, and L'Esterre in the Grenadines.

At all collection localities, animals were removed from their shells and the most distal tips of the digestive glands and gonads were excised, placed in 2-cc plastic vials with screw tops, and submersed in liquid nitrogen. These samples were shipped on dry ice to the laboratory, where they were stored at −70°C. An equal volume of grinding buffer (Place and Powers, 1978) was added prior to homogenization with ultra sound. Homogenates were absorbed onto Watman #1 paper wicks and inserted into starch gels.

Variation at 18 enzyme systems was assayed with horizontal starch gel electrophoresis using a series of buffer systems. The systems most useful for resolving polymorphic loci were (1) the discontinuous lithium hydroxide

buffer, pH 8.1–8.4, of Selander *et al.* (1971), (2) the discontinuous lithium hydroxide, pH 8.5, of O'Malley *et al.* (1979), and (3) the continuous tris citrate buffer, pH 6.3–6.7, of Selander *et al.* (1971).

Seven of the 18 loci were polymorphic, and these are used here to describe the population structure of *Strombus gigas*. Their names, abbreviations, and the buffer systems used to resolve them are as follows: 6-phosphogluconate dehydrogenase, 6Pgd, buffer 3; phosphoglucomutase, Pgm-1, buffer 2; phosphoglucomutase, Pgm-2, buffer 1; glycerate dehydrogenase, Gdh, buffer 2; aminopeptidase, Ap, buffer 1; leucine aminopeptidase, Lap, buffer 2; malate dehydrogenase, Mdh, buffer 3. Alleles were numbered by electrophoretic mobility, with the fastest migrating allele designated "1."

Our stain for phosphoglucomutase is similar to that of Shaw and Prasad (1970) except that we used a form of glucose-6-phosphate dehydrogenase that is more active with NAD than with NADP (Sigma G 5760). Pgm-1 stained quite well with only NAD, but Pgm-2 had insufficient activity with NAD, and good activity with NADP. Our stain for glycerate dehydrogenase was the same as any other NAD-dependent dehydrogenase, but the substrate solution was made as follows: 0.2 g glyceric acid plus 0.5 g L-histidine dissolved in 50 ml water, adjusted to pH 9.0 with 1 *M* NAOH.

Heterogeneity of allelic frequencies was tested as in Workman and Niswander (1970). F_{st}, a standardized measure of variation in allelic frequencies, was calculated as

$$F_{st} = S^2/p(1 - p) \qquad (1)$$

where S^2 is the observed variance in allelic frequencies among localities, and p is the mean allelic frequency. Nm, the product of population size and migration rate, is estimated, following Slatkin (1985a, b, 1987), as

$$Nm = (1/F_{st} - 1)/4 \qquad (2)$$

Thus, genetic variation at each polymorphic locus is used to estimate the number of individuals exchanged between populations each generation.

Results

Macrogeographic variation

Two alleles were segregating at Pgm-1, Ap, and Mdh. A rare (0.03) fast allele was found at 6Pgd, but only at Gros Islet on St. Lucia. A slow allele at Pgm-2 was found at Bermuda and Barbados, but these alleles appeared in single heterozygotes. Four alleles were detected at Gdh. At all localities the slow allele was most common, and in some localities, it was the only allele present. A single very slow allele was detected at Basse-Terre, St. Kitts; this allele was not found at other localities. The fast and medium alleles had similar mobilities, and their similarity, in combination with the low activity of this locus, made it difficult to differentiate these alleles. For a conservative estimate of differentiation of populations, the fast and medium alleles at Gdh were pooled (Table I). A rare, slow allele at the Ap locus appeared in one individual from Barbados, but nowhere else. Allelic frequencies for the 7 polymorphic loci in 17 population samples are summarized in Table I.

Although the differentiation of allelic frequencies among populations is generally statistically significant, most populations are quite similar. For example, the same allele is generally the most abundant at all collection localities (minor exceptions are 6Pgdh and Ap at Vieux Fort, St. Lucia, and Ap at Bermuda). Thus, a first impression from Table I is of general genetic similarity of populations throughout the range of *Strombus gigas*.

Gene flow

In addition to the allelic frequencies, F_{st} and the derived estimate of Nm for each locus are also presented in Table I. Values of Nm for 6Pgd, Pgm-1, Pgm-2, Gdh, Ap, Lap, and Mdh are 6.4, 11.5, 19.0, 2.9, 12.9, 1.5, and 0.9, respectively. The geographic distribution of genetic variation at Mdh is patchy, for there is a substantial level of genetic variation in Bermuda, but little variation within the Caribbean. If Bermuda is dropped from this analysis, the value of Nm for Mdh jumps to 6.8. The disparity in these estimates suggests that Bermuda is isolated from populations in the Caribbean. Using the second estimate, the mean value for Nm is 8.7.

Private alleles, defined as allelic variants restricted to single populations (Neel, 1973), may be used to estimate Nm using the formula of Slatkin (1985a):

$$\ln (p) = -.505 * \ln (Nm) - 2.44 \qquad (3)$$

in which p is the average frequency of private alleles, N is population size, and m is the migration rate. Three alleles appear to be candidates for private alleles. A very fast allele at 6Pgd reaches a frequency of 0.051 in Gros Islet, St. Lucia, a very slow allele at Gdh has a frequency of 0.01 in Basse-Terre, St. Kitts, and a very slow allele at Ap has a frequency of .018 at Oistens, Barbados. When the mean of these frequencies (.026) is used in Equation 3, the estimate of Nm is 11.0. Both this estimate and the estimate derived from Equation 2 (Nm = 8.7) suggest that gene flow is or has been relatively high throughout the range of this species.

Allelic frequencies in Bermuda are representative of the Caribbean populations for 6Pgd, Pgm-1, Pgm-2, Ap, and Gdh. But the allelic frequencies of Lap and Mdh are both outside the range seen in the Caribbean (Table I). For example, the frequency of the fast allele is .30 in Ber-

Table I

Allelic frequencies, Fst and Nm, in queen conch

		6Pgd			Pgm-1		Pgm-2			Gdh			Ap			Lap		Mdh	
Locality allele	n	1	2	3	1	2	1	2	3	1+2	3	4	1	2	3	1	2	1	2
Bermuda	41	.00	.25	.75	.23	.77	.31	.68	.01	.28	.72	.00	.51	.49	.00	.38	.62	.30	.70
Turks & Caicos																			
Pine Cay	56	.00	.28	.72	.44	.56	.40	.60	.00	.28	.72	.00	.47	.53	.00	—	—	.00	1.00
French Cay	53	.00	.36	.64	.28	.72	.31	.69	.00	.16	.84	.00	.44	.56	.00	—	—	.00	1.00
Plandon Cay	40	.00	.28	.72	.35	.65	—	—	—	.23	.77	.00	.39	.61	.00	—	—	.00	1.00
Six Hill Cay	25	.00	.30	.70	.20	.80	—	—	—	.30	.70	.00	.23	.77	.00	.06	.94	—	—
St. Kitts																			
Major's Bay	31	.00	.42	.58	.35	.65	.35	.65	.00	.04	.96	.00	.42	.58	.00	.00	1.00	—	—
Basse-Terre	48	.00	.25	.75	.35	.65	—	—	—	.04	.95	.01	—	—	—	.23	.77	—	—
Nevis	48	.00	.29	.71	.32	.68	.32	.68	.00	.19	.81	.00	.46	.54	.00	—	—	—	—
St. Lucia																			
Gros Islet	71	.03	.31	.66	.42	.58	.47	.57	.00	.34	.66	.00	.44	.56	.00	.23	.77	.04	.96
Vieux Fort	48	.00	.51	.49	.39	.61	.32	.68	.00	.00	1.00	.00	.52	.48	.00	.31	.69	.02	.98
Bequia	29	.00	.21	.79	—	—	.36	.64	.00	—	—	—	.38	.62	.00	—	—	.00	1.00
Grenadines																			
Petit St. Vincent	47	.00	.33	.67	.24	.76	—	—	—	—	—	—	.48	.52	.00	.25	.75	.00	1.00
Saline Cay	63	.00	.33	.67	.33	.67	—	—	—	.02	.98	.00	.42	.58	.00	.24	.76	.00	1.00
L'Esterre	40	.00	.21	.79	.38	.62	—	—	—	.17	.83	.00	.41	.59	.00	—	—	.00	1.00
Barbados	27	.00	.30	.70	.29	.71	.31	.68	.01	.40	.60	.00	.48	.50	.02	—	—	.05	.95
Belize																			
(normal)	24	.00	.28	.72	.27	.73	—	—	—	.17	.83	.00	.44	.56	.00	.00	1.00	.00	1.00
(samba)	23	.00	.32	.68	.33	.67	—	—	—	.24	.76	.00	.49	.51	.00	.00	1.00	.00	1.00
Mean allelic frequency		.00	.31	.69	.32	.68	.35	.65	.00	.19	.81	.00	.44	.56	.00	.17	.83	.03	.97
F_{st}			.038		.021		.013			.080			.019			.142		.220	
Nm			6.4		11.5		19.0			2.9			12.9			1.5		0.9 (6.8)	

Note: — indicates missing data. Value in parentheses for Nm was calculated excluding Bermuda. Alleles are listed in decreasing eletrophoretic mobility.

muda, but this allele is not seen in most of the Caribbean populations, and where it is found it does not have frequencies higher than 0.05. Once again, these data suggest that Bermuda is isolated from the Caribbean populations.

Microgeographic variation

Although gene frequencies at most loci do not differ strikingly among populations, and the estimate of gene flow is estimated to be relatively high, allelic frequencies at some loci are heterogeneous among population samples taken within island groups (Table II). For example, St. Lucia is a small, oval island, and although Gros Islet and Vieux Fort are localities at opposite ends of the island, they are only 40 km apart. Despite this geographic proximity, the population samples from these localities were significantly differentiated for 6Pgd, Pgm-2, and Gdh. Similarly, Pgm-1 and Ap allelic frequencies were heterogeneous in the Turks and Caicos, and 6Pgd, Gdh, and Lap allelic frequencies were heterogeneous in St. Kitts and Nevis. In the Grenadines, allelic frequencies at Gdh were heterogeneous. Thus, there are numerous examples of microgeographic variation within island groups.

Samba

In Belize, we collected samples of both normal conch and samba, a smaller, melanic form that is generally shunned by fishermen because of its size and dark meat. Allelic frequencies are similar for these samples for all loci except Gdh. Table I presents the sum of alleles 1 and 2, but the frequencies of these alleles differ between the

Table II

Tests of homogeneity of allelic frequencies within island groups in queen conch

Area	Locality	6Pgd	Pgm-1	Pgm-2	Gdh	Ap	Lap	Mdh
Turks and Caicos	Pine Cay French Cay Plandon Cay Six Hill Cay	NS	*	NS	NS	*	—	NS
St. Kitts and Nevis	Basse-Terre Major's Bay Butlers	*	NS	NS	**	NS	**	—
St. Lucia	Gros Islet Vieux Fort	**	NS	*	***	NS	NS	NS
Grenadines	Petit St. Vincent Saline Cay L'Esterre	NS	NS	—	***	NS	NS	—

Note: — indicates missing data. *= $P < .05$, **= $P < .01$, ***= $P < .001$.

morphs. For samba, the frequencies (and standard errors) of alleles 1, 2, and 3 are 0.22 (0.06), 0.02 (0.02), and 0.76 (0.06), while the corresponding frequencies for the normal conch are 0.00, 0.17 (.05), and 0.83 (0.05). The samba and the normal conch do not appear to be random samples from a randomly mating population ($P < 0.01$). We also sampled samba from French Cay, but all of the mature animals obtained were samba, so we could not replicate the comparison of normal and samba conch from Belize. Samples from other localities in the Turks and Caicos contain only normal conchs. There are differences between French Cay and the other Cays in the Turks and Caicos, especially at Gdh and 6Pgd, but these might be attributable to microgeographic variation rather than differentiation of normal and samba conch.

Discussion

Marine molluscs with planktonic larvae are known for their capacity to disperse, yet their effective range of dispersal may be much more limited than their presence in the plankton implies (Scheltema, 1971). Transoceanic dispersal of larvae has been suggested (Scheltema, 1971, 1972, 1978, 1986a, b; Pechenik *et al.*, 1984; Scheltema and Williams, 1983), but the crucial question—whether significant proportions of the larvae found in the middle of the ocean are capable of metamorphosis and survival, and contribute significantly to down-stream gene pools—has not been answered (Laursen, 1981). Unfortunately, studies of gene flow have not been carried out on teleplanic species. The advent of biochemical genetic techniques and modern statistical methods (*e.g.*, Slatkin, 1985a, b) now makes this possible.

Larvae attributed to the genus *Strombus* have been collected from both nearshore (Berg, 1975, 1976, and unpub. data) and oceanic waters (Laursen, 1981; Scheltema, pers. comm.) of the Atlantic and Pacific oceans. The effective duration of larval life under normal planktonic conditions is unknown. D'Asaro (1970) reared *S. gigas* larvae for 60 to 75 days on natural phytoplankton supplemented with laboratory reared species, but no conch metamorphosed and it is not known if the larvae were competent to do so. Repeated rearings of extensive numbers of larvae in laboratories throughout the Caribbean have shown that metamorphosis occurs between 12 days (Ballantine and Appledoorn, 1983) and 35 days (Davis and Hesse, 1983), with an average duration of 21 days. Thus, larvae of *S. gigas* have the potential to be transported throughout the Caribbean. Extensive gene flow throughout the Caribbean is consistent with the similarity of allelic frequencies in that region (Table I).

Estimates of Nm derived from F_{st} and from the frequency of private alleles are concordant, and they are also in agreement with predictions based on the life history of this species. The extended larval stage provides the potential for long distance dispersal, and the population structure of *S. gigas* indicates either that dispersal among localities is relatively common (on the order of 10 individuals exchanged among localities per generation), or was so in the recent past.

Although extensive gene flow is suggested, conchs are certainly not a single randomly mating population, for there are clear discontinuities in allelic frequencies. For example, Bermuda appears to be isolated from the populations in the Caribbean. Currents from the Caribbean and Gulf of Mexico sweep past the Florida Keys as the Florida Current and then north along the Atlantic coast as the Gulf Stream, passing far west of Bermuda in an arc northeastward to form the North Atlantic drift. Gulf Stream rings occasionally approach Bermuda (Robinson, 1983; Hogg *et al.*, 1978) bearing other teleplanic lar-

vae (Scheltema, 1986b), but it is not known if they carry *Strombus* larvae. As might be predicted, decimated conch stocks in Bermuda have not recovered despite 10 years of protection. Abbott and Jensen (1967) report cyclic disappearances of species in shell collections from Bermuda over the previous 110 years, including the congeneric *S. costatus*, which has a larval period similar to that of *S. gigas* (Brownell, 1977; Ballantine and Appeldoorn, 1983). Although *Strombus alatus* is the most common species of *Strombus* in northern areas and its planktonic larvae occur in the neritic waters off North Carolina (Thiriot-Quievreux 1983), it disappeared from Bermuda sometime since the Pleistocene, when glaciers forced the Gulf Stream to the south and into a more east-west orientation, bringing it closer to Bermuda (Keffer *et al.*, 1988). Bermuda now lies in the central oceanic gyre of the North Atlantic, more than 1500 km from the Gulf Stream. It is doubtful that viable larvae of the genus *Strombus* are ever carried to Bermuda and therefore the population in Bermuda must be self sustaining. The same may be true for the upstream population on Barbados that exhibits rare slow alleles at Pgm-2 and Ap. The population around Barbados was decimated in the 1930's and has never regained its previous size. Consequently, traditional recipes for its cooking have been lost to native cooks. Animals are breeding around both of these islands (Berg, pers. obs.), and retention of their offspring in local circulations (Farmer and Berg, in press) may be sufficient to maintain the populations at low densities.

Unlike Bermuda and Barbados, the Turks and Caicos Islands, Cuba, and the Bahamas are all downstream of the eastern Caribbean conch populations and appear to experience high annual recruitment. These populations support large fisheries, but even when decimated by over fishing they recover quickly if management measures are followed (Munoz *et al.*, 1987; Berg, pers. obs.).

Variation among islands within archipelagos is apparent in our samples taken from the Turks and Caicos, St. Kitts and Nevis, St. Lucia, and the Grenadines. St. Lucia is an elipse with a long axis (north-south) perpendicular to prevailing winds and strong ocean currents (Kinder *et al.*, 1985). Despite the close proximity of Gros Islet and Vieux Fort, and the lack of obvious differences in habitat or gross morphology of *S. gigas* from these two areas, their populations are significantly differentiated. A possible explanation may be that the east-west currents prohibit exchange of larvae between these localities; mixing of larvae may occur far in the lee of islands, but not near shore. Eddies formed in the lee of islands (Emery, 1972) and current reversals (Mazeika *et al.*, 1983) could retain larvae and allow differentiation in these upstream areas, while downstream populations may receive larvae from many sources. Complex currents may restrict gene flow among localities in close proximity in other areas of the Caribbean.

Acknowledgments

We would like to thank the many people in the islands who helped with the collection of samples used in this study. These include the personnel of Bermuda Division of Fisheries, the Fisheries Department of St. Kitts/Nevis, the Fisheries Management Unit of St. Lucia, the Belize Fisheries Unit, the Bellairs Research Institute, and numerous divers and boatmen including Paul Hudson, Julius Jennings, Ken Gonzales, Mel Goodwin, and others from Bequia, the Grenadines, and Barbados. Dr. Sheldon Segal offered both encouragement and financial support when it was needed most.

Dr. Terrie Bert provided a critical review of a draft of the manuscript.

This project was supported by funds from the World Wildlife Fund—U. S., the Rockefeller Foundation, the Oakleigh L. Thorne Foundation, the National Geographic Society, and by a John Simon Guggenheim Fellowship to J. B. M.

Literature Cited

Abbott, R. T., and R. Jensen. 1967. Molluscan faunal changes around Bermuda. *Science* **155:** 687–688.

Ballantine, D. L., and R. S. Appeldoorn. 1983. Queen conch culture and future prospects in Puerto Rico. *Proc. Gulf Caribbean Fish. Inst.* **35:** 57–63.

Berg, C. J., Jr. 1975. Behavior and ecology of conch (Superfamily Strombacea) on a deep subtidal algal plain. *Bull. Mar. Sci.* **25:** 307–317.

Berg, C. J., Jr. 1976. Growth of the queen conch *Strombus gigas*, with a discussion of the practicality of its mariculture. *Mar. Biol. (Berl.)* **34:** 191–199.

Berger, E. 1973. Gene-enzyme variation in three sympatric species of *Littorina*. *Biol. Bull.* **145:** 83–90.

Berger, E. M. 1983. Population genetics of marine gastropods and bivalves. In *The Mollusca*. W. D. Russell-Hunter, ed. Academic Press, New York. **6:** 563–596.

Brownell, W. N. 1977. Reproduction, laboratory culture, and growth of *Strombus gigas*, *S. costatus*, and *S. pugilus* in Los Roques, Venezuela. *Bull. Mar. Sci.* **27:** 668–680.

Davis, M., and C. Hesse. 1983. Third world level conch mariculture in the Turks and Caicos Islands. *Gulf Caribbean Fish. Inst.* **35:** 73–82.

D'Asaro, C. N. 1970. Egg capsules of prosobranch mollusks from South Florida and the Bahamas and notes on spawning in the laboratory. *Bull. Mar. Sci.* **20:** 414–440.

Ehrlich, P. R., R. A. White, M. C. Singer, S. W. McKechnie, and L. E. Gilbert. 1975. Checkerspot butterflies: a historical perspective. *Science* **188:** 221–228.

Emery, A. R. 1972. Eddy formation from an oceanic island: ecological effects. *Carib. J. Sci.* **12:** 121–124.

Endler, J. A. 1973. Gene flow and population differentiation. *Science* **179:** 243–250.

Endler, J. A. 1977. *Geographic Variation, Speciation, and Clines.* Princeton University Press, Princeton, NJ.

Farmer, M. W., and C. J. Berg Jr. Circulation around islands and gene flow. *Proc. Gulf Caribbean Fish. Inst.* (in press).

Hilbish, T. J., and R. K. Koehn. 1985. Dominance in physiological phenotypes and fitness at an enzyme locus. *Science* **229:** 52–54.

Hogg, N. G., E. J. Katz, and T. B. Sanford. 1978. Eddies, islands, and mixing. *J. Geophy. Res.* **83:** 2921–2938.

Keffer, T., D. G. Martinson, and B. H. Corliss. 1988. The position of the Gulf Stream during quaternary glaciations. *Science* **241:** 440–442.

Kinder, T. H., G. W. Hebrun, and A. W. Green. 1985. Some aspects of the Caribbean circulation. *Mar. Geol.* **68:** 25–52.

Koehn, R. K., B. L. Bayne, M. N. Moore, and J. F. Siebenaller. 1980. Salinity related physiological and genetic differences between populations of *Mytilus edulis*. *Biol. J. Linnean Soc.* **14:** 319–334.

Koehn, R. K., and T. J. Hilbish. 1987. The adaptive importance of genetic variation. *Am. Sci.* **75:** 134–140.

Koehn, R. K., R. Milkman, and J. B. Mitton. 1976. Population genetics of marine pelecypods. IV. Selection, migration and genetic differentiation in the blue mussel *Mytilus edulis*. *Evolution* **30:** 2–32.

Koehn, R. K., R. I. E. Newell, and F. Immerman. 1980b. Maintenance of an aminopeptidase allele frequency cline by natural selection. *Proc. Natl. Acad. Sci. USA* **77:** 5385–5389.

Laursen, D. 1981. Taxonomy and distribution of teleplanic prosobranch larvae in the North Atlantic. *Dana Rept.* **89.** 43 pp, 3 plts.

Lessios, H. A., D. R. Robertson, and J. D. Cubit. 1984. Spread of *Diadema* mass mortality through the Caribbean. *Science* **226:** 335–337.

Levin, D. A., and H. W. Kerster. 1974. Gene flow in seed plants. *Evol. Biol.* **7:** 139–220.

Mayr, E. 1963. *Animal Species and Evolution.* Harvard University Press, Cambridge, Mass.

Mayr, E. 1970. *Populations, Species, and Evolution* Harvard University Press, Cambridge, Mass.

Mazeika, P. A., T. H. Kinder, and D. A. Burns. 1983. Measurements of subtidal flow in passages of the Lesser Antilles. *J. Geophys. Res.* **88**(c7): 4483–4488.

Munoz, L., P. Alcolado, I. Fraga, and P. Llorente. 1987. Status of populations and fisheries of *Strombus gigas* in Cuba, with some results of juvenile rearing in pens. *Proc. Gulf. Carib. Fish. Inst.* **38:** 353–361.

Neel, J. V. 1973. "Private" genetic variants and the frequency of mutation among South American Indians. *Proc. Natl. Acad. Sci. USA* **70:** 3311–3315.

O'Malley, D. M., F. W. Allendorf, and G. M. Blake. 1979. Inheritance of isozyme variation and heterozygosity in ponderosa pine. *Biochem. Genet.* **17:** 233–250.

Pechenik, J. A., R. S. Scheltema, and L. S. Eyster. 1984. Growth stasis and limited shell calcification in larvae of *Cymatium parthenopeum* during trans-Atlantic transport. *Science* **224:** 1097–1099.

Place, A. R., and D. A. Powers. 1978. Genetic bases for protein polymorphism in *Fundulus heteroclitus* (L.). I. Lactate dehydrogenase (Ldh-B), malate dehydrogenase (Mdh-A), glucosephosphate isomerase (Gpi-B), and phosphoglucomutase (Pgm-A). *Biochem. Genet.* **16:** 577–591.

Robinson, A. R. 1983. *Eddies in Marine Science.* Springer-Verlag, New York, 609 pp.

Scheltema, R. S. 1971. Larval dispersal as a means of genetic exchange between geographically separated populations of shallow-water benthic marine gastropods. *Biol Bull* **140:** 284–322.

Scheltema, R. S. 1972. Dispersal of larvae as a means of genetic exchange between widely separated populations of shoal-water benthic invertebrate species. *Fifth Eur. Mar. Biol. Symp., Padua.* Pp. 101–114.

Scheltema, R. S. 1978. On the relationship between dispersal of pelagic larvae and the evolution of marine prosobranch gastropods. Pp. 391–397 in *Marine Organisms—Genetics, Ecology and Evolution,* B. Battaglia and J. A. Beardmore, eds. Plenum, New York.

Scheltema, R. S. 1986a. Long distance dispersal by planktonic larvae of shoal-water benthic invertebrates among Central Pacific Islands. *Bull. Mar. Sci.* **39:** 241–256.

Scheltema, R. S. 1986b. On dispersal and planktonic larvae of benthic invertebrates: an eclectic overview and summary of problems. *Bull. Mar. Sci.* **39:** 290–322.

Scheltema, R. S., and I. P. Williams. 1983. Long-distance dispersal of planktonic larvae and the biogeography and evolution of some polynesian and western pacific mollusks. *Bull. Mar. Sci.* **33:** 545–565.

Selander, R. K., M. H. Smith, S. Y. Yang, and W. E. Johnson. 1971. Biochemical polymorphism and systematics in the genus *Peromyscus.* I. Variation in the old-field mouse *Peromyscus polionotus.* Pp. 49–90 in *Studies in Genetics VI,* M. R. Wheeler, ed. University of Texas Press, Austin.

Shaw, C. R., and R. Prasad. 1970. Starch gel electrophoresis of enzymes—a compilation of recipes. *Biochem. Genet.* **4:** 297–320.

Slatkin, M. 1985a. Rare alleles as indicators of gene flow. *Evolution* **39:** 53–65.

Slatkin, M. 1985b. Gene flow in natural populations. *Ann. Rev. Ecol. Syst* **16:** 393–430.

Slatkin, M. 1987. Gene flow and the geographic structure of natural populations. *Science* **236:** 787–792.

Thiriot-Quievreux, C. 1983. Summer meroplanktonic prosobranch larvae occurring off Beaufort, North Carolina. *Estuaries* **6:** 387–398.

Williams, G. C., R. K. Koehn, and J. B. Mitton. 1973. Genetic differentiation without isolation in the American eel, *Anguilla rostrata*. *Evolution* **27:** 192–204.

Workman, P. L., and J. D. Niswander. 1970. Population studies on southwestern Indian tribes. II. Local differentiation in the Papago. *Am. J. Hum. Genet.* **22:** 24–29.

Wright, S. 1931. Evolution in Mendelian populations. *Genetics* **16:** 97–159.

Reference: *Biol. Bull.* 177: 363–371. (December, 1989)

Hindsight and Rapid Escape in a Freshwater Oligochaete

C. D. DREWES[1] AND C. R. FOURTNER[2]

[1]*Department of Zoology, Iowa State University, Ames, Iowa 50011, and* [2]*Department of Biological Sciences, State University of New York at Buffalo, Buffalo, New York 14260*

Abstract. A novel escape reflex involving the posterior end of a freshwater oligochaete worm, *Lumbriculus variegatus*, is described. Electrophysiological recordings and videotape analysis from submersed, freely behaving worms show that either a moving shadow or sudden decrease in light intensity evokes repetitive spiking in lateral giant nerve fibers (LGFs) and rapid tail withdrawal when the worm's posterior end is positioned at the air-water interface, to facilitate gas exchange. Because comparable electrical and behavioral response patterns occur in isolated posterior body fragments, but not in midbody or anterior fragments, we conclude that the LGF shadow-sensitivity is localized in posterior segments. Added support for this idea is provided by electron microscopic observations demonstrating the presence of candidate photoreceptor cells in the epidermis of posterior segments. These cells are invaginated distally to form a cavity (phaosome) filled with microvilli, and resemble the known photoreceptors in anterior segments of earthworms and leeches.

Introduction

Rapid escape responses to stimulus modalities such as touch and substrate vibration are widespread in polychaete and oligochaete worms (Mill, 1975, 1978; Dorsett, 1978, 1980; Drewes, 1984). However, relatively few annelid species exhibit rapid escape responses to photic stimulation (Steven, 1963; Mill, 1978), and these have not been extensively studied.

Examples of polychaetes with photically activated escape responses include several species of nereids (Clark, 1960; Evans, 1969, Gwilliam, 1969), sabellids, and most serpulids (Nicol, 1948, 1950; Krasne, 1965). In all of these groups, key features of the responses are: (1) adequacy of abrupt decreases, but usually not increases, in light intensity for eliciting escape; (2) localization of photosensitivity into anterior segments; (3) rapid withdrawal of the worm's anterior end or branchial crown which is often modified for respiration as well as feeding; (4) apparent mediation of escape by giant nerve fibers; and (5) rapid habituation with repeated stimuli.

Although rapid escape reactions to mechanosensory modalities exist in many species of terrestrial and freshwater oligochaetes (Drewes *et al.*, 1983; Drewes, 1984; Zoran and Drewes, 1987), escape sensitivity to the modality of light appears to be rare. Although behavioral observations (Darwin, 1881; Hess, 1925; Nomura, 1926; Unteutsch, 1937; Howell, 1939), suggest that at least a few earthworm species withdraw their anterior ends when stimulated by sudden changes in background illumination, the possibility that such reactions may be mediated by giant nerve fibers has not been studied.

In this study we provide the first correlated electrophysiological and behavioral description of a rapid escape response to photic stimulation in an oligochaete worm. The worm, *Lumbriculus variegatus*, lives in the shallow margins of ponds, and conspicuously positions its tail segments at the air-water interface to facilitate gas exchange via the dorsal blood vessel. We show that the worm's tail is rapidly withdrawn in response to an abrupt decrease in light intensity or moving shadow, that sensitivity to such stimuli is restricted to posterior segments, and that such tail responses appear to be mediated by the lateral giant nerve fiber system. We have used electrophysiological and video recordings *in situ* to characterize the timing of electrical and behavioral events during shadow-evoked escape, and have compared these to touch-evoked responses. In addition, we have identified

Received 5 June 1989; accepted 24 August 1989.

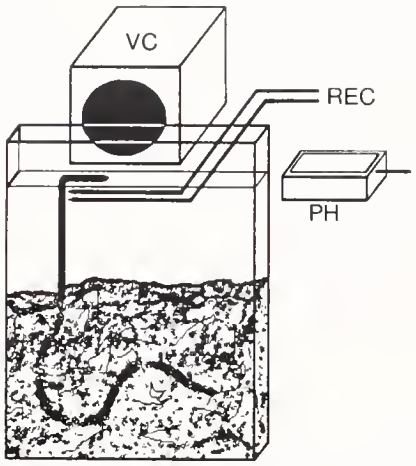

Figure 1. Test chamber for recording electrical and behavioral correlates of rapid escape in intact worms. The worm's tail protruded above the sediments and laid horizontally at the air-water interface. Recording electrodes (REC), submersed in the water and next to the tail, detected giant nerve fiber spikes while the video camera (VC) recorded escape movements. The photocell (PH) detected changes in the intensity of lighting from above.

candidate photoreceptor and mechanoreceptor cells in tail segments of the worm.

Materials and Methods

Animals

Freshly collected and fully grown specimens of *Lumbriculus variegatus* (Order Lumbriculida; Family Lumbriculidae) were used in all experiments. The average length of worms ranged from 5 to 7 cm and from 0.5 to 1.0 mm in diameter. The worms were collected during June–August from a pond adjacent to West Lake Okoboji (Gull Point), Iowa, and maintained as laboratory colonies in bowls containing debris (*i.e.*, leaf litter, wood fragments, and sediment) from the natural habitat. The water level was adjusted to approximately 3 cm above the debris, thus simulating typical habitat conditions. No aeration or supplemental food was provided.

Escape reflexes in intact worms

Worms were placed into individual glass-walled test chambers (75 mm high, 25 mm wide, 7 mm deep) containing debris from the natural habitat (Fig. 1). The water level was adjusted to 2–3 cm above the debris, and the chamber was placed on shock absorbing material.

Electrical recordings were obtained by mounting a pair of teflon-coated silver wire electrodes (0.01 inch diameter; 2 mm spacing between electrode tips) on a micromanipulator, immersing the electrodes into the water, and positioning the uninsulated electrode tips to within 1 mm of the worm's posterior end. Recorded activity was amplified (AC coupling; differential inputs), filtered, and displayed on an oscilloscope using a Tektronix 5D10 waveform digitizer. The digitized displays were either photographed on the oscilloscope screen or transferred, in analog form, from the digitizer to a chart recorder.

To study responses to a moving shadow, the test chamber was illuminated with four 15-W white fluorescent lamps placed 0.5 m above the water level. A moving shadow was created by interrupting the light path with a black shade attached to the end of a rigid arm. The arm was mounted on the rotating post of a pen driver motor driven by ramp voltages from a waveform generator.

Responses to abrupt decreases in light intensity were studied using a video camera (Panasonic Model WV-1400), fitted with a 100-mm camera lens and positioned at the side of the chamber. In addition to the main lighting previously described, a weakly lit white backdrop was positioned behind the chamber, providing sufficient contrast for videotaping escape movements even without the main lighting. The intensity of this lighting combination was 90-ft candles at the level of the water surface. The test stimulus was delivered by remotely switching off power to the main lighting, causing an abrupt decrease in light intensity to 6-ft candles at the water level. Stimulus onset was detected with a photocell, and interstimulus intervals were 30 min. All tests were at room temperature (22–24°C).

Escape responses in isolated body fragments

Since asexual reproduction by fragmentation is common in this species, most body fragments survive and regenerate into complete worms within several weeks. Body fragments ranging in length from 5 to 10 mm were obtained from anterior, middle, and tail regions using a dissecting scissors. All except 1 of 21 anterior fragments, 1 of 31 middle fragments, and 9 of 77 tail fragments survived at least 24 h after cutting.

Preliminary screening for behavioral responses to moving shadows was done between 8 and 12 h after cutting. Each fragment was placed into a flat glass dish containing a thin layer of water. The dishes were covered with a glass plate and illuminated as previously described. At 30-min intervals, a hand-held black screen was passed over each dish. Three replicate tests were done for each fragment. Escape responses to such shadow stimuli were clearcut; fragments either showed a vigorous shortening response or no overt response occurred.

Fragments that responded in preliminary screening tests were then used for studying the critical rate of shadow movement required for escape behavior, and the

responsiveness to mechanosensory stimuli or abrupt decreases in light intensity. Electrical recording were made as described for intact worms, but light conditions for videotaping behavioral responses were modified by positioning backdrop illumination below the flat dishes and reflecting the image of the fragment at a right angle into the video camera. Thus neither the mirror nor the camera interfered with the path of the main lighting from above. Mechanosensory stimuli to the fragments were delivered with the rounded head of an insect pin that was glued to the diaphragm of a small speaker. The speaker was mounted on a micromanipulator and driven by 1-ms pulses from a square pulse generator.

Microscopy

Fragments (5–10 segments long) were obtained from the tail and mid-body regions of worms. Fragments were fixed in 100-m*M* sodium cacodylate solution (pH 7.2) containing 2.5% glutaraldehyde and postfixed in osmium. The tissue was then dehydrated in an alcohol-propylene oxide series, and embedded in epon-araldite plastic. Cross-sections (1-μm thick) were cut, stained with 0.5% toluidine blue, and screened for candidate photoreceptor cells. Thin sections of those areas containing possible photosensitive regions were then prepared for transmission electron microscopy using slotted grids and uranyl acetate staining. For scanning electron microscopy, the tissues were fixed in 4% glutaraldehyde, dehydrated, and critically point dried for later viewing in a Hitachi S-800 field emission scanning electron microscope.

Results

Escape responses in intact worms

In many aquatic oligochaetes, including *Lumbriculus variegatus*, waveforms of all-or-none spikes from the medial (MGF) and lateral (LGF) giant nerve fibers are highly stereotyped and readily detected by non-invasive (transcutaneous) electrophysiological recordings using printed circuit board recording grids (Zoran and Drewes, 1987, 1988). The following are reliable diagnostic criteria for identifying LGF spikes and distinguishing them from MGF spikes in such recordings: (a) the LGF sensory field for mechanosensory stimuli includes the posterior two-thirds of the body, while the MGF field includes slightly more than the anterior one-third; thus there is only a small region of sensory field overlap; (b) LGF spikes are diphasic and often twice the amplitude and duration of the monophasic MGF spikes; (c) a single LGF spike is not usually followed by any detectable electrical potential from muscle, although two closely spaced LGF spikes often evoke a large muscle potential; in contrast, a single MGF spike is invariably followed after a few milliseconds by a small muscle potential; and (d) LGF conduction velocity is much slower than MGF velocity in the anterior and middle regions of the body.

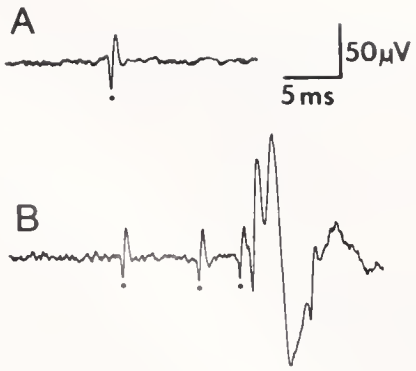

Figure 2. LGF spikes from intact worms. (A) One LGF spike (dot) was evoked by very light touch near the tip of the tail. (B) Repeated LGF spiking (dots) was evoked by a shadow moving across the worm's tail. The response was accompanied by a vigorous escape withdrawal of the tail.

To study the efficacy of mechanosensory and photic stimuli in evoking escape responses within a behavioral context, worms were placed individually into test chambers (Fig. 1). Within a few hours the worms had burrowed their anterior ends into the debris and projected their posterior ends vertically toward the water surface. Once the tip of the tail reached the surface, the terminal 15–30 segments of the tail became flexed ventrally, at a right angle, so that the dorsal surface of the body wall in these segments laid horizontally just above the surface of the water. In this position, the dorsal blood vessel, which lies just beneath the epidermis, began high-frequency, anterograde pumping of blood. Unless disturbed, worms remained in this stereotyped position for up to several hours, only occasionally readjusting their position.

A pair of recording electrodes was then very gradually positioned to less than 1 mm from the body wall of the projecting tail. LGF spikes, identical in waveform and other criteria described above, were readily detected in response to abrupt water displacement, direct touch to any portion of the tail, a moving shadow, or abrupt decrease in light intensity. Occasionally, only a single LGF spike was evoked in response to very light touch or moving shadow (Fig. 2A); however, such responses were insufficient to produce any detectable muscle electrical response or movement and, therefore, appeared to be subthreshold for overt behavior. Most commonly, however, these stimuli evoked two or more closely spaced LGF spikes (Fig. 2B) that were followed by larger, slower potentials (presumably from longitudinal muscle) and rapid escape shortening of the tail. Onset of these larger

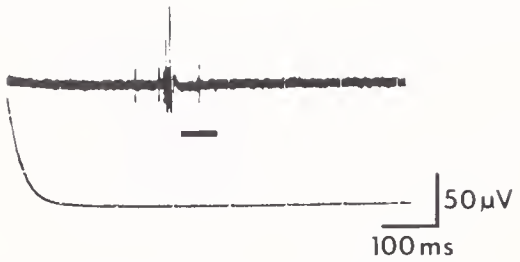

Figure 3. LGF response to an abrupt decrease in light intensity. In the upper trace, two LGF spikes (at least) preceded a burst of presumed muscle activity. The short bar below the trace designates when behavioral shortening occurred, as determined from videotape recordings. The lower trace shows the decreased output from the photocell, corresponding to onset of the stimulus.

potentials usually made it difficult to resolve any later LGF spiking in the response.

An example of LGF spiking in response to an abrupt decrease in light intensity is shown in Figure 3. Such responses were always accompanied by rapid escape shortening. The mean latency from stimulus onset to the first LGF spike was 314 ms ± 48 SD (n = 24 measurements; 11 worms).

An example of a videotape sequence of rapid escape withdrawal in response to an abrupt decrease in light intensity is shown in Figure 4. Here, marked tail withdrawal occurred between the ninth to eleventh frames after the stimulus onset. The mean latency from stimulus onset to detectable tail withdrawal was 389 ms ± 99 SD (58 measurements; 15 animals).

Animals were also tested for responsiveness to moving shadows or decreased light intensity at times when their tails were protruded vertically above the sediments, but not lying horizontally at the air-water interface. Care was taken to ensure that sufficient time had elapsed (>30 min) for recovery from previous test stimuli. Nevertheless, no escape withdrawal was observed in response to such stimuli, suggesting that the worm's responsiveness to moving shadow or abruptly decreased light intensity is dependent on its behavioral state.

Escape responses in body fragments

Isolated body fragments were screened for behavioral responsiveness to a moving shadow. The results (Fig. 5) showed that nearly half of the tail fragments, but no anterior or middle fragments, rapidly shortened in response to at least one of three test stimuli delivered at 30 min intervals. Failure of some test stimuli to evoke responses in otherwise responsive fragments did not appear to result from insufficient recovery time. Rather, the lack of responsiveness appeared to be related to variations in the behavioral state of the fragment. For example, we noted that if tail fragments were quiescent just before testing, then rapid escape responses were often evoked. However, if fragments were crawling or wriggling just before testing, then no rapid escape responses were evoked. These observations suggest that responsiveness to shadow may be reduced during such movements.

Next, electrical correlates of rapid escape movements were examined in tail fragments exhibiting shadow responsiveness. A very light touch stimulus anywhere on the fragment evoked one or more LGF spikes. As in intact worms, a single spike was never accompanied by a detectable muscle electrical response or movement (Fig.

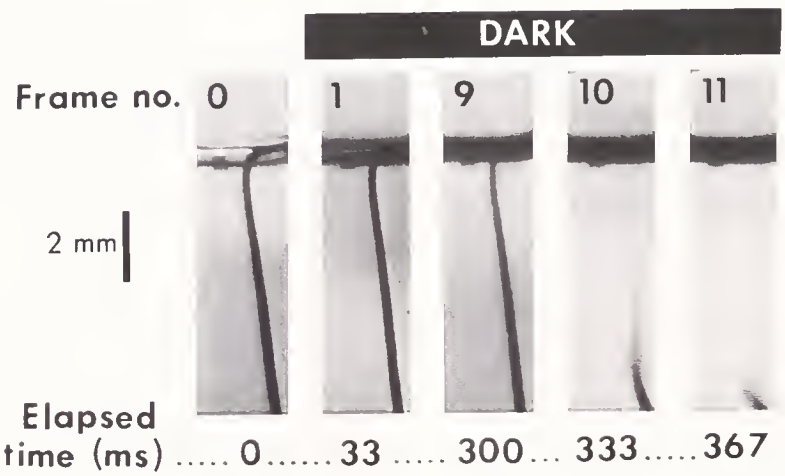

Figure 4. Frame-by-frame analysis of an escape response to an abrupt decrease in light intensity. Frame 0 shows the worm's tail lying at the air-water interface before onset of the stimulus. By the next frame (1) the lighting from above had been switched off, and between frames 9–11 the worm's tail rapidly withdrew from the water surface.

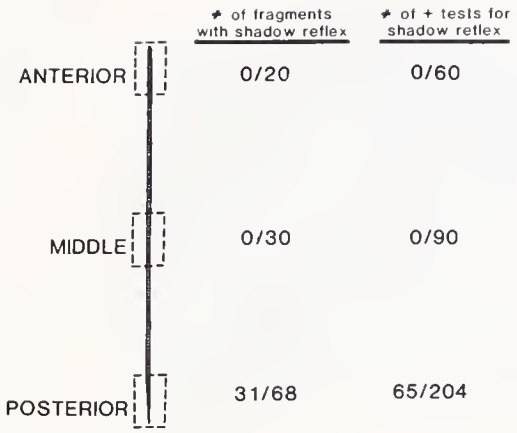

Figure 5. Results from behavioral screening tests with isolated fragments from anterior, middle, and posterior locations.

6A), but two or more closely spaced spikes usually evoked such responses (Fig. 6B). The latency from a touch stimulus to the first LGF spike ranged from 3–12 ms.

A moving shadow or abrupt decrease in light intensity also reliably evoked multiple LGF firing and muscle responses (Fig. 6C), resembling those obtained in intact worms. The minimal rate of shadow movement required for reliably evoking escape shortening was determined by passing a shadow at varying speeds over the tail fragments. The mean minimal rate was 4.4 mm/s ± 2.1 SD (n = 7 worms). This value appeared unaffected by changes in the orientation of the shadow relative to the longitudinal axis of the exposed tail.

The latencies of electrical and behavioral responses to abrupt decreases in light intensity were also determined, as described for intact worms. The mean latency from stimulus onset to the first LGF spike was 375 ms ± 96 SD (n = 23 measurements; 13 worms). A videotaped sequence of the behavioral response to the same stimulus is shown in Figure 7. The mean latency to the onset of such responses was 449 ms ± 67 SD (n = 24 measurements; 9 worms). Thus, although latencies to electrical and behavioral responses were somewhat longer in tail fragments than intact worms, the same general pattern of LGF responsiveness to photic stimulation was seen in both tail fragments and intact worms.

Since results from isolated tail fragments suggested that the sensitivity of escape responses to shadow was localized in tail segments, these fragments were examined for candidate photoreceptor cells.

Candidate photo- and mechanoreceptors in posterior fragments

Since physiological and behavioral results from isolated body fragments suggested that tail fragments were particularly responsive to shadow (as well as touch) these fragments were microscopically examined for candidate photoreceptors and mechanoreceptor cells.

Light microscopy and scanning electron microscopy revealed no obvious ocellar-like structures on the cuticular surface, although many complex arrangements of long and short ciliary processes, intermingled with large numbers of short microvillar projections, were evident on the cuticular surface (Fig. 8A). However, transmission electron microscopy of the epithelial surface revealed candidate photoreceptor cells. These were similar to the simple phaosomal-type photoreceptors described in the anterior segments of leeches and earthworms (reviews by Sawyer, 1986, and Jamieson, 1981). These cells were located on the dorsal surface of the tail and were sparsely distributed. Usually two, but occasionally as many as four, were found per segment. Cursory observations in mid-body segments of three animals revealed no evidence of comparable cells.

Figure 8B–C shows the candidate photoreceptors from two different worms. The cells have a large apical phaosome (varying in size from 1.5 to 4.0 μm) with a broad opening to the external cuticle. The phaosome contains numerous microvilli (0.10 to 0.15 μm in diameter), most projecting centrally into the phaosome cavity and a few projecting through the phaosomal opening and into the cuticular layer. Other features of these cells include: (1) extensive tight junctions with surrounding epithelial

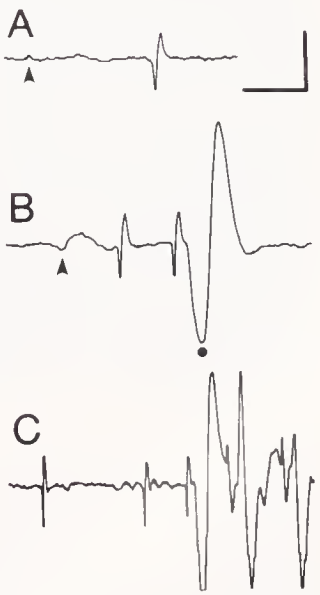

Figure 6. LGF responses in isolated tail fragments. (A) One LGF spike was evoked by a mechanical stimulus (arrow). (B) Two LGF spikes, followed by a presumed longitudinal muscle potential (dot), were evoked by another, slightly stronger mechanical stimulus. (C) A train of LGF spikes and muscle response were evoked by a moving shadow. Time scale: 5 ms (A, B); 10 ms (C). Voltage scale: 50 μV.

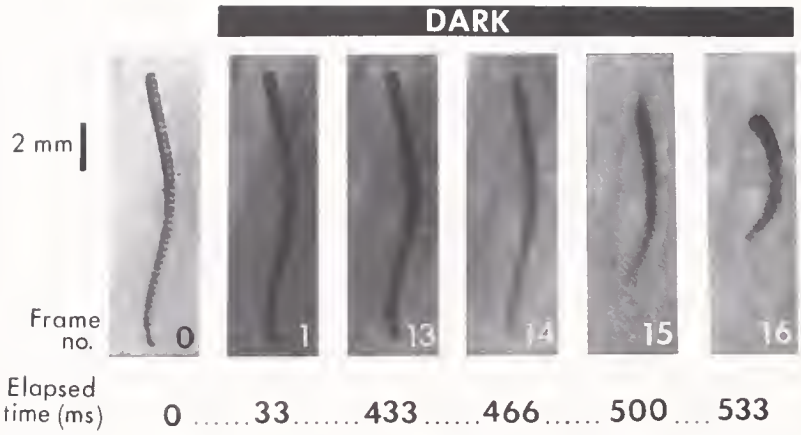

Figure 7. Frame-by-frame videotape sequence of rapid shortening in an isolated tail fragment in response to an abrupt decrease in light intensity. Frame 0 shows the tail fragment before onset of the stimulus. Rapid shortening occurred between frames 13 to 16.

cells (Fig. 8C); (2) a basal nucleus; and (3) basal projections into a radial nerve plexus directly beneath the epithelial layer.

Thin sections through the body wall also provided details regarding the ciliated epithelial cells (Fig. 8D, E). Both uniciliate and multiciliate cells were evident. The multiciliate cells generally have four to six cilia with a corresponding number of basal bodies. In the uniciliate cells, the cilium arises from a pit in the apical region of the cell and is surrounded by 10 microvillar projections, each containing an abundance of microfilaments and an electron-dense region adjacent to the ciliary process. The microvilli (approximately 0.3 μm in cross-sectional area and 0.15 μm in width) are also interconnected via an organized, electron-dense material (Fig. 8E). These two ciliated cell types are nearly identical to the proposed epithelial mechanoreceptors described in the anterior segments of earthworms (Knapp and Mill, 1971; Mill, 1982) and an aquatic oligochaete, *Rhynchelmis limosella* (Moritz and Storch, 1971), the latter representing the same family as *Lumbriculus (i.e.,* Lumbriculidae).

Discussion

Adaptive significance and timing of the shadow reflex

Stimulus modalities that elicit rapid tail withdrawal in *L. variegatus* include touch, moving shadow, and abrupt decrease in light intensity. These modalities, as well as the specific escape movements they elicit, appear well matched to the worm's specific lifestyle and habitat. The worms are especially abundant in the shallow margins of ponds where their tails protrude several centimeters above the sediments and lie horizontally at the air-water interface (Fig. 1), a position that apparently facilitates gas exchange via the dorsal blood vessel. In this position, the exposed tail would be vulnerable to attack by subsurface, surface, or aerial predators.

Because pond water is often highly turbid, and candidate photoreceptor cells in exposed segments tend to be located in a dorsolateral position, mechanosensory, rather than photosensory, cues may be more important in the detection of subsurface predators (*e.g.,* aquatic insects or fish). On the other hand, photosensory cues may be important in signalling the approach of surface or aerial predators (*e.g.,* amphibians or birds). This idea is consistent with observations that moving shadows above the water surface reliably elicit rapid tail withdrawal, either in small laboratory aquaria containing natural sediments (Fig. 4), or in actual field settings (C. Drewes, unpub.).

Although the electrophysiological and behavioral events during responses to photic stimuli appeared indistinguishable from those elicited by mechanosensory stimuli, the timing of escape responses to these two stimulus types differed markedly with respect to onset latency. The latency between a mechanical stimulus and the onset of LGF spiking was usually less than 12 ms, a value comparable to those in other terrestrial and aquatic oligochaetes (Drewes, 1984; Zoran and Drewes, 1987). In contrast, latencies following a photic stimulus were much longer, ranging from 250–375 ms. Such values are similar to those seen in other annelid escape responses to photosensory stimuli, such as giant fiber responses to shadow in polychaetes (Gwilliam, 1969) and S-cell responses to light flashes in leech (Laverack, 1969; Bagnoli *et al.,* 1973).

Several possible factors could contribute to these relatively long latency values. (1) The response time of the photoreceptors may be relatively slow. For example, in leech photoreceptor cells, the time from onset of a photic

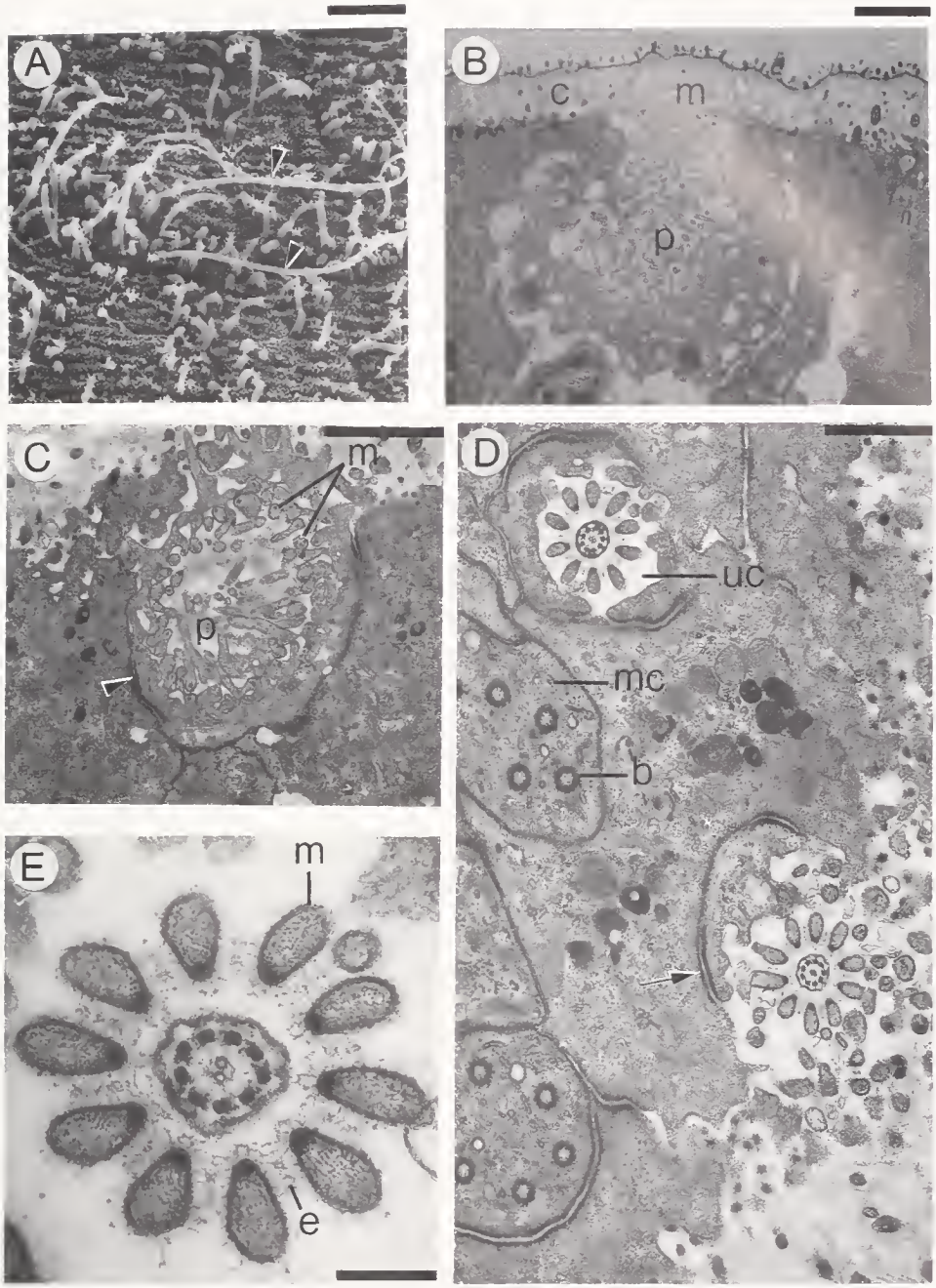

Figure 8. Scanning and transmission microscopy of body wall of the tail of *L. variegatus*. The scanning image (A) reveals a rough cuticular surface and an abundance of microvilli and cilia protruding from the surface. Note the long cilia (arrows) lying parallel to the surface. The cross-section (B) and frontal section (C) through the phaosomal region of the presumed photoreceptor reveals numerous microvilli (m) projecting into the phaosome cavity (p) and cuticle (c). The presumed photoreceptors are linked to adjacent epithelial cells via tight junctions (arrows in C and D). A frontal section (D) of the body wall shows uniciliary (uc) and multiciliary cells (mc). Note the basal bodies (b) of the multiciliary cell. A cross-section (E) of the cilium from a uniciliary cell reveals the standard 9 + 2 cilium surrounded by ten microvillar processes. Adjacent microvilli are connected via a circular complex of extracellular fibers (e). Scale bars: A, C, 2.0 μm; B, D, 1.0 μm; E, 0.25 μm.

stimulus to the first spike in the photoreceptor cells is approximately 80 ms (Lasansky and Fuortes, 1969; Fioravanti and Fuortes, 1972; Peterson, 1984). (2) Conduction and synaptic transmission from the peripheral photoreceptors to through-conducting fibers in the central nervous system may be time-consuming, especially if

pathways are small in caliber and include interposed sensory interneurons, as proposed in the leech (Kretz *et al.*, 1976). (3) Additional time may be consumed for spatial integration and parallel processing of segmental inputs onto giant fibers.

These factors, although detrimental in terms of increasing response time, may be advantageous by providing an opportunity for appropriate modulation of escape response sensitivity. For example, our results suggest that escape response sensitivity depends on the worm's behavioral state, with tail segments being especially responsive to shadows when positioned horizontally at the air-water interface. This suggests that specific combinations of sensory cues may somehow interact to modulate escape responsiveness, a phenomenon that has been experimentally demonstrated for converging photosensory and mechanosensory inputs onto S-cell interneurons in the leech (Bagnoli *et al.*, 1973).

Candidate photoreceptor cells

Photoreception in oligochaete worms is predominantly mediated by extraocular, dermal photoreceptors (Steven, 1963; Yoshida, 1979; Welsch *et al.*, 1984). Evidence from two lumbricid earthworm species, *Lumbricus terrestris* and *Eisenia foetida*, indicate that the photoreceptor cells have a characteristic microvillar organization. That is, the receptor cell contains a large, membrane-bound cavity (termed the "phaosome") which is lined by microvilli (review by Jamieson, 1981). Our results (Fig. 8) indicate that this same type of receptor cell exists in the epidermis of tail segments in the aquatic oligochaete, *L. variegatus*. Because isolated tail fragments are capable of reacting to decreased light intensity (Fig. 5), and because we have been unable to find other candidate photoreceptor cells in these fragments, we infer that the phaosomal photoreceptors somehow mediate the worms' reactions to these stimuli.

The ultrastructural organization of these epidermal photoreceptor cells closely resembles that of the earthworm, *Eisenia foetida*, in having a relatively apical position in the epidermis, a free space in the center of the phaosome, and a microvillar-lined canal, which joins the phaosomal cavity with the extracellular space beneath the body wall cuticle (Hirata *et al.*, 1969). These features are also evident in photoreceptors of the medicinal leech (review by Sawyer, 1986) but not in the common earthworm, *Lumbricus terrestris*. In the latter case, the microvillar photoreceptor cells are located in the basal portion of the epidermis and the phaosome does not open to the outside (Rohlich *et al.*, 1970; Myhrberg, 1979).

Based on microelectrode studies of leech photoreceptor cells (Lasansky and Fuortes, 1969; Fiorvanti and Fuortes, 1972; Peterson, 1984), an abrupt increase in light intensity causes a large depolarizing receptor potential and marked increase in action potential firing in the cell. Since the adequate stimulus for eliciting an escape response in *L. variegatus* is an abrupt decrease in intensity, an interesting question arises as to the polarity of its photoreceptor electrical response. If the polarity is identical to that in the leech, then a shadow stimulus would be expected to hyperpolarize the receptor cell and excitation of the LGF system would therefore necessitate a step of disinhibition somewhere along the afferent pathway. Progress in resolving this question will require developing a reliable means of identifying and recording from the photoreceptor cells in dissected preparations. This may be difficult in view of the relatively sparse distribution of receptors cells in the epidermis and the proclivity for segmental autotomy when attempting to dissect this species. On the other hand, the associated high capacity for segmental regeneration by body fragments, in combination with a segmental respecification (morphallaxis) during regeneration (Drewes and Fourtner, in prep.), may offer unusual opportunities for investigating behavioral, anatomical, and physiological correlates of developmental plasticity in the shadow reflex of this species.

Acknowledgments

Some of this research was carried out at Iowa Lakeside Laboratory and we thank Dr. R. V. Bovbjerg, Director, for generously providing space and services there. We also thank A. J. Siegel, P. Bush, and R. Barone for assistance with electron microscopy.

Literature Cited

Bagnoli, P., M. Brunelli, and F. Magni. 1973. Afferent connections to the fast conduction pathway in the central nervous system of the leech *Hirudo medicinalis*. *Arch. Ital. Biol.* **111:** 58–75.

Clark, R. B. 1960. Habituation of the polychaete *Nereis* to sudden stimuli. I. General properties of the habituation process. *Anim. Behav.* **8:** 83–91.

Darwin, C. 1881. The formation of vegetable mould through the action of worms, with observations of their habits. Murray, London.

Dorsett, D. A. 1978. Organization of the nerve cord. Pp. 115–160 in *Physiology of Annelids*, P. J. Mill, ed. Academic Press, New York.

Dorsett, D. A. 1980. Design and function of giant fibre systems. *Trends Neurosci.* **3:** 205–208.

Drewes, C. D. 1984. Escape reflexes in earthworms and other annelids. Pp. 43–91 in *Neural Mechanisms of Startle Behavior*, R. C. Eaton, ed. Plenum, New York.

Drewes, C. D., C. A. Callahan, and W. M. Fender. 1983. Species specificity of giant nerve fiber conduction velocity in oligochaetes. *Can. J. Zool.* **61:** 2688–2694.

Evans, S. M. 1969. Habituation of the withdrawal response in nereid polychaetes. I. The habituation process in *Nereis diversicolor*. *Biol. Bull.* **137:** 95–104.

Fioravanti, R., and M. G. F. Fuortes. 1972. Analysis of responses in visual cells of the leech. *J. Physiol.* **227:** 173–194.

Gwilliam, G. F. 1969. Electrical responses to photic stimulation in

the eyes and nervous system of nereid polychaetes. *Biol. Bull.* **136:** 385–397.

Hess, W. N. 1925. Photoreceptors of *Lumbricus terrestris*, with special reference to their distribution, structure and function. *J. Morphol* **41:** 63–93.

Hirata, K., N. Ohsako, and K. Mabuchi. 1969. Fine structure of the photoreceptor cell of the earthworm, *Eisenia foetida*. *Rep. Fac. Sci. Kagoshima Univ. (Earth Sci. Biol.)* **2:** 127–142.

Howell, C. D. 1939. The response to light in the earthworm, *Pheretima agrestis* Goto and Hatai, with special reference to the function of the nervous system. *J. Exp. Zool.* **81:** 231–259.

Jamieson, B. G. M. 1981. *The Ultrastructure of the Oligochaeta.* Academic Press, New York.

Knapp, M. F., and P. J. Mill. 1971. The fine structure of ciliated sensory cells in the epidermis of the earthworm *Lumbricus terrestris*. *Tissue Cell* **3:** 623–636.

Krasne, F. B. 1965. Escape from recurring tactile stimulation in *Branchiomma vesiculosum*. *J. Exp. Biol.* **42:** 307–322.

Kretz, J. R., G. S. Stent, and W. B. Kristan. 1976. Photosensory input pathways in the medicinal leech. *J. Comp. Physiol.* **106:** 1–37.

Lasansky, A., and M. G. F. Fuortes. 1969. The site of electrical responses in visual cells of the leech, *Hirudo medicinalis*. *J. Cell Biol.* **42:** 241–252.

Laverack, M. S. 1969. Mechanoreceptors, photoreceptors and rapid conduction pathways in the leech, *Hirudo medicinalis*. *J. Exp. Biol.* **50:** 129–140.

Mill, P. J. 1975. The organization of the nervous system in annelids. Pp. 211–264 in *"Simple" Nervous Systems*, P. N. R. Usherwood and D. R. Newth, eds. Edward Arnold, London.

Mill, P. J. 1978. Sense organs and sensory pathways. Pp. 63–114 in *Physiology of Annelids*, P. J. Mill, ed. Academic Press, New York.

Mill, P. J. 1982. Recent developments in earthworm neurobiology. *Comp. Biochem. Physiol.* **73A:** 641–661.

Moritz, K., and V. Storch. 1971. Elektronenmikroskopische Untersuchungen eines Mechanorezeptors von Evertebraten (Priapuliden, Oligochaeten). *Z. Zellforsch. Mikro. Anat.* **117:** 226–234.

Myhrberg, H. E. 1979. Fine structural analysis of the basal epidermal receptor cells in the earthworm (*Lumbricus terrestris*). *Cell Tiss. Res.* **203:** 257–266.

Nicol, J. A. C. 1948. The function of the giant axon of *Myxicola infundibulum*. *Canad. J. Res.* **26:** 212–222.

Nicol, J. A. C. 1950. Responses of *Branchiomma vesiculosum* (Montagu) to photic stimulation. *J. Mar. Biol. Assoc. U. K.* **29:** 303–320.

Nomura, F. 1926. Effect of light on the movements of the earthworm, *Allolobophora foetida* (Sav.). *Sci. Rep. Tohoku Imp. Univ. IV.* **1:** 294–409.

Peterson, E. L. 1984. Photoreceptors and visual interneurons in the medicinal leech. *J. Neurobiol.* **15:** 413–428.

Rohlich, P., B. Aros, and S. Viragh. 1970. Fine structure of photoreceptor cells in the earthworm, *Lumbricus terrestris*. *Z. Zellforsch. Mikro. Anat.* **104:** 345–357.

Sawyer, R. J. 1986. *Leech Biology and Behavior, Vol. 1. Anatomy, Physiology, and Behavior.* Oxford University Press, New York.

Steven, D. M. 1963. The dermal light sense. *Biol. Rev.* **38:** 204–240.

Unteutsch, W. 1937. Uber den Licht- und Schattenreflex des Regenwurms. *Zool. Jahrbuch. Allg. Zool. Physiol. Tiere* **58:** 69–112.

Welsch, U., V. Storch, and K. S. Richards. 1984. Epidermal cells. Pp. 269–296 in *Biology of the Integument, Vol. I. Invertebrates*, J. Bereiter-Hahn, A. G. Matolsty and K. S. Richards, eds. Springer-Verlag, New York.

Yoshida, M. 1979. Extraocular photoreception. Pp. 581–640 in *Handbook of Sensory Physiology*, Vol. VII/6A, H. Autrum, ed. Springer-Verlag, New York.

Zoran, M. J., and C. D. Drewes. 1987. Rapid escape reflexes in aquatic oligochaetes: variations in design and function of evolutionarily conserved giant fiber systems. *J. Comp. Physiol.* (A) **161:** 729–738.

Zoran, M. J., and C. D. Drewes. 1988. The lateral giant fibers of the tubificid worm, *Branchiura sowerbyi*: structural and functional asymmetry in a paired interneuronal system. *J. Comp. Neurol.* **275:** 76–86.

Reference: *Biol. Bull.* **177:** 372–385. (December, 1989)

Autotrophic Carbon Fixation by the Chemoautotrophic Symbionts of *Riftia pachyptila*

CHARLES R. FISHER[1], JAMES J. CHILDRESS[1], AND ELIZABETH MINNICH[2]

[1]*Oceanic Biology Group, Department of Biological Sciences and Marine Science Institute, University of California, Santa Barbara, California 93106; and* [2]*Panlabs, 11804 N. Creek Parkway S., Bothell, Washington 98011*

Abstract. Preparations of trophosome tissue from *Riftia pachyptila* containing viable endosymbiotic bacteria were incubated with several substrates under a variety of conditions to characterize the symbionts physiologically. Of all the potential substrates tested, only sulfide stimulated carbon fixation by the trophosome preparations; neither hydrogen, ammonia, nor thiosulfate were effective. Trophosome preparations did not oxidize ^{14}C-methane to either ^{14}C-organic compounds or $^{14}CO_2$, nor did they reduce acetylene under the conditions tested. Carbon fixation by the endosymbionts appears barotolerant. The symbionts require both sulfide and oxygen to fix carbon through autotrophic pathways, but are inhibited by free oxygen and by sulfide concentrations in the 300 μM range. Maximal rates of carbon fixation were documented in incubations in dilute *Riftia* blood, which protects the symbionts from the inhibitory effects of free sulfide and oxygen while providing them with an abundant pool of both substrates, bound by the vestimentiferan hemoglobins.

Introduction

Symbioses between marine invertebrates and endosymbiotic chemoautotrophic sulfur bacteria were first discovered at deep sea hydrothermal vents (Cavanaugh *et al.*, 1981; Felbeck, 1981). Similar associations are now well documented in several phyla of worms and in five molluscan orders found in a variety of habitats where redueed chemical species are present (Fisher, 1990). In all groups except the Vestimentifera, symbionts are housed in close proximity to the external environment. They are found in gill cells (most molluses), in internal cells in very small animals (pogonophorans), or extracellularly, on the surface of the animal (oligochaetes, alvinellids, and thyasirids). These symbionts are therefore in close contact with the necessary metabolites carbon dioxide, sulfide, and oxygen (Fisher, 1990). In contrast, the vestimentiferans examined to date harbor abundant endosymbiotic, sulfide-oxidizing, chemoautotrophic bacteria in an internal organ—the trophosome. This organ is highly vascularized and is located in the trunk of the worm; it has no close connections to ambient seawater (Jones, 1981).

The trophosome comprises about 15% of the wet weight of the hydrothermal vent tubeworm, *Riftia pachyptila*, and hemoglobin-containing vascular and coelomic fluids account for at least another 30% (Childress *et al.*, 1984). The bacterial volume is between 15 and 35% of the total volume of the trophosome, and estimates of bacterial density range from 3.7 to 10×10^9 cells/g trophosome (Cavanaugh *et al.*, 1981; Powell and Somero, 1986). Because this organ is located in a coelomic cavity in the trunk of the animal, metabolites must be transported to the bacteria through the circulatory system. Vestimentiferan hemoglobins, found in both the hemolymph and coelomic fluid, bind hydrogen sulfide and oxygen independently and reversibly, preventing spontaneous oxidation of the sulfide while transporting it to the trophosome for use as an electron donor by the chemoautotrophic endosymbionts (Arp and Childress, 1983; Childress *et al.*, 1984; Fisher and Childress, 1984; Arp *et al.*, 1987). The high affinity of the hemoglobins for sulfide also protects the animal cytochrome *c* oxidase system from poisoning by this potentially toxic molecule (Powell and Somero, 1983, 1986).

Few studies have been done on the physiology of vestimentiferan symbionts, most likely because it is difficult

Received 2 August 1989; accepted 25 September 1989.

to obtain living material. Belkin *et al.* (1986) demonstrated that the symbionts from several individuals of *R. pachyptila* used sulfide, and not thiosulfate, as an electron donor to fuel chemoautotrophic carbon fixation. Fisher *et al.* (1988a) reported sulfide stimulated carbon fixation by the symbionts of another vestimentiferan. Wilmot and Vetter (1990) recently reported that only exogenously supplied sulfide (not thiosulfate or sulfite) is oxidized by the symbionts, and that oxygen consumption by both trophosome preparations and partially purified symbionts is not inhibited by atmospheric levels of oxygen, or by sulfide concentrations below 2 m*M*. All of the vestimentiferans tested (including numerous individuals of *R. pachyptila*) have contained appreciable activities of RuBP carboxylase/oxygenase, ATP sulfurylase, and adenosine-5′-phosphosulfate (APS) reductase in their trophosomes indicating that the symbionts are chemoautotrophic sulfur oxidizers (Felbeck, 1981; Felbeck *et al.*, 1981; Brooks *et al.*, 1987; Fisher *et al.*, 1988b; Cary *et al.*, 1989). While one study suggested that *R. pachyptila* trophosome homogenates could oxidize methane (Fisher and Childress, 1984), another demonstrated that the intact symbiosis did not take up methane and that the hemolymph lacked a binding protein for methane (Childress *et al.*, 1984). In addition, stable carbon isotope studies have led some investigators to suggest that methane may be oxidized by some vestimentiferans (Kulm *et al.*, 1985).

The role of vestimentiferan blood in protecting the endosymbionts of an unnamed hydrocarbon-seep escarpid (phylum Vestimentifera) from the toxic effects of hydrogen sulfide, while supplying the endosymbionts with a large pool of bound hydrogen sulfide, has recently been reported (Fisher *et al.*, 1988a). Although carbon fixation by the symbionts of *R. pachyptila* is dependent on the availability of oxygen (Belkin *et al.*, 1986), investigators have only speculated about the role of vestimentiferan blood in protecting the symbionts from oxygen inhibition of carbon fixation, while simultaneously providing a large pool of this required substrate, (Childress, 1987; Fisher *et al.*, 1988a).

Here we report the results of several experiments carried out with trophosome preparations from *Riftia pachyptila*. A variety of potential electron donors were tested for suitability as an electron donor for the endosymbionts. Methane oxidation by the endosymbionts was investigated using both ^{14}C methane and $NaH^{14}CO_2$. The symbionts' ability to fix molecular N_2 was tested by the acetylene reduction method under a variety of conditions. Barotolerance of symbiont autotrophy was studied in incubations of trophosome preparations at high pressure. Finally, sensitivity of symbiont carbon fixation to free oxygen and sulfide, and the role of vestimentiferan blood in providing these substrates at appropriate activities for maximal rates of autotrophic carbon fixation, was investigated.

Materials and Methods

Experimental material

The *Riftia pachyptila* used in these experiments were collected during three cruises: two to the Galapagos Rift (Galapagos 1985, and Galapagos 1988), and one to 13°N on the East Pacific Rise (Hydronaut in 1987). On all cruises, the animals were collected by submersible (either ALVIN or NAUTILE) and brought to the surface in a temperature insulated container. Upon recovery, the animals were placed in fresh, chilled seawater and transferred to a refrigerated van for processing. Most of the animals used in this study were dissected immediately after recovery; some were transferred to flow-through pressurized aquaria (Quetin and Childress, 1980) for short term maintenance (less than three days) before being used.

The experiments reported here were conducted on tissue from living worms. Trophosome tissue is extremely fragile and deteriorates rapidly when the organ is even slightly damaged. When damaged, the tissue begins to take on a fuzzy pink appearance. In the early stages, this is just visible between the lobes of the trophosome tissue. This "fuzzy pink" effect may be due to the effects of lysozymes on the blood, which is normally a deep red color. Tissue from damaged individuals has always shown very low rates of carbon fixation in our studies. About 25% of externally undamaged animals (especially larger individuals) dissected immediately upon recovery contained a substantial portion of visibly degraded trophosome tissue. The incidence of degradation, and its intensity, increased dramatically in animals held at ambient pressure for even a few hours before dissection. No damaged tissue was used in this study.

Preparation of Riftia *saline*

Riftia saline was prepared based on the average concentrations of inorganic salts measured in both vascular and coelomic fluids. The saline was titrated to pH 7.5 with NaOH before use. One liter of *Riftia* saline contains: 20.48 g NaCl (0.4 *M*); 0.194 g KCl (2.6 m*M*); 6.22 g $MgCl_2*6H_2O$ (30.6 m*M*); 1.65 g $CaCl_2*2H_2O$ (11.2 m*M*); 4.53 g Na_2SO_4 (31.9 m*M*); and 11.915 g HEPES (50 mM) (Fisher *et al.*, 1988a).

Preparation and analysis of Riftia pachyptila *blood*

The *Riftia pachyptila* blood used in these experiments was collected from living worms and, unless otherwise specified, was kept frozen at either −20 or −70°C until used. This blood was a mixture of coelomic fluid and

hemolymph from a number of individuals. Bound sulfide was removed from the blood by acidifying to pH 5.5 with HCl, and purging the chilled blood (7°C) with a stream of nitrogen for 24 h. The blood was diluted with vestimentiferan saline solution before use in the trophosome homogenate incubations.

In two sets of experiments, fresh blood was used in the incubations. Blood from freshly collected *R. pachyptila* was neither acidified to remove bound sulfide, nor frozen, before use in the experiments in which free oxygen was varied in blood incubations (Fig. 2C and Table II). For these experiments, the chilled blood (pH 7.5) was saturated with oxygen by stirring under a stream of air for 15 min and then stripped of free (unbound) oxygen by stirring under a stream of nitrogen for an additional 45 min before use. Because it is difficult to strip the hemoglobins of oxygen, this treatment has little effect on the amount of oxygen bound by the hemoglobin. The result, therefore, is blood with the hemoglobin virtually saturated with oxygen, but containing very low concentrations of free oxygen in solution. This blood stock was then loaded into a gas-tight syringe, and added to incubation syringes containing saline solution with various concentrations of oxygen to generate variable concentrations of free oxygen in the experimental syringes. In the experiments shown in Figure 5 (testing symbiont sulfide sensitivity), fresh coelomic fluid from worms maintained in pressure aquaria in the absence of sulfide was used because it contained very low levels of bound sulfide (28 μM), and therefore did not require the acidification treatment to remove bound sulfide.

The heme content of the blood mixture was determined from the absorbance of a cyanomet hemoglobin derivative (Tentori and Salvati, 1981). We determined the capacity of separate aliquots of the bloods for sulfide by equilibrium dialysis of the blood in 30 mM citric acid phosphate buffer at 7°C and pH 7.5 (Arp and Childress, 1983). Samples of the blood in dialysis tubing were allowed to come to equilibrium (24 h) with sulfide in the dialysate (1 mM). The concentrations of sulfide in both blood and dialysate were analyzed with a gas chromatograph (Childress *et al.*, 1984). The difference between the sample sulfide and the dialysate sulfide was the amount of sulfide bound.

Preparation and analysis of Calyptogena magnifica *serum*

Dilute *Calyptogena magnifica* serum was used as an incubation medium in several experiments because the clam serum binds sulfide but not oxygen (Arp *et al.*, 1984). The clam serum was collected during the "Galapagos 1985" expedition and was used in experiments conducted during the "Hydronaut" expedition. Clam blood was collected from freshly recovered clams and centrifuged for 3 min in a bench top centrifuge at about 2000 × *g*. Dissection of the clams, collection of the blood, and centrifugation was all conducted in a refrigerated van (6–8°C). The serum was transferred to plastic scintillation vials, frozen at −20°C on board ship, then transferred to −70°C for storage in the laboratory. Before use, the serum was concentrated and cleared of precipitates by dialysis against distilled water for 16 h in a vacuum concentrator. Binding capacity of the serum for sulfide was determined as above for the *Riftia* blood. The binding capacity of the concentrated serum was 8.43 mM, and it was diluted with *Riftia* saline to a binding capacity of 2.0 mM before use as a serum stock in the trophosome incubations.

Preparation of the trophosome homogenates

Trophosome tissue containing symbiotic bacteria was dissected from living *Riftia pachyptila* and separated from the major blood vessels and gonads also present in this organ. A portion of the tissue (0.4–1.0 g) was blotted for a few seconds on a paper towel to remove excess blood, weighed on a motion compensated shipboard balance system (Childress and Mickel, 1980), and then submerged in about 7 ml of chilled, deoxygenated (nitrogen purged) *Riftia* saline solution (Fisher *et al.*, 1988a). The tissue was gently homogenized for 5–10 s in a chilled, loose fitting Dounce type ground glass tissue homogenizer (2–4 passes), to rupture most of the bacteriocytes and disperse the symbionts. The homogenate was diluted to either 30 or 60 ml with additional deoxygenated saline and loaded into one or two glass 30-ml syringes, equipped with three-way valves, containing marbles to mix the homogenate. This entire procedure takes between 5 and 10 min and, except for weighing, was conducted in a refrigerated van (6–8°C). A portion of this homogenate (0.1 ml) was fixed in 0.9 ml of 3% glutaraldehyde in 0.1 M phosphate-buffered 0.35 M sucrose (pH 7.35) for later examination using epifluorescence microscopy (Hobbie *et al.*, 1977).

For the experiments in which the effect of free oxygen concentration on carbon fixation was examined, the weighed tissue was transferred to a glove bag (in the refrigerated van), and the homogenate was prepared and loaded into the 30-ml syringe under a nitrogen atmosphere.

$NaH^{14}CO_3$ incubations

The incubations were conducted in 10-ml glass syringes (except the Galapagos 1985 experiments, which were conducted in disposable 10-ml plastic syringes) fitted with low dead volume teflon valves. Experiments were conducted in a refrigerated van that was main-

tained between 6 and 8°C (the incubation temperature during an experiment was constant, but the temperature inside the van varied slightly from day to day). Prior to preparation of the homogenate, between 6 and 18 syringes were loaded with the incubation media and substrate concentrations appropriate for a given experiment. All media and substrate stock solutions were titrated to pH 7.5 before use. The incubation media contained variable amounts of *Riftia* blood or *Calyptogena magnifica* serum diluted with *Riftia* saline, or else *Riftia* saline alone. The various sulfide concentrations used in the experiments were generated in the experimental syringes by adding appropriate amounts of a sulfide stock solution (7 to 15 m*M*) to the experimental syringes, using a three-way valve on the stock syringe. Similarly, variable oxygen concentrations were generated in the experimental syringes by introducing a mixture of saline stock solutions of variable oxygen concentrations (also contained in syringes and introduced through three-way valves). Stock solutions of methane and hydrogen were prepared by bubbling a saline solution with the appropriate gas. The stock solutions of thiosulfate and ammonia were prepared from sodium thiosulfate and ammonium chloride, respectively. Sulfide, methane, and inorganic carbon concentrations in the blood and saline stock solutions, and oxygen concentration in the saline stocks, were determined using a gas chromatograph (Childress *et al.*, 1984). (O_2 concentrations were not directly quantifiable in blood by this method.) Ammonium concentration in the stock solution was verified by flow injection analysis (Willason and Johnson, 1986). To confirm that stimulated carbon fixation was through autotrophic pathways, 10 m*M* DL-glyceraldehyde (a feedback inhibitor of RuBP carboxylase-oxygenase; Stokes and Walker, 1972) was added to one syringe in most of the experiments (Fisher *et al.*, 1988a).

To start the incubations, $NaH^{14}CO_3$ was added to the trophosome preparation, and 2.5 ml of the labeled preparation was drawn into each of the syringes, which already contained incubation media with the desired levels of sulfide, oxygen, or other substrates. The final concentrations of $NaH^{14}CO_3$ used in these experiments ranged from 0.1 to 1.0 μCi/ml depending on the experiment. Activity of $NaH^{14}CO_3$ in the syringes was determined by scintillation counting of replicate samples of the trophosome preparation stabilized with hyamine hydroxide. After all the experimental syringes had been filled and the contents mixed (a process that took between 4 and 7 min), replicate samples (0.1 ml) were removed from each syringe and acidified for scintillation counting of the fixed carbon. Replicate samples (0.1 ml) were similarly removed and assayed from each syringe at 10- to 20-min intervals for the next 60 to 80 min. Carbon fixation rates were calculated, following the methods of Strickland and Parsons (1972), from the measured concentration of inorganic carbon in the incubation media, the measured specific activity of that inorganic carbon pool, and the amount of acid-stable ^{14}C found in the samples at each time point.

Fixation rates were calculated after subtracting first sample values from the values measured at the later time points. This method of analysis compensated for the variable rates of carbon fixation before, and during, the first few minutes that the preparations were exposed to the substrates in the experimental syringes (Fisher *et al.*, 1988a). Trophosome preparations that failed to show a carbon-fixation rate greater than 0.2 μmol/g/h under any experimental conditions were considered to contain, at best, only marginally viable symbionts, and no data from these preparations are reported here.

Incubations under pressure

In the experiments designed to test the effect of pressure on the carbon fixation rate by the trophosome preparations, identical paired syringes were prepared, and one of each pair was incubated in a pressure vessel at 100 atm. One hundred atm was considered a sufficient pressure because this pressure supports extended survival of the tubeworms that cannot survive at 1 atm (Childress *et al.*, 1984). For pressure incubations, the glass syringes were suspended in an acrylic pressure vessel (Quetin and Childress, 1980), with a fine teflon tube extending from a luer lock fitting on the syringe to the outside through high pressure valves. Thus, samples could be taken from the syringes without releasing the pressure around the incubations. The pressure vessel was inverted repeatedly so that the marbles in the syringes would mix the samples.

Rate calculations

Determination of the appropriate carbon fixation rate for analysis was often problematic because, under some conditions, the fixation rates were distinctly non-linear over the course of the incubation. These situations were handled as follows: if the carbon fixation showed no systematic increases or decreases during the incubation (did not appear to increase or decrease significantly as a function of time), then rates were calculated by linear regression of all data points. This was the situation in most of the incubations in *Riftia* blood, and some of the saline experiments. If the rates in all of the syringes during an experiment decreased over time, then rates were calculated from the same portion of the experiment for all syringes (the first two, three, or four time points). In some of the saline and serum incubations, where either sulfide or oxygen was low, the rates decreased as the limiting substrate was exhausted, and the rates were therefore cal-

culated from the first two or three points. In a few incubations where the substrate (oxygen or sulfide) was initially present in slightly inhibitory concentrations, the rates increased over the course of the incubations as the substrate was depleted. The rates in these experiments were also calculated from the first few time points. Examples of these situations can be seen in Fisher *et al.* (1988a). The specific experiments in which rates were calculated from less than all five points are indicated in the results section. Data were always treated consistently within an experiment.

^{14}C-methane incubations

Trophosome samples from two individuals of *R. pachyptila* were also tested for the ability to use methane as a carbon or energy source. $^{14}CH_4$, synthesized microbiologically as described by Daniels and Zeikus (1983), having a specific activity of 4×10^5 dpm/μl, was used as a tracer for methane oxidation by trophosome preparations. Contamination of the labeled methane was less than 0.01% as determined by gas proportion counting.

Trophosome homogenates were prepared as described above, and 10 ml of the homogenate was placed in each of six 35-ml serum vials. The headspace was flushed with a stream of nitrogen for 1 min, then the vials were capped with butyl rubber stoppers and crimped with aluminum seals. The headspaces over the vials were adjusted using a gas-tight syringe to remove nitrogen and inject air and methane to produce the desired concentrations of dissolved oxygen ($\sim$100 μM) and methane, as estimated from Bunsen coefficients. Two methane concentrations were tested in each experiment: 10 and 100 μM in the first experiment and 5 and 10 μM in the second. $^{14}CH_4$ tracer stock (500 μl) was added to each vial 30 min after injecting the cold methane to initiate the incubations. Duplicate samples and a formalin-killed control were incubated for each methane concentration. The incubations were terminated 1 h after introducing the labeled methane by adding 200 μl of 5 *N* NaOH to each. The seals were then removed from each vial and the stoppers replaced by another, with a piece of Whatman #1 filter paper soaked with 100 μl of phenethylamine suspended from a wire into the headspace. The vials were re-sealed, and 500 μl of concentrated H_2SO_4 was added to each vial by injection. The filters were allowed to absorb the CO_2 released from the liquid for 24 h, and then removed and placed in 10 ml of 3a70 fluor (National Diagnostics) and counted in a liquid scintillation counter. Replicate 100-μl samples of the homogenate were degassed and assayed for acid stable ^{14}C by liquid scintillation counting.

Results

Potential symbiont substrates

The results of experiments conducted during the Galapagos 1985 expedition should be regarded as preliminary because these techniques were developed during this expedition. Nine sets of experiments were conducted during this expedition, with preparations of trophosome material from nine individuals of *Riftia pachyptila*. In each of these experiments, six to ten syringes were run simultaneously. Only hydrogen sulfide (among electron donors tested in these experiments) significantly stimulated carbon fixation: by as much as 140% in saline, and by as much as 880% when incubations were conducted in 50% *Riftia* blood. (Control syringes containing blood but no trophosome preparation did not fix carbon.) Considerably higher rates of carbon fixation (ten- to twenty-fold) were found when the incubations were conducted in dilute *Riftia* blood as compared to incubations in saline alone. Neither methane (140–500 μM, 10 incubations, 5 worms), hydrogen ($\sim$⅓ saturated, 5 incubations, 3 worms), ammonia (50 and 100 μM, 6 incubations, 3 worms), nor thiosulfate (0.05 and 0.5 mM, 6 incubations, 3 worms) had a significant effect on the rate of carbon fixation in these experiments. All of these comparisons were conducted under both aerobic (0.1–0.2 mM oxygen) and micro-aerobic (0.02–0.04 mM oxygen) conditions.

Trophosome tissue from two individuals of *R. pachyptila* tested during the Galapagos 1988 expedition did not oxidize ^{14}C-methane to either ^{14}C-organic compounds or $^{14}CO_2$.

Trophosome tissue from two individual worms was tested for the ability to fix N_2 by the acetylene reduction method during the Galapagos 1985 expedition. Tissue from both individuals was tested under both aerobic and micro-aerobic conditions in both saline and dilute *Riftia* blood, with and without sulfide (100 μM) as an energy source. Results were negative (no appearance of ethylene) in all 12 incubations, which lasted either 9 or 16 hours.

Effects of pressure on carbon fixation

Seven experiments, conducted during the Hydronaut expedition, were designed to test the effects of pressure on carbon fixation by *Riftia pachyptila* trophosome preparations (Table 1). The carbon fixation rates for the incubations conducted in saline (3 experiments) were calculated from the first three points only, because the rates decreased significantly during the incubations (Fig. 1a). Similar decreasing rates were observed during many of the other incubations in saline, but the phenomenon was most pronounced in these incubations; a possible cause was the increased time involved in beginning the experiments in pressure vessels, an additional 15–20 min after preparing the homogenate. No significant rate decrease was observed in the blood incubations during the experiments (Fig. 1B). Typical results of this study are

Table I

Effects of pressure on carbon fixation rate of Riftia pachyptila *trophosome tissue*

Exp.	Pres. (ATM)	[Sulfide] (μM)			Carbon fixation rates [μmol $^{-1}$ h $^{-1}$ (r^2)]				Ratio of P/A*		
		Low	Med.	High	Low	Med.	High	Inhib.**	Low	Med.	High
S 1	100	35	65	260	2.40 (1.0)	2.49 (.72)	2.80 (.83)		1.26	1.00	1.35
	1	35	65	260	1.91 (.63)	2.49 (.62)	2.07 (.18)				
S 2	100	25	50	200	1.63 (.25)	2.19 (.27)	1.33 (.16)		1.55	1.60	1.06
	1	25	50	200	1.05 (.28)	1.37 (.53)	1.26 (.31)	0.49 (.22)			
S 3	100	30	60	230	3.82 (.25)	3.38 (.15)	2.32 (.08)		1.12	1.02	1.63
	1	30	60	230	3.41 (1.05)	3.32 (.60)	1.42 (.68)	1.27 (.20)			
B 1	100	55	230	570	5.8 (.32)	8.7 (1.33)	7.7 (.77)		0.69	0.94	0.91
	1	55	230	570	8.4 (.26)	9.3 (1.12)	8.5 (.71)	2.7 (.17)			
B 2	100	85	335	840	9.3 (.56)	10.3 (.67)	5.0 (.56)		0.89	1.00	0.98
	1	85	335	840	10.4 (.66)	10.3 (1.65)	5.1 (.91)	5.0 (.35)			
B 3	100	110	395	1060	7.22 (.57)	6.11 (.87)	2.46 (.32)		0.99	1.04	1.08
	1	110	395	1060	7.30 (.72)	5.90 (.74)	2.27 (.19)	3.83 (.18)			
B 4	100	110	395	1060	8.5 (.11)	9.0 (.40)	2.5 (.12)		0.90	0.98	1.19
	1	110	395	1060	9.4 (.26)	9.2 (.39)	2.1 (.12)	3.0 (.08)			

Standard errors of the slopes of the linear regressions are presented in parentheses next to the rates. Linear regressions (and rates) were calculated from the first three time points only for the saline incubations.

S—experiments conducted in *Riftia* saline.

B—experiments conducted in dilute *Riftia* blood (binding capacity about 330 μM).

Low, Med., and High are related to each other within an experiment and refer to the sulfide concentrations given in the table for each experiment.

* P/A is the ratio of the rate at 100 ATM to the rate at 1 ATM in that experiment.

** The inhibitor (10 mM D,L-glyceraldehyde) was added to a syringe containing the "Med." level of sulfide in the saline experiments and "Low" level of sulfide in the blood experiments.

depicted in Figure 1. In the saline incubations, the carbon fixation rates under pressure were the same or slightly higher (averaging 30% higher) at all three sulfide concentrations (Table I), but there were no significant differences in the slopes of the linear regressions (rates) in pairwise comparisons within experiments. When the incubations were conducted in blood, carbon fixation rates were slightly lower under pressure. The only significant differences in the slopes of the paired pressure and ambient incubations occurred in run B1 at 55 μM sulfide (Table I).

Effects of oxygen concentration on carbon fixation rates

Ten experiments conducted during the Hydronaut expedition were designed to determine the effect of free oxygen on the carbon fixation rates of trophosome preparations. The results of three experiments conducted in saline and four experiments conducted in 8% *Calyptogena magnifica* serum were substantially the same (Table II). Maximal fixation rates in saline and dilute clam serum were recorded at initial oxygen concentrations between 72 and 154 μM, with higher oxygen concentrations significantly inhibiting carbon fixation. These rates were calculated from the first two or three points when the carbon fixation pattern was distinctly non-linear, as it was at all limiting oxygen concentrations (see Fig. 2A). The difference between limitation and inhibition was evident from the shape of the curves at the different oxygen concentrations (compare the fixation patterns at 53 and 160 μM O_2 in Fig. 2A). The rates presented in Table II for the saline and clam serum experiments are higher than the actual measured inorganic carbon incorporation rates for the 60 to 70 min incubations because they were calculated from the initial, linear portion of the curves (see Fig. 2A).

When incubations were conducted in dilute *Riftia* blood (with O_2 saturated hemoglobin), none of the incubations appeared oxygen limited (the carbon fixation rates were linear at all oxygen concentrations throughout the experiments, Fig. 2B), and oxygen inhibition of carbon fixation was evident at much lower free (unbound) oxygen concentrations than in the saline and clam serum experiments (data shown in Fig. 2B are typical of the blood incubations). This is most easily visualized in Figure 3, where all of the experiments are summarized. Each point in Figure 3 represents a rate calculated from one incubation, and the rates are presented as a percent of the maximal rate observed with that preparation. The maximum rates calculated from each experiment are given in Table II.

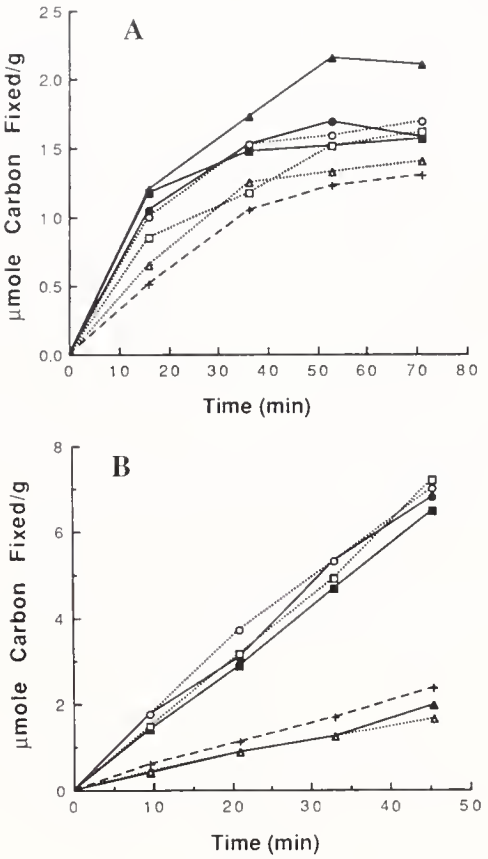

Figure 1. Effects of 100 atm pressure on carbon fixation by *Riftia pachyptila* trophosome preparations at three sulfide concentrations. Open symbols and dotted lines represent data from incubations at ambient pressure and closed symbols represent data from incubations at 100 atm: (A) incubations in *Riftia* saline without blood (Saline 1, Table I): squares, 35 μM initial sulfide; circles, 65 μM initial sulfide; triangles, 260 μM initial sulfide; +, 1 atm, 65 μM initial sulfide and 10 mM D,L-glyceraldehyde. (B) Incubation in dilute *Riftia* blood with binding capacity of about 330 μM (Blood 4, Table I): squares, 110 μM initial sulfide; circles, 395 μM initial sulfide; triangles, 1060 μM initial sulfide; +, 1 atm, 110 μM initial sulfide and 10 mM D,L-glyceraldehyde.

Effects of sulfide concentration on carbon fixation rates

Experiments were conducted during the 1988 Galapagos expedition to determine the optimum concentrations of sulfide for chemoautotrophic carbon fixation by *Riftia pachyptila* trophosome preparations. The results of the four experiments conducted in saline, in which the maximal carbon fixation rates were greater than 1 μmole $g^{-1}\,h^{-1}$, are shown in Figure 4. Remember that the actual concentrations during the incubation are lower than the initial concentrations presented in the figure legends due to spontaneous oxidation of sulfide in the saline incubations. The inhibitory levels of sulfide in the saline incubations are, therefore, maximum values. The initial sulfide concentrations that were maximally stimulatory to carbon fixation by the trophosome preparations incubated in saline ranged from 250 to 350 μM in the four experiments (Fig. 4). The trophosome preparations were sulfide limited at initial concentrations below 175 to 250 μM, and sulfide inhibition became apparent at concentrations of 350 to 500 μM in these experiments (Fig. 4).

Ten experiments were conducted in various concentrations of *Riftia* blood that had been collected during the Hydronaut expedition, stored at −20°C for several months, and treated as described in the methods section to remove bound sulfide. We consider the results of these experiments preliminary because subsequent analysis of the blood used indicated that it did not have the affinity,

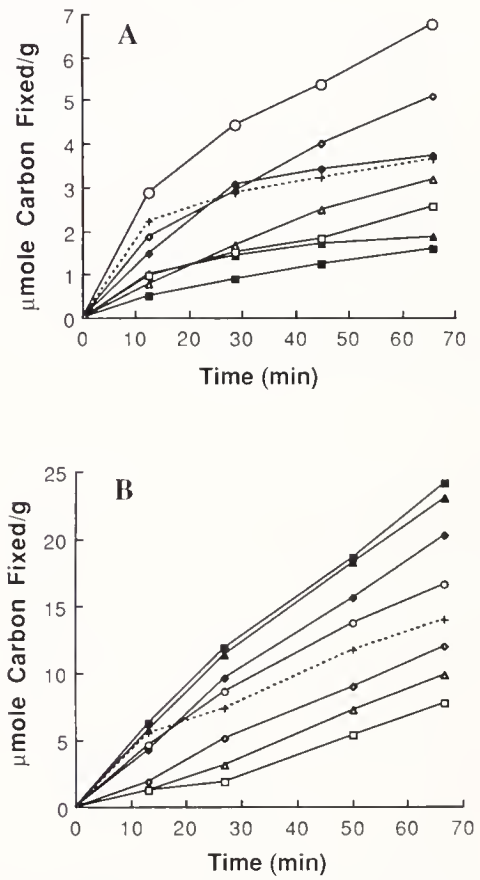

Figure 2. Effects of free oxygen concentration on carbon fixation by *Riftia pachyptila* trophosome preparations. (A) Incubations in *Riftia* saline without blood: closed square, trace oxygen; closed triangle, 27 μM initial oxygen; closed diamond, 53 μM initial oxygen; open circle, 107 μM initial oxygen; open diamond, 160 μM initial oxygen; open triangle, 213 μM initial oxygen; open square, 267 μM initial oxygen; plus with dotted line, 107 μM initial oxygen and 10 mM D,L-glyceraldehyde. (B) Incubations in 18% *Riftia* blood and balance saline: closed square, trace unbound oxygen; closed triangle, 47 μM initial unbound oxygen; closed diamond, 94 μM initial unbound oxygen; open circle, 140 μM initial unbound oxygen; open diamond, 187 μM initial unbound oxygen; open triangle, 234 μM initial unbound oxygen; open square, 292 μM initial unbound oxygen; plus with dotted line, 47 μM initial unbound oxygen and 10 mM D,L-glyceraldehyde.

Table II

Effect of oxygen concentration on carbon fixation by Riftia pachyptila *trophosome preparations*

	Incubation conditions			Maximum rate of C fixation	
Run #	Media	$[H_2S]$ (μM)	$[\Sigma CO_2]$ (mM range)	Rate (μmol g^{-1} h^{-1})	$[O_2]$ (μM)*
S 1	Saline	60	2.51–2.56	13.73	107
S 2	Saline	100	2.58–2.59	11.60	107
S 3	Saline	65	2.01–2.41	1.20	90
CS 1	8% Serum	160	1.16–1.35	5.63	154
CS 2	8% Serum	160	1.42–1.48	3.60	108
CS 3	8% Serum	110	1.71–1.83	3.31	72
CS 4	8% Serum	110	1.71–1.83	13.80	108
RB 1	18% Blood	140	3.58–3.61	28.03	Trace
RB 2	18% Blood	140	3.58–3.61	20.48	Trace
RB 3	9% Blood	85	2.27–2.30	13.47	38

S—*Riftia* Saline; CS—*Calyptogena magnifica* Serum; RB—*Riftia pachyptila* Blood.

* Oxygen concentration in the syringe which produced the rate of carbon fixation given in the previous column; oxygen concentrations in blood incubations refer to free oxygen, the hemoglobins are saturated with oxygen in all three experiments.

or capacity, for sulfide that heme content and experience indicates it should (Arp *et al.*, 1987; Fisher *et al.*, 1988a). Although the results were variable with respect to the absolute levels of sulfide that were inhibitory to carbon fixation in the different experiments, carbon fixation was never inhibited by sulfide levels below the estimated blood binding capacity.

When it became apparent that this frozen, treated blood was damaged, two experiments were conducted using fresh coelomic fluid from two worms that had been maintained in pressure aquaria without sulfide for several days. Sulfide concentration in their mixed, undiluted coelomic fluid was 28 μM, and the binding capacity of the fluid was 910 μM. Results of these experiments are shown in Figure 5. The lowest sulfide concentrations tested in these experiments depended on the concentration of blood used in the incubations. At a blood dilution resulting in a sulfide binding capacity of 120 μM, the lowest sulfide concentration tested was 4 μM; at a binding capacity of 360 μM, the lowest sulfide concentration tested was 11.2 μM; and at a binding capacity of 480 μM, the lowest sulfide concentration tested was 14.9 μM. The level of total sulfide (bound and unbound) that inhibited carbon fixation was dependent on the concentration of the blood used in the incubations and was always above the binding capacity of the dilute blood (Fig. 5). Inhibition of carbon fixation in the parallel saline incubations occurred below 350 μM sulfide, and the carbon fixation rates were generally higher when the homogenates were incubated in blood.

Discussion

Potential symbiont substrates

Early work with trophosome preparations, as well as bacterial isolates from high dilutions of trophosome material, suggested that a variety of different types of symbiotic bacteria might be present in the trophosome of *R. pachyptila* (Jannasch, 1983; Fisher and Childress, 1984; Jannasch and Nelson, 1984; *cf* Jannasch, 1989). Similarly, the recent work of Cary *et al.* (1989), Southward (1988), and Jones and Gardiner (1988) all suggest nonvertical transmission of symbionts (both fertilized eggs and early juveniles appear symbiont-free), a situation which, if true, could facilitate the occurrence of a variety of symbionts in *R. pachyptila*. On the other hand, analysis of the 16S rRNA sequences of the symbionts from two specimens of *R. pachyptila* indicate that at least 90% of the symbionts in each individual are of the same species, and that the symbionts in the two individuals are the same (a unique symbiont constituting less than 10% of the bacterial biomass might not be recognized by this technique) (Distel *et al.*, 1988).

The present study confirms the results of Belkin *et al.* (1986); that symbiont carbon fixation is stimulated by sulfide, but not thiosulfate. Similarly, Wilmot and Vetter (1990) demonstrate that sulfide (and not thiosulfate or sulfite) stimulates oxygen consumption by both trophosome preparations and partially purified symbionts of *R. pachyptila*. Furthermore, our results indicate that neither hydrogen nor ammonia stimulate carbon fixation by trophosome preparations. As a test for methanotrophic symbionts, trophosome material from two worms collected at 13°N on the East Pacific Rise was tested for the ability to oxidize ^{14}C-methane, again with negative result. The present study does not directly address the question of symbiont heterogeneity in vestimentiferans, however it does indicate that *R. pachyptila* symbionts from all individuals analyzed are similar in that they use only sulfide as an electron donor to fuel chemoautotrophic carbon fixation.

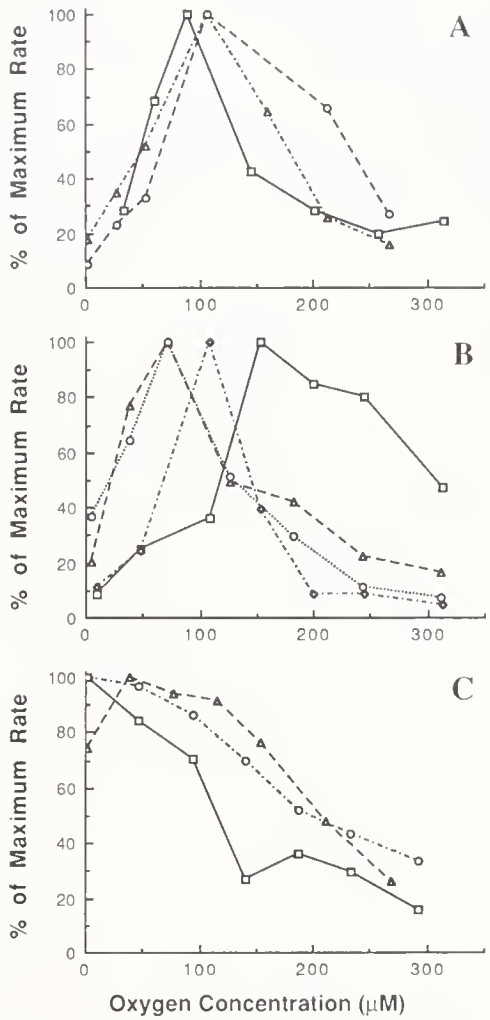

Figure 3. Rate of carbon fixation by *Riftia pachyptila* trophosome preparations as a function of free (unbound) oxygen concentration in three incubation media. Conditions for each incubation are described in Table II. (A) Incubations in saline: triangles, saline #1; circles, saline #2; squares, saline #3. (B) Incubations in 8% *Calyptogena magnifica* serum in saline (sulfide binding capacity, 675 μM): squares, serum #1; triangles, serum #2; circles, serum #3; diamonds, serum #4. (C) Incubations in dilute *Riftia* blood in saline: squares, blood #1; circles, blood #2; triangles, blood #3.

Because of the limited number of experiments conducted previously to test for nitrogen fixation by trophosome preparations (Fisher and Childress, 1984), several additional experiments were conducted with material from the Galapagos Rift. These experiments were conducted under several concentrations of both oxygen and sulfide, and under no condition was there any evidence of nitrogen fixation (acetylene reduction). These results agree with earlier, similar experiments (Fisher and Childress, 1984), enzyme activity measurements (Felbeck, 1981), measurements of $\delta^{15}N$ in *R. pachyptila* tissue (Rau, 1981; Fisher *et al.*, 1988b), and changes in *in situ* nitrate concentration around vent animals (Johnson *et al.*, 1988a). All of these suggest that nitrate is the nitrogen source for the intact symbiosis.

Pressure effects

The results of this study indicate that *Riftia pachyptila* symbionts are barotolerent but not barophilic, although pressure did slightly affect the carbon fixation rate of trophosome preparations (discussed below). These results agree, in general, with ones showing that oxygen consumption by trophosome preparations was not affected by pressure of 100 atm (Fisher and Childress, 1984), and with the fact that all free-living sulfur-oxidizing bacteria isolated from hydrothermal vent waters (and tested) are barotolerant (Jannasch, 1989). Although the actual environmental pressure for these organisms is about 250 atm, 100 atm was considered sufficient for this test because this is enough pressure to keep the tubeworm hosts, as well as other barophilic vent animals, alive (Mickel and Childress, 1982a, b; Arp *et al.*, 1984; Childress *et al.*, 1984).

One effect of increasing pressure is on the dissociation constant for H_2S. Higher pressure favors dissociation of H_2S because of the negative volume change associated with this reaction in water ($\Delta V = -16.3$ cm^3 mol^{-1}) (Isaacs, 1981). Although H_2S is probably the species that crosses cell surfaces (since it is uncharged) and is the species toxic to cytochromes (Smith and Gosselin, 1979), HS^- is the species bound by the hemoglobins of *R. pachyptila* (Childress *et al.*, 1984; Arp *et al.*, 1987). Pressure will also affect the abundance of total sulfide because, by changing relative abundances of charged and uncharged species, it will affect the rate of abiotic oxidation of sulfide. We believe a combination of these variables is responsible for the inconsistent effect of pressure on carbon fixation by the preparations in saline.

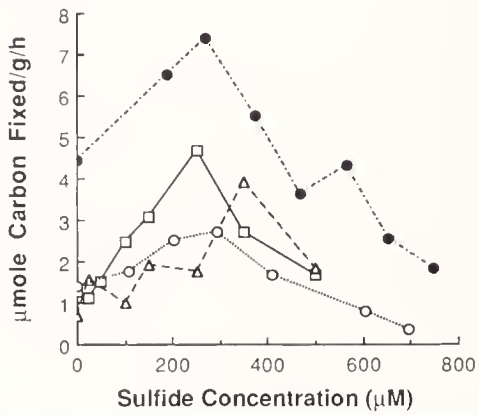

Figure 4. Rate of carbon fixation by *Riftia pachyptila* trophosome preparations in saline as a function of initial sulfide concentration. Each different symbol and line represents a separate experiment.

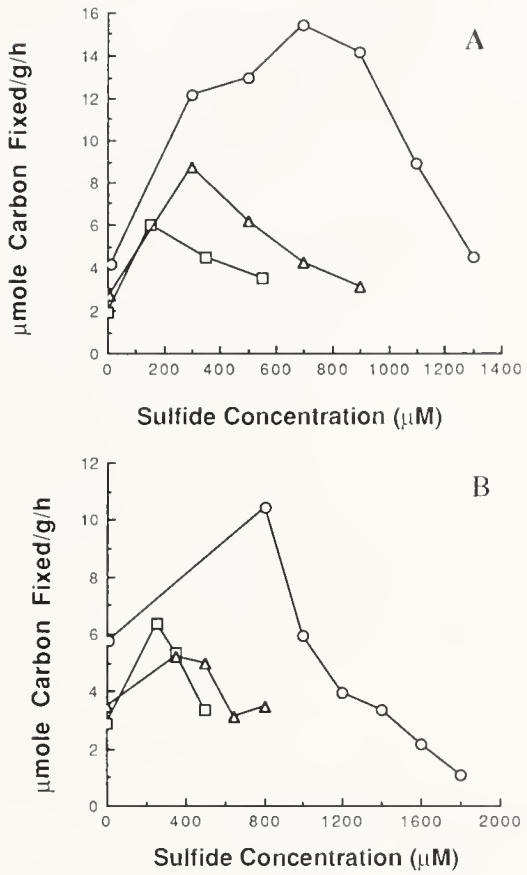

Figure 5. Rate of carbon fixation by *Riftia pachyptila* trophosome preparations as a function of initial total sulfide concentration. A and B represent two separate experiments with trophosome preparations from different worms. Incubations under all three conditions in each experiment were conducted simultaneously. Squares are rates from incubations in saline without added blood; triangles are rates from incubations in dilute (13%) fresh coelomic fluid with a binding capacity of 120 μM sulfide; circles are rates from incubations in more concentrated (53% in A and 40% in B) fresh coelomic fluid with a binding capacity of 360 and 480 μM sulfide, respectively.

The effects of pressure on the blood incubations are also slight. It significantly inhibited carbon fixation at lowest sulfide concentration tested (55 μM), with only slight effects at sulfide concentrations above that, and no effect at concentrations that were clearly inhibitory to carbon fixation. These small effects could be due to either a direct pressure effect on blood sulfide binding or an indirect effect stemming from the altered equilibrium between HS^- and H_2S.

Effects of oxygen concentration on carbon fixation

The possibility that vestimentiferan endosymbionts might be sensitive to free (unbound) oxygen is suggested by the observation that many free-living sulfur bacteria are microaerophilic (Krieg and Hoffman, 1986). Although Wilmot and Vetter (1990) found no oxygen inhibition of oxygen consumption by trophosome preparations, their study does not address the possibility that oxygen may inhibit autotrophic carbon fixation by the symbionts, as oxygen consumption (or sulfide oxidation) and carbon fixation are not tightly coupled in sulfur bacteria (Kelly, 1989). Experiments designed to explore the sensitivity of vestimentiferan symbiont carbon fixation to oxygen were conducted in *Riftia* saline. In these experiments, the maximum rate of carbon fixation was recorded at oxygen concentrations of approximately 100 μM (Table II, Fig. 3A), but the shape of the curves (carbon fixation *vs.* time) suggested increasing substrate limitation over time at the lower oxygen concentrations (Fig. 2A). Due to the reactivity of sulfide and oxygen, either of these substrates could have become limiting during the experiments under those conditions. In a first attempt to stabilize the sulfide without affecting the free oxygen in the experiments, incubations were conducted in dilute *Calyptogena magnifica* serum. This serum was used because it binds sulfide but not oxygen (Arp *et al.*, 1984). The results of the experiments in dilute *C. magnifica* serum were essentially the same as those in saline alone (Table II, Fig. 3B). This suggests that oxygen—not sulfide—is the limiting substrate.

With variable substrate limitation removed from the experimental design by the presence of *Riftia* hemoglobin, the effects of free oxygen on the carbon fixation rate of the trophosome preparations were easily visible (Fig. 3C). At free oxygen levels around air saturation (220 μM), carbon fixation by the trophosome preparations was inhibited by 60 to 70%, while at the maximum ambient oxygen levels the animals are exposed to *in situ* (100 μM), inhibition ranged from about 10 to 40% (Fig. 3C).

Oxygen inhibition of carbon fixation may be caused by the well-documented oxygenase function of the primary carboxylating enzyme in the symbionts, ribulose 1,5-bisphosphate carboxylase/oxygenase (RuBPC/O, EC 4.1.139) (Tabita, 1988). However, the experimental conditions of high total inorganic carbon concentration used in these experiments (Table II) would minimize that effect, especially at the lower oxygen concentrations. The predicted inhibition of carbon fixation due to the oxygenase function of RuBPC/O can be calculated using a substrate specificity factor, which compares the relative rates of the carboxylase and oxygenase reactions at any given concentrations of CO_2 and O_2 (Tabita, 1988). The specificity factor has not been experimentally determined for RuBPC/O of *Riftia pachyptila* symbionts, but a factor of 50 is in the range of the lowest values reported for prokaryotic RuBPC/O with both large and small subunits (Tabita, 1988); *R. pachyptila* symbiont RuBPC/O contains both large and small subunits, (Stein *et al.*, 1989). Using this factor to predict the percent of oxygen

inhibition of carbon fixation due to the oxygenase function of the enzyme (RuBPC/O) would, therefore, result in a maximum estimate. Based on the free CO_2 concentrations [calculated from the ΣCO_2 concentrations measured in the experimental syringes (Table II), our experimentally determined relationship between P_{CO_2} and ΣCO_2 in the saline, and the solubility of CO_2 in the saline], we predict no more than 8.4% inhibition of carbon fixation at 220 μM oxygen at the lowest CO_2 concentration employed (in the serum incubations, Table II). A range of 2.5 to 5.7% inhibition by 220 μM O_2 in the other incubations is due to RuBPO. The same calculations predict between 1.2 and 4.2% inhibition of carbon fixation by 110 μM O_2 due to the oxygenase function of RuBPC/O in these experiments.

The most probable explanation for the degree of oxygen inhibition of carbon fixation found in this study is that the symbionts, like many free-living microaerophiles, are sensitive to toxic forms of oxygen, such as H_2O_2, O_2^- or $OH\cdot$ (Krieg and Hoffman, 1986), even though activity of some detoxifying enzymes has been demonstrated in extracts of *R. pachyptila* trophosome (Blum and Fridovich, 1984). Catalase is not present in *R. pachyptila* trophosome, but moderate levels of peroxidase have been demonstrated in trophosome extracts and might defend against H_2O_2 (Blum and Fridovich, 1984). Activity of superoxide dismutase against superoxide ions has also been demonstrated in *R. pachyptila* trophosome, but the activity was substantially lower than that in muscle tissue. Furthermore, the activity was nonlinear after less than 1 min in cell-free preparations (Blum and Fridovich, 1984), and, therefore, may be inactive in our longer term trophosome experiments. Several microaerophiles contain activities of these protective enzymes and yet are sensitive to toxic forms of oxygen (reviewed by Kreig and Hoffman, 1986). One possible explanation for this is that intracellular protective enzymes of the microaerophile *Campylobacter fetus* are apparently ineffective against exogenous O_2^- and H_2O_2, which could be adversely affecting the microbial cell surface (Hoffman *et al.*, 1979). The subcellular location of the protective enzymes in *Riftia* symbionts is unknown. The possibility that symbionts are sensitive to toxic forms of oxygen is further substantiated by three other observations. (1) Exposure to moderate levels of oxygen during preparation of a trophosome homogenate substantially lowers the activity of the preparation. (2) Highest rates of carbon fixation in saline incubations occurs when homogenates were prepared under virtually anaerobic conditions (Table II). (3) When the same preparation is incubated in dilute *Riftia* blood and in saline, the incubations in blood fix carbon at consistently higher rates. Unequivocal demonstration of symbiont sensitivity to toxic forms of oxygen awaits studies that demonstrate relief of oxygen inhibition by substances that quench toxic forms of oxygen (see review by Kreig and Hoffman, 1986).

Whatever the cause of the observed reduction in carbon fixation rate as a function of free oxygen concentration, the role of blood in mitigating this effect, while providing an abundant pool of oxygen, is evident (Table II, Figs. 2, 3). That the highest carbon fixation rates were observed when free oxygen in solution approached zero (the P50 of *Riftia* hemoglobin is around 2 μM at 7.5°C; Arp and Childress, 1981) indicates that the symbionts have an even higher affinity for oxygen and can remove it from the blood. The maximum levels of free oxygen possible in the blood of living worms *in situ* would be equal to the maximum oxygen levels in the surrounding water—110 μM in the ambient (non-vent) bottom water (Johnson *et al.*, 1988a). According to detailed surveys of oxygen and sulfide conditions at the central clump of *R. pachyptila* at the Rose Garden vent on the Galapagos Rift, the worms are exposed to levels of oxygen that vary from 110 μM to undetectable over very short or moderate time scales (Johnson *et al.*, 1988b). Thus, levels of oxygen in blood fresh from the plume would be expected to vary considerably. The anatomy of *Riftia* and the properties of its blood buffer its symbionts from the extremes in ambient oxygen concentration (which range from limiting to inhibitory), and allow maximal rates of carbon fixation by providing the symbionts with an abundant pool of oxygen, while maintaining low levels of free (unbound) oxygen in the trophosome.

Effects of sulfide concentration on carbon fixation

The experiments designed to address this question can be divided into three groups: experiments in saline; experiments in mixed blood with reduced sulfide binding capacity; and comparative experiments in saline and fresh coelomic fluid.

The maximum rates of carbon fixation in experiments in saline occurred at initial sulfide concentrations between 250 and 350 μM (Fig. 4). The differences in the sulfide concentrations yielding maximum carbon fixation rates could be due to real differences in sulfide sensitivity of the symbionts from different individuals. However, the inherent instability (and unpredictability) of unbound sulfide and oxygen in solution cast some doubt as to the actual levels of sulfide present during these incubations; the apparent differences could be due to differing rates of auto-oxidation of sulfide in the different incubations and resultant variations in actual sulfide concentrations during the incubations.

Two general conclusions stand out from the data collected in the incubations with blood of reduced binding capacity. First, even this blood protects the symbionts

from the inhibitory effects of sulfide demonstrated in the saline incubations (Fig. 4). Second, carbon fixation by *R. pachyptila* symbionts is not inhibited by levels of sulfide below the binding capacity of the blood.

In the experiments with fresh coelomic fluid, as found in the other experiments reported here and in previous work (Fisher *et al.*, 1988a), the blood protected the symbionts from the inhibitory effects of sulfide at sulfide concentrations below the binding capacity of the blood. The maximal rates of carbon fixation in the blood incubations were also higher than the maximum rates in the corresponding saline incubations. However, unlike the symbionts of a hydrocarbon seep escarpid vestimentiferan which were inhibited by total sulfide concentrations greater than 70% of capacity (Fisher *et al.*, 1988a), *Riftia pachyptila* symbionts were not inhibited by sulfide until the concentration surpassed the binding capacity of the dilute blood (Fig. 5). The exact level of free sulfide that was inhibitory to *R. pachyptila* symbionts cannot be determined due to the paucity of data points around the carbon fixation maxima (Fig. 5). However, it is clearly above the 100 μM that is inhibitory to the seep escarpid (Fisher *et al.*, 1988a), and more likely closer to 350 μM as suggested by the saline incubations (Fig. 4). Another recent study (conducted during the same cruise as these experiments) demonstrated that oxygen consumption by trophosome preparations was not inhibited by sulfide concentrations up to 2 mM (Wilmot and Vetter, 1990). The results of that study and this one are not contradictory; most likely they reflect the relatively "loose" coupling between sulfide oxidation and carbon fixation, and indicate that trophosome preparations can oxidize sulfide without concomitant carbon fixation. An earlier study of sulfide stimulation of carbon fixation by *Riftia* symbionts showed an optimum of 600 μM, however, these workers' trophosome preparations had very low levels of activity and apparently no effort was made to exclude or quantify blood contamination in the preparations (Belkin *et al.*, 1986). Thus, while their results are in general agreement with ours, a precise comparison cannot be made.

The lesser sensitivity to free sulfide of autotrophic carbon fixation by the symbionts of *R. pachyptila*, as compared to the seep escarpid, is probably a reflection of the ambient sulfide levels the animals are exposed to in their respective environments. The highest sulfide levels measured around the plumes of the seep escarpid are below 3 μM, and even if these vestimentiferans take up sulfide across their body wall, as has been suggested (MacDonald *et al.*, 1989), the symbionts are likely never exposed to sulfide levels in the blood approaching saturation. In fact, the highest level reported in the blood of freshly collected seep vestimentiferans is 114 μM (Childress *et al.*, 1986) which, assuming the blood has similar capacities to *R. pachyptila* blood, corresponds to a free sulfide concentration below 1 μM (Fisher *et al.*, 1988a). This assumption is validated by preliminary experiments with blood from the seep escarpid, which indicate that the blood binds sulfide and is of similar concentration to that of *R. pachyptila* (A. J. Arp, pers. comm.). *R. pachyptila* is exposed to sulfide levels in the 300 μM range *in situ* (Johnson *et al.*, 1988a), and total sulfide levels in the blood of freshly collected *R. pachyptila* as high as 9 mM have been reported (Childress *et al.*, 1984). Therefore, free sulfide levels in the blood of *R. pachyptila* are apt to be much higher than those found in the seep escarpid, and *R. pachyptila* symbionts are apparently adapted to these higher concentrations.

The symbionts of both species are located in vacuoles within host cells (bacteriocytes) in the trophosome, and not directly exposed to the blood *in situ*. The conditions inside the vacuole and host bacteriocyte will certainly affect both the total amount of sulfide and the ionic species to which the symbionts are exposed. However, the high degree of vascularization of the trophosome (Jones, 1988) implies that the blood exerts considerable influence on the concentrations of sulfide and oxygen in the bacteriocytes, and that the maximum concentrations to which the symbionts are exposed are almost certainly a reflection of the highest free concentrations of these substances in the blood.

Despite the differences between the species, the role of the blood with respect to sulfide in the intact *R. pachyptila* symbiosis is basically the same as for the seep escarpid (Fisher *et al.*, 1988a). That role is to provide the symbionts with an abundant supply of sulfide, while maintaining free sulfide at levels that allow maximal rates of carbon fixation.

Conclusion

R. pachyptila individuals appear to grow rapidly (Fustec *et al.*, 1987; Hessler *et al.*, 1988; Roux *et al.*, 1989). Because these animals are apparently dependent upon their symbionts for at least their bulk nutritional carbon requirements (see review by Fisher, 1989), the trophosome must be a very productive chemoautotrophic organ. Shipboard studies with live animals under pressure suggest that the oxygen consumption rate of *R. pachyptila* is in the range of 0.44 to 1.52 μmole oxygen g^{-1} h^{-1} in the absence of sulfide (Childress *et al.*, 1984). Assuming a RQ of 1, these data suggest that the intact symbiosis requires an input of organic carbon at about the same rate. Since the trophosome accounts for 15.3 ± 4.9% of the worms wet weight (Childress *et al.*, 1984), the trophosome must incorporate inorganic carbon into organic compounds at at least 10 μmole carbon g trophosome^{-1} h^{-1} to meet the metabolic needs of the intact symbiosis.

The higher rates reported in this study (20 to 28 μmole C g^{-1} h^{-1}) suggest that the symbionts can meet the bulk nutritional carbon requirements of the intact symbiosis through chemoautotrophy, even assuming an efficiency of 50% or less in the transfer of nutritional carbon from symbiont to host. This calculation also supports the contention that the activities of the preparations used in this study are reasonable, and that preparations with significantly lower activity are suboptimal.

The stable carbon isotope composition of these animals has been interpreted as reflecting carbon limited symbionts (Rau, 1981, 1985; Fisher *et al.*, 1988c). This interpretation implies a high rate of consumption of inorganic carbon by the symbionts and also suggests a trophosome with high metabolic activity (both of which are supported by this study). The high sulfide and oxygen binding capacities of the hemoglobins of *R. pachyptila* are therefore necessitated by both the relatively large quantity of trophosome and its high autotrophic capacity. Additionally, the affinity of the blood for sulfide and oxygen allows the symbionts access to these large pools of bound substrates without exposing the symbionts to high free concentrations of either substance, thereby supporting maximal rates of carbon fixation by the symbionts.

Vestimentiferans rely on a finely tuned symbiosis for their survival. Both their anatomy and the properties of vestimentiferan hemoglobins are adapted for symbiosis with a specific type of sulfide-oxidizing symbiont. The host tube-worms reap the benefits of an autotrophic life style, while providing their symbionts with an environment which free-living sulfide-oxidizing bacteria can only regard with envy.

Acknowledgments

This work was supported by NSF grants OCE83-11257 and OCE86-09202 to JJC and OCE86-10514 to JJC and CRF. We would like to thank M. Wells and J. Favuzzi for technical assistance with apparatus and R. Van Buskirk, V. Vanderveer, R. Kochevar, and D. Gage for technical assistance during the cruises. Thanks are also due to the captains and crews of the RV Melville, RV Thomas Thompson, and N/O Nadir, Drs. A. Alayse-Danet and H. Felbeck the expedition leader and chief scientist of the RV Thomas Thompson respectively during project Hydronaut, as well as the sub crews and pilots of the submersibles Alvin and Nautile, without whom this work would not have been possible. This manuscript has benefited from discussions with and comments by R. Kochevar, J. Favuzzi, G. Somero, and R. Trench.

Literature Cited

Anthony, C. 1982. *The Biochemistry of Methylotrophs.* Academic Press, London. 431 pp.

Arp, A. J., and Childress, J. J. 1981. Blood function in the hydrothermal vent vestimentiferan tube worm. *Science* **213:** 342–344.

Arp, A. J., and J. J. Childress. 1983. Sulfide binding by the blood of the deep-sea hydrothermal vent tube worm *Riftia pachyptila*. *Science* **219:** 559–561.

Arp, A. J., J. J. Childress, and C. R. Fisher Jr. 1984. Metabolic and blood gas transport characteristics of the hydrothermal vent bivalve *Calyptogena magnifica*. *Physiol. Zool* **57:** 648–662.

Arp, A. J., J. J. Childress, and R. D. Vetter. 1987. The sulphide-binding protein in the blood of the vestimentiferan tube-worm *Riftia pachyptila*. *J. Exp. Biol.* **128:** 139–159.

Belkin, S., D. C. Nelson, and H. W. Jannasch. 1986. Symbiotic assimilation of CO_2 in two hydrothermal vent animals, the mussel *Bathymodiolus thermophilus* and the tube worm *Riftia pachyptila*. *Biol. Bull.* **170:** 110–121.

Blum, J., and I. Fridovich. 1984. Enzymatic defenses against oxygen toxicity in the hydrothermal vent animals *Riftia pachyptila* and *Calyptogena magnifica*. *Arch. Biochem. Biophys.* **228:** 617–620.

Brooks, J. M., M. C. Kennicutt, C. R. Fisher, S. A. Macko, K. Cole, J. J. Childress, R. R. Bidigare, and R. D. Vetter. 1987. Deep-sea hydrocarbon seep communities: evidence for energy and nutritional carbon sources. *Science* **238:** 1138–1142.

Cary, S. C., H. Felbeck, and N. D. Holland. 1989. Observations on the reproductive biology of the hydrothermal vent tube worm, *Riftia pachyptila*. *Mar. Ecol. Prog. Ser.* **52:** 89–94.

Cavanaugh, C. M., S. L. Gardiner, M. L. S. Jones, H. W. Jannasch, and J. B. Waterbury. 1981. Prokaryotic cells in the hydrothermal vent tube worm, *Riftia pachyptila*: possible chemoautotrophic symbionts. *Science* **213:** 340–342.

Childress, J. J. 1987. Uptake and transport of sulfide in marine invertebrates. Pp. 231–239 in *Comparative Physiology: Life in Water and on Land*, P. Dejours, L. Bolis, C. R. Taylor, and E. R. Weibel, eds. 1X-Liviana Press, Padova.

Childress, J. J., and T. J. Mickel. 1980. A motion compensated shipboard precision balance system. *Deep-Sea Res.* **27a:** 965–970.

Childress, J. J., A. J. Arp, and C. R. Fisher Jr. 1984. Metabolic and blood characteristics of the hydrothermal vent tube-worm *Riftia pachyptila*. *Mar. Biol.* **83:** 109–124.

Childress, J. J., C. R. Fisher, J. M. Brooks, M. C. II. Kennicutt, R. Bidigare, and A. E. Anderson. 1986. A methanotrophic marine molluscan (Bivalvia, Mytilidae) symbiosis: mussels fueled by gas. *Science* **233:** 1306–1308.

Daniels, L., and J. G. Zeikus. 1983. Convenient biological preparation of pure high specific activity ^{14}C-labelled methane. *J. Labelled Comp. Radiophar.* **20:** 17–24.

Distel, D. L., D. J. Lane, G. J. Olsen, S. J. Giovannoni, B. Pace, N. R. Pace, D. A. Stahl, and H. Felbeck. 1988. Sulfur-oxidizing bacterial endosymbionts: analysis of phylogeny and specificity by 16S rRNA sequences. *J. Bacteriol.* **170:** 2506–2510.

Felbeck, H. 1981. Chemoautotrophic potential of the hydrothermal vent tube worm, *Riftia pachyptila* Jones (Vestimentifera). *Science* **213:** 336–338.

Felbeck, H., J. J. Childress, and G. N. Somero. 1981. Calvin-Benson cycle and sulphide oxidation enzymes in animals from sulphide-rich habitats. *Nature* **293:** 291–293.

Fisher, C. R. 1990. Chemoautotrophic and methanotrophic symbioses in marine invertebrates. *Rev. Aquat. Sci*

Fisher, C. R., Jr., and Childress, J. J. 1984. Substrate oxidation by trophosome tissue from *Riftia pachyptila* Jones (Phylum Pogonophora). *Mar. Biol. Lett.* **5:** 171–183.

Fisher, C. R., J. J. Childress, and N. K. Sanders. 1988a. The role of vestimentiferan hemoglobin in providing an environment suitable for chemoautotrophic sulfide-oxidizing endosymbionts. *Symbiosis* **5:** 229–246.

Fisher, C. R., J. J. Childress, A. J. Arp, J. M. Brooks, D. Distel, J. A. Favuzzi, S. A. Macko, A. Newton, M. Powell, G. N. Somero, and T. Soto. 1988b. Physiology, morphology, and biochemical composition of *Riftia pachyptila* at Rose Garden in 1985. *Deep-Sea Res.* **35:** 1745–1758.

Fisher, C. R., J. J. Childress, and J. M. Brooks. 1988c. Are hydrothermal-vent Vestimentifera carbon limited? *Am. Zool.* **28:** 128a.

Fustec, A., D. Desbruyères, and S. K. Juniper. 1987. Deep-sea hydrothermal vent communities at 13°N on the East Pacific Rise: microdistribution and temporal variations. *Biol. Ocean.* **4:** 121–164.

Hessler, R. R., W. M. Smithey, M. A. Boudrais, C. H. Keller, R. A. Lutz, and J. J. Childress. 1988. Temporal change in megafauna at the Rose Garden hydrothermal vent. *Deep-Sea Res.* **35:** 1681–1710.

Hobbie, J. E., Daley, R. J., Jasper, S. 1977. Use of nucleopore filters for counting bacteria by fluorescence microscopy. *Appl. Environ. Microbiol* **33:** 1225–1228.

Hoffman, P. S., H. A. George, N. R. Krieg, and R. M. Smibert. 1979. Studies of the microaerophilic nature of *Campylobacter fetus* subsp. *jejuni*. II. Role of exogenous superoxide anions and hydrogen peroxide. *Can. J. Microbiol.* **25:** 8–16.

Issacs, N. S. 1981. *Liquid Phase High Pressure Chemistry.* John Wiley and Sons. 414 pp.

Jannasch, H. W. 1983. Microbial processes at deep sea hydrothermal vents. Pp. 677–709 in *Hydrothermal Processes at Seafloor Spreading Centers*, P. A. Rona *et al.*, eds. Plenum Press New York.

Jannasch, H. W. 1989. Chemosynthetically sustained ecosystems in the deep sea. Pp. 147–166 in *Autotrophic Bacteria*, H. G. Schlegel and B. Bowien, eds. Science Tech. Publ., Madison and Springer-Verlag, Berlin.

Jannasch, H. W., and D. C. Nelson. 1984. Recent progress in the microbiology of hydrothermal vents. Pp. 170–176 in *Current Perspectives in Microbial Ecology*, M. J. Klug and C. A. Reddy, eds. Am. Soc. Microbiol., Washington.

Johnson, K. S., J. J. Childress, R. R. Hessler, C. M. Sakamoto-Arnold, and C. L. Beehler. 1988a. Chemical and biological interactions in the Rose Garden hydrothermal vent field. *Deep-Sea Res.* **35:** 1723–1744.

Johnson, K. S., J. J. Childress, and C. L. Beehler. 1988b. Short term temperature variability in the Rose Garden hydrothermal vent field. *Deep-Sea Res.* **35:** 1711–1722.

Jones, M. L. 1981. *Riftia pachyptila* Jones: observations on the vestimentiferan worms from the Galapagos Rift. *Science* **213:** 333–336.

Jones, M. L. 1988. The vestimentifera, their biology and systematic and evolutionary patterns. *Oceanol. Acta* **SP 8:** 69–82.

Jones, M. L., and S. L. Gardiner. 1988. Evidence for a transient digestive tract in vestimentifera. *Proc. Biol. Soc. Wash* **101:** 423–433.

Kelly, D. P. 1989. Physiology and biochemistry of unicellular sulfur bacteria. Pp. 193–218 in *Autotrophic Bacteria*, H. G. Schlegel and B. Bowen, eds. Science Tech. Pub. Madison, WI.

Krieg, N. R., and P. S. Hoffman. 1986. Microaerophily and oxygen toxicity. *Ann. Rev. Microbiol.* **40:** 107–130.

Kulm, L. D., E. Suess, J. C. Moore, B. Carson, B. T. Lewis, S. D. Ritger, D. C. Kadko, T. M. Thornburgh, R. W. Embley, W. D. Rugh, G. J. Massoth, M. G. Langseth, G. R. Cochrane, and R. L. Scamman. 1985. Oregon subduction zone: venting, fauna, and carbonates. *Science* **231:** 561–566.

Macdonald, I. R., G. S. Boland, J. S. Baker, J. M. Brooks, M. C. Kennicutt II, and R. R. Bidigare. 1989. Gulf of Mexico hydrocarbon seep communities. II. Spatial distribution of seep organisms and hydrocarbons at Bush Hill. *Mar. Biol* **101:** 235–247.

Mickel, T. J., and J. J. Childress. 1982a. Effects of pressure and pressure acclimation on activity and oxygen consumption in the bathypelagic mysid *Gnathophausia ingens*. *Deep-Sea Res.* **29:** 1293–1301.

Mickel, T. J., and J. J. Childress. 1982b. Effects of temperature, pressure and oxygen concentration on the oxygen consumption rate of the hydrothermal vent crab *Bythograea thermydron* (Brachyura). *Physiol. Zool.* **55:** 199–207.

Powell, M. A., and G. N. Somero. 1983. Blood components prevent blood poisoning of respiration of the hydrothermal vent tube worm *Riftia pachyptila*. *Science* **219:** 297–299.

Powell, M. A., and G. N. Somero. 1986. Adaptations to sulfide by hydrothermal vent animals: sites and mechanisms of detoxification and metabolism. *Biol. Bull.* **171:** 274–290.

Quetin, L. B., and Childress, J. J. 1980. Observations on the swimming activity of two bathypelagic mysid species maintained at high hydrostatic pressures. *Deep-Sea Res.* **27A:** 383–391.

Rau, G. H. 1981. Hydrothermal vent clam and tube worm 13C/12C: further evidence of nonphotosynthetic food sources. *Science* **213:** 338–340.

Rau, G. H. 1985. 13C/12C and 15N/14N in hydrothermal vent organisms: ecological and biogeochemical implications. *Bull. Biol. Soc. Wash.* **6:** 243–248.

Roux, M., M. Rio, E. Schein, R. A. Lutz, L. W. Fritz, and L. M. Ragone. 1989. Mesures *in situ* de la croissance des bivalves et des vestimentifères et de la corrosion des coquilles au site hydrothermnal de 13°N (dorsale du Pacifique oriental). *C. R. Acad. Sci. Paris, Sér. III* **308:** 121–127.

Smith, R. P., and R. E. Gosselin. 1979. Hydrogen sulfide poisoning. *J. Occup. Med.* **21:** 93–97.

Southward, E. C. 1988. Development of the gut and segmentation of newly settled stages of *Ridgeia* (Vestimentifera): implications for relationship between Vestimentifera and Pogonophora. *J. Mar. Biol. Assoc. U. K.* **68:** 465–487.

Stein, J., M. Haygood, and H. Felbeck. 1989. Diversity of RuBP carboxylase genes in sulfur oxidizing symbioses. *Proc. 4th Endocytobio. Coll.*, Lyon, France. July, 1989 (in press).

Stokes, C. M., and D. A. Walker. 1972. Photosynthesis by isolated chloroplasts: inhibition by DL-glyceraldehyde of carbon dioxide assimilation. *Biochem. J.* **128:** 1147–1157.

Strickland, J. D. H., and T. R. Parsons. 1972. A practical handbook of seawater analysis, 2nd ed. *Bull. Fish. Res. Board Can.* **167:** 1–310.

Tabita, F. R. 1988. Molecular and cellular regulation of autotrophic carbon dioxide fixation in microorganisms. *Microbiol. Rev.* **52:** 155–189.

Tentori, L., and A. M. Salvati. 1981. Hemoglobinometry in human blood. In *Hemoglobins*, E. Antonni, L. Rossi-Bernardi, and E. Chiancone, eds. *Meth. Enzymol.* **76:** 707–714.

Willason, S. W., and K. S. Johnson. 1986. A rapid, highly sensitive technique for the determination of ammonia in seawater. *Mar. Biol.* **91:** 285–290.

Wilmot, D. B. Jr., and R. D. Vetter. 1990. The bacterial symbiont from the hydrothermal vents tubeworm *Riftia pachyptila* is a sulfide specialist. *Mar. Biol.*

Reference: *Biol. Bull.* 177: 386–395. (December, 1989)

Gills as Possible Accessory Circulatory Pumps in *Limulus polyphemus*

M. A. FREADMAN[1] AND W. H. WATSON III[2,*]

[1]*Marine Biological Laboratory, Woods Hole, Massachusetts 02543 and* [2]*Department of Zoology, University of New Hampshire, Durham, New Hampshire 03824*

Abstract. Heart electrical activity (ECGs), gill closer muscle potentials (EMGs), and blood pressures in the heart and the branchiocardiac canals, were measured in adult horseshoe crabs (*Limulus polyphemus*) during various activities. During ventilation, hyperventilation, and swimming, large transient increases in pressures (10–35 cm H_2O) occur in the branchiocardiac canals, which carry blood from the gills to the heart. These pulses of positive pressure are related to, and apparently caused by, gill plate closing. During quiescent periods, with no ventilatory activity, there are no pressure pulses in the canals, but the pressure is still greater than zero. We found covariation of heart and ventilation rates during intermittent ventilation, hyperventilation, gill cleaning, and swimming, as well as evidence of transient periods of phasic coordination. The heart appears to be weakly entrained to the gill rhythm by phasic cardioregulatory nerve input. The preferred phase of heartbeats, with respect to gill rhythm, was 0.5, or 180 degrees out of phase. In some animals, intra-cardiac pressures were enhanced when the heart and gill rhythms were entrained. We suggest that rhythmic movements of the gill plates enhance the flow of low pressure blood returning from the body to the heart. Thus, ventilatory appendage movements may constitute an accessory blood pumping mechanism in *Limulus*.

Introduction

Many invertebrates, including annelids, molluscs, arthropods, and echinoderms, have highly developed circulatory and respiratory systems. In many cases the morphology is well known, but the functional properties and interactions of these convective systems during normal behavior have not been examined in detail. Evidence from research on decapod crustaceans suggests that investigations of the respiratory and circulatory systems of aquatic arthropods might yield valuable information for understanding the operating conditions and physiological role of coupling between these systems. Close coordination and coupling between circulatory and respiratory systems under a variety of environmental conditions has been reported frequently (*Homarus americanus, Cancer productus,* McMahon and Wilkens, 1975, 1977; Young and Coyer, 1979; *Cancer magister,* Wilkens *et al.*, 1974; *Carcinus maenus,* Young, 1973; *Cancer borealis, Cancer irroratus,* Coyer, 1977). Nevertheless, the physiological significance of respiratory/circulatory coupling is not fully understood.

The coordination of cardiac and ventilatory activity in *Limulus polyphemus* presents another interesting example, worthy of further investigation. Watson and Wyse (1978) reported frequency covariation (heart and ventilation rates changed together) and phasic coordination (heart beats occurred in phase with the gill plate movements) of heart and ventilatory systems under normoxic and hypoxic conditions, as well as during intermittent ventilation, hyperventilation, gill cleaning, and swimming. The frequency covariation observed in *Limulus*, as well as many other organisms, may serve primarily to adjust the volume of blood circulated to the rate of oxygen uptake. On the other hand, the adaptive significance of phasic coordination between the gills and heart is not clear. Watson and Wyse (1978) suggested that phasic coordination makes the two blood pumping systems more efficient. While the role of the gills as an accessory "heart" has been suggested previously (Patten and

Received 24 March 1989; accepted 22 September 1989.
* Address for correspondence.

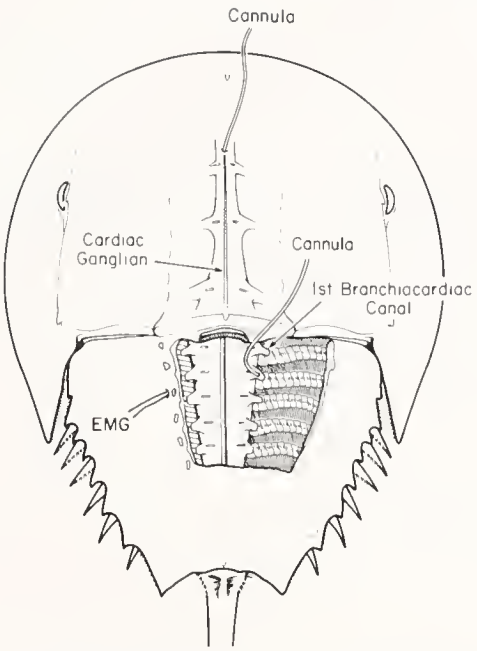

Figure 1. Dorsal cutaway illustration of *Limulus polyphemus*, illustrating the position of catheters and electrodes.

Redenbaugh, 1899; Lockhead, 1950), little physiological evidence is available to support these interpretations. The present contribution provides evidence that the gill plates help circulate the blood in *Limulus*, and documents the hemodynamic relationships between the cardiac and ventilatory systems of intact horseshoe crabs during all of their known respiratory behaviors. In addition, we present evidence suggesting that, in some cases, phase coupling between the heart and gill rhythms enhances cardiac output.

In crustaceans, there is good evidence that frequency covariation between the gills and heart is mediated by the cardioregulatory nerves (Field and Larimer, 1975a, b; Young, 1978). In a few instances investigators recorded phasic activity in the cardioregulatory nerves that appeared to be coupled to the ventilatory rhythm; they suggested that this type of activity would help phase-lock the heart rhythm to scaphognathite movements. In *Limulus* the cardioregulatory nerves also appear to be important in the tonic regulation of heart rate and in the coordination between the cardiac and ventilatory rhythms (Watson, 1979). However, phase coupling between the heart and gills could also be mediated by direct pressure cues. In this study we found that phase coupling between heart and gill rhythms was associated with rhythmic bursts in the cardioregulatory nerves. These data suggest that in *Limulus* both tonic and phasic coordination between the heart and gills is regulated by the nervous system.

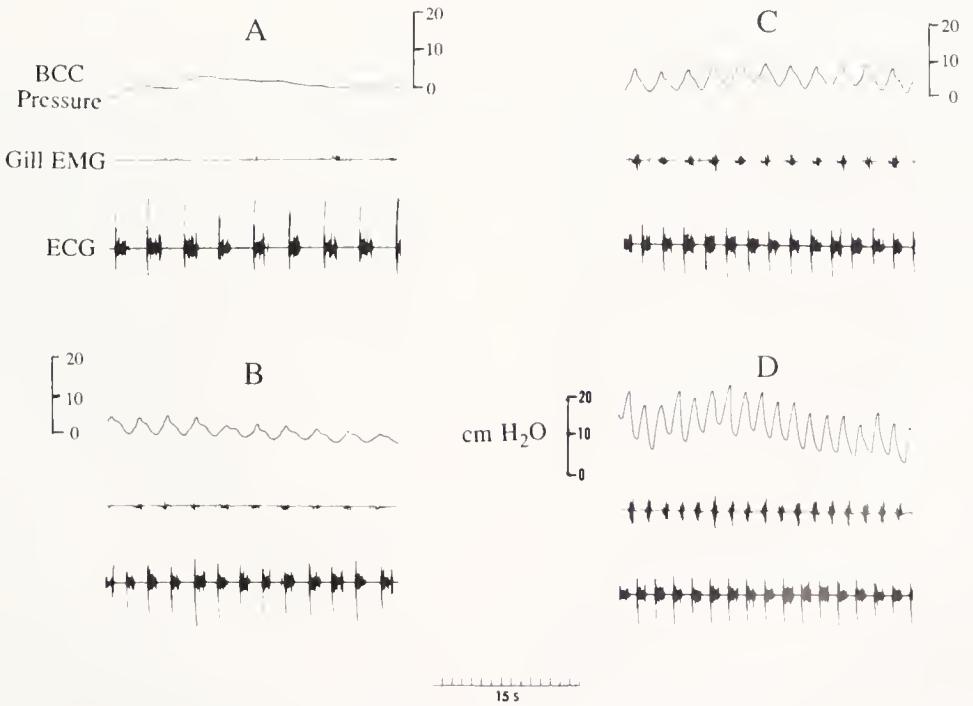

Figure 2. The relationship between pressure (cm H_2O) in a branchiocardiac canal (BCC, 2nd canal), the electromyogram (EMG) of the gill closer muscle (20) of the 2nd gill plate and heart activity (ECG) during rest (A) and increasing amplitudes of ventilation (B–D). Similar records obtained during hyperventilation and swimming are presented in a subsequent figure. Pressures are relative to ambient in the water column.

Materials and Methods

Specimens of *Limulus polyphemus* (18–25 cm carapace width) were either obtained from the Marine Biological Laboratory or collected from Buzzards Bay, Falmouth, Massachusetts. Animals were maintained in either a recirculating seawater system (University of New Hampshire, Durham, New Hampshire) or a 1200-liter tank continuously supplied with fresh seawater (MBL, Woods Hole, Massachusetts) at 13–15°C (30–33‰) and fed mussel bits every few days. Survival and health of the animals in the laboratory over several months were excellent. Twelve animals were used in our blood pressure experiments; and six were used for neurophysiology.

Electrical activity of the heart was recorded with pairs of 40- or 45-gauge stainless steel wire (annealed, epoxy coated for insulation) inserted through small holes in the dorsal midline of the opisthosoma, adjacent to the cardiac ganglia. Electrical activity of ventilatory muscles was recorded with similar wires inserted into muscle 20 (Patten and Redenbaugh, 1899) through small holes in the overlying cuticle (Fig. 1). Implants were held in place on the cuticle surface with a small amount of methylcyanoacrylic adhesive or dental wax.

Pressures in the heart and in the branchiocardiac canals (which convey blood from the gills to the pericardial cavity) were measured with polyethylene tubing (PE 100) and pressure transducers (Statham P23ID). Catheters with beveled tips were inserted into the heart or one of the branchiocardiac canals through small holes drilled in the overlying cuticle, and cemented in place with quick-drying epoxy (Fig. 1). Prebranchial blood pressure was also measured at the junction of the mesosoma and telson. Catheters were kept as short as feasible (about 18 cm), and their insertion positions were confirmed at the termination of experiments by dissection. At times, we noted reduced frequency and amplitude responses in the pressure records irrespective of the activity of the animal; this was due to clotting at the proximal end of the catheters and was alleviated by gentle flushing. Most experiments were conducted in cold seawater (13°C) to reduce the tendency of blood clotting in the catheters.

Following surgical procedures, animals were allowed to rest for 4–5 h or overnight before measurements were made. Oxygen in the seawater of the test chamber was maintained above 90% saturation during the acclimation period and the experiments. Experiments were carried out in 80-liter Plexiglas chambers filled with seawater and arranged with a mirror underneath the test chamber for observation of the gill appendages. Wire electrodes were attached to a sliding rack above the chamber to prevent fouling of the implants. Some of the crabs were restrained in the chamber on a Plexiglas shelf with a hole situated under the animals abdomen, so the gill appendages could ventilate freely. Others were allowed to move and swim freely about the chamber. Signals of heart and ventilatory muscle electrical activity, as well as the pressure waveforms from the heart and branchiocardiac canal catheters, were recorded individually, or simultaneously, on adjacent channels of a Grass Polygraph (Model 7D).

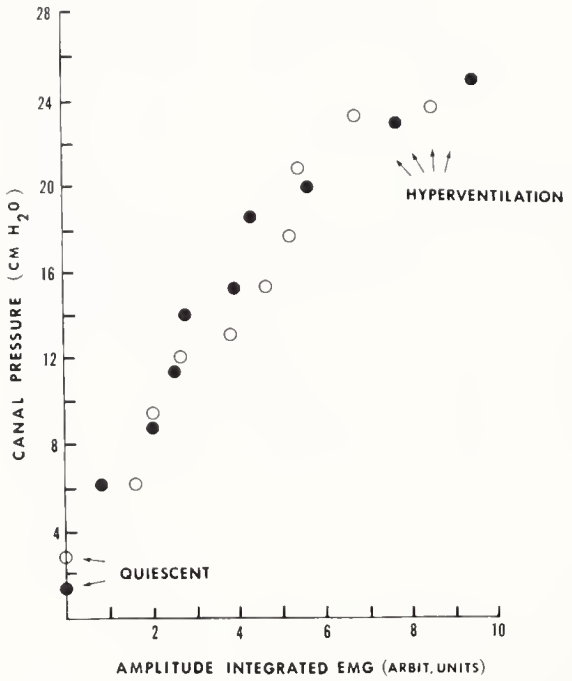

Figure 3. The relationship between strength of gill contractions and peak BCC pressure. Pressure in the 2nd branchiocardiac canal and integrated electromyogram (EMG) of a gill closer muscle were obtained during quiescent behavior, increasing ventilatory activity and hyperventilation in two different animals (open and closed circles). The pressures recorded from the BCC's were proportional to the strength of gill plate contractions.

Cardioregulatory nerve recordings were obtained using suction electrodes from animals restrained in a Plexiglas chamber as described above. A small window was cut in the carapace to expose the cardioregulatory nerves. All signals (EMG, ECG, and extracellular potentials) were detected with Grass P511 amplifiers, displayed on an oscilloscope, photographed with a Grass C4 camera, and recorded on magnetic tape. Recordings from isolated ventral nerve cords were carried out as described in Wyse *et al.* (1980).

Results

General respiratory behavior

During experiments lasting 7–16 h, most specimens of *Limulus polyphemus* exhibited several types of ventilatory activity: intermittent ventilation, hyperventilation, gill cleaning, and swimming. Intermittent ventilation in

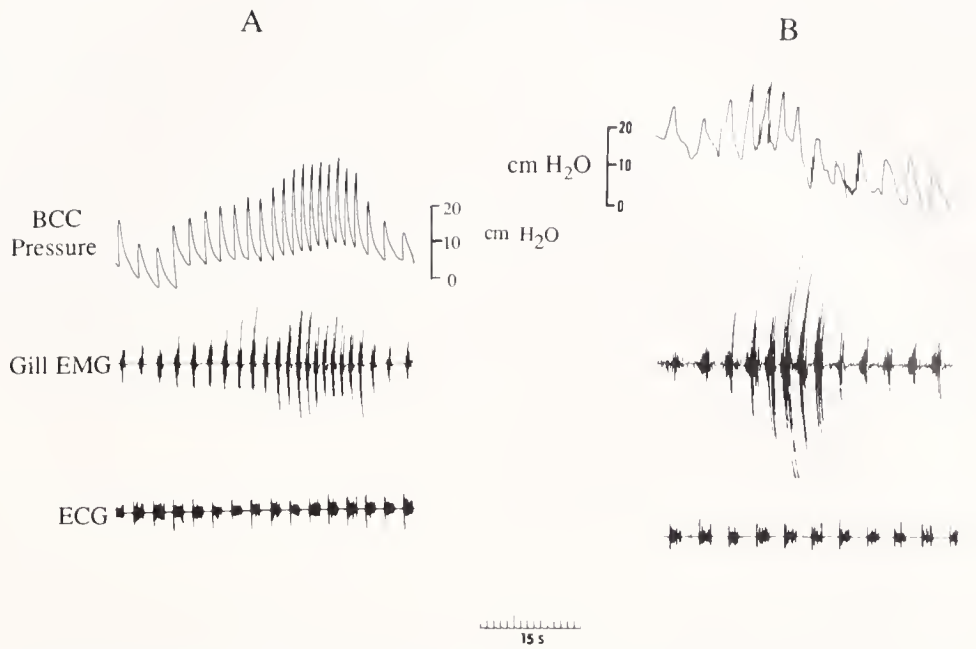

Figure 4. Pressure in one branchiocardiac canal, gill EMG and ECG during hyperventilation (A) and swimming, as indicated by the large amplitude gill EMG's (B).

Limulus occurs as alternating bouts of ventilation and apnea. Both hyperventilation and swimming are characterized by a large increase in rates of gill plate movements over that observed in shallow ventilation (Knudsen, 1973). The major difference between the two behaviors is that during swimming the legs also move in phase with the gills, while during hyperventilation leg movements are independent of gill activity. During gill cleaning, the gill plates move across the midline and flick the inner lobe of a gill plate between the book gill lamellae of the opposite side. In all the aforementioned ventilatory activities, heart rate was always positively correlated with the rate of ventilation. These respiratory and locomotor behaviors of *Limulus* have also been reported in earlier papers (Watson and Wyse, 1978; Watson, 1980a, b).

Pressures in the branchiocardiac canals during rest, ventilation, hyperventilation, and swimming

The branchiocardiac canals (BCCs), as the term implies, carry blood from the gills to the pericardial cavity and heart. Five pairs of canals correspond to the five gill appendages (Fig. 1). Blood from the venous circuit passes through an extensive gill network (Lockhead, 1950; Johansen and Petersen, 1975) before returning to the heart. We measured pressures in one canal, while simultaneously recording the electrical activity of that gill's closer muscle, during rest (*i.e.*, no ventilatory activity occurring), ventilation, hyperventilation, and swimming. During rest, no pressure pulses occur in the canal, although the pressure may be greater than zero (Fig. 2A). As the amplitude of ventilation increases, pressure in the canal rises substantially (3–20 cm H_2O), as does the amplitude and frequency of the recorded EMG and the heart rate (Fig. 2B–D).

To examine more closely the relationship between the strength of gill contractions (as monitored by EMG activity) and the resulting BCC pressures, we plotted integrated EMG amplitudes *versus* the magnitude of canal pressures, during several different intensities of ventilatory activity, ranging from shallow ventilation to hyperventilation. There is a direct relationship throughout the range of pressures measured (Fig. 3). This relationship was consistent during all of our experiments, whether the animals were restrained or freely moving.

We also recorded pressures in a BCC during hyperventilation and swimming. Examples of these results are shown in Figure 4. Hyperventilation was sometimes intermittent, and with the onset of this behavior, large pressure pulses occur in the canal (Fig. 4A). During swimming, which is also periodic, the record shows essentially the same result, but the recorded pressures are more erratic (Fig. 4B). This is probably due to movement artifacts introduced to the liquid-filled pressure catheter system during swimming as the animal moved up and down in the chamber.

Prebranchial pressures (junction of soma and telson) are low during rest (1–2 cm H_2O, n = 9) and increased only slightly during ventilatory periods (2.5–3 cm H_2O). Therefore, the blood reaching the gills is at a low pres-

sure, and the rhythmic movements of the gills are likely important for circulating venous blood dorsally to the heart.

Frequency covariation between heart and gill rhythms

To assess the relationship between heart pressures and BCC pressures, we obtained simultaneous recordings of closer muscle electrical activity (EMG), BCC pressures, heart electrical activity (ECG), and intracardiac blood pressure (Fig. 5A). Throughout all of our experiments, a strong frequency coordination existed between the two rhythmic systems. When gill ventilation increased, so did the pressures in the BCC's (Figs. 2–5), and, presumably, the rate of venous return. Thus, from a hemodynamic perspective, frequency covariation between heart and gill pumps insures that the venous return is coordinated with the tonic output of the heart.

Phasic coordination between heart and gills

Most of the animals examined did not exhibit strong phase coupling between the heart and gill rhythms (see Fig. 6 for illustration of how phase coupling was determined). However, a small proportion (10–20%) of the animals examined either strongly phase coupled, or drifted in and out of the coupling mode. When phase coupling did occur, the preferred phase was usually close to 0.5 (Fig. 6), indicating that the heart beat 180° out of phase with the gills. Why is 0.5 the preferred phase? If there is some hemodynamic advantage, then the output of the heart should be maximal when the two pumps are 180° out of phase. To test this hypothesis, we recorded heart and BCC pressures for approximately 1 h, and then plotted peak cardiac pressures *versus* phase of the heartbeat with respect to the gill rhythm, on a beat-to-beat basis. We found that, in some of the animals, intra-cardiac pressure remained relatively constant regardless of ventilatory activity (Fig. 7B). In three animals, however, the cardiac pressures were greatest when the heart and ventilatory rhythms were 180° out of phase (Fig. 7A). Thus, at least in some animals, phase coupling may enhance cardiac output.

Cardioregulatory nerve activity during phase coupling

If the heart is entrained by the nervous system, it must receive phasic timing cues through the cardioregulatory nerves. Furthermore, this timing information must have a fixed phase relationship to the ventilatory rhythm so it can entrain the two oscillatory systems. We recorded cardioregulatory nerve activity from intact, immobilized animals while monitoring heart ECGs and gill plate EMGs (Fig. 8). During periods when the gill plates were making large, rapid movements, there was a phasic component to the cardioregulatory nerve activity (Fig. 8A, C). Bursts comprising several different units tended to occur during and just after contractions of the gill plate closer muscle. Periods of silence followed for the remainder of the gill interburst interval. When this type of cardioregulatory nerve activity was present the heart was phase locked to the ventilatory cycle (see top plot, Fig. 8). But when ventilation slowed and became weaker, cardioregulatory nerves lacked phasic activity, and phase coupling did not occur (Fig. 8B, D, and top of Fig. 8).

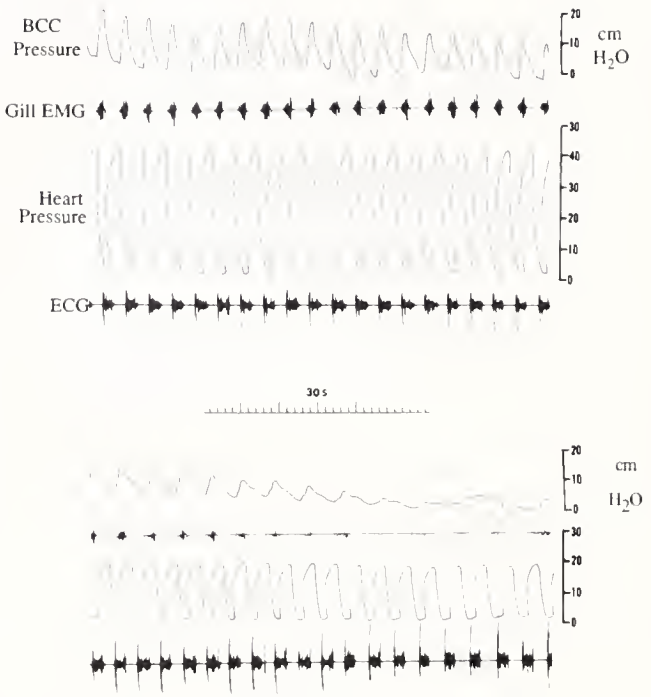

Figure 5. Pressures (cm H_2O) and electrical activity in the respiratory and circulatory systems of *Limulus*. The top four records show pressure in 1st branchiocardiac canal (BCC), EMG of the 1st gill muscle, pressure in the heart and the ECG. The bottom four traces are the same physiological processes and include a section where ventilatory activity ceased. Pressures are relative to ambient in the water column.

To eliminate the possibility that phasic activity was due to sensory modulation, we recorded cardioregulatory nerve activity from isolated ventral nerve cords. When there were strong bursts in the ventilatory motor nerves, we also recorded bursts in the cardioregulatory nerves that were phase locked to the ventilatory central pattern generator (CPG) (Fig. 9). During quiet ventilation, however, only tonic firing was present. Thus, phasic cardioregulatory nerve activity is a component of the ventilatory central pattern generator. Although these data do not prove that the phasic cardioregulatory nerve activity is responsible for entraining the heart to the ventilatory rhythm, we suggest that phase coupling is most

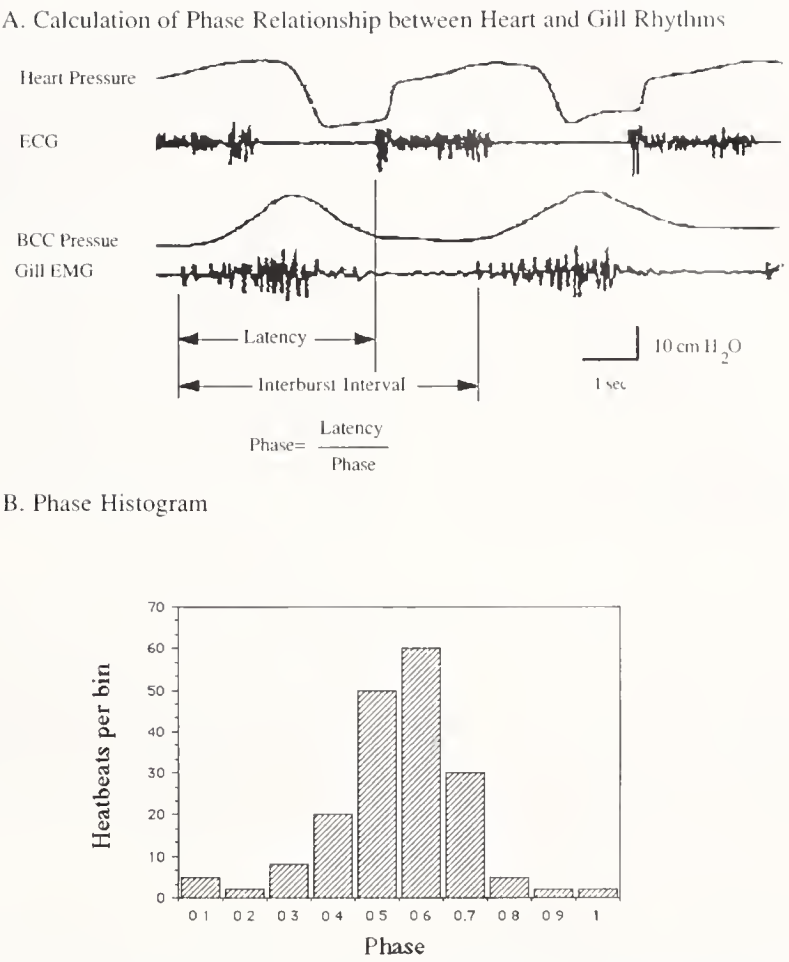

Figure 6. Phase relationships between heart and gill rhythms. A. Actual records of BCC and heart pressures, gill EMG, and ECG, showing how the phase relationship between the two rhythms was calculated. Phase is calculated by dividing the latency (time between onset of a gill muscle burst and onset of cardiac ganglion burst) by the duration of the concurrent gill interburst interval (time between the beginning of one burst and the beginning of the next burst). B. Histogram demonstrating phase preference of a cardiac ganglion burst (recorded as ECG) with respect to concurrent ventilatory event. The number of heartbeats from a particular phase were then totaled and a histogram constructed. Heartbeats per bin indicates number of events falling in each decile of phase (*e.g.*, between 0.2 and 0.3). In this experiment, there was a very strong phase preference of 0.5 indicating the heartbeat was 180° out of phase with ventilatory activity. We did not find such strong phase preference in all animals or in any single animal at all times. But, when phase preferences existed, they were usually close to 0.5.

likely mediated by neural rather than hemodynamic mechanisms.

Discussion

Circulatory systems have traditionally been divided into two types: closed systems, in which the blood is always in distinct vessels separated physically from intercellular fluids; and open systems, with large, ill-defined cavities, in which the blood is not separated from the intercellular fluids. The open systems have been regarded as poorly developed and capable of generating only low pressures and low blood flow velocities. The open circulatory system of *Limulus polyphemus* is well developed and appears to have few of the large sinuses normally found in open circulatory systems (Shuster, 1978; Redmond *et al.*, 1982). Our study indicates that high pressures occur in various portions of the circulatory system, particularly in the heart and branchiocardiac canals. Sumwalt (1933) and Abbott *et al.* (1969) also reported high pressures in the heart of *Limulus*.

Redmond *et al.* (1982) measured blood pressures in and around the heart and body of resting horseshoe crabs in water and air. They attributed the moderate variability

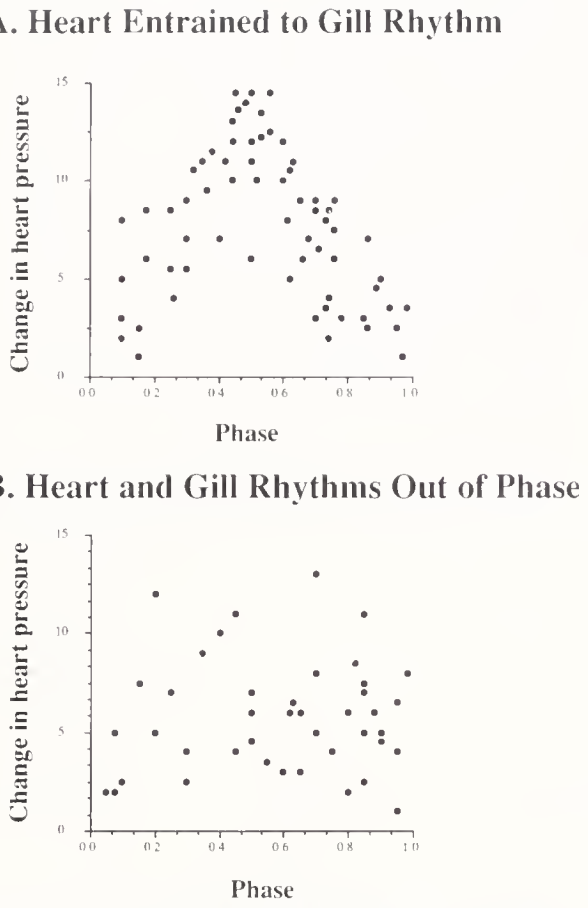

Figure 7. Influence of heart/gill phase relationship on cardiac pressures. On a beat-to-beat basis the phase relationship between the heart and the gill rhythms was calculated and plotted *versus* the amplitude of the pressure change during the subsequent heartbeat. In some animals, when the heart and gills were approximately 180° out of phase (0.5), the pressures recorded from the heart were higher (as illustrated by data from the animal plotted in A). In other animals there was no apparent influence of heart/gill phase on cardiac output (as shown by data from a different animal plotted in B).

of their data to differing activity levels. We monitored ventilatory muscles and, from previous experience (Watson and Wyse, 1978), could identify quiescent behavior, intermittent ventilation, hyperventilation, gill cleaning, and swimming. These are the most characteristic activities that involve the gill appendages (Watson and Wyse, 1978; Watson, 1980a, b). Rhythmic pressure changes in the BCCs were always associated with movements of the gills, and their amplitudes varied with the type and strength of gill movements. Thus, variability in pressures recorded in the heart and BCCs are probably due to the animal switching from one type of respiratory activity to another.

It is likely that the rhythmic movements of the gill appendages of *Limulus* serve to enhance gas exchange and to pump oxygenated venous blood to the pericardial cavity. It has been reported that blood moves from the large ventral sinuses through the gill lamillae and BCCs to the pericardial cavity (Patten and Redenbaugh, 1899; Lockhead, 1950; Redmond *et al.*, 1982). We have also observed blood moving in this manner in juvenile horseshoe crabs. In this study we recorded large pressure pulses in the branchiocardiac canals during normal ventilation, hyperventilation, and swimming—all important components of the daily activities of horseshoe crabs. These changes in pressure always occur during contraction of the gill closer muscles, and their amplitudes are proportional to the magnitude of the gill plate movements. We never detected pressure surges in the branchiocardiac canals during quiescent behavior, when the gill plates were not moving, but the heart was still beating. Thus, it is likely that venous return to the heart is assisted by the gill appendages, which may serve as an accessory heart in *Limulus*.

Although pressure pulses recorded from the BCC's are likely caused by movements of the gill appendages and result in the flow of blood from the gills to the pericardial cavity, additional studies will be required to prove this hypothesis. In particular, it is important to determine if valves are present in the BCCs to rectify flow, and to continuously monitor the dynamics of blood flow in the canals.

Apparently, enhanced blood flow from ventilatory movements in horseshoe crabs is established in early life stages. We had the opportunity to observe blood flow in young specimens of *Limulus* (5 mm carapace width) under a dissecting microscope, because animals this small are quite transparent. With each ventilatory movement and during swimming activity, blood rapidly pulses into the pericardial cavity and heart. We also observed covariation of heart and ventilatory rates.

Occasionally, horseshoe crabs exhibit phase coupling between the heart and gill rhythms. Our analyses suggest that, in some animals, this coupling may increase cardiac output. It may also allow the animal to do the same amount of circulatory work more efficiently, but we have no data to support this hypothesis at present. The preferred phase of almost all animals that demonstrated phase coupling was approximately 0.5, or 180° out of phase. Why would this relationship between two systems lead to enhanced blood flow? When the gill plates close, due to the contraction of gill muscle 20, oxygenated blood is forced dorsally through the BCCs to the pericardial cavity. If the heart and gills are 180° out of phase, then the heart will be relaxing as blood enters the pericardial cavity (see Fig. 6). When the heart relaxes, blood enters the heart through the ostia. Thus, maximal blood is available to the heart during the filling phase of its contraction-relaxation cycle. This appears to increase the

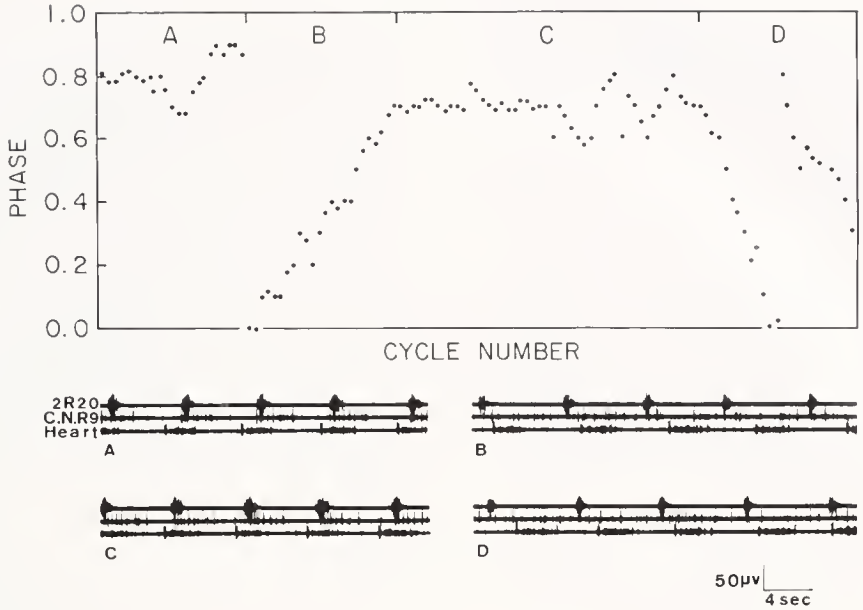

Figure 8. The relationship between bursting in the cardiac nerves and the degree of coupling between the heart and gill rhythms. The top graph shows a sequential phase plot of heartbeats with respect to the concurrent gill interburst intervals (Phase = heart latency/duration of the gill burst interval). In this particular experiment, there was good coupling between the heart and gill rhythms during segments A and C, and drifting, or no phase coordination during B and D. Representative segments of records from these periods are shown below (A–D). During periods of coupling (A and C) there was discrete bursting in cardiac nerve 9, while during periods of drifting (B and D), the cardiac nerve activity was more weakly phasic. This suggests that coupling may be related to the degree of phasic activity in the cardiac nerves.

force of the next heartbeat (Fig. 7) and, as a consequence, may lead to an increase in cardiac output.

We cannot estimate the quantitative contribution of blood flow to the heart from ventilatory movements of the gill appendages, or cardiac output from our data because we did not measure blood flow. Measurements of cardiac output in *Limulus* at rest, calculated from the Fick equation, are reasonably high (Mangum *et al.*, 1975) and we expect the values to increase during activity. The use of microcatheter tip flow probes should allow measurements of cardiac output; then the possibility that phase coupling in *Limulus* leads to enhanced cardiac output can be more rigorously tested.

Phase coupling between *Limulus* heart and gills appears to be mediated by the cardioregulatory nerves. Bursts of action potentials, which are phase locked to the ventilatory CPG, can be recorded from the cardioregulatory nerves in intact animals and in isolated preparations (Figs. 8, 9). When bursts are present in some animals, the heart is coupled to the gill rhythm; when the bursts are

Figure 9. Rhythmic bursts recorded from cardioregulatory nerves in isolated ventral nerve cords. It is possible to monitor motor patterns which represent ventilation by recording from the External (E), Medial (M) and Internal (I) branchial nerves in the isolated nerve cord. Strong ventilatory motor patterns produced by the isolated ventral nerve cord are accompanied by rhythmic bursts in cardioregulatory nerve #10 (CN), which emanates from the 2nd abdominal ganglion. This indicates that the ventilatory central pattern generator may also provide timing information to the cardioregulatory nerves, and thus to the heart.

not present, the two pattern generators run independently. But the heart may also be receiving timing input from the blood pressure pulses in the BCCs. To separate these two influences and to determine which is the controlling factor, we used a motor to move all the gill plates at a frequency that was slightly different from the output of the ventilatory CPG. We monitored the output of the ventilatory CPG by recording EMGs in the gill muscles. We found that the heart was phase coupled to the ventilatory CPG, but not to the imposed gill movements. In other words, the heart was entrained by some type of neural input that was phase locked to the ventilatory CPG, but was out of phase with pressure pulses from the BCCs (unpub. data). Thus, we conclude that phase coupling between the heart and gills in *Limulus* is mediated by the cardioregulatory nerves.

The coordination between cardiac and ventilatory rhythms in *Limulus* is very similar to that in decapod crustaceans. Decapods also exhibit frequency and phase coordination between the two systems (Wilkens *et al.*, 1974; McMahon and Wilkens, 1975; Wilkens, 1976; Field and Larimer, 1975a, b; Young and Coyer, 1979). The frequency coupling in decapods is not as tight as in *Limulus*, but the phase coupling is very similar. It only occurs in a small percentage of the animals studied and ranges from strong coupling to a drift and lock mode, to nonexistent. In decapods, cardioregulatory nerves also appear to mediate phase coupling. Young (1978) showed that cardioinhibitory units, and perhaps cardioaccelleratory units as well, occasionally fired in bursts that were phase locked to the scaphognathite rhythm. In *Limulus*, the inhibitory and excitatory units in the cardioregulatory nerves have not yet been identified. Nevertheless, in both decapods and *Limulus*, phase coupling appears to be mediated by cardioregulatory nerves that transmit information from ventilatory CPGs in the CNS to the cardiac ganglion. Further experiments are necessary to demonstrate which units are involved and to examine why coupling strength is so variable.

The movement of fluids in circulatory systems of invertebrates is accomplished by a variety of mechanisms, including tubular "hearts," sac-like hearts, chambered hearts, contracting blood vessels, several types of accessory pumps and body movements (Schmidt-Nielsen, 1983). In general, locomotion and associated body movements are important in blood flow in many small and large animals, coupling metabolic needs with delivery of nutrients and oxygen to the tissues. This strategy appears to be an important facet of hemodynamics. The horseshoe crab provides yet another example of the efficiency of this organization. The rapid movements of the gill plates that are associated with swimming also serve to ventilate the book gill lamellae and pump the oxygenated blood to the pericardial canal.

Acknowledgments

We thank Dr. Arthur B. DuBois (John B. Pierce Foundation, New Haven, Connecticut), the Grass Instrument Company (Quincy, Massachusetts), and Dr. John Sasner (University of New Hampshire) for loaning pressure transducers for our initial experiments. Dr. Daniel G. Gibson (Worcester Polytechnic Institute) taught us how to collect very young horseshoe crabs in the field and also pointed out their transparent character. Some of the experiments were conducted in Dr. Gordon Wyse's laboratory (University of Massachusetts, Amherst) as part of W.H.W. III's thesis work. We are extremely grateful to him for his advice and the use of his facilities. Dr. John Sasner and Dr. Gordon Wyse also made numerous helpful criticisms on earlier versions of this manuscript. This research was supported in part by the Ocean Industries Program at Woods Hole Oceanographic Institution (M.A.F.), a Grass Fellowship to W.H.W. III, a Faculty Research Grant from the University of New Hampshire (W.H.W. III), and a grant from NINCDS (19053, W.H.W. III).

Literature Cited

Abbott, B. C., F. Lange, I. Parnas, W. Parmley, and E. Sonnenblick. 1969. Physiological and pharmacological properties of *Limulus* heart. Pp. 232–243 in *Experientia Supplement 15, Comparative Physiology of the Heart. Current Trends.* Birkhauser Verlag, Stuttgart.

Coyer, P. E. 1977. Responses of heart and scaphognathite rates in *Cancer borealis* and *C. irroratus* to hypoxia. *Comp. Biochem. Physiol.* **56A:** 165–167.

Field, L. H., and J. L. Larimer. 1975a. The cardioregulatory system of crayfish: neuroanatomy and physiology. *J. Exp. Biol.* **62:** 519–530.

Field, L. H., and J. L. Larimer. 1975b. The cardioregulatory system of crayfish: the role of circumesophageal interneurons. *J. Exp. Biol.* **62:** 531–544.

Johansen, K., and J. A. Petersen. 1975. Respiratory adaptations in *Limulus polyphemus* (L.). Pp. 129–145 in *Eco-physiology of Estuarine Animals*, F. J. Vernberg, ed. University of South Carolina Press, South Carolina.

Knudsen, E. I. 1973. Muscular activity underlying ventilation and swimming in the horseshoe crab, *Limulus polyphemus*. *Biol. Bull.* **144:** 355–367.

Lockhead, J. H. 1950. *Xiphosura polyphemus.* Pp. 360–381 in *Selected Invertebrate Types*, F. A. Brown, ed. John Wiley, New York.

Mangum, C. P., M. A. Freadman, and K. Johansen. 1975. The quantitative role of hemocyanin in aerobic respiration of *Limulus polyphemus*. *J. Exp. Biol.* **191:** 279–285.

McMahon, B. R., and J. L. Wilkens. 1975. Respiratory and circulatory responses to hypoxia in the lobster *Homarus americanus*. *J. Exp. Biol.* **62:** 637–655.

McMahon, B. R., and J. L. Wilkens. 1977. Periodic respiratory and circulatory performance in the red rock crab *Cancer productus*. *J. Exp. Biol.* **202:** 363–374.

Patten, W., and W. A. Redenbaugh. 1899. Studies on *Limulus*. II. The nervous system of *Limulus polyphemus* with observations upon the general anatomy. *J. Morphol.* **16:** 91–200.

Redmond, J. R., D. D. Jorgensen, and G. B. Bourne. 1982. Circulatory physiology of *Limulus*. Pp. 133–146 in *Physiology and Biology of Horseshoe Crabs*, J. Bonaventura, C. Bonaventura, and S. Tesh eds. Alan R. Liss, New York.

Schmidt-Nielsen, K. 1983. *Animal Physiology*. Cambridge University Press, New York, 619 pp.

Shuster, C. N. Jr. 1978. The circulatory system and blood of the horseshoe crab. U. S. Department of Energy, Federal Energy Regulatory Commission, 14 pp.

Sumwalt, H. M. 1933. The blood pressure of *Limulus*. *Biol. Bull.* **65:** 372.

Watson, W. H. III, and G. A. Wyse. 1978. Coordination of the heart and gill rhythms in *Limulus*. *J. Comp. Physiol.* **124:** 267–275.

Watson, W. H. III. 1979. The respiratory behavior of *Limulus polyphemus*. PhD Thesis, University of Massachusetts, Amherst.

Watson, W. H. III. 1980a. *Limulus* gill cleaning behavior. *J. Comp. Physiol.* **141:** 67–75.

Watson, W. H. III. 1980b. Long-term patterns of gill cleaning, ventilation and swimming in *Limulus*. *J. Comp. Physiol.* **141:** 77–85.

Wilkens, J. L., L. A. Wilkens, and B. R. McMahon. 1974. Central control of cardiac and scaphognathite pacemakers in the crab, *Cancer magister*. *J. Comp. Physiol.* **90:** 89–104.

Wilkens, J. L. 1976. Neuronal control of respiration in decapod crustacea. *Fed. Proc.* **35:** 2000–2006.

Wyse, G. A., D. H. Sanes, and W. H. Watson III. 1980. Central neural motor programs underlying short- and long-term patterns of *Limulus* respiratory behavior. *J. Comp. Physiol.* **141:** 87–92.

Young, R. E. 1973. Nervous control of ventilation in the shorecrab *Carcinus maenus*. Ph.D. Thesis, University of St. Andrews.

Young, R. E. 1978. Correlated activities in the cardioregulatory nerves and ventilatory system in the Norwegian lobster, *Nephrops norvegicus* (L.). *Comp. Biochem. Physiol.* **61A:** 387–394.

Young, R. E. and P. E. Coyer. 1979. Phase coordination in the cardiac and ventilatory rhythms of the lobster *Homarus americanus*. *J. Exp. Biol.* **82:** 53–74.

Reference: *Biol. Bull.* 177: 396–400. (December, 1989)

Inactivation of the Corpora Allata in the Final Instar of the Tobacco Hornworm, *Manduca sexta*, Requires Integrity of Certain Neural Pathways from the Brain

LOUIS SAFRANEK AND CARROLL M. WILLIAMS

Department of Cellular and Developmental Biology, Harvard University, Cambridge, Massachusetts 02138

Abstract. Neither the implantation of active CA nor treatment with O-ethyl,S-phenylphosphoramidothiolate (EPPAT), a potent inhibitor of the juvenile hormone esterase (JHE), prevented metamorphosis of final instar tobacco hornworms. However, a combination of the two treatments often blocked metamorphosis and caused the formation of supernumerary larvae or larval-pupal intermediates. So also, in conjunction with EPPAT treatment, unilateral severance of the medial nerve from the brain to the corpus cardiacum-corpus allatum complex often resulted in abnormal supernumerary or intermediate larval forms. Thus, clearance of JH from mature hornworm larvae prior to metamorphosis appears normally to depend on two mechanisms: (1) cessation of JH production by inhibition of the CA *via* the innervation of these glands, and (2) destruction of previously secreted existing JH *via* production of JHE. In the present experiments, each of these mechanisms appeared fully able to clear JH sufficiently to permit normal metamorphosis, because only simultaneous interruption of both mechanisms led to formation of supernumerary larvae. Acting in concert as they do late in larval life, these two mechanisms ensure the timely and thorough clearance of JH in preparation for metamorphosis.

Introduction

Juvenile hormone (JH) is indispensable for maintenance of the larval condition in Lepidoptera as it is in many other orders of insects. Conversely, metamorphosis normally presupposes the virtual absence of JH and can regularly be derailed by the timely application of JH or JH analogs to mature larvae. Thus the transition from the larva's feeding life-style to the metamorphic sequence entails elimination of JH. This prerequisite could potentially be satisfied either by curtailing production of JH or by augmenting its destruction. In fact, persuasive evidence supports regulation by both pathways. Thus, production of JH by the corpora allata (CA) declines late in larval life (for review, see Feyereisen, 1985); simultaneously, breakdown of JH to inactive metabolites is enhanced by the increased production of enzymes inactivating JH such as the so-called "juvenile hormone esterase" (JHE) (for review, see Hammock, 1985).

In the present communication, we focus on regulation of JH clearance in the final instar of the tobacco hornworm *Manduca sexta*. Prior studies of this species have documented a rapid increase in the activity of JHE during the final instar (Vince and Gilbert, 1977; Sparks *et al.*, 1983). The importance of this increase has been supported by the demonstration that administration of specific JHE inhibitors can delay metamorphosis by prolonging the final instar just as can be accomplished by administering JH or its active analogs (Sparks *et al.*, 1983). Moreover, studies on hornworm CA have shown that their activity declines during the final larval instar (Bhaskaran *et al.*, 1980). JH bioassays have directed attention to multiple avenues of CA regulation, including deployment of humoral and neural inhibitors as well as withdrawal of humoral and neural stimulators (Bhaskaran and Jones, 1980; Bhaskaran *et al.*, 1980; Bhaskaran, 1981). However, neither interruption of JH breakdown nor interference with CA regulation has successfully pro-

Received 6 September 1988; accepted 25 September 1989.

Abbreviations: JH = juvenile hormone; JHA = juvenile hormone analog; JHE = juvenile hormone esterase; br-cc-ca = brain-corpora cardiaca-corpora allata complexes; CA = corpora allata; EPPAT = O-ethyl,S-phenylphosphoramidothiolate; LD = long day; SD = short day; *bl* = black larva strain of the tobacco hornworm.

voked supernumerary larval molts or done more than delay the normal pupation of final instar hornworms. Thus, the normal regulatory mechanisms that are critical for JH clearance in mature hornworm larvae remain uncertain. In the experiments described here, we document the key role played by JHE, as well as that of a brain-centered neural inhibition of JH secretion by the CA.

Materials and Methods

Hornworms were reared as previously described (Safranek and Williams, 1980) under a long-day (LD, 17L: 7D) or a short-day (SD, 12L:12D) photoperiod at 25°C. The first day of each instar was termed Day 1. Bioassays of brain-corpora cardiaca-corpora allata complexes (br-cc-ca) were performed in *black* (*bl*) hornworm larvae during the first half of the photophase as previously described (Safranek and Riddiford, 1975). Implantation of these complexes occurred 1–6 h prior to the onset of head capsule slipping in host larvae, and hosts were scored 48 h later after completion of the molt. The scoring system was derived from that previously described (Truman *et al.*, 1973) and is summarized here under Results.

Denervation of the CA was accomplished in CO_2- anesthetized larvae under Ringer's solution (Safranek and Williams, 1980). A small, three-sided flap of integument was raised near the center of the head capsule, thereby exposing the brain in the center of the field. With forceps placed behind the brain, the latter was delicately tipped forward—a maneuver that permitted adequate exposure of the two small nerves from one hemisphere of the brain to the ipsilateral corpus cardiacum-corpus allatum complex. After both nerves had been inspected, the one to be transected was securely grasped with forceps and carefully severed with scissors. The integumentary flap was replaced and the wound sealed by melted wax. In sham-operated preparations, both nerves were identified on one side but not manipulated. In all experiments, individuals were carefully examined after completion of the molt at the end of the fifth instar for JH-dependent morphological abnormalities of the types previously described (Truman *et al.*, 1974).

The juvenile hormone esterase inhibitor O-ethyl,S-phenylphosphoramidothiolate (EPPAT) was a gift of Drs. T. C. Sparks and B. D. Hammock. It was dissolved in ethanol for topical administration to the dorsal thorax or anterior abdomen using a Hamilton syringe and a repeating dispenser.

Results

Larval hornworm CA are inactivated prior to metamorphosis

To document inactivation of hornworm CA prior to metamorphosis, br-cc-ca complexes were dissected from SD fifth-instar hornworms and implanted for bioassay directly into fourth-instar *black* hornworm larvae as described under Materials and Methods. All operations were performed on *bl* larvae during the first half of the photophase so that the implanted complexes were present shortly before the onset of head capsule slipping by the *bl* larvae, at which stage the *bl* fifth-instar pigmentation can be modified by exposure to JH. The *bl* assay is useful when comparing the activity of br-cc-ca complexes producing amounts of hormone less than that required to generate the assay's maximum score of +3. As summarized in Figure 1, the complexes of larvae weighing less than 8 g on the morning of assay were nearly always active, whereas those from larvae weighing more than 8 g at that stage of the photocycle were nearly always inactive. Larvae weighing over 8 g during the first half of the photophase usually initiated metamorphosis (signaled by dorsal vessel exposure and onset of the wandering behavior) during the next scotophase; smaller larvae delayed metamorphosis for one or more days. Thus, in these experiments, complexes actively secreting JH were

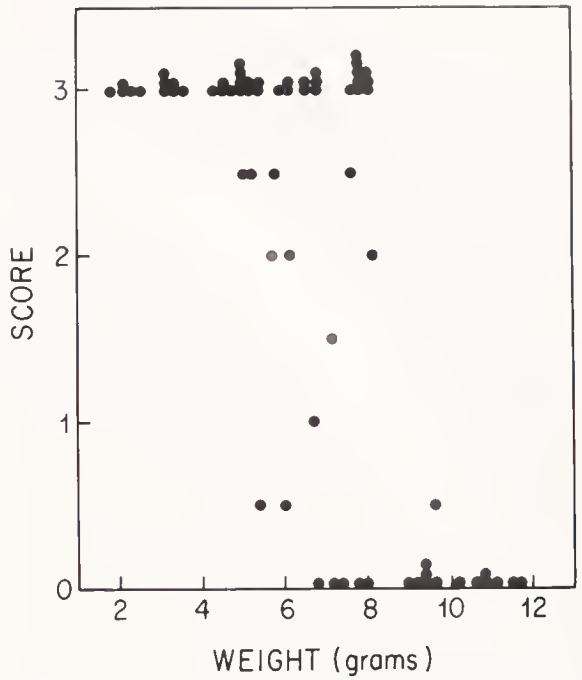

Figure 1. Activity of fifth-instar larval corpora allata in the *black* larval assay as a function of fifth-instar larval weight. Brain-cc-ca complexes from feeding fifth-instar larvae of various weights were singly implanted for assay into pharate fifth *black* hornworm larvae. These assay larvae were scored after completion of the molt to the fifth instar using the following scoring system: 0 = fully black pigmentation; 0.5 = grey head or thorax; 1.0 = green head or thorax; 1.5 = green head or thorax with faint green pigmentation apparent in the abdomen; 2.0 = grey-green abdomen; 2.5 = excessive melanization restricted to cuticular creases across the abdomen; and 3.0 = normal pigmentation. Each point represents assay of one brain-cc-ca complex.

regularly identified from larvae that were at least 36 h before the onset of the wandering period, whereas inactive complexes were found when donor larvae would have initiated wandering in less than 12 h. Thus, inactivation of the CA occurs from 12 to 36 h before the visible onset of the wandering period.

Denervated active CA block metamorphosis only in conjunction with EPPAT administration

A series of experiments were designed to evaluate the developmental responses to implantation of denervated CA in the presence or absence of EPPAT. For these studies we selected Day 2 LD fifths weighing 3.3–5.0 g, because the above data suggested that all larvae of this stage would have CA actively secreting JH. One group received implants of single CA from larvae of a similar weight and stage. A second group received application of 20 nmol of EPPAT (2 μl) every 8 h, beginning late on Day 2 and continuing until dorsal vessel exposure signaled the onset of metamorphosis. This dose and schedule of administration had been shown in preliminary experiments neither to delay the onset of metamorphosis by intact fifth-instar hornworms nor to give rise to morphological aberrations in the resulting pupae. A third group received implantation of a single CA on Day 2 followed by 20 nmol of EPPAT (2 μl) every 8 h beginning on Day 3 and continuing until the appearance of dorsal vessel exposure or of head capsule slipping. Three control groups received either a sham-operation or topical ethanol application (2 μl) every 8 h or a combination of sham-operation and topical EPPAT application (20 nmol EPPAT in 2 μl ethanol every 8 h). All larvae were restored to diet after initiation of treatment.

Results of these experiments are summarized in Table I. Larvae that received both implantation of isolated CA as well as topical application of EPPAT were the only group substantially different from the controls. Of the 23 larvae in this group, 12 formed larval-pupal intermediates similar to those seen after JH treatment of late fifth-instar larvae. Among these individuals, head capsule slipping occurred on average at Day 10 of the instar. Even the 11 larvae in this group that did not form intermediates appeared, nevertheless, to have been affected by the treatment: wandering was typically delayed until Day 10 of the instar and only 7 of the 11 pupated normally; 3 others died prior to pupation; and 1 displayed multiple abnormalities but no larval features. These findings were in contrast to the development of the control groups and of the groups in which either implantation of denervated CA or topical EPPAT application were singly employed: all groups initiated metamorphosis with, at most, slight average delays, and all individuals survived to form normal pupae.

Table I

Effects of treatment with EPPAT, denervated CA, or both

Treatment	Number	Days to wander or molt*	% Larval-pupal intermediate#
Sham operation	9	7/0	0
Sham (ethanol) application	19	6/0	0
Implantation of active CA	9	7/0	0
EPPAT application	19	6/0	0
Sham operation plus EPPAT application	20	8/0	0
CA implantation plus EPPAT application	23	10/10	52

* Mean day of fifth instar on which initiation of the wandering period or of head capsule apolysis was first noted. Treatment was initiated on LD fifth-instar larvae weighing 3.3–5.0 g late on Day 2.

Intermediates ranged from sixth-instar larvae of nearly normal appearance to largely pupal forms with retained prolegs and mandibles. The remainder exhibited patches of larval and pupal cuticle distributed in patterns characteristic of fifth-instar larvae treated with JH analogs (Truman *et al.*, 1974). Few supernumerary larvae or intermediates were able successfully to complete ecdysis at the end of the fifth instar, nor did any feed substantially or undertake further development before death.

We also attempted to abort the normal metamorphosis of fifth-instar larvae similar to those above (LD, Day 2, 3.5–5.0 g) by implanting individual loose CA from fourth-instar larvae (n = 22), or Day 1 fifth-instar larvae (n = 13), or adult females (n = 7). CA from all these stages are highly active in the *black* larval bioassay or in a pupal bioassay (Safranek and Williams, 1987; unpub. results). In no instance did the implanted CA prevent pupation or provoke retention of larval features.

Another experiment used older LD fifth instars approximately 30 h prior to the onset of the wandering period. Implantation of a single CA from a Day 1 fifth-instar (n = 13) or treatment with EPPAT (100 nmol every 8 h) (n = 9) did not prevent normal pupation. By contrast, combination of the two treatments once again led to the occurrence of sixth-instar larvae or larval-pupal intermediates in 5 of 8 larvae. Thus, as in the previous experiments, neither implantation of CA nor administration of EPPAT deployed individually substantially altered either the time course or character of metamorphosis: only combination of the two treatments regularly prevented normal pupation and led to retention of larval characteristics.

Not all EPPAT-treated preparations containing denervated CA formed larval-pupal intermediates or supernumerary larvae. Though we are uncertain of the reason for this, we suspect that the dosage of EPPAT used here may have been inadequate to ensure a response by all larvae. Our limited supply of EPPAT prevented extensive exam-

Table II

Effects of in situ *denervation of the CA coupled with EPPAT application*

Operation	Number of larvae#	% Larval-pupal intermediates*
Sham	27	0
Sever a lateral nerve to an active CA	19	11
Sever a medial nerve to an active CA	25	64

The numbers represented include only those surviving to molt. Four sham-operated preparations died postoperatively, as did three preparations with a severed lateral nerve, and five with a severed medial nerve.

* All individuals not forming larval-pupal intermediates formed pupae that were normal except for minor aberrations about the head believed secondary to the surgery. Larval-pupal intermediates demonstrated the same range of forms described in Table I. The heads of all preparations forming largely larval intermediates were dissected after the molt and in every case the persistent section of the originally operated nerve was confirmed.

ination of the response to higher EPPAT dosages. Moreover, we wished to avoid the use of EPPAT at higher dosages that cause developmental delays even in intact larvae without denervated CA (Sparks *et al.*, 1983; pers. obs.). Our limited experience with higher EPPAT dosages up to 200 nmol every 8 h suggests that more aggressive EPPAT-treatment to larvae with loose or denervated CA might well result in an even higher percentage of larval-pupal intermediates than described in the present experiments.

Denervation of CA in situ *can block metamorphosis in conjunction with EPPAT administration*

Table II summarizes a final series of experiments on fifth-instar hornworms; here we succeeded in unilaterally denervating active CA without otherwise disturbing them. In these experiments we used mature SD fifth instars 24–36 h prior to the outset of the wandering period. Larvae at this stage could be removed from diet postoperatively without the significant developmental delay routinely encountered after operation and starvation of younger larvae. Either the medial or the lateral nerve from the brain to the corpus cardiacum of one side was transected as described under Materials and Methods. After the operation, all individuals were removed from diet and received an initial dose of 120 nmol of EPPAT followed by 50 nmol every 8 h. As shown in Table II, transection of a medial nerve to a CA resulted in the formation of a larval-pupal intermediate by the majority of larvae.

Discussion

Denervation of the CA figured critically in the aborted metamorphosis of the larval-pupal intermediates generated in the present experiments. Either implantation of active CA or denervation of *in situ* CA often generated supernumerary larvae and larval-pupal intermediates when these maneuvers were deployed along with administration of the potent JHE inhibitor EPPAT. These aberrant forms were indistinguishable from the supernumerary larvae and larval-pupal intermediates seen after administration of large doses of JHA to mature feeding fifth-instar larvae (Truman *et al.*, 1974). We attribute the present findings to the inability of the brain to inactivate the denervated CA: the latter's continued secretion of JH could not be countered by the EPPAT-inactivated JHE. Hence, the secreted JH remained active and caused retention of larval features.

The present experiments document inactivation of hornworm CA late in the feeding portion of the final instar. Suppression of JH synthesis by the CA through the neural circuitry to those glands has been suggested in earlier work on the hornworm (Bhaskaran *et al.*, 1980) as well as in other species (for review, see Feyereisen, 1985). The anatomical basis for neural inhibition of the CA by the brain has also been documented: the hornworm CA demonstrate a complex innervation arising from the brain, including axons from multiple neurosecretory cells whose cell bodies lie in several regions of the brain (Nijhout, 1975; Carrow *et al.*, 1984). Most of the documented neurosecretory innervation of the CA from the brain is *via* the medial nerve (termed NCC I–II in the work of Nijhout, 1975) whose section in the present experiments coupled with EPPAT treatment often resulted in the production of larval-pupal intermediates.

Implantation of active CA can alone effectively prevent the pupation of allatectomized fourth-instar larvae and starved immature fifth-instar larvae (Bhaskaran and Jones, 1980; Bhaskaran *et al.*, 1980). The efficacy of implanted CA in these cases contrasts with our inability to block the pupation of mature, feeding fifth-instar larvae merely by implantation of active CA. In the present experiments denervation of the CA was of morphogenetic consequence only when deployed concurrently with the JHE inhibitor EPPAT. This is presumably explained by the high levels of JHE activity found in feeding fifth-instar larvae, levels manifestly sufficient to inactivate JH produced by denervated CA of every stage examined.

These experiments highlight the important role of JHE in the elimination of circulating JH prior to metamorphosis. Nevertheless, production of JHE does not seem to be required for clearance of JH sufficient to permit metamorphosis. For example, while treatment of fifth-instar larvae with EPPAT in dosages larger than

those deployed here can slightly delay the onset of metamorphosis (Sparks *et al.*, 1983; pers. obs.). EPPAT administration alone does not prevent metamorphosis or lead to the production of larval-pupal intermediates. This failure presumably reflects the concurrent suppression of JH production by the CA and the clearance of residual JH by alternative routes.

Thus, the present experiments document that the disappearance of JH necessary for the onset of metamorphosis normally occurs through two mechanisms: the inactivation of JH secretion by the CA and the production of JHE. Each mechanism can apparently alone clear sufficient JH to permit metamorphosis. Together they establish a potent system for the timely and thorough elimination of JH during the final days of larval life.

Acknowledgments

This work was initially supported by the N.I.H., continued with the generous support of Rohm and Haas, Inc., and completed with support from the N.S.F.

Literature Cited

Bhaskaran, G., and G. Jones. 1980. Neuroendocrine regulation of corpus allatum activity in *Manduca sexta:* the endocrine basis for starvation-induced supernumerary larval moult. *J. Insect Physiol.* **26:** 431–440.

Bhaskaran, G., G. Jones, and D. Jones. 1980. Neuroendocrine regulation of corpus allatum activity in *Manduca sexta:* sequential neurohormonal and nervous inhibition in the last-instar larva. *Proc. Natl. Acad. Sci. USA* **77:** 4407–4411.

Bhaskaran, G. 1981. Regulation of corpus allatum activity in last instar *Manduca sexta* larvae. Pp. 53–82 in *Current Topics in Insect Endocrinology and Nutrition,* G. Bhaskaran, S. Friedman, and J. G. Rodriguez, eds. Plenum Publishing, New York.

Carrow, G. M., R. L. Calabrese, and C. M. Williams. 1984. Architecture and physiology of insect cerebral neurosecretory cells. *J. Neurosci.* **4:** 1034–1044.

Feyereisen, R. 1985. Regulation of juvenile hormone titer: synthesis. Pp. 391–429 in *Comprehensive Insect Physiology, Biochemistry, and Pharmacology,* Vol. 7, G. A. Kerkut and L. I. Gilbert, eds. Pergamon Press, New York.

Hammock, B. D. 1985. Regulation of juvenile hormone titer: degradation. Pp. 431–472 in *Comprehensive Insect Physiology, Biochemistry, and Pharmacology,* Vol. 7, G. A. Kerkut and L. I. Gilbert, eds. Pergamon Press, New York.

Nijhout, H. F. 1975. Axonal pathways in the brain-retrocerebral complex of *Manduca sexta* (L.) (Lepidoptera: Sphingidae). *Int. J. Insect Morphol. Embryol.* **4:** 529–538.

Safranek, L., and L. M. Riddiford. 1975. The biology of the black larval mutant of the tobacco hornworm, *Manduca sexta*. *J. Insect Physiol.* **21:** 1931–1938.

Safranek, L., and C. M. Williams. 1980. Studies of the prothoracicotropic hormone in the tobacco hornworm, *Manduca sexta*. *Biol. Bull.* **158:** 141–153.

Safranek, L., and C. M. Williams. 1987. Studies of the ecdysiotropic activity of juvenile hormone in pupae of the tobacco hornworm, *Manduca sexta*. *Biol. Bull.* **172:** 299–306.

Sparks, T. C., B. D. Hammock, and L. M. Riddiford. 1983. The haemolymph juvenile hormone esterase of *Manduca sexta* (L.)—inhibition and regulation. *Insect Biochem.* **13:** 529–541.

Truman, J. T., L. M. Riddiford, and L. Safranek. 1973. Hormonal control of cuticle coloration in the tobacco hornworm, *Manduca sexta:* basis of an ultrasensitive bioassay for juvenile hormone. *J. Insect Physiol.* **19:** 195–203.

Truman, J. T., L. M. Riddiford, and L. Safranek. 1974. Temporal patterns of response to ecdysone and juvenile hormone in the epidermis of the tobacco hornworm, *Manduca sexta*. *Dev. Biol.* **39:** 247–262.

Vince, R. K., and L. I. Gilbert. 1977. Juvenile hormone esterase activity in precisely timed last instar larvae and pharate pupae of *Manduca sexta*. *Insect Biochem.* **7:** 115–120.

INDEX

D

E

F

G

H

I

J

K

L

M

N

O

P

Q

R

S

T

U

V

W

Y

Z

CONTENTS